

**PROCEEDINGS
INTERNATIONAL
SOLVENT EXTRACTION
CONFERENCE
1974**

VOL. 1



S.C.I.

PROCEEDINGS
OF THE
INTERNATIONAL SOLVENT EXTRACTION
CONFERENCE

I.S.E.C. 74

INTERNATIONAL SOLVENT EXTRACTION CONFERENCE 1974

Sponsored by: The Society of Chemical Industry

In Association with:

Societe de Chimie Industrielle
The Institution of Chemical Engineers
The European Federation of Chemical Engineering

PRESIDENT

The President Elect of The Society of Chemical Industry

VICE PRESIDENT

Professor L. Denivelle

Conference Committee

Chairman: Professor J.D. Thornton, University of Newcastle upon Tyne.

Monsieur R. Barbe, Societe de Chimie Industrielle.

Dr. G. Davies, University of Manchester Institute of Science and Technology

Dr.D.S.Flett, Department of Trade and Industry

Mr. C. Gauger, Glaxo Laboratories Ltd.

Monsieur R.Guillet, Societe de Chimie Industrielle

Professor C. Hanson, University of Bradford.

Dr. C.R.Howarth, (Assistant Secretary), University of Newcastle upon Tyne.

Professor G.V.Jeffreys, University of Aston in Birmingham

Dr.H.A.C.McKay, United Kingdom Atomic Energy Authority.

Mr. A. Newton, Imperial Chemical Industries Ltd.

Monsieur P.Regnaud, Commissariat a L'Energie Atomique.

Dr.H.Sawistowski, Imperial College, London

Mr. J.B.Scuffham, Davy Powergas Ltd.

Dr.D.H.Sharp, Society of Chemical Industry

Mr.L.G.Sherrington, Thorium Ltd.

Monsieur Y. Sousselier, Commissariat a L'Energie Atomique

Mr.B.F.Warner, British Nuclear Fuels Ltd.

Mr.J.E.White, Esso Europe Inc.

Secretary: Dr.A. Naylor, British Nuclear Fuels, Ltd.

U.K. Working Group

Chairman: Professor J.D.Thornton

Monsieur R.Barbe

Mr.C.Gauger

Dr.C.R.Howarth (Assistant Secretary)

Professor G.V.Jeffreys

Dr.H.A.C.McKay

Mr.B.F. Warner

Secretary: Dr.A. Naylor

French Working Group

Chairman: Monsieur C.Long, President de la Section Centre-Est de la Societe de Chimie Industrielle.
Monsieur Germain, Director de l'Ecole Superieure de Chimie Industrielle de Lyon.
Monsieur Jaymond, Director du Laboratoire de Recherches de Rhone-Progil (Decines).
Monsieur Vachet, President du Syndicat des Produits Chimiques de Lyon et de sa Region.

Secretary: Mademoiselle Girod, Secretaire General du Syndicat des Produits Chimiques de Lyon et de sa Region.

Editorial Committee

Professor J.D. Thornton
Dr. A. Naylor
Dr. H.A.C. McKay
Professor G.V. Jeffreys

Corresponding Members

Dr. R. Blumberg, Israel Mining Industries, Israel.
Dr. E. Detilleux, Eurochemic, Belgium.
Professor S. Hartland, Technisch-Chemisches Laboratorium, Switzerland.
Professor P.M.Heertjes, Delft University of Technology, The Netherlands
Mr. J. E. House, General Mills Chemical Inc., U.S.A.
Professor R. C. Kintner, Illinois Inst. of Technology, U.S.A.
Dr. W. Knoch, Gesellschaft Fur Kernforschung M.B.H., Germany.
Dr. T. Misek, Research Inst.Chemical Equipment, Czechoslovakia.
Professor D. F. Peppard, Argonne National Laboratory, U.S.A.
Dr. H.R.C. Pratt, University of Melbourne, Australia.
Mr G.M.Ritcey, Department of Energy, Mines and Resources, Canada.
Professor J. Rydberg, Chalmers University of Technology, Sweden.
Professor S.Stemerding, Lab v Technische Scheikunde, The Netherlands.
Professor M. Tanaka, Nagoya University, Japan.
Professor R. E. Treybal, New York University, U.S.A.
Mr.T.H.Tunley, National Institute of Metallurgy, South Africa.
Mr.J. Wilson, ICI Europa Ltd., Belgium.
Dr. M.Zifferero, Comitato Nazionale Per L'Energia Nucleare, Italy.
Professor F.I.Zuiderweg, University of Delft, The Netherlands.



SOLVENT EXTRACTION

Proceedings
of the
International Solvent Extraction Conference
I.S.E.C. 74

Lyon; 8-14th September 1974

SOCIETY OF CHEMICAL INDUSTRY
LONDON
1974

SOCIETY OF CHEMICAL INDUSTRY

14 BELGRAVE SQUARE

LONDON S.W.1.

Editorial Committee

Prof. J. D. Thornton

Dr. A. Naylor

Dr. H. A. C. McKay

Prof. G. V. Jeffreys (Editor)

© 1974 SOCIETY OF CHEMICAL INDUSTRY

In Four Volumes

ALL RIGHTS RESERVED

Printed in England by Page Bros (Norwich) Ltd., Printers

PREFACE

These three volumes contain all the papers which have been accepted for presentation at the 1974 International Solvent Extraction Conference in Lyon. In one respect, this publication represents a slight departure from the 1971 Proceedings in that all the papers have been preprinted in their final form before the Conference. This action has been forced upon us by rising costs and is a compromise between the need to supply Conference delegates with reprints and yet provide a permanent record of the Conference. A consequence of this decision is the absence of recorded Discussions following the presentation of the various papers. It is hoped however that this deficiency will be more than offset by the reduced cost of these Proceedings.

The 1974 International Solvent Extraction Conference is the triennial successor to Conferences held previously in the Hague, Israel, Sweden, the U.K., Belgium and the U.S.A. It is by now an internationally recognised forum for all those scientists, engineers and technologists concerned with the many facets of solvent extraction. In particular, the industrial applications of extraction have always been well represented and the 1974 Conference is no exception in this respect. The present volumes contain over 165 papers from workers in thirty countries and to this extent this publication can be said to reflect current interests in extraction technology. It is perhaps slightly disappointing to note the small number of contributions relating to droplet behaviour and mass transfer phenomena but, on the other hand, this fact alone might serve to encourage a few more research workers to devote some of their efforts to this important and rewarding area of extraction science.

Once again, the Solvent Extraction Group of the Society of Chemical Industry has been responsible for initiating I.S.E.C.74. The Society has very generously sponsored the Conference in Association with the Societe de Chimie Industrielle, the Institution of Chemical Engineers and the European Federation of Chemical Engineering. We are particularly indebted to the U.K. and French Working Groups for all the hard work that they have put into the organisation of this event and to the Conference Committee for their advice and guidance as arrangements proceeded. A new departure has been the appointment of a number of international

Corresponding Committee Members. This has enabled the Committee to sound a wide range of opinions quickly as the need arose.

It will be appreciated that an enormous amount of work has been involved in the refereeing and processing of the authors' papers and in this connection thanks are due to the various Session Chairmen and Secretaries for their unfailing help and enthusiasm. Thanks are also due to our French colleagues for arranging the industrial visits and the Ladies Programme. Finally our thanks are due to Dr. D.H. Sharp and Miss Jane Bovier of the Society of Chemical Industry for their continued support during the organisation of the Conference.

J.D. Thornton,
Chairman, Conference Committee,
The University of Newcastle
upon Tyne,
A. Naylor,
Secretary, Conference Committee,
British Nuclear Fuels Ltd.
Cumbria.

CHAIRMEN

Professor H M N H Irving
Professor F J Zuiderweg
Professor S Hartland
Professor J Rydberg
Professor C Hanson
Dr H Sawistowski
Professor A S Kertes
Dr W Schuller
Mr A Trambouze
Mr M Porthault
Dr A Naylor
Professor L G Schill
Dr H A C McKay
Dr T Misek
Mr A Fontine
Mr A Chesne
Professor D Wasan
Mr G M Ritcey
Ing O Braaten
Dr R Blumberg
Professor G V Jeffreys
Professor A C Pappas
Mr J Dolfus
Professor J D Thornton
Mr B F Warner

SESSION SECRETARIES

1. Dr. V. Lakshmanan	&	Dr. H. Latreille
2. Dr. G.A. Davies	&	Mr. P. Rouyer
3. Dr. M.P. Wilson	&	Mr. M. Perrut
4. Dr. D.F.C. Morris	&	Mr. A. Balhellier
5. Dr. G.A. Davies	&	Mr. J. Breysse
6. Mr. G.J. Lawson	&	Mr. C.P. Battu
7. Dr. G.J. Lawson	&	Dr. H. Latrielle
8. Dr. P.J. Bailes	&	Mr. H. Van Landeghem
9. Dr. G. Stewart	&	Mr. J. Breysse
10. Dr. D.F.C. Morris	&	Mr. P. Patigny
11. Mr. A.L. Mills	&	Mr. P. Claudy
12. Dr. J. Ingham	&	Mr. M. Perrut
13. Dr. N.M. Rice	&	Mr. P. Boero
14. Mr. A.L. Mills	&	Mr. P. Patigny
15. Dr. C.J. Mumford	&	Mr. H. Van Landeghem
16. Dr. V. Lakshmanan	&	Mr. C.P. Balfu
17. Mr. T.V. Healy	&	Mr. P. Michel
18. Dr. M. Cox	&	Mr. R. Joly
19. Dr. P.G.M. Brown	&	Mr. P. Michel
20. Dr. M. Streat	&	Mr. J.C. Leroy
21. Dr. M.A. Hughes	&	Mr. J.C. Leroy
22. Dr. W.J. Korchinski	&	Mr. C. Euzen
23. Mr. J.D. Griffin	&	Mr. C. Lackme
24. Mr. T.V. Healy	&	Mr. P. Claudy
25. Dr. E. Rushton	&	Mr. C. Lackme
26. Dr. M.A. Hughes	&	Mr. A. Bathellier
27. Dr. P.J. Bailes	&	Mr. J. Coste

EDITORIAL NOTE

The papers published in these proceedings have been printed by photoreducing the authors typescript and then reproducing by off-set lithography. The resulting publication is therefore not as elegant as ~~one~~ that would be printed in the normal manner. However, this method of production is far less costly, and the conference committee were insistent that the cost of I.S.E.C.74 should be reduced to a minimum so that a larger number of younger scientists and engineers would be able to attend. The editorial committee is of the opinion that an economic publication has been produced which they hope will be satisfactory to all participants.

The onerous work of organising refereeing the papers submitted was done by the session secretaries. In addition they arranged the papers in preparation for publication, and this made the work of the editorial committee much less difficult. We therefore express our gratitude to all the secretaries for the excellent work they have done in getting the papers ready for publication. Also we are most indebted to Mrs. M. Evans for retyping many of the papers which were not in a form suitable for printing and also to Mr. D. Austin of the University of Aston for reproducing many of the diagrams.

G.V. Jeffreys

Editor in Chief

The University of Aston in Birmingham

SESSION 1 CHEMISTRY OF EXTRACTION (MECHANISM AND STRUCTURE)

- 37 ZAGORETS P A and OCHKIN A V - Moscow Institute of Chemical Technology, USSR - non-polar solvents.
- 80 GORBANEV A I, SERGEEV V P, DZEVITSKII B E and MARGULIS V B - Moscow Academy of Sciences, USSR - Mechanism of cluster compounds extraction.
- 135 SPIVAKOV B Ya, PETRUKHIN C M and ZOLOTOV A - Moscow of Sciences, USSR - On the extraction of halide complexes of metals from the point of view of co-ordination chemistry.
- 204 MRNKA M, SATROVA J, JEDINAKOVA V and CELEDA J - Prague Institute of Chemical Technology, Czechoslovakia - Extraction of monobasic acids by amines.
- 237 LASKARIN B N, YAKSHIN V V and SHARAPOV B N - State Committee for the Utilization of Atomic Energy, Moscow, USSR - The intermolecular hydrogen bond and donor-acceptor properties of the phosphorous-and-nitrogen-containing extraction agents.

SESSION 2 EQUIPMENT (MIXER SETTLERS)

- 45 ROWDEN G A, SCUFFHAM J B and WARWICK G C I - Davy Powergas Ltd, Stockton on Tees, UK - The effect of changes in operating organic/aqueous ratio on the operation of a mixer-settler.
- 49 SLATER M J Bradford University, UK, RITCEY GM and PILGRIM R F - Department of Energy, Ottawa, Canada - Aspects of copper extraction in mixer-settlers.
- 102 MIZRAHI J, BARNEA E and MEYER D - IMI Institute for Research and Development, Israel - The development of efficient industrial mixer-settlers.
- 106 MATTILA T K - Oulu Research Laboratory, Finland - The Kemira mixer-settler extractor.
- 219 ALY G S - Lund University, Sweden - Dynamic behaviour of mixer-settlers.
- 233 KARPACHEVA S M, RAGINSKY L S, MURATOV V M, IVANOV V D and SHELOUMOV M V - State Committee for the Utilization of Atomic Energy, Moscow, USSR - Development and experience of industrial operation and optimisation of pulsed mixer-settler extractor.
- 247 JOHANNISBAUER W and KAISER G - G Kernforschungsanlage Julich mbH, W Germany - Scale-up of air pulsed mixer-settlers for the reprocessing of nuclear fuels.

SESSION 3 DROPLET PHENOMENA

- 265 11 JEFFREYS G V and ALLAK A - Birmingham University,
UK - Study of coalescence and phase separation in
bands.
- 289 18 RUSHTON E and DAVIES G A - Manchester University, UK -
The motion of liquid droplets in settling and
coalescence.
- 62 WASAN D T, ROSENFELD J I and LANGDON W M - Illinois
Institute of Technology, USA - The removal of a
dispersed liquid phase by fibrous bed coalescence.
- 90 EDGE R M and KALAFATOGLU - Strathclyde University
UK - The break-up of chlorobenzene drops falling
freely through water.
- 115 DZUBER I and SAWISTOWSKI H - Imperial College London,
UK - Effect of direction of mass transfer on break-
up of liquid jets.
- 121 IZARD J, A, Royal Military College, Victoria, CAVERS
S D and FORSYTH J S - Vancouver University, Canada -
Production of liquid drops of discontinuous injection.
- 417 147 FORSYTH J S, FISH L W and CAVERS S D - Vancouver
University, Canada - A simulation study of wake
behaviour in spray columns.

SESSION 4 CHEMISTRY OF EXTRACTION (NUCLEAR)

- 15 GUILLAMONT R, GENET M and GALIN M - Paris University,
France - Pentavalent neptunium extraction by chelate
formation from basic media.
- 46 MACASEK F, MIKULAJ and KOPUNEC R - Comenius University,
Czechoslovakia - Distribution of the daughter species
resulting from chelates by α -decay in two-phase
systems.
- 57 HEALY T V and PILBEAM A - AERE, Harwell, UK - Metal
retention by hydroxamic acids in irradiated TBP solutions.
- 143 LUNDQVIST R - Chalmers University of Technology,
Sweden - Ionic species of Pa(IV) in aqueous perchlorate
solutions.
- 202 MALEK Z, SCROTTEROVA, JEDINAKOVA V, MRNKA M and
CELEDA J - Prague Institute of Chemical Technology,
Czechoslovakia - On the extraction of zirconium by
amines from sulphate media.
- 203 SLADKOVSKA J, JEDINAKOVA V and MRNKA M - Prague
Institute of Chemical Technology, Czechoslovakia -
The composition of the organic phase in the extraction
systems tri-n-decylphosphin oxide - C_6H_6 - $HC1$ - H_2O

- 226 PUSHLENKOV M F, SHCHEPETILNIKOV N N, KUZNETSOV G I, KASIMOV F D, JASNOVITSKAYA A L and MAKOVLEV G N - Khlopin Radium Institute, USSR - Kinetics of uranium, plutonium, ruthenium, zirconium extraction with tributylphosphate.

SESSION 5 EQUIPMENT (Settler characteristics)

- 81 GORBANEV A I, DZEVITSKY B E and MARGULIS V B - Moscow Academy of Sciences, USSR - Thermodynamic nature of hyperfine emulsion formation at the extraction.
- 87 DOULAH M S and DAVIES G A - Manchester University, UK - A queue model to describe separation of liquid dispersions in vertical settlers.
- 130 EUZEN J P, cedi, RIPOCHE J and GUTTIEPREZ - Centre de Recherche Elf de Solaize, France - Comparative study of industrial coalescing packing performances in petroleum industry.
- 567 138 JACKSON I D, SCUFFHAM J B, WARWICK G C I, Davy Powergas Ltd and DAVIES G A - Manchester University, UK - An improved settler design in hydrometallurgical solvent extraction systems.
- 591 263 VIJAYAN S and PONTER A B - Swiss Federal Institute of Technology of Laysanne, Switzerland - Coalescence in a Laboratory continuous mixer-settler unit: Contributions of drop/drop and drop/interface coalescence rates on the separation process.

SESSION 6 EXTRACTION TECHNOLOGY (Common Metals)

- 100 BRUIN S, HILL J S and VAN DER MEER D - Shell Research, Holland - Solvent extraction of cobalt chloride in rotating disc contactors.
- 107 NYMAN B G, Metallurgical Research Centre and HUMMELSTEDT L, Institute of Industrial Chemistry, Finland - Use of liquid cation exchange for separation of nickel (II) and cobalt (II) with simultaneous concentration of nickel sulphate.
- 125 CHRISTIE P G, LAKSHMANAN V I and LAWSON G J - Birmingham University, UK - The liquid-liquid extraction of copper (II) and iron (III) from chloride solutions using Lix 64N in kerosene.
- 126 LAKSHMANAN V I, LAWSON G J and NYHOLM P S - Birmingham University, UK - The extraction of copper (II) and iron (III) with Kelex 100 from aqueous media containing chloride ions.

- 127 LAWSON G J and PRIDDEN B J - Birmingham University, UK.- Extraction of copper, nickel and cobalt with versatic acid from ammoniacal solutions.
- 137 MANFROY W and GUNKLER T - Dow Chemical, USA - Use of high density hydrocarbons as diluents in copper solvent extraction.
- 222 HARTLAGE J A and CRONBERG A D - Ashland Chemical Co, USA - Correlation of Kelex (R) copper distribution data with extraction and stripping mixer-settler performance.

THURSDAY, 10th September

SESSION 7 CHEMISTRY OF EXTRACTION (Common Metals)

- 7 GRIMM R and ZOLARIK Z - Institut für Heisse Chemie, W. Germany - Acidic organophosphorus extractants-XXII. Complexes of some bivalent transition metals with di (2-ethylhexyl) phosphoric acid in highly loaded organic phases.
- 50 HANSON C, Bradford University, UK and MURTHY S L N - Bombay Institute of Technology, India - Recovery of magnesium chloride from sea water concentrates.
- 67 CRABTREE H E and RICE N M - Leeds University, UK - A spectrophotometric study of the organic phase complexes formed in the extraction of cobalt (II) with carboxylic acids.
- 75 NAKASUKA N, TANAKA M, Nagoya University and YAMADA H, Gifu University, Japan - Formation of mixed metal complexes in the extraction of metals with capric acid.
- 131 HUMMELSTEDT L, SUND H, KARJALUOTO J, BERTS L and NYMAN B G - Institute for Industrial Chemistry, Finland Use of extractant mixtures containing Kelex 100 for separation of nickel (II) and cobalt (II).
- 157 TORGOV V G, MIKHAILOV V A, DROZDOVA M K, MARDEZHNOVA G A and GALTISOVA E A - Novosibirsk Institute of Inorganic Chemistry, USSR - The extraction ability of oxygen-containing extractants of class R_nXO with respect to cobalt (II) chloride.
- 181 SATO T and UEDO M - Shizuoka University, Japan - The complexes formed in the divalent metals-hydrochloric acid - di-(2-ethylhexyl)-phosphoric acid extraction systems - manganese (II), iron (II), cobalt (II), nickel (II), copper (II) and zinc (II) complexes.

SESSION 8 EXTRACTION TECHNOLOGY (Organic Processes)

- 26 ANWAR M M, COOK S T M, Teeside Polytechnic,
HANSON C and PRATT M W T - Bradford University,
UK - Separation of mixtures of 2-6 lutidine with
3- and 4-picoline by liquid-liquid extraction.
- 65 CROIX J M, LABROCHE C, LACKHE C and MERLE A -
Department de Transfert et Conversion D'Energie
Service des Transferts Thermiques, France -
Dense bed in a spray column. An application to the
extraction of phenol from waste water.
- 113 JOHANSSON G and HARTMAN A - Umea University, Sweden -
Partition of proteins in aqueous biphasic systems.
- 193 RITCEY G M, LUCAS B H and ASHBROOK A W - Extraction
Metallurgy Division, Mines Branch, Canada - Treatment
of Solvent Extraction raffinate for Removal of
organic Reagents
- 265 KICIK I and ALESSI P - Trieste University, Italy -
Liquid-Liquid equilibrium of ternary systems.
Hydrocarbons-fluorocarbon
- 267 MILNES M H - Coalite and Chemical Products Ltd, UK -
The separation of dichlorophenols by dissociation
extraction.

SESSION 9 MASS TRANSFER PHENOMENA I

- 23 PAULES B, Centre de Cinetique Physique et Chimique
du CRNS and PERRUT M, Centre de Recherches ELF,
France - Heat or mass transfer in liquid-liquid spray
columns: Wake phenomena and entrainment flow.
- 32 BAILES P J, Bradford University and THORNTON J D,
Newcastle University, UK - Electrically augmented
liquid-liquid extraction in a two-component system II-
multidrop studies.
- 114 IYER P V R and SAWISTOWSKI H - Imperial College of
Science and Technology UK - Effect of electric field
on mass transfer across a plant interface.
- 185 MEKOVAR P and VACEK V - Prague Institute of Chemical
Technology, Czechoslovakia - Single Drop oscillations
and mass transfer

SESSION 10 CHEMISTRY OF EXTRACTION (Rare Earths and Transplutonium
Elements)

- 79 MIKHAILICHENKO A I, KOTLIAROV R V, SOKOLOVA N P and
ABRAMOV L A - Institute of Rare Metals, Moscow,
USSR - Extraction of the rare earth elements with
phosphine-, amine- and sulfoxides.

- 134 FIDELIS I - Warsaw Institute of Nuclear Research, Poland - Double-double effects in the free energy and enthalpy changes of the extraction of heavy lanthanides in the HDEHP-HNO₃ system.
- 141 ALSTAD J, AUGUSTSON, J H, DANIELSEN T and FARBU L - Oslo University, Norway - A comparative study of the rare earth elements in extraction by HDEHP/Shell Sol T from nitric and sulphuric acid solutions.
- 167 MYASOEDOV B F, CHMUTOVA M K, KOTCHETKOVA H E and PRIBYLOVA G A - Moscow Academy of Sciences, USSR - Extraction of trivalent transplutonium elements and europium by a mixture of di-2-ethylhexylorthophosphoric acid and phosphorus pentoxide from strongly acid media.
- 206 KORPUSOV G V, DANILOV N A, KRYLOV Yu S, KORPUKOVA R D, DRYGIN A I and SHVARTSMAN V Ya - Moscow Academy of Sciences, USSR - Investigation of rare-elements extraction with different carboxylic acid.
- 228 PUSHLENKOV M F, VODEN V G and OBUKHOVA M E - State Committee for the Utilization of Atomic Energy, USSR - The extraction of americium, thorium and europium with capryl-hydroxamic acid (CHA)

SESSION 11 EXTRACTION TECHNOLOGY (Common Metals)

- 2 HUGHES M A and LEAVER T M - Bradford University, UK - The solvent extraction of anions from chromium bearing liquors - binary equilibria.
- 124 LAKSHMANAN V I and LAWSON G J, Birmingham University, UK - The extraction of cadmium (II) and zinc (II) from sulphate and chloride solutions with Kelex 100 and Versatic 911 in kerosene.
- 152 CUER J P, STUCKENS W and TEXIER N - Produits Chimiques Ugine Kuhlmann, France - The technique of solvent extraction applied to the treatment of industrial effluents.
- 201 BOZEC C, DEMARTHE J M and GANDON L - Societe le Nickel, France - Recovery of nickel and cobalt from metallurgical waste by solvent extraction.
- 223 MERIGOLD C R and JENSEN W H - Minerals Industries, USA - The separation and recovery of nickel and copper from a laterite-ammonia leach solution by liquid ion exchange.
- 246 MIHALOP P, Charter Consolidated Ltd, Mrs C J BARTON, LOGSDAIL D H, McKAY H A C and SCARGILL D - AERE, Harwell, UK - Design of a process for the purification of cobalt by means of di-2-ethylhexyl phosphoric acid.
- 251 DEMARTHE J M, TATNERO M, MIQUEL P and GOUONDIY J P - CEA, France - Example of nitric acid recovery by solvent extraction.

SESSION 12 EQUIPMENT (Axial Mixing Phenomena)

- 77 INGHAM J, Bradford University, UK, BOURNE J R, Zurich
1299 2 Technisch Chemisches Laboratorium and MOGLI A Kuhnli
A.G, Switzerland - Backmixing in a Kuhnli Liquid-liquid
extraction column.
- 119 CHOUDHURY P R, AMBROSE P T, McNAB G S, FISH L W and
1319 2 CAVERS S D - University of British Columbia, Canada -
Liquid-liquid spray columns: Correction of driving
force for axial mixing.
- 140 BORRELL A, MURATET G and ANGELINO H - Laboratoire
1341 2 Associe CNRS, France - Contribution of the dispersed
phase to the longitudinal mixing in a rotating disc
contactor.
- 191 WATSON J S and McNEESE L E - Oak Ridge National
1371 2 Laboratory, USA - Hydrodynamic behaviour of packed
liquid-liquid extraction columns with fluids of
different densities.

WEDNESDAY, 11th September

SESSION 13 CHEMISTRY OF EXTRACTION (Thermodynamics)

- 41 IVANOV I M, GINDIN L M and CHICHAGOVA G N - The
Siberian Branch of the Academy of Sciences, USSR -
Thermodynamic characteristics of the extraction
of anions.
- 59 O'BRIEN W G and BAUTISTA R G - Iowa State University,
USSA - A thermodynamic activity model for a single
lanthanide nitrate liquid-liquid extraction system.
- 74 KRASNOV K S, KASAS T S and KUZNETSOV V S - Ivanov
Institute of Chemistry and Technology, USSR - Thermo-
dynamics of extraction of salts with noble gas ions.
- 142 ALLARD B, JOHNSON S and RYDBERG J - Chalmers University
of Technology, Sweden - Thermodynamics and solvent
influence in zinc and copper acetylacetonate extraction
- 177 TSIMERING L and KERTES A S - The Hebrew University,
Israel - Correlation of excess enthalpies of mixing in
tributylphosphate - N - alkane system.
- 178 GRAUER F and KERTES A S - The Hebrew University,
Israel - Formation of trialkylammoniumchlorides in
dry and wet benzene.

SESSION 14 EXTRACTION TECHNOLOGY (Nuclear Processes I)

- 14 DWORSCHAK H and HALL A - CNEN - Eurex Plant, Italy -
Experiences of highly enriched uranium reprocessing
in the Eurex pilot plant.
- 61 WARNER B F, NAYLOR A, DUNCAN A and WILSON P D - BNFL,
UK - A review of the suitability of solvent extrac-
tion for the reprocessing of fast reactor fuels.
- 110 MILLS A L and LILLYMAN E - UKAEA, Dounreay, UK -
Fast reactor fuel reprocessing at Dounreay.
- 150 TUNLEY T H, Johannesburg, National Institute for
Metallurgy and NEL V W - Palabora Mining Co Ltd.,
South Africa - The recovery of uranium from uranatoria-
nite at the Palabora Mining Co. Ltd.
- 153 LEWIS L C and ROHDE K L - Idaho Chemical Processing
Plant, USA - Fission product behaviour in a two-solvent
extraction system for enriched uranium.
- 253 BOUDRY J C, CENF and MIQUEL P - CEA, France - Adapta-
tion of the purex process to the reprocessing of fast
reactor fuel

SESSION 15 EQUIPMENT (Contactor Performance I)

- 17 BAIRD M H I, McMaster University and RITCEY G M -
Department of Energy, Canada - Air pulsing techniques
for extraction columns.
- 24 MUMFORD C J and AL-HEMERI A A A - Birmingham University
UK - The effect of wetting characteristics upon the
performance of a rotating disc contactor.
- 25 ARNOLD D R, JEFFREYS G V and MUMFORD C J - ^{Aston} Birmingham
University, UK - Droplet size distribution and inter-
facial in agitated contactors.
- 55 OLDSHUE J Y, HODGKINSON F and AGOUTIN M - Mixing
Equipment Co Inc, USA - Mixing effects in a multi-
stage mixer column.
- 78 HAFEZ M M, NEMECEK M and PROCHAZKA J - Academy of
Sciences, Czechoslovakia - Hold-up and flooding in
reciprocating-plate extractors.

SESSION 16 CHEMISTRY OF EXTRACTION (Common Metals)

- 47 EINAGA H - National Institute for Researches in Inorganic Materials, Japan - Distribution characteristics of iron (III) as benzoic acid complex between benzene and 1.0 M (Na, H) C_{10}H_8 aqueous solution.
- 73 RAIS J, KYRS M and KADLECOVA L - Institute of Nuclear Research, Czechoslovakia - Extraction of some univalent and bivalent metals in the presence of macrocyclic polyether.
- 94 MUHL P, GINDIN L M, KHOLKIN A I, GLOE K and LUBOSHNIKOVA K S - Dresden Academy of Science and Siberian Branch of Academy of Science, USSR - Investigations on the mechanism of Fe (III) extraction by n-caprylic acid.
- 163 EGER I - Negev University, Israel - Salting out effect of some metal perchlorides on FeCl_3 extraction from aqueous phase with methyl isobutyl-ketone.
- 205 BREZHNEVA N E, KORPUSOV G V, PROKHOROVA N P, PROKOPCHUK Yu Z, SVETLAKOV V I and TRUKHANOV S Ya - Moscow Academy of Sciences, USSR - Investigation of extraction and some processes of separation of alkali-earth elements.
- 213 DANESI P R, MEIDER-GORICAN H, CHIARIZIA R, CAPUANO V and SCIBONA G - CNEN, Italy - Alkali metals extraction by the cyclic polyether dibenzo-18-crown-6.
- 236 LASKARIN B N, YAKSHIN V V, UL'YANOV V S and MIROKHIN A M - Moscow Academy of Sciences, USSR - The effect of structure of 2 - hydroxyphenonoximes on the formation of their copper complexes.

SESSION 17 CHEMISTRY OF EXTRACTION (General and other Interactions)

- 34 FROLOV Yu G and SERGIEVSKY V V - Moscow Institute of Chemical Technology, USSR - The hydration of organic phase components and its influence on extraction equilibrium.
- 69 SEKINE T, KOKISO M and HASEGAWA Y - Tokyo University, Japan - Effect of inert salts on the solvent extraction of metal complexes.
- 117 ASHTON N, SOARES L de J and ELLIS S R M - Birmingham University, UK - Prediction of multicomponent liquid equilibria data.
- 218 MAKSIMOVIC Z B and Mrs MIOCINOVIC - Boris Kidric Institute, Yugoslavia - Solvent extraction of PETN and RDX from nitric acid solution.

- 227 KOMAROV E V and KOMAROV V N - Leningrad State University, USSR - Peculiarities of solvent extraction by deeply associated reagents.
- 229 SHMIDT V S, MEZHOV E A and SHESTERIKOV V N - State Committee for the Utilization of Atomic Energy, USSR - Prediction and analysis of extraction system properties with linear free energies relations (LFER)
- 242 BAGREEV V V, ZOLOTOV Yu A, TSERYUTA Yu S, YUDUSHKINA L M and KUTYREV I M - Moscow Academy of Sciences - FISCHER G and MUHL P - Dresden Academy of Sciences GDR - Mutual effects of elements in the extraction by long-chain amine salts.

THURSDAY, 12th September

SESSION 18 CHEMISTRY OF EXTRACTION (New and Unusual Extractants)

- 28 DZIOMKO V M, IVANOV O V, ANVILINA V N, IVASHCHENKO A V and KASAKOVA T S - All-Union Scientific Research Institute, USSR - Recent developments in the study of heterocyclic amine extraction chemistry. Application of the formation of intramolecular hydrogen bonding between ligand and co-ordinated anions in the salt extraction.
- 82 GORBANEV A I, MARGULIS V B, DZEVITSKII B E - Moscow Academy of Sciences and SHALYGIN V M - All-Union Research Institute of Petrochemical Processes, Leningrad, USSR - Principle of systematic activation and its application for synthesis of extractants with predicted selectivity.
- 83 ZOLOTOV Yu A, SERYAKOVA I V and VOROBYEVA G A - Moscow Academy of Sciences, USSR - New sulphur-containing extractants.
- 139 MAKSIMOVIC Z B, RUVARAC A Lj and HALASI R - Boris Kidric Institute of Nuclear Sciences, Yugoslavia - Solvent extraction of metal chloride complex by tri-n-laurylamine oxide.
- 154 LAURENCE G J, Mrs T L THAI, ENSCP France, BOURGUIGNON J R and MICHEL P - CENF, France - Metals extraction by and -monosubstituted tetrahydrofurans in chlorhydric medium
- 224 UHLEMANN E - Potsdam College of Education, E Germany - The extraction and photometric determination of metals by means of thiodibenzoylmethane.
- 264 PROSKURYAKOV V A and GAILE A A - Leningrad Institute of Technology, USSR - New extractive agents for aromatic hydrocarbons.

SESSION 19 EXTRACTION TECHNOLOGY (Nuclear Processes II)

- 72 TSUBOYA T, TANAKA T, NEMOTO S and HOSHINO T -
Tokai-mura, Japan - Some modification of a Purex
process for the recovery of neptunium.
- 109 SCHMIEDER H, BAUMGARTNER F, GOLDBACKER H, HAUSBERGER H
and WARNECKE E - Institute für Heisse Chemie, W.
Germany - Electrolytic methods for application in the
Purex process.
- 197 PATIGNY P, REGNIER G, TAILLARD D and MIQUEL P - CEA,
France - Utilisation of hydroxylamine nitrate for the
final concentration and purification of plutonium in
the irradiated fuel processing factory at La Hague
- 220 SCHULZ W W, BOUSE D F and KUPFER M J - Atlantic Rich-
field Hanford Co, USA - Reflux amine flowsheet for
plutonium recovery from metallurgical scrap.
- 241 HUPPERT K L, ISSEL W and KNOCH W - G Wiederaufarbeitung
von Kernbrennstoffen mbH, W. Germany - Performance
of extraction equipment in the WAK-pilot plant.
- 257 GERMAIN M, BATHELLIER A, CENF and BERARD P - Centre
de Marcoule, France - Use of formic acid for the
stripping of plutonium.

SESSION 20 EXTRACTION CHROMATOGRAPHY AND ANALYTICAL APPLICATIONS

- 56 KROEBEL R and MEYER A - Bayer A G, W. Germany -
Application of newly developed materials for extrac-
tion chromatography of inorganic salts in columns.
- 66 BENMALEK M, CHERMETTE H, MARTELET C, SANDINO D and
TOUSSET J - Institute Physique Nucleaire, France -
The selective extraction of halide traces.
- 148 McDOWELL W J and COLEMAN C F - Oak Ridge National
Laboratory, USA - Combined solvent extraction - liquid
scintillation methods for radio-assay of alpha emitters
- 187 LEVIN I S, SERGEEVA V V, RODINA T F, TARASOVA V A,
YUKJIN Yu M, VARENTSOVA V I, VORSINA I A, BALAKIREVA N A,
BYKHOVSKAYA I A, NOVOSELTSEVA L A, TISCHENKO L I
and FRID O M - Institute for Mineral Treatment, USSR -
Di-2-ethylhexyldithiophosphoric acid application to rare
and non-ferrous metal analytical chemistry and hydro-
metallurgy; mechanism of extraction and exchange
interphase interaction of metals of the copper, zinc,
gallium, germanium, arsenic sub-groups.

- 194 EKSBERG S and SCHILL G - Uppsala University, Sweden - Ion-pair chromatography of organic components.
- 209 BORG K O, GABRIELSSON M and JOHNSON T E - A B Hassle, Sweden, Ion-pair partition chromatography applied to separations in the bioanalytical field.

SESSION 21 CHEMISTRY OF EXTRACTION (Rare metals)

- 27 MARKILAND S Aa - Research Establishment Riso, Denmark - Separation of niobium and tantalum by solvent extraction with tertiary amines from sulphuric acid solutions
- 33 FROLOV Yu G, MORGUNOV A F and SOLDATENKOVA N A - Mendeleev Institute of Chemical Technology, USSR - The state of niobium when extracted from solutions of sulphuric and hydrochloric acids.
- 36 YAGODIN G A, SINEGRIKOVA O A and CHEKMAREV A M - Mendeleev Institute of Chemical Technology, USSR - Zirconium and hafnium polymerization effect on their extraction by different class organic compounds.
- 128 BRONZAN P and MEIDER-GORICAN H - Institute Rudjer Bosovic, Yugoslavia - Solvent extraction of zirconium and hafnium with some trifunctional phosphine oxides.
- 182 SATO T, KOTANI S and TERA O - Shizuoka University, Japan - The extraction of anionic vanadium (IV)-thiocyanato complex from aqueous solutions by long-chain alkyl quaternary ammonium compound.
- 186 JORDANOV N, PAVLOVA M - Institute of General and Inorganic Chemistry and BOIKOVA D - High Institute of Chemical Technology, Bulgaria - Mechanism of solvent extraction of perhenate ions by cyclohexanone.

SESSION 22 EQUIPMENT (Contactor Performance II)

- 155 LAURENCE G, HABSINGER D, TALEOT J - ENSCP, France and CHAIEB M T - Tunis University, Tunisia and MICHEL P, Centre d'Etudes Nucleaires, France - Metal extraction by di-n-heptyl phosphide (DH_2SO); applications in a pulsed column.
- X 216 STEINER L and HARTLAND S - Federal Institute of Technology, Switzerland - Calculation of mass transfer coefficients in extraction columns under non-ideal-flow conditions.
- 2315 248 WEISS, S, SPATHE R, WURFEL R and MOHRING D - Technische Hochschule fur Chemie, E. Germany - Hydrodynamic behaviour and mass transfer of extraction columns with various rotating parts.

256

3 2339

ROWYER H, LEBOUHELLEC J, HENRY E and MICHEL P -
CEA, France - Present study and development of
extraction pulsed columns.

258

3 2365

SEIDLOVA B and MISEK T - Research Institute of
Chemical Equipment, Czechoslovakia - Liquid flow
study in the cross-section of ARD extractor.

266

TODD D B and DAVIES G R - Baker Perkins Inc. USA -
Performance of centrifugal extractors.

SESSION 23 MASS TRANSFER PHENOMENA II

51

HANSON C, HUGHES M A and MARSLAND J G - Bradford
University, UK - Mass Transfer with chemical reaction
in liquid-liquid systems.

53

COX P R and STRACHAN A N - Loughborough University,
UK - The influence of chemical reaction (nitration)
on the rate of surface renewal at a liquid-liquid
interface.

95

FARBW L, McKAY H A C and WAIN A G - Atomic Energy
Research Establishment, UK - Transfer of metal nitrates
between aqueous nitrate media and neutral organo-
phosphorus extractants.

174

RITCEY G M and LUCAS B H - Mines Branch, Canada -
Diluents and modifiers - their effect on mass transfer
and separation.

192

CLINTON S D - Oak Ridge National Laboratory, USA -
Mass transfer of water from single aqueous sol droplets
fluidized in a partially miscible alcohol.

FRIDAY, 13th September

SESSION 24 CHEMISTRY OF EXTRACTION (Synergism and Kinetics)

6

AMMON R V - Institut für Heisse Chemie, W. Germany -
 ^1H - and ^{31}P -NMR study of ligand exchange kinetics in
the systems $\text{UO}_2(\text{NO}_3)_2$ -TBP and $\text{Pu}(\text{NO}_3)_4$ -TBP.

12

SPINK D R and OKUHARA D N - University of Waterloo,
Canada - The effect of diluents on the extraction
of tracer level copper by an alkyl hydroxy quinoline
(Kelex 100).

35

YAGODIN G A, TARASOV V V and KIZIM N F - Mendeleev
Institute of Chemical Technology, USSR - The state of
substances in the organic phase and stripping micro-
kinetics.

91

FLETT D S, COX M and HEELS J D - Warren Spring Laboratory
UK - Extraction of nickel by hydroxyoxime/carboxylic
acid mixtures.

- 136 SPIVAKOV B Ya, MYASOEDOV B F, SHKINEV B M, KOTCHETKOVA N E and CHMUTOVA M K - Moscow Academy of Sciences, USSR
Synergic extraction of metals by the mixtures of tri-n-octylamine with a neutral extractant from nitrate and chloride solutions.
- 195 NAVRATIL O - Purkyne University, Czechoslovakia -
Synergistic effects in liquid-liquid extraction of some heavy metals by 1-phenyl 3-methyl-3-benzoyl-pyrazol-5-one.
- 269 KOLARIK Z and KUHN W - Institut fur Heisse Chemie, W. Germany - Acidic organophosphorus extractants-XXI. Kinetics and equilibria of extraction of Eu(III) by di(2-ethylhexyl) phosphoric acid from complexing media.

SESSION 25 EXTRACTION TECHNOLOGY (Process Modelling and Control)

- 9 McDONALD C R and WILKINSON W L - Bradford University, UK - Control studies on a solvent extraction column.
- 211 GAUDERNACK B, MULLER T B, NULAND S and ORJASAETER O - Institutt for Atomenergi, Norway - Simulation of the static and dynamic behavior of a solvent extraction process for rare earth separation.
- 250 BOYADZHIEV L and ANGELOV G - Academy of Sciences, Bulgaria - On the multicomponent extraction with backmixing.
- 260 ARMFIELD R N and AGNEW J B - Monash University, Australia
Application of a two-variable-search optimisation scheme to the on-line control of a continuous extraction process.

SESSION 26 CHEMISTRY OF EXTRACTION (Rare Metals)

- 64 FOUCHE K F, LESSING J G V and P A BRINK - Atomic Energy Board, South Africa, Extraction of platinum group metals from cyanide melts with liquid metals.
- 88 SINITZIN N M, TRAVKIN V F, PLOTINSKY G L, SVETLOV A A and ROVINSKY F J - Moscow Institute of Fine Chemical technology, USSR - Extraction of ruthenium and osmium nitrosocomplexes.
- 123 GROENEWALD T - Chamber of Mines, South Africa, - A modified diluent for the solvent extraction of gold (I) cyanide from alkaline solution.
- 129 SEVDIC D - Institute "Rudjer Boskovic", Yugoslavia - Solvent Extraction of silver (I) and mercury (II) with sulphur containing ligands.

- 158 MIKHAILOV V A, KOROL N A and BOGDONOVA D D -
Institute of Inorganic Chemistry, USSR - The
chemical equilibria at distribution of mercury
chloride between water and solutions of TBP and
di-n-octyl sulphoxide in different diluents.
- 252 ESNAULT F, ROBAGLIA M, LATARD J M and DEMARTHE J M -
CEA, France - Separation of molybdenum and tungsten
by a liquid-liquid ion-exchange method.

GENERAL SESSION 27 INDUSTRIAL PROCESSES (Development,
Performance and Economics)

- 103 BLUMBERG R, GAI J E and HAJDU K - IMI Institute for
Research and Development, Israel - Interesting aspects
in the development of a novel solvent extraction
process for producing sodium bicarbonate.
- 145 KUYLENSTIERNA U - Stora Kopparbergs AB - and OTTERTUN
H - Chalmers University of Technology, Sweden - Solvent
extraction of HNO_3 -HF from stainless steel pickling
solutions.
- 199 DASHER J - Bechtel, USA - Economics of SX and its
alternatives for uranium and copper.
- 261 BIRCH C P - Nchanga Consolidated Copper Mines, Zambia
The evaluation of the new copper extractant "P-1"
- 274 RITCEY G M, LUCAS B H and ASHBROOK A W - Extraction
Metallurgy Division, Mines Branch, Canada - Some
Comments on the, and Environmental Effects of Solvent
Extraction Reagents used in Metallurgical Processing.

SESSION 1

Monday 9th September: 9.00 hrs

C H E M I S T R Y O F E X T R A C T I O N
(Mechanism and Structure)

Chairman

Professor H.M.N.H. Irving

Secretaries

Dr. V. Lakshmanan

Dr. H. Latreille

The Statistical Theory of Substituted Ammonium Salt
Solutions in Non-polar Solvents

by P.A.Zagorets, A.V.Ochkin

McMillan - Mayer statistical theory of solutions has been applied for describing extraction systems with substituted ammonium salts. The second virial coefficient has been computed by using of the potential of central point dipole inside hard sphere. Other potentials are also discussed. Dipole moments of some substituted ammonium salts have been measured. Effective diameters of ammonium salt molecules have been calculated from concentration dependence of activity coefficients and dielectric constant of solution.

D.I.Mendelev Institute of Chemical Technology,
Moscow, USSR.

The characteristic feature of amine extraction systems is nonideality of organic phase. Large dipole moments of alkylammonium salts and low dielectric constant of diluents used in extraction result in the fact that solute-solute interaction greatly exceeds solute-solvent or solvent-solvent interaction. As a result the strong association and the hydration of amine salts is observed. There are several approaches for describing such systems. We think one of the most progressive to be the application of McMillan-Mayer statistical theory¹. After us²⁻⁷ this theory was used by Levy⁸.

McMillan-Mayer Statistical Theory of Solutions.

According to McMillan-Mayer statistical theory the thermodynamic functions of solutions can be expressed in power series of component concentrations. Thus the following equations have been derived for vapour pressure over solution P and solvent activity α :

$$P = P_0 + RT \left[\frac{\Delta\alpha}{\gamma} + \sum_s c_s - \sum_{j,n} (1 + \sum_s n_s - 1) B_{jn} \left(\frac{\Delta\alpha}{\gamma} \right)^j \prod_s c_s^{n_s} \right] \quad (1)$$

$$\ln \alpha = \ln \rho - \frac{\gamma}{\Delta\alpha} \sum_{j,n} j B_{jn} \left(\frac{\Delta\alpha}{\gamma} \right)^j \prod_s c_s^{n_s} \quad (2)$$

where ρ and γ are a concentration and an activity coefficient of solvent; $\gamma = \alpha/\rho$; at infinite dilution $\alpha_0 = \rho_0$ and $\gamma_0 = 1$; $\Delta\alpha = \alpha - \alpha_0$;

c_s is a concentration of component s in solution; B_{jn} is irreducible integral characterizing interaction of j solvent molecules and n solute molecules in infinitely dilute solution. Calculation of B_{jn} can be made by means of equations like those used in the theory of imperfect gases. For example, for the same molecules 1 and 2

$$B_2 = \frac{N_0}{2 \cdot 10^3} \int_V [\exp(-u_{12}/kT) - 1] dq_{12} \quad (3)$$

where u_{12} is average force potential; q_{12} is the generalized co-ordinate characterizing the relative position of molecules 1 and 2; $N/10^3$ is normed multiplier allowing to use molar concentrations in the equations (1) and (2); N_0 is Avogadro's number.

To apply the equations (1) and (2) for describing extraction systems it is reasonable to transform them as shown earlier⁵.

1) Let's introduce mole fraction x_1 , activity a_1 and mole activity coefficient $f_1 = a_1/x_1$ of solvent. As $x_1 = \frac{\rho}{\rho_0 + \sum c_s}$ and

$a_1 = \frac{\alpha}{\rho_0}$ then

$$\ln f_1 = \ln(\rho + \sum c_s) - \ln \rho_0 - \frac{1}{\Delta \alpha} \sum_{n=1}^{\infty} B_{1n} \left(\frac{\Delta \alpha}{\gamma}\right)^n \prod_r c_r^{n_r} \quad (4)$$

2) Applying (1) for constant $P, \Delta \alpha / \gamma$ is expanded in series in c_s

$$\frac{\Delta \alpha}{\gamma} = - \sum_s c_s + \sum_{n=2}^{\infty} L_n \prod_s c_s^{n_s} \quad (5)$$

where L_n is easily calculated by substituting (5) in (1) and by equalizing sums of terms with the same powers of c_s to zero. For example

$$L_2 = B_{02} - B_{11} + B_{20} \quad \text{and} \quad L_{11} = B_{011} + 2B_{200} - B_{110} - B_{101} \quad (6)$$

3) As $\frac{\Delta \alpha}{\gamma} = \frac{\alpha - \alpha_0}{\gamma} = \rho - \frac{\rho_0}{\gamma}$ then we find from (5)

$$\rho + \sum c_s = \frac{\rho_0}{\gamma} + \sum_{n=2}^{\infty} L_n \prod_s c_s^{n_s} \quad (7)$$

and expressing γ from (2)

$$\rho + \sum c_s = \rho_0 \exp \left[\frac{1}{\Delta \alpha} \sum_{n=1}^{\infty} B_{1n} \left(\frac{\Delta \alpha}{\gamma}\right)^n \prod_r c_r^{n_r} \right] + \sum_{n=2}^{\infty} L_n \prod_s c_s^{n_s} \quad (8)$$

4) Substitution (8) in (4) and expansion of $\ln(\rho + \sum c_s)$ in Taylor's series lead for two-component system to

$$\ln f_1 = A_2 c^2 + A_3 c^3 + \dots \quad (9)$$

where $A_2 = \frac{1}{\rho_0} (B_{02} - B_{11} + B_{20})$; $A_3 = \frac{2}{\rho_0} (B_{03} - B_{12} + B_{21} - B_{30})$ etc. (10)

Thus the evaluation of thermodynamic functions comes to the calculations of irreducible integrals.

Calculation of Irreducible Integrals.

It has been shown⁵ that the irreducible integrals B_{20} and B_{11} can be expressed by means of partial molar volumes of solvent V_{01} and solute V_{02} and isothermal compressibility of solvent β :

$$B_{20} = \frac{1}{2}(RT\beta - V_{01}) \quad \text{and} \quad B_{11} = RT\beta - 2V_{01} + V_{02} \quad (11)$$

Table 1 gives B_{20} and B_{11} for solutions of some salts in benzene, the data being taken from literature. As values $\rho_0 A_2$ (Table 7) are usually much more than 50 it is evident that B_{20} and B_{11} can be ignored in (10) i.e.

$$\rho_0 A_2 \approx B_{02} \quad (12)$$

The equation (12) shows the interaction between two amine salt molecules in solution to exceed greatly the interaction of a salt molecule with a solvent molecule or the interaction between two solvent molecules.

Calculation of B_{02} is rather complicated and greatly depends on the form of the chosen average force potential u_{12} . As the first approximation it is possible to use interaction energy of two point dipoles μ placed in center of hard spheres of diameter σ :

$$u_{12} = +\infty \quad \text{at } r < \sigma$$

$$u_{12} = -\frac{\mu^2}{\epsilon_0 r^3} (2\cos\theta_1 \cos\theta_2 - \sin\theta_1 \sin\theta_2 \cos\varphi) \quad \text{at } r > \sigma \quad (13)$$

where r is the distance between dipoles, θ_1 and θ_2 are the angles between the direction of dipoles and their connecting line, φ is the angle of their relative rotation, ϵ_0 is the dielectric constant of solvent. It is clear that this potential rather

roughly reflects true picture of interaction in solution. Nevertheless at present the choice of potential according to (13) is fully justified because of following reasons:

1) As mentioned above ($B_{02} \gg B_{20}$ or B_{11}) the interaction between amine salt molecules is much stronger than that of solvent molecules. Therefore the solvent can be treated as continuum of dielectric constant ϵ_0 .

2) Lack of necessary data does not allow to take into account true geometrical form and charge distribution in salt molecules.

3) Complication of intermolecular potential results in some mathematical difficulties which are often impossible to overcome.

To calculate B_{02} we substitute (13) in (3), expand the exponent in series and make integration.

$$B_{02} = \frac{N_0}{4 \cdot 10^3} \int_0^{2\pi} \int_0^\pi \int_0^\pi \int_0^\infty [\exp(-u_{12}/kT) - 1] r^2 dr \sin \theta_1 d\theta_1 \sin \theta_2 d\theta_2 d\varphi =$$

$$= \frac{2\pi N_0}{3 \cdot 10^3} \sigma^3 \left[-1 + \sum_{n=1}^{\infty} \beta_n x^{2n} \right] \quad (14)$$

$$\text{where } x = \frac{\mu^2}{\epsilon_0 kT \sigma^3}; \beta_n = \frac{2^{2n}}{(2n+1)!(4n^2-1)} \left[1 + \frac{n}{2(2n-1)} + \dots + \frac{n!}{2^n(2n-1)(2n-3)\dots 3 \cdot 1} \right]$$

Table 1.

Values B_{20} and B_{11} for some solutions in benzene.

Salt	$t^\circ C$	V_{02} l /mole	$RT\beta$ l/mole	V_{01} l/mole	B_{20} l/mole	B_{11} l/mole
$(C_4H_9)_4NCNS$	20	0.3119 ^a	0.0023 ^b	0.089 - 0.043	0.089 - 0.043	0.136
	25	0.3124 ^a				
	30	0.3129 ^a				
$(C_{12}H_{25})_3NHBr$	25	0.65 ^c		0.089 - 0.043		0.47
$(C_{12}H_{25})_3NHNO_3$	25	0.65 ^c		0.089 - 0.043		0.47

^a Reference 9.

^b Reference 10.

^c Reference 11.

Values $\frac{B_{02}}{\sigma_3} \cdot 10^{-24}$

[illegible]

By means of computer we calculated β_n till $n = 30$ and B_{02}/σ^3 for $x = 5.0 \div 10.0$ through 0.1 (Table 2).

It is evident from table 2 that B_{02}/σ^3 is monotonous increasing function of x . Therefore the association of amine salts is to increase with growth of dipole moment, with diminishing of dielectric constant, temperature and amine radical length. These regularities are in good conformity with data on association of amine salts.

Dipole Moments of Amine Salts.

The values μ and σ are necessary for B_{02} calculation. The former may be measured tentatively from independent data the latter being "effective" values and can't be determined from experiment. Due to this it is reasonable to determine σ on activity coefficient values of solvent and to compare them with other molecular parameters, for example, with anion radii.

Dipole moments of compounds in solutions are usually determined by Debye's method. In one of the modifications of this method¹², the dielectric constant of solution ϵ is dealt with as a linear function of solute gravimetric concentration w :

$$\epsilon = \epsilon_0 + \alpha' w \quad (15)$$

The concentration range w (where equation (15) is correct) is rather small due to a very strong association of amine salts in non-polar solvents. Dependence ϵ on w was curvilinear in most researches where dipole moments of ammonium salts were measured. Application of curvilinear areas is found to result in lower values of parameter α' and dipole moment μ . To avoid

this difficulty we used concentrations which are 10 times less those usually applied. Thus for tertiary amine salts $w = 0.00008 + 0.0006$ and for quaternary ammonium salts $w = 0.00001 + 0.0002$. For sake of comparison let's point out that in recent work¹¹ the minimum concentration of amine salts w was about 0.001. In mentioned above concentration range the equation (15) was applied for tertiary amine salts whereas the dependence ϵ on w was curvilinear for quaternary ammonium salts and approximated as

$$\epsilon = \epsilon_0 + \alpha' w + \alpha'' w^2 \quad (16)$$

The results of measurements are given in Tables 3 and 4.

Table 3

Dipole moments of some tertiary amine salts in benzene¹³.

Salt	$t^{\circ}\text{C}$	α'	μ_D	μ_D reported
$(\text{C}_4\text{H}_9)_3\text{N HCl}$	25	35.52	8.53	7.2 ^a 8.1 ^b
$(\text{C}_6\text{H}_{13})_3\text{N HCl}$	25	25.59	8.50	
$(\text{CH}_3)(\text{C}_8\text{H}_{17})_2\text{N HCl}$	25	25.59	8.27	
$(\text{C}_{12}\text{H}_{25})_3\text{N HCl}$	25	13.88	8.47	7.6 ^c
$(\text{C}_6\text{H}_{13})_3\text{N HBr}$	25	26.16	9.19	
$\text{CH}_3(\text{C}_8\text{H}_{17})_2\text{N HBr}$	25	25.30	8.85	
$(\text{C}_{12}\text{H}_{25})_3\text{N HBr}$	25	14.86	9.11	
"	40	13.67	9.09	
$(\text{C}_{12}\text{H}_{25})_3\text{N HNO}_3$	25	15.80	9.24	
$(\text{C}_{12}\text{H}_{25})_3\text{N H}_2\text{SO}_4$	25	4.206	4.92	6.4 ^c
$(\text{C}_{12}\text{H}_{25})_3\text{N HClO}_4$	25	20.84	10.95	10.1 ^c

^a Reference 14.

^b Reference 15 (solvent is toluene)

^c Reference 11.

Table 4

Dipole moments of quaternary ammonium salts
in benzene⁷.

Salt	t °C	α'	$\alpha' \cdot 10^3$	μ D
$(C_5H_{11})_4NCl$	25	37.06	107.1	10.7
	40	37.54	84.7	11.2
$(C_6H_{13})_4NJ$	25	43.88	210.5	13.9
	40	44.26	153.2	14.6
$C_8H_{17}(C_4H_9)_3NJ$	25	43.0	215	13.0
$(C_8H_{17})_4NJ$	25	36.5	150	14.1
	40	35.2	114	14.4
$CH_3(C_8H_{17})_3NJ$	25	15.35	20.7	8.11
$(CH_3)_2(C_8H_{17})_2NJ$	40	13.6	22.5	7.0
$(C_8H_{17})_4NNO_3$	25	31.86	91.1	12.5
	40	35.31	97.9	13.6
$C_3H_7(C_8H_{17})_3NBr$	25	25.9	64	10.7

Figures listed in Table 3 show that dipole moments of tertiary amine salts practically do not depend on radical length. Only introduction of methyl radicals diminishes dipole moment on $\sim 0,3$ D. As the dependence ϵ on w for quaternary ammonium salts was not linear in the involved concentration range the values μ in Table 4 appear to be lowered. Nevertheless the sharp lowering of dipole moment when methyl radical is introduced can be considered to be certain.

Calculation of Effective Diameters of Salt
Molecules on Activity Coefficient Data

Values $\rho_o A_2 \approx B_{o2}$ and also values σ were calculated on experimental data of solvent activity coefficients. The results are summerized in Table 5.

Table 5.

Effective diameters of some alkylammonium salts

Salt	Conditions	Ref.	$\rho_o A_2(B_{o2})$ l/mole	μ_D	σ_A
$(C_8H_{17})_3N HBr$	$C_6H_6-78.6^0C$	4	45.3	9.1	4.9I
"	$CCl_4-75.3^0C$	4	I35	9.1	4.76
$(C_8H_{17})_3NHCl$	"	2	83.7	8.5	4.6I
$(C_8H_{17})_3N HClO_4$	"	2	287	II.0	5.34
$CH_3(C_8H_{17})_2NHCl$	"	4	I22	8.3	4.47
$(C_{12}H_{25})_3N HBr$	"	4	II6	9.1	4.79
$(C_6H_{13})_4NJ$	"	2	I4IO	I4.3	6.I7
"	$C_6H_6-78.6^0C$	4	629	I4.3	6.25
$(i-C_5H_{11})_4NCNS$	$C_6H_6-5.5^0C$	I6,I7	3434	I5.4	6.75

Values σ given in Table 5 have a reasonable order and, in particular, they are larger than the diameters of salt anions. They also increase with increase of anion radius and at less degree with the growth of radical length.

Calculation of Effective Diameters of Salt Molecules
on dielectric Data.

One of the main reasons of nonlinear dependence of dielectric constant of amine salt solutions on their concentration is the solute association. The values α'' in (16) which are measures of deviation from linearity can be used to calculate effective diameters of salt molecules.

The orientational polarization P_2 of solute in dilute solutions can be expressed as

$$P_2 = \frac{4\pi\mu^2 N_0}{9\kappa T} (1 + B'_2 C + \dots) \quad (17)$$

where B'_2 is the second virial coefficient of dielectric polarization which can be deduced from following equation¹⁸:

$$B'_2 = \frac{N_0}{10^3} \int \cos \psi \exp(-u_{12}/\kappa T) dq_{12} \quad (18)$$

where ψ is the angle between directions of two dipoles. Using (13), expanding the exponent in series and making integration we find

$$B'_2 = \frac{4\pi N_0}{3 \cdot 10^3} \sigma^3 \sum_{n=1}^{\infty} \beta'_n x^{2n+1} \quad (19)$$

where $x = \frac{\mu^2}{\epsilon_0 \kappa T \sigma^3}$; $\beta'_n = \frac{2^{2n} (n-3)!}{2! (2!+1)^2 (2!+3)^2 \dots (2n+3)^2}$

Computed values B'_2/σ^3 for $x = 5.0 + 10.0$ through 0.1 are presented in Table 6. Values B'_2 may be also calculated from experimental data according to next equation¹⁹:

$$B'_2 = \frac{M_2}{10^3} \left\{ \frac{3}{(\epsilon_0+2)^2} \cdot \frac{\alpha'' V_0^2 M_2}{P_2} + \gamma' - \frac{\alpha' V_0}{\epsilon_0+2} - \frac{P_2 \epsilon (\epsilon_0+2)}{3 M_2} + \frac{(V_0+\gamma')(\epsilon_0-1)}{3} \right\} \quad (20)$$

where M_2 and P_{2E} are correspondingly mol. wt. and electronic polarization of solute, V_0 is the specific volume of solvent, γ' is a coefficient in equation $V = V_0 + \gamma' w$. Comparison of values B'_2 calculated on equation (20) with tabulated data in Table 6 allows to determine σ . The results are given in Table 7. and have reasonable value. As might be expected they increase with growth of amine radical length and anion radius. At the same time

Table 6

Values - $\frac{B_2'}{\sigma^3} \cdot 10^{-24}$

$x = \frac{\mu^2}{\epsilon_0 K T e^2}$	0.0	0.1	0.2	0.3	0.4	0.5	0.6	0.7	0.8	0.9
5.	0.036946	0.042846	0.049709	0.057698	0.067003	0.077846	0.090488	0.105236	0.12245	0.14256
6.	0.16605	0.19351	0.22563	0.26323	0.30724	0.35880	0.41923	0.49009	0.57322	0.67078
7.	0.78534	0.91991	1.07806	1.26401	1.4827	1.7401	2.0431	2.3999	2.8203	3.3158
8.	3.9000	4.5890	5.4021	6.3618	7.4949	8.8335	10.4151	12.2846	14.495	17.109
9.	20.203	23.864	28.198	33.331	39.412	46.617	55.157	65.283	74.291	91.537

Table 7.

Effective diameters of salt molecules on dielectric
data

Salt	t °C	μ D	$-B'_2$ l/mole	σ Å
$(C_5H_{11})_4NCl$	25	11.0	1100	5.38
	40	11.0	876	5.34
$(C_6H_{13})_4NJ$	25	14.3	2640	6.34
	40	14.3	1940	6.31
$C_8H_{17}(C_4H_9)_3NJ$	25	13.1	2440	5.98
$(C_8H_{17})_4NJ$	25	14.3	2780	6.34
	40	14.3	2220	6.29
	25	8.11	735	4.36
$CH_3(C_8H_{17})_3NJ$	40	7.0	716	3.87
$C_3H_7(C_8H_{17})_3NJ$	25	10.7	1350	5.25
$(C_8H_{17})_4NO_3$	25	13.1	1730	6.03
	40	13.1	1700	5.95
$(C_{12}H_{25})_3NHClO_4$	25	11.0	45.4	5.96
$(C_{12}H_{25})_3NHBr$	40	9.1	9.23	5.44

one can observe the continual decrease σ with temperature increase which might be caused by

- 1) errors in values α'' and μ due to curvilinearity of dependence ϵ on w ;
- 2) in-accuracy of involved average force potential (13).

Conclusion

The statistical theory of solutions considered above describes rather well qualitative regularities which are observed in alkylammonium salt solutions in solvents with low dielectric constant. To reach better agreement the theory with experiment it is necessary to consider other forms of average force potential instead of (13). It should be noted that the potential (13) can't be used for describing amine salt hydration because it predicts wrongly growth of hydration with increase of salt dipole moment. Now we carry out research to describe hydration phenomenon with use of patterns in which amine salt molecule is treated as a pair of spherical ions. Main problem in using more complicated potentials than (13) is a difficulty to make integration. Application of more powerful computers is likely to let overcome this problem.

References

1. McMillan, W.G., and Mayer, Y.E., J.chem.Phys., 1945, 13, 276.
2. Zagorets P.A., Ochkin A.V., Trudy mosk.khim. - tekhnol.Inst, 1965, 49, 206.
3. Zagorets P.A., Ochkin A.V., Trudy mosk.khim. - tekhnol.Inst., 1968, 58, 48.
4. Zagorets P.A., Ochkin A.V., Teor.exper.khim., 1969, 5, 484.
5. Ochkin A.V., Zagorets P.A., Teor.exper.khim., 1965, 2, 489.
6. Frolov, Yu.G., Ochkin A.V., and Sergievsky V.V., Atom. Energy Rev., 1969, 7, 71.
7. Ochkin A.V., Zagorets P.A., Zh.fiz.khim., 1973, 47, 2010.
8. Levy O., J.phys.Chem., Ithaca, 1972, 76, 1752.
9. Poltoratzky G.M. Dissertation, Mosk.Khim.Tekhnol.Inst. Moscow, 1964.
10. Pena, M.D., and Cavero B., Anales Real.Soc.Expan.Fis. Quim (Madrid), Ser.B. 1964, 60, 357.
11. Levy O., Markovits G., and Kertes, A.S., J.phys.Chem., Ithaca, 1971, 75, 512.
12. Halverstadt, I.F., and Kumler, W.D., J.Amer., Chem.Soc., 1942, 64, 2988.
13. Ochkin A.V., Zagorets P.A., Zh.fiz.khim., 1972, 46, 2911.
14. Geddes, J.A., and Kraus, C.A., Trans.Faraday Soc., 1936, 32, 585.
15. Deitz V., and Fuoss, R.M., J.Amer.Chem.Soc., 1938, 60, 2394.
16. Batson, E.M., and Kraus, C.A., J.Amer.Chem.Soc, 1934, 56, 2017.
17. Copenhafer D.T., and Kraus C.A., J.Amer.Chem.Soc., 1951, 73, 4557.
18. Fuoss, R.M., J.Amer.Chem.Soc., 1934, 56, 1031.
19. Buckingham, A.D., and Raab, R.E., Trans.Faraday Soc., 1959, 55, 377.

MECHANISM OF CLUSTER COMPOUNDS EXTRACTION

A.I. Gorbanev, V.P. Sergeev, B.E. Dzevitskii, V.B. Margulis

Baikov Institute of Metallurgy of the Academy of Sciences
of the USSR, Moscow, USSR

ABSTRACT

A systematic study has been carried out on the extraction of platinum metals in the presence of tin dichloride from aqueous solutions of hydrochloric acid with tributyl phosphate and a number of oxygen-containing solvents belonging to basic classes of organic compounds. The formation of clusters via platinum metal-to-tin bonding and the transfer of these to an organic phase in the form of cluster anions ion-paired to oxonium cations is the basis of the process, as established by the concentration dependence measurements and spectral (optic and Mössbauer) evidence. The above scheme is adequate for all the platinum metals in general. The character of intermetallic bonds in the clusters is discussed.

INTRODUCTION

Ivanov (1) was the first to report the formation of coloured complexes of platinum with tin dichloride. Since then this phenomenon has been used as a sensitive test reaction (2, 3).

Later, the reaction was extended to other platinum metals and the ability of coloured species to transfer to organic phase was demonstrated (4). The extraction mechanism and structures of the compounds formed represented an interesting problem. Isolation and analysis of the solid-phase platinum complexes along with data on their structures were first reported in the communication (5).

In the present work this investigation is extended to other platinum metals. To this effect a thorough study of the concentration dependences was carried out and spectroscopic properties of complexes both in solid phase and in solution were determined, which enabled us to identify species present in the extracts and provided a key to the extraction mechanism.

EXPERIMENTAL

Materials. The concentration of the initial hydrochloric acid of "Pure" grade was 10.5M as measured alkalimetrically.

It was brought to an adequate dilution by an estimated volume of distilled water.

A purity grade "Analytically Pure" $\text{SnCl}_2 \cdot 2\text{H}_2\text{O}$ was used, weighted amounts of it being dissolved in hydrochloric acid to obtain solutions of required concentration.

For the most part preparation of platinum metal-containing solutions followed the procedures recommended in (6). Operating solutions of Pt(IV), Pd(II), Rh(III) and Ir(IV) were those of H_2PtCl_6 , PdCl_2 , RhCl_3 , and $(\text{NH}_4)_2\text{IrCl}_6$ in hydrochloric acid.

To obtain Os-containing solution, osmic acid (5.66 g osmium content) was refluxed with 20% HCl and a few ml of ethanol until the solution changed in colour from light-yellow to deep brown and then to reddish-yellow. On cooling the liquid evaporated to a syrup-like consistence, large crystals of $\text{H}_2(\text{OsCl}_6)$ were separated. The bulk of the product was dissolved in water to give 200 ml of stock solution. In case of Ru a portion of the metal was added to the KOH/ KNO_3 (8:2) saturated solution. The mixture was water-bathheated in a Wurtz flask while passing chlorine through it to generate RuO_4 . This was distilled into concentrated HCl yielding a reddish-brown solution of $\text{Ru}(\text{OH})\text{Cl}_3$. The latter was treated with an excess of ethanol and boiled until the conversion to a red solution of aquoruthenium trichloride $\text{Ru}(\text{H}_2\text{O})\text{Cl}_3$ was achieved. The solution was gently evaporated adding ethanol upon darkening. 1 ml of Os or Ru stock solutions were diluted with HCl to obtain operating solutions which were mixed with that of SnCl_2 for extraction experiments, the concentration of platinum metal being of the order of 10^{-4} g/ml.

Purity grade "Pure" organic solvents were used. No special purification was carried out excepting that ethers were shaken with SnCl_2 to remove peroxides. Extractants employed

Table 1

Operating Concentrations of Platinum Metals and Detectable
Concentrations of Cluster Compounds

Metal	Concentration (mg/ml)	Detectable concentration (μ g/ml)
Pt	0.311	0.4
Pd	0.202	-
Rh	0.211	0.1
Ir	0.148	0.5
Os	0.283	0.5
Ru	0.078	0.02

were tributyl phosphate (b.p. 289°C), primary hexanol (b.p. 153.5°C), dibutyl ether (b.p. 142°C), isobutyl acetate (b.p. 115 - 118°C), methyl hexyl ketone (b.p. 172.9°C).

Experiment was carried out under static conditions. Partition column technique was also used in case partition coefficient didn't exceed 10. Fluoroplastic-4 was employed as an organic phase carrier.

A centrifugal separation of phases was needed since stable emulsions were readily formed.

Analytical determination of platinum metals was carried out spectrophotometrically with the help of the CQ-8 model spectrometer and the ФЭKH-57 model photocolorimeter equipped with quartz cells, using the intrinsic coloration of the tin dichloride complexes. Special experiments showed the

identity of the absorption spectra of the compounds in organic and aqueous phases and the dependence of optical density on the acidity and concentration for which the correction was made. Standard solutions for the calibration were prepared in 3M HCl. Optical density followed the Beer's law over the range 0.020 to 0.520. Measurements were limited to metal-sensitive band maxima (Table 2).

Optical absorption spectra were recorded with the SF-8 model spectrophotometer using 1 cm path length quartz cells in the spectral region from 280 to 800 nm.

Mössbauer ^{119}Sn spectra of the solid-phase complexes and of their frozen solutions (extracts) were measured with a variable-speed common type spectrometer equipped with a multi-channel analyser AM-256, ^{119}Sn source of 10 μCurie activity and absorber of 10-15 mg/cm^2 specific thickness with respect to natural tin. Spectra were recorded at the liquid nitrogen temperature. SnO_2 and $\beta\text{-Sn}$ were used as reference samples. Channel loading was in the range of 100 to 500 thousand pulses.

Solid-phase complexes were isolated as tetramethylammonium salt precipitates (5, 7).

Analytical procedures followed technique described in (8). Platinum metal content was calculated by difference method, control tests being carried out by colorimetric measurements.

RESULTS

Extraction. Preliminary tests indicated that the conversion of platinum metals to a transferable (cluster) form demanded an excess of tin dichloride, hydrochloric acid medium, and boiling. Otherwise, the complexing is slow. At 100:1 Sn/platinum metal ratio by weight all the metals were converted after five minutes of boiling. Cooled solutions were used for the extraction experiments. Partition coefficient (K_p) was calculated using the equation:

$$K_p = (Q_{\text{initial}} - Q_{\text{aq}})/Q_{\text{aq}} \times V_{\text{aq}}/V_{\text{organic}}$$

where Q_{initial} , Q_{aq} are the quantities of the solute in initial aqueous phase and in raffinate respectively;

V_{aq} , V_{organic} are the phase volumes.

In Fig.1, partition coefficients for Ru and Os clusters are plotted against concentration of HCl. The other platinum metals display similar dependences. In case of tributyl phosphate, all the clusters were extracted with K_p exceeding 200, beginning with the HCl concentration of 0.5M.

The analysis of possible errors allows the conclusion that the overall accuracy of partition coefficient determinations was estimated to be $\pm 50\%$ for $K_p \approx 1$, $\pm 8\%$ for $K_p = 10-40$, and $\pm 20\%$ for K_p 's exceeding 100.

Optical absorption spectra were composed of two broad high-intensity bands. The first, very strong one, has the absorption maximum at the short wave-length boundary (280-300 nm) in all the spectra investigated. The second band is characteristic of every individual given platinum metal except Pd,

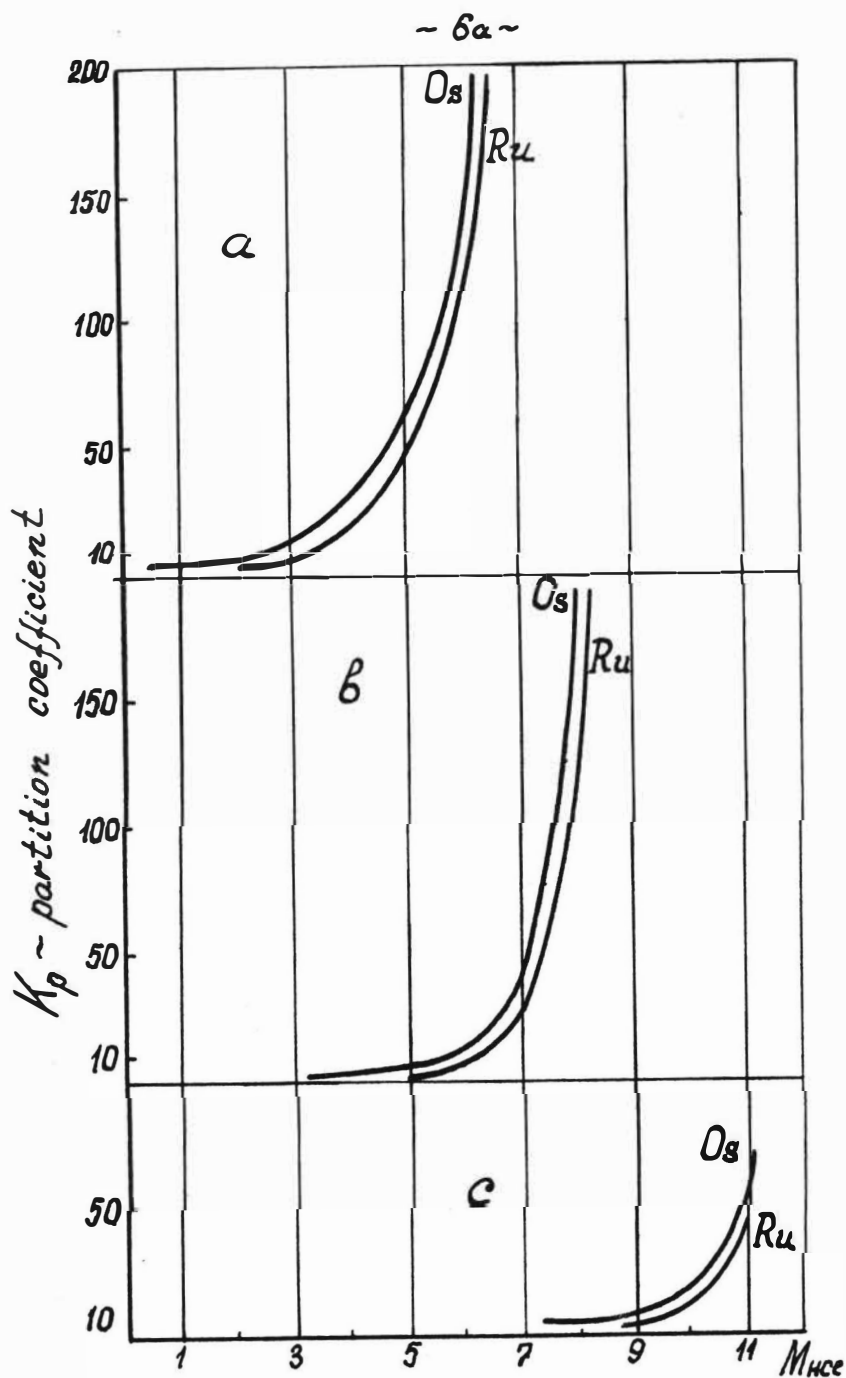


Fig. 1. Partition coefficient K_p vs acidity of solution for *Os* and *Ru*: a - methyl-heptyl ketones; b - hexyl alcohol; c - dibutyl ether.

and is associated with the inherent colour of the cluster. Values of absorption maxima wave-lengths and molar extinction for this band are presented in Table 2.

Provided that the experimental procedure described was strictly followed, reproducible and time-stable results were obtained. As mentioned above, the absorption spectra of solutions, extracts, and solid-phase samples were identical.

Mössbauer ^{119}Sn spectra were essentially the same for isolated complexes and extracts within the measurement error. A well-shaped not broadened doublet line was observed in all the patterns. Values of chemical shifts and splittings are summarised in Table 3 along with platinum metal initial valences and platinum metal to tin molar ratios used for isolation of clusters.

Table 2

Absorption Spectra of Platinum Metal-to-Tin Clusters

Metal	$\lambda_{\text{max}}, \text{nm}$	$\epsilon_0 (\times 10^4)$
Ru	443	1.10
Rh	475	0.38
Pd	330	0.30
Os	383	0.25
Ir	359	1.30
Pt	403	0.78

Table 3

Mössbauer Parameters of the Extractable Platinum Metal
Clusters with SnCl_2

Metal	M:Sn ratio	State	Chemical shifts with respect to $\alpha\text{-Sn}$, mm/sec	Quadrupole splittings, mm/sec
Pt(IV)	1:2	cryst.	-0.40	2.08
Pt(II)	1:2	cryst.	-0.39	2.08
Pt(IV)	1:5	cryst.	-0.49	2.06
Pt(II)	1:5	cryst.	-0.44	2.16
Pt(IV)	1:10	cryst.	-0.44	2.00
Pt(II)	1:10	cryst.	-0.44	2.08
Pt(IV)	1:5	solution	-0.38	2.07
Pt(II)	1:5	solution	-0.41	2.12
Pt(IV)	1:10	solution	-0.38	2.07
Pt(II)	1:10	solution	-0.52	2.05
Ru(III)	1:5	cryst.	-0.05	1.73
Ru(III)	1:5	solution	-0.16	1.70
Pd(II)	1:10	cryst.	-0.60	2.20
Pd(II)	1:10	solution	-0.58	2.21
Ph(III)	1:10	cryst.	-0.31	2.00
Ph(III)	1:10	solution	-0.26	1.98
Ir(IV)	1:10	cryst.	0.53	2.13
Ir(IV)	1:10	solution	-0.44	2.23
Os(IV)	1:10	cryst.	-0.15	1.72
Os(IV)	1:10	solution	-0.25	1.83
$[(\text{CH}_3)_4\text{N}][\text{SnCl}_3]$		cryst.	+1.41	1.08

Data refer to solid-state complexes and their solutions in hexanol, as is indicated. Platinum metal to tin ratios correspond to different cluster compositions resulting from substitution of halogen anion for SnCl_3 in the inner sphere of the metal. Experimental values are believed to be correct to ± 0.05 mm/sec and ± 0.1 mm/sec for shifts and splittings respectively.

DISCUSSION

Our results indicate that the formation of cluster complexes and the transfer of their soluble forms to an organic phase is the basis of the mechanism of platinum metals extraction from a hydrochloric acid medium in the presence of the dichloride. To validate this view it was essential (i) to identify the extractable compounds and (ii) to demonstrate that the transferable species represented clusters, i.e. complexes with metal-to-metal bonding. Spectral studies provided sufficient information to clarify the second point and what is more to get insight into the nature of this peculiar type of bonding. Then, it was necessary to explain the observed concentration dependences.

First of all, the extractibility of platinum metals in itself is closely associated with their interaction with tin dichloride. The reaction may proceed in different ways depending on the conditions. Using platinum as an example, it has been shown (5) that the composition of the reaction product, i.e. the extent of substitution of ligand for complex anions, varies with Pt:Sn ratio. This was illustrated by isolation

of $[(CH_3)_4N][Pt(SnCl_3)_5]$ and $[(CH_3)_4N]_2[PtCl_2(SnCl_3)_2]$. The same is true for other platinum metals. This work deals with complexes of the highest extent of substitution. Provided a large excess of tin is used, these are readily obtained, platinum metal being reduced to the lowest valence state, and the products exhibit reproducible and time-stable spectral and extraction characteristics. Only fully substituted complexes are extracted well. Mostly, the saturation was accomplished at the formation of mixed ligand complexes by substitution of usually 2 or 4 chlorines for $SnCl_3^-$ in the inner sphere, the fully substituted platinum compound being the only exception. All of the species represented complex anions. The same anions occurred in extracts, as was evidenced by composition determinations, extraction behaviour studies, and by the fact that extracts gave spectra identical to those of solid-phase compounds. This view is supported by a well-known tendency of tributyl phosphate and oxygen-containing extractants to extract complex acids in the form of ion-pairs with onium cations (9). Next evidence comes from a typical form of K_p vs acidity dependence displayed by Os and Ru (Fig. 1).

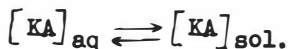
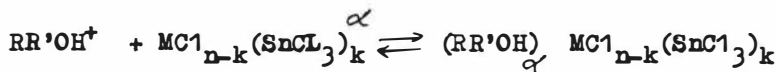
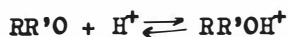
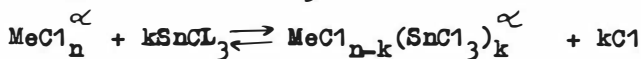
Now, it has to be demonstrated that the complex anions in question are clusters in fact, that is, involve a direct metal-to-metal bonding (platinum metal-to-tin in our case). This follows from spectroscopic evidence. According to arguments in (5), platinum metal is in the lowest oxidation state and tin is formally bivalent. As a rule, the latter is characterized by a positive chemical shift with respect to α -Sn, whereas the investigated clusters exhibit negative shifts both in solid phase and in solution (Table 3).

On the other hand, the observed shifts cannot be assigned to the presence of Sn(IV) since it gives shifts in the range of -1.2 to -2 with respect to α -Sn. Also, electron balance considerations rule out this possibility. Thus, we are driven to the conclusion that we deal with an unusual coordination state of Sn(II). It is more correct to treat its electronic state as an intermediate one between electronic states of Sn(II) and Sn(IV). Since bonding through halogen bridges is inconsistent with Sn(II) stereochemistry (10) and cannot account for the observed shifts and splittings, the only alternative is to assume a direct platinum metal-to-Sn(II) (in SnCl_3^- anion) coordination bonding. X-ray structural analysis of the platinum cluster compound confirms this conclusion (11). The cluster model accounts for changes in s-electron density on tin due to s-electron participation in σ -bonding as well as for increase in splitting originating from metal-to-tin donation. It suggests an electron transfer from d-orbital of platinum metal to π^* level of SnCl_3^- , this being essentially Sn P_x and P_y orbitals and some depopulation of Sn P_z orbital since P_z electrons contribution to σ -bonding. These two effects are responsible for all the spectral phenomena associated with coordination bonding of SnCl_3^- with platinum metals (for details see ref. 5).

In addition, it should be emphasized that the dative $\pi \rightarrow \pi^*$ bonding also provides an explanation for the character of optic spectra. Actually, according to the above consideration, SnCl_3^- represents a ligand of high spectrochemical activity for it acts as a weak σ -donor and strong π -acceptor. Lack of data on cluster structures makes it impossible

to determine SnCl_3 position in spectrochemical series. The assumption of square-planar configuration of Pt and Pd complexes, which is very likely, results in SnCl_3 field strength close to that of strong π -acceptors (CN^- , CO , $\text{S}_2\text{O}_3^{2-}$). Thus, the bond character considerations suppose the assignment of sensitive to metal bands in spectra of clusters to $d \rightarrow d$ ligand field and $P_L \rightarrow d$ ligand-to-metal charge transfer transitions. These transitions are nearly equal in energy, as suggested by the analysis of SnCl_3 electronic structure, though the ligand-to-metal transitions contributes predominantly into the band intensities. The short-wave-length maxima originate from intraligand transitions and therefore are observed in free of platinum metal solutions of SnCl_2 in HCl . The overall consistency of spectroscopic and chemical characteristics of clusters favours the suggested extraction mechanism.

To return to the concentration dependences of the extraction, the following scheme is supposed to explain the observed relationships according to the law of mass acting:



The data presented in Fig. 1 may be utilized to calculate the equilibrium constants of oxonium salt formation and the corresponding partition coefficients for different solvents.

There are several possible ways of explaining the anomalous extraction behaviour of oxygen-containing reagents in comparison to that of simple complex acids, e.g. HFeCl_4 (9). Further investigation is needed to choose between them. Solvent effect on ion pair stability, differences in proton affinity, and to a lesser degree competition of HCl may be of primary importance.

CONCLUSIONS

The existence of general mechanism of extraction of platinum metals was demonstrated. It is based on the formation of cluster compounds with metal-to-metal bonding which are transferred to the organic phase. The mechanism is observed in the extraction process in the presence of SnCl_2 . Its existence was supported by the overall spectroscopic and chemical evidence. Mössbauer spectral data were utilized to form an opinion on the coordination bond nature in the clusters. The bond is a covalent one with a considerable π -character due to a dative electron transfer from d-orbital of platinum metal to ligand π^* level.

REFERENCES

1. V.N. Ivanov, Zhurn. Russk. Fiz.-Khim. Obshch., 49, 7-9, 601 (1917) (Russ).
2. G.H. Ayres, B.L. Tuffly, G.S. Forrester, Anal. Chem., 27, N11, 1742 (1955).
3. S.S. Berman, E.C. Goodhue, Canad. J. Chem., 37, 370 (1959).
4. G.S. Katykhin, M.K. Nikitin, V.P. Sergeev. XV1 Vsesoyuznoe soveshchanie po yadernoi spektroskopii i strukture atomnogo yadra (XV1 All-Union Conference on Nuclear Spectroscopy and Atomic Nuclear Structure), Proceedings, Moscow, "Nauka" Press, 1966. (Russ).

V.P. Sergeev, V.I. Baranovskii, B.E. Dzevitskii. 8-e Vsesoyuznoe soveshchanie po khimii, analizu i tekhnologii blagorodnykh metallov (The 8-th All-Union Conference on Chemistry, Analysis and Technology of Noble Metals), Proceedings, p. 42, Novosibirsk, 1969. (Russ).
5. V.I. Baranovskii, V.P. Sergeev, B.E. Dzevitskii, Doklady Akad. Nauk SSSR, 184, N3, 632-634 (1969) (Russ).
6. Sintez kompleksnykh soedinenii metallov platinovoi gruppy (The Handbook on Synthesis of Platinum Metal Complex Compounds), ed. by acad. Chernyaev, Moscow, 1964 (Russ).
7. G.F. Young, R.D. Gilland, G. Wilkinson, J. Chem. Soc., 12, 5176 (1964).
8. K.G. Bauer. Analysis of Organic Compounds, The 2-nd Ed., Moscow, 1953.
9. D.Y. Tuck, R.M. Diamond, Progr. Inorg. Chem., 2 (1960), Interscience Publ., N.-Y. - L.
10. J.D. Donaldson, Progr. Inorg. Chem., 8, 287 (1967), Interscience Publ., N.-Y. - L.
11. J.R. Lindsay, Private Communication.

On the extraction of halide complexes of metals from the point of view of co-ordination chemistry

B.Ya.Spivakov, C.M.Petrukhin, and Yu. A.Zolotov
Vernadsky Institute of Geochemistry and Analytical
Chemistry, U.S.S.R.Academy of Sciences, Moscow

It is necessary to know the composition of the compounds extracted for solving different problems of solvent extraction including quantitative description of extraction equilibria. The examination of physical-chemical properties of halide complexes of metals and the extractants enables us to estimate in many cases the composition of the compounds extracted from halide solutions depending on the nature of the metal, halide and extractant.

The estimation of the type of the compound being extracted (extraction mechanism) and its exact composition is one of most important problems of the solvent extraction chemistry. The selection of an extractant and conditions for the extraction depends on the type of the extracted compounds, the knowledge of their composition is necessary for quantitative description of the extraction equilibria.

Very many data on the extraction of halide complexes of metals including data on the composition of the compounds extracted have been published. Correlations between certain properties of halo complexes of metals—stability, charge and hydration, size and others with their extraction behaviour have been discussed¹⁻⁴. In this work an attempt has been made to find regularities which can explain why this very extractable com-

pound is formed, to estimate critically experimental data on the composition of the complexes being extracted and to predict the extraction mechanism for unstudied systems. Modern co-ordination chemistry seems to enable us (i) to determine a type of the compound extracted from some properties of the metal, halide and extractant and (ii) to estimate the most probable composition of the extracted compound by the co-ordination number (CN) of the metal.

Halogeno complexes of metals are extracted via three mechanisms: as co-ordinatively unsolvated neutral compounds MeX_m (X^- is the halide ion), co-ordinatively solvated compounds $MeX_m S_p$ (S is the extractant molecule), and complex anions which form part of the composition of ion associates. Any extractable compound, independent of its composition, must have two necessary properties: weak interaction with components of the aqueous phase and sufficient stability. The compound must be co-ordinatively saturated with regard to present in the system ligands, including water and halide ions. A co-ordinatively saturated extractable compound corresponds to a molecule whose electronic configuration is a system with filled atomic orbitals of the metal valence-shell and binding molecular orbitals and with a rather high energy of vacant orbitals⁵.

To estimate the extraction mechanism it is convenient to proceed from some properties of neutral halides which have been studied in detail. Co-ordinatively saturated compounds can be extracted into "inert" solvents as co-ordinatively unsolvated complexes. Co-ordinatively unsaturated metal halides, having energetically available vacant orbitals, can, on the contrary, interact with ligands-donors L (L is the

halide ion, water or extractant molecule), and can be extracted as anions of ion associates $Kat_n MeX_{m+n}^{n-}$ or co-ordinatively solvated molecules $MeX_m S_p$. The nature of the compound being extracted depends on the relative affinity of MeX_m to extractant molecules S and halide ions X^- and on extraction conditions.

Thus the estimation of the possibility of forming $MeX_m L_t$ from MX_n and L can be reduced to the estimation of the acceptor ability of MeX_m and electronodonor one of L. That is why the theoretical consideration of the electronic structure of MeX_m and L and estimation of their donor-acceptor properties seem to be a natural way for solving the problem. However, modern calculation methods of the quantum chemistry do not make it possible to estimate the vacant orbital energy of the molecules by their atomic properties and ionization potentials can at best serve as a characteristic of the electronodonor ability of the ligand for a certain class of the ligands⁶. This makes to use more qualitative approaches of the co-ordination chemistry and data on physicochemical properties of MeX_m molecules.

Data on the electronic structure and characteristics, that point to a weak acceptor ability of the metal halides, permit to select molecules which can be extracted into "inert" organic solvents. For instance, it follows from the electronic structure of GeX_4 ($X=Cl, Br, I$) that these molecules can be acceptors only on σ^* -antibonding MO or vacant 4d AO of germanium. Therefore, GeX_4 molecules (except GaF_4) are weak acceptors. Generally, only metal halides with filled d orbitals are acceptors solely to np and nd AO and σ^*_{ant} MO. That is why metal halides with a weak acceptor ability can be found only among halides of metals with filled d orbitals.

Compounds of the class being considered form molecular crystals with discrete molecules. For example, AsX_3 ($\text{X}=\text{Cl}, \text{Br}, \text{I}$) are monomer molecules in both gas and solid phase. A weak intermolecular interaction is reflected in low melting points of such metal halides, for instance, in those of germanium, arsenic, antimony⁸.

Such a consideration enables to point out those few metal halides which can be extracted as unsolvated neutral molecules. These are halides of Hg(II) , Ge , Sn(IV) , As , Sb(III) and, probably, of some other metals.

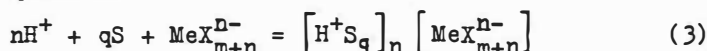
Depending on the conditions, co-ordinatively unsaturated metal halides can form corresponding solvates



or complex anions



the extraction of which by a neutral extractant is described by the equation^{x)}



The distribution coefficients of the ion associate as a complex acid or a solvate are expressed by the equations

$$D_a = \frac{K_{ex}^a \gamma_a^{-1} (\text{H}^+)^n (\text{X}^-)^{m+n} (\text{S})^q}{\sum_{i=0}^{m+n} \beta_i (\text{X}^-)^i \gamma_i^{-1}} \quad (4)$$

$$D_s = \frac{K_{ex}^s \gamma_s^{-1} (\text{X}^-)^m (\text{S})^p}{\sum_{i=0}^{m+n} \beta_i (\text{X}^-)^i \gamma_i^{-1}} \quad (5)$$

where the round brackets denote thermodynamic activities, β_i and

^{x)} The extraction of metal complexes by amines and other cationic extractants can be described as a process of forming the ionic associate from a co-ordinatively unsaturated neutral metal halide and an amine halide.

γ_1 the overall stability constants of the halide complexes and their activity coefficients in the aqueous phase, K_{ex}^a and K_{ex}^s the extraction constants for the associate and the solvate, and γ_a and γ_s denote their activity coefficients in the organic phase. The probability of the extraction via the first or the second mechanism is determined by the ratio

$$\frac{D_a}{D_s} = \frac{S_{ex}^a}{K_{ex}^s} \frac{\gamma_s}{\gamma_a} (H^+)^n (X^-)^n (S)^{a-p} \quad - (6)$$

A contribution of the ratio of the activity coefficients for the extracted forms in the organic phase can be essential if polymerization or dissociation of the forms occurs or in the case of a large difference in the energy of their interaction with the diluent⁹.

To examine the effect of other factors, we assume that $\gamma_s/\gamma_a=1$ and that the solvate numbers for both mechanisms are about the same and express K_{ex} through the stability constants and partition constants. Then

$$\frac{D_a}{D_s} = \frac{P_a \beta_a}{P_s \beta_s} k (H^+)^n (X^-)^n \quad - (7)$$

Where P_a and P_s are the partition constants of the complex acid and the solvate, β_a and β_s are the equilibrium constants for reactions (2) and (1), k is the constant for the formation of the cationic part of the associate. The value of D_a depends strongly on the anion charge. The P_a/P_s value shifts the equilibrium to the solvate mechanism if the metal extracted forms a double charged or a multicharged anion. The dilution of the extractant with a non-polar diluent can lead to a similar shift. The values of D_a and D_s can be comparable in the case of a single charged anion, and the ratio of β_a/β_s can play the decisive role for the extraction via the first or the second mechanism. This

very ratio conditions the order of the D_a/D_s value in most cases because the values of β_a and β_s , unlike all other parameters in equations (6) and (7), can change very much with the change in the nature of the metal, halide ion and extractant.

The division of metal ions into classes A and B¹⁰ and the principle of hard and soft acids and bases (PHSAB)^{11,12} can be used to estimate the interaction of MeX_m with X^- and S. According to PHSAB, metal ions, their complexes as well as ligands can be divided into hard (class A), soft (class B) and borderline. Hard acids interact preferably with hard bases, soft acids with soft bases. Neutral metal halides are Lewis acids. Those formed by hard and soft ions can be respectively considered as hard and soft¹³ although the change of the hardness (softness) of MeX_m with changing the nature of X should be taken into account. The decrease of the electronegativity of the halide ion from fluoride to iodide results in the decrease of the hardness of MeX_m due to the decrease of the effective charge of the central atom in the order $MeF_m > MeCl_m > MeBr_m > MeI_m$ in spite of the occurrence of the metal-ligand π -back donation for metals with filled $(n-1)d-AO$.

The estimation of the relative affinity of the neutral metal halide to corresponding halide ions and to extractant molecules can be carried out by means of a series in which halide ligands and extractant donor atoms follows the order of decreasing their hardness (increasing softness)¹²; $F > O > N > Br > I > S$. The series, in spite of its conventional character, proved to be useful for estimating the extraction mechanism. The authors of work¹⁴ estimate the affinity of hard metal halides to X^- by the nucleophilicity parameter of the latter.

The hardness and softness of the extractant is first of all conditioned by the donor atom nature. Hence, oxygen-bearing extractants are most hard and sulphur-bearing ones are most soft. Any characteristic, somehow connected with the electronic density of the donor orbital of the extractant, can be used as a measure of its hardness within one class of the extractants. The donor-acceptor ability of the extractant with a given donor atom is conditioned by its structure and the nature of the substituents.

The possibility of the formation and stability of complexes with a mixed co-ordination sphere, that is the interaction between the extractant and a neutral metal halide, is conditioned by the mutual effect of X and S. The mutual effect of the ligands is considerably connected with the change of the charge of the complex central atom. That's why the affinity to hard bases, for example to oxygen-bearing extractant for which the electrostatic interaction is essential, must increase in the order: MeI_m , MeBr_m , MeCl_m . The decrease of the covalency of the Me-X bond in this series can lead to strengthening the bond of the metal halide with a soft extractant as well if the contribution of the metal-extractant π -back donation is small¹⁵.

The considered regularities combined with data on the structure and some properties of halo complexes allows to explain the experimental results known and to predict the extraction mechanism.

As has been shown, the relative affinity of the neutral metal halide to corresponding halide ions and extractant molecules, that is the value of β_a/β_s , can be estimated by means of the above mentioned qualitative series for the complex stability. It follows from the series that fluoride ions are more hard

ligands than oxygen-bearing extractants ($\beta_a \approx \beta_s$). That's why class A ions are extracted from fluoride solutions, apparently, only as ion associates^{x)}. Thus, tributyl phosphate (TBP) extracts tantalum as HTaF₆ already at the ratio of Ta:F=1:6. Class A metal ions with the electronic shell of inert gases-scandium, rare earths, zirconium and hafnium - are extracted via the solvate mechanism from solutions of any halide ion concentration because less hard chloride and bromide ions are weak competitors in comparison, for instance, with TBP for such metals ($\beta_a < \beta_s$).

The covalent interaction with ligands becomes essential for borderline and hard ions of the transition metals and metals with filled d orbitals (Co(II), Ni, Cu(II), Fe(III), Zn, Ca, In). In this case chloride and bromide ions are more preferable ligands than more hard oxygen-bearing extractants ($\beta_a > \beta_s$). Not a single metal of this group, probably, is extracted with TBP as a solvate from halide solutions with concentration of more than 3-4 M, that is if X⁻ concentration is comparable with extractant concentration or higher. Less effective oxygen-bearing extractants, such as ethers or some esters, extract all these elements as acido complexes over the whole range of HCl or HBr concentration.

Sulphur-bearing extractants badly extract borderline metal ions (and certainly hard ones) from chloride, bromide and iodide solutions as solvates because sufficiently hard ligands are optimal for such elements as Co, Ni or Cu(II). As can be seen from the ligand hardness series, chloride and bromide ions are more preferable than very soft sulphur from this point of view ($\beta_a > \beta_s$).

^{x)} Extraction data are given from¹⁶.

During the extraction of class B ions by oxygen-bearing extractants the solvates, if any, are formed only at very low X^- concentration as the inequality of $\beta_a > \beta_s$ is valid for chloride, bromide and surely iodide systems. In the case of soft ions the effective positive charge of the metal decreases as a result of the formation of the neutral metal halide from the ion that confirms the validity of the ratio. Thus Ag(I), Hg(II), Au(III) are extracted as solvates with TBP only at low concentration of chloride, bromide or iodide ions while for Au(III) such a mechanism has not been observed even in the case of tri-octylphosphine oxide. The inequality $\beta_a < \beta_s$ is valid for class B ions and sulphur-bearing extractants as, according to the series given above, sulphur is the optimal ligand for soft ions and their neutral halides. In the case of such systems the solvate mechanism is also predominant because sulphur atoms of practically used extractants is protonated weakly, that is the value of k in equation (7) is small. That is why Ag(I), Hg(II), Pd(II) and other such elements are extracted with alkyl sulphides and their analogs as solvated neutral halides.

A relatively high affinity to proton is a specific peculiarity of most wide-spread extractants containing trivalent nitrogen. A high value of k in equation (7), conditioned by this, results in $D_a > D_s$, that is most elements are extracted from HX solutions as ion associates (steric hindrances can also prevent from the formation of the solvates). The solvate mechanism is possible only for elements with a high affinity to nitrogen, for example for the platinum metals during their extraction by primary amines from HCl solutions¹⁷.

Thus the approach suggested enables to estimate the type of the compound being extracted (extraction mechanism) by certain

metal, halide ion and extractant properties and extraction conditions. The estimation of the exact composition of the neutral solvate (solvate number) or the anionic part of the ion associate should be the next step. This problem can be solved by estimating CN of the metal in the compound being extracted using literature data on the composition of its complexes. For this purpose it is necessary to analyze data of physical and chemical methods on the structure of corresponding halide complexes in each particular case. We may consider here only few examples.

A lot of papers have been devoted to the study of the extraction mechanism of scandium with TBP. It has been suggested in early works that scandium is extracted as a complex acid $H_3ScCl_6 \cdot 3TBP$ or $HScCl_4 \cdot 2TBP$. More detailed studies have shown that a solvate of $ScCl_3(TBP)_p$ is extracted where $p=3,2$ or even 1. As has been shown above, the solvate mechanism is much more probable for such an element as scandium. It is known that $ScCl_3$ has vacant $(n-1)d$ AO and, hence, should be a comparatively strong acceptor. In fact solid $ScCl_3$ is a coordination crystal (m.p. is $960^\circ C$) with CN of six for scandium. That's why a solvate of $ScCl_3 \cdot 3TBP$ is the most probable compound being extracted. The suggestion on the formation of the monosolvate seems to be groundless.

One more example. It is known that palladium is extracted with soft extractants from halide solutions via the solvate mechanism. Most chemists have come to the conclusion that compounds of $PdX_2 \cdot 2S$ ($X=Cl, Br, I$) are extracted. However, the authors of one work have experimentally shown that the monosolvate $PdX_2 \cdot S$ is extracted. Meanwhile, plane square complexes are typical for palladium (II) as well as for other metals with

d⁸ structure. Such a structure is observed in all palladium compounds. The main fragment of the structure of PdCl₂ is the plane square co-ordination. Complexes with dialkylsulphides and phosphines are also plane and square. That's why we can think that the authors, who observed the extraction of the monosolvate (if their experiments were correct) dealt most probably with dimer molecules of the extracted compound with two bridge chlorine atoms.

The authors, dealt with the determination of the composition of cobalt (II) halo complexes being extracted with oxygen-bearing extractants, faced some difficulties. The information on the mechanism of the extraction of cobalt(II) from chloride solutions is contradictory. According to some works, only CoCl₄²⁻ passes to the organic phase from HCl, LiCl, CaCl₂ solutions as well as merely from CoCl₂ solutions. Some other authors have come to the conclusion that TBP and ketones extract CoCl₂·pTBP, Li(CoCl₃)·pTBP and Li₂(CoCl₄)·pTBP. The authors of work¹⁸ believe that a complex of CoCl₂·3TBP is extracted at HCl concentration of less than 5 M and that of HCoCl₃·3TBP at higher concentration. The analysis of data on the structure of solid complexes (CoX₂, where X=Cl, Br, I, forms octahedral structures, complexes of CoX₂·2S do molecular tetrahedral and polymer octahedral structures) enables us to think that solvates of CoCl₂·2S or CoCl₂·4S can be extracted from solutions with low Cl⁻ concentration (the formation of the disolvate seems to be more probable). As has been shown above, H₂CoCl₄ must be the main extractable form in the extraction from solutions with high HCl concentration. The extraction of HCoCl₃ is also possible from solutions with moderate Cl⁻ concentration but only if the fourth co-ordination

position of cobalt is occupied by an extractant molecule because Co(II) does not form complexes with $CN=3$. If co-ordinatively solvated anions are not formed under extraction conditions, one can believe that the composition of $HCoCl_3$ is not valid.

A mixture of a cationic extractant and a neutral one can be used for effective extraction of metals forming co-ordinatively unsaturated anionic halo complexes under extraction conditions. Trivalent transplutonium elements (TPE) from anions such as $(MeCl_4^-)$ or $(MeCl_5^{2-})$ in extraction systems with amines. CN of the metal in these complexes does not correspond to the potential co-ordination of the TPE ions which have a number of energetically available vacant orbitals. The co-ordination sphere of such hard ions is added with water molecules (hard ligands) that prevents from the extraction of the complexes. That's why a suggestion has been expressed and experimentally confirmed that a mixture of tri-n-octylamine with TBP extracts americium (III) from LiCl solutions much better than alone extractants. The solvation of anionic chloro complexes of Am(III) with TBP molecules leads to an increase in their extraction with amines¹⁹.

For the last example of using PHSAB and data on CN of ions for the explanation of the extraction behaviour of halo complexes, it is well known that indium is extracted with oxygen-bearing extractants and amines from chloride solutions much worse than gallium and indium (III). At the same time all three elements are extracted into the organic phase as $MeCl_4^-$ complexes whose stability follows the order: $Ga < In < Tl$. Such "anomalous" behaviour of indium becomes clear if we compare the change of CN and the ion softness from Ga to Tl(III). Gallium is most hard of three ions but the complex $GaCl_4^-$ is not hydrated in the

inner sphere as the small size of the metal ion prevents from the formation of a complex with $CN > 4$. The size of In and $Tl(III)$ enables them to add two water molecules to a $MeCl_4^-$ anion ($CN=6$) but indium is a rather hard ion and it retains them firmly while a soft thallium ion in $TlCl_4^-$ is whether not hydrated or forms a very weak bond with water molecules.

References

1. Spivakov B.Ya., Petrukhin O.M., Zolotov Yu.A. Dokl.Akad.Nauk SSSR, 1972, 204, 887; Zh.analit.khimii, 1973, 27, 1584.
2. Diamand R.M., Tuck D.G., in: Progress in Inorganic Chemistry. Ed.F.A.Cotton. 1960. Vol.II. (Interscience Publ.,New-York-London).
3. Zolotov Yu.A., Zh.analit.Khimii, 1971, 26, 20.
4. Iofa B.Z., Dokl.Akad.Nauk SSSR, 1969, 188, 1053.
5. Petrukhin O.M. Zh.neorgan.khimii, 1972, 17, 2257.
6. Briegleb G. Elektronen - Donator-Akzeptor-Komplexe. 1961. (Springer-Verlag, Berlin).
7. I.Narai-Sabo. Inorganic Christallchemistry. 1969. (Acad. Kiad6. Budapest).
8. Spravochnik khimika. 1971. V.2. (Moscow, Khimiya.).
9. Rozen A.M., Yurkin V.G., Fedoseev D.A. In book: Khimiya protsessov ekstraktsii.Ed.by Yu.A.Zolotov and B.Ya.Spivakov. 1972, p.88. (Moscow, Nauka).
- 10.Ahrland S., Chatt J., Davies N.R., Quart.Rev., 1958, 12,265.
- 11.Pearson R.G., J.Amer.Chem.Soc.,1963,85, 3533.
- 12.Basolo F., Peerson R.Mechanisms of Inorganic Reactions.1967. Second Edition, (New-York-London).
- 13.Satchell D.P.N., Satchell R.S.Chem.Rev.,1969,69, 251.
- 14.Shmidt V.S., Shesterikov V.N.Radiokhimiya, 1971, 13, 815.
- 15.Yatsimirsky K.B.Zh.neorgan.khimii,1970, 15, 925.
- 16.Zolotov Yu.A., Iofa B.Z., Chuchalin L.K. Ekstraktsiya galo-genidnykh kompleksov metallov, 1973, (Moscow, Nauka),
- 17.Gindin L.M., Bobikov P.I., Kouba E.F. Izv.Sibirsk.Otd.Acad. Nauk SSSR, 1961, N10, 84.
- 18.Levin V.I., Kozlova M.D., Sevast'yanova A.S. Radiokhimiya, 1972, 14, 48.
19. Spivakov B.Ya., Myasoedov B.F., Shkinev V.M., Kochetkova N.E. Shmutova M.K. This conference.

Miroslav Mrnka, Jana Šatrová, Věra Jedináková and Jiří Čeleda
Prague Institute of Chemical Technology, Department of Nuclear
Fuel Technology and Radiochemistry, Czechoslovakia

From the results obtained by the chemical analysis of the organic phase as well as by cryoscopic and viskosimetric measurements and from infra-red spectra the authors conclude that amine salts of strong mineral acids are forming six-membered rings in the organic phase. At a high water activity in the system these rings consist of the ions R_3NH^+ , X^- and of water molecules. With decreasing water activity in the system a dehydration sets in and the rings of the hydrated salts are transformed into equally six-membered rings of the trimeric anhydrous salts. A similar formation of cyclic structures seems to be responsible also for the excess acid extraction.

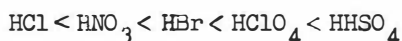
The mechanism of the extraction of acids by amines is not yet fully elucidated, in spite of the numerous investigations done in this field. From this point of view, the following three questions are essential:

- 1/ the association of the salt in the organic phase
- 2/ the co-extraction of water
- 3/ the extraction of the excess acid

So far there does not exist any uniform opinion on the part played by water in the extraction process, where contradictory results have been published, neither there are any exactly for-

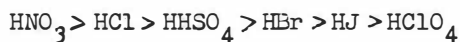
mulated conclusions on the structure of the extracted species in the organic phase.

The aggregation of the amine salts has actually been stated nearly in all cases of the extraction of mineral acids by amines. From the published experimental data it may be inferred as a general rule that the association is enhanced by the same factors as those which influence the polarity of amine salts: by the strength of the acid and by the basicity of the amine. Markovits and Kertes /1/ find the following order of the dimerization constants of amine salts:



which is nearly exactly the order in which the polarity of the salt is increasing. The majority of experimental results show that aggregation comes to stop at the stage of low oligomers, with association degrees within the range of 2 - 4. This fact has been established for salts of secondary and tertiary amines.

The extraction of the excess acid has also been observed with all mineral acids. According to Keder and Wilson /2/ the tendency to bind additional amounts of the acid decreases in the following order:



which is the order of increasing strength of the acid.

This direct dependence of the excess acid extraction on the affinity of the anion of the salt for the proton indicates that the molecules of the acid extracted in excess are bonded to the salt of the amine by hydrogen bonding of their proton to the anion of the salt. Conforming to these conclusions on the mechanism

of the excess acid extraction the formation of the complex anion HX_2^- is assumed, in the case of monobasic acids.

If this conclusion is right, then we might expect that the perturbation of the $N-H^+$ bond in the hydrogen-bonded cations should decrease on excess acid extraction as result of this formation of the more basic simple anion X^- into the weakly basic complex anion. This has been confirmed by Keder's and Wilson's measurements of the infra-red spectra /2/.

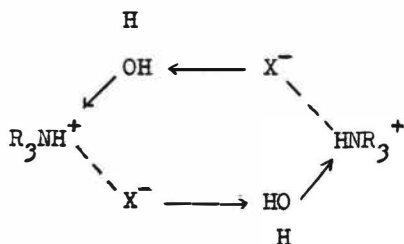
For the co-extraction of water there are so far no complete data about the way in which the water molecules are incorporated into the structure of the salt of the amine. It may, however, be assumed that the water molecules are hydrogen-bonded by one of their OH's to the anion of the salt since it cannot be bonded to the cation of the amine where no free electron pair is available. As evidence for the formation of the $OH-X^-$ bond may serve the fact that the affinity for water increases with the proton-accepting tendency of the anion, i.e. with the basicity, as well as with the tendency of the amine salt to bind molecules of alcohols ROH, where the formation of the hydrogen bond $O-H...X^-$ has been established from shifts of the stretching frequencies of the O-H bond. In the case of the excess acid extraction of some acids an increase of the co-extraction of water has been observed. This indicates that the first additional amounts of the acid pass into the organic phase as the hydrated ion pair $H_3O^+-X^-$. So far it is not known, which is the relation between the way of binding of these pairs and the binding of the anhydrous HX molecules. The authors only agree in the statement that no simple

relation between the water content and the content of the excess acid in the organic phase can be found. Neither it is possible to say that there exists a stoichiometric displacement of water by the excess acid, nor to interpret the observed fact in terms of a stoichiometric hydration of this acid. Sometimes there exists a certain parallelity between these two processes, in other cases, however, there appear diametral differences, supporting the view that the addition of water and the excess acid extraction are two independent reactions.

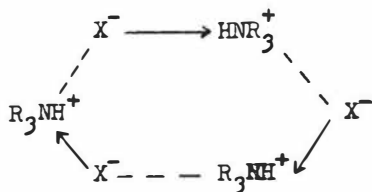
We have found by comparatory cryoscopic measurements that the polymerization degree of the amine salt in the organic phase depends on the water activity in the system and that it is in connection with the co-extraction of water /directly determined by the analysis of the content in the organic phase/. When hydrochloric acid is extracted from diluted aqueous solutions, where the activity of water in the system is high, water is being co-extracted by trioctylamine in an equimolar ratio, i.e. 1 H_2O molecule to each molecule of the amine salt formed in the organic phase, and the polymerization degree of the salt is equal to 2 in this case. Contrary to this, there is no extraction of water from concentrated acid solutions /as far as we do not reach the region of the excess acid extraction/, and the polymerization degree of the amine salt tends towards 3 in this case. In the transition region between these two extremes the polymerization degree changes with the water content in the organic phase in such a way as if there existed a mixture of an anhydrous trimer of the amine salt with a dimerized hydrated salt containing 1 H_2O molecule for each $\text{R}_3\text{NH}^+ - \text{X}^-$ ion pair.

If each cation R_3NH^+ and each anion X^- as well as each water molecule is taken as one link in the polymer chain /which is possible to do here regarding the fact that the hydrogen bonds $O-H \dots X$ and $N-H \dots X$ behave as rigid connections we obtain the number of members in the polymer molecule of the amine salts equal to 6 in all cases, no matter what is its hydration degree. This high stability of the six-membered chains has lead us to the conclusion that the chains undergo cyclization to six-membered rings.

Respecting the fact that the aminium cation does not dispose any free electron pair to act as an acceptor of the hydrogen bond, it is possible to involve this cation into structural considerations only as a donor of hydrogen bonds. Anions of strong acids are as a rule weaker acceptors of hydrogen bonds than the relatively strongly basic water molecules; on the other hand, they dispose of a stronger electrostatic field than the electro-neutral water molecules whose electrostatic action is limited to the short-range dipole field. From this we have inferred that the amine cations in the hydrated salts will preferently form hydrogen bonds with the water molecules, whereas the anions in the polymer chain they will be held by bonds of prevailing electrostatic character /"ionic-bonds"/. In this way we have come to assume the following structure of the dihydrate amine salt:



where the ionic bonds are represented by dotted connection lines while the dative electron shifts in the hydrogen bonds are marked by arrows. In the case of the anhydrous salt the formation of six-membered rings is possible only through association of three molecules of the salt:



When the concentration of the acid is lowered /i.e. with increasing activity of water the anhydrous trimer rings are converted into dimetric hydrated rings.

A point of favour of these structures are also the infra-red spectra. To the non-disturbed N-H^+ bond in the amonium cation should correspond, according to published data, the stretching frequency N-H^+ in the vicinity of $3\,200\text{ cm}^{-1}$. The perturbation of the bond will shift this band to lower frequencies. In the case of the extraction of perchloric acid the perturbation is rather weak due to the very low basicity of the anion ClO_4^- ; the region of stretching frequencies is shifted here only to $3\,000 - 3\,100\text{ cm}^{-1}$, where can still be distinguished the peak of symmetrical and asymmetrical vibrations. In the case of HCl the shift is larger both peaks are strongly broadened and melt together to a broad band with absorption maximum at $2\,400\text{ cm}^{-1}$, corresponding to the stretching mode of the N-H bond in the amonium cation strongly perturbed by hydrogen-bonding. The protons of the absorption maxima of

the NH band in other salts of TOA in the organic phase are given for comparison:

HClO ₄	3 050 cm ⁻¹	DClO ₄	2 280 cm ⁻¹
HNO ₃	2 650 "	DNO ₃	2 110 "
HJ	2 600 "	DCI	2 090 "
HBr	2 500 "		
HCl	2 400 "		
HF	2 250 "		

Nitric acid assumes here an anomal position among other mineral acids. In spite of being a relatively weak acid, its NH stretching frequency comes near to that of stronger hydroiodic acid. The observed shifts are in agreement with the values found by many authors.

The big shifts of the band found for trioctylamine chloride indicates a perturbation of the N-H⁺ bonds by their participation in strong hydrogen bonds between the N-H⁺ cations and their neighbours in the cyclic chain. In the case of the dimeric hydrates these neighbours are the ions X⁻ and the H₂O molecules. Since the anions X⁻ can be bond to the N-H⁺ cations as well by electrostatic forces as by hydrogen bonds whereas to water molecules they can practically be bonded only by hydrogen bonds, it may be assumed as already mentioned before - that the only proton available in the alkylaminium cation R₃NH⁺ will be turned towards the H₂O link in the hydrated ring and form a hydrogen bond with this molecule, whereas to the anion X⁻ the R₃NH⁺ cation will be held mainly by electrostatic forces. The water molecules are then going to close the ring by forming a hydrogen bond between one of their two O-H bonds

and another anion X^- , as shown in the formula. The second O-H bond remains free, since the NH^+ group does not dispose of free electron pairs by which it could bind additional protons and act towards the OH group, as an acceptor of the hydrogen bond. By such formation of hydrogen bonds between the links H_2O and X^- it may be then easily explained why the hydrogen bond $NH^+ - OH_2$ varies in strength in different salts of the same amine. The stronger base is the anion X^- , the stronger it will perturb the O-H bond in water. It will polarize by attracting the proton more to its own side, which results in larger electron density on the oxygen atom and, consequently, a stronger perturbing action of the last on the amine proton in the $NH - OH_2$ hydrogen bond.

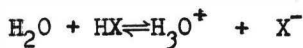
Infra-red spectra of trioctylamine chloride have fully confirmed these conclusions. They show a sharp peak of the free OH bonds on $3\ 660\text{ cm}^{-1}$ an intensive broad absorption band of the hydrogen-bonded OH groups with maximum on $3\ 400\text{ cm}^{-1}$. With other salts this splitting is somewhat different. In the case of trioctylamine perchlorate this band is considerably narrowed and its shift is smaller, proportionally to the narrowing of the band and to the decrease of its own shift. This shows that the action of the anions in hydrated amine salt is transferred by inductomeric effects along the whole chain as well to the H_2O links as to the R_3NH^+ cations. This is well consistent with the cyclic structure, with hydrogen bonds /connecting all the participating components/. These conclusions have been tested on synthetically prepared amine salts.

Cryoscopic measurements have clearly shown that anhydrous amine salts, independently of the acid applied, are polymerized to the mean association degree $\bar{n} = 3$. Adding water to the anhydrous solution leads to the transformation into hydrated dimers. This was best seen with TOA chloride in benzene solutions where it was possible to prepare a hydrate in the ratio $\text{TOA}:\text{HCl}:\text{H}_2\text{O} = 1:1:1$ and where the mean polymerization degree fell gradually on additions of water from the value 3, corresponding to the anhydrous salt to the value 2, attained at the hydration ratio 1:1. With other TOA salts it was not possible to prepare the solutions of a stoichiometric monohydrate of the salt in benzene. However in these cases too the decrease of the association degree from the value $\bar{n} = 3$ for an anhydrous salt was proportional to the water concentration in the organic phase and correspondent to the amount of dimeric monohydrate calculated from the amount of water added.

The extraction of excess amounts of the acid is paralleled by increase of the water concentration in the organic phase even in cases, where there was already a dehydration of dimeric hydrate beginning, before the excess acid extraction has set in. This shows that the excess amounts of the acid are transferred into the organic phase in the form of a monohydrate, i.e. $\text{H}_3\text{O}^+\text{X}^-$ ion pairs. The mean association degree of the amine salt is simultaneously increasing, as may be seen from the decrease of the freezing point depression as well as from further increase of the viscosity of the organic phase. Hence it may be assumed that the excess acid is forming ion-pair bridges linking the cycles mutually into larger units.

As to the way in which the $\text{H}_3\text{O}^+\text{X}^-$ bridges are incorporated between the two adjacent rings, it is possible to start with the assumption that the cationic pole of the ion pair is hydrogen-bonded to the anionic member in the ring transforming it into a voluminous complex anion with a lowered electron density, thus weakening its hydrogen bond with the NH^+ cation. Therefore, the perturbation of the NH^+ bonds should be weakened and their band originally shifted towards low frequencies, should be return near the value corresponding to the non-perturbed bond. In the spectrum there should furthermore appear a new band in the region of low frequencies belonging to the hydrogen-bonded H_3O^+ cations. Both these effects were actually found in the i.r. spectra. This shows that the excess acid extraction actually starts in such way bonding of $\text{H}_3\text{O}^+\text{X}^-$ ion pairs to the X^- members of a hydrated ring, excess acid side chains are formed to the anionic poles of which a second ring is then associated by means of its free OH groups. In this way the side chains, in their turn, are closed to a ring and get stabilized. Such bonding of a hydrated ring to another hydrated ring may give rise to a condensed tricyclic molecule containing 4 R_3NH^+ cations and 2 excess acid unites. The mutual association of the anhydrous ring alone, however, should not be possible, due to the disappearance of the H_2O members being essential for this mechanism. This would mean that the association of cycles in the course of excess acid extraction should proceed only to such extent, insofar the decrease in the water activity in the system has not reached the degree at which an extensive transformation of the hydrated dimeric cycles into anhydrous trimers set in. The extraction of further amounts of excess acid should then proceed in an anhydrous form and without mutual association of rings. This

is fully consistent with the cryoscopic data, which show an increase of the association degree of the amine salt in presence of hydrated excess acid in the organic phase towards 4 and subsequent decrease to 3, when the water content in the organic phase is decreasing towards $c_{\text{H}_2\text{O}}' = 0$ on further increase of the concentration of the acid in the aqueous phase. Hence we have inferred that the $\text{H}_3\text{O}^+\text{X}^-$ side chains, having lost the opportunity to bond with their anionic poles to the H_2O links in a second hydrated ring, are being transformed by further uptake of anhydrous HCl molecules into longer acid side chains which get cyclized on the same trimer ring. Owing to the considerable stability of the condensed structures it may be assumed that the water remaining in the organic phase at those high concentrations will be preferentially concentrated into the remaining tricyclic molecules. Anhydrous HX molecules will be preferentially incorporated into the acid side chains. Water is going to be bond there only to the extent necessary for the cyclization of these side chains into stable side rings by forming ionic bonds between the anionic end of the chains and the R_3NH^+ cations in the trimeric cycles. The results of chemical analysis and cryoscopy have confirmed this pattern. Furthermore, if these conclusions are right, then the entrance of the anhydrous molecules into the cycles should be detectable in the infra-red spectra by a new absorption band. From the existence of the equilibrium which in the systems with comparable water and HX concentrations



is considerably shifted towards the centre, it may be concluded that

the strength of the HX bond is comparable with that of the O-H bond in the H_3O^+ ion so that the band of hydrogen-bonded HX molecules might be expected in the vicinity of the band of hydrogen-bonded H_3O^+ ions. Since the O-H and NH band are widely perturbed by the bands of C-H bonds we have employed deuteration for checking these conclusions. In this way it is actually possible to detect in the i.r.spectra in the region of highest acid concentrations as a shoulder on the very broad hydroxonium ion band. That it is really the band of anhydrous HX molecules becomes obvious from the fact that the total absorption intensity in the long wave region is continually increasing with increacing excess acid extraction, although the concentration of hydroxonium ions begins already to drop at these high acidities due to the strong dehydration of the organic phase. In deuterated systems the bands of all these types of hydrogen bonds are quite distinct. This formation of side cycles bonded to the anions of the acid results in a decrease in the electron density at these anions similarly as the substitution of this anions by anions of a stronger acid. In this way also the anomalous position of the NH bands observed in the case of the extraction of the nitric acid may be easily explained. This acid is being extracted already from low concentrations in high over-stoichiometrical proportion as anhydrous molecules, and the cryoscopic polymerization degree of the amine salt is 3 in wide $\text{TOA}:\text{HNO}_3$ range. This shows that the anhydrous molecules HNO_3 form side cycles on the anions NO_3^- simultaneously with the formation of the amine salt, so that the anions in the rings are not NO_3^- , but big complex anions $[\text{NO}_3/\text{NHO}_3]^-$ of lowered basicity.

Conclusions

It was found from chemical analyses of the organic phase and from cryoscopic and viscosimetric data as well as from infra-red spectra that hydrochloric, hydrobromic, hydroiodic, nitric and perchloric acids are extracted by benzene solutions of TOA in the form of six-membered rings of the amine salt consisting of the ions R_3NH^+ , X^- and of the water molecules partly associated by hydrogen bonds and partly bounded by forces of prevailing electrostatic character. To the anions in these cyclic chains the "over-stoichiometric" amounts of the acid are bonded. At higher activities of water they are transferred into the organic phase as $H_3O^+-X^-$ pairs. As long as there are hydrated cycles of the amine salt present in the organic phase, able to bind by their free OH groups the anionic ends of these $H_3O^+-X^-$ pairs the rings are associated by the $H_3O^+-X^-$ side chains of excess acid to give tricyclic condensed molecules and the polymerization degree of the salt is increasing. When at high acid concentration in the aqueous phase the hydrated cycles have been converted into anhydrous trimeric rings, the acid side chains cyclize under intake of anhydrous HX molecules to side rings by bonding their free anionic end to the same trimere ring without increasing the polymerization degree of the trimeric anhydrous salt. This double mechanism of excess acid extraction, in which the proportion of both alternative reactions varies in dependence on the activity of water in the system, on the acido-basic characteristics of both the amine and the acid as well as on the diluent used, may account for the contradictory results reported in the literature.

References

- 1/ Markovits G., Kertes A.S. : Internat. Conference on Solvent
Extraction Chemistry, Göteborg 1966
- 2/ Keder W.E., Wilson A.S. : Nucl. Sci. and Engg /1963/, 17, 287

THE INTERMOLECULAR HYDROGEN BOND AND DONOR-ACCEPTOR
PROPERTIES OF THE PHOSPHOROUS - AND NITROGEN -
CONTAINING EXTRACTION AGENTS

B.N. Laskorin, V.V. Yakshin, B.N. Sharapov

At the present time it should be commonly accepted that the donor-acceptor mechanism of the interaction is general for both interaction in a pair of complexing agent - ligand and for an intermolecular hydrogen bond (IHB) formation. Thus an approach based on the extraction properties of compounds interpreted in terms of IHB thermodynamic parameters is quite promising.

The equilibrium constants, free energies, enthalpies and entropies of IHB's were determined for 40 neutral organophosphorous compounds of the type X_3PO (where $X=R, RO, NR_2, NHR$) with phenol and water using the method of IR spectroscopy. The values were computed that describe quantitatively an electron-donor activity of the molecules and satisfactorily correlate with their extraction properties. The proposed principle could be easily extended to polydentate extraction agents.

The way of isolating compounds by means of extraction has found a wide application in the various fields of science and technology. Extraction permits study of the states of elements and compounds in the aqueous solutions at macro and micro concentration levels. It also gives an opportunity for designing automatic plants for processing irradiated fuel with a minimum number of staff which is of great importance for theoretical and applied radiochemistry⁽¹⁾.

Besides its traditional application in hydrometallurgy extraction plays a leading role in good and drug production. The extraction spectrophotometric method opens new possibilities for analytical chemistry. At the present time extraction processes are used in protecting the biosphere and their role will increase in the future.

The extraction type of processes are not properly understood in the complex and multilateral living activities of man, animals and plants studied by biochemistry although the final success in this field is hardly reestimated.

Thus it is necessarily to make steps towards developing the theory of choosing the extraction agents and quantitatively describing the principal reactions accompanying an extraction, in particular the donar-acceptor complexing agent - ligand interaction. The quantum-chemical calculations of the complexes could give the most complete information. However, nowadays there are rather few sufficiently reliable results (ab initio calculations and computations within the Hattwee-Fock-Roothaan approximation⁽²⁾) for deriving a reasonable theory. Most of the work carried out using the zero-differential overlap and its different modifications afforded quite contrary results⁽³⁾.

In our opinion a perspective explanation and forecasting of the specifics of extraction interactions is afforded by the study of energetic parameters of the hydrogen bond formation (H-bonds) between an acid standard and some bases which may serve as extraction agents. Actually the first papers have been published a quarter of a century ago which propose and prove a donor-acceptor model of the hydrogen bond⁽⁴⁾. Most parts of the theory have been studied in detail and modified and now the model itself is approved by a majority of the specialities⁽⁵⁾. A great number of experiments were conducted that enable from thermodynamical studies deduction of a relation between the molecular electronic structure and the macroproperties of the compounds available.

The present authors used phenol and water as standard acids (electron acceptors) because of the following reasons: Reactions with phenol have been studied in sufficient detail. Thus one may compare the electron donor properties of the phosphorous- and nitrogen-containing extraction agents to those of a large number of compounds that belong to different classes. The energy of hydration of the extraction agents is interesting in itself and water could also be used as a standard acid^(6,7).

The thermodynamic measurements were performed by means of the infrared spectroscopic method. The dilute solutions of acceptor (A) - electron donor (D) in carbon tetrachloride were investigated. According to our data and those already reported⁽⁸⁾ phenol in CCl_4 solution is by more than 99.9% monomeric (at $C_A = 3-5 \times 10^{-3}$ mole/l). The C_D concentration of the extracting agents was such that provide the ratio $C_D/C_A = 0.5-0.15$. In the study of the interaction between the neutral organophosphorous compounds (NOPC) and water the binary solutions H_2O - NOPC ($C_D/C_A = 1-3$) were prepared and then diluted ten-fold with CCl_4 .

In the region of $4000-2000\text{ cm}^{-1}$ the IR spectra were obtained on the double - beam IKC-14 spectrophotometer with an LiF prism. Frequency calibration was performed using the chloroform and polystyrene spectra.

The IR spectra of the system phenol - NOPC- CCl_4 showed a narrow band $\nu_{fr} = 3611\text{ cm}^{-1}$ assigned to the OH stretch in phenol and a broad band corresponding to ν_{as} of OH stretching mode of phenol associated through an intermolecular hydrogen bond with the phosphoryl oxygen of the donor. The last band has several satellites in the low-frequency part; but their number is independent of the donor type and intensities increase with increasing $\Delta\nu = \nu_{fr} - \nu_{as}$. Similar behaviour of ν_{as} has been cited⁽⁹⁻¹²⁾ and explained by its Fermi resonance. This is quite in agreement with the theoretical structure of the band ν_{as} in hydrogen bond complexes predicted⁽¹³⁾ on the basis of simple models of H - complexes using published results⁽¹⁴⁾. Spectroscopic titration has demonstrated that under such conditions phenol reacts with $X_3P=O$ ($X=R, RO, NR_2, NHR$) in CCl_4 to give an 1:1 complex.

Badger and Bauer^(17,18) were the first who tried to obtain the thermodynamic characteristics of H-bond formation from spectral parameters.

They have observed a linear dependence between enthalpy ΔH and frequency difference $\Delta \nu$ for absorption of the free and associated groups. Now a large number of dependences of the type $H = a\Delta \nu + b$ with different a and b are known which describe a limited set of donors interacting with an acceptor. Drago et al.⁽¹⁹⁾ have observed a linear correlation between the shift and enthalpy for one base and different acceptors. Iogansen⁽²⁰⁾ has doubted the validity of a linear dependence of ΔH with $\Delta \nu$ for the ΔH region investigated (0-11 kcal/mole) and assumed a quadratic relationship between ΔH and $\Delta \nu$ with an observed deviation from linearity at $\Delta H \leq -3$ kcal/mole.

We suggest that the literature data available allow us to ascertain that for $\Delta H \geq -4$ kcal/mole the enthalpy versus frequency shift is linear. Using published ratios⁽²¹⁻²⁴⁾ we estimated the enthalpy of H-bond formation between phenol and phosphorous - and nitrogen-containing extraction agents as a mean of four values. The equilibrium constants were computed by three methods²⁵⁻²⁷. The graphical solution of the system of equations proposed⁽²⁵⁾ was replaced by a more accurate analytical one. The free energy and entropy were found from the relations (ΔG°) (ΔS°):

$$\Delta G^\circ = RT \ln K \quad (1)$$

$$\Delta S^\circ \times T = \Delta H^\circ - \Delta G^\circ \quad (2)$$

where R is the universal gas constant,

and $T = 298^\circ \text{ K}$

The hydration enthalpies of extraction agents were computed using known equations⁽²⁸⁾ derived on the basis of theoretical formalism⁽²⁹⁾ and computation^(30,31) of vibration spectra of water in solutions.

Table 1 shows the spectral and thermodynamic parameters of complex formation between the neutral organophosphorous extraction agents and phenol and water.

Statistical analysis of the experimental data was performed by the method⁽³²⁾ for avoiding rough measurement errors. The values in Table 1 are measured at an accuracy of 20%.

TABLE 1

The spectral and thermodynamic characteristics of complex formation between the neutral organophosphorous extraction agents and phenol and water in CCl_4

No.	Electron donor	Electron acceptor								
		phenol					water			
		ΔV	$-\Delta H^\circ$	K	$-\Delta G^\circ$	$-\Delta S^\circ$	E_t	ΔV	$-\Delta H_{ex}^\circ$	$-\Delta H_{cal}^\circ$
1	$(CH_3)_3PO$	307	5.7	120	2.8	9.7	1.08	224	4.0	3.8
2	$(CH_3O)_2P(O)CH_3$	334	6.1	203	3.1	10.1	1.15	236	4.0	4.0
3	$(CH_3)P(O)(CH_3)_2$	400	7.0	295	3.4	12.1	1.32	278	4.8	4.6
4	$(CH_3)_3PO$	450	7.6	687	3.9	12.4	1.43	298	5.1	5.0
5	$(CH_3O)_2P(O)N$									
	$(CH_3)_2$	361	6.5	196	3.1	11.4	1.23	239	4.2	4.3
6	$CH_3OP(O)-$									
	$(N(CH_3)_2)_2$	416	7.2	524	3.7	11.7	1.36	255	4.5	4.8
7	$(N(CH_3)_2)_3PO$	462	7.8	736	3.9	13.1	1.47	332	5.8	5.2
8	$(CH_3)_2P(O)-$									
	$N(CH_3)_2$	442	7.5	332	3.4	13.8	1.42	283	5.0	5.0
9	$CH_3P(O)-$									
	$(N(CH_3)_2)_2$	460	7.7	653	3.8	13.1	1.45	273	4.8	5.1

10	$\text{CH}_3\text{P}(\text{C})\text{CH}_2\text{O}$ $\text{N}(\text{CH}_3)_2$	379	6.7	458	3.6	10.4	1.26	241	4.2	4.4
11	$(\text{C}_4\text{H}_9)_3\text{PO}$	320	6.0	150	3.0	10.1	1.13	211	3.8	4.0
12	$(\text{C}_4\text{H}_9)_2\text{P}(\text{O})\text{C}_4\text{H}_9$	383	6.7	261	3.3	11.4	1.25	257	4.3	4.4
13	$(\text{C}_4\text{H}_9)_2\text{P}(\text{O})-$ $(\text{C}_4\text{H}_9)_2$	451	7.6	316	3.4	14.1	1.43	282	4.9	5.0
14	$(\text{C}_4\text{H}_9)_3\text{PO}$	496	8.2	664	3.8	14.8	1.55	3.06	5.3	5.4
15	$(\text{C}_4\text{H}_9)_2\text{P}(\text{O})-$ $\text{N}(\text{C}_4\text{H}_9)_2$	368	6.5	253	3.3	10.7	1.23	251	4.2	4.3
16	$\text{C}_4\text{H}_9\text{OP}(\text{C})-$ $[\text{N}(\text{C}_4\text{H}_9)_2]_2$	427	7.3	326	3.4	13.1	1.38	273	4.6	4.8
17	$[\text{N}(\text{C}_4\text{H}_9)_2]_3\text{PO}$	468	8.0	1104	4.1	13.1	1.51	283	5.1	5.3
18	$(\text{C}_4\text{H}_9)_2\text{P}(\text{O})\text{N}-$ $(\text{C}_4\text{H}_9)_2$	454	7.7	561	3.7	13.7	1.45	303	5.1	5.1
19	$\text{C}_4\text{H}_9\text{P}(\text{C})-$ $[\text{N}(\text{C}_4\text{H}_9)_2]_2$	443	7.5	533	3.7	12.8	1.42	281	4.8	5.0
20	$\text{C}_4\text{H}_9\text{P}(\text{O})\text{N}(\text{C}_4\text{H}_9)_2$ $\text{C}_4\text{H}_9\text{O}$	377	7.1	262	3.3	12.8	1.34	265	4.5	4.7
21	$(\text{C}_4\text{H}_9)_2\text{P}(\text{O})-$ NHC_4H_9	513	8.4	735	3.9	14.8	1.56	3.13	5.3	5.5
22	$\text{C}_4\text{H}_9\text{P}(\text{C})(-$ $\text{NHC}_4\text{H}_9)_2$	504	8.3	871	4.0	14.8	1.55	319	5.4	5.5
23	$(\text{NHC}_4\text{H}_9)_3\text{PO}$	541	8.8	1104	4.4	15.8	1.66	344	5.8	5.8
24	$\text{C}_4\text{H}_9\text{CP}(\text{C})-$ $(\text{NHC}_4\text{H}_9)_2$	496	8.2	828	4.0	14.1	1.53	313	5.3	5.4
25	$(\text{C}_4\text{H}_9\text{C}_2)\text{P}(\text{O})-$ NHC_4H_9	337	6.1	310	3.4	9.1	1.15	233	3.9	4.0

26	$(C_4H_9O)_2P(O)NH_2$	335	6.1	266	3.3	9.4	1.15	269	4.3	4.0
27	$(C_4H_9O)_2P(O)-$ NHC_4H_9	344	6.2	305	3.4	9.4	1.17	242	4.0	4.1
28	$(C_4H_9O)_2P(O)NHC_3H_7$	361	6.5	443	3.6	9.7	1.23	239	4.1	4.3
29	$(C_4H_9O)_2P(O)-$ $NHC_{12}H_{25}$	354	6.4	443	3.6	9.4	1.21	271	4.5	4.2
30	$(C_6H_{11}O)_2P(C)-$ NHC_4H_9	361	6.5	338	3.4	10.4	1.23	254	4.3	4.3
31	$(C_8H_{17}O)_2P(C)-$ NHC_4H_9	361	6.5	263	3.3	10.7	1.23	254	4.3	4.3
32	$(C_4H_9O)_2P(O)NHC_4H_9$	307	5.7	305	3.4	7.7	1.08	248	4.1	3.8
33	$(C_4H_9O)_2P(C)NH-$ C_4H_9-t	292	5.6	355	3.5	7.0	1.06	246	4.1	3.7
34	$(C_4H_9O)_2P(C)-$ $NHC_6H_{11}-cis$	318	5.9	443	3.6	7.7	1.11	249	4.1	3.9
35	$(n-C_4H_9O)_2P(C)-$ NHC_4H_9	322	5.9	482	3.6	7.7	1.11	245	4.1	3.9
36	$(EG)_2P(O)NHC_4H_9$	401	7.0	118	2.8	4.2	1.32	265	4.5	4.6
37	$(C_4H_9O)_2P(C)-$ $N(C_4H_9-I)_2$	350	6.3	285	3.3	10.1	1.19	246	4.0	4.2
38	$(C_4H_9)_2P(O)N(C_4H_9h)$	322	5.9	466	3.6	7.7	1.11	235	3.9	3.9
39	$(C_4H_9C)_2P(O)N-$ $(C_6H_{11}-c)_2$	332	6.1	210	3.2	9.7	1.15	253	4.3	4.0
4.0	$(i-C_4H_9O)_3PO$	329	6.1	165	3.0	10.4	1.15	223	3.8	4.0

Notes to table 1, $^{x}_{EG} - C_4H_9\overset{C_2H_5}{CH} - CH_2O$

Units: $\Delta V - cm^{-1}$, ΔH^0 and ΔG^0 kcal/mole, ΔS^0 e.u., $K - l/mole$
Measured at 25°C.

The reaction of NOPC with water and phenol has the same nature. Thus it is naturally to expect⁽¹⁹⁾ that the strengths of the H-bonds produced would vary linearly. Actually, such a linear dependence is observed

$$H_{\text{phenol}} = 2.0 H_{\text{H}_2\text{O}} - 2.3 \quad (r=0.92) \quad (3)$$

Thus it is quite obvious that one may introduce the parameter specifying the electron donor ability of the given compound in all donor-acceptor interactions. Iogansen has shown⁽³³⁾ that the enthalpy of an H-bond is almost proportional to the product

$$H_{ij} = H_{11} P_i E_j$$

where H_{11} is the proportionality coefficient equal to the enthalpy of a standard complex with an H-bond,

P_i - the factor of the i -th acid,

E_j - the factor of the j -th base.

Phenol and diethyl ether were used as the standard reacting pair for which $P_i = E_j = 1$ and $H_{11} = -5.3$ kcal/mole. The values of E_j unluckily called the basicity factors⁽³³⁾ were computed for NOPC (Table 2). Using E_j 's, the hydration enthalpies of NOPC were found which agree well with the experimental data (table 1). Acceptor properties of water could be estimated from equation (4) and E_j :

$$P_{\text{H}_2\text{O}} = 0.66.$$

Of practical interest is a comparison of E_j 's with extraction characteristics. Table 2 lists the logarithms of some known extraction constants of nitric acid⁽³⁴⁻³⁷⁾, $\text{HTICl}_3 \cdot 2\text{S}$ ⁽³⁸⁾ and uranium from nitric acid solutions⁽³⁹⁾ and the sum of charges on the nitrogen, phosphorous and oxygen atoms given in the literature

TABLE 2

Factors E_j , extraction characteristics and atomic charges sums at N, O, P in some phosphorous - and nitrogen-containing extraction agents.

Extraction agent	E_j	$\log K_{\text{HNO}_3}$	$\log K_{\text{HTTC}_1}$	$\log K_{\text{UO}_2}$	$\sum_{i=\text{N,O,P}} q_i$
$(\text{C}_4\text{H}_9\text{O})_3\text{PO}$	1.13	-1.06	1.18	2.2	1.695
$(\text{C}_4\text{H}_9\text{O})_2\text{P(O)}\text{O}_4\text{H}_9$	1.26	-0.86	2.24	3.3	1.766
$\text{C}_4\text{H}_9\text{OP(O)}(\text{C}_2\text{H}_9)_2$	1.43	-0.35	3.34	6.0	1.862
$(\text{C}_4\text{H}_9)_3\text{PO}$	1.55	-0.10	3.97	8.3	2.00
$\text{C}_4\text{H}_9\text{O}$ $\text{P(O)}\text{N}(\text{C}_4\text{H}_9)_2$	1.34				1.899
$(\text{C}_4\text{H}_9)_2\text{P(O)}\text{N}(\text{C}_4\text{H}_9)_2$	1.23				1.818
$\text{C}_4\text{H}_9\text{OP(O)}(\text{N}(\text{C}_4\text{H}_9)_2)_2$	1.38				1.916
$(\text{N}(\text{C}_4\text{H}_9)_2)_3\text{PO}$	1.51	-0.32			2.000
$\text{C}_4\text{H}_9\text{P(O)}(\text{N}(\text{C}_4\text{H}_9)_2)_2$	1.42				2.000
$(\text{C}_4\text{H}_9)_2\text{P(O)}\text{N}(\text{C}_4\text{H}_9)_2$	1.45				1.997
$(\text{NHC}_4\text{H}_9)_3\text{PO}$	1.66	0.08			
$\text{C}_4\text{H}_9\text{OP(O)}(\text{NHC}_4\text{H}_9)_2$	1.53	-0.56			
$(\text{C}_4\text{H}_9\text{O})_2\text{P(O)}\text{NHC}_4\text{H}_9$	1.15	-0.11			
$\text{C}_4\text{H}_9\text{OP(O)}(\text{NHC}_4\text{H}_9)_2$	1.55	0.11			
$(\text{C}_4\text{H}_9)_2\text{P(O)}\text{NHC}_4\text{H}_9$	1.56	0.03			

Unfortunately only a rather limited amount of extraction data are known for the most investigated NOPC. Thus table 2 gives a comparison of accuracy of the correlating equations for a series of phosphate-phosphonate-phosphinate-phosphineoxide compounds to that of the same equations used for all compounds in table 2 (the dependence $\log K_{\text{HNO}_3}(E_j)$ is presented most completely.

The correlation coefficient is taken as a measure of accuracy. Thus for the first four extraction agents

$$\log K_{\text{HNO}_3} = 2.3 E_j - 3.7 \quad (r = 0.94) \quad (5)$$

Extending equation (5) to all compounds in table 2 we have the best correlation coefficient $r = 0.98$. Analogously

$$\log K_{\text{HTlCl}_{1.2}\text{S}} = 6.9 E_j - 6.5 \quad (r=0.999) \quad (6)$$

$$\log K_{\text{UO}_2^+} = 15.2 E_j - 15.4 \quad (r=0.990) \quad (7)$$

$$\sum q_i = 0.8 E_j + 0.85 \quad (r=0.92) \quad (8)$$

The value of the isoequilibrium temperature ⁽⁴²⁾ is an important factor in the extraction technique. In a majority of cases the equilibrium constant K is used as the parameter specifying the stability of complexes. But if temperature T of the equilibrium constant measurement is close to an isoequilibrium one then one can not make a conclusion that the energies of molecular bonds in the complexes discussed are close or that such complexes have similar stabilities ⁽⁴³⁾. Moreover the family of curves $\Delta G_i(T) = \Delta H_i - T \Delta S_i$ ($i=1, 2, \dots, n$, n is the number of investigated compounds) invert at the point $T = \beta$. Thus the order of relative reactivity of the compounds at $T > \beta$ is opposite to that observed at the experimental temperature $T < \beta$.

In our case for the first twenty compounds of table 1 the equation of compensational effect has the form

$$\delta \Delta G = 0.23 \delta \Delta H + 0.32 \quad (r = 0.91) \quad (9)$$

where δ is the Lefler operator. Thus the equilibrium temperature is $\beta = 441^\circ\text{K}$ (168°C). (Measurements were performed at $T = 298^\circ$).

We note that the presence of a compensative effect should be checked for each reaction series otherwise erroneous conclusions could be drawn. Thus Lopes and Thompson⁽⁴⁴⁾ have obtained the thermodynamic characteristics of the H-bond between phenol, tert-butanol, 2,6-ditert-butylphenol and cyanides. These values have been compared with published data^(27,45) on complex formation between thiocyanic acid and alcohols and ethers, ketones, amides, nitriles. The authors have assumed the presence of a compensative effect with $\Delta S^\circ = 540^\circ$ valid in the region of $-\Delta H = 1 - 9$ kcal/mole. However, from the more detailed analysis of the results⁽⁴⁴⁾ an isoentropic reaction series is observed instead of a symbathic change of ΔH and ΔS . The authors themselves⁽⁴⁴⁾ have adopted an isoentropic character for interaction of phenol with nitriles. In the case of complex formation of tert-butanol with nitriles Lopes and Thompson described it by the function $\Delta S(\Delta H) \neq \text{const}$, while our computation using their data gave $\Delta S = \text{const} = -6.6$ e.u. with a mean square deviation of $\sigma = +0.8$ (smaller than in⁽⁴⁴⁾) ($\sigma = \pm 1.1$ e.u.) One can not interpret unequivocally the thermodynamic characteristics of reaction between 2,6-ditert-butylphenol with nitriles because of the close values and the use of only two reacting pairs.

Assuming that the presented results may serve not only for predicting an extraction ability of compounds we support Palm⁽⁴⁶⁾ in a possibility of changing many of our concepts on reaction mechanism, the effect of structure and solvent on chemical reactions and other processes. And we have to pay more attention (than we do now) to the effect of specific solvation and particularly hydrogen bonds. For example the H-bond formation may be discussed as a standard reaction series for determining the numerical values of substituent constants. Such considerations have been advanced⁽⁴⁶⁾.

Starting from the principle of additivity of properties we computed the values conventionally called donor coefficients (e) (table 3).

TABLE 3

The donor coefficients of different functional groups.

No.	Group	e	No.	group	e
1	CH_3O	0.35	12	$\text{NHC}_4\text{H}_9\text{-n}$	0.57
2	$\text{n-C}_4\text{H}_9\text{O}$	0.34	13	$\text{NHC}_{12}\text{H}_{25}\text{-n}$	0.53
3	$\text{n-C}_6\text{H}_{13}\text{O}$	0.33	14	$\text{C}_4\text{H}_9\text{O-iso}$	0.38
4	$\text{n-C}_8\text{H}_{17}\text{O}$	0.33	15	$\text{C}_8\text{H}_{17}\text{O-sec}$	0.27
5	CH_3	0.48	16	$\text{C}_4\text{H}_9\text{CH}(\text{C}_2\text{H}_5)\text{CH}_2\text{O}$	0.38
6	$\text{n-C}_4\text{H}_9$	0.52	17	$\text{N}(\text{C}_4\text{H}_9\text{iso})_2$	0.51
7	$\text{N}(\text{CH}_3)_2$	0.49	18	$\text{N}(\text{C}_4\text{H}_9\text{-sec})_2$	0.43
8	$\text{N}(\text{C}_4\text{H}_9\text{-n})_2$	0.49	19	$\text{N}(\text{C}_6\text{H}_{11}\text{-cyclo})$	0.47
9	NH_2	0.47	20	$\text{NHC}_4\text{H}_9\text{-sec}$	0.40
10	NHCH_3	0.49	21	$\text{NHC}_4\text{H}_9\text{-tert}$	0.38
11	$\text{NHC}_3\text{H}_7\text{-n}$	0.55	22	$\text{NHC}_6\text{H}_{11}\text{-cyclo}$	0.43

The donor coefficients introduced allow computation of the extraction constants from equations (5-7) for NOPC which were not included in table 1 if the molecules of such compounds contain the groups shown in table 3.

In the same manner e's could be obtained for other classes of compounds.

Then

$$\text{Log } K = A \sum e + b \quad (10)$$

where K is the extraction constant

$\sum e$ is the sum of the donor coefficients of functional groups in the molecule.

A and B numerical parameters.

Equation (10) is valid when the extraction and its modelling by means of the thermodynamics of H-bond are performed in the same solvent or in those having similar donor-acceptor properties.

REFERENCES

1. M.F.Pushlenkov, Atomnaya Energiya, 33 (1972) 625
2. C.C.J.Roothaan, Rev.Mod.Phys. 23 (1951) 69.
3. M.E.Dyatkina, Zh.Vsesoyuz.KhimObshch.im.D.I.Mendeleeva, 17 (1972) 285.
4. N.D. Sokolov, Dokl.Akad.Nauk.SSSR, 58 (1947) 611.
5. "Vodorodnaya svyaz" Coll.papers, Ed. N.D.Sokolov and V.M.Chulanovskii, "Nauka"Publ.House, Moscow. 1964, p.8.
6. A.V.Karyakin, G.A.Muradova, Zh.Fiz.Khim., 45 (1971) 1054.
7. A.V.Karyakin, G.A.Kriventsova, Dokl.Akad.Nauk SSSR, 208 (1973) 107.
8. M.D. Joesten, R.S.Drago, J.Am.Che.,Soc., 84 (1962) 2037.
9. A.V.Iogansen, E.V.Rassadin, Zh.Prikld.Spectr., 6 (1967) 492.

10. B.V.Rassadin, A.V.Iogansen, Zh.Prirkld.Spediz.,
1C (1969) 290.
11. A.V.Iogansen, B.V.Rassadin, Zh.Prirkld.Spediz.,
11 (1969) 828.
12. S.E.Odinokov, A.V.Iogansen, A.K.Dzhenko, Zh.Prirkld.
spediz, 14 (1971) 418.
13. A.B.Iogansen, in "Optika i Spektroskopiya" III, "Nauka",
Leningrad, 1967, p 228.
14. G.Herzberg, Infrared and Raman Spectra of Polyatomic
Molecules, New York, 1945
15. A.V.Nikolaev, Yu.A.Dyadin, Z.A.Grankina, I.I.Yakovlev,
E.V.Sobolev, Izv.Sib.Otd.Akad.Nauk SSSR, Ser.Khim.nauk.,
7, (1969) 3.
16. D.C.Whitney, R.M.Diamond, J.Phys.Chem., 67(1963)209
17. R.M.Badger, S.H.Pauer, J.Chem.Phys., 5(1937) 839.
18. R.M.Badger, J.Chem.Phys., 8(1940) 288.
19. R.S.Drago, N.O'brien, G.C.Vogel, J.Am.Chem.Soc., 92
(1970) 3924.
- 20 A.V.Iogansen, Doctoral Thesis, Moscow, 1969.
21. M.D.Joesten, R.S.Drago, J.Am.Chem.Soc., 84(1962)3817.
22. S.Singh, A.S.N.Murthy, C.N.R.Rao, Trans.Faraday Soc.,
62 (1966)1056.
23. T.D.Epley, R.S.Drago, J.Am.Chem.Soc., 89(1967)5770.
24. T.Gramstad, Spectrochim.Acta, 19(1963)497.
25. H.J.Rose, R.S.Drago, J.Am.Chem.Soc., 81(1959)6138
26. H.A.Fenesi, J.H.Hildebrand, J.Am.Chem.Soc., 71(1949)
2703
27. E.D.Becker, Spectrochim.Acta, 17(1961)436

28. A.V.Karyakin, G.A.Muradova, L.Ya.Golishnikova, in
Kolebatel'nye spektry v neorganicheskoi khimii",
"Nauka" , Moscow, 1971, p.267.
29. G.V.Yukhnevich, A.V.Karyakin, A.V.Petrov, Zh.Prirod.
Soedin, 3, (1965) 142.
30. G.V.Yukhnevich, in "Optika i Spektroskopiya," II, Izd.
Akad.Nauk SSSR, Moscow-Leningrad, p 223.
31. G.V.Yukhnevich, A.V.Karyakin, Dokl.Akad.Nauk SSSR,
156 (1964) 631.
32. G.N.Kassandrova, V.V.Lebedev, Obrabotka Rezul'tatov
Nablyudenii, "Nauka2, Moscow, 1970.
33. A.V.Iogansen. Teor. i.experim.Khim., 7,(1971) 302.
34. B.N.Laskorin, V.V.Yakshin, V.V.Shatalov, E.P.Buchikhin,
L.I.Sokal'skaya, V.I.Medvedev, Report at the 10-th annual
Czechoslovak conference on radiation chemistry, Marian-
skie Lazni, 1970.
35. V.G.Voden, Radiokhimiya, 2, 121 (1959).
36. M.F.Pushlenkov, Radiokhimiya, 2, 215 (1960)
37. B.N.Laskorin, V.V.Yakshin, E.P.Buchikhin, L.I.Sokal'skaya,
V.I.Medvedev, Teor. i experim. Khim., 9 (1973) 245
38. S.P.Khranenko, L.K.Chuchalin, Izv. Sib. Otd. Akad. Nauk SSSR,
Ser. Khim. Nauk, 14, n.6 (1972) 3
39. A.V.Nikolaev, L.N.Mazalov, I.A.Gal'tsova, A.P.Sadovski, Izv.
Sib. Otd. Akad. Nauk SSSR, Ser. Khim. Nauk, 12, n.5 (1972) 7
40. M.A.Landau, V.V.Sheluchenko, S.S.Dubov, Dokl. Akad. Nauk
SSSR, 182 (1968) 1934
41. M.A.Landau, V.V.Sheluchenko, S.S.Dubov, Zh. Strukt. Khimi,
11 (1970) 513

42. J.F.Leffler, J. Org. Chem., 20 (1955) 1202
43. E.N.Gur'yanova, I.P.Goldshtein, I.P.Romm, Donorno-acceptornaya svyaz, "Chimia" Publ. House, Moscow, 1973
44. M.C.S.Lopes, H.W.Thompson, Spectrochim. Acta, 24A, (1968) 1367
45. T.M.Barakat, M.J.Nelson, S.M.Nelson, A.D.E.Pullin, Trans. Faraday Soc., 62 (1966) 2674
46. V.A.Palm, Osnovi colchestvenoi teori organicheskikh reacsi, "Chimia" Publ. House, Leningrad, 1967, p.311

SESSION 2

Monday 9th September: 9.00 hrs

E Q U I P M E N T

(Mixers & Settlers)

Chairman:

Professor F.J. Zinderweg

Secretaries:

Dr. G.A. Davies

Mr. P, Ronyer

"THE EFFECT OF CHANGES IN OPERATING ORGANIC/AQUEOUS RATIO ON THE
OPERATION OF A MIXER SETTLER"

G A Rowden, J B Scuffham, G C I Warwick

ABSTRACT

The effects of changes in the operating organic/aqueous ratio under both organic and aqueous continuous mixer conditions were studied at laboratory scale. The significant influence of the operating organic/aqueous ratio on such parameters as specific flow/dispersion bed depth relationships, mass transfer efficiency and entrainment values is illustrated and possible mechanisms proposed.

Davy Powergas Limited
Research & Development Division
STOCKTON-ON-TEES
England

INTRODUCTION

Entrainment, both of the aqueous phase in the organic phase and of the organic phase in the aqueous phase, has been an area of major concern in metallurgical solvent extraction technology. Attempts have been made to contain the problem by such techniques as flotation, first practised on a commercial scale by Ranchers Exploration at their Bluebird Mine operation in Miami (1), centrifugation or by coalescence devices, as practised by Anglo American at their Western Reefs plant where coke beds are used after the settlers to coalesce out the entrained organic solution. Such systems do not deal with the cause of the problem, which originates in the contacting/settling equipment and is a function of the design of that equipment and of its operation.

Features of the Davy Powergas Limited design of mixer settler have been developed to minimise secondary haze. One such feature, which has been described previously (2), is an introductory baffle. This device is included to obtain beneficial effects on entrainment values and settling rates by introducing the dispersion into the correct portion of the dispersion bed in the settlers.

However, a major factor influencing separation rate and entrainment values is the phase ratio in the mixer and this effect is the subject of this paper.

In metallurgical solvent extraction systems, there is usually a metal value concentration effect between the feed and strip aqueous streams. Therefore the overall phase ratios in these two sections of the plant will be different. It rarely occurs that the operating overall phase ratio is the optimum phase ratio, as will be discussed below, and in these systems, individual stage recycle is practised in one section or the other to achieve an optimum. The choice of this optimum can be of major importance in determining capital and operating costs of the plant.

Treybal (3) and Davies and Jeffreys (4) have suggested a packing ratio in water-kerosene systems in which the proportion of each phase present in the dispersion is a function of the phase continuity imposed. The systems described are ones in which mass transfer is of small consequence.

During experiments carried out by Davy Powergas Limited using a laboratory scale mixer discharging into a rectangular settler, it was observed that the organic/aqueous ratio in the mixer had a dramatic influence on the organic and aqueous entrainment values in the settler discharge streams and also on the dispersion bed depth.

Quantitative experiments were therefore conducted to establish the magnitude of the effect of the organic/aqueous ratio in the mixer upon extraction efficiency, dispersion bed depth and entrainment values.

EXPERIMENTAL WORK

Two series of laboratory based experiments were carried out; one to examine the effect of organic/aqueous ratio on the operation of a single mixer-settler and the other to investigate the effects occurring in a multistage, linked solvent extraction circuit comprising three extraction and three strip stages.

The single and multistage experiments were carried out using Perspex mixer-settlers having mixer boxes of dimensions 10 cm x 10 cm x 10 cm and settler dimensions 8 cm wide, 20 cm deep and 12.5 cm long. Fig 1.

The pump-mix impeller used in the experiments was of a double shrouded, backward swept vane type incorporating additional shear blades on the external surfaces of the upper and lower shrouds. Throughout the experiments the impeller was operated at a tip speed of 2.61 M/sec. In all cases the impeller was situated at the vertical mid-point of the mixing box on top of the integral draught tube in such a way that internal recirculation of the dispersion in the mixer box was at a minimum.

The dispersion discharging from the mixer box flowed into its integral settler down an inlet baffle, capable of vertical adjustment. The baffle was positioned so that the inlet flow entered the dispersion bed on the dispersion side of the coalescing interface. The settler was fitted with an adjustable aqueous weir and this controlled the position of the dispersion in the settler.

At the total flow rate used in the single stage experiments, $3 \times 10^{-2} \text{ m}^3/\text{hr}$, the available settler area gave a specific flow of approximately $2.3 \text{ M}^3/\text{M}^2 \text{ hr}$. To increase this specific flow to a more realistic value for the LIX/copper system used in the investigation, a dam baffle was fitted which effectively reduced the area of the settler available for settling. Thus the extraction experiments were carried out with a specific flow of $3.5 \text{ M}^3/\text{M}^2 \text{ hr}$ and the strip experiments with a specific flow of $3.1 \text{ M}^3/\text{M}^2 \text{ hr}$.

The multistage experiments were carried out with a variety of specific flows covering the range 1.15 to $3.5 \text{ M}^3/\text{M}^2 \text{ hr}$. This range was achieved by variation of both the total inlet flow to the mixer and the available settler area.

As a result of decreasing the settler length, a 'dead' volume existed between the dam baffle and organic weir box. To eliminate errors in the entrainment measurement due to settling-out in this area, permanently situated organic and aqueous glass sample tubes, fitted with Teflon/glass valves, were placed immediately downstream of the dam baffle in their respective phases.

The variation in the operating organic/aqueous ratio in the single stage extraction experiments, i.e. the ratio of the total flow of organic and aqueous solution entering the mixer, was achieved by keeping the overall organic/aqueous ratio constant, i.e. the ratio of the organic and aqueous flow entering the mixer but excluding any recycle flow, and varying the flow of recycled aqueous or organic phase. The total flow and therefore the mixer retention time were also constant. For the extraction experiments, the overall organic/aqueous ratio was 1.0 and the mixer retention time two minutes. The comparable figures for the strip experiments were an overall organic/aqueous ratio of 3.0 and a mixer retention time of three minutes.

In the multistage experiments, the overall organic/aqueous ratio in the extraction section was 11.25 and that in the strip section 3.0. Recycle of aqueous phase, when used, was sufficient to decrease the operating organic/aqueous ratio to unity in both cases. Unlike the single stage experiments, which were carried out under constant mixer retention time conditions, the mixer retention times in the multistage experiments were varied over the range 2 - 6 minutes for both the extraction and strip sections.

In those experiments requiring recycle of aqueous phase, the aqueous effluent from the settler passed to a glass vessel of approximately 1 litre capacity, which was equipped with two outlets. One of these was connected to the recycle pump, while the other was connected either to a polypropylene aspirator used as a spent solution storage tank or to the relevant mixer-settler. The phase not recycled passed directly to a polypropylene aspirator or to the relevant mixer-settler.

The aqueous solution used in the single stage extraction experiments contained approximately 0.10 gpl Cu^{2+} and approximately 3.50 gpl (free) H_2SO_4 and simulated a typical raffinate extraction stage. The multistage experiments were carried out with an aqueous feed containing 45 gpl Cu^{2+} and 0.5 gpl free H_2SO_4 . The aqueous feed solution used in both the single and multistage strip experiments simulated a typical solvent extraction/electrowinning spent electrolyte concentration and contained 25 gpl Cu^{2+} and 150 gpl free H_2SO_4 .

0.7 M³ batches of solution were prepared in town's water using commercial grade copper sulphate and sulphuric acid. The raffinate and advance electrolyte solution from each experiment were discarded.

The organic solution used in the single stage experiments was 18 vol % LIX 64N* in Napoleum 470**. After use in each extraction experiment, the loaded organic solution was contacted with sulphuric acid and washed with water. Before storage and use, the stripped organic solution was passed through a glass-wool packed coalescer to remove entrained water and then analysed for copper. The partially loaded organic phase used as feed in the strip experiments and containing 0.6 gpl Cu^{2+} , was reused by reloading to the required copper level with ammoniacal copper sulphate solution and washing out the entrained aqueous phase and contained ammonia with water. Additional coalescence treatment was then applied before analysis and reuse as described for the extraction experiments. The organic phase used in the multistage experiments was a 40 volume % solution of LIX 73* in Napoleum 470**.

In all the experiments the organic and aqueous feed and recycle flows were controlled by Watson Marlow peristaltic pumps in conjunction with calibrated flow meters. The pumps were operated in a manner which avoided pulsing.

Each single stage experiment was of 2 hours duration whilst the multistage mixer-settler circuit operated for continuous periods of up to 50 hours. During the test period which was 1 hour for the single stage experiments and 4 hours for the multistage system, the solution flow rates, dispersion bed depths, clear organic and aqueous depths, and the head developed by the impeller were measured at 15 minute intervals.

Samples of aqueous raffinate were taken at 15 minute intervals and samples of organic extract at 30 minute intervals. Their copper contents were determined by the analytical procedures described below.

At the completion of each of the single stage and multistage experiments, the determination of the equilibrium solution copper concentrations was carried out as follows. Samples of aqueous and organic phase from each of the settlers were taken in the same ratio as that used in the experiment, (operating organic/aqueous ratio) and equilibrated for a minimum of 30 minutes at the experimental temperature. The solutions were then separated and analysed.

* Registered Trade Mark of General Mills Incorporated

** Registered Trade Mark of Kerr McGee Corporation

Analysis of both phases for copper values of less than 1 gpl were carried out by atomic absorption spectrophotometry, care being taken to eliminate entrainment of one phase in the other. The free sulphuric acid concentrations of the solutions and the copper concentration of those solutions containing greater than 1 gpl were determined volumetrically.

Samples for organic and aqueous entrainment were taken at 30 minute intervals. The determinations of aqueous entrainment were carried out by means of a centrifuge using calibrated tubes. The determination of organic entrainment was carried out by infra-red spectrophotometry.

DEFINITIONS

1. a OVERALL ORGANIC/AQUEOUS RATIO

The overall organic/aqueous ratio is given by

$$\frac{\text{organic feed flow (ml/min)}}{\text{aqueous feed flow (ml/min)}}$$

where the feed flows do not include any recycle flow

b OPERATING ORGANIC/AQUEOUS RATIO

The operating organic/aqueous ratio is given by

$$\frac{\text{total flow of organic to mixer (ml/min)}}{\text{total flow of aqueous to mixer (ml/min)}}$$

where the total flows include any recycle.

2. PERCENTAGE EXTRACTION

The percentage extraction was calculated using the following formula:

$$\% \text{ Extraction} = \frac{C_{\text{Faq}} - C_{\text{R}}^{\text{Ep}}}{C_{\text{Faq}}} \times 100$$

where C_{Faq} = copper concentration of the aqueous feed

C_{R}^{Ep} = copper concentration of the aqueous raffinate

3. EXTRACTION STAGE EFFICIENCY (% Approach to Equilibrium)

The stage efficiency was calculated using the following formula:

$$\text{Stage efficiency} = \frac{C_{\text{Faq}} - C_{\text{R}}^{\text{Ep}}}{C_{\text{Faq}} - C_{\text{R}}^{*\text{Ep}}} \times 100$$

where $C_{\text{R}}^{*\text{Ep}}$ = copper concentration in equilibrated raffinate

4. PERCENTAGE STRIP/STRIP STAGE EFFICIENCY (% Approach to Equilibrium)

Analogous to that described above for extraction but using experimental and equilibrium organic phase copper concentrations.

RESULTS

The results of the experimental work are given in Tables 1, 2 and 3 and have been presented in Graphs 1 to 10.

TABLE 1

Single Stage Extraction Section

Aqueous Feed	:	100 ppm Cu^{2+} , 3.5 gpl H_2SO_4
Organic Feed	:	18 vol % LIX 64N* in Napoleum 470**
Impeller	:	Double shrouded, sweptback vaned, externally spoiled
Impeller tip speed	:	2.61 M/s
Specific Settler Flow	:	$3.5 \text{ M}^3/\text{M}^2 \text{ hr}$
Overall O/A Ratio	:	1 to 1
Mixer Retention Time	:	2 minutes
Total Solution Flow	:	$0.03 \text{ M}^3/\text{hr}$

Overall O/A Ratio	Operating O/A Ratio	Mixer Continuity	Stage Efficiency %	Dispersion bed depth cm	*** Aqueous Entrain- ment ppm	Organic Entrain- ment ppm
0.99:1	0.99:1	Organic	92.5	13.0	600	14
0.98:1	0.98:1	Aqueous	83.9	1.4	450	38
1.01:1	1.98:1	Organic	91.8	11.0	4000	13
1.01:1	1.97:1	Aqueous	90.9	1.8	225	30
1.02:1	3.02:1	Organic	93.6	6.4	7500	12
1.02:1	3.00:1	Aqueous	93.6	1.7	7500	35
1.01:1	3.90:1	Organic	91.3	1.5	15000	13
0.99:1	1:2.01	Organic	95.8	13.3	10	8
0.98:1	1:2.03	Aqueous	87.2	0.8	2100	425
1.00:1	1:3.00	Organic	96.7	8.1	10	20
1.00:1	1:2.98	Aqueous	84.6	0.4	1350	525
0.99:1	1:4.01	Organic	95.7	5.9	40	25
0.99:1	1:3.99	Aqueous	84.6	0.2	2200	470

*** The values quoted refer to the primary dispersion and not to the diffuse secondary dispersion that formed at high operating organic/aqueous ratios.

TABLE 2

SINGLE STAGE STRIPPING SECTION

Spent Electrolyte	:	25 gpl Cu^{2+} , 150 gpl free H_2SO_4
Organic Feed	:	18 vol % LIX 64N* in Napoleum 470** containing 0.6 gpl Cu^{2+}
Impeller	:	Double shrouded, swept back vaned, externally spoiled
Impeller tip speed	:	2.61 M/sec.
Specific Settler flow	:	$3.1 \text{ M}^3/\text{M}^2 \text{ hr}$
Overall O/A Ratio	:	3 to 1
Mixer Retention Time	:	3 minutes
Total Solution Flow	:	$0.02 \text{ M}^3/\text{hr}$

Overall O/A ratio	Operating O/A Ratio	Percentage Strip	Stage Efficiency %	*** Dispersion bed depth cms	Aqueous Entrain- ment ppm	Organic Entrain- ment ppm
3.00	3.00	56.6	86.3	1.7	4200	41
3.00	1.99	61.5	93.5	3.4	3750	30
3.05	1.50	64.7	95.7	4.6	1400	45
3.10	1.32	65.1	98.4	4.4	900	30
2.91	0.98	65.6	98.6	5.2	50	23
3.08	0.51	63.2	99.2	6.2	50	58
2.69	0.34	63.4	99.7	5.8	20	55

*** The values quoted refer to the 'primary' dispersion and not to the diffuse secondary dispersion that formed at high operating organic/aqueous ratios.

TABLE 3

MULTISTAGE CIRCUIT RESULTS

Aqueous Feed	:	45 gpl Cu^{2+} , 0.5 gpl free H_2SO_4
Organic Phase	:	40 volume % LIX 73* in Napoleum 470**
Spent Electrolyte	:	25 gpl Cu^{2+} , 150 gpl free H_2SO_4
No of Extraction Stages:		Three
No of Strip Stages	:	Three
Overall O/A Ratio -		
Extraction	:	11.25 to 1
Overall O/A Ratio -		
Strip	:	3.00 to 1
Temperature	:	25°C

Effect of Recycle on % stage efficiency

Mixer retention time - min	Average Extraction Single Stage % Efficiency		Average Strip Single Stage % Efficiency	
	Recycle	No recycle	Recycle	No recycle
2	89.9	75.1	95.2	86.1
3	98.7	80.4	95.9	96.3
4	98.0	85.2	91.6	93.8
5	97.1	86.0	94.4	95.8

Effect of recycle on entrainment

	Extraction Section		Strip Section	
	Organic Entrainment ppm	Aqueous Entrainment ppm	Organic Entrainment ppm	Aqueous Entrainment ppm
Recycle	62	190	63	260
No recycle	11	>5000	15	>5000

DISCUSSION

DISPERSION BED DEPTH

The results from the experiments show the marked dependence of dispersion bed depth on phase ratio (Graphs 1 - 4). The results were in agreement with earlier observations and a possible explanation is as follows.

For the systems under study, there exists a 'preferred' organic/aqueous ratio in the dispersion bed, i.e. a 'preferred' packing ratio. From the results obtained in earlier qualitative experiments, this 'preferred' organic/aqueous ratio appeared to be 1:2 as evidenced by the constancy of the distribution of the dispersion bed around the settled interface and its independence of the operating organic/aqueous ratio of the mixer settler. A 'preferred' organic/aqueous ratio of 1:2 under organic continuous operation for the water/kerosene system can be inferred from evidence in the literature (3) (4).

As a result of this 'preferred' packing ratio, at high operating organic/aqueous ratios under organic continuous conditions there is an excess of organic over that required in the dispersion bed, the volume of dispersed aqueous phase being low. This excess organic phase therefore rapidly disengages from the dispersion on leaving the mixer and there results a large, upward flow of organic at the settler inlet. This large flow carries with it a considerable proportion of the very small dispersed aqueous droplets which are produced in the mixer. These droplets remain suspended in the organic phase as a result of the natural organic drainage from the dispersion bed, forming diffuse 'secondary' dispersion bands and giving rise to the high aqueous entrainments recorded.

As the total solution flow was kept constant throughout the single stage experiments, there was only a small volume of dispersed aqueous phase present when using a high operating organic/aqueous ratio. At the 'preferred' packing ratio of 1:2, this small volume of dispersed aqueous phase would be associated with half its volume of organic phase and the resulting volume of dispersion would be only a small proportion of the total mixed flow entering the settler. Assuming that the coalescence rate was substantially the same in all cases, and remembering that the total flow and settler area were constant throughout the single stage experiments, operation at a high organic/aqueous ratio would result in the small dispersion bed depth recorded. Therefore decreasing the operating organic/aqueous ratio has two major effects. Reducing the amount of excess organic over that required in the dispersion to form the 'preferred' ratio results in a reduction in the flow of organic out of the dispersion at the settler inlet, thus decreasing the 'carry out' of dispersed aqueous droplets and reducing the depth of the diffuse 'secondary' dispersion bed. Simultaneously the increase in the volume of dispersed aqueous phase plus its associated organic phase results in an increase in the dispersion bed depth.

The above trends continue with a rapidly decreasing diffuse 'secondary' dispersion bed depth and a rapidly increasing 'primary' bed depth until the operating organic/aqueous ratio approximates to the 'preferred' packing organic/aqueous ratio, i.e. 1:2 under organic continuous conditions.

On further decreasing the operating organic/aqueous ratio there is insufficient organic phase to form the 'preferred' packing ratio, since the amount of dispersed aqueous phase has increased and that of the continuous organic phase has decreased. This reduced amount of continuous organic phase must, of necessity, envelope an increased volume of dispersed aqueous phase assuming a constant particle size distribution with the result that the average interdrop distance decreases. As the rate of coalescence is strongly influenced by the time taken for the interdrop distance to decrease to a given value, the rate of coalescence increases as a result of the decreasing operating organic/aqueous ratio, so decreasing the dispersion bed depth.

Thus the effect of the operating organic/aqueous ratio on dispersion bed depth is to give a curve of the type shown in Graphs 1 and 2, with a maximum at the 'preferred' packing organic/aqueous ratio.

The sharpness of the peak in the curve will depend upon the dispersion bed depth/specific settler flow relationship. Thus if a small change in specific flow results in a large change in dispersion bed depth, then the peak will be sharp. Alternatively if the specific flow is such that a large change results in only a small change in dispersion bed depth then the peak will be broad and flat. The latter appears to be the case for the curve obtained during the single stage extraction experiments under aqueous continuous conditions, shown in Graph 1. The specific flow of $3.5 \text{ M}^3/\text{M}^2 \text{ hr}$ used throughout the experiments is very conservative for aqueous continuous operation and a peaked curve is not obtained.

For the above proposition to be correct, the aqueous continuous dispersion bed/operating phase ratio curve should show a peak at an operating organic/aqueous ratio of approximately 2:1. The existing curve does show a tendency to peak at this value but this could only be confirmed by another series of experiments at a higher specific settler flow.

Although the multi-stage experiments were not carried out in the same manner as were the single stage experiments, the results clearly illustrate the dispersion bed/phase ratio relationship. Thus a study of Graphs 3 and 4 shows that, under comparable conditions of specific flow, both extraction and strip stages have larger dispersion bed depths when operating with recycle than when operating without.

One consequence of the above concerns changing the continuity of an industrial scale plant by drastically altering the operating organic/aqueous ratio. Thus, if a mixer operating with aqueous continuity inverts to organic continuity when running at an operating organic/aqueous ratio of 1:1 and the organic/aqueous ratio is then changed to less than 1:1 to re-establish aqueous continuity without decreasing the total flow, the operating organic/aqueous ratio will pass through the maximum in the dispersion bed depth curve. If the dispersion bed depth/specific flow is already in the critical region, flooding of the settler may occur both on decreasing the organic/aqueous ratio to invert the continuity and again when reverting to the original value. In case where the dispersion bed depth/specific flow relationship is very critical even small changes in the operating organic/aqueous ratio may be sufficient to cause flooding of the settler at constant total flow.

ORGANIC ENTRAINMENT IN THE AQUEOUS PHASE

Under organic continuous mixer conditions, the values of organic entrainment in the aqueous phase appear to be virtually independent of the operating organic/aqueous ratio as illustrated in Graphs 5 and 7. There is, however, an indication from Graph 5 that the organic entrainment increases as the operating organic/aqueous ratio decreases from 1:1 to 1:4.

It is believed that under organic continuous mixer conditions the presence of organic entrainment in the aqueous phase is primarily a function of the coalescence mechanism and general settler operation rather than mixer operation. It has been experimentally confirmed that coalescence in the settler gives rise to entrainment of the continuous phase in the bulk disperse phase by several mechanisms. (5). Thus, providing that the coalescence rate and the nature of the dispersion remain the same, the organic entrainment values should be constant at constant mixing conditions. This is indicated by the independence of the organic entrainment values with respect to operating organic/aqueous ratios over the range 4:1 to 1:2. At organic/aqueous ratios below 1:2, the nature of the dispersion changes as the organic film surrounding each aqueous particle decreases in thickness, thus increasing the coalescence rate. This increased rate of coalescence could increase the degree of organic entrainment in the aqueous phase as a result of the increased violence of the coalescence mechanisms.

The values of organic entrainment under organic continuous conditions for the multi-stage experiments, listed in Table 3, indicate that the effect of recycle has a deleterious effect upon the values obtained. Typical figures were 62 ppm in the raffinate with recycle, 11 ppm without, and 63 ppm in the advance electrolyte with recycle and 15 ppm without. No satisfactory explanation for these results can be forwarded at this time.

The relationship between organic entrainment and operating organic/aqueous ratio under aqueous continuous mixer conditions is completely different from that under organic continuous conditions as shown in Graph 5. This is because, in this case, the organic entrainment primarily originates in the mixer box. The shape of the observed curve can be explained as follows.

At the lowest organic/aqueous ratio studied, there is an excess of aqueous over that required to form the 'preferred' organic/aqueous ratio of 2:1 in the dispersion bed. This 'excess' aqueous phase therefore 'flashes-off' on leaving the mixer and, on entering the settler, immediately joins the bulk continuous phase, carrying with it many of the smaller dispersed organic droplets. As the operating organic/aqueous ratio increases, the volume of 'excess' aqueous phase decreases and the reduced flow of this phase through the dispersion bed results in a reduction in the amount of entrained organic droplets.

This sequence continues with increasing organic/aqueous ratio until the organic/aqueous ratio equals the 'preferred' ratio of 2:1 in the dispersion bed. At this point there is no 'excess' aqueous phase present and the only flow of aqueous phase out of the dispersion bed is that draining from the result of coalescence.

At operating organic/aqueous ratios greater than the 'preferred' ratio, it could be deduced that there will be little change in the amount of organic entrainment, if it is assumed that the entrainment is a function of the amount of aqueous phase passing from the bed. However, due to the fact that stable operation with organic/aqueous ratio in excess of 3:1 was not possible under aqueous continuous conditions, insufficient results are available to enable this proposition to be confirmed.

AQUEOUS ENTRAINMENT IN THE ORGANIC PHASE

The values of aqueous entrainment under organic continuous mixer conditions for the single and multi-stage laboratory circuits show the opposite trends to those described for organic entrainment under aqueous continuous operation in the preceding section. The shape of the curves obtained in these cases and shown in Graphs 6 and 7 can be explained by an analogous mechanism to that proposed in the preceding section.

No such clear analogy is evident for the results obtained under aqueous continuous mixer conditions as illustrated in Graph 6 or the single stage laboratory study. The mechanism previously proposed would predict a low and constant entrainment in the operating organic/aqueous range 2:1 to 1:4 with perhaps a slight increase on increasing the operating organic/aqueous ratio above 2:1. However, the results show an extremely high entrainment value at an operating ratio of 3:1 and an increasing value on decreasing the operating O/A from 2:1 to 1:4.

Additional factors present in this system which could be affecting the results obtained were the relative instability of the system at high organic/aqueous ratios and the shallow dispersion bed depths which were invariably obtained. Thus the former could have an effect on the results at the organic/aqueous ratio of 3:1 as a result of the tendency of the dispersion to revert to organic continuity while the shallow dispersion beds could be sufficiently disturbed by the increasing flow of 'excess' aqueous phase at the low organic/aqueous ratios to give the results noted. These possibilities were not investigated further.

EXTRACTION EFFICIENCY

For any mixer-settler system it can be shown that at constant mixer retention time, recycle of any phase will increase the efficiency of the stage above that obtained without recycle. Thus the curve of efficiency against recycle rate should show a minimum under conditions of no recycle.

The curves in Graph 8 indicate that the improvement in efficiency with recycle is most marked when recycle results in an increase in the proportion of dispersed phase present in the mixer. Thus, under organic continuous mixer conditions, there is an increase in efficiency on decreasing the organic/aqueous ratio from 1:1 to 1:4. Under aqueous continuous mixer conditions, the largest increase in efficiency is shown when the proportion of organic dispersed is increased by increasing the operating organic/aqueous ratio from 1:1 to 3:1.

The very small increase in efficiency when the increased recycle rate results in a decrease in the proportion of dispersed phase present in the mixer is contrary to expectations and can only be explained by proposing an additional mechanism.

The efficiency of a mixer system is a function of many variables amongst which are particle size distribution, mixing pattern, power input, residence time distribution and temperature. The degree of coalescence/redispersion taking place affects the particle size distribution and is known to have a large effect on the mass transfer efficiency of a system (6).

For a constant total flow of solution into the mixer, recycling the continuous phase will reduce the proportion of dispersed phase present. This reduction will decrease the chance of interdroplet collision and thus decrease the coalescence/redispersion rate. A fall in mass transfer and extraction efficiency will therefore result.

On recycling the phase which is dispersed the frequency of interdrop collision will increase and the extraction efficiency therefore increases. Thus it can be proposed that there are two major mechanisms affecting the efficiency of any mixer-settler system. Recycle, which increases the efficiency independently of which phase is recycled and the amount of coalescence/redispersion occurring, which can either decrease or increase depending upon the phase recycled and the operating continuity. For organic continuous mixer conditions, recycling the organic phase dilutes the dispersion, decreasing the amount of coalescence/redispersion and mass transfer and thus opposing the expected increase in mass transfer due to recycle. Alternatively recycling the aqueous phase concentrates the dispersion, increasing the amount of coalescence/redispersion and mass transfer in support of the expected increase due to recycle.

Under organic continuous mixer conditions, therefore, the resulting curve should show a rapid increase in efficiency on decreasing the operating organic/aqueous ratio from 1:1 to 1:4, and a change in efficiency on increasing the operating organic/aqueous ratio from 1:1 to 4:1 which is a balance between the opposing effects detailed above. The experimental results suggest that for the system under study, the two effects are equal in magnitude, as the efficiency varies very little with change in operating organic/aqueous ratio over the range 1:1 to 4:1. The curve obtained under aqueous continuous operation can be explained in an analogous manner.

The percentage strip and efficiency results obtained from the single stage strip experiments, and illustrated in Graph 9, are in agreement with the mechanism proposed above. Thus, the strip experiments were carried out with aqueous recycle only, so that under the conditions of organic continuity employed, an increase in percentage strip and efficiency would be expected. Unlike those from extraction, the experimental curves obtained under stripping conditions do not show a minimum and this is due to the fact that organic recycle was not employed to increase the operating organic/aqueous ratio above the 3:1 overall organic/aqueous ratio used as the standard condition.

The efficiency results from the laboratory scale multi-stage circuit also confirm the effect of recycle as illustrated in Graph 10. Thus, over the whole range of mixer retention times studied, operation of the extraction section under conditions of recycle to an operating organic/aqueous ratio of 1:1 gave single stage efficiencies averaging approximately

12% more than the efficiencies obtained without recycle under comparable mixer retention times at an operating organic/aqueous ratio of 11.25:1. The distinction between efficiencies obtained under recycle and non-recycle conditions in the strip section was not so clearly defined due to the smaller amount of recycle employed and the more rapid mass transfer rate of the strip system compared to that in extraction. However at the lowest mixer retention time used, the difference is still significant.

CONCLUSIONS

The effect of changes in the operating organic/aqueous ratio on the performance of mixer-settler systems at laboratory scale have been shown to be very marked. At commercial plant scale, disregard of the effect of this parameter could lead to serious operational problems and the operating organic/aqueous ratio is thus to be considered as a major design parameter.

ACKNOWLEDGEMENTS

The authors wish to thank their colleagues in the R & D Division of Davy Powergas Limited for their assistance in the preparation of this paper and to the Directors of Davy Powergas Limited for their permission to publish.

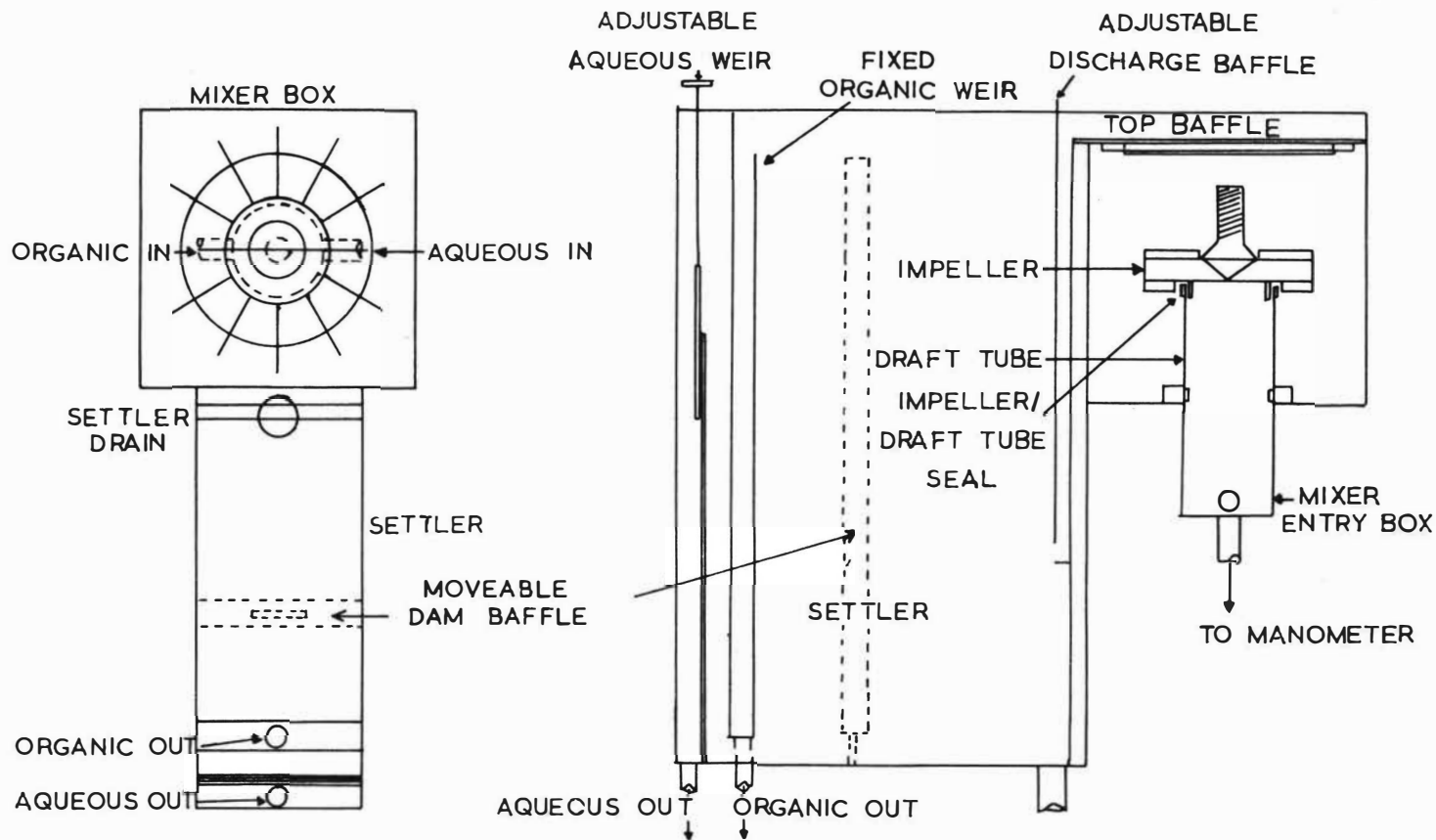
REFERENCES

1. Power K L. Operation of first commercial copper liquid ion exchange plant. Proc. of the Extractive Metallurgy Div. Sym. Denver, Colorado, Feb 15, 1970.
2. J B Lott, G C I Warwick & J B Scuffham. Soc. of Min. Eng. AIME. Trans Vol 252, March 1972. 27.
3. Treybal RE. Liquid Extraction 2nd Edition, McGraw-Hill Company, New York, 1963.
4. Jeffreys G V, Davies G A and Pitt K, AIChE., Journal Vol 16, No 5. 1970. 823.
5. Davies GA, Jeffreys GV and Ali FA. Can J Chem Eng Vol 48, 1970. 328.
6. Hanson C. Recent advances in liquid-liquid extraction. Pergamon Oxford 1971.

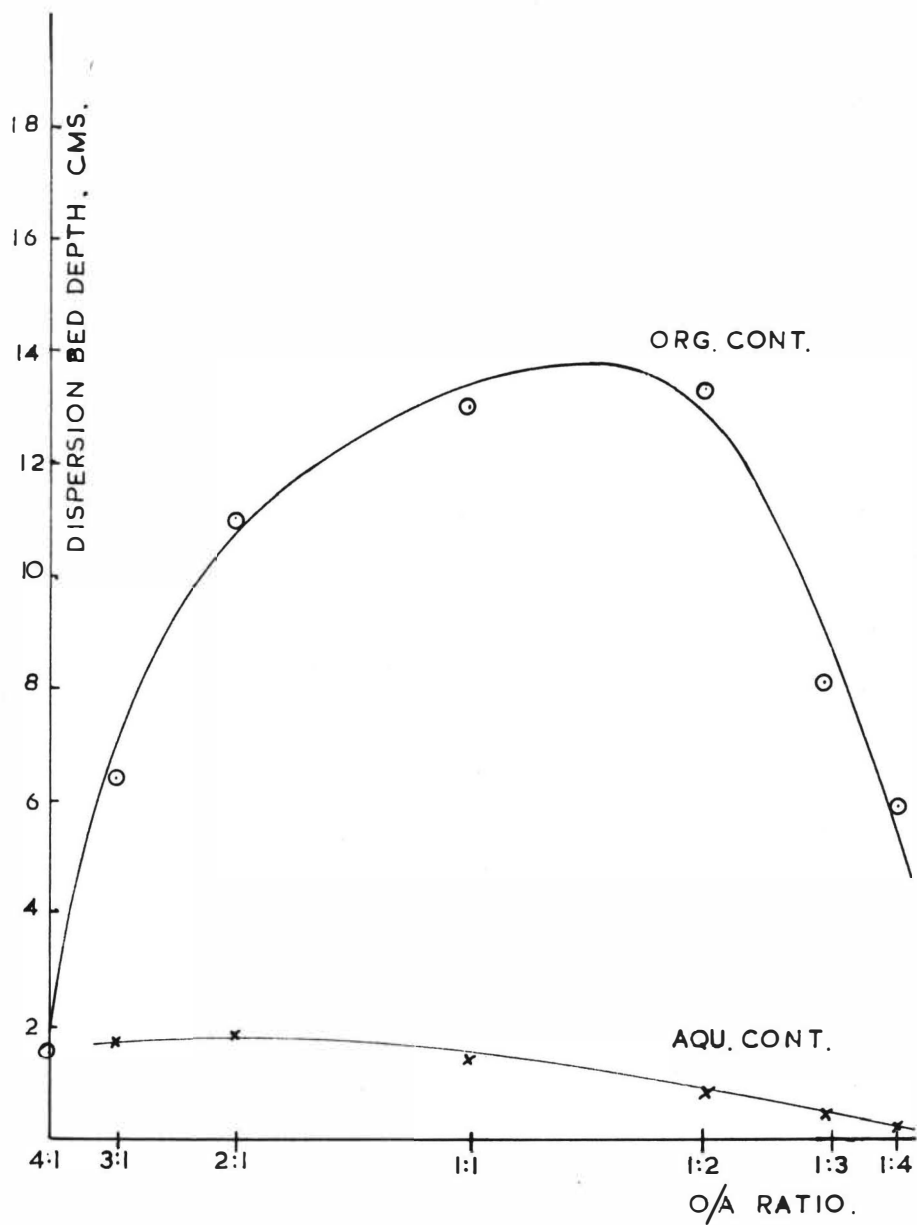
FIG. 1

LABORATORY MIXER SETTLER

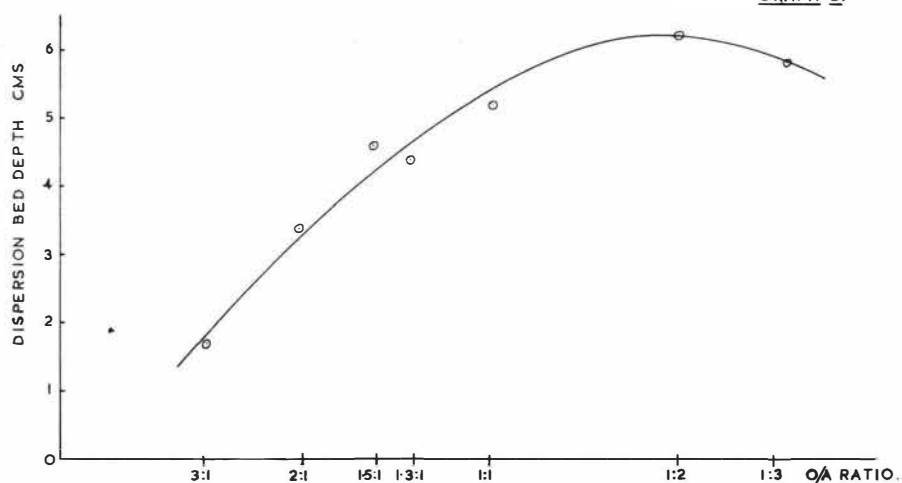
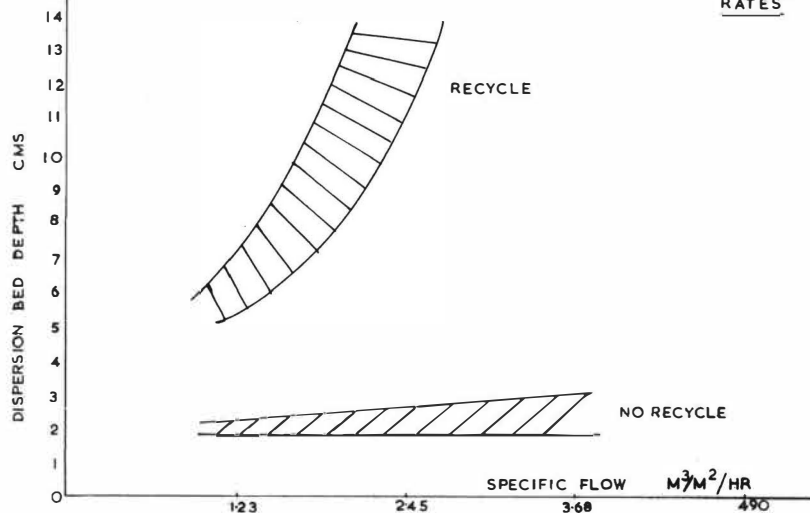
101

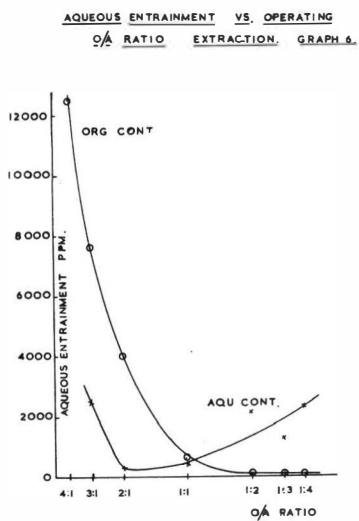
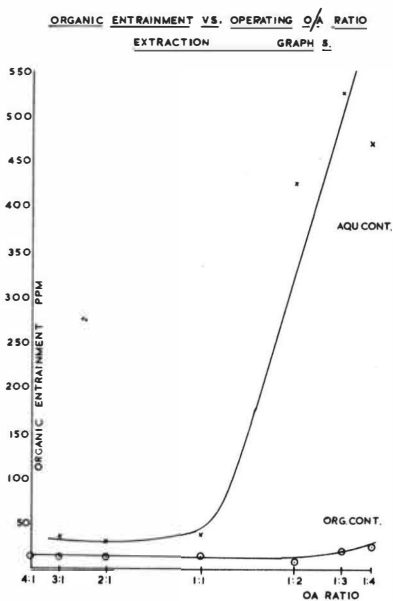
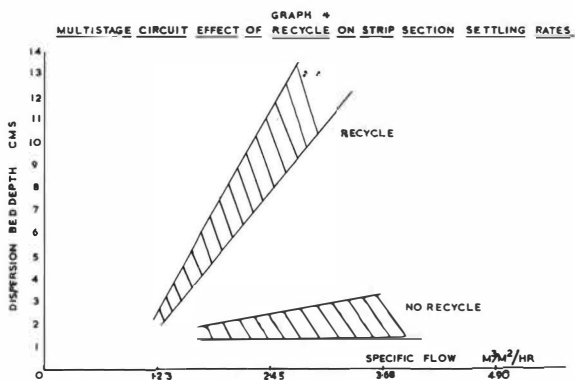


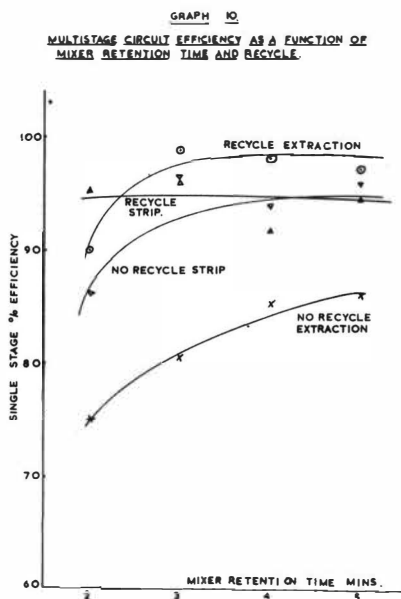
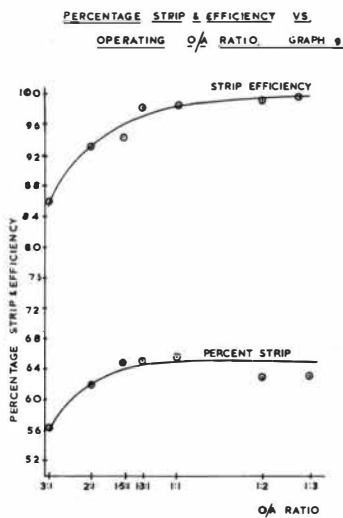
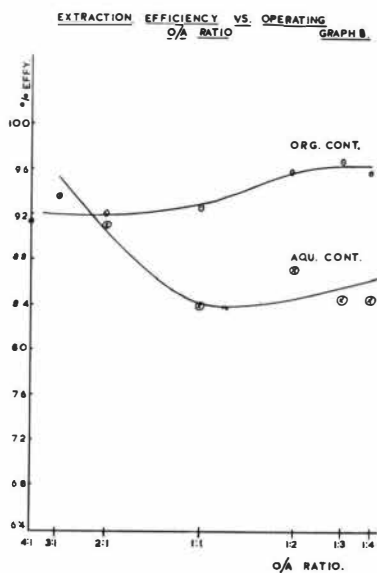
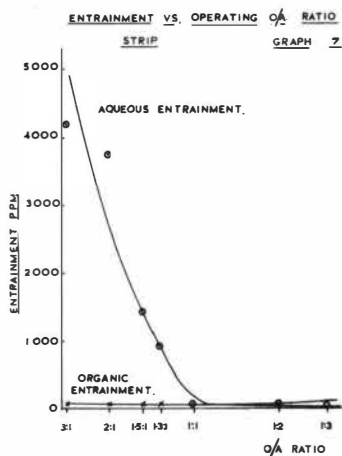
DISPERSION BED DEPTH VS. OPERATING O/A RATIO
EXTRACTION. GRAPH I.



GRAPH 2.

GRAPH 3
MULTISTAGE CIRCUIT EFFECT OF RECYCLE ON EXTRACTION SECTION SETTLING RATES





ASPECTS OF COPPER EXTRACTION IN MIXER-SETTLERS

M.J. Slater

G.M. Ritcey*

and

R.F. Pilgrim*

Abstract

Techniques are described for investigating the performance of continuous flow mixer-settlers using batch data on mass transfer kinetics and on phase separation after mixing of aqueous and solvent phases in a tank. Illustrations of the techniques proposed are drawn from the field of solvent extraction of copper from sulphuric acid solutions using various commercial extractants and diluents on a non-comparative basis.

A statistically designed set of experiments can be used to develop an empirical equation to predict the degree of copper extraction in a batch stirred tank test as a function of stirring speed, stirring time and phase ratio. From this data the stage efficiency in a flow system may be estimated. Measurements of sedimentation and coalescence rates can also be obtained from batch tests to aid settler design and to understand the relationship between mixer and settler operating conditions.

Schools of Chemical Engineering
University of Bradford
Bradford
Yorkshire
England

*Extraction Metallurgy Div.
Mines Branch,
Dept. of Energy, Mines and Resources
300, Le Breton Street,
Ottawa, Ontario, Canada

Introduction

The design of mixer-settlers has been improved gradually in recent years in response to applications of solvent extraction in metals recovery¹ and phosphoric acid production² for example. Now that very large scale mixer-settlers are being built for copper recovery it is apparent that the design of both mixer and settler must be critically examined to minimize overall costs, and particularly the cost of the initial solvent inventory, since the extractants for copper are relatively expensive.

This paper describes experimental techniques based on batch tests for exploring the behaviour of both mixer and settler using two commercial copper extractants, to obtain equipment design data with a minimum of experimental work. It must be strongly emphasized that each combination of extractant and diluent is appropriate for a particular type of leach solution and operating temperature, and comparison cannot be made fairly on the basis of the work reported here. The paper aims to illustrate general principles using examples of copper extraction under a variety of conditions.

Operating Variables

For the mixer the operating variables considered are the impeller speed, stirring time, volume fraction of the phase dispersed, and the type of dispersion (organic continuous or aqueous continuous phase). The key parameter is the average drop size. The drop size distribution is also important but this is also dependent on impeller design which was not varied.

The rate of separation of the dispersion in a settler is expected to depend primarily on the drop sizes in the dispersion leaving the mixer, the volume fraction of the dispersed phase in the feed dispersion and the nature of the dispersion (organic or aqueous phase dispersed). If mass transfer in the mixer is incomplete, continuing mass transfer in the settler will also affect the separation rate by enhancing or inhibiting droplet coalescence³.

Physical Properties

The droplet size developed in the mixer and the drop coalescence rates depend partly on phase densities, viscosities and interfacial tension. The latter two were measured using the capillary tube method and a Du Noüy ring tensiometer respectively. The values are given in Tables 1 and 2 for the materials used.

The diluents and the General Mills reagents were used in the condition received but the Ashland Chemicals Kellex 100 was first dissolved with the modifier in the diluent, then was loaded with copper and stripped with sulphuric acid before use.

Mass Transfer Rate Experiments

A plexiglass rectangular mixing vessel was constructed to the measurements already used in a mixer-settler for continuous flow studies. The vessel was 7.6 cm square and 12.0 cm deep with a liquid level of 6.2 cm (350 ml). A three-bladed marine impeller, 5 cm in diameter, 45° blade angle, with upthrust was positioned centrally and 3.0 cm above the base. A simulated draught tube 2.5 cm high and 1.6 cm outside diameter was glued to the base in the centre. Tests comprised adding a measured volume of an aqueous phase to the tank, switching on the stirrer motor, previously set to the required speed, and adding a known volume of organic phase quickly. After stirring for a measured time the stirrer was switched off and the phases were allowed to disengage. When a relatively clear interface was observed the time elapsed after mixing was noted and samples of both phases were removed, filtered and analysed for copper and pH. The time taken (after ceasing to stir) for discontinuities in the drop layer at the interface to appear was identified as the primary break time. The work was carried out at an ambient temperature of 20°C .

To characterize the performance of a solution of 20% Kellex 100 plus 10% isodecanol in Solvesso 150 diluent with particular synthetic aqueous acid copper sulphate solutions a set of 140 tests were carried out for a range of

aqueous/organic (A/O) volume ratios, stirring speed and stirring time. The pH of each aqueous feed was 1.0 but the copper content was adjusted assuming that the maximum loading of the organic phase, about 11.6 g Cu/l, could ideally be achieved with sufficient contact time. This would be the basis for deciding flow ratios in a flow system; in practical cases, however, a recycle of one phase may be used to ensure that a particular phase is the continuous phase, or to obtain a flow ratio through the mixer near unity to maximise interfacial area for mass transfer. The laboratory batch tests are necessarily limited in application and can only serve to guide selection of operating conditions. This limitation justifies the sampling of phases after phase disengagement (during which period some further mass transfer occurs) since sampling immediately after mixing is difficult and rapid phase separation is required using sophisticated equipment. Knowledge of the extent of mass transfer achieved in mixing and settling stages combined is required in practice but analysis in terms of mass transfer coefficients is obscured if there is substantial mass transfer in the settling period compared to the mixing period.

The results obtained are given in Table 3. For the first 70 tests the aqueous phase was continuous and in the next 70 tests the organic phase was continuous (indicated by the direction of drop sedimentation).

The data were analysed statistically to indicate the importance of the variables on the degree of extraction achieved, defined as the fractional amount of copper removed from the aqueous feed into the organic phase. Variations in kinetics and equilibrium loading of the organic phase affect the degree of extraction. The equations developed are empirical; various power series in each variable with interactions between variables were examined. Early assessment, coupled with graphical relationships, gave rise to more complex logarithmic terms. Standard deviations of less than 5% on the predicted parameter were sought with high degree of correlation.

The equations developed for the 140 tests were:

For the aqueous phase continuous,

$$C_{s\theta} = -25.8 - 3.63 \log_{10} r + 9.20 \log_{10} (\theta + 20) + 6.09 \log_{10} (N - 165) \quad (1)$$

For the organic phase continuous,

$$C_{s\theta} = -7.11 + 2.94 \log_{10} r + 3.36 \log_{10} (\theta + 20) + 3.83 \log_{10} (N - 165) \quad (2)$$

The values of $C_{s\theta}$ predicted may be used in the equations shown below to calculate the degree of copper extraction from a given aqueous feed and the degree of approach to equilibrium.

The extensive data for extraction with Kelex 100 could be analysed further in terms of a mass transfer coefficient. It may be shown⁴ that the approach to equilibrium in a stirred tank test as described above is given by

$$E_b = \frac{C_{s\theta} - C_{so}}{C_{se} - C_{so}} = \frac{C_{ao} - C_{a\theta}}{C_{ao} - C_{ae}} = 1 - \exp \left[- \frac{K_s a V \left(1 + \frac{mv_a}{v_s} \right) \theta}{v_s} \right] \quad (3)$$

where the overall mass transfer rate coefficient based on the solvent phase, for example only, is defined by

$$V \frac{dC_{s\theta}}{d\theta} = K_s a V (C_s^* - C_{s\theta}) \quad (4)$$

and C_{se} and C_s^* are related, in the case of a straight equilibrium line of slope m , by

$$\frac{C_s^* - C_{se}}{C_{se} - C_{s0}} = \frac{mv_s}{v_a} \quad (5)$$

where the equilibrium line is

$$C_s^* = mC_a \quad (6)$$

In some cases slight variation in the slope, m , is compensated by variations in the mass transfer coefficient, K_s , and the specific interfacial area, a , and for a given phase ratio we may use

$$E_b \approx 1 - \exp [-k\theta] \quad (7)$$

to evaluate a rate coefficient, k , which is approximately constant. By analysing a multi-stage flow system it may also be shown⁴ that the Murphree stage efficiency may be written

$$E_{ms} = E_f / \left[1 + (1 - E_f) \frac{mF_s}{F_a} \right] \quad (8)$$

where $E_f = k\theta / (1 + k\theta) \quad (9)$

and where k is the same as in the batch test for the conditions used and θ is now the contact time in the mixer. The number of real stages required in a flow system may now be estimated using a McCabe-Thiele diagram.

Typical plots of the batch rate data are given in Figure 1 and the derived rate coefficients are shown in Figure 2 as a function of stirring speed. Although the coefficients are only approximate the strong effect of

stirring speed is noticeable. The data show little effect of the aqueous/organic solvent volume phase ratio, but dispersion of the solvent gives poorer kinetics than dispersion of the aqueous phase. This suggests that the mass transfer rate is diffusion controlled not chemically controlled. Some values of E_f are given in Table 4.

The effort required to determine the map of degree of copper extraction for the ranges of variables considered is substantial and a statistically designed set of 18 tests was proposed to reduce the cost of such exercises. These tests were carried out for an aqueous continuous phase condition and the results are given in Table 5.

The regression analysis gives the following equations. For the degree of extraction, defined by

$$\phi = (C_{ao} - C_{a\theta})/C_{ao} \quad (10)$$

the equation is

$$\begin{aligned} \phi = & -236.0 - 2.84 \log_{10} r + 83.2 \log_{10} (\theta + 20) \\ & + 49.3 \log_{10} (N - 165) \end{aligned} \quad (11)$$

For the pH of the aqueous product,

$$\begin{aligned} \text{pH}_f = & 1.344 + 0.669 \log_{10} r - 0.232 \log_{10} (\theta + 20) \\ & - 0.212 \log_{10} (N - 165) \end{aligned} \quad (12)$$

and for the primary break time

$$\begin{aligned} \tau = & -35.38 - 32.6 \log_{10} r + 24.8 \log_{10} (\theta + 20) \\ & + 11.5 \log_{10} (N - 165) \end{aligned} \quad (13)$$

The predicted responses are shown in Table 5. For the degree of extraction the standard deviation is $\pm 3.0\%$ and the coefficient of multiple determination is 0.986; for the final pH, the standard deviation is ± 0.046 and the coefficient is 0.844; for the primary break time the figures are ± 5.0 sec and 0.864.

A similar set of 18 tests was carried out using a 20% by volume solution of LIX64N in Escaid 100 diluent. The aqueous copper feed solution pH was 1.9 and the copper content was varied assuming that a solvent loading of about 3.7 g Cu/l could ideally be reached. The Kelex and LIX64N extractants are not being compared here because of the different nature of the aqueous feeds. The experimental data are given in Table 6 and equations similar to (11), (12) and (13) have been developed. (Appendix)

The degree of extraction, ϕ , may be related to the batch efficiency, E_b , by

$$\phi C_{ao} / (C_{ao} - C_{ae}) = E_b \quad (14)$$

The equilibrium relationship between C_a and C_s is required to establish C_{ae} for given conditions. The Murphree stage efficiency may then be calculated for those conditions and applied to a McCabe-Thiele construction to determine how many real stages are required in a flow system.

Discussion of Mixing Tests

Extensive test work can be avoided by using a limited set of statistically designed experiments to determine the effect on kinetics of mass transfer of major operating variables. The data obtained can be used to estimate Murphree stage efficiencies in flow systems. Optimum operating conditions may be established for consequent trials using laboratory-scale continuous flow mixer-settlers.

The low significance of the phase ratio in determining the degree of extraction is principally due to favourable equilibrium for extraction (a high value of m) as can be seen from equation (3).

The rate coefficient calculated from a batch test appears to decrease as time progresses. This is in part due to equilibrium line curvature and possibly due to reductions in the mass transfer coefficient, K_g , as the driving force decreases or as interdroplet coalescence rate decreases.

The use of an equation to represent the mixer behaviour is important in optimizing a mixer-settler if the consequent behaviour of the settler can also be mathematically modelled.

The phase separation process

Two aspects of the separation process require consideration, sedimentation and interface coalescence. Droplets in a dispersion fed into a settling vessel will move under the influence of buoyancy and gravitational forces towards an interface where coalescence with the homophase will occur. The continuous phase associated with the feed of dispersion must be released at some stage in this sedimenting process. If the droplets assume a denser packing arrangement during travel to the interface a counter-flow of displaced continuous phase must arise, and when droplets coalesce with the homophase the associated continuous phase, dependent on the packing of drops, must be released to flow counter to droplets arriving at the interface. The ratio of droplet flow and the net continuous phase flow must equal the volume ratio in the feed dispersion.

The flow patterns in settlers are complex and may disturb the sedimentation process in an adverse manner. Sedimentation under quiescent non-flow conditions, as in a batch tank after stirring, may however represent ideal conditions against which settler performance may be compared. The rates of sedimentation and coalescence are important in the settler and both of

these may be measured under non-flow conditions to give guidance in settler design.

After mixing two phases in the mixer described above, under specified conditions of phase ratio, stirring speed and time of stirring, the stirrer motor is switched off. The dispersion now begins to disengage by the two independent processes of drop sedimentation and droplet coalescence with the interface. Photographs were taken of the two demarcation lines of the sedimentation front and the coalescence front moving towards each other at different rates. Photographs were taken every two seconds using an automatic camera. The position of each front was measured as a function of time from the photographs; typical results are given in Fig. 3. The slope of the lines represents a velocity.

Existing theory of sedimentation of particles can be used to relate the measured sedimentation velocity to average droplet size and fractional volume hold-up of dispersed phase. The initial sedimentation velocity is assumed to be taking place at a hold-up the same as that of the feed dispersion. In a dense dispersion the droplets tend to move with the same velocity as that of the average size of drop and if the average drop size and the hold-up remain constant the sedimentation velocity remains constant. If droplets coalesce with each other during sedimentation the sedimentation velocity may increase; if droplets have to queue at the interface before coalescence with the interface occurs a packed condition of drops may develop and droplets may coalesce with each other. Under packed conditions sedimentation theory does not apply but a counter-flow of continuous phase still occurs.

Little is known about the coalescence process at the interface and a means of measuring the rate with real systems is required. A velocity of coalescence may be obtained from the batch tests but it must be recognised that the rate is a function of the depth of dispersion above or below the

interface; laboratory coalescence velocity data must therefore not be used for calculating the throughput of a larger scale mixer-settler but can give guidance on the depth of settler required.

Experimental Results

Tests were carried out using various extractants at different concentrations to demonstrate in principle the development of a settler design. An aqueous feed of copper sulphate in sulphuric acid was used, of 5 kg Cu/m³ and 19% H₂SO₄. The high acidity allows no copper transfer. The solvents comprised LIX64N, LIX70, LIX71 and LIX73 (General Mills Inc.) all dissolved in the Exxon diluent Escaid 100.

Solvents and the aqueous feed were mixed together at various phase ratios, stirring speeds of 800 and 1200 rpm and stirring times of 30, 60 and 120 seconds. Only the condition of having an organic continuous phase was studied and the phase ratio was limited to values not far removed from unity. The initial sedimentation velocities were measured with an uncertainty of about $\pm 10\%$ and an average coalescence velocity was measured over the whole coalescence period, with an accuracy of about $\pm 10\%$ also.

Discussion of Results

(a) Stirring Time and Stirring Speed

Some influence of stirring time and speed on the drop size developed is possible but the effects are not clear from the data on sedimentation velocities in Tables 6 and 7.

(b) The effect of phase ratio or dispersed phase hold-up

In the range of hold-up studied, from 0.41 to 0.50, the coalescence rate is insensitive to hold-up in the feed dispersion (Fig. 4). This is believed due to the denser packing achieved at the coalescence front which is little dependent on initial hold-up.

The hold-up of dispersed phase has a marked effect on the sedimentation

rate of the droplets, as shown by the experimental points on Figs. 5 and 6. This aspect of the work is amenable to theoretical analysis based on sedimentation theory.

A relative velocity or slip velocity, V_{SLIP} , may be defined for two-phase counter-flow systems as

$$V_{SLIP} = V_s / (1 - h) + U_s / h \quad (15)$$

where V_s and U_s are superficial velocities of the continuous and dispersed phases respectively and h is the volume fraction hold-up of dispersed phase. It has been found that the slip velocity can be experimentally determined as a function of hold-up in the form⁵

$$V_{SLIP} = V_T (1 - h)^{n - 1} \quad (16)$$

for monosize particles where V_T is the terminal velocity of drops and the exponent is a function of Reynolds number at the terminal velocity. By applying the equation to each drop size for a given size distribution it is possible to relate velocities, hold-up and average drop size for non-coalescing systems⁶. Using this method for a batch sedimentation process with the sedimentation front as a moving frame of reference we may write

$$V_{bs} / (1 - h) = V_{SLIP} \quad (17)$$

where V_{bs} is the measured velocity of the sedimentation front. For a given drop size distribution and specified physical properties (density, viscosity, interfacial tension) the average terminal velocity may be calculated from existing correlations. For a given hold-up the sedimentation velocity may

be predicted. Alternatively, if the sedimentation velocity is measured the average drop size may be estimated. Earlier work⁷ has established that close agreement on measured and calculated drop sizes can be achieved. For the systems used in this work the computed relationship of drop size, sedimentation velocity and hold-up is presented on Figs. 5, 6, 7 and 8. Very little difference in calculated sedimentation velocities is apparent between the systems used since the viscosities and densities are so similar, apart from the Kelex system (Fig. 8) which is more viscous but has a higher loading capacity.

It is seen from Figs. 5 and 7 that the measured sedimentation rates in batch tests suggest that for 20% LIX64N stirred at 800 rpm for up to 120 seconds, drop sizes of about 0.06 cm to 0.085 cm exist immediately after mixing; the possibility of some interdroplet coalescence immediately after stirring cannot be ruled out and it is not known how closely these values approximate the drop sizes during mixing. For the LIX70, 71 and 73 at 20% concentration in Escald 100 and the same stirring conditions an average drop size of about 0.02 cm is achieved (Fig. 6). This would suggest that interdroplet coalescence with LIX64N is more frequent than with LIX70, 71 or 73 under these highly acidic conditions since the densities and viscosities are similar.

The effect of recycling continuous phase to lower the hold-up of dispersed phase will enhance settler throughput markedly if sedimentation controls the separation rate.

(c) The effect of extractant concentration

The coalescence rates of LIX64N, 70, 71 and 73 are shown on Fig. 9 as a function of extractant concentration at constant dispersed phase hold-up. Knowledge of the densities, viscosities, interfacial tensions and drop sizes is insufficient to explain the relationship of the measured velocities

to each other. Other factors must affect the coalescence rate.

The sedimentation velocities are shown on Fig. 10. Whereas the LIX70, 71 and 73 systems are little affected, the LIX64N shows remarkable increase in sedimentation velocity as the extractant is diluted. The average drop size is assumed to be increasing as dilution of LIX64N proceeds whereas little change occurs in the other systems. This again points to a rapid inter-droplet coalescence rate for LIX64N but not for LIX70, 71 and 73.

The copper carrying capacity of the solvent decreases as the extractant is diluted if the phase ratio is held constant. If the phase ratio is changed as the extractant is diluted the copper carrying capacity can be made approximately constant. For these circumstances (Fig. 11) the effects described above still appear. As the extractant is diluted higher sedimentation and coalescence rates are experienced. However, as the extractant is diluted the size of the mixer must increase to cope with the higher flow rate of solvent and the specific interfacial area in the mixer decreases. The settler area is proportional to the aqueous flow rate divided by the controlling velocity, (sedimentation velocity or coalescence velocity), if the aqueous phase is dispersed. Significant reductions in settler area may be achieved if sedimentation controls the separation rate, by operating with dilute extractants.

(d) Primary break time

In every experiment a delay occurred before coalescence began; this delay is the period of droplet packing and droplet growth by coalescence. The coalescence with an interface then proceeds virtually at a constant velocity until all drops have coalesced. The primary break time is usually taken as the time required for clear patches to appear in the interface. This is not a reliable measurement and has no fundamental meaning because

generally it comprises the packing time and interface coalescence time, two independent processes. However, as shown on Fig. 12, the primary break time, calculated as the sum of the measured packing time and the time of coalescence assuming a constant velocity until complete separation is ideally achieved, is related to the coalescence velocity. It is this link which allows systems to be compared on a basis of primary break time, but measurement of the coalescence velocity is much to be preferred.

During the tests on mass transfer rates with Kelrex and LIX64N primary break times were estimated. The conclusions to be drawn are that the break time is generally independent of stirrer speed but decreased as hold-up of dispersed phase decreased for hold-up less than 0.33 and the organic phase dispersed. As the stirring time increased the primary break time increased.

The data were correlated statistically.

Continuous Flow Systems

The slip velocity concept may be applied to sedimentation of the dispersion entering a settler at a known hold-up of dispersed phase (calculated from the phase ratio in the mixer). We may write

$$V_s/(1-h) + U_s/h = V_{bs}/(1-h) \quad (18)$$

together with the condition imposed by the flow ratio that

$$V_s/U_s = (1-h)/h \quad (19)$$

assuming that U_s refers to the dispersed phase. Therefore

$$V_s = V_{bs}/2 \quad (20)$$

$$\text{and} \quad U_s = V_{bs} h/2(1 - h) \quad (21)$$

These values of V_s and U_s in a flow system can be plotted on Figs. 4, 5 and 6 using the batch sedimentation data. The value of V_s represents the maximum possible continuous phase vertical superficial velocity in the settler and U_s represents the dispersed phase superficial coalescence velocity required if the maximum allowable sedimentation velocity is to be reached. The coalescence velocity is known to be a function of dispersion band depth in a flow system so the band must be allowed to build up to a level to satisfy the maximum throughput criterion. If this is not possible without approaching flooding conditions lower throughputs must be accepted.

By comparing measured coalescence velocities in a small batch tank with required velocities in a flow system an idea of the depth of dispersion band required on a larger scale may be obtained.

Summary

Procedures for investigating mixer and settler performance using a batch stirred tank have been described with the objective of reducing experimental work to a minimum in the investigation of a new process for which mixer-settlers are considered the appropriate apparatus to use on a large scale.

Using examples of copper extraction, attention is drawn to a procedure for using data on kinetics of mass transfer to estimate Murphree stage efficiencies in continuous counter-current mixer-settlers so that the number of real contacting stages can be calculated for a wide range of operating conditions. Further work using a continuous mixer-settler system may then be minimized and used mainly for determining solvent losses and degradation for example.

A new procedure is proposed for estimating maximum throughput in a

settler. The effects on the throughput of the principal variables of stirring speed, contact time, dispersed phase hold-up and extractant concentration are demonstrated for a particular system.

In general it is considered that batch tests in stirred tanks can provide much of the data required to design a large scale mixer-settler. The techniques described also provide a foundation for further work on the optimization of a series of mixers and settlers.

Acknowledgements

Miss D. McDonald and K.T. Price carried out the mass transfer tests at the Mines Branch, Ottawa, and the numerous chemical analyses were carried out by the Mines Branch Analytical Section. The work on coalescence was carried out at the University of Bradford.

The authors gratefully acknowledge the supply of materials from Ashland Chemicals Co., (Kellex 100 and isodecanol), Exxon (Escaid 100), General Mills Inc. (LIX64N, 65N, 70, 71, 73), I.C.I. Ltd. (isodecanol), Power-Gas Ltd. (LIX reagents), and Shell Chemicals Ltd. (Solvesso 150).

References

1. Lott, J., Warwick, G., Scuffham, J., paper 71851, AIME/SME meeting, New York, March 1971.
2. Barnea, E., Mizrahi, J., The Chem. Eng. J., 1973, 5, 171.
3. Jeffreys, G., Davies, G., Chapter 14 in "Recent Advances in Liquid-Liquid extraction", ed. C. Hanson, pub. Pergamon, 1971.
4. Treybal, R., Liquid Extraction, pub. McGraw-Hill, 1963.
5. Richardson, J., Zaki, W., Tr. Inst. Chem. Eng., 1954, 32, 35.
6. Slater, M., Mines Branch Report EMA 72-15, Dept. of Energy, Mines and Resources, Ottawa, Canada.
7. Current work.

Nomenclature

C_a	Copper concentration in aqueous phase , gm Cu/l
C_s	Copper concentration in solvent phase , gm Cu/l
E_b	Batch efficiency
E_f	Flow system efficiency
E_{MS}	Murphree stage efficiency based on solvent phase
F_a	Aqueous flow rate
F_s	Solvent flow rate
h	Dispersed phase volume fraction hold-up
K_{sa}	Overall mass transfer coefficient times specific interfacial area
k	Rate coefficient
m	Equilibrium line slope
n	Exponent
N	Stirrer speed, rpm
r	Volume phase ratio (aqueous/solvent)
U_c	Superficial coalescence velocity, cm/s
U_s	Superficial dispersed phase velocity, cm/s
V	Total volume of phases in mixer
V_{SLIP}	Slip velocity, cm/s
V_s	Superficial continuous phase velocity, cm/s
V_{bs}	Superficial measured sedimentation velocity, cm/s
V_T	Terminal velocity, cm/s
v_a	Volume of aqueous phase in mixer
v_s	Volume of solvent in mixer
ϕ	Degree of copper extraction
τ	Primary break time, s
θ	Contact time in mixer, s

Subscripts

- o Initial value
- θ Value at time θ
- e Equilibrium value in batch test

Appendix

Equations developed from a set of 18 tests on 20% LIX64N in Escaid 100 with an aqueous continuous phase, feed pH 1.9.

The degree of extraction is given by

$$\begin{aligned} \phi &= -108.06 - 16.2 \log_{10} r + 29.0 \log_{10} \theta \\ &\quad + 43.7 \log_{10} (N - 165) \end{aligned}$$

The loading of the organic phase is

$$\begin{aligned} C_{a\theta} &= -3.98 - 0.522 \log_{10} r + 1.06 \log_{10} \theta \\ &\quad + 1.60 \log_{10} (N - 165) \end{aligned}$$

The final pH is

$$\begin{aligned} \text{pH}_f &= 2.094 + 0.652 \log_{10} r - 0.104 \log_{10} \theta \\ &\quad - 0.261 \log_{10} (N - 165) \end{aligned}$$

The primary break time is

$$\begin{aligned} \tau &= -13.92 - 79.3 \log_{10} r - 3.68 \log_{10} \theta \\ &\quad + 40.5 \log_{10} (N - 165) \end{aligned}$$

TABLE 1

VISCOSITIES AND DENSITIES AT 20%

Solution	Density g/ml	Viscosity cp
Acid CuSO ₄ ^{*5}	1.127	1.462
Escaid 100	0.792	1.440
LIX 64N	0.899	-
20% Kelex 100/10% Isodecanol/ Solvesso 150	0.941	4.10
10% LIX64N/Escaid 100	0.802	1.695
14% "	0.804	1.780
16% "	0.807	1.792
18% "	0.810	1.848
20% "	0.812	1.916
25% "	0.817	2.100
20% LIX65N "	0.808	2.055
10% LIX70 "	0.802	1.680
15% "	0.809	1.903
20% "	0.816	2.087
25% "	0.821	2.247
10% LIX73 "	0.802	1.714
15% "	0.808	1.878
20% "	0.814	2.007
25% "	0.820	2.220

solvents in hydrogen form

^{*5} 5 g Cu/l, 19% H₂SO₄

TABLE 2

INTERFACIAL TENSION AT 20°C

Phase 1	Phase 2	Interfacial Tension, dyne/cm
20 % LIX64N [†]	Acid/CuSO ₄ ⁵	14.3
10 % LIX64N	Acid/CuSO ₄	15.5
"	Air	26.8
20 % LIX70	Acid/CuSO ₄	14.7
10 % LIX70	Acid/CuSO ₄	15.6
"	Air	26.7
Escaid 100	Air	27.0
Acid/CuSO ₄	Air	46.8

⁵ 5 g Cu/l, 19% H₂SO₄

[†] Escaid 100 diluent

TABLE 3

RESULTS OF MIXING AND SETTLING TESTS USING 20% KELEX 100 WITH AN AQUEOUS
COPPER FEED AT PH 1.0

Test No.	A/O Ratio	Stirring Speed RPM	Stirring Time secs	Organic Analysis G/L	† Extraction %	PBT(%) secs
Calculated Feed = 3.64 G/L						
1	4	300	10	0.65	4.46	7
2			30	1.23	8.44	10
3			60	2.49	17.1	10
4			120	4.38	30.1	12
5			180	5.36	36.8	15
6			300	7.15	49.1	12
7		600	600	10.1	69.4	15
8			10	1.62	11.1	15
9			30	3.47	23.8	20
10			60	5.12	85.2	22
11			120	8.0	54.9	28
12			180	9.33	64.1	33
13	900	300	10.72	73.6	34	
14		600	11.69	80.3	37	
15		10	2.45	16.8	22	
16		30	5.21	35.8	22	
17		60	7.81	53.6	24	
18		120	10.23	70.2	34	
19		180	11.19	76.8	35	
20		300	11.8	81.0	37	
21		600	11.84	81.3	38	
22		1200	10	2.78	19.1	18
23	30		5.18	35.6	23	
24	60		7.84	53.8	30	
25	120		9.91	68.0	35	
26	180		10.92	75.0	38	
27	300		11.64	79.9	40	
28	1400	600	12.01	82.5	43	
29		10	3.48	23.9	20	
30		30	6.75	46.4	26	
31		60	9.38	64.4	35	
32		120	11.23	77.1	37	
33		180	11.89	81.6	42	
34		300	12.09	83.0	46	
35		600	12.07	82.9	48	
Calculated Feed = 4.92 G/L						
36	3	300	10	.87	5.90	15
37			30	1.7	11.5	20
38			60	3.27	22.2	23
39			120	5.34	36.2	30
40			180	7.1	48.1	35
41			300	9.33	63.2	40

Test No	A/O Ratio	Stirring Speed RPM	Stirring Time secs	Organic Analysis G/L	† Extraction %	PBT(τ) secs
42	3	600	600	11.08	75.1	60
43			10	2.14	14.5	
44			30	3.83	26.0	
45			60	5.91	40.0	
46			120	8.55	57.9	
47			180	10.0	68.1	
48			300	11.1	75.7	
49			600	11.57	78.4	
50		900	10	2.16	14.6	15
51			30	4.72	32.0	18
52			60	6.92	46.9	21
53			120	9.73	65.9	30
54			180	10.75	72.8	33
55			300	11.29	76.5	37
56			600	11.41	77.3	38
57		1200	10	2.88	19.5	16
58			30	6.31	42.8	21
59			60	8.62	58.4	29
60			120	10.52	71.3	33
61			180	11.26	76.3	36
62			300	11.41	77.3	38
63			600	11.87	80.4	39
64		1400	10	3.01	20.4	26
65			30	6.29	42.6	29
66			60	8.70	59.0	32
67			120	10.85	73.5	34
68			180	11.57	78.4	35
69			300	11.73	79.5	38
70			600	11.98	81.2	38

Calculated Feed = 14.58 G/L

71	1	300	10	2.27	15.6	180
72			30	4.13	28.4	240
73			60	7.34	50.4	275
74			120	9.72	66.8	306
75			180	9.97	68.5	278
76A			300	10.98	75.4	220
76B				11.0	75.6	210
77A			600	11.17	76.7	210
77B				11.2	76.9	205
78		600	10	8.12	55.8	358
79			30	10.16	69.8	360
80			60	10.35	71.1	301
81A			120	11.11	76.3	240
81B				11.0	75.6	235
82A			180	9.81	67.4	475
82B				11.2	76.9	200
83A			300	10.86	74.6	380
83B				11.1	76.2	197

Time No	A/O Ratio	Stirring Speed RPM	Stirring Time secs	Organic Analysis G/L	† Extraction %	PBT (τ) secs
84A			600	11.06	76.0	285
84B				11.1	76.2	195
85	1	900	10	2.04	14.0	32
86			30	10.2	70.1	420
87			60	10.52	72.3	405
88A			120	11.06	76.0	350
88B				11.1	76.2	150
89B			180	11.3	77.6	145
90			300	11.44	78.6	240
91			600	11.38	78.2	150
92		1200	10	9.3	63.9	211
93			30	10.1	69.4	139
94			60	10.9	74.9	100
95			120	11.1	76.2	99
96			180	10.9	74.9	95
97			300	10.9	74.9	94
98			600	11.1	76.2	90
99		1400	10	8.7	60.0	205
100			30	10.1	69.4	119
101			60	11.0	75.6	110
102			120	11.3	77.6	191
103			180	11.1	76.2	175
104			300	11.2	76.9	179
105			600	11.5	79.0	174

Calculated Feed = 29.5 G/L

106	.5	300	10	1.78	12.1	23
107			30	3.19	21.6	90
108			60	5.6	38.0	150
109			120	5.29	35.9	
110			180	9.36	63.4	180
111			300	10.5	71.2	
112			600	10.5	71.2	135
113		600	10	4.0	27.1	191
114			30	9.22	62.5	235
115			60	10.1	68.5	210
116			120	10.5	71.2	145
117			180	10.8	73.2	133
118			300	10.6	71.9	128
119			600	10.6	71.9	120
120		900	10	7.4	50.2	174
121			30	9.9	67.1	181
122			60	10.4	70.5	145
123			120	10.7	72.5	104
124			180	10.7	72.5	95
125			300	10.9	73.9	110
126			600	11.2	75.9	90
127		1200	10	9.5	64.4	167
128			30	10.7	72.5	125

Test No	A/O Ratio	Stirring Speed RPM	Stirring Time secs	Organic Analysis G/L	† Extraction %	PBT(%) secs
129			60	11.1	75.2	105
130			120	11.5	78.0	98
131	.5	1200	180			108
132			300	11.4	77.3	85
133			600	11.5	78.0	81
134		1400	10	9.72	65.9	168
135			30	10.4	70.5	105
136			60	10.7	72.5	72
137			120	10.5	71.2	70
138			180	10.8	73.2	80
139			300	10.9	73.9	60
140			600	11.0	74.6	

† % Copper Extraction Computed From 'Best' Mean Calculated Feeds For Each A/O Ratio, And From Organic Analyses

TABLE 4VALUES OF E_f

Phase Dispersed	Stirring Time θ , s	Stirring Speed N, r.p.m.			
		300	600	900	1200
Solvent	30	0.13	0.22	0.28	0.32
	60	0.23	0.36	0.44	0.49
	120	0.37	0.53	0.61	0.66
Aqueous	30	0.32	0.50	0.60	0.68
	60	0.49	0.66	0.75	0.81
	120	0.66	0.80	0.85	0.89

TABLE 5

RESULTS OF MIXING AND SETTLING TESTS USING 20% KELEX-100 WITH AN AQUEOUS COPPER FEED AT PH 1.0

Test No	A/O Ratio	Retention Time Secs	Impeller Speed RPM	Copper Analyses-G/L % Extraction						Final PH PBT (Secs)			
				Feed	Raff	Org	Calcd Feed	Measd	Pred	Meas	Pred	Meas	Pred
1	2	40	300	5.78	4.82	1.79	5.72	15.5	14.8	0.75	0.66	24	28.8
2			900		2.95	6.07	5.98	52.5	52.5	0.5	0.53	27	29.2
3		120	300		3.36	4.80	5.76	41.5	45.4	0.6	0.63	40	38.2
4			900		1.24	9.53	6.00	82.4	83.1	0.45	0.43	40	39.4
5	4	40	300	2.89	2.45	1.70	2.88	14.7	14.8	0.8	0.87	18.4	19.6
6			900		1.46	5.82	2.92	50.3	52.5	0.7	0.73	25	20.0
7		120	300		1.66	5.10	2.94	44.1	45.4	0.75	0.84	30	28.9
8			900		0.56	9.52	2.94	82.4	83.1	0.65	0.63	30	30.2
9	3	80	600	3.95	1.80	6.71	4.04	56.6	58.7	0.65	0.65	28	27.9
10					1.74	6.80	4.00	57.4	58.7	0.65	0.65	28	27.9
11					1.75	6.96	4.07	58.7	58.7	0.65	0.65	28	27.9
12					1.62	7.03	3.96	59.3	58.7	0.6	0.65	28	27.9
13	1.5			7.67	2.90	7.53	7.92	65.4	58.7	0.4	0.44	43	39.9
14	4.5			2.50	1.03	7.21	2.63	64.1	58.7	0.85	0.75	23	26.1
15	3	30		3.95	2.72	3.71	3.96	31.3	34.3	0.75	0.69	23	20.4
16		130			1.20	8.58	4.06	72.4	73.7	0.6	0.61	30	32.6
17		80	200		3.40	1.06	3.75	8.94	7.16	0.9	0.83	5	
18			10000		1.04	8.88	4.00	74.9	73.6	0.6	0.60	28	28.4

The % Extractions Are Calculated From The Measured Organic/Mean Feed Analysis and Predicted by the Best-Fitting Mathematical Model.

TABLE 6

RESULTS OF MIXING AND SETTLING TESTS USING 20% LIX64N IN ESCAID 100

Test No	A/O Ratio	Retention Time, Secs	Impeller Speed, RPM	Feed*	Copper Raff.	Analyses - g/L Org.	Calcd. Feed	Measured † Extraction%	Final PH	Primary Break Time, Secs
1	2	90	300	1.810	0.950	1.56	1.730	47.5	1.55	38
2	"	"	900	"	0.402	2.48	1.642	77.9	1.34	70
3	"	210	300	"	0.899	1.62	1.709	50.2	1.49	29
4	"	"	900	"	0.302	2.63	1.617	83.4	1.34	61
5	4	90	300	0.916	0.677	0.85	0.890	25.7	1.76	15
6	"	"	900	"	0.201	2.46	0.816	78.2	1.51	59
7	"	210	300	"	0.488	1.50	0.863	46.4	1.67	23
8	"	"	900	"	0.158	2.72	0.838	82.5	1.48	39
9	3	150	600	1.230	0.347	2.39	1.144	71.6	1.51	44
10	"	"	"	"	0.331	2.41	1.134	73.2	1.45	49
11	"	"	"	"	0.336	2.41	1.139	72.4	1.52	49
12	"	"	"	"	0.328	2.44	1.141	73.2	1.47	49
13	1.5	"	"	2.390	0.529	2.48	2.182	77.8	1.25	90
14	4.5	"	"	0.788	0.238	2.30	0.749	69.6	1.61	35
15	3	60	"	1.230	0.605	1.71	1.175	50.4	1.52	43
16	"	240	"	"	0.258	2.51	1.095	78.8	1.48	55
17	"	150	200	"	1.000	0.60	1.204	17.8	1.76	3
18	"	"	1000	"	0.201	2.66	1.088	83.8	1.42	46

*Aqueous feed pH = 1.9

†Based on aqueous concentrations

TABLE 7

EFFECT OF STIRRING SPEED ON SEDIMENTATION 20 ∇ /o LIX64N

h_A	Stirring Time, θ		V_s , cm/s
	sec	800 RPM	1200 RPM
0.50	30	0.48	0.30
"	60	0.44	0.35
"	120	0.52	0.37
0.47	30	0.35	0.45
"	60	0.52	0.43
"	120	-	0.46

TABLE 8

EFFECT OF STIRRING SPEED ON COALESCENCE 20 ∇ /o LIX64N

h_A	Stirring Time, θ		U_c , cm/s
	sec	800 RPM	1200 RPM
0.50	30	0.070	0.064
"	60	0.078	0.073
"	120	0.084	0.077
0.47	30	0.066	0.077
"	60	0.064	0.076
"	120	-	0.089
0.44	30	0.110	-
	60	0.093	-
	120	0.081	0.078
0.41	30	0.076	-
"	60	0.093	0.058
"	120	0.089	0.060

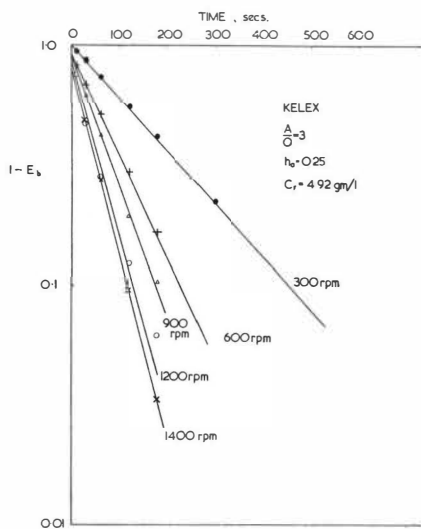


FIG. 1 BATCH RATE EXPERIMENTS

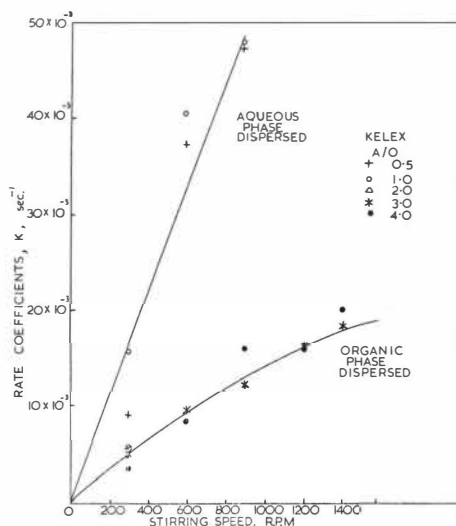
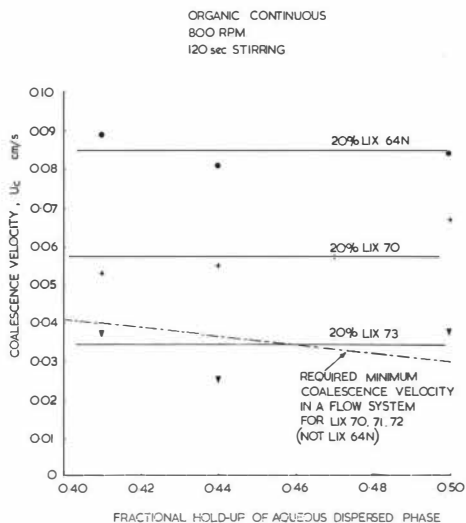
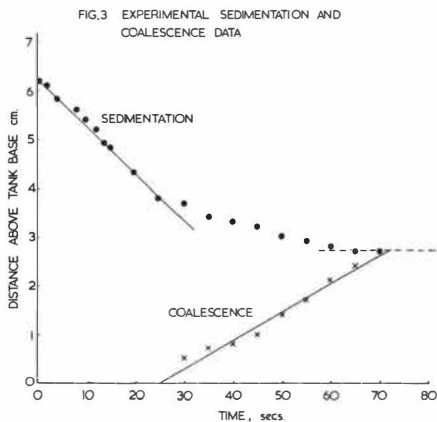


FIG. 2 RATE COEFFICIENTS

FIG. 4 EFFECT OF PHASE RATIO ON COALESCENCE



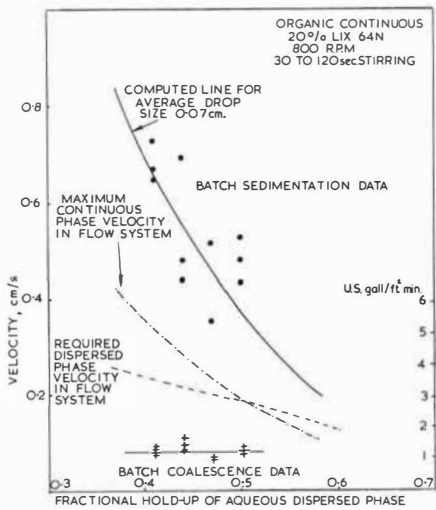


FIG. 5 MAXIMUM SEPARATION VELOCITIES IN CONTINUOUS COUNTERFLOW SYSTEM

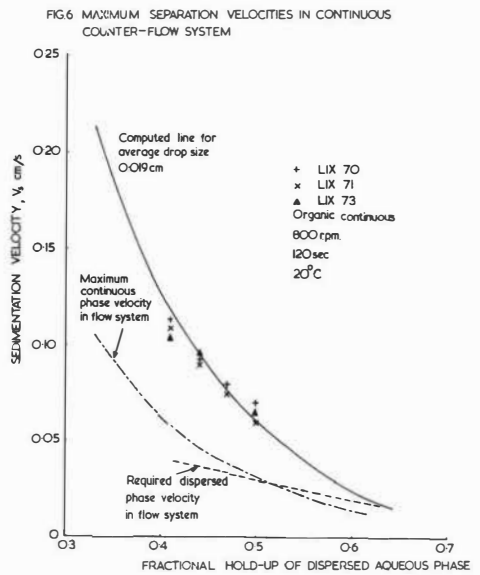


FIG. 7 ESTIMATION OF DROP SIZES

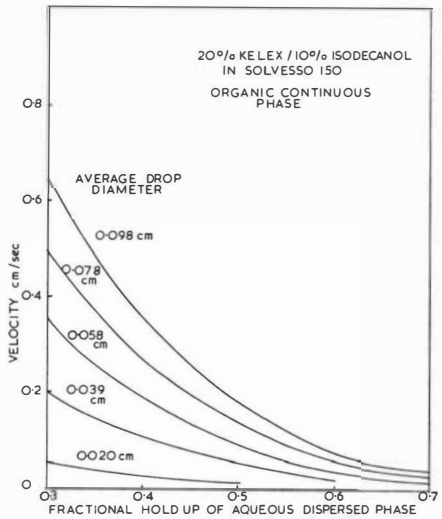
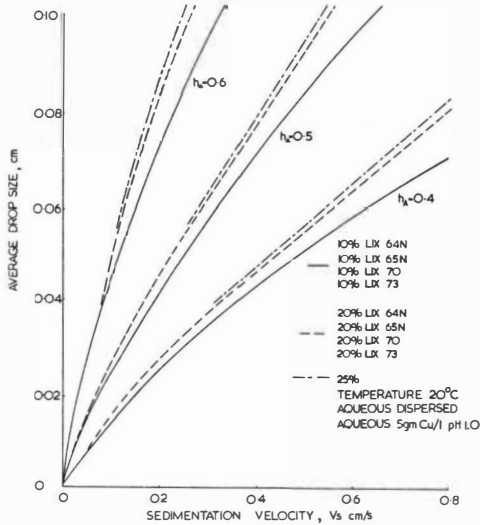


FIG. 8 CALCULATED SEDIMENTATION VELOCITIES FOR A KELEX SOLUTION

FIG.9 EFFECT OF EXTRACTANT CONCENTRATION ON COALESCENCE

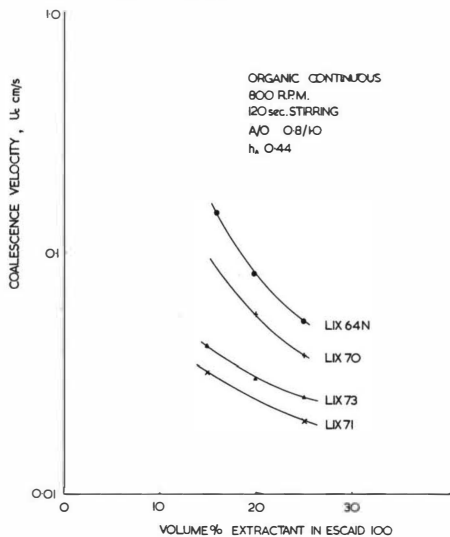
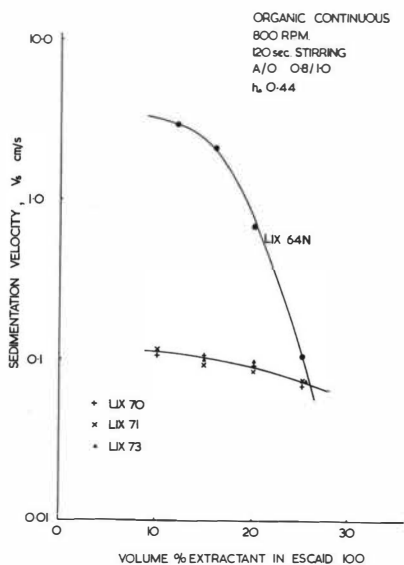


FIG.10 EFFECT OF EXTRACTANT CONCENTRATION ON SEDIMENTATION



ORGANIC CONTINUOUS
800 R.P.M.
120 sec. STIRRING

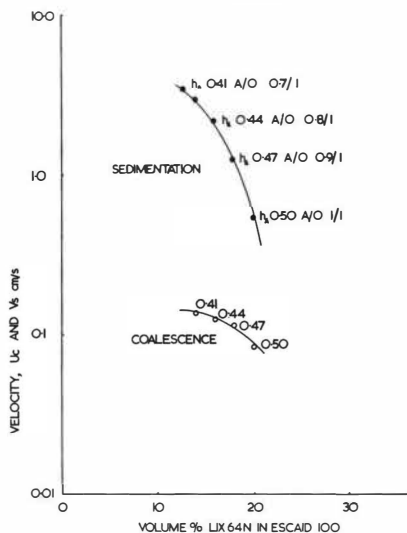
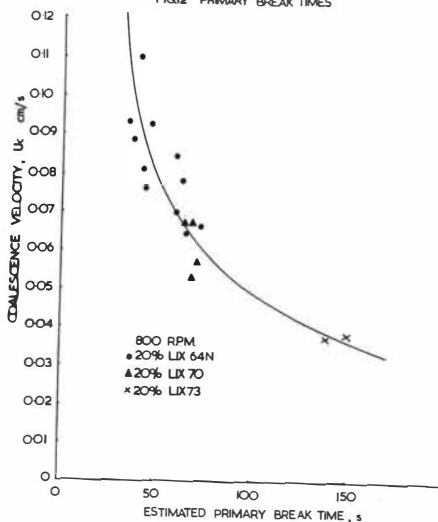


FIG.11 EFFECT OF VARYING HOLD UP WITH VARYING EXTRACTANT CONCENTRATION

FIG.12 PRIMARY BREAK TIMES



THE DEVELOPMENT OF EFFICIENT INDUSTRIAL MIXER-SETTLERS

J. Mizrahi, E. Barnea and D. Meyer

IMI Institute for Research and Development

POB 313, Haifa, I s r a e l

Abstract

The considerations affecting the choice of mixer-settlers of the hydraulically-independent type, for the industrial implementation of large-scale solvent extraction processes are reviewed from the process, design, operation and economic points of view.

The design requirements for industrial pump-mixers are listed and the various approaches analysed; an industrially proven pump-mixer model having separate mixing and pumping elements on the same shaft and a new turbine-pump mixer are schematically described.

Settler design problems, as well as the different routes to higher separation efficiency, are reviewed on the basis of a fundamental model of the separation mechanism. The practical advantages of the improved settlers for industrial operation are outlined.

Paper presented to the International Solvent Extraction Conference 1974 (ISEC 74).
Lyon, September 1974.

1. INTRODUCTION

1.1 Many types of liquid-liquid contacting equipment have been proposed and used, including both differential and stagewise contactors of various configuration. Each has a specific area of application, and has characteristics peculiar to it ^{1,2,3}. Of all these, the only type which approaches the characteristics of a set of ideal contact stages is the hydraulically-independent battery of mixer-settlers (Fig. 1). Its basic design concept is unidirectional flow, both from a mixer to its settler and from adjacent settlers into a mixer. Backmixing is thus eliminated, and each mixer-settler can, if properly designed, closely approach the equilibrium attained in an ideal stage.

The hydraulic design of these countercurrent batteries requires either a lifting device for the mixed phases from the mixers (Fig.1-a)^{2,6,7} or external pumps on either one or both streams for each stage (Fig.1-b, and 1-c). When the lifting device in Fig.1-a and the mixing device are connected on the same shaft or incorporated in the same impeller, the mixer is classified as a pump-mix type.

1.2 This paper is concerned with the design of efficient, industrial scale batteries of hydraulically-independent mixer-settlers of the pump-mix type operating in countercurrent. The relatively recent implementation of large scale solvent extraction processes in the hydrometallurgical and heavy chemical industries has revealed the need for a basic design philosophy for such equipment.

IMI has been active in this field as a result of the implementation of its own solvent extraction processes in many plants in the last twelve years, and the present concepts and know-how result from the intensive efforts, contributions and industrial experience of many members of IMI staff during this time.

1.3 When evaluating contacting equipment for the implementation of a solvent extraction process, the following features weigh very heavily in favour of mixer-settlers of the type described:

a) Process reasons

- the use of nearly ideal contact stages, both in pilot development work and in the plant, allows process design on the basis of pilot results with great confidence, without having to introduce corrections for stage efficiency and back-mixing (which characterise the equipment and not the process).
- Extraction processes operating with very steep concentration profiles are notoriously sensitive to back-mixing effects; in many cases, a relatively mild back-mixing can almost nullify the desired separation. This is particularly critical when sharp separations are required.

b) Design reasons

- Many processes are characterised by significant changes in the physical properties of the phases (viscosity, specific gravity etc.) from one end of a battery to another, necessitating the adaptation of the mixing and separation conditions to each stage individually.
- The phase ratio deriving from mass-balance considerations may be unfavourable from the mixing-separation point of view, requiring the internal recirculation of one phase within the stage to reach an operable phase ratio.
- A stage-wise configuration makes it easier to introduce or withdraw side streams in the middle of a battery, at the place most convenient from the process point of view.
- A stage-wise design conveniently allows for possible changes in the flow-sheet configuration, by transferring stages from one battery to another, or by adding stages as needed. This flexibility is specially important for processes which might have to operate with raw materials of varying grades.
- In many cases, the corrosion-resistant materials of construction impose practical limitations on the height or mechanical features of the contacting equipment; mixer-settlers can generally be designed within these limitations using conventional fabrication methods.

- For very large throughputs in a single line, the design and fabrication problems for separate mixer-settlers are less complex than for large diameter columns.
- Mixer-settlers of the hydraulically-independent type can be practically tested in closed-cycle rigs with a full-scale prototype, since the mixing, settling and hydraulic behaviour of each stage is independent of the adjacent stages. All the stages can be simulated in a single prototype unit by changing the fluid compositions, thus avoiding scale-up hazards.

c) Operating Reasons

- Mixer-settler batteries can be started up rapidly, by filling the equipment in a cross-current fashion; the production of "off-spec" material is minimized.
- When the plant is stopped for any reason, the contents of each stage remain at equilibrium and the battery profile is preserved; operation can thus be resumed directly without the loss of time and production necessary to reestablish steady-state. This is especially important during plant start-up.
- The possibility of opening the units without emptying makes routine maintenance much easier.

d) Economic Considerations

The comparative evaluation of all the above points may still leave a reasonable choice between several types of equipment, (mixer-settlers being one possible choice). In this case, an economic evaluation will have to take investment and operating costs into consideration, including such aspects as downtime, technical obsolescence, etc.

From the investment aspect, mixer-settlers may suffer from apparent handicaps compared to other types of equipment: greater built area, higher solvent inventory, many separate motors, etc. While some of these handicaps are inherent in the nature of mixer-settlers, many have been carried over from the inadequate design methods used

in the past and from the rather weak theoretical background in this field. Recent advances in the basic understanding of the operating mechanism have resulted in improved design procedures and industrial models; the weight of these handicaps has been considerably reduced and the mixer-settlers have now become more competitive on the investment level as well.

2. LIQUID-LIQUID MIXERS

2.1 General Considerations ^{4,5}

The design of continuous liquid mixers has been strongly influenced by the theories and practices previously developed for solid-liquid mixers; many such models were used in solvent extraction work without questioning whether their features were desirable for mass transfer operations between two liquids, where the dispersed phase particles can be sheared, broken into smaller droplets and then recoalesced. The specific gravity difference is generally lower in the present case and the requirement of homogeneity is not directly relevant. Thus, most liquid-liquid mixing experiments were done with turbines of the "standard" configuration or with marine propellers, in baffled cylindrical tanks.

It is now well established that the bulk mechanism of mass transfer in liquid-liquid mixers involves two zones. In the immediate vicinity of the impeller, drops are sheared into smaller droplets, passing through film and filament stages. The best conditions for mass transfer occur here, but the residence time of the droplets in this zone is very small and equilibrium is not generally obtained in one pass. In the rest of the vessel, mildly turbulent conditions obtain, in which further mass transfer occurs at a lower rate; drop recoalescence also occurs to a certain extent. The flowlines deriving from the vortex pattern and determined by the mixer geometry recirculate part of the dispersion through the shearing zone, so that each element of dispersed or continuous phase has a statistical opportunity of passing through it one or more times. The relative amount of mass transfer occurring in each zone depends on the liquid system, both zones contributing to the final result; they also affect the final drop size distribution according to a dynamic equilibrium between the shearing and recoalescence mechanisms.

The logical corollary of this mechanism concept is that improvement of the mass transfer efficiency (rate per unit volume) must derive from the enlargement of the relative space occupied by the shearing zone, as well as inducing a large number of dispersion-recoalescence cycles for each element of dispersed phase by controlled and forced circulation between the two zones inside the mixer.

2.2 Requirements for an Industrial Pump-Mixer

It is useful to start this discussion by clearly defining the practical requirements for continuous liquid-liquid pump-mixers incorporated in an industrial battery of countercurrent mixer-settler units, in the light of many years of industrial development.

Mass Transfer Considerations: The exit composition of the two liquid phases should be as near as possible to equilibrium, giving a stage efficiency close to unity. This can be achieved by :

1. - High interfacial area and shear forces in the mixing zone.
2. - High recoalescence rate in the other parts of the mixer, and high circulation rate through the mixing zone, allowing many dispersion-recoalescence cycles for each element of dispersed phase.
3. - A narrow residence time distribution of both phases, that is minimum segregation and/or short-circuiting of the mixing zone.

Phase Separation Considerations: The outlet dispersion should be in the form best suited for settler operation, that is:

4. - The outlet dispersion should have a quiet flow, a maximum average drop size and a narrow drop size distribution, particularly without a significant "tail" of the smallest droplets which are detrimental to settler performance (see below).

Operational Considerations

5. - The pump-mixer should develop a differential hydraulic head, between the level of the inlet of the heaviest phase to the discharge level, sufficient for the operation of a counter-current battery with "deep-layer" settlers (that is 60 - 120 cm head). Excess head can be used to advantage for passing the dispersion through coalescence aids.

6. - The pump-mixer should operate in a wide range of throughputs, without requiring adjustment after a flow change and without affecting the mixing action.
7. - The mixer volume should be minimal in relation to the mass transfer operations, thus requiring flow renewal through all parts of the mixer (no "dead-space") and efficient mass-transfer. This requirement is important in high throughput equipment in order to:
 - have a lower solvent inventory, and to
 - match the mixer and the settler heights without significant denivellation between them; this would complicate the plant construction and layout.
8. - The energy consumption should be minimized by preventing inefficient turbulence and obtaining a higher pumping efficiency.
9. - Steady state operation should be reached with minimum response time.
10. - The pump-mixer should be capable of stable operation with a wide range of phase ratios without inversion of the dispersed phase, to accommodate fluctuations in the phase ratio.
11. - The pump-mixer should be capable of handling incidental solids (i.e. chips, aggregates from incrustations, etc.) without breakage or damage.

Design Considerations

12. - The conceptual understanding of the pump-mix operation and the factual information should allow safe design for various systems, scaling-up and down and separate consideration of the mixing and pumping action. This is specially important, since many ideas can be proposed or tested on a small scale or with a single system. The development work required to test and understand a new model reasonably is very lengthy and expensive, but, without this effort, it cannot be considered for industrial application.

13. - The possibility of building small models and large prototype units on the basis of similarity principles; otherwise every new application will involve an intuitive extrapolation.
14. - Finally all these requirements should result in low-investment equipment of simple design and construction, adapted to an industrial environment and allowing unsophisticated maintenance.

It is apparent that there are inherent contradictions between these requirements; in each practical case, the relative importance of each consideration will be weighed in the light of the available data, to reach a compromise bridging these contradictions. It follows, of necessity, that no single model of pump-mixer can be universally recommendable. Different models may fit different cases best. It is only important that the choice of the preferred model be based on a thorough analysis of the case, taking into account the actual testing of the mixing-settling behaviour of the liquid-liquid system under consideration according to established procedures and all the accumulated experience.

2.3 Design and Operation of Pump-Mixer with Separate Mixing and Pumping Elements on the Same Shaft.

While it is apparent that the easiest design and maximum mechanical efficiency will be obtained with a mixing impeller and a vertical, low pressure pump on separate vertical shafts, this solution was found too complicated and expensive for plants involving a large number of relatively small size mixer-settlers, and development efforts were concentrated in a design involving a common shaft^{6,7,8}.

This design (Fig. 2) was developed and prototyped in 1965. Since then, hundreds of units have been operating satisfactorily in nine industrial plants producing phosphoric acid, potassium nitrate and uranium, in a wide variety of liquid-liquid systems with through-puts of mixed phases of 20 - 500 m³/hr. The mixing element (upthrust marine impeller) is located in the lowest part of the baffled cylindrical tank and the feed streams are introduced at that level by means of inlet baffles.

The pumping element⁸ consists of an axial flow impeller, housed in a draft tube between two static sets of antiscirl guide vanes. The draft tube is submerged in the dispersion, at some vertical distance from the mixing impeller, and discharges the dispersion onto a horizontal deck, from which it flows quietly, by gravity, to the settler in a rectangular channel. This type of pump imparts minimum additional shear to the dispersion.

The size of the mixing impeller and the rotational speed are the result of compromises to satisfy both mixing and pumping requirements as well as the requirement that the entire pump and agitator assembly be capable of being withdrawn and replaced with minimum time loss, for ease of maintenance. The synthesis of these requirements resulted in models with a relatively small mixing zone, and a fairly large recoalescence zone. This has proved to be satisfactory for many systems characterized by a relatively rapid rate of mass transfer, and insensitivity to energy input, with average residence times in the mixer of the order of 2 minutes. In these conditions, a relatively wide range of fluctuations in throughputs and phase ratios could be allowed, requiring, in certain cases, adjustment of the rotating speed of the mixer. The main problem was the damage to PVC-made pumps caused by incidental solids, principally during running-in.

However, as the range of application has progressively widened, it became apparent that this pump mixer model was not suitable for a number of processes. These were mainly :

- Processes involving phase systems sensitive to energy input, in which the mixing intensity should be rigorously controlled and excessive shearing avoided, to prevent production of difficultly separable emulsions .
- Processes where mass transfer is difficult, in which more intensive "scrubbing" is needed to achieve practical results .
- Processes implemented on a very large scale, in which the mere size of the mixers (based on 2 minutes residence time) would either be an economic incentive for smaller equipment and smaller solvent inventory or create design problems, as regards the relative height of the mixers and the settlers .

For these cases, it seemed worthwhile to develop a new type of liquid-liquid mixer to obtain the required results with an effective residence time of 10 - 20 seconds.

2.4 Design and Operation of Pump-Mixers with a Single Impeller fulfilling both Functions.

It is well known that a rotating impeller can produce both shearing forces (dispersing one liquid into another) and pressure differences. In principle, this allows a wide range of design possibilities.

At one extreme of this range, one can consider an ordinary centrifugal pump sucking two liquid phases and discharging an emulsion; this possibility (which is sometimes used) is characterised by a very short residence time in severe shearing conditions in a once-through pattern and is accompanied by an unnecessarily high discharge pressure. These characteristics are generally not relevant to solvent extraction processes and, to correct them in the desired direction, one should make the pump "less efficient", by increasing the casing in relation to the impeller size, decreasing the rotating speed and allowing internal recirculation.

At the other extreme of this range, one can use the well-known suction effect at the centre of a rotating turbine, giving a negative pressure difference sucking one or both of the inlet streams into the mixing vessel. This is a useful design feature for pilot-size mixer-settlers, where denivellations are small and rotating speeds can be high. Upon scaling-up, the constraints deriving from the link between the suction pressure difference, the rotating speed and the turbine diameter become critical and present serious design and operating problems.

Between these two extremes, a number of attempts to accomodate these constraints have been published for particular cases, using a special internal pump-mix geometry. Four of these are briefly reviewed; in the first three, the mixing and the settling take place in the same vessel:

- Gordon and Zeigler's design⁹ (Fig.3-A) much resembles a flotation machine, closely following the first extreme.

- Mensing's design ¹⁰ (Fig.3-B) has an axial flow impeller in a draft tube, with some possibility of recycle. The residence time in the mixing zone is still low.
- Coplan, Davidson and Zebrosky ¹¹ (Fig.3-C) used a low-head, high capacity centrifugal impeller, confined between two horizontal discs and connected to a rotating hollow dip leg. Recirculation of dispersion to the impeller is possible through an annular slit.
- The mixer model developed by the Power-Gas Co. ¹² (Fig.3-D) for large scale copper extraction plants is a further development in this direction. Both feeds are introduced in a static draft tube below the impeller; the latter is a shrouded, low shear impeller; circulation to the impeller is possible through an adjustable slit between the draft-tube and the impeller. The impeller may also have external blades. The dispersion is discharged from a central hole in a horizontal upper baffle.

With all these considerations in mind, IMI developed a new type of turbine-pump-mix and tested it both on a small-scale model and on an industrial scale prototype of 127 cm diameter, operating in the range of 80 - 200 m³/hr at 80 - 120 RPM. This mixer ¹³ embodies the following features (Fig.3) :

- a) Mixing and pumping are both performed by a single turbine of large diameter relative to the tank diameter (70 - 90%) rotating at a relatively low RPM. The turbine is shrouded and includes a large number of blades on one or both sides. Above and/or below the turbine, there are two static recirculation chambers of the same diameter as the turbine, separated by static discs.
- b) The two inlet streams are fed from the adjacent settlers through separate channels below the mixing vessel (or through a false bottom) to the centre of the turbine.
- c) A coaxial cylindrical baffle, closed from the bottom except for the passage of the shaft, limits the mixer volume and creates a cylindrical annulus between this baffle and the mixer wall.

The exit suspension is discharged upwards through this annulus and out through a tangential rectangular channel to the settler. This annulus may be equipped with one or more helicoidal baffles to enhance rotation of the exit stream (at the expense of excess head, if available). The centrifugal action and flow pattern in this annulus can be used to generate significant pre-coalescence.

- d) The turbine action creates strong radial currents, centrifugally between the blades towards the wall and then, after a reversal of radial flow, centripetally below and above the turbine in the recirculation chambers to close the loops, since the pumping rate exceeds the net flow rate by at least an order of magnitude. The centripetal flow is ensured by fitting the recirculation chambers with curved vertical vanes, tangential to the rims of the recirculation chambers. This recirculation is essential for efficient mass transfer by passing the dispersion many times through the shearing zone. The forced vortex caused by reversed flow enhances coalescence in the internal recycled stream, thus equalising the concentration in the dispersed phase and producing bigger drops to be sheared again.
- e) The centrifugal head available at the turbine discharge is partly converted into gravitational head, pushing part of the dispersion into the annular zone in an helicoidal path. The hydraulic head between the fixed discharge channel at the top and the head of the heaviest inlet phase was correlated with the net-throughput, for parametric values of the RPM and internal geometry. Changes in head caused by throughput fluctuations are absorbed in the level of the inlet channels leaving the mixer always full and therefore not affecting the mixing action.
- f) The mixer does not include vertical baffles hampering the circular action, since secondary turbulence more than that produced by reversal of the radial flow is not required.

Testing on the industrial prototype has fully established the feasibility of this equipment. Flows of the order of 80-200 m³/hr were handled, with a head in excess of 100 cm, at 80-120 RPM. The power consumption is dependent to a great extent on the recirculation rate allowed. The pumping head is relatively insensitive to throughput. Mixing efficiency, flow pattern and liquid hold-up are all practically independent of throughput and pumping head. It is specially important to note that, since both feeds are fed directly to the high shear zone and recirculation rates are high, stable operation is achieved with dispersions containing up to 80% of dispersed phase. This allows the choice of the type of dispersion which is more easily separated. This type of pump-mix has been specified for a plant manufacturing a food product, at present under construction, and is being adapted to two new large capacity plants. More details on its operation will be published elsewhere.

3. LIQUID-LIQUID SETTLERS

3.1 General considerations

The settlers represent the major part of the investment, of the plant area and of the liquid inventory in a mixer-settler battery, yet their function is only accessory to that of the mixer. All that is required from a settler is the ability to separate a given throughput of dispersion, having certain separation characteristics, in a particular set of process conditions. Since no phase separation can be absolutely complete in industrial conditions, the separation requirement will be expressed as a fixed maximum entrainment level allowable in each discharged stream. Depending on the process, this level can be between a few ppm up to one percent per volume.

The economic efficiency of the settler lies in obtaining these results with the minimum erected equipment cost, the most compact layout and the smallest volume (minimising the solvent inventory cost). On the other hand, since good phase separation results are critical for plant operation and since settler behaviour is not generally understood or predictable with changing conditions, generous overdesigning factors are introduced as a rule. The economic value of this overdesign becomes

quite significant in larger plants and its reduction represents an incentive for better and more efficient designs, based on fundamental studies.

In the early development stages, designers' attention was apparently mostly devoted to eliminating the detrimental effects of hydrodynamic macro-currents near the inlet and outlet connections on the separation efficiency, by empirical geometrical design. Inlet turbulence is damped by some kind of diffuser (perforated or slotted partition) to reduce and spread the horizontal velocity of the entering stream evenly. Similarly, the overflow and underflow stream outlets are spread as evenly as practically possible to reduce the horizontal velocity components. The location of the feed inlet was found to have an optimum level in certain cases. At the same time, a good design practice was developed as regards those very important "details" of industrial equipment, such as underflow level regulators, drains, seals, vents, grounding cables, sight glasses and floating level indicators, intermediate layer nozzles, recycling lines, by-pass loops with or without automatic non-return valves, air-tight sampling devices and sampling taps, manholes, etc. All these have to be adapted for each case, taking into account the convenience of plant operation and maintenance. The final result is an efficient deep-layer settler of the simple gravitational type^{6,7}.

Further improvements in settler efficiency involve one or more of the following approaches:

- improving the separation characteristics of the dispersion entering the settler by :
 - changing the mechanical design of the mixer.
 - introducing a "precoalescer" element between the mixer and the settler.
- accelerating the separation rate of the dispersion by:
 - adjusting the process conditions, wherever possible (temperature, pH, change of solvent/diluent, elimination of harmful impurities from the solvent and aqueous phases, etc.).

- adjusting the phase ratio and/or the type of dispersion, by internal recycle of one phase within each stage.
- adding coalescence aids within the dispersion band in the settler, such as powders with suitable surface properties^{28,29}.
- better functional use of the settler volume by means of specially designed internal partitions (compact settler).

Each of these approaches has its range of usefulness and its limitations. Before discussing this, it will be useful to review briefly the present knowledge on the separation mechanism of a deep-layer settler, resulting from recently published fundamental work¹⁴⁻¹⁷.

3.2 Model of the separation mechanism in a deep-layer settler.

When a liquid-liquid settler operates in steady state, a dispersion band exists between the upper and lower layers of separated phases, limited by the "active interface" (or "coalescence front") and the "passive interface" (or "settling front"). In a "deep-layer" industrial settler, the thickness of the dispersion band (ΔH) is substantially even, between 40 and 100 cm (not less than 15 cm) and the ratio of settler length (or radius) to ΔH does not exceed 10 P. In these conditions, a well-defined relationship (the settler characteristic) exists between ΔH and the specific throughput of dispersion separated in the settler (Q/A), including parametric values depending on dispersion characteristics and operating conditions. For all practical purposes, each unit of horizontal area of settler separates an equal throughput of dispersion at a given ΔH . This has been found to be reasonably accurate for well-designed settlers having the above-mentioned limitations and represents a very useful scale-up tool ("area principle")¹⁷⁻²¹.

In settlers operating with lower nominal specific throughputs and with much thinner dispersion bands (both in the absolute sense and relative to settler length) a wedge-shaped dispersion band is obtained; this represents a limiting condition of the deep-layer settler. These conditions have been studied extensively^{22,23}

and are relevant mostly to pilot-installations; they are rarely purposely included in large-scale industrial operations and will not be discussed further in this paper.

A systematic investigation of the hold-up of the dispersed phase within the dispersion band¹⁴ showed that it consists of two main sub-layers, defined as :

- the "dense layer" near the active interface, in which the hold-up is much higher than in the feed and increases sharply towards the active interface, where it reaches unity;
- the "even-concentration layer", where the hold-up level is almost constant and slightly lower than in the feed; the actual hold-up decreases moderately and roughly linearly towards the passive interface, where it drops more or less sharply to zero.

The hold-up profiles for varying ΔH were found to be very similar, and could be reduced to a single function by dividing the vertical height by ΔH . In all cases when ΔH exceeded 20 - 30 cm, the "dense layer" occupied only 10 - 20% of the total volume of the dispersion band.

Investigations¹⁴ on both continuous and batch separations indicate that the instantaneous rate of coalescence on the active interface is proportional to the overall effective weight of the dispersed droplets in the dense layer, and that the thickness and hold-up gradient of the dense layer is self-adjusting to allow the required coalescence rate in each set of conditions (throughput, phase ratio, temperature, etc.).

Determination of the flow patterns of both the dispersed and continuous phases within the dispersion band resulted in the following simplified picture¹⁵.

The entering dispersion flows as a bulk, in what is termed the "chimney" current, to the level between the "dense" and the "even concentration" layers. From there, the continuous phase is drained more or less evenly towards the passive interface. The majority of the larger dispersed drops penetrate directly into the even concentration

layer and pass rather rapidly through the active interface. The remaining smaller drops are entrained towards the passive interface by the continuous phase: however after some time the entrained droplets were found to reverse their vertical direction and to flow against the draining continuous phase towards the dense layer, where they eventually coalesce. This reversal can only be explained by increase of the drop diameter of the drop due to drop-to-drop coalescence in the "even-concentration" layer. Since the settler is operated in steady-state conditions without entrainment and with a ΔH depending on the throughput, it follows that the thickness of the "even concentration" layer is self-adjusting to provide the residence time and conditions for the droplet growth up to the critical diameter, allowing the reversal of vertical direction..

The mathematical analysis of this method ¹⁶, based on the concept of average size and average residence time, took into account two main physical mechanisms:

- the hindered settling of drops in a concentrated liquid-liquid dispersion which was analysed by the present authors ^{24,25} on the basis of an extended definition for the modified drag coefficient and particle Reynolds numbers. The universal correlation developed allowed the calculation of the relative velocity of spherical particles in a dense crowd, knowing the average particle diameter, particle hold-up and physical properties of both phases. For liquid particles, an empirical coefficient has to be included for the surface effects of adsorbed impurities ("retardation" of internal circulation).
- The rate of drop-to-drop coalescence, which must take into account and accommodate two mechanisms ("collision" and "bouncing"), including empirical coefficients in their expression.

Semi-quantitative mathematical expressions were developed for these aspects, from which the previously established empirical expression ^{17,18,19,20,26}, of the settler characteristic:

$$\Delta H \text{ proportional to } (Q/A)^Y \quad (1)$$

was reconstituted. It was deduced that Y should be constant, minimum

and equal to 2.5 when the settling conditions are in the creeping flow region and the droplet growth rate is entirely controlled by the collision rate. These conditions are by no means exceptional^{17,18-20,27}. Values of y apparently lower than 2.5 have been obtained from points in the very low ΔH range, with higher empirical values being obtained for other conditions. In these cases, theoretical arguments indicate that there may be a more or less significant increase in y , as ΔH increases, indicating that the settler "characteristics" (that is the plot of ΔH versus (Q/A) on logarithmic coordinates), would be an upwards concave curve. The degree of curvature depends on the balances of the various mechanisms prevailing for each case. In many systems, for a given range of ΔH , the characteristics may be approximated by a straight line for all practical purposes. There is however an inherent danger in straight-line extrapolation from experimental data obtained in the lower ΔH range to high ΔH values; this could yield very sizable errors.

3.3. Effect of mixer operation on settler characteristics

The above investigations indicated that the main factor affecting ΔH (that is, mostly the thickness of the "even-concentration" layer) is the fraction of smaller size droplets of the dispersed phase in the settler feed. This size distribution results from a dynamic equilibrium between opposing mechanisms determined by mixer action. Even when the mixing regime is kept unchanged, increasing throughput results in a smaller residence time in the mixer, with smaller energy input per unit volume of suspension. This is a fundamental aspect of mixer-settler design.

The accumulated empirical experience shows that, in general, liquid systems can be classified as "sensitive" or "insensitive", according to the dependence of the dispersion separation rate on the amount of mixing energy input, i.e. mixing intensity and/or residence time in the mixing zone. With "sensitive" systems, phase separation rates decrease systematically as the mixing parameters i.e. residence or mixing time, impeller diameter or rotational speed, turbulence-inducing baffles, etc. are increased. However, even with "sensitive" systems, the separation rate

decreases towards an asymptotic value, and a range of variables can be attained in which further increase in mixing intensity does not measurably affect the separation rate. In the rigorous sense, all systems are "sensitive", but the practical difference between "sensitive" and "insensitive" systems is that for the latter, this asymptotic value is reached with a mild mixing intensity. Thus, for "insensitive" systems, the separation rate, either batch or continuous, does not change significantly with increasing mixing intensity in the "normal" range of operations (say, mixing time of 10 - 200 seconds and agitation intensity between that required to produce an apparently homogeneous dispersion to 2-3 times this minimum value.

Fortunately, many of the systems encountered (in IMI practice) were relatively "insensitive". This can be explained as follows: the final drop size is the result of the dynamic equilibrium between droplet break-up and coalescence, both mechanisms being simultaneously affected by increasing mixing intensity, in such a way that the final drop size distribution at the mixer exit is only moderately affected. On the other hand, equations which have been developed¹⁵ for the rate of drop-to-drop coalescence in the "even concentration layer" show that the effect of average drop diameter in the feed tends to become negligible in many cases.

Experimentation, testing, design and operation of mixer-settlers with systems which are practically "insensitive" to energy input are very much simplified, since the mixing and settling operations can be conducted separately, within reasonable limits, without interactions between them. The different values of ΔH obtained in a given mixer-settler for different (Q/A) are all obtained with dispersions having essentially the same separation behaviour.

On the other hand, similar operations with "sensitive" systems are most complicated and delicate, since exact scale-up, or even duplication of mixing regimes, is doubtful. "Sensitive" systems also tend to be unstable, i.e. their properties drift with time. Systems incorporating kerosene in the solvent are generally quite "sensitive"¹². These systems will always require flexible designs, to be "tuned" at the prototype scale, and very thoughtful operating procedures, to avoid unnecessary turbulence.

3.4 Precoalescing elements between the mixer and the settlers

The use of the packed beds, fibrous mats and porous media for enhancing coalescence is well known in practice, mainly for dilute dispersions of very small droplets³⁰. The mechanism of operation of such coalescers has been related to the extended packing surface preferentially wetted by a film of dispersed phase and to the tortuous flow channels causing the impact of the droplets on this film which, after growing in thickness, is drained from the packing in the form of larger drops. Apart from the surface characteristics of the packings, other factors are relevant, such as bed thickness, superficial velocity, pressure drop, phase ratio and physical properties of the phases.

Despite this knowledge, coalescers were rarely incorporated in mixer-settlers batteries of the hydraulically-independent type until recently, mainly for the following reasons:

- Very little information existed on their contribution to the mechanism of partial pre-coalescence of concentrated dispersions (of the order of 30 - 70% dispersed phase by volume).
- the obvious limitation on the superficial velocity of the dispersion, requiring a large cross-section area and complicated physical arrangements.
- the possible plugging of the elements with solid particles (always present to some extent in any industrial plant), in particular in view of the filtering effect of these porous elements.
- the very limited extra hydraulic head which can be designed into pump-mixer batteries, and be available to compensate the necessary pressure drop between the mixer and the settler.
- the very high price required for sophisticated elements of the types used for mist separation made the saving in settler area an uncertain economic proposition.

These are inherent problems for any type of pre-coalescer; the pre-coalescer required should give significant partial pre-coalescence with superficial velocities of the order of 50 - 100 m³/hr.m², with pressure

drops of the order of a few cm of liquid. Such elements should have rather large openings, limited thickness and small specific area, and should be of simple and cheap construction. The dispersion residence time in it will be a few seconds.

Extensive experimentation has been carried out at IMI in recent years on the improvement caused by a rather thin layer of standard packing material (Baschig rings etc.) on settler capacity. Increasing superficial velocity through the element decreased the improvement factor, up to a certain limiting velocity. Results showed that there is an optimum bed thickness, above which presumably the redispersion process becomes predominant at relatively high velocities. There is also a systematic effect of the particle size. It is however most interesting to note that, in our experience, the surface properties of the packing material had very little effect, and packings similar in all respects, made from hydrophilic or hydrophobic materials or mixture of both kinds, had practically the same effect.

The improvement must be attributed to the drop-to-drop coalescence caused by the rapid and frequent changes in the velocity magnitude and direction inside the concentrated dispersion as it passes through the packing. In one particular system, intensively tested, improvements in the range of 30 - 100% in nominal settler capacity were recorded, at superficial velocities of 40 - 80 m³/hr m² and pressure drops of 1-2 cm. This type of packing is relatively cheap and easy to instal inside the settler and can hardly be plugged by fine solids.

3.5 Effect of process conditions

Increase in the operating temperature always results in increasing settler capacity. The reasons for this effect have been extensively analysed¹⁷ and its practical implication is that the process should be designed to operate at a higher temperature, whenever this is compatible with other considerations. As a rough rule of thumb, settler capacity can be doubled when operated at 40°C instead of 20°C. Obviously, there is a limit where other problems (solvent stability, vapour pressure etc.) would nullify the value of the increase in capacity.

Other relevant process conditions may be the acidity or electrolyte

level at various stages, the choice of the extending solvent, the presence of various impurities in "commercial-grade" components of the solvent system, the presence of solid or colloid precipitates, etc.

This emphasises the need for preliminary mixing-settling tests at early stages of process development, according to established procedures, to avoid spending time and effort on unsuitable choices of solvents and conditions.

3.6 Effect of phase ratio and dispersion type

For each pair of liquid phases at equilibrium, there is a particular dispersion type and phase ratio which gives the highest settler capacity, calculated on the basis of throughput of either phase. This has been extensively discussed¹⁷. There is a practical possibility of adapting the phase ratio (and indirectly affecting the type of stable dispersion at this ratio) by internal recycle between the settler and the mixer of each stage, in order to reach the optimum settler capacity. In the new turbine-pump-mix discussed above, either type of dispersion can be maintained with almost any phase ratio, up to 80% of dispersed phase. This effect is however difficult to predict exactly at this stage and must be established experimentally for each practical case.

3.7 Effect of solid particles of suitable surface properties in the separation mechanism in the dispersion band.

As discussed in previous publications^{28,29}, this effect can result in very significant improvements in specific cases: however, purposely added powders are not used in industrial settlers to our knowledge, since the deriving operational complications do not seem to make it of practical value.

3.8 Compact settler

The principle of the compact settler resides in a better utilisation of the settler volume, deriving from the fact that the volumetric separation capacity of thicker dispersion bands is lower than that of thinner bands, the incremental contribution of increasing thickness to the separation capacity being even less. The settler is divided into

40 - 50 superimposed thin settlers of 2 - 3 cm thickness each, separated by thin rigid partitions slightly inclined in a direction perpendicular to the axis of the flow of the dispersion, with common "manifold" space for the introduction of the feed dispersion and withdrawal of the two separated phases. The flow lines of the feed dispersion are essentially horizontal and parallel to the plates, while the separated liquid is drained in a vertical direction by the plate inclination. The design of this patented settler³¹ has been described in a previous publication³², and the explanation of its mechanism can be based on the above mentioned theoretical model in view of the decrease in the vertical draining velocity of the continuous phase. It is now in operation in three plants, and two other plants are at the design and construction stage. The improvement in settler capacity, on the basis of surface area, is of 3 - 8-fold and it is important to note that this effect is independent of that obtained by other methods. Thus, if the capacity of a simple gravitational settler in a particular set of conditions is $C \text{ m}^3/\text{m}^2 \text{ hr}$, and a capacity increase of 1.5 may be obtained by the described precoalescer, the capacity of a compact settler could be 4 C, and the capacity of a compact settler with precoalescer would be $1.5 \times 4 \times C = 6 C$. This additivity is a most powerful design tool³³.

Another important point is the fact that, with the increase of the separation capacity per unit area, the vertical and radial velocities of the separated phases become quite significant, in particular near the overflow weir and underflow outlet. These local velocities may disturb the flow patterns inside the dispersion band and cause its "swelling". To remedy this, special precautions must be taken to spread the vertical streams across the horizontal area, by means of perforated plates, extended overflows, etc. as described in Reference 32.

3.9 The methods of improving settler efficiency can be divided in 3 groups:

- a) those affecting the size distribution of the feed dispersion (mixer geometry, precoalescers)

- b) those affecting the separation rate inside the settler: (compact settler, non-gravitational fields of forces, "active" solid powders, etc.).
- c) those affecting both mixing and coalescence at the same time (temperature, phase ratio, process conditions, physical properties, etc.).

Evidently, methods from group (c) are most effective; methods from groups (a) and (b) can generally be combined with additive results; combinations of methods within group (a) or (b) cannot be expected to be much more effective than each method separately.

4. FINAL REMARKS

The paper lists the fundamental considerations in the choice, development, design and operation of industrial mixer-settlers. As in all other fields of industrial innovation, these considerations are complex and require fundamental know-how and practical expertise to make a reasonably well-based decision.

It seems that this field has now reached the stage of maturity, both in the scientific approach and in the industrial practice. It is only to be hoped that the industries concerned recognise and take advantage of these achievements.

Acknowledgement

This summarizing review is published by permission of the Managing Director of IMI Institute for Research and Development and incorporates contributions made at various times during the past decade by a large number of members of IMI staff. In particular, A. Baniel, R. Blumberg, E. Blumenthal, M. Elroy and D. Gonen made leading contributions in the earlier stages of this development program.

Nomenclature

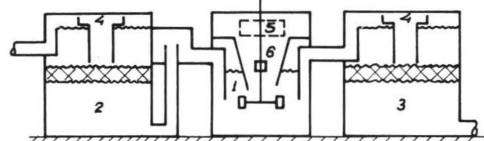
- A: horizontal area of the settler.
- Q: volumetric throughput of dispersion.
- ΔH : thickness of the dispersion band.
- y: exponent defined by Equation 1.

R e f e r e n c e s

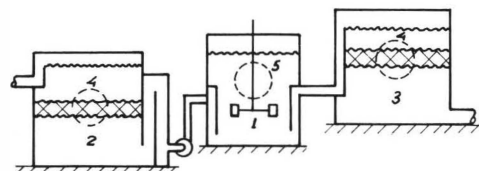
1. Warwick, G.C.I., Chem. and Industry, 403, May (1973)
2. Hanson, C., Chem.Eng., Aug.26, Sept. 9 (1968)
3. Bailes, P.J. and Winward, S., Trans.Instn.Chem.Eng. 50,240 (1972).
4. Oldshue, J.Y., Solvent Extraction Review 1 (2), 195 (1971)
5. Schindler, H.D. and Treybal, R.E., AIChE Journ., 14, 790 (1968).
6. IMI Patent, Israel 23,539 (1969).
7. IMI Staff, Proc.Eng. Plant & Cont., Sept. (1967).
8. IMI Patent Application, Israel. 34096 (1970)
9. Gordon, J.J. and Zeigler, J.H. US Pat.2,176,899 (1934).
10. Mensing, L.E. US Pat. 2,405,158 (1945)
11. Coplan, J.V., Davidson, J.H. and Zebroski, E.S., Chem.Eng.Progress 50, 403 (1954).
12. Warwick, G.C.I., Scuffham J.B. and Lott, J.B., Proceedings Intn.Solvent Extraction Conf., Vol. 2, 1373, Society of Chem.Industry, London (1971)
13. IMI Patent Application, Israel 43692 (1973).
14. Barnea, E. and Mizrahi, J., Transactions Instn.Chem.Eng.(London).Part/in press (1974).
15. Ibid - Part 2
16. Ibid - Part 3
17. Ibid - Part 4
18. Ryon, A.D., Daley, F.L. and Lowrie, R.S. Chem.Eng.Progress 55 (10), 70 (1959).
19. Ibid, Report No. ORNL-2951 Oak Ridge National Laboratory, Tennessee (1960)
20. Ryon, A.D. and Lowrie, R.S., Report No. ORNL-3381, Oak Ridge National Laboratory, Tennessee (1963).
21. IMI Staff, Proc.Intern.Solvent Extraction Conference, Vol. 2, 1386, Society of Chem.Industry, London (1971).
22. Jeffreys, G.V., Davies, G.A. and Pitt, K., AIChEJ, 16, 823 (1970).
23. Jeffreys, G.V., Davies, G.A., Chap. 14 in "Recent Advances in Liquid-Liquid Extraction" edited by C.Hanson, Pergamon Press (1971).
24. Barnea, E. and Mizrahi, J. The Chem.Engng.J., 5, 171 (1973).
25. Ibid (in publication)
26. Gondo, S. and Kusunoki, K. Hydrocarbon Processing, 48, 209, 4 (1969).

27. Naylor, A. and Larkin, M.J. Proc.Intern.Solvent Extraction Conference, Vol. 2, 1356, Society of Chem.Industry, London (1971).
28. Mizrahi, J. and Barnea, E., British Chem.Eng., 15 (4) 497 (1970)
29. Mizrahi, J. and Barnea, E., Progress in Heat and Mass Transfer, vol. 6, 717, Pergamon Press (1972)
30. Spielman, L.A. and Goren S.L., Ind. Eng.Chem. 62, 10 (1970).
31. IMI Patent, Israel 30,304 (1968).
32. Mizrahi, J. and Barnea E., Process Engng. p.60, Jan. 1973.
33. IMI Patent Application, Israel 43,693 (1973)

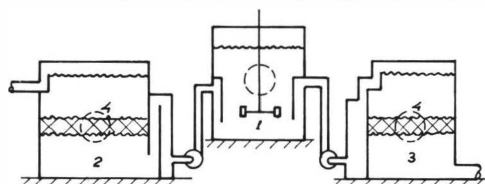
FIG 1



a: GRAVITY FLOW FOR BOTH PHASES, MIXTURE LIFTED



b: HEAVY PHASE PUMPED, LIGHT PHASE CASCDED

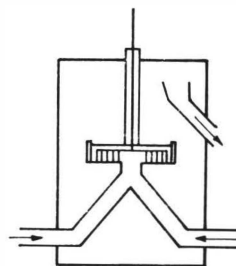


c: BOTH PHASES PUMPED

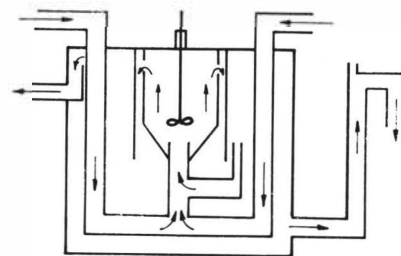
LEGEND

- | | |
|--------------------------------------|----------------------|
| 1: MIXER | 4: DISPERSION INLET |
| 2: SETTLER DELIVERING
HEAVY PHASE | 5: DISPERSION OUTLET |
| 3: SETTLER DELIVERING
LIGHT PHASE | 6: LIFTING DEVICE |

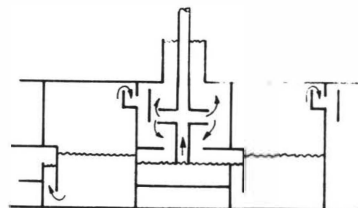
FIG. 2



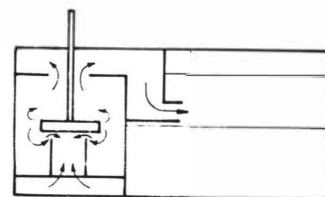
a



b

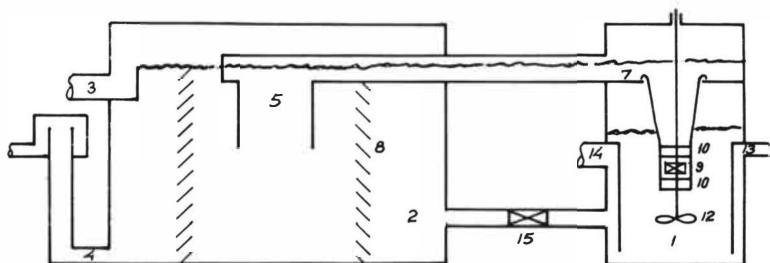


c



d

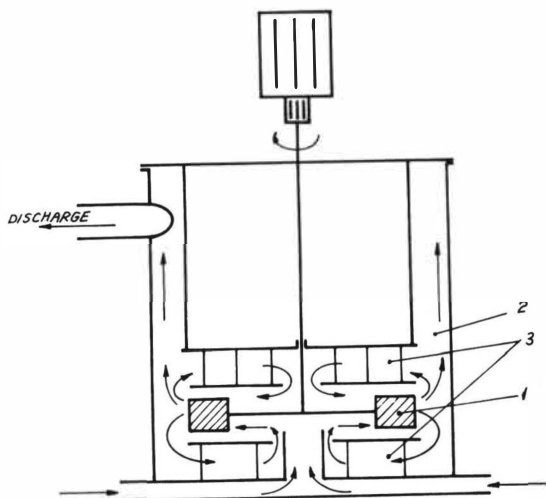
FIG. 3



IMI LIQUID-LIQUID CONTACTOR
SCHEMATIC DIAGRAM
LEGEND

- | | |
|------------------------------------|------------------------------------|
| 1. MIXER BODY | 9. PUMPING DEVICE |
| 2. SETTLER BODY | 10. STRAIGHTENING VANES |
| 3. LIGHT PHASE OUTLET | 11. DRAUGHT TUBE |
| 4. HEAVY PHASE OUTLET (ADJUSTABLE) | 12. MIXING IMPELLER |
| 5. DISPERSION INLET | 13. HEAVY PHASE INLET |
| 6. DISPERSION CHANNEL | 14. LIGHT PHASE INLET |
| 7. PUMP DISCHARGE DECK | 15. OPTIONAL RECYCLE (HEAVY PHASE) |
| 8. ANTI-TURBULENCE BAFFLE | |

FIG. 4: SCHEMATICAL SKETCH OF THE NEW PUMP-MIXER



- 1 TURBINE
2 MIXING CHAMBER AND ANNULUS
3 RECIRCULATION ZONES

THE KEMIRA MIXER-SETTLER EXTRACTOR

T.K.Mattila

Kemira Oy, Oulu Research Laboratory

Oulu, Finland

Kemira Oy has developed a new mixer-settler extractor, which is an improvement of the normal pump-mix mixer-settler extractor. It has the following principal features:

- the heavy phase only is pumped into the bottom of the mixing space whilst the lightweight phase is allowed to flow freely from the settling space to the top of the mixing space without any pumping,
- a larger than normal auxiliary space has been connected between the mixing space and the settling space to act as an effective stopping/starting system.

The Kemira extractor has many advantages compared with known conventional mixer-settler extractors. It is trouble-free in operation; the possibilities of phase inversion are slight, moreover it is easy to start. The stopping/starting system guarantees the formation of the right dispersion when starting the mixer-settler, and to a large extent shortens the starting and breakdown periods.

1. Introduction

The latest and most effective mixer-settler extractors are designed according to the following principles:

- ensure that the maximum degree of mass transfer takes place without creating so fine a dispersion that the two phases settle only with difficulty;
- the phases can be transferred from stage to stage without any external pumping;
- the controlled recycle of the phases within a stage is possible.

In most cases this is achieved by bringing both phases together as soon as possible after phase separation, which means that the phases contact with each other before reaching the mixing space. For example in the normal pump-mix apparatus, the phases are brought into contact whilst in the pipe and then pumped together into the mixing space, where the phases are dispersed and then the dispersed liquids are lifted through the top of the mixing space into the settling space. Such flow arrangements may often be very unstable in operation.

A situation may arise, where one phase is pumped by the pump-mix device for a longer time than the other phase. This may lead to great hold-up variations in the mixing space, which in turn may produce phase inversion. Phase inversion invariably leads to decreased mass transfer efficiency, and most often decreases phase separation. Furthermore, the normal pump-mix construction generally tends to produce plenty of organic micro-drops, which settle very slowly.

In designing the mixer-settler extractor, the flexible and rapid stopping and restarting of the apparatus is often forgotten. In conventional mixer-settler extractors when pumping and mixing is interrupted for some reason, the heavy and lightweight phases separate in the mixing space. If mixing is now continued in this

situation, the previously mentioned phase inversion may be formed immediately after restarting the system.

In order to be certain of the formation of the right dispersion in restarting the system, the following time consuming operation must be carried out:

- stop the feeding of the intended drop phase (phase 1),
- let the other phase (phase 2) flow through the apparatus so long as all the mixing spaces have been filled by it, i.e. the continuous phase,
- restart the feeding of the phase (phase 1), i.e. the drop phase.

In the Kemira mixer-settler extractor we have made improvements on the previously mentioned pump-mix apparatus, which have eliminated those disadvantages characteristic of normal pump-mix apparatus. This report describes an auxiliary device included in the Kemira extractor, namely the so-called stopping/starting system which reduces the lengthy stopping and restarting operation, and guarantees the formation of the right dispersion when restarting the extractor.

2. Description of the apparatus and its operation

The principle drawing of the Kemira extractor is shown in figure 1. The drawing represents a part of the countercurrent multistage extraction apparatus provided with Kemira mixer-settler units. Extraction stages have been marked by numbers $n-1$, n , and $n+1$. Every stage has a mixing space M, a settling space S, and an auxiliary space A. The lower part of the settling space S has been connected to the auxiliary space A through an overflow pipe 10, which in turn has been fitted into the auxiliary space A, and which can be regulated in the vertical direction to control the interface level in the settling space. The lower part of the auxiliary space A has been connected to the lower part of the mixing space M by the connection pipe 5.

Mixing space M contains a vertical shaft rotated by motor Mo. At the end of the shaft there is a heavy phase pump turbine 2, and at its centre point there is a mixing impeller 1.

The heavy phase flows by pipe from stage to stage firstly by overflowing from the bottom of the settling space into the auxiliary space and then by flowing from the auxiliary space into the bottom of the mixing space due to the pumping effect of turbine 2. The liquid surface level of the heavy phase in the auxiliary space is kept low, the volume and position of the auxiliary space being such that it can receive all the heavy phase which has settled in the mixing space.

The lightweight phase flows countercurrently along the overflow pipe 4 from the top of the settling space S to the top of the mixing space M. The mixing impeller 1 disperses the phases entering the mixing space, holds them there for some time and then moves them into the settling space through the head pressure pipe 7, and the dispersion pipe 3. Both phases may be recirculated within a stage through pipes 8 and 9. The lightweight phase flows through pipe 9 as an overflow, because the liquid surface level in the settling space is higher than the liquid surface level in the mixing space, due to the difference between phase densities, and to head pressure in pipe 7 caused by the rotation of mixing impeller 1. The heavy phase flows through pipe 8 due to the pumping effect created by pump turbine 2.

The whole mixer-settler apparatus has been stepped slightly stage by stage in the direction of the lightweight phase flow.

3. Operation of the stopping/starting system

Figure 2 shows the schematic drawing of the stopping/starting system. The function has been described in a series of drawings. The normal stopping/starting action

in the Kemira extractor has been taken as our example. This stopping/starting system is suitable only for those operations in which the heavy phase is the drop phase; this kind of operation being the most common in the field of inorganic extractions. The function of the stopping/starting system can be divided into five different stages:

1. Operation
2. Stopping
3. Phase separation
4. Levelling
5. Starting

These stages have been described in this order in figure 2.

Operation

This is a normal operation stage. The head of the pump turbine has been regulated so that the auxiliary space is practically empty of the heavy phase.

Stopping

Mixing is stopped in this stage and the valve in the connection pipe which is between the auxiliary space and the mixing space is shut to prevent dispersed liquids flowing into the auxiliary space. The liquid surface level in the auxiliary space stays the same as during normal operation.

Phase separation

In the mixing space dispersed liquids are separated.

Levelling

The valve in the connection pipe is opened after phase separation and the heavy phase separated in the mixing space is allowed to flow entirely into the auxiliary

space. The lightweight phase flowing from the settling space replaces the heavy phase in the mixing space entirely.

The exit end of the dispersion pipe in the settling space is located within the lightweight phase above the interface.

Starting

Only after mixing has begun is the valve in the connection pipe opened slowly in order that the heavy phase can flow into the mixing space now full with the lightweight phase. Right dispersion is now guaranteed. The normal operation is soon achieved.

4. Hydraulics of the apparatus

The hydraulic conditions under which the Kemira extractor is operated are presented in the following text. Fig. 3 shows necessary height differences and pressure drops and gives their symbols for the following hydraulic calculations.

The following hydraulic equations are valid provided that:

- the heavy phase is the drop phase,
- phase interface in the settling space is below the exit end of the dispersion pipe,
- phase densities are almost constant from stage to stage.

4.1 The stepping of the stages

Minimum stepping:

$$\Delta h_{1\min} = \Delta p_1 / \rho_L g - \Delta h_2 \quad (1)$$

$$(h_2 - \Delta h_2) \rho_M g + \Delta p_H = \Delta p_2 + h_2 \rho_L g \quad (2)$$

$$\Delta h_{1\min} = \Delta p_1 / \rho_L g + \Delta p_2 / \rho_M g - h_2 (1 - \rho_L / \rho_M) - \Delta p_H / \rho_M g \quad (3)$$

where

$$\rho_M = \rho_L \Phi_L + \rho_H (1 - \Phi_L) \quad (4)$$

and Φ_L is the lightweight phase hold-up in the mixing space and Δp_H is the pressure built up in the head pressure pipe caused by the rotation of the mixing impeller. ρ_L and ρ_H are the lightweight and heavy phase densities and g is the acceleration of gravity.

Equation (3) shows that stepping is necessary ($\Delta h_{1\min} > 0$), if pressure drops Δp_1 and Δp_2 are high compared with the other terms in the equation, namely apparatus height (h_2), phase density difference (ρ_L/ρ_M), and head pressure (Δp_H).

Because of the use of head pressure Δp_H there is less need for stage stepping, moreover it permits the use of relatively low apparatus.

However, stage stepping in the Kemira extractor mainly guarantees high flow capacity.

4.2 Pumping of the heavy phase

When this type of apparatus is used without the stopping/starting system it may be proven that heavy phase pumping is not always necessary:

$$h_3 \rho_L g = \Delta p_3 + (h_3 - h_5) \rho_H g \quad (5)$$

$$h_4 \rho_M g + \Delta p_4 = h_7 \rho_H g \quad (6)$$

$$\Delta h_3 = h_4 - (\Delta h_1 - \Delta h_2) - h_5 - h_7 \quad (7)$$

$$\begin{aligned} \Delta h_3 = h_4 (1 - \rho_M/\rho_H) - h_3 (1 - \rho_L/\rho_H) + \Delta h_2 \\ - \Delta h_1 - (\Delta p_3 + \Delta p_4) / \rho_H g \end{aligned} \quad (8)$$

According to the equation (8) pumping is necessary ($\Delta h_3 > 0$) when for example pressure drops Δp_3 and Δp_4 in the pipes are high, and stepping of the stages is marked. On the other hand less pumping is needed when there is an increase in head pressure (Δh_2 is increasing).

The heavy phase surface level in the auxiliary space has to be at the same level as the bottom of the mixing space when using the stopping/starting system, and at the same time the volume of the auxiliary space has to be adequate enough to receive all the heavy phase from the mixing space. Therefore, the minimum pumping head is:

$$h_{pmin} = (h_4 \rho_M g + \Delta p_4) / \rho_W g \quad (9)$$

where ρ_W is the density of water.

The maximum pumping head is determined by the fact that the liquid surface level of the heavy phase in the connection pipe is not allowed to fall beneath the lowest point in the pipe. Otherwise unstable pumping occurs resulting from an intake of air.

$$h_{pmax} = (h_4 \rho_M g + h_6 \rho_H g + \Delta p_4) / \rho_W g \quad (10)$$

4.3 The function of the head pressure pipe

The end of the head pressure pipe is located so near the mixing impeller that the mixing impeller rotation produces head pressure. Head pressure is dependent on many variables.

Fig. 4 illustrates how the head/flow curves vary as the rotation speed of the mixing impeller is changed, and fig. 5 illustrates how these curves vary as the distance between the head pressure pipe and the mixing impeller is changed. The head/flow curves in these figures have been measured in an apparatus where the mixing space has been standard configuration stirred tank type, and where the mixing impeller has been the normal 6-bladed, disk-type flat blade turbine. It can be seen clearly from these figures how head pressure increases much more when increasing the mixing impeller rotation speed than decreasing the distance between the head pressure pipe and the impeller.

It has been observed also that the angle of the head pressure pipe end, and the head pressure pipe diameter/impeller blade height-ratio have optimum values, which give the maximum head pressure.

4.4 Pump turbine

The shape of the pump turbine has to be such that its head/flow characteristic curves are stable. The head should increase as little as possible when the heavy phase flow rate changes from its nominal operating rate to the zero flow rate. Furthermore, the pump turbine is not allowed to reduce any possible organic drops in the heavy phase into micro-drops which settle only with difficulty.

Stability in this respect means that the head/flow curves do not have any maximum point, but the head decreases gradually or is almost constant; if not possible variations in the heavy phase flow rate might lead to unstable pumping.

The four-blade turbine shown in figure 6 is known to be one of the best. Figure 6 shows the typical head/flow characteristic curves for this kind of turbine, which were measured in a normal mixer-settler unit, where the volume of the mixing space was 80 litres. Thus, referring to the figure 6, the heavy phase pumping is stable provided that the increase in the pumping head during possible flow interruptions (from the normal operation point O to zero point O') is less than the height (h_6) of the connection pipe 5 (see fig. 1 and 3).

Furthermore, it has been observed that the distance from the pump turbine to the bottom of the mixing space has great influence on the pumping head. The head increases as the distance decreases, and this influence may be used to regulate the pumping head if the rotation speed of the pump turbine has been fixed already.

5. Mass transfer efficiency of the Kemira extractor

Mass transfer efficiencies were measured in apparatus of three different sizes: in the bench-scale apparatus, where the volume of the mixing space was one litre, in the pilot-plant apparatus with a mixing space volume of 35 litres, and in the final scale prototype unit with a mixing space volume of 1.75 m^3 . The overall efficiency of a stage (mixing space + settling space) was measured with real liquids as percentage approach to equilibrium.

The pilot scale measurements for stage efficiencies were carried out in connection with the piloting of a process where a liquid-liquid extraction method was developed for making nitrophosphate fertilizers.¹ In this process phosphoric acid and nitric acid are extracted by tertial amyl alcohol from a nitric acid solution of phosphate rock, while calcium and other impurities remain in the water phase. The transfer of phosphoric acid to amyl alcohol is rapid and the state of equilibrium is achieved within one minute. The approximate retention times in the mixing spaces of this pilot plant were about one minute, and the mixing power was about 1 kW/m^3 . Under these circumstances stage efficiencies of nearly 100 % were obtained.

The measurements of stage efficiencies in the mixer-settler prototype were carried out with real liquids as used in pilot plant experiments. The retention time and the mixing power in the prototype mixer were the same as in the pilot scale. Both phases were recirculating. The heavy phase flowed back from the settling space through the auxiliary space into the mixing space and the lightweight phase flowed from the settling space through a fairly big reservoir vessel into the mixing space.

Stage efficiency was measured by feeding phosphoric acid into the auxiliary space for about 5 minutes after the equilibrium state was achieved, and by taking samples at intervals of one minute from the phases leaving the

dispersion pipe. These phase samples were divided into two parts, and the concentration of phosphoric acid was measured before and after they were equilibrated. At the same time the concentration of the organic phase flowing into the auxiliary space was measured. The results of a mass transfer measurement are shown in figure 7. Mass transfer efficiency is about 90 %.

6. Applications

The Kemira mixer-settler extractor has been developed mainly in connection with the development of an extraction process for manufacturing nitrophosphate fertilizers.¹ It has been used and tested in piloting this process for several years. A full scale prototype unit (one extraction stage), has been built to obtain reliable data for scale-up and design. The Kemira extractor has proved to be very flexible and safe in operation in this rather difficult process, in which flow rates vary considerably from stage to stage.

The Kemira extractor is used mainly for inorganic extractions where it is particularly flexible especially when there are great variations in the flow rate from stage to stage.

The Kemira extractor has been used successfully in many metal extractions in production- and bench-scale. More specifically it has been used for many years in the process for separating rare earths from a phosphate rock by means of liquid-liquid extraction.

7. Conclusions

The Kemira extractor has been designed with the greatest possible flexibility and operational safety in mind.

It has those normal advantages, typical of all conventional mixer-settler extractors, furthermore it has the following advantages:

- The probability of phase inversion during the operation has been minimized by changing the basic flow arrangements as in normal pump-mix mixer-settlers, by separating the lightweight phase flow from the heavy phase flow at the point where they are flowing into the mixing space.
- The safe and rapid restarting is guaranteed even after possible troubles because of the simple stopping/starting principle, which produces the right dispersion. The time to achieve the normal operation after restarting is approximately one third of the time required in an extractor without stopping/starting system. Much valuable production time is saved when using our stopping/starting system.

8. Acknowledgements

The author wishes to thank Messrs. J.Örjans, H.Ahonen, and M.Lamberg for the contributions to the development of the Kemira mixer-settler extractor. The permission of Kemira Oy to publish this paper is gratefully acknowledged.

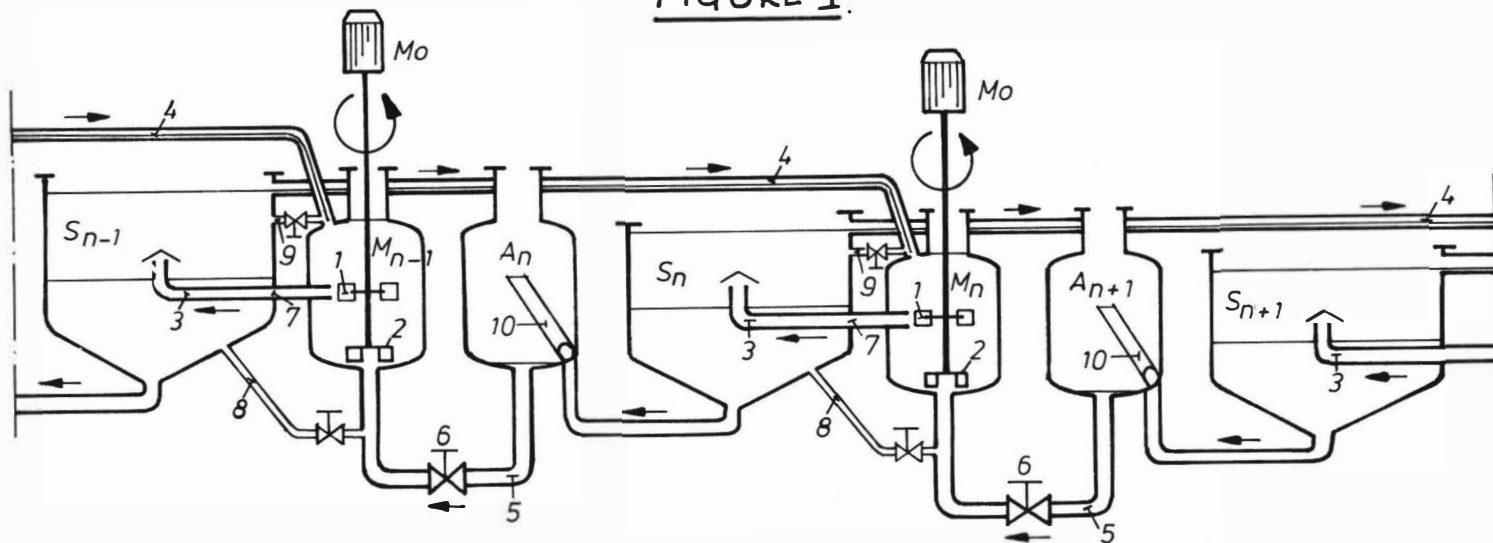
References:

1. Niinimäki, L. and Örjans, J.R., Solvent Extraction Scores in Making Nitrophosphates, Chem. Eng. 1971, 11, 63.

List of used symbols

g	= acceleration of gravity, m/s^2
$h_i (i = 2,7)$	= heights (see fig. 3), m
h_p	= pumping head, m H_2O
$\Delta h_i (i = 1,3)$	= height differences (see fig. 3), m
$\Delta p_i (i = 1,4)$	= pressure drops in pipes (see fig. 3), N/m^2
Δp_H	= pressure caused by the mixing impeller rotation into the head pressure pipe, N/m^2
ρ_H	= heavy phase density, kg/m^3
ρ_L	= lightweight phase density, kg/m^3
ρ_W	= water density, kg/m^3
ρ_M	= dispersion mean density in the mixing space, equation (4), kg/m^3
Φ_L	= lightweight phase hold-up in the mixing space

FIGURE 1.



KEMIRA MIXER-SETTLER.

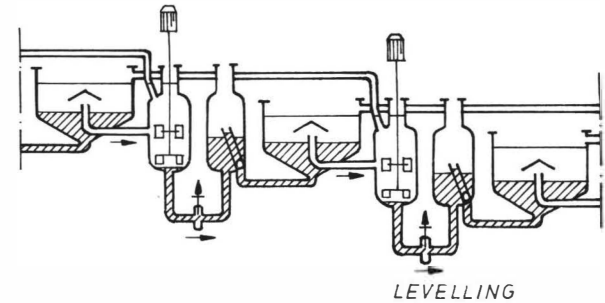
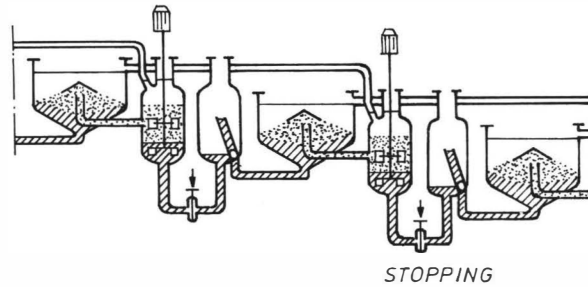
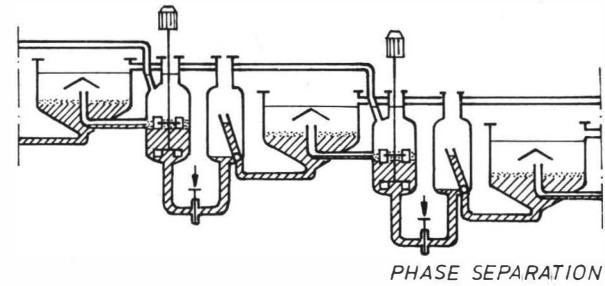
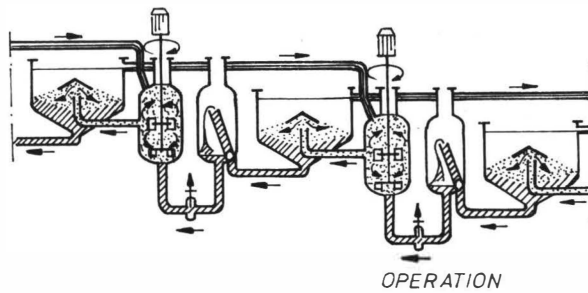
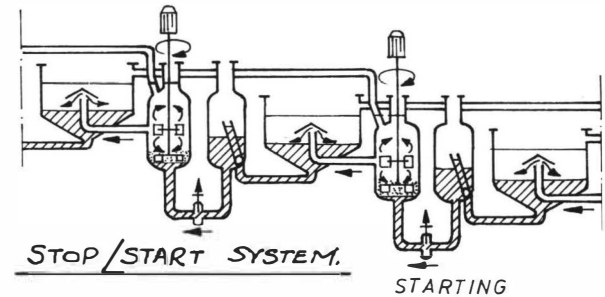


FIGURE 2.



STOP/START SYSTEM.

FIGURE 3.

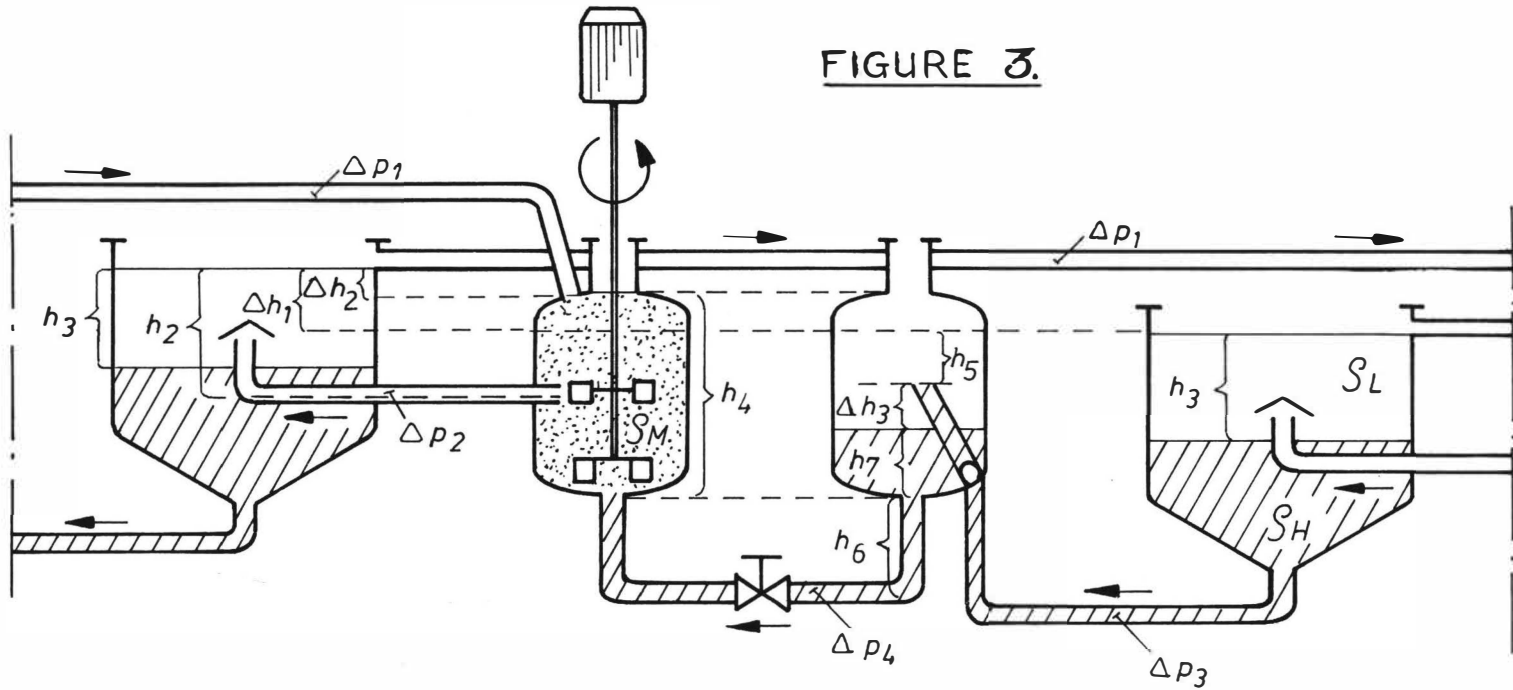
HYDRAULICS OF A KEMIRA MIXER-SETTLER.

FIGURE 4

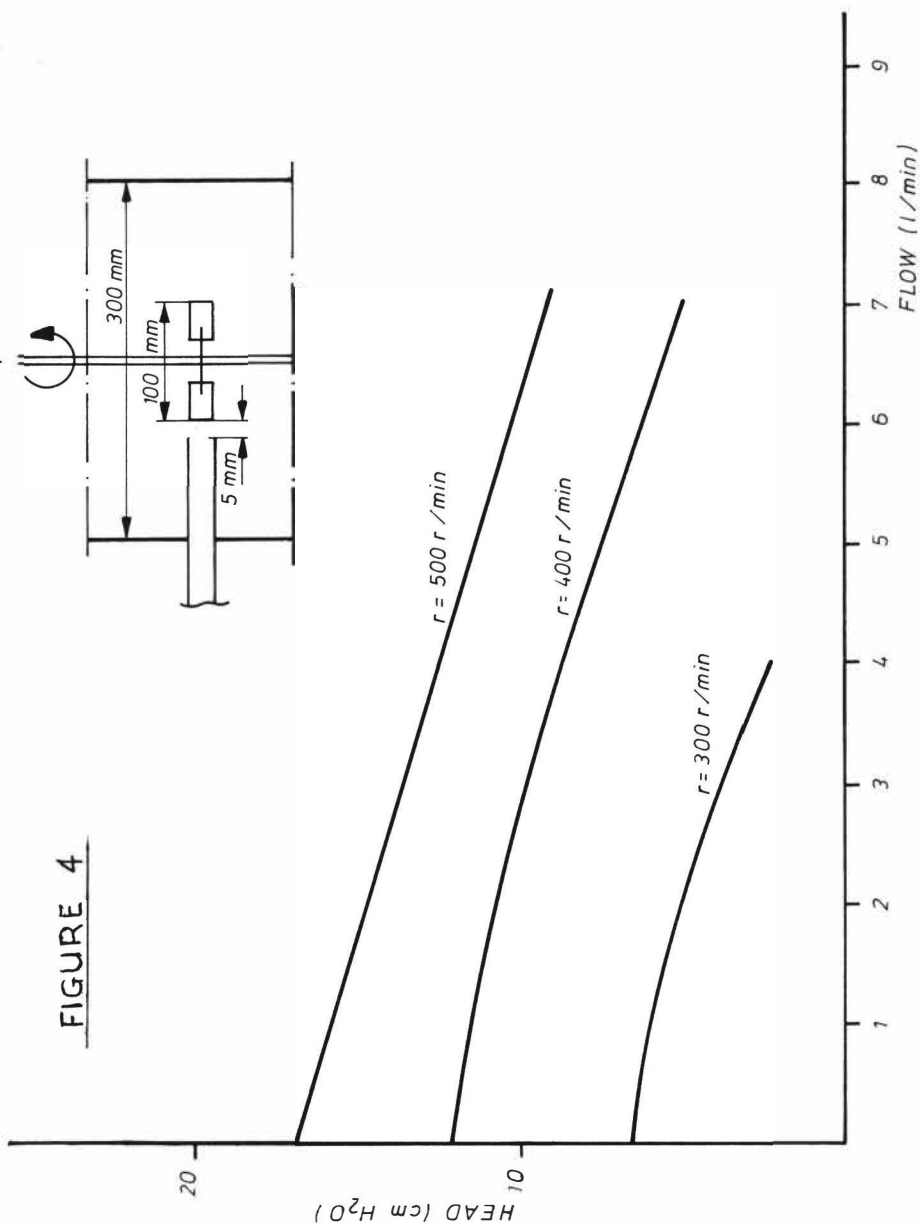


FIGURE 5

HEAD / FLOW CHARACTERISTICS

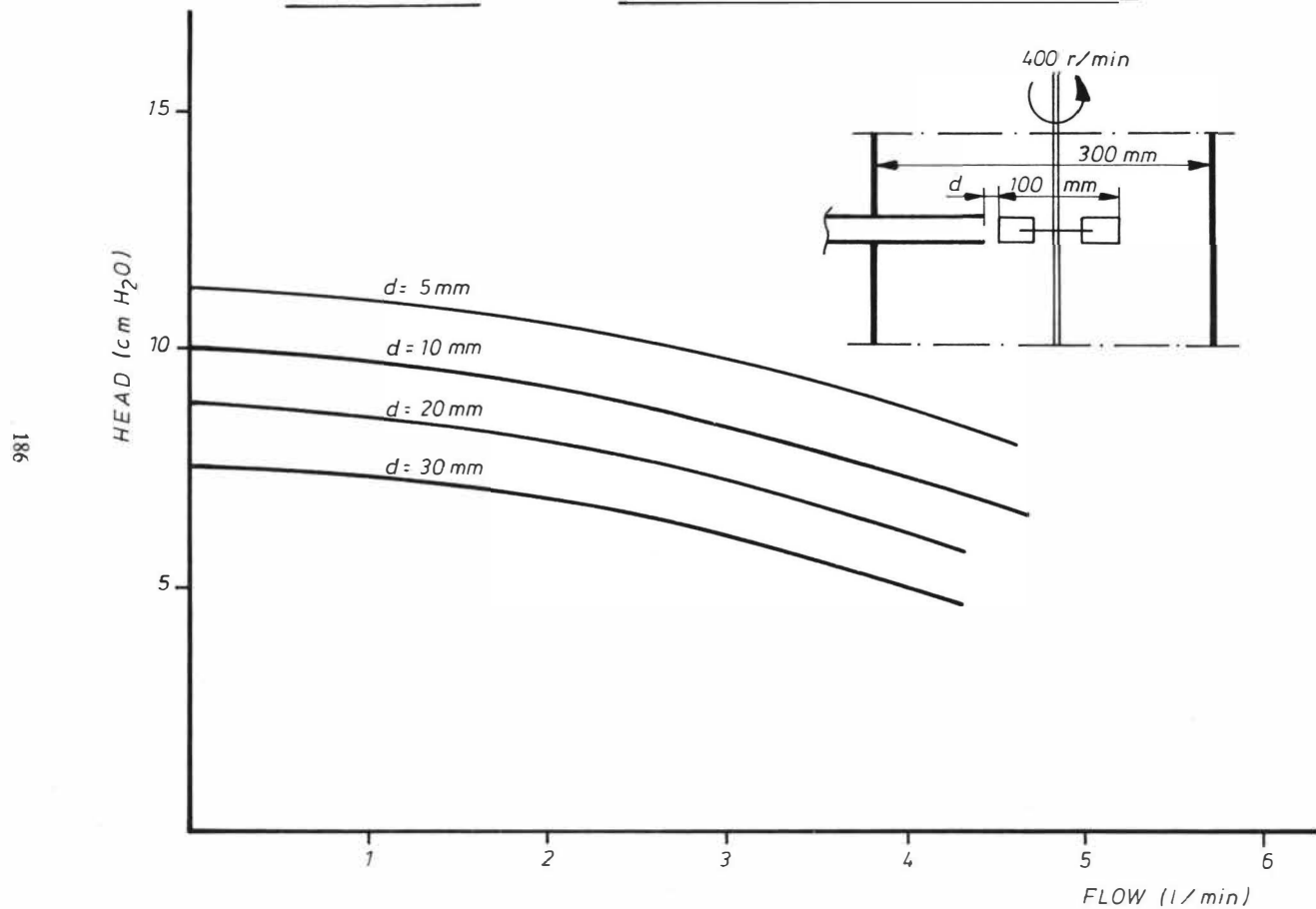


FIGURE 6. HEAD / FLOW CHARACTERISTICS.

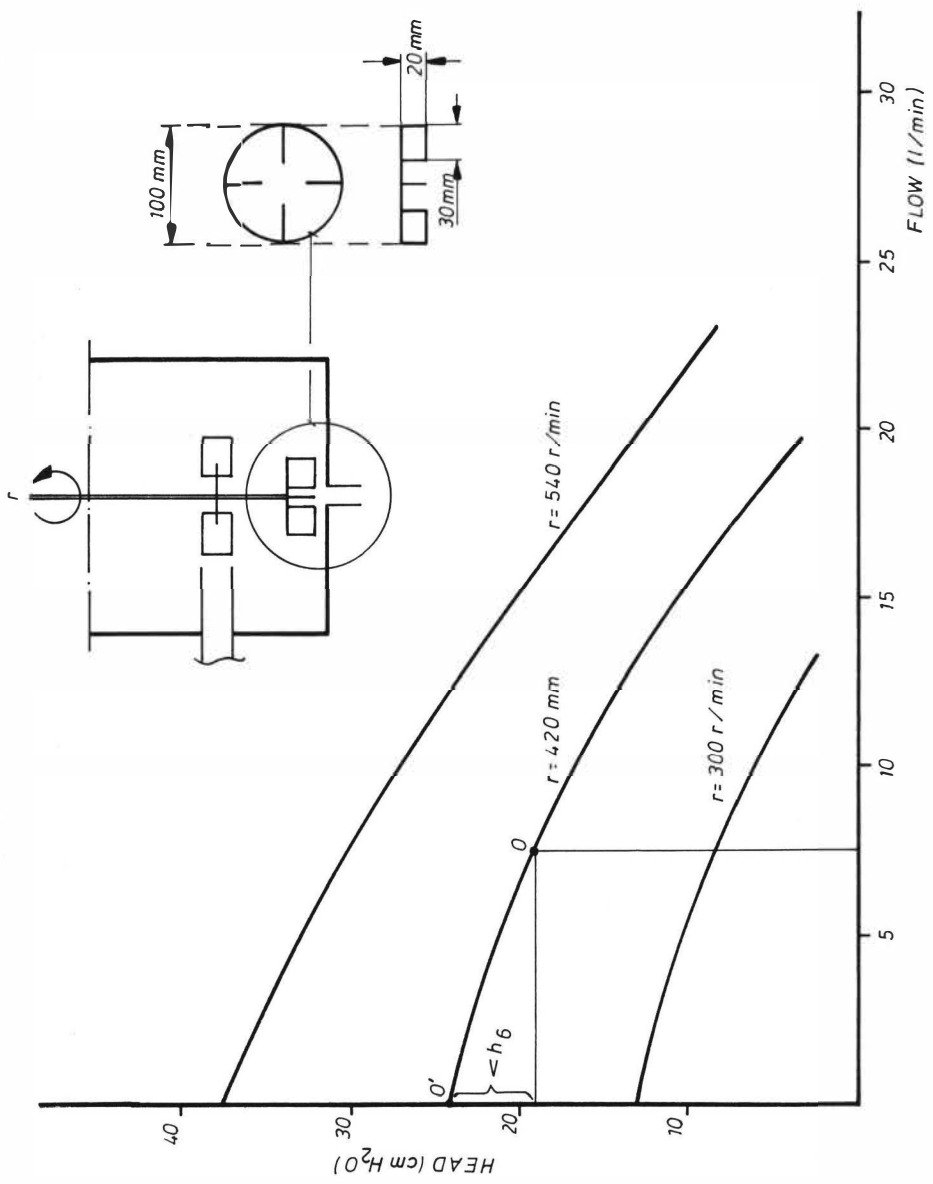
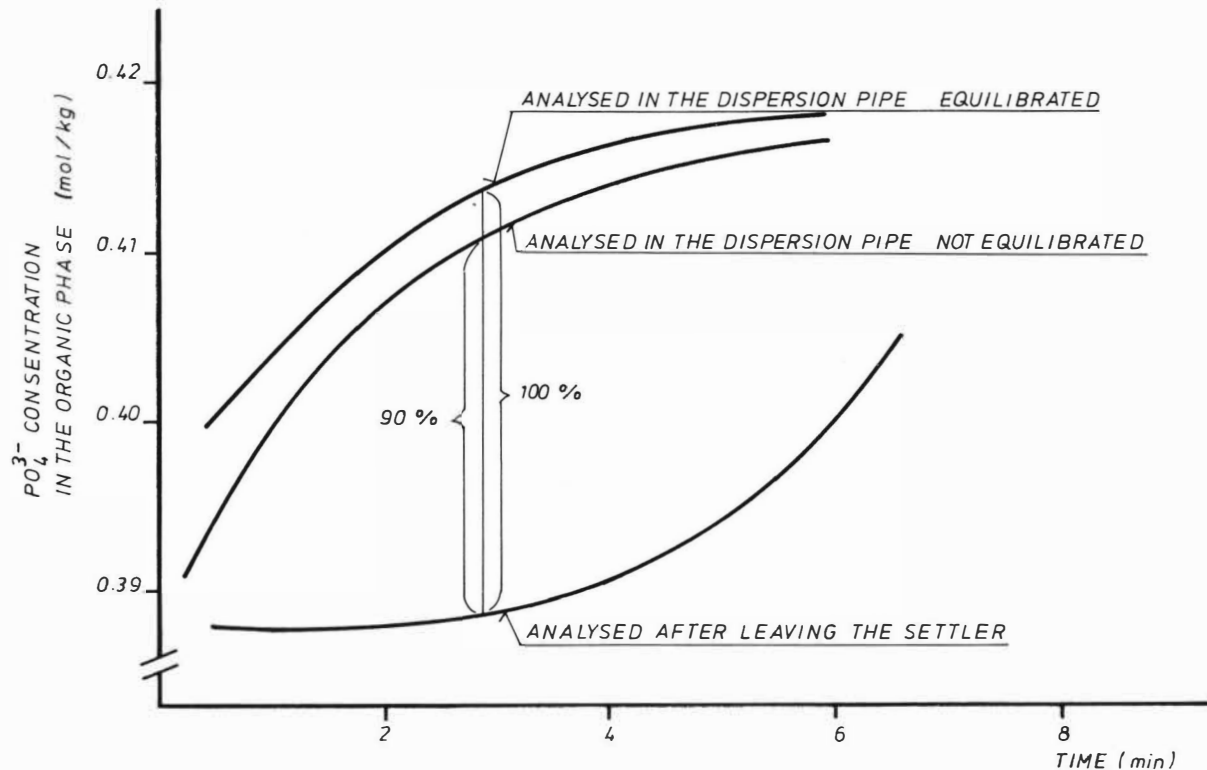


FIGURE 7

MASS TRANSFER DATA FOR A SINGLE STAGE

IV. The Cadman - Hsu model

Gharib S. Aly

Department of Chemical Engineering, University of Lund, Box 740,
S-220 07 Lund, Sweden.

Synopsis

A straightforward solution for the Cadman-Hsu model, allowing simulation of the dynamic behaviour of multi-stage mixer-settler extractors, is presented. The applicability of this solution was tested on copper extraction in a four-stage unit. Comparison of this model with a simpler one shows that chemical systems with fast kinetics can be described almost as well using the simple model.

1. INTRODUCTION

The present series of investigations on the dynamic behaviour of mixer-settlers is concerned with a theoretical and experimental examination of how well various simple mathematical models describe the dynamic behaviour of extractors of this type. A simpler model would have strong practical advantages. For many present extraction systems, it is necessary to restrict the complexity of the mathematical model describing the process, especially when the computer memory available is limited. Moreover many extraction processes in practice often contain loading, scrubbing and stripping sections which may further complicate computer simulation. If the solvents used in such processes are valuable or expensive, as in metal extractions, other unit operations such as distillation and evaporation will also be involved. A research team in the Department of Chemical Engineering at the University of Lund is engaged in developing generalised computer programs for the simulation of steady state and dynamic characteristics of some unit operations. The main overall goal of this project, of which the present investigation is a part, is to link together these computational programmes in order to simulate complete chemical processes.

Two different mathematical models describing the dynamic behaviour of mixer-settlers were presented earlier.^{1,2} These 4-input, 2-output linearised models have been thoroughly tested by two identification methods. In part II of this series¹ the experimental data used represented the response to different input signals with the inlet aqueous phase solute concentration as control variable. The identification was made on both the organic and the aqueous phase solute concentrations leaving the first stage of a 4-stage mixer-settler unit. In part III², the aqueous and organic phase flow rates were used as control variables while the response consisted of the outlet concentrations from the fourth stage. These two investigations showed good agreement between the theoretical and experimental responses, provided that the linearity assumption is not violated. It was concluded that these linearised simple models are adequate for simulating the dynamics of mixer-settler units when the chemical system in question possesses fast kinetics. The simplicity of these models is largely due to the fact that every mixer-settler stage is treated as a black-box with inlet and outlet streams. However, some of the assumptions were not sufficiently realistic to be easily accepted in practice.

Cadman and Hsu have recently presented a substantial theoretical dynamic study using a mathematical model based on more solid assumptions, which was separated into two parts, one describing the mixer, and the other describing the settler. This work was a thorough examination of the dynamics and control of multi-stage mixer-settler extractors using non-linear dynamic models based on instantaneous overall and component mass balances and on generalised liquid-liquid equilibrium relationships. The model was linearised and on solution using the Laplace transformation technique, yielded the frequency transfer functions of the multi-stage system. A two-stage mixer-settler unit with a hypothetical ternary extraction system was examined numerically. The method of solution was chosen with the primary objective of quantifying the steps of theoretical feedforward and feedback control design. Consequently the numerical solution in the frequency domain is too complex for complete analysis. It was the purpose of the present work to find an easier and more straightforward solution and to code this in a FORTRAN IV computing program simulating the dynamic behaviour of multi-stage mixer-settler systems. The program obtained has been used to compare theoretical results from the Cadman-Hsu model with the experimental responses of a four-stage mixer-settler unit. The experimental dynamic behaviour studies were made on the extraction of copper using Alamine 336⁵ and LIX 64N⁶.

2. Mathematical Models

Models for both variable and constant liquid levels in the mixer and settler were described by Cadman and Hsu.³ However only the constant level models were investigated in the present study. These models are based on the following assumptions:

- (i) perfect mixing
- (ii) 100% stage efficiency – any degree of approach to equilibrium in the system can be applied using pseudo-equilibrium diagrams, but 100% stage efficiency is assumed for simplicity
- (iii) negligible density variation with composition.

These assumptions imply that most of the assumptions specified in Part II¹ are relaxed, so that:

- (i) the liquids can be partially miscible
- (ii) the equilibrium relationship is not necessarily linear
- (iii) the flow rates change with time
- (iv) the hold-up volumes in the settler part can vary with stage number.

2.1 Mixer

Overall and component mass balances for the mixer shown in Figure 1 give the following equations

$$F_t(K) = L_t(K-1) + V_t(K+1) \quad (1)$$

$$H_m(K) \cdot (dZ_{A_t}(K)/dt) = X_{A_t}(K-1) \cdot L_t(K-1) + Y_{A_t}(K+1) \cdot V_t(K+1) - Z_{A_t}(K) \cdot F_t(K) \quad (2)$$

$$H_m(K) \cdot (dZ_{B_t}(K)/dt) = X_{B_t}(K-1) \cdot L_t(K-1) + Y_{B_t}(K+1) \cdot V_t(K+1) - Z_{B_t}(K) \cdot F_t(K) \quad (3)$$

2.2 Settler

Two different cases were investigated for the settler³

- (a) constant overall hold-up volume and constant internal hold-up volumes
- (b) constant overall hold-up volume and non-constant internal hold-up vols.

Only case (a) will be considered here. Case (b) is however also included in the computer program developed.⁶ Overall and component mass balances for the settler shown in Figure 2 yield the following equations

$$F_t(K) = V_t(K) + L_t(K) \quad (4)$$

$$Z A_t(K).F_t(K) = Y Z A_t(K).V_t(K) + X Z A_t(K).L_t(K) \quad (5)$$

$$Z B_t(K).F_t(K) = Y Z B_t(K).V_t(K) + X Z B_t(K).L_t(K) \quad (6)$$

$$H V(K).(d Y A_t(K)/dt) = [Y Z A_t(K) - Y A_t(K)].V_t(K) \quad (7)$$

$$H V(K).(d Y B_t(K)/dt) = [Y Z B_t(K) - Y B_t(K)].V_t(K) \quad (8)$$

$$H L(K).(d X A_t(K)/dt) = [X Z A_t(K) - X A_t(K)].L_t(K) \quad (9)$$

$$H L(K).(d X B_t(K)/dt) = [X Z B_t(K) - X B_t(K)].L_t(K) \quad (10)$$

2.3 Equilibrium relationships

Let us consider a ternary extraction system in which the feed solution consists of (A+B) where A is the solute. Component C is the extractant, i.e. the extract will contain only (A+C) if the liquids are immiscible and (A+C+B) if these are partially miscible.

The equilibrium relationships were considered for simplicity as second-order polynomial functions in the original models, but, as mentioned above, these can take any form. These are

$$Y C_t(K) = b_1 + b_2.Y A_t(K) + b_3.Y A_t^2(K) \quad (11)$$

$$X B_t(K) = c_1 + c_2.X A_t(K) + c_3.X A_t^2(K) \quad (12)$$

$$Y A_t(K) = a_1 + a_2.X A_t(K) + a_3.X A_t^2(K) \quad (13)$$

In a triangular diagram, the first two equations represent the solubility curves while the third equation represents the tie-line relationship using equilibrium concentrations for the solute A. Thus if $X A(K)$ is known, the remaining concentrations can be obtained directly.

3. Model Solution

Neglecting the mass balances for component C, there are 13 equations for every mixer-settler stage. Consequently, 13 unknowns can be evaluated by this model. These are:

$$L, X_A, X_B$$

$$V, Y_A, Y_B$$

$$F, Z_A, Z_B$$

$$Y_{ZA}, Y_{ZB}, X_{ZA}, X_{ZB}$$

The non-linear model can thus be solved exactly but it is better linearised around some steady state operating conditions. It was shown earlier^{1,2} that linearised models are adequate for simulation of the dynamics of such extractors.

3.1 Matrix notation

For convenience in presentation a matrix notation is used and the linearised time-invariant system is presented by a modified state model $S(A,B,C,D)$ defined by the equations

$$dX/dt = A.X + B.U$$

$$XVL = C.X + D.U$$

where

X = the state vector containing $6.n$ concentrations

U = the input vector containing 6 control variables

A = the dynamic matrix ($6.n \times 6.n$)

B = the input matrix ($6.n \times 6$)

XVL = a state vector containing $2.n$ flow rates

C = a $2.n \times 6.n$ matrix

D = a $2.n \times 6$ matrix

n = number of mixer-settler stages

3.2 Linearised model

If the above 13 equations are linearised taking into consideration only the first derivatives in the Taylor series expansion, then the following equations can be obtained:

$$F(K) = L(K-1) + V(K+1) \quad (14)$$

$$\begin{aligned} H_m(K). (dZA(K)/dt) &= XA(K-1). \overline{L}(K-1) + YA(K+1). \overline{V}(K+1) + \\ &+ [\overline{XA}(K-1) - \overline{ZA}(K)] . L(K-1) + [\overline{YA}(K+1) - \overline{ZA}(K)] . V(K+1) \\ &- ZA(K). \overline{F}(K) \end{aligned} \quad (15)$$

$$\begin{aligned} H_m(K). (dZB(K)/dt) &= XB(K-1). \overline{L}(K-1) + YB(K+1). \overline{V}(K+1) + \\ &+ [\overline{XB}(K-1) - \overline{ZB}(K)] . L(K-1) + [\overline{YB}(K+1) - \overline{ZB}(K)] . V(K+1) \\ &- ZB(K). \overline{F}(K) \end{aligned} \quad (16)$$

$$F(K) = V(K) + L(K) \quad (17)$$

$$ZA(K). \overline{F}(K) + F(K). \overline{ZA}(K) = \alpha(K) + \gamma(K) \quad (18)$$

$$ZB(K). \overline{F}(K) + F(K). \overline{ZB}(K) = \beta(K) + \delta(K) \quad (19)$$

$$HV(K). (dYA(K)/dt) = \alpha(K) - YA(K). \overline{V}(K) - V(K). \overline{YA}(K) \quad (20)$$

$$HV(K). (dYB(K)/dt) = \beta(K) - YB(K). \overline{V}(K) - V(K). \overline{YB}(K) \quad (21)$$

$$HL(K). (dXA(K)/dt) = \gamma(K) - XA(K). \overline{L}(K) - L(K). \overline{XA}(K) \quad (22)$$

$$HL(K). (dXB(K)/dt) = \delta(K) - XB(K). \overline{L}(K) - L(K). \overline{XB}(K) \quad (23)$$

$$YC(K) = DB(K). YA(K) \quad (24)$$

$$XB(K) = DC(K). XA(K) \quad (25)$$

$$YA(K) = DA(K). XA(K) \quad (26)$$

where

$$\alpha(K) = YZA(K). \overline{V}(K) + V(K). \overline{YZA}(K) \quad , \quad \gamma(K) = XZA(K). \overline{L}(K) + L(K). \overline{XZA}(K)$$

$$\beta(K) = YZB(K). \overline{V}(K) + V(K). \overline{YZB}(K) \quad , \quad \delta(K) = XZB(K). \overline{L}(K) + L(K). \overline{XZB}(K)$$

$$DB(K) = b_2 + 2b_3. \overline{YA}(K)$$

$$DC(K) = c_2 + 2c_3. \overline{XA}(K)$$

$$DA(K) = a_2 + 2a_3. \overline{XA}(K)$$

In the above equations, the superscript $\bar{}$ indicates the steady state value of the variable. Variables without superscript $\bar{}$ refer to deviations from steady state conditions, i.e.

$$L(K) = L_t(K) - \bar{L}(K)$$

where $\bar{L}(K)$ is the steady state value of the aqueous phase flow rate from stage number K.

3.3 Solution of linearised model for one stage

The solution procedure presented by Cadman and Hsu was chosen³ so that after Laplace transformation of the linearised equations it allowed the derivation of overall transfer functions for a mixer, a settler, for one stage, for two stages, and finally for any number of stages.⁴ Because of the complexity of the model, the overall transfer functions were obtained by numerical calculations in the frequency domain. It should however be mentioned here that thirty six such functions are required to completely specify a two-stage mixer-settler system.

In the present work, the number of state variables is reduced from 13 to 6 in order to simplify the model, especially for systems with more than two stages. The variables which will be eliminated are the concentrations XZA, XZB, YZA and YZB and the flow rates L, V and F.

The elimination procedure is given in Appendix 1 and the final result can be written for stage number K shown in Figure 3 in the form (see section 3.1):

$$dX(K)/dt = A(K).X(K) + B(K).U(K) \quad (27)$$

$$XVL(K) = C(K).X(K) + D(K).U(K) \quad (28)$$

where

$$A(K) = \begin{bmatrix} x & 0 & 0 & 0 & 0 & 0 \\ 0 & x & 0 & 0 & 0 & 0 \\ x & x & x & 0 & 0 & 0 \\ x & x & 0 & x & 0 & 0 \\ x & x & 0 & 0 & x & 0 \end{bmatrix}, \quad B(K) = \begin{bmatrix} \overbrace{x \ x \ 0}^{\tau_1(K)} & \overbrace{x \ x \ 0}^{\tau_2(K)} \\ x \ 0 \ x & x \ 0 \ x \\ x \ 0 \ 0 & x \ 0 \ 0 \\ x \ 0 \ 0 & x \ 0 \ 0 \\ x \ 0 \ 0 & x \ 0 \ 0 \\ \underbrace{x \ 0 \ 0}_{\omega_1(K)} & \underbrace{x \ 0 \ 0}_{\omega_2(K)} \end{bmatrix}$$

$$C(K) = \begin{bmatrix} x & x & x & | & 0 & 0 & 0 \\ x & x & x & | & 0 & 0 & 0 \end{bmatrix}, \quad D(K) = \begin{bmatrix} x & 0 & 0 & | & x & 0 & 0 \\ x & 0 & 0 & | & x & 0 & 0 \end{bmatrix}$$

$$X(K) = \begin{bmatrix} ZA(K) \\ ZB(K) \\ XA(K) \\ XB(K) \\ YA(K) \\ YB(K) \end{bmatrix}, \quad U(K) = \begin{bmatrix} L(K-1) \\ XA(K-1) \\ XB(K-1) \\ V(K+1) \\ YA(K+1) \\ YB(K+1) \end{bmatrix}, \quad XVL(K) = \begin{bmatrix} V(K) \\ L(K) \end{bmatrix}$$

where

0 represents zero elements

x represents non-zero elements

3.4 Solution of the linearised model for two stages

For the second stage, stage number (K+1), of the extraction system shown in Figure 4, equations (27) and (28) are written as

$$dX(K+1)/dt = A(K+1).X(K+1) + B(K+1).U(K+1) \quad (29)$$

$$XVL(K+1) = C(K+1).X(K+1) + D(K+1).U(K+1) \quad (30)$$

where the input vector $U(K+1)$ contains the following elements

$$U(K+1) = \begin{bmatrix} L(K) \\ XA(K) \\ XB(K) \\ V(K+2) \\ YA(K+2) \\ YB(K+2) \end{bmatrix}$$

In order to link together the two stages, the intermediate flow rates $L(K)$ and $V(K+1)$ must be eliminated since the input vector contains only 6 elements representing the inlet streams to the system, i.e. $L(K)$ and $V(K+2)$. The detailed derivation of this elimination is reported in the literature,⁷ and will not be repeated here. The elements of the system matrices are however given in Appendix 2. The resulting system can be written as:

$$dX/dt = A.X + B.U$$

$$XVL = C.X + D.U$$

where

$$A = \begin{bmatrix} A(K) & \begin{bmatrix} 0 & 0 & \omega_2(K) \end{bmatrix} \\ \begin{bmatrix} 0 & \omega_1(K+1) & 0 \end{bmatrix} & A(K+1) \end{bmatrix} + \begin{bmatrix} \begin{bmatrix} x & x & x \\ x & x & x \\ x & x & x \\ x & x & x \\ x & x & x \\ x & x & x \end{bmatrix} & 0 & \begin{bmatrix} x & x & x \\ x & x & x \\ x & x & x \\ x & x & x \\ x & x & x \\ x & x & x \end{bmatrix} & 0 \\ 0 & 0 & 0 & 0 \end{bmatrix} \quad (31)$$

A' AL
 $(6n \times 6n)$ $(6n \times 6n)$

$$B = \begin{bmatrix} \begin{bmatrix} \tau_1(K) & 0 \end{bmatrix} \\ 0 & \begin{bmatrix} \tau_2(K+1) \end{bmatrix} \end{bmatrix} + \begin{bmatrix} \begin{bmatrix} x & x \\ x & x \\ x & x \\ x & x \end{bmatrix} & \begin{bmatrix} x & x \\ x & x \\ x & x \\ x & x \end{bmatrix} \\ \begin{bmatrix} x & x \\ x & x \\ x & x \\ x & x \end{bmatrix} & \begin{bmatrix} x & x \\ x & x \\ x & x \\ x & x \end{bmatrix} \end{bmatrix}, \quad X = \begin{bmatrix} X(K) \\ X(K+1) \end{bmatrix} \quad (32)$$

B' BL X
 $(6n \times 6)$ $(6n \times 6)$ $(6n \times 1)$

$$C = \begin{bmatrix} \begin{bmatrix} x & x & x \\ x & x & x \\ x & x & x \\ x & x & x \end{bmatrix} & 0 & \begin{bmatrix} x & x & x \\ x & x & x \\ x & x & x \\ x & x & x \end{bmatrix} & 0 \end{bmatrix}, \quad U = \begin{bmatrix} L(K-1) \\ XA(K-1) \\ XB(K-1) \\ V(K+2) \\ YA(K+2) \\ YB(K+2) \end{bmatrix} \quad (33)$$

$(2n \times 6n)$ (6×1)

$$D = \begin{bmatrix} x & 1x & & & \\ x & 1x & & & \\ x & 0 & 1x & & 0 \\ x & & 1x & & \\ x & & 1x & & \end{bmatrix}, \quad XVL = \begin{bmatrix} V(K) \\ L(K) \\ V(K+1) \\ L(K+1) \end{bmatrix} \quad (34)$$

(2nx6) (2nx1)

where

- 0 represents zero elements
- x represents non-zero elements

The elements of the above matrices are given in Appendix 2 for a two-stage unit.

3.5 Solution of the linearised model for multi-stage systems

As in the above equations, the system matrices can be systematically expanded for any number of stages. Multi-stage systems are illustrated by the presentation below for a four-stage system showing matrices A' and B' only. The elements of these matrices are given in Appendix 2.

$$A' = \begin{bmatrix} A(K) & 0 & \omega_2(K) & 0 & 0 \\ 0 & \omega_1(K+1) & 0 & A(K+1) & 0 & \omega_2(K+1) & 0 \\ 0 & 0 & A(K+2) & 0 & \omega_2(K+2) \\ 0 & 0 & \omega_1(K+3) & 0 & A(K+3) \end{bmatrix}, \quad B' = \begin{bmatrix} \tau_1(K) & 0 \\ 0 & 0 \\ 0 & 0 \\ 0 & \tau_2(K+3) \end{bmatrix}$$

4. Results

Two numerical examples illustrating the application and applicability of the model and the simplicity of the solution are presented below.

4.1 Numerical example No.1

The model was tested on a two-stage mixer-settler unit with the ternary system³ ethylene glycol - n-amyl alcohol - water. In this system, ethylene glycol is the solute, A, and water is the solvent, C. This means that the light phase was chosen as the raffinate and the heavy phase as the extract. Equilibrium data for this system is available in the literature,⁸ and was used to determine the polynomial coefficients of the equations (11), (12) and (13). Diagrammatically, this system is presented here in the form of a triangular diagram (Figure 5) and an equilibrium curve (Figure 6).

The steady state values of the intermediate and outlet streams can be iteratively calculated if the inlet streams to the system are fixed. This calculation is done by using the steady state material balances, both stagewise and overall.

The selected input variables (streams L(1) and V(4)), output variables (streams L(3) and V(2)) as well as the calculated steady state values are summarized in Figure 7.

Two input signals in the form of small variations around the steady state operating conditions of the process were used to test the dynamic behaviour of the system. The responses to the first input signal, a step change in $XA(1)$, are plotted in Figure 8. The system responses to the second input signal, a step change in $YA(4)$, are shown in Figure 9.

As can be seen from these two figures, the "hypothetical" experiment was chosen to last for 60 minutes. A comparison of the solution method presented by Cadman and Hsu³ and that adopted in the present work is shown in Figures 10 and 11. Since only the early response period was given by Cadman and Hsu Figures 10 and 11 show the first minutes of the experiment for both cases. It should be pointed out that the difference between the two methods, although very small, is probably due to the accuracy with which the responses were read. Points on the Cadman and Hsu curves were obtained from photographic enlargements and fed to the computer system. This redetermination of points from the published curves involves some sources of uncertainty which will decrease accuracy.

4.2 Numerical example No.2

Copper extraction by Alamine 336 in a four-stage mixer-settler unit⁵ is used in this example to test the reliability of the model. This experiment, which consists of two input signals in the form of instantaneous step changes in both the inlet aqueous phase flow rate (-10%) and the inlet organic phase flow rate (+10%), has been reported earlier² and is not repeated here. The model outputs, model errors, input signals and experimental outputs are shown in Figure 12. A comparison between the results obtained from this complicated model and those obtained from the simpler model², is shown in Figure 13. This shows the close resemblance between the two models. This resemblance is not surprising because in the Cadman-Hsu model discussed here (where the hold-ups of both light and heavy phases are constant) the dynamic effect of the feed stream, F , from the mixer is not amplified in the settler, since

$$V' = V, \quad L' = L \quad (35)$$

5. Conclusions

From the simulation results presented above, especially in Figure 13, it can be seen that the complicated Cadman-Hsu model has shown similar static and dynamic characteristics to one of the simple models presented in Part III of this series². Thus it can be concluded that both models give similar results for chemical systems with fast kinetics.

Part V in this series⁶ will include an analysis of the model for copper extraction with LIX 64N.

Acknowledgements

The author is greatly indebted to Professor A.Jernqvist, Head of the Chemical Engineering Department at the University of Lund, for his encouraging support and invaluable help during the course of this work. I would also like to express my sincere gratitude to Mr A.Axelsson for his fruitful cooperation, during the work on his M.Sc. in the Department, as well as the computational work involved in this study. The financial support of this project by the Swedish Board for Technical Development is gratefully acknowledged.

References

1. Aly, G.; Wittenmark, B. *J. appl. Chem. Biotechnol.* 1972, 22, 1165.
2. Aly, G.; Ottertun, H. *J. appl. Chem. Biotechnol.* 1973, 23, 643.
3. Cadman, T.W; Hsu, C.K. *Trans. Instn Chem. Engrs* 1970, 48, T209.
4. Hsu, C.K. *Trans. Instn Chem. Engrs* 1971, 49, 251.
5. Aly, G.; Jernqvist, A.; Reinhardt, H.; Ottertun, H. *Chem Ind.* 1971, 1046.
6. Aly, G. To be published.
7. Axelsson, A. M.Sc. Thesis, Department of Chemical Engineering, University of Lund. *Simulation of Dynamics in a Mixer-Settler Unit* (In Swedish), 1973.
8. Jaswon, M.A.; Smith, W. *Proc.R.Soc.*, 1954, 225, A226.

Appendix 1

Elimination of the concentrations XZA, XZB, YZA and YZB

These concentrations are eliminated by substituting expressions obtained for $\alpha(K)$, $\beta(K)$, $\gamma(K)$ and $\delta(K)$ from equations (20), (21), (22) and (23) respectively in equations (18) and (19). These will then take the following form, the index K being dropped for simplicity:

$$ZA.\bar{F} + F.\bar{ZA} = [HV.(dYA/dt) + YA.\bar{V} + V.\bar{YA}] + [HL.(dXA/dt) + XA.\bar{L} + L.\bar{XA}] \quad (36)$$

$$ZB.\bar{F} + F.\bar{ZB} = [HV.(dYB/dt) + YB.\bar{V} + V.\bar{YB}] + [HL.(dXB/dt) + XB.\bar{L} + L.\bar{XB}] \quad (37)$$

It follows from equations (25) and (26) that

$$XB = DC.XA \quad \text{thus} \quad dXB/dt = DC.(dXA/dt) \quad (38)$$

$$YA = DA.XA \quad \text{thus} \quad dYA/dt = DA.(dXA/dt) \quad (39)$$

From equation (11) it can be easily seen that

$$YB = DD.XA \quad \text{thus} \quad dYB/dt = DD.(dXA/dt) \quad (40)$$

where

$$DD = - (1 + DB).DA$$

Substituting equation (17) together with the above relationships in equations (36) and (37) one can get

$$(HV.DA + HL).(dXA/dt) + (DA.\bar{V} + \bar{L}).XA + (\bar{YA} - \bar{XA}).V + (\bar{XA} - \bar{ZA}).F - ZA.\bar{F} = 0 \quad (41)$$

$$(HV.DD + HL.DC).(dXA/dt) + (DD.\bar{V} + \bar{L}.DC).XA + (\bar{YB} - \bar{XB}).V + (\bar{XB} - \bar{ZB}).F - XB.\bar{F} = 0 \quad (42)$$

Using equations (41) and (42) we may extract dXA/dt and V as linear functions of the four variables XA , ZA , ZB and F . Thus

$$dXA/dt = R(1).ZA + R(2).ZB + R(3).XA + R(4).F \quad (43)$$

$$V = Q(1).ZA + Q(2).ZB + Q(3).XA + Q(5).F \quad (44)$$

Equation (17) can be used once again to yield

$$L = - Q(1).ZA - Q(2).ZB - Q(3).XA + Q(4).F \quad (45)$$

where

$$R(1) = - [\bar{Y}B - \bar{X}B] \cdot \bar{F}/K3$$

$$R(2) = [\bar{Y}A - \bar{X}A] \cdot \bar{F}/K3$$

$$R(3) = - 1/K2$$

$$R(4) = [(\bar{Y}A - \bar{X}A)(\bar{Z}B - \bar{X}B) - (\bar{Y}B - \bar{X}B)(\bar{Z}A - \bar{X}A)]/K3$$

$$Q(1) = (HV.DD + HL.DC) \cdot \bar{F}/K3$$

$$Q(2) = - (HV.DA + HL) \cdot \bar{F}/K3$$

$$Q(3) = [(DD.\bar{V} + DC.\bar{L})(HV.DA + HL) - (DA.\bar{V} + \bar{L})(HV.DD + HL.DC)] \cdot K3$$

$$Q(4) = [(\bar{Y}A - \bar{Z}A)(HV.DD + HL.DC) - (\bar{Y}B - \bar{Z}B)(HV.DA + HL)]/K3$$

$$Q(5) = - (\bar{X}A - \bar{Z}A)(HV.DD + HL.DC) - (\bar{X}B - \bar{Z}B)(HV.DA + HL) /K3$$

$$K1 = (\bar{Y}A - \bar{X}A)(DD.\bar{V} + DC.\bar{L}) - (\bar{Y}B - \bar{X}B)(DA.\bar{V} + \bar{L})$$

$$K2 = K3/K1$$

$$K3 = (\bar{Y}A - \bar{X}A)(HV.DD + HL.DC) - (\bar{Y}B - \bar{X}B)(HV.DA + HL)$$

It should be observed that $Q(4) + Q(5) = 1$ for every stage in the mixer-settler unit.

The system has been reduced from 13 to 6 equations, by eliminating L, V, F, XZA, XZB, YZA and YZB. This enable us to obtain the final form of the system matrices by replacing the variable F in equation (43) using equation (14) and then substituting in equations (38), (39) and (40) to obtain expressions for (dXB/dt) , (dYA/dt) and (dYB/dt) respectively. Expressions for the remaining concentrations (dZA/dt) and (dZB/dt) are obtained from equations (15) and (16). The index K can now be retained and the system is written in the following way:

$$\begin{aligned} dZA(K)/dt = & M(K).ZA(K) + MA(K,1).L(K-1) + MA(K,2).XA(K-1) + \\ & + MA(K,4).V(K+1) + MA(K,5).YA(K+1) \end{aligned} \quad (46)$$

$$\begin{aligned} dZB(K)/dt = & M(K).ZB(K) + MB(K,1).L(K-1) + MB(K,3).XB(K-1) + \\ & + MB(K,4).V(K+1) + M(K,6).YB(K+1) \end{aligned} \quad (47)$$

$$\begin{aligned} dXA(K)/dt = & R(K,1).ZA(K) + R(K,2).ZB(K) + R(K,3).XA(K) + \\ & + R(K,4).[L(K-1) + V(K+1)] \end{aligned} \quad (48)$$

$$\begin{aligned} dXB(K)/dt = & DC(K).R(K,1).ZA(K) + DC(K).R(K,2).ZB(K) + \\ & + R(K,3).XB(K) + DC(K).R(K,4).[L(K-1) + V(K+1)] \end{aligned} \quad (49)$$

$$\begin{aligned} dYA(K)/dt = & DA(K).R(K,1).ZA(K) + DA(K).R(K,2).ZB(K) + \\ & + R(K,3).YA(K) + DA(K).R(K,4).[L(K-1) + V(K+1)] \end{aligned} \quad (50)$$

$$\begin{aligned} dYB(K)/dt = & DD(K).R(K,1).ZA(K) + DD(K).R(K,2).ZB(K) + \\ & + R(K,3).YB(K) + DD(K).R(K,4).[L(K-1) + V(K+1)] \end{aligned} \quad (51)$$

where

$$\begin{aligned} M(K) &= -\bar{F}(K)/H_m(K) \\ MA(K,1) &= (\bar{XA}(K-1) - \bar{ZA}(K))/H_m(K) & MB(K,1) &= (\bar{XB}(K-1) - \bar{ZB}(K))/H_m(K) \\ MA(K,2) &= (\bar{L}(K-1))/H_m(K) & MB(K,2) &= 0 \\ MA(K,3) &= 0 & MB(K,3) &= (\bar{L}(K-1))/H_m(K) \\ MA(K,4) &= (\bar{YA}(K+1) - \bar{ZA}(K))/H_m(K) & MB(K,4) &= (\bar{YB}(K+1) - \bar{ZB}(K))/H_m(K) \\ MA(K,5) &= (\bar{V}(K+1))/H_m(K) & MB(K,5) &= 0 \\ MA(K,6) &= 0 & MB(K,6) &= (\bar{V}(K+1))/H_m(K) \end{aligned}$$

The system matrices

$$\begin{aligned} A(K) &= \begin{bmatrix} M(K) & 0 & 0 & 0 & 0 & 0 \\ 0 & M(K) & 0 & 0 & 0 & 0 \\ R(K,1) & R(K,2) & R(K,3) & 0 & 0 & 0 \\ DC(K).R(K,1) & DC(K).R(K,2) & 0 & R(K,3) & 0 & 0 \\ DA(K).R(K,1) & DA(K).R(K,2) & 0 & 0 & R(K,3) & 0 \\ DD(K).R(K,1) & DD(K).R(K,2) & 0 & 0 & 0 & R(K,3) \end{bmatrix} \\ B(K) &= \begin{bmatrix} MA(K,1) & MA(K,2) & 0 & MA(K,4) & MA(K,5) & 0 \\ MB(K,1) & 0 & MB(K,3) & MB(K,4) & 0 & MB(K,6) \\ R(K,4) & 0 & 0 & R(K,4) & 0 & 0 \\ DC(K).R(K,4) & 0 & 0 & DC(K).R(K,4) & 0 & 0 \\ DA(K).R(K,4) & 0 & 0 & DA(K).R(K,4) & 0 & 0 \\ DD(K).R(K,4) & 0 & 0 & DD(K).R(K,4) & 0 & 0 \end{bmatrix} \end{aligned}$$

$$C(K) = \begin{bmatrix} Q(K,1) & Q(K,2) & Q(K,3) & 0 & 0 & 0 \\ -Q(K,1) & -Q(K,2) & -Q(K,3) & 0 & 0 & 0 \end{bmatrix}^*$$

$$D(K) = \begin{bmatrix} Q(K,5) & 0 & 0 & Q(K,5) & 0 & 0 \\ Q(K,4) & 0 & 0 & Q(K,4) & 0 & 0 \end{bmatrix}$$

Appendix 2

It is to be noticed that unmentioned matrix elements throughout this Appendix are zero elements.

Elements of matrix A'

$$A'(K+1, K+1) = A'(K+2, K+2) = -\overline{F}(I)/H_m(I)$$

$$A'(K+3, K+1) = -(\overline{YB}(I) - \overline{XB}(I)) \cdot \overline{F}(I)/K3(I)$$

$$A'(K+4, K+1) = DC(I) \cdot A'(K+3, K+1)$$

$$A'(K+5, K+1) = DA(I) \cdot A'(K+3, K+1)$$

$$A'(K+6, K+1) = DD(I) \cdot A'(K+3, K+1)$$

$$A'(K+3, K+2) = (\overline{YA}(I) - \overline{XA}(I)) \cdot \overline{F}(I)/K3(I)$$

$$A'(K+4, K+2) = DC(I) \cdot A'(K+3, K+2)$$

$$A'(K+5, K+2) = DA(I) \cdot A'(K+3, K+2)$$

$$A'(K+6, K+2) = DD(I) \cdot A'(K+3, K+2)$$

$$A'(K+3, K+3) = A'(K+4, K+4) = A'(K+5, K+5) = A'(K+6, K+6) = -1/K2(I)$$

$$A'(J-5, J+5) = A'(J-4, J+6) = \overline{V}(I)/H_m(I-1)$$

$$A'(J+1, J-3) = A'(J+2, J-2) = \overline{L}(I-2)/H_m(I-1)$$

The values of the indices K, I and J are tabulated below.

No of stages	J	K	I
1		0	2
2	6	0	2
		6	3
3	6 12	0	2
		6	3
		12	4
4	6 12 18	0	2
		6	3
		12	4
		18	5

Table 1. Values of indices in matrix A'.

and so on

Elements of matrix B'

$$\begin{aligned}
 B'(1,1) &= (\overline{XA}(1) - \overline{ZA}(2))/H_m(2) \\
 B'(2,1) &= (\overline{XB}(1) - \overline{ZB}(2))/H_m(2) \\
 B'(3,1) &= [(\overline{YA}(2) - \overline{XA}(2)). (\overline{ZB}(2) - \overline{XB}(2)) - \\
 &\quad (\overline{YB}(2) - \overline{XB}(2)). (\overline{ZA}(2) - \overline{XA}(2))]/K3(2) \\
 B'(4,1) &= DC(2). \quad B'(3,1) \\
 B'(5,1) &= DA(2). \quad B'(3,1) \\
 B'(6,1) &= DD(2). \quad B'(3,1) \\
 B'(1,2) &= B'(2,3) = \overline{C}(1)/H_m(2) \\
 \\
 B'(K+1,4) &= (\overline{YA}(I+1) - \overline{ZA}(I))/H_m(I) \\
 B'(K+2,4) &= (\overline{YB}(I+1) - \overline{ZB}(I))/H_m(I) \\
 B'(K+3,4) &= [(\overline{YA}(I) - \overline{XA}(I)). (\overline{ZB}(I) - \overline{XB}(I)) - \\
 &\quad (\overline{YB}(I) - \overline{XB}(I)). (\overline{ZA}(I) - \overline{XA}(I))]/K3(I) \\
 B'(K+4,4) &= DC(I). \quad B'(K+3,4) \\
 B'(K+5,4) &= DA(I). \quad B'(K+3,4) \\
 B'(K+6,4) &= DD(I). \quad B'(K+3,4) \\
 B'(K+1,5) &= B'(K+2,6) = \overline{V}(I+1)/H_m(I)
 \end{aligned}$$

The values of the indices K and I are tabulated below.

No of stages	1	2	3	4	-	-	-	-	-
I	2	3	4	5	-	-	-	-	-
K	0	6	12	18	-	-	-	-	-

Table 2. Values of indices in matrix B'

Elements of matrix C

$$C(1,I) = Q(1,I) \cdot Q(2,4)$$

$$C(2,I) = - Q(1,I)$$

$$C(3,I) = - Q(1,I) \cdot Q(2,5)$$

$$C(4,I) = - Q(1,I) \cdot Q(2,4)$$

$$C(1,J) = Q(2,I) \cdot Q(1,5)$$

$$C(2,J) = Q(2,I) \cdot Q(1,4)$$

$$C(3,J) = Q(2,I)$$

$$C(4,J) = - Q(2,I) \cdot Q(1,5)$$

Values of I are 1,2 and 3 while those of J are (I+6)

Elements of matrix D

$$D(1,1) = Q(1,5)$$

$$D(2,1) = Q(1,4)$$

$$D(3,1) = Q(1,4) \cdot Q(2,5)$$

$$D(4,1) = Q(1,4) \cdot Q(2,4)$$

$$D(1,4) = Q(1,5) \cdot Q(2,5)$$

$$D(2,4) = Q(1,4) \cdot Q(2,5)$$

$$D(3,4) = Q(2,5)$$

$$D(4,4) = Q(2,4)$$

Elements of matrices C and D will be divided throughout by the factor $(1 - Q(1,4) \cdot Q(2,5))$:

Elements of matrices AL and BL

$$AL(1,I) = C(3,I) \cdot BM(1,2)$$

$$AL(2,I) = C(3,I) \cdot BM(2,2)$$

$$AL(3,I) = C(3,I) \cdot BM(3,2)$$

$$AL(4,I) = C(3,I) \cdot BM(4,2)$$

$$AL(5,I) = C(3,I) \cdot BM(5,2)$$

$$AL(6,I) = C(3,I) \cdot BM(6,2)$$

$$AL(7,I) = C(2,I) \cdot AM(1,2)$$

$$AL(8,I) = C(2,I) \cdot AM(2,2)$$

$$AL(9,I) = C(2,I) \cdot AM(3,2)$$

$$AL(10,I) = C(2,I) \cdot AM(4,2)$$

$$AL(11,I) = C(2,I) \cdot AM(5,2)$$

$$AL(12,I) = C(2,I) \cdot AM(6,2)$$

where the index I takes the values 1,2,...12. The elements of matrix BL are obtained from those of AL by replacing AL and C by BL and D respectively while the index I in this case will take the values 1,2,...6. In these elements, the values of matrices BM and AM are as follows.

$$BM(1,I) = (\overline{YA}(I+1) - \overline{ZA}(I))/H_m(I)$$

$$BM(2,I) = (\overline{YB}(I+1) - \overline{ZB}(I))/H_m(I)$$

$$BM(3,I) = [(\overline{YA}(I) - \overline{XA}(I)) \cdot (\overline{ZB}(I) - \overline{XB}(I)) - (\overline{YB}(I) - \overline{XB}(I)) \cdot (\overline{ZA}(I) - \overline{XA}(I))] / K3(I)$$

$$BM(4,I) = DC(I) \cdot BM(3,I)$$

$$BM(5,I) = DA(I) \cdot BM(3,I)$$

$$BM(6,I) = DD(I) \cdot BM(3,I)$$

$$AM(1,I) = (\overline{XA}(I-1) - \overline{ZA}(I))/H_m(I)$$

$$AM(2,I) = (\overline{XB}(I-1) - \overline{ZB}(I))/H_m(I)$$

$$AM(L,I) = BM(L,I) \quad \text{for } L = 3,4,5 \text{ and } 6$$

In these elements, which originate from the B' matrix, the index $I = 2$ for 2 stages.

Appendix 3

List of symbols

A, B, C	Components in ternary liquid system; ethylene glycol, n-amyl alcohol, and water respectively in numerical example No. 1
A, B, C, D	System matrices defined in equations (27) and (28)
A', B'	Matrices defined in equations (31) and (32) respectively
a_1, a_2, a_3	Polynomial coefficients, equation (13)
b_1, b_2, b_3	Polynomial coefficients, equation (11)
c_1, c_2, c_3	Polynomial coefficients, equation (12)
AL, BL	Matrices defined in equations (31) and (32) respectively
AM, BM	Matrix elements defined in Appendix 2
DA, DB, DC, DD	Constants defined in equations (24), (25), (26) and (40) respectively
H_m	Mixer hold-up
K	Stage number
K1, K2, K3	Constants defined in Appendix 1
MA, MB	Matrix elements defined after equation (51)
n	Number of stages
Q, R	Matrix elements defined after equation (45)
t	Time
U	Input vector, defined in equation (27) and (28)
X, XVL	State vectors defined in equations (27) and (28)

Time varying quantities (subscript t)

F	Exit stream from mixer
HL	Hold-up of heavy phase in settler
HV	Hold-up of light phase in settler
h_l	liquid height in heavy phase of settler
h_v	liquid height in light phase of settler
L	Exit heavy phase stream from settler
L'	Portion of exit stream from mixer entering heavy phase of settler
V	Exit light phase stream from settler
V'	Portion of exit stream from mixer entering light phase of settler
$\left. \begin{matrix} XA \\ XB \\ XC \end{matrix} \right\}$	Heavy phase concentrations from settler
$\left. \begin{matrix} XZA \\ XZB \\ XZC \end{matrix} \right\}$	Concentrations of stream L'
$\left. \begin{matrix} YA \\ YB \\ YC \end{matrix} \right\}$	Light phase concentrations from settler
$\left. \begin{matrix} YZA \\ YZB \\ YZC \end{matrix} \right\}$	Concentrations of stream V'
$\left. \begin{matrix} ZA \\ ZB \\ ZC \end{matrix} \right\}$	Concentrations of exit stream from mixer

Superscripts

—	Steady state value
---	--------------------

- Figure 1 : The mixer in stage number K
- Figure 2 : The settler in stage number K
- Figure 3 : Mixer-settler stage number K
- Figure 4 : Schematic diagram of a two-stage mixer-settler unit
- Figure 5 : Triangular diagram for the system ethylene glycol – n-amyl alcohol – water^a
- Figure 6 : Equilibrium curve for the system ethylene glycol – n-amyl alcohol – water^a
- Figure 7 : Steady state values in numerical example No.1
Concentrations in weight fraction, flow rates in kg/min and hold-ups in kg
- Figure 8 : Results of numerical example No.1
(a) input step signal in XA(1)
(b) model outputs, extract phase concentrations
(c) model outputs, raffinate phase concentrations
(d) model outputs, flow rates
- Figure 9 : Results of numerical example No.1
(a) input step signal in YA(4)
(b) model outputs, extract phase concentrations
(c) model outputs, raffinate phase concentrations
(d) model outputs, flow rates
- Figure 10 : Comparison between Cadman-Hsu and present work
Input: step signal in XA(1)
- Figure 11 : Comparison between Cadman-Hsu and present work
Input: step signal in YA(4)

Figure 12 : Results of numerical example No.2:

- (a) input step signals
- (b) experimental and theoretical outputs
- (c) model error (organic phase)
- (d) model error (aqueous phase)

Figure 13 : Comparison between Cadman-Hsu and the simple model²

- (a) input step signals
- (b) theoretical outputs
- (c) difference between the two models (organic phase)
- (d) difference between the two models (aqueous phase)

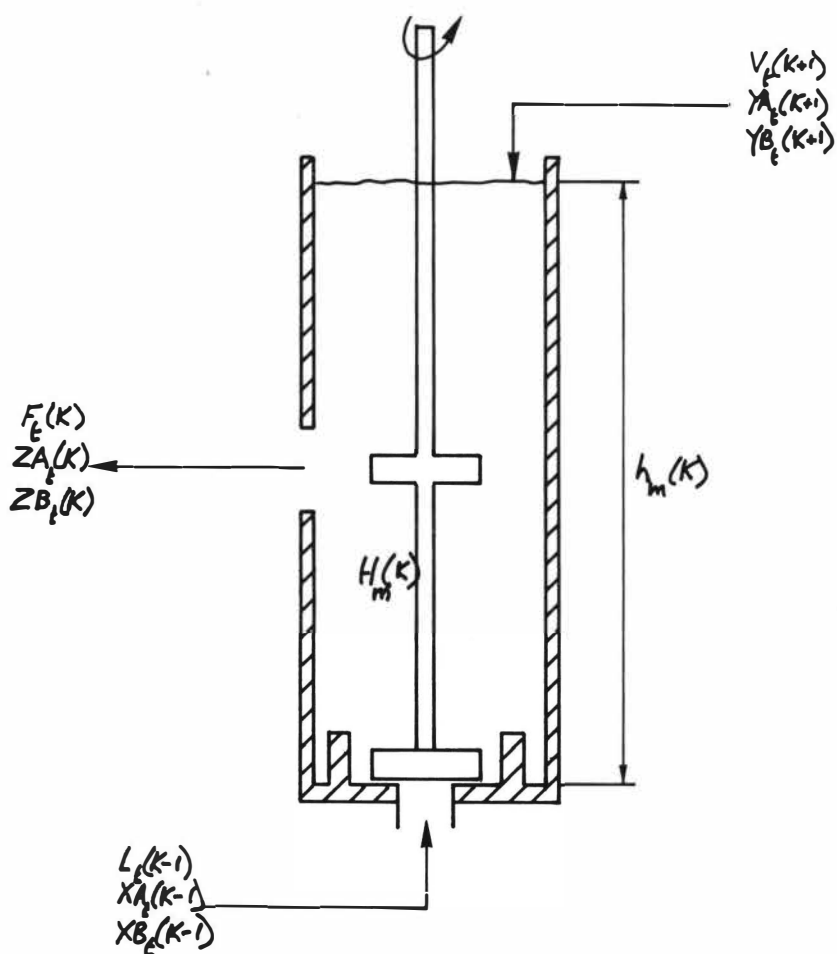


Fig.1 K^{th} STAGE : Dynamic Behaviour of Mixer-Settlers

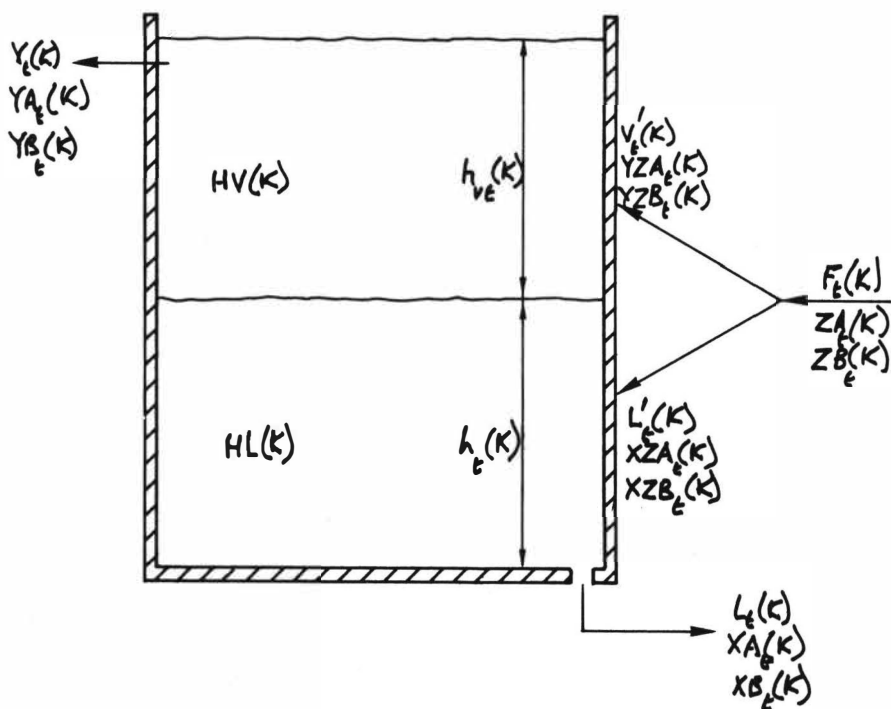
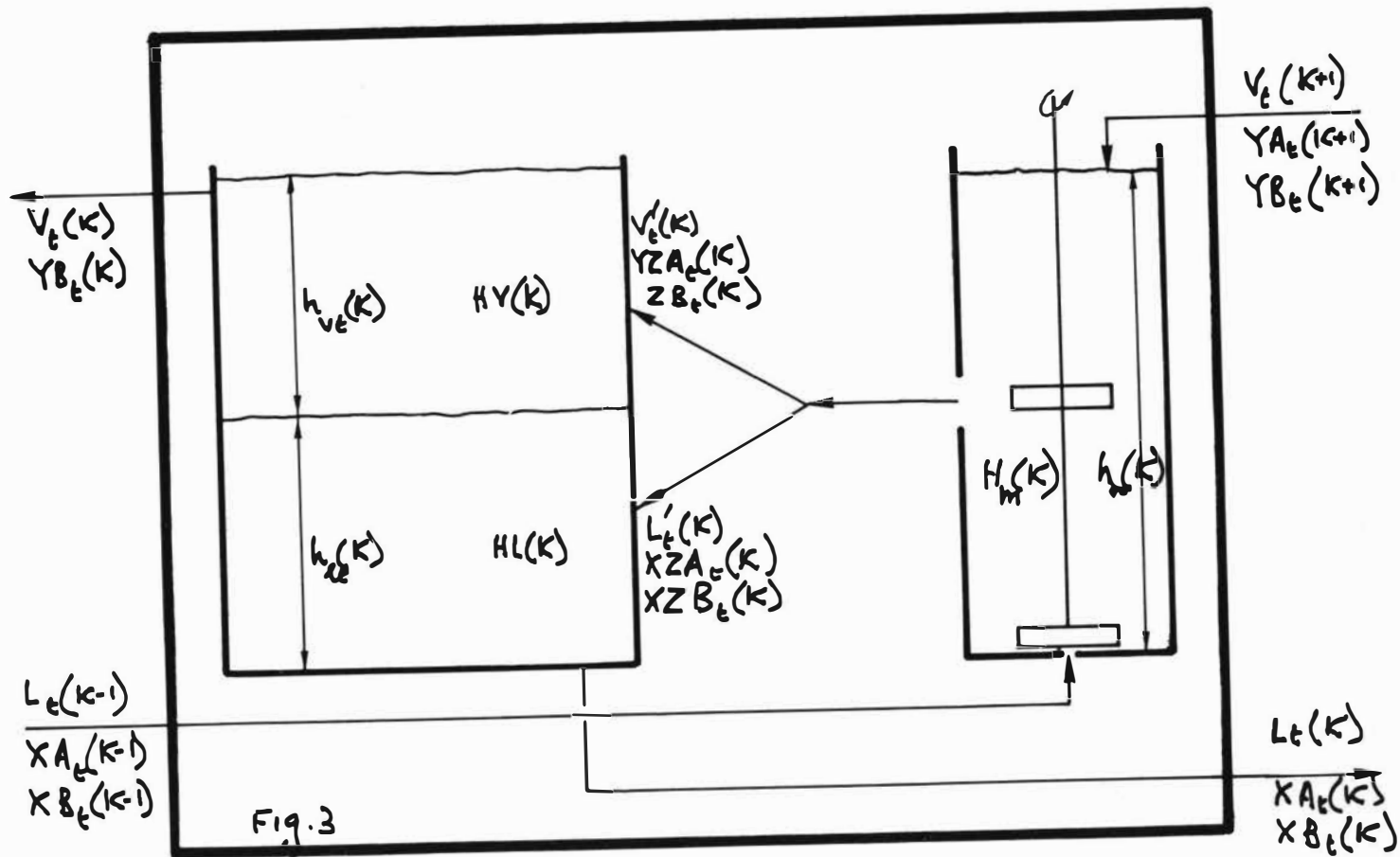


Fig.2. SETTLER : Kth STAGE



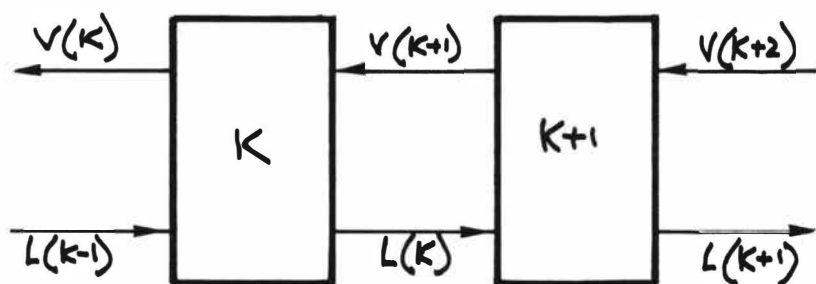


Fig. 4: 2 STAGES, K th / $(K+1)$ th

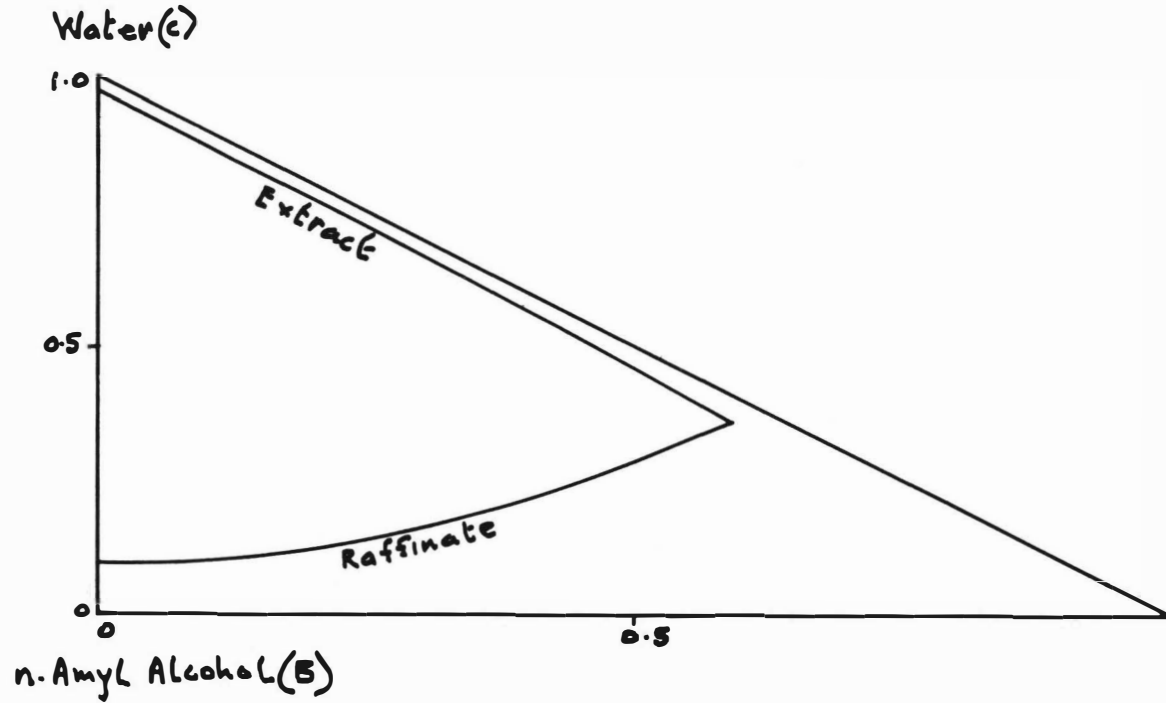


Fig 5. Equilibria. Ethylene Glycol - n Amyl Alcohol - Water

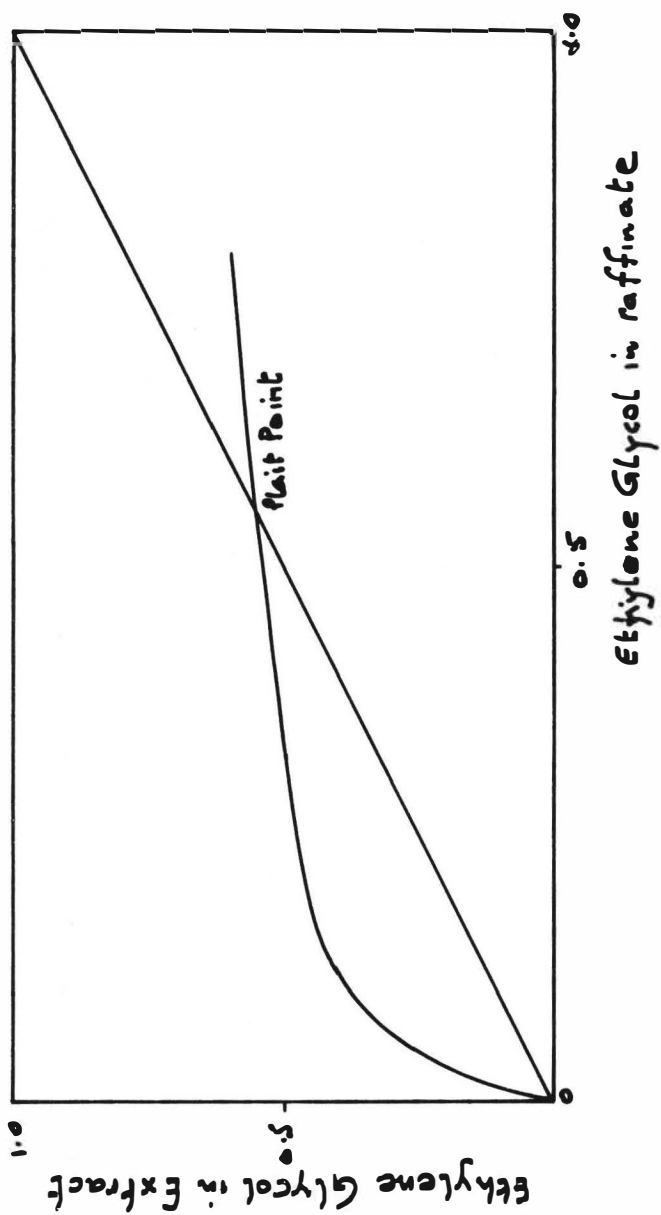
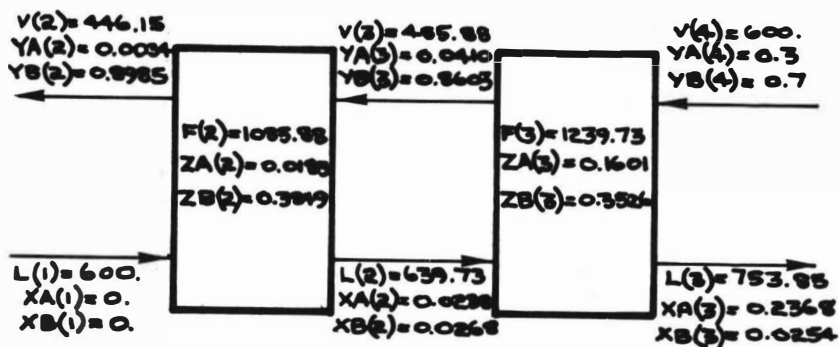


Fig 6. Equilibria:- Ethylene Glycol System



$$H_m(2) = 2000.$$

$$HV(2) = 1000.$$

$$HL(2) = 1000.$$

$$H_m(3) = 2000.$$

$$HV(3) = 1000.$$

$$HL(3) = 1000.$$

FIG. 7 EXAMPLE NO. 1 STEADY STATE VALUES OF STREAMS

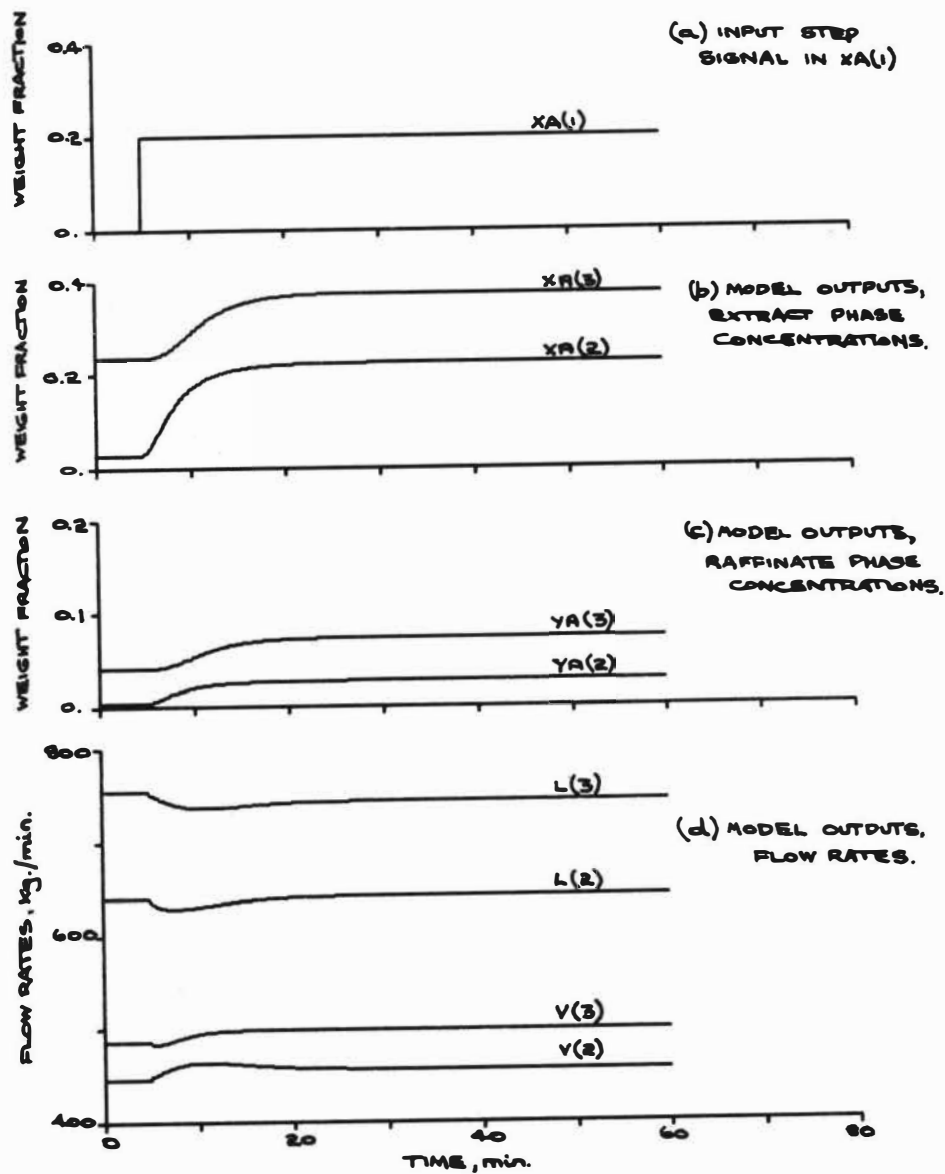


FIG. 8 EXAMPLE NO. 1 RESPONSE CURVES

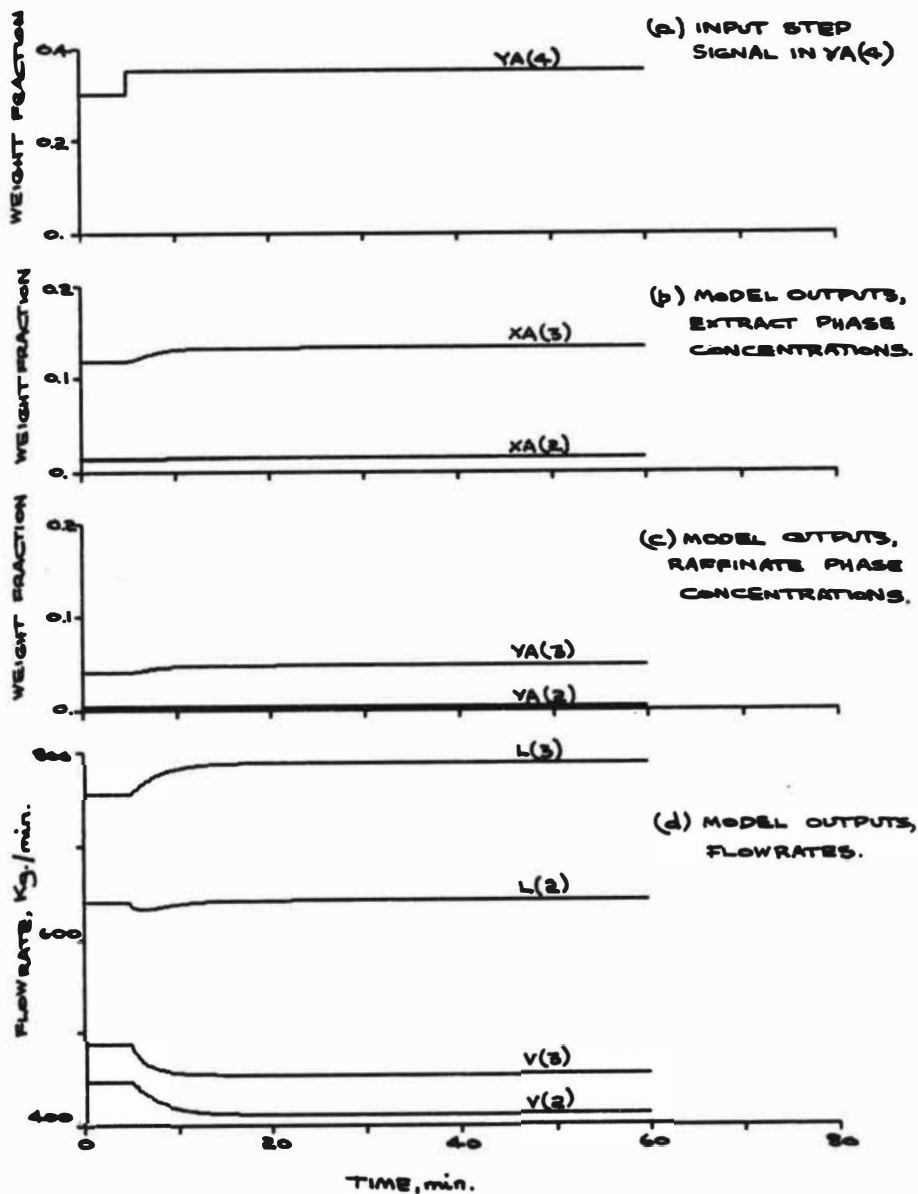


FIG. 9 EXAMPLE NO. 1 RESPONSE CURVES.

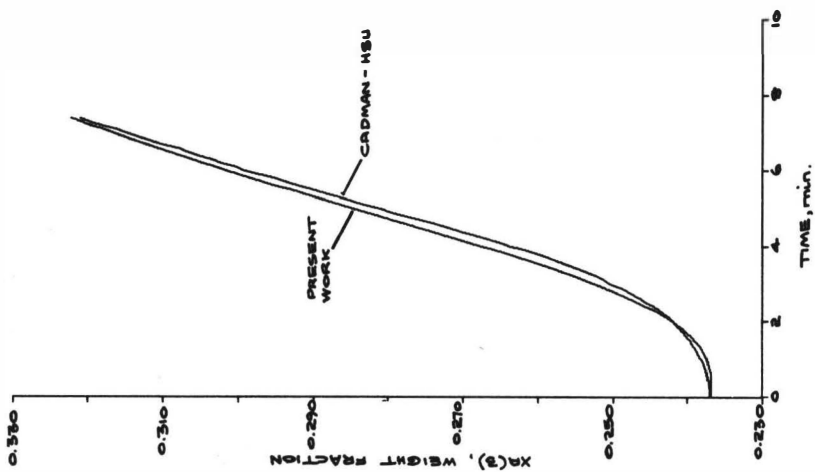


FIG. 10 COMPARISON OF CADMAN-HSU MODEL WITH PRESENT WORK.

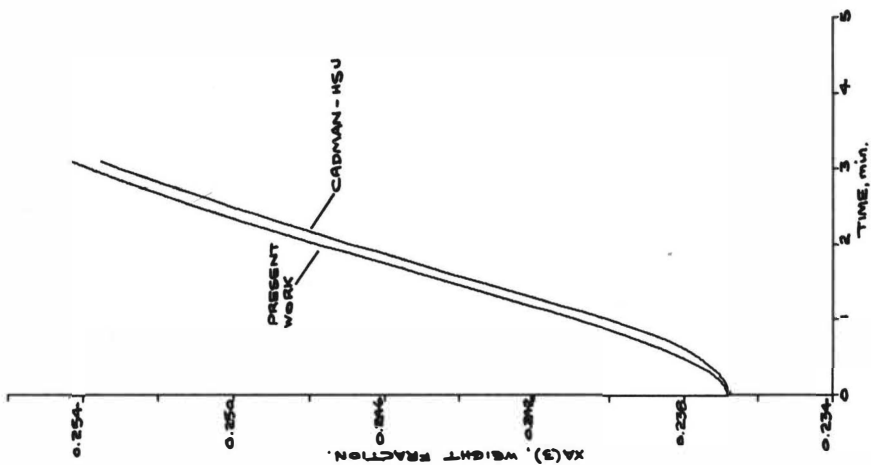


FIG. 11 COMPARISON OF CADMAN-HSU MODEL WITH PRESENT WORK.

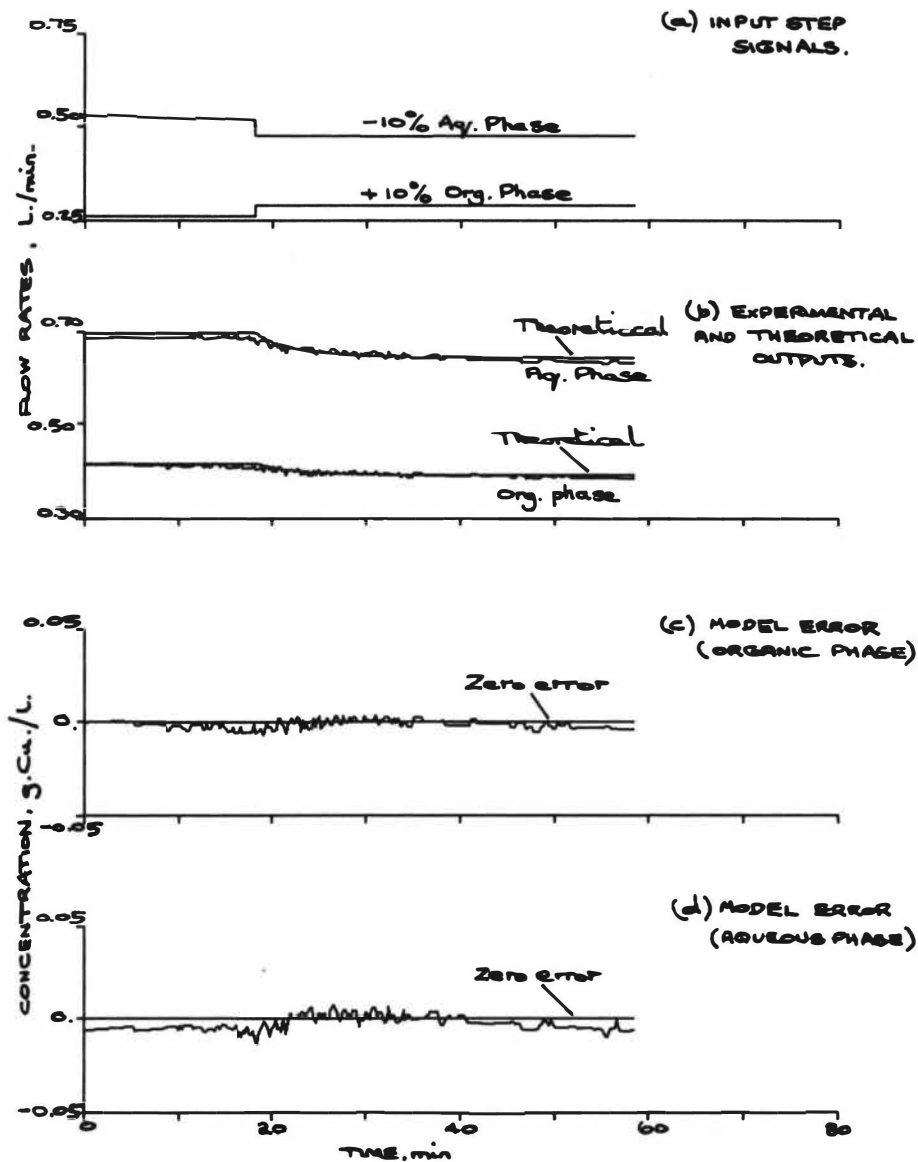


FIG. 12 EXAMPLE No. 2 RESPONSE CURVES

FLOW RATES, L./min.

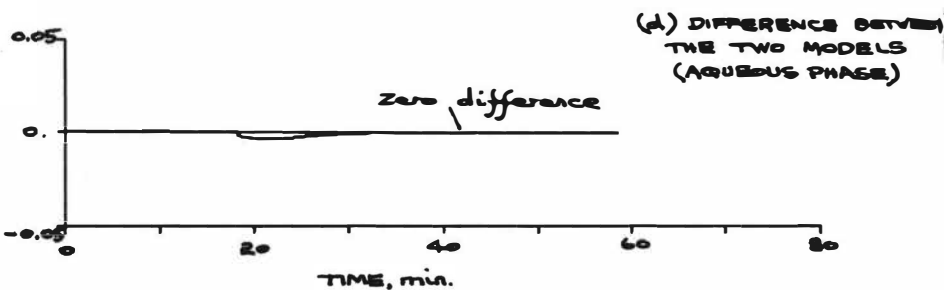
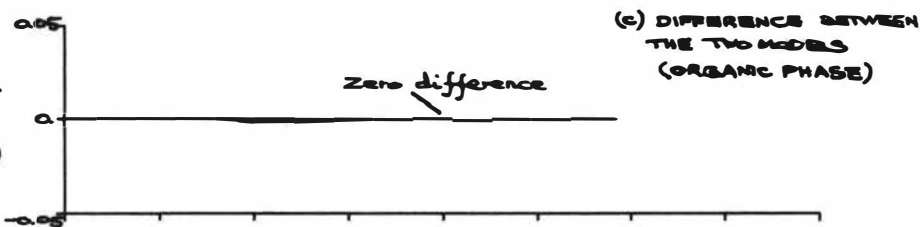
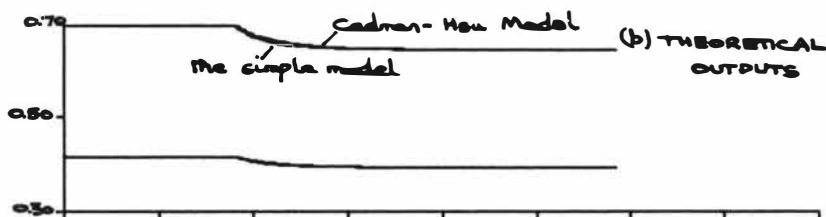
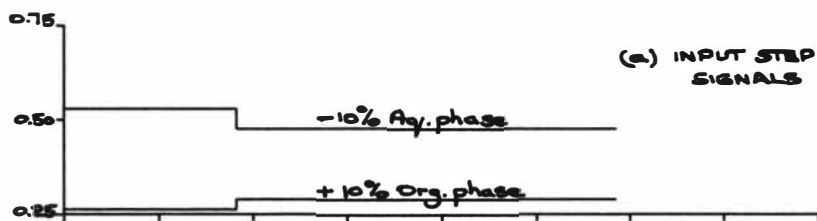


FIG. 13 COMPARISON OF CADMAN-HSU MODEL AND THE SIMPLE MODEL (2)

Development and Experience of Industrial
Operation and Optimisation of Pulsed
Mixer - Settler Extractor

S.M. Karpacheva, L.S. Raginsky,
V.M. Muratov, V.D. Ivanov, M.V. Sheloumov

ABSTRACT

The paper analysis operating experiences with mixer settler extractors. It has been shown that the dimensions may be substantially reduced by optimization of mixing and settling processes.

The optimized "Honeycomb" design has been suggested which has a cocurrent mixing chamber and a settling chamber arranged arbitrarily with respect to the former.

The results of hydraulic and engineering tests on the bench optimized extractor and the $16 \text{ m}^3/\text{hr}$ pilot plant model, based on these data, are presented. The extractor has demonstrated high efficiency at the least entrainment.

INTRODUCTION

Column and mixer-settler type extractors have found the widest use in industry.

The main advantage of mixer-settlers is a definite number of stages having relatively high efficiency (70-90%) and small height (1-2m). On the other hand, mixer-settlers take more space and volume than columns. At the same time, for most commercial columns HETS is vague and cannot be determined from laboratory data because the scaling up factor does not yield to calculation (except for the pulse KRMZ-packed column described elsewhere¹). This uncertainty presents difficulties when designing extraction equipment and is responsible for the preference often given to less effective mixer-settlers. The larger volume of a mixer-settler is dictated, firstly, by the availability of settling zones for each stage compared to only two in a column with many stages and, secondly, by finer dispersion of drops in the transfer zone, requiring larger area for phase separation in each settling zone. Moreover, the flow pattern in a mixer-settler requires positioning settling zones in line with mixing ones, which further increases the floor area.

A decrease in the mixing intensity enables the settling chamber size to be reduced but in these cases the transfer volume may increase due to a decrease in the mass transfer surface. However, the mixing conditions fitting the optimal total volume of settling and mixing chambers are likely to be found as in the objective of the work.

In a mixer-settler, to obtain high efficiency the whole volume of the transfer zone should be mixed. This is accomplished by a stirrer inducing circulatory flows wherein dispersion occurs. Transporting and mixing are usually handled by the same unit, so the capacity depends on the stirrer intensity. In this case even the minimum energy used to obtain uniform mixing throughout the volume and to transport the emulsion over the section causes the dispersed phase to break up to small droplets 0.1mm and less.

Until recently, the problem of possibility and necessity of a decrease in the mixing intensity received no attention as high efficiency was believed to be obtained only with fine drops.

Meanwhile, such a fine dispersion is unnecessary for high efficiency. When studying pulse columns², the optimal drop size was found to be equal to 0.8-1.0mm.

Further dispersion results in a mutual screening of the drop surfaces, i.e. they are partially out of reach of the second phase. An emulsion containing such drops is laminated 3-5 times as fast as that with 0.1mm drops.

EXPERIMENTAL

The foregoing shows that the optimization of contacting and separating processes in a mixer-settler requires first of all a different power supply, so as to control the dispersion intensity within the desired limits, provided the uniform drop distribution is retained and the emulsion is transported.

In pulse columns operating in a piston-like mode, mixing should cover the cross-section area rather than the whole volume. This enables the power consumption to be reduced. Moreover, the power is supplied not locally as in a mechanical mixer but over the cross-sections, this allowing for the intensity to be further reduced and controlled so as to produce the optimal drop size and (with KRMZ-packing) the uniform drop size.

Therefore, it is quite tempting to use a cocurrent pulse column of small height as a mixing zone. Apart from a less power consumption for dispersion, this would allow some latitude in arranging settling zones and the whole assembly.

Settlers could be positioned over, under or next to mixing chambers and the whole assembly could be one-row or multi-serial (fig. 1a,b).

The design is dependent on the way of transporting the liquid phases from one section to another without affecting the optimal mixing conditions in the transfer zone. Pulse control in several columns (mixing chambers) by a single pulsator is also of practical importance.

The design of a mixer-settler with optimized dispersion has been possible by using separate centrifugal pumps for each phase³. Work has been done on the pulse control in the pumps by a common pulsator. Fig.1 shows the diagram of the optimized mixer-settler "Honeycomb".

In such a design, the drop size is readily controlled and kept as a rule the same as in columns at 0.8-1.2mm. The appropriate pulsation intensity is maintained by the pumps or a pulsator if the pump-generated pulsation is inadequate.

Transportation of each phase singly prevents the formation of secondary dispersions often which are formed by stirrers and pumps when passing two immiscible liquids through them. The phase separation velocity is several times higher than that in a conventional mixer-settler.

Hydrodynamic and engineering characteristics of the simulated extractor (900mm high, the transfer zone is $176 \times 176\text{mm}^2$) have been studied without and with mass transfer. For hydrodynamic tests a mutually saturated system of 0.4-ON nitric acid and 100% TBP or 25% TBP in kerosene was used.

Mass transfer was studied when extracting uranyl nitrate from solutions with its low or high content by 25% TBP in Kerosene.

Table 1

Hydraulic Test Data for the Simulated Extractor at $n=1$.

Pulsation Intensity 1, mm/min		Specific Flow Rate, $\text{m}^3/\text{m}^2\text{hr}$					
		10	15	20	25	30	35
700	i	0.01	0.02	0.02	0.02	0.02	0.03
	j	0.01	0.01	0.01	0.01	0.02	0.02
850	i	0.01	0.02	0.02	0.03	0.05	
	j	0.01	0.01	0.01	0.02	0.02	
1100	i	0.02	0.03	0.03			
	j	0.02	0.02	0.02			

i - the aqueous phase entrainment by the organic phase, %

j - the organic phase entrainment by the aqueous phase, %

Table 2

Test Data for the Extractor Using Low Uranyl-nitrate Solution at $n=1$

Pulsation Intensity, 1, mm/min		Specific Flow Rate, $\text{m}^3/\text{m}^2\text{hr}$						
		10	20	25	30	35	40	50
300	η				75			79
	i				0.01			0.03
	j				0.02			0.03
700	η	100		95	95	93		94
	i	0.01		0.02	0.02	0.02		0.02
	j	0.01		0.02	0.02	0.02		0.03
500	η				86		86	86
	i				0.01		0.02	0.02
	j		100	100	0.02		0.03	0.03
850	η		100	100	100			
	i		0.01	0.02	0.02			
	j		0.01	0.02	0.02			

- efficiency, %

i - the aqueous phase entrainment by the organic phase, %

j - the organic phase entrainment by the aqueous phase, %

Table 3

Test Data for the Extractor Using High Uranyl-nitrate
Solutions at $n=4$

Pulsation Intensity, 1,mm/min		Specific Flow Rate, $m^3/m^2 \text{ hr}$				
		10	15	20	25	30
300	h					96
	i					0.07-0.10
	j					0.02
500	h	88.5		87		95
	i	0.02		0.02		0.10
	j	0.01		0.02		0.02
700	h			94	92.5	94
	i			0.05	0.08	0.12
	j			0.01	0.02	0.02
850	h		97.5	98	96.5	
	i		0.02	0.055	0.13	
	j		0.02	0.02	0.03	
1000	h			95		
	i			0.07		
	j			0.03		

- efficiency, %

i - the aqueous phase entrainment by the organic phase, %

j - the organic phase entrainment by the aqueous phase, %

The flow, ratio; n , was equal to 1 in the former case and to 4 in the latter one.

To assess the extractability the mutual entrainment was determined assuming the entrainment of no more than 0.1% to be tolerable. The total efficiency was estimated from the stage efficiency by a graphical method.

Results and Discussion

The data obtained are given in tables 1,2,3. It follows that with a limited entrainment of 0.1% the flow rate can be as high as $25\text{m}^3/\text{m}^2\text{hr.}$ at $n=4$ and more than $50\text{m}^3/\text{m}^2\text{hr.}$ at $n=1$. These flow rates exceed those in conventional mixer-settlers by an order or magnitude and those in countercurrent pulse columns using the same systems. If the aqueous phase entrainment of more than 0.1% is allowable the extractor capacity further increases. In all cases the organic phase entrainment did not exceed 0.03%.

As it is seen from table 2, with the flow ratio of 1 the entrainment, being no more than 0.02%, is actually unaffected by the pulsation intensity up to $850\text{mm}/\text{min}$ and the flow rates up to $50\text{m}^3/\text{m}^2\text{hr.}$ indicating the margin of capacity.

The extraction at $n=4$ (table 3) indicates the effect of the pulsation intensity and flow rate on the aqueous phase entrainment. This fact may be attributed, firstly, to the higher organic phase flow rate in the latter case at the same total capacity and, secondly, to the higher viscosity and surface tension of a concentrated uranyl-nitrate solution.

The data presented show the proposed extractor is a new type of a mixer-settler which together with its main advantage, a definite number of stages, offers high efficiency and capacity, i.e. the space occupied and the extractant feed are small.⁺).

Mixing and separation data obtained from the simulated extractor with a total capacity of $1\text{m}^3/\text{hr.}$ formed the basis of the $16\text{m}^3/\text{hr.}$ pilot plant extractor.

The phases were transported by pulse centrifugal pumps driven by a pulsator, and mixed by another pulse system with another pulsator.

The three-section pilot plant test data (table 5) substantiated the results from the simulated extractor tests. The low uranyl-nitrate solution at the phase ratio, $n=1$, was used for these tests.

Table 5

Pilot - plant Test Data

Conditions Variables	Hydraulic Tests		Engineering Tests at capacity of $16m^3/hr$	
	$16m^3/hr$	$20m^3/hr$	Extraction	Stripping
Aqueous phase entrainment, % (pulse intensity - $540mm/min$)	0.02	0.04	0.025-0.03	0.02-0.03
Organic phase entrainment, % (pulse intensity - $540mm/min$)	0.02	0.04	0.02	0.03-0.04
, %			(1= $400\overset{85}{mm}/min$) (1= $1000mm/min$)	
Dispersed phase hold-up, , %			19-21	15-23

The volume of settling zones and hence, the solvent amount in them is 4-5 times lower than in ordinary mixer-settlers.

Moreover, the new extractor "Honeycomb" is capable of bringing into contact solutions with like specific weights, which presents problem for most other extractors except for centrifugal ones.

As specific weights become similar from stage to stage during extraction in columns, this would lead to an unsteady operation of the transfer zone and its flooding.

In cocurrent mixer-settlers the converging of specific weights may be responsible for little or even absence of lamination of an emulsion containing very fine drops.

With the cocurrent flows in a mixer of the new extractor the mixing process is unaffected by decreasing in the difference in specific weight, $\Delta\rho$, the phase separation, though less effective with decreasing $\Delta\rho$, takes place due to relatively large drops.

The tests showed the total specific flow rate per a settling zone under optimal operating conditions was equal to $1.0-1.5\text{m}^3/\text{m}^2\text{hr}$ in a mixer-settler, $10\text{m}^3/\text{m}^2\text{hr}$ in a counter-current extraction column and up to $30\text{m}^3/\text{m}^2\text{hr}$ in the extractor ("Honeycomb") with optimized mixing and settling.

The comparative tests were performed using the 1.5N nitric acid - 100% TBP system with some amount of nitrates. The difference in specific weights between aqueous and organic phases was equal to 0.03.

Conclusions

On the basis of the research into column and mixer-settler type extractors the "Honeycomb" unit was optimized mixing and settling has been developed. It offers high performance with a lower settling volume and lower solvent inventory.

Various models, from small to industrial scale ($16\text{m}^3/\text{hr}$), have been tested.

Reliability and efficiency of the proposed design have been substantiated.

List of Literature

1. Karpacheva S.M., Zaharov E.I., Raginsky L.S., Muratov V.M., Romanov A.V. Avtorskoe Svidetelstvo (Licence) 175489. Bulletin izobreteny 5 (1965).
2. Karpacheva S.M., Zaharov E.I. "Hydravlicheskie i technologicheskie harakteristiki pulsatsionnyh kolonn s nasadkoy KRIMZ", ChISA, 1972.
3. Raginsky L.S., Muratov V.M., Ivanov V.D., Baulin Y.N. Avtorskoe Svidetelstvo (Licence) 293139, Bulletin izobreteny 5 (1971).

List of Figures

Fig.1. Basic diagram of the pulse extractor "Honeycomb".

- a) design with a top-mounted settler
- b) design with a bottom-mounted settler

- 1. Transfer chamber;
- 2. Settling chamber;
- 3. Transporting units for light and heavy phases;
- 4. Pulse chamber;
- 5. Packing KRMZ;
- 6. Channel for emulsion;
- 7. Channel for light phase;
- 8. Channel for heavy phase;
- 9. Pulse main;
- 10. Baffle.

Note: Nos. 1-10 above should be listed as captions for Fig.1.

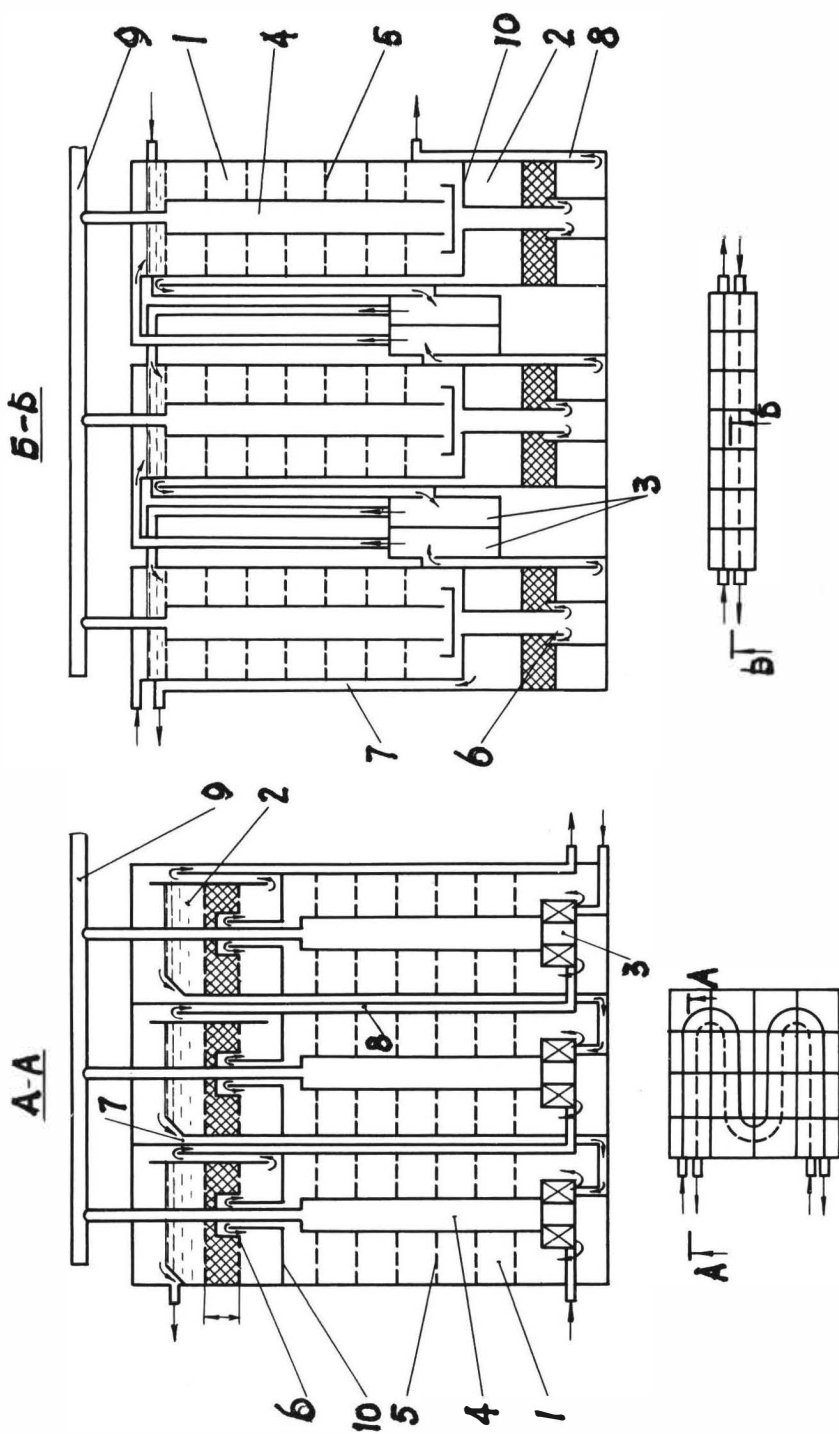


FIGURE 1.

Scale-up of air pulsed mixer-settlers for the reprocessing of nuclear fuels

W. Johannisbauer and G. Kaiser

Kernforschungsanlage Jülich GmbH,
Institut für chemische Technologie, 517 Jülich, F. R. Germany

A bench scale air pulsed mixer-settler was developed from a small scale stirred model. Experiments with it demonstrated that it could in principle be used in the JUPITER pilot plant, which is to be built for the reprocessing of thorium containing nuclear fuels. For a more exact determination of the dimensions necessary for the JUPITER model, a study was made of the mass transfer in the mixing chamber, the phase separation characteristics in the settling chamber and the transport of fluids through a mixer-settler stage using two additional mixer-settlers of increasing size. The data obtained were used to establish general criteria for still larger scale-ups.

Introduction

In the Federal Republic of Germany, the Institute for Chemical Technology of the Nuclear Research Centre Jülich, in cooperation with several industrial firms, has developed a method for the reprocessing of fuel elements containing thorium after several years' research [1]. This process consists of a combustion and dissolution step and a solvent extraction process, the THOREX or INTERIM process. With the construction of the pilot plant JUPITER the process is to be tested on a semi-technical scale under conditions approximating as closely

as possible to the practice [2].

Starting from data gained during the development of the extraction processes [3], a suitable extraction apparatus was to be selected for JUPITER and its dimensions determined for a five-fold throughput of 2 kg heavy metals per day.

The extraction apparatus selected was then to be studied to find a method of expanding it for the capacity of a prototype and an industrial reprocessing plant.

Selection of an extraction apparatus

The choice of an extraction apparatus for JUPITER was determined on the one hand by the requirements arising from the processing of radioactive material and fissionable substances. On the other hand, the experimental programme and the size of the hot cells restricted the choice.

In the reprocessing of nuclear fuels three types of extraction apparatus are mainly used:

mixer-settlers

pulsed columns

centrifugal extractors.

Mixer-settlers are particularly suitable for pilot plants, in which the process conditions frequently change and operation and shut-down phases alternate in short intervals. Each stage of a mixer-settler battery remains in extraction equilibrium, independent of the others, even if the plant is temporarily shut down. Due to their small height, mixer-settler batteries can be arranged in stages one above the other, so that the liquids can flow by gravity from one stage to the next.

Air pulsed mixer-settlers which have the basic advantage that they require no moving parts within the shielded area are used in various versions for nuclear applications. The UKAEA in Great Britain has patented such an apparatus [4]. At EUROCHEMIC in Mol, Belgium, an air pulsed mini-mixer-settler was also developed. The apparatus consists of a row of mixing chambers

with a row of settling chambers, inclined at 45° , in front. Each mixing chamber is connected through openings with three settling chambers. To mix the two phases the liquid is alternately sucked into two pulse tubes, which dip into the mixing chamber, and released. The pulse tubes end in a jet near the phase boundary. Therefore both the heavy and light phases are sucked into the tube and the former is broken up into droplets. The falling liquid column strikes the phase boundary and disperses the aqueous phase further.

Encouraged by the good experience in the Institute for Chemical Technology in laboratory and hot cell experiments with the air pulsed mixer-settler, this type was therefore chosen for use in JUPITER.

Preliminary tests

In order to obtain quick information on whether the air pulsed mixer-settler, previously known only as laboratory apparatus, could be expanded for the required capacity, and to arrive at approximate dimension values for the plant planning, a few preliminary tests were carried out.

The laboratory and hot cell experiments for the development of the extraction processes were performed in 16-stage, stirred mixer-settlers. The flowrates were chosen so that the product quality satisfied the requirements with regard to fission product decontamination and heavy metal losses. The heavy metal throughput was about 0.4 kg per day for all tests. The mixer-settler to be developed was to have five times this throughput, i.e. 2 kg heavy metal per day, with the same product quality.

Since the product quality of an extraction process under given operating conditions depends only upon the number of stages and the stage efficiency, the stage efficiency of the stirred mixer-settler was compared with that of an enlarged air pulsed mixer-settler. As a test system uranyl nitrate / nitric acid and 30 % TBP / Dodecane was used.

The results of a test series with a stirred and a pulsed mixer-settler are shown in fig. 1. Both apparatus show the same stage

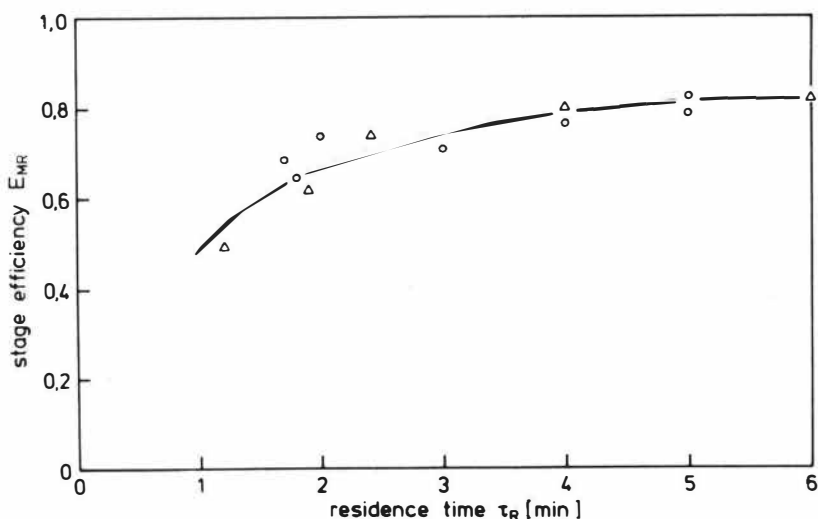


Fig. 1 Comparison of the stirred with the pulsed mixer-settler

\circ stirred MS, $n = 1400 \text{ min}^{-1}$

Δ pulsed MS, $H = 20 \text{ cm}$, $f = 50 \text{ min}^{-1}$
 $\emptyset = 0.5$

efficiency at the given mixing intensities, if the residence times in the mixing chambers are constant.

Thus it has been shown that the air pulsed mixer-settler can be enlarged in such a way that the same efficiency as in the stirred mixer-settlers is attained. A 16-stage mixer-settler can therefore process the required throughput at the specified product quality.

Two test runs in a 16-stage air pulsed mixer-settler battery with the THOREX process and a throughput of 2 kg thorium in 24 hours confirmed this opinion [5].

Scale-up criteria for air pulsed mixer-settlers

In order to determine the exact dimensions of the JUPITER extraction batteries and, in addition, the size of mixer-settlers for a prototype or industrial reprocessing plant, further experiments were necessary. In the end they were to lead to criteria which enable the individual elements of an air pulsed mixer-settler to be enlarged from model scale to full scale. These elements are:

mixing chamber with pulse tubes
settling chamber
ports.

The experiments were carried out in two acryl glass mixer-settlers of different size, a 3-stage mini-mixer-settler and a 3-stage midi-mixer-settler with the following dimensions (in cm):

mixing chamber	mini	midi	settling chamber	mini	midi
width	3.2	8		2.6	4.2
depth	3.2	11.5		2.6	8.2
height	10	8.5		11	9.5
inclination				45°	35°

pulse tubes	mini	midi	openings	mini	midi
diameter	0.8	3.0		1.0	2.5
length	30	25		2.3	1.5
nozzle diameter	0.5	0.5			
nozzle number	1	7			

The pulsation was produced by air jets, whose driving air was controlled by a magnetic valve and a pulse timer. In the midi-mixer-settler compressed air was blown into the pulse tubes out of phase with vacuum, which accelerated the dropping of the

liquid column (fig. 2). The extraction tests were again made with the system uranyl nitrate / nitric acid and 30 % TBP / Dodecane.

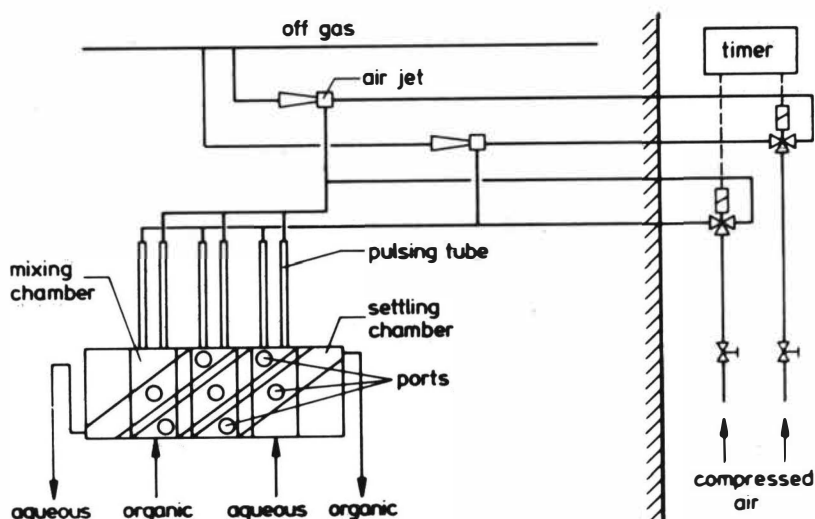


Fig. 2 Experimental set-up of the air pulsed midi-mixer-settler

The stage efficiency was determined as a function of the residence time, suction height, pulse frequency and nozzle and tube diameter.

The theory of mass transfer between two phases in an ideal mixing vessel and the definition of the stage efficiency lead to the equation [6]:

$$\frac{E_{MR}}{1 - E_{MR}} = k_R \cdot a \cdot \tau_R$$

With the aid of the similarity theory two dimensionless parameters were formed, which describe the mass transfer in the

mixing chamber with sufficient accuracy.

$$\frac{k_R a d^2}{D} = K \left[\frac{P/V d^2 \rho_c}{(g d)^{0,5} \sigma \Delta \rho} \right]^\alpha$$

The specific power is:

$$P/V \sim \rho_c d_R^2 H^3 f^3 / V$$

For pulse tubes with several nozzles an equivalent nozzle diameter is calculated from the equation

$$\frac{\pi}{4} d_{ae}^2 = \sum_{i=0}^{i=z} d_i^2 \frac{\pi}{4}$$

The experimental results may be described by a potential function with $K = 3 \cdot 10^4$ and $\alpha = 0.58$ (fig. 3). The scatter of the experimental points about this function must be compensated by a subsequent optimisation in operation. For this purpose the pulse frequency and the suction height should be variable by $\pm 20\%$.

The scale-up criteria for the mixing chambers and the pulse tubes of a mixer-settler are therefore

$$\tau_R = \text{constant}$$

$$\frac{(P/V)^{0,58}}{d^{1,13}} = \text{constant}$$

if the same extraction process takes place in both the model and full-scale versions.

The investigation on the performance of the settling chamber was confined to the mini-mixer-settler. Nitric acid and 30 % TBP / Dodecane were used as test system. In the experiments the

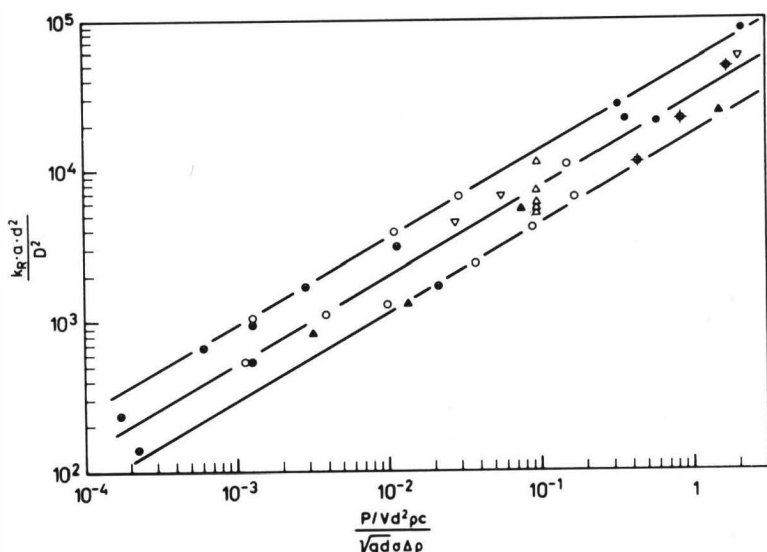


Fig. 3 Plot of the mass transfer results
 mini-mixer-settler: \circ $F(f)$, \square $F(H)$, \bullet $F(d)$, \oplus $F(d_R)$
 midi-mixer-settler: Δ $F(\tau)$, \blacktriangle $F(H)$, ∇ $F(f)$

thickness of the dispersion layer in the settling chamber was determined as a function of the throughput, chamber depth, phase ratio, suction height and pulse frequency.

With the aid of the model of the coalescence of a dispersion modified for the vertical settling chamber [7] a calculation equation for the thickness of the dispersion layer was developed.

Starting from the drop and volume balance in the dispersion layer

$$\frac{\partial d}{\partial h} = - \frac{\varphi}{6} \frac{d}{v_d t_d}$$

and at the phase boundary, and from empirical equations [8] for the life expectancy of the individual drops, one obtains the

equation

$$h_d = K_1 \frac{v_d}{\sqrt{V_d}} \left[K_2 v_d^{1,06} - d_o^{2,64} \right]$$

With the aid of the potential equation

$$\frac{d}{d_o} = K_3 \left[\frac{P/V d^2 \rho_c}{\sqrt{gd} \sigma \Delta \rho} \right]^\beta$$

the drop diameter on entering the settling chamber can be expressed as a function of the mixing intensity.

The experimental results (figs. 4 and 5) confirm the theoretical equation and the model concepts on which it is based. Further, with the aid of this equation the scale-up criteria for the settling chambers of an air pulsed mixer-settler can be derived.

When mixer-settlers are used for the reprocessing of nuclear fuels, the height of the apparatus must not exceed a certain limit, in order to avoid a critical configuration when processing fissionable material. This requirement of geometrically safe mixer-settlers means that the dispersion thickness in the settling chamber of the full-scale version must remain constant when the equipment is enlarged.

The thickness of the dispersion layer is certainly not greater than that of the model version if

$$\frac{P/V d^2 \rho_c}{\sqrt{gd} \sigma \Delta \rho} = \text{constant}$$

and

$$v_d = \text{constant}$$

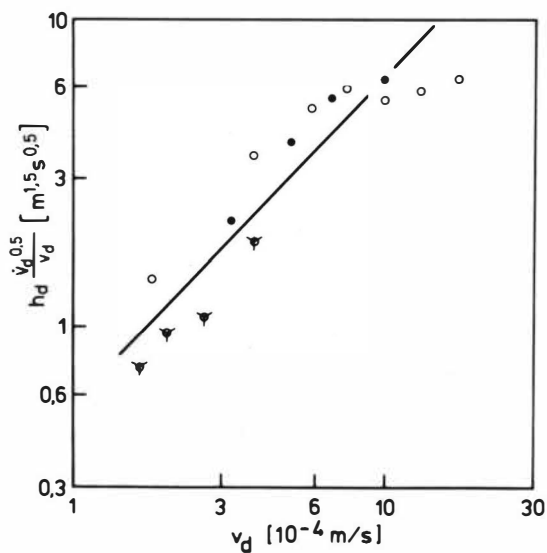


Fig. 4 Influence of the throughput and the dispersion velocity on the dispersion thickness
 $\circ F(\dot{V}_d)$, $\bullet F(0)$ $C_a = 0.01 \text{ Mol H}^+/\text{l}$
 $\nabla F(W)$ $C_a = 1.06 \text{ Mol H}^+/\text{l}$

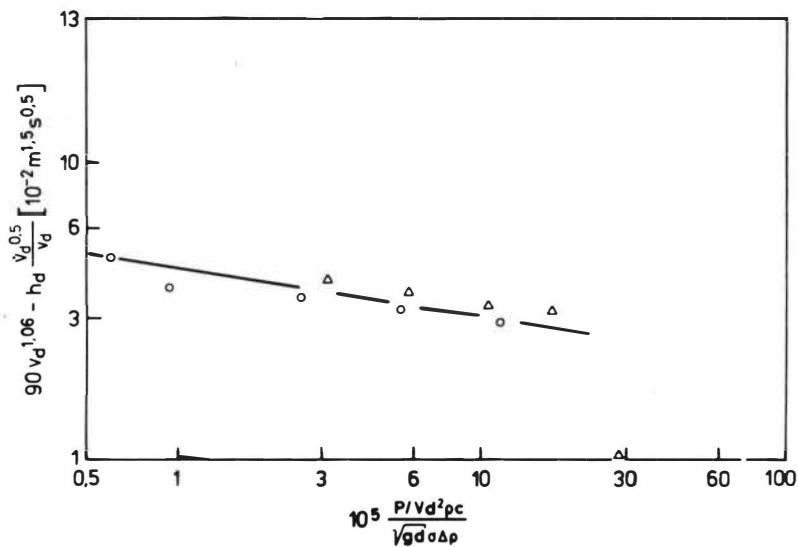


Fig. 5 Dispersion thickness as a function of the power number
 $\Delta F(H)$, $\circ F(f)$, $v_d = 0.1 \text{ cm/s}$

The form and size of the ports between the mixing and settling chambers influence the transport of both phases through a mixer-settler battery. If the pressure drop for a particular throughput is too high, the phase boundary or the liquid level in the settling chamber may rise to such an extent that a transport is impossible or the battery overflows.

Since the air pulsed mixer-settler cannot suck in both phases like the impeller in stirred mixer-settlers, the factors influencing the transport of the two liquids were investigated.

For this purpose, the level of the phase boundary in the middle settling chamber was measured during the extraction tests with both air pulsed mixer-settlers as a function of the phase ratio, the throughput and the mixing intensity.

On the basis of the theory of hydrodynamic equilibrium [9, 10], equations were developed which describe the level of the phase boundary as a function of the geometrical dimensions of the mixer-settler (fig. 6) and the operating conditions.

$$h_i = \frac{\Delta p_u + \Delta p_m}{g(\rho_s - \rho_l)} + h_p [\phi + (1 - \phi)(1 - \psi)] - \phi h_d$$

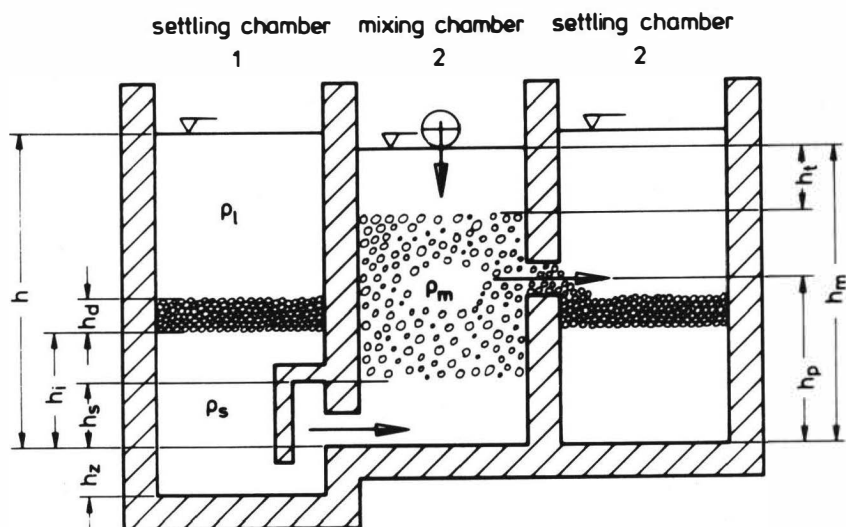


Fig. 6 Schematic diagram of the liquid transport

The comparison of theory and experimental results in fig. 7 shows that the pressure drop in the equipment used was negligibly small.

The mixing proportion, i.e. the ratio of the actual dispersed volume to the maximum possible dispersed volume of the mixing chamber, is given approximately by the power number (fig. 8).

The level of the light phase may rise from stage to stage in a multistage extraction battery if the pressure drop in the middle opening is greater than

$$(h - h_t - h_p) (\rho_s - \rho_l) \phi g$$

The difference in level of two neighbouring stages is then

$$h_3 - h_2 = \frac{\Delta p_o}{\rho_l g} + \frac{\Delta p_m}{\phi (\rho_s - \rho_l) + \rho_l} - (h - h_t - h_p)_3 \left[1 - \frac{\rho_l}{\phi (\rho_s - \rho_l) + \rho_l} \right]$$

The scale-up of mixer-settlers with regard to the transport of the two phases through the apparatus must be carried out in such a way that the phase boundary remains below the middle opening and the level of the light phase does not rise so far that the battery overflows.

From the above equations for the height of the phase boundary and the level of the light phase the only new condition for scale-up is

$$\Delta p \ll h = \text{constant}$$

The remaining criteria have already been set up for the enlargement of the mixing or settling chambers.

From the dependence of the pressure drop on the flow velocity and the geometry of the ports one obtains the enlargement

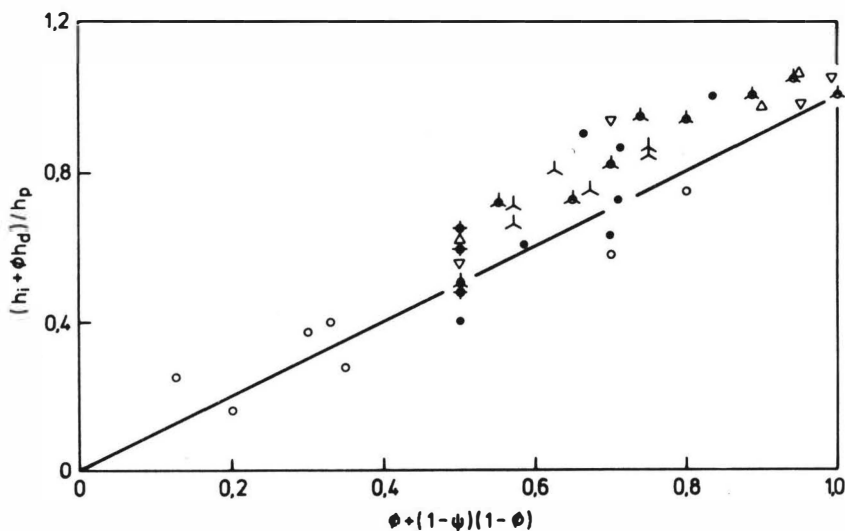


Fig. 7 Test of the theory of hydrodynamic equilibrium
 mini-mixer-settler: $\diamond F(\tau_R)$, $\circ F(0)$, $\bullet F(f)$, $\blacktriangle F(H)$
 midi-mixer-settler: $\nabla F(\tau_R)$, $\triangle F(H)$, $\times F(f)$

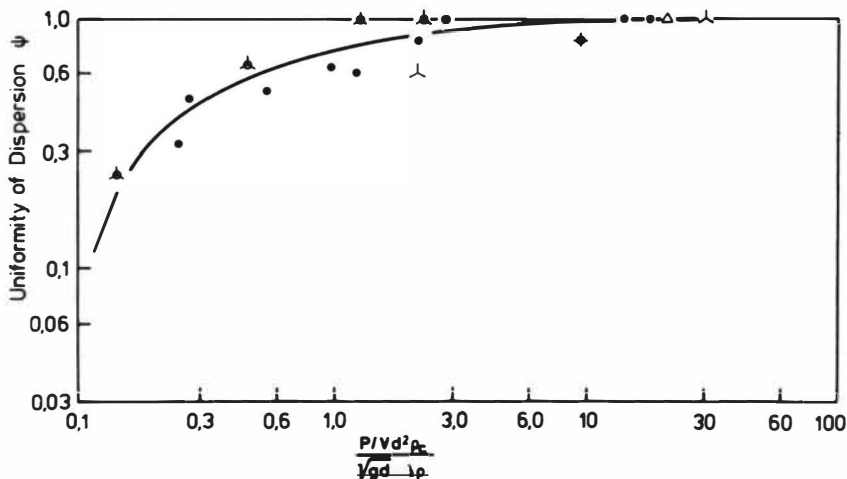


Fig. 8 Mixing proportion as a function of the power number
 mini-mixer-settler: $\bullet F(f)$, $\blacktriangle F(H)$
 midi-mixer-settler: $\triangle F(f)$, $\nabla F(H)$, $\diamond F(\tau_R)$

condition for the ports:

$$\Delta p \sim \frac{1}{d} v^2 \quad \frac{1}{d} \left[\frac{\dot{V}}{A} \right]^2 = \text{constant}$$

Design of an air pulsed mixer-settler for a prototype plant

After the operation of the JUPITER plant with a heavy metal throughput of 2 kg/day the individual components of a reprocessing plant for fuel elements containing thorium will very probably have to be tested on a larger scale. A throughput of approximately 150 kg/day, representing an enlargement by a factor 75, is being considered.

On the basis of the above scale-up criteria, the extraction apparatus must have approximately the following dimensions and operating data:

mixing chamber			settling chamber	ports
width	25	cm	25 cm	16 cm
depth	20	cm	30 cm	0.6 cm
height	7	cm	7 cm	1.2 cm
stages	16		16	

pulse tubes			operating data	
No. per chamber	4		pulse frequency	25 min ⁻¹ ± 10
diameter	3	cm	suction height	30 cm
length	30	cm		
nozzle diameter	0.3	cm		
nozzles p. head	7			

The higher mixing energy was attained by doubling the number of pulse tubes and reducing the nozzle diameter. The dimensions of the mixing and settling chamber were adjusted to one

another in such a way that a "compact box" arrangement is possible.

Summary

An air pulsed mixer-settler for nuclear application is presented, which works without moving parts behind shielding. Comparative tests with a stirred mixer-settler and this apparatus show that it is suitable for the JUPITER pilot plant. Further, theoretical equations for the mass transfer in the mixing chamber, the coalescence in the settling chamber and the hydrodynamic behaviour of the mixer-settler are developed and confirmed by experiments with the test system uranyl nitrate / nitric acid - 30 % TBP / Dodecane. On the basis of the equations scale-up criteria for the individual elements of an air pulsed mixer-settler are derived and used for the calculation of an extraction apparatus for a prototype re-processing plant.

Nomenclature

A	area
a	specific area
C	concentrations
D	diffusion coefficient
d	diameter
E	efficiency
F	function
f	frequency
g	acceleration due to gravity
H	height of suction
h	height
K	overall mass transfer coefficient, constant
k	mass transfer coefficient
l	length
P	power
p	pressure
V	volume
\dot{V}	throughput
ρ	density
σ	interfacial tension
τ	mean residence time
Φ	volume fraction of the aqueous liquid
φ	packing efficiency
ψ	uniformity of dispersion

Subscripts

a	aqueous phase
ae	aequivalent
c	continuous phase
d	dispersed phase
i	interface
l	light
M	Murphree
m	middle, mixing
o	top
p	port
R	raffinat, tube
s	heavy
t	dipping (see figure 6)
u	bottom
α, β	exponent
Δ	difference

Acknowledgments

The authors gratefully acknowledge the encouragement of Prof. E. Merz and the work of Dr. B. G. Brodda of the Chemical Analysis Section for the chemical analysis.

References

- [1] Schäfer, L., Wojtech, B., Kaiser, G., Merz, E.,
& Sckuhr, P.,
Proc. 4th int. Conf. peaceful Uses atom. Energy,
Geneva, 1971, 8, pp. 349
- [2] Kaiser, G., Merz, E., & Sckuhr, P.,
ANS Transactions, Vol. 14, No. 1, June 1971, p. 79
- [3] Schäfer, L., Wojtech, B., Brodda, B.G., Kirchner, H.,
& Riedel, H.J.,
Tagungsbericht Reaktortagung, Bonn, 1971, p. 710
- [4] Tanner, M.C., & Lowes, L.,
Brit. Patent No. 831 383 (1960)
- [5] Johannisbauer, W.,
to be published in Report Jül (1974)
- [6] Treybal, R.E.,
"Liquid-Liquid Extraction", 1963, Vol. II
(New York: McGraw-Hill)
- [7] Jeffreys, G.V., Davies, G.A., & Pitt, K.,
A.I.Ch.E. Jour. 16 (1970), p. 823
- [8] Davies, G.A., Jeffreys, G.V., & Smith, D.V.,
Proc. Int. Conf. Solvent Extraction, The Hague, 1971,
Vol. I, p. 385
- [9] Williams, J.A., Lowes, L., & Tanner, M.C.,
Trans. Instn. Chem. Engrs. 36 (1958), p. 464
- [10] Lowes, L., & Larkin, M.J.,
Instn. Chem. Engrs., London, Symposium Series No. 26
(1967), p. 111

SESSION 3

Monday 9th September: 9.00 hrs

D R O P L E T P H E N O M E N A

Chairman:

Professor S. Hartland

Secretaries:

Dr. M.P. Wilson

Mr. M. Perrut

PHASE SEPARATION IN THICK DISPERSION BANDS

By

A M A Allak & G V Jeffreys

Chemical Engineering Dept
University of Aston
Birmingham

SUMMARY

A refractive index matching technique has been developed to study the behaviour and coalescence of drops in dispersion bands. The frequency of interdrop coalescence has been estimated and correlated, and a model, based on film rupture thickness, has been solved by computer to predict dispersion band thickness as a function of inlet drop size, flow rate and the physical properties of the system.

INTRODUCTION

In previous studies of the behaviour of droplets in dispersion bands the characteristics of the beds have been established from observations made on the drops residing at the wall and at the coalescing interface. Drop behaviour inside the dispersion has been assumed to be identical with that seen at the periphery because the opacity of the dispersion prevented observation of droplets inside. Therefore in this study in order to investigate coalescence behaviour inside dispersion bands systems have been chosen in which the refractive index of the dispersed and continuous phases are the same, then one or more coloured drops have been introduced into the transparent dispersion and their behaviour followed. The coloured drops must have identical properties with all the other drops in the dispersion band. Consequently 'Red Oil O', which Kintner⁽⁴⁾ reported to be non surface active, was used to produce discrete coloured drops, and these were studied as they passed through the bed. A second method used in this investigation was to generate the colour in the drops, in situ, at particular positions in the bed. This was done by dissolving a small quantity of a phototropic dye in one, or other, of the phases, and irradiating the particular section of the dispersion band to generate colour. Claude and Rumpf⁽²⁾ reported that most spirans are very sensitive phototropic dyes and 1.3.3 trimethyl-indolino-6' nitrobenzopyrylspiran was selected for this work because preliminary experiments revealed that a 1.0% solution of this compound was sufficient to produce a quite intense colour change when irradiated with ultra violet light. In addition the colour was sustained for only about 10 minutes after exposure to the U.V. light. After this period it rapidly reverted to its colourless form but could be irradiated repeatedly, so that the solutions containing the dye could be recirculated through the apparatus continuously. Furthermore neither form of the spiran was surface active, and at the concentrations employed, had no affect on the physical properties of the system. This spiran was also insoluble in water; hence by making one of the phases aqueous mass transfer losses and effects were eliminated.

Finally the Christiansen Effect⁽³⁾ was also used to identify drops in the dispersion band. This consisted of matching the refractive index of each phase against the sodium D line to obtain a transparent dispersion,

and then passing beams of red light, produced by a gas laser, through the bed. Since the phases will not be matched for all wave lengths, the drops within the beam become opaque and are easily seen so that their behaviour is readily followed.

The object of the present investigation is to apply the techniques described above to observe the phase separation occurring in thick dispersion bands of the kind encountered in liquid extraction and effluent treatment processes. From the mechanisms revealed, to develop a model to predict the dispersion band thickness as a function of flow rate, inlet drop size and the physical properties of the system.

EXPERIMENTAL

The systems chosen for study were solutions of glycerine in water for the aqueous phase, with refractive indices in the range 1.333 to 1.47, and either iso octane, n-hexane, amyl acetate or ethylacetate, whichever had the same refractive index as that of the aqueous phase. Details of the systems studied are given in Table 1.

The apparatus employed for this study is illustrated schematically in Figure 1. It consisted of a glass column (1) 5.0 cm in diameter, 60.0 cm long to which was attached a 5.0 cm - 7.5 cm reducer to accommodate the dispersed phase distributor. The column was connected to the dispersed phase reservoir (2) via a pump (3), a sintered glass filter (4), constant head tank (5) and the rotameters (6) as shown. The pump was an all glass centrifugal pump possessing P.T.F.E. seals and the sintered glass filter was inserted to trap any scum and solids. The dispersed phase reservoir was constructed from a glass pipe section 22.5 cm in diameter, 22.5 cm long with stainless steel flanges attached to each end. The constant head tank was similarly constructed from a glass pipe section 15.0 cm in diameter, 15.0 cm long, and the interconnecting pipework was entirely of glass of nominal bore 1.5 cm. The distributor was constructed from stainless steel and details are presented in Figure 2. That is, the apparatus was constructed from glass, stainless steel and P.T.F.E. in order to reduce the possibility of contamination to a minimum.

A typical experiment was carried out by thoroughly cleaning the apparatus, by first flushing with tap water, soaking in a concentrated solution of Decon for 24 hours, draining, and flushing again with distilled water. Following this the column was filled with the continuous phase to a predetermined height and the reservoirs were filled with the dispersed phase. The pump was started so that the dispersed phase formed a dispersion band, and after coalescence, filled the remainder of the column. The coalesced dispersed phase was circulated continuously through the apparatus and its flow rate was adjusted to produce a dispersion band of suitable thickness. The thickness of the band was determined by injecting a coloured drop from the special nozzle in the distributor, or, when one of the phases contained the phototropic dye, by exposing the bed to U.V. light from a mercury arc lamp so that the bed became blue in colour. After a number of experiments had been conducted, the location of the band and its thickness could be estimated from the dispersed phase flow rate, although because of the 'matched' refractive index of the phases, the bed could not

be seen in the column.

When steady state had been attained one or more coloured drops were injected into the bed and their behaviour photographed as they passed through the dispersion, using a high speed camera. Alternatively the spiran was dissolved in the organic liquid which could be either the dispersed or continuous phase. The dispersed phase was again circulated until steady state conditions had been attained, then the band, or parts of it, were exposed to U.V. light for a few seconds. This produced a layer, or cluster, of blue drops and their progress through the bed was similarly photographed.

From these experiments the mean drop residence time and the frequency of coalescence between a drop and the wall, a pair of drops and the drop and the interface was obtained, and these have been reported in detail as a function of band thickness by Allak ⁽¹⁾.

RESULTS

Experiments were carried out with a number of distributors having nozzles of uniform size in the range 1.0 mm to 4.0 mm, and the dispersed phase flow rate was controlled to produce uniform sized drops. The drop size was estimated from photographs of the coloured drops entering the dispersion band and these were compared with the drop size predicted from the procedures recommended by Meister and Scheele ⁽⁵⁾. In all cases the agreement between the estimated and predicted value was very good.

Observation of the bed when steady state had been attained revealed that there were three zones as shown in Figure 3.

(i) A flocculating zone, at the droplet entrance: Thus, when the drops enter the bed they are jostled about with the result that, although they remain spherical, they arrange themselves in the most compact way and trap the continuous phase in the interstices. This is the flocculating zone and the dispersed hold-up is probably close to 0.74, i.e. the so-called 'Oswaldt's ratio.'

(ii) A packing zone: As the drops pass into the band they are squeezed together extruding the continuous phase. Figure 4 shows a coloured drop inside the band. There it will be seen that the drop is deformed into the shape of a pentagonal dodecahedra. The faces are pentagonal and reasonably flat, and the continuous phase is squeezed into plateau borders which form a drainage network throughout this zone. Considerable interdrop coalescence

occurs in this zone.

(iii) Interface coalescing zone one or two drops thick, in which the drops are still dodecahedra in shape but tend to coalesce with the interface, more than with each other.

The thickness of the dispersion band depended on the inlet drop size and dispersed phase flow rate, and typical plots showing the relationship between these variables are presented in Figure 5 for the system iso-octane- aqueous glycerine. These are similar in shape to results reported by other workers, and confirm that the bed height increases as the inlet drop size decreases, and the dispersed phase flow rate increases. All the results have been correlated by dimensional analysis as shown in figure 6. There it can be seen that 85% of the results are within $\pm 5.0\%$ of the correlation curve and 97.5% are within 10%. In this correlation the predominant group is the Capillary Number suggesting that drainage of the continuous phase controls the bed height. This is further discussed below.

The packing zone extends over most of the dispersion band, and in this zone drop coalescence occurs with the walls of the vessel in addition to coalescence with each other. The frequency of drop-wall coalescence was found to be remarkably constant throughout the band, but varied with the system. The frequency of interdrop coalescence varied with bed height and frequencies obtained for the above system is presented in Figure 7. These frequencies are the mean values of 75 repeated observations of interdrop coalescence at each plane in the bed. They are typical of all the experimental results obtained and give an insight into the coalescence processes. Thus it will be seen that the frequency of interdrop coalescence is periodic and increases as the drops pass through the bed. That is, at a particular plane in the band the drainage of the continuous phase will proceed to such an extent that the film between the drops rupture and interdrop coalescence ensues. There will be slight differences in the film thickness in between different drops in a layer so that coalescence occurs only between the drops separated by the thinnest film. This interdrop coalescence disturbs the drops around the coalescing pair, with the result that the film surrounding the neighbouring drops is partly regenerated by flow from above and tension in the film from the lower layers. Consequently the film between the drops is renewed and stabilised temporarily, and must drain again to a critical thickness before further coalescence can occur. During this period this layer continues to pass through the bed, and is a region in which the frequency of interdrop

coalescence is low. When the film has again drained to a critical thickness further drop-drop coalescences occur, and these processes are repeated until all of the continuous phase trapped at the entrance of the bed has drained. At this point interdrop coalescence is complete and an interface is formed. This plane is the drop-interface coalescence zone.

The frequency of interdrop coalescence in the packing zone was correlated against the Capillary Number since this is an index of the rate of drainage of the continuous phase in the films and through the plateau borders; the drop size, and the band thickness. The result correlation was:-

$$\lambda = 1 - 0.559 \left(\frac{\gamma}{\mu V_d} \right)^{0.054} \left(\frac{d}{H} \right)^{0.19} \quad 1$$

where λ represents the frequency, or probability, of coalescence expressed as a fraction of the total number of drops residing at a plane in the bed. A comparison of the experimental and predicted probability of coalescence is shown in Figure 8 for all the systems studied. There it will be seen that there is some scatter between the predicted and experimental results, and as 'smoothing' is necessary in developing the correlation, the agreement is considered to be quite good and is satisfactory for the analysis of the phase separation process.

It has been postulated above that interdrop coalescence occurs in the packing zone of the dispersion band when the continuous phase film, in between the pentagonal faces adjacent drops, drains to a critical thickness. This was substantiated by examination of high speed cine films of the dispersion band that contained the phototropic dye in the continuous phase, and which had been irradiated with U.V. light. It was noticed that as the film thinned, the intensity of the blue colour decreased proportionately and disappeared immediately before coalescence. This suggests that when the film just cannot sustain the blue colour it has been reduced to its critical thickness and rupture takes place.

It is not possible to measure the film thickness in the dispersion band but the thickness of the film that is just unable to sustain the blue colour of the phototropic dye was estimated as follows.

Three cells of thickness 50.0; 25.0 and 7.0 microns were used to measure the absorption of light by the continuous phase in the excited and unexcited state in a U.V. absorptiometer, and the absorption was plotted versus cell thickness for the system isobutyl acetate-aqueous glycerine. Extrapolation of the two curves resulted in their intersection at 2.0 microns, suggesting that this is the critical film thickness. This thickness was confirmed by placing the continuous phase with the phototropic dye in between two optical flats; irradiating with U.V. light in the absorptiometer and then reducing the thickness until the colour just disappeared. Then measuring the thickness between the optical flats by counting the interference fringes. The film thickness was confirmed to be 2 microns for the system and this was concluded to be a reasonable estimate of the critical film thickness. This, together with the above correlation of probability or frequency of interdrop coalescence form the basis for a model to predict the thickness of dispersion bands.

PREDICTION OF DISPERSION BAND THICKNESS

The drops in a dispersion band are distorted to the shape of dodecahedra with flat pentagonal faces, and the continuous phase film drains radially between the adjacent faces of a pair of drops since, even for very thick films, the ratio of the surface forces to gravity forces always exceeds 50:1. Therefore the rate of drainage of the continuous phase film from in between adjacent drops into the plateau borders can be expressed by the equation

$$\frac{dh}{dt} = \frac{0.21F h^3}{\mu R^4} \quad 1$$

irrespective of the inclination of the pair of faces. The rate of drainage through the plateau borders can be predicted from the equation of Lenard & Lemlick ⁽⁶⁾

$$q = 0.0005 r_o^4 \cdot \frac{\Delta P}{\Delta l} \quad 2$$

and therefore the total rate of drainage of the continuous phase film per unit area at any plane in the dispersion band is, by equations 1 & 2

$$Q_{\text{down}} = \frac{0.0041 r_o^4 \rho g \phi}{-\mu d^2} \quad 3$$

This flow rate must equal the flow rate of the continuous phase film carried upwards with the drops in the dispersion band moving towards the coalescing interface. This flow rate of the continuous phase per unit cross sectional area is (7).

$$Q_{up} = \frac{3.32 Vh}{d}$$

where the film thickness h is

$$h = 0.3 \left(\frac{1-\phi}{\phi} \right) d \tag{5}$$

Also the radius of the plateau border has been shown to be related to the characteristics of the system by the equation (7)

$$r_o = 2.44 \times 10^3 \frac{Vh\mu d}{\rho g \phi^2} \tag{6}$$

and from this the force causing drainage has been evaluated from Laplace's equation to be

$$F = 0.042 \left(\frac{\rho g \phi^2 d^7}{Vh\mu} \right)^{\frac{1}{4}} \tag{7}$$

Substituting equations 2 to 7 into equation 1 and integrating between the limits that

when $t = 0$: $h = h$

and

when $t = t$; $h = h_c$ (Rupture thickness)

gives

$$t = 0.056 \left(\frac{V\mu^5 d^9}{\rho g \phi^2 h} \right)^{\frac{1}{4}} \tag{8}$$

Equations 2 to 8 have been formulated into a computer program to perform the iterative calculations and the computer flow chart is presented in figure 9. The calculation procedure was started by assuming that the dispersed phase flow rate in the flocculating zone was 0.74 i.e. Ostwaldt's ratio for face centred cubic packing. This is considered to be realistic from observations of the zone, that the drops were very near spherical, and had formed a stable configuration. Thereafter the drops were simply squeezed together forming a dodecahedra confirming that twelve drops surrounded each drop. Initially the critical film thickness was set at 2.0μ and the program processed. Then the value of the critical film thickness was adjusted by 0.5μ increments

until the predicted band thickness matched the experimental thickness. This film thickness was then used to predict the band thickness at other flow rates for each system. The comparison between the experimental and predicted results are presented in Figure 10 for the system quoted above. There it will be seen that the agreement between the experimental band thickness and the predicted thickness is very good for each flow rate. Furthermore the critical film thickness computed for each system agreed to within 0.5μ of that estimated by light transmission in the Absorptiometer.

Finally in order to confirm the validity of the derivation of the model Christiansen's effect was used to photograph the plateau borders, and to measure the radius of the arc making up the walls of the plateau border. The measured radius was then compared with the predicted value obtained by solution of equation 11. The plateau borders were photographed with a cine camera because the drops in the bed were in motion so that it was not possible to be absolutely certain that the plateau border being photographed and the camera film were absolutely parallel. The slightest deviation would greatly distort the photographed plateau border radius. A photograph of the plateau border is shown in figure 11. This is an enlargement of a 2.0 mm square field corresponding to the diameter of the collimated laser beam. The mean value of the radius r_o , measured from 24 consecutive frames of the movie film, and taken at a plane 4 cm from the band entrance when the dispersed phase flow rate was 0.67 cm s^{-1} and the total bed thickness was 12.0 cm, was 3.1 mm. The value predicted from equation 11 was 3.9 mm and this is considered to be exceptionally good considering the difficulties in making the measurements. Similar quality agreement was obtained from the other estimations. Therefore this is considered to further confirm the soundness of the model and together with Figures 10 and 11 confirm the reliability of the procedure of basing the prediction of the thickness of deep dispersion bands on a critical film thickness and a frequency of coalescence curve. This is considered to be more reliable than attempting to analyse bed thickness from a drop-drop coalescence time for the bed as a whole, and for each system to be considered.

In concluding the discussion of the results presented here it should be mentioned that no secondary drops of the dispersed phase were seen at any time; although these have been observed by other workers in bands and by ourselves in single layers of drops. However with the experiments in which the phototropic dye was in the continuous phase it was noticed that very small blue satellite drops appeared above the interface in the

coalesced dispersed phase. An allowance was made for this loss in the computer program. Nevertheless it is a finding not previously confirmed and should be considered in the design of phase separating vessels.

CONCLUSIONS

New techniques have been developed for examining the phase separation processes inside thick dispersion bands, based on matching the refractive indices of the phases and then discriminating the drops to be studied using phototropic dyes, lasers and the Christiansen effect.

A model describing the coalescence processes occurring in thick dispersion bands has been developed, based on the thickness of the continuous phase film at rupture and the shape of drops packed in the bed. The film thickness has been verified using a light absorption technique, and a computer program was written to predict band thickness as a function of drop size, flow rate and the physical properties of the system. Agreement between predicted and experimental results are very good.

TABLE 1

SYSTEM	DISPERSED PHASE	CONTINUOUS PHASE	REFRACTIVE INDEX	VISCOSITY cp		DENSITY gm/cm^3		INTERFACIAL TENSION γ dynes/cm
				DISP. μ_d	CONT. μ_c	DISP. ρ_d	CONT. ρ_d	
I	*AMYLACETATE	52% Wt.G	1.460	1.350	8.00	0.870	1.140	14.2
II	*ETHYLACETATE	37% Wt.G	1.372	0.455	3.60	0.900	1.090	7.0
III	*ISO OCTANE	48% Wt.G	1.395	0.433	5.45	0.692	1.122	35.6
IV	*HEXANE	37% Wt.G	1.372	0.326	3.60	0.660	1.090	34.5
V	*17% Wt.G	DIETHYLETHER	1.355	1.60	0.233	1.042	0.713	10.0
VI	*46% Wt.G.	ISOBUTYLACETATE	1.392	5.25	0.732	1.118	0.870	12.5
VII	ISOPROPYLETHER	27% G	1.367	0.470	2.15	0.730	1.065	15.0

*Systems that have been investigated.

SYSTEMS STUDIED

NOTATION

A	Area of plateau border
d	Drop diameter
D	Hydraulic mean diameter
F	Force causing drainage
g	Acceleration
h	Film thickness
H	Total band thickness
K	Constant in Lenard-Lemlick Equation
l	Length of side of face of dodecahedra
N	Number of drops
P	Pressure in film
q	Incremental flow rate
Q	Continuous phase flow rate
r	Radius of plateau border
R	Radius
t	Time
U	Drainage velocity
V	Superficial velocity
Z	Coordinate perpendicular to film
γ	Interfacial tension
θ	Angle of inclination of plateau border
λ	Frequency, or probability of coalescence
ϕ	Hold-up

Subscripts

c	Continuous phase
d	Dispersed phase
	Downward flow
o	Plateau border
u	Upward flow

LITERATURE CITED

1. Allak, A.M.A.:Ph.D.Thesis,Aston University, Birmingham 1973.
2. Claude, O. & Rumpf, P.:Compte Rend, 236, 697, 1953.
3. Christiansen, C.:Ann.Phys.,23, 294, 1884.
4. Kintner,R.C.:Advances in Chemical Engineering,4,87,1968,Acad.Press,
New York.
5. Meister,B.J. & Scheele,G.F.:A.I.Ch.E.J.,14,5,1968.
6. Lenard,R.A. & Lemlick,R.:Chem.Eng.Sci,20,79, 1965.
7. Allak, A.M.A. & Jeffreys G.V.: To be published.

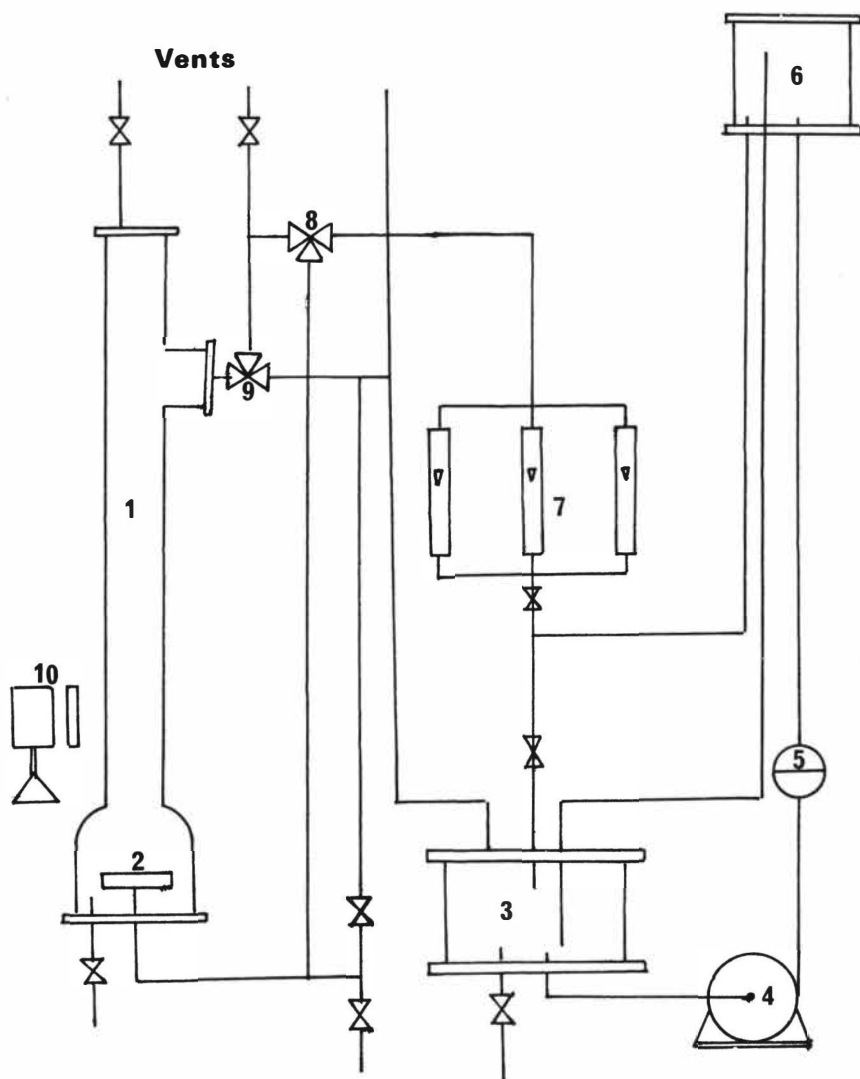


Figure 1 Arrangement of the Column

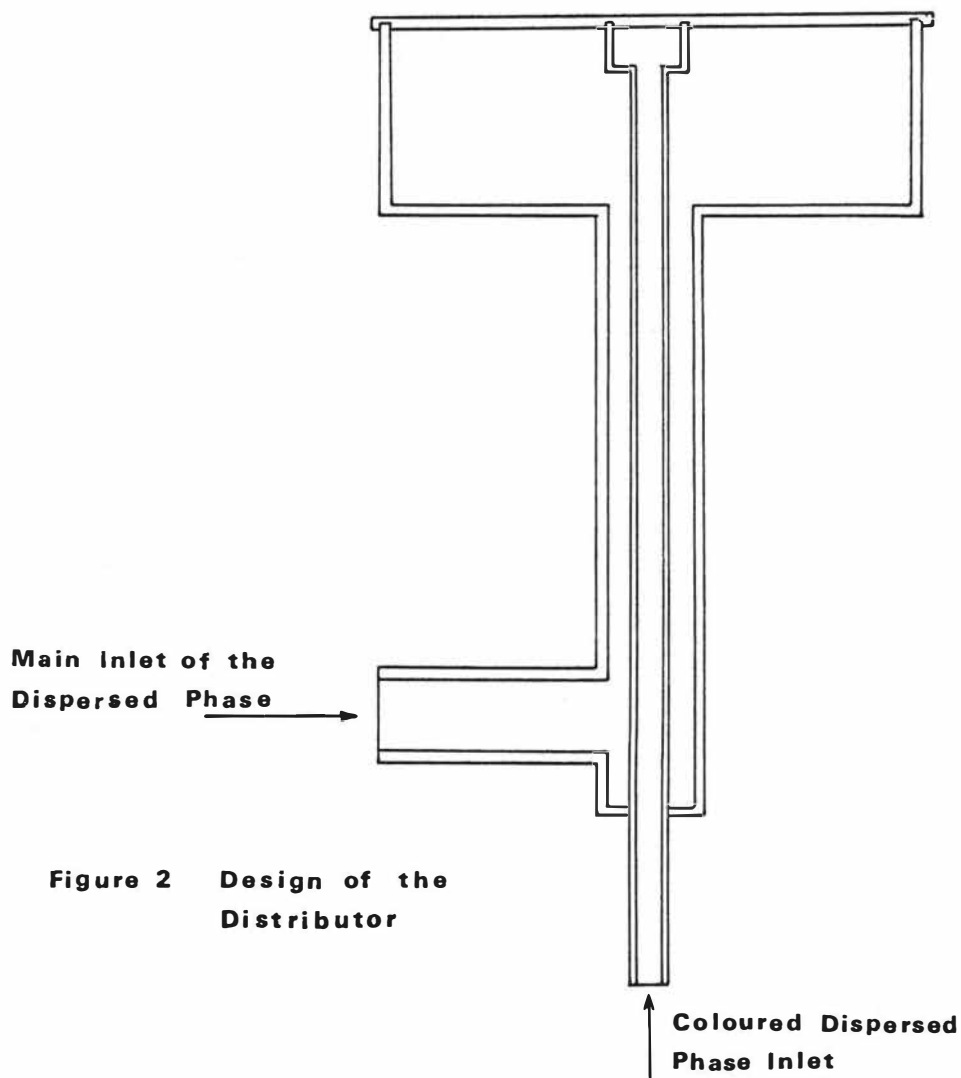


Figure 2 Design of the Distributor

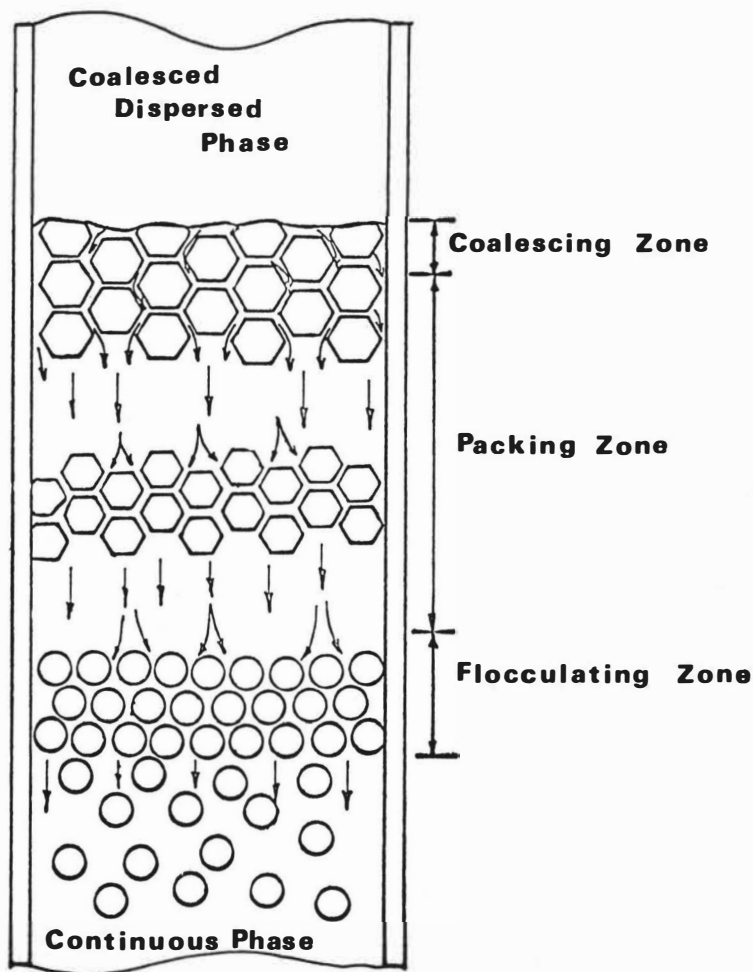


Figure 3 Illustration of Zones in a Closely Packed Dispersion Band

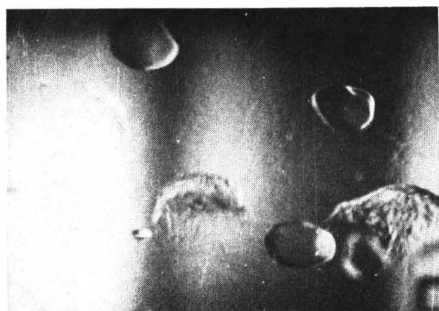


Figure 4 Coloured Drop Inside the Bed

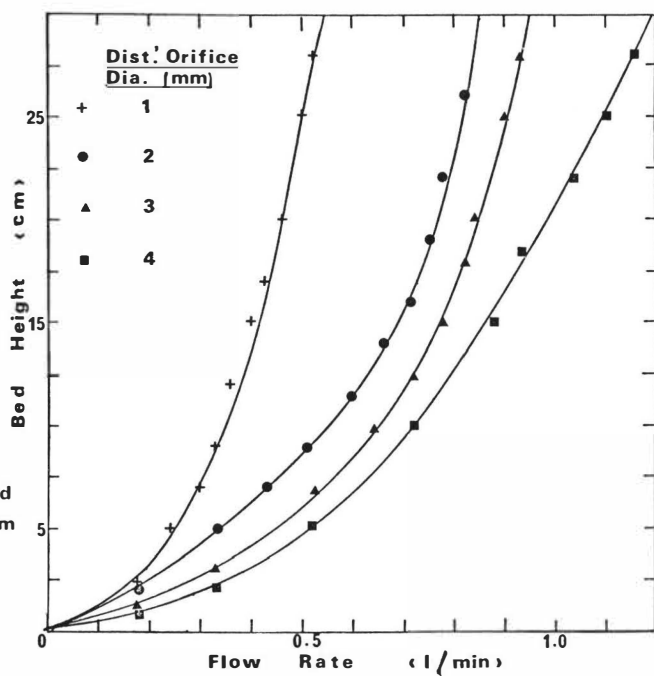


Figure 5 Relationship Between Bed Height and Flow Rate for the System Iso Octane

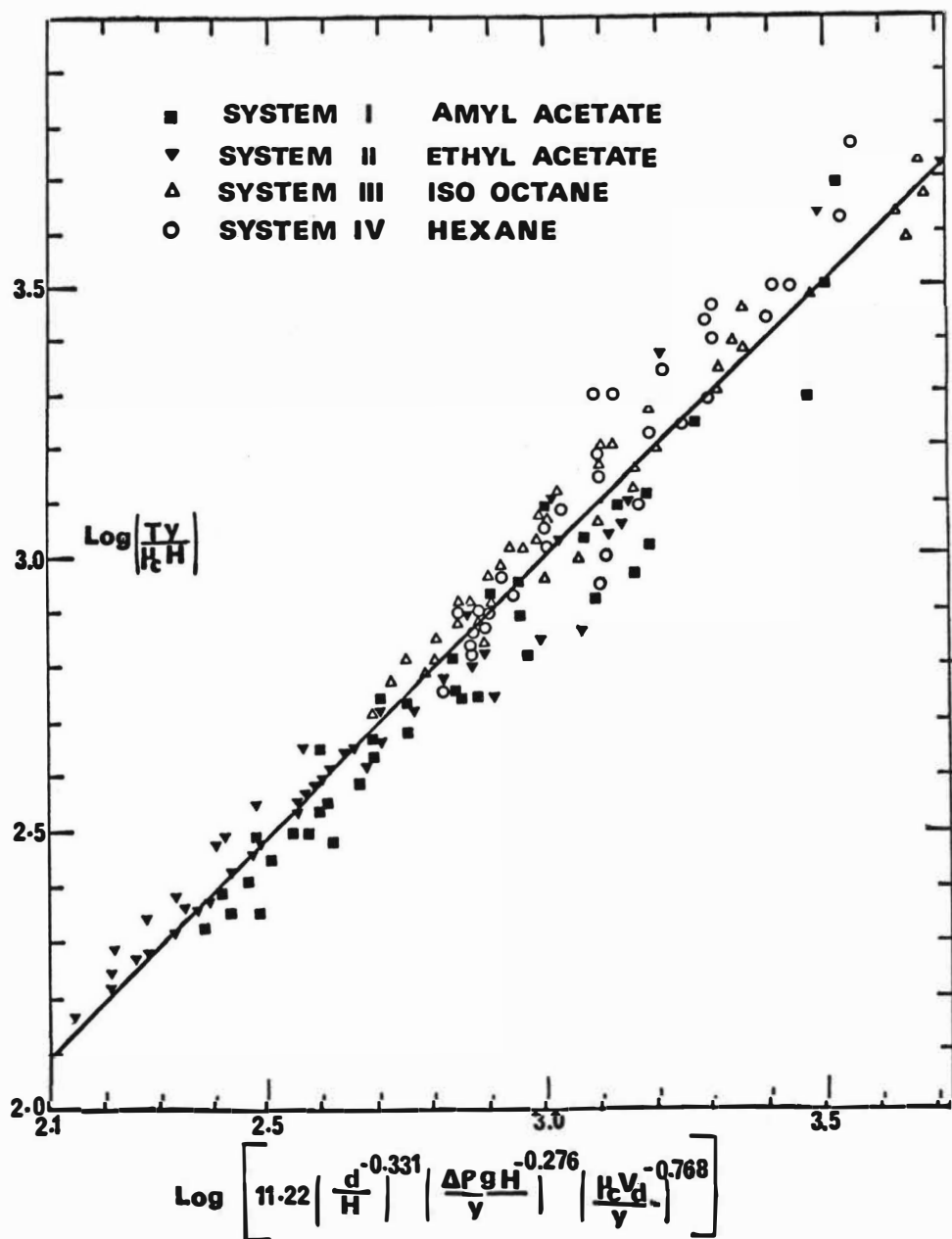


Figure 6 Correlation of Parameters

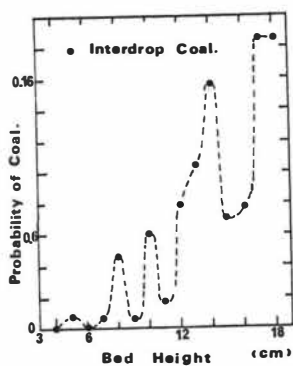


Figure 7 Probability of Coalescence for the System Iso Octane

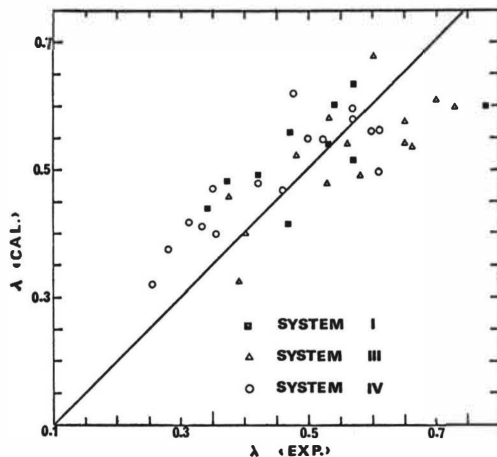


Figure 8 Comparison Between Experimental and Calculated Probability of Coalescence

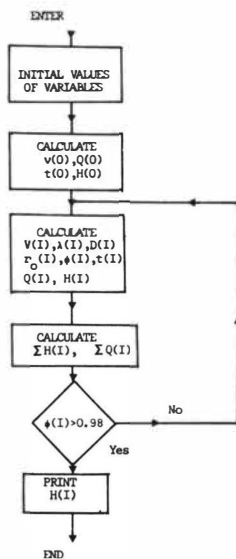


Figure 9 Block Diagram of Computer Programme

Figure 10 Comparison Between Experimental and Predicted Bed Heights for System Iso Octane

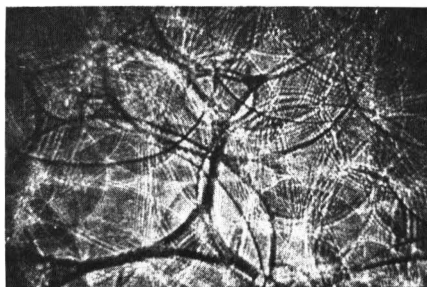
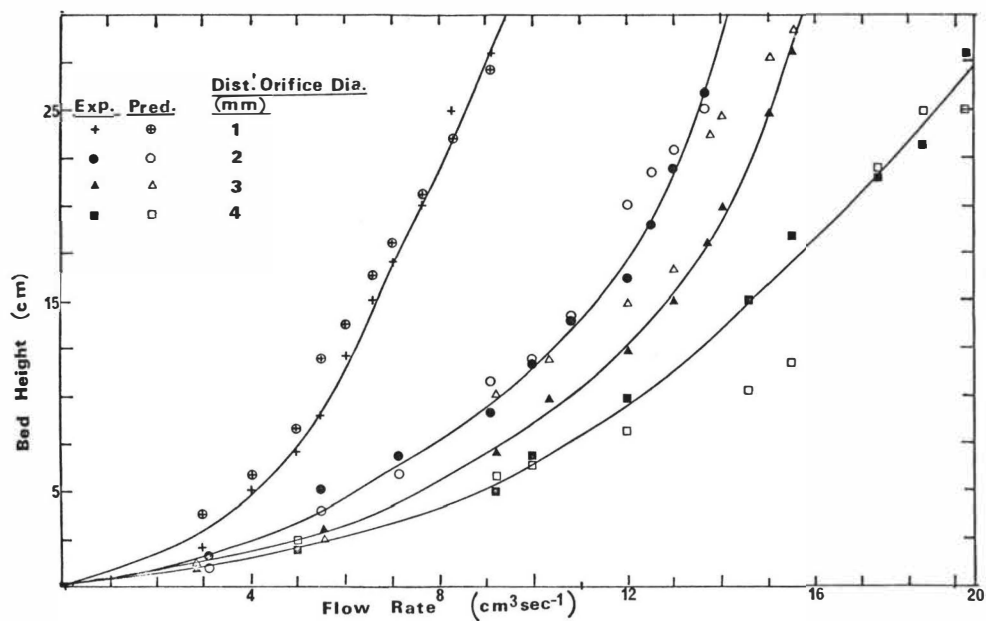


Figure 11 Photograph of a Plateau Border Inside the Bed

The motion of liquid droplets in settling and coalescence

E. Rushton & G.A. Davies

Department of Chemical Engineering,
University of Manchester
Institute of Science and Technology,
Manchester, 1. England.

Abstract

The relative motion of pairs of droplets along their line of centres is considered and solutions presented for settling and approach prior to coalescence. The influence of fluid viscosities, drop size, separation and approach velocity on flow in both the continuous phase fluid between the droplets and circulation within the droplets are investigated. It is shown that simple analyses presented in most 'film drainage' models are not correct. Internal circulation within droplets set up as a consequence of interfacial shear forces significantly influence the flow field particularly in the continuous phase fluid in the region separating the drops. Results are presented for settling representing the three limiting conditions; constant interdroplet separation, droplet separation and coalescence.

1. Introduction

The settling of droplets through an immiscible liquid phase is important in liquid extraction and particularly so in phase separation and coalescence. Settling is usually affected by the presence of rigid walls, free surfaces and adjacent droplets and thus, although prevailing conditions can be interpreted by the theory of low Reynolds number hydrodynamics, the simple Stokes law is not applicable. To formulate a description for a dispersion of droplets one must proceed beyond the case of a single droplet. This brings with it many complications. However, some assessment of interaction effects can be acquired by considering the case of doublets. This is amenable to analysis and the case of motion of two drops along the line of centres through each drop is the subject of the present paper. Apart from interpretation of settling phenomena the case considered is of some interest to droplet coalescence. If one considers coalescence between two droplets or a drop at an interface four stages can be distinguished viz. the approach of the droplets, drainage of the film of continuous phase trapped between the droplets, rupture of this film and finally transference of content of one drop into the other or, in the case of interface coalescence, into the bulk phase. Of these four sequences film drainage is the rate limiting step and thus any factors which influence film drainage will have immediate bearing on coalescence. In this context the approach of droplets is important particularly the flow conditions inside the droplets. If one considers a single drop settling through a second liquid, then it is well known that a secondary flow is established inside the droplet which not only modifies the drag forces on the droplet and the droplet terminal velocity but also modifies the surface velocity around the droplet^(1,2). In analysing the conditions of film drainage between a single droplet and an interface the internal circulation inside the droplet must be accounted for, unless it is immediately damped out on arrival at the interface (which is not possible), since it will modify the boundary conditions at the various fluid interfaces. In all models proposed

for film drainage this is not considered, indeed most workers⁽³⁻⁷⁾ have used boundary conditions requiring that the radial component of the surface velocity at both fluid-fluid interfaces is zero. Not only does this ignore the possibility of internal circulation but also requires that the fluid interfaces can sustain a finite shear stress, a condition applicable to fluid-solid interfaces and not to clean fluid-fluid interfaces.

The solutions of Hadamard and Rybczynski cannot be used directly to determine the internal circulation conditions in a droplet for the case of either approach towards a flat interface or towards a second droplet. This can only be obtained by allowing for the presence of a second droplet or interface. Thus the motion of two droplets has to be considered and this is the topic of the present paper. A short resumé of work relevant to this will first be presented.

The problem of the motion of two spherical particles along their line of centres was first considered by Stimson and Jeffrey⁽⁸⁾. They analysed the case of motion of two unequal solid spheres moving in the same direction with equal parallel particle velocities along their line of centres through a viscous fluid and obtained expressions for the drag force opposing the motion of each particle. This method of solution was extended by Pshenay-Severin⁽⁹⁾ to consider the case of unequal particle velocities and the corresponding drag forces associated with each particle determined.

The problem of the approach of a particle towards a flat interface, which is in fact a limiting case of the doublet problem obtained by letting the radius of curvature of one of the droplets approach infinity, has also been considered. Brenner⁽¹⁰⁾ and Maude⁽¹¹⁾ both analysed the problem of a solid particle approaching a solid plane and free surface whilst Bart⁽¹²⁾ has extended this to a solid and fluid sphere approaching a solid and fluid interface.

In all cases cited the authors have computed drag forces acting on the particles and the modifications required to use a simple Stokes law. The extension to compute (from the stream functions obtained from the solution of the flow equations) local velocities and velocity profiles in the various fluid regions has not been reported. These velocities are particularly important in settling and coalescence processes. The problems considered in the present paper will be analysed to provide information on velocity profiles in the various fluid regions - continuous and dispersed phases.

2. Formulation of the problem

The problem considered, motion of two spherical droplets through an immiscible liquid phase, is represented on figure 1. For incompressible Newtonian fluids fluid motion is described by the Navier Stokes equations and in this system three separate regions can be considered in which these equations must be satisfied viz. droplet phases 1 and 2 and the continuous phase fluid 3. In extraction and coalescence phases 1 and 2 may be identical thus only two separate phases exist. In developing the analysis however, the system will be kept general and three regions defined.

Under flocculation and gravity settling conditions the Navier Stokes equations can be linearised since the quadratic inertia terms $\vec{u} \cdot \nabla \vec{u}$ are small compared with the viscous term $\nabla^2 \vec{u}$ (13). Thus the equations describing fluid motion and the continuity equation are:-

$$\frac{\partial \vec{u}}{\partial t} + \frac{1}{\rho} \nabla p = \nu \nabla^2 \vec{u} \quad (1)$$

$$\nabla \cdot \vec{u} = 0 \quad (2)$$

where \vec{u} is the local fluid velocity and p the pressure. The problem considered here of approach of two droplets is inherently unsteady but the time dependent terms, $\frac{\partial \vec{u}}{\partial t}$, can be neglected if the dimensionless group incorporating the droplet translational Reynolds number (Ua/ν) $(a/h) \ll 1$ (10).

In this group U is a characteristic velocity - approach velocity of the droplets, $a (=2r)$ is a characteristic diameter and h a characteristic distance in the direction parallel to the flow - distance between the centre of the droplets. Thus when this condition and the condition of creeping flow is satisfied equations (1) reduce to the quasi-steady creeping flow equations,

$$\frac{1}{\rho} \nabla p = \nu \nabla^2 \vec{u} \quad (3)$$

For axisymmetric motion the velocity components in cylindrical co-ordinates (R, Z, θ) may be expressed in terms of the Stokes stream function, ψ . Thus

$$u_R = \frac{1}{R} \frac{\partial \psi}{\partial Z}, \quad u_Z = -\frac{1}{R} \frac{\partial \psi}{\partial R} \quad \& \quad u_\theta = 0 \quad (4)$$

and the quasi-steady creeping flow equations become

$$\left[\frac{\partial^2}{\partial Z^2} + R \frac{\partial}{\partial R} \left(\frac{1}{R} \frac{\partial}{\partial R} \right) \right] \psi = 0 \quad (5)$$

Due to the geometry of the fluid boundaries it is more convenient to express the fluid motion in a bi-polar co-ordinate system (ξ, η, θ) related to the cylindrical co-ordinates, (R, Z, θ) by

$$R = \frac{c \sin \eta}{\cosh \xi - \cos \eta}, \quad Z = \frac{c \sinh \xi}{\cosh \xi - \cos \eta}, \quad \theta = \theta \quad (6)$$

Two settling drops, figure 1, external to each other and travelling in the negative Z direction correspond to the values $\xi = \alpha$ (> 0) and $\xi = \beta$ (< 0) where α , β and c (which is also greater than zero) are defined by the relations:-

$$\alpha = \cosh^{-1} (h_1/r_1) \quad (6i)$$

$$\beta = \cosh^{-1} (h_2/r_2) \quad (6ii)$$

$$c = r_1 \sinh \alpha = -r_2 \sinh \beta \quad (6iii)$$

The solution, ψ_1 , of equation (5) where the subscript corresponds to the flow region 1, 2 or 3 (figure 1), is (8)

$$\psi_1 = (\cosh \xi - x)^{3/2} \sum_{n=0}^{\infty} U_{ni}(\xi) C_{n+1}^{-1/2}(x) \quad (7)$$

where $x = \cos \eta$,

$$U_{ni}(\xi) = a_{ni} \cosh(n-1/2)\xi + b_{ni} \sinh(n-1/2)\xi + c_{ni} \cosh(n+3/2)\xi + d_{ni} \sinh(n+3/2)\xi$$

and $C_{n+1}^{-1/2}(x)$ is a Gegenbauer polynomial of order $(n+1)$ and degree $-1/2$.

The constants a_{ni} , b_{ni} , c_{ni} and d_{ni} are to be determined from the boundary conditions.

For fluid interfaces (in the absence of surface active agents) the boundary conditions must allow for the continuity of velocity and shear stress at each fluid interface. It is assumed that the discontinuity in the normal stresses is balanced by the interfacial tension forces. In addition to these requirements the velocity components must remain finite at the centres of the droplets. These conditions have been considered in a previous paper in which the drag forces opposing the motion of two arbitrary fluid spheres were evaluated⁽¹⁴⁾. By applying the boundary conditions, a system of linear algebraic equations for the constants a_{ni} , b_{ni} , c_{ni} and d_{ni} can be generated. By solving these equations, values for the stream function over a range of values of ξ and η can be generated. In the present paper we are interested in computing velocity profiles in the various fluid regions. These can be obtained from the stream functions ψ_1 since,

$$u_{\xi i} = - \frac{(\cosh \xi - x)^2}{c^2} \frac{\partial \psi_1}{\partial x} \quad (8i)$$

$$u_{\eta i} = - \frac{(\cosh \xi - x)^2}{c^2 \sin \eta} \frac{\partial \psi_1}{\partial \xi} \quad (8ii)$$

$$u_{\theta i} = 0 \quad (8iii)$$

In interpreting the results, and to compare them with previously published data, it is convenient to also compute velocity components in cylindrical co-ordinates u_{R1} , u_{Z1} , $u_{\theta 1}$. These are related to the corresponding bi-polar components by:-

$$u_{R1} = -\frac{1}{(\cosh \xi - x)} \left[u_{\xi 1} \sin \eta \sinh \xi + u_{\eta 1} (1-x \cosh \xi) \right] \quad (9i)$$

$$u_{Z1} = \frac{1}{(\cosh \xi - x)} \left[u_{\xi 1} (1 - x \cosh \xi) - u_{\eta 1} \sin \eta \sinh \xi \right] \quad (9ii)$$

$$u_{\theta 1} = 0$$

Thus from equation 7 the stream function ψ_1 can be evaluated for appropriate values of ξ and η in each of the three fluid regions. By substitution into equations 8 or 9 the local fluid velocities can be computed and velocity profiles constructed. At this stage no limitations, apart from the droplets remaining spherical, have been imposed and by selecting values of droplet velocities U_1 and U_2 the conditions for settling of the droplets by reason of resulting buoyancy forces, for which case U_1 and U_2 will have the same sign, or coalescence when U_1 and U_2 will generally have opposite signs can be considered.

Furthermore no restrictions have been placed on the radii of the droplets. By allowing the radius of one of the droplets to approach infinity the conditions for a droplet approaching a flat fluid interface prior to coalescence can be investigated. Some inter-relation of the parameters U and r however exist and for example in the case of settling of droplets of one liquid through a second liquid the settling velocities are functions of the droplet radii and cannot be selected arbitrarily. To allow for this, recourse must be made to the drag forces acting on each droplet⁽¹⁴⁾. Settling of a pair of liquid droplets is considered, in this paper the drag forces for the conditions examined were first computed and the appropriate ratio U_1/U_2 arising from this used in com-

puting the velocity profiles (see ref. 14 equation 51).

3. Results and Discussion

Numerical evaluation of equations 8 has been obtained for conditions of settling of drops and coalescence. These are presented for a range of conditions to show the effect of droplet diameter, droplet relative velocities, interdroplet separations and most important the viscosities of the fluid phases on the velocities in the continuous phase fluid, separating the droplets, and inside the drops. Before presenting the results it is perhaps instructive to discuss the relationship between bipolar and cylindrical co-ordinates. ξ_i ($i = 1, 2$ and $\xi_1 = \alpha$, $\xi_2 = \beta$), equation 6i and 6ii, represents a dimensionless geometric separation. The single or combined effect of either increasing the droplet radius, r_i , or reducing the geometric separation of the drop from the plane $Z = 0$ ($\xi = 0$), h_i , decreases the corresponding value of ξ_i (see equations 6i and 6ii). Hence solutions for different values of ξ_i may be compared to assess either the relative geometric separations or the drop radii on the velocities in each phase.

The solutions presented are displayed in reduced dimensionless cylindrical co-ordinates ($R^* = R/c$, $Z^* = Z/c$) and are functions of the dimensionless separations α and β and the viscosity ratio μ^* defined as μ_2/μ_1 . The limiting case of $\mu^* = 0$ corresponds to the motion of solid particles and satisfies the boundary conditions of zero radial velocity at the particle surfaces. Results will be presented first for settling of droplets through an immiscible liquid phase due to the action of buoyancy forces and then for approach of droplets travelling towards each other with arbitrary velocities prior to coalescence.

a) Settling

In examining settling of two droplets in an immiscible fluid phase three cases can be considered. Denoting the upper droplet by subscript 1 and the lower by subscript 2 these are:- case 1) $U_1 = U_2$, i.e the relative velocity between the droplets is zero thus the interdroplet distance will

remain constant; case 2) $U_1 > U_2$, here the interdroplet distance will decrease leading to droplet coalescence, and finally case 3) when $U_2 > U_1$, the separation between the droplets will increase with time. All cases can be investigated by inserting appropriate values of physical properties, radii and particle terminal velocities into the equations in Section 2.

For the two fluid problems considered here i.e. phase 1 = phase 2 it is important to realise that the settling velocities and radii of the droplets are inter-related and cannot be selected arbitrarily. Results for each of the three cases described are presented to show the influence of the viscosities of the fluid phases. The velocities of the droplets were first computed from expressions for the drag forces⁽¹⁴⁾ and then substituted into equations 8 to obtain velocities in the continuous phase fluid separating the droplets, $U_{R3} = f(Z)$ and inside the drops, $U_{Z1}, U_{Z2} = f(R)$. To generalise, velocities relative to an approach velocity U are presented. To simplify, the presentation the radial velocity profile is presented at a constant radial position $R^* = 0.5$ and the velocities inside droplets are computed across a diameter perpendicular to the direction of settling.

Case 1 $U_1 = U_2 = U$

For this case with $v_1 = v_2$ the radii of the droplets are equal. The effect of the viscosity ratio, μ^* , on both velocities U_R and U_Z is shown in figure 2. For the case of solid particles, $\mu^* = 0$, the radial velocity component U_R is zero at the surfaces of the spheres and as we proceed in the positive Z direction from the surface of the second particle the velocity becomes negative denoting flow of continuous phase fluid into the region between the particles. U_R continues to decrease to minimum then increases to be zero at the origin, $Z/c = 0$, which is midway between the particles. It then continues to increase to a maximum velocity before finally decreasing to zero at the surface of the upper sphere. The profile is made up of two parabolas about the midpoint of separation of the particles

the one being a reflection of the other such that the net flow of phase 3 into this region is zero. This satisfies the physical conditions. As the viscosity ratio increases the parabolic shape flattens and the surface velocities on each sphere become non zero, a consequence of internal motion in the drop phases. On the surface of the lower droplet the surface velocity is in the direction of reduced R^* since the internal circulation is towards the near stagnation point at $R^* = 0$, $\xi = \beta = -1.0$. At the near stagnation point the surface velocity must of course become zero thus $U_R \big|_{\xi=\beta=-1.0}$ must decrease as one proceeds around the sphere towards $R^* = 0$. In all cases the radial velocity profile is similar about the axis $R^* = 0$ thus satisfying the physical condition of constant droplet separation and thus zero net flow of continuous phase in this region. The development of internal motion in the droplet with increasing μ^* is seen from figures 2b and 2c. The absolute velocity (that is as seen by an observer at a fixed position), U_Z , is symmetric about the axis $R^* = 0$. The maximum velocity increases with μ^* , at $\mu^* = 10$ the maximum velocity is 35% greater than the settling velocity U . Again to satisfy the physical conditions $\int_0^{+r} U_Z \, dR^2 = U r^2$ for all cases.

Case 2 $U_1 = U > U_2$

In settling this will result in interdroplet coalescence and is a condition often observed in a flocculating dispersion. If the fluid phases 1 and 2 are identical then solution of the equation relating the velocity ratios for $U_1 - U_2 > 0$ must result in $r_1 > r_2$. To illustrate the variation of the velocities U_{R3} and U_{Z1} with μ^* calculations have been carried out for $\xi = \alpha = 0.5$ and $\xi = \beta = -1.0$. The situation is shown in figure 3. Consider first the radial velocity in phase 3. If $U_1 > U_2$ then a net flow of continuous phase fluid from the region between the particles must take place, and as seen in all cases for $\mu^* = 0$ to $\mu^* = 10$, \bar{U}_R/U is always positive. In the case of $\mu^* = 0$, representing settling of two solid spheres,

the surface velocity as in case 1 above is zero. Again as μ^* increases so the effect of surface velocity becomes more pronounced and the velocity profile flattens. The effect of internal circulation on the radial velocity profile is perhaps seen most clearly at the surface of the upper droplet. The surface velocity is in the positive direction and increases as μ^* increases. On the lower droplet however the surface velocity is in the negative direction towards the near stagnation point, this effect becomes pronounced as μ^* increases. In figure 3d a flow reversal is evident in the region next to the surface of the lower droplet. This is similar to case 1 and is due to internal circulation in the droplets, the development of which can be assessed from the profiles of U_z in figure 3. It is worth noting the point made earlier that U_1 , U_2 , r_1 and r_2 are not independent in settling. As μ^* increases from 0 to 10 for constant drop radii the ratio of the settling velocities U_1/U_2 decreases from $1/0.71$ to $1/0.82$.

Case 3 $U_1 = U < U_2$

This case will result in increasing particle separation with time and again is a situation observed in flocculation, particularly in spray columns when interdroplet coalescence has taken place. As is evident from case 2 above if phases 1 and 2 are identical and $U_1 - U_2 < 0$ then $r_2 > r_1$. The velocity profiles for $\mu^* = 0, 0.1, 1.0$ and 10 are shown in figure 4. The trends discussed above for the surface velocities, radial velocity profiles and axial velocity profiles in the droplet are again observed. In this case to satisfy the physical condition of net flow of continuous phase into the region separating the droplets. \bar{U}_R is negative. For the solid/solid case the profile at any instant of time is symmetric about the midpoint of separation of the particles and is approximately parabolic. As μ^* increases the profile flattens. A similar condition to that in case 2 is observed as μ^* increases, a flow reversal can take place brought about solely by the action of internal droplet circulation. This may be seen in figure 4d (compare 3d), in this case the reversal takes place near the surface of

the upper droplet.

The analysis of the settling of two droplets shows clearly that the fluidity of the droplets must be taken into account. Velocities in both phases are influenced by the relative viscosities. It is not satisfactory to use results for solid spheres to interpret droplet behaviour. In these results spherical droplets only are considered, the position will be further accentuated if distortion takes place.

b) Coalescence

The approach of droplets prior to the film drainage period can be investigated. Equations 8 can be evaluated for a range of conditions to investigate the effects of droplet approach velocities, droplet diameters and separation and the viscosity of the phases. Arbitrary values of approach velocities will be chosen but if coalescence takes place by gravity settling alone then, as in the previous section, the droplet approach velocities are not independent and must be calculated. In the cases considered the velocities in both dispersed and continuous phase fluids will be calculated relative to an approach velocity U ($U = U_1$).

The influence of the fluidity of the droplet will first be considered for the special case of approach of equal sized drops. This was first discussed by McAvoy and Kintner⁽⁵⁾ in an attempt to analyse conditions prior to interdroplet coalescence. The flow of continuous phase fluid in the region separating the drops was considered. McAvoy and Kintner, following an earlier treatment of Charles and Mason⁽⁴⁾ for the analogous drop-interface problem, postulated a parabolic velocity profile in this region of the continuous phase fluid. This, as stated in the introduction, implies that the radial component of velocity is zero at the interface of drops. In the present work this has been re-examined and solutions of equations 8 obtained over a range of fluid viscosities from $\mu^* = 0$ (the solid sphere-fluid problem) to $\mu^* = 10$. The results are shown in figure 5. In this figure the radial velocity profile in the continuous

phase fluid is shown computed at $R/c = 0.5$. In addition the absolute velocity inside the upper droplet is shown computed across the diameter perpendicular to the line of motion of the drop. For the case considered where each droplet is allowed to approach at the same velocity U the velocity profile inside the lower droplet is merely a mirror image of that shown for the upper drop. It should be emphasised that any values for U_1 and U_2 can be chosen, it is not necessary that $U_1 = U_2$. Considering the velocity in the continuous phase fluid first the conditions for $\mu^* = 0$ result in a parabolic velocity profile in accord with the analysis of McAvoy and Kintner. This is only correct for solid spheres and for this case the velocity in the sphere, U_2 , is constant and equal to the approach velocity U . This is shown in figure 5a. As μ^* increases two things are apparent. First that the radial velocity profile in the continuous phase fluid flattens and at $\mu^* = 1.0$ this is approaching plug flow. At $\mu^* = 10$ this velocity profile becomes concave. This change is brought about by the increasing fluidity of the drop, as μ^* increases so the internal circulation inside the drop increases. The absolute motion inside the drops in the direction Z are shown in figure 5(a)-(d). As the viscosity of the dispersed phase is reduced the centre line velocity at $R/c = 0$ increases until at $\mu^* = 10$ this is 70% greater than the approach velocity U . The relative velocity inside the droplets (that is as seen by an observer moving with the droplet) is shown in figure 6. This is again computed across the diameter at $Z/c = 1.313$. As μ^* increases from zero the relative velocity itself develops and the velocity in a central zone about $R/c = 0$ increases in the direction of motion of the droplet. As a consequence of the shear forces acting at the interface of the drop at the periphery the flow is in the negative direction. As would be expected this increases with increasing μ^* . Thus the results show that the radial velocity profile in the continuous phase fluid is influenced by the

fluidity of the drop and parabolic profiles are only correct for solid spheres approaching. The influence of internal droplet circulation must be considered.

The effect of approach velocity and drop size has been considered and results for approach of particles radii r_1 and r_2 at velocities U and $U/2$ and U and 0 are shown in figures 7 and 8.

Only two cases $\mu^* = 0$ and $\mu^* = 10$ are shown but results follow a similar trend as for equal sized drops. Again the parabolic velocity profile for the cases $\mu^* = 0$ are modified as μ^* increases. The surface velocity in each drop is determined by the approach velocity and as this is reduced the radial velocity profile in the continuous phase fluid is modified. This can be seen from figures 5d, 7b and 8b i.e. as U_2 decreases from U to 0 . Also clearly as the relative approach velocity between the drops decreases so the displacement flow of continuous phase decreases and thus the curvature of the profile changes, compare 7a and 8a. The conditions inside the drops show the same trend as for equal sized drops. It is interesting to note that again as the relative approach velocity decreases so the relative velocity inside the drops is modified and as seen from figures 7d and 8d the maximum velocity (at $R/c = 0$) is reduced. This is a direct consequence of a reduction in the surface velocities of the drops.

From the present analysis the surface velocity u_η can be calculated. Results for approach of different sized particles are shown in figure 9. In 9a the relative surface velocity u_η/U on the smaller particle is shown. The difference in conditions between a solid particle and fluid drop is well demonstrated. For the solid sphere the surface velocity u_η is determined only by the component of the approach velocity U and is always positive. For liquid droplets this can be quite different, u_η/U is again zero at $\eta = \pi$ but then becomes negative (as a result of internal circulation) increases to take on a maximum value before decreasing to zero again at

the near stagnation point $\eta = 0$. As μ^* increases this trend becomes more pronounced. A limiting case of this above work, to consider a spherical drop approaching a flat fluid interface (the extension of the simple Charles and Mason model), has already been considered⁽⁵⁾. In this paper radial velocity profiles and surface velocities were computed and show exactly the same trend. One extension to this is to compute equation 8 for conditions inside the droplet. These are shown in figure 10. A similar trend is observed and by comparing figures 5 and 8 with this the effect of the radius of curvature of the lower interface in increasing from R_2 to ∞ can be observed.

Conclusions

A solution to the creeping flow equations is presented for the motion of droplets along their line of centres and results for typical cases in free settling and conditions of droplet approach prior to coalescence presented. For limiting cases such as approach of solid spheres the solutions agree with previously published data. It is shown that effect of internal circulation on the liquid velocities at the interfaces is important in modifying the velocity profile in the continuous phase fluid between the drops. This effect increases as the ratio of the viscosity of the continuous phase liquid to dispersed phase liquid increases and becomes very significant when this ratio is of the order 10. As this ratio increases internal circulation can cause flow reversal in the continuous phase fluid separating the drops.

Finally the results show the limitations of simplified models presented to represent film drainage prior to coalescence in which a parabolic velocity profile is postulated.

NOMENCLATURE

a_n, b_n, c_n, d_n	constants of integration (equation (7))
c	constant (equation (6))
$C_{n+1}^{-\frac{1}{2}}(s)$	Gegenbauer polynomial of order $(n+1)$ and degree $-\frac{1}{2}$ with argument μ
h	characteristic distance, distance of centre of sphere $\xi = \text{constant}$ from $\xi = 0$
i	subscript denoting fluid regime, i ($i = 1, 2, 3$) (see figure 1)
n	summation index (equation (7))
p	pressure
r	characteristic radius, radius of sphere $\xi = \text{constant}$
R, Z, θ	cylindrical co-ordinates
t	time
U	characteristic velocity, approach velocity of sphere $\xi = \text{constant}$
\vec{u}	vector fluid velocity
U_R, U_Z, U_θ	velocity components in cylindrical co-ordinates
\bar{u}_R	mean velocity in radial direction
u_ξ, u_η, u_θ	velocity components in bipolar co-ordinates
$U_n(\xi)$	mathematical function (equation (7))

Greek symbols

σ	dimensionless distance (equation (5))
β	dimensionless distance (equation (5))
μ_1	fluid viscosity of region 1
μ^*	dimensionless viscosity group μ_3/μ_1
ξ, η, θ	bipolar co-ordinates
ν	kinetic viscosity
ψ	stream function
x	$\cos \eta$

References

1. Hadamard, J.S., C.r hebdomadaire Académie des Sciences, 152, 1735 (1911) and 154, 109, (1912)
2. Rybczynski, W., Bull. Acad. Sci. Cracovie Ser. A 40, (1911)
3. Gillespie, T. & Rideal, E.K., Trans. Faraday Soc., 52, 173 (1956)
4. Charles, G.E. and Mason, S.G., J. Coll. Sci., 15, 105, 236, (1960)
5. McAvory, R.H. & Kintner, R.C., J. Coll. Sci., 20, 188, (1965)
6. Jeffreys, G.V. & Hawksley, J.L., A.I.Ch.E.J. 11, 413, (1965)
7. Hartland, S. Chem. Eng. Sci., 22, 1675, (1967)
8. Stimson, M & Jeffrey, G.B. Proc. Roy. Soc., A111, 110, (1926)
9. Pshenay-Severin, S.V., Bull. Acad. Sci. USSR, Geophys. Ser. 10, 724, (1958)
10. Brenner, H. Chem. Eng. Sci., 16, 242, (1961)
11. Maude, A.D., Br. J. Appl. Phys., 12, 293, (1961)
12. Bart, E., Chem. Eng. Sci., 23, 193, (1968)
13. Happel, J. & Brenner, H., "Low Reynolds Number Hydrodynamics"
Prentice Hall Book Co (1965)
14. Rushton, E. & Davies, G.A., Appl. Sci. Res. 28, 37 (1973)
15. Rushton, E. & Davies, G.A., A.I.Ch.E. Annual Meeting Philadelphia
Symposium on Interfacial Phenomena, Nov. 1973.

CAPTIONS

- Figure 1 Geometric Configuration
- Figure 2 Settling of Identical Drops $U_1 = U_2 = U$, Effect Of Fluid Viscosities on Velocity Profiles
- Figure 3 Settling of Drops $U_1 = U > U_2$, Effect of Fluid Viscosities on Velocity Profiles
- Figure 4 Settling of Drops $U_1 = U < U_2$, Effect of Fluid Viscosities on Velocity Profiles
- Figure 5 Approach of Identical Drops Prior to Coalescence
 $U_1 = -U_2 = U$, Effect of Fluid Viscosities on Velocity Profiles
- Figure 6 Approach of Identical Drops Prior to Coalescence
 $U_1 = -U_2 = U$, Effect of Fluid Viscosities on Relative Velocity, U_z/U , inside a drop.
- Figure 7 Approach of Unequal Drops Prior to Coalescence. Effect of Fluid Viscosities on Absolute and Relative Motion.
- Figure 8 Approach of a Drop Towards a Stationary Drop, Effect of Fluid Viscosities on Absolute and Relative Motion.
- Figure 9 Variation of Surface Velocity on Drops, Effect of Fluid Viscosities.
- Figure 10 Approach of a Drop towards a Plane Interface, Effect of Fluid Viscosities on Relative Velocity, U_z/U , inside drop.

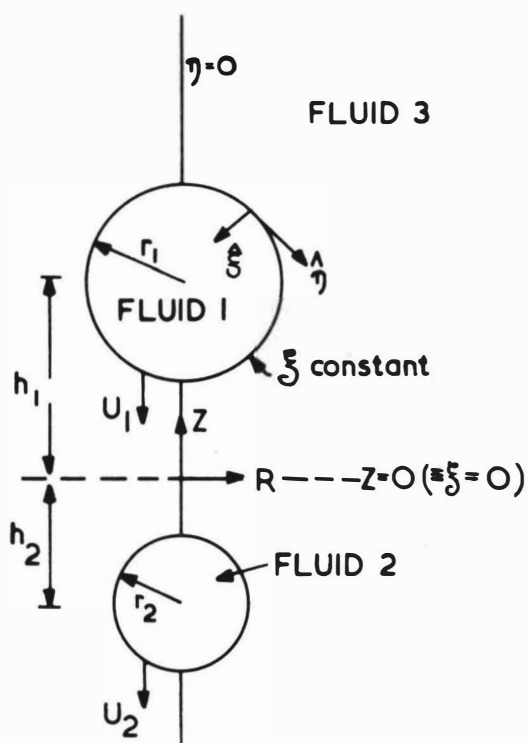


FIGURE 1. GEOMETRIC CONFIGURATION.

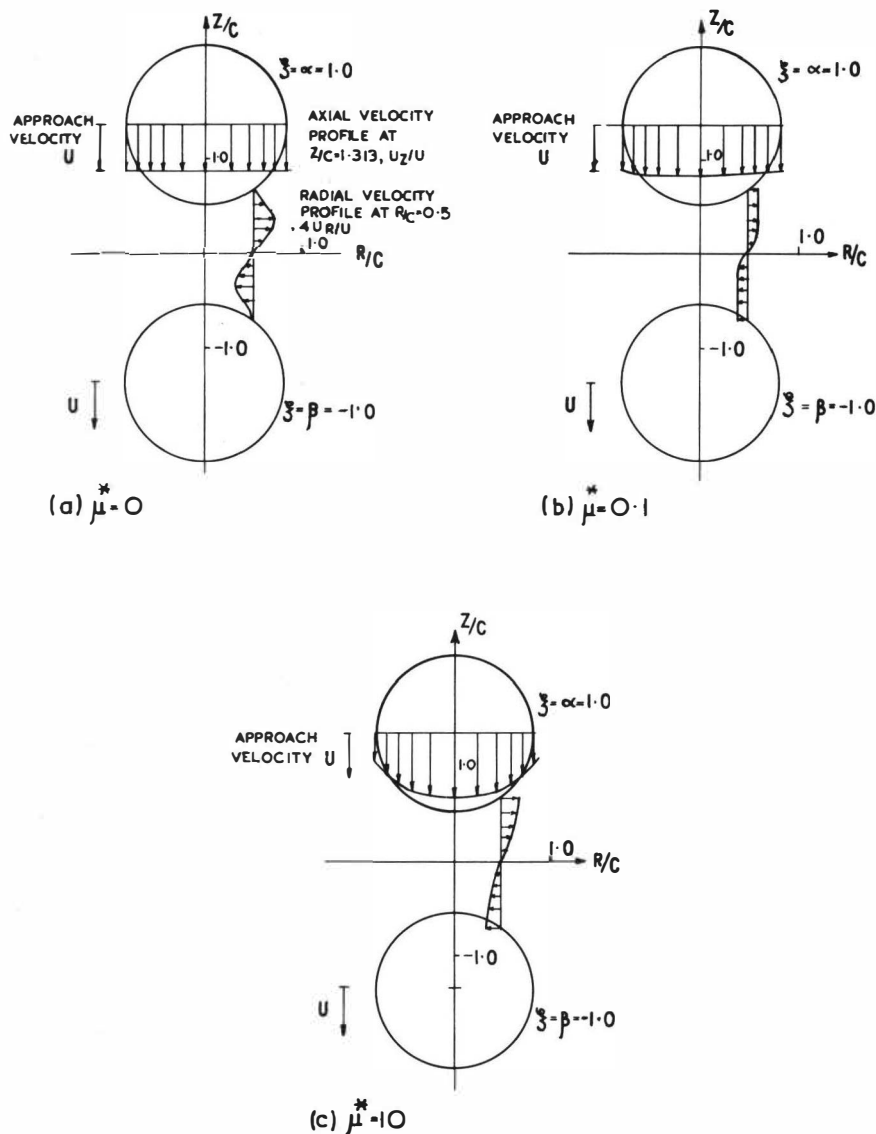


FIGURE 2. SETTLING OF IDENTICAL DROPS $u_1 = u_2 = u$
EFFECT OF FLUID VISCOSITIES ON VELOCITY PROFILES

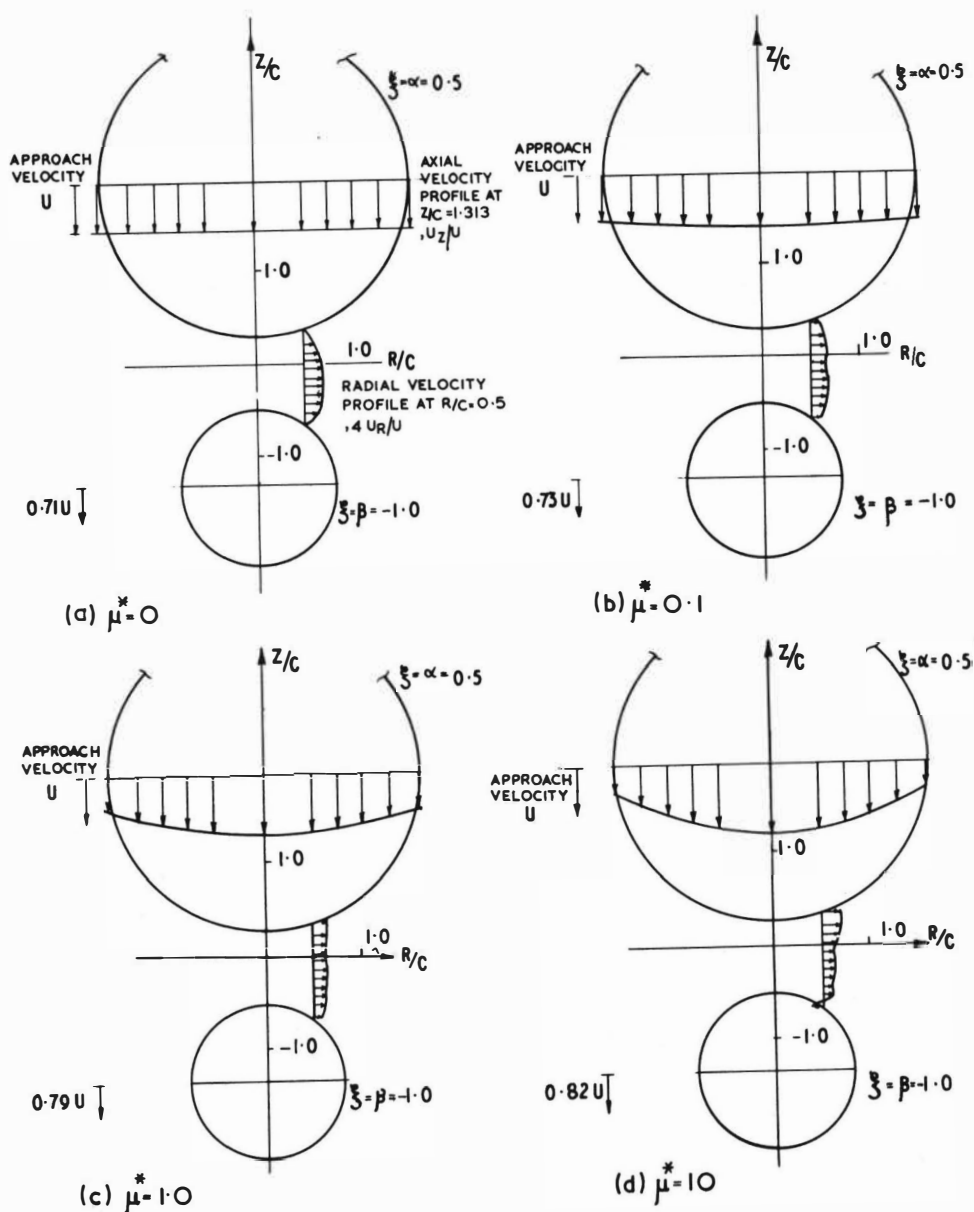


FIGURE 3. SETTLING OF DROPS $U_1 = U > U_2$,
EFFECT OF FLUID VISCOSITIES ON VELOCITY PROFILES.

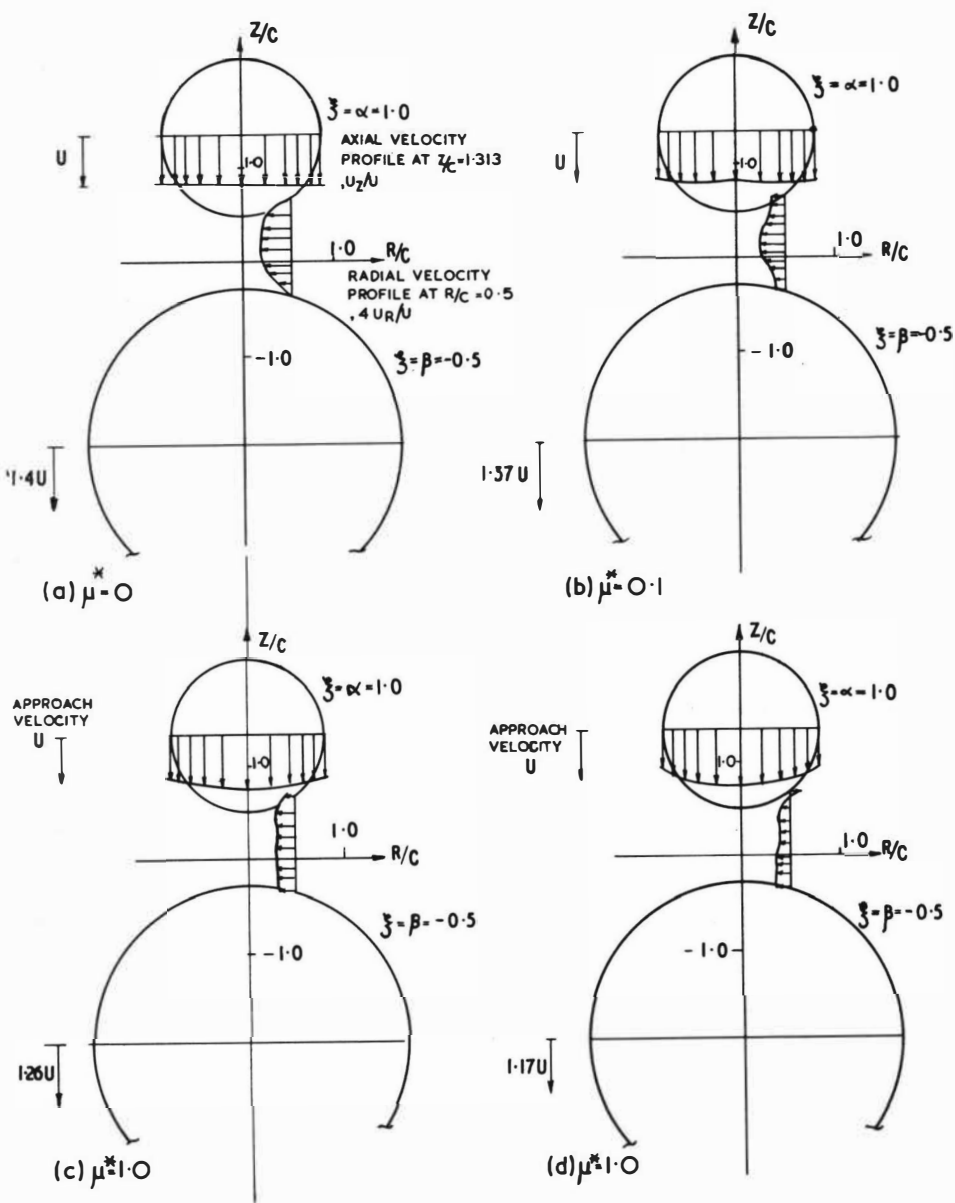


FIGURE 4. SETTLING OF DROPS $u_1 = U < u_2$,
EFFECT OF FLUID VISCOSITIES ON VELOCITY PROFILES.

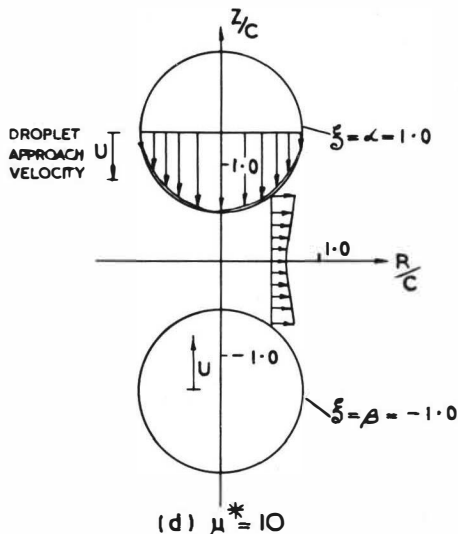
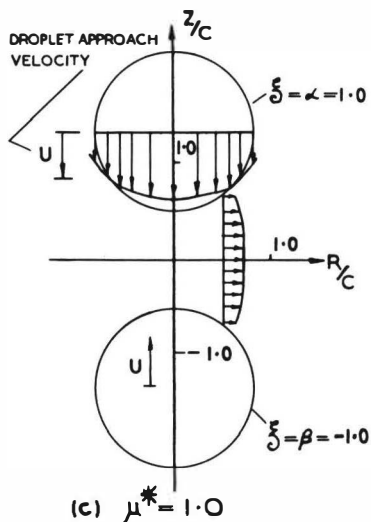
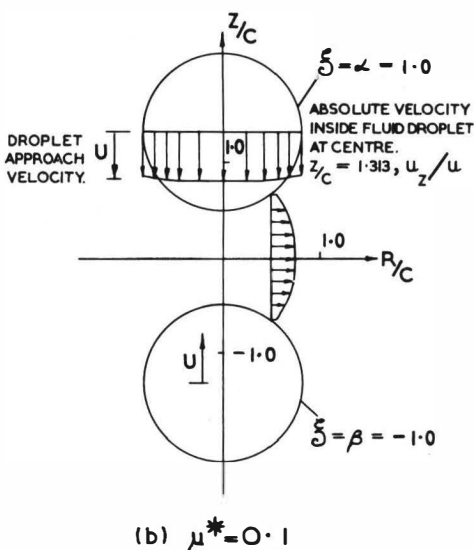
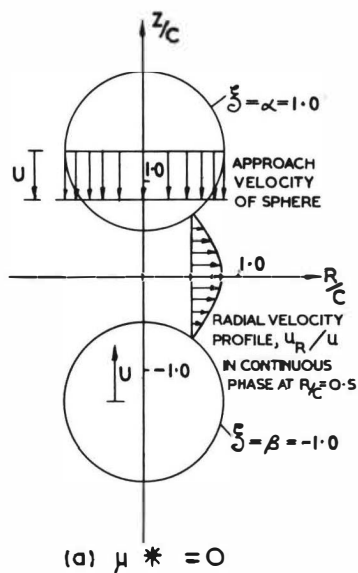


FIGURE 5. APPROACH OF IDENTICAL DROPS PRIOR TO COALESCENCE $u_1 = -u_2 = u$, EFFECT OF FLUID VISCOSITIES ON VELOCITY PROFILES.

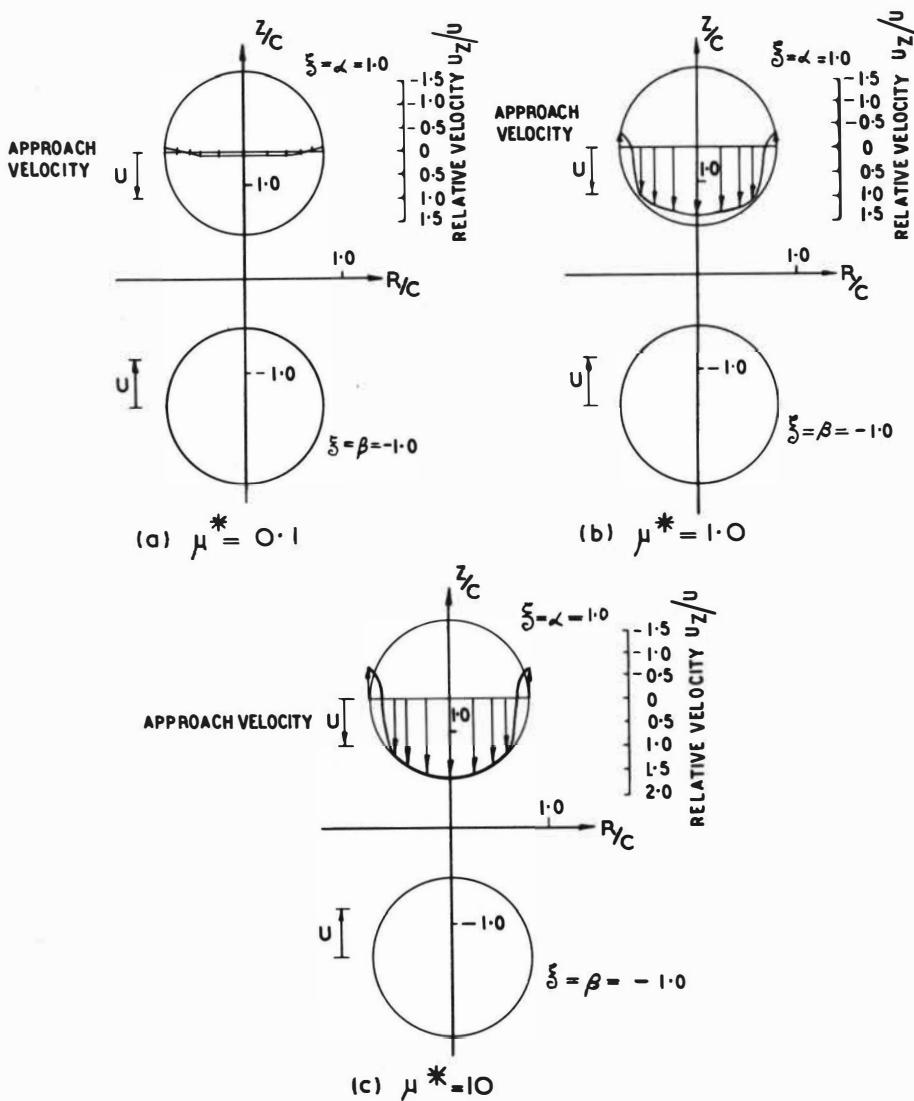
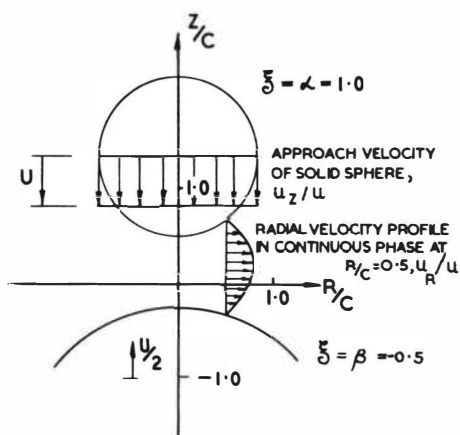
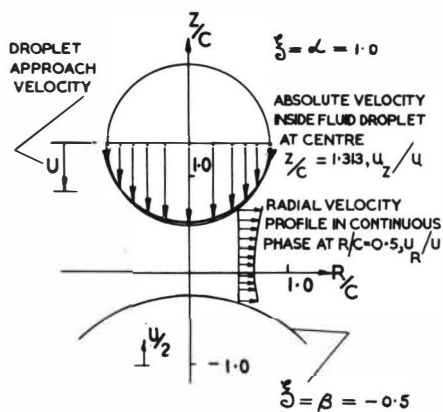


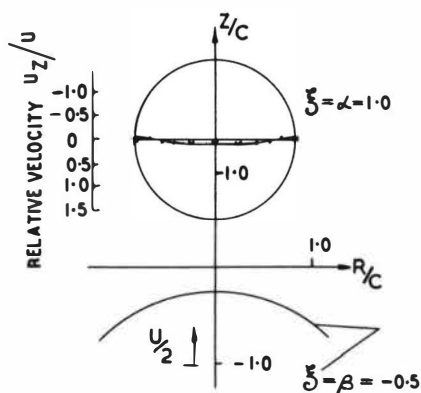
FIGURE.6. APPROACH OF IDENTICAL DROPS PRIOR TO COALESCENCE $U_1 = -U_2 = U$, EFFECT OF FLUID VISCOSITIES ON RELATIVE VELOCITY u_z/u , INSIDE DROP.



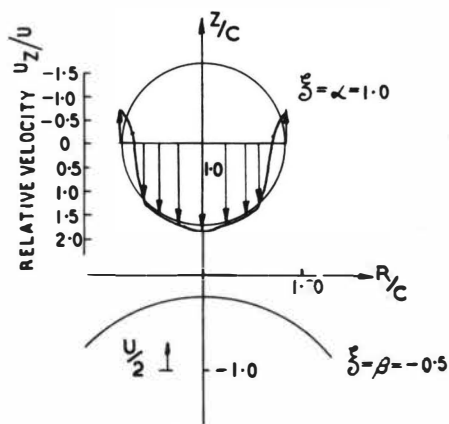
(a) $\mu^* = 0$. (SOLID-SOLID CASE)



(b) $\mu^* = 10$

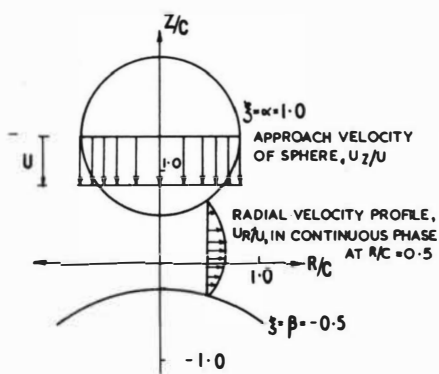


(c) $\mu^* = 0.1$

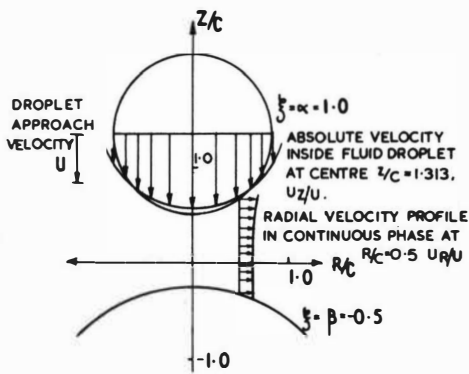


(d) $\mu^* = 10.0$

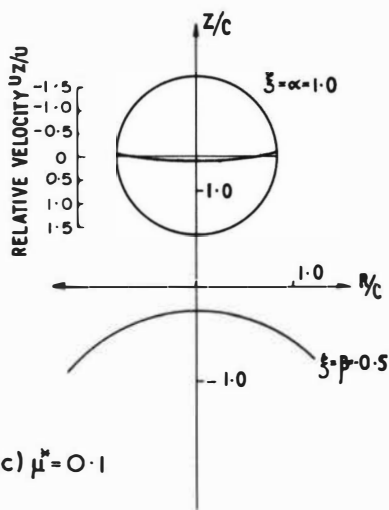
FIGURE 7. APPROACH OF UNEQUAL DROPS PRIOR TO COALESCENCE, EFFECT OF FLUID VISCOSITIES ON ABSOLUTE AND RELATIVE MOTION.



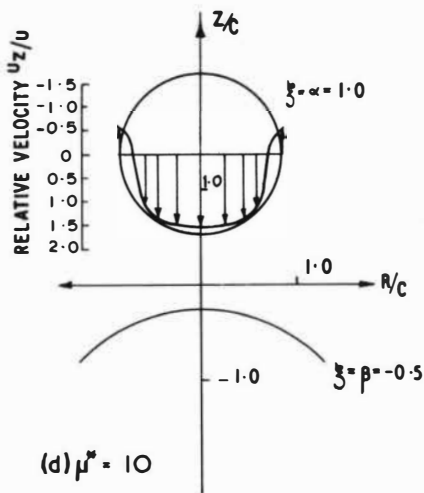
(a) $\mu^* = 0$ (solid-solid case)



(b) $\mu^* = 10$



(c) $\mu^* = 0.1$



(d) $\mu^* = 10$

FIGURE 8. APPROACH OF A DROP TOWARDS A STATIONARY DROP
EFFECT OF FLUID VISCOSITIES ON ABSOLUTE AND
RELATIVE MOTION.

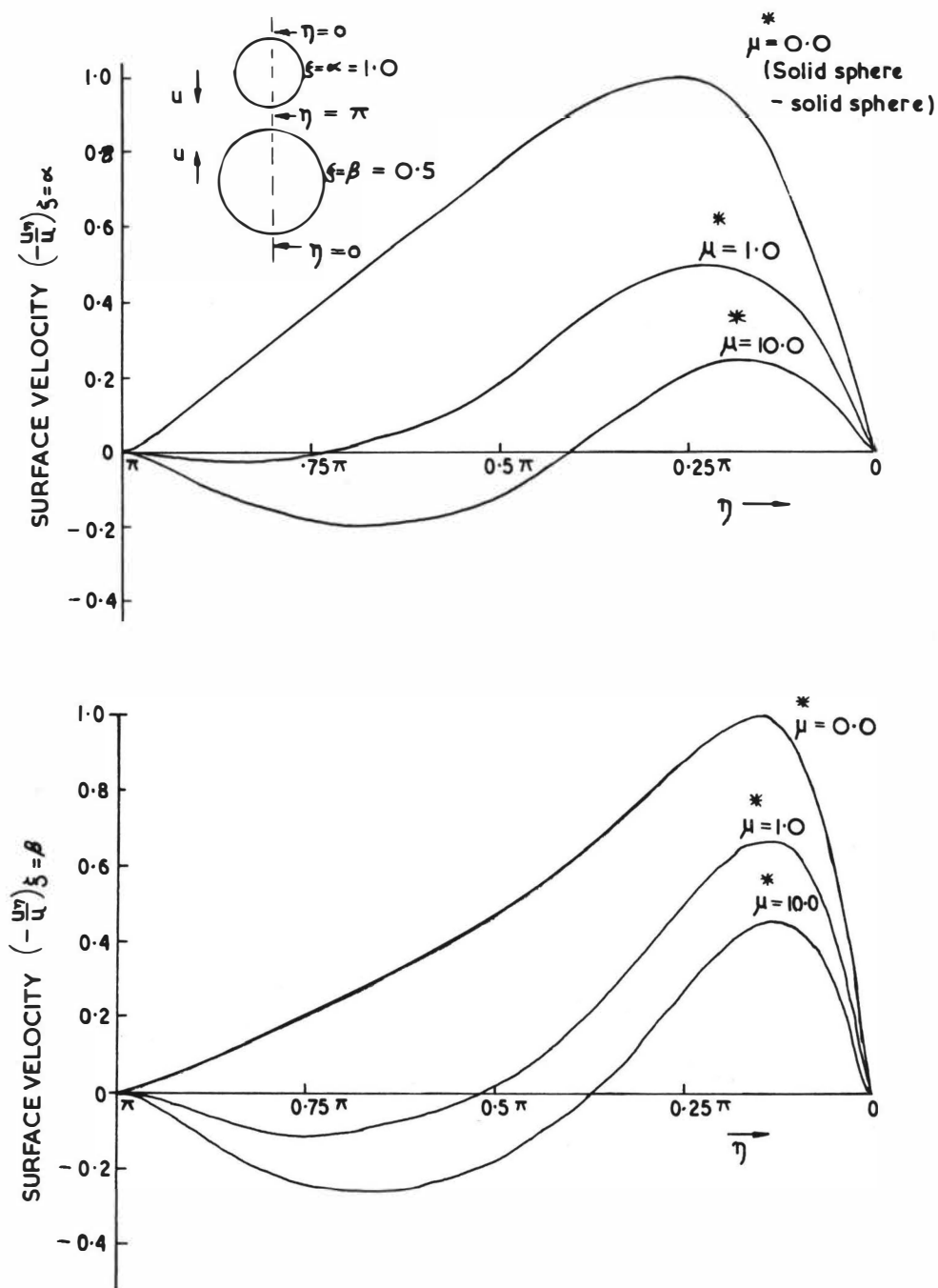


FIGURE 9. VARIATION OF SURFACE VELOCITY ON DROPS, EFFECT OF FLUID VISCOSITIES.

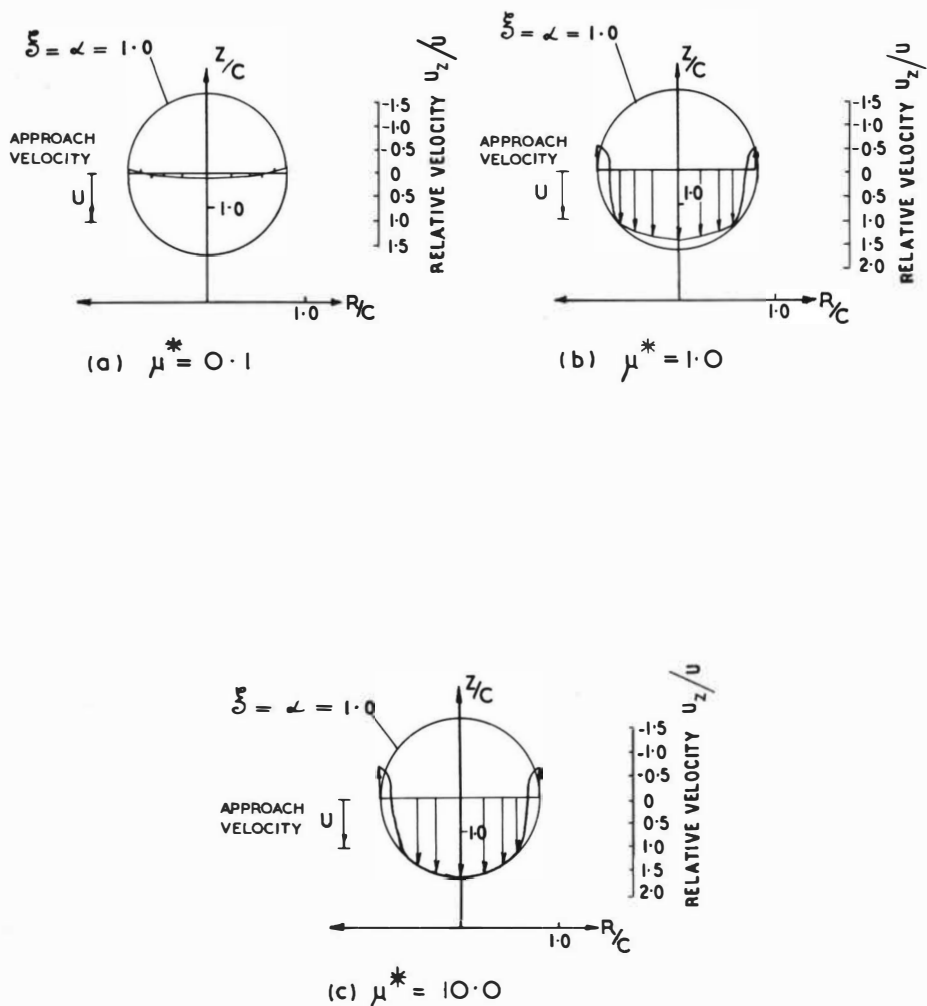


FIGURE 10. APPROACH OF A DROP TOWARDS A PLANE INTERFACE, EFFECT OF FLUID VISCOSITIES ON RELATIVE VELOCITY, u_z / u , INSIDE DROP.

THE REMOVAL OF A DISPERSED LIQUID PHASE
BY FIBROUS BED COALESCENCE

BY

D. T. Wasan, J. I. Rosenfeld, and W. M. Langdon

ABSTRACT

Liquid-liquid dispersions are often formed in chemical engineering operations as a result of solvent extraction. When the drops of the dispersed liquid phase are sufficiently large, this phase can be readily removed by settling. If, however, the dispersed phase consists of small drops under $10\ \mu$, other means must be used. Among these is a fibrous bed coalescer, in which small drops pass through and coalesce on fibers packed in a bed. The large drops leaving the exiting surface can be readily settled. The available models for describing the operation of a fibrous bed, including our present model, are presented and analyzed. A procedure is also presented which allows the optimum values to be selected for the design of a fibrous bed coalescer. Among those variables which are considered are the mat thickness, the fiber diameter, the bed porosity, and the superficial velocity.

Illinois Institute of Technology
Department of Chemical Engineering
Chicago, Illinois 60616, U. S. A.

INTRODUCTION

Liquid-liquid dispersions are commonly encountered in chemical engineering as well as other operations. These dispersions result from liquid-liquid extraction, direct contact heat transfer, condensation of azeotropes, vacuum distillation using steam jets, breathing of oil tanks, and caustic washing of light distillates. In many cases it is desired to remove the dispersed liquid phase because of economics. However, when the continuous liquid phase is water which is to be discharged into a stream or lake, the dispersed phase must be removed to meet effluent standards. A similar situation occurs when water is used to ballast the fuel tanks of ships. Before this oil-contaminated water can be pumped out of the tanks for refuelling, it is necessary to remove the oil. Also, it is sometimes necessary to remove emulsified water in aviation fuel to prevent flame out from ice formation.

When the droplets of the dispersed phase are large (greater than $10\ \mu$), and a significant density difference exists, the dispersion is called a primary emulsion, and the dispersed phase can generally be removed by gravity alone. However, for the case of a secondary emulsion, where the droplets are small, the time required to remove the dispersed phase droplets makes the gravity settling system uneconomical. Various other methods must then be used. Among these are: the use of alternating electrical fields, centrifugation, the addition of chemical coagulants, and coalescence by flow through porous solids.

The last of these methods will be considered here. The specific porous solids which will be discussed are fibers. In this method, which has been described by Treybal ⁽¹⁾, the emul-

sion flows through a bed which is packed with fibers. As the emulsion flows through the fibrous bed, some of the droplets of the dispersed phase are captured and held by the fibers. These held drops or films are then struck by flowing drops, and coalescence occurs on the fluid collected on the fibers. The held liquid grows to a size sufficient for drag forces to cause it to flow through the bed. The liquid leaves the disengaging surface as a large drop which can then be economically removed by gravity. The bed does not act as a sieve on the small drops since the pore size of the bed is much larger than the drop size. Thus the bed is not a filter and is called a fibrous bed coalescer.

In order to assist in the design of fibrous bed coalescers, a description of the models of fibrous bed coalescers will be presented. Each of these will be analyzed so as to point out its shortcomings. Then, as an example, the present model will be used to design a fibrous bed coalescer for an actual system.

MODELS DESCRIBING THE OPERATION OF A FIBROUS BED COALESCER

Davies and Jeffreys Model

One of the first attempts to describe the operation of a fibrous bed coalescer was made by Davies and Jeffreys⁽²⁾ in 1969. They stated that drops above the sub-micron range coalesce on the surface of the fibers to form a film onto which subsequent drops coalesce. Film drainage occurs in the bed and drops leave the bed at 'drip points'. For the case where the dispersed phase does not wet the fibers, interdrop coalescence takes place in the interstices of the packing. Direct interception is considered to be the mechanism of approach. Surface roughness is important in determining how long a drop will reside on a fiber. In this model it is assumed that above a maximum velocity the drops will not

adhere to the fiber surface long enough to allow for interdrop coalescence. However, film studies at Illinois Institute of Technology^(3, 4) have shown that it is the size of the drop which determines when it will detach from a fiber. Thus the length of time a drop remains on a fiber is not the critical point, since at the time the drop detaches it will have attained a specified size. However, as Davies and Jeffreys mentioned, if the velocity is too large the drop will be too small when it detaches.

Hazlett Model

Also in 1969, Hazlett⁽⁵⁾ presented a model of a fibrous bed coalescer. In his model there are three main steps. These are: the approach of a droplet to a fiber or to a droplet attached to a fiber; the attachment of the droplet to the fiber or to a droplet attached to the fiber; and the release of the enlarged droplet from the fiber. As in the previous model, direct interception is assumed to be the principle mechanism of approach. An equation developed by Langmuir⁽⁶⁾ is used to describe the approach of the drops. This equation is:

$$E_s = 1/2(2 - \ln N_{Re}) \left[2(1 + R) \ln(1 + R) - (1 + R) + 1/(1 + R) \right] \quad (1)$$

where E_s is the efficiency of collection by a single isolated fiber from a fluid stream of a width equal to the diameter of the fiber; N_{Re} is the Reynolds number; and R is the ratio of the drop diameter to the fiber diameter. Unfortunately, this equation predicts that as the velocity increases, the efficiency increases. This is the direct opposite of what has been experimentally observed^(7, 8, 9, 10, 11, 12). The extension of the efficiency of one fiber to that of a fibrous bed can be made by

considering the area coverage fraction. This is the total projected area of fibers in the bed.

After the drop approaches the fiber, attachment occurs when the film is thinned to a certain minimum thickness so that rupture can take place. Surfactants which lower the interfacial tension may cause the drainage time to increase. Before the drop is released, it is assumed that the droplet has become large enough to bridge to a downstream fiber to which it attaches before being released from the first fiber. It is also assumed that threads of the dispersed phase snake through the coalescer rather than discrete drops. However, this notion probably arose from viewing the back of the front support plate which was wetted by the dispersed phase and assuming that this represented the entire bed.

The drop size at the time of release depends upon the flow velocity, the surfactant content and the fiber size. The hydrodynamic force is balanced against the adhesive force to determine the size of the drop at detachment. Three possible mechanisms for release are considered. Drop-volume rupture equates the drag force with the restraining force of the interfacial tension. This yields:

$$C\rho_c v^2 \pi[d_p^2/4-a^2]/2 = 2\pi a\sigma \quad (2)$$

where C is the drag coefficient, ρ_c is the continuous phase density, v is the velocity through the bed, d_p is the drop diameter, a is the orifice radius, and σ is the interfacial tension. Unfortunately this equation neglects the van der Waals force, and limits the analysis to systems where the equilibrium contact angle is 90° . Also in the analysis, an unrealistic drag coefficient is assumed. Thus the final equation for the drop size at

the time of release is inapplicable.

Another release mechanism is the elongation affected by the moving fluid surrounding a droplet. This leads to a rupture of the threads which are formed. For the viscosity ratio which is frequently encountered, the elongation at small distortions is proportional to a dimensionless number F such that:

$$F = 2G \mu_c (d_p/2)/\sigma \quad (3)$$

where G is the shear rate, and μ_c is the continuous phase viscosity.

The last mechanism is considered to be the most realistic. This is ejection of the dispersed phase from the bed by jet action. Small drops are formed due to Rayleigh instability.

As in the previous model, no overall equation is presented. Thus Hazlett's model is of very limited use in designing a fibrous bed system.

Vinson and Churchill Model

In 1970, Vinson and Churchill⁽¹³⁾ presented yet another model. The model assumes that drops collide with fibers and have a probability of being retained. They then move along the fiber onto other fibers, and coalesce with other retained drops. This idea however has been found experimentally⁽¹⁴⁾ to be invalid. The model further assumes that the drops are captured by interception and the thinning of the continuous phase film results from the normal stresses due to the flow and the van der Waals attraction. The drop-filament adhesion along with the wettability determines whether a drop will remain on the fiber long enough to coalesce with other drops. In the case of strong adhesion, cohesive failure may occur. In this case only a part of the drop disengages.

This leads to a drop phase which will be attenuated to sheets or threads downstream of the fibers by fluid forces. The size of the drops at disengagement depends upon the thickness of the sheets or threads.

Although an equation is presented to describe the performance of the fibrous bed, it is not based on the model. It is simply the best fit of the data which was taken for a system where photo-etched screens were used to simulate a fibrous bed. The equation is:

$$\text{Fractional Removal} = -0.089 + 0.128 (U d_f \mu_c)^{-0.4} \quad (4)$$

where U is the superficial velocity, and d_f is the fiber diameter.

However, there is no basis whatsoever for using this equation to design a fibrous bed.

Spielman and Goren Model

Also in 1970, Spielman and Goren^(15, 16, 17) developed a model. They attempted to use this model along with some experimental data to arrive at a semi-theoretical design equation. The model assumes that when a dispersion flows through a fibrous bed, the suspended drops are transported to the fibers and entrapped liquid interfaces where they are captured and coalesced into the bulk of previously captured liquid. This coalesced liquid drains through the bed and leaves the bed at the same rate as the rate at which suspended drops are coalesced within the bed. Each immiscible fluid is considered to flow within a fixed channel, with the nonwetting fluid flowing on the inside. The pressure difference across the interface is called the capillary pressure and each channel is described by Darcy's law.

There appear to be several shortcomings in this model. First the idea of a continuum of the dispersed phase seems

unlikely since this phase is so dilute. Also, the concept of channels in a bed with a porosity greater than 90 percent has generally been rejected^(18, 19, 20).

While there are several other shortcomings in the qualitative model, such as the arbitrary assumptions that two phase capillary equilibrium determines the distribution of the flowing fluids, the rate of capture of drops is directly proportional to their number concentration, and all of the coalesced dispersed phase exists as discrete spherical globules of a uniform radius which is related to the fiber radius, it is the final design equation which is of interest. This equation is:

$$\lambda d_f^3 / d_p^2 = 0.29 (A d_f^2 / \mu_c U d_p^4)^{0.25} \quad (5)$$

where λ is the filter coefficient, and A is Hamaker's constant. This equation is completely independent of the model. It is based purely on the capture of a drop by a fiber. However the model states that drops are captured by coalesced drops. A modification⁽²¹⁾ of the classical interception theory is used to obtain the correlating function in Equation (5). Then the constant and exponent are chosen from the data. However, there is no justification for the assumption that the modified interception term can be used as the correlating function for the entire process. Thus this is in fact essentially an empirical equation. Since considerable data is needed to determine the exponent, this equation is only of limited help in designing a fibrous bed.

Sherony and Kintner Model

Sherony and Kintner⁽²²⁾ were the first authors to develop a model of a fibrous bed and use this to arrive at a design equation. In their work, which appeared in 1971, the final equation results directly from the model. The model assumes that there is

a population of drops which adhere to the fibers, and the emulsion does not form a continuum. When a drop which is flowing in the bed collides with a drop which is held by a fiber it is assumed that coalescence will occur a certain percent of the time. After coalescence, the enlarged drop is released and a new drop equal in size to the original held drop is attached to the fiber. The number of collisions between two drops is assumed to be proportional to the number of each of the drops.

In order to develop an equation from this model, various questionable assumptions had to be made. The shortcomings of these are that: when a drop leaves the fiber it is unlikely that an identical drop will immediately replace the original drop, when two drops coalesce the drop may not detach from the fiber if it has not reached a large enough size, and the probability of a collision between two drops is probably not independent of the drop size.

Using the method of moments described by Hulburt and Katz⁽²³⁾ the number density of drops (the zeroth moment) is obtained. However, in order to design a fibrous bed, it is necessary to know the complete size distribution. Thus, insufficient information is available.

The design equation which is derived from this model can be written as:

$$\left(\frac{\text{Outlet}}{\text{Inlet}} \right) \text{ Particle } N^{\circ} \text{ Density} = \text{Exp} \left[-\frac{3}{2}(1-\epsilon)s \cdot \left(1 + \frac{d_{10}}{d_f} \right) \eta_c \frac{L}{4d_f(1-s)} \right] \quad (6)$$

where ϵ is the void fraction of the bed, s is the saturation, d_{10} is the mean inlet particle size, η_c is the overall coalescence efficiency which is a parameter which varies with velocity, and L is the bed length.

Present Model

This model⁽²⁴⁾ which appeared in 1973 assumes the interception mechanism, such that drops flow along the streamlines of the fluid and if they come close enough to a held drop or fiber, they will strike it. There is then a probability that this will lead to coalescence. When the diameter of the held drop has grown by coalescing to a size which is greater than that which can be held by the fiber, it is released. Each drop size is considered independently and thus, knowing the inlet size distribution, the outlet size distribution can be found. Hence, enough information is given so that a fibrous bed can be designed. In order to solve the equations which arise, it is necessary to only consider drops which are smaller than the critical diameter. This is the largest diameter which can be held by a fiber. The final theoretical equation is:

$$\lambda = (8\beta(1-\epsilon)d_p/\pi^2d_f^2\epsilon(1-S))(2d_{fe}+d_p)/(d_{fe}+d_p) \quad (7)$$

where β is a parameter which tells the percentage of collisions which lead to coalescence and d_{fe} is the effective fiber diameter which includes the influence of held drops. Comparison of this equation with data shows that it is only valid at low velocities where the turbulence in the bed is insignificant. At larger velocities a purely empirical extension of Equation (7) is made to fit the data. This leads to the equation:

$$\lambda = (8\beta(1-\epsilon)d_p/\pi^2d_f^2\epsilon(1-S))(U_{cr}/U)^{0.5}(2d_{fe}+d_p)/(d_{fe}+d_p) \quad (8)$$

where U_{cr} is the velocity at which the filter coefficient begins to decrease. This is referred to as the critical velocity and is an adjustable parameter. U is the actual superficial velocity.

Some typical values for the filter coefficient are shown in

Figures 1 and 2. In these figures, the data of Spielman⁽¹¹⁾ are shown. In Figure 1, the effect of varying the drop diameter is demonstrated. While in Figure 2, the variation with the fiber diameter is shown. In each case a theoretical curve is also indicated. Equation (7) is used in the lower velocity region, and Equation (8) is used in the larger velocity region, where the filter coefficient depends on the velocity. The values for the parameters which were selected to fit the data are $\beta = 0.24$, and the critical velocity equal to 0.15 cm/sec. As expected, the filter coefficient increases as the drop size increases, and as the fiber diameter decreases. Since the filter coefficient is multiplied by the bed length to determine the coalescer performance, it is obvious that smaller fibers and larger drops will lead to a thinner bed. Although the curves for the filter coefficient in the two figures consist of two lines, it seems reasonable to believe that in actuality the filter coefficient is one continuous curve which only approaches these lines at the velocity extremes.

In order to find the region of applicability of Equations (7) and (8), an expression for the critical diameter d_c is obtained. This expression is:

$$d_c = d_f \left\{ \left[\frac{A^2}{144} \pi^2 r_o^4 [3\mu_c v K (1 + 2\mu_c / 3\mu_D) / (1 + \mu_c / \mu_D) - \sigma (1 + \cos \theta_e)]^2 \right] - 1 \right\} \quad (9)$$

where r_o is the closest distance between the drop and the fiber, μ_D is the viscosity of the dispersed phase, and θ_e is the equilibrium contact angle for the three phase system. K is an adjustable parameter which accounts for the influence of the neighboring fibers in the bed.

Equation (9) was found by considering the undeformed drop on

a fiber, and including the effect of the drag force F_D , the van der Waals force F_V , and the adhesion force F_A . The fact that the undeformed drop could be considered was found by observing the expressions for the various forces as a function of deformation. It was found that the critical condition occurs at zero deformation. The expressions for the forces are:

$$F_D = [3\pi a_p v \mu_c (1+2\mu_c/3\mu_D)/2 (1+\mu_c/\mu_D)] \cdot \quad (10)$$

$$[5 - 3h/a_p - (1 - h/a_p)^3]$$

$$F_V = A(8a_p^3 - 12a_p^2h + 6a_ph^2 - h^3)/12r_o^2(2a_p - h + r_o)^2 \quad (11)$$

$$F_A = 2\pi\sigma(2a_p - h)[a_p(1 + \cos \theta_e) - h]/(2a_p + h) \quad (12)$$

where a_p is the radius of a deformed drop, and h is the truncation of the drop. Since the undeformed drop can be used, an improvement of the expression for the van der Waals force can be made. This leads to the expression:

$$F_V = [2Ar_p^3/3(2r_p + r_o)^2 r_o^2] [r_f/(r_p + r_f + r_o)]^{1/2} \quad (13)$$

where r_p is the radius of the drop, and r_f is the radius of the fiber. This equation is valid if:

$$\text{Fiber Half Length} > 2 r_f (1 + r_p/r_f)^{1/2} \quad (14)$$

The equations which were developed from this model represent the best equations available for the design of a fibrous bed. Only two parameters are needed and these can be found by one experiment which measures the filter coefficient as a function of velocity. However, since an empirical expression is needed for the large velocity it is apparent that further improvements can be made so that theoretical expressions are

available for all velocities.

DESIGN OF A FIBROUS BED SYSTEM

In order to show how the present model can be used to design a fibrous bed system, an example will be presented.

Required Information

In order to design a system for the removal of a dispersed liquid phase it is necessary to specify certain terms. In the example which will be presented, it will be assumed that:

The size distribution of oil in water is as specified in Table 1 where it is arbitrarily assumed that the total concentration is 100 ppm, and it is desired to remove 95% of the dispersed phase at a flow rate of 10 000 gpm.

The saturation in the bed, which is the volume of the dispersed phase which is held by the bed per volume of bed voids, can be represented by:

$$S = 0.8 (1-\epsilon) U^{-0.2}/\epsilon \quad (15)$$

where U is the superficial velocity in ft/min. This represents a system of oil in water with an interfacial tension of 23.7 dynes/cm, a dispersed phase density of 0.840 gm/cm³ and a dispersed phase viscosity of 23.2 centipoise.

The pressure drop for single phase flow through the bed can be expressed as:

$$\Delta P_1 = 1125 UL \propto F(\alpha)/d_f^{3/2} \quad (16)$$

where ΔP_1 is the pressure drop in psi, L is the bed length in inches, α is the volume fraction of fibers, and d_f is the fiber diameter in microns.

The coalescer is operating in the region where the filter coefficient depends on the velocity. Thus, Equation (8) is

applicable. Further, it will be assumed that:

$$U_{cr} = 0.295 \text{ ft/min} \quad (17)$$

and:

$$\beta = 0.01 \quad (18)$$

The basis for these assumptions is described elsewhere⁽²⁴⁾.

Economic Considerations

The costs which enter into the design of the system are the pumping cost, the cost of the fibers, and the cost for the filter coalescer. Each of these can be considered separately and the total cost can then be minimized to obtain the optimum design.

The pumping cost can be found from the pressure drop. The pressure drop for heterogeneous flow through a bed is given⁽²⁴⁾ as:

$$\Delta P_2 = \alpha' F(\alpha') \Delta P_1 / \alpha F(\alpha) \quad (19)$$

where α' is the volume fraction of fibers plus the held drops on the fibers. If Equation (19) is combined with Equation (16), the result is:

$$\Delta P_2 = 1125 \alpha' F(\alpha') UL/d_f^{3/2} \quad (20)$$

Further, if a linear approximation is made then:

$$F(\alpha) = 16.25 \alpha^{1.3} \quad (21)$$

Also it is known that:

$$\alpha' = \alpha + \epsilon S \quad (22)$$

If Equations (15), (20), (21), and (22) are combined, then:

$$\Delta P_2 = 18 \ 281.25 UL \alpha^{2.3} (1 + 0.8U^{-0.2})^{2.3} / d_f^{3/2} \quad (23)$$

If the cost of electricity is assumed to be \$0.01/KWH, and the overall efficiency is 75%, then:

$$\text{Pumping Cost} = 1.765 \text{ UL } \alpha^{2.3} (1 + 0.8 \text{ U}^{-0.2})^{2.3} / d_f^{3/2} \quad (24)$$

$$\$/10^3 \text{ gal}$$

The cost of the coalescing fibers can also be found. If it is assumed that glass fibers are to be used, the costs are as shown in Table 2. These are the costs of uncompressed fibers with a volume fraction of 0.00365. In actual practice, the fibers are compressed some 10-20 fold to increase the volume fraction. If the costs are normalized on the basis of one-half inch uncompressed thicknesses, and are represented by the term C, then the cost of A ft² of fibers with a thickness of L inches is:

$$\text{Actual Cost of Fibers} = \$0.548 \text{ C } \alpha \text{ AL} \quad (25)$$

If the time between fiber replacement in hours is T, the cost of the fibers for a flow rate of 10 000 gpm is:

$$\text{Cost of Fine Fibers} = 9.133 \times 10^{-4} \text{ C } \alpha \text{ AL/T} \quad (26)$$

For each coalescing layer which is used, coarse glass lead-in and lead-off layers are required to act as filters for the excess oil, to act as a diffuser to distribute the drops, and to lead off the drops at the exit. This results in a cost of \$300/10³ ft². Treating the cost with straight line amortization over 10 years with a 90 percent stream factor:

$$\text{Cost of Coarse Fibers} = 6.34 \times 10^{-9} \text{ A } \$/10^3 \text{ gal} \quad (27)$$

Finally the cost of the filter press itself can be found. The cost of a completely automated filter press with an area of 2100 ft² has been given as \$50 000⁽²⁵⁾. Hooton and Thomas⁽²⁶⁾ have found that the cost of a filter press varies as the area

raised to the 0.9 power. Also, Peters and Timmerhaus⁽²⁷⁾ list a factor of 3.12 for the ratio of the capital investment to the delivered equipment cost for solid-liquid processing. Using a spare coalescer for continuous operation and straight line amortization over 10 years with a 90 percent stream factor:

$$\text{Cost of Filter Coalescer} = 6.75 \times 10^{-6} A^{0.9} \$/10^3 \text{gal} \quad (28)$$

Optimum Design

The design which reduces the effluent concentration to less than 5 ppm with the minimum cost is the optimum design. To find the minimum cost, it is merely necessary to add the costs of the various components. The total cost for the system is the sum of Equations (24), (26), (27), and (28). If it is noted that for a flow rate of 10 000 gpm:

$$A = 1337/U \quad (29)$$

then the total cost which must be minimized is:

$$\begin{aligned} \text{Total Cost} = & [1.765 UL \alpha^{2.3} (1 + 0.8U^{-0.2})^{2.3} / d_f^{3/2} \quad (30) \\ & + 1.22 C\alpha L/TU + 8.48 \times 10^{-6} / U + 4.39 \times 10^{-3} / U^{0.9}] \\ & \$/10^3 \text{gal} \end{aligned}$$

The minimum cost is found from Equation (30) by varying the independent variables and calculating the resulting cost. The independent variables are the thickness, L, the fiber diameter, d_f , and the volume fraction of fibers, α . The velocity, U, can then be found by calculating the velocity needed to reduce the outlet concentration to a value less than 5 ppm.

If this procedure is used, the optimum design is:

$$d_f = 2.39 \mu \quad (31a)$$

$$\alpha = 0.05 \quad (31b)$$

$$L = 0.511 \text{ inches} \quad (31c)$$

$$U = 1.91 \text{ ft/min} \quad (31d)$$

This is equivalent to 24 layers of one-quarter inch mats which have been compressed by a factor of 13.7. The most economical filter press which meets these conditions is a 36 in press with 44 plates, and an area of 701 ft². The outlet oil concentration is 4.94 ppm, and is distributed as shown in Table 3. For this system, the pressure drop is 16.65 psi, the saturation is 0.037, and the effective fiber diameter is 3.12 μ . The costs of the various components are:

$$\text{Pumping Cost} = 1.61 \times 10^{-3} \text{ \$/10}^3\text{gal} \quad (32a)$$

$$\text{Fine Fibers} = 1.81/T \text{ \$/10}^3\text{gal} \quad (32b)$$

$$\text{Coarse Fibers} = 4.44 \times 10^{-6} \text{ \$/10}^3\text{gal} \quad (32c)$$

$$\text{Filter Coalescer} = 2.45 \times 10^{-3} \text{ \$/10}^3\text{gal} \quad (32d)$$

The labor cost is due to the replacement of the fine fibers.

If it is assumed that it takes 1 min to change one plate, and if the direct labor cost is 5.75 \$/hr with supervision 50 percent of labor⁽²⁵⁾, then:

$$\text{Cost for Labor} = 0.0106/T \text{ \$/10}^3\text{gal} \quad (33)$$

If Equations (32) and (33) are combined, the final result is:

$$\text{Total Cost} = (4.1 \times 10^{-3} + 1.82/T) \text{ \$/10}^3\text{gal} \quad (34)$$

In Table 4, the costs in dollars per thousand gallons are shown for various fiber lifetimes.

DESIGN OF AN ALTERNATE SYSTEM

In order to determine the economic attractiveness of the

fibrous bed system, it will be compared to an alternate method for reducing a 100 ppm concentration to less than 5 ppm. In this system⁽²⁸⁾ chemical coagulants are added to assist in the removal of the dispersed phase. A flow diagram of this process is shown in Figure 3.

For a flow rate of 1500 gpm, the total fixed cost of the system can be found⁽²⁷⁾. This cost is itemized in Table 5, and is nearly \$241 000. Using straight line amortization over 10 years and a 90 percent stream factor, the total fixed cost is equivalent to $0.0339 \text{ \$/10}^3 \text{ gal}$. The costs of the additives are listed in Table 6. When these costs are added to the equivalent total fixed cost, the overall cost for the process is found to be $0.165 \text{ \$/10}^3 \text{ gal}$. When this is compared to Equation (34), a coalescer with a fiber lifetime greater than 11.3 hours is more economical than the chemical coagulation system. Since it has been found⁽²⁹⁾ that typical lifetimes range between 14 and 305 hours, it can be concluded that the fibrous bed system is generally the more economical.

CONCLUSIONS

A review of the models which are available to describe the operation of a fibrous bed coalescer has been made. It has been shown that only the equations derived from the present model can be used to design an actual system. For the sake of example, an actual fibrous bed system has been designed using this model. The costs of this system have been compared with those of an alternate system with the conclusion that the fibrous bed system is generally more economical.

ACKNOWLEDGMENT

The authors wish to acknowledge the many helpful

suggestions provided by Dr. R. C. Kintner of Illinois Institute of Technology.

NOMENCLATURE

- a = orifice radius, used in Equation (2), cm
- a_p = radius of a deformed drop, cm
- A = Hamaker's constant, ergs
- A = cross-sectional area of a fibrous bed, cm^2
- C = drag coefficient, used in Equation (2), dimensionless
- C = the cost of 1 000 ft^2 of a one-half inch thick fibrous mat, dollars
- d_c = critical diameter, the largest drop which can remain attached to a fiber, cm
- d_f = fiber diameter, cm
- d_{fe} = effective fiber diameter, $d_f[(1-\epsilon+\epsilon S)/(1-\epsilon)]^{1/2}$, cm
- d_p = drop diameter, cm
- d_{10} = the mean inlet particle size, cm
- E_s = efficiency of collection by a single isolated fiber from a fluid stream of a width equal to the diameter of the fiber, defined in Equation (1), dimensionless
- F = a dimensionless number defined by Equation (3), dimensionless
- F_A = adhesion force, dynes
- F_D = drag force, dynes
- F_V = van der Waals force, dynes
- $F(\alpha)$ = dependence of a dimensionless pressure gradient on the fraction of solids, dimensionless
- G = shear rate, sec^{-1}
- h = truncation of a drop, cm
- K = term which represents the effect of neighboring fibers in

a bed on the drag force, used in Equation (9),
dimensionless

- L = length or thickness of a fibrous bed, cm
- N_{Re} = Reynolds number, dimensionless
- ΔP_1 = pressure drop for single phase flow through a fibrous bed, g/cm^2
- ΔP_2 = pressure drop for heterogeneous flow through a fibrous bed, g/cm^2
- r_f = fiber radius, cm
- r_o = the closest distance between a drop and a fiber, cm
- r_p = drop radius, cm
- R = the ratio of the drop diameter to the fiber diameter, dimensionless
- S = saturation, the volume of dispersed phase held by the bed per volume of bed voids, dimensionless
- T = time between fiber replacement, sec
- U = superficial velocity, cm/sec
- U_{cr} = critical velocity, the velocity at which the filter coefficient begins to decrease, cm/sec
- v = velocity through the bed, cm/sec

Greek Letters

- α = volume fraction of fibers, dimensionless
- α' = volume fraction of fibers plus the held drops on the fibers, dimensionless
- β = a parameter which tells the percentage of collisions which lead to coalescence, dimensionless
- ϵ = void fraction of the bed, dimensionless
- η_c = the overall coalescence efficiency, dimensionless
- θ_e = equilibrium contact angle for the three phase system, dimensionless

- λ = filter coefficient, the negative of the natural logarithm of the ratio of the number of drops at the outlet to the number at the inlet, divided by the length of the bed, cm^{-1}
- μ_c = viscosity of the continuous phase, g/cm-sec
- μ_D = viscosity of the dispersed phase, g/cm-sec
- ρ_c = density of the continuous phase, g/cm^3
- σ = interfacial tension between the continuous phase, and the dispersed phase, dynes/cm

REFERENCES

- (1) Treybal, R.E., Liquid Extraction, (1963), 2nd ed. pp. 447-448, (McGraw-Hill Book Company, Inc., New York).
- (2) Davies, G.A., Jeffreys, G.V., Filtr. Separ., (1969), 6, 349.
- (3) Sherony, D.F., M.S. Thesis, (1967), Illinois Inst. of Tech., Chicago, Ill.
- (4) Tan, C.B., M.S. Thesis, (1968), Illinois Inst. of Tech., Chicago, Ill.
- (5) Hazlett, R.N., Ind. Eng. Chem. Fundam. (1969), 8, 625.
- (6) Langmuir, I., OSRD Report No. 865, (1942).
- (7) Bitten, J.F., Report No. IITRI-C6088-12, (1969), IIT Research Institute, Chicago, Ill.
- (8) Burtis, T.A., Kirkbride, C.G., Trans. Amer. Inst. Chem. Eng. (1946), 42, 413.
- (9) Farley, R., Valentin, F.H.H., AIChE-I.C.E.Symp. Series 1, (1965), 1.
- (10) Patel, J.G., M.S. Thesis, (1970), Illinois Inst. of Tech., Chicago, Ill.
- (11) Spielman, L.A., Ph.D. Thesis, (1968), Univ. of California, Berkeley, Calif.

- (12) Vinson, C.G., Ph.D. Thesis, (1965), Univ. of Michigan, Ann Arbor, Mich.
- (13) Vinson, C.G., Churchill, S.W., Chem.Eng. J., (1970), 1, 110.
- (14) Bitten, J.F., J. Colloid Interface Sci., (1970), 33, 265.
- (15) Spielman, L.A., Goren, S.L., Ind. Eng. Chem., (1970), 62, 10.
- (16) Spielman, L.A., Goren, S.L., Ind. Eng. Chem. Fundam., (1972), 11, 66.
- (17) Spielman, L.A., Goren, S.L., Ind. Eng. Chem. Fundam., (1972), 11, 73.
- (18) Chen, C.Y., Chem. Reviews, (1955), 55, 595.
- (19) Iberall, A.S., J. Res. Nat. Bur. Stand (1950) 45, 398.
- (20) Wong, J.B., Ranz, W.E., Johnstone, H.F., J. Appl. Phys., (1956), 27, 161.
- (21) Spielman, L.A., Goren, S.L., Environ. Sci. Technol., (1970), 4, 135.
- (22) Sherony, D.F., Kintner, R.C., Can. J. Chem. Eng. (1971), 49, 314.
- (23) Hulburt, H.M., Katz, S., Chem. Eng. Sci. (1964), 19, 555.
- (24) Rosenfeld, J.I., Ph.D.Thesis,(1973), Illinois Inst. of Tech., Chicago, Ill.
- (25) Langdon, W.M., Naik, P.P., Wasan, D.T., Final Report, (1971) Environmental Protection Agency, Grant No. 12050 DRC.
- (26) Hooton, J.A., Thomas, C.M., paper presented at The Filtration Society's Conference at Filtech, (1967), Olympia, London.
- (27) Peters, M.S., Timmerhaus, K.D., Plant Design and Economics for Chemical Engineers, (1968) 2nd ed., (McGraw-Hill, New York).
- (28) Barker, J.E., Foltz, V.W., Thompson, R.J., Chem. Eng. Progr. Symp. Ser., No. 107, (1970), 67, 423.

(29) Langdon, W.M., Naik, P.P., Wasan, D.T., Environ.Sci.Technol.
(1972), 6, 905.

TITLE OF TABLES

Table 1: Inlet size distribution

Table 2: Costs for various fiber mats (Jan. 1973)

Table 3: Outlet size distribution

Table 4: Total costs for various fiber lifetimes

Table 5: Total fixed cost for a chemical coagulation and
flotation system

Table 6: Costs of the additives for a chemical coagulation
system

TABLE 1

INLET SIZE DISTRIBUTION

Drop Dia. (μ)	1	2	3	4	5	6	7	8	9	10
PPM	0.3	2.1	5.3	8.9	12.4	15.8	18.7	17.5	15.5	3.5

TABLE 2

COSTS FOR VARIOUS FIBER MATS (JAN. 1973)

Diameter (μ)	Thickness (in)	Cost ($\$/10^3 \text{ ft}^2$)
2.39	0.25	55.20
3.20	0.25	40.80
8.45	0.50	50.40

TABLE 3

OUTLET SIZE DISTRIBUTION

Drop Dia. (μ)	1	2	3	4	5	6	7	8	9	10
PPM	.15	.58	.88	.91	.79	.64	.49	.30	.17	.03

TABLE 4

TOTAL COSTS FOR VARIOUS FIBER LIFETIMES

Time (Hr)	1	2	5	10	100	1 000	10 000
Cost (\$/10 ³ gal)	1.824	0.914	0.368	0.186	0.022	0.006	0.004

TABLE 5

TOTAL FIXED COST FOR A CHEMICAL COAGULATION AND FLOTATION SYSTEM

Components	Cost
Rapid Mix Tanks	\$26 800
Flocculation Tanks	26 800
Flotation Tanks	19 600
Metering Pumps	1 265
Recycle Pumps	<u>2 620</u>
Total Purchased Cost	\$77 085
Capital Inv./Delivered Cost	<u>x3.12</u> (27)
Total Fixed Cost	\$240 505

TABLE 6

COSTS OF THE ADDITIVES FOR A CHEMICAL COAGULATION SYSTEM

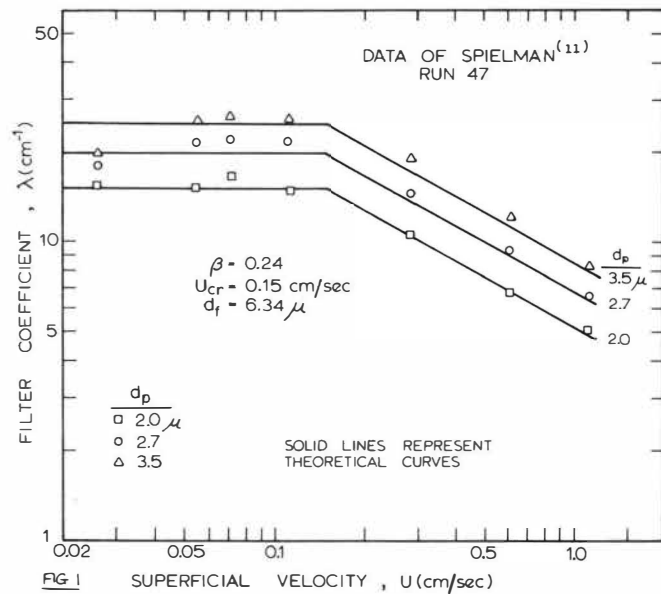
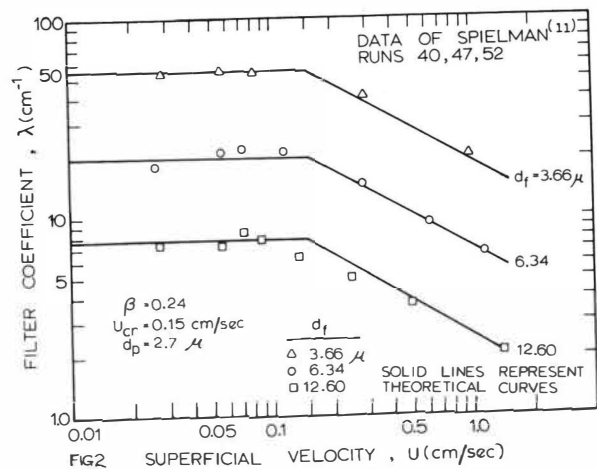
Additive	Cost (\$/lb)	Amount (lb/gal)	Cost (\$/10 ³ gal)
Alum	0.077	1.46×10^{-3}	0.112
Clay	0.06	1.34×10^{-4}	0.008
Coagulant Aid	0.73	4.17×10^{-6}	0.003
Lime	0.0255	3.01×10^{-4}	<u>0.008</u>
Total Cost			0.131

FIGURE CAPTIONS

Figure 1: Filter coefficient as a function of the superficial velocity for various drop sizes.

Figure 2: Filter coefficient as a function of the superficial velocity for various fiber sizes.

Figure 3: Flow diagram of a chemical coagulation system.



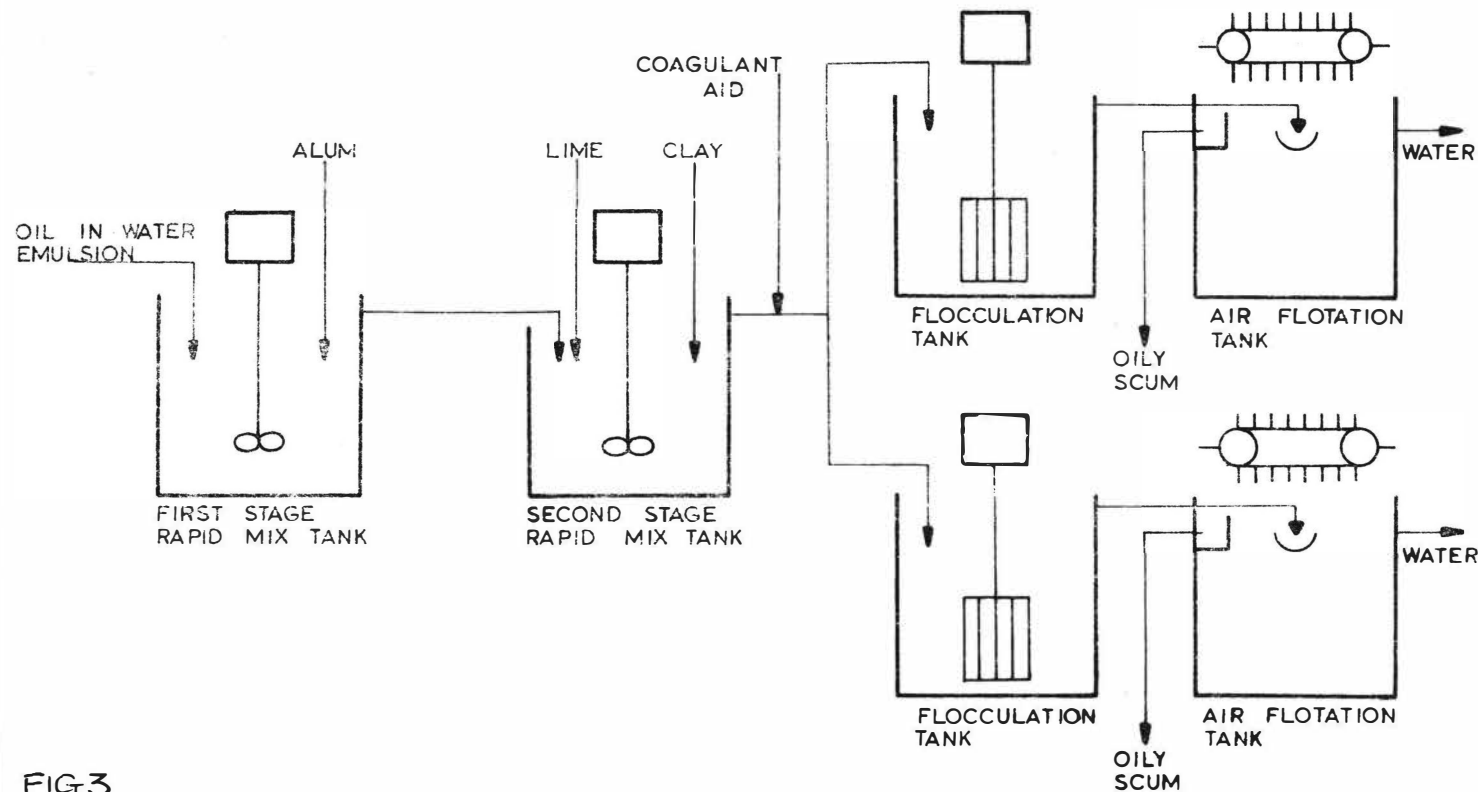


FIG 3

R.M. Edge and I.E. Kalafatoglu*

ABSTRACT

The breakup of drops of chlorobenzene falling freely through water is described and discussed. Drops in the size range $0.896 \text{ cm} \leq D_{E,1} \leq 1.146 \text{ cm}$ are considered and it is shown that breakup occurs during the oscillation which follows the first shedding of a class III attached wake. Secondary drops are formed by a necking process from both rear and front formed columns and their occurrence and size are related to the size and oscillations of the primary drop. Theoretical predictions are made of the onset of necking and the rate of necking using respectively surface free energy considerations and a momentum balance on the liquid in the column.

* Department of Chemical Engineering,
University of Strathclyde, Glasgow G1 1XJ, Scotland.

INTRODUCTION

The mechanism of the break up of liquid drops has interested research workers in several fields, including liquid-liquid extraction, atomisation and meteorology. Both liquid-liquid and gas-liquid systems have been studied but most of the work has been concentrated on two hydrodynamic systems, namely: drops in a steady sheared motion (1-4) and drops in free fall in air (5-9). Work on the break up of liquid drops which are falling freely through a liquid phase has been of a fragmentary nature and consists mainly of observations made during the study of other facets of drop hydrodynamics.

From the literature it appears that drops falling freely through a liquid phase may break in several ways. Schroeder and Kintner (10) report that in some systems nozzle induced oscillations are violent and cause the rupture. However, they deduce that in other systems the rupture is not caused by drop oscillations because at drop diameters just less than the critical for break up, oscillations are not present and random wobbling occurs. Stuke (11) and O'Brien (12) have reported a break up mechanism which is similar to that observed for liquid drops falling through air. Here a cavity is formed at the rear of the drop and this penetrates the drop, causing it to shatter. The present paper is concerned only with the breakup of drops which is caused by drop oscillations.

The mechanism of the breakup caused by oscillations has been little studied. Kintner (13) reported that for drops of chlorobenzene of diameter 0.985 cm rupture occurred 5 in. below the nozzle and that two types of breakup occurred. In the one type of breakup a secondary droplet was formed at the front of the drop and in the second the secondary droplet was formed at the rear of the drop. The rear formed droplet was always larger than the front

formed droplet. Occasionally they observed two successive droplets formed at the rear of the drop and also the formation of both front and rear droplets from the same drop.

Elzinga and Banchero⁽¹⁴⁾, following a suggestion by Gunn⁽¹⁵⁾, proposed that an oscillating drop breaks only when the frequency, with which it sheds its wake, is equal to the natural frequency of oscillation of the drop. They estimated the frequency of oscillation from Lamb's equation⁽¹⁶⁾ for the oscillation of a spherical inviscid drop at rest in an inviscid continuous phase. As Edge and Grant⁽¹⁷⁾ have shown that the frequency of oscillation of the drop and the frequency of wake shedding are the same, this proposal means that the drop breaks only when its frequency of oscillation is equal to that given by Lamb's equation. Hu and Kintner⁽¹⁸⁾ used a different approach, which was based on the theoretical work of Hinze⁽⁵⁾ and other workers⁽²⁾. These workers, who had studied breakup of drops in gas-liquid systems and in simple shear flow systems, proposed that the ratio of the stress on the surface of the drop caused by the flow of the bulk fluid to the stress caused by the interfacial tension was of great importance in determining whether a drop would break, and Hinze has shown that for drops of liquid systems falling through air the critical Weber number for breakup is approximately constant and equal to 10. Hu and Kintner modified this equation to $We_{CD} = \text{constant}$ and found that when their experimental results were fitted into this equation they obtained the relationship

$$(D_{E,1})_{crit} = \left[1.452 \times 10^{-2} \frac{\sigma}{\Delta \rho} \right]^{\frac{1}{2}} \quad (1)$$

However, Edge and Grant⁽¹⁹⁾ have shown that both the frequency and amplitude of oscillation are affected by the purity of the system. Therefore, when

applying equation (1) it must be remembered that the systems used by Hu and Kintner were not specially purified and that equation (1) will probably not apply to purified systems.

EXPERIMENTAL

The apparatus, which is shown in Figure 1, and the experimental techniques have been described in detail in previous papers (19,20). The drops were formed in the continuous phase from stainless steel tips which had sharp circular ends. A stainless steel rod was inserted down the inside of the larger sizes of tip. The diameter of this rod was somewhat less than the inside diameter of the tube and it stopped any tendency for the continuous phase to enter the tip. The rate of formation was one drop every 10 seconds

The motion of the drops was recorded on cine film at a nominal 1000 frames/sec using a Fastax cine camera and a focussed shadow optical system. The drops were visible in the optical systems for the first 12 cm of fall.

Great care was taken to avoid adventitious contamination of the system. The apparatus was cleaned with chromic acid using the procedure described in the previous papers. The drop phase liquid was chlorobenzene which was of analar quality and was fractionated before use in a 30 plate all glass Oldershaw column. The continuous phase was double-distilled water. The properties of the system are given in Table 1. All experiments were carried out at $25^{\circ}\text{C} \pm 0.1^{\circ}\text{C}$.

RESULTS

Measurements were made of D_H and D_V , the lengths of the major and minor axes respectively (Figure 2), for class IV drops during the period between

detachment from the forming tip and breakup. Typical results are presented in Figure 3 for three sizes of drop. Also included are values of E , the eccentricity, which is defined as D_H/D_V . During the period immediately before breakup, measurements were made of the length and diameter of the column of fluid formed behind each drop (Figure 2) and typical results are presented in Figure 4 for four sizes of drop. Four drops were analysed in detail for each of the ten sizes of drops which were studied.

Initially, all drops fell from the tip in a vertical path. Tip induced oscillations resulted from the deformation of the drop on the tip prior to detachment. These oscillations decayed and in no case did they cause rupture. At some distance below the tip there was a sudden increase in the amplitude of the oscillations. This finding is in agreement with the results of Edge and co-workers⁽²¹⁾ for non-breaking drops. It was found that if a drop did not break during this oscillation then it would not break subsequently during its free fall. This oscillation will be called the critical oscillation. Secondary drops were formed from both the front and the rear of the primary drops and Table 2 gives details of the position of breakup.

A typical formation of a secondary drop from the rear of a primary drop is illustrated in Figure 5 by tracings which were taken from a cine-film and Figure 4c presents data for the shape of this drop during the critical oscillation. At the start of the critical oscillation the horizontal extremes of the drop move forward to produce a saucer-like shape with a rear cavity and a forward protrusion. The edge of the saucer continues to move forward and the front protrusion is drawn back into the drop so that the drop has cavities at both its front and rear surfaces. The drop then begins to elongate rapidly, the cavities disappear, and it forms itself into a shape resembling a cylinder with

hemispheroidal ends. The cylinder necks at approximately midway along its length but, after a short period, the rate of necking decreases and, with several sizes of drop, becomes zero. The rear volume of the drop shrinks and, except in the case of the two larger drops, it forms itself into a shape resembling a cylinder with a hemispheroidal cap. After a short period this column necks where it joins the main volume of the primary drop and a secondary drop is formed. During this necking period the diameter D_C remains approximately constant which indicates that there is little drainage from the hemispheroidal cap. The drop which had a diameter of 0.896 cm (Figure 4a), which is close to the critical volume for breakup, showed a similar behaviour except that D_C remained constant for only part of the necking period. After this there was a race between necking and drainage and the resulting secondary drop was small in volume. The diameter D_C also decreased during the necking period of the 0.998 cm diameter drop (Figure 4b). The reason for this will be discussed later in this paper. With the two larger sizes of drop, the dimensions of the drainage columns and the sizes of the secondary drops were less reproducible. In these cases the neck persisted throughout the period of drainage (Figure 4d) and only one drop of each size produced a column which resembled a cylinder with a hemispheroidal cap.

Shortly after the necking and draining process of the rear protrusion has been completed, a combination of the oscillations of the drop and the forward movement of the liquid near the minor axis of the drop cause a protrusion to form on the forward surface of the drop. This forms itself into a column which both shrinks and is withdrawn into the drop. During this process a secondary drop may be formed by a necking process (Figure 5).

DISCUSSION

The critical oscillation and the formation of secondary drops

It was shown previously that as a class IV drop falls freely from a tip there is a transition of the wake through the various classes until the wake class of the terminal region is established⁽²¹⁾. Whilst the drop has either a class I or a class II wake the oscillations are of a damped type and it is not until the class III wake is formed that oscillations, which are characteristic of the terminal region, are initiated. The first of these oscillations is the critical oscillation and this occurs immediately after the first shedding of a class III attached wake. At the start of the critical oscillation the eccentricity of the drop reaches its maximum value (Figure 3) and this accounts for the high amplitude of the oscillation. Measurements made of non-breaking drops showed that subsequent oscillations were of lower amplitude and this accounts for the finding that no drops broke outwith the critical oscillation.

The critical oscillation did not occur at a fixed distance below the forming tip, as reported by Schroeder and Kintner⁽¹⁰⁾ for breaking drops of chlorobenzene. It was found that, as the diameter of the primary drop was increased, there was a decrease in the number of oscillations which occurred before the critical oscillation (Figure 3, Table 2). With drops of chlorobenzene no breakup occurred until the critical oscillation corresponded with the fourth D_V peak. Both the 0.896 cm and 0.906 cm drops broke on the fourth peak and Figure 6 shows the rapid rise of $D_{E,2}$ which occurred as $D_{E,1}$ was increased above the critical value. Also, although 0.906 is not greatly above the critical diameter, this drop produced a rear formed column which broke in a manner similar to that shown in Figures 5 and 4c. However, when the drop diameter was increased to 0.932 cm, the rear formed column just failed to

produce a secondary drop. This can be attributed to the transition of the critical oscillation between the fourth and third peaks. In this transition region neither the third nor the fourth D_V peaks were of sufficient amplitude to cause breakup of the rear-formed column. However, secondary drops were formed in this transition region by breakup from a front formed column which was produced after the third D_V peak. This occurred when $D_{E,1} = 0.969$ cm. When the size of the primary drop was increased to 0.998 cm the rear column, which now occurred at the third D_V oscillation, was again of sufficient size to produce a small rear-formed secondary drop. Further increase in $D_{E,1}$ produced a corresponding increase in the amplitude of the third D_V peak which resulted in a large increase in $D_{E,2}$. All drops which had diameters between 1.013 cm and 1.088 cm produced rear formed drops by a process which was similar to that shown in Figures 5 and 4c.

Figure 6 also shows a discontinuity in the relationship between $D_{E,2}$ and $D_{E,1}$ for front-formed secondary drops. When the fluid from the rear column is drawn back into the drop after the third D_V peak, it jets along the vertical axis of the drop. This partly explains the formation of the succeeding front column. As the size of the primary drop is increased, the size of the rear formed secondary drop increases and therefore the amount of this jetting liquid is reduced. This could explain the discontinuity. However, it is thought that this is only a part explanation because, if it was the sole cause of the discontinuity, it would be expected that the discontinuity should occur closer to the critical diameter for rear breakup on the third D_V peak than is shown in Figure 6.

The results for the two larger sizes of drop showed an anomaly. The largest drop produced a front formed secondary drop which had a diameter of

approximately the expected size. However, when $D_{E,1} = 1.124$ no front formed secondary drop was formed. The reason for this is not known, but it was noticed that with these two sizes of drop the measurements of the drop and column dimensions during the necking process were much less reproducible than with the other drops studied.

Size of the rear-formed secondary drop

Figure 6 shows that there is no single relationship between $D_{E,2}$ and $D_{E,1}$. However, for drops breaking on the third D_V peak, the following simple empirical relationship was found to give a good correlation for rear formed secondary drops:

$$V = 3.6 (D_{E,1} - D_{E,1}^*) \quad (2)$$

where V is the volume of the secondary drop and $D_{E,1}^*$, the critical diameter for breakup on the third D_V peak, is 0.9978 cm. This correlation is shown in Fig.6.

The critical value of R_C for necking to occur

The authors know of no theoretical study of the breakup of a column of liquid behind a falling drop during the critical oscillation. However, it was observed that there are many similarities between the above breakup and the formation of a secondary drop during the coalescence of a drop at a plane liquid-liquid interface and this latter phenomenon has been studied theoretically by Charles and Mason⁽²²⁾. They based their theory on existing theories of the breakup of a cylindrical jet of fluid and it is useful to consider these theories first.

The first theoretical study of the breakup of a cylindrical jet of fluid appears to have been made by Plateau⁽²³⁾ and this theory was clarified and extended by Rayleigh⁽²⁴⁾. These authors considered a long cylinder of fluid

into which there was no net flow and they examined whether a disturbance on the surface of the cylinder would grow. The criterion for growth which they used was that if the disturbance results in a smaller surface area than that of the cylinder, then the disturbance will grow. If it results in a larger surface area then it will die out and the liquid will revert to the original cylindrical shape. It was shown that only disturbances which are symmetrical about the axis of the jet will grow. The shape of the disturbed surface can be represented by a Fourier series.

$$r = r_0 + \sum_n \alpha_n \cos 2\pi z / \lambda_n$$

and it was shown that only terms where $\lambda_n \gg \lambda_{n,\text{crit}}$ result in a disturbance which will grow and that $\lambda_{n,\text{crit}} = 2\pi r_c$ where r_c is the radius of the undisturbed cylinder. From an energy balance it was also shown that for a cylinder of a perfect fluid $d\alpha_n/dt$, the rate of increase of the amplitude of the wave represented by the n^{th} term of the above series, is a maximum when $\lambda_n = \lambda_{n,\text{opt}} = 2.87\pi r_c$ and it was deduced that a long cylinder of fluid will tend to divide itself into portions of fluid whose length is equal to $2.87\pi r_c$.

In subsequent papers Rayleigh⁽²⁵⁾ and Weber⁽²⁶⁾ considered a disturbance on the surface of a cylinder of a viscous fluid and Tomotika⁽²⁷⁾ has examined the effect of a surrounding viscous fluid. By solving the Navier-Stokes equations and neglecting inertial terms these authors deduced equations which predict $\lambda_{n,\text{opt}}$ for the various systems studied.

Charles and Mason, in their study of coalescence, suggested that a secondary drop is formed during coalescence by the following process. Immediately after the rupture of the continuous phase film, which separates the drop from the plane interface, the drop deflates and forms itself into a column (Figure 7). The radius of the column then decreases until the height becomes

less than $\lambda_{n,crit} (= 2\pi r_c)$ and a Rayleigh disturbance can grow. From here on there is a race between the drainage and the neckingdown process which determines the size of the secondary drop. However, in order to estimate the size of the secondary drop, they assumed that the height of the column of liquid was equal to $D_{E,1}$, the equivalent spherical diameter of the drop before coalescence, and that the column drained as a cylinder until $\lambda_{n,opt} = D_{E,1}$, and not $\lambda_{n,crit} = D_{E,1}$, and that subsequently there was no drainage of fluid from the column. Thus, using $\lambda_{n,opt}$ calculated from the theory of Rayleigh, they estimated that the volume of the secondary drop would be equal to the volume of a cylinder of diameter $D_{E,1}/1.435\pi$ and of length $D_{E,1}$. This gave a value of 0.42 for the ratio $D_{E,2}/D_{E,1}$ where $D_{E,2}$ is the equivalent spherical diameter of the secondary drop. This fell within the range 0.13 to 0.54 found experimentally. Charles and Mason also used values of $\lambda_{n,opt}$ calculated from Tomotika's theory in similar calculations and found that there was reasonable agreement between theory and experiment when the viscosity ratio of the dispersed to the continuous phase was greater than 1.

Although the above indirect evidence supports the use of Rayleigh's theory of jet breakup in coalescence studies there are no published measurements of the column height and diameter immediately before necking with which to test its use directly. Examination of photographs published by Charles and Mason indicate that, immediately prior to the onset of necking, the ratio of the length of the column of liquid to diameter is much less than 1.435π , the value used by Charles and Mason in their theory. Also the length of the column appears to be less than D_E .

In the present work on the breakup of drops, measurements show that immediately before necking the column length and circumference are in the ratio

of approximately 0.4 (Table 3). This is not in agreement with the theory of Charles and Mason which predicts that the column will not neck until $\frac{H}{D_C} > \pi$. When assessing the value of the Charles and Mason model in the present work, the original criterion used by Rayleigh for stability must be kept in mind and it should be noted that the change in surface area which occurs during necking is not great. This means that unless the model describes accurately the surface area of the system its use will not be valid. As an illustration of the invalidity in the present work of the pictorial model used by Charles and Mason (Figure 8, model A), the breakup of a drop with a diameter of 1.088 cm will be used. Immediately prior to necking the column had the dimensions $D_C = 0.52$ cm, $H = 0.75$ cm. This gave a secondary drop which had a surface area of 0.93 cm^2 . The model gives an area before necking of 1.23 cm^2 and a secondary drop with a surface area of 1.42 cm^2 . Therefore the difference in surface area between the experimental and predicted secondary drops is greater than the change in surface area predicted by the model. The Charles and Mason model also neglects the changes in area of the surfaces attached to the liquid column which result from the necking process. This is illustrated in Figure 8. In the present work these are of a similar magnitude to the changes which occur in the surface area of the column. It is hoped to compare in a future paper the Charles and Mason theory with results obtained for secondary drop formation during coalescence.

Visual observations of the shape of the column during necking suggested that the surface is better represented by a section of the surface $r = r_0 + \alpha \cos(2\pi z/4h)$ of length h joined to a section of the surface $r = R_C$ (Figure 8, model B). It is interesting to note that if Rayleigh's result $\lambda_{n,\text{crit}} = 2\pi R_C$ is used to predict the onset of necking of the cylindrical column, where $\lambda_{n,\text{crit}} = 4h_{\text{crit}} = 4(H - R_C)_{\text{crit}}$, then the predicted value of $(H/R_C)_{\text{crit}}$ is $\pi/2 - 1$. This is in fair

agreement with the experimental results which are given in Table 3. However, a close examination of the mathematical implications of this procedure shows that it is unjustified. The changes in surface area which occur during necking were investigated for model B with surface waves represented by either $r = (R_c - \alpha) + \alpha \cos \frac{\pi z}{2h}$, $0 < z < h$ and $\frac{\alpha}{R_c} \ll 1$ (model B₁); or $r = R_c - \sin \frac{\pi z}{2h}$, $0 < z < h$ and $\frac{\alpha}{R_c} \ll 1$ (model B₂), and no drainage of the column during necking. Both gave an increase in surface area during necking for all cases of practical interest and therefore predict that the column will not neck. The case of a draining column was then examined and it was noted that the surface of the primary drop, to which the column is attached, is approximately spherical at the onset of necking. The system was represented by models C₁, C₂ and C₃ (Figure 9). For a system of constant volume these models give respectively

Model C₁ with $(\frac{R_c}{R_1})^2 \ll 1$

$$\frac{dA}{dR_c} = 2\pi H + 2\pi \frac{R_c^2}{R_1} - \frac{4\pi R_c H}{R_1} - 2\pi R_c \tag{3}$$

Model C₂ with $\alpha/R_c \ll 1$ and $(R_c/R_1)^2 \ll 1$

$$\frac{dA}{d\alpha} = (4 - 2\pi)(H - R_c) + 2\pi R_c + (4\pi - 8) \frac{(H - R_c)R_c}{R_1} \tag{4}$$

Model C₃ with $\alpha/R_c \ll 1$ and $(R_c/R_1)^2 \ll 1$

$$\frac{dA}{d\alpha} = -4H + (4 + 2\pi)R_c + 8 \frac{R_c H}{R_1} - 8 \frac{R_c^2}{R_1} \tag{5}$$

where R_1 is the radius of the primary drop immediately before necking. Using the previously discussed criterion for stability, for the drainage to occur by column shrinkage $\frac{dA}{dR_c} > 0$ and for drainage to occur by necking $\frac{dA}{d\alpha} < 0$. As a first approximation it was assumed that $R_1 = R_{E,1}$. The values of R_c given in Table 3 were calculated using this assumption and measured values of H . They show that drainage of the column can occur by either shrinking or necking and

that drainage by shrinking can occur at higher values of R_c than can drainage by necking. This is in agreement with the experimental results. The theoretical values of the critical R_c for drainage by both shrinking or necking are low. However, this was expected because of the difficulty of describing the surface of a breaking drop. These difficulties were discussed earlier in this paper. Also, it must be borne in mind that, because of the relatively high kinetic energy of the fluid in both the column and the drop during the draining process, surface energy considerations alone may not predict correctly the critical diameter for column shrinkage or necking.

Estimation of da/dt at the onset of necking

An estimate of da/dt , the rate of necking, at the onset of necking was obtained from a momentum balance. The column was approximated to a frustum of a cone plus a non-draining hemispheroidal cap (Figure 10) and it was assumed that the velocity profile across a z plane in the frustum was parabolic and given by the expression:

$$U_z|_r = U_z|_{r=0} \left(1 - \left(\frac{r}{r_s}\right)^2\right) \quad (5)$$

where $r_s = R_c - z/h(R_c - a)$ a mass balance gives:

$$U_z|_{r=0} = \frac{-2z^2}{r_s^2 h} \frac{da}{dt} \left(R_c - \frac{2z}{3h}(R_c - a)\right) \quad (6)$$

The results presented in Figure 4c show that at the onset of necking $d^2a/dt^2 = 0$ and therefore the momentum balance for the element δz , when $a \rightarrow R_c$, is given by the expression

$$\begin{aligned} -\frac{2\pi\rho_d z^3}{3h^2} \left(\frac{da}{dt}\right)^2 = & -\frac{d}{dz} \left[\frac{\frac{4\rho_d z^2}{3h} \left(\frac{da}{dt}\right) \left(R_c - \frac{2z}{3h}(R_c - a)\right)}{\left(R_c - \frac{z}{h}(R_c - a)\right)^2} \right]_{a \rightarrow R_c} \\ & - d/dz (P\pi R_c^2) + \pi\rho_d g R_c^2 \end{aligned} \quad (7)$$

Integrating between the limits $z = 0$ and $z = h$ gives ΔP_f , the change in pressure between the ends of the frustum:

$$\Delta P_f = -\frac{7\rho_d h}{6R_c^2} \left(\frac{da}{dt}\right)^2 + \rho_d g h \quad (8)$$

Therefore, if the pressure drop due to the flow of fluid in the primary drop is neglected, ΔP_w , the pressure drop in the continuous phase between the points A and B, is given by the expression

$$\Delta P_w = -\frac{7\rho_d h}{6R_c^2} \left(\frac{da}{dt}\right)^2 + \rho_d g D_v + 2\sigma \left(\frac{1}{C_B} - \frac{1}{C_A}\right) \quad (9)$$

where C_A and C_B are the radii of curvature at points A and B respectively. There are no published measurements for the pressure drop across a falling droplet, but Jenson and co-workers ⁽²⁸⁾ have published data for the pressure distribution around a sphere immersed in a fluid which is flowing horizontally and this data will be used to estimate ΔP_w . Over a range of Reynolds numbers similar to those used in the present work, the data for the pressure drop between the forward and rear stagnation points of the sphere may be represented by the equation

$$\Delta P = 1.12 \left(\frac{1}{2} \rho_w U_\infty^2\right)$$

Therefore $\Delta P_w = 1.12 \left(\frac{1}{2} \rho_w U_\infty^2\right) + \rho_w g D_v$

and because $1.12 \left(\frac{1}{2} \rho_w U_\infty^2\right) \approx 105 \text{ dyn/cm}^2$, equation (9) becomes

$$\frac{7\rho_d h^2}{6R_c^2} \left(\frac{da}{dt}\right)^2 = (\rho_d - \rho_w) g D_v - 105 + 2\sigma \left(\frac{1}{C_B} - \frac{1}{C_A}\right) \text{ dyn/cm}^2 \quad (10)$$

Values of da/dt were calculated from equation (10) using the experimental values of H and R_c at the onset of necking, and with $h = H - R_c$. There was difficulty in obtaining values for C_A and C_B . Measurements were made of C_A but, because of the large scatter of the readings, a mean value of 0.85 cm was used in the calculations for all sizes of drop. It was assumed that, as there was no drainage from the hemispheroidal cap, $C_B \approx 2R_c$. The calculated

values of da/dt are compared with the experimental values in Table 4. No results are presented for the 0.998 cm diameter drops because at no time did they neck at a constant R_C . Nor are results presented for the two larger sizes of drop because they did not form a cylindrical column. Table 4 shows that the calculated and experimental values of da/dt are in fair agreement, in spite of the many simplifying assumptions which were made in the calculations.

Similar calculations were also made to determine dR_C/dt for a column which drained by shrinkage (Model C, with a hemispheroidal end). These gave values of dR_C/dt which were numerically much smaller than $d\alpha/dt$ and therefore which predict that in the region where shrinking and necking are possible, then necking will predominate. This prediction is supported by the experimental results.

CONCLUSIONS

The following conclusions were made concerning the breakup of freely falling drops of chlorobenzene in the size range 0.896 cm $\leq D_{E,1} \leq$ 1.146 cm.

1. The breakup occurs during the critical oscillation which follows the first shedding of a class III attached wake. Drops which do not break up during this oscillation will not break subsequently during their free fall.
2. Secondary drops are formed from both front and rear formed columns by a necking process. The volume of the secondary drops, which are formed from the rear column when the critical oscillation corresponds with the third D_V peak after detachment, can be predicted by the equation

$$V = 3.6 [D_{E,1} - D_{E,1}^*]$$

3. The rate of necking of the rear column at the onset of necking may be predicted from a momentum balance on the fluid in the column.

4. Theoretical considerations of the surface free energy of the drop, da/dR_C and $da/d\alpha$, during secondary drop formation, predict that the rear column will drain initially by shrinkage and finally by necking.

NOTATION

A	total surface area of the drop and rear column, cm^2
a	radius of the rear column at the point of necking, cm
C	radius of curvature, cm
D_C	maximum diameter of the rear column at any instant, cm
$D_{E,1}$	equivalent spherical diameter of the primary drop, cm
$D_{E,2}$	equivalent spherical diameter of the secondary drop, cm
$(D_{E,1})_{\text{crit}}$	critical $D_{E,1}$ for breakup (equation 1), cm
$D_{E,1}^*$	critical $D_{E,1}$ for breakup on the third peak (equation 2), cm
D_H	length of the major axis (Figure 2), cm
D_V	length of the minor axis (Figure 2), cm
E	eccentricity ($= D_H/D_V$)
V	volume of the secondary drop, cm^3
H	length of the column (Figure 2) cm
h	length of the column (Figures 8, 9), cm
P	pressure, dynes/ cm^2
ΔP_w	pressure drop in the continuous phase between points A and B (Figure 10), dynes/ cm^2
ΔP_f	change in pressure between the ends of the frustum (Figure 10), dynes/ cm^2
R_C	maximum radius of the rear column at any instant, cm
R_1	radius (Figure 9), cm
$R_{E,1}$	equivalent spherical radius of the primary drop, cm
r	radius

r_0	a constant, cm
r_c	radius of a cylindrical column of fluid prior to necking, cm
r_s	radius of the column at z (Figure 10), cm
t	time, sec
U_z	fluid velocity in the z direction, cm/sec
U_∞	terminal velocity of the sphere or drop, cm/sec
z	distance along the column (Figure 10), cm

Greek symbols

α	amplitude of the disturbance, cm
λ	wavelength of the disturbance, cm
ρ	density, gm/cm ³
$\Delta\rho$	density difference between the phase, gm/cm ³
δ	interfacial tension, dynes/cm

Subscripts

c	column
w	continuous aqueous phase
d	dispersed phase
$crit$	critical for necking
opt	optimum for necking

REFERENCES

1. Taylor, G.I., Proc.R.Soc.(London), 1932, A138, 41
2. Taylor, G.I., Proc.R.Soc.(London), 1934, A146, 501
3. Hinze, J.O., AIChE.Jl., 1955, 1, 289
4. Karam, H.J., and Bellinger, J.C., Ind.Engng.Chem. Fundamentals, 1968, 7, 576
5. Hinze, J.O., Appl.Scient.Res., 1948, A1, 273
6. Blanchard, D.C., Trans.Am.Geophys.Un., 1950, 31, 836
7. Lane, W.R., Ind.Engng.Chem., 1951, 43, 1312
8. Magarvey, R.H. and Taylor, B.W., J.Appl.Phys., 1956, 27, 1129
9. Lenard, P., Met.Z., 1904, 21, 248
10. Schroeder, R.R., and Kintner, R.C., AIChE.Jl., 1965, 11, 5
11. Stuke, B., Z.Phys., 1954, 137, 376
12. O'Brien, V., J.Met., 1961, 18, 549
13. Kintner, R.C., Adv.Chem.Engng., 1963, 4, 51
14. Elzinga, E.R., and Banchemo, J.T., AIChE.Jl., 1961, 7, 394
15. Gunn, R., J.Geophys.Res., 1949, 54, 383
16. Lamb, H., 'Hydrodynamics', 1945, 6th edn (Dover)
17. Edge, R.M., and Grant, C.D., Proc. of the International Solvent Extraction Conference, 1971, 1, 82
18. Hu, S., and Kintner, R.C., AIChE.Jl., 1955, 1, 42
19. Edge, R.M., and Grant, C.D., Chem.Engng.Sci., 1972, 27, 1709
20. Edge, R.M., and Grant, C.D., Chem.Engng.Sci., 1971, 26, 1001
21. Edge, R.M., Flatman, A.T., Grant, C.D., and Kalafatoglu, I.E., Symposium on Multi-Phase Flow Systems, April 1974
22. Charles, G.E., and Mason, S.G., J.Colloid Sci., 1960, 15, 105
23. Plateau, 'Statique Experimentale et Theorique des Liquides soumis aux seules Forces Moleculaires', 1873, (Paris)

- 24. Rayleigh, Proc.R.Soc.(London), 1879, 29, 71
- 25. Rayleigh, Phil.Mag., 1892, 34, 145
- 26. Weber, C., Z.Angew.Math.Mech., 1931, 11, 136
- 27. Tomotika, S., Proc.R.Soc.(London), 1935, A150, 322
- 28. Jenson, V.G., Horton, T.R., and Wearing, J.R., Trans.Instn.Chem. Engrs., 1968, 46, 177

TABLE 1 Physical properties at 25°C of the liquids used

Liquid	Density	Viscosity	Interfacial tension
	g/ml	cP	dyn/cm
Water	0.997	0.894	-
Chlorobenzene	1.099	0.756	36.5

TABLE 2 The D_y peaks at which the critical oscillation occurred and the position at which the drop broke

$D_{E,1}$	Critical Oscillation	Position of breakup
cm	D_y peak after detachment	
0.620	9	no breakup
0.674	7	no breakup
0.769	5	no breakup
0.896	4	rear breakup
0.906	4	rear breakup
0.932	4	no breakup
0.969	3-4	front breakup
0.998	3	rear and front breakup
1.013	3	rear and front breakup
1.056	3	rear and front breakup
1.088	3	rear and front breakup
1.124	3	rear breakup
1.146	3	rear and front breakup

TABLE 3 Dimensions of the rear formed column immediately prior to necking

EXPERIMENTAL					THEORETICAL		
$D_{E,1}$	H	R_C	Value of R_C for drainage to occur by:				
			column shrinkage		necking	necking	
			Model C1	Model C2	Model C3		
cm	cm	cm			cm	cm	cm
0.896	0.37	0.15	0.39	2.5	0.16	0.072	0.099
0.906	0.40	0.175	0.36	2.3	0.165	0.077	0.103
0.998	0.35	0.165	0.34	2.25	0.17	0.072	0.097
1.013	0.445	0.175	0.405	2.55	0.185	0.085	0.115
1.056	0.665	0.235	0.45	2.8	0.21	0.114	0.146
1.088	0.75	0.26	0.46	2.8	0.225	0.125	0.158

TABLE 4 Experimental and theoretical values of da/dt , the rate of necking, at the onset of necking

$D_{E,1}$	da/dt experimental	da/dt equation 10
cm	cm/sec	cm/sec
0.896	- 5.8	- 8
0.906	- 5.7	- 8.7
1.013	- 5.0	- 7.2
1.056	- 6.05	- 5.5
1.088	- 6.05	- 5.2

DIAGRAMS

- Figure 1 Column.
- Figure 2 Drop dimensions.
- Figure 3 The variation of D_H and D_V , the lengths of the major and minor axes of the drop respectively and of E , the eccentricity with time for chlorobenzene drops falling from rest.
- Figure 4 The dimensions of the rear column during breakup.
- Figure 5 The shape of a 1.056 cm diameter drop during the critical oscillation.
- Figure 6 The equivalent spherical diameter of the secondary drop.
- Figure 7 The model used by Charles and Mason to examine secondary drop formation during coalescence,
- Figure 8 Models used to represent the necking of a non-draining column behind a drop.
- Figure 9 Models used to represent the necking of a draining column behind a drop.
- Figure 10 The drainage model which is used to give an estimate of da/dt .

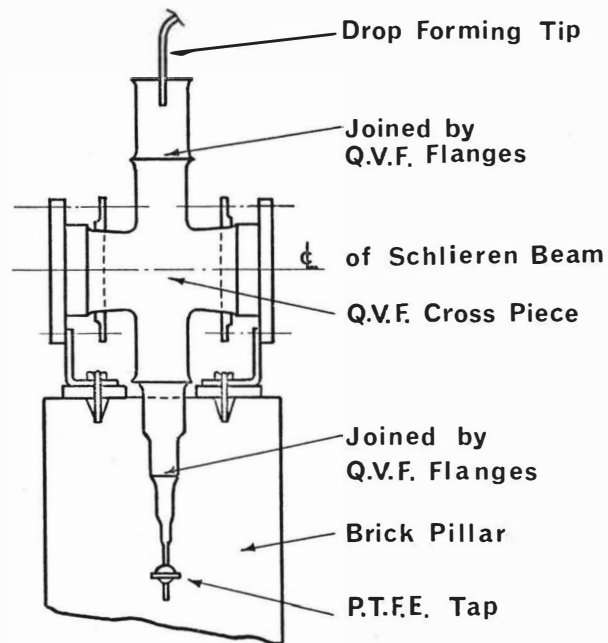


Fig.1 Column.

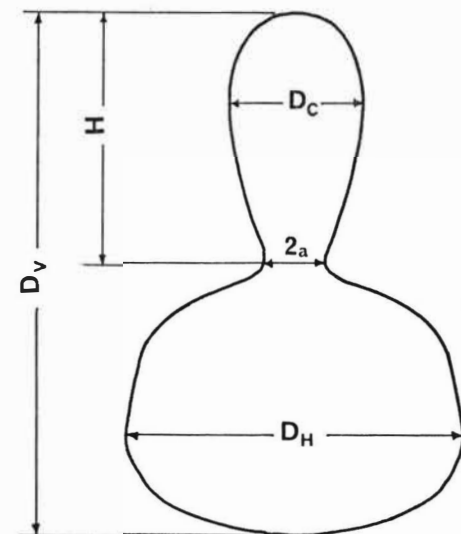


Fig.2. Drop dimensions

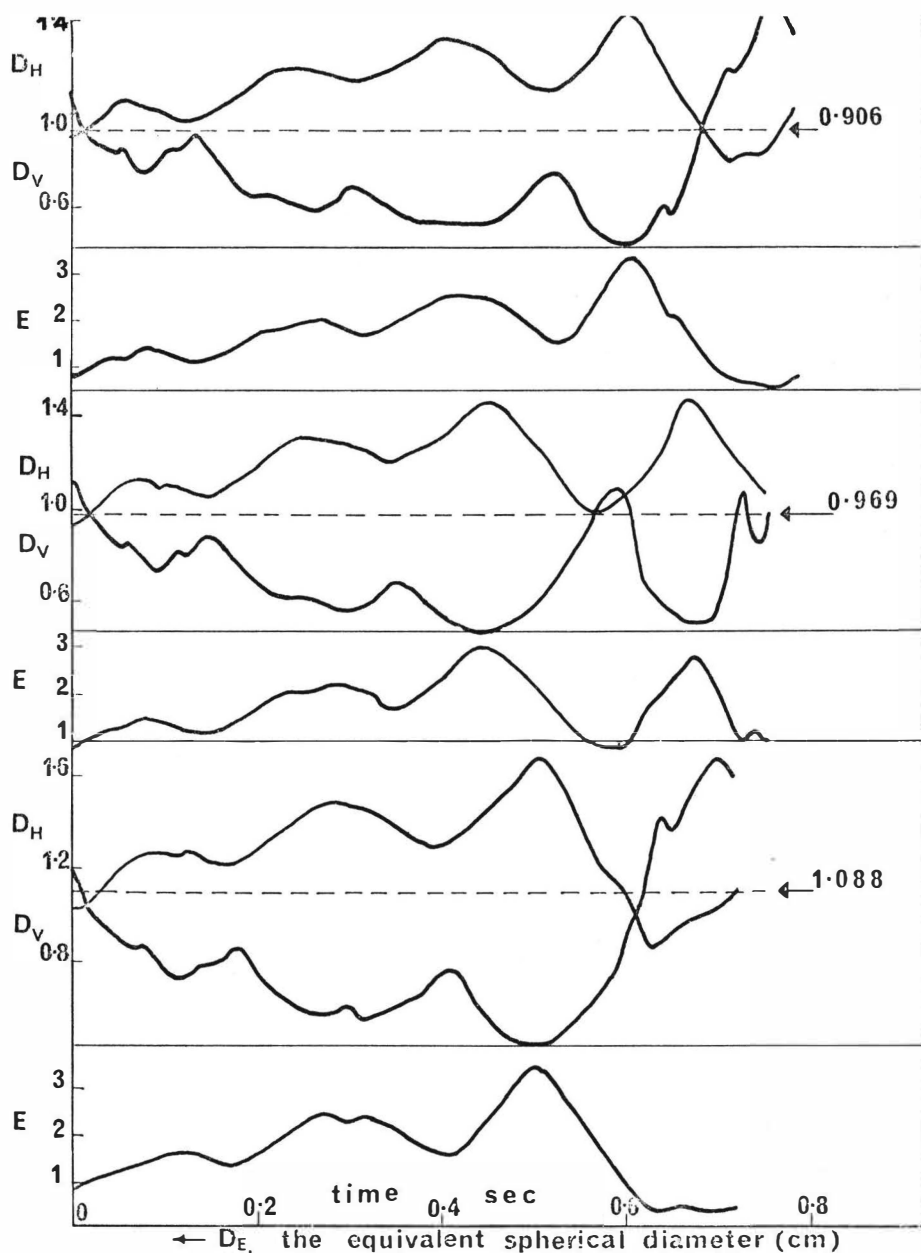


Fig. 3. The variation of D_H and D_V , the lengths of the major and minor axes of the drop respectively (cm), and of E , the eccentricity with time for chlorobenzene drops falling from rest.

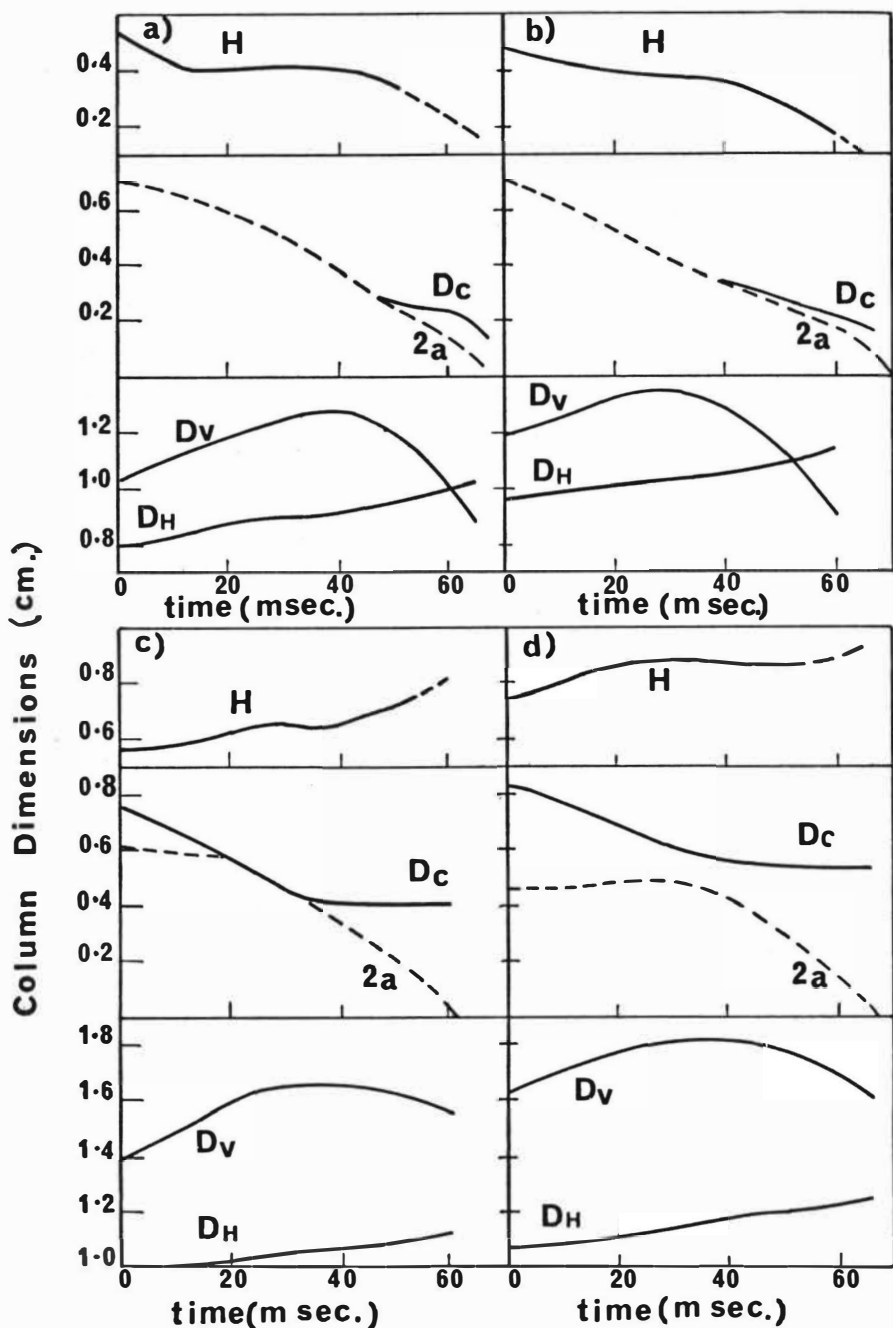


Fig. 4. The dimensions of the rear column during breakup. (a) $D_E = 0.896$ cm. (b) $D_E = 0.998$ cm. (c) $D_E = 1.056$ cm. (d) $D_E = 1.146$ cm.

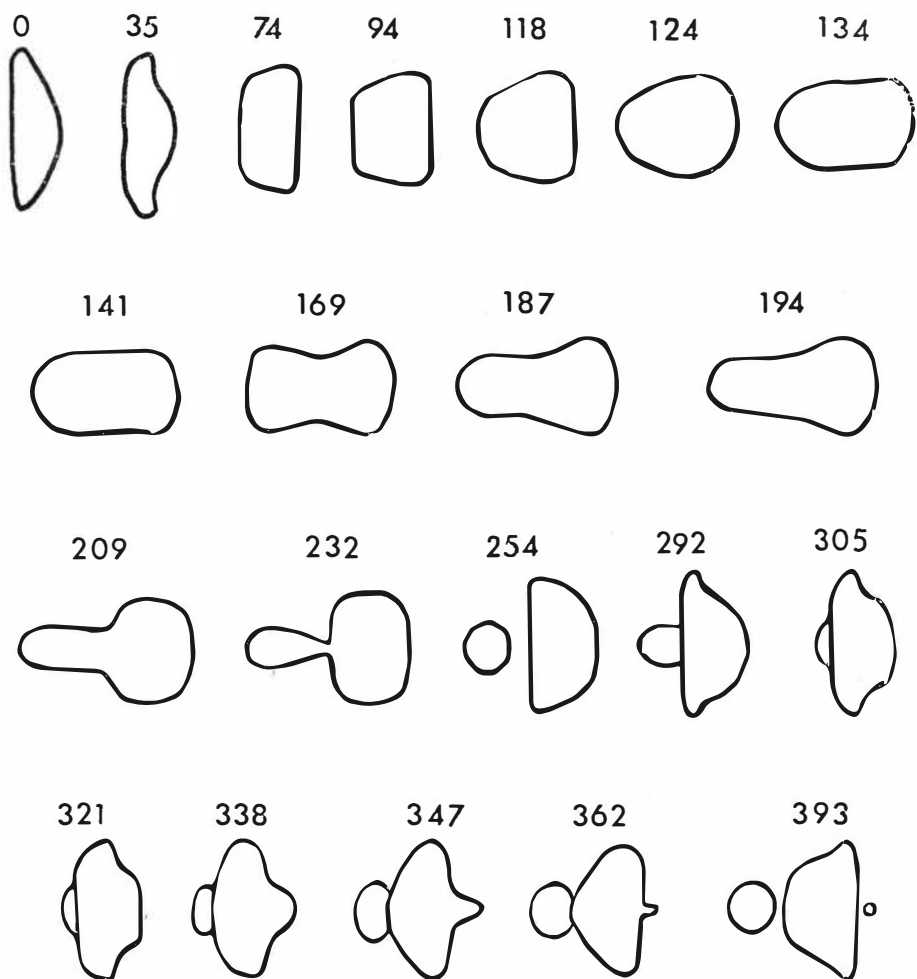


Fig.5. The shape of a 1.056 cm. diameter drop of chlorobenzene during the critical oscillation. numbers indicate time in m.secs.

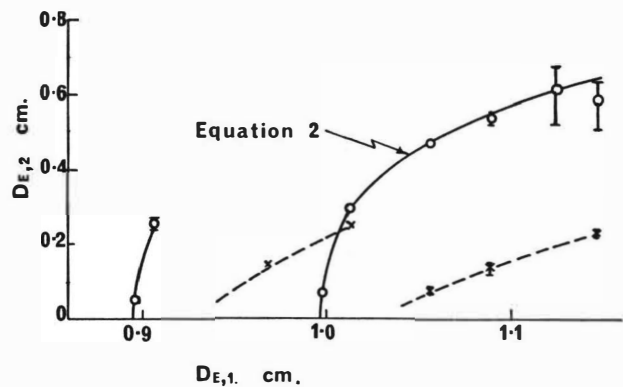


Fig.6. The equivalent spherical diameter of the secondary drop —○— rear formed secondary drop; —x— front formed secondary drop; I limits of the scatter.

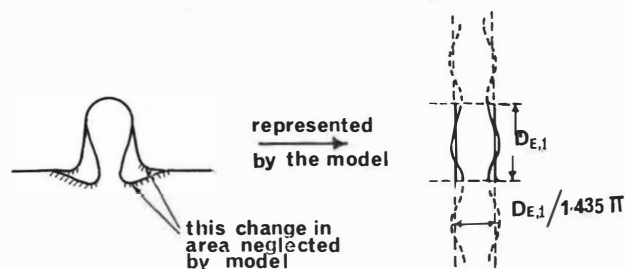


Fig.7. The model used by Charles and Mason²² to examine secondary drop formation during coalescence.

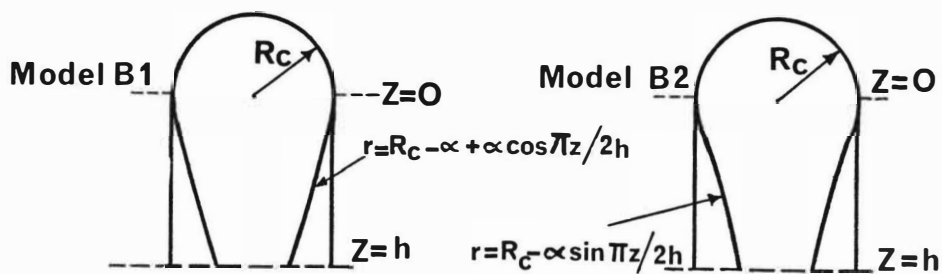
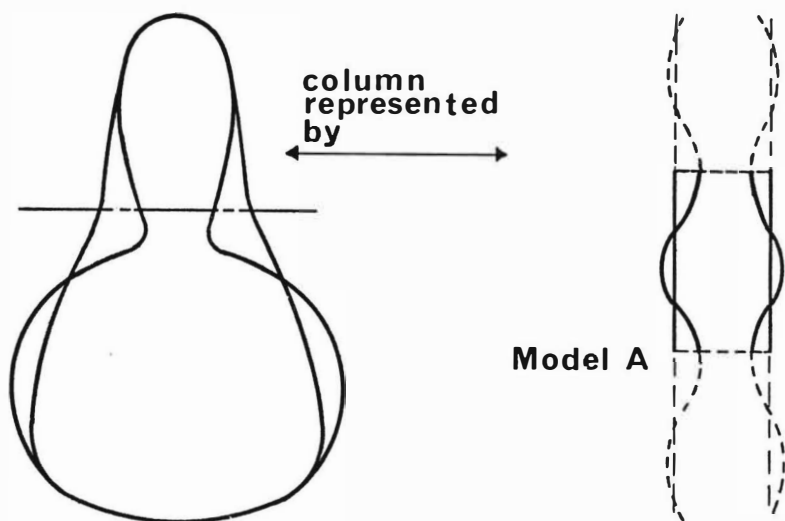
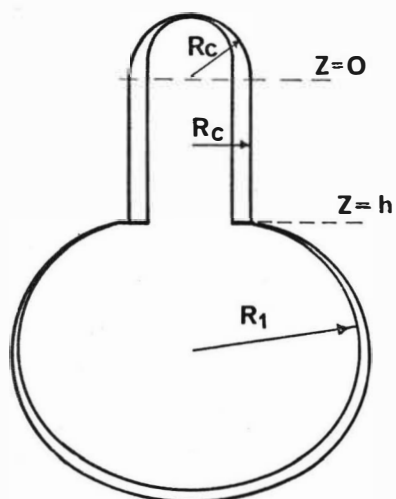
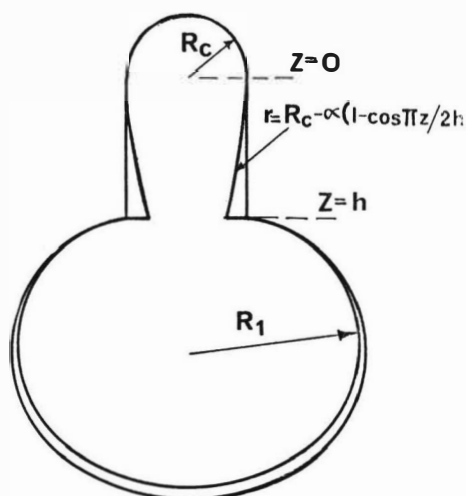


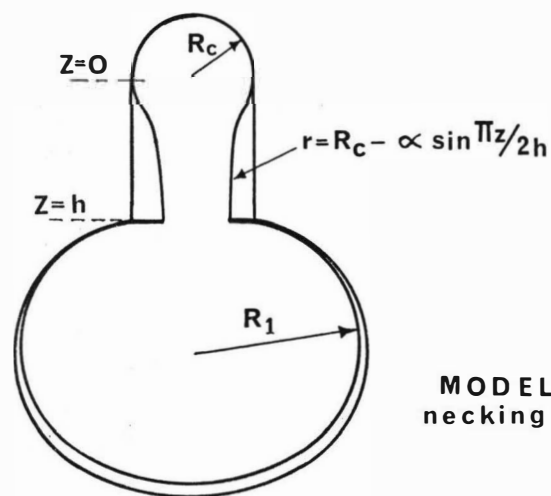
Fig.8 Models used to represent the necking of a nondraining column behind a drop.



MODEL C 1
shrinking column



MODEL C 2
necking column



MODEL C 3
necking column

Fig.9. Models used to represent the necking of a draining column behind a drop.

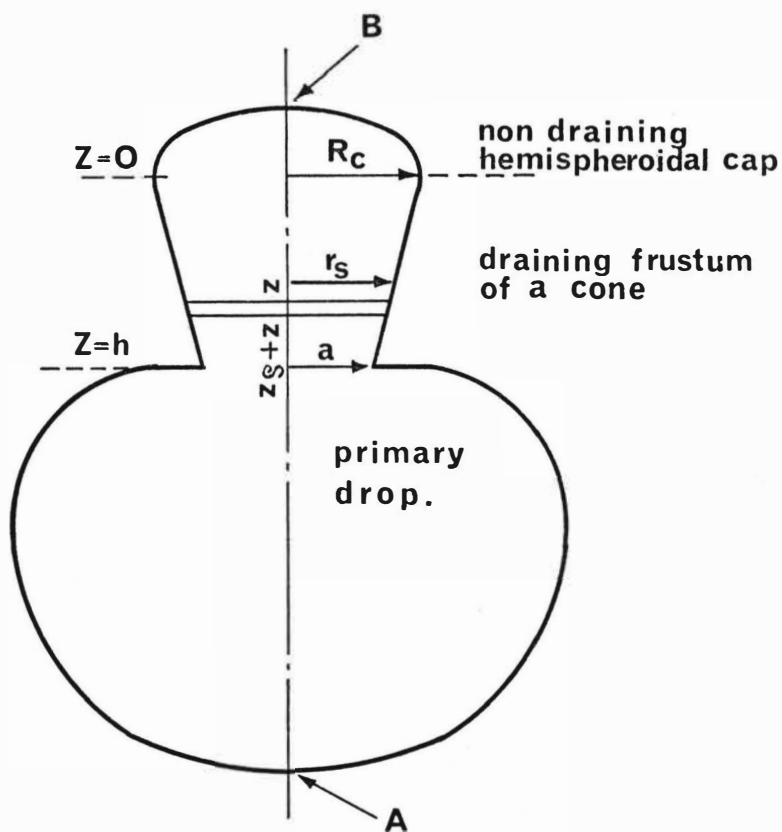


Fig 10. The drainage model which is used to give an estimate of $\frac{da}{dt}$

EFFECT ON DIRECTION OF MASS TRANSFER ON
BREAK-UP OF LIQUID JETS

by: I. Džubur* and H. Sawistowski,
Department of Chemical Engineering and Chemical
Technology, Imperial College of Science and
Technology, London SW7

SYNOPSIS

Experiments were conducted on the effect of the presence of a solute, propionic acid, on the break-up of liquid jets in liquid-liquid systems. The main parameters studied were jet length and the surface/volume ratio of resulting drops. It was found that results obtained in the absence of mass transfer and with solute in phase equilibrium are in good agreement with theory. Contrary to expectations, however, no significant effect could be detected of the action of 'thin-film' Marangoni phenomena on jet stability in the presence of mass transfer. The results were best explained in terms of difference in interfacial tension produced by assuming a specific distribution of resistances to mass transfer between the phases. The significantly lower surface/volume ratio for transfer out of the jet can also be explained in a similar way.

* Present address: ENERGOINVEST - ITEN, Sarajevo,
Yugoslavia

INTRODUCTION

The problem of hydrodynamic instability, and hence of the break-up of axisymmetric jets, has received a lot of attention both theoretical and experimental. Its practical significance rests on the fact that the size of drops formed in the break-up of cylindrical jets is controlled by the amplification of interfacial perturbations and related to the magnitude of the dominant wave number. However, jet stability affects not only drop size but also jet length. Both these interrelated problems are of great importance in liquid-liquid extraction, particularly in spray columns, where dispersion of one phase in another is achieved by injection through nozzles.

The stability theories and their semi-empirical simplifications refer generally to gas-liquid and immiscible liquid-liquid systems in the absence of mass transfer. For such a case equations exist for the prediction of jet length and drop sizes formed by the break-up of cylindrical jets. The comprehensive work of Meister and Scheele^(1,2) seems to provide the best correlations and also a good summary of previous work.

The occurrence of mass transfer introduces a twofold affect; Firstly, the presence of solute lowers, in general, the interfacial tension. Since interfacial tension is a stabilizing force in jet-break up, its decrease results in smaller drops and hence larger surface to volume ratios. On the other hand jet length is inversely proportional to the growth constant of the disturbance which, in turn, is proportional to $\gamma^{\frac{1}{2}}$. Consequently, a decrease in interfacial tension increases the jet length. However, the problem is complicated by the distribution of resistances to mass transfer between the phases, which governs the magnitude of the interfacial tension.

The second mass transfer effect is the appearance of Marangoni phenomena. As was discussed by Bainbridge and Sawistowski⁽³⁾ with reference to distillation, the narrowing of the jet at the nodes leads to the appearance of concentration

gradients and thus interfacial tension gradients. The resulting surface flow will, in the case of liquid-liquid extraction^(4,5), accelerate break-up for transfer into the jet (if $d\gamma/dc < 0$) and decelerate it for transfer out of the jet. This will affect the growth constant and hence, for a system of constant interfacial tension, mass transfer into the jet should decrease the jet length and mass transfer out of the jet increase it, provided $d\gamma/dc < 0$. Reverse effects are to be expected if $d\gamma/dc > 0$. Drop sizes are, however, affected by the wavelength of the disturbances and assumed to be controlled by symmetrical disturbances. As these arise before Marangoni effects can be effective, there should be no effect of the latter on drop sizes.

There is very little information on the effect of mass transfer on disintegration of liquid jets. Experimentally only a short paragraph is devoted to it in the work of Meister and Scheele, whereas a theoretical treatment was outlined by Berg⁽⁶⁾ at a recent discussion meeting. There is a need, therefore, for the presentation of more experimental data, which the present work is intended to fulfil.

EXPERIMENTAL

Two systems were employed for the experimental investigation: benzene/water and chlorobenzene/water with propionic acid as solute. In each case the organic phase was dispersed. The equilibrium relation and the variation of interfacial tension with concentration for the system chlorobenzene/propionic acid/water are shown in Figs. 1 and 2 respectively.

The experiments on benzene/water were preliminary in nature⁽⁷⁾ and the set-up employed consisted of a nozzle, 1.6mm inside diameter, located centrally in a glass tube, 45 mm in diameter, with the tube surrounded by a parallel-sided channel of water to facilitate photography. A systematic study⁽⁸⁾ was conducted on the system chlorobenzene/water. For this purpose a nozzle, 2.0mm inside diameter was employed placed centrally inside a rectangular column, 10 cm by 15 cm in cross-section and 45 cm high, fitted with two parallel glass windows.

In each set-up a millimetre scale was placed in the chamber, parallel to the jet, to facilitate measurement of jet length and drop size. The flow rate of the dispersed phase was controlled by a needle valve and measured by a rotameter. Facilities also existed for simultaneous flow of the continuous phase.

The analysis of jet length was conducted and checked by means of photography. For the benzene/water set-up a polaroid camera was employed using polaroid film of ASA 3000 and a shutter speed of 1/500s. The back of the channel was painted blue and illuminated from behind using a 500w lamp. Best results were obtained with aperture f 5.6. In the chlorobenzene/water set-up a white, diffusely reflecting, surface was positioned behind the column and illuminated by two light sources placed in the plane of the camera but at an angle of 60° to the camera-column axis. An ordinary camera was employed with a shutter speed of 1/500s and aperture f 7.2 using a FP4 film. Drop sizes were measured from photographs and only drops close to the jet were employed for analysis.

RESULTS

The work was concentrated on investigating (a) the variation of jet length with Reynolds number and direction of transfer, and (b) the variation of drop size with the same parameters. The first variation is shown in Figs. 3 and 4 for benzene/water and chlorobenzene/water respectively. Jet length is expressed in a dimensionless form as L/d_N , where L is the jet length and d_N the nozzle diameter. The Reynolds number is also based on conditions in the nozzle, i.e. $Re = u_N d_N \sqrt{\rho/\mu}$. The second variation is represented in Figs. 5 and 6 as a plot surface/volume ratio, which is inversely proportional to the mean drop diameter, against Reynolds number with mass transfer and its direction as parameter.

DISCUSSION AND CONCLUSIONS

Jet Length

In all investigated cases the jet length passed through a maximum with Reynolds number. This is illustrated visually in Fig.7, which also shows that turbulent jet break-up occurs at the expected Reynolds number of 2200. The corresponding Reynolds numbers for turbulent break-up in the presence of mass transfer were, however, much lower and nearer to 1000 than 2000. This lowering of the critical value could not be attributed to the effect of reduced interfacial tension as no corresponding lowering was observed in the equilibrium runs. It must, therefore, be a feature of the mass transfer process itself, which may introduce random and asymmetrical disturbances through the action of Marangoni-induced interfacial turbulence. The concentration levels were sufficiently high for such phenomena to occur.

The comparison of results in the absence of mass transfer, that is obtained in pure systems and under equilibrium conditions, indicate that the presence of solute in phase equilibrium shifts the curve towards lower Reynolds numbers and produces a sharper and higher peak (Fig.6). This behaviour can be explained purely in terms of changes in interfacial tension. Thus, it has been shown that the jetting velocity u_J , that is nozzle velocity below which a jet will not form, is given by

$$u_J = A (1 - d_N/d_P) \gamma / \rho_D d_N \quad (1)$$

and hence is directly proportional to interfacial tension. (This is not quite correct since drop diameter, d_P , also depends on γ). Consequently a decrease in γ will allow jets to form at lower Re and shift the curve to the left.

It is generally assumed that when a disturbance on the jet surface attains an amplitude equal to the jet radius a drop is formed which is shed by the jet. However, drag resistance to the motion of such a drop is larger than to the motion of the jet. The drop is thus unable to escape and conditions exist for rapid lengthening of the jet. Jet disruption occurs then not as a result of symmetrical disturbances but of sinuous waves which throw the drops away from the path of the jet. It is reasonable to suppose that the critical velocity for jet disruption by sinuous waves will correspond to the maximum in the variation of jet length with jet velocity. According to Ranz⁽¹⁾ jet "thrashing" and formation of non-uniform drops begins when

$$u_N (\rho_c d_N / \gamma) = 2.83 \quad (2)$$

In the present case, for the system chlorobenzene/water the interfacial tension is 0.0365 N/m for the pure system and 0.015 N/m for the equilibrium run. Thus, using equation (2), the critical Reynolds number for maximum jet length becomes 1050 and 680 for the two cases. This is in good agreement with Fig.4.

In the preliminary work a few runs were conducted with the addition of a small amount of a surfactant, Teepol, to the benzene for transfer out of the jet. This resulted in a spectacular increase in jet length, considerably beyond the equilibrium run, but without a corresponding shift in the jetting velocity (Figs. 3, 8 and 9).

The mass transfer results are more difficult to interpret due to interactions of changes in interfacial tension and Marangoni phenomena. The change in interfacial tension depends on the distribution of resistances between the phases. This is shown in Table 1 for various assumed values of ratios of mass transfer coefficients for the system chlorobenzene/water.

The corresponding interfacial concentrations were obtained from Fig.1, the interfacial tensions from Fig.2, and the critical Reynolds numbers Re' , calculated with the help of equation 2.

Table 1

Effect on distribution of resistances on interfacial tension

K_C/K_D	∞	4	1	0.25	0
Transfer out of jet					
C_{Ci} (kmol/m ³)	0	0.18	0.57	1.00	1.27
$\gamma \times 10^3$ (N/m)	36.5	28.0	20.0	16.4	14.5
Re'	1050	940	790	710	670
Transfer into jet					
C_{Ci} (kmol/m ³)	1.16	1.03	0.82	0.40	0
$\gamma \times 10^3$ (N/m)	15.5	16.3	17.5	23.0	36.5
Re'	620	640	660	750	1050

The interpretation of results from Fig. 4 with the help of values from Table 1 leads to a reasonable assumption of approximately equal resistances in the two phases. This locates the maximum in jet length at Reynolds number of 660 for transfer into jet and at 790 for transfer out of jet. It also predicts a lower jetting velocity for transfer into the jet. All these predictions are reasonably consistent with results in Fig.4. The difficulty arises in relating the mass transfer curves to those of no mass transfer.

The Marangoni phenomenon can affect the process in two distinctive ways. By affecting the 'strength' of the nodes it stabilises the jet for mass transfer out of it, but the jet is destabilized for transfer into it. This however, is in disagreement with results in Figs. 3 and 4 as well as with the results of Meister and Scheele⁽¹⁾.

Also, it is the transfer from water to chlorobenzene which is the unstable direction of transfer in terms of the Sternling-Scriven criterion. Any presence of interfacial turbulence should, therefore, be more pronounced in this direction of transfer and lead to shorter jet lengths. Another possible Marangoni effect must also be discounted: As a drop detaches from the jet, a 'thin-film' type of Marangoni effect⁽⁵⁾ begins to act in a different direction. A thin film exists momentarily between the drop and the front of the jet. Mass transfer out of the drop (jet) would facilitate coalescence and increase the difficulty of the drop getting away from the jet. Mass transfer into the drop (jet) would, however, increase the resistance to coalescence and eliminate any coalescence effects. But such coalescence effects would again produce lengthening of the jet for mass transfer out of it, which is not consistent with experimental observation.

There is thus only one possible way of explaining these apparently anomalous results: The distribution of resistances to mass transfer is different from that assumed, e.g. $K_G/K_D = 3$, and the resulting differences in interfacial tension have a stronger effect on jet stability than the Marangoni effect. However, more experimental work is required for conclusive proof of this postulate.

Drop Size

The characteristic equation obtained by Tomotika⁽¹¹⁾ for the case of equilibrium of a long cylindrical thread of a viscous liquid surrounded by another viscous liquid incorporating the effect of interfacial tension and of viscous forces was solved for the pure chlorobenzene/water system using the Imperial College CDC 6400 computer. This gave the dimensionless wave number of the dominant disturbance as

$$ka = 2\pi a/\lambda = 0.57$$

By assuming $a = d_N/2$ and making the usual assumption that drop volume is equal to the volume of a liquid cylinder of radius a and length λ

$$d_p = 2.02 \quad d_N = 4.04 \text{ mm}$$

This prediction is compared with actual results in Fig.10. The agreement is very good indeed.

For the presence of solute the analysis of Figs. 5 and 6 shows that the surface/volume ratio is significantly smaller for mass transfer out of the jet than into the jet (data on pure systems were omitted for the sake of clarity). This can also be noticed visually in Figs. 11 and 12. Further, there is very little difference between transfer into the jet and the equilibrium run. Figs. 13 and 14 also indicate that there is, in addition, a significantly greater standard deviation for transfer into the jet than for the other two cases, between which there is again little difference.

At first it would appear that the results could be explained solely in terms of Marangoni effect and the thereby induced resistance to drop formation. However, in view of the negligible effect of Marangoni phenomena on jet length and the knowledge that drop diameter decreases with decreasing interfacial tension it was decided to examine the latter effect first.

It has already been established in discussion on jet length that by assuming $K_C/K_D = 3$ there is little difference in interfacial tension for transfer into the jet and the equilibrium run but that the interfacial tension for transfer out of the jet may be significantly higher. Consequently, on consideration of interfacial tension alone, it follows that surface/volume ratios (specific surface areas) should be similar for transfer into the jet and under equilibrium conditions but lower for transfer out of jet. This agrees with experimental observations. Again the general validity of these findings requires further investigations as does the possibility that the results may have been affected by coalescence between drops already detached from the jet.

NOMENCLATURE

A	constant in equation 1
a	jet radius
C	molar concentration of solute
d_N	internal diameter of nozzle
d_P	drop diameter
K	mass transfer coefficient
k	wave number
L	jet length
Re	Reynolds number
S	surface/volume ratio (specific surface area)
u_J	jetting velocity
u_N	liquid velocity in nozzle
γ	interfacial tension
λ	dominant wave length
ν	kinematic viscosity
ρ	density
σ	standard deviation

Subscripts

C	continuous phase
D	dispersed phase
i	interfacial condition

References

1. Meister, B.J. and Scheele, G.F., A.I.Ch.E. J1, 1969, 15, 689.
2. Meister, B.J. and Scheele, G.F., A.I.Ch.E. J1, 1969, 15, 700.
3. Bainbridge, G.S., and Sawistowski, H., Chem. Engng Sci., 1964, 19, 992.
4. Sawistowski, H., Interfacial Phenomena, in Hanson, C. (Ed), Recent Advances in Liquid-Liquid Extraction, 1971 (Oxford: Pergamon Press).
5. Sawistowski, H., Chemie-Ingr-Tech, 1973, 45, 1114.
6. Berg, J.C., 66th Annual Meeting of A.I.Ch.E., Philadelphia, 1973.

7. Comyn, J. and Swainson, G., B.Sc. report, Imperial College, London, 1969
8. Dzubur, I., M.Sc. report, Imperial College, London, 1972.
9. Scheele, G.F., and Meister, B.J., A.I.Ch.E. J1, 1969, 14, 9.
10. Ranz, W.E., Can. J. Chem. Engng, 1958, 36, 1958.
11. Timotika, S., Proc. Roy. Soc., 1935, A150, 332.

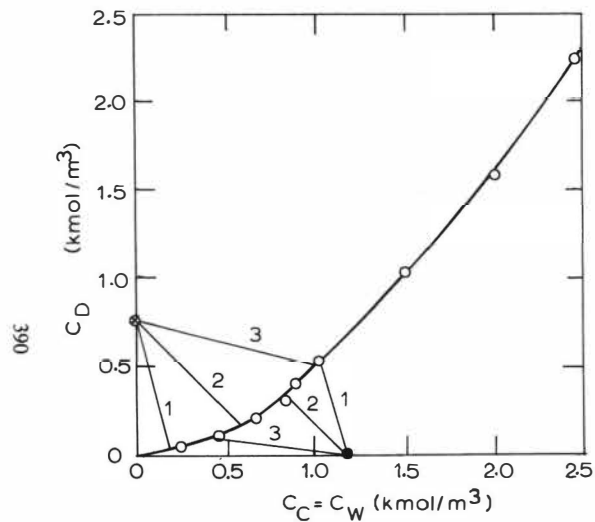


FIG. 1. EQUILIBRIUM AND OPERATING RELATIONS FOR THE SYSTEM CHLOROBRNENE/WATER WITH PROPIONIC ACID AS SOLUTE.

○ OPERATING POINT FOR TRANSFER OUT OF JET

● OPERATING POINT FOR TRANSFER INTO JET

1 - $K_C/K_D = 4$; 2 - $K_C/K_D = 1$; 3 - $K_C/K_D = 0.25$.

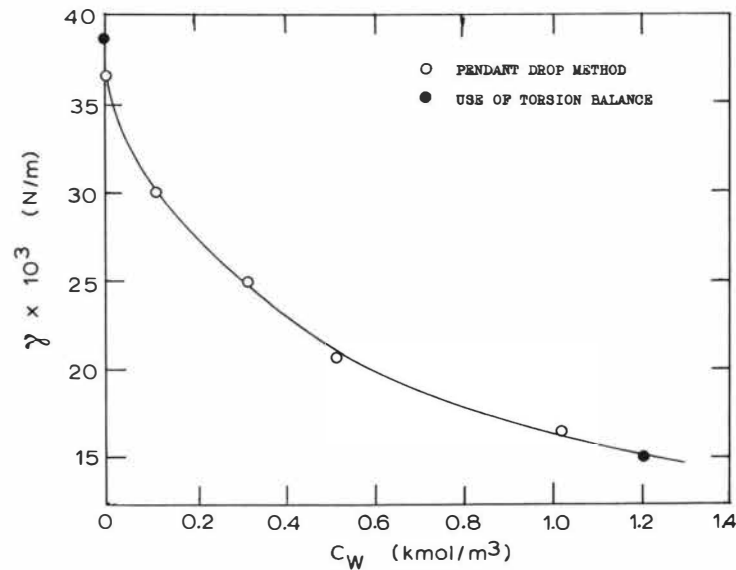


FIG. 2. VARIATION OF INTERFACIAL TENSION WITH CONCENTRATION OF PROPIONIC ACID.

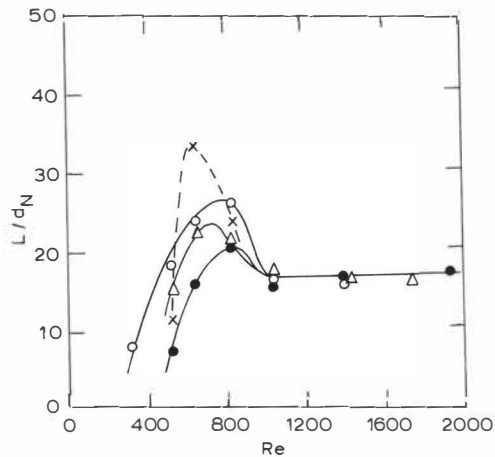


FIG. 3. VARIATION OF JET LENGTH WITH REYNOLDS NUMBER FOR THE SYSTEM BENZENE/PROPIONIC ACID/WATER. ○ EQUILIBRIUM CONDITIONS, $C_D = 0.77$, $C_C = 1.16$; ● TRANSFER OUT OF JET, $C_D = 0.77$, $C_C = 0$; △ TRANSFER INTO JET, $C_D = 0$, $C_C = 1.16$; × TRANSFER OUT OF JET IN PRESENCE OF SURFACTANT, $C_D = 0.77$, $C_C = 0 \text{ KMOL/M}^3$.

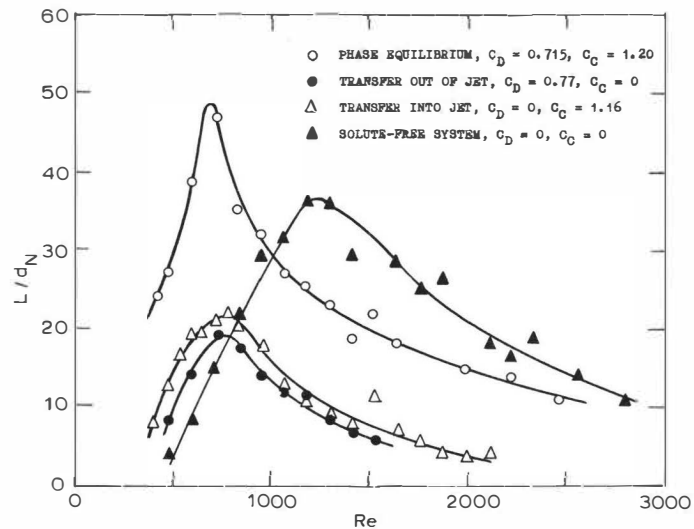


FIG. 4. VARIATION OF JET LENGTH WITH REYNOLDS NUMBER FOR CHLOROBENZENE/PROPIONIC ACID/WATER.

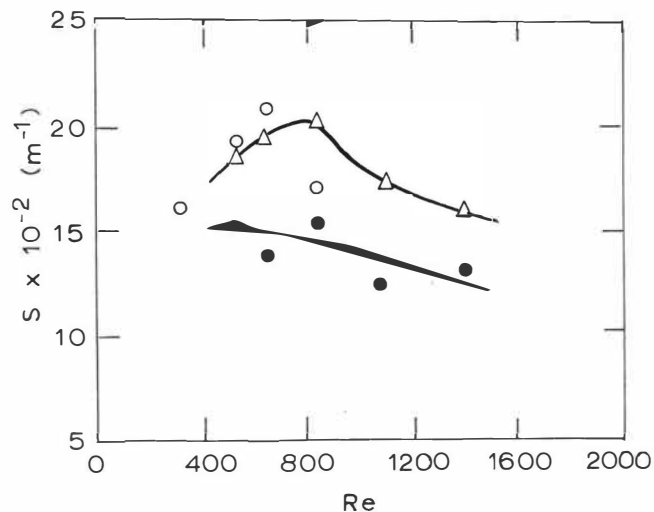


FIG. 5. VARIATION OF SURFACE/VOLUME RATIO WITH REYNOLDS NUMBER FOR TRANSFER OF PROPIONIC ACID IN THE SYSTEM BENZENE/WATER.

- SOLUTE IN PHASE EQUILIBRIUM, $C_D = 0.77$, $C_C = 1.16$;
 ● TRANSFER OUT OF JET, $C_D = 0.77$, $C_C = 0$;
 △ TRANSFER INTO JET, $C_D = 0$, $C_C = 1.16$ KMOL/M³.

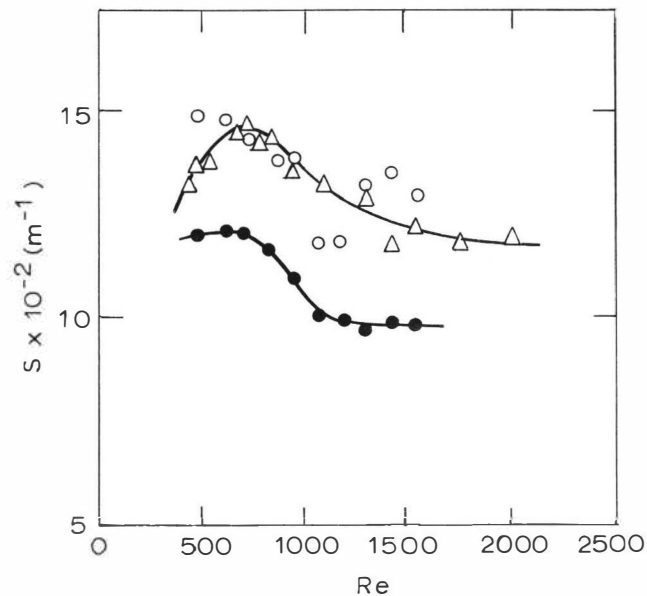


FIG. 6. VARIATION OF SURFACE/VOLUME RATIO WITH REYNOLDS NUMBER FOR TRANSFER OF PROPIONIC ACID IN THE SYSTEM CHLOROBENZENE/WATER. ○ SOLUTE IN PHASE EQUILIBRIUM, $C_D = 0.715$, $C_C = 1.16$; ● TRANSFER OUT OF JET, $C_D = 0.77$, $C_C = 0$; △ TRANSFER INTO JET, $C_D = 0$, $C_C = 1.16$ KMOL/M³.

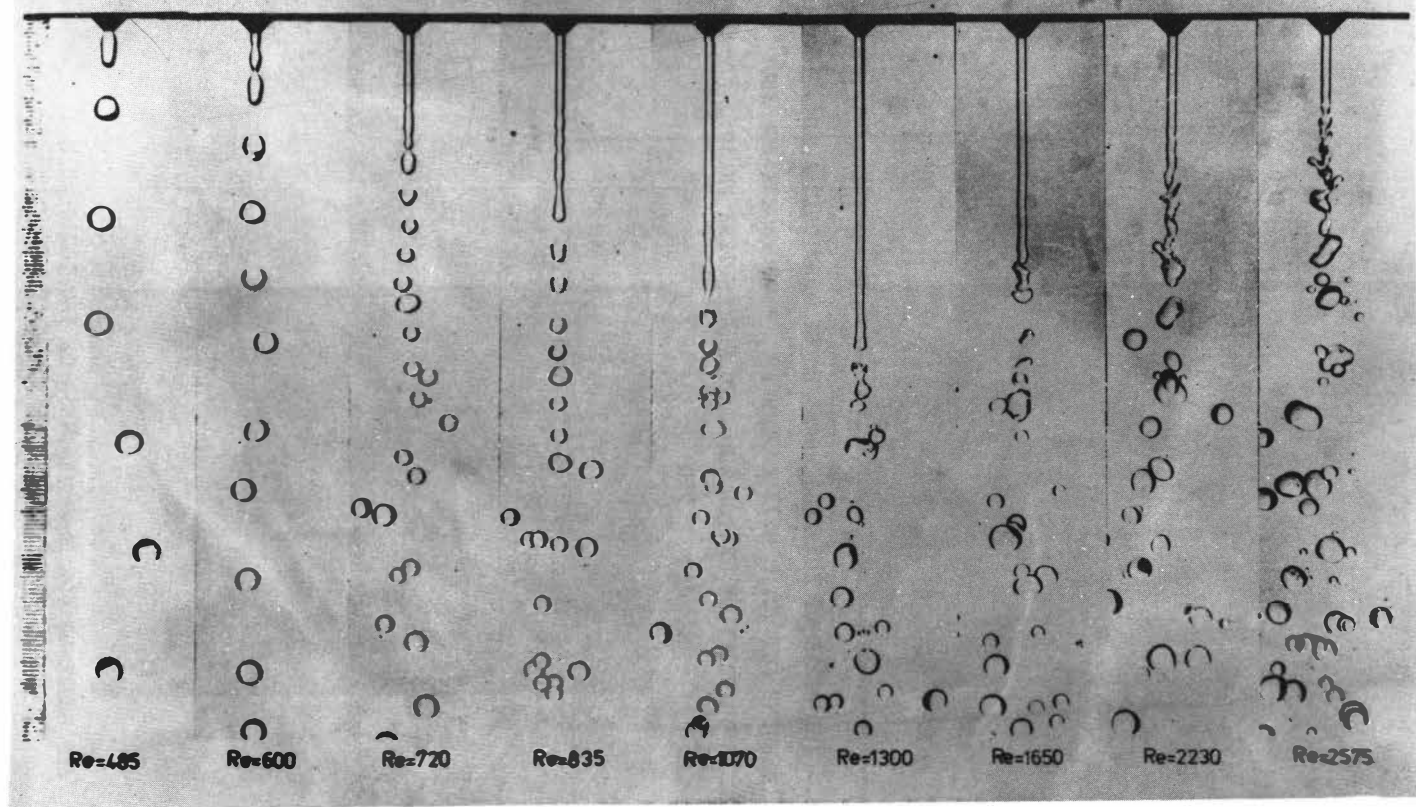


FIG. 7. VARIATION IN LENGTH OF A CHLOROBENZENE JET IN WATER
WITH REYNOLDS NUMBER.

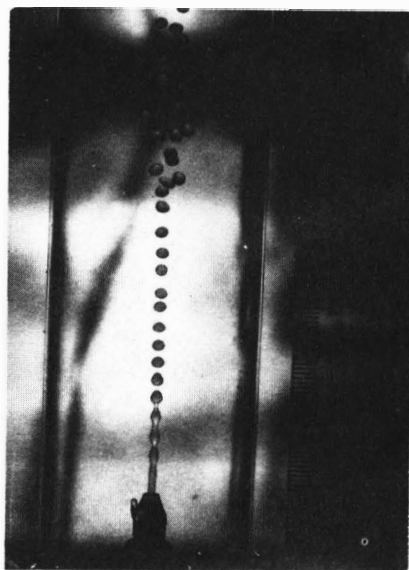


FIG. 8. JET BREAK-UP FOR MASS TRANSFER OF PROPIONIC ACID
OUT OF BENZENE JET ($C_D = 0.77 \text{ KMOL/M}^3$, $C_C = 0$) IN THE PRESENCE
OF A SMALL QUANTITY OF TEEPOL ADDED TO THE BENZENE PHASE.
($Re = 530$)

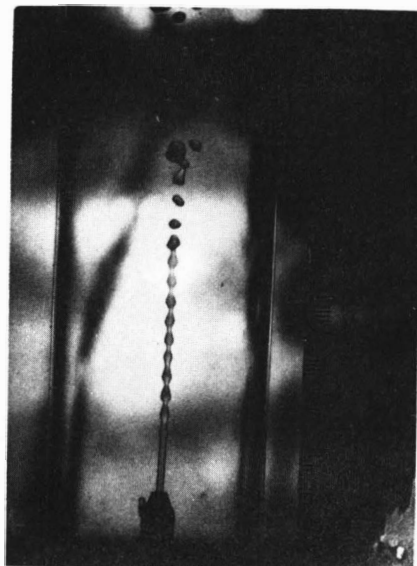


FIG. 9. JET BREAK-UP FOR MASS TRANSFER OF PROPIONIC ACID
OUT OF BENZENE JET ($C_D = 0.77 \text{ KMOL/M}^3$, $C_C = 0$) IN THE PRESENCE
OF A SMALL QUANTITY OF TEEPOL ADDED TO THE BENZENE PHASE.
($Re = 650$)

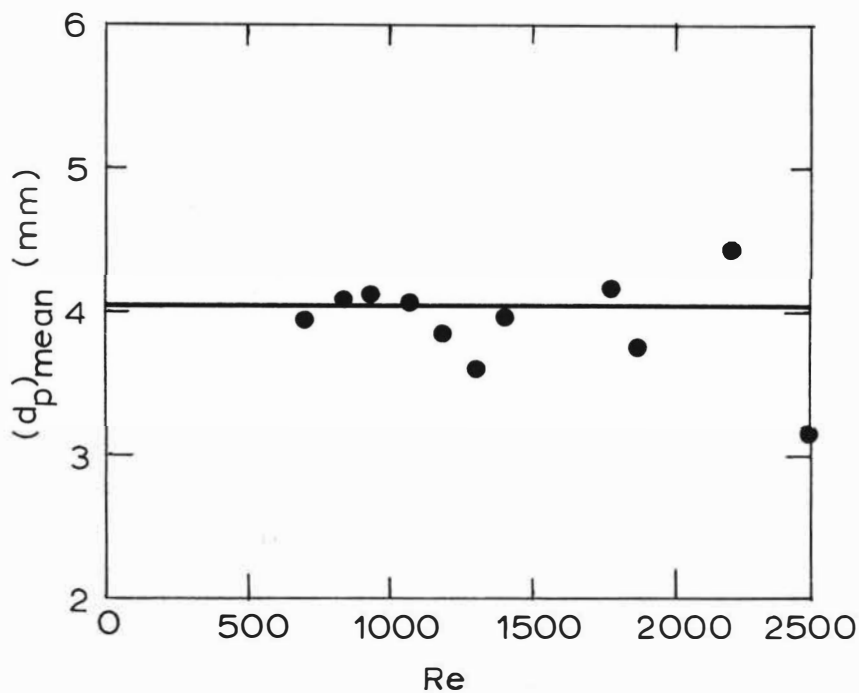


FIG. 10. COMPARISON OF THEORETICALLY PREDICTED AND EXPERIMENTAL DROP DIAMETER FOR THE SOLUTE-FREE SYSTEM CHLOROBENZENE/WATER.

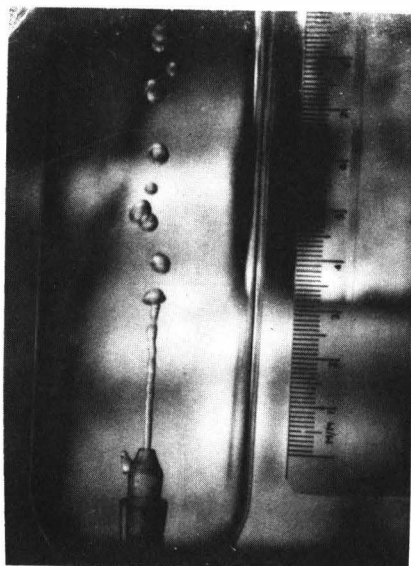


FIG. 11. JET BREAK-UP FOR MASS TRANSFER OF PROPIONIC ACID
OUT OF BENZENE JET ($C_D = 0.77 \text{ KMOL/M}^3$) INTO SOLUTE-FREE
WATER AT $Re = 830$.

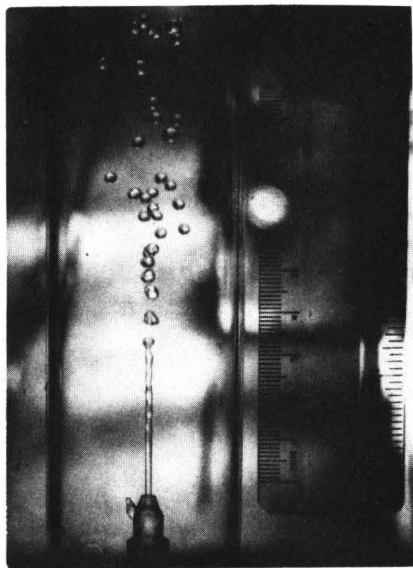


FIG. 12. JET BREAK-UP FOR MASS TRANSFER OF PROPIONIC ACID
OUT OF WATER ($C_C = 1.16 \text{ KMOL/M}^3$) INTO SOLUTE-FREE JET AT
 $Re = 830$.

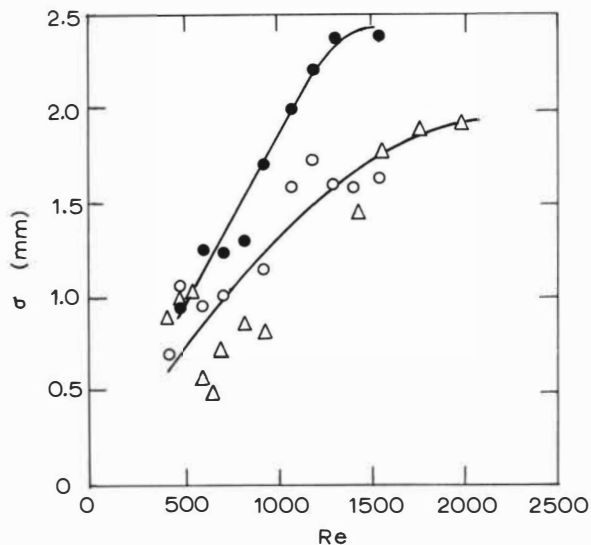


FIG. 13. STANDARD DEVIATION OF DROP DIAMETER FOR TRANSFER OF PROPIONIC ACID BETWEEN CHLOROBENZENE AND WATER. ○ PHASE EQUILIBRIUM, $c_D = 0.715$, $c_C = 1.20$; ● TRANSFER OUT OF JET, $c_D = 0.77$, $c_C = 0$; △ TRANSFER INTO JET, $c_D = 0$, $c_C = 1.16$.

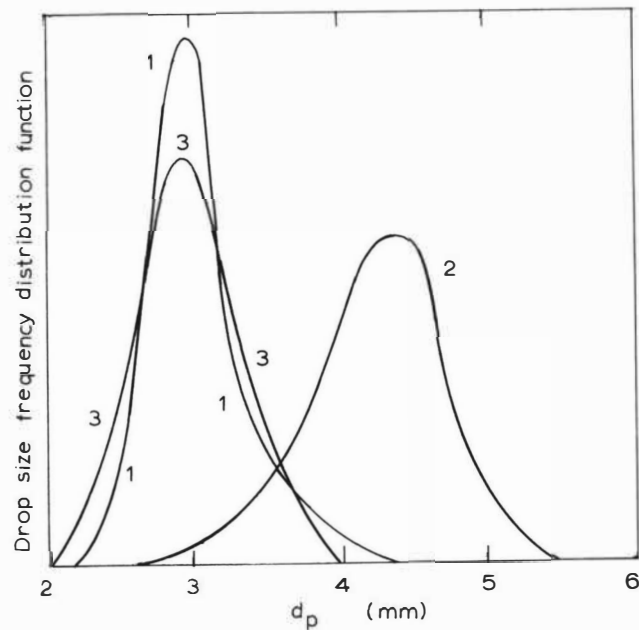


FIG. 14. DROP SIZE FREQUENCY DISTRIBUTION FUNCTION FOR TRANSFER OF PROPIONIC ACID BETWEEN BENZENE AND WATER AT $Re = 650$. 1 - PHASE EQUILIBRIUM, 2 - TRANSFER OUT OF JET, 3 - TRANSFER INTO JET.

Production of Liquid Drops by Discontinuous Injection

*Izard, J. A., +Cavers, S. D., and +Forsyth, J. S.

Abstract

A technique for producing uniform-sized drops by discontinuous injection of organic liquids into water is examined. The effect of nozzle characteristics and velocity-time profile of injection are investigated for benzene, 4-methyl-2-pentanone (MIBK) and 1-butanol. The behaviour is described of a single nozzle, producing a sparse dispersion of drops, and of an assembly of six nozzles, producing a dispersion of drops sufficiently copious for use in a spray extraction column.

Experimentally determined conditions for the production of uniform-sized drops by discontinuous injection are in agreement with theoretical predictions based on continuous injection.

*Royal Roads Military College, FMO Victoria, B. C., Canada

+Department of Chemical Engineering, The University of British Columbia, Vancouver, B. C., Canada.

Introduction

Research extending over many years has been carried out on spray liquid-liquid extraction columns. In general, the "spray" of dispersed phase has been formed by passing that phase into the continuous phase as a continuous stream through one or more cylindrical nozzles, or through holes in a plate. The jet of dispersed phase so formed continues as an uninterrupted column for some distance and then breaks up into drops.¹

In spray-column research it is clearly of advantage to have a dispersion in which every drop has the same volume. Although much attention has been given to producing such a uniform dispersion, success has been limited and uncertain in liquid-liquid systems.^{1,2,3,4.}

An earlier paper by the present authors described a preliminary investigation of the successful production of a uniform dispersion by a process of injecting the dispersed phase into the continuous as recurring discrete fixed volume increments, each giving rise to only one drop.⁵ Magarvey and Taylor⁶ used a somewhat similar method to form liquid drops in a gas phase. Also for the liquid in gas case, Park and Crosby⁷ produced uniform drops by vibrating a liquid jet by sonic means.

The first part of this present paper reports in a quantitative way results obtained by discontinuous injection through single sharp-edged nozzles with several mechanical arrangements for three binary systems. The second part re-

norts results obtained from dispersing benzene into water through an array of nozzles in order to obtain a sufficiently copious supply of uniform sized drops for use in an experimental spray-column.

Injection through single nozzles

Experimental

The essential elements of the apparatus used are shown schematically in Figure 1. Column A held stagnant continuous phase within which drops were formed. Vessel B, which communicated with metering burette C, was used to store dispersed phase. This passed through the positive displacement pump D to a dispersion nozzle E. After passing through the continuous phase, dispersed phase coalesced near the column top and returned to storage vessel B. The apparatus did not lend itself to thermostating other than by control of room temperature. The results quoted for 1-butanol, and 4-methyl-2-pentanone (MIBK) span a temperature range from 20°C to 24.5°C. In the case of benzene, a temperature range from 20°C to 22°C was achieved.

Pump and Drive

In the early stages of the work concern about leaks and contamination led to the use of sealed bellows pump D.

Cam H operated a cam follower J which in turn acted

against a lever K. This lever was held by a spring L against a fulcrum M and operated the push rod F. The location of the fulcrum M could be varied, thereby making possible a range of pump strokes, and, therefore, delivered volumes, while using the same cam. The time average volumetric rate of pumping over a number of strokes was measured by reading the rate of removal of liquid from burette C while valve G was closed. The number of strokes was counted mechanically.

Cams

Three different cams were used. Cam 1 gave uniform acceleration of the cam follower from 0° to 30° of cam rotation, and thereafter a uniform velocity up to 90° at which point the movement of the cam follower suddenly ceased. Cam 2 gave uniform acceleration of the follower between 0 and 30° , uniform velocity from 30° to 90° , and uniform deceleration to rest from 90° to 120° . Cam 3 gave simple harmonic motion between 0° and 180° . The linkage mechanism transmitted proportional, but undistorted, cam movement to the bellows. The form of the return stroke was of no significance because this was the suction stroke of the pump and no delivery was being made to the nozzle. Provision was made for driving the cams at various speeds so that injection strokes of various durations could be obtained.

Observation Column

The drops were formed in a square glass column (optically ground, 4.0 x 4.0 cm) to aid in photography used to check for drop uniformity.

Nozzles

Brass nozzles with converging, with diverging, and with cylindrical bores, and stainless steel nozzles with cylindrical bores were tried. A stainless steel nozzle tipped with Teflon also was used. Except where otherwise stated, the results quoted here are for brass nozzles with cylindrical bores of 0.18, 0.28, 0.32, 0.41, 0.45 and 0.49 cm.

Materials

Experiments were made with each of reagent grade benzene, technical grade MIBK, and technical grade 1-butanol as the dispersed phase. The continuous phase always was distilled water. Both the continuous and the dispersed phases were mutually saturated. The three systems studied are ones which have been used in liquid-liquid extraction research. They vary considerably in interfacial tension.

Results

The 1-butanol and the MIBK systems were studied first. As a result of improved equipment and techniques the data for the benzene system, studied subsequently, are more

reliable.

The Teflon-tipped nozzle proved unsatisfactory because of being wet preferentially by the dispersed phase.⁵ Of the metal nozzles, those of brass and of cylindrical bore were easiest to manufacture. These were chosen for the bulk of the work for this reason, and because none of the others gave more stable performance when dispersing the organic phase. In order to preserve desirable wetting characteristics heat-treating of the nozzles was resorted to from time to time.⁵

Results obtained for the system benzene/water are shown in Figures 2 and 3. The choice of abscissa as "duration of discharge stroke" rather than strokes/sec. is to permit comparison of the results for the different cams used, each of which required a different fraction of the cam revolution to complete the delivery stroke. The ordinate is the liquid volume delivered by each stroke of the pump.

For the conditions corresponding to any point within an envelope such as a b c d e in Figure 2, for the 0.45 cm nozzle, every stroke of the pump produces one drop, and successive drops are of the same volume (within about $\pm 2\%$): the interesting case.

Outside such an envelope a wide range of discharge patterns occur. With small delivery volumes the quantity

of liquid provided by a single pump stroke may be insufficient to form even one drop which can separate itself from the nozzle tip. After a number of pump strokes sufficient liquid volume will have collected at the nozzle tip for separation to occur. As this takes place the liquid body may rupture and two unequally sized drops result. At larger delivery volumes, but, of course, outside a b c d e, the discharge pattern for a given ordinate and abscissa usually is reproducible from stroke to stroke. However, more than one drop is produced, and these are of unequal size. Ordinarily at least one of the drops formed is relatively small: a trailer.⁵

Envelopes analogous to a b c d e of the 0.45-cm diameter nozzle are shown in Figure 2 for benzene dispersed into water through nozzles of diameters 0.32 and 0.18 cm when supplied by a positive displacement pump driven by cam 3. The required drop formation time (duration of the pump discharge stroke) is much the same for all nozzles, but the volume of the drop varies markedly with nozzle diameter. Envelopes for the 0.41-cm and the 0.28-cm diameter nozzles have been left out for the sake of clarity but occupy appropriate intermediate positions.

The form of the envelope produced by injecting benzene into water was studied for a wide range of nozzles and all

cams. The results for the 0.32-cm nozzle are shown in Figure 3. In this, as in all other cases cam 3, the simple harmonic motion cam, gave the largest envelope. For this reason, and because of the simplicity of manufacture, all subsequent work made use of SHM drive.

Also shown in Figure 2 (and in Figure 4) are drop volumes calculated by the method of Izard⁸ for predicting drop volumes in liquid-liquid systems when using continuous injection of the dispersed phase. This method has been used rather than others,^{3,9,10,11,12} since it is less empirical in nature. This method and the other correlations neglect the existence of small trailer drops as well as the variation in size of drops produced by continuous injection.

The Izard⁸ method is based upon the calculation of a shape for the forming drop. A pressure balance across the interface is used, and also a balance of the buoyancy, interfacial tension, viscous drag, and momentum change forces. This method was not developed for injection in discrete increments as employed in the experiments described in the present paper, but rather for steady flow. In calculating the drop-volumes for Figures 2 and 4 by means of this method, the use of steady mass flow input naturally was required. For the purposes of these figures, this was taken to be the average mass flow rate during the pump discharge stroke.

Table 1 summarizes the results obtained using the three systems, six cylindrical brass nozzles, and cams 2 and 3. Figure 4 illustrates the effect of system for the specific case of 0.45-cm nozzles and cam 3.

Table 1. Conditions for formation of uniform drops

Cylindrical sharp-edged brass nozzles with cams 2 and 3

System	Nozzle diameter, cm					
	0.18	0.28	0.32	0.41	0.45	0.49
Benzene-water	Y*	Y	Y	Y	Y	N
MIBK-water	NT	NT	Y	Y	Y	N
1-butanol-water	NT	NT	N	Y	Y	N

Legend:	Y	Uniform drop region exists
	N	No uniform drop region exists
	*	Very narrow uniform drop region
	NT	Not tested

It will be noticed that the calculated lines in Figures 2 and 4 lie mostly within the experimentally determined envelopes of uniform drops. However, for the 1-butanol/water system the method failed to calculate drop volumes for the

0.45-cm and the 0.41-cm nozzles, although reference to Table 1 reveals that uniform drops can be produced with these nozzles by discontinuous injection. The problem with 1-butanol/water seemed to arise because of its low interfacial tension (about 2.4 dyne/cm). Indeed, with MIBK/water (about 10 dyne/cm) the maximum nozzle size for which drop volumes could be calculated by the method was 0.45 cm. The benzene-water system presents no problem.

Injection through an array of nozzles.

Experimental

In the work already described, only one nozzle and one pump were in use at a time, and the resulting drop dispersion was sparse. In order to achieve the copious supply of drops needed for spray-column extraction studies, two modifications were made. The first was to increase the number of nozzles in use, and the second to arrange that each nozzle be fed by more than one pump.

The use of an array of nozzles, although clearly of great help must be limited ultimately by considerations of geometry, and probably more important, by the effect of interactions between several drops in various stages of formation. An array of six 0.32-cm I.D. nozzles equally spaced on a circle of 2.4 cm diameter was fitted into a Teflon plug which was installed at the bottom of the observation column

described earlier. Discontinuous injection was retained, but the arrangement used to feed the nozzles was modified to make fuller use of each.

It seemed advisable to make use of commercially available pumps. Of those available, Series 2 DCL 0-0.5 cm³ per stroke micro metering pumps seemed most suitable. The movement of the piston in these pumps is simple harmonic motion, a pumping mode which is shown to be satisfactory in the first part of the paper. Several pumps were used and all were driven by the same Graham variable speed drive.

Preliminary work with these pumps indicated that a discharge of 0.45 cm³ per stroke, equally provided to two 0.32 cm nozzles (that is 0.225 cm³ per nozzle) would give uniform drops. Equal sharing of the discharge between the two nozzles was achieved by using flow restrictors, one for each nozzle. These restrictors consisted of 2.5-cm lengths of 1.00-mm I.D. micro tubing. Thus, for one pump supplying one pair of nozzles, two drops are injected into the column per delivery stroke.

A nozzle fed by only one pump is unemployed during the suction stroke. By feeding a pair of nozzles from a manifold supplied by three pumps, each 120° out of phase with the others, and by eliminating a portion of the initial part of the discharge stroke, it proved possible for each pair of nozzles to inject six drops per pumping cycle. The

paired nozzles were located diametrically opposite in the circle.

Each of the other two pairs of nozzles was fed similarly by an additional bank of three pumps. By mechanically coupling the three banks 30° out of phase, it was possible to produce 18 drops per pumping cycle, the drops breaking away at equal time intervals from each pair of nozzles in succession.

Results

Shown in Figure 5 are envelopes for which uniform-sized drops are produced by multiple injection when benzene is being dispersed into water through the six nozzles. Plotted in this figure are both individual drop size and total volumetric flow for various rates of drop production. Observation revealed that drops were formed at each nozzle in succession, and there was no apparent interference between the drops at breakaway. Within the column a superficial dispersed-phase velocity of $45 \text{ ft}^3/\text{hr ft}^2$ or $0.38 \text{ cm}^3/\text{sec cm}^2$ was achieved. Larger pumps were not available. Therefore larger nozzles were not tested. However, it is reasonable to expect that considerably higher superficial velocities could have been achieved by using 0.41 and 0.45-cm nozzles.

Conclusions

Simple harmonic pump drive proved to be the most satis-

factory. It provided the greatest volume range of uniform-sized drops, and also was, the simplest to produce.

For systems of interfacial tension greater than about 10 dynes/cm, the Izard method⁸ based upon continuous injection can be used to estimate nozzle diameters suitable for producing uniform drops of a given size by discontinuous injection.

The use of multiple nozzles, combined with the elimination of dead time during the suction strokes of the displacement pumps, makes it feasible to produce a supply of uniform-sized drops sufficiently copious for use in the study of spray column operation.

Acknowledgements

The research for this paper was supported in part by the Defence Research Board of Canada, Grant No. 9530-44. The authors wish to thank also the National Research Council of Canada, and the President's Committee on Research of The University of British Columbia, both of which provided additional financial assistance, and to Susan Izard for her work on the calculations.

References

1. Keith, F. W.; Hixson, A. N. Ind.Engng Chem. 1955, 47, 258.
2. Johnson, H. F.; Bliss, H. Trans.Am.Inst.chem.Engrs 1946, 42, 331.
3. Hayworth, C. B.; Treybal, R. E. Ind.Engng Chem. 1950, 42, 1174.
4. Rocchini, R. J. M.A.Sc. Thesis, The University of British Columbia, 1961.
5. Izard, J. A. W.; Cavers, S. D.; Forsyth, J. S. Chem. Engng Sci. 1963, 18, 467.
6. Magarvey, R. H.; Taylor, B. W. Rev.Scient.Instrum. 1956, 27, 944.
7. Park, R. W.; Crosby, E. J. Chem.Engng Sci. 1965, 20, 39.
8. Izard, J. A. A.I.Ch.E. J1 1972, 18, 634.
9. Null, H. R.; Johnson, H. F. A.I.Ch.E. J1 1958, 4, 273.
10. Scheele, G. F.; Meister, B. J. A.I.Ch.E. J1 1968, 14, 9.
11. deChazal, L. E. M.; Ryan, J. T. A.I.Ch.E. J1 1971, 17, 1226.
12. Heertjes, P. M.; deNie, L. H.; deVries, H. J. Chem. Engng Sci. 1971, 26, 441.

List of diagrams
with captions

- Figure 1. Schematic layout of the apparatus.
- Figure 2. The effect of nozzle size when producing uniform drops ^{by} dispersing benzene into water and using a SHM cam pump drive.
- Figure 3. The effect of cam profile when producing uniform drops by dispersing benzene into water through a 0.32-cm nozzle.
- Figure 4. The effect of system for production of uniform drops when dispersing the organic phase through a 0.45-cm nozzle and using a SHM cam pump drive.
- Figure 5. The dispersion of benzene into water through six 0.32-cm nozzles by multiple injection.

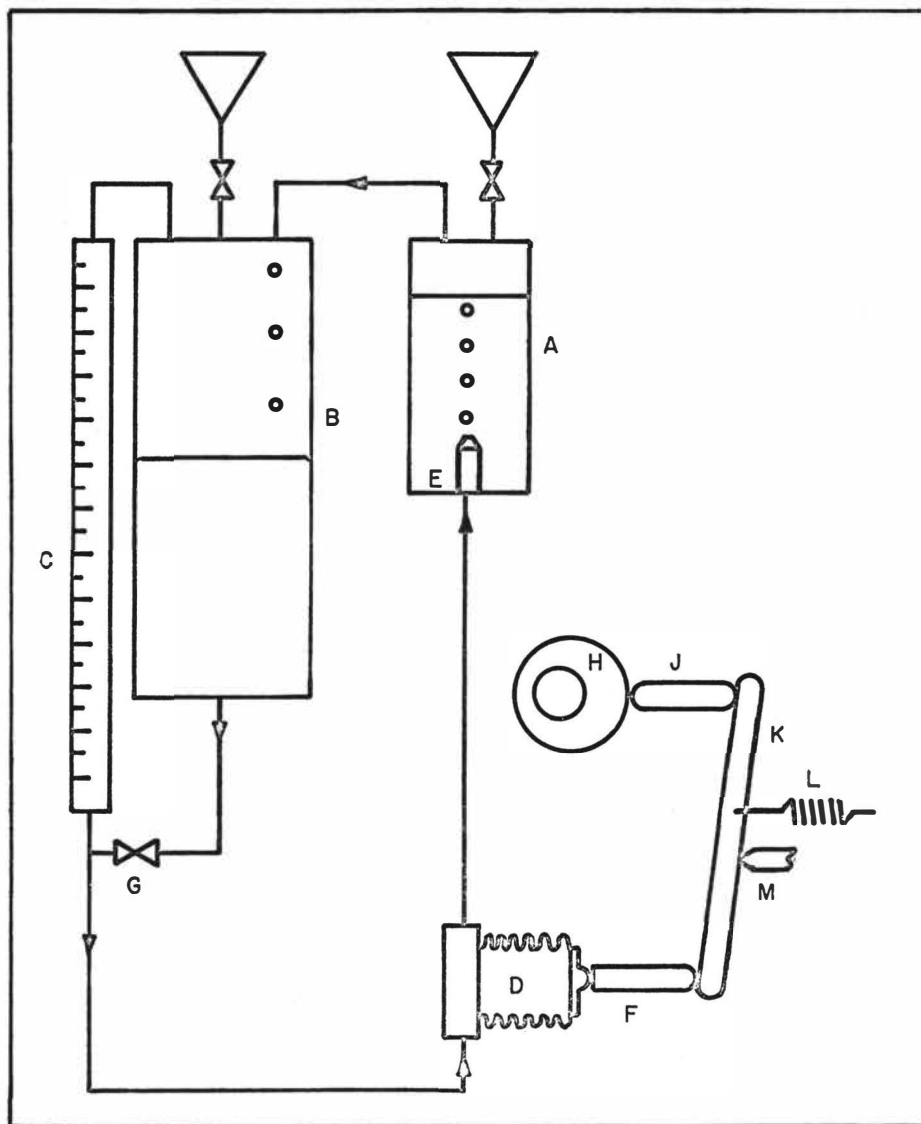


FIGURE I
SCHEMATIC LAYOUT OF THE APPARATUS

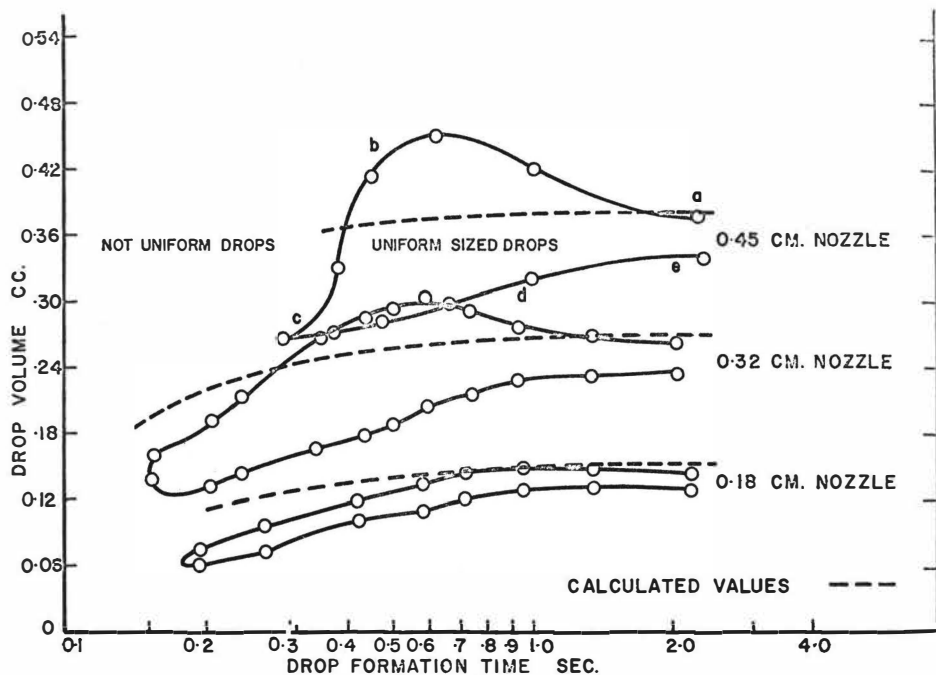


FIGURE 2
EFFECT OF NOZZLE SIZE
BENZENE-WATER CAM 3.

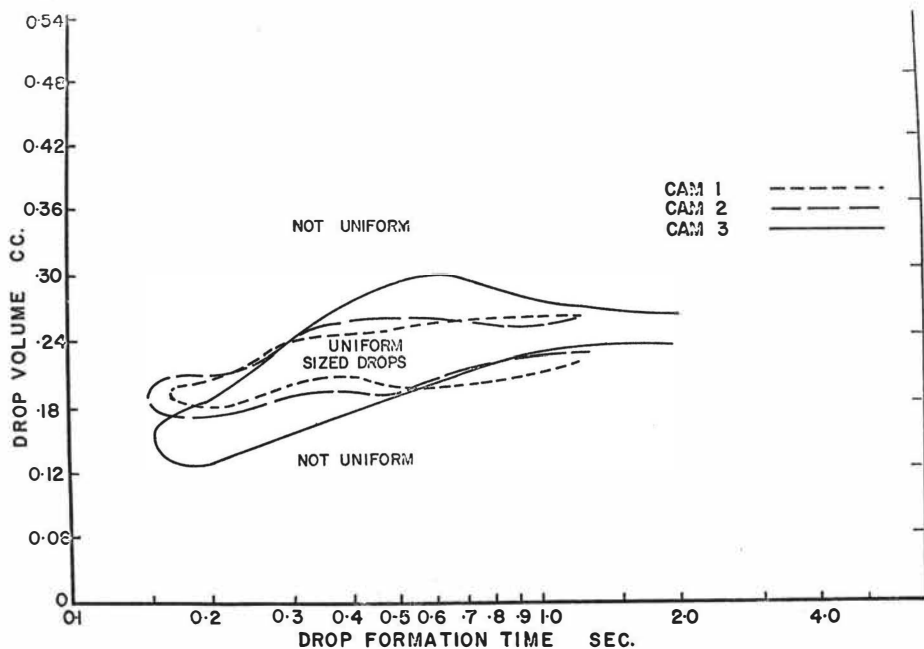


FIGURE 3
EFFECT OF CAM PROFILE — 0.32 CM. I.D. NOZZLE
BENZENE-WATER SYSTEM

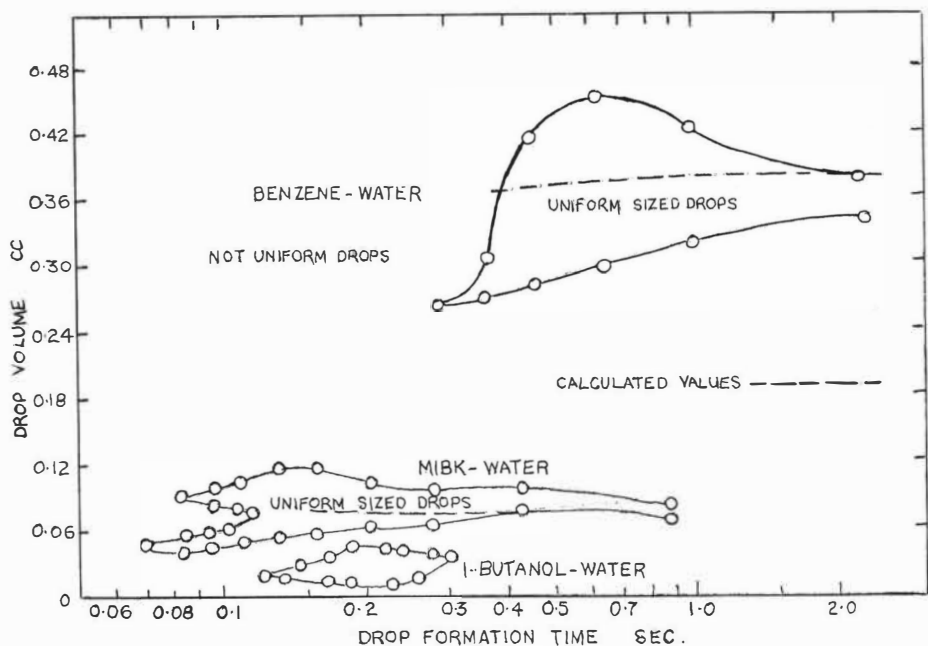


FIGURE 4
EFFECT OF SYSTEM
0.45 cm NOZZLE CAM 3

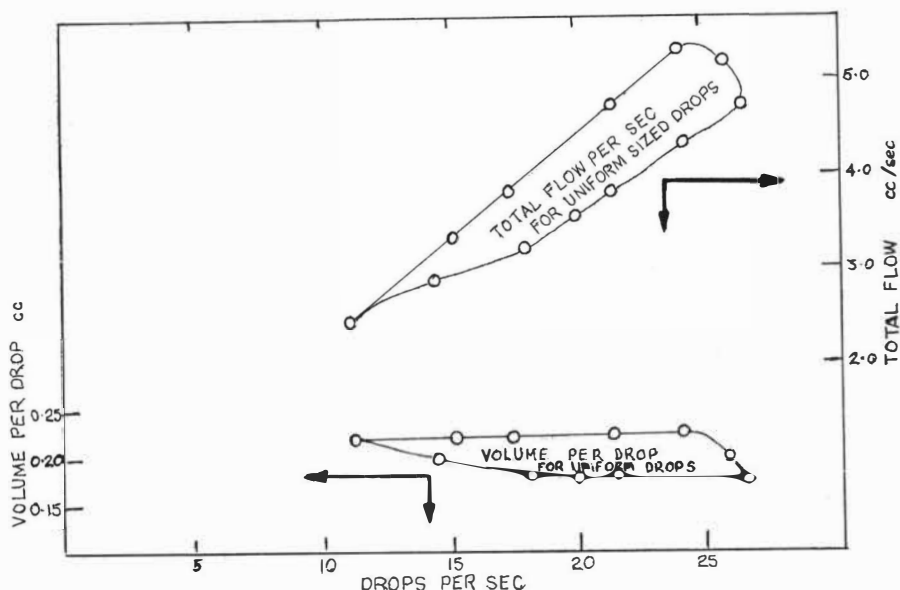


FIGURE 5
MULTIPLE INJECTION
BENZENE-WATER SYSTEM
6-0.32-cm NOZZLES

A SIMULATION STUDY OF WAKE BEHAVIOUR IN SPRAY COLUMNS

J.S. Forsyth; L.W. Fish; and S.D. Cavers

Department of Chemical Engineering, The University of British Columbia, Vancouver 8, B.C.

Concentration profiles of a solute in the continuous and in the dispersed phase of a liquid-liquid extraction spray column have been calculated using a simple simulation technique. These profiles are compared with profiles determined experimentally. Good agreement can be achieved. Although it is possible to determine by the simulation the value of the height of the column equivalent to a theoretical stage, it is not possible, within the precision of the present experimental data, to recognize a unique value of the ratio of wake volume to drop volume. The experimental data available are discussed with respect to their suitability for the present purposes.

INTRODUCTION

The authors have been concerned for sometime with the experimental measurement of backmixing in spray columns. They have become impressed by the difficulty of making unambiguous measurements and of making useful generalizations. They decided, as an activity parallel to their experimental work, to investigate the usefulness of numerical simulation as a guide to the possible sensitivity of response of column behaviour to a set of imposed operating parameters. The work now reported describes a simple simulation and the results given by it.

The process of simulation was chosen as being easy to construct by direct appeal to physical principles. Also it seemed that simulation might require little a priori knowledge of the mathematical formulation of the behaviour of the parameters involved. The intention was to vary parameters to find how sensitively the column behaviour depended on such changes, rather than to obtain definitive values of the parameters. By assessing such sensitivity, guidance applicable to the design of further experimental work might become available. Of course, any conclusions drawn are appropriate only to the extent that the model is appropriate.

MODEL

2.1. The apparatus to be modelled is described elsewhere^{1,2,3} and, for reference, is shown in Figure 1a in simplified form. Briefly, a solute is transferred from a downward-flowing continuous phase to rising drops of dispersed phase. These phases are introduced and removed at the extremities of the apparatus. A tracer substance, soluble in the continuous phase but insoluble in the dispersed phase, may be introduced at some intermediate level of the column. All tracer must leave in the outgoing continuous phase. The experimental results with which the results of the simulation will be compared also are described elsewhere^{4,5,6,7}.

2.2. Mass Transfer features

The model used for the simulation is very simple. It is assumed that the spray column can be represented by a number of "contact stages" (shown as squat rectangles in Figure 1b). Each contact stage accepts dispersed phase from the stage below and continuous phase from that above, and allows mass transfer of solute between phases. Such transfer is limited to a fraction of that possible in an equilibrium stage. The partly equilibrated phases are passed on to the appropriate adjacent stages.

This series of contact stages is terminated at the upper end by a "coalescence stage" (shown as an elongated rectangle in Figure 1b). In this stage, rising drops of dispersed phase recombine to become a single stream and then leave the apparatus. The experimentally observed fact^{2,8,9} that mass transfer does occur during coalescence is recognized in the model by representing the coalescence process by a contact stage with its own, less than equilibrium, performance.

2.3. Wakes

In addition to the mass transfer of solute between phases, which is the principal object of operating an extraction column, there also occurs transport of portions of continuous phase in the direction opposite to that of the main flow of that phase. This transport is brought about by the existence of wakes being trailed behind the rising drops¹⁰. Each wake is visualized as continually picking up and shedding liquid to the non-wake portion of the continuous phase. This process results in wakes of constant volume but of changing composition. The composition of each wake must be that of the non-wake continuous phase existing at a lower position in the column. Shedding of part of the wake constitutes backmixing of continuous phase from a lower to a higher position.

2.4. Main column wakes

The combined wakes at a given stage are shown as circles in Figure 1b. By way of example, take from circle $n-1$, one wake. It may be regarded as being associated with a drop which is at stage $n-1$. This wake is considered to discard a volume (v_t) into the continuous phase flowing from stage n to stage $n-1$. It then picks up an equal volume from the continuous phase flowing from stage $n-1$ to $n-2$. The combined wake (for all the drops passing through a stage) is fully mixed. (Wakes at the top, and those at the bottom of the column, are treated in special ways to be described presently).

Once all combined wakes have had their composition calculated they are all moved up one station. That is, the combined wake which has been numbered $n-1$ is now numbered n , and so on. This calculational procedure is the analogue of the physical upward movement of wakes as their associated drops rise through the continuous phase.

2.5. Terminal wakes

When the combined wake corresponding to the top stage (n_g) is moved upward all its volume is added to, and completely mixed with, the incoming continuous phase.

A drop entering stage 1 at the bottom of the column is newly created and has no wake. However, at stage 1 the drop is considered to collect a small wake (volume = v_t), the composition of which is $C_{c,1}$. None of this wake is cast off as the wake is moved upwards. When associated with stage 2, it picks up a second volume increment v_t , this time of composition $C_{c,2}$. This process of moving up, acquiring additional increments of volume at each stage, but never shedding volume, continues for some predetermined number of stages (n_i). Thus

$$v_W = n_i v_t$$

A somewhat similar mode of wake development is described by Letan and Kehat¹⁰. Once the predetermined number of initial stages has been passed, the wake becomes a "main column" wake, of volume constant at v_W , because accretion is exactly offset by shedding.

2.6. Numerical procedures

To obtain numerical results, the following procedure was used. All compositions were initialized to reasonable values, the superficial velocities were inserted, and calculation was begun. For each stage material balances were solved with due regard for the conservation of material, solute equilibrium between phases, and the efficiency of the stage. The appropriate adjustment of wake concentration was made. The resulting compositions were used by direct substitution in the next iteration. No special procedures were used to accelerate convergence. No simulation results have been used which have

material balances poorer than 0.02%.

2.7. Selection of parameters

Consider Table 1. The parameters in the upper part of the table are fixed for a given data set. However, the following are available for manipulation:

n_s , n_i , P , E_s , and E_a . These somehow must be chosen so that the behaviour of the experimental column with respect to both solute and tracer concentration is reflected faithfully in the numerical solution. The selection of the five parameters is done in three steps. The first consists simply of setting a value of n_s , the number of contact stages; the second is to select the parameters n_i and P , which describe the wake associated with one drop; the third is to choose E_s and E_a , the stage efficiencies.

The first step, the selection of n_s , is easy. In principle any value of n_s can be used to reproduce the experimentally-observed rates of tracer decay. As will be seen later, when Figures 2 and 3 are inspected, $n_s = 22$ and $n_s = 45$ give almost identical results, although it might have been expected that $n_s = 45$ would have reduced effects associated with the stagewise representation of a differential process. From the point of view of computer costs $n_s = 22$ is desirable.

The rate of decay (D) on a distance basis can be related to the rate of decay (D_s) on a stage basis by

$$D_s = D \frac{h_o}{n_s} \quad (2)$$

The second step, the specification of the wake parameters to reproduce the observed rate of decay of tracer, is done by determining, in effect, the size of the wake associated with each drop (v_w), and the volume from that wake (v_t) which will be case off, and replaced by other continuous phase, over a given height of the column: for present purposes, the height of one stage.

In the actual simulation it is n_i and P that are set. That this is equivalent to specifying v_W and v_t can be seen by considering Equation 1, and the equations listed below. First, the ratio of v_t to the volume of the drop (v_D) is defined to be P .

$$P = \frac{v_t}{v_D} \quad (3)$$

Substitution into Equation 1 gives

$$v_W = n_i P v_D \quad (4)$$

In the simulation, then, v_W and v_t are specified by setting n_i and P . The values used must, of course, result in D_s given by the simulation agreeing with the value from Equation 2.

Although v_D appears in Equation 4, its absolute value is of no importance in the simulation. To see this, let Q be the number of drops passing through unit area of a horizontal cross section, per unit time. Because

$$Q v_D = L_d \quad (5)$$

and

$$Q v_W = L_W \quad (6)$$

where L_W is the superficial velocity of the flow of continuous phase as wakes toward the top of the column, then, from Equation 4,

$$L_W = L_d P n_i \quad (7)$$

Note that L_d is available at a known experimental value (Table 1) independent of whether or not the actual drop volume (v_D) is available. It was convenient, then, to work with the superficial velocities L_d and L_W in the simulation instead of basing the calculations directly on v_D and v_W . Similarly when multiplied by Q , Equation 1 becomes

$$L_t = \frac{L_W}{n_i} \quad (8)$$

where L_t , although a radial flow, is based on the cross section of the column perpendicular to the axis. The combined wakes of figure 1 are given correspondingly by Qv_w . Also, v_t for a single drop becomes L_t for the combined wakes on the diagram. (Notice that L_c (based on the rate of entry of the continuous phase into the column) plus L_w gives the superficial velocity of descending continuous phase at any stage above n_i (L_{des})).

Once D_g has been reproduced, n_i and P have been determined for the transport of tracer. However, the wakes carry all components of the continuous phase. Therefore n_i and P apply also to the transport up the column of solute in wakes.

The third step in the selection of the parameters relates to the transfer of solute between phases. In the simulation this occurs continuously between the drop and the continuous phase in contact with it because the phases are not in equilibrium. The present simple simulation does not address itself to the niceties of the model of Letan and Kehat¹⁰ as to the particular route by which the transferring solute goes between a drop and the continuous phase. Instead, the simulation represents the mass transfer process as taking place in stages of efficiency E_g . The third step consists of selecting the value of this efficiency, and of the efficiency of the coalescence stage, and adjusting these values, until acceptable agreement is obtained between calculated and experimental solute concentration profiles. Since all the parameters except these two efficiencies have been fixed already, and since the efficiencies must lie between 0.0 and 1.0 only a fairly simple 2-dimensional search is required.

When tracer concentrations are obtained by sampling, the result is a volumetric average concentration¹, which is an average of the wake and the non-wake (descending) continuous phase concentrations, weighted according to the volume of each present in a thin slice of column. The same weighting procedure is used in the simulation program to provide average tracer concentrations ($C_{c,av}$) for comparison with measured tracer decay lines. In present notation,

$$C_{c,av} = \left(\frac{1}{1-H} \right) (C_w H n_i P + C_{des} (1 - H - H n_i P)) \quad (9)$$

Now, whereas tracer concentration in a wake arises only as a result of transport of tracer from lower down the column (back mixing), solute concentration in a wake results from a combination of backmixing and solute transfer between phases. Nevertheless, in the simulation model, where solute transfer is taken into account via E_s , the solute concentration in wakes still is considered to arise only from backmixing. It is assumed that experimentally measured concentrations are volumetric averages in this case also, and Equation 10 is used again. With solute transfer from continuous to dispersed phase, and if it is accepted for the purposes of argument that the mechanism of Letan and Kehat¹⁰ does describe experiment, then the solute concentration in wakes is higher in the simulation than it would be in an experiment, but the solute concentration in the non-wake continuous phase is lower. Thus the two effects tend to offset one another. The results which follow seem to indicate that Equation 10 is adequate for comparing simulated and measured concentration profiles.

As a more detailed example of the procedures used in selecting the parameters, consider Data Set 1 of Table 1 ($n_s = 22$). Experimentation³ shows that the concentration of tracer falls off exponentially above the point of injection in conformity with the diffusion model. In Data Set 1, D is -5.83 ; thus D_s is -0.593 . With n_i set at 1 (Run 1), P had to be 0.309.

For the particular values $n_s = 22$, $n_i = 1$, and $P = 0.309$ applied to Data Set 1, the choice of $E_s = 0.25$ and $E_a = 0.3$ gives good agreement between calculation and experiment, as will be seen in Figure 2. Figure 2 was chosen from a number of graphs produced during the search for suitable values of E_s and E_a . The choice was, as always, subjective. With n_s still at 22, putting $n_i = 2$ requires a new computation of P and a new search for E_s and E_a . (See Run 2).

If instead of $n_s = 22$ one selects a value of 45, corresponding values of n_i , P , E_s and E_a can be determined. See Table 1, Runs 3, 4 and 5. (The existence of more than one run which reproduces the experimental results for a data set will be considered later).

Parameter values are shown in Table 1 for a second data set also.

RESULTS

3.1. Experimental data used for purposes of comparison

All the comparisons made in this work are between values calculated from the model, and experimental results obtained by Gavers and co-workers^{4,5,6,7}.

All these results are for the system 4-methyl-2-pentanone (MIBK/acetic acid/water. Because of the small concentrations of solute involved, and because the continuous and dispersed phases entered mutually saturated, it is assumed that no volume change of either phase occurs in the apparatus. The required equilibrium relationship was taken to be¹¹

$$\frac{C_d^*}{C_c} = 0.4487 + 0.1162 C_c - 0.01861 C_c^2 + 0.001987 C_c^3 \quad (10)$$

Sodium chloride was used as tracer in the experimental work, but at concentrations such that the use of the above expression (for salt-free solutions) was appropriate.

In attempting to compare calculated with experimental results difficulties immediately arise. Although a considerable number of solute and of tracer concentration profiles exist, these were determined by different workers at different times, in apparatus which was from time to time dismantled and reassembled in different configurations (particularly with respect to height and locations of sample points). Few real replicates are available, and those which do exist show solute profiles differing by more than do the best calculated profiles from the mean of the experimental determinations. In the case of tracer decay profiles, it was the slopes of the lines of $\ln C_{tr}$ versus h which was of principal interest to the workers involved^{3,5,7}. These slopes agree only fairly well between replicates. However, the slopes do form a consistent pattern when considered as a function of L_c and L_d , a fact which enabled them to be used for the purpose for which the experiments were done. Nevertheless, the individual lines are found to be displaced up or down, a matter of little moment to measuring axial mixing coefficients, but of importance in the present work. This point will be discussed later.

Finally, like all experimental runs, those used here for comparison had errors in material balances, whereas the simulation is arranged to provide almost perfect material balances. In short, it is difficult to obtain experimentally and therefore to find in the literature, trustworthy experimental data with which meaningful comparisons can be made of data computed from the model. Nevertheless, the results now reported do give very clear indications as to what well-authenticated experimental data should be sought.

3.2. Validity of comparisons

To assist comparison, all data presented graphically have been normalized with respect to the concentration of solute in the entering continuous phase ($C_{c,in}$ for the appropriate data set). Heights are normalized also, by dividing by h_o . Thus the entering continuous phase is located on Figures 2, 3, 4, 5 and 6 at (1.0, 1.0) without further identification. The value of $C_{c,in}$ (also $C_{d,in}$) is assumed to be accurate. Errors in experimental material balances thus must appear in the output streams.

3.3. Data Set 1

Data Set 1 is the average of the experimental data of two tests which agreed quite closely. Thus, at least with respect to solute concentrations, the points used probably are fairly reliable. However, the value of the tracer decay rate used was determined in a quite separate experiment, and some mismatch between solute profiles and tracer profile is possible. Simulation runs 1 and 3, both using $n_i = 1$, but having 22 and 45 stages respectively, give excellent agreement between calculated and experimental results. (See Figures 2 and 3).

Consideration of Data Set 1 shows that v_w/v_D is very sensitive to n_i . For example, values vary by a factor of ten between Run 3 and Run 5. (Run 5 is shown in Figure 4). Notwithstanding the factor of ten, Figures 3 and 4 are not very different. It would appear that for the numbers of stages used, the best runs are 1 and 3, although Run 4 is almost as good as 3. Runs 2 and 5 are noticeably poorer.

3.4. Data Set 2

Data Set 2 uses the experimental results from a single test. In this case no determination of tracer decay was available for the superficial velocities used in the experiments. The required decay rate was determined by extrapolation and cross-plotting. Figure 5 shows the results for Run 7. Agreement between experimental and simulated results is good.

3.5. Other data sets

The results for two other sets of data are shown in Figures 6a and b. For one reason or another the experimental data used were regarded as less trustworthy than those used for Figures 2 through 5, and, accordingly, Figure 6 does not show much detail. The agreement between simulated and experimental results, although poorer than for Data Sets 1 and 2 in one or more respects is still fairly good.

DISCUSSION

Table 1 shows that several simulation runs, all reproducing the tracer decay rate, and all giving reasonable agreement with experimental solute concentration data, may show substantial differences in the values of the parameters used. It might be expected that E_a would be constant for any data set, although between sets, and therefore referring to different phase flows, it might change. This expectation broadly is fulfilled. Results obtained during the search for best values showed that E_a does not influence column performance strongly. It might be expected also that, for any one data set, the values of E_s would vary in such a way that the height equivalent to one theoretical stage would remain constant. Again broadly this is so. However, when n_1 is changed, the height equivalent to a perfect stage also changes somewhat. This may arise from representing a differential contacting operation by stages.

Much greater variations occur in the value of v_W/v_D . Only one value of v_W/v_D can be correct for one data set; yet values differing by an order of magnitude are reported. Nevertheless, within each data set all give almost equally good reproduction of experimental results. It is apparent that some additional restraint applies that has not been imposed in the simulation. Some indication as to the nature of this restraint is revealed by consideration of the rate of decay of concentration of tracer.

Figure 7 is a graph of the logarithm of tracer concentration versus height above the nozzle tips, as might be given by a typical simulation. The graph has been orientated to make "upwards" in the graph correspond to upwards in the column. The line FEGB is drawn with ordinate equal to the height of the plane of injection of tracer. The line EM is for concentration in wakes (C_W). A tracer balance around the top of the column gives

$$\frac{C_{des}}{C_W} = \frac{L_W}{L_{des}} = \frac{L_W}{L_W + L_c} \quad (11)$$

which is less than unity and is constant. Hence on Figure 7 the line EO, representing C_{des} , is parallel to EM. Substituting Equations 7 and 11 into Equation 10 gives

$$\frac{C_{c,av}}{C_W} = \left(\frac{1}{1-H} \right) \left(H \frac{L_W}{L_d} + \left(\frac{L_W}{L_W + L_c} \right) (1-H - H \frac{L_W}{L_d}) \right) \quad (12)$$

which also is constant and less than unity, so that line G₁ representing $C_{c,av}$ is parallel to EM and EO. GN lies between EM and EO. The line AB represents the constant tracer concentration in the continuous phase below the point of injection. Notice that experimentally measured tracer concentrations should exhibit a discontinuity at the plane of FEGB. In principle, therefore, it should be possible to determine L_W/L_d , i.e. v_W/v_D , by selecting, from a family of lines given by various values of P, that line which most nearly coincides with one determined experimentally.

Unfortunately the real situation does not permit of such action. The experimental determination of tracer decay was made in order to evaluate axial mixing coefficients³, and only the slope of the plot of $\ln C_{tr}$ versus h was of importance at that time. As has been said earlier, these slopes are fairly consistent from run to run. If a figure like Figure 7 were drawn using experimental tracer decay lines, it would be found that these usually would intersect a line corresponding to FB to the left of B, but on occasion the best fit to the points would result in an intersection to the right (an impossible physical situation). Although scatter is considerable, the concentration at G is on average close to that at B. Hence, from Equation 12, the data would seem to favour the existence of a large v_w/v_D ratio. These arguments are complicated by the uncertainty of the location of line FB. Although the height at which tracer is injected is, of course, known, the tracer may not instantaneously disperse uniformly across the column in a radial direction. Thus doubt exists as to the proper zero point from which tracer can be considered to decay exponentially.

If further experimental work is undertaken in the hope of evaluating v_w/v_D from tracer decay data, attention should be given to at least two points. First, considerable replication of experiments should be undertaken so that statistical analysis can be applied to locate the concentration corresponding to point G. Second, the possibility should be examined of achieving radially uniform tracer concentration over the plane of injection.

ACKNOWLEDGEMENTS

Financial support from the National Research Council, and from the Dean's Committee on Research, Faculty of Graduate Studies, The University of British Columbia, is gratefully acknowledged.

References

1. Henton, J.E.; Hawrelak, R.A.; Forsyth, J.S.; Cavers, S.D. Proc. Int. Solvent Extraction Conference 1971, II, 1302.
2. Cavers, S.D.; Ewanchyna, J.E. *Can. J. chem. Engng* 1957, 35, 113.
3. Henton, J.E.; Cavers, S.D. *Ind. Engng Chem. Fundamentals* 1970, 9, 384.
4. Choudhury, P.R. M.A.Sc. Thesis, The University of British Columbia, 1959.
5. Henton, J.E. Ph.D. Thesis, The University of British Columbia, 1967.
6. Bergeron, G. M.A.Sc. Thesis, The University of British Columbia, 1963.
7. Lim, C.J. M.A.Sc. Thesis, The University of British Columbia, 1971.
8. Geankoplis, C.J.; Hixson, A.N. *Ind. Engng Chem. Fundamentals* 1950, 42, 1141.
9. Choudhury, P.R.; Ambrose, P.T.; McNab, G.S.; Fish, L.W.; Cavers, S.D. submitted to Proc. Int. Solvent Extraction Conference 1974, Paper 119.
10. Letan, R.; Kehat, E. *A.I.Ch.E. J* 1968, 14, 398.
11. Fish, L.W.; Errico, J.E.; Lim, C.J.; Cavers, S.D. submitted for publication.

Nomenclature

C_c	concentration in continuous phase (normalized, or kgmole/m^3)
C_d	concentration in dispersed phase (normalized, or kgmole/m^3)
C_{des}	concentration of the non-wake (descending) continuous phase (normalized, or kgmole/m^3)
C_{tr}	concentration of tracer (p.p.m., or kgmole/m^3)
C_W	concentration in wakes (p.p.m., or kgmole/m^3)
D	rate of decay of tracer per unit of height = $d \ln C_{tr}/dh$ (1/m)
D_s	rate of decay of tracer per stage; see Equation 2
E_a	efficiency of the coalescence stage: concerned with agitation of drops prior to coalescence into the interface at the top of the column
E_s	efficiency of a contact stage within the column
h	vertical distance above nozzle tips (m)
h_o	total vertical height of column (nozzle tips to coalescence interface) (m)
h_s	height of a contact stage (m)
H	holdup: volume fraction of column occupied by dispersed phase
L_c	continuous phase superficial velocity based on the feed stream to the column ($\text{m}^3/\text{s m}^2$)
L_d	dispersed phase superficial velocity ($\text{m}^3/\text{s m}^2$)
L_{des}	superficial velocity of non-wake (descending) continuous phase ($\text{m}^3/\text{s m}^2$)
L_t	superficial velocity of transfer of wake material into or out of the non-wake continuous phase, based on the cross section of the column perpendicular to the axis ($\text{m}^3/\text{s m}^2$)
L_W	superficial velocity of transport of continuous phase in drop wakes ($\text{m}^3/\text{s m}^2$)
n	the number of an individual contact stage
n_i	number of contact stages through which wake is forming
n_s	the number of the highest stage, excluding the coalescence stage. Therefore there are n_s stages in the column proper.
P	volume of wake transferred to or from wake per stage per unit drop volume (m^3)

v_D	volume of a single drop (m^3)
v_t	volume of wake per drop transferred per stage into or out of the non-wake continuous phase (m^3)
v_W	volume of wake associated with a single drop (m^3)

Subscripts not included above

av	volumetric average
in	inlet of phase
1,2,etc.	(from) stage 1,2,etc.

Superscript

*	equilibrium value
---	-------------------

Table 1. Data sets used for comparison, and parameters from the simulation model

Exp'tl variables	Data Set 1					Data Set 2	
L_c	0.00154					0.00464	
L_d	0.00617					0.00616	
h_o	2.24					2.25	
D	-5.83					-16.7	
E	0.0747					0.0797	
$C_{c,in}$	0.808					0.807	
$C_{d,in}$	0.1046					0.1081	
Simulation & derived parameters							
n_s	22		45			22	45
h_s	0.1017		0.0497			0.1023	0.0500
D_s	-0.593		-0.290			-1.72	-0.836
Run	1	2	3	4	5	6	7
n_i	1	2	1	2	3	1	1
P	0.308	0.0148	0.746	0.123	0.0266	0.167	0.578
E_s	0.25	0.30	0.10	0.13	0.15	0.35	0.175
E_a	0.3	0.4	0.4	0.4	0.4	0.1	0.1
v_w/v_D	0.308	0.0296	0.746	0.246	0.0798	0.167	0.578

Notes:

Data Set 1. Solute concentrations are averages of those from Runs 67 and 68 of Reference 4.

Tracer decay rate is from Run 57 of Reference 5.

Data Set 2. Solute concentrations are from Run 8 of Reference 6. Tracer decay rate was obtained graphically from data of Reference 5.

In all data sets column diameter = 38 mm, and drop size³ = 3.4 mm.

Captions for figures

A Simulation Study of Wake Behaviour in Spray Columns

J.S. Forsyth; L.W. Fish; and S.D. Cavers

Figure 1. Schematics.

- a. Experimental column.
- b. Simulation model.

Figure 2. Comparison of solute concentration profiles for Run 1.

(Circles are experimental; lines are calculated. Ordinate of horizontal arrow = calculated dispersed phase concentration leaving column.)

Figure 3. Comparison of solute concentration profiles for Run 3.

(Circles are experimental; lines are calculated. Ordinate of horizontal arrow = calculated dispersed phase concentration leaving column.)

Figure 4. Comparison of solute concentration profiles for Run 5.

(Circles are experimental; lines are calculated. Ordinate of horizontal arrow = calculated dispersed phase concentration leaving column.)

Figure 5. Comparison of solute concentration profiles for Run 7.

(Circles are experimental; lines are calculated. Ordinate of horizontal arrow = calculated dispersed phase concentration leaving column.)

Figure 6. Comparison of solute concentration profiles for data sets other than 1 and 2.

Figure 7. Tracer decay lines for various streams.

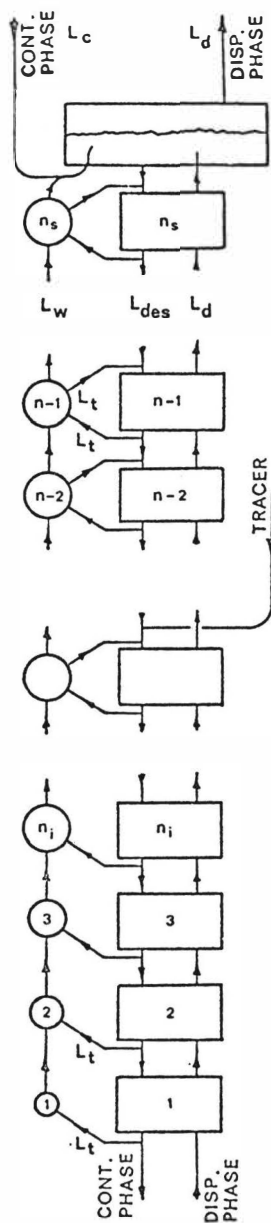
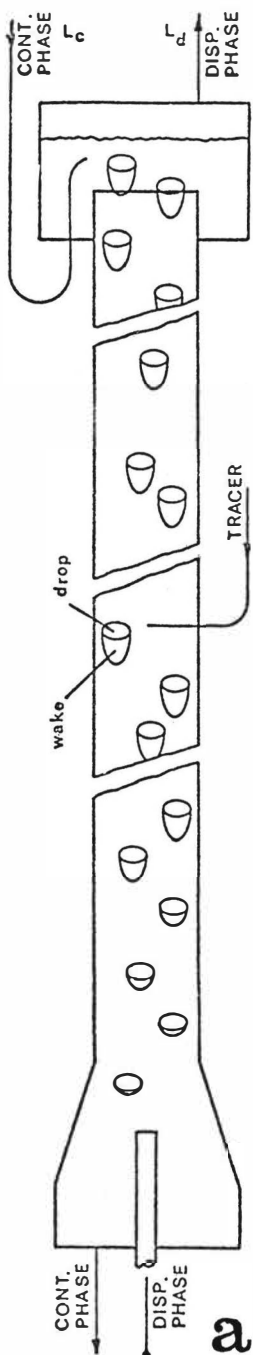


Figure 1. Schematics.

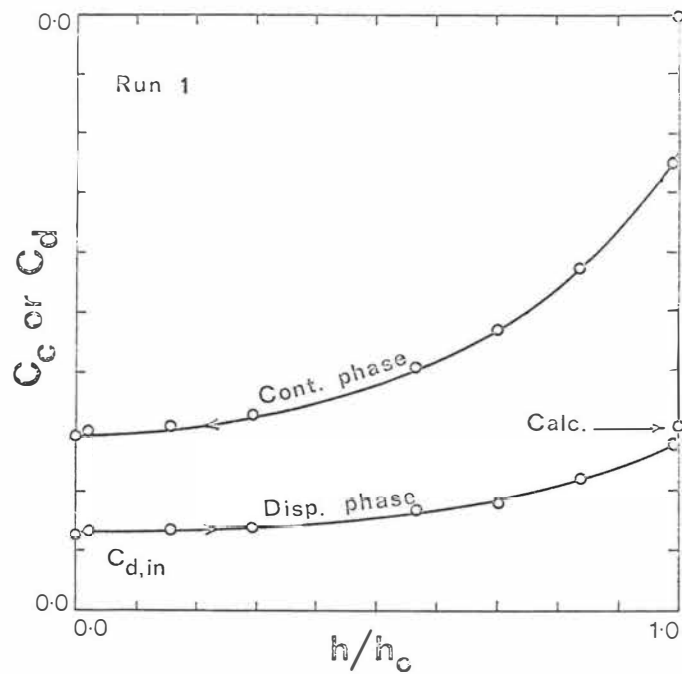


Figure 2. Comparison of solute concentration profiles for Run 1. (Circles are experimental; lines are calculated. Ordinate of horizontal arrow = calculated dispersed phase concentration leaving

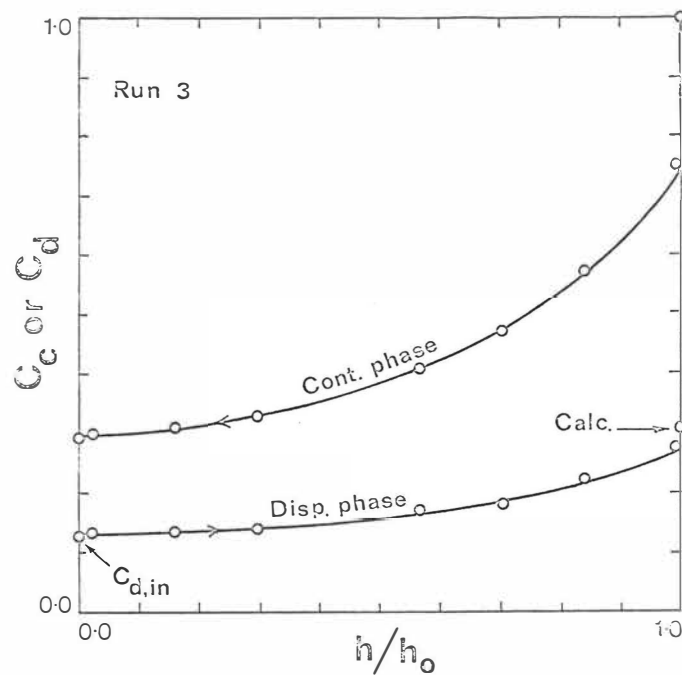


Figure 3. Comparison of solute concentration profiles for Run 3. (Circles are experimental; lines are calculated. Ordinate of horizontal arrow = calculated dispersed phase concentration leaving column.)

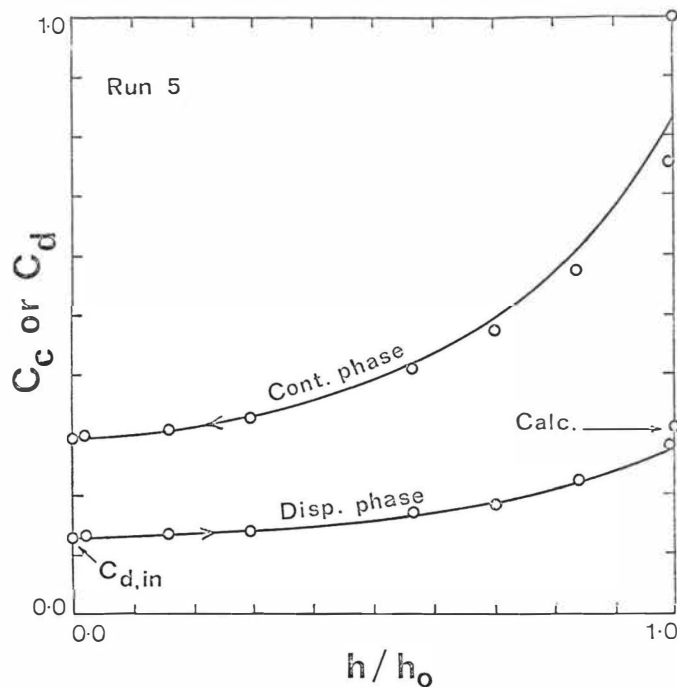


Figure 4. Comparison of solute concentration profiles for Run 5. (Circles are experimental; lines are calculated. Ordinate of horizontal arrow = calculated dispersed phase concentration leaving column.)

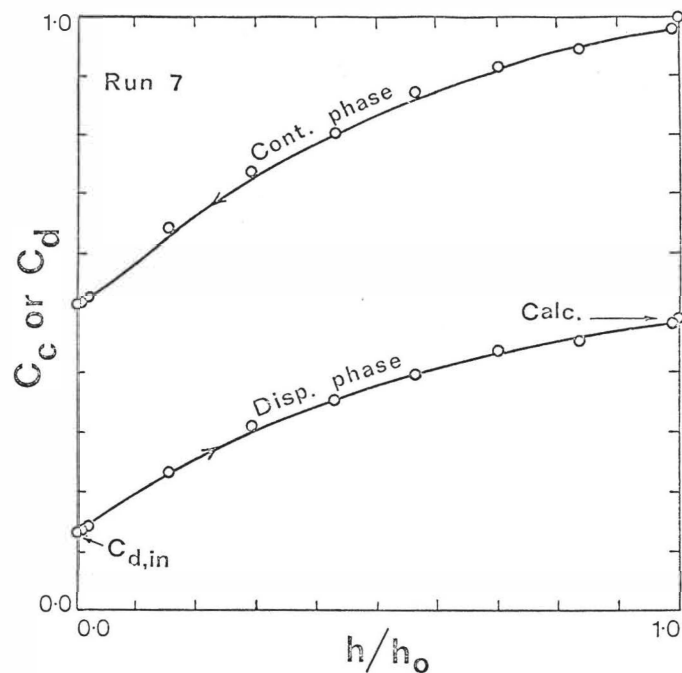


Figure 5. Comparison of solute concentration profiles for Run 7. (Circles are experimental; lines are calculated. Ordinate of horizontal arrow = calculated dispersed phase concentration leaving column.)

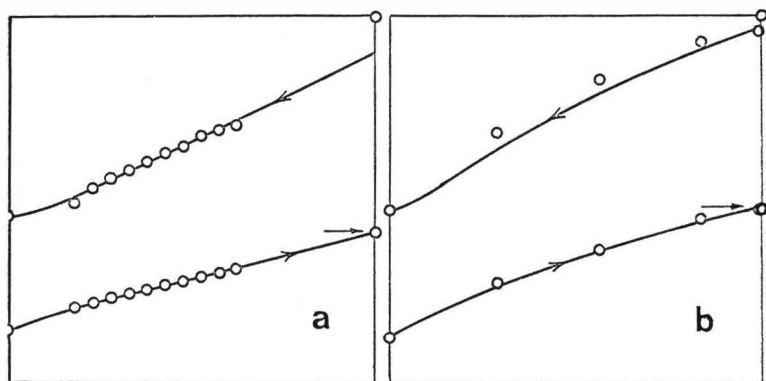
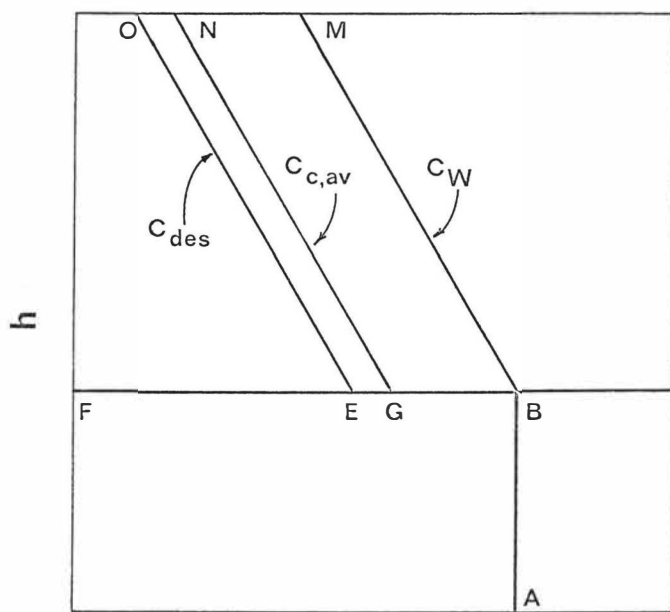


Figure 6. Comparison of solute concentration profiles for data sets other than 1 and 2.



$\ln C_{tr}$
 Figure 7. Tracer decay lines for various streams.

SESSION 4

Monday 9th September: 14.00 hrs.

C H E M I S T R Y O F E X T R A C T I O N

(Nuclear)

Chairman:

Mr. A. Chesne

Secretaries:

Dr. D.F.C. Morris

Mr. A. Bathellier

R. Guillaumont, M. Genet and M. Galin

Laboratoire de Radiochimie, I.P.N., Université de Paris XI,
B.P. No. 1, 91406 Orsay, France.Abstract

The solvent extraction of Np(V) from NaOH solutions into *tert*-butyl acetate-*tert*-butyl alcohol (S) organic phases by chelate formation with dibenzoylmethane (HA) has been investigated. Variation of D_{Np} with pH and with the chelating reagent or alcohol concentration indicates that the species extracted are NpO_2A_3HA and $NpO_2A_2HA.S$ near pH 14, and $NpO_2A.nS$ ($n = 0, 1, 2$ and 3) between pH 12 and 13.

Introduction

Symbols: C, stoichiometric concentration; [X], concentration of species X. \bar{A} (e.g. \bar{C}) denotes the organic phase.

Solvent extraction of ions from basic aqueous solutions by chelate formation has not received much attention. This is partly due to complications such as (i) an increasing concentration of the chelating reagent or chelates in the aqueous phase with rising pH, (ii) coextraction of the alkali cation, and (iii) hydrolysis of aqueous metallic ions resulting in formation of inextractable radio-colloids and/or adsorption on surfaces at tracer concentrations, and in formation of polymeric species at higher concentrations.

As Np(V) is easily obtained in basic media and the solutions (10^{-3} to $10^{-10} M$) are quite stable both towards ageing (because hydrolysis of NpO_2^+ starts at pH ~ 9 - 10 ⁽¹⁾ and NpO_2OH is amphoteric) and towards redox processes, we have investigated the partition of $10^{-10} M$ $^{239}Np(V)$ in the system: 0-1M NaOH (aq)/*tert*-butyl acetate, *tert*-butyl alcohol (S), dibenzoylmethane (HA). Such a system was selected on the basis of previous studies by Zolotov et al.,^(2,3) Novikov et al.⁽⁴⁾ and Espinosa et al.,⁽⁵⁾ which show *inter alia* that halogen derivatives of hydrocarbons fail to extract Np(V) by chelate formation from basic solutions. The organic phase must contain both chelating and oxygen donor reagents, such as alcohols, ketones, esters or ethers.

Experimental

All reagents were "Fluka" products. The alcohol content may be increased up to 6-7M without significant change in the volumes of the aqueous and organic phases.

Alkaline $^{239}Np(V)$ solutions were obtained by dilution of a drop of Np(V) stock solution in 0.5M $HClO_4$ with 50 cm³ of the appropriate NaOH solution containing only about 0.05M CO_3^{2-} , which is too low to yield carbonate complexes of Np(V).⁽⁵⁾ The stock solution was prepared once a week by separating 0.5M $HClO_4$ which was in contact with 500 mg cation resin (Dowex 50, 400 mesh) loaded with 300 μg of ^{243}Am .⁽⁵⁾ The oxidation state of the neptunium in basic media was checked by electrophoresis on glass paper;⁽⁵⁾ no reduction occurred.

In all cases, partition equilibrium for Np(V) or Na at 25°C was reached after one hour's shaking of 5 cm³ of each of the phases in a stoppered glass tube. D_{Na} was determined by γ -radiometry using ^{24}Na . No absorption on glass was detected.

The variation of D_{HA} with the alcohol content of the organic phase was determined by a spectrophotometric method. Beer's law was checked up to $8 \cdot 10^{-5} M$. The enol form of HA shows a broad absorption at 350 nm with ϵ decreasing slowly from 26,000 to 22,000 l/mole.cm as C_S increases up to 6M (in C_6H_{12} , $\epsilon_{337} = 24,700$ l/mole.cm). In the spectrum of the aqueous phase, two bands appear around 245-250 (ketone) and 350 nm (enol). D_{HA} values were calculated from the $[HA]$ values combined with a calculation of $[HA]$ at the observed pH, based on $pK_a = 9.35$.⁽⁶⁾ Interpolated values from many determinations are given in table 1.

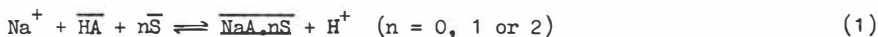
Table 1

\bar{C}_S	0.5	1.5	2.5	3	4	5	6
$\log D_{HA}$	4.4	4.5	4.6	4.65	4.85	5.2	5.8

Results and Discussion

Saponification. *Tert*-butyl acetate was selected as diluent because its saponification is a relatively slow reaction. After one hour of equilibration heterogeneous saponification causes the consumption of 15 to 30% of the initial 1, 0.1 or 0.01M hydroxide ion whatever the value of \bar{C}_S . Equivalent quantities of *tert*-butyl acetate ions appear in the aqueous phase, but are non-complexing, and the content of *tert*-butyl alcohol slowly increases with time. Data without any alcohol in the organic phase cannot be obtained at high pH. HA has no influence on the saponification.

Sodium extraction. The sodium extraction results are given in Figs. 1 and 2. $[HA]$ was calculated from formula I in the appendix, which assumes that NaA is the extracted chelate, and $[S]$ was equated with \bar{C}_S , which is valid for sufficiently low sodium extraction. It will be seen that as much as 10% of the sodium is sometimes extracted. The graphs on the left-hand side of Fig. 1 are all straight lines of slope unity, indicating that one HA molecule reacts with each Na^+ ion during the extraction, as assumed in formula I. The graphs to the right show $\partial \log D_{Na} / \partial \log [S]$ increasing from zero to 2, indicating the attachment of 0, 1 or 2 molecules of S to the chelate. The reaction involved is thus



so that

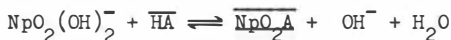
$$D_{Na} = [HA](K_e + K_1[S] + K_2[S]^2)/[H^+] \quad (2)$$

where K_e , K_1 and K_2 are the formation constants of $NaA.n\bar{S}$ for $n = 0, 1$ and 2 respectively. The best fit with the experimental data is obtained with $\log K_e = -13.8$, $\log K_1 = -13.3$ and $\log K_2 = -13.4$. These results are consistent with those obtained by Healy in the synergic extraction of alkali metal ion by thenoyltrifluoroacetone.⁽⁷⁾

Neptunium extraction. The neptunium extraction results are given in Figs. 3 and 4. $[HA]$ was again calculated from formula I in the appendix, while $[S]$ was obtained from formula II when \bar{C}_{Na} was high. At the two lower pH's, $\partial \log D_{NP} / \partial \log [HA] = 1$ at sufficiently low $[HA]$, while $\partial \log D_{NP} / \partial \log [S]$ increases from zero to 3, indicating formation of $NpO_2A.n\bar{S}$ ($n = 0, 1, 2$ or 3). These should possibly be formulated $[NpO_2(H_2O)_{3-n}n\bar{S}]A$; the hydration would help to explain why the chelates are not extracted when halogenated hydrocarbons are used as diluents. At pH 13.90, $\partial \log D_{NP} / \partial \log [HA] = 3.5$ at $[S] = 0.15-0.3M$, suggesting a mixture of, say, $NpO_2A.2HA.S$ and $NpO_2A.3HA$; at $[S] = 7M$, the slope

is smaller, probably because S replaces HA to give, say, $\text{NpO}_2\text{A} \cdot \text{HA} \cdot 2\text{S}$.

When $[\overline{\text{HA}}] \leq 0.001\text{M}$, $\partial \log D_{\text{Np}} / \partial \text{pH} = -1$ at pH 12-13. This indicates $\text{NpO}_2(\text{OH})_2^-$ as the predominant neptunium species in the aqueous phase, reacting according to



after which $\text{NpO}_2\text{A} \cdot n\text{S}$ can be formed when alcohol is present. At higher $[\overline{\text{HA}}]$ levels rather complicated relations are found, as Fig. 4 shows.

Of possible value in analysis is the strong extraction of neptunium (V) from 1M NaOH (pH ~ 13.90) shown in Fig. 4. We hope to exploit this in studying neptunium VI and VII, and preparing them on a tracer scale.⁽⁵⁾

In conclusion, we may comment that it seems useful to investigate solvent extraction by chelate formation from basic media, in spite of the complications which occur.

Appendix

Formula I

$$[\text{HA}] = [\overline{\text{C}}_{\text{HA}} - \text{C}_{\text{Na}} / (1 + 1/D_{\text{Na}})] / [1 + (1 + 10^{-9.35} / [\text{H}^+]) / D_{\text{HA}}]$$

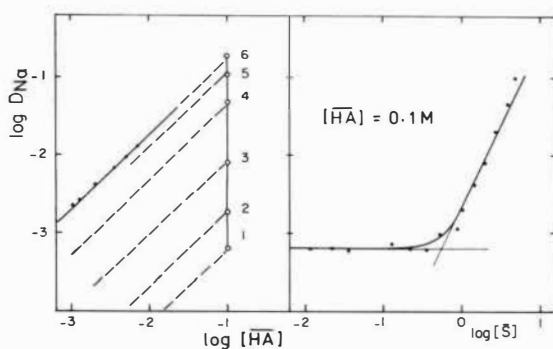
Formula II

$$[\overline{\text{S}}] = \overline{\text{C}}_{\text{S}} - \text{C}_{\text{Na}} \left[\frac{[\overline{\text{HA}}](K_1[\overline{\text{S}}] + 2K_2[\overline{\text{S}}]^2) / [\text{H}^+]}{1 + [\overline{\text{HA}}](K_e + K_1[\overline{\text{S}}] + K_2[\overline{\text{S}}]^2) / [\text{H}^+]} \right]$$

References

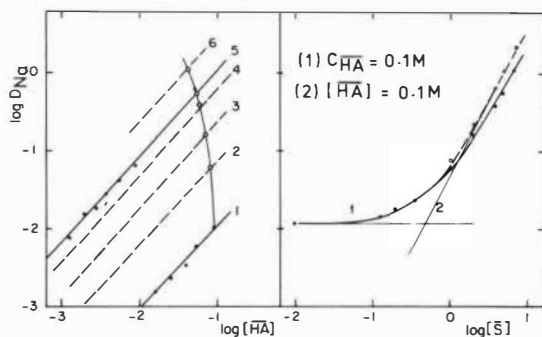
1. Moskin A.I., Radiokhimiya (1971) 13, 700.
2. Zolotov Y.A. and Alimarin I.P., J. Inorg. Nucl. Chem. (1963) 25, 691.
3. Zolotov Y.A. and Alimarin I.P., Radiokhimiya (1962) 4, 272.
4. Novikov Y.P., Mjasoedov B.F. and Ivanova S.A., Radiochem. Radioanal. Letters (1972) 9, 85.
5. Espinosa E., Genet M. and Guillaumont R. (submitted to Radiochimica Acta); Espinosa E., thesis 3e cycle (1973), Paris VI University.
6. Stary J., The Solvent Extraction of Metal Chelates, Pergamon 1964, p.197.
7. Healy T.V., J. Inorg. Nucl. Chem. (1968) 30, 1025.

Curve	[S]
1	0 M
2	1 M
3	2 M
4	4 M
5	5 M
6	7 M



$pH = 11.85$
 $(C_{NaOH} = 0.01 M)$

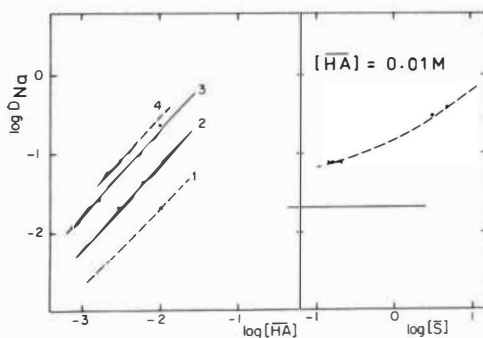
Curve	[S]
1	0.025 M
2	1 M
3	2 M
4	4 M
5	5 M
6	7 M



$pH = 12.80$
 $(C_{NaOH} = 0.1 M)$

Curve	[S]
1*	0 M
2	0.15-0.3 M
3	3 M
4	5 M

*From Fig.2 by extrapolation as indicated



$pH \sim 13.90$
 $(C_{NaOH} = 1 M)$

Fig. 1.

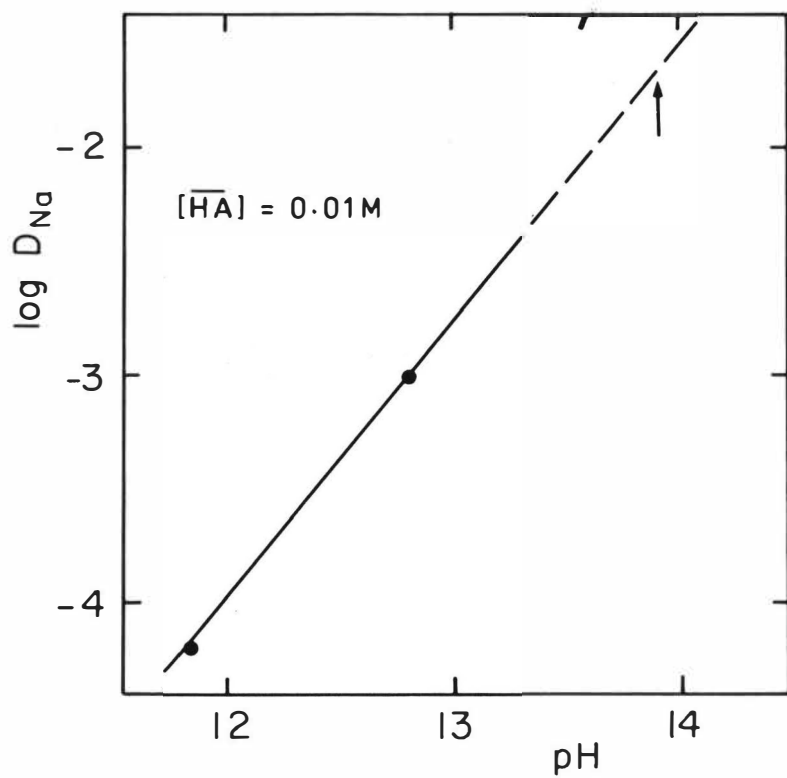
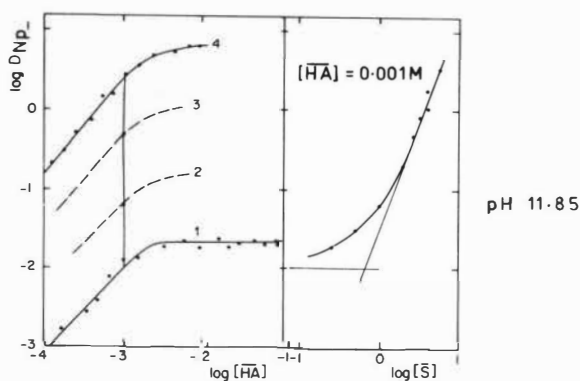
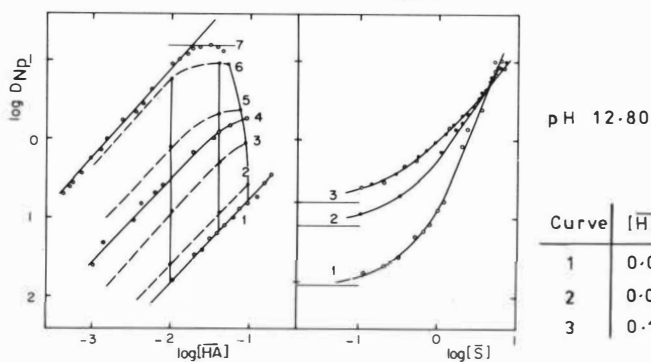


Fig. 2.

Curve	$[\bar{S}]$
1	0 M
2	1 M
3	3 M
4	7 M



Curve	$[\bar{S}]$
1	0.025 M
2	0.2 M
3	1 M
4	1.5 M
5	2 M
6	5 M
7	7 M



Curve	$[\overline{HA}]$
1	0.01 M
2	0.05 M
3	0.1 M

Curve	$[\bar{S}]$
1	0.15 - 0.3 M
2	7 M

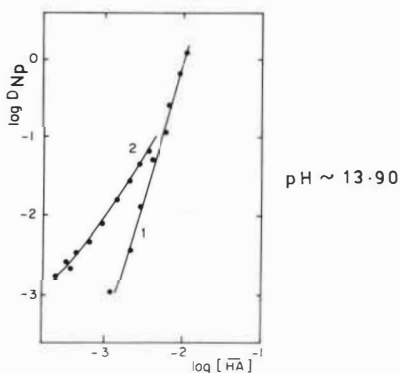


Fig. 3.

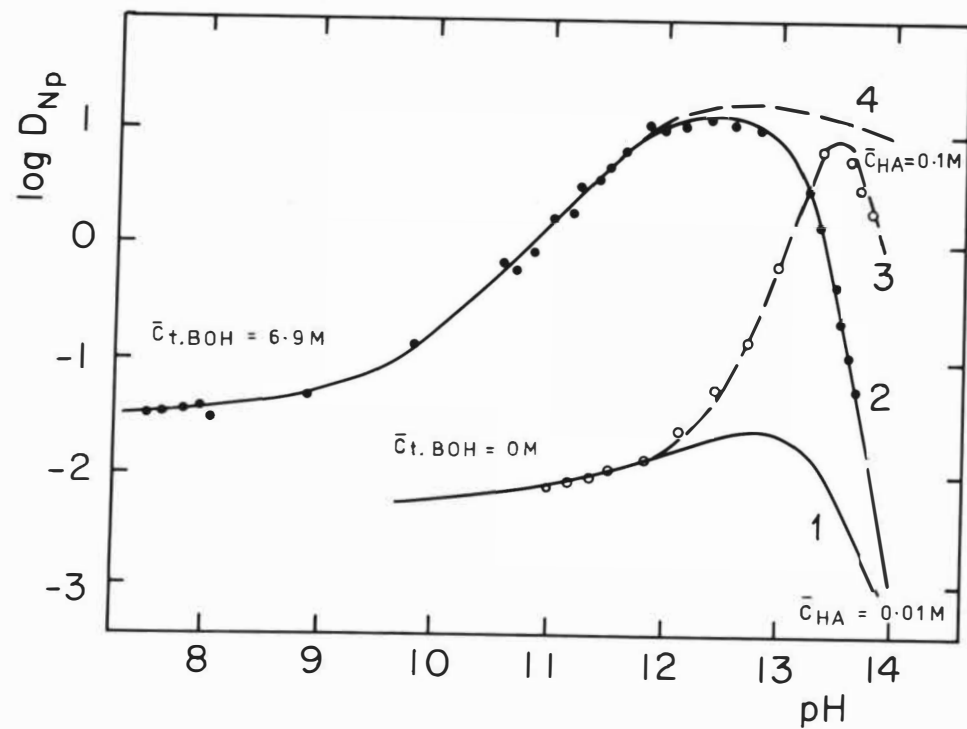


Fig. 4.

Distribution of the Daughter Species resulting from Chelates by β^- -Decay in Two-Phase Systems

F. Macášek, V. Mikulaj, R. Kopunec

Department of Nuclear Chemistry, Comenius University,
Bratislava, Czechoslovakia

Abstract

The β^- -decay of a radionuclide bound in a neutral chelate gives rise to a molecular ion containing the daughter nuclide even in a non-polar organic phase. The daughter species in the ^{99}Mo - $^{99}\text{Tc}^{\text{m}}$, ^{144}Ce - ^{144}Pr and ^{234}Th - $^{234}\text{Pa}^{\text{m}}$ decays may be unusual in respect to their coordination and oxidation states. Their steady state distribution is of interest, generally differing from a conventional extraction equilibrium of the daughter elements (Tc, Pr, Pa) in their normal valency states in the same systems, and a model for this distribution is proposed.

Introduction

A daughter nuclide formed by pure β^- -decay from a neutral molecule may, on account of the small recoil energy and in the absence of multiple autoionization, appear in a molecular ion. The primary molecular ion is isoelectronic with the parent molecule and the original chemical bonds will be to a great extent preserved if the ion is a stable form of the daughter element. When the recoil energy and electron shake-off are not negligible, and especially when the β -decay is accompanied by internally converted γ -transitions, the daughter atoms arise in a chemical form which is quite different from the parent compound.⁽¹⁻³⁾

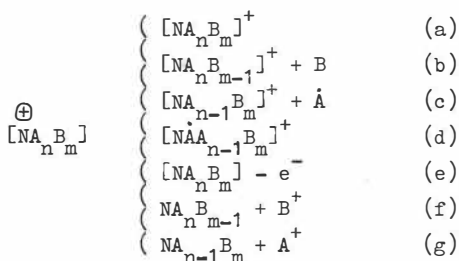
We have studied the distribution of daughter $^{234}\text{Pa}^{\text{m}}$ following β -decay of ^{234}Th in extraction systems with thenoyltrifluoroacetone⁽⁴⁾ and $^{99}\text{Tc}^{\text{m}}$ in systems with several [^{99}Mo] molybdenyl chelates.⁽⁵⁾ The behaviour of the daughter species may be more complicated in these chelate systems than, for example, in those with phthalocyanine⁽⁶⁾ owing to the possible variety of secondary reactions. A kinetic treatment of ^{144}Pr behaviour during the β -decay processes in $^{144}\text{Ce}(\text{III})$ -aminopolycarboxylate complexes has been given by Glentworth and Wiseall⁽⁷⁾ and Shiokawa and Omori.⁽⁸⁾ In the present paper an attempt is made to give a simple model describing the liquid-liquid distribution of the daughter radionuclide, based upon results obtained with the radioactive chains mentioned above.

The Model

The β -decay of a radionuclide M bound in a complex MA_nB_m , with anionic and electroneutral ligands A^- and B respectively, must result initially in a molecular ion of the daughter nuclide N with additional positive charge localized on the central atom N:



Within a time shorter than 10^{-7} s, these primary molecular ions may be expected to undergo charge-distribution and bond-rupture processes, e.g.



which imply immediate collisional reactions of the ions. It is important that in reactions (c)-(f) the oxidation state of the daughter element is the same as that of the parent atom but after processes (a) and (b) it increases and after fragmentation (g) it decreases by one unit.

Now let us consider what happens when a phase, say an aqueous phase, containing a relatively long-lived parent M in radioactive equilibrium with its daughter N is shaken with another, immiscible phase, say an organic phase. We will assume that M distributes rapidly between the two phases, the equilibrium being characterised by $R_M = m'/m$ where m' is the number of M atoms in the organic phase, and m is the total number of M atoms. R_M , m' and m are substantially constant. We will also assume that atoms of the daughter N undergo an immediate distribution when first produced, and then redistribute on a longer timescale as the initial chemical forms revert to more normal species. Of N atoms formed in the organic phase, let a fraction α remain there (presumably those in neutral products, e.g. from reactions (e)-(g)), and let a fraction $(1 - \alpha)$ transfer to the aqueous phase immediately (presumably those in ionic products, e.g. from reactions (a)-(d)). On the other hand we suppose that all N atoms formed in the aqueous phase remain there initially. We also assume that the later redistribution can be described by means of two first-order rate constants, k_1 (extraction) and k_2 (stripping).

The rate of change of n' , the number of atoms of N in the organic phase, is then given by

$$\begin{array}{cccc}
dn'/dt = & \alpha \lambda_M m' & - \lambda_N n' & + k_1 (n - n') - k_2 n' \\
& (A) & (B) & (C) \quad (D)
\end{array}$$

(λ 's are decay constants, and n is the total number of N atoms) where the terms on the right-hand side refer to the following:

- (A) N atoms formed by decay of M in organic phase, and remaining there initially.
- (B) N atoms decaying in organic phase.
- (C) Subsequent mass transfer of N from aqueous to organic phase.
- (D) Subsequent mass transfer of N from organic to aqueous phase.

Dividing through by n , which is constant, putting $R = n'/n$, and introducing the relation $\lambda_M m = \lambda_N n$ for radioactive equilibrium, we obtain

$$dR/dt = \alpha \lambda_N R_M - \lambda_N R + k_1 (1-R) - k_2 R \quad (1)$$

On integration this gives

$$R = (\alpha \lambda_N R_M + k_1) [1 - \exp(-\lambda t)] / \lambda + R_0 \exp(-\lambda t) \quad (2)$$

where $\lambda = \lambda_N + k_1 + k_2$, and $R = R_0$ at $t = 0$.

After a sufficiently long time ($t \rightarrow \infty$) eq. (2) reduces to

$$R_\infty = (a \lambda_N R_M + k_1) / \lambda \quad (3)$$

In the particular case when the secondary redistribution processes are fast in comparison with the rate of decay of N (k_1 and $k_2 \gg \lambda_N$)

$$R_\infty = k_1 / (k_1 + k_2), \quad (4)$$

which is the value R_∞ would assume if N were not part of a radioactive decay chain. When, on the other hand, the secondary redistribution processes are relatively extremely slow (k_1 and $k_2 \ll \lambda_N$),

$$R_\infty = a R_M \quad (5)$$

It may be noted that

$$R/R_M = (n'/m')(m/n) = n' \lambda_N / m' \lambda_M = A'_N / A'_M,$$

where the A' 's are organic phase activities.

Experimental

All chemicals used were of analytical grade. ^{99}Mo (~ 100 mCi/g MoO_3), and carrier-free ^{144}Ce and ^{143}Pr were purchased from the Institute of Research, Production and Utilization of Radioisotopes, Prague, and ^{234}Th was prepared from uranyl nitrate.⁽⁴⁾ Both daughter and parent nuclide activities were measured with scintillation counters by the method of growth curve extrapolation⁽⁴⁾ or by channel counting.⁽⁵⁾ The extractions were performed in hydrophobised glass test-tubes of the same size and liquid contents, which were vigorously shaken in a vibrational shaker at the temperature $22 \pm 1^\circ\text{C}$. The other experimental procedures employed were substantially the same as those described previously.^(4,5)

Results and Discussion

When the aqueous solutions of $1.7\text{--}3.3 \times 10^{-3} \text{ M } ^{99}\text{Mo(VI)}$ in equilibrium with the daughter $^{99}\text{Tc}^{\text{m}}$ ($\lambda_{\text{Tc}} = 0.115 \text{ h}^{-1} = 1.93 \times 10^{-3} \text{ min}^{-1}$) were shaken with 5,7-dichlor-8-hydroxyquinoline (HOx) solutions in chloroform, molybdenum was extracted rather rapidly and an increasing extraction of technetium followed (Fig. 2). Here we have the same picture as was observed in extractions with α -benzoinoxime and 8-hydroxyquinoline⁽⁵⁾ and its other dihalogen derivatives.⁽⁹⁾ Tc(VII) , which may formally be expected as the β -decay product of Mo(VI) , has been proved to be extracted with a negligible yield under these conditions. Hence, the daughter technetium must be retained in the organic phase in a lower oxidation state, owing to a rapid process of type (g) above, viz. $\text{MoVI} \cdot \text{Ox}_2 \rightarrow \text{TcO}_2 \cdot \text{Ox}_2 \rightarrow \text{TcO}_2 \cdot \text{Ox} + \text{Ox}^+$. The accumulation of $^{99}\text{Tc}^{\text{m}}$ in the organic phase corresponds to its growth from extracted parent ^{99}Mo , indicating that k_1 and $k_2 \ll \lambda_{\text{Tc}}$ so that a values (see Table 1) can be evaluated by means of eq. (5).

Table 1

Equilibrium aqueous phase	a
0.1N NaCl, pH 7.2	1.04
0.1N NaCl, pH 2.0	0.87
0.1N HCl	0.95
0.2N HCl	0.88
1.0N HCl	0.92
$\text{Av} = 0.93 \pm 0.06$	

It can be seen that the a values are more or less independent of the aqueous phase composition and, though the presence of oxygen and a low HCl concentration prevent Tc(V) from being extracted in conventional extraction systems because of its oxidation, the pentavalent technetium chelate remains in the organic phase once it is formed there. Thus, the β -decay of [^{99}Mo] molybdenyl chelate is a useful tool for identifying the inert complexes of Tc(V).

The behaviour of daughter ^{144}Pr ($\lambda_{\text{Pr}} = 4.01 \times 10^{-2} \text{ min}^{-1}$) at the steady state in ^{144}Ce -8-hydroxyquinoline systems (Table 2) is somewhat less clear cut. It is helpful to compare it with ^{143}Pr , which undergoes a simple isotopic exchange when introduced into one of the phases in the same system in presence of inactive praseodymium carrier. For the exchange reaction we can apply the McKay equation to determine ($k_1 + k_2$):

$$\ln(1 - F) = -(k_1 + k_2)t \quad (7)$$

(F = degree of exchange), and we can then use eq. (4) to obtain the separate values of k_1 and k_2 . The results are given in the left-hand part of Table 2.

Table 2

^{143}Pr and ^{144}Pr behaviour in the system:

Initial aqueous phase: 10^{-4}M Ce(III) , 10^{-7}M Pr(III) , acetate buffer, NaClO_4 to ionic strength 0.1M

Initial organic phase: 0.1M oxine in CHCl_3

^{143}Pr undergoes isotopic exchange. ^{144}Pr is formed by decay of ^{144}Ce in Ce(IV) oxinate.

pH	^{143}Pr				^{144}Pr				
	R_∞	k_1+k_2	k_1	k_2	R_{Ce}	R_∞	$k_1+k_2(+\lambda_{\text{Pr}})$	k_1	k_2
Rate constants in min^{-1}									
5.85	0.57	0.34	0.19	0.15	0.85	0.10	-	-	-
6.23	0.80	0.47	0.38	0.09	0.97	0.22	2.0 ± 0.2	0.44	1.6
6.93	0.94	0.56	0.53	0.03	0.99	0.73	-	-	-

In the case of the ^{144}Ce - ^{144}Pr chain we can determine the steady-state distribution of both species (R_{Ce} and R_∞), but the steady state is reached so rapidly that kinetic data are difficult to obtain. Nevertheless one result is given in Table 2. The parameter measured is actually ($k_1 + k_2 + \lambda_{\text{Pr}}$), but this does not differ significantly from ($k_1 + k_2$). We can again obtain k_1 and k_2 with the aid of eq. (4).

The high values of R_{Ce} indicate that the cerium is extracted in the tetravalent state, since no trivalent lanthanide is so highly extracted.⁽¹⁰⁻¹²⁾ Despite this high extraction of the cerium, however, more of the ^{144}Pr goes into the aqueous phase than in the case of purely chemical equilibrium, since R_∞ is lower for ^{144}Pr . This in turn is due to a much higher value of k_2 for ^{144}Pr than for ^{143}Pr , whereas the k_1 -values are essentially the same. The probable explanation is that some product, probably charged, containing ^{144}Pr is ejected from the organic phase, whereas in the ^{143}Pr case there is only the common extractable neutral chelate PrOx_3 to consider.

Charged products could be formed from the ^{144}Ce chelate during decay as a result of internal conversion of γ -rays or electron shake-off (about 30%⁽⁸⁾), or

by intramolecular reduction of Pr(V) as in reaction (d) given earlier.

Rapid reactions in the organic phase, however, may reasonably be taken to explain our results for the distribution of $^{234}\text{Pa}^{\text{III}}$ in the system of carrier-free parent ^{234}Th -0.01M thenoyltrifluoroacetone in benzene-chloride (buffered at pH 2), where $R_{\infty} = R_{\text{Th}} = 0.53$ was found. Because $k_1 + k_2 < 0.03 \lambda_{\text{Th}}$ in this system, α should be close to unity. The daughter protactinium might be expected to appear in the organic phase as a molecular ion PaTTA_4^+ . Unlike technetium, there is no reason to expect reduction and the molecular ion should undergo further neutralization reactions by collision with HTTA or H_2O molecules present in benzene, before it is stripped into the aqueous phase. The kinetic details are difficult to ascertain, owing to the short half-life of $^{234}\text{Pa}^{\text{III}}$ ($\lambda_{\text{Pa}} = 0.593 \text{ min}^{-1}$). It is interesting to remark that the daughter ^{95}Nb formed by β^- -decay of ^{95}Zr extracted by HTTA in benzene was found to transfer into the aqueous phase (1M HNO_3) when the phases were contacted.⁽¹⁴⁾

It is clear that the extensive simplification in our model of the behaviour of the daughter species formed by β^- -decay in extraction systems should not detract from an intelligent understanding of the overall picture. Its aim, however, has been to explain the main features connected with specific phenomena of molecular ion formation in the organic phase and to allow a classification of such systems. The study of the distribution of the daughter species may be useful, especially when combined with isotope exchange data, from the point of obtaining new extractable compounds of daughter elements, and of the extraction kinetics of short-lived isotopes and their behaviour in radionuclidic generators, because a proportion of the daughter nuclide enters into chemical reactions in an unusual form.

References

1. Nefiodov V.D., Zaitsev V.M., Toropova M.A., Usp. Khim. 1963, 32, 1367.
2. Stöcklin G., Chemie heisser Atome, 1969, p.34 (Weinheim, Verlag Chemie).
3. McKay H.A.C., Principles of Radiochemistry, 1971, p.464 (London, Butterworths).
4. Macásek F., Drienovský P., Kopunec R., Mikulaj V., Acta Facultatis Rerum Naturalium Universitatis Comenianae-Chimia, 1971, 15, 33.
5. Mikulaj V., Rajec P., Fábervová V., Chem. Zvesti, in press.
6. Stentström J., Jung B., Radiochim. Acta, 1965, 4, 3.
7. Glentworth P., Wiseall B., Chemical Effects of Nuclear Transformations, 1965, Vol. II., p.483 (Vienna, IAEA).
8. Shiokawa T., Omori T., Bull. Chem. Soc. Japan, 1969, 42, 696.
9. Mikulaj V., to be published.
10. Alimarin I.P., Przhivalskii E.S., Puzdrenkova I.V., Solovina A.P., Trudy Komissii po analit. khimii ANSSSR, 1958, 8, No. 11, 152.
11. Kopunec R., Kotočová A., Chem. Zvesti, in press.
12. Kopunec R., to be published.
13. Edwards R.R., Coryell C.D., 1961, USAEC Report TID 13 363.
14. Fletcher, J.M., Morris D.F.C., Wain A.G., Bull. Inst. Mining and Metallurgy, 1956, No. 597, 487.

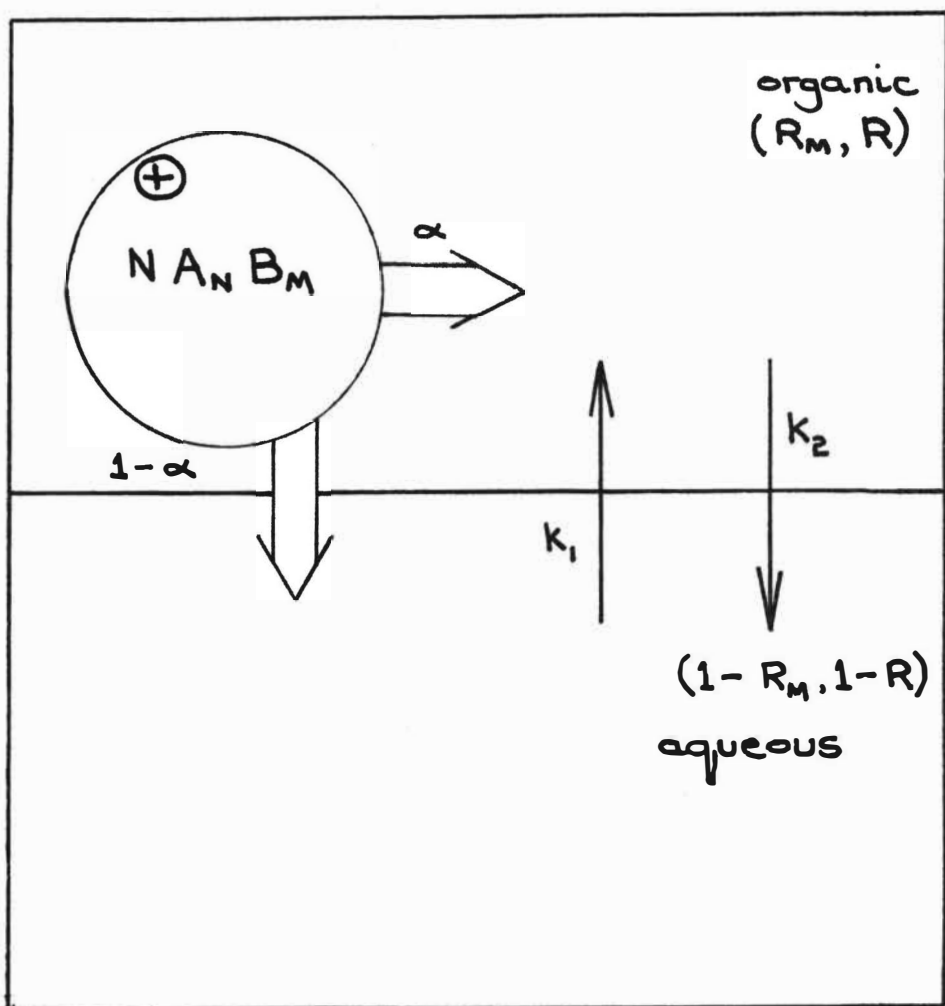
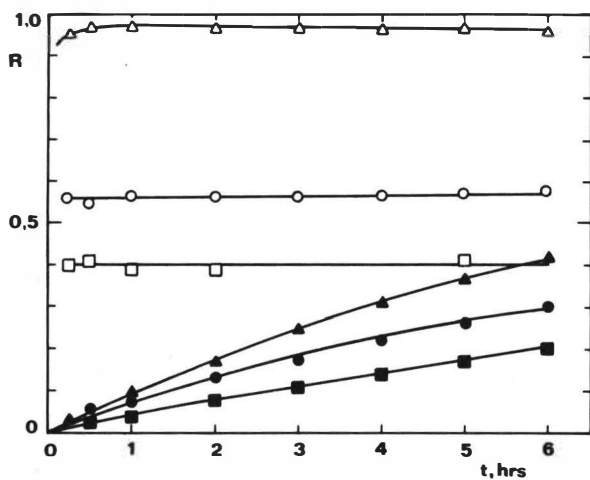


FIG. 1 MODEL FOR DISTRIBUTION OF DAUGHTER N FORMED BY β -DECAY OF M .



^{99}Tc ^{99}Mo
 0.1 N NaCl, pH 7.26 ▲ △
 0.1 N NaCl, pH 2.00 ● ○
 0.1 N HCl ■ □

FIG. 2 EXTRACTION WITH 0.03 M
5,7- DICHLOR- 8- HYDROXYQUINOLINE IN CHCl_3

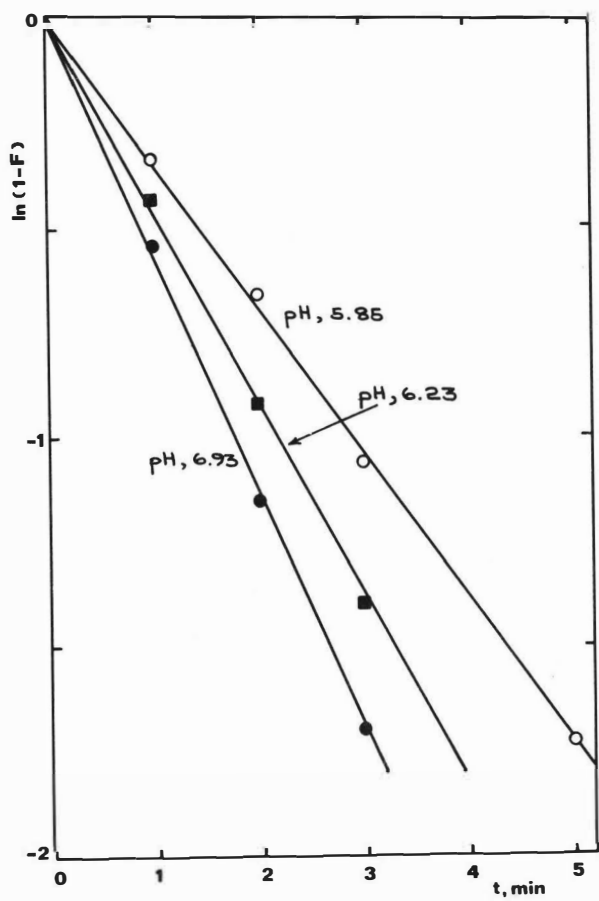


FIG. 3 ^{143}Pr EXCHANGE.

Metal Retention by Hydroxamic Acids in Irradiated TBP Solutions.

T.V. Healy and A. Pilbeam

Atomic Energy Research Establishment, Harwell, Didcot, Berks., U.K.

This paper attempts to show the effects of hydroxamic acids on metal retention by tributyl phosphate/kerosene in nuclear fuel reprocessing under both simulated and actual conditions,

Introduction

During the reprocessing of nuclear fuel by tributyl phosphate/ odourless kerosene (TBP/OK), solvent degradation, both radiolytic and chemical, causes an increasing retention of fission products particularly zirconium by the solvent, together with retention of plutonium. The higher levels of radiation produced in the burn-up of fast reactor fuels plus higher reprocessing temperatures should increase the degree of undesirable metal retention by the degraded solvent. Because alkali washing of recycled solvent only removes some of the degradation products, the activity level of the solvent builds up, contamination of the uranium and plutonium products occurs and the reprocessing plant performance is impaired by poor phase separation.

Among the main primary degradation products of the diluent - organic nitrates, nitroparaffins, aldehydes, ketones and carboxylic acids - only nitroparaffins have been considered as leading to metal retention by the solvent. Blake et al.¹ consider that nitroparaffin enol adducts or salts cause metal retention in degraded solvents. Stieglitz², using hafnium tests, found no relation between the amount of hafnium complexed in the solvent and the concentration of nitroparaffins. Lane³ and Huggard and Warner⁴ considered that none of the primary products of solvent degradation are responsible for fission product retention, but suggested that secondary products, hydroxamic acids, could be formed and, under favourable conditions, could produce appreciable fission product retention, in particular, zirconium retention. Stieglitz² concluded from his work that carbonyl containing compounds were mainly responsible for increased hafnium retention by degraded solvent. The infra red absorption peak at 1660 cm^{-1} , assigned by Stieglitz to the carbonyl group in ketones, could equally well be ascribed to the carbonyl group in hydroxamic acids⁵.

Hydroxamic acids are assumed to be formed from primary nitro-paraffins by the Victor Meyer rearrangement or by cumulative formation via the Nef reaction on alternate acid and alkali treatment³. There has been no real identification of hydroxamic acids in recycled solvent, but Hughes (quoted in reference 4) and Ohwada⁶, both using the rather insensitive ferric chloride spot test believe there may be evidence for the presence of hydroxamic acids at ca. $10^{-5}M$. The amount of zirconium retained in a typical solvent extraction plant is estimated to be about $10^{-8}M$ per pass, so the amount of ligand combined with the zirconium even after 100 passes would only be about $10^{-6}M$, and hydroxamic acid at this level would not be detected. To test whether hydroxamic acids are in fact responsible for zirconium retention in Windscale recycled solvent, we have synthesised a number of them and examined their behaviour in HNO_3 /TBP/OK systems and, in particular, the effect on zirconium partition of the C_{12} acid, laurohydroxamic acid (LHA).

Experimental

TBP, obtained from Albright and Wilson Ltd., London, was purified by steam stripping in the presence of 0.1M NaOH, using a nitrogen bleed. Equal volumes of TBP and 0.1M NaOH were heated until half the aqueous volume had distilled over. After two one-volume washes with 0.1M NaOH and with water, the TBP was dried under vacuum and made up to 20% vol/vol TBP/OK using Shell Mex kerosene. This diluent has a boiling range of about 200 - 250°C, and consists mainly of paraffins (62%) and naphthenes (36%), with about 2% of aromatics.

Degraded TBP/OK solutions were obtained either directly from Windscale recycled solvent from the BNFL plant or by irradiations (1) in the Technological Irradiation Group fuel element pond at Harwell or (2) from Cobalt-60 irradiations in the Harwell Gamma Irradiation Facility. In all irradiations TBP/OK solutions were stirred continuously with an aqueous nitric acid phase, usually 3M. Dibutyl phosphoric acid (DBP) was obtained from Albright and Wilson Ltd., London and purified according to the method of Hardy and Scargill⁷. Where it was desirable to remove DBP from TBP solutions, two equal volume washed with 0.1M Na_2CO_3 were carried out at room temperatures, followed by a water wash. Nitrous acid

was removed from TBP solutions by an equal volume wash with 0.05M sulphamic acid, followed by a water wash. Nitrous acid was removed from aqueous HNO_3 solutions by addition of small amounts of sulphamic acid. The acids laurohydroxamic (LHA), decanohydroxamic (C_{10}HA), octanohydroxamic (C_8HA) and caprohydroxamic (C_6HA) were all synthesised from the appropriate commercially available carboxylic acid esters plus hydroxylamine hydrochloride, using slight modifications of the method for the preparation of benzohydroxamic acid⁸. The acids, all obtained in about 80% yield, were recrystallized two to three times from ethyl acetate as lustrous white plates with m.p.'s similar to those in the literature. The detection and estimation of hydroxamic acids by the ferric chloride colorimetric spot test⁴ is somewhat insensitive, the detection limit being about $2 \times 10^{-4}\text{M}$ LHA, and the determination is also strongly affected by the presence of zirconium. A much more sensitive vanadium colorimetric method has been developed by one of us⁹ from a vanadium spot test for hydroxamic acids^{5,10}. The detection limits of this method are of the order of $5 \times 10^{-6}\text{M}$ and the method is not affected by the presence of zirconium or uranium. This method has been used throughout this work for estimation of hydroxamic acids. A Unicam SP 500 UV Spectrophotometer was used to measure the colour at 575 nm.

Chemicals used, such as ammonium vanadate, hydrochloric, nitric acid and sulphamic acids and sodium nitrite, were all of reagent grade. Lauryl nitrate, 1-nitrododecane, methyl decyl ketone and caproic acid were all obtained from BDH and used without further purification. Stock solutions of inactive zirconium in 3M HNO_3 were prepared from BDH "zirconium nitrate" by initially heating for several hours with concentrated HNO_3 , then diluting the filtered solution to give a final solution of 3M HNO_3 , after estimating the acid present using 0.1M NaOH . After a few days standing the solution was centrifuged and the zirconium estimated gravimetrically as pyrophosphate. Active $^{95}\text{Zr}/^{95}\text{Nb}$ tracer was obtained from R.C.C. Amersham as the oxalate. Niobium was separated using a solvent extraction method¹¹ to give a stock solution of ^{95}Zr at about 10^{-9}M in 8M HNO_3 for use as tracer. A number of Z tests were carried out based on the standard Windscale Z test⁴, but incorporating a refinement¹² whereby each cycle of a typical process for the multi-stage extraction, including scrubbing and back extraction of uranium, is carried

out in the presence of zirconium. The test results are expressed as Z numbers, that is, the number of moles of zirconium retained in 10^9 l of degraded solvent.

Results and Discussion

Zirconium distribution data with hydroxamic acids.

A study has been made of the effect of different concentrations of LHA on the distribution of zirconium between 20% TBP/OK and nitric acid. The results are given in Table 1, which also gives one result for octanohydroxamic acid (C_8HA). The shorter carbon chain acid has a smaller effect on zirconium distribution. Caprohydroxamic acid (C_6HA) was too water soluble to be used meaningfully in this table. Synergistic effects were looked for with LHA in conjunction with primary degradation products of the diluent and also with DBP. All the distribution coefficients (D_{Zr}) represent back extraction data for zirconium, after an original forward extraction into an equal volume of 20% TBP/OK plus additives. Except where otherwise stated, separated tracer ^{95}Zr only ($10^{-9}M$), was used.

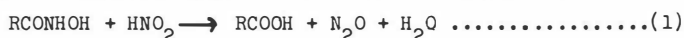
This table shows that concentrations of the order of 10^{-4} to $10^{-3}M$ LHA can and do lead to strong metal retention in TBP mixtures. LHA has a much larger effect than DBP. There appears also to be no appreciable synergic effect between LHA or DBP and any of the additives.

Table 1

<u>Effect on Zr Distribution of Added Hydroxamic Acid and Primary Degradation Products in 20% TBP/OK.</u>				
LHA Molarity	DBP Molarity	Other Additives (All $10^{-2}M$)	3M HNO_3 D_{Zr}	0.5M HNO_3 D_{Zr}
	-	-	0.08	0.10
10^{-5}	-	-	0.12	0.11
10^{-4}	-	-	2.0	-
10^{-3}	-	-	40	60
$10^{-3}(C_8HA)$	-	-	4.8	5.2
10^{-3}	-	Lauryl Nitrate(LN)	43	90
10^{-3}	-	1-nitrododecane(ND)	45	110
10^{-3}	-	Methyl Decyl Ketone(MDK)	38	-
10^{-3}	-	Caproic Acid (CA)	42	150
10^{-3}	-	LN + ND	50	150
10^{-3}	-	MDK + CA	50	150
10^{-3}	-	LN + ND + MDK + CA	50	79
10^{-3}	10^{-2}	LN + ND + MDK + CA	15	30
-	10^{-3}	LN + ND + MDK + CA	0.9	1.6
-	10^{-3}	-	0.9	1.7
-	10^{-2}	-	21	-
10^{-3}	-	$10^{-3}M$ Zr	5	-

Effect of nitrous acid on hydroxamic acid behaviour

The large effect of hydroxamic acid on the retention of zirconium by TBP/OK, as discussed in the previous paragraph, can be counteracted by the addition of nitrite to the system. For example Table 1 shows that D_{Zr} for 20% TBP/OK/0.5M HNO_3 is increased from 0.10 to 60 by making the organic phase 10^{-3} molar in LHA. If this phase is also made 10^{-2} molar in nitrous acid, D_{Zr} drops again to 0.15, indicating destruction of the LHA. The reaction of hydroxamic acids with nitrous acid has been reported in the literature¹³ as liberating nitrous oxide as in equation (1)



Schenck¹³ reported that a little nitrogen is produced, possibly through a diazotization stage. Work at Harwell, to be reported elsewhere¹⁴, indicates that on contacting LHA in TBP/OK with nitrous acid in 0.5M HNO₃, one mole of nitrous acid is required to destroy one mole of LHA, as in equation (1). At high acidity, say 3M HNO₃, four moles of LHA are destroyed per mole of nitrous acid, the reaction probably following equation (2).



This destruction of hydroxamic acid by nitrous acid is illustrated below (Table 2) in the 20% TBP/OK/3M HNO₃ system, where LHA is added to the organic phase and sodium nitrite to the aqueous phase. The remarkable protection of LHA from nitrite attack by initial formation of the zirconium salt¹⁴ is also illustrated in the table, but great excess of nitrite destroys even this protection. In the experiments with zirconium present, the nitrite was added to the mixture a half hour after the addition of LHA and zirconium, the time of mixing being taken after the nitrite addition.

Table 2

Destruction of LHA by Nitrite and its Protection by Zirconium (Two phase system 20% TBP/OK/3M HNO ₃)					
M LHA x 10 ⁴ At Start	At End	% LHA Destroyed	M HNO ₂ x 10 ⁴	M Zr x 10 ⁴	Mixing Time min
300	300	0.0	None	None	10
300	19	93.7	100	"	2
90	4.5	95.0	100	"	2
33	1.95	94.1	100	"	2
33	1.40	95.7	100	"	3
33	1.05	96.8	100	"	10
11	0.62	94.4	33	"	3
11	5.8	47.3	33	16	3
*9	4.5	50.0	33	16	3
8	0.1	98.5	1000	10	3

The asterisk refers to the use of 20% TBP/OK/3HNO₃ which had been

previously irradiated in a cobalt source to 40 wh/l. After separation this degraded solvent was alkali and water washed, prior to the addition of LHA, zirconium in HNO_3 and finally nitrite. In this experiment with degraded solvent the LHA is protected by the zirconium to about the same degree as when pure TBP/OK is used. Huggard and Warner⁴ had previously noted that the Z number of 20% TBP/OK, to which a hydroxamic acid had been added, was much lower than that to which a zirconium hydroxamate was added. This phenomenon can also be explained as protection of the acid by zirconium from the nitrite concentration normally encountered in these tests, namely $2 \times 10^{-3}\text{M}$.

The effect of nitrite concentration on the zirconium distribution coefficient using pure TBP/OK, Windscale recycled solvent, and irradiated TBP/OK have also been compared, both in the presence and absence of LHA, and results are shown in Table 3.

Table 3

Effect of HNO_2 and LHA on D_{Zr} for Treated TBP/OK (Aqueous Phase is 3M HNO_3)			
Solvent Treatment	LHA	HNO_2	D_{Zr}
Pure 20% TBP	None Added	None Added	0.08
" " "	$3 \times 10^{-4}\text{M}$	" "	6.0
Windscale Recycled Solvent (20% TBP/OK)	None detected	" "	6.4
" " "	" "	$3 \times 10^{-4}\text{M}$	11.4
" " "	" "	$100 \times 10^{-4}\text{M}$	16.6
Pure 30% TBP/OK	None added	None Added	0.2
" " "	10^{-3}M Added	" "	100
30% TBP/OK Irrad(42 wh/l)	None Detected	" "	100
" " "	10^{-3}M Added	" "	300

As shown above, Windscale recycled solvent contains no

detectable hydroxamic acid ($< 5 \times 10^{-6}M$) and yet has a D_{Zr} value rather similar to that of pure solvent with $3 \times 10^{-4}M$ LHA added. Also addition of nitrite to the recycled solvent, which would be expected to destroy LHA, actually increases D_{Zr} . Similarly, highly irradiated TBP/OK contains no detectable hydroxamic acid but its D_{Zr} value is similar to that for pure solvent with $10^{-3}M$ LHA added.

Using the improved Z test¹², Z numbers have been obtained for 20% TBP/OK to which LHA has been added, in the presence and absence of nitrous acid. These results are shown in Table 4. The LHA concentrations at the beginning and end of the Z test are also recorded.

Table 4

The Effect of Nitrite on LHA and Z Number in 20% TBP/OK			
LHA Molarity		Nitrite Molarity	Z Number
Initial	Final		
None	None	2×10^{-3}	40
10^{-4}	$< 5 \times 10^{-6}$	2×10^{-3}	340
10^{-4}	0.9×10^{-4}	None	1280
10^{-3}	$< 5 \times 10^{-6}$	2×10^{-3}	400
10^{-3}	10^{-3}	None	1500

The nitrite concentration ($2 \times 10^{-3}M$) is the level usually reported for the Windscale aqueous nitric acid feed solution. This table gives further evidence of the destruction of hydroxamic acids if originally present in recycled solvent. Even when the LHA is protected from nitrite attack during the Z test, by elimination of nitrous acid, the Z numbers obtained, using 10^{-3} and 10^{-4} molar LHA, are much lower than those obtained on test bed recycled solvent⁴ or on highly irradiated solvent which contains no detectable hydroxamic acid concentration.

Conclusions

Hydroxamic acids, if present in concentrations of the order of 10^{-3} to $10^{-4}M$, could have appreciable effects on metal retention by

solvents. At this level, they could be easily detected in recycled solvent or in highly irradiated TBP/OK/aqueous HNO_3 systems. The authors have been unable to find any evidence for their presence although many samples of both types of irradiated solvent have been examined. We have also found no evidence for any synergic metal retention effects of these acids plus primary solvent degradation products.

Hydroxamic acids are very quickly destroyed by nitrous acid on a basis of four moles per mole of nitrous acid and there is usually a fairly high concentration (10^{-3}M) of nitrous acid present during solvent extraction of nuclear fuel. Although zirconium salt formation does have a protective effect on hydroxamic acids, this occurs only if nitrous acid is present at low concentrations. Nevertheless, if hydroxamic acid were formed under process conditions, zirconium salt formation should afford some measure of protection. The zirconium distribution data presented in the paper also provide further evidence for the statement of Huggard and Warner⁴ that hydroxamic acids are not the only strong complexing agents produced during solvent degradation and that to obtain substantial yields of these acids requires extreme conditions. Our work indicates that some other species must be largely responsible for metal retention in degraded TBP/OK solutions.

References.

1. Blake, C.A., Davies Jr., W., and Schmitt, J.M., Nucl. Sci. Engng., 1963, 17, 626.
2. Stieglitz, L., Proc. Int. Solvent Extraction Conf., the Hague, 1971, p. 155, Society of Chemical Industry, London (1971)
3. Lane, E.S., Nucl. Sci. Engng., 1963, 17, 620.
4. Huggard, A.J. and Warner, B.F., Nucl. Sci., Engng., 1963, 17, 638.
5. Agrawal, Y.K., The Analyst, 1973, 98, 147.
6. Ohwada, K.J., Nucl. Sci. Tech., 1968, 5(4), 163.
7. Hardy, C.J. and Scargill, D., J. inorg. nucl. Chem., 1959, 10, 323.
8. Hauser, C.R. and Renfrow, Jr., W.B., Organic Syntheses, Coll. Vol II, ed. A.H. Blatt, John Wiley and Sons, New York (1946)
9. Pilbeam, A., UKAEA Document, AERE R 7065, 1973.
10. Battacharyya, S.C. and Tandon, S.G., Anal. Chem. 1961, 33, 1267 and 1964, 36, 1378.
11. Moore, F.L., Anal. Chem., 1956, 28, 997.
12. Brown, P.G.M., Naylor, A. and Smith, J.K., unpublished work.

13. Hantzsch, C. and Sauer, E., *Ann. der Chemie*, 299, 83.
Schenck, M. and Resche, A., *Ber.* 1940, 73, 202, 205.
Schenck, M., *Ber.*, 1944, 77, 29.
14. Healy, T.V. and Barton, C.J., unpublished work.

R. LUNDQVIST

Department of Nuclear Chemistry, Chalmers University of Technology, Fack, S-402 20 Goteborg 5, Sweden

Tetravalent protactinium in perchlorate solution was studied by different extraction systems. The complexation with acetylacetone, sulphate, ethylenediaminetetraacetic acid, perchlorate and tri-n-octylphosphine oxide suggests that the dominant hydrolysed protactinium species, in the pH range 0-3, is PaO^{2+} (or $\text{Pa}(\text{OH})_2^{2+}$). Equilibrium and thermodynamic constants are given for the extraction processes.

Information on Pa(IV) hydrolysis and complex formation in solution is very limited although it is of interest for comparison with other tetravalent ions.¹ Most investigations have been made in very acid media (e.g. 3 M HClO_4 ^{2,3}) where the hydrolysis is expected to be low^{1,4}. The method chosen for this study was the liquid-liquid distribution technique, because it allows one to work with trace concentrations of protactinium, thus avoiding polynuclear hydrolysis products.

EXPERIMENTAL

As a detailed description of the experimental techniques employed in the solvent extraction investigations has been presented earlier^{5,6,7} only a summary is given here. The organic and aqueous phases in the Pa(IV) extraction system were of equal volume (15 ml) and consisted of a dilute solution of the extraction agent (acetylacetone or tri-n-octyl phosphine oxide) in benzene and a dilute solution of the complexing agent (sodium sulphate or EDTA) in aqueous perchlorate solution. The protactinium (^{233}Pa or $^{234\text{m}}\text{Pa}$) was reduced to the tetravalent state either electrolytically at a mercury cathode ($\text{pH} \geq 7-8$) or by 0.01 M Cr^{2+} ($\text{pH} 0-3$).

The system was equilibrated in an oxygen free atmosphere of N_2 or Ar and under controlled pH ($= -\log(H^+)$) and temperature. The distribution of Pa(IV) was determined by measuring the gamma activity of samples of each phase. All chemicals used were of analysis quality.

Liquid-Liquid distribution investigations of Pa(IV)

1. Extraction with acetylacetone (HAA)

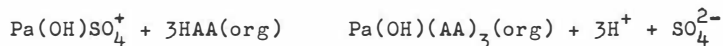
The distribution of Pa(IV) between dilute solutions of HAA in benzene and 1 M $(Na,H)ClO_4$ was investigated at different concentrations of HAA and H^+ and at different temperatures. All distribution data could be fitted to the function $\log D = f(pAA)$, where $D = (Pa)_{org}/(Pa)$ and $pAA = -\log(AA^-)$, see Fig.1. From the limiting slope $\log D / pAA = -2$ at high pAA it was concluded that the complexes formed were of the type $M L_n$ according to the general theory⁸ for evaluating the composition of the composite metal complex $M_m L_n (OH)_p (HL)_r (org)_s (H_2O)_t \dots$ in a liquid-liquid distribution system. The species formed in aqueous phase were M^{2+} , MAA^+ and uncharged $M(AA)_2$, the latter being distributed between the organic and aqueous phases. M^{2+} here denotes the Pa(IV) ion in the aqueous phase which must be either PaO^{2+} or $Pa(OH)_2^{2+}$. The stability constants for the Pa(IV)-acetylacetone complexes were calculated as $\log K_1 = 6.1$, $\log K_2 = 13.15 \pm 0.13$ and $\log K_3 ((M(AA)_2)_{org} / (M(AA)_2)) = 2.07 \pm 0.10$. For the extraction reaction $M^{2+} + 2HAA(org) \rightleftharpoons M(AA)_2(org) + 2H^+$, the constants $\log K_D = -4.13 \pm 0.05$, $\Delta H = 30 \pm 2$ kJ/mole and $S = 22 \pm 9$ J/mole deg were calculated.

2. Extraction with acetylacetone in the presence of sulphate

The distribution of Pa(IV) between a dilute solution of HAA in benzene and 1 M $(Na,H)ClO_4$ was drastically changed in the presence of sulphate, see Fig.1. A new extraction system $M(AA)_3$ was progressively developed, at the expense of the $M(AA)_2$ system, with increasing sulphate concentration (at constant pH).

It was concluded, from the sulphate dependence of the distribution of Pa(IV) ($\log D / \log (\text{SO}_4) = -1$), that there was only one sulphate molecule per Pa(IV) complex.

The combined results from the investigations of the influence of the concentrations of acetylacetone, sulphate and hydrogen ions led to the conclusion that the dominating reaction is



with the equilibrium constants $\log K_D = -8.17 \pm 0.06$, $H = 14.3 \pm 0.3$ kJ/mole and $S = 110 \pm 11$ J/mole/deg. The stability constants for formation of the Pa(IV) acetylacetone complexes from the Pa(IV) sulphate complex $n = (\text{Pa}(\text{OH})(\text{AA})_n^{(3-n)+} (\text{SO}_4^{2-})^n) / (\text{Pa}(\text{OH})\text{SO}_4^+ (\text{AA}^-)^n$ were calculated to be $\log K_2 = 12.3 (\pm 0.1)$ and $\log K_3 = 18.34 \pm 0.10$. The distribution constant $K_3 = (\text{Pa}(\text{OH})(\text{AA})_3)_{\text{org}} / (\text{Pa}(\text{OH})(\text{AA})_3)$ was found, as expected, to be greater than the corresponding K_2 ($\log K_3 = 2.54 \pm 0.06$ compared to $\log K_2 = 2.07 \pm 0.10$).

3. Extraction with tri-n-octylphosphine oxide (TOPO)

The distribution of Pa(IV) between dilute solutions of TOPO (0.0003-0.05 M) in benzene, and perchlorate media of different molarity (0.1-5.9), see Fig.2, shows that Pa(IV) is extracted as an ion-pair solvated with two TOPO molecules ($\log D / \log (\text{TOPO}) = 2$) over the pH range 0-3. This indicates that the dominating ionic form of Pa(IV) in the aqueous phase does not alter over this interval. The distribution of Pa(IV) was constant for pH 1-3 but for pH 1 there was a sharp decrease in the extraction of Pa(IV); this was a result of the extraction of HClO_4 at higher acidities than 0.1 M.

The very strong dependence on the extraction of the perchlorate concentration ($\log D / \log (\text{ClO}_4) = 2$) suggests that the extracted Pa(IV) aggregates contain two perchlorate anions, which implies that Pa(IV) exists as a doubly charged cation M^{2+} , i.e. $\text{Pa}(\text{OH})_2^{2+}$ or PaO^{2+} . The extraction constant and the corresponding thermodynamic constants for the extraction reaction $\text{M}^{2+} + 2\text{ClO}_4^- + 2\text{TOPO}(\text{org}) \rightleftharpoons (\text{M}^{2+}(\text{TOPO})_2)(\text{ClO}_4^-)_2(\text{org})$ at 25°C (pH 1-3) were calculated to be $K_D = 4.41 \pm 10$, $H = -72 \pm 9$ kJ/mole and $S = -157 \pm 31$ J/mole/deg.

4. Extraction with acetylacetone in the presence of EDTA

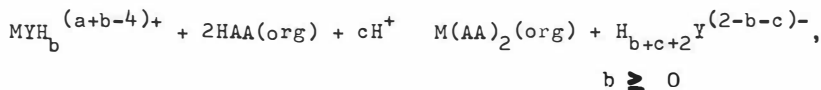
The influence of the presence of EDTA (ethylenediaminetetraacetic acid, 10^{-5} - 10^{-3} M) on the distribution of Pa(IV) between 2.16 M acetylacetone in benzene and 1M (Na,H)ClO₄ (pH 0-2, at 25°C) was investigated.

The following limiting dependences on the extraction, as the complexation of Pa(IV) with EDTA increases, were found (see Fig.3):

$$\log D / \log (\text{EDTA})_{\text{tot}} = -1, \quad \log D / \log (\text{HAA})_{\text{org}} = 2 \text{ and}$$

$$\log D / \log (\text{H}^+) = 2$$

A general extraction reaction is proposed based on the dominating species in the two phases:



where $\text{H}_4\text{Y} = \text{EDTA}$ and $\text{M}^{2+} = \text{Pa}(\text{OH})_2^{2+}$ or PaO^{2+}

The main Pa(IV) - EDTA complexes may be derived from the extraction reaction by considering that in the pH range 1.3-1.9, $c = 2$ ($\log D / \log (\text{H}^+) = 2$) and that the dominating EDTA species⁹ are H_3Y and H_5Y^+ .

Consequently, MY^{2-} and MYH^- are suggested to be the dominating Pa(IV)-EDTA species.

The experiments are still in progress and more detailed information will be published elsewhere.

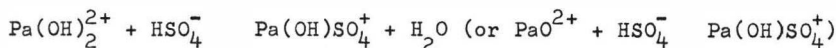
5. Extraction with TOPO in presence of sulphate

The influence of sulphate on the TOPO extraction system (see part 3) was investigated at 25°C in the pH range 0.6-2.7. The TOPO concentration was 0.0066 M and the aqueous phase consisted of mixtures of 1 M (Na,H,0.01 Cr)ClO₄ and 1 M Na₂SO₄. The ionic strength was somewhat increased (1.0 to 1.2) and the perchlorate concentration decreased (1.0 to 0.9) by the

addition of 1 M Na_2SO_4 . The influence of these changes on the distribution was, however, neglected as they have opposite effects.

A plot of the distribution ($\log D$) against $\log (\text{Na}_2\text{SO}_4)$ (Fig.4) shows a maximum slope, $\log D / \log (\text{Na}_2\text{SO}_4)$, of -1 which indicates that a 1:1 Pa(IV) sulphate complex is formed. As the complexation between Pa(IV) and sulphate was decreased at increased pH the ionic form of the sulphate molecule involved in the reaction formula must be HSO_4^- , as (HSO_4^-) is also decreased at increased pH.

The complex formation can be expressed as



The same reaction was found in the pH range 0.4-1.1 at an ionic strength of 0.50 and a temperature of 10°C , from a solvent extraction investigation¹⁰ using HTTA (thenoyl trifluoroacetone) as extracting agent.

The stability constant calculated from the present data $K = 10^{2.8 \pm 0.1}$ ($\mu = 1$, pH 0.6-2.7, 25°C) is not very different from that obtained in the HTTA investigation $K = 10^{2.50}$ ($\mu = 0.50$, pH 0.50, 10°C). (The concentration of HSO_4^- was calculated using $K(\text{HSO}_4^-)/(\text{H}^+)(\text{SO}_4^{2-}) = 10^{1.00}$, literature values are $K = 10^{0.76}$ (ref. 11) and $K = 10^{1.02}$ (ref. 12).

DISCUSSION

The present study of the aqueous chemistry of tetravalent protactinium shows that Pa(IV) exists as a doubly-charged cation $\text{Pa}(\text{OH})_2^{2+}$ or PaO^{2+} in the pH range from 0 up to at least 3. This pH range was studied using both HAA (Fig.3 and 1) and TOPO as extracting agents (with HAA even higher pH was investigated but no further hydrolysed species were observed for pH 6). However, solvent extraction investigations using HTTA (Thenoyl trifluoroacetone) indicate⁴ that a progressive hydrolyzation of Pa(IV) occurs so that $\text{Pa}(\text{OH})_2^+$ (or $\text{PaO}(\text{OH})^+$) is developed already at pH 1. Another study¹⁰ indicates, however, that $\text{Pa}(\text{OH})_2^{2+}$ (or PaO^{2+}) is the dominating species in the pH range 0.4-1.1.

The oxygen (or the hydroxyl groups) on Pa(IV) must be firmly attached because neither EDTA nor HAA was able to remove it (or any of them). HTTA, however, seems to have enough complexing power to achieve this and to form tetrakis complexes $\text{Pa}(\text{TTA})_4$. Normally, only two HAA molecules can be bound to Pa(IV), but a third HAA molecule was found to enter after protonization (or dehydrolysatation) of Pa(IV) with sulphate (forming $\text{Pa}(\text{OH})\text{SO}_4^+$).

The very broad pH range where $\text{Pa}(\text{OH})_2^{2+}$, or PaO^{2+} , diminishes, together with the very high stability of this ion towards EDTA and HAA, makes the PaO^{2+} more probable than $\text{Pa}(\text{OH})_2^{2+}$.

ACKNOWLEDGEMENT

The author is indebted to Professor J. Rydberg, Dr. J.O. Liljenzin and civ.ing. S. Wingefors for valuable discussions and suggestions and to ing.M.Ohlson for experimental help. The EDTA part of this study was based on diploma work by civ.ing. J-E.Anderson. Ph.D. C. Coombes revised the English of the manuscript and Miss.C. Hard af Segerstad kindly made the typewriting.

REFERENCES

1. Noren, B. Acta Chem. Scand. **27** (1973) 1369
2. Guillaumont, R., Bouissieres, G. and Muxart, R. Actinides Rev. **1** (1968) 135
3. Pal shin, E.S., Myasoedov, B.F. and Davydov, A.V. "Analiticheskaya khimiya protaktiniya", Analiticheskaya Khimiya Elementov, Moscow, Izdatel stvo Nauka, 1968.
4. Guillaumont, R. Compt. Rend. Acad. Sci. Paris, **260**(1965)1416
5. Lundqvist, R. "Aqueous Chemistry of Protactinium(IV). 1. "Acta. Chem. Scand. A, **28** (1974), in press.
6. Lundqvist, R. and Rydberg, J. "Aqueous Chemistry of Protactinium(IV). 11." Acta Chem. Scand. A, in press.
7. Lundqvist, R. "Aqueous Chemistry of Protactinium(IV). 111." Acta Chem. Scand. A, in press.
8. Rydberg, J. Rec. Trav. Chim. **75** (1956) 737
9. Anderegg, G. Helv. Chim. Acta. **50** (1967) 2333.
10. Mitsuji, T. Bull. Chem. Soc. Japan **41** (1968) 115
11. Reynolds, W.L. and Fukushima, S. Inorg. Chem **2** (1963) 176
12. Eichler, E. and Rabideau, S.J. Amer. Chem.Soc. **77** (1955)5501.

Figure 1. Distribution of $^{233}\text{Pa}(\text{IV})$, at 25°C , between dilute solutions (0.1-2.5 M) of acetylacetone HAA in benzene and 1 M $(\text{Na,H})\text{ClO}_4$ (line 1) and 0.94 M $(\text{Na,H})\text{ClO}_4$ + 0.059 M Na_2SO_4 (line 2) as a function of pAA ($= -\log(\text{AA}^-)$). The solid lines are calculated from estimated stability constants.

Figure 2. Distribution of $^{233}\text{Pa}(\text{IV})$ between dilute solutions of tri-n-octyl-phosphine oxide (TOPO) in benzene and perchlorate media at pH 1 and 25°C .

$$(\text{ClO}_4^-) = 5.93 \text{ M}$$

$$(\text{ClO}_4^-) = 1.03 \text{ M}$$

$$(\text{ClO}_4^-) = 0.13 \text{ M}$$

Figure 3. Distribution of $^{233}\text{Pa}(\text{IV})$, at 25°C , between 2.16 M acetylacetone in benzene and dilute solutions of EDTA in 1 M $(\text{Na,H})\text{ClO}_4$ as a function of pH ($= -\log(\text{H}^+)$).

$$(\text{EDTA}) = 0 \text{ M}$$

$$(\text{EDTA}) = 10^{-3.92} \text{ M}$$

$$(\text{EDTA}) = 10^{-3.25} \text{ M}$$

Figure 4. Distribution of $^{233}\text{Pa}(\text{IV})$, at 25°C , between 0.0066 M tri-n-octyl-phosphine oxide (TOPO) in benzene and mixtures of 1 M Na_2SO_4 and 1 M $(\text{Na,H})\text{ClO}_4$ at different pH ($= -\log(\text{H}^+)$)

$$\text{pH } 0.65$$

$$\text{pH } 1.99$$

$$\text{pH } 1.07$$

$$\text{pH } 0.65$$

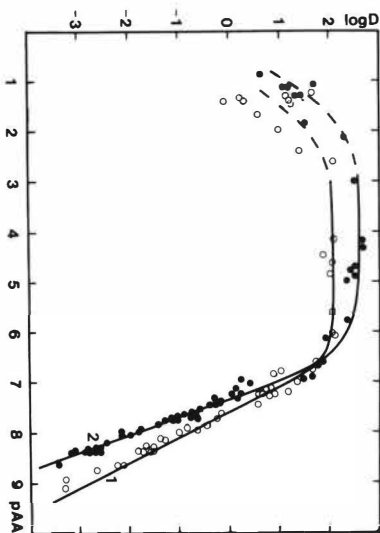


Figure 1. Distribution of $^{233}\text{Pa(IV)}$, at 25°C , between dilute solutions (0.1–2.5 M) of acetylacetone HAA in benzene and 1 M $(\text{Na,H})\text{ClO}_4$ (line 1) and 0.94 M $(\text{Na,H})\text{ClO}_4 + 0.059 \text{ M Na}_2\text{SO}_4$ (line 2) as a function of pAA ($= -\log[\text{AA}]$). The solid lines are calculated from estimated stability constants.

Figure 4. Distribution of $^{233}\text{Pa(IV)}$, at 25°C , between 0.0066 M tri-n-octyl-phosphine oxide (TOPO) in benzene and mixtures of 1 M Na_2SO_4 and 1 M $(\text{Na,H})\text{ClO}_4$ at different pH ($= -\log[\text{H}^+]$).

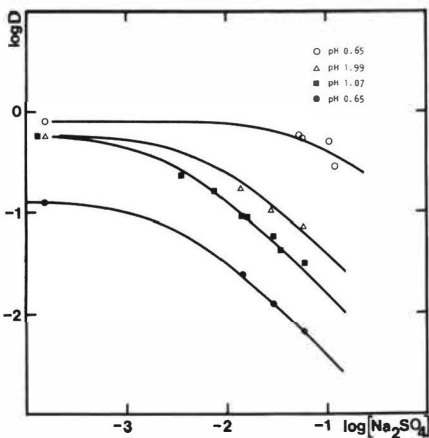


Figure 2. Distribution of $^{233}\text{Pa(IV)}$ between dilute solutions of tri-n-octyl-phosphine oxide (TOPO) in benzene and perchlorate media at pH 1 and 25°C .

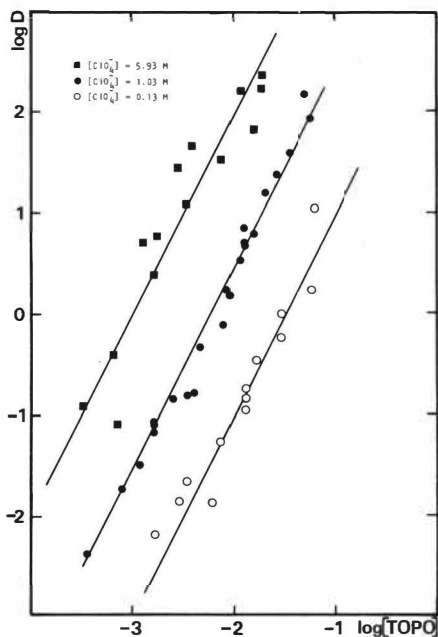
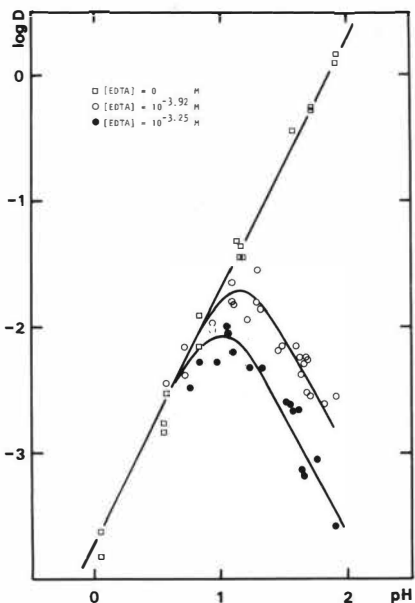


Figure 3. Distribution of $^{233}\text{Pa(IV)}$, at 25°C , between 2.16 M acetylacetone in benzene and dilute solutions of EDTA in 1 M $(\text{Na,H})\text{ClO}_4$ as a function of pH ($= -\log[\text{H}^+]$).



MEDIA

Zdenek Malek, Daria Schrotterova, Vera Jedinakova,
Miroslav Mrnka, Jiri Celeda,
Prague Institute of Chemical Technology, Department of
Nuclear Fuel Technology and Radiochemistry, Czechoslovakia.

The mechanism of the extraction of zirconium from aqueous sulphate solutions by tri-n-octylamine (TOA) dissolved in benzene has been investigated using chemical and radiometric analysis of the organic phase (with results evaluated by means of the saturation method and logarithmical analysis of the extraction curves). Infrared spectrometry and cryoscopic and viscometric measurements have also been employed. Evidence has been obtained for zirconium being extracted as a dimeric hydrated sulphato-zirconate of TOA containing 8 R_3NH^+ cations and 8 H_2O molecules per 2 Zr atoms. The ratio of the ligands SO_4^{2-} and OH^- (or O^{2-}) has not been determined.

INTRODUCTION

The mechanism of the extraction of rare metal salts by organic amines from sulphate media has not yet been successfully elucidated. Moreover, there is not satisfactory knowledge of the degree of formation of the various zirconium complexes occurring in the aqueous phase, nor on the nature of the extracted species. Even information on the formula of the extracted complex is incomplete and ambiguous. In determining the composition of the extracted species, contradictory results are obtained depending on the method used.

The first question which has to be decided in investigating the amine extraction of sulphate complexes of metals is the structure and chemical composition of the sulphate of the amine in the organic phase, this salt acting as the actual extractant.

We have investigated this problem in our laboratory ¹⁾, using a number of methods, and have obtained the evidence that at low H_2SO_4 concentrations of the aqueous phase ($c_{\text{H}_2\text{SO}_3}^0$ c_A) the prevailing species in the benzene phase is the monomeric sulphate hydrate $(\text{R}_3\text{NH})_2\text{SO}_4 \cdot x\text{H}_2\text{O}$ where $x=4$ to 6 (as found from the Karl Fischer determination of the water content in the organic phase). The free amine is present in anhydrous benzene solutions as monomeric molecules. At higher H_2SO_4 concentrations ($c_{\text{H}_2\text{SO}_4}^0$ c_A) there is an excess acid extraction in the proportion of 1 molecule of H_2SO_4 per 2 molecules of the sulphate, and the cryoscopic degree of polymerization of amine in this salt is equal to 4. These results indicate the formation of a mixed normal and acid salt, the predominating species being $(\text{R}_3\text{NH})_2\text{SO}_4 \cdot 2(\text{R}_3\text{NH})\text{HSO}_4$, which is hydrated by several H_2O molecules. A comparison with the amine salts of other acids shows that the moiety responsible for this increased hydration is the doubly charged anion SO_4^{2-} . When the acidity of the aqueous phase has exceeded the limits corresponding to 1 to 2 mol/dm⁻³ H_2SO_4 , the predominant species in the organic phase is the dimeric monohydrate of the amine hydrosulphate $(\text{R}_3\text{NHHSO}_4 \cdot \text{H}_2\text{O})_2$, which at concentrations of the acid as high as 5 or 6 mol dm⁻³, i.e. in the region where the water activity is lowered to some 50%, transforms into an anhydrous trimer of the amine hydrosulphate $(\text{R}_3\text{NHHSO}_4)_3$.

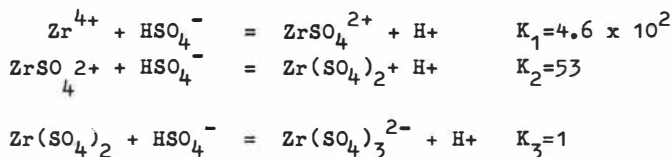
Of course, the regions of existence of these species overlap and there are ranges where two or more individual species co-exist in the organic phase. In principle, the exact proportion in which each of them is present may be determined from a detailed investigation of all corresponding extraction equilibria in the system $\text{H}_2\text{SO}_4\text{-H}_2\text{O-TOA-benzene}$.

Sulphate solutions of zirconium have been the subject of investigation of a number of authors. Quite a number of salts with various metal-anion ratios have been prepared. Studies of infra-red spectra and other methods have shown that the Zr=O bond, characteristic for the zirconyl cation, does not occur in the sulphate complexes of zirconium (IV) in aqueous solutions.

* C^0 refers to an initial concentration in the aqueous phase.

_A refers to the formed conc. of amine.

Even at relatively low concentrations of sulphuric acid there exist neutral or anionic complexes $\text{Zr}(\text{SO}_4)_x / 2^{(x-2)-}$. The following equilibrium constants for complex formation have been found:



Hydrolysis of sulphate-complexes of zirconium was found at concentrations of sulphuric acid lower than 0.5 mol dm^{-3} . The predominant form of zirconium (IV) in the concentration range of sulphuric acid around 1 mol/dm^{-3} is the $\text{Zr}(\text{SO}_4)_3^{2-}$ complex.

The extraction of sulphato-complexes of zirconium has been investigated by Yagodin, Chekmarev and Vladimirova²⁾, who determined the amine-to-metal ratio in the organic phase saturated with metal to be 4:1. The composition of the extracted species was studied by the saturation method, as well as by the method of the logarithmic dependence of the metal distribution ratio on the concentration of the amine salt. The authors assume the extraction of $(\text{R}_3\text{NH})_4\text{Zr}(\text{SO}_4)_4$ species, however, without giving any detailed data about the degree of polymerization in the organic phase, nor about the co-extraction of water an attempt to elucidate these details has been made in the present work.

EXPERIMENTAL

The dependence of zirconium (IV) extraction on the concentration of acid, sulphate ions, and amine was measured. By the method of saturating the organic phase with the metal, the amine-to-metal ratio in the extracted compound was determined. The zirconium concentrations in the organic and aqueous phases were determined either radiometrically, employing ^{95}Zr , or by complexometric titration (xylene orange as indicator).

Cryoscopic and viscometric measurements were carried out by standard methods. The water in the organic phase was determined by use of the Karl Fischer reagent.

Infra red spectra of the organic phases were recorded by using a 325 Perkin-Elmer instrument with AgCl cells in the range of $800-4000\text{cm}^{-1}$ for the following conditions.

- a) 0.2 mol dm^{-3} amine equilibrated with $1.5\text{ mol dm}^{-3}\text{ H}_2\text{SO}_4$ as aqueous phase.
- b) zirconium (IV) extracted at varying sulphuric acid concentrations ($c_{\text{Zr}}^0\ 9\text{g dm}^{-3}$, $c_{\text{TOA}}\ 0.2\text{ mol dm}^{-3}$, $c_{\text{H}_2\text{SO}_4}^0\ 0.3-3\text{mol dm}^{-3}$)
- c) ditto with higher zirconium and amine concentration ($c_{\text{Zr}}^0\ 18\text{g dm}^{-3}$, $c_{\text{TOA}}\ 0.5\text{mol dm}^{-3}$, $c_{\text{H}_2\text{SO}_4}^0\ 0.9-2.0\text{mol dm}^{-3}$ $c_{\text{Zr}}^0\ 3\text{ to }24\text{gdm}^{-3}$).

RESULTS AND DISCUSSION

In Fig.1. is shown the dependence of zirconium extraction on the initial concentration of metal in the aqueous phase (system of 0.25 mol dm^{-3} TOA benzene - 1 mol dm^{-3} sulphuric acid). The results correspond with those of Yagodin and co-workers²⁾, i.e. at a sulphuric acid concentration of 1 mol dm^{-3} the amine is saturated at an amine-to-metal ratio of 4:1. Very different results are obtained for zirconium extraction in the system TOA-kerosene- $1\text{ mol dm}^{-3}\text{ H}_2\text{SO}_4$ (where the amine-to-metal ratio in the organic phase has been found to be 6:1). Moreover, in extraction by benzyloctylamine, a secondary amine, (0.1mol dm^{-3} amine-kerosene- $2\text{mol dm}^{-3}\text{ H}_2\text{SO}_4$) the amine-to-metal ratio is still higher. For further investigations we have chosen the system with benzene as solvent, where it is possible to carry out studies by infra-red spectroscopic as well as cryoscopic methods.

From the dependence of the metal distribution ratio D_{Zr} on the concentration of the extracting agent at very low metal concentrations (radioisotope ^{95}Zr) it was found that the slope of the curve $\log D_{\text{Zr}}$ vs. $\log c_{\text{A}}$ does not reach the expected value 4, as would have corresponded to the results obtained by the saturation method at macroscopic concentrations of zirconium, but only the value 1. The same result is referred to in paper²⁾. The authors explain this discordance by the non-ideality of the

organic phase, i.e. by the aggregation of the amine salt. They assume that the amine salt present in the organic phase exists as aggregates, consisting of m monomeric salt molecules; the exponent in the dependence of D_{Me} on c_A would not be n (the number of molecules of the extractant in the extracted complex species) but n/m . Therefore, the observed slope 1 may be explained on the basis that the four TOA molecules are not combining with the zirconium ion separately as free particles, but that they are bonded in a single aggregated particle. The only form of the sulphates of TOA which suits this requirement (from all those which have been detected in the organic phase, is the species $(R_3NH)_2SO_4 \cdot 2R_3NHHSO_4$ hydrated by several water molecules. From this it follows that the results of logarithmic analysis of distribution curves cannot be applied for the determination of the formula of the extracted species. If we consider (in agreement with the results hitherto obtained in connection with sulphato-complexes of zirconium, only $Zr-SO_4$ complexes and no extraction of mixed sulphato-oxo or sulphato-hydroxo complexes, then the results obtained by the saturation method, together with those obtained from slope analysis of the extraction curves at trace concentrations of zirconium may be interpreted in terms of the overall reaction scheme

$$\begin{aligned} & /Zr(SO_4)_x /^{2(x-2)-} + / (R_3NH)_2SO_4 \cdot 2(R_3NH)HSO_4 /_{org} = \\ & = / (R_3NH)_4Zr(SO_4)_4 /_{org} + (3-x)H^+ + (x-1)HSO_4^- \end{aligned}$$

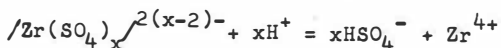
At higher H_2SO_4 concentrations where bisulphate is the predominant species in both the organic and aqueous phase, the extraction process may be described by the equation

$$\begin{aligned} & /Zr(SO_4)_x /^{2(x-2)-} + 2/(R_3NH \cdot HSO_4)_2 /_{org} = \\ & = / (R_3NH)_4Zr(SO_4)_4 /_{org} + (4-x)H^+ + xHSO_4^- \end{aligned}$$

with the dimeric hydrated TOA bisulphate prevailing in the organic phase.

According to these two equations, H^+ ions should have an unfavourable effect on the extraction of zirconium in all cases where the metal is present in the aqueous phase as sulphato-complexes with x lower than 3 or 4. Increasing concentration of sulphat has initially a positive influence, as long as there are no sulphato-complexes in the solution (i.e. $x=0$), or, in the case of the normal TOA sulphate co-existing with the bisulphate, as long as the complexing of the metal has not exceeded the value $x=1$ in the aqueous phase. Further increase of sulphate above this limit has a negative effect on the extraction of zirconium.

The H^+ ions compete with Zr^{4+} for the ligand SO_4^{2-} in displacing the metal ion from the complex:



This is a simple competition of two acidic ions (H^+ and Zr^{4+}) for a common base (SO_4^{2-}). This fact becomes obvious from fig.2 as well as from the i.r. spectra.

In the infra-red spectra of the organic phase containing extracted sulphuric acid the band corresponding to the stretching vibration of bisulphate becomes visible at $850cm^{-1}$ which is in good agreement with the values $844-877cm^{-1}$ found for similar systems by other authors. Furthermore, the entering of sulphate into association with TOA resulted in the appearance of distinct absorption bands at $1235, 1156, 1056cm^{-1}$ (published values $1232, 1156$ and $1060cm^{-1}$).

The absorption band of S-OH ($850cm^{-1}$) characteristic of extracted amine bisulphate gradually diminishes with extraction of the metal, although it is particularly evident at the lower concentrations of zirconium in the organic phase. At metal concentrations c_{Zr}^o higher than $6g\ dm^{-3}$ it is completely absent. At constant initial concentrations of the metal the appearance of the bisulphate band is shifted with higher concentrations of sulphuric acid and its intensity increases with increasing acid concentrations in the range of $c_{H_2SO_4}$ between 1.45 and $3.0mol\ dm^{-3}$.

This may serve as evidence that there is no bisulphate present in the organic phase at sulphuric acid concentrations lower than 1.5 mol dm^{-3} and c_{Zr}° higher than 6 g dm^{-3} .

The extraction of zirconium is connected with the appearance of new absorption bands at 943 and 998 cm^{-1} , corresponding to the Zr-O-S stretching vibration; these increase in intensity simultaneously with the weakening of the HSO_4^- band at 850 cm^{-1} as the metal concentration is increased. At the same time there is an increase of the intensity of the SO_4^{2-} band at 1162 cm^{-1} as well as of the other two sulphate stretching vibrations which are shifted from 1158 and 1235 cm^{-1} to 1150 and 1260 cm^{-1} , respectively. When the concentration of sulphuric acid is increased at constant metal concentration (e.g. $c_{\text{Zr}}^{\circ} = 9 \text{ g dm}^{-3}$), the intensity of the sulphate-zirconate bands at 943 and 998 cm^{-1} decrease, the HSO_4^- band on 850 cm^{-1} appears with growing intensity and the bands at 1150 and 1260 cm^{-1} are shifted back again to their original positions. This shows that the ions H^+ actually destroy the sulphato-complexes of Zr^{4+} in the organic phase by displacing the ions Zr^{4+} and converting the ligands SO_4^{2-} into free bisulphate ions.

The amount of water extracted into the organic phase is proportional to the concentration of the amine and does not depend on the metal concentration. When comparing the i.r. spectra of the $\text{TOA-H}_2\text{SO}_4$ system with the spectra of the organic phases containing zirconium, a slight shift becomes visible in the OH band of water from some 3450 to 3495 cm^{-1} , which shows that the hydrogen bond between water and the complex anion is weaker than in the case of the simple SO_4^{2-} anion. From the determination of water in the organic phase by using the Karl Fischer reagent, it was observed that in the concentration range of the acid and metal investigated in the present work, water is always present and the constant amine-to- H_2O ratio $1:1$ remains unchanged. Hence one may infer that the basic structure of the amine salt remains unaffected by the metal extraction. The metal complex seems only to associate with the salt, without any substantial changes in its structure and degree of hydration.

Cryoscopic measurements of the organic phase over a broad concentration range of sulphuric acid and zirconium (IV) have shown that the extracted metal complex is present as a dimer at macroscopic concentrations of the metal; this is in contrast to the 1:1 slope observed at micro-concentrations, where the dimers must necessarily dissociate into monomeric species.

CONCLUSIONS

1. It has been deduced from results obtained by the saturation method, that the metal-to-amine ratio in the case of zirconium, extracted by solutions of tri-n-octylamine in benzene from aqueous solutions of sulphuric acid is equal to 1:4.

2. At H_2SO_4 concentrations in the aqueous phase lower than 1.5 mol dm^{-3} the protons in the TOA bisulphate present in the organic phase are quantitatively displaced by Zr^{4+} , and the HSO_4^- ions are thus converted into deprotonated SO_4^{2-} ligands bound to zirconium.

3. At higher H_2SO_4 concentrations there is a competition between the cations H^+ and Zr^{4+} for the anions SO_4^{2-} , the result of which is a decrease of the metal extraction due to the sulphatozirconate of TOA in the organic phase being destroyed and the ligands SO_4^{2-} transformed back into TOA bisulphate.

4. Water is coextracted at higher H_2SO_4 concentrations, giving a water-to-amine ratio of 1:1, independently of the amount of zirconium extracted by the TOA sulphate. At very high H_2SO_4 concentrations (above 6 mol dm^{-3}) a dehydration of the organic phase sets in.

5. From the results it is inferred that zirconium is extracted at macroconcentrations of the metal in the form of the hydrated dimeric TOA sulphatozirconate $/(R_3^{\text{NH}})_4\text{Zr}(\text{SO}_4)_4 \cdot 4\text{H}_2\text{O}/_2$.

6. These conclusions cannot be generalized to apply to the amine extraction of zirconium sulphates in diluents other than benzene.

REFERENCES

- 1) Mrnka, M., Satrova, J., Jaderna energie (to be published)
- 2) Yagodin, G.A. Chekmarev, A.M., Vladimirova, L.M.
Zh.neorg.khim., 14, 1603 (1969).

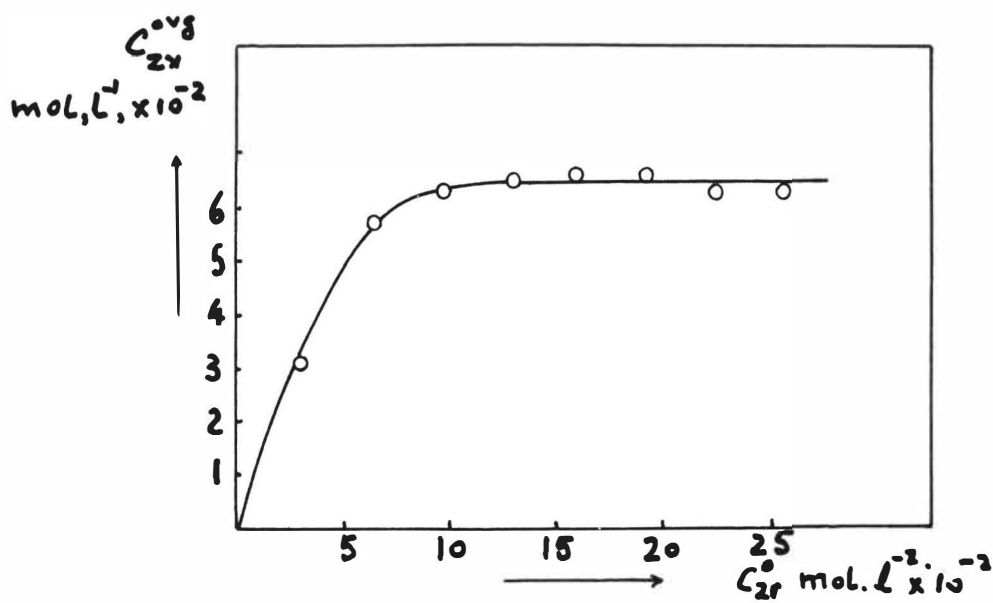


Figure 1.

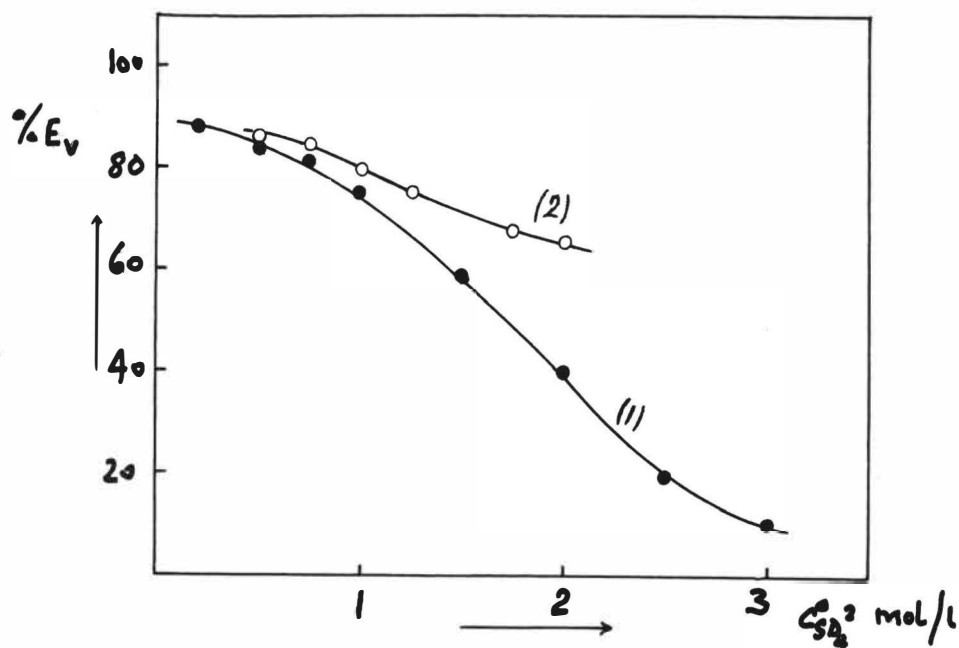


Figure 2.

Abstract

From chemical analysis of the organic phase and from cryoscopic and viscosity measurements, as well as from the infra-red spectra of the organic phase in the normal (H₂O-HCl) and the deuterated (D₂O-DCl) system, it is concluded that as the HCl concentration increases, HCl adducts of TDPO.H₂O are first formed, and then anhydrous adducts of TDPO. The adducts are in some degree polymerised.

Introduction

It has been shown⁽¹⁾ that among organic derivatives of orthophosphoric acid the polarity of the PO group increases in the order phosphate < phosphonate < phosphinate < phosphine oxide. On this account special attention has been paid to the phosphine oxides, which for the majority of metals give the highest values of the distribution ratio and in some cases high selectivity for particular metals.

The extraction of metals and acids is usually accompanied by the extraction of water and water is indeed soluble in the phosphine oxide/diluent mixtures themselves, where it bonds with the phosphine oxide molecules. The degree of hydration of the phosphine oxide increases with its concentration⁽²⁾ and depends on the type of the diluent⁽³⁾ and on the temperature.⁽⁴⁾ In < 0.1M TBPO or TOPO the monohydrates TBPO.H₂O⁽⁵⁾ and TOPO.H₂O⁽⁶⁾ predominate. At higher concentrations of the extractant associates of the type mTXPO.nH₂O (X = alkyl) have been found, where m,n > 1.⁽⁴⁻⁶⁾

In experiments on mineral acid extraction by phosphine oxides (HNO₃,⁽⁷⁻¹⁰⁾ H₂SO₄,^(7,11,12) HCl^(8,13)) it was found that associates between the phosphine oxide and the acid may be anhydrous as well as hydrated: the degree of hydration depends on the concentrations of the acid and the extractant, and on the diluent used. Thus in the extraction of HCl by 1.25M TOPO in octane⁽⁸⁾ the species found in the organic phase were 2TOPO.2H₂O.HCl at < 2M HCl (aq), and 2TOPO.2H₂O.2HCl at 4M HCl (aq). Similarly in the extraction of HCl by TBPO in CCl₄ at < 2.5M HCl (aq) the prevailing species in the organic phase⁽¹³⁾ are TBPO.HCl.nH₂O and 2TBPO.HCl.nH₂O (n = 1-3), the latter being formed by dipole-dipole interaction between the former species and molecules of free TBPO.

In the present work the mechanism of the extraction of HCl by tri-*n*-decyl phosphine oxide (TDPO) solutions in benzene has been investigated by determining the co-extraction of water and the degree of association of the extractant in the organic phase as measured cryoscopically. As an auxiliary guide in evaluating the experimental results, the infra-red spectra of the organic phases in the systems HCl-H₂O-TDPO-benzene and ²HCl-²H₂O-TDPO-benzene were examined.

Materials and Methods

Hydrochloric acid was of A.R. grade. The deuterated acid was prepared

from POCl_3 by reaction with $^2\text{H}_2\text{O}$, and the degree of deuteration was tested mass spectrometrically.

The TDPO was of commercial purity and was used without further purification and dissolved in A.R. benzene.

The freezing point of the organic phase was determined by a standard cryoscopic method and its viscosity was measured by means of an Ubbelohde viscometer at 25°C . Water was determined by the Karl Fischer method.

Infra-red spectra between $700\text{--}4000\text{ cm}^{-1}$ were recorded with a Perkin-Elmer 325 instrument.

The extraction experiments were carried out at $25 \pm 2^\circ\text{C}$. Equal volumes of the aqueous and organic phases (20 ml of each in the case of HCl and 1 ml of each in the case of ^2HCl) were shaken for 10 min, this time having been established as sufficient for full equilibration.⁽¹⁾ Three TDPO concentrations were used: 0.12M, 0.25M and 0.30M.

Results and Discussion

Fig. 1 shows that $[\text{HCl}]_{\text{org}}$ increases steadily with $[\text{HCl}]_{\text{aq}}$ and that the $[\text{HCl}]_{\text{aq}} : [\text{TDPO}]_{\text{org}}$ ratio reaches unity at 6-7M HCl (aq). It also shows that the $[\text{H}_2\text{O}]_{\text{org}} : [\text{TDPO}]_{\text{org}}$ ratio is approximately unity over the range 0-4M HCl (aq), and thereafter decreases. These results strongly suggest the formation of monohydrates, viz. $\text{TDPO} \cdot \text{H}_2\text{O}$ in the absence of HCl, and of $\text{TDPO} \cdot \text{mHCl} \cdot \text{H}_2\text{O}$ as HCl is added to the system up to 4M HCl (aq). At higher HCl concentrations, anhydrous compounds must be formed.

The results in Fig. 2 indicate increasing polymerisation as the HCl concentration increases, although they are difficult to interpret quantitatively. If in the range 0-4M HCl (aq) the HCl entering the organic phase adds on to $\text{TDPO} \cdot \text{H}_2\text{O}$, as we have suggested, then the fall in Δt as $[\text{HCl}]_{\text{org}}$ increases, implies that the $\text{TDPO} \cdot \text{mHCl} \cdot \text{H}_2\text{O}$ species must be more highly polymerised than $\text{TDPO} \cdot \text{H}_2\text{O}$. The continuing fall in Δt at higher HCl concentrations implies a still greater degree of polymerisation of the anhydrous $\text{TDPO} \cdot \text{mHCl}$ compounds. How far $\text{TDPO} \cdot \text{H}_2\text{O}$ itself is polymerised, if at all, cannot be stated, because it is not known how well TDPO-water-benzene solutions obey Raoult's law.

The infra-red results support the conclusions so far reached. There is a sharp peak at 3680 cm^{-1} (OH stretch), indicating the presence of free OH groups, not bonded for example to TDPO, and a broad band at 3360 or 3400 cm^{-1} due to hydrogen-bonded OH groups. The former is produced only by the species $\text{TDPO} \cdot \text{H}_2\text{O}$, and disappears as expected at $> 6\text{M}$ HCl (aq). The latter remains, but shifts to the higher of the frequencies indicated, presumably because the hydrogen bond is weaker in $\text{TDPO} \cdot \text{mHCl} \cdot \text{H}_2\text{O}$ than in $\text{TDPO} \cdot \text{H}_2\text{O}$. At still higher acidities, the broad band also tends to disappear, as anhydrous species are formed.

A similar pattern is observed in deuterated systems, but at lower frequencies, viz. 2700 cm^{-1} (free OD) and about 2480 cm^{-1} (bonded OD).

The PO stretch peak at 1168 cm^{-1} in the absence of HCl is gradually replaced by one at 995 cm^{-1} as HCl is added. Such a large shift cannot be ascribed merely to hydrogen bonding, and indicates protonation of the strongly basic PO group by direct reaction with the extracted HCl. No sharp peak corresponding to free PO-H^+ bonds could be detected either in the non-deuterated or deuterated system, but instead there was a broad absorption continuum in the region $1000\text{--}2500\text{ cm}^{-1}$. A very broad absorption below 2200 cm^{-1} was also observed at high acidities, when the anhydrous adducts are formed.

References

1. Marcus Y., Kertes A.S.: Ion Exchange and Solvent Extraction of Metal Complexes, 1969 (New York, Wiley-Interscience).
2. Higgins C.E., Baldwin W.H.: Anal. Chem. 1960, 32, 233.
3. Klofutar C., Paljk S., Senegachniko M., Jerkovich B.: J. Inorg. Nucl. Chem. 1972, 34, 3873.
4. Lodhi M.A., Danesi P.R., Scibona G.: J. Inorg. Nucl. Chem. 1971, 33, 1889.
5. Rolland G., Duyckaerts, G.: Spectrochim. Acta 1966, 22, 793.
6. Bucher J.J., Diamond R.M.: J. Inorg. Nucl. Chem. 1972, 34, 3531.
7. Martin B., Ockenden D.W., Foreman J.K.: J. Inorg. Nucl. Chem. 1961, 21, 96.
8. Mikhaylichenko A.I.: Radiokhimiya 1970, 12, 594.
9. Zingaro R.A., White J.C.: J. Inorg. Nucl. Chem. 1960, 12, 315.
10. Goffart J., Duyckaerts G.: Anal. Chim. Acta 1967, 38, 529.
11. Goffart J., Duyckaerts G.: Anal. Chim. Acta 1966, 36, 499.
12. Higgins C.E., Baldwin W.H., Ruth J.M.: USAEC Rept. ORNL 1952, 1338.
13. Nikitina G.B., Pushlenkov M.F.: Radiokhimiya 1963, 5, 445.
14. Pinchas S., Laulicht I.: Infra-red Spectra of Labelled Compounds, 1971, p.42 (Academic Press, London and New York).
15. Bellamy L.J.: Novyie dannyye po IK-spectram slozhnykh molekul, 1971, p.258 (Moscow, Mir).

Fig.1 The Extraction of HCl by TDPO in Benzene and the Co-extraction of Water at the Extraction of HCl

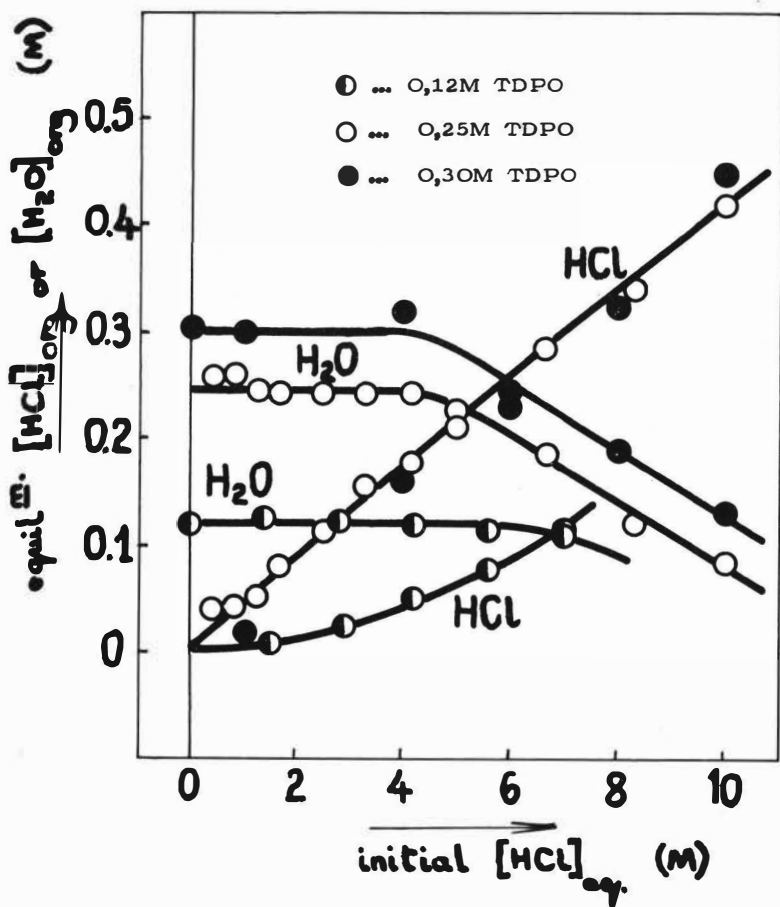
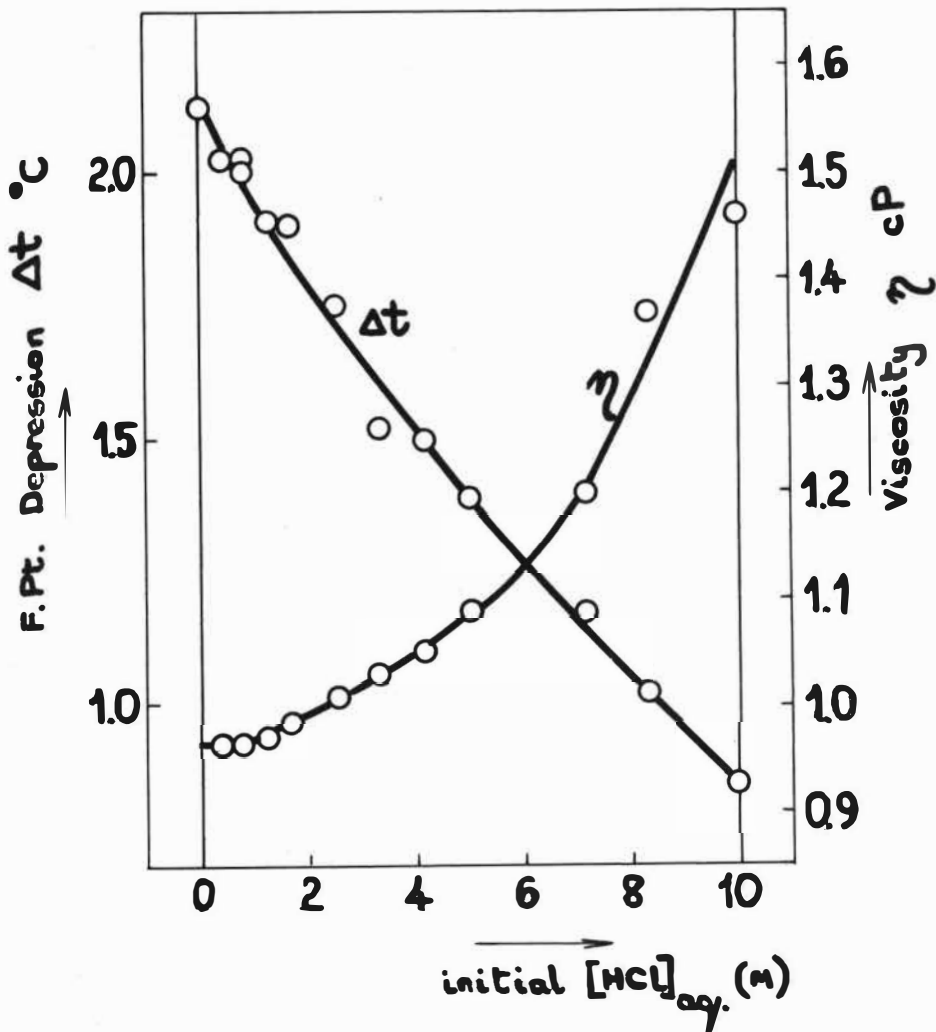


Fig.2 The Dependence of the Freezing Point and Viscosity of the Organic Phase on Starting Concentration of HCl in the Aqueous Phase

The TDPO Concentration : 0,25M



THE KINETICS OF URANEUM, PLUTONIUM, RUTHENIUM AND
ZIRCONIUM EXTRACTION WITH TRIBUTYLPHOSPHATE

by - M.F. Pushlenkov, N.N. Shchepetilnikov, G.I. Kuznetsov,
F.D. Kasimov, A.L. Yasnovitskaya, G.N. Yakovlev

ABSTRACT

The kinetics of the centrifugal extraction of uranium, plutonium, ruthenium, zirconium and nitric acid with tributylphosphate have been investigated. An experimental technique has been developed for making these measurements. It has been established that the rate of uranium plutonium and nitric acid extraction is diffusion controlled. The period of mass transfer (98-99% of the equilibrium state) varies from 0.6-6 sec. The rate of ruthenium extraction is limited by slow chemical reactions in the aqueous phase. It is shown that the centrifugal extractor can be effectively used for uranium and plutonium extraction. In some cases the distribution ratios of the elements can be changed by taking into account the differences in the rate of their extraction.

V.G. Khlopin Radium Institute, Leningrad

INTRODUCTION

Centrifugal extractors have been developed for radiochemical production in the USSR, USA, France, FDR and in some other countries. The high output of these extractors and their comparatively small size, the possibility of using them for work with viscous solutions, the 30-50 fold reduction of phase contact period as compared to gravitational extractors and the corresponding lowering of extractants radiolysis all make the centrifugal apparatus especially effective. Hence, they offer the facility for processing highly radioactive solutions of "hot" fuel elements by extraction with short contact times. Moreover, they may be particularly useful for processing fuel elements from fast neutron reactors.

The duration of the phase contact time in the centrifugal extractor is a few seconds. For example, in small centrifugal extractors (SCE), the phase contact time is 3 sec^{/1/} and 1.8 sec^{/2/}. Therefore, under these conditions, it is necessary to know the period required for the essentially complete mass transfer of the components concerned. It seems impossible to calculate the period necessary for mass transfer in centrifugal extractors from the results of several papers which have been published on the kinetics of extraction of the actinides of uranium, for example^{/3/6}, as the experiments were carried out under conditions that were quite different from the mixing conditions appertaining to a centrifugal apparatus.

This work is dedicated to the investigation of the kinetics of the extraction of uranium, plutonium, ruthenium and zirconium with tributylphosphate in a diluent when the process is carried out in the centrifugal extractor (SCE).

EXPERIMENTAL

Methods - Methods based on a SCE were worked out and the installation was set up for the investigation of the extraction process kinetics in the centrifugal apparatus with a phase contact time from 0.6 to 18 sec. The working solutions were fed under gravity from the thermostated pressure vessels into the centrifugal extractor and were collected in the receiving vessels. The feed stock was regulated by means of needle valves and the volumes were measured using rotameters. The temperature control at the inlet and outlet from the extractors was carried out by means of thermometers. The extractor was driven by an electric motor. The extractor rotation rate was regulated by a laboratory autotransformer and was checked by means of a tacho-generator and a voltmeter. The principle of the extractor action has been described in detail ref /1/, but the volume of the mixing chamber in this work was decreased to $5 \cdot 10^{-6} \text{ m}^3$. Experiments were carried out at an extractor rotation rate of 22-67 rev/sec. The temperature at which the experiments were carried out was $295 \pm 1^\circ \text{K}$, except in the case of the experiments on the temperature dependence of the extraction kinetics. The total rate of flow of the aqueous and the organic solutions was varied between $3.7 \times 10^{-6} \text{ m}^3/\text{sec}$ and $1.1 \times 10^{-4} \text{ m}^3/\text{sec}$, which corresponds to a change in the phase contact time from 18 to 0.6 sec. In the majority of the experiments the fraction of the aqueous phase in the total stream of the working solutions (φ_{aq}) was 0.6; for other cases the value of φ_{aq} is given where the results of the experiments are shown. Calculation of the extraction process efficiency (E) and of the degree of reaction was made according to the methods described in reference /7/.

In order to mix the liquids in the gravitation at field, the vessel used was in the form of a glass cylinder of diameter 0.018 m with a stirrer of diameter 0.010 m equipped with a mercury shutter. The working volume of the vessel was 10^{-5} m^3 . The rotation rate of the stirrer was 20 rev/sec.

Analysis and compounds - Uranium was analysed at concentrations using the gravimetric method in the form of U_3O_8 . At low concentrations, uranium was determined colorimetrically. Nitric acid in the presence of uranium was determined by the conductometric titration with alkali. The plutonium concentration was determined by α -counting. Plutonium was separated from uranium by means of plutonium co-precipitation with the double sulphate of potassium and lanthanum in a reducing medium. The ruthenium and zirconium content was separately calculated by γ -counting. The ruthenium concentration in the aqueous feed solution was determined according to the methods described in reference /9/. The samples of solutions for analysis were taken under standardised operating conditions of the centrifugal extractor work which corresponded to tenfold exchange of solutions in the apparatus.

Repeatedly recrystallized uranyl nitrate was used in our work. The ^{239}Pu was in nitric acid solution. The plutonium was stabilised in the tetra valent state by means of sodium nitrate /8/. The ferrous sulphamate used for the experiments on the reductive plutonium stripping was prepared by heating sulphamic acid with metallic iron for 8 hours at a temperature of 333 K.

The feed solution containing nitrosoruthenium nitrates labelled with ^{106}Ru was prepared according to the methods described in reference /10/. This solution contained a mixture of radioactive and stable ruthenium isotopes and had a ruthenium content of $3.4 \times 10^{-3}\text{M}$ and γ -equivalent $2.5 \times 10^{-3}\text{g-eq/l}$. It was kept in 8M nitric acid for several days. The ruthenium distribution ratio (D_{Ru}) was periodically determined during the course of its extraction into 1.1 M tributylphosphate in carbon tetrachloride for a phase contact time (τ) of 5 minutes in glass vessels:

τ_{res} (days)	2	3	4	5	6	7	11
$D_{\text{Ru}} \cdot 10^3$	1,2	1,0	0,9	1,1	0,9	1,4	1,2

It is evident from the results shown that a two-day residence time measured from the moment of finishing the synthesis, is sufficient to obtain a feed solution in which all the forms of ruthenium complexes being extracted are in equilibrium.

The zirconium nitrate feed solution, labelled with ^{95}Zr , was prepared in the following way. An oxalic acid solution containing the $^{95}\text{Zr} - ^{95}\text{Nb}_3$ was evaporated down several times with the concentrated nitric acid in order to destroy the oxalate ions. The nitric acid solution obtained was kept above processed glass wool in order to separate the niobium.^{/11/} In order to mix the isotopes a sample of zirconyl nitrate prepared and an aliquot of radioactive zirconium solution prepared by the above method were evaporated down together four times in 10M nitric acid. All evaporations were carried out on a water bath. As a result of this, the concentration of the feed solution was 10^{-3}M zirconium in 10M nitric acid. Before commencing the experiments the solution was diluted to give the required nitric acid concentration, and the period for which the solution had been kept was checked upon. It was established that the zirconium distribution coefficient in 2M nitric acid remained practically instant over the two days beginning from the moment of dilution.

Tributylphosphate and carbon tetrachloride were purified according to the methods^{/12/} for the dilution of the former. The mixture of aliphatic hydrocarbons (AHC) with the specific gravity 0.72 g/cm^3 (at 293K) and boiling point in the range 383-543K and the n-decane that were used as tributylphosphate diluents were treated with concentrated sulphuric acid and phosphorous anhydride, and then washed with a 1M solution of caustic soda and with distilled water until they gave a neutral reaction. After the uranium has been stripped out, the organic solution was washed with a 0.5M sodium carbonate solution, followed with 0.5M caustic soda and finally with distilled water. It was subsequently acidified with nitric acid until the equilibrium in the aqueous phase concentration was 2M with respect to nitric acid. The nitric acid and all the reagents were chemically pure. The solutions were prepared with distilled water. The density of the solutions was measured using a hydrometer. The viscosity of the solutions was determined with a viscometer.

All the results are the average of three parallel determinations. The time required for the establishment of 98-99% equilibrium between the phases was defined as the period of practically complete mass transfer.

Results

A typical series of curves showing the changes in uranium extraction efficiency vs. phase contact time is given in Fig.1. As is evident from Fig.1., the time required for practically complete mass transfer (period of setting up the equilibrium between phases) at centrifugal extractor rotation rates of 22, 30 and 67 rev/sec. is 6, 3.5 and 0.8 sec. respectively for the system 0.011M uranyl nitrate - 2M nitric acid - 1.1M TBP in AHC.

The time required to attain equilibrium between the phases in the case of nitric acid which is necessary for the extraction of uranium, plutonium and other elements, as well as for uranium is shown in Fig.2 and 1).

When the uranium concentration in the aqueous feed solution was increased up to 0.43M, the time necessary to establish equilibrium also increases as shown in Fig.3. The experimental activation energy is about 6 Kcal/mole if the assumption is made that the area of interfacial surface is independent of temperature.

When carbon tetrachloride is used as diluent (Fig.4), the time required to establish equilibrium during the course of the uranium extraction is 1.5 times shorter than if the mixture of aliphatic hydrocarbons (AHC) is used as the diluent.

The time required for the practically complete mass transfer in the extraction and stripping of plutonium (IV) (Fig.5.), is almost the same as that for uranyl nitrate at a concentration of 0.11M.

Fig.6 shows the uranium and plutonium concentrations in the organic phase during their co-extraction as a function of the phase contact time. When the centrifugal extractor rotation rate was 43 rev/sec, plutonium was more rapidly transferred into the organic phase than uranium. Further saturation of the extractant with uranium resulted in a decrease in the plutonium concentration in the organic phase. An extractant saturation of 86% with respect to uranium was achieved.

The rate of plutonium stripping with divalent iron is less than in the processes discussed above; it depends on the nitric acid concentration and in the ferrous ion concentration (Fig.7). The experimental activation energy in 2M nitric acid is 18 kcal/mole for a reducing agent concentration of 0.05M.

Since it is known that the properties of nitrosonitrate ruthenium complexes and their ratio depend on the methods used for the preparation of the solutions and on the time for which they have been allowed to stand, the time required to establish equilibrium between the ruthenium complexes in aqueous solution (Fig.8) were determined before any experiments were carried out on the investigation of the ruthenium extraction kinetics. The time required to establish equilibrium as the nitric acid concentration is changed from 8, 6 and 4M to 2M (curves 1-3) is 2-3 days, 6-7 hours and 2-3 hours respectively. The experimental activation energy for ruthenium transition from the state present in 2M nitric acid to the state present in 4M nitric acid is 21 kcal/mole.

The dependence of D_{Ru} on the phase contact time () in the extraction of nitrosoruthenium complexes from nitric acid solutions with 1.1M tributylphosphate in CCl_4 using a centrifugal extractor.

τ , sec	Nitric acid concentration, M		
	2	4	5.2
0.6	0.041	0.0105	0.0030
1.2	0.042	0.0104	0.0032
4.8	0.040	0.0106	0.0028
9.0	0.043	0.0103	0.0029
22	0.043	0.0109	0.0031

The dependence of the ruthenium distribution on the phase contact time (τ) is shown in Table 1 and in fig.9. Because of the difficulties associated with these methods, experiments were carried out in the centrifugal extractor for values of $\tau = 0.6-24$ sec, and for values of $\tau > 24$ sec, they were carried out in a gravitational extractor. A change in the dependence of D_{Ru} on the rate of rotation of the stirrer (n) in the gravitational apparatus for an aqueous phase nitric acid concentration equal to 4M.

D_{Ru}		n , rev/sec.
= 60 sec	= 300 sec	
0.0132	0.0167	20
0.0134	0.0187	30
0.0134	0.0182	38

Ruthenium distribution is only observed in the case when the phase contact time is greater than 60 sec. The rate of ruthenium extraction decreases as the acidity increases. (Fig.9). The dependence of the rate of ruthenium on the intensity of phase mixing is shown in Table 2. The experimental activation energy with 2M nitric acid is 16 kcal/mole.

The dependence of the efficiency of zirconium extraction on the phase contact time is shown in Fig.10. The time required to achieve the practically complete mass transfer of zirconium is longer than 6 sec.

Discussion

In order to determine the optimum working conditions for the extraction apparatus it is necessary to define the factors that affect the time of mass transfer, which, in turn, controls the overall rate of the process. The limiting factors is either the rate of diffusion of the compounds to the reaction zone and the rate of diffusion of the products from the reaction zone or it is the rate of the chemical reaction associated with the extraction process. The main variables which provide information to which of these possibilities is the rate determining step are the intensity of mixing and temperature. It is known that it is characteristic of extraction processes in which the rate determining step is the chemical interaction of the compounds taking part in the reaction that the rate is strongly dependent on the temperature and is almost independent of the intensity of mixing /13, 14/. The rate of diffusion is strongly dependent on the intensity of mixing and only slightly dependent on the temperature.

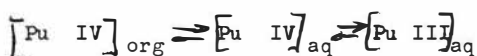
The dependence of the uranium, plutonium and nitric acid extraction rates on the intensity of mixing (Fig. 1-5), lead us to conclude that the rate determining step is that involving the diffusion of the reactants. The time required for the practically complete mass transfer of each of these compounds for $n = 42$ rev/sec is almost the same and is about 2 sec., (Fig. 1, 2, 5). It is to be noted that this conclusion concerning the diffusion controlled kinetics of nitric acid extraction in a centrifugal extractor (Fig.2) is in accordance with conclusions which have been drawn in reference /12/ concerning the rate determining step in the kinetics of the nitric acid extraction; the latter conclusion was drawn on the basis of data obtained using different phase mixing conditions.

The small value of the activation energy, which is 6kcal/mole, for the system 0,42M uranyl nitrate - 2M nitric acid - 1.1M tributylphosphate in AHC provides additional confirmation that convective diffusion is the rate determining step in the processes under investigation. The decrease in the rate at which equilibrium is established during the course of uranium extraction, as the concentration of the latter is increased, (Fig.1, 3), can be explained by the increase in the viscosity of the solutions.

The time required to establish equilibrium in the stripping of plutonium is almost the same as it is in the extraction process; in both cases, the process is diffusion controlled (Fig.5), and the time required to establish equilibrium is independent of the nitric acid concentration.

It follows from Fig.6 that the uranium and plutonium distribution depends on the phase contact time, thus, when τ is changed from 18 to 1.5 sec distribution increases by a factor of 3.5. This fact provides an example of how the partition of elements whose distribution ratios are similar under equilibrium conditions can be improved when the process is carried out under non-equilibrium conditions.

The reductive stripping of plutonium can be represented in the following manner:



According to this formula the rate determining step for these processes is controlled by the rate at which plutonium IV is transferred from the organic into the aqueous phase and by the rate at which plutonium IV is reduced by ferrous ions in the aqueous phase. This latter process is a very slow one; it depends on the nitric acid and reducing agent concentration (Fig.7) and to a considerable extent, on the temperature. Plutonium IV is rapidly transferred from the organic to the aqueous phase (Fig.5). From a consideration of all the data obtained we may conclude that, at high nitric acid concentrations, and at low concentrations of the reducing agent, the rate determining step in the reductive stripping of plutonium is the slow chemical

reaction involving the reduction of plutonium in the aqueous phase.

The kinetics of the reduction of plutonium IV by Fe(II) is represented by the equation:

$$V = K' (Fe(II)) (Pu(IV))_{aq}$$

where K' - is the effective rate constant in
4M HNO_3 .

since $(Fe(II)) (Pu(IV))_{aq}$, it can be written:

$V = K(Pu(IV))_{aq}$, where $K = K'(Fe(II))$. According to the data in Fig.7 (curve 1), the rate constant is 0.76×10^{-7} mole/sec. The equilibrium concentration of Pu(IV) in the aqueous phase in the absence of the reducing agent was 1.9×10^{-6} M. Thus, in the first approximation, $K^1 = 40$ rev/mole sec. hence $K = 40(Fe(II))$ rev/sec. When the nitric acid concentration in aqueous phase is ≤ 1 M the rate of plutonium reduction becomes comparable with its rate of diffusion (Fig.7 and 5). When the nitric acid concentration is decreased in the aqueous phase at rather high concentrations of Fe(II), the process may take place under such conditions that the rate determining step is either the rate of reduction of the plutonium into the trivalent state or the rate of diffusion of the tetravalent plutonium from the organic to the aqueous phase.

The data of various authors concerning the time required to establish equilibrium in ruthenium complexes is rather contradictory /15/18/. It is known that a solution of ruthenium nitrosocomplexes in nitric acid is a mixture of generically related complexes with different extraction properties. when the acidity of the solution is changed, their ratio is changed and a new equilibrium state is achieved after the elapse of some time. The slope of the curves in Fig.8 is indicative of the reversible character of the process being observed and, accordingly suggests that true equilibrium is being attained. Equilibrium is established rather slowly and the time required to establish the new equilibrium is proportional to the magnitude of the change in the acid concentration.

It is evident from the data given in Fig.9 that the values for ruthenium distribution ratios obtained by extrapolation to $= 0$ are not equal to zero. This testifies to the rapid initial stage of the process which is finished in less than 0.6 sec (Table 1) according to the data obtained using the centrifugal extractor. This is in agreement with the data for the diffusion of uranium and plutonium and nitric acid. Hence the conclusion can be drawn that the first step in the extraction of ruthenium is diffusion controlled.

As a result of the diffusion of highly extractable nitroso-ruthenium complexes into the organic phase, the equilibrium in the aqueous phase is upset. The second step in the process is the chemical transformation of weakly extracted complexes into readily extractable ones. The rate of this second step of the process depends on the nitric acid concentration (Fig.9). According to the data presented in Fig.9, the process in the second stage has a reaction order of 2.2. with respect to (HNO_3) . The rate constant for this process in 1M HNO_3 is 0.0018 rev/min. The large value for the experimental activation energy may be taken as confirmation of the fact that the rate determining step involves a chemical reaction. The fact that the ruthenium distribution ratio is independent of the intensity of mixing (Table 2) is one more piece of evidence in support of the chemical character of the second step.

The time required for the practically complete mass transfer of zirconium is more than the time required to establish equilibrium for the diffusion process, Fig.10 and 1-5. This is probably due to the slow chemical transformation of non-extractable zirconium complexes into extractable ones, in case of ruthenium.

A time of two seconds is sufficient to extract uranium and plutonium in the centrifugal extractor at a rotation rate of 42 rev/sec. It is evident that, in this case, the distribution ratios of uranium and plutonium can be relatively increased with respect to those of ruthenium and zirconium.

CONCLUSIONS

1. That kinetics of the extraction of uranium, plutonium, zirconium and nitric acid by tributylphosphate in a diluent have been investigated using a centrifugal apparatus.
2. The rate of mass transfer of uranium plutonium, and nitric acid under the conditions studied is determined by the rapid convective diffusion step which is finished in 0.6 to 6 sec.
3. The rate of mass transfer of ruthenium as well as of plutonium during reductive stripping is determined by the slow chemical reactive steps.
4. The use of a centrifugal extractor allows one to carry out the uranium and plutonium extraction process quite effectively using a short phase contact time.
5. It is shown that, in some cases, the distribution ratios of the elements can be increased if the process is operated under non-equilibrium conditions.

REFERENCES

1. Yakovlev G.N., Pushlenkov M.F., Kuznetsov G.I., Shchepetilnikov N.N., Feofanov A.P., Atomnaya Energiya, 1971, 28, 244.
2. Kuznetsov G.I., Pushlenkov M.F., Yakovlev G.N., Atomnaya energiya, 1971, 30, 410.
3. Lewis J.B., Pratt H.R.C., Nature, 1953, 171, 1155.
4. Lewis J.B., Chemi.Eng.Sci., 1958, 8, 295.
5. Hahn H.T., J.Amer.Chem.Soc., 1957, 79, 4625.
6. Murdoch R., Pratt H.R.G., Trans.Inst.Chem.Eng., 1953, 31, 307.
7. Treiball R., Liquid extraction, 1966, Chimia, 447 (Moscow).
8. Milyukova M.S., Gusev N.I., Senturin I.G. Sklyarenko I.S., Plutonium analytical chemistry, 1965, Nauka (Moscow).
9. Sandell E.G., Colorimetric determination of traces of metals, 1959, Goskhimizdat (Moscow).
10. Zvyagintsev O.E., Kolbin N.I., Ryabov A.N., Avtokratova T.D., Goryunov A.A., Ruthenium chemistry, 1965. Nauka (Moscow).
11. Vdovenko V.M., Lazarev L.N., Chvorostin Ya.S., Radiokhimiya, 1959, I, 364.
12. Pushlenkov M.F., Shchepetilnikov N.N., Radiokhimiya, 1969, II, 19.
13. Glasstone S., Laidler K., Eyring H., Theory of absolute reaction rates. McGraw. Hill Book Co., New York, 1941.
14. Frank-Kamenetskii D.A., Diffusion and heat transfer in chemical kinetics, 1967 Nauka (Moscow).
15. Fletcher J.M., Brown P.G.M., Gardner B.R., Hardy C.J., Wain A.G., Woodhead J.L., J.Inorg.Nucl.Chem., 1959, 12, 154.
16. Nikolskii B.D., Shmidt, B.C., Zh.Neorgan.Khim., 1957, 2, 2746.
17. El-Guebeily M.A., Hallaba E., Azzam R.A., Proceedings of the Third International Conference on the Peaceful Uses of Atomic Energy, 1965, 10, United Nations, 452 (New York).
18. Rudstam G., Acta Chem.Scand., 1959, 13, 1481.

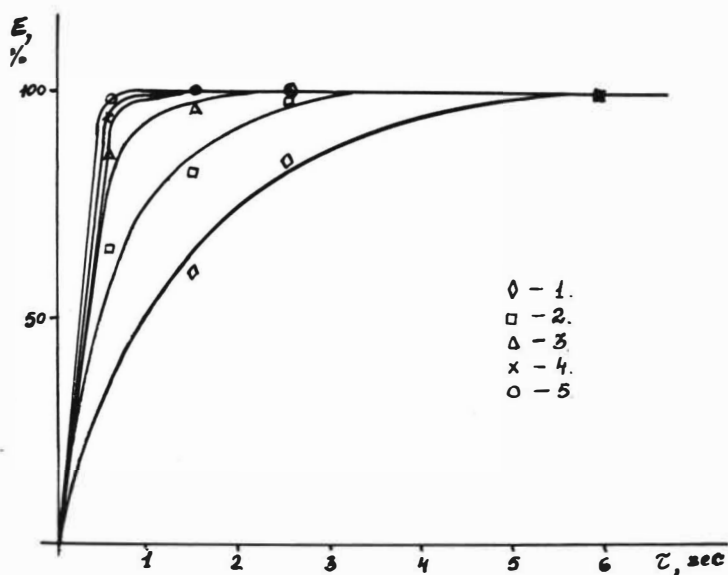


Fig.1. The dependence of the efficiency of uranyl nitrate extraction on the phase contact time in a centrifugal extractor. The system was as follows: 0.011M uranyl nitrate in the feed stock aqueous phase - 2M nitric acid - 1.1M tributylphosphate in a mixture of aliphatic hydrocarbons (AHC). Rotation rate, in rev/sec: 1) 22, 2) 30, 3) 42, 4) 50, 5) 58, 6) 67.

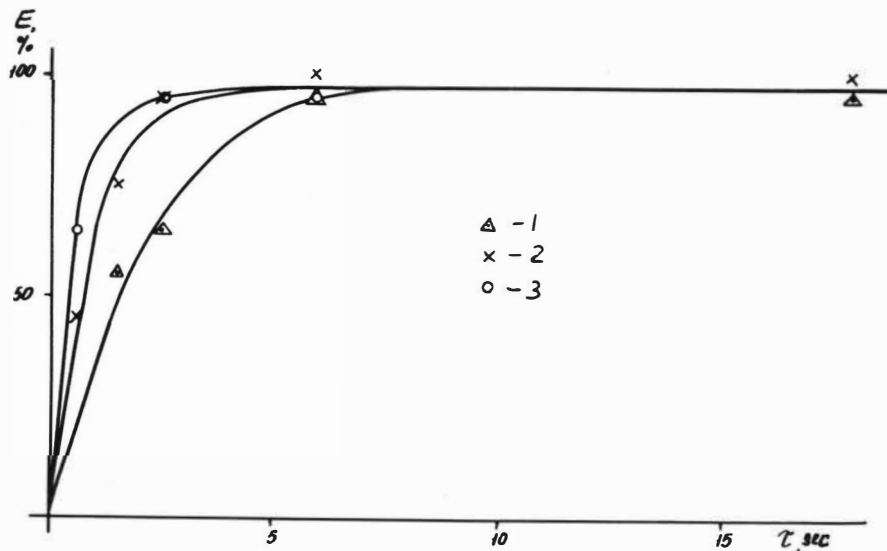


Fig.2. The dependence of the efficiency of nitric acid extraction on the phase contact time in a centrifugal extractor. The system was as follows: 2M nitric acid - 1.1M tributylphosphate in AHC. Rotation rate, in rev/sec: 1) 22, 2) 30, 3) 42.

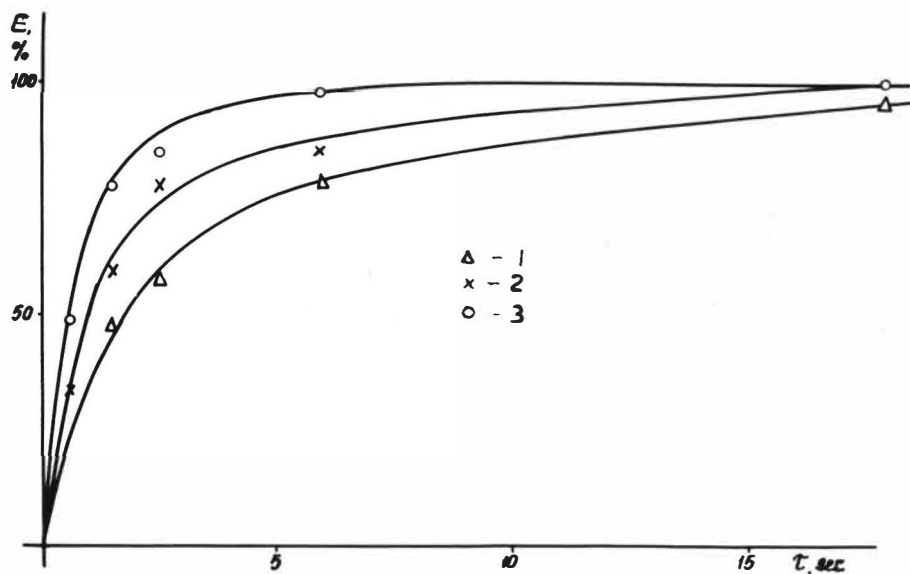


Fig.3. The dependence of the efficiency of uranyl nitrate extraction on the phase contact time in a centrifugal extractor. The system was as follows: 0.42M uranyl nitrate - 2M nitric acid - 1.1M tributylphosphate in AHC. Rotation rate, in rev/sec: 1) 22, 2) 30, 3) 42.

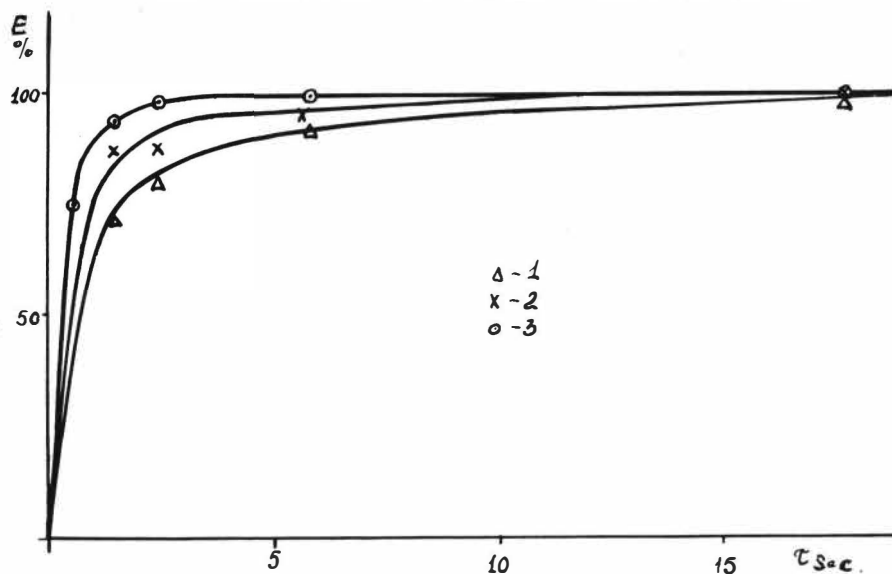


Fig.4. The dependence of the efficiency of uranyl nitrate extraction on the phase contact time in a centrifugal extractor. The system is as follows: 0.42M uranyl nitrate - 2M nitric acid - 1.1M tributylphosphate - carbon tetrachloride. Rotation rate, in rev/sec: 1) 22, 2) 30, 3) 42.

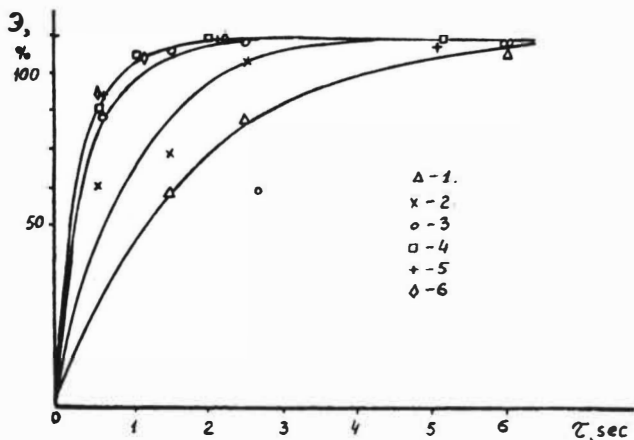


Fig. 5

Fig.5. The dependence of the efficiency of plutonium extraction and stripping on the phase contact time in a centrifugal extractor. 1 to 3. Plutonium extraction. The system is as follows: 6.8×10^{-4} M plutonium (IV) nitrate - 2M nitric acid - 1.1M tributylphosphate in AHC. Rotation rate in rev/sec: 1) 22, 2) 30, 3) 42. 4 to 6. Plutonium stripping: 4.2×10^{-5} M plutonium (IV) nitrate in organic feed solution (1.47M tributylphosphate in d-decane). The rotation rate was 47 rev/sec. Nitric acid concentration in the aqueous phase, in M : 1) 1, 2) 2.5, 3) 4.

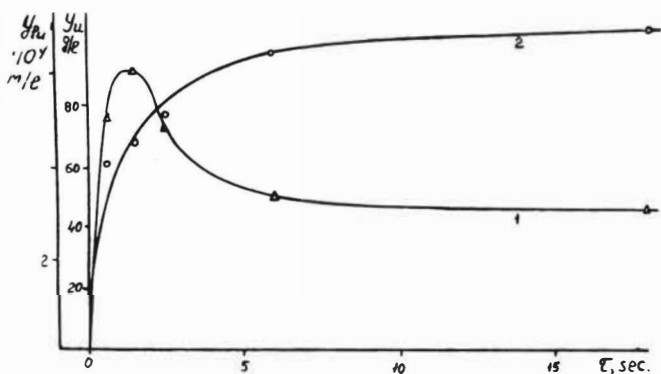


Fig. 6

Fig.6. Uranium VI and plutonium IV concentration in the organic phase and its dependence on the phase contact time in a centrifugal extractor. The system was as follows: 1M uranyl nitrate - 1.2×10^{-4} M plutonium (IV) nitrate-2M nitric acid 1.1M tributylphosphate in AHC, $\varphi_{aq} = 1.5$ 1) plutonium (IV), 2) uranium (VI). The rotation rate was 42 rev/sec.

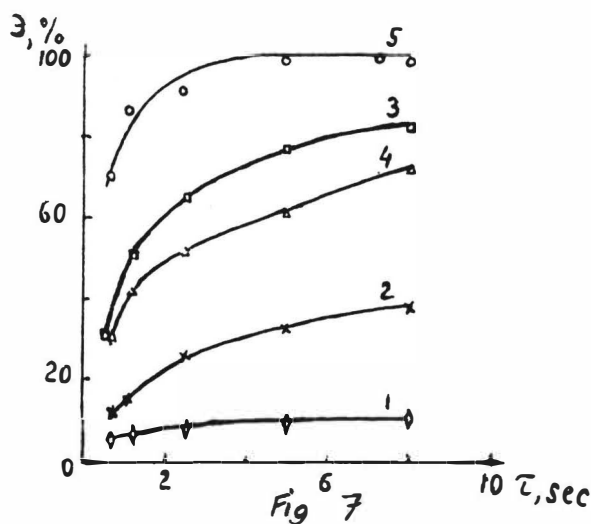


Fig.7. The dependence of the efficiency of the reductive stripping of plutonium on the phase contact time in a centrifugal extractor. 1 to 3 the system was: 4.2×10^{-5} M plutonium (IV) (in organic feed phase) - 1.47M tributylphosphate-n-decane-4M nitric acid Fe(II). Fe(II) sulphamate concentration in aqueous feed solution, in M : 1) 0.001, 2) 0.05, 3) 0.02. 4 to 5.

The system was: 4.2×10^{-5} M plutonium (IV) in organic feed phase - 1.47M tributylphosphate-n-decane-nitric acid - 0.05M Fe(II). The nitric acid concentration in the aqueous phase in M was: 4) 2.5, 5) 1. 1 to 6. The rotation rate was 47 rev/sec.

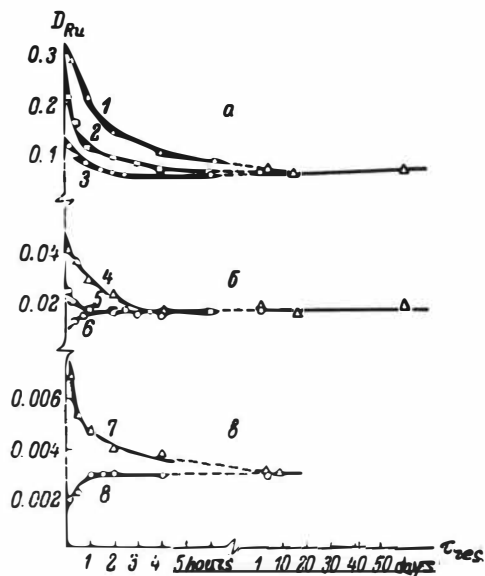


Fig. 8

Fig.8. The dependence of the distribution ratio for Nitrosoruthenium complexes on the time for which the aqueous solution had been allowed to stand after preparation. Nitric acid concentration after the preparation of the solutions from (in M): a) 2, b) 4, c) 5.2. Nitric acid concentration in feed solutions (in M): 1) 8, 2) b, 3) 4, 4) 8, 5) 52, 6) 2, 7) 11.6, 8) 4. The phase contact time was 5 min in the gravitational apparatus (curves 1-6) and 1.4 sec in the centrifugal apparatus (curves 7-8). The organic phase was 1:1M tributylphosphate in carbon tetrachloride,

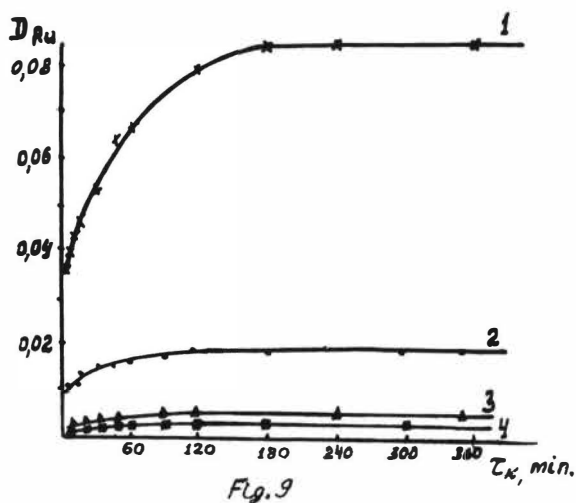


Fig. 9. The dependence of the distribution ratio for the extraction of nitrosoruthenium complexes with tributylphosphate in carbon tetrachloride. The rate of rotation of the stirrer was 20 rev/sec.

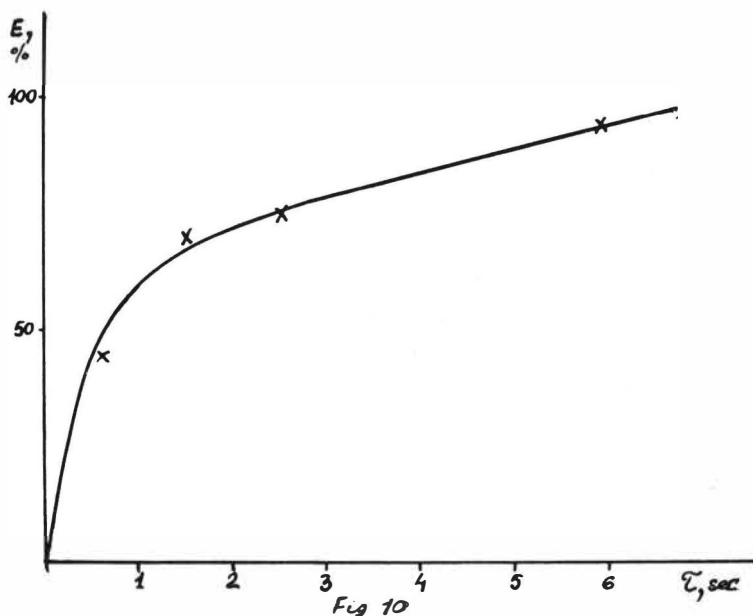


Fig. 10. The dependence of the efficiency of zirconium nitrate extraction on the phase contact time. This system was 2×10^{-4} M zirconium nitrate - 2M nitric acid - 1.1M tributylphosphate - AHC. The rotation rate was 42 rev/sec.

LISTS OF DESIGNATIONS

- E - extraction process efficiency, the degree of transformation.
- AHC - mixture of aliphatic hydrocarbons.
- D_{Ru} - ruthenium distribution ratio that was obtained as the ratio of ruthenium analytical concentration in the aqueous phase at a given phase contact time (τ), generally, it is a non-equilibrium distribution ratio.
- n - rotation rate, rev/sec.
- y_U - uranium concentration in the organic phase at a given phase contact time, .
- y_{Pu} - plutonium concentration in the organic phase at a given phase contact time, .
- Pu(IV), Pu(III) represent tetra - and trivalent plutonium, respectively.
- φ_{aq} - aqueous phase fraction in the combined stream of aqueous and organic phases.
- τ - phase contact time, sec.
- τ_{res} - time for which the nitrosoruthenium nitrate solution was left standing measured from the moment of its preparation.
- R - constant rate of the process.
- V - process rate.

SESSION 5

Monday 9th September: 14.00 hrs

E Q U I P M E N T

(Settler Characteristics)

Chairman:

Professor D. Wasan

Secretaries:

Dr. G.A. Davies

Mr. J. Breysse

THERMODYNAMIC NATURE OF HYPERFINE EMULSIONS FORMATION AT THE EXTRACTION

A.I. Gorbanoz, B.N. Dzovitsky and V.B. Margulis

Institute of Metallurgy of the Academy of Sciences of the USSR,
Moscow, USSR.

ABSTRACT

The problem of formation and stability of hyperfine emulsions during extraction is discussed in terms of thermodynamics of heterogeneous systems. Thermodynamical difference between microemulsions and conventional macroemulsions is demonstrated. A hyperfine emulsion is a disperse phase comprising spherical particles of surface layers of finite thickness distributed in the bulk of a liquid phase. Such isolated surface layer particles which can exist independently are stable in any multicomponent systems due to thermodynamical factors. The same factors are responsible for microemulsions being monodisperse.

For various emulsions differential equations of equilibrium are derived and some of the corollaries are discussed. Formation of microemulsions is one of the causes of the extractant losses and determines the excess solubility of immiscible liquids obtained by mechanical dispersion, as compared to the solubility at ordinary phase contact.

INTRODUCTION

As is well known, mutual dispersion of liquid phases is promoted by lowering the interphase surface tension ($\sigma_{12} \rightarrow 0$) /1/. This is the main factor in emulsion stabilization by emulsifiers. Thermodynamics are not needed to study formation and stability of microemulsions and the processes of phase reversal. But the thermodynamic approach is necessary to analyze the relative capillary activities of the components in multicomponent systems encountered in extraction phenomena. Moreover, a thermodynamic approach should be used to understand why fine stable emulsions are formed in the absence of emulsifiers. The modern thermodynamics of surface phenomena treat the surface layers at the interface as surface phases, that is, of infinite thickness /2/. This treatment implies an universal dispersion mechanism for surface layers leading to formation of a microemulsion.

As the processes of emulsion formation are of great importance in liquid extractors /3/ we analyzed this problem in thermodynamic terms.

THERMODYNAMICAL

A thermodynamical treatment of microemulsion should take into account, besides the finite thickness of the boundary layers, curvature of the interface.

At first, consider the number of degrees of freedom. According to the phase rule, for an n -component system consisting of two liquid phases and the equilibrium vapour (that is, with three boundary phases) the number of degrees of freedom f is

$$f = n - 3 + 2 = n - 1$$

For constant p , T we have $f = n - 2$.

Thus, the bulk-surface phase processes with variation of an surface extensive parameter can occur only in a multicomponent system (n > 6). When the number of components is less than 6 these processes are necessarily nonequilibrium ones. For small numbers of components, emulsification is rigorously restricted by the phase rule due to the purely thermodynamic factors. These restrictions are not important in the real extraction systems. Kusanov /2/ put forward a generalized phase rule with variance expressions accounting for surface phenomena and external conditions. For a two-phase system he demonstrated a possibility for the surface layer to curve, its area being constant, and for the area to change at a expense of mass of the bulk phases, the curvature being constant. Thus, dispersion of phases with emulsification does not contradict the phase rule.

A surface layer of finite thickness and its energy

This method was suggested by Van der Waals and Kohnstamm /4/. The effective thickness of the surface layer is specified by the deviation of the local properties near the surface from their value in the bulk of the phase. It is assumed that at the boundary of the surface layer the local and the bulk properties are identical so that there should be an asymptotic formula for the thickness of the layer. Using statistical methods /5/ the strict expression for layer thickness in the case of Van der Waals interaction was obtained:

$$\tau_0 = \left[\frac{\pi \rho_0 x_0 (B' \rho' - B_0 \rho_0) (\rho' - \rho_0)}{6} \right]^{1/3}$$

where ρ' and ρ_0 are the phase densities, B' and B_0 are the constants of dispersion interaction, and x_0 is the mean isothermal compressibility of the phases.

For systems with strong interaction no rigorous analysis has been performed but, evidently, they have layers of greater thickness than in the above case. It may be assumed that the parameter r_0 determines the radius of dispersed particles in microemulsions.

The specific energy of the surface layer identical to the interface surface tension is related to the work of deformation by the following expression:

$$\delta W = -P_N \delta V + \sigma \delta A = -P_N \delta V + \delta A \int_{-r_0}^{+r_0} (P_N - P_T) dz$$

For a homogeneous liquid phase we obtain

$$P_A = P_N = P, \quad \sigma = 0 \quad \text{and} \quad \delta W = -P \delta V.$$

For a two-phase system we obtain

$$\sigma = \int_{-r_0}^{+r_0} (P_N - P_T) dz$$

Now we shall determine δW for the spherical layer between the dispersion phase (1) and the dispersion medium (2) in the solid angle ω between the concentric boundaries of the surface layer of radii r_1 and r_2 ($r_2 > r_1$). Introducing new variable r_x we obtain ($r_2 \geq r_x \geq r_1$):

$$\sigma_x = \frac{1}{r_x^2} \left[\int_{r_1}^{r_x} (P^{(1)} - P_T) r^2 dr + \int_{r_x}^{r_2} (P^{(2)} - P_T) r^2 dr \right]$$

The relationship between σ_x and r_x is given by the Kondo equation [5]:

$$\frac{\partial \sigma_x}{\partial r_x} + \frac{2\sigma_x}{r_x} = P^{(1)} - P^{(2)}$$

This equation yields the minimum of γ for a given value of r_0 , which we consider to be identical to r_0 in microemulsions on the strength of the above argument. The presence of the surface energy minimum for a given curvature of the surface is of a general nature as the Kondo equation follows from the fundamental Gibbs equations. This, too, shows that microemulsions are monodisperse.

Conditions of equilibrium and stability for microemulsions

The particles of the conventional (macro)emulsions consist of a disperse phase core, an enveloping surface layer of finite thickness and an ambient dispersion medium with a bounding surface of negative curvature. Actually, this is a three-phase system with several interfaces of varying curvature.

Such aggregates are difficult to consider thermodynamically. On the other hand, their formation and stability are determined, basically, by non-thermodynamic factors so that thermodynamic treatment is needed only when considering the macroproperties of a system of such aggregates.

We assume that the particles of a hyperfine emulsion consist only of a surface layer separating two liquid phases. This layer is the disperse phase while each of the liquid phases may act as the dispersion medium.

For the processes of extractant loss aqueous phase is the dispersion medium.

Without loss of generality we may assume that particle diameter for hyperfine emulsions is twice the radius of the tension surface:

$$d = 2r_0.$$

As r_0 is found from the process of virtual motion of the interface we take r_0 to be equal to the thickness of the flat surface layer at the interface of two liquid phases which can be measured experimentally.

Thus it follows that there are two possible mechanisms of formation of hyperfine (micro)emulsions:

- mechanical dispersion of surface layers with high curvature radius, and
- nucleation of one liquid phase in the bulk of another one.

In the real extractors the first mechanism is predominant as their operation involves intensive turbulization and dispersion of two-phase systems /1/.

Let us consider the conditions of equilibrium and stability for microemulsions assuming that their particles (disperse phase) consist only of the surface layer material. In fact, in this way we obtain a two-phase system with one spherical interface. Index 1 denotes the disperse phase and index 2 denotes the dispersion medium. Our two-phase is, apparently, thermodynamically metastable (that is, stable in respect to the infinitesimal variations of its state).

For our system the equilibrium conditions can not be expressed by mere equality of temperatures, pressures and chemical potentials of the phases as the system is highly nonuniform. The equilibrium conditions in terms of local variables are expressed by the following equations:

$$\left. \begin{array}{l} \text{grad } P = 0 \\ \text{grad } \sigma = 0 \end{array} \right\} \text{mechanical equilibrium}$$

$$\text{grad } T = 0 \quad \text{thermal equilibrium condition (in the absence of non-stationary mass transfer)}$$

$$\text{grad } \mu_i = 0 \quad (i = 1, 2, \dots) \quad \text{mass-transfer equilibrium for individual components}$$

Accordingly, the fundamental thermodynamic equations below will be written down using the local variables (depending on X, Y and Z).

Naturally, we shall take into account the degrees of freedom associated with the interface area and curvature.

The following is the fundamental equation valid for each of the phases considered, for their parts and for the system as a whole:

$$dU = Tds = \int_V dV \sum_k P_k \delta \rho_k + \int_V dV \delta \rho_k \frac{\partial \rho_k}{\partial r} r dr + \sum_i \mu_i da_i.$$

This equation yields the equilibrium principle:

$$(dU)_{S,V,A_r,r,\mu_i} = 0$$

Subdividing the system into the identical microhomogeneous parts and integrating over their volume we obtain

$$U = TS - p^{(1)}V_1 - p^{(2)}V_2 + \int_V dV \delta \rho_k \frac{\partial \rho_k}{\partial r} r dr + \sum_i \mu_i m_i$$

This relation and the fundamental equation yield the differential equation of equilibrium:

$$A_r d\delta \rho_k = -s dT + V_1 dp^{(1)} + V_2 dp^{(2)} - \sum_i m_i \mu_i + A_r \frac{\partial \delta \rho_k}{\partial r} r dr$$

The problem is to obtain from these equations information on composition and other properties of the disperse phase which we assume to be identical to the surface layer.

Treated formally, the microemulsion may be considered to be monodisperse. In physical terms this means that the curvature of the surface layer particles provides for the minimum of energy.

In this case the treatment is simplified as $dr = 0$ and the term dependent on $\frac{1}{r}$ can be dropped from the equation. Thus, we obtain the Gibbs equations whereby a real two-phase system is replaced by an aggregate of phases with a distinct interface of zero thickness (the Gibbs tension surface).

However, we shall take into the account explicitly the curvature of the interface dropping the condition of pressure equality in the phases.

$$(*) \Lambda_0 dG_0 = -SdT + V_1 dp^{(1)} + V_2 dp^{(2)} - \sum_i m_i d\mu_i$$

In contrast to the equilibrium condition, the condition of stability is expressed by the inequality $\Delta U > 0$, and as, $dU = 0$, it is evident that $d^2U \geq 0$, or

$$\begin{bmatrix} D(T, -p^{(1)}, -p^{(2)}, \mu_1, \dots) \\ D(S, V_1, V_2, \mu_1, \dots) \end{bmatrix} > 0$$

(follows from the theory of quadratic forms).

The notation $\begin{bmatrix} D(x) \\ D(y) \end{bmatrix}$ is used to designate a determinant of derivatives $\frac{\partial x}{\partial y}$.

Derivation of equations of microequilibrium

+ Let us find the relationship between T , $p^{(1)}$, $p^{(2)}$, and the mole fractions. Proceeding from the fundamental equation (*) we write down for the unit mass of the disperse phase:

$$ad = -SdT + V_1 dp^{(1)} + V_2 dp^{(2)} - \sum_i X_i d\mu_i \text{ where } a = \frac{\Lambda}{m}, V_1 = \frac{1}{m}, V_2 = \frac{V}{m}, X_i = \frac{m_i}{m}, V_1 + V_2 = V$$

We obtain for the macroheterogeneous system (equilibrium of two phases with flat interface):

$$\begin{aligned} (1) \quad V^{(1)} dp^{(1)} &= S^{(1)} dT^{(1)} + \sum_{i=1}^n m_i^{(1)} d\mu_i^{(1)} \\ (2) \quad V^{(2)} dp^{(2)} &= S^{(2)} dT^{(2)} + \sum_{i=1}^n m_i^{(2)} d\mu_i^{(2)} \end{aligned} \quad \begin{array}{l} \text{internal equilibrium of} \\ \text{phases} \end{array}$$

The internal equilibrium of the surface layer:

$$(3) \quad Ad = -S^{(\sigma)} dT^{(\sigma)} + V^{(\sigma)} dP_N - \sum_{i=1}^n m_i^{(\sigma)} d\mu_i^{(\sigma)};$$

$$T^{(1)} = T^{(2)} = T^{(\sigma)}; \quad P^{(1)} = P^{(2)} = P^{(\sigma)};$$

$$\mu_1^{(1)} = \mu_1^{(2)} = \mu_1^{(\sigma)}.$$

Adding (1), (2) and (3) we obtain the equilibrium equation for the whole system:

$$AdG = -SdT + VdP_N - \sum_{i=1}^n m_i d\mu_i$$

To express the concentrations in mole fractions we introduce

$$\left(\frac{\partial G}{\partial x_1} \right)_{T, P_N, \sigma} = \mu_1 - \mu_n \quad (i = 1, 2, \dots, n-1).$$

For conservation of equilibrium when the state of the system is varying we have the following equations:

$$(\dots) \quad d\mu_1^{(1)} = d\mu_1^{(2)} = d\mu_1^{(\sigma)} = d\mu_1;$$

$$d\left(\frac{\partial G}{\partial x_1} \right)^{(1)} = d\left(\frac{\partial G}{\partial x_1} \right)^{(2)} = d\left(\frac{\partial G}{\partial x_1} \right)^{\sigma},$$

where G is the Gibbs potential.

N degrees of freedom are represented by the following independent variables:

$$T, P, \sigma, (n-1)x_1.$$

The superscripts 1, 2 and σ designate various functional relationships. There are two independent equations for each of them and two equations for the system as a whole (respectively, there are composition variables for each case). Let us derive these equations. For unit mass of the surface layer,

$$adG = -S^{(\sigma)} dT + V^{(\sigma)} dP - \sum_{i=1}^n x_i^{(\sigma)} d\mu_i^{(\sigma)}$$

where a , S , V and X represent mean values as their local values vary in different points. Using the equation (**) we obtain two independent equations:

$$ad\zeta = -s^{(\zeta)}dT + v^{(\zeta)}dP - \sum_{i=1}^n x_i^{(\zeta)}d\mu_i^{(1)}$$

$$ad\zeta = -s^{(\zeta)}dT + v^{(\zeta)}dP - \sum_{i=1}^n x_i^{(\zeta)}d\mu_i^{(2)}$$

Let us introduce the partial derivatives with respect to mole fractions: $d\mu_1 = SdT + VdP - \sum_{j=1}^{n-1} x_j d(\frac{\partial \zeta}{\partial x_j}) + d(\frac{\partial \zeta}{\partial x_1})$;

$$d\zeta_1 = -SdT + VdP - \sum_{j=1}^{n-1} x_j d(\frac{\partial \zeta}{\partial x_j}), \quad i = 1, 2, \dots, n-1.$$

Writing down these equations for the phases 1 and 2 and substituting them into the equation for () we obtain

$$ad\zeta = (s^{(1)} - s^{(\zeta)})dT - (v^{(1)} - v^{(\zeta)})dP + \sum_{i=1}^{n-1} (x_1^{(1)} - x_1^{(\zeta)})d(\frac{\partial \zeta}{\partial x_1})^{(1)};$$

$$ad\zeta = (s^{(2)} - s^{(\zeta)})dT - (v^{(2)} - v^{(\zeta)})dP.$$

Similar equations may be obtained for the parameters of the system as a whole (without superscripts):

$$a_0 d\zeta = (s^{(1)} - s)dT - (v^{(1)} - v)dP + \sum_{i=1}^{n-1} (x_1^{(1)} - x_1)d(\frac{\partial \zeta}{\partial x_1})^{(1)};$$

$$a_0 d\zeta = (s^{(2)} - s)dT - (v^{(2)} - v)dP + \sum_{i=1}^{n-1} (x_1^{(2)} - x_1)d(\frac{\partial \zeta}{\partial x_1})^{(2)}$$

$$\text{where } a_0 = \frac{1}{m}, \quad S = \frac{s}{m}, \quad V = \frac{v}{m}, \quad x_1 = \frac{m_1}{m}, \quad m = \sum_{i=1}^n m_i.$$

$$i = 1$$

Using the second equations (**) and the total difference trials for $\partial \zeta / \partial x_1$ we obtain the relationship between T , P , ζ and X for the emulsions:

$$d(\frac{\partial \zeta}{\partial x_1}) = -\frac{s}{\partial x_1}dT + \frac{\partial v}{\partial x_1}dP + \sum_{k=1}^{n-1} s_{1k}dx_k = \frac{\partial a}{\partial x_1}d\zeta$$

(for the bulk phases the last term is absent)

$$ad\zeta = -s_{1\zeta} dT + v_{1\zeta} dP + \sum_{i,k=1}^{n-1} (x_i^{(1)} - x_i^{(\zeta)}) s_{ik}^{(1)} dx_k^{(1)}.$$

$$ad\zeta = (s_{12} - s_{1\zeta}) dT - (v_{12} - v_{1\zeta}) dP + \sum_{i,k=1}^{n-1} (x_i^{(2)} - x_i^{(\zeta)}) s_{ik}^{(1)} dx_k^{(1)}$$

$$\text{where } s_{12} = s^{(2)} - s^{(1)} = \sum_{i=1}^{n-1} (x_i^{(2)} - x_i^{(1)}) \left(\frac{\partial s}{\partial x_i} \right)^{(1)}$$

with the similar expressions for $s_{1\zeta}$, v_{12} and $v_{1\zeta}$.

These values determine the differential molar volume and entropy effects of the phase formation processes $1 \rightarrow 2$, $1 \rightarrow \zeta$. Similar expressions may be obtained for the processes $2 \rightarrow 1$ and $2 \rightarrow \zeta$.

Let us exclude from the last two equations first dP and then dT :

$$ad\zeta = (s_{12} \frac{v_{1\zeta}}{v_{12}} - s_{1\zeta}) dT + \sum_{i,k=1}^{n-1} \left[(x_i^{(2)} - x_i^{(1)}) \frac{v_{1\zeta}}{v_{12}} - (x_i^{(2)} - x_i^{(1)}) \right] s_{ik}^{(1)} dx_k^{(1)};$$

$$ad\zeta = (v_{1\zeta} - \frac{s_{1\zeta}}{s_{12}} v_{12}) dP + \sum_{i,k=1}^{n-1} (x_i^{(2)} - x_i^{(1)}) \frac{s_{1\zeta}}{s_{12}} - (x_i^{(\zeta)} - x_i^{(1)}) s_{ik}^{(1)} dx_k^{(1)}.$$

These equations give the dependence of the surface energy on the temperature, pressure and phase composition, not allowing for the interface curvature, that is, for the flat interfaces. In the case of microemulsion we shall take into account the curvature of the interface.

Consideration of the interface curvature

As mentioned above, to take into account the interface curvature we drop the condition of equality of the phase pressures. For a system of liquid phases these pressures are osmotic in nature.

Proceeding from the equation (*) for unit mass of the surface layer and using the same transformations as in the flat case we obtain two independent equations:

$$ad\zeta = -s_{1\zeta} dT + (v_{1\zeta} - v_2^{(\zeta)}) dP^{(1)} + v_2^{(\zeta)} dP^{(2)} + \sum_{i,k=1}^{n-1} - \\ - (x_i^{(1)} - x_i^{(\zeta)}) \varepsilon_{ik}^{(1)} dx_k^{(1)};$$

$$ad\zeta = (s_{12} - s_{1\zeta}) dT + (v_{1\zeta} - v_{12} - v_2^{(\zeta)} + v^{(2)}) dP^{(1)} + \\ + (v_2^{(\zeta)} - v^{(2)}) dP^{(2)} + \sum_{i,k=1}^{n-1} (x_i^{(2)} - x_i^{(1)}) \varepsilon_{ik}^{(1)} dx_k^{(1)};$$

$$\text{where } v_1^{(\zeta)} + v_2^{(\zeta)} = v^{(\zeta)}.$$

These equations give the relationship between ζ , T , $P^{(1)}$, $P^{(2)}$ and composition of phases. Similar equations may be derived for phase 1, phase 2 and for the composition of the surface layer.

We may pass on to the other variables according to a relation which follows from the Kondo equation:

$$dP^{(1)} = dP^{(2)} + \frac{2}{r} d - \frac{2}{r} dr.$$

Rearranging the superscripts 1, 2 and excluding some of the differentials we may obtain all the thermodynamic equations for the equilibrium of a disperse system. One of these equations contains only the superscripts 1 and 2, thus, describing a microemulsion (that is a system where the surface layer is one of the two equilibrium phases):

$$(v_{12} - v^{(2)}) dP^{(1)} + v^{(2)} dP^{(2)} = s_{12} dT + \sum_{i,k=1}^{n-1} (x_i^{(2)} - x_i^{(1)}) \\ \times \varepsilon_{ik}^{(1)} dx_k^{(1)}$$

This is an analogue of the generalized Van der Waals equation.

Nonspecified variables are convenient to use (superscript 0) to derive the equations describing the effect of the interface curving in the phase fragmentation on the state of the disperse phase and the dispersion medium in our case (when one of the phases is the surface layer):

$$S_{12} \left[a + \frac{2}{r} (v_2^{(0)} - \frac{s_{10}}{s_{12}} v^{(2)}) \right] dT - v_{12} \left[a + \frac{2}{r} (v_2^{(0)} - \frac{s_{10}}{s_{12}} v^{(2)}) \right] dP(1) - \frac{2}{r} \frac{v^{(2)} a}{r} dr + \sum_{1,k=1}^{n-1} \left[(x_1^{(2)} - x_1^{(1)}) (a + \frac{2}{r} v_2^{(0)}) - \frac{2}{r} (x_1^{(0)} - x_1^{(1)}) v^{(2)} \right] g_{1k}^{(1)} dx_k^{(1)} = 0$$

$$S_{12} \left\{ a + \frac{2}{r} \left[v_2^{(0)} - v_{10} - \frac{s_{10}}{s_{12}} (v^{(2)} - v_{12}) \right] \right\} - v_{12} a + \frac{2}{r} (v_2^{(0)} - \frac{s_{10}}{s_{12}} v^{(2)}) dP(2) - \frac{2G(v^{(2)} - v_{12})}{r} dr + \sum_{1,k=1}^{n-1} \left\{ (x_1^{(2)} - x_1^{(1)}) \left[a + \frac{2}{r} (v_2^{(0)} - v_{10}) - \frac{2}{r} (x_1^{(0)} - x_1^{(1)}) (v^{(2)} - v_{12}) \right] \right\} g_{1k}^{(1)} dx_k^{(1)} = 0$$

$$\left\{ a + \left[\frac{2}{r} v_2^{(0)} - v_{10} - \frac{s_{10}}{s_{12}} (v^{(2)} - v_{12}) \right] \right\} dP(1) - \left[a + \frac{2}{r} (v_2^{(0)} - \frac{s_{10}}{s_{12}} v^{(2)}) \right] dP(2) + \frac{2G a}{r^2} dr - \frac{2}{r} \sum_{1,k=1}^{n-1} \left[(x_1^{(2)} - x_1^{(1)}) \frac{s_{10}}{s_{12}} - (x_1^{(0)} - x_1^{(1)}) g_{1k}^{(1)} dx_k^{(1)} \right] = 0$$

The main corollaries

a) We may find the temperature dependence of the microemulsion particle size if its composition and pressure over one of the phases are kept constant:

$$\left(\frac{dr}{dT} \right)_{P(1)}, x_1^{(1)} = \frac{r^2 s_{12}}{2G v^{(2)} a} \left[a + \frac{2}{r} (v_2^{(1)} - \frac{s_{10}}{s_{12}} v^{(2)}) \right],$$

$$\left(\frac{dr}{dT} \right)_{P(2)}, x_1^{(2)} = \frac{r^2 s_{12}}{2G (v^{(2)} - v_{12}) a} \left[a + \frac{2}{r} \left[v_2^{(0)} - v_{10} - \frac{s_{10}}{s_{12}} (v^{(2)} - v_{12}) \right] \right]$$

These expressions are simplified for the limiting cases of small and large radii of the disperse phase. At small radii the derivatives turn to zero demonstrating the mutual compensation of the effects of temperature and composition.

At large radii the signs of the derivatives are determined by the sign of excess entropy S_{12} or by the sign of the molar differential heat of the phase transition $H_{12} = TS_{12}$. we obtain

$$\left(\frac{dr}{dT}\right)_{p_1}^{(1)} \gtrless 0 \text{ for } H_{12} \gtrless 0.$$

The effect of temperature on microemulsion stability is of the opposite character in two coexisting macrophases. A similar treatment for a liquid-vapour system is given in /2/.
b) The similar derivatives with respect to pressures (for constant temperature) depend on the bulking effect V_{12} (for large r).

For small r the sign of the derivatives is determined by the ratio between the volume of the dispersion medium and the volume of the whole system:

$$\left(\frac{dr}{dp}\right)_T^{(1)} \gtrless 0 \quad \text{for } v(1) \gtrless v(2)$$

$$\left(\frac{dr}{dp}\right)_T^{(2)} \gtrless 0$$

c) The equations derived yield, also, the inequalities describing the relationship between the composition and the size of the microemulsion particles. The following rule may be stated: if the disperse phase has a higher concentration of a certain component (relative to the gross composition), increasing concentration of this component gives rise to decreasing size of the microemulsion particles, the temperature and pressure being constant.

In other words, increasing concentration of this component promotes dispersion of the surface layers and formation of microemulsions.

So it may be said that this component plays the part of a surface-active substance. Qualitatively, this follows from Gibbs conception of adsorption.

CONCLUSIONS

The basic thermodynamic equations were used to consider emulsification at extraction. It is shown that the conception of surface layers of finite thickness, accounting for their curvature, permits thermodynamic approach to be used to analyse the formation and stability of emulsions in multi-component systems without recourse to the concept of adsorption. The qualitative results obtained are equivalent to the conception of adsorption of the surface-active components at the interfaces.

The differential equations obtained describe rigorously emulsion equilibrium and conditions of emulsion stability, and indicate the presence of the universal mechanism of hyperfine emulsion formation in the extraction systems. In these systems the amount of the disperse phase is directly proportional to time and intensity of dispersion. It is shown that the microemulsions are highly monodisperse and data are obtained on the influence of various factors on the particle size.

A QUEUE MODEL TO DESCRIBE SEPARATION OF LIQUID DISPERSIONS IN VERTICAL SETTLERS

M.S. Doulah, G.A. Davies

Department of Chemical Engineering, University of Manchester

SUMMARY

A statistical model is presented to describe the continuous steady state separation of droplet dispersion bands formed in vertical gravity settlers and in countercurrent extraction columns. The model is based on queue theory and after review of the birth-death equation describing the process, a numerical simulation is described from which the depth of the droplet dispersion band can be calculated. Results were computed for a range of dispersion flowrates for five liquid-liquid systems. Satisfactory agreement with experimental data was obtained and the results compared favourably with those from deterministic models. The need for more data on interdrop coalescence within a dispersion is apparent from this work.

INTRODUCTION

In gravity settlers droplets flocculate to form a heterogeneous zone at the phase boundary between the two liquids. The final separation of the phases is achieved by droplet coalescence both within this zone and at the phase boundary. The depth of this dispersion band increases with flowrate and also depends on the size of droplets entering the settler^{1,2}. The capacity of a unit is determined by the separation in the dispersion band, if this is less than the incoming flow then the settler rapidly floods.

Similar conditions are experienced in all liquid extractors when the dispersion generated in the contact zone has finally to be separated at the phase boundary between the liquids. It is of interest therefore to be able to predict the performance of settlers. Surprisingly little data are available for this. Design methods are based on a required residence in the settler. This may vary from seconds up to 60 minutes³ without clear definitions of how to calculate the appropriate value in a particular system. The residence time will determine the settler volume, the other parameter settler area is frequently computed from the specific settling rate, ξ , (the settling rate per unit area), Again this may vary from less than $1 \text{ m}^3/\text{m}^2 \text{ hr}$ to $10 \text{ m}^3/\text{m}^2 \text{ hr}$. ξ varies with system physical properties and the droplet size or interfacial area per unit volume of the dispersion. At the present time little data is available from which either ξ or the residence time can be determined without recourse to pilot scale experiments.

In this paper the problem of coalescence and phase separation in a dispersion band in a vertical settler is examined and a statistical model proposed to simulate coalescence behaviour.

Description of the Separation Process

Under steady state conditions droplets continually arrive at the phase boundary and form a close packed array termed the dispersion band, figure 1. In this band droplets coalesce together and hence increase in diameter whilst at the phase boundary droplets coalesce with the bulk fluid to finally leave the dispersion zone. At steady conditions the rate at which material enters the dispersion band must balance the volumetric coalescence rate at the phase boundary. Within the dispersion band countercurrent flow of the continuous phase liquid takes place as this drains back to the bulk continuous phase. In this paper we propose to consider these conditions at steady state.

The process of coalescence of drops at an interface and formation of dispersion bands of drops in spray columns and gravity settlers may be considered analogues to a queue operation. Arriving units (in this case droplets) accumulate to form a queue and are subsequently 'serviced' and leave the queue by coalescence. In the case of dispersion bands the hold time for a certain droplet may be either the time between arriving and drop-drop coalescence or drop-interface coalescence at the phase boundary. In the latter case this results in removal of dispersed phase from the band. Drop-drop coalescence results in a net reduction of the number of drops, for binary coalescence the reduction is one drop, but the volume of dispersed phase in the band remains unchanged. Whilst the coalescence time of a single drop depends on the system physical properties and size of drop there is no one unique coalescence time but a distribution is always observed.

Model

With this analogy with a queue operation the gravity separation of a dispersion may be expressed. Consider the close packed dispersion band formed in a gravity settler made up of a series of droplet queues. Several modes for distribution of droplets entering the dispersion band into these queues can be postulated. In this context let us consider that arriving droplets choose between adjacent queues equally at random then the system can be simplified into independent single channel systems and if the average drop arrival rate into the dispersion band is λ (drops/sec) then if there are m queues the arrival rate into each queue or channel will be $\frac{\lambda}{m}$. (Other possibilities could be considered; for example that droplets rearrange at the inlet to the bed to settle and form the shortest queue and that rearrangement between queues takes place. Clearly in practice the situation is complex). With the simplifications suggested the process can be reduced to that of examining the behaviour of a single queue with the view to predicting the steady state queue length and therefore the depth of the dispersion band.

Let the probability of there being n droplets in the queue at time t be $P_n(t)$. The change in P_n will be caused by new arrivals, by coalescence into the bulk phase at the interface and by interdrop coalescence in the dispersion. This change will of course be equal to zero when steady operation is achieved. A complication exists in representing interdrop coalescence. Account must be made of whether a drop coalescence with an adjacent drop in the queue or whether coalescence takes place between drops in adjacent queues. It is not possible to consider the latter case in formal analysis of the resulting birth-death equations to describe queue behaviour although the possibility can be incorporated in numerical simulation. In a gravity settler the distribution of droplets across the section of the vessel ahead of the dispersion band will not usually be constant at a particular instant. Furthermore although one can define an average drop arrival rate, λ , the frequency of droplets crossing a given plane in the flocculating region will not be constant. Thus the frequency of arrival into each channel will vary and will be represented by a Poisson distribution such that the probability density $p(t)$ is

$$p(t) = \lambda e^{-\lambda t} \quad (1)$$

where $\lambda = \frac{\text{area under curve}}{m}$

If the service time of coalescence time is represented by an exponential distribution function such that the probability density that coalescence of a droplet at the interface is completed in time t , i.e. rate of coalescence, is

$$c_i(t) = \theta e^{-\theta t} \quad (2)$$

where θ is the mean coalescence time at the interface and by analogy for interdroplet coalescence the probability density, $c_d(t)$, is

$$c_d(t) = \gamma e^{-\gamma t} \quad (3)$$

then the birth-death equation for the process relating the probability of finding n droplets in the queue, P_n , may be simplified to:-

$$d [P_n] = [\lambda P_{n-1} + [\theta + \gamma] P_{n+1} - [\lambda + \theta + \gamma] P_n] dt \quad (4)$$

with $n \geq 2$

If the probability P_n is independent of time leading to a statistically steady state then

$$\lambda P_{n-1} + [\theta + \gamma] P_{n+1} - [\lambda + \theta + \gamma] P_n = 0 \quad (5)$$

The solution to the simultaneous algebraic equation contained in (5) is then

$$P_n = a_n \left(\frac{\lambda}{\theta + \gamma} \right)^n P_0 \quad (6)$$

$$\text{where } a_n = \prod_{j=0}^{n-2} R (j+2)$$

$$\text{and } R_n(n) = \left(\frac{\lambda}{\theta + \gamma} \right) \quad (7)$$

where R is the loading factor

In the absence of interdrop coalescence equation (4) gives

$$P_n = P_0 (1 - R) \quad (8)$$

$$R \leq 1$$

The expected number of drops in the system at steady state, L , is then

$$L = \sum_{n=1}^{\infty} n P_n = \frac{R}{1-R} \quad (9)$$

$$R \leq 1$$

The equilibrium state probabilities given in equations (6) and (8) and the expected queue length are valid only when the system has been operating for an infinite time. The problem for finite time operation or for non-exponential probability density functions is not amenable to formal analytical solution of the equations. However an alternative procedure can be adopted using a simulation based on a Monte Carlo method. This is used in the present paper and results of the simulation will be compared with experimental data obtained in a vertical settler.

Consider a vertical section through the dispersion band making up a queue in which droplets enter singly one at a time. If V_o is the volume flow of dispersed per unit cross section entering the dispersion band then the average number of drops entering the settler per unit time, N_o , is

$$N_o = V_o \left(\frac{\pi d_o^2}{4} \right) / \epsilon d_o^3 \quad (10)$$

where ϵ is the surface packing efficiency of drops at the inlet of mean diameter d_o .

$$d_o = \frac{\sum n_i d_i}{\sum n_i} \quad (11)$$

The average time between entering drops, T , is

$$T = \frac{1}{N_o} \quad (12)$$

Simulation of the process is based on this time T . At the phase boundary assume that a drop then occupies an area of the interface equal to the area of a circle having diameter d_H plus a free area around the drop related to the area packing efficiency at this point, ϵ . Thus the interface may be divided into equal units. The assembly of drops above each unit then comprises the queue from which service takes place by coalescence. It is required to calculate the number of drops coalescing and thus leaving the queue by both drop-interface and drop-drop coalescence during the time interval T . To do this information is required on coalescence frequency. Considering the drop interface problem representing service at the head of the queue recourse is made to data reported on single drop coalescence. Many workers⁽⁴⁾ have presented data on this and equations of the form

$$\ln \left(\frac{N}{N_s} \right) = - \left(\frac{C}{O^2} \right) t_c^2 \quad (13)$$

have been found to fit the data for coalescence time distributions for a particular system. N_s is the number of drops in the population with a mean coalescence time O and N is the number of drops coalesced in time t_c .

Equation (13) is the probability density function of the coalescence time t_c . This was used in the simulation and t_c was calculated by the rejection technique for sampling⁽⁵⁾.

It is necessary in computing data for different physical systems to have some method of calculating Θ . This has been found to depend on the physical properties of the system, notably phase densities and viscosities and interfacial tension. A correlation for Θ_n proposed by Davies, Jeffreys and Smith⁽⁶⁾ was used in the present work to calculate Θ , thus:-

$$\Theta = 6.20 \times 10^3 \frac{\mu d}{\sigma} \frac{d^2 \Delta \rho g}{\sigma}^{-1.14} \quad (14)$$

Equation 14 was used to calculate Θ_m for a given system and this value was then used in equation (13) to estimate the coalescence frequency at the interface in the time interval T in the simulation.

Interdrop coalescence must next be considered since drops can leave the queue by this process. Furthermore interdrop coalescence results in a progressive increase in droplet size though the dispersion band which then affects coalescence and service at the phase boundary.

Interdrop coalescence is more difficult to handle since very little data is available either in the form of a probability density function or mean coalescence times. To overcome this deficiency the following procedure was adopted in the present work. First only binary coalescence is accounted for. That is not to say that simultaneous multiple drop coalescence does not take

place but merely to put a very low probability on such events. Then the effect on interdrop coalescence on the mean drop size in the queue and in particular on the mean drop at the phase boundary, since this has direct influence on Θ , can be assessed. Thus the mean drop size after M coalescence events, \bar{d}_m can be related to the mean drop size of entering drops d_0

$$\bar{d}_m = \frac{(M d_m^3 + (n_o - 2M) d_o^3)}{n_o - M} \quad (15)$$

Similarly after $M + 1$ coalescence events

$$\bar{d}_{m+1} = \frac{d_{m+1}^3 + (n_o - M - 2) \bar{d}_m^3}{n_o - M - 1} \quad (16)$$

For binary coalescence of two equal sized drops

$$d_m = \bar{d}_m (2)^{\frac{2}{3}}$$

Equation (16) represents a difference equation in \bar{d} . Rearranging it can be shown that (16) reduced to

$$\bar{d}_{m+1} - \bar{d}_m = \bar{d}_m \left[\left(1 - \frac{1}{n_o - M} \right)^{\frac{2}{3}} - 1 \right] \quad (17)$$

Expanding the right hand side and neglecting powers greater than 1 gives:-

$$\Delta \bar{d}_m = \bar{d}_m \left[\frac{1}{3 n_o (1 - M/n_o)} \right] \quad (18)$$

Defining $\omega = \frac{M}{n_o}$ and $d\omega = \frac{dM}{n_o}$

$$\Delta \bar{d}_m = \frac{\bar{d}_m}{3 n_o (1 - \omega)} \Delta M \quad (19)$$

where $\Delta M = 1$

This difference equation may be reduced to a differential equation.

Thus $\lim_{\Delta M \rightarrow 0}$

$$\frac{d \bar{d}_m}{d\omega} = \frac{\bar{d}_m}{3 (1 - \omega)} \quad (20)$$

This may be integrated over the queue since $\bar{d}_m = d_o$ at $\omega = 0$, the inlet, and $\bar{d}_m = \bar{d}_H$ at $\omega = \omega$, the phase boundary. This gives

$$\omega = \frac{\bar{d}_H^3 - d_o^3}{\bar{d}_H^3} \quad (21)$$

The extent of interdroplet coalescence, w , as stated effects not only the droplet size but also the overall separation rate of the dispersion since $\theta = f(h_H)$.

Thus at steady state

$$V_o = V_H = \frac{2}{3} \eta^1 \frac{\bar{d}_H}{\theta} \quad (22)$$

θ can be calculated using equation (14) which gives for a particular physical system:-

$$\bar{d}_H = C_1 V_o^{0.44} \quad (23)$$

This equation can be used for obtaining information on the extent of interdrop coalescence in a particular system from experimental data on steady state settling. Such data has been published by Smith and Davies⁽⁸⁾. Using this data for w can be generated. It was found that values for w obtained could be represented by Weibull distribution function thus

$$w = 1 - \exp \left(- (H/d_o)^B / \delta \right) \quad (24)$$

The simulation procedure used to model steady state settling can now be described. The simulation time, T was set. At time zero simulation was commenced. After time T the probability of coalescence at the interface was determined by selecting t_c (by random selection) and substituting into the probability density function equation (13). The simulation time was then advanced by a further increment T during which time a drop arrives and joins the queue. The queue length or dispersion band depth is then calculated the change in mean drop size at the interface taking place as a result of interdrop coalescence during this time period. This up dated value of \bar{d}_H is then used to calculate θ and then the probability of coalescence at the phase boundary as before. This procedure was repeated and the queue allowed to develop. The simulation was continued for 400 to 600 seconds real time by which time a 'steady state' value for queue length had normally been achieved. The value of the queue length was recorded at 20 second intervals after the start of the simulation.

Results and Discussion

The apparatus used and experimental data has been published in an earlier paper⁽⁷⁾. In this, data for steady state operation of a vertical settler is recorded and the variation of dispersion band bed depth with flowrate and inlet drop size is presented for a range of liquid systems. In all cases as the dispersed phase flowrate was increased or the inlet mean drop size d_o decreased the depth of the dispersion band increased. It was further shown that H varied exponentially with flowrate V ($H = A e^{BV}$), a result which has subsequently been confirmed by other workers (2,8). Because of the variation of H with d_o it was convenient to represent data by combining these to give a dimensionless group (H/d_o). In comparing the data from the present model with the experimental results the steady state queue length computed (representing H) was divided by d_o .

The operating conditions analysed in the present work covered a range of flowrates from 3.6 to 45 M^3/M^2HR , inlet mean drop diameters over the range 2mm to 6.5mm for five liquid-liquid systems. The discussion on the choice of systems may be found in reference (7).

The results obtained are compared with experimental data in figure 2. The depth of the dispersion band predicted from the model is plotted along the ordinate. Complete agreement between experiment and theory would correspond to a line through the origin with slope 1.0 i.e. $y = x$. As is evident some scatter is obtained. The line on the graph was obtained by a linear regression analysis on the data. The equation for regression of y , the values predicted from model, on x the experimental data is

$$y = 1.0442x + 0.31528 \quad (25)$$

and the 95% confidence limits for the slope are 0.9756 and 1.1129.

The scatter is seen to be random about the regression line for all the systems. The majority of data predicted from this queue model is however consistently greater than the experimental data. Possible reasons for this may include the method employed to account for interdrop coalescence, interactions between adjacent droplets in the vicinity of a coalescence event both within the dispersions and in the phase boundary and the simplified structure assumed for the arrangement of droplets within the dispersion band. Considering these there is clearly a need to provide more information on interdrop coalescence within a dispersion. If data were available in the form of a probability density function and mean coalescence times then this could readily be included in an analysis. Without such information both statistical and deterministic models which may be formulated for this process will have to include some simplifying assumptions. The difficulty lies in the measurement techniques. A non disturbing technique is required to obtain information within the dispersion away from solid surfaces. This is necessary since wall effects can completely obscure the measurements⁽⁹⁾. Recently a technique using iso-optic systems has been developed⁽¹⁰⁾ from which this data can be obtained and more work is being carried out. Some workers have suggested that interdroplet coalescence is of minor significance in dispersion separation and that drop interface coalescence is the controlling mechanism^(11,12). More recent experimental work in laboratory and pilot plant equipment has refuted this^(7,8). In the present model results were computed for the case when only drop-interface coalescence took place. Results were obtained from the analytical solution, equations 8 and 9 and by numerical simulation. In both cases the predicted results for all five liquid systems considered were much greater (factors of between 1.5 to 4 times) than the experimental values.

The other problems mentioned may also be investigated by using the same techniques. In the model presented here it has been assumed that the system can be reduced to essentially independent parallel queues. Information gained in earlier work on signal layers of drops (i.e. $H d_0$) indicated that interaction effects are evident⁽⁶⁾. If these are significant within dispersion bands then the overall effect would be to effectively reduce the queue length. Again further work may elucidate this.

Notwithstanding these points reasonable agreement between experiment and the model was obtained. The experimental data for bed depth H may vary by 10%. The predictions of this statistical model are as good as those of deterministic models published earlier ⁽¹³⁾ and when more data is available further improvements may be possible.

CAPTION FOR FIGURES

Fig.1. Diagram of dispersion band in a continuous gravity settler

Fig.2. Comparison of simulated results from model with experiment

NOMENCLATURE

C	constant, equation (13)
C_1	constant, equation (23)
$C_d(t)$	rate of drop-drop coalescence
$C_i(t)$	rate of drop interface coalescence
d	droplet diameter, Sauter mean diameter
g	gravitational constant
H	depth of dispersion band
L	expected number of drops in queue
M	number of interdroplet coalescence events
m	number of queues or number of interdrop coalescence events
N_o	number of drops entering settler per unit time
N	number of drops coalesced in time t_c
N_s	number of drops in sample population
n	number of droplets
p	probability
$p(t)$	probability density function
R	loading factor, equation (7)
T	simulation time
t_c	coalescence time
v	volumetric flow rate per unit cross section area
x	experimental value, H/d_o
y	simulated value, H/d_o
\hat{y}	predicted value from regression analysis
Λ	drop arrival rate d
s	constant equation (24)
s	constant equation (24)
γ	mean drop-drop coalescence time
	settling rate per unit area
λ	drop arrival rate into queue

θ	mean drop-interface coalescence time
η'	surface packing efficiency
σ	interfacial tension
ρ	density
μ	viscosity
ω	extent or degree of interdrop coalescence, equation (21)

Subscripts

o	conditions at the inlet of the dispersion bed
H	conditions at the outlet of the dispersion bed
d	dispersed phase

REFERENCES

1. Jeffreys G.V., Davies G.A. & Pitt K., A.I.Ch.E.J. 16, 823, (1970)
2. Gondo S., & Kusanoka I., Hydrocarbon Processing No.9, 210, (1969).
3. Treybal, R.E., "Liquid Extraction" 2nd ed. McGraw Hill Book Co., New York (1963).
4. Jeffreys G.V., & Davies G.A., Ch.14 "Recent Advances in Liquid Extraction" Ed. C. Hanson, Pergamon Press, (1971).
5. Shreider Yu. A., "The Monte Carlo Method", Pergamon Press, London (1966).
6. Davies G.A. Jeffreys G.V., & Smith D.V., I.S.E.C. 1, 385, (1971).
7. Smith D.V. & Davies G.A., Can.J.Chem.Eng. 48, 628, (1970).
8. Warwick G.C.I., Scuffham J.B., & Lott J.B., I.S.E.C. 2, 1373, (1971).
9. Smith D.V., Ph.D. Thesis University of Manchester (1969).
10. Sui S.M., M.Sc. Thesis University of Manchester (1972).
11. Ryon A.D., Daley F.L., & Lowrie R.S. Chem.Eng.Prog., 55, 70 (1959).
12. Lee J.C., & Lewis G., Inst.Chem.Eng.Symposium Series No.26, 13, (1967),
13. Smith D.V., & Davies G.A., A.I.Ch.E. Symposium Series 68, 124,1 (1972).

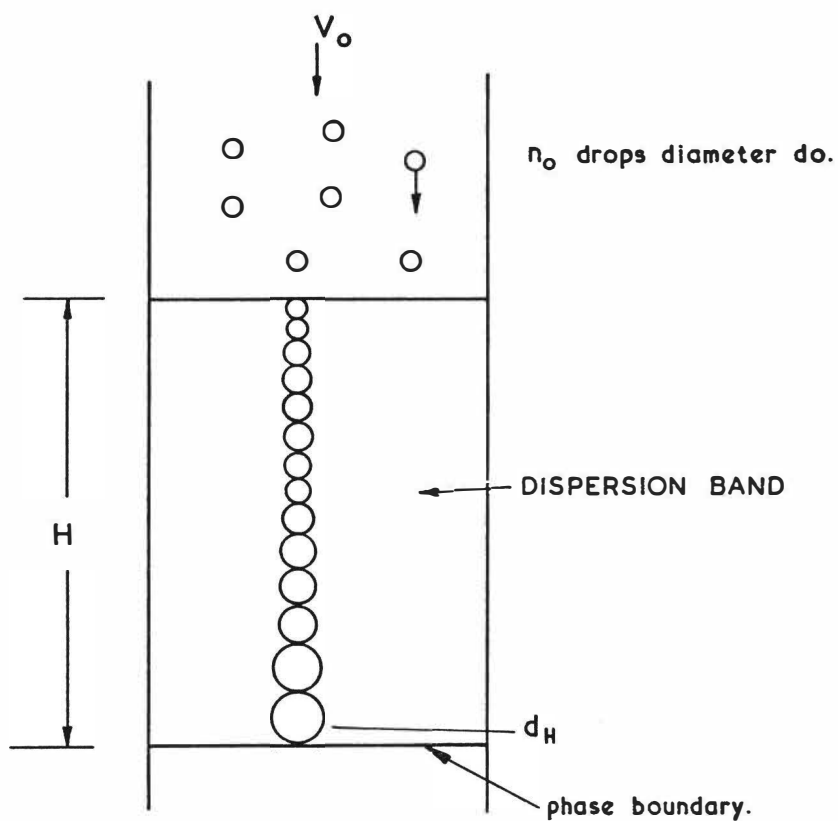


FIGURE 1. DIAGRAM OF DISPERSION BAND IN A CONTINUOUS GRAVITY SETTLER .

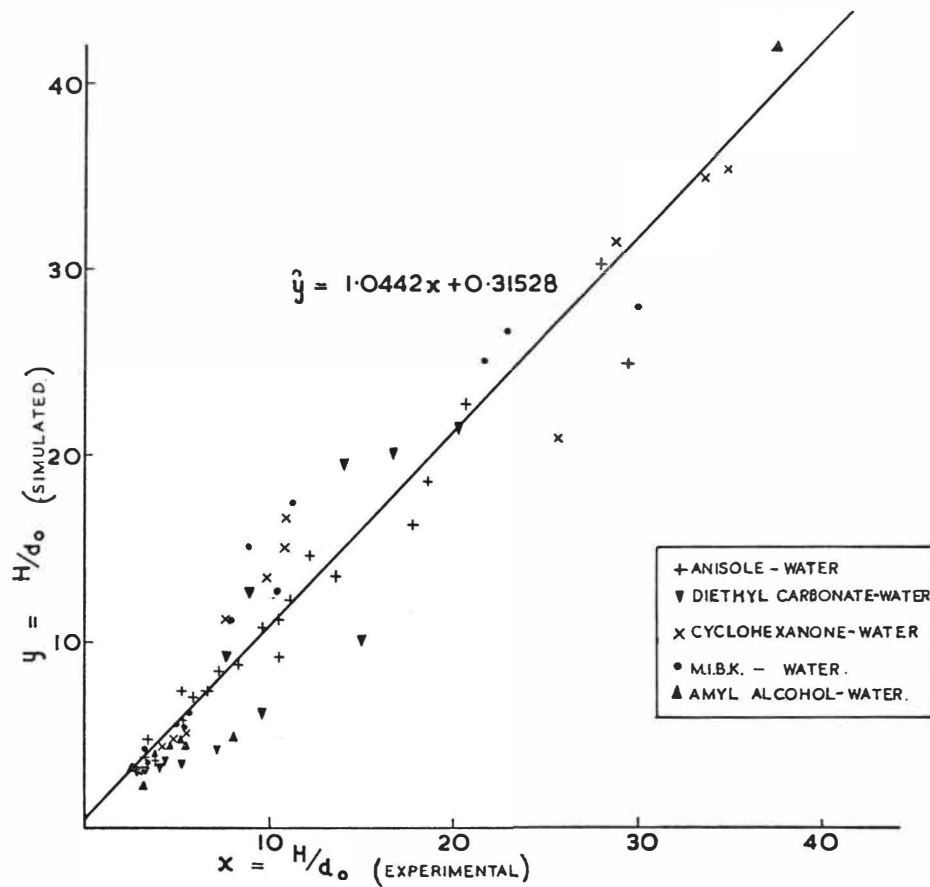


FIGURE 2.

COMPARISON OF SIMULATED RESULTS FROM MODEL
WITH EXPERIMENT.

COMPARATIVE STUDY OF INDUSTRIAL COALESCING
PACKINGS PERFORMANCES IN PETROLEUM INDUSTRY

J.P. EUZEN,

J. RIPOCHE,

M.J. GUTTIERREZ

ABSTRACT

The removal of free water from jet fuel and diesel fuel oil by coalescence has been studied both on laboratory scale and in an on-line pilot plant. The most efficient packing materials and optimal operating conditions have been selected.

During the laboratory work screening tests on various materials have been operated. Thereafter, the best of them have been used in a more systematic research on the influence of bed thickness and superficial velocity.

The most attractive materials have been tested on a pilot plant in order to determine their endurance in industrial environment. It has been found out that the most effective systems were made up by thin fiber glasswool followed by a packing of coarse polyester felt.

x : Institut Francais du Petrole - C.E.D.I. - B.P. n° 3 - 69390
VERNAISON

xx : Centre de Recherche Elf de Solaize - B.P. n° 22 - 69360
SAINT SYMPHORIEN D'OZON

In petroleum refining, straight-run products such as kerosene and diesel fuel oil contain water in two fashions: dissolved water and free water in very small (3 to 20 μ) droplets. The whole water content is about 1000 p.p.m., the dissolved water concentration being only of 100 to 200 p.p.m., according to the temperature and the type of hydrocarbons. In order to meet commercial specifications, the refiners try to remove, first of all, the undissolved water. The coalescence on fibre beds is known to be an interesting way to separate the two components of a liquid-liquid suspension. We therefore started a research program in order to find cheap industrial materials which could be used in this particular case.

The INSTITUT FRANCAIS DU PETROLE (I.F.P.) and E.R.A.P. successfully cooperated during this study.

The mechanism of coalescence in fibrous materials is not yet well established. However the parameters most frequently mentioned as important ones are :

- the nature and the size of the droplets of the dispersed phase (3.7.8),
- the nature and the diameter of the fibers (1.2.3.5.6.8),
- the thickness of the packing (6.7),
- the superficial velocity of the liquid in the fiber bed (2.4.5.8).

Although it has been recognized that this set of parameters governs mainly the performance of a coalescer, a quantitative prediction of their influence does not seem to be possible.

EXPERIMENTAL SECTION

LABORATORY : According to the conclusions of the literature survey, we focused our studies to the influence of the following parameters :

- the nature of the fiber
- the diameter of the fiber,
- the thickness of the packing bed,
- the superficial velocity.

During screening tests, we compared fibers of different kind, keeping constant all the other parameters.

So we used the following fibers :

- fiber glass (woven or felt),
- polyester (woven or felt),
- polypropylene (felt),
- chlorinated fiber (P.V.C. felt),
- steel (knitted),
- polytetrafluoroethylene (felt).

The experimental apparatus (see fig.1) consisted essentially on an emulsion generator and of the test coalescer. The emulsion "water in gasoil" was produced in a loop-line composed by a centrifugal pump and a small tank. Droplets of about 5 μ of diameter, like ones in industrial gasoil, were obtained with a good reproductibility. The undissolved water content was about 1 000 p.p.m. The coalescer was a cylindrical vessel wherein the coalescing material could be fixed and more or less compacted. The coalesced water was collected in a water accumulator sump. Input and output water concentrations were measured by the Karl-Fisher method. For small concentrations, a capacitance hygrometer was used. The visual aspect of the suspension was also evaluated by the experimenter. The superficial velocity studied ranged from 0 to 1.75 cm/s.

In table 1, the performances of various packings are shown, classified in four sections, according to their visual aspects. So coalescence can be Total (T), Good (G), Partial (P), Bad (B).

In a second step, selected materials were tested more accurately for various thickness and superficial velocities. For industrial purposes, one has to consider two important response variables :

- the pressure drop in the coalescer ΔP ,
- the relative residual free water content ($R = 100 \times$ residual free water in output flow/initial free water in input flow).

We tried therefore to compile correlations between this two responses variables and the operational conditions of the coalescer (thickness of the fiber bed and superficial velocity).

This attempt has been successful for several materials. The result can be summarized as follows.

The pressure drop was accurately predicted by the formula:

$$P = k \times (L \times V)^{0.86}.$$

where :

- ΔP : pressure drop in packing (g/cm^2),
- L : thickness of the packed bed (cm),
- V ; superficial velocity of the liquid (cm/s),

The values of k depend on the type of material. So we found:

- 43 for chlorinated fiber,
- 66 for polyester felt,
- 480 for fiber glass.

Concerning the residual free water content, R , two quite different behaviours could be observed, according to the values of the superficial velocity:

- for small velocities (≤ 0.2 cm/s), R is influenced only by the thickness of the fiber bed (Fig.3). In the case of chlorinated fibers for example, the results can be correlated by $R = 30 \cdot 10^{-0.03L}$;
- for higher velocities (above about 0.2 cm/s, R varies with both thickness and velocity, according to the relation $R = 238 V/L$ (for chlorinated fibers).

Starting from the required values of the response variables,
- ΔP (obtained from economical and mechanical considerations),
- R (given by commercial specification),
we can get the highest velocity acceptable for the ΔP value and realizing the necessary coalescence. The estimation of the corresponding bed thickness is quite straightforward. The procedure is shown in the nomograph of fig.4.

The fiber glass packing had been shown to give interesting results during the laboratory tests, but more complex beds made by associating more loose materials to the already studied packings were much more efficient. This kind of association has therefore been used during the endurance test in an industrial environment.

INDUSTRIAL CONDITIONS

The experimental apparatus (fig. 5) consisted of a pump to assure a steady flow, a rotometer, a filter (magnetic + 10 μ cartridge) and a coalescer. The main part was a commercial coalescer modified to receive layers of coalescing materials. Special perforated trays were used to prevent the layers from collapsing. Input and output lines were connected to the same stream of gasoil. The superficial velocity could be chosen between 0 and 2 cm/s.

Some preliminary runs were carried out in order to fix the most convenient values for the parameters. We decided to perform all the runs with the same velocity of 0.3 cm/s, corresponding to a liquid flow of 0.5 m³/h.

The analysis of the total water content in the input and output flow gave the every day performances of the apparatus. The run was continued until the output water concentration showed a sharp increase (example of fig.6). From time to time, we determined the actual efficiency i.e. the ratio of the free water content in the output, on the free water in the input.

Five runs have been performed until today and interesting results have been observed. In a first step, we tried beds containing only one material; the association of materials were tested later on. Results are summarized in table 2 and figure 5. The tests of endurance took a lot of time, but their results with beds of associated materials were very encouraging. For instance, a packing made of fibreglass followed by some polyester felt layers, gave performances equivalent to coalescing cartridges designed for our unmodified commercial apparatus, but the home made packing was cheaper than cartridges.

We can also note that a decrease of efficiency corresponds to an increase of the pressure drop in the packing. The warping of fibrous material is the main problem we shall try to solve in the near future.

CONCLUSION

Our studies, carried out on laboratory scale and on a refinery pilot plant, gave us a selection of cheap and efficient materials for coalescing free water present in straight-run gasoil.

The association of different materials proved to be frequently the most attractive solution for this kind of problems ; e.g. the coupling of a bed of thin fiber glass with some polyester felt layers was very efficient in our particular case.

The laboratory studies allowed to define a design procedure for an industrial coalescer equipped with fibrous materials.

TABLE 1

MATERIALS	NUMBER OF LAYERS	THICK- NESS (mm)	EFFICIENCY FOR A VELOCITY OF (cm/s)			
			0.25	0.5	1	1.5
Polypropylene	10	115	G	B		
(felt)	25	310	T	T	G	G
Polyester						
(felt n° 1)	15	30	T	G	P	B
(felt n° 2)	70	5	B			
(woven)		0,5	G	B	B	B
Chlorinated fibers	5	9	P	B	B	B
	10	14	G	P	B	B
	15	20	T	T	G	P
	15	35	B	B	B	B
	25	15	T	P	B	B
Polytetrafluorethy- lene (wool 50 μ)		5	B	B	B	
		35	B			
Steel (woven 5 μ)		0.5	B			
(knitted 250 μ)		145	B	B	B	
Fiber glass						
(woven)	16	35	G			
	17	35	T	G	B	B
	10	21	G	G	B	B
	16	32	G	G	B	
(roving)	5	5	B	B	B	B
	15	13	B	B	B	
Fiber glass (felt)						
(\emptyset 3.5 μ)	15	33	T	T	T	T
(\emptyset 1.5 μ)	5	35	T	G	B	B
(\emptyset 1.5 μ)	10	20	T	T	G	
(\emptyset 1.5 μ)	15	5	T	G		

ASSOCIATION OF MATERIALS

Compound fiber glass + metal (knitted)		20	B	B	B	B
Fiber glass (felt)						
(3.5 μ)	5		T	G	G	
(1.5 μ)	5					
Fiber glass (3.5 μ)	15		T	G	B	
+ polyester	1					
Fiber glass (3.5 μ)	10	30	T	T	G	
+ polyester	2	10				
+ métal (knitted)		15				

Total (T), Good (G), Partial (P), Bad (B).

BIBLIOGRAPHY

- 1 BELK T.E., Chem. Eng. Prog. 61 (1965), p. 72
- 2 DAVIES G.A., JEFFREYS G.V., Filtration and separation, 6, 349-354 (1969)
- 3 DAVIES G.A., JEFFREYS G.V., PRYCE-BAYLEY D., Print of Knitmesh Ltd,
Greenfield
- 4 SPIELMAN L.A., GOREN S.L., Ing. Eng. Chem. Fund., 11,1, p. 66 and p.73 (1972)
- 5 SAREEN S.S., ROSE P.M., GUDESEN R.G., KINTNER R.C., A.I.Ch.E. Journal, 12
1966, p. 1045
- 6 THOMAS R.J., MUMFORD C.J., Tome 1, Proceedings of Int. Solv. Ext. Conf.
La Haye (1971)
- 7 SHERONY D.F., KINTNER R., Can. J. Chem. Eng., 49, 314-325, June 1971
- 8 HAZLETT R.N., Ind. Engng. Chem. Fund., 8, 625-633, Nov. 1969

-:-:-:-:-

TABLE 2

	TOTAL TREATED VOLUME (m ³)	ON STREAM DAYS	AVERAGE PRESSURE DROP IN PACKING (bars)	AVERAGE FLOW- RATE (m ³ /h)
Polypropylene felt 23 layers	164	17	0.1	0.4
Fiber glass				
20 layers	100.8	7	0.25	0.6
40 layers	127	12	0.50	0.45
4 P.V.C. felt + 20 fiber glass	137		0.2	0.55
20 fiber glass + 10 polyester felt	458	40	0.4	0.47

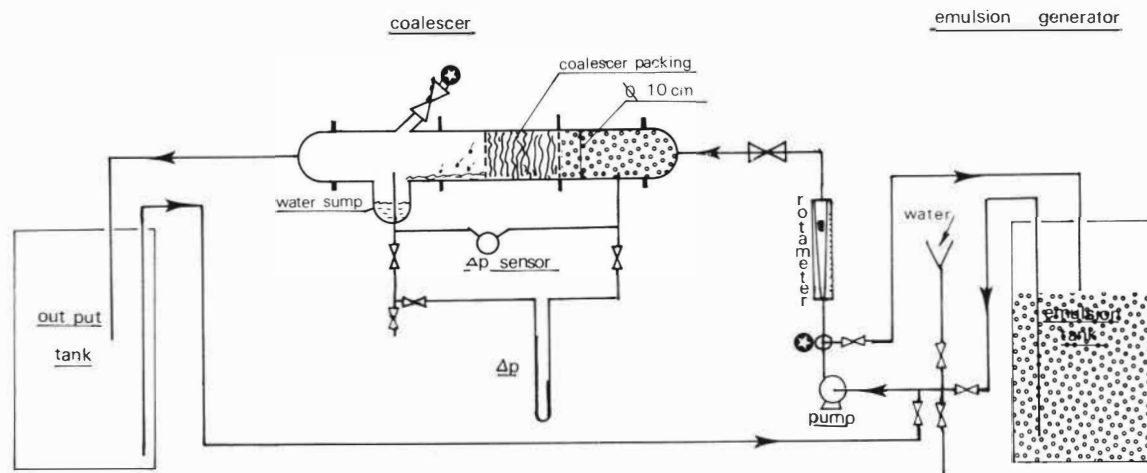
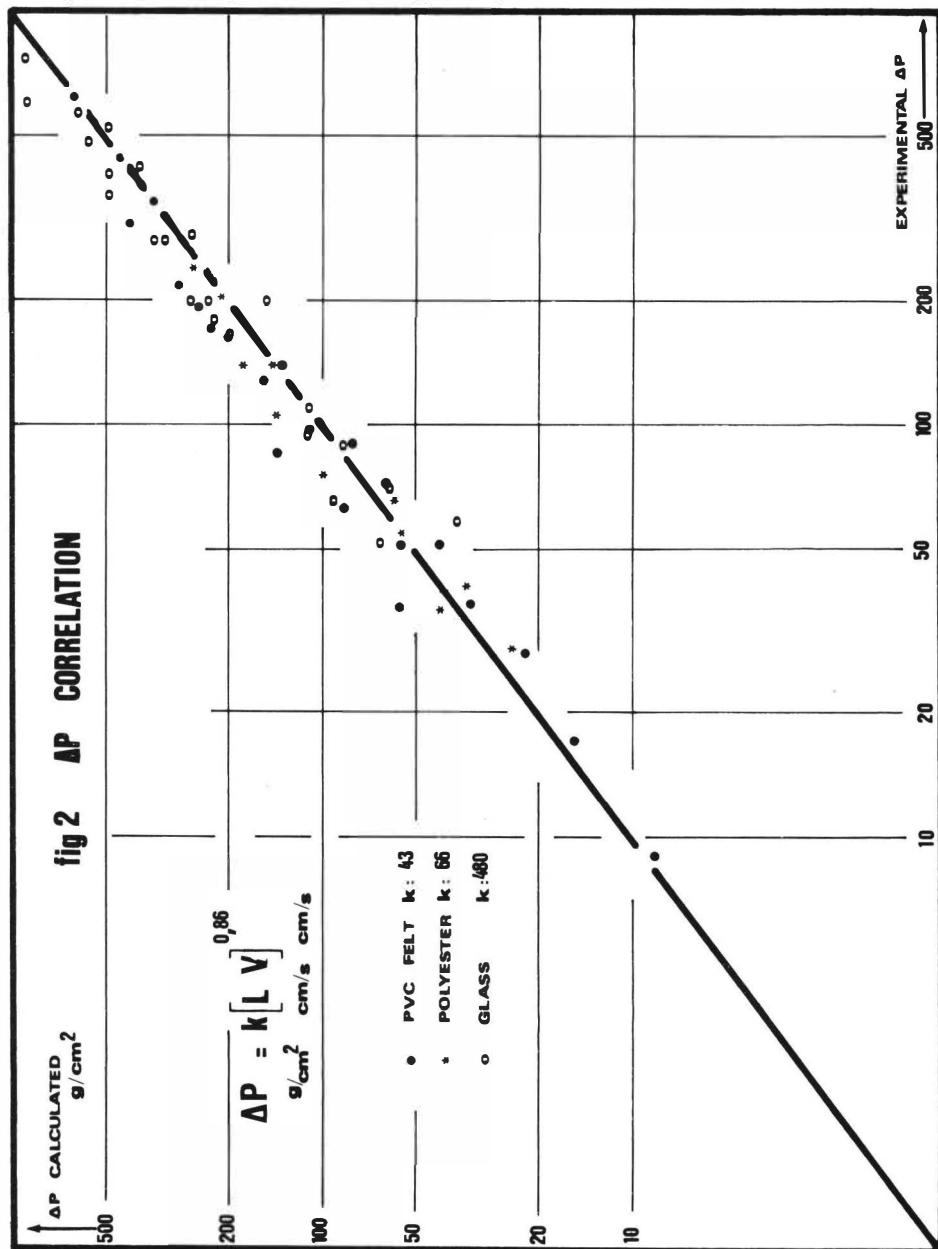
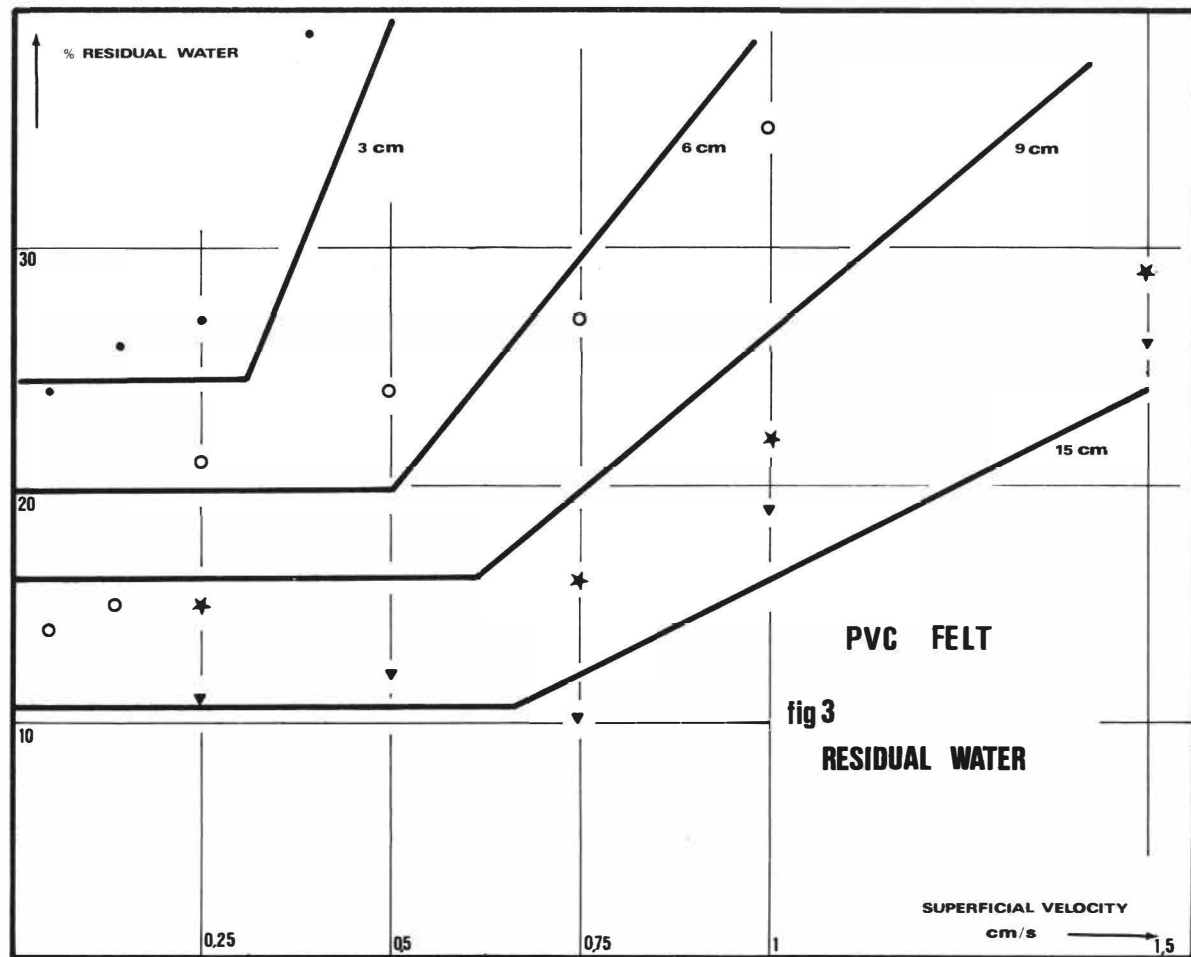
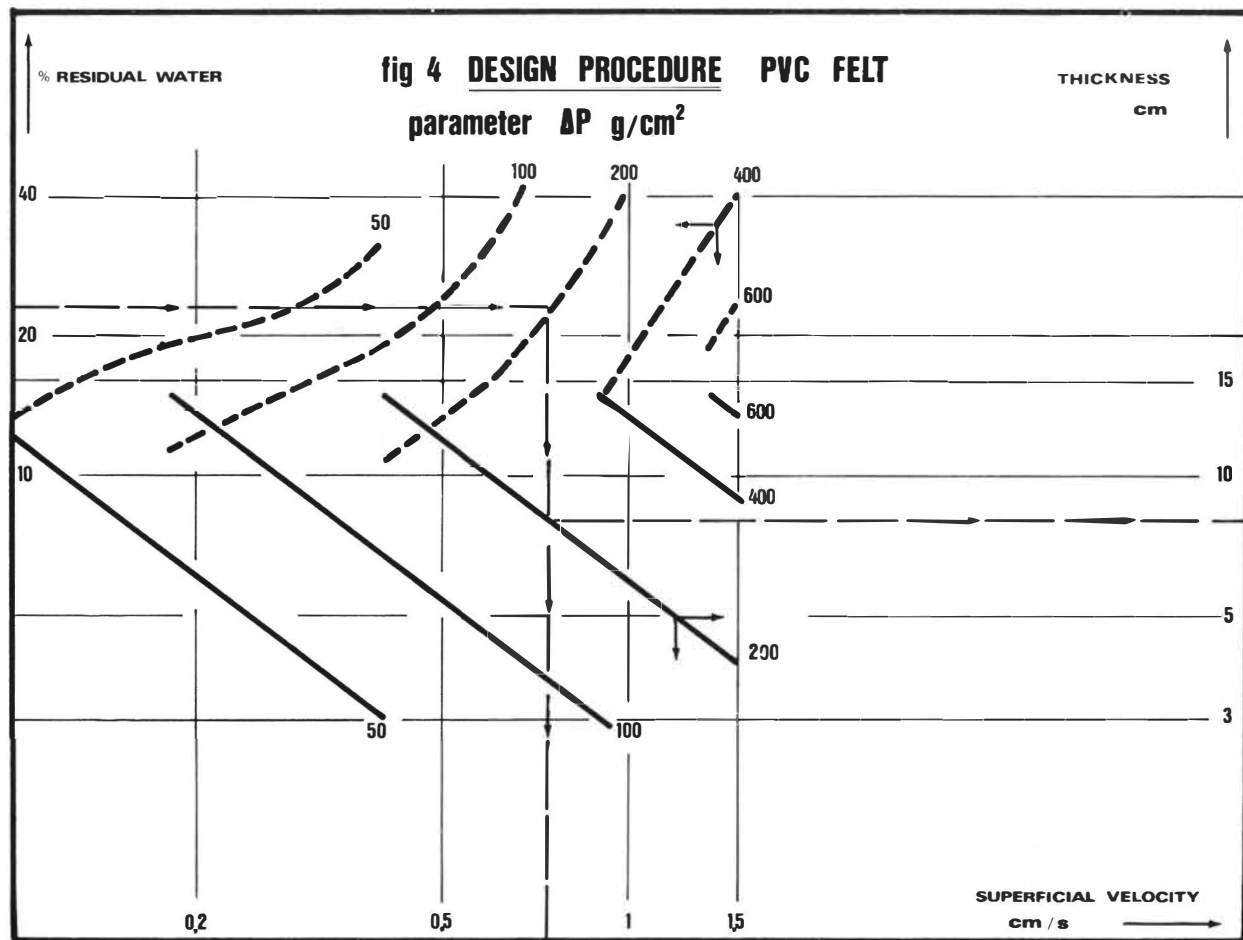


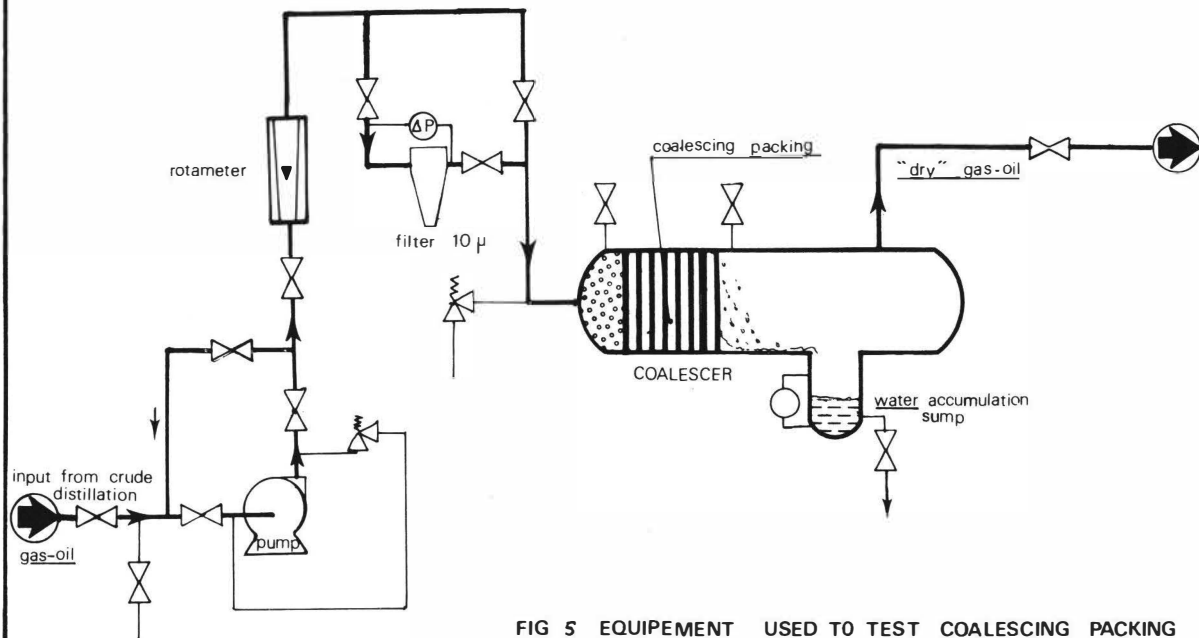
FIG 1 PILOT APPARATUS FOR COALESCING PACKING STUDY

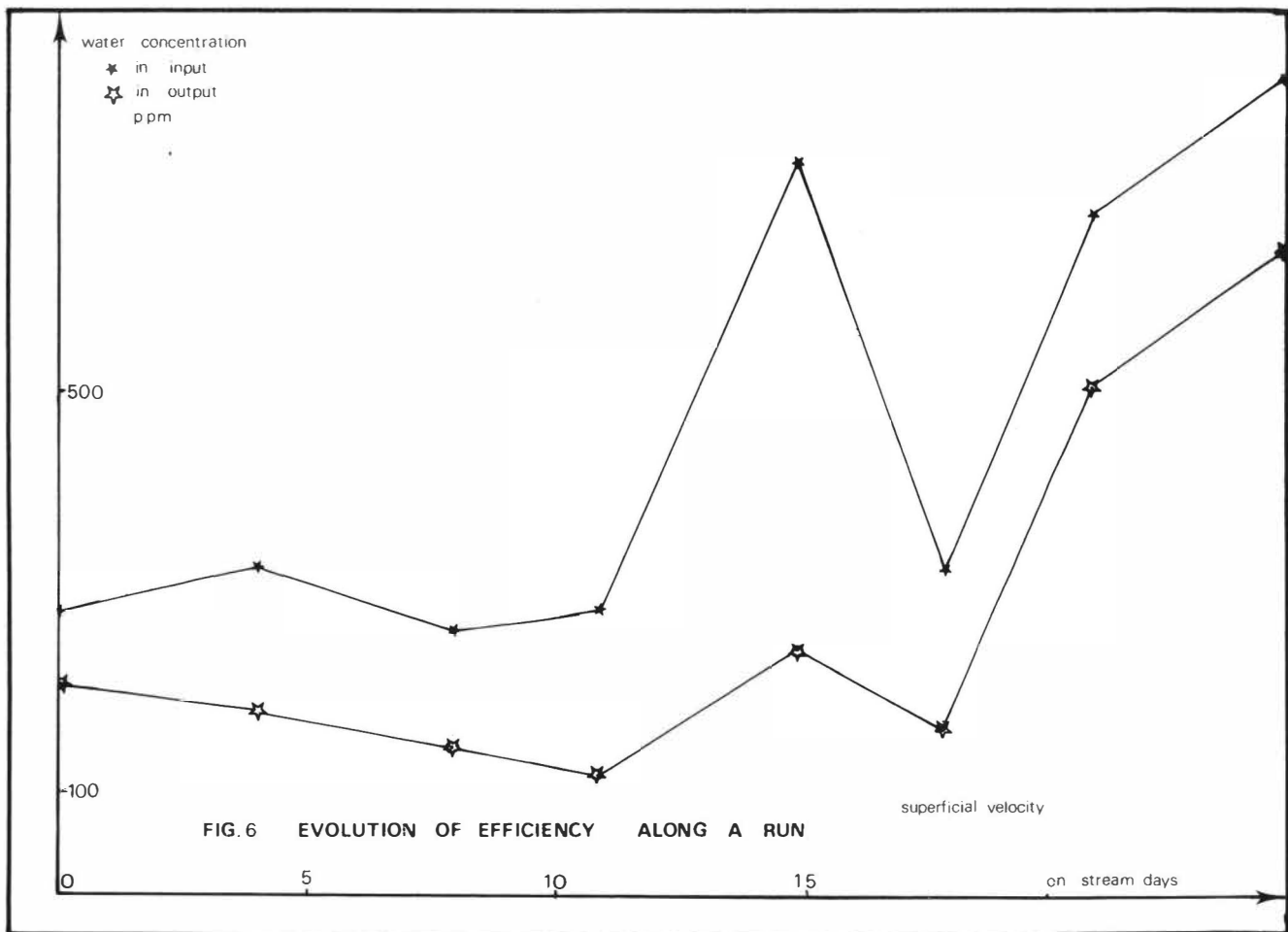
\oplus analysis point











"AN IMPROVED SETTLER DESIGN IN HYDROMETALLURGICAL SOLVENT
EXTRACTION SYSTEMS" *

I D Jackson; J B Scuffham; G C I Warwick & G A Davies *

Davy Powergas Limited
Research & Development Division
Stockton on Tees
England

ABSTRACT

The design and operating characteristics of settlers associated with large scale hydrometallurgical solvent extraction plant are reviewed and problems of scale and solvent inventory discussed. Major improvements on simple gravity settlers are shown to be possible by the use of recently developed coalescer aids. These are described and pilot plant data presented. The advantages in capital costs gained by such improved designs are reviewed.

* Dept. of Chemical Engineering, University of Manchester
Institute of Science and Technology, Manchester, England.

INTRODUCTION

The development of solvent extraction processes over recent years has led to their use on an increasing scale in metal extraction plants. In recent applications for copper and uranium recovery, for instance, total flow rates have been of the order of several thousands of litres per minute. Large scale operation brings with it problems which are not always evident in smaller scale plant and some of these problems will be highlighted in the present paper.

Mixer-settlers are almost universally used for metallurgical extraction processes and this paper will review factors important in the design of large scale mixer-settler systems with particular reference to the design of settlers. Some improvements in the design of settlers have been made recently by the use of coalescer aids and these will be described. Laboratory work using these coalescer aids will be presented and, finally, the costs of systems incorporating these aids will be compared with the costs of conventional systems.

The liquid-liquid system chosen for the experimental work was the extraction of copper from aqueous solutions by Lix 64N * dissolved in Napoleum 470.

* Trade mark for a General Mills solvent

Economic Factors in the Design of Mixer-Settlers

In order to arrive at the most economic design of a mixer-settler system for a given application, it is necessary to consider all the factors which affect the capital and operating costs of the system.

Factors having a significant effect on the capital costs are :

- a) the number of stages
- b) the mixer volume per stage
- c) settler area required
- d) solvent inventory
- e) solvent recovery system
- f) construction costs and
- g) ancillary equipment such as pumps, pipework, instrumentation, etc.

Operating costs are made up of :

- a) solvent loss - make-up costs
- b) acid loss
- c) power costs, mixing and pumping
- d) operating labour costs

In addition, the economics of the process are greatly affected by the extraction efficiency achieved which determines the value of unextracted metal in the raffinate.

Most of the variables which affect both capital and operating costs of a plant rely upon relationships between the degree of mixing to which the phases are subjected, the extent of mass transfer which occurs and the subsequent degree and rate of phase separation which can be achieved.

Mixing

Some consideration has been made of design of mixer systems for these large throughput plants (1). A pump-mix system which eliminates the need for interstage pumps has been successfully scaled-up to give stream throughputs of 28 M³/min of mixed phase. Having selected a mixing system, capital and operating costs dependent on the mixer are fixed. Factors affecting mixing will not be considered further in this paper.

Settling

In addition to the physical properties of the system, the main factors which influence settling are the phase continuity, the droplet size distribution produced in the mixer, the flow conditions and the interface control in the settler. In the settler, complete phase disengagement must be achieved if extraction efficiency is to be maximised. Entrainment between stages means loss of efficiency and entrainment in the outlet streams results in the loss of either solvent or acid which directly affects operating costs. In addition, the presence in product streams of entrained droplets of the opposite phase can have chemical side effects on subsequent process stages. For example, the entrainment of organic phase in the aqueous stripping solution in copper extraction can lead to contamination of the cathode copper produced by electrolysis from that solution. This phenomenon is known as "organic burn". (2). The type of dispersion formed during mixing, either organic in aqueous (o/w) or aqueous in organic (w/o) is of great importance since coalescence and separation rates are not the same for each system. Other factors being equal, it would be desirable to operate a system such that the dispersion resulting in the highest possible separation rate was formed in the mixer. This is largely determined by the phase ratio and degree of mixing. However, choice of a single optimum operating condition is not always possible since in most systems a significant ambivalence range exists (ie a range of phase ratios within which either o/w or w/o dispersions can be formed). Thus the settler must be designed for the worst operating conditions, ie to handle the most stable dispersion. In addition, the settlers must be designed for the lowest seasonal temperature since settling rates usually decrease with temperature (3). To illustrate the effect of phase continuity on settler performance, Fig 1. shows how, in copper extraction, the dispersion band thicknesses in the extraction settlers are substantially greater when the mixer is operating with an organic continuous dispersion than they are when the organic is dispersed. Mixer impeller speed is also important in directly affecting the settler performance. Whilst increasing impeller speed can improve extraction efficiency, the loading on the settler increases (with increasing interfacial area in the dispersion). This can also be seen in Figure 1 where the dispersion band thickness in a settler increases with increasing impeller speed.

The phase continuity of the dispersion and the impeller speed both influence the degree of entrainment in the streams discharging from a settler. Providing the settler is correctly designed and operated such that the primary dispersion is separated, entrainment is entirely of the very small droplets (diameters $<10\text{-}30\text{ }\mu\text{m}$)

constituting the secondary dispersion. Since secondary dispersions can be produced during both mixing and coalescence of primary dispersions it is not surprising that phase continuity and mixer speed influence entrainment. Results of entrainment from a gravity settler are shown in Figure 2. With a w/o dispersion aqueous entrainment is significantly higher and covers a broad range which increases with impeller speed (illustrated as tip speed). The organic entrainment produced during coalescence in the settler is much lower. If the dispersion inverts to become a o/w dispersion in the mixer, high organic entrainments are experienced. Thus it is common practice to run a mixer settler organic continuous if the organic entrainment is to be kept low. This is utilised in the last extraction stage and in the first stripping stage to minimise solvent loss and organic carryover to the electrowinning cells.

Gravity Settlers

In designing gravity settlers, the factors discussed above are all important. For the development of designs of an extraction plant for the treatment of copper leach liquors, studies on bench scale equipment (capacities up to $5.0 \times 10^{-4} \text{ M}^3/\text{min}$) and pilot scale ($1.9 \times 10^{-1} \text{ M}^3/\text{min}$) were carried out in order to provide information for the scale up to a full scale plant ($28 \text{ M}^3/\text{min}$). In common with other design procedures, a specific settling rate i.e. $\text{gal}/\text{ft}^2 \text{ min}$ or $\text{M}^3/\text{M}^2 \text{ hr}$ was determined from experimental work and this was used, in conjunction with constraints on the mean horizontal velocity of the bulk phases through the settler to establish the overall size of the settlers required for a particular throughput. As mentioned above, mixing conditions, phase continuity, entrainment levels and permissible limits were all considered in the experimental work carried out to determine specific settling rates. Also, the effects of crud and particulate matter, especially calcium sulphate which is often present in leach liquors were studied. The results of scale-up are illustrated in Figure 3 which shows mixer and settler sizes and configurations up to production plant scale. The development work has been borne out in practice and the plant capacity has been realised. However certain factors arise in such high throughput solvent extraction plants which hitherto have not perhaps appeared to be significant. For a total throughput of $28 \text{ M}^3/\text{min}$, the settlers required are 36.6M long and 12.2M wide. Fabrication costs in themselves are significant but the solvent inventory of the settler also represents a considerable capital investment. By the reduction of settler area, benefits accrue not only from capital saving but also from the fact that vapour losses and fire hazards are diminished.

Assisted Settling

Methods of increasing coalescence and phase separation have been developed from time to time and these vary from tilted plate separators and simple baffles to random or regular packings. Some significant increases in separation rates can be achieved using these techniques. For example, gravity settlers normally operate in the range of $3-5 \text{ M}^3/\text{M}^2 \text{ hr}$ (flowrate per unit settling area). This can be increased to $15-20 \text{ M}^3/\text{M}^2 \text{ hr}$ using random or regular packing as a coalescer aid. Therefore the potential to reduce settler sizes and solvent inventory exists. That this has not been applied in practice is due to a number of reasons. It has been shown that the effectiveness of these types of coalescer aids depends upon their preferential wetting by the dispersed phase (3,4). If the type of dispersion is constant this does not present a problem, but, when phase inversion takes place, the preferred conditions cannot be maintained and the performance of the coalescer decreases. If conventional packings were used in operating plant, settlers designed for a specific phase continuity would flood if phase inversion took place. This is a major disadvantage in their use particularly if the process is operated within the ambivalence range. The other problem related to the use of packings is the effect of crud and particulate matter which is present in most industrial systems. Both could affect coalescence efficiency and cause blockage in the packing. The consequent need for periodic removal, cleaning and replacement of the coalescer aids must therefore be considered. This adds to the operating costs of the process and reduces both the overall plant availability and reliability.

New Packing Materials

Recently, improvements in the design of coalescer aids have been made which make them sufficiently attractive to consider their use in industrial solvent extraction processes. The inherent difficulty of being effective for one specific type of dispersion has been overcome whilst at the same time, the capacity has been increased such that loadings up to $50-60 \text{ M}^3/\text{M}^2 \text{ hour}$ can be achieved. Their operation depends on the use of two dissimilar materials, usually a high surface free energy material, eg metal or glass fibre together with a low surface free energy material, eg. polymeric materials such as polypropylene, PTFE etc (5). At the junction between these surfaces, it has been shown that enhanced droplet coalescence can take place and, as stated, if this concept is used in packings, coalescence of both w/o and o/w dispersions can be achieved (6). Development of packings using this concept has resulted in their application in extraction processes in the petrochemical field, particularly for the reduction of entrainment

from counter current extractors (eg RDC). However, their potential in large scale operations, particularly in reducing solvent inventory and settler size, is perhaps more important. Before examining the effects on plant size and economics some results for the copper-LIX system will be presented.

Experimental Work

It has been established that when regular packings are used higher throughputs can be achieved. To utilise the "junction" effect in regular packing, a knitted mesh packing made of dissimilar materials, KnitMesh, was chosen for examination. Results confirmed the increase in capacity but indicated that the horizontal velocity of the dispersion entering the coalescer was important and that it should be greater than that normally used in a gravity settler. Therefore a completely redesigned settler was required to house the KnitMesh coalescer.

A small experimental mixer-settler unit, shown in Figure 4 was used. Mixing and settling experiments were conducted using an acidified aqueous phase of pH 2 and containing 100 ppm copper, and an organic solution of 18% LIX 64N in Napoleum 470, the two phases being equilibrated at 21°C. In the first part of the work, measurements were made of the pressure drop across and the entrainment from the settler fitted with a KnitMesh DC coalescer type 9201 consisting of 30 swg stainless steel wire and polypropylene filament of diameter 0.013 cm. These functions were measured for a range of flowrates, coalescer thicknesses and positions of the coalescer relative to the inlet to the settler. The impeller speed was maintained constant throughout the work at 400 rpm. For the impeller used the dispersion mean drop size produced was of the order of 0.2 mm. The drop size or inter-facial area per cent volume of the dispersion influences the performance of the coalescer but to a lesser degree than in a gravity settler.

Experimental Results

The proposal that this form of coalescer can successfully handle both o/w and w/o dispersions was confirmed in this work, separation of the primary dispersion being achieved in both cases at flowrates up to 55 M³/M² hour. Typical conditions before and after fitting a coalescer (in this case a coalescer 7.62 cm thick) are shown in Figure 5. In Figure 5a, the dispersion is not separated and the settler is flooding. When the coalescer is fitted (shown in Figure 5b) separation of the primary dispersion to give two phases is attained. Measurements of pressure drop across the settler are shown in Figures 6 & 7. As would be expected the pressure drop increases with both total flowrate and depth of the coalescer pad. Furthermore the pressure drop varies with the position of the coalescer pad in the settler, increasing as the distance between the front face of the pad and

and settler inlet is reduced, Figure 8. This will be the subject of further investigations but is probably due to some drainage having taken place before the coalescer pad is reached. A uniform dispersion flow into the coalescer is required. If this is not achieved, non-uniform loading of the coalescer at the inlet face results, which gives not only an increase in pressure but also a loss of efficiency. Thus as with gravity settlers, the design of the settler inlet is important. A further significant point is that with this system, the pressure drop across the coalescer is affected very little by a phase inversion. If the pressure drop across the packing were to change markedly on phase inversion then this would normally result in changes of flow in the system with consequent system instability.

In none of the experiments was flooding in the settler observed and therefore the maximum flowrate reported, viz $55 \text{ M}^3/\text{M}^2$ hour, does not represent the maximum attainable flow through the coalescer. Indeed satisfactory phase separations in this system have been attained at flows up to $100 \text{ M}^3/\text{M}^2$ hour. An important factor not yet discussed is the efficiency of phase separation measured by the entrainment in the phases leaving the settler. Results are shown in Figures 9a, b & c for pad depths of 7.6 cm, 15.2 cm and 30.5 cm. It is evident that, as was found with pressure drop, the entrainment, particularly of the discontinuous phase liquid leaving the settler, is dependent on the position of the pad. If, however, the distance between the settler inlet and the coalescer pad is greater than 25 cm then both the entrainment and pressure drop tend to constant values (Figure 10).

Earlier work using coalescers showed that a minimum depth of packing was required and that for knitted mesh coalescers, this is of the order of 25 cm. This is confirmed in the present work. In both the 7.6 cm and 15.2 cm pads, breakthrough of the dispersion was evident above a certain flow rate, shown on Fig. 9. When this occurred, a dispersion band was found behind the coalescer and entrainment of dispersed phase increased rapidly. With a pad 30.5 cm thick, no breakthrough occurred, and entrainments remained low (< 250 ppm in the worst case).

The basic finding therefore is that with a correctly positioned coalescing pad of optimum thickness, the settler loading can be increased by as much as ten times over that achievable in a gravity settler, without increasing entrainment values.

A major question with respect to the application of such coalescers in full scale solvent extraction plant is the effect of crud and particulate matter in the feed liquors. Ultimately, this question can only be resolved in industrial systems since it is difficult in laboratories to simulate particular field conditions; nevertheless some quantitative laboratory testwork was carried out to establish the general behaviour of simulated process liquors. Prolonged operation in which crud was deliberately allowed to build up has shown that the coalescer can still be operated effectively even under conditions of increased pressure drop. A photograph, Fig. 11., shows crud inside the coalescer and at the interface between the phases upstream of it. In no test did the presence of crud affect the performance of the coalescer significantly. The crud was effectively removed by simply backflushing or washing through with aqueous phase. Therefore, crud of this form does not appear a major problem.

The effect of particulate matter has also been examined. Two conditions can exist:

- a) that particulate matter is carried into the plant in suspension in the leach liquors and
- b) that material can be precipitated out of aqueous solution in the extraction process.

Both depend on ore, location, and leach conditions.

Gypsum for example can be introduced into the system by particulate carryover in the feed liquor or it can arise through supersaturation of the feed liquor. To investigate suspended material, various grades and sizes of silicacious materials were introduced in the aqueous feed to the mixer settler loop. Solids separated out in the settler. The circuit was operated under the worst conditions during these tests i.e. at high total throughputs. The position of the pad in the settler was found to be significant. When the pad was positioned near the settler inlet, precipitation took place, within the pad, and as the deposit built up, the pressure drop increased. Although the rate of coalescence was not affected and entrainment levels remained fairly constant, a point was reached when the pressure drop increased beyond the discharge capability of the pump mix impeller. At this point in a practical system, the coalescer would need cleaning. This effect was less as the pad was moved away from the inlet. With silica particles of size 150 μm and the pad positioned 25 cm from the inlet, heavy depositions were formed in front of the mesh. In practice this is a less troublesome condition since the precipitate could be removed through a blow-down line. The final design of cleaning system will depend on the type of solids expected to be present. Considerable latitude in coalescer design is possible since the voidage and free volume of the coalescer can be varied over a wide range by changes in either stitch length, filament or wire diameter and crimp depth.

Prolonged tests have also been carried out to investigate the effect of deposition of material inside the coalescer, particularly calcium sulphate. Supersaturated aqueous solutions of calcium sulphate were circulated through the equipment and the build up of deposit within the settler was recorded. The pressure drop characteristics are shown in Figure 12. Figure 13 is a photograph showing the deposition of precipitated calcium sulphate within the coalescer. Results were recorded for a system using a 30.5 cm pad positioned 30 cm from the inlet. The calcium sulphate deposited only in that part of the coalescer occupied by the bulk aqueous phase. Again the pad was effectively cleaned by back-washing with aqueous phase.

Improved designs have recently been tested in which the coalescer was shaped to eliminate the lower section, which during operation was within the bulk coalesced aqueous phase. In this way deposition within the pad was considerably reduced. Laboratory testwork on the behaviour of particulate matter cannot be exhaustive. Final tests must be made in the field and these are currently being carried out. At this stage, it appears that problems associated with crud and particulate matter are not critical. On the contrary, results have been encouraging.

Cost Data

The discussion so far has centred on the operational performance and advantages of KnitMesh. However, the particular incentive for the experimental work was the possible financial advantages which could be achieved by the use of the material.

A cost comparison has been carried out and the results are shown in Table 2. In the comparison the LIX 64N copper extraction system has been used as the example since it is in this type of operation - using a relatively high cost solvent for the extraction of a relatively cheap metal (compared with uranium systems for instance) - that costs are particularly crucial. Costs are compared for gravity settlers and KnitMesh assisted settlers. The costs for mixers are, of course, the same for both systems so that these have been excluded from the study.

The gravity settler is of conventional longitudinal design and costs include structural support, weir systems, and protective covers. For the KnitMesh assisted settler to accommodate the various derived design parameters most conveniently, a cylindrical settler designed to be concentric with the mixer, has been chosen (7). The KnitMesh coalescer sits in the settler as a concentric cylinder and the dispersion is caused to flow radially through it from the mixer, the separated phases being collected from the annular space between the outer face of the KnitMesh and the settler walls. A totally enclosed design is proposed, with provision for access for cleaning.

An important part of the saving made by the use of KnitMesh settlers is the reduction in solvent inventory. This depends to a large extent on the settler area and Table 1 shows the significant reduction in settler area which is achieved.

Table 1 - Plan Area of Gravity & KnitMesh Settlers

Basis - $250 \text{ M}^3/\text{hr}$ of mixed phase flow at an o/w ratio of 1:1

Settler Specific Flow $\text{M}^3/\text{M}^2 \text{ hr}$	Settler Plan Area (M^2)	
	Gravity	KnitMesh
1	250	5.2
3	83.3	5.2
5	50.0	5.2
7	36.0	5.2
9	27.0	5.2

The depth of organic layer in the settlers depends on a variety of factors. In the case of the gravity settler, it depends mainly on the allowable organic velocity relative to the dispersion band. From experimental work carried out by DPG, this is of the order of 12 cm/sec at a clear organic depth of 15 cm. Above this velocity, severe carryover of dispersion can occur.

For KnitMesh settlers the organic hold-up depends on the mean velocity of dispersion entering the coalescer.

In the settler cost comparison, these factors have been allowed for in determining the volume and cost of organic phase held up in the settler.

Table 2 - Comparative Total Installed Costs of Gravity & KnitMesh Settlers (Including Solvent Inventory)

$$R = \frac{\text{Total cost of settler + solvent (KnitMesh)}}{\text{Total cost of settler + solvent (Gravity)}}$$

Organic System: LIX 64N dissolved in Napoleum 470

Reagent Concentration (Vol % LIX 64N)	10	20	30	40
	1.0	0.67	0.53	0.47

It can be seen from Table 2 that for the more dilute systems the cost advantage of the use of KnitMesh is diminished. However, when recovering large quantities of metal from dilute liquors, very high flowrates are encountered. For gravity settlers, this means very large surface areas, even requiring multi-streaming in some cases, whereas, as has been shown in Table 1, KnitMesh settler plan areas are comparatively very small even when specific flows as high as $9 \text{ M}^3/\text{M}^2 \text{ hr}$ can be achieved in a gravity settler.

Conclusions

At this time, all the various parameters required for the design of full scale settlers using DC KnitMesh have been established in the laboratory and some of this work has been described in this paper. When the current field trials have been completed, it is expected that the laboratory work will have been verified to the point where full scale practical application of the new coalescer will be put into immediate operation.

The experimental work has shown that use of the material can produce benefits not only in capital savings, but also in reduction of space requirements and ease of implementing safety systems in large scale metallurgical solvent extraction plants.

Potential problems of the use of the material, such as solid build-up, have been recognised and investigated. To date, none of these problems has proved insuperable and the practical application of the material can be predicted with confidence even though it is recognised that each metal recovery problem is unique in some way.

Acknowledgements

The authors wish to acknowledge the assistance of colleagues in the R & D Division of Davy Powergas Limited in the preparation of this paper and also to thank the Directors of Davy Powergas Limited and KnitMesh Limited for their permission to publish.

REFERENCES

1. Lott J B, Warwick G C I & Scuffham J B
Trans SME, 252, 27 (1972).
2. Hopkins W R, Eggett G and Scuffham J B
Ch 7 "International Symposium on Hydrometallurgy"
Eds. Evans, Shoemaker: AIME New York 1973.
3. Davies G A & Jeffreys G V
"Coalescence of droplets and Separating Dispersions"
Ch 14 "Recent Advances in Liquid Extraction" Ed C Hanson,
Pergamon Press (1971).
4. Davies G A & Jeffreys G V
Filtration and Separation 6, 349, (1969).
5. Davies G A, Jeffreys G V, Ali F & Afzal M, Chem Eng
266, 392, (1972).
6. Davies G A, Jeffreys G V & Afzal M, Brit Chem Eng.
17, 709, (1972).
7. British Provisional Patent No 40473/72.

FIG. 1

THE EFFECT OF VARIATION OF PHASE CONTINUITY AND MIXER
 $N^3 D^2$ ON SETTLER DISPERSION BAND DEPTH

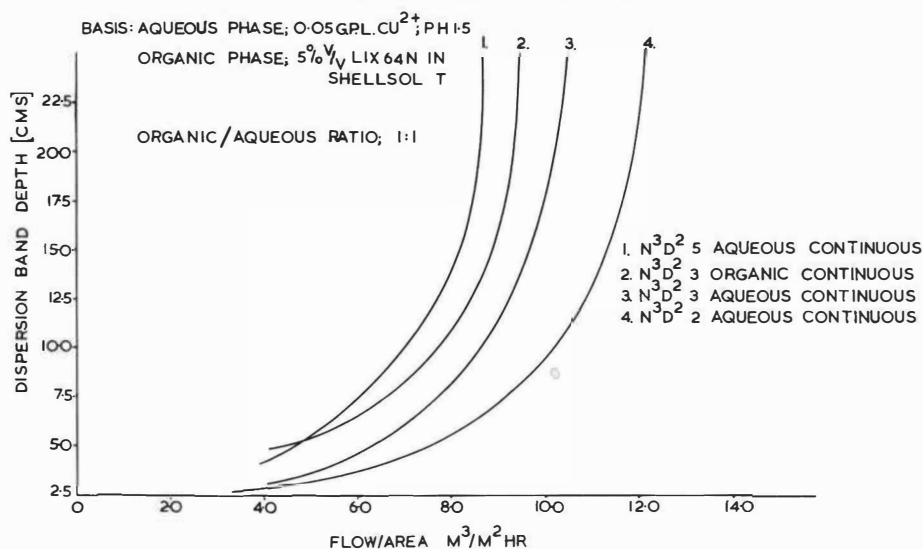


FIG. 2

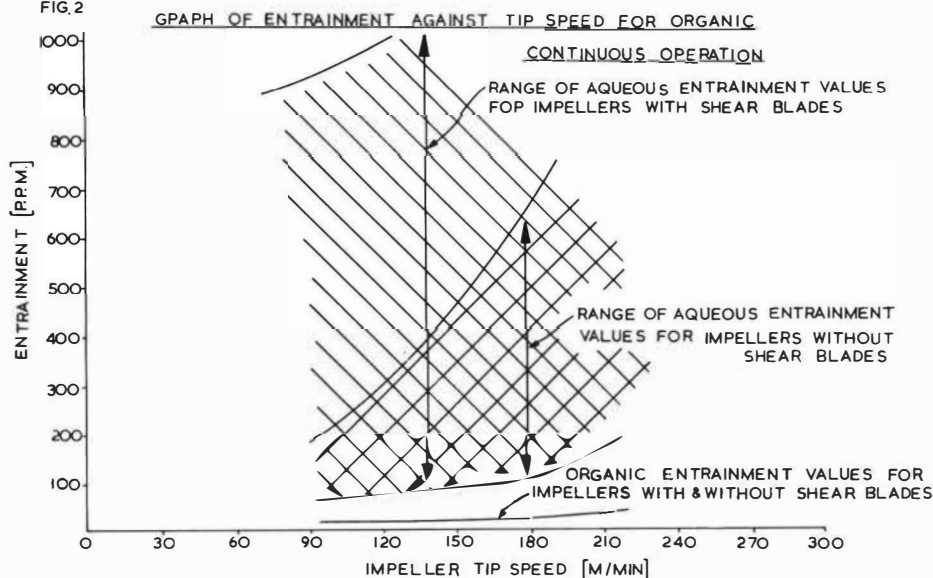
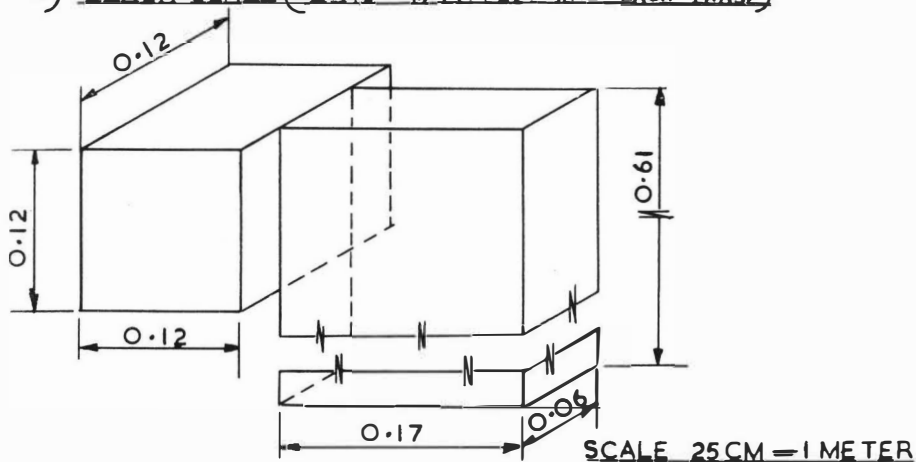
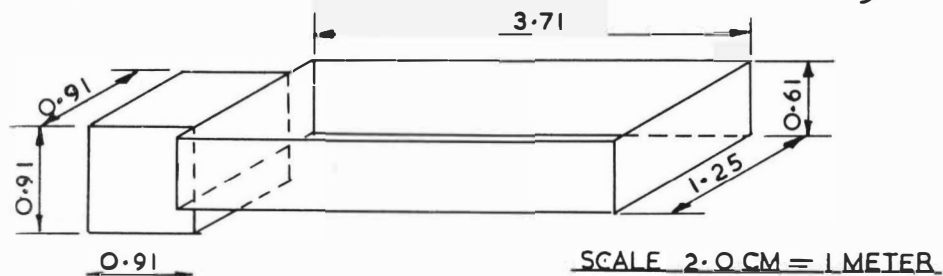


FIG 3 COMPARISON OF THREE SIZES OF MIXER-SETTLERS
TO SHOW EFFECT OF SCALE UP

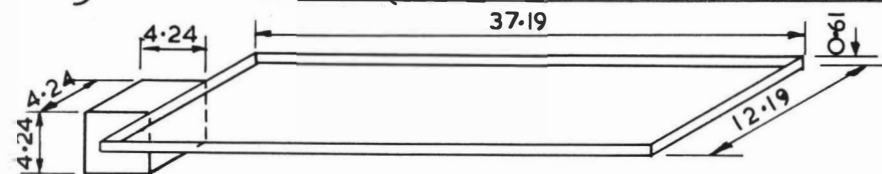
a) BENCH SCALE ($4 \times 10^{-3} \text{ M}^3 \text{ PM}$ FLOWRATE EACH PHASE)



b) PILOT PLANT SCALE ($1.89 \times 10^{-1} \text{ M}^3 \text{ PM}$ FLOWRATE EACH PHASE)

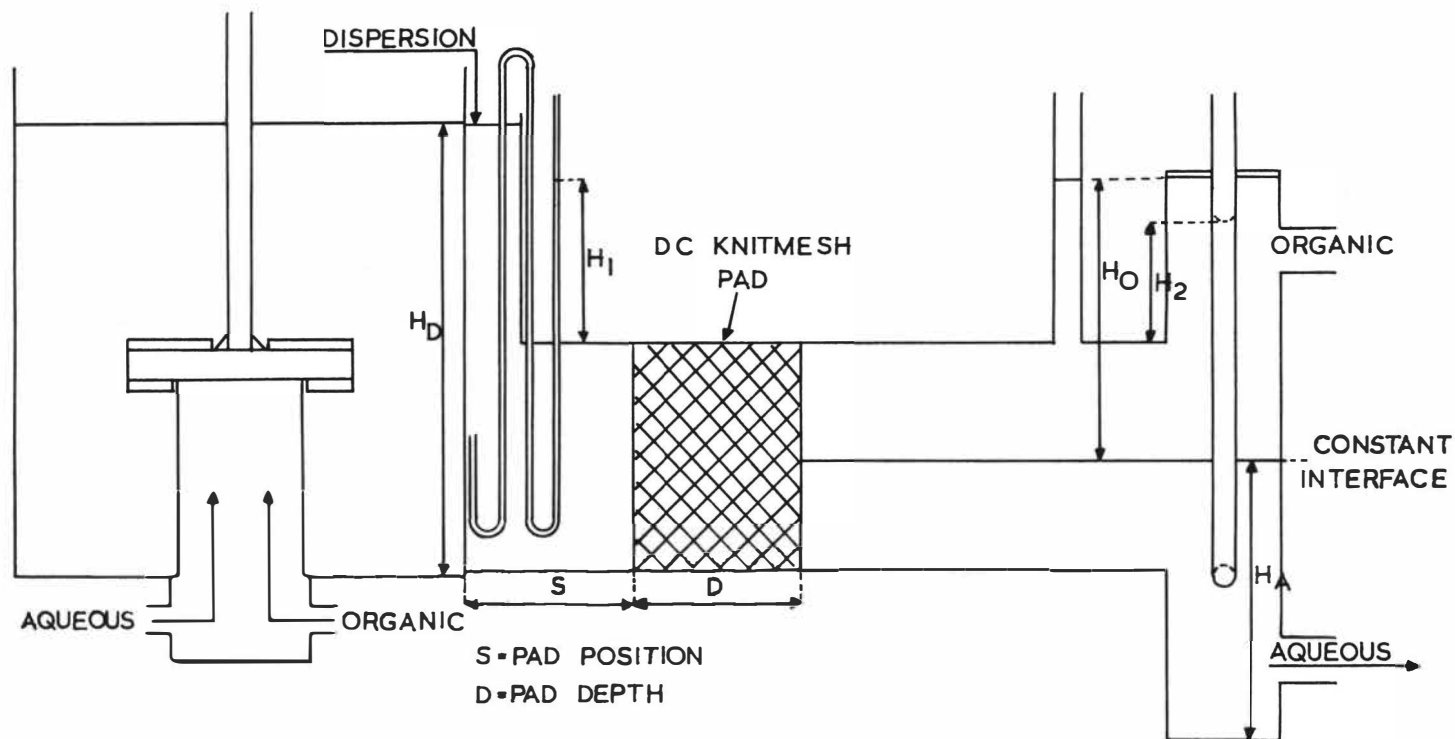


c) MAIN PLANT SCALE ($18.9 \text{ M}^3 \text{ PM}$ FLOWRATE EACH PHASE)



ALL DIMENSIONS ARE IN METERS SCALE 0.25 CM = 1 M

FIG. 4



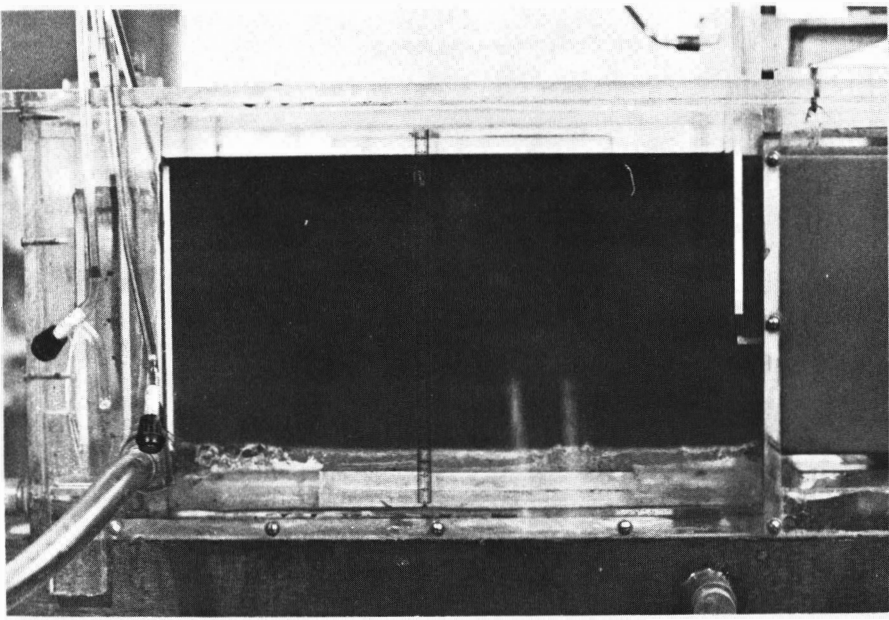


FIG. 5A. GRAVITY SETTLER AT FLOODING POINT

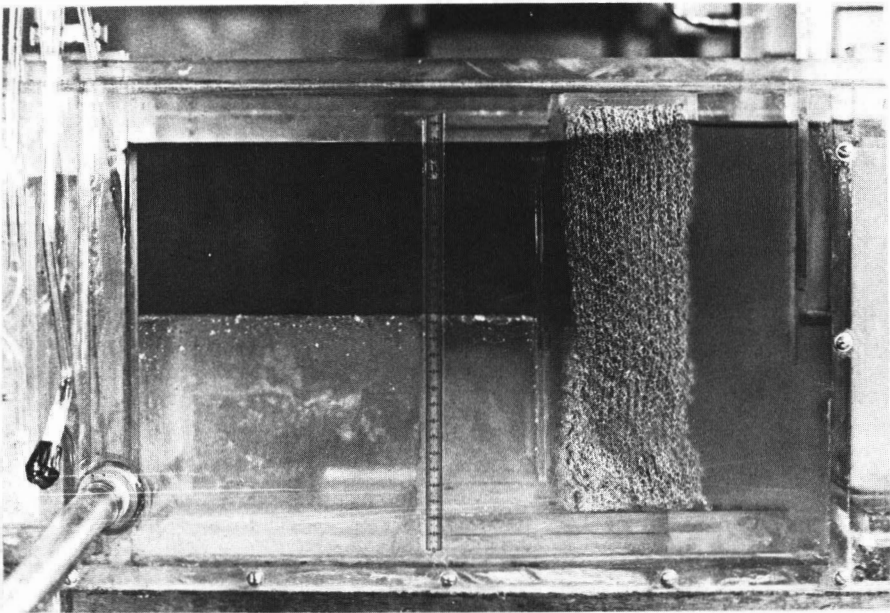


FIG. 5 B. KNITMESH ASSISTED SETTLING AT SAME FLOW
CONDITIONS AS IN 5A

FIG. 7

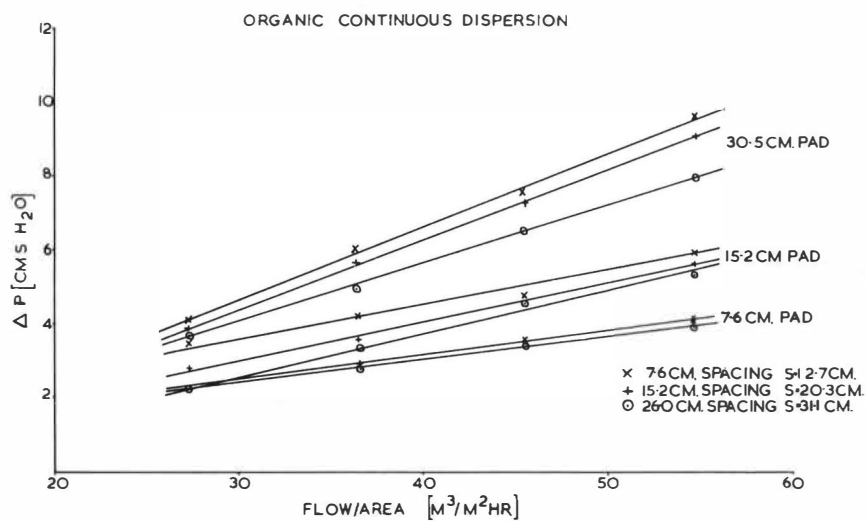


FIG. 6

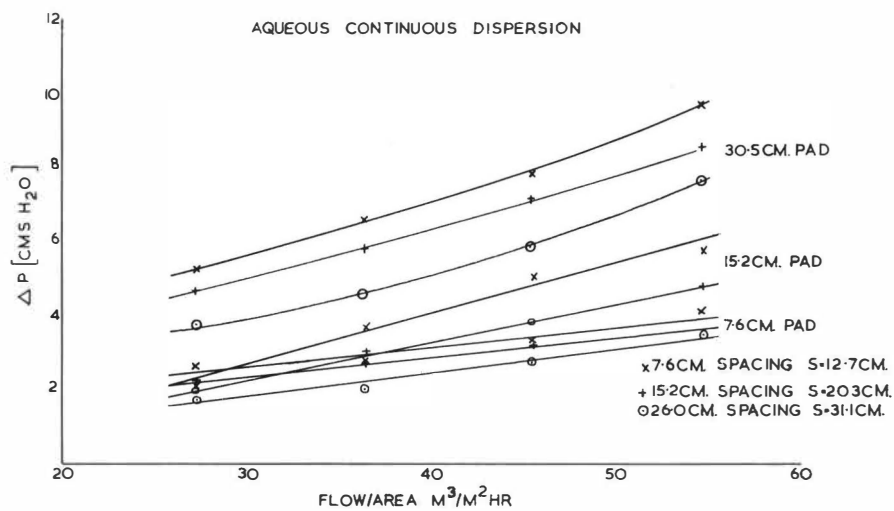
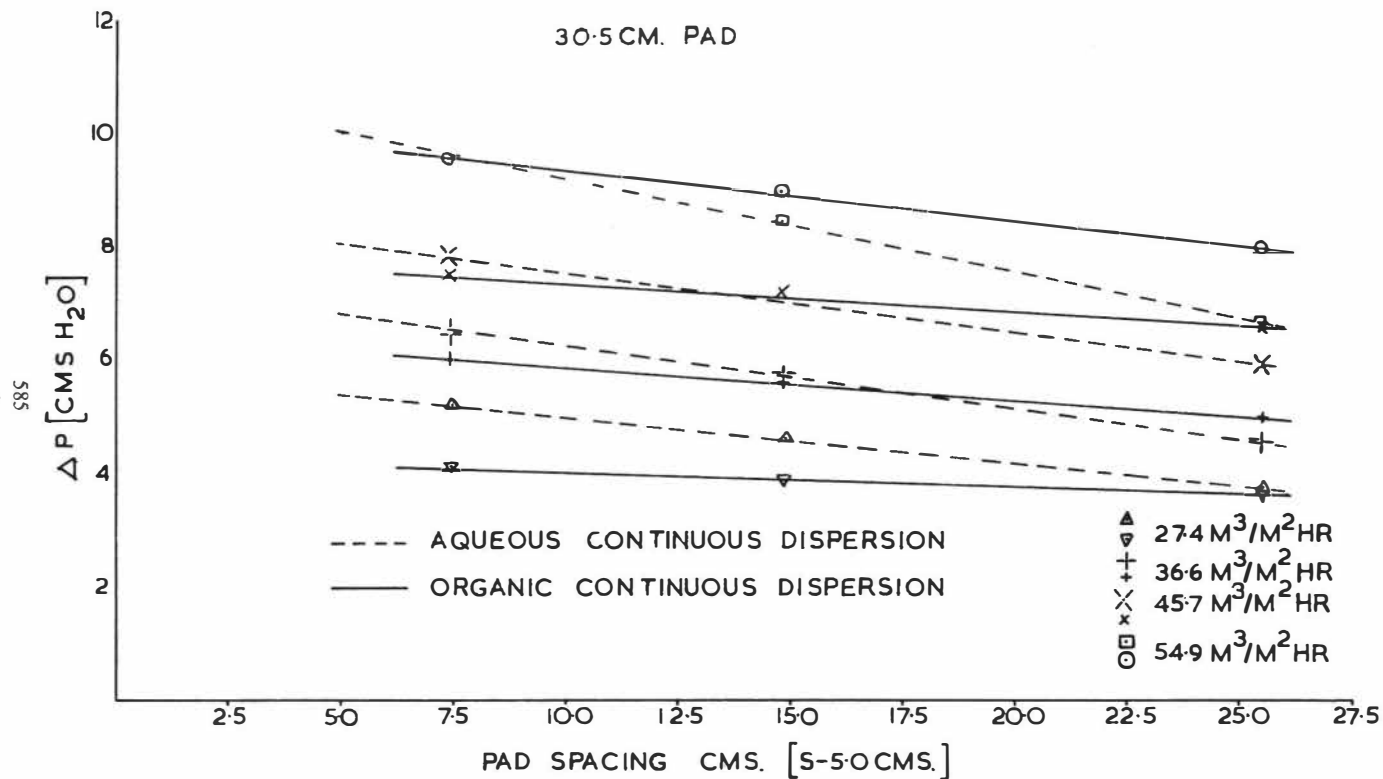


FIG. 8



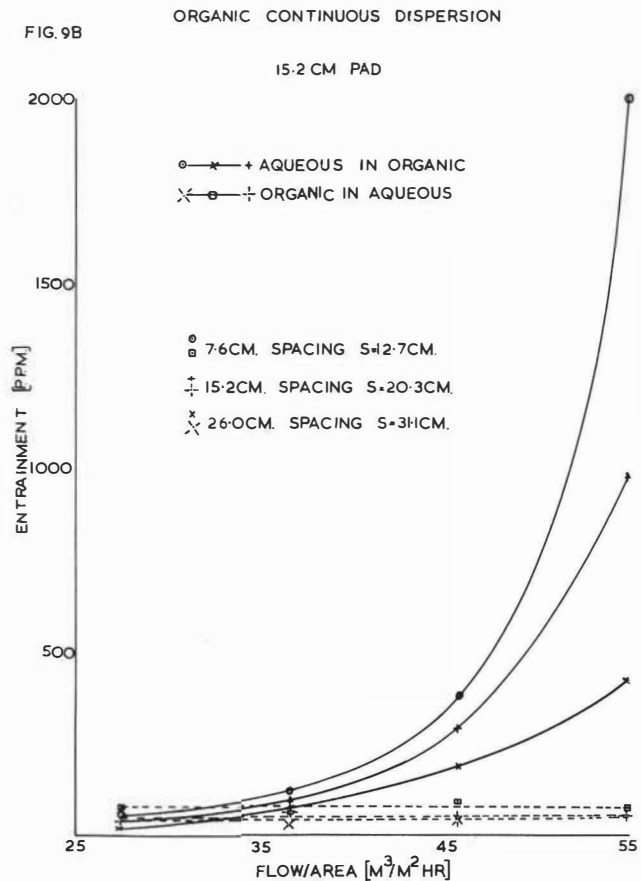
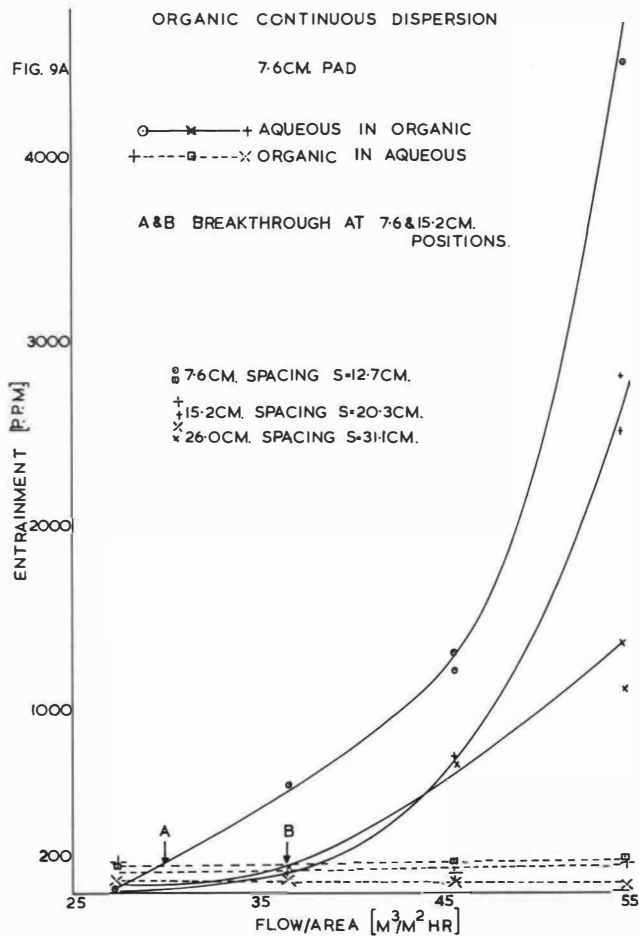


FIG. 9C

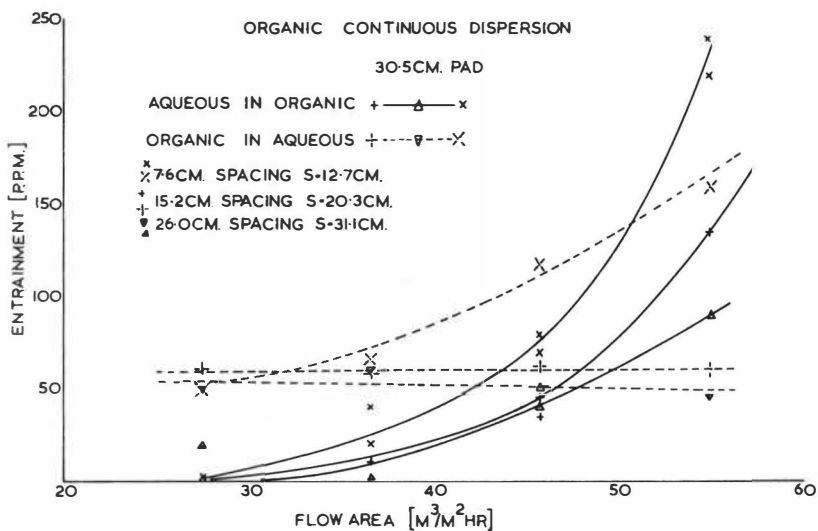
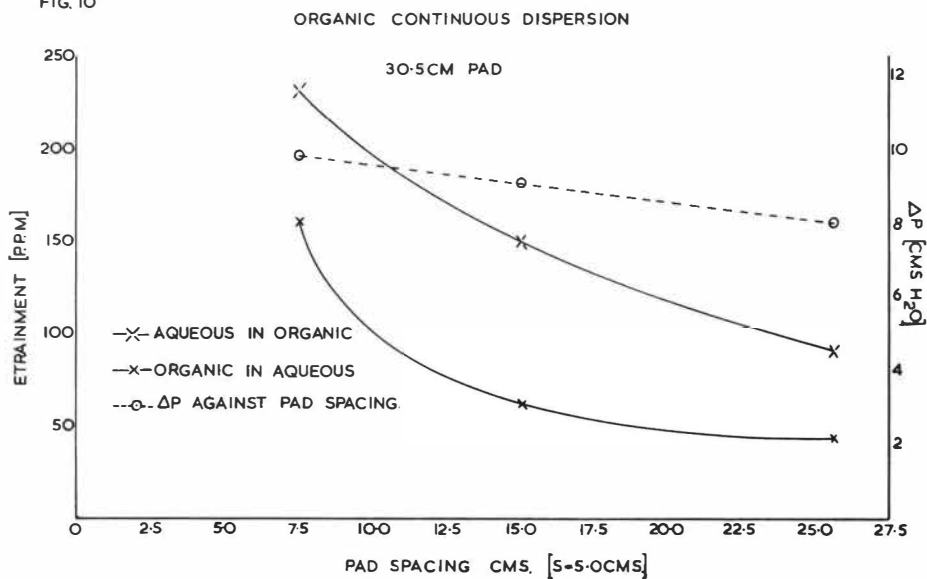


FIG. 10



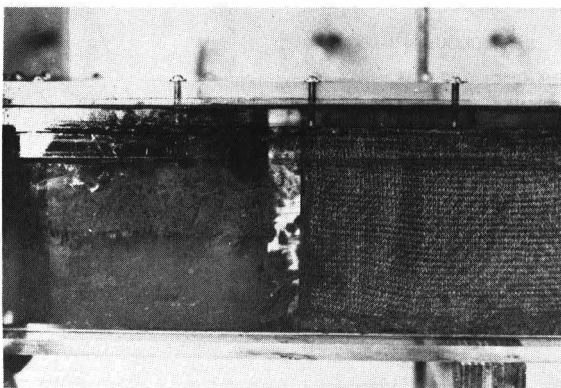
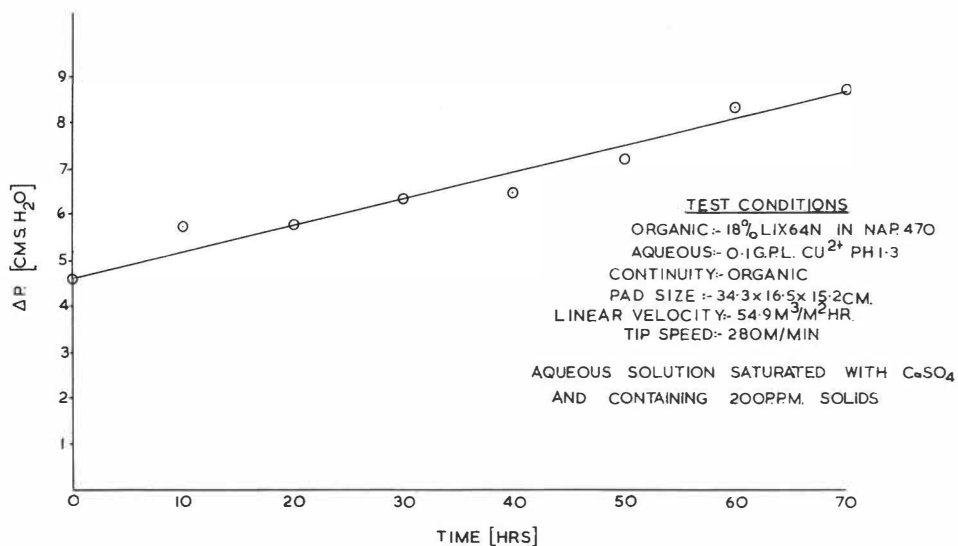


FIG. 11.

CRUD BUILD UP IN KNITMESH SYSTEM

FIG. 12



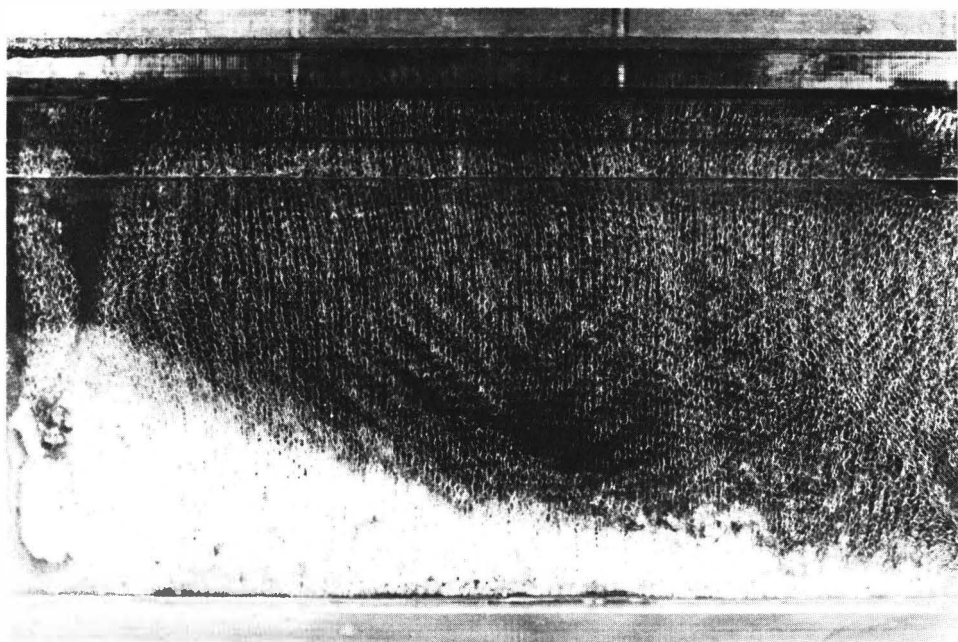


FIG. 13.

CALCIUM SULPHATE DEPOSITION IN KNITMESH

COALESCENCE IN A LABORATORY CONTINUOUS MIXER-SETTLER UNIT :
CONTRIBUTIONS OF DROP/DROP AND DROP/INTERFACE COALESCENCE
RATES ON THE SEPARATION PROCESS

S. VIJAYAN and A.B. PONTER

Chemical Engineering Institute

Swiss Federal Institute of Technology of Lausanne

CH-1024, ECUBLENS, SWITZERLAND

ABSTRACT

A deterministic model coupled with the differential model proposed by Jeffreys et al is presented which allows the behaviour of a horizontal gravity settler, where drop/drop and drop/interface coalescence prevail, to be analysed. Data obtained from an experimental investigation with a laboratory single-stage mixer-settler unit using the n-heptane/water system enables the relative contributions of the two coalescence processes to be ascertained.

INTRODUCTION

Few dispersion studies have been described, and most of these have been restricted to batch systems. Meissner and Chertow⁽¹⁾ investigated the effect of phase ratio on separation times, and found that secondary droplets were always present in the phase occupying the greater volume fraction. As a result of this study, a method of removing secondary hazes by dilution was proposed.

Davies and Jeffreys⁽²⁾ showed that secondary droplets can be formed of both phases by coalescence within a dispersion. They demonstrated that partial coalescence takes place within a dispersion which results in the formation of secondary droplets of the dispersed phase, and proposed a qualitative explanation to account for coalescence of a drop at the phase boundary and inter-drop coalescence within the dispersion band. Ryan et al⁽³⁾ studied the scale-up aspects of settlers to coalesce dispersions of sulphate solutions with kerosine containing di-2-ethyl hexyl phosphoric acid and tri-butyl phosphate. The emulsion was formed in a variable input mixer and passed continuously to one of a variety of settlers ranging in diameter from 6 in. to 48 in. They developed a scale-up criteria on the basis of nominal capacity based on the phase boundary where the drop phase did not wet the settler walls,

and subsequently Davies et al⁽⁴⁾ confirmed this criterion with a mathematical model.

Rodgers et al⁽⁵⁾ and later Smith⁽⁶⁾ reported that solvent dispersions gave higher capacities than aqueous dispersions although it has been generally found that the converse was true. They also reported that the separation took place by coalescence of drops only at the interface. Later Williams et al⁽⁷⁾ and Smith⁽⁶⁾ observed considerable drop/drop coalescence within the dispersions.

Jeffreys et al⁽⁸⁾ studied the separation of dispersions in a single mixer settler designed so that the drops moved axially along the settler in plug flow. They proposed an idealized mathematical model to predict the dimensions of the heterogeneous wedge in the settler using coalescence data. In spite of a number of shortcomings in the model, this study contributed much to the design of separation equipment from fundamentals. Following this, Jeffreys et al⁽⁹⁾ carried out a detailed study using a rectangular mixer-settler and proposed a differential model, taking into account both modes of coalescence mechanism to predict the dimensions of the wedge. It is of note that they applied for the first time single drop/interface coalescence data to analyse the results.

For bulk studies Mizrahi and Barnea⁽¹⁰⁾ have recently reported design and operation procedures using a compact liquid/liquid settler, whilst the dynamic behaviour of mixer-settlers have been reported by Aly et al⁽¹¹⁻¹³⁾ by applying

electrical analogue models and experiments.

In the present investigation, a single stage continuous horizontal mixer settler unit has been chosen in view of its popularity in industry as one of the more efficient devices for carrying out extraction operations.

The available design procedures for the gravity settlers are based either on hydraulic balances of the two phase flows or upon empirically determined mean residence times. However, very little attempt has been given to the development of design procedures for liquid/liquid gravity settlers from fundamental principles.

The objective of this paper is to investigate further theoretically and by experiment, the microscopic and macroscopic separation mechanisms of a liquid/liquid dispersion in order to establish the contributions of drop/drop and drop/interface coalescence times to the separation process.

BASIC DETERMINISTIC MODEL OF THE COALESCENCE RATE PROCESS

The problem considered is concerned with the overall behaviour of the coalescence process excluding the nature of the interface and the physical properties of the fluids. The analysis is developed from a coalescence model used to determine size distribution where binary collisions of the species take place⁽¹⁴⁾

but which now takes into account the two coalescence mechanisms namely drop/drop and drop/interface coalescence modes.

A schematic representation of the coalescence process is given in Figure 1. If the dispersed phase consists of drops of the denser liquid, then the band of drops is formed above the interface. It is assumed that at the lower surface of the band, drops are coalescing with the bulk liquid phase by a drop/interface coalescence mechanism whilst within the band and at the top surface, drop/drop coalescence occurs. The life of the drops in the band is controlled by these two processes and a knowledge of the time spent by the drops before disappearance is a critical factor in the design of the settler. A restricted-in-space configuration where a given drop can coalesce only with a restricted number of drops within a characteristic neighbourhood, defined by the appropriate volume, is assumed for drops with random size distribution.

Let n_k be the average number of drops of size k in a characteristic unit volume. Since the movement of a given drop is very much restricted by the high population density, a drop of size k can encounter only the drops which immediately surround it. Hence the theoretical number of collisions between drops of size k and ℓ can be written as,

$$C_{k\ell} = \frac{n_k n_\ell}{N} \quad (1)$$

where N is the total number of drops of all sizes present and defined as

$$N = \sum_{k=\ell}^{\infty} n_k \quad (2)$$

Assuming no breakage of drops to form secondary droplets, where coalescence is the only prevailing mechanism and $n_k \gg 1$, the basic deterministic equation for the number balance of drops of size k becomes :

$$\begin{aligned} \frac{dn_k(t)}{dt} = & - \frac{\lambda(t)}{k/\text{interface}} \cdot n_k(t) \\ & - \sum_{\ell=1}^{\infty} \lambda_{k\ell}(t) \cdot \frac{n_k(t)n_{\ell}(t)}{N(t)} \\ & + \frac{1}{2} \sum_{\ell=1}^{k-1} \lambda_{k-\ell,\ell}(t) \cdot \frac{n_{k-\ell}(t)n_{\ell}(t)}{N(t)} \end{aligned} \quad (3)$$

where $\lambda_{k/\text{interface}}$ is the rate constant for drop/interface coalescence defined as the fraction per unit time of the theoretical number of drops disappearing by drop/interface coalescence and is a function of drop/interface characteristics, physico-chemical nature of the interface etc. $\lambda_{k\ell}$ is the collision - coalescence rate constant equal to the fraction per unit time of the theoretical total number of collisions and is a function of the mobility of drops, geometry and physical chemistry of their mutual interaction on close approach etc.

The first term on the right-hand side accounts for the number of drops of size k that are disappearing per unit time because of drop/interface coalescence. The second term accounts for the number of drops of size k that are disappearing per unit time because of drop/drop coalescence with all other sizes present at time t , while the third term gives the number of drops being created per unit time of size k by coalescence of drops of sizes ℓ and $k-\ell$.

It was assumed by previous investigators^(14,15), for a variety of dispersed phase coalescing processes that $\lambda_{k\ell}$ can be considered a constant, at least as a first approximation. Other investigators⁽¹⁶⁻¹⁸⁾ have also assumed that $\lambda_{k\ell} = \lambda$ for all k and ℓ values. $\lambda_{k/\text{interface}}$ is now assumed to equal $\alpha\lambda$, where α is a constant and greater than zero for a specified range of drop sizes.

With the assumptions made above, equation (3) can now be re-written as

$$\begin{aligned} \frac{dn_k(t)}{dt} = & -\lambda(t)n_k(t) \quad (1 + \alpha) \\ & + \frac{1}{2} \sum_{\ell=1}^{k-1} \lambda(t) \frac{n_\ell(t) n_\ell(t)}{N(t)} \end{aligned} \quad (4)$$

Equation (4) can be summed from $k = 1$ to ∞ , and combining with equation (2) yields :

$$\frac{dN(t)}{dt} = -N(t) \lambda(t) \left[\frac{1}{2} + \alpha \right] \quad (5)$$

Equations (4) and (5) are the two important and basic expressions of the deterministic model. Introducing the transformations,

$$\theta = \frac{N(t)}{N(0)} \quad (6)$$

and

$$f_k(\theta) = \frac{n_k(t)}{N(t)} \quad (7)$$

where $f_k(\theta)$ represents the mean fraction of drops of size k at dimensionless time θ , θ is a measure of the degree of coalescence, the solution of equation (4) can be obtained by a generating function technique⁽¹⁹⁾ subject to the following initial conditions :

$$\begin{aligned} f_k(\theta) &= 1 \text{ for } k = 1 \\ &= 0 \text{ for } k > 1 \end{aligned} \quad \text{at } \theta = 1 \quad (8)$$

Thus, the solution of equation (4) becomes :

$$f_k(\theta) = \theta^{(A-1)} \left[\frac{(\theta^{1-A} - 1)}{\theta^{1-A}} \right]^{k-1} \quad (9)$$

where

$$A = \frac{2(1 + \alpha)}{1 + 2\alpha} \quad (10)$$

and when $A = 2$, i.e., $\alpha = 0$

$$f_k(\theta) = \theta(1 - \theta)^{k-1} \quad (11)$$

Equation (11) is a particular case of equation (9) and is identical to one given by Sastry and Fuerstenau⁽²⁰⁾ who considered solid particle agglomeration.

It can be readily shown that

$$\sum_{k=1}^{\infty} f_k(\theta) = \sum_{k=1}^{\infty} \theta^{A-1} \left[\frac{\theta^{1-A} - 1}{\theta^{1-A}} \right]^{k-1} = 1 \quad (12)$$

Hence the cumulative fraction $\chi_k(\theta)$, larger than a specified drop size k is

$$\chi(\theta) = 1 - \left[\frac{1}{\theta^{1-A}} \right]^k \quad (13)$$

The characteristics of the drop size distribution given by equation (9) can be analysed using statistical methods involving moments and cumulants of the random variable-drop size. Thus, at $t=0$, there is only one size of drops present in the system and at $t > 0$, there is a distribution of drops in multiples of the original size. This shows that the drop size distribution proposed by the above random coalescence model is self preserved. Further, this model can be extended to a situation where $k = 1, 2 \dots$ up to a finite value at $t = 0$, as an initial condition in solving equation (4).

It can be observed from equation (9) that for a given degree of coalescence, the size distribution of the resulting drops is exactly the same irrespective of the kinetics, resulting from the random behaviour of the coalescence processes considered. This model does not take into account

the fluctuations of the number of species of any given size, but the assumption of large number of drops in the system makes the fluctuations in the distribution from the mean number of drops, n_k of size k , unimportant. For a given θ and $f_k(\theta)$, the model developed usefully predicts the relative contributions of the drop/interface and the drop/drop coalescence processes taking place in a dispersion band.

COUPLING OF EQUATION (5) WITH THE DIFFERENTIAL MODEL PROPOSED

BY JEFFREYS ET AL⁽⁹⁾

Owing to the difficulties encountered in measuring $f_k(\theta)$ experimentally at the present time, the kinetics of the coalescence processes described in equation (5) are coupled with the differential model of Jeffreys et al⁽⁹⁾ which is essentially derived by drawing two balances on the system - (1) a material balance for the dispersed phase. (2) a total drop-number balance with the following assumptions :

- (1) inlet stream of the settler is composed of uniform size drops.
- (2) the drops are considered as rigid spheres
- (3) drop size at any position in the wedge is characterized by an average drop diameter defined as $d_{av} = \Sigma nd / \Sigma n$
- (4) multiple drop coalescence is ignored
- (5) volume packing efficiency in the wedge and area packing efficiency at the interface are identified as

average values over time and position

(6) local disturbances in the vicinity of a coalescence step do not have an adverse effect on the coalescence mechanism

(7) only axial flow of drops in the settler is considered

Material balance for the dispersed phase :

Consider a settler of unit width opening under steady state conditions. In the differential element as shown in Figure 1, therefore, the volume of dispersed phase entering per second is equal to the volume of dispersed phase leaving the element plus the volume of dispersed phase coalesced with the lower interface. Thus,

$$\begin{aligned} \frac{n \pi d_{av}^3}{6} &= \left(n - \frac{dn}{dl} \delta l \right) \cdot \frac{\pi}{6} \left[d_{av} + \frac{d(d_{av})}{dl} \delta l \right]^3 \\ &= \frac{\pi d_{av}^3}{6} \left[\frac{\bar{n}_d/I}{\bar{t}_{d/I}} \cdot \frac{\delta l \cdot l}{\left(\frac{\pi}{4} d_{av}^2 \right)} \right] \end{aligned} \quad (14)$$

Similarly a drop-number balance gives :

$$\begin{aligned} n &= \left(n - \frac{dn}{dl} \delta l \right) + \frac{\bar{n}_d/I}{\bar{t}_{d/I}} \cdot \left(\frac{\delta l \cdot l}{\frac{\pi d_{av}^2}{4}} \right) \\ &+ \frac{1}{2} \frac{\bar{n}_d/d}{\bar{t}_{d/d}} \cdot \left(\frac{\delta l \cdot h \cdot l}{\frac{\pi}{6} d_{av}^3} \right) \end{aligned} \quad (15)$$

That is the number of drops entering the differential element per second is equal to the number of drops leaving plus the number of drops coalescing at the interface and half the number of drops coalescing by a drop/drop coalescence mechanism.

Rearranging equations (14) and (15), considering only first order terms and combining them (for details see reference 9) with the following boundary conditions :

$$\begin{aligned} L = 0; n &= n_0, d_{av} = d_0 \\ \lim_{l \rightarrow L} n &= 0 \\ \lim_{l \rightarrow L} d &= d_L \text{ and } h = d_L \end{aligned} \quad (16)$$

we get,

$$\frac{d(d_{av})}{dl} = \frac{\bar{n}_{d/d} h}{\pi \bar{t}_{d/d} n d_{av}^2} \quad (17)$$

The volume of the wedge per unit width at any position is given by

$$v_{av} h \bar{n}_{d/d} = \frac{\pi}{6} n d_{av}^3 \quad (18)$$

Substituting equation (18) into equation (17),

$$\frac{d(d_{av})}{dl} = \frac{1}{6} \frac{d_{av}}{v_{av} \bar{t}_{d/d}} \quad (19)$$

Comparison of equation (19) with equation (5) reveals that for a given $dN(t)/dt$, $N(t)$, $\bar{t}_{d/I}$, $d(d_{av})/dl$ and d_{av} which can be determined experimentally, $\bar{t}_{d/d}$ can be obtained by solving

equations (19) and (5). However, since direct measurement of $dN(t)/dt$ is not feasible, equation (5) is modified as

$$\frac{dN(t)}{dt} = -N(t) \left(\lambda_{d/I} + \frac{1}{2} \lambda_{d/d} \right) \quad (20)$$

Defining $t = l/v$ and taking v , the velocity of drops in the wedge to be a constant equal to v_{av} , equation (20) becomes :

$$v_{av} \frac{dN(l)}{dl} = -N(l) \left(\frac{1}{\bar{t}_{d/I}} + \frac{1}{2} \frac{1}{\bar{t}_{d/d}} \right) \quad (21)$$

It should be pointed out that since v_{av} is not equal to the dispersed phase flow rate divided by the cross-sectional area occupied by the dispersed phase in the settler, v_{av} becomes a variable parameter like $\bar{t}_{d/I}$ which has to be determined experimentally. However, the above coupling eliminates the experimental determination of v_{av} which can be calculated together with $\bar{t}_{d/d}$ by solving equations (19) and (21) simultaneously.

An experimental programme was designed to study the dispersion behaviour in a continuous gravity settler which allowed the measurement of the system parameters - dN/dl , d_{av} , $d(d_{av})/dl$ and $\bar{t}_{d/I}$. The following sections describe the experimental techniques employed and the results of the investigation.

EXPERIMENTAL

The experimental programme comprised four parts :

- (1) A macroscopic study of the single stage mixer-settler system. This involved an investigation of the effects of initial drop size and volumetric input rates on the rate of coalescence of dispersions in the settlers,
- (2) Single drop/interface coalescence study in the settler under no-flow conditions,
- (3) Single drop/interface coalescence study in the settler where the drop is subjected to a relative axial boundary velocity,
- (4) Measurement of single drop/interface coalescence times when surrounded by other drops.

APPARATUS

The experiments were carried out in a single stage mixer-settler unit (a development of that described by Jeffreys et al ⁽⁹⁾), as shown in Figure 2. The mixing vessel comprised an acrylic vertical cylindrical beaker 15 cm diameter and 30 cm high fitted with light and heavy phase inlet ports and an emulsion discharge port made of glass of 1.5 cm diameter, fitted at 90 degrees to the inlet ports, 8 cm above the base.

The heavy and light phase inlet ports were constructed from 1.25 cm diameter stainless steel tubing and placed diametrically opposite to each other at a height of 3.5 and 12.5 cm respectively above the base of the beaker. Four removable baffles, each 1.25 cm wide, made of stainless steel were inserted vertically in the mixing vessel at positions 45 degrees to the inlet and outlet ports. A four bladed stainless steel paddle impeller 6 cm diameter and 3 cm wide, attached to a stainless steel shaft was used as stirrer. The shaft was connected to a 0.05 hp. electric Cole Parmer Master Servodyne motor system - model 4425G. The speed of the stirrer could be varied between 6 and 300 rpm by means of a speed and torque regulating electronic drive system controller.

The rectangular settler was constructed of acrylic polymer of dimensions 60x30x10 cm. The separated phase leaving the settler were recirculated back into the mixing vessel through 0.95 cm diameter stainless steel tube by means of two centrifugal pumps and two rotometers with fine control needle valves having a flow range up to 1200 cm³/min. The pumps were isolated from the apparatus by mounting on shock resisting rubber sheets. The circulating liquids were maintained at 25°C by allowing each phase to pass through long stainless steel coils immersed in a constant temperature water bath.

N-heptane and water were selected with phase ratios maintained at 1:1 for agitator speeds of 200 and 250 rpm. The n-heptane was spectroscopically pure with a surface tension of 19.8 dyne/cm at 20°C. This system was shown not to affect the acrylic walls since no measurable changes in the physical properties of the n-heptane were detected after prolonged periods of exposure. The water was deionized and double distilled in alkaline permanganate solution and gave a product with a surface tension of 72.2 dyne/cm at 20°C.

PROCEDURE

As the coalescence process is highly sensitive to surfactant impurities, strict precautions were undertaken in the cleansing procedures. The acrylic parts were rinsed with n-heptane, dried in a current of hot air and thoroughly flushed with distilled water. Following this operation, a 10% alcoholic solution of sodium hydroxide was placed in the settler and mixer for about one hour before being thoroughly rinsed with distilled water to remove all traces of caustic soda. Finally, the vessels were carefully dried in a current of hot air.

The impeller, baffles and stainless steel pipe lines were degreased using n-decane and washed consecutively in dilute nitric acid, water and acetone before being rinsed with distilled water and dried.

Following the cleansing procedure described above, the apparatus was assembled. The pipe lines and pumps were primed with the appropriate liquid. The valve in the transfer line between the mixer and the settler was closed and the required volumes of distilled water and n-heptane to give a phase ratio of 1:1 were added to the settler. A requisite amount of distilled water was placed in the mixer and the agitator then switched on, the speed being set to a predetermined value for the particular experiment. N-heptane was added to the mixer slowly to maintain the 1:1 phase ratio and in this way n-heptane was dispersed. The n-heptane was maintained as the dispersed phase throughout this investigation. After half an hour agitation, the valve in the transfer line between the mixer and the settler was opened and the phases were circulated at the desired flow rates at 25°C for atleast for 2 to 3 hours to reach steady state conditions and to ensure temperature equilibrium and mutual saturation of the phases.

A check on the purity of the system was performed by withdrawing samples of both phases periodically and measuring the surface tension. No measurable changes in surface tension of the phases were noted compared with the initial values.

MEASUREMENT TECHNIQUE

Under steady state conditions, the position and thickness of the dispersion band was fixed and the band took the form of a wedge. The heterogeneous wedge thus formed was photographed to obtain information of the dispersion along the settler length. The lower surface was photographed with the aid of a mirror placed at 45 degrees below the wedge. The photographic negatives were magnified to 15X and the diameters of the drops were measured using a plexi scale by applying proper corrections to the magnification. At the same time the number of drops in a given area were also counted.

SINGLE DROP/INTERFACE COALESCENCE TIMES UNDER NO-FLOW AND FLOW CONDITIONS IN THE SETTLER

In an attempt to study the coalescence taking place in dispersions, investigators⁽²¹⁻²⁷⁾ have examined the behaviour of a single drop resting on a plane liquid/liquid interface. Film thinning and rupture have been shown to determine the drop/interface coalescence time. In all the studies reported, experiments were performed in small coalescence cells of about 5 cm diameter and drops only coalesced under static conditions. These experiments gave considerable insight into understanding certain fundamental aspects of coalescence but not the situations such as encountered in the settler operating at steady state conditions where bulk momentum exists in the phases. As the

drops in the band are constantly subjected to a velocity at the interface, it is expected that this effect would interfere with the coalescence mechanism. Hence single drop/interface coalescence times with and without velocity fields were measured with n-heptane drops using a stop watch with an accuracy of ± 0.1 sec. The drop radii employed in the investigation varied from 0.182 cm to 0.372 cm and the relative boundary velocities, Δv (drop phase velocity - continuous phase velocity) from -0.03 to + 0.15 cm/sec.

DROP/INTERFACE COALESCENCE TIMES FOR A SINGLE DROP SURROUNDED BY NEIGHBOURING DROPS

Multi-drop systems which form a drop-layer at an interface have been investigated as supplementary studies whilst analysing performances of liquid/liquid extraction systems⁽²⁸⁻³¹⁾. Otake and Komasa⁽³²⁾ analysed the characteristics of longitudinal dispersions of liquid in a modified pulse sieve-plate column. Komasa and Otake⁽³³⁾ studied the stabilities of both a single drop at liquid/liquid interface and of multidrops in a drop layer by following the decrease in height of the dispersion photographically. They concluded that no large difference was observed between the stabilities of a single drop and

multi-drop in a layer in the absence of stabilizing agents. However, the stability of drops in a layers was found to be less than that of a single drop in the presence of stabilizing agents. Cockbain and McRoberts⁽³⁴⁾ found while studying the coalescence of layers of drops on a plane interface that the relatively large disturbance propagated by the coalescence of one of the drops tended to stabilize the others. Following this Lawson⁽³⁵⁾ showed that single drop/interface coalescence times surrounded by other drops were greater than single drop/interface coalescence times in the absence of other drops.

EXPERIMENTAL TECHNIQUE AND PROCEDURE

An organic soluble phototropic dye (a spirane derivative) was used which gave a distinct blue colour when exposed to a strong beam of light. Taking advantage of this effect, a pencil beam of light from a carbon arc lamp-collimator iris diaphragm set was shone on to the single drop layer of the dispersion over a 1 cm diameter field. This field area was monitored carefully by visual observations. Since the dye coloured only that part of the dispersion where the light was focussed, the movements of a single drop could be followed. As soon as a rearrangement took place at the active phase boundary of the dispersion, a hole was formed and one drop

from the near vicinity entered this new position. A stop watch was started at this instant and the time taken between this instant and its disappearance was recorded. A large number of measurements were made and an average value was determined.

A second set of experiments was conducted where coloured n-heptane drops containing 'Oil Red O' organic soluble dye were released through the dispersion. The rest time of this coloured drop was measured between the impact of the drop at the interface and its disappearance. The time between the arrival of the drop at the first layer of the active zone and its complete coalescence with the interface was recorded as the residence time.

The concentration of the dye used was less than 20 mg/liter and it has been shown⁽³⁶⁾ that the presence of the dye does not affect the surface properties at these concentrations and this has been confirmed by the authors.

RESULTS

Although methods are available⁽³⁷⁾ which predict drop size in agitated emulsions, in this work the size of drops entering the settler d_o , was measured by photographing the dispersion at the entrance of the settler. From the photographs of the front, top, bottom and side views, the drop size was found to be about 95% uniform. Thus for $N = 200$ rpm, d_o is 1.3 mm and

for $N = 250$ rpm, d_o is 1.1 mm. This method of measurement of drop size entering the settler eliminates complexities such as coalescence of drops due to fluid turbulence that would otherwise have resulted in the transfer line connecting the mixer and the settler. Agitator speeds were selected such that both a uniform emulsion was produced and entrainment of air into the liquid was prevented.

The drop sizes of the active (upper) and the passive (lower) dispersion surfaces in the settler were measured at every 5 cm distance from the inlet of the settler for different volumetric flow rates and agitator speeds.

The drop sizes were averaged from the relation $d_{av} = \sum nd / \sum n$ over a 1 cm^2 area. Results obtained from these calculations for agitator speeds of 200 rpm and 250 rpm are presented in Figure 3 and 4.

From the over-all photograph of the wedge, wedge heights were measured at different distances from the inlet of the settler. The results are plotted as wedge height versus wedge length and shown in Figures 5 and 6.

Drop concentration N , defined as the number of drops per unit volume in the wedge at a given position of the wedge was obtained by constructing a unit cube which included the top and the bottom wedge surfaces. From the photographs and experimental procedure described earlier, the number of drops

present in that volume were counted. Information on drops residing inside the cube was obtained by taking pictures of atleast one drop layer below the top surface of each view and extrapolating. Similarly, drop diameters were measured in a unit volume and the average drop diameter determined. These results are presented in Figures 7 and 8 for an agitator speed of 200 rpm and in Figures 9 and 10 for a stirrer speed of 250 rpm.

RESULTS FOR SINGLE DROP/INTERFACE COALESCENCE EXPERIMENTS

The mean primary coalescence time $\bar{t}_{d/I}$ for a range of drop sizes and relative axial boundary velocities Δv , are listed in Table 1. With a freshly assembled unit, primary coalescence times were low for drop radii 0.182, 0.322 and 0.372 cm. These values are in fact comparable to those obtained using water drops. However, unlike water drops, as the age of the system increased the distribution of rest times became very large. As noted by previous workers⁽²¹⁾, secondary droplets were formed-sometimes these droplets were stable whilst in other cases the droplets coalesced in rapid succession at least for several minutes, and had to be removed before continuing the experiment. For a fresh system, cleaning the interface gave short and reproducible coalescence times with a narrower distribution than before cleaning. Confirming the observations

of Hodgson and Lee⁽²⁴⁾ large interface ages resulted in longer coalescence times for small drops (radius = 0.182 cm) than for drop sizes of 0.322 and 0.372 cm.

In the presence of axially imposed relative boundary velocities, the primary coalescence times of single heptane drops did not vary appreciably. Drop movements were noted for some values of Δv (see Table 1). In these cases, out of 50 counts about 30% of drops showed a linear motion whilst the rest coalesced without any movement. It is important to note that the mean coalescence time increased in relation to the distance travelled by the drop.

Drop/interface coalescence time measurements at the down stream end of the n-heptane dispersion in the settler using the photographic dye technique gave a distribution of coalescence times from 1.4 sec to 11.5 sec with a mean coalescence time of 4.5 sec when the average drop diameter was 0.32 cm. This was so for all the dispersed phase volumetric input rates studied. Preliminary experiments conducted using 'Red oil 0' dye in the n-heptane drop of 0.2 cm diameter at 7 cm from the inlet of the settler gave a mean drop/interface coalescence time of 1.5 sec. Only a small number of drops released through the water reached the active phase boundary. Some travelled within the wedge trying to reach the active interface whilst others in the process of doing so, disintegrated within the

wedge. The exact location of where the coloured (pink) drop coalesced in the wedge could be easily identified by observing the origin of the vortex shredding.

DISCUSSION

The relationships between drop size in the upper and lower surfaces of the wedge with position in the settler and the dispersed phase flow rates are represented for the dispersion of n-heptane in water in Figures 3 and 4. From these plots, it can be seen that the drop size increases in the active and passive wedge surfaces are almost parallel from the inlet of the settler. For $N = 200$ rpm and dispersed phase flow rate of $620 \text{ cm}^3/\text{min}$ (Figure 3), the drop size increases more in the passive surface than in the active surface. This suggests that the drop/drop coalescence is very significant in the system.

Figures 5 and 6 confirm the presence of a region near the dispersion inlet in which turbulence due to sudden expansion and other inlet effects are smoothed out and the drops rearrange to pack together closely giving a stable structure. This section is seen to extend upto 5 cm of the settler length. Drop size measurements within the section showed that no coalescence occurred and the section can be considered as a 'dead zone' in which the local drop concentration equals that of the feed. The relatively fast flow in this section causes a disturbance

in the neighbourhood and as the result, a strong diagonally-oriented velocity field results in the first 10 cm (from single coloured drop experiments). This forced feeding of the dispersion causes a swelling⁽³⁸⁾ of the dispersion and hence a thicker dispersion band because of the changes in the drop concentration.

From Figure 11, it can be seen that the length of the coalescence wedge is proportional to the drop input rate which agrees with the observations of Jeffreys et al⁽⁹⁾ when using the kerosine/water system. This signifies that the drainage of the continuous phase from the interstices of the drop band is dependent upon the number of drops present in the wedge, and hence length of the wedge is controlled by the drop input rate to the settler.

For agitator speed of 250 rpm, a minor portion of the feed to the settler contained very small droplets formed during the mixing process and visual observations indicated that the small droplets flowed with appreciable velocity to below the passive interface and accumulated at the leading edge of the wedge. A minor portion of these droplets were entrained in the continuous phase and finally reached the free interface (down stream end of the settler) by buoyancy.

It was found that such droplets filled the free area of the leading edge and also surrounded the bigger drops at the leading edge of the wedge. This gave a stabilizing effect by preventing the drops from coalescing with the interface. Photographs of the active surface shown in Figure 12 illustrates this phenomenon. Removal was expected to result in an increase of the settler's capacity, but it was found that the tiny droplet layer occupying the free interface of the settler also prevented the dispersion from further spreading. Periodic interface cleaning in this investigation minimized this effect.

Although the n-heptane/water system is known to form secondary droplets, there was no indication of the presence of secondary droplets in the dispersion, suggesting that the secondary droplets probably coalesced with the neighbouring bigger drops almost instantaneously. Jeffreys et al⁽⁹⁾ suggested that the smallest droplets in the wedge are secondary droplets formed during the coalescence in the active interface, but the probability that these could have escaped from the densely packed bed is very small as demonstrated in Figure 13 (for an agitator speed of 200 rpm and dispersed phase flow rate of 1000 cm³/min).

Analysis of the active surface revealed that the area packing efficiency gradually increased from the inlet of the settler to the outlet. Near the inlet and the middle sections,

the average area packing efficiency $\bar{\eta}_{d/I}$ was approximately 75% whilst at the down stream end, the value lay close to 100%. The 75% efficiency is apparently due to the interaction effect of the sublayer of drops beneath the top layer to congregate more closely. Often, it was observed that drops from the top layer coalesced with the drops in the sublayer very effectively. Also, the disturbance created by this mode of coalescence leads to oscillation of the interface giving rise to appreciable mobility. There were also occasions where drops escaped completely through the wedge and coalesced by a drop/interface mode with the free interface. Volume packing efficiency of the wedge, excluding the active interface was found to have an average value of 95 %.

DETERMINATION OF $\bar{t}_{d/I}/\bar{t}_{d/d}$ FROM EQUATIONS (19) AND (21)

USING THE EXPERIMENTAL DATA

Figures 8 and 10 show that the average drop size per unit volume increases along the length of the settler rapidly for $N = 200$ rpm and 250 rpm. Figures 7 and 9 show the decrease of drop concentration along the length of the wedge. From the model (equation (19) and (21)), it can be seen that three systems parameters must be evaluated - $\bar{t}_{d/d}$, $\bar{t}_{d/I}$ and v_{av} . To overcome the difficulties of assigning a value of v_{av} , the equations were solved by eliminating this parameter which

resulted in an expression for the ratio $\bar{t}_{d/d}/\bar{t}_{d/I}$ in terms of $dN/d\ell$, N , d_{av} and $d(d_{av})/d\ell$. Values of $dN/d\ell$, N and $d(d_{av})/d\ell$, d_{av} at any length of the wedge were obtained by measuring the slopes of the curves in Figures 7-10 for a given dispersed phase flow rate. From this, the ratio $\bar{t}_{d/d}/\bar{t}_{d/I}$ was calculated and plotted as shown in Figure 14. Figure 15 represents the variation of $v_{av} \cdot \bar{t}_{d/d}$ with the length of the wedge. From Figure 13, $\bar{t}_{d/d}/\bar{t}_{d/I}$ tends to zero in the middle part of the wedge and less than one at about 7 cm from the inlet and 5 cm from the down stream end of the wedge. In some cases, this ratio took a negative value in the middle section of the wedge which was probably due to errors in slope measurement and to the limitation of the model itself. However, the results demonstrate the important drop/drop coalescence contribution to the separation process.

SINGLE DROP/INTERFACE COALESCENCE TIMES

Results obtained from drop/interface coalescence time measurements with no-flow and flow conditions showed that $\bar{t}_{d/I}$ did not vary appreciably for both conditions for the range of drop sizes studied (see Table 1). It has been recently⁽³⁹⁾ shown that $\bar{t}_{d/I}$ obtained from small coalescence cells (about 6 cm diameter) were at least 2 to 3 fold higher than obtained in the settler (50x10 cm) under identical conditions such as drop size, material of construction of the cell, mode of measurement etc. The lower

values of $\bar{t}_{d/I}$ in the absence of any velocity field was attributed to the larger available interface than the coalescence cell. Consequently, for a given descent distance, the surface waves produced by the impact of the drop at the interface propagate over the available interface rather unrestrictedly. Since these waves travel radially, it enhances the film drainage and hence gives low rest times. The narrow coalescence time distribution (unlike small cell data) suggested that either the contamination level was low or evenly spread.

$\bar{t}_{d/I}$ measured in the presence of an relative axial boundary velocity in the settler showed (Table 1) that mean coalescence times did not show any appreciable change with changes in Δv . However, for certain values of Δv , the drop moves along the interface for a certain distance in which case the $\bar{t}_{d/I}$ increased in relation to the distance travelled by the drop. A comparison of these values with single drop/interface coalescence times obtained in the absence of flow show no appreciable difference between these values. It is of note that drop movement increases the rest time values.

Single drop/interface coalescence times in the presence of other drops at the active surface of the wedge show that $\bar{t}_{d/I}$ increased from 1.5 sec at the inlet to 4.5 sec at the down stream end of the wedge. This can be attributed to both an increase in the area packing efficiency and also to an increase in the drop size. Drop rupture was observed within

the wedge using single coloured drops. Thus, single drop studies have shown the influence of surface extent whilst in the real situation existing in the settler unit, the drops are subjected to a flow field and to the interaction of adjacent drops. The former effect is expected to sweep away surface tension lowering impurities so reducing the drainage time whilst the latter is expected to reduce the film thinning. Local agitation at coalescing points may decrease or increase film thinning. Therefore, because of the complex effects of these phenomena, a multi-drop system together with the influence of surface extent on single drop coalescence, it is evident that the data from experiments employing single drops which were designed to predict events in a realistic multi-drop situation have to be viewed with considerable caution and emphasises the need for more multi-drop studies to be made.

The deterministic model proposed here is a case of a restricted-in-space type configuration for drops. For a given degree of coalescence, the size distribution of the resulting drops is exactly the same irrespective of the kinetics and it is the result of the random behaviour of the coalescence processes considered. This model does not take into account

- (1) mobility of drops and its influence on the coalescence times
- (2) drop deformation
- (3) secondary droplet formation

(4) and breakage of drops in the wedge. The model accounts, not for the over-all length of the wedge but only the length of the coalescing section. The assumption of an average velocity of drops is incorrect as a drop in the wedge is found to have both horizontal and vertical velocity components. Therefore, this problem should be dealt as a two dimensional case while seeking for a general solution to predict the wedge dimensions. Also, experiments have shown differences in drop velocities at the upper and lower interfaces attributed to vertical displacements of drops within the wedge. The experiments and the model have shown that the velocity of drops in the wedge together with $\bar{t}_{d/d}/\bar{t}_{d/I}$ form the system parameters which control the coalescence processes in the wedge. Thus, a detailed investigation is inevitable to determine v_{av} in the wedge. Nevertheless, the experiments reported and the model described here usefully brings out the importance of the contributions of drop/drop and drop/interface coalescence processes in the dispersion. The model presented is expected to be a good tool to describe these processes, if due information is available on $f_k(\theta)$ and θ . This suggests that new experimental programme is necessary to determine these quantities.

CONCLUSION

The deterministic model presented together with the differential model of Jeffreys et al⁽⁹⁾ usefully analyses the relative

contributions of the drop/drop and drop/interface coalescence processes. Comparison of the model with the experiments has revealed that drop/drop coalescence is very significant for the n-heptane/water system.

ACKNOWLEDGEMENT

The authors express thanks to Professor G.V. Jeffreys for many helpful discussions and for providing the dyes.

NOMENCLATURE

A	extent of drop/interface to drop/drop coalescence.
$C_{k\ell}$	theoretical number of pairs (or collisions) that can be realized between drops of size k and ℓ
d	diameter of drop, cm
$f_k(\theta)$	distribution function of drops of size k = $n_k(t)/N(t)$
H	height of wedge at inlet, cm
h	height of wedge, cm
L	over-all length of wedge, cm
ℓ	wedge length, cm
n	number of drops per second
$n_k(t)$	average number of drops of size k present at time t
N	agitator speed, revolutions per minute
$N(0)$	total number of drops in system at time 0 per unit volume of wedge
Q	volumetric flow rate, cm ³ /min
T	temperature, °C
t	time, sec
\bar{t}	mean coalescence time, sec
v	velocity of drops in the wedge, cm/sec
Δv	relative axial boundary velocity, cm/sec

GREAK LETTERS

α	defined as $\lambda_{d/d}/\lambda_{d/I}$
λ	coalescence rate efficiency
$\bar{\eta}$	packing efficiency
θ	dimensionless time variable = $N(t)/N(0)$ denotes degree of coalescence
χ	cumulative size fraction

SUBSCRIPTS

av	average values
o	inlet conditions
k, l	referring to drops of size k or l
d/I	drop/interface coalescence mode
d/d	drop/drop coalescence mode

REFERENCES

1. H.P. Meissner and B. Chertow, *Ind. Eng. Chem.*, 1946, vol. 38, pp. 856.
2. G.A. Davies, G.V. Jeffreys, D.V. Smith and F.A. Ali, *Can. J. Chem. Eng.*, 1970, vol. 48, pp. 328.
3. A.D. Ryan, F.L. Daley and R.S. Lowrie, U.S. Atomic Energy Commission Rept. NO ORNL 2591 (1960); *Chemical Eng. Prog.*, 1959, vol. 55, pp. 70.
4. G.A. Davies, G.V. Jeffreys and F.A. Ali, *Inst. Chem. Symposium on Process Development*, Birmingham, England, 1969.
5. M.A. Rodgers, V.G. Trice and J.H. Rushton, *Chem. Eng. Prog.*, 1966, vol. 52, pp. 12.
6. D.V. Smith, Ph.D. Thesis, Univ. of Manchester, England, 1969.
7. J.A. Williams, L. Lowes and M.C. Tanner, *Trans. Inst. Chem. Eng.*, 1958, vol. 36, pp. 466.
8. G.V. Jeffreys, D.V. Smith and K. Pitt, *I. Chem. E. Symposium Series*, No 26 (1967, *Instn. Chem. Engrs.*, London) 1967, pp. 11.
9. G.V. Jeffreys, G.A. Davies and K. Pitt, *A.I.Ch.E. Journal*, 1970, vol. 16, No 15, pp. 823-831.
10. J. Mizrahi and E. Barnea, *Chem. Proc. Eng.*, 1973, January, pp. 60-65.
11. G. Aly and B. Wittenmark, *J. Appl. Chem. Biotechnol.*, 1972, vol. 22, pp. 1165.
12. G. Aly, A. Jerngvist, H. Reinhardt and H. Ottertun, *Chem. Ind.*, 1971, pp. 1046.
13. G. Aly and H. Ottertun, *J. Appl. Chem. Biotechnol.*, 1973, vol. 23, pp. 643-660.

14. P.E. Kapur and D.W. Fuerstenau, Ind. Eng. Chem. Process Design Develop., 1969, vol. 8, pp. 56-62.
15. E.O. Knuston, K.W. Pontinen and L.W. Rees, Am. Ind. Hyg. Assoc. J., 1967, vol. 28, p. 83.
16. S.K. Friedlander and C.S. Wang, J. Colloid and Interface Sci., 1967, vol. 24, pp. 170.
17. Z.A. Melzak, Appl. Math., 1953, vol. 11, pp. 231.
18. W.T. Scott, J. Atmospheric Sci., 1968, vol. 25, pp. 54.
19. A.T. Bharuche-Reid, Elements of the theory of Markov Processes and their Applications, McGraw-Hill, New York, 1960.
20. K.V.S. Sastry and D.W. Fuerstenau, Ind. Eng. Chem. Fundamentals, 1970, vol. 9, pp. 145-149.
21. G.E. Charles and S.G. Mason, J. Colloid Sci., 1960, vol. 15, pp. 236.
22. G.V. Jeffreys and J.L. Hawksley, A.I.Ch.E. Journal, 1965, vol. 11, pp. 413.
23. S. Hartland, Trans. Instrum. Chem. Engrs., 1967, vol. 45, T 97, T 102, T 109.
24. T.D. Hodgson and J.C. Lee, J. Colloid and Interface Sci., 1969, Vol. 30, pp. 94.
25. T.D. Hodgson and D.R. Woods, J. Colloid and Interface Sci., 1969, vol. 30, pp. 429.
26. K.A. Burril and D.R. Woods, J. Colloid and Interface Sci., 1969, vol. 30, pp. 511.

27. S.B. Lang and C.R. Wilke, Ind. Eng. Chem. Fundamentals, 1971, vol. 10, pp. 341.
28. S. Gondo, K. Hisatomi, K. Kusunoki and I. Nakamori, Kagaku kogaku, 1968, vol. 32, pp. 923.
29. D.H. Logsdail, J.D. Thornton and H.R.C. Pratt, Trans. Instn. Chem. Engrs. (London), 1957, vol. 35, pp. 301.
30. G. Sege and F.W. Woodfield, Chem. Eng. Progr. Symposium Ser., 1954, No 13, pp. 179.
31. A.R. Smith, J.E. Caswell, P.P. Larson and S.D. Cavers, Can J. Chem. Eng., 1963, vol. 41, pp. 150.
32. T. Otake and I. Komasaawa, Kagaku kogaku, 1968, vol. 32, pp. 583.
33. I. Komasaawa and T. Otake, J. Chemical Eng. Japan, 1970, vol. 3, No 2, pp. 243.
34. E.G. Cockbain and T.S. McRoberts, J. Colloid Sci., 1953, vol. 8, pp. 440.
35. G. Lawson, Ph. D. Thesis, Univ. Manchester, England, 1967.
36. G.V. Jeffreys, Private Communications, 1973.
37. R. Shinnar and J.M. Church, Ind. Eng. Chem., 1960, vol. 52, pp. 1960.
38. K.D. Manchanda and D.R. Woods, Ind. Eng. Chem. Process Design and Development, 1968, vol. 7, pp. 182.
39. S. Vijayan and A.B. Ponter, Paper submitted, 1973.

TABLE 1 Mean coalescence time of n-heptane drops at n-heptane/
water interface at 25°C in the settler

Drop radius (cm)	Velocity (cm/sec)		Δv (cm/sec)	$\bar{t}_{d/I}$ (sec)	Observation
	n-heptane	Water			
0.182	0	0	0	≤ 1.0	
0.322	0	0	0	1.53	
0.372	0	0	0	1.73	
0.182	0.2	0.05	+0.15	0.78	no drop movement
				2.12	drops travelled from 1-6 cm
	0.15	0.18	-0.03	0.7	
0.322	0.03	0.28	-0.25	0.85	
	0.20	0.11	+0.09	0.99	
	0.09	0.11	-0.02	0.95	
	0.20	0.23	-0.03	1.14	
0.372	0.14	0.28	-0.14	1.2	no drop movement
				2-7	drops travelled from 1.5-4.5 cm
	0.03	0.28	-0.25	1.55	
	0.20	0.10	+0.09	1.23	no drop movement
				2-6	drops travelled from 1-3 cm
	0.20	0.05	+0.15	1.25	

FIGURE CAPTIONS

- Figure 1 Coalescence wedge (heavy phase dispersed).
- Figure 2 Schematic diagram of apparatus.
- Figure 3 Variation of drop size into active and passive interfaces with distance from settler inlet.
- Figure 4 Variation of drop size in the active and passive interfaces with distance from settler inlet.
- Figure 5 Variation of wedge height with distance from settler inlet.
- Figure 6 Variation of wedge height with distance from settler inlet.
- Figure 7 Variation of average drop concentration with distance from settler inlet.
- Figure 8 Variation of average drop size per unit volume with distance from settler inlet.
- Figure 9 Variation of average drop concentration with distance from settler inlet.
- Figure 10 Variation of average drop size per unit volume with distance from settler inlet.
- Figure 11 Effect of drop input rate on wedge length.
- Figure 12 Photographs of active interface for different wedge lengths when n-heptane is dispersed for $N = 250_3 \text{ rpm}$ and dispersed phase flow rate = $1000 \text{ cm}^3/\text{min}$.

- Figure 13 Photographs of active interface for different wedge lengths when n-heptane is dispersed for $N = 200$ rpm and dispersed phase flow rate = $1000 \text{ cm}^3/\text{min}$.
- Figure 14 Variation of $\bar{t}_{d/d}/\bar{t}_{d/I}$ with distance from settler inlet.
- Figure 15 Variation of $v_{av} \times \bar{t}_{d/d}$ with distance from settler inlet.

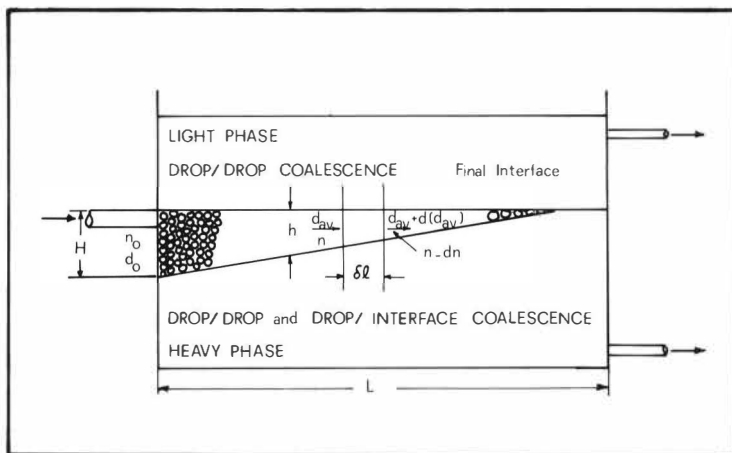


Figure 1 -

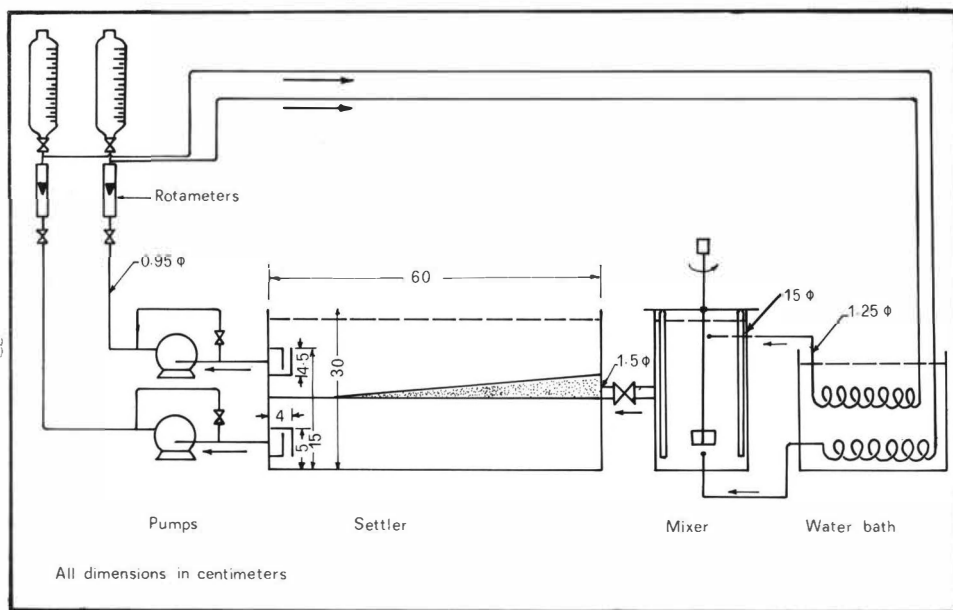


Figure 2 -

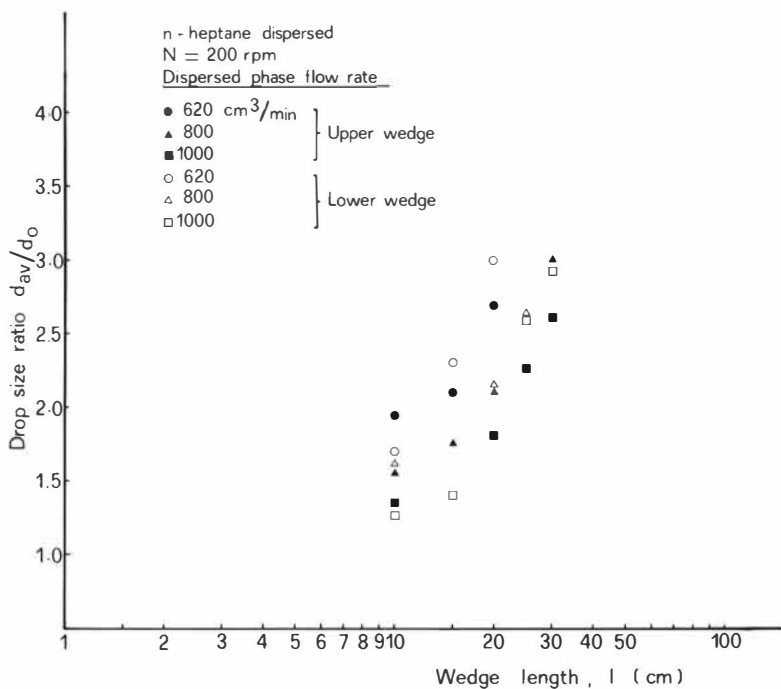


Figure 3-

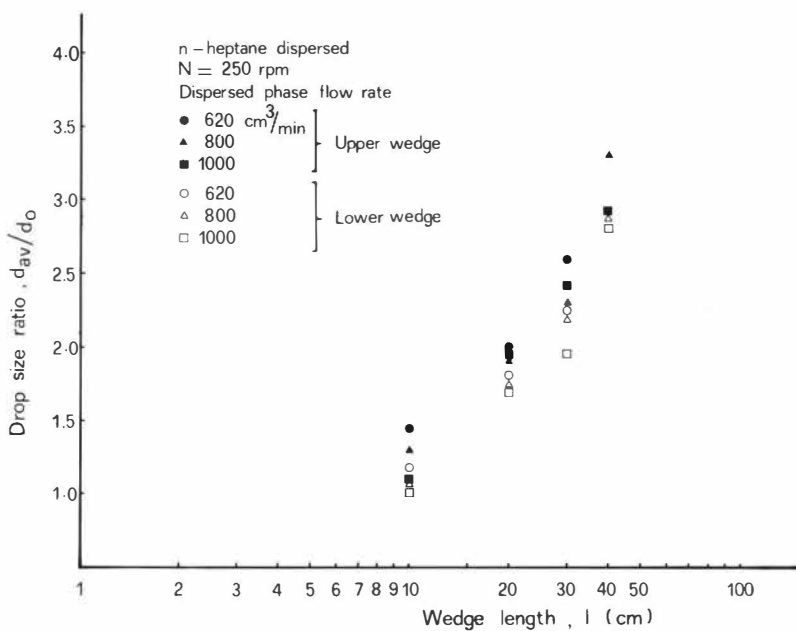


Figure 4 -

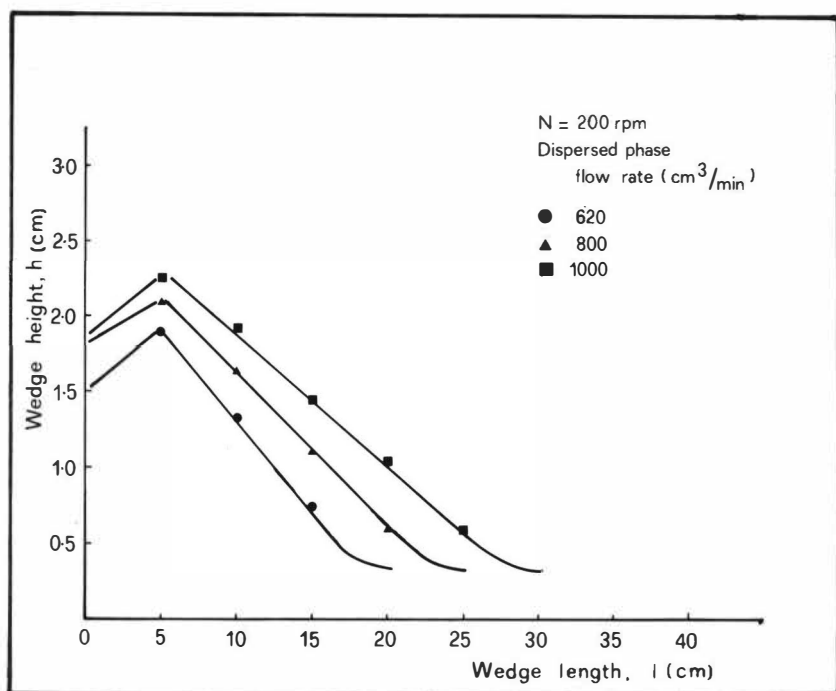


Figure 5 -

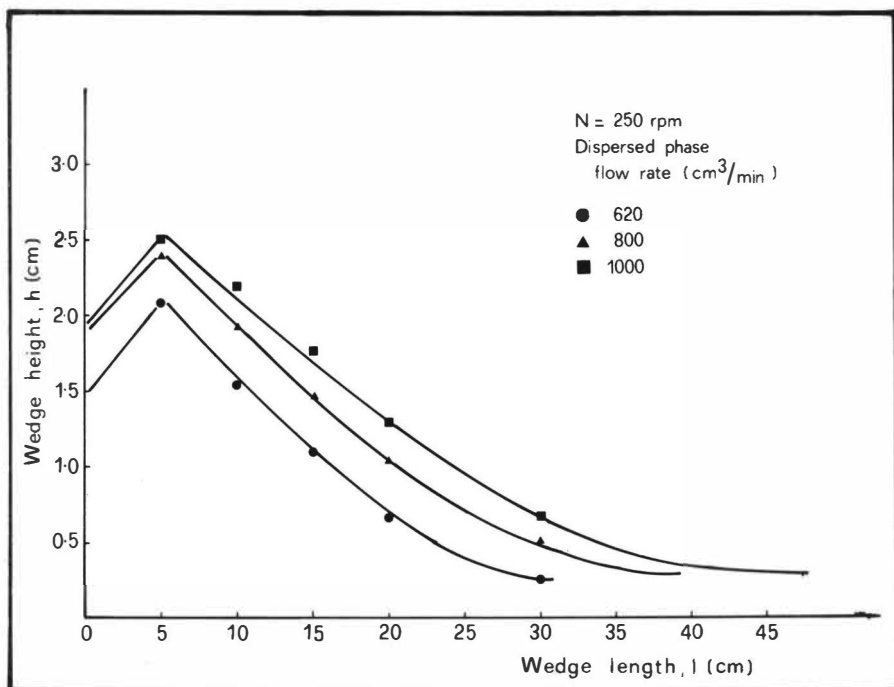


Figure 6 -

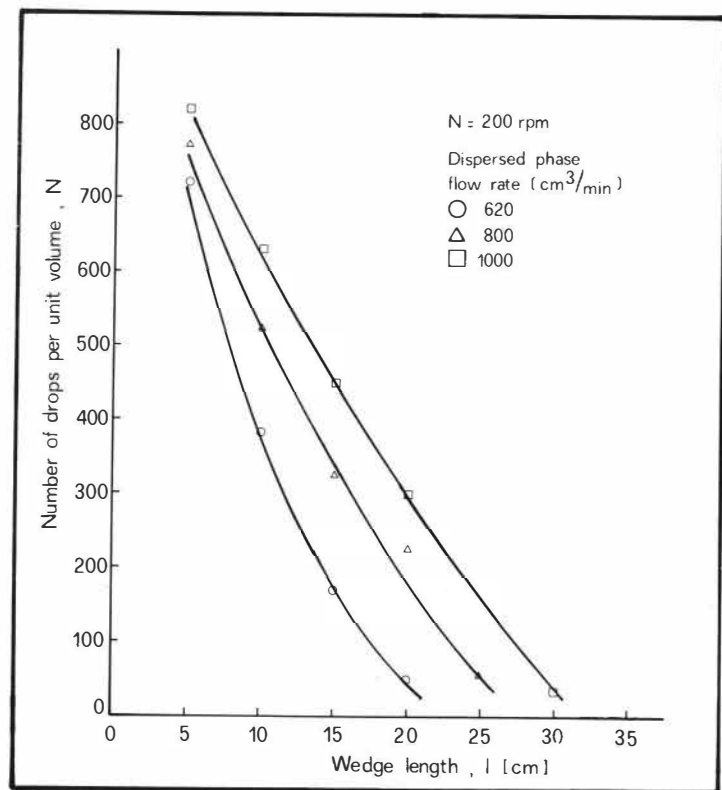


Figure 7

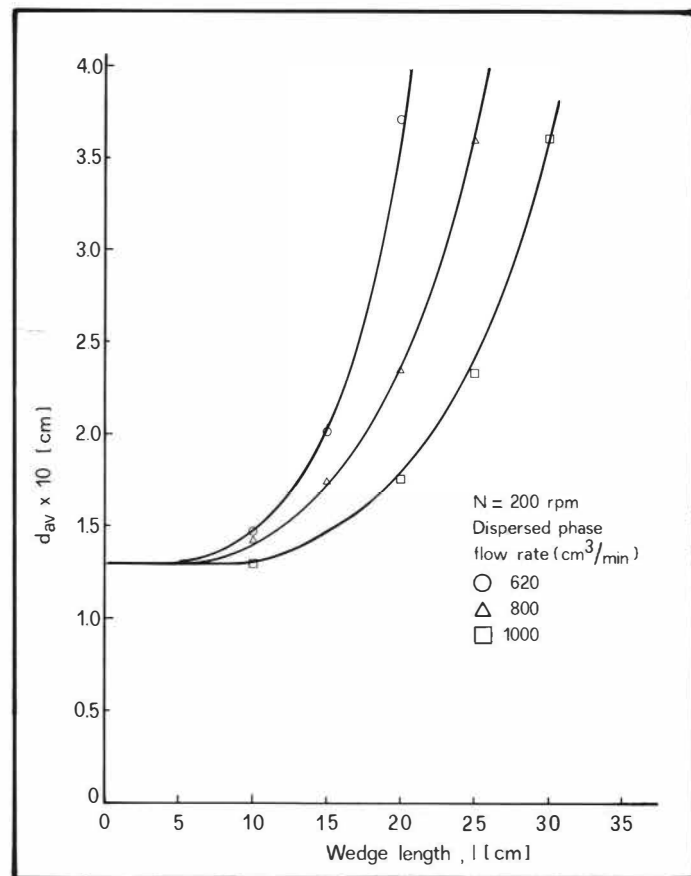


Figure 8

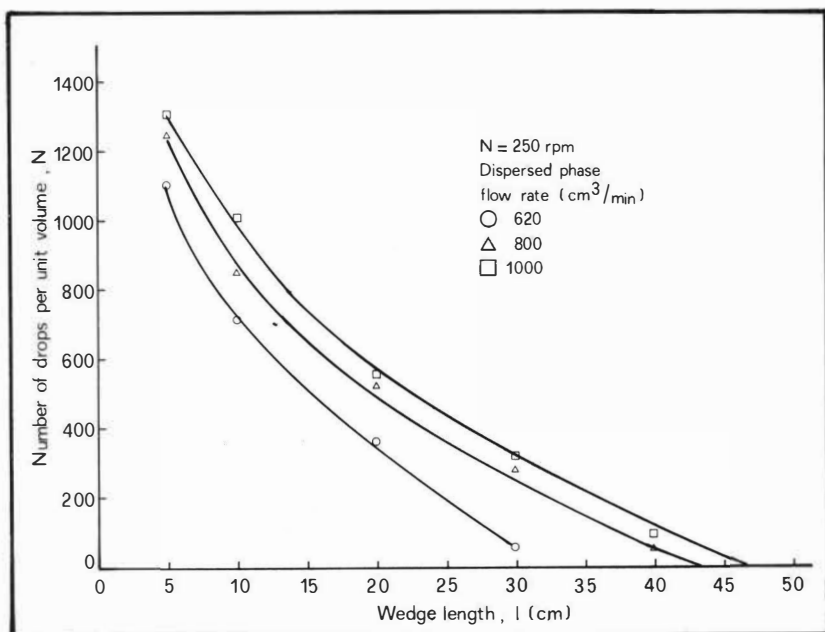


Figure 9-

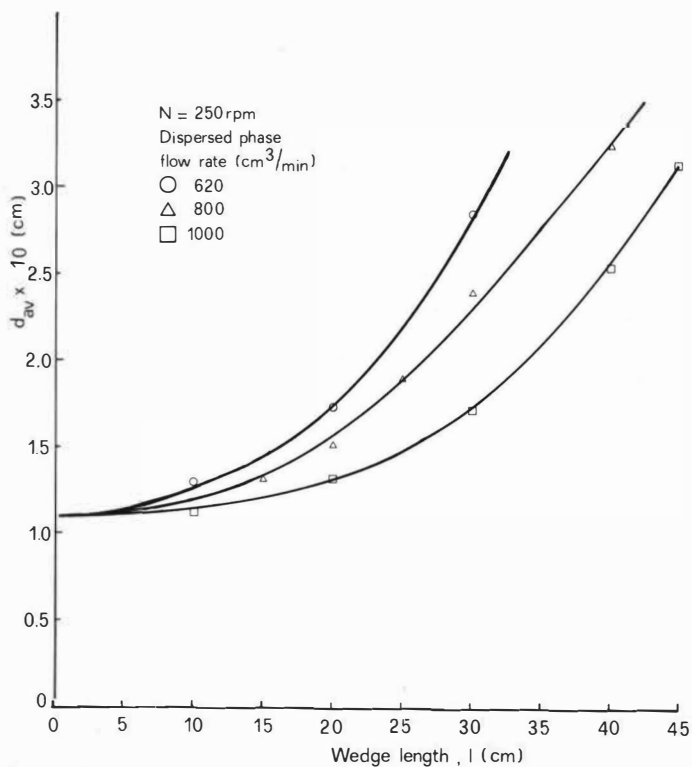


Figure 10-

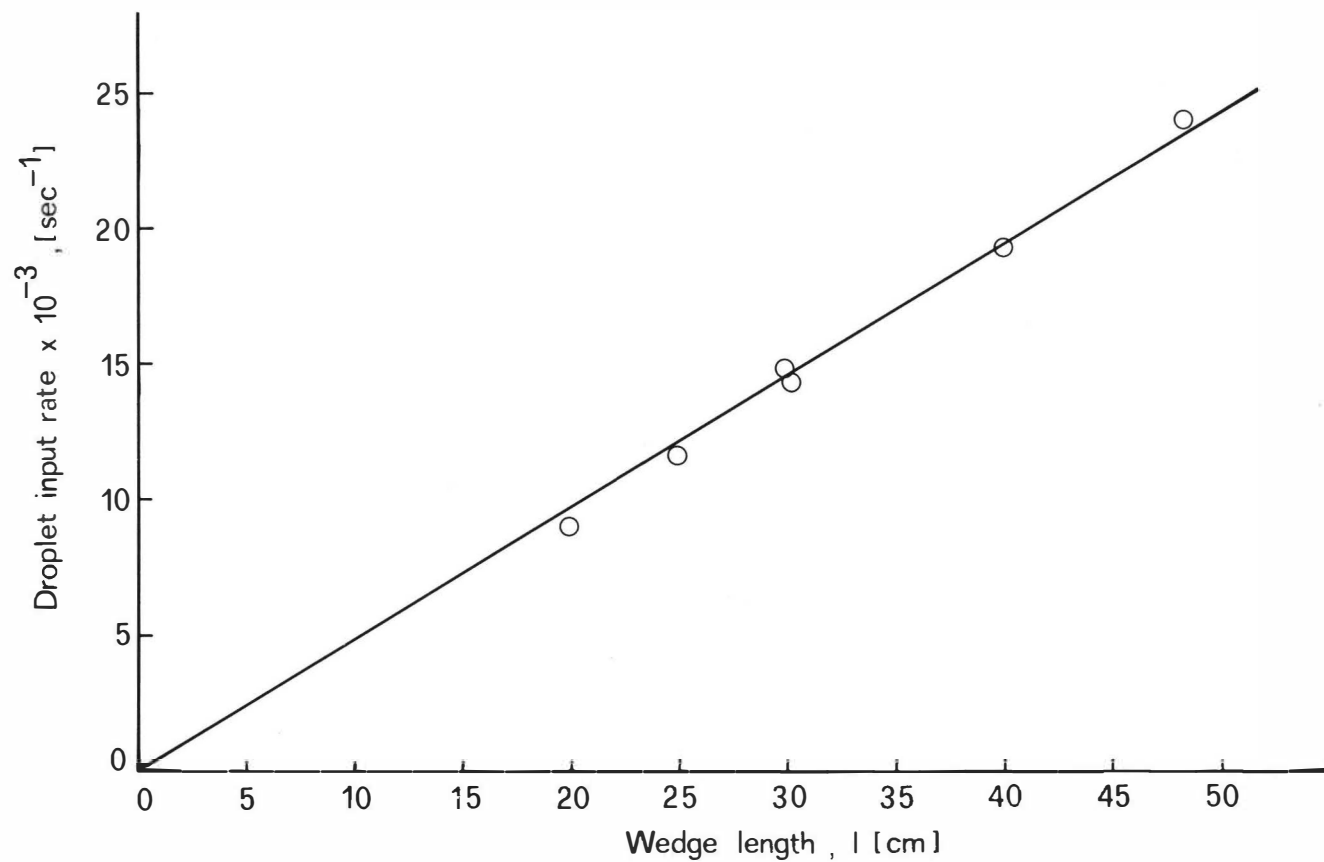
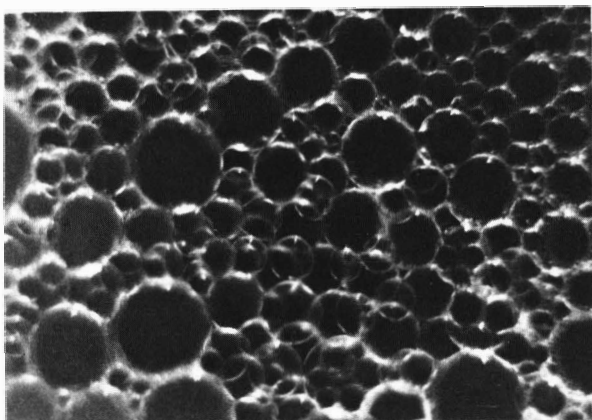


Figure 11 -

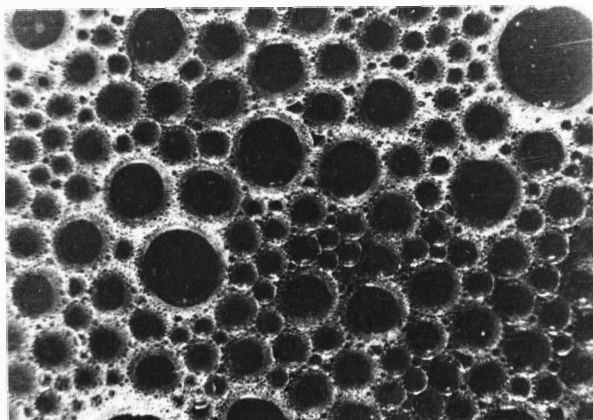
$l = 5 \text{ cm}$



$l = 40 \text{ cm}$



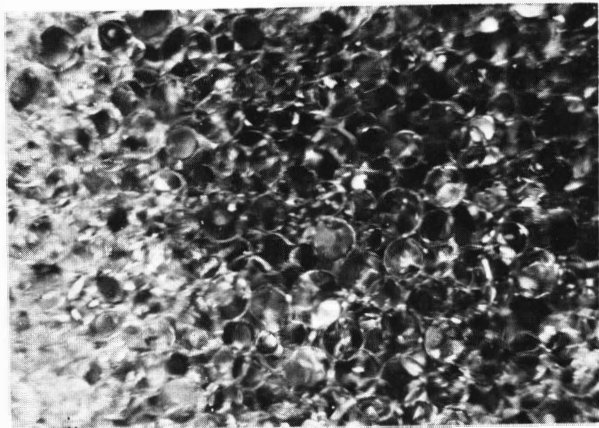
$l = 47 \text{ cm}$



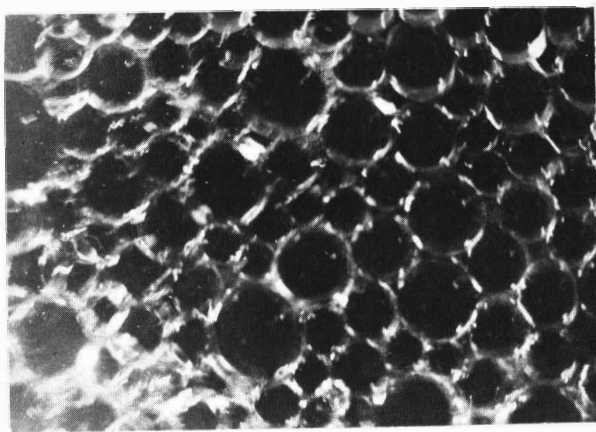
magnification 5x

Figure 12 -

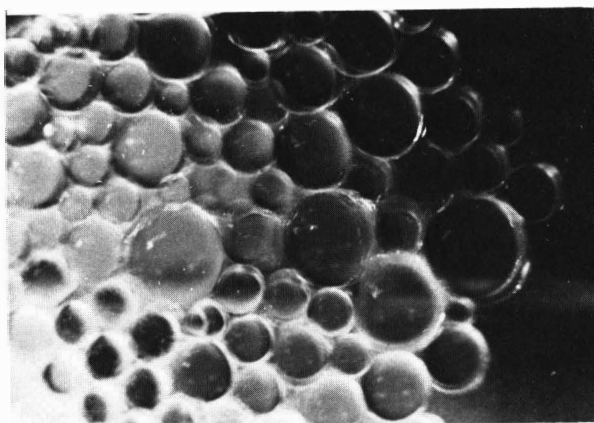
$l = 5 \text{ cm}$



$l = 25 \text{ cm}$



$l = 30 \text{ cm}$



magnification 5x

Figure 13 -

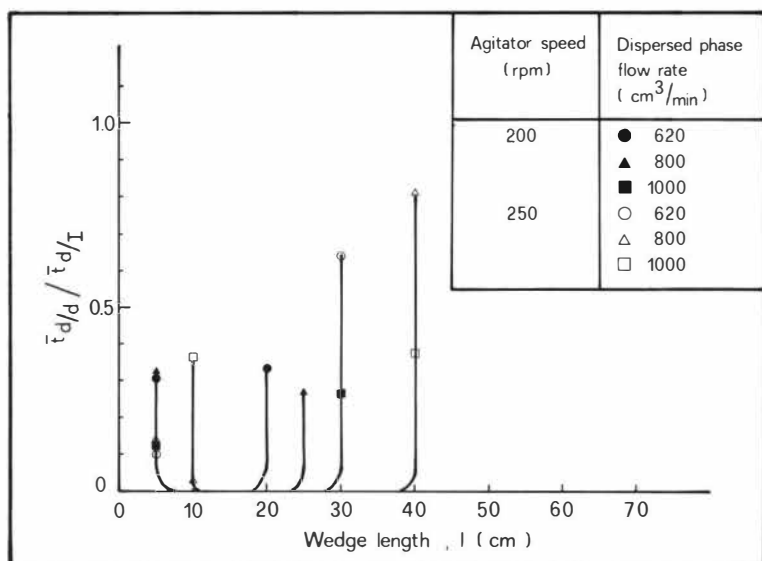


Figure 14 -

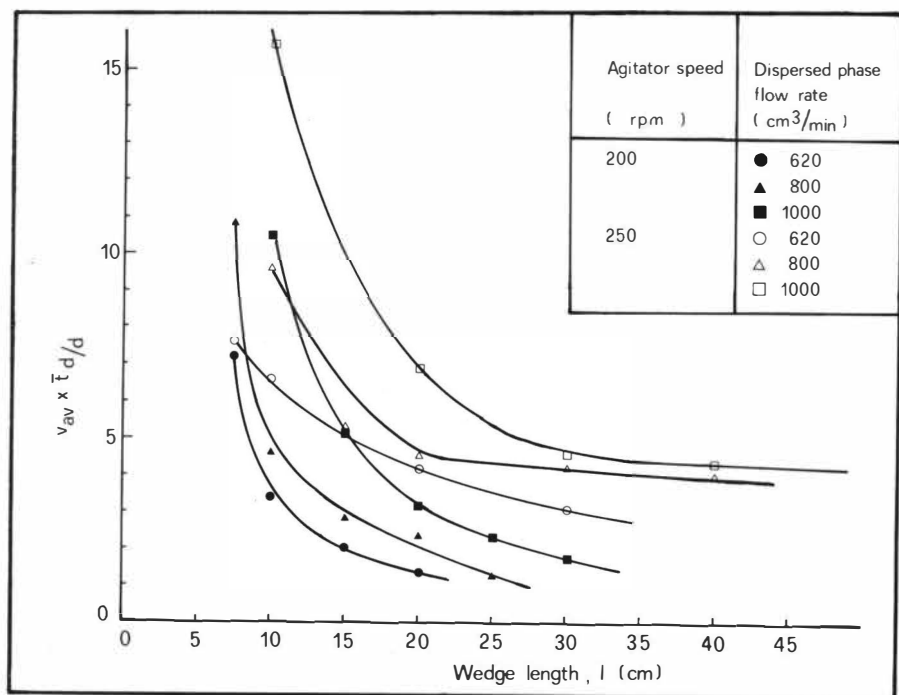


Figure 15-

SESSION 6

Monday 9th September: 14.00 hrs

E X T R A C T I O N T E C H N O L O G Y

(Common Metals)

Chairman:

Mr. G.M. Ritcey

Secretaries:

Dr. G.J. Lawson

Mr. C.P. Batten



SOLVENT EXTRACTION OF COBALT CHLORIDE IN ROTATING
DISC CONTACTORS

by

S. Bruin, J.S. Hill and D. van der Meer
KONINKLIJKE/SHELL-LABORATORIUM, AMSTERDAM
(Shell Research B.V.)

SUMMARY

A brief survey is given of pilot plant experience with solvent extraction of cobalt chloride from aqueous process streams containing nickel chloride and hydrochloric acid. Aliquat 336 in toluene was used as the extractant solution. The pilot plant comprises two rotating disc contactors (RDC's), one for the extraction/scrubbing steps, and the other for solvent regeneration, in an integrated circuit. The technical feasibility of such a system was proved in a series of runs in which throughputs and mass transfer efficiencies were measured.

INTRODUCTION

An investigation was conducted into the potentialities of the rotating disc contactor (RDC) for solvent extraction of cobalt chloride from aqueous process streams containing this salt, together with nickel chloride and hydrochloric acid. Suitable extractants include triisooctylamine (Alamine), tri-n-propylmethylammonium chloride (Aliquat 336) and alkyl sulphonium compounds in appropriate diluents. We used Aliquat 336 in the work reported here. Such applications of solvent extraction become increasingly attractive in hydrometallurgical operations and the extraction of cobalt chloride in particular appears in two fields of application: recovery and purification of nickel values from lateritic ores and recycling of cobalt and nickel containing scrap materials¹⁻¹². These processes involve the dissolution of the metals of interest in a leach step, followed by further process steps to separate the various metals present in the aqueous pregnant leach liquor from each other and from impurities and finally the metal production proper by reduction, either in the gas phase or by electrolysis.

DESCRIPTION OF PILOT PLANT

The pilot plant, consisting of two extractors of 0.06 m diameter and 3.2 m long, is schematized in Fig.1. In the rotating disc contactor RDC-1 cobalt chloride is extracted from the feed flowing down by the extractant phase (Aliquat 336, ex General Mills, in toluene as diluent) which becomes loaded with cobalt while flowing up. The top part of the RDC can be used as scrubbing section, if needed. The (scrubbed) loaded extractant phase then flows to the second RDC where it is stripped of its cobalt in countercurrent flow with a diluent CoCl_2 strip solution. The regenerated extractant phase (solvent) is then recycled to the extraction section of RDC-1.

The RDC's are built up in four segments of 0.3 m length, interconnected by flanges provided with bearings and sample connections between the compartments. The internals (rotor discs and stator rings) are constructed from Hastelloy B and the extractors are glass-walled. Top and bottom settling compartments are again constructed from Hastelloy B. Tubes are made in PTFE and

vessels in glass or polyethylene. The pumps have glass housings and PTFE impellers.

EQUILIBRIUM DATA

In the RDC experimental programme phase ratios, concentrations, etc., were only considered as variables to a limited extent. They were generally fixed on the basis of equilibrium data (see Appendix 1) such that reasonably effective and selective extraction of cobalt could be expected. The investigation was then limited to determining the height of a transfer unit as a function of the RDC operating variables (throughput, power input, choice of dispersed phase). Some of the more important features of the extraction of cobalt/nickel chloride solutions with Aliquat 336 in toluene are summarised here.

The distribution coefficient of cobalt ($K_{Co^{2+}}$) is proportional to the fifth power of the chloride concentration over the range 3 to 8 kmol/m³. At ambient temperature with an extractant concentration in the range 0.2-0.6 kmol/m³ a chloride concentration of 5 kmol/m³ or higher is indicated for efficient extraction of cobalt (i.e. in a limited number of stages and with a small excess of extractant). $K_{Co^{2+}}$ is directly proportional to the extractant concentration and increases markedly with temperature.

Considerable co-extraction of nickel occurs from aqueous solutions containing high concentrations of nickel chloride. The separation factor, β ($= K_{Co^{2+}}/K_{Ni^{2+}}$) can be improved by increasing the chloride concentration ($K_{Ni^{2+}}$ is roughly constant over the range of interest) and by minimising the excess of extractant over cobalt (i.e. approaching saturation of the extractant with cobalt). Co-extracted nickel can also be removed by scrubbing loaded extractant phase with a nickel-free chloride solution which can also act as a source of additional chloride when required. In this case scrubbing with HCl will usually be preferable since the introduction of extraneous metal ions into the raffinate is then avoided.

Scrubbing with HCl offers an additional advantage in that the separation factor is also enhanced by an increase in the ratio, E, of HCl to total chloride. The influence of loading and chloride source is illustrated in Fig.2 where β is plotted against the load factor, L, for two extreme values of E corresponding to aqueous phases containing (apart from traces of cobalt chloride) only nickel chloride (E = 0) or HCl (E = 1). The separation factor is given by the equation

$$(1) \quad \beta = \frac{\bar{c}_{Co^{2+}} / \bar{c}_{Ni^{2+}}}{c_{Co^{2+}} / c_{Ni^{2+}}} = c_1 (c_{Cl^-})^5 \frac{\sqrt{10E + 1} [(8E^{-8E} + 4.4)L + 1]}{(1 - L)}$$

where

$$(2) \quad E = \frac{(c_{Cl^-})_{HCl}}{(c_{Cl^-})_{tot}}$$

$$(3) \quad L = \frac{2\bar{c}_{Co^{2+}}}{c_a}$$

$$(4) \quad c_1 = 3.3 \times 10^{-2} \text{ (roughly a constant)}$$

EXTRACTION EXPERIMENTS

Two solutions, A and B, containing cobalt chloride, nickel chloride and hydrochloric acid were used in pilot plant runs. The compositions are given in Table 1. A was a dilute solution whose chloride concentration was rather too low for efficient extraction. In this case we applied a scrub with 6N HCl, partly to make up for the chloride deficiency and partly to reduce co-extraction of nickel. Solution B was much more concentrated than A. This solution required no scrub with HCl and was injected via the top nozzle into RDC-1 (see Fig.1).

Solution A ($0.54 \text{ kmol/m}^3 \text{Co}$) was extracted throughout with a 0.4M extractant solution at a phase ratio of 5:1 (org/aq). The extractant/cobalt molar ratio was about 4 compared with the stoichiometric requirement of 2 (see Appendix). This favours high cobalt extraction but also results in high nickel co-extraction, hence the application of a scrub.

TABLE 1

COMPOSITIONS AND PHYSICAL PROPERTIES OF THE
FEED SOLUTIONS AND EXTRACTANT MIXTURES

Solution	ρ	$\nu \times 10^6$	c_{Co}	c_{Ni}	c_{Fe}	c_{H^+}	c_{Cl^-}
	kg/m^3	m^2/s	kg/m^3	kg/m^3	kg/m^3	kmol/m^3	kmol/m^3
A	1100	1.62	32	74	-	1.25	7.8
B	1350	3.12	48.4	115	0.01	1.5	7.6
strip solution	1031	1.0	5.10	-	-	-	0.17-0.34
0.4M Aliquat in toluene	886	1.83	-	-	-	-	-
0.6M Aliquat in toluene	891	3.44	-	-	-	-	-

Solution B ($0.82 \text{ kmol/m}^3 \text{Co}$) was generally treated with a slight excess of extractant (0.4M extractant at a phase ratio 5:1 or 0.6M extractant at 3.3:1. A few runs were also performed with 0.6M extractant at a phase ratio of 5:1, under which conditions co-extraction of nickel was considerable.

In each run, after steady state had been reached, we measured the compositions of the various aqueous and organic streams into and out of both RDC's. Dispersed phase hold-ups were determined from samples taken along the columns (see Fig.1). In a series of runs we varied flow rates and rotor speed in order to find the optimum operating conditions of both RDC's. From the results of the runs we deduced the capacities and mass transfer rates in both RDC's. Capacity is expressed in the usual fashion as the sum of the superficial velocities of continuous and dispersed phase at incipient flooding:

$$(v_c + v_d)_f = 4(Q_c + Q_d) / (\pi D^2) \quad (5)$$

The mass transfer rate was characterised by the height of a true transfer unit, $(HTU)_{\text{true}}$. Corrections for axial mixing of both the continuous and the dispersed phase were made using standard axial mixing correlations for RDC's (see also Appendix 1).

4.1. Capacity measurements

Flooding of the column occurs when the dispersed phase droplets can no longer overcome the velocity of the continuous phase and thus are entrained with the latter relative to the equipment. This leads to a build-up of droplets which eventually leave the column with the continuous phase. In Fig.3 we have plotted the measured capacities against the group $N^3 R^5 / (HD^2)$ which is proportional to the power input per unit mass in the contactor. The capacity $(v_c + v_d)_f$ will be proportional to the slip velocity v_s between the two phases.

$$(v_c + v_d)_f = v_s (1 + v_d/v_c) \left[\frac{v_d/v_c}{(1 - h_f)} + 1/h_f \right] \quad (6)$$

If we combine the Hu and Kinter correlation for settling velocities¹³ with the Hinze/Sleicher correlations¹⁴ for average drop size we have the following series of proportionalities for $(v_c + v_d)_f$ and v_s :

Hu/Kinter correlation (approximate)

$$v_s \sim d_{av}^{0.7} g^{0.7} \mu_c^{-0.1} \rho_c^{-0.2} \quad \text{if } T \leq 10 \quad (7a)$$

$$v_s \sim 4 \rho^{0.27} g^{0.17} \mu_c^{0.2} \rho_c^{-0.55} g^{0.27} \quad \text{if } T > 10 \quad (7b)$$

where T is defined as

$$T = v_s d_{av} g^{0.15} \rho_c^{0.7} 4 \rho^{0.15} \mu_c^{-0.4} g^{-0.45} \quad (7c)$$

$$d_{av} \sim \epsilon_m^{0.6} \rho_c^{-0.6} \mu_c^{-0.4} \quad (8)$$

Combining these correlations with equation (6) gives the following forulae. If $T = 10$:

$$(v_c + v_d)_f \sim \epsilon_m^{0.5} \Delta \rho^{0.7} \rho_c^{-1.0} \mu_c^{-0.2} \epsilon_m^{-0.4} \quad (9)$$

If $T = 10$:

$$(v_c + v_d)_f \sim \epsilon_m^{0.17} \Delta \rho^{0.27} \rho_c^{-0.55} \mu_c^{0.10} \epsilon_m^{0.27}$$

The implication of equation (9) is that under operating conditions where turbulent drop break-occurs (small droplets with low v_s and hence a low T -value) a plot of $\log (v_c + v_d)_f$ against $\log (\epsilon_m)$ should approach a slope of -0.4 . The curves in Fig.3 roughly follow this trend. Fig.4 shows how the hold-up of the dispersed phase in stripper and extractor is affected when solution A is processed under various conditions. The hold-up rises sharply if the power input group approaches flooding conditions. The flooding conditions are reached at considerably lower power inputs if the phase ratio $v_d/v_c > 1$ and hindered settling apparently prevails. Fig.5 shows the capacity curves for extracting and stripping RDC when processing solution B. The capacity tends to be somewhat higher than for solution A, presumably because of the greater difference in density, $\Delta \rho$, between organic phase and water phase.

4.2. Mass transfer rates

The height of a true transfer unit¹⁵, $(HTU)_{true}$, was used as a measure of the mass transfer rates we were able to obtain in the equipment. A difficulty in using the concept is that the extraction factor, F , varied from one stage to another because of changes in the slope of the equilibrium line over the range of concentrations of interest. We calculated an average extraction factor by means of a computer program for multicomponent solvent extraction discussed in Appendix 1. The $(HTU)_{true}$ is defined as ¹⁴ column length divided by the number of true transfer units $N_{of, t}$:

$$(\text{HTU})_{\text{true}} = \frac{v_f}{k_{\text{of}} a) = \frac{L}{N_{\text{of}, t}} \quad (10)$$

where v_f is the superficial velocity of the (dispersed) feed phase, k_{of} an "effective" mass transfer coefficient (including possible chemical effects) on overall feed phase basis and a the specific area of contact between drops and continuous phase in m^2/m^3 .

The main results are given in Figs. 6-9 as plots of $(\text{HTU})_{\text{true}}$ against the power input group $N^3 R^5 / (\text{HD}^2)$. Fig. 6 pertains to the dilute feed A, which was the dispersed phase in the extraction column at $v_d/v_c = 0.20$. The $(\text{HTU})_{\text{true}}$ decreases with increasing power input to about 0.2 m at the highest power input level we used. Substitution for v_f ($\approx 1.2 \times 10^{-3}$ m/s) at the condition where $(\text{HTU})_{\text{true}} = 0.2$ m gives a $(k_{\text{of}} a)$ of about $0.6 \times 10^{-2} \text{ s}^{-1}$. Spherical drops of 2 mm diameter would give an interfacial area of $300 \text{ m}^2/\text{m}^3$ at 10% holdup, hence $k_{\text{of}} \approx 0.2 \times 10^{-4}$ m/s, which is in the right order of magnitude for a mass transfer limited transport of the component in question.

Fig. 7 gives the results obtained for stripping of the cobalt-laden extract phases from solutions A and B with a dilute aqueous cobalt chloride solution (for composition see Table 1). In this stripping step the strip solution is continuous and the loaded organic phase dispersed. The lowest $(\text{HTU})_{\text{true}}$ measured now was 0.40 m at power inputs of $N^3 R^5 / (\text{HD}^2) = 0.2-0.3 \text{ m}^2/\text{s}^3$. For these conditions we had $v_f = 4 \times 10^{-3}$ m/s and thus $k_{\text{of},a} = 10^{-2} \text{ s}^{-1}$, giving roughly $k_{\text{of}} \approx 0.3 \times 10^{-4}$ m/s.

In Figs. 8 and 9 measured $(\text{HTU})_{\text{true}}$ is plotted against power input for the extraction of feed B with 0.4M and 0.6M Aliquat 336 in toluene as extractant solutions. The results strikingly differ from those of Figs. 6 and 7: the $(\text{HTU})_{\text{true}}$ is much more sensitive to an increase in power input than in the previous cases. Partly this could be explained by interfacial tension effects. The interfacial tension of both the 0.4M and 0.6M Aliquat extractant phases towards feed solution 3 decreases with increased loading of the extractant phase (see Fig. 10). Now, roughly speaking, the product $(k_{\text{of}} a)$ is inversely proportional to drop size squared and the drop size is proportional to the interfacial tension to the power 0.6; see equation (8).

We may therefore expect from equation (10) that the height of a transfer unit decreases with decreasing interfacial tension. But a decrease in the height of a transfer unit means better mass transfer of cobalt and hence a higher loading of the organic phase, which in turn leads to a still lower interfacial tension. In consequence, at an increase in power input, drop size will decrease more rapidly than one would expect from the influence of mean drop size alone. Thus also the $(HTU)_{true}$ will decrease more sharply when compared with cases where no loading effect on interfacial tension is present (solution A).

DISCUSSION AND CONCLUSIONS

The use of an RDC for the extraction of cobalt chloride from aqueous solutions containing nickel chloride and hydrochloric acid with Aliquat 336 in toluene as extractant solution is technically feasible. To illustrate this further we calculated, with the aid of the data presented in this paper, the extractor volume needed, and the solvent inventory to be expected, in the extraction of $4 \text{ m}^3/\text{h}$ of solution B with $12 \text{ m}^3/\text{h}$ 0.6M Aliquat in toluene with a 99.9% cobalt recovery. Calculations for a number of power inputs are represented in Fig. 11. At very low power inputs the $(HTU)_{true}$ is so high that long slender columns are needed. At high power inputs the $(HTU)_{true}$ is so low that axial mixing effects (which increase with increasing power input and column diameter) become length-determining, and because of the low flooding velocities a large-diameter column is needed. This results in a long, large diameter column. Both situations mean a relatively big volume of the contactor. There is an optimum volume at a power input of roughly $0.1\text{--}0.2 \text{ m}^3/\text{s}$ where further efforts to reduce mass transfer limitation are thwarted by increasing axial mixing and lower capacity.

From this sample calculation we conclude that reasonable capacities can be obtained at sufficient efficiency levels. This indicates that the rotating disc contactor, which can be and has been constructed on a technical scale from corrosion resistant materials such as glass reinforced Epikote, should be considered as an alternative in designing cobalt extraction systems under conditions similar to those discussed in this paper.

ACKNOWLEDGEMENT

Measurements were performed by Messrs. J.M. van der Klaauw
and R. Kok

FIGURE 1
FLOW SHEET OF PILOT PLANT FOR COBALT EXTRACTION

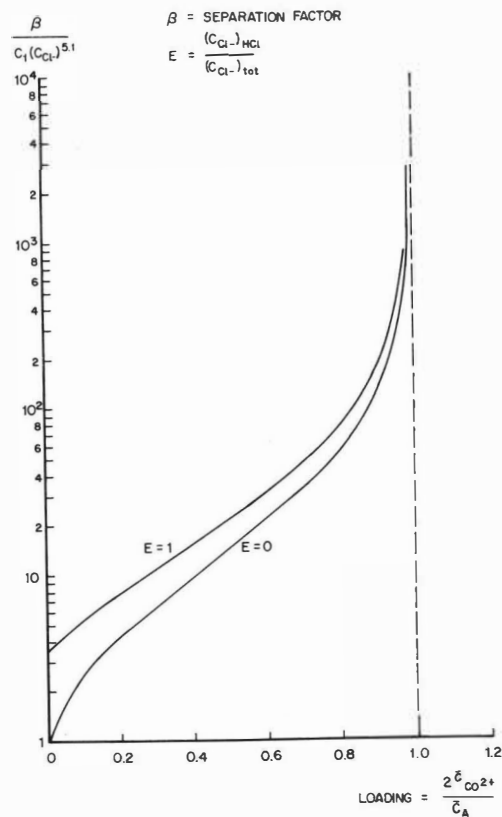


FIGURE 2
COBALT/NICKEL SEPARATION FACTOR AS A FUNCTION OF LOADING

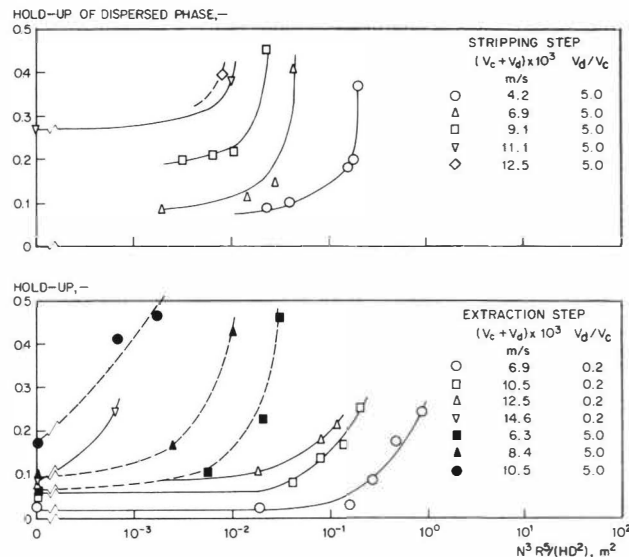


FIGURE 4
HOLD-UP FOR EXTRACTION AND STRIPPING OF SOLUTION ①
WITH 0.4M ALIQUAT 336 IN TOLUENE

SYSTEM	V_d/V_c	CONT. PHASE
▽ ① + 0.4M ALIQUAT	0.2	ORGANIC
□ ① + 0.4M ALIQUAT	5.0	AQUEOUS
△ KEROSENE/WATER	0.2	AQUEOUS
○ STRIP SOLUTION/ 0.4M ALIQUAT	0.2	ORGANIC
● STRIP SOLUTION/ 0.4M ALIQUAT	5.0	AQUEOUS

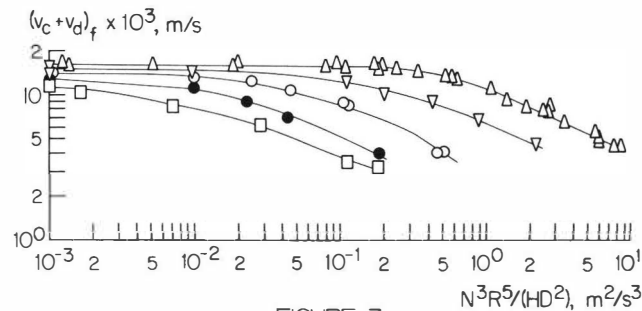


FIGURE 3
CAPACITY CURVES FOR COBALT EXTRACTION
WITH ALIQUAT 336, SOLUTION ①

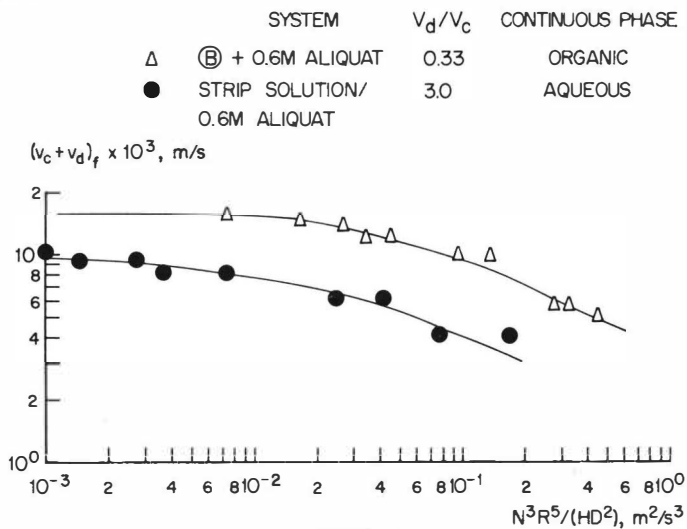


FIGURE 5
CAPACITY CURVES FOR COBALT EXTRACTION
WITH ALIQUAT 336, SOLUTION (B)

DWG. 74.01.1108

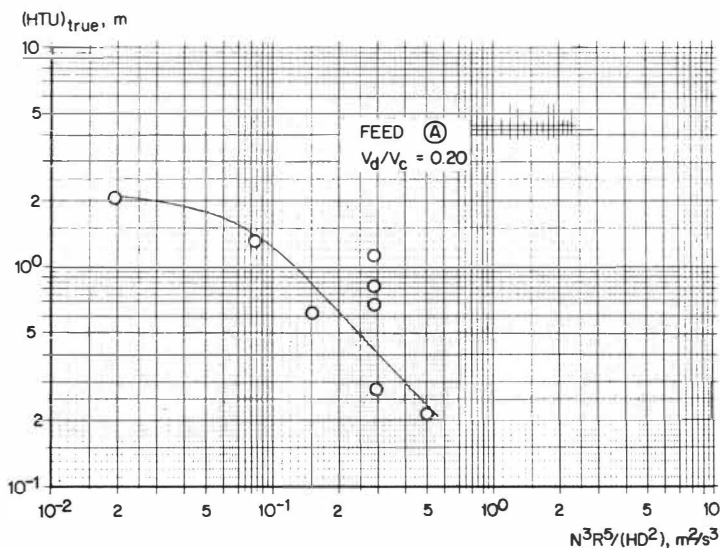


FIGURE 6
 $(HTU)_{true}$ AGAINST SPECIFIC POWER INPUT FOR FEED (A)

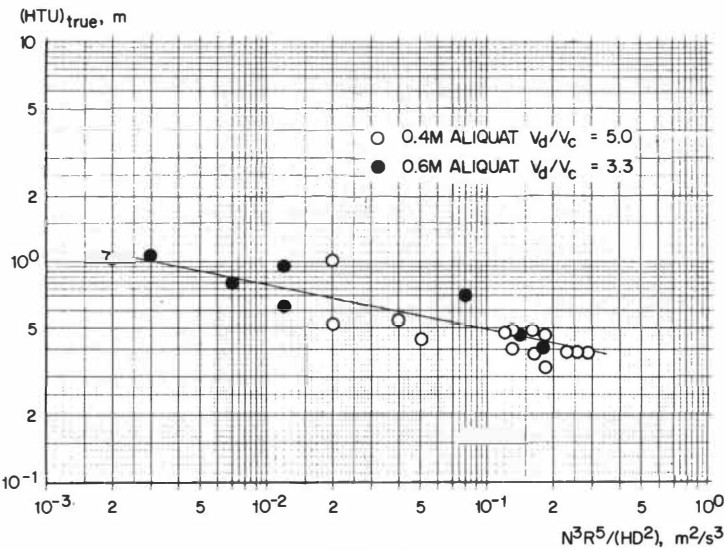


FIGURE 7
 $(HTU)_{true}$ AGAINST POWER INPUT FOR STRIPPING OF ALIQUAT 336/TOLUENE

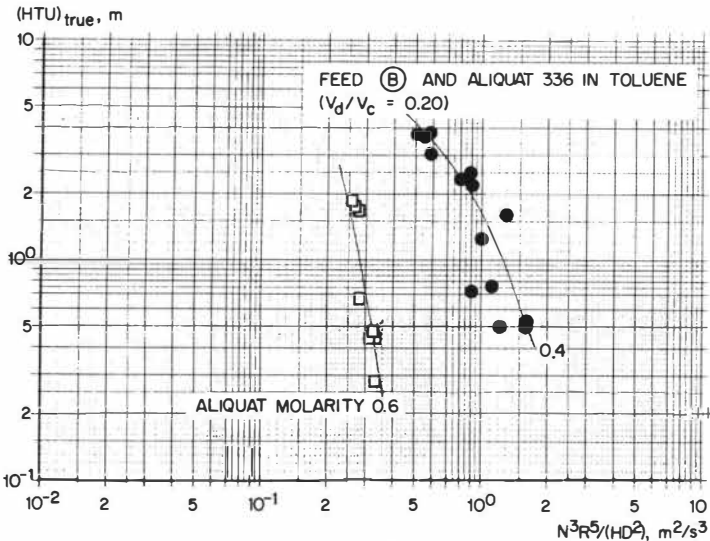


FIGURE 8
 $(HTU)_{true}$ AGAINST POWER INPUT FOR FEED SOLUTION (B)

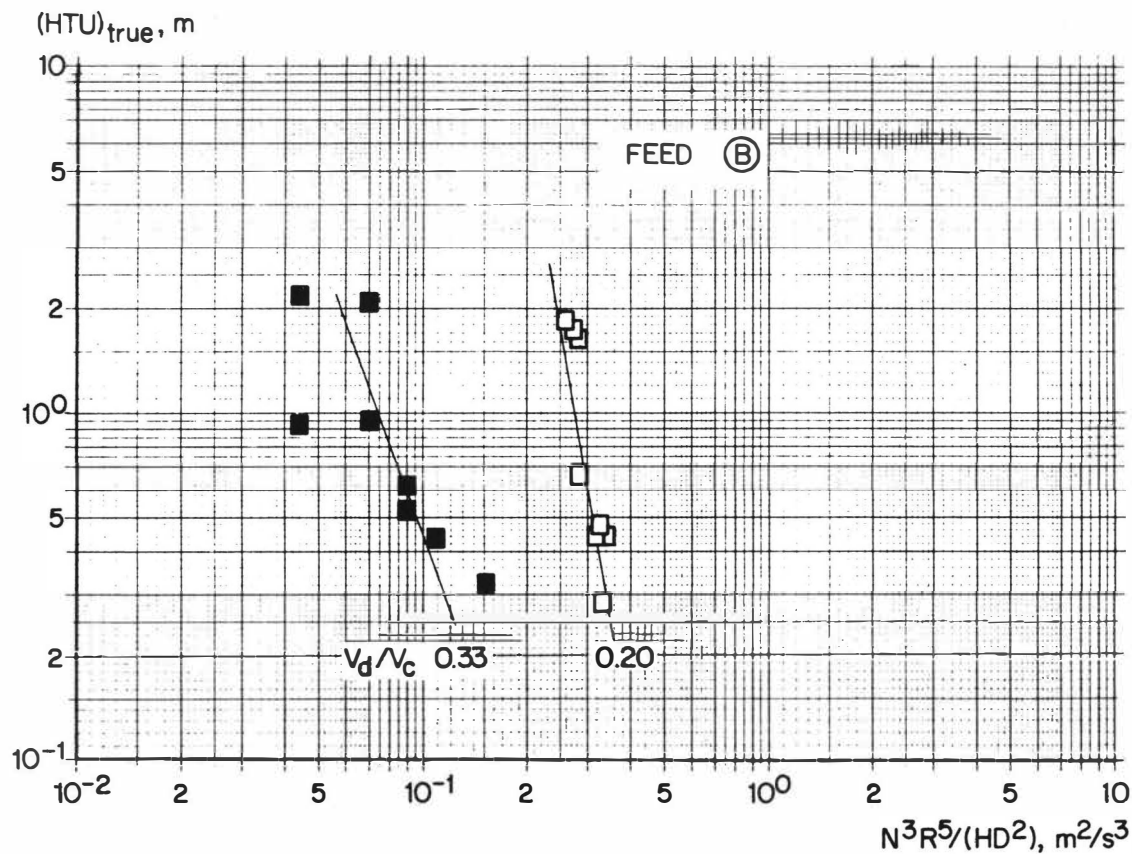


FIGURE 9

$(HTU)_{true}$ AGAINST POWER INPUT FOR FEED SOLUTION (B)

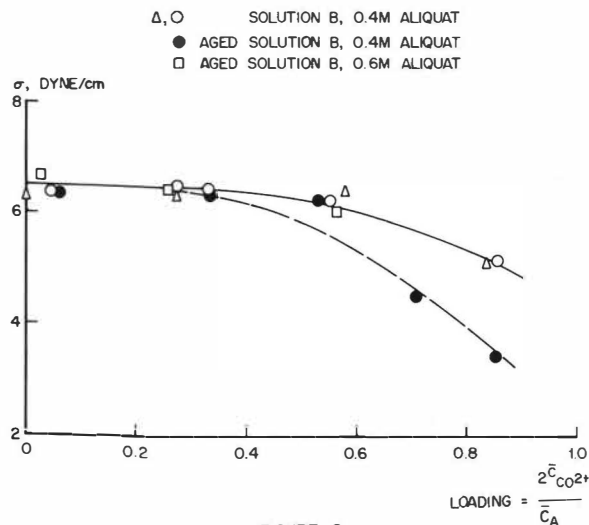


FIGURE 10
INTERFACIAL TENSION AS A FUNCTION OF LOADING OF ORGANIC PHASE

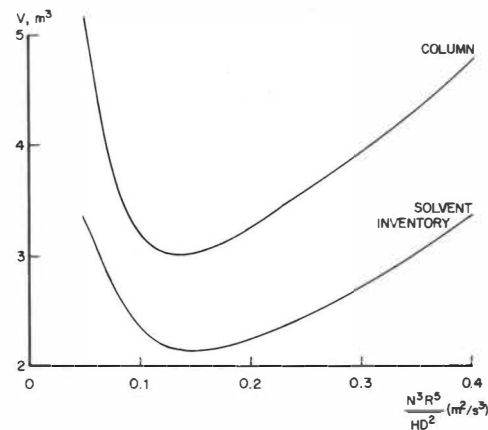


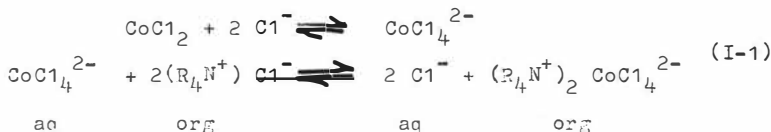
FIGURE 11
TYPICAL CALCULATIONS OF COLUMN VOLUME
REQUIRED FOR EXTRACTION OF $CoCl_2$ AT A CAPACITY OF $4 m^3/h$
 $4 m^3/h$ PLANT, SOLUTION B
 99.9% Co^{2+} RECOVERY
 0.6M ALIQUAT IN TOLUENE

DRAWN BY
 DWS 74 01.1113

A P P E N D I X

ANALYSIS OF EXTRACTION RESULTS

The extraction of cobalt from aqueous to organic phase is based on the following postulated reaction scheme (reaction occurs at the interface aqueous/organic):



The phase equilibrium of cobalt chloride solutions with nickel chloride and hydrochloric acid present was measured against Aliquat 336 in toluene as the solvent phase.

Fig. I-1 gives an example of cobalt distribution curves for an aqueous phase with a chloride ion concentration of 5 kmol/m^3 . One curve pertains to pure HCl as the chloride source, the other to pure nickel chloride. Similar curves were collected for solutions where only part of the chloride present stems from nickel chloride, the remainder being from hydrochloric acid. The curves were summarised in an equation relating the cobalt concentration in the organic phase, $\bar{c}_{\text{Co}2+}$, explicitly to the cobalt chloride concentration in the aqueous phase, $c_{\text{Co}2+}$, the chloride concentration in the aqueous phase from nickel chloride, $(c_{\text{Cl}^-})_{\text{Ni}}$, and from hydrochloric acid, $(c_{\text{Cl}^-})_{\text{HCl}}$, the molarity of Aliquat 336 in organic phase and the temperature. Also, the distribution of nickel chloride and hydrochloric acid was measured and summarised in equations of the same type as indicated above for cobalt.

Since cobalt, hydrogen, nickel and chloride ions are all distributed between the phases during extraction, we found that a simple McCabe-Thiele diagram is only an approximation to the actual extraction, especially if a HCl scrub is applied. The slope of the equilibrium curve, m , may vary widely from one equilibrium stage to the next, a fact which greatly complicates the analysis of extraction data in terms of transfer units, because one has to calculate an average value for the extraction factor F . Accordingly, we adapted a multicomponent stage-to-stage computer program¹⁶

to this particular extraction problem. The program calculates concentration profiles, component recoveries and the like, taking into account the simultaneous transfer of all the ionic species with all their thermodynamic interactions. The resultant print-out was then used to calculate an average value for the extraction factor, ψ , for every pilot plant run. We took the geometric mean value of the extraction factors for the individual stages. From this ψ value, supplemented with the analyses of cobalt concentrations in feed and exit streams, the exterior apparent number of transfer units, N_{of} , was calculated.

$$N_{of} = \frac{1}{\langle F \rangle - 1} \ln \left(\frac{1 - \psi}{1 - \langle F \rangle \psi} \right), \quad (I-1)$$

where ψ is the extent of extraction defined as

$$\psi = \frac{c_{Co^{2+}}^f - (c_{Co^{2+}})_{out}}{c_{Co^{2+}}^f - (c_{Co^{2+}})^*_{out}} \quad (I-2)$$

The Peclet numbers for the axial mixing in both phases were calculated from standard RDC correlations and defined as

$$Pe_c = \frac{v_c H}{(1-h) E_{a,c}} \quad (I-3)$$

$$Pe_d = \frac{v_d H}{h E_{a,d}} \quad (I-4)$$

The height of a true transfer unit was then calculated on the basis of the model for plug flow with axial dispersion by means of the correlations of Stermerding and Zuideweg¹⁷ which are readily solved without iteration because contactor length is given:

$$\frac{1}{(Pe)_1} = \frac{\langle F \rangle}{Pe_f} + \frac{1}{Pe_s}$$

$$\frac{1}{(Pe)_2} = \frac{1}{Pe_f} + \frac{\langle F \rangle}{Pe_s}$$

$$(Pe)_0 = (Pe)_1 \cdot \frac{0.1 L / (HTU)_{true} + 1}{0.1 L / (HTU)_{true} + (Pe)_1 / (Pe)_2} \quad (I-5)$$

$$HDU = \frac{1}{\frac{(Pe)_0}{H} + \frac{0.8}{L} \frac{\ln \langle F \rangle}{\langle F \rangle - 1}}$$

$$(HTU)_{true} = \frac{L}{N_{of}} - HDU$$

The resultant value is, of course, still a function of phase ratio, slip velocity and power input per unit mass in the column.

Fig.I-2 shows a typical family of concentration profiles for hydrogen, c_{H+} , and cobalt, $c_{Co^{2+}}$, in an extraction with a scrubbing section (solution A). Each curve represents a different number of equilibrium stages in the extraction section (1 to 6 stages) with two scrubbing stages.

NOMENCLATURE

- a specific phase contact area, m^2/m^3
- \bar{c}_a concentration of Aliquat 336 in toluene, kmol/m^3
- c_{Cl^-} concentration of chloride ions, kmol/m^3
- $c_{\text{Co}^{2+}}$ concentration of cobalt ions, kmol/m^3
- $c_{\text{Ni}^{2+}}$ concentration of nickel ions, kmol/m^3
- D diameter of RDC, m
- d_{av} Sauter mean droplet diameter, m
- E ratio of chloride from HCl to total chloride in aqueous phase, -
- E_a axial mixing coefficient, m^2/s
- $F(= m Q_f/Q_s)$ = extraction factor, -
- g acceleration of gravity, m/s^2
- h volumetric hold-up of dispersed phase, -
- H height of a compartment in the RDC, m
- HDU height of a dispersion unit, m
- $(\text{HTU})_{\text{true}}$ = height of a true transfer unit, m
- K distribution coefficient (kmol/m^3 solvent phase)/
(kmol/m^3 feed phase)
- k_{of} mass transfer coefficient on overall feed phase basis,
including chemical effects, m/s
- L length of stirred height in column, m
- $m(=dc_{\text{Co}^{2+}}/d\bar{c}_{\text{Co}^{2+}})$ = slope of equilibrium curve (kmol/m^3)/(kmol/m^3)
- N_{of} number of exterior apparent transfer units on overall
feed phase basis, -
- N rotor speed, s^{-1}
- Pe_c, Pe_d = Peclet numbers of continuous and dispersed phase,
respectively, -
- Q_c, Q_d = flow rates of continuous and dispersed phase, respectively
 m^3/s

R rotor diameter, m
 T dimensionless group defined in eq. (7c)
 v superficial velocity, m/s
 v_s slip velocity, m/s

Greek symbols

β separation factor, -
 ϵ_m power input per unit, mass, m²/m³
 $\Delta\rho$ difference in density between continuous and dispersed
 phase (absolute), kg/m³
 ρ density, kg/m³
 ψ extent of extraction, -
 μ viscosity, kg/ms
 ν kinematic viscosity, m²/s

Superscripts

- organic phase
 * at thermodynamic equilibrium

Subscripts

c continuous phase
 d dispersed phase
 f "at flooding", or "feed phase"
 s "slip", or "solvent phase"
 of on overall feed phase basis

REFERENCES

1. Fletcher, A.W., Chem. Ind., 5 May 1973, 414-419.
2. Queneau, P.E. and Roorda, H.J., De Ingenieur 83, July 16 (1971), M1-9.
3. Rey, M., De Ingenieur, 83, Nov. 12 (1971), M13-22.
4. Tougarinoff, B., 36^e Congrès Chim. Ind., Brussels 1966, Ind. Chim. Belge T32 (1967) 2^e vol.
5. van Peteghem, A., Willekens, M. and Tougarinoff, B., Symp. Nickel, September 1970, Wiesbaden, pp. 147-154 (Clausthal-Zellerfeld, 1970).
6. Boldt, J.R. and Queneau, P.E. (Eds.), "The Winning of Nickel", 1967 (Toronto, Longmans Canada Ltd.).
7. Thornhill, P.G., Wigstøl, E. and van Weert, G., J. Metals, July 1971, 131-8.
8. Wigstøl, E. and Frøland, K.E., "Solvent Extraction in Nickel Metallurgy: the Falconbridge Matte Leach Process", Int. Symp. Solvent Extraction, Antwerp, May 1972, pp. 62-72.
9. Brooks, P.T. and Rosenbaum, J.B., U.S. Bur. Mines Rept. of Inv. 6159, 1963.
10. Brooks, P.T., Potter, G.M. and Martin, D., U.S. Bur. Mines Rept. of Inv. 7316, 1969.
11. Brooks, P.T. and Potter, G.M., U.S. Bur. Mines Rept. of Inv. 7402, 1970.
12. Aue, A., Skjutare, L., Björling, G., Reinhardt, H. and Rydberg, J., ISEC 1971 Proceedings, pp. 447-450.
13. Treybal, R., "Liquid Extraction", 1963, 2nd ed., p. 185 (New York, McGraw-Hill).
14. Collins, S.B. and Knudsen, J.G., A.I.Ch.E.Jl. 16, 1970, 1072.
15. Miyauchi, T. and Vermeulen, Th., Ind. Engng. Chem. Fundamentals 2 (2) 1963, 113-126.
16. Hanson, D.N., Duffin, J.H. and Somerville, G.F., "Computation of Multi-stage Separation Processes", 1962, Reinhold Chemical Engng. Series,

(New York, Reinhold Publ. Corp.).

17. Stemerding, S. and Zuiderweg, F.J., Chem. Engr. 1963, CE 156.

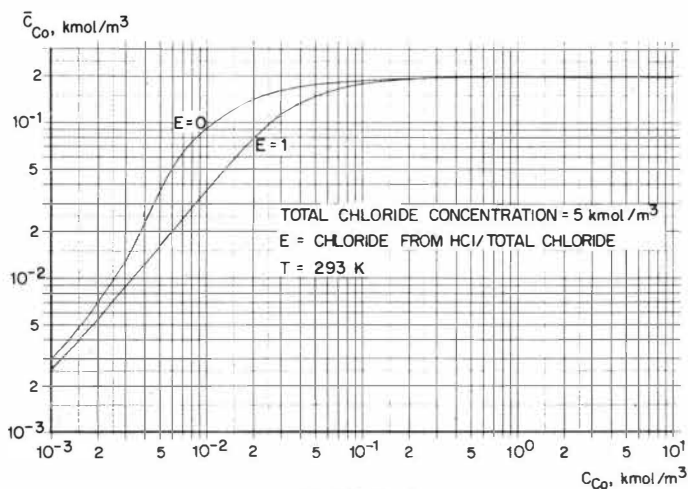


FIGURE I-1
EQUILIBRIUM CURVE FOR 0.4M ALIQUAT IN TOLUENE AND
VARIABLE AQUEOUS CHLORIDE SOURCE

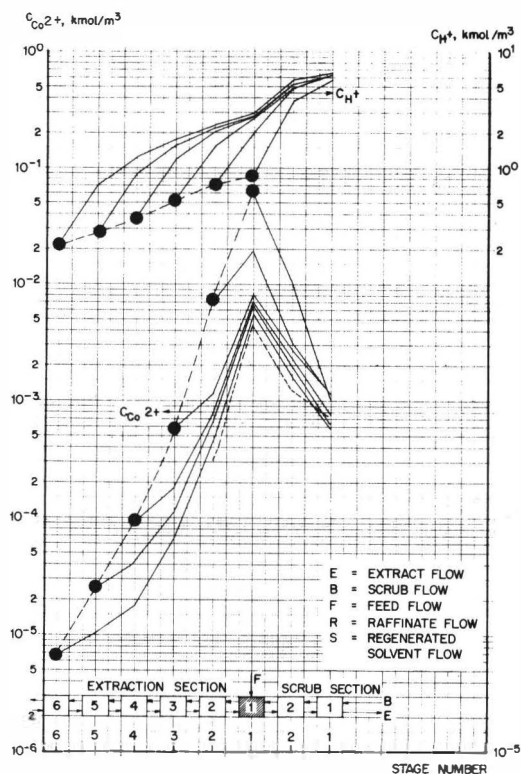


FIGURE I-2
EXTRACTION PROFILES FOR FEED (A) (TWO SCRUBBING STAGES)
IN THE RAFFINATE PHASE

USE OF LIQUID CATION EXCHANGE FOR SEPARATION OF NICKEL(II) AND COBALT(II) WITH SIMULTANEOUS CONCENTRATION OF NICKEL SULPHATE

by B.G. Nyman^x and L. Hummelstedt^{xx}

^{xx} Institute of Industrial Chemistry, Åbo Akademi, Åbo, Finland

^x Metallurgical Research Centre, Outokumpu Oy, Pori, Finland

A discovery according to which it is possible to increase considerably the rate at which certain mixtures of hydroxyoximes and carboxylic acids extract nickel has been utilized in the development of a method for separation of nickel and cobalt and for concentration of nickel solutions. Using the described solvents, which consist of mixtures of commercially available reagents, separation factors $S_{Ni,Co}$ of the order of magnitude 30-260 have been obtained. A solvent extraction process for the separation of nickel from a cobalt sulphate solution is outlined on the basis of batch phase mixing tests and confirming mixer-settler experiments. According to the results it will be quite possible to produce a cobalt solution with a cobalt/nickel ratio of for example 3000 while at the same time producing solid nickel sulphate of high purity.

Introduction

Much research effort has been devoted to the problem of separation of nickel and cobalt by solvent extraction. Some successful developments of amine extraction^{1,2} have been based on the ability of cobalt to form anionic complexes with the chloride ion at a high chloride ion concentration. Tri-isooctylamine has turned out to be a suitable reagent for the extraction of the produced species $CoCl_4^{2-}$. Because neither nickel nor cobalt in sulphate solutions generally obtained in

hydrometallurgical operations forms a corresponding complex extractable by amines several attempts to separate the metal ions by liquid cation exchange have been made³⁻⁸. The separation of nickel and cobalt has however proved difficult especially in acid sulphate solutions. Ritcey and Ashbrook⁵ reported a successful separation of cobalt from nickel at pH 5-6 using di-(2-ethylhexyl)-phosphoric acid (HDEHP), although the value of the obtained separation factor $S_{Co, Ni}$ was rather low.

According to the literature on solvent extraction, there thus still seems to be a need for a selective extractant for nickel. Because it was felt that the extraction of nickel usually preferably would be carried out in as low a pH range as 2-4, also some synergic extractant mixtures capable to extract nickel at a low pH were tested for this separation. Certain mixtures of hydroxyoximes and carboxylic acids were discovered to show an attractive selectivity for nickel⁹. As also Flett and West¹⁰ have reported, the rate at which such a mixed extractant extracts nickel is, however, too slow to encourage development of a separation process.

According to results described in this paper it has proved to be possible to considerably increase the rate at which nickel is extracted by a mixture of a hydroxyoxime and a carboxylic acid using a small addition of a strong organic acid. A method for the separation of nickel from cobalt was developed based on investigations of the extraction properties of different combinations of hydroxyoxime, carboxylic acid and the discovered most promising kinetic synergist.

Experimental

A suitable mixture of extractants for separation of nickel and cobalt was determined on the basis of batch phase mixing tests using propeller stirred spherical separatory retorts equipped with a glass calomel combination electrode and an inlet for air or nitrogen diluted ammonia for continuous pH control. Comparative extraction experiments were also performed in a similar gas tight apparatus, in which nitrogen atmosphere was maintained. Data were also collected from series of small-

scale continuous tests in pump-mix mixer settlers having a 150 ml mixer capacity and a 400 ml settler capacity. An enhanced separation was obtained by maintaining different appropriate pH values in the discrete extraction stages. The pH regulation was based on a discovery according to which ordinary glass calomel electrodes in this case could be used for stable pH measurement over a long period of time in a mixer dispersion not only of the aqueous continuous but also of the organic continuous type. According to the preferred pH control performance separate control units of the type Metrohm E 450 coupled to a magnetic valve were used for each pH regulated stage. As neutralisation agent, nitrogen diluted ammonia was chosen. It can be mentioned that in dispersions and in corresponding separated aqueous solutions measured pH values showed good agreement.

In this investigation laboratory separation tests were performed on mixtures of a hydroxyoxime (LIX-63, LIX-65N, LIX-64N or LIX-70, General Mills Chemicals, Inc.), a tertiary carboxylic acid (Versatic 9-11, Shell Chemical Co. Ltd.) and a sulphonic acid (dinonyl naphthalene sulphonic acid (DNNS), R.T. Vanderbilt Co., Inc. or a mixture of alkylsubstituted benzene sulphonic acids, ECA 6414, Esso Chemicals) diluted in an aliphatic hydrocarbon solvent (Shellsol K or Isopar M, Esso Chemicals) or an aromatic solvent (Solvesso 150).

Results

Enhanced rate of nickel extraction

The separation tests were performed on a synthetic sulphate solution containing 10 g of nickel/l, 25 g of cobalt/l and 33 g of ammonium sulphate/l. According to preliminary results the chosen hydroxyoxime had a much stronger effect on the nickel selectivity of the prepared mixed extractant than the used carboxylic acid. Owing to this Versatic 9-11, a stable tertiary carboxylic acid, was fixed as one of the main components of the investigated extractant mixtures.

Although LIX-63 does not show a good stability to temperatures above ambient, which could be expected to be used to speed up the extraction of nickel, some work was done with

the mixture LIX-63/Versatic 9-11/Shellsol K, the extraction properties of which were considered interesting because LIX-64N and LIX-70 were known to contain some LIX-63. The use of this mixture did not, however, appear attractive, because besides that the obtained separation of nickel and cobalt was rather poor, the stripping of co-extracted cobalt caused difficulties.

The sensitivity of the rate of nickel extraction to a temperature change was tested for the reagent mixture LIX-65N/Versatic 9-11. The found temperature dependence is presented in Fig. 1. As could be expected the temperature showed a considerable influence on the extraction rate, which however still at 62°C was unsatisfactorily low. In this connection it was noticed that the chosen diluent has a remarkable effect on the extraction rate. According to the obtained results, which also are shown in Fig. 1, Isopar M, a highly branched aliphatic hydrocarbon, gave a slower rate of extraction than Shellsol K. With Solvesso 150, an aromatic diluent, a still longer contact time was required to obtain separation equilibrium, the position of which however owing to a depressed co-extraction of cobalt was shifted in an advantageous direction.

Finally it was discovered that the rate of nickel extraction could be considerably increased by a small addition of some sulphonic acids to the hydroxyoxime/carboxylic acid mixture. In Fig. 2 the rate at which a LIX-70-based extractant mixture without an addition of DNNS at 50°C extracts nickel can be compared with the nickel extraction rate obtained at the same temperature by the same mixture, to which an addition of DNNS was made corresponding to a concentration level of only 0.01 M of sulphonic acid. Also the sulphonic acid product ECA 6414 was found to show a similar but not as strong an effect as DNNS, which obviously owing to its molecular structure to a higher extent causes exchange reactions to occur between molecules at the interphase and molecules in the bulk of the organic phase¹¹.

While it could be expected that also the LIX-63 present in LIX-70 might act as a kinetic synergist on the extraction of nickel, the preceding experiment was repeated with the LIX-63

removed from the used LIX-70 product according to a method developed by Tammi¹². This time the contact time required to obtain equilibrium without an addition of DNNS was 4-5-fold compared with the earlier results while only a slight difference could be observed in the presence of some DNNS. It was also interesting to note that the value of the separation factor $S_{Ni, Co}$ now increased from a level 120 obtainable using commercial LIX-70 to an order of 250.

pH-controlled separation

The nickel is extracted by a mixture 25 vol-% LIX-70/1.0 M Versatic 9-11/0.01 M DNNS/Shellsol K at an advantageously low pH range 2-5 as is shown in Fig. 3, which also gives the pH dependence of the corresponding $S_{Ni, Co}$. The chosen carboxylic acid concentration of 1.0 M has to be considered as a compromise. It was observed that the value of $S_{Ni, Co}$ gradually decreases while the rate of nickel extraction slightly increases with an increasing concentration of Versatic 9-11. The overwhelmingly most important feature of the carboxylic acid was however to depress the tendency of the co-extracted cobalt to remain in the organic phase, which probably was caused by an air-oxidation of the extracted divalent cobalt.

In Fig. 4 a series of related equilibrium lines is presented for the extraction of nickel in the presence of a constant amount of cobalt, which means that the pH-dependent internal circulation of cobalt within the separation section has been neglected in the performed graphical stage-to-stage construction. The usefulness of pH-control is clear from the advantageous jumps between equilibrium lines, which can be made owing to easily maintained stage-pH-values.

Scrubbing and stripping

Preliminary tests showed that the Ni/Co ratio in the extract could be considerably increased above the limiting value, which was determined by the composition of the main feed, using a nickel sulphate solution as scrubbing agent. It was noticed that no pH control of the scrubbing performance was required, if the pH of the used nickel sulphate solution had been adjusted

to a value above 3.5.

Great importance was attached to obtained stripping results according to which nickel can be stripped almost completely in one stage provided that the pH is maintained below a value of about 2. The stripping ability of a sulphuric acid solution is demonstrated by determination of a stripping isotherm at a pH 0.35 and at a temperature of 50°C. The discovered closeness of the obtained isotherm to the abscissa in Fig. 5 exceeded the most optimistic expectations. Thus, only 1-2 stages are required for production of a saturated nickel sulphate solution. To this it can be added that the rate, at which nickel is stripped, is of an attractive order of magnitude. That is also the case with the rate, at which the main part of the extracted cobalt is stripped. It was however noticed that a complete stripping of cobalt could not rapidly be obtained, especially if the extract had been in an unstripped condition under exposure to air for several hours. The appearance of traces of difficultly stripped cobalt was accompanied by a considerable darkening of the organic phase. According to performed tests it was on the contrary quite easy using a dilute solution of sulphuric acid to bring about a complete stripping of cobalt from a loaded organic phase, which had been prevented from coming into contact with oxygen and in which the formed cobalt complex had remained deeply red in colour.

Continuous separation tests

A synthetic sulphate solution containing 9.60 g/l of nickel, 25.5 g/l of cobalt and 33 g/l of $(\text{NH}_4)_2\text{SO}_4$ was fed into a six-stage counter-current extraction unit with the mixed extractant 25 vol-% LIX-70/1.0 M Versatic 9-11/0.02 M DNNS/Shellsol K, the main part of which had been prepared and used for the first time in a similar experiment 7 months ago. This test was the last in a series of tests, in which the organic phase before re-use only was stripped in one stage with a sulphuric acid solution and in which the contactor was completely uncovered thus allowing an intimate contact between mixer-dispersion and air to take place. The separation was performed at a temperature of 50°C, at a contact

time of 7 min and with an organic phase to aqueous phase flow ratio (O:A) of 2.5. While the pH in the feed was adjusted to a value 3.87 the pH in the second, the fourth and the sixth stage (numbering of the stages made in the direction of the aqueous flow) was maintained by automatic pH control at values shown in the following table together with the obtained separation results.

While a raffinate with a cobalt/nickel ratio of 3000 was produced, the cobalt/nickel exchange reaction proceeded with some reluctance, which partly however was due to the used combination of a high extractant/nickel ratio and a maintained high pH level. It can be considered encouraging that the level of the cobalt concentration in the mixed extractant, which

Countercurrent separation of nickel (II) and cobalt (II)
in six stages

Feed: 9.60 g/l Ni, 25.5 g/l Co, 33 g/l $(\text{NH}_4)_2\text{SO}_4$, $\text{pH}_{23^\circ\text{C}} = 3.87$

Mixed extractant: 25 vol-% LIX-70, 1.0 M Versatic 9-11,

0.02 M DNNS, Shellsol K

Organic to aqueous phase flow ratio: 2.5

Temperature: 50°C

Neutralisation agent: nitrogen diluted ammonia

pH controlled stages: 2nd, 4th, 6th

Stage	1	2	3	4	5	6
$\text{pH}_{23^\circ\text{C}}$	3.54	3.87	3.73	4.01	3.62	3.73
Organic phase:						
Ni g/l	4.09	3.26	1.29	0.31	0.16	0.069
Co g/l	1.10	1.76	2.53	3.41	2.40	2.40
Aqueous phase:						
Ni g/l	8.2	2.7	0.53	0.083	0.018	0.009
Co g/l	28.8	31.1	33.4	30.7	30.9	26.1
Extracted Ni g/h	0.56	2.06	0.80	0.16	0.024	0.0035
Extracted Co g/h	-0.58	-0.67	-0.78	0.88	0.00	1.82

still was stripped in only one stage with sulphuric acid, at the end of the described countercurrent experiment was determined to be 0.58 g/l. Thus it might be possible especially in process conditions including scrubbing, which has been found to promote stripping, to avoid the requirement of taking a bleed stream of the organic phase to a complete cobalt stripping section, which according to works in progress could be based on slightly modified conventional liquid-liquid methods or on sulphide precipitation¹³.

Finally it can be mentioned that the determined stripping equilibrium according to which a saturated nickel solution can be produced using a closed stripping circuit has been confirmed by further mixer-settler experiments.

Flowsheet for a separation process

A proposed flowsheet for a separation process of nickel from cobalt with simultaneous concentration of nickel sulphate is shown in Fig. 6. After the feed has been contacted with the mixed extractant LIX-70/Versatic 9-11/DNNS/kerosene at a controlled pH level of 3-4 and at a temperature of above 40°C small amounts of co-extracted cobalt are removed from the extract by scrubbing with a nickel sulphate solution at the same pH and temperature level. No pH-control is required during scrubbing provided that the pH of the used nickel sulphate solution is adjusted to a value somewhat above the wanted. The obtained scrub solution is combined with the feed while the purified extract is stripped with mineral acid for example sulphuric acid. If a closed stripping circuit is used as shown in the flowsheet, the recovery of nickel can be made from any suitable concentration level for example in the form of solid nickel sulphate from a saturated solution. A bleed of the produced nickel sulphate is used for scrubbing of the loaded mixed extractant.

Conclusions

Small amounts of a suitable sulphonc acid have proved to considerably improve the rate at which a mixture of hydroxyoxime and carboxylic acid extracts nickel. Of the tested sulphonc acid products DNNS acted as the strongest kinetic synergist while LIX-70 in presence of Versatic 9-11 gave a good separation of nickel from cobalt. A still higher separation factor could be obtained in absence of LIX-63, the addition of which to the used LIX-product is not required for nickel extraction.

A proposed process has been described for the separation of nickel from an acidic cobalt solution. Temperatures above 40°C are used throughout the process. The extraction is carried out over a pH range 3-4 using automatic stage-to-stage pH control while the scrubbing of any co-extracted cobalt is performed with a nickel sulphate solution, the pH of which has been adjusted to a value of about 3.5. Owing to an advantageous stripping equilibrium solid nickel sulphate can be produced in a closed stripping circuit, the acid content of which can be varied over a wide range, the lower limit corresponding to a pH value close to 3.

It is still open to doubt whether the organic phase has to be bled to a complete cobalt stripping section, because the cobalt shows a quite low tendency to be retained by the LIX-70-based mixed extractant in the used low pH range.

In view of certain major advantages offered by the LIX-70/Versatic 9-11/DNNS mixture it cannot be considered to be quite out of the question that this type of a mixed extractant also could be useful for recovering nickel values.

References

- 1 Thornhill, P.G., Wigstol, E., Van Weert, G., J. Metals Vol. 23, No. 7, 13-18 (1971)
- 2 Aue, A., Skjutare, L., Björling, G., Reinhardt, H., Rydberg, J., Proceedings International Solvent Extraction Conference 1971. Vol. 1, 447-450, Society of Chemical Industry, London 1971
- 3 Fletcher, A.W., Flett, D.S., Trans. AIME, Vol. 247, No. 4, 294-299 (1970)

- 4 Hawes, W.B., B.P. 959,813
- 5 Ritcey, G.M., Ashbrook, A.W., U.S.P. 3,399,055
- 6 Drobnick, J.L., Millsap, W.A., U.S.P. 3,276,863
- 7 Coltrinary, L.E., Ger. Offen. 2,152,696
- 8 Kane, W.S., Cardwell, P.H., Ger. Offen. 2,126,223
- 9 Rainio, K., M.Sc. Thesis, Åbo Akademi (1970)
- 10 Flett, D.S., West, D.W., Proceedings International Solvent
Extraction Conference 1971. Vol. 1, 214-223 (1971).
Society of Chemical Industry, London 1971
- 11 Van Dalen, A., RCN (Reactor Cent. Ned.) Rep. 1971, RCN-141
- 12 Tammi, T., Private communication, Åbo Akademi (1972)
- 13 Merigold, C.R., Sudderth, R.B., "Recovery of nickel by
liquid ion exchange technology", Paper presented at
the AIME Annual Meeting, Chicago, 1973

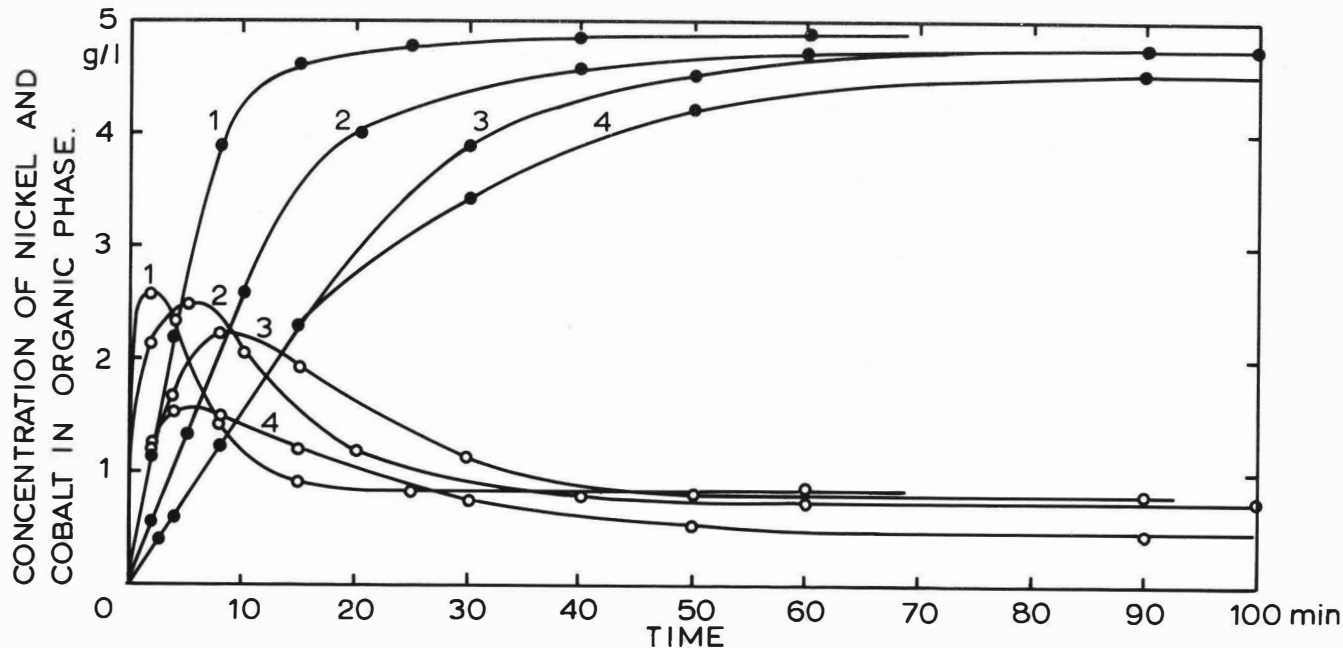


Fig.1. Rate of nickel extraction in presence of cobalt

Organic solution: 25 vol-% LIX-65N/1.0 M Versatic 9-11/diluent.

Sulphate solution: 10 g/l Ni^{2+} ; 25 g/l Co^{2+} ; 33 g/l $(\text{NH}_4)_2\text{SO}_4$

O/A = 1.6; neutralisation agent: N_2 -diluted NH_3 ; atmosphere: N_2 ; ● nickel; ○ cobalt

1. diluent Shellsol K; 62°C; $\text{pH}_{23^\circ\text{C}} = 4.96$

2. diluent Shellsol K; 50°C; $\text{pH}_{23^\circ\text{C}} = 4.85$

3. diluent Isopar M; 50°C; $\text{pH}_{23^\circ\text{C}} = 4.88$

4. diluent Solvesso 150; 50°C; $\text{pH}_{23^\circ\text{C}} = 4.83$

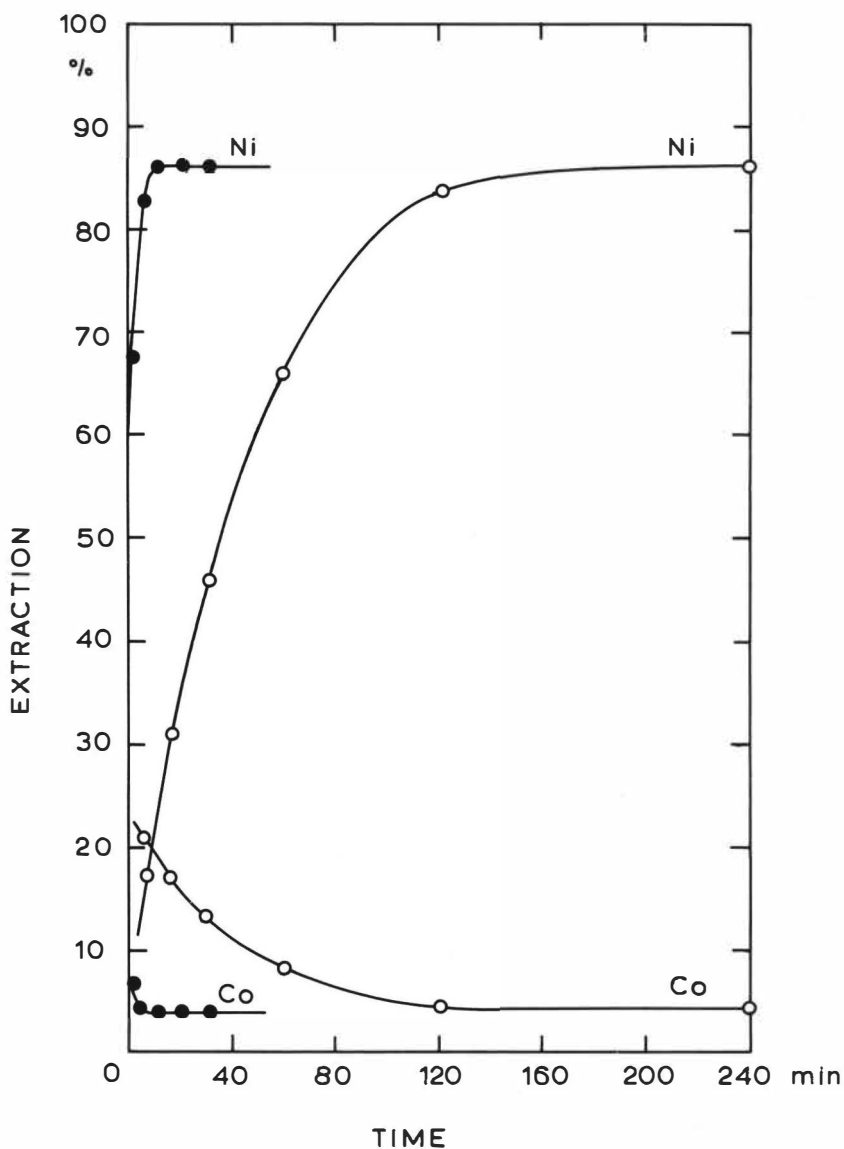


Fig.2. Rate of Nickel extraction in presence of cobalt

○ 25 vol-% LIX-70/1.0 M Versatic 9-11/Shellsol K

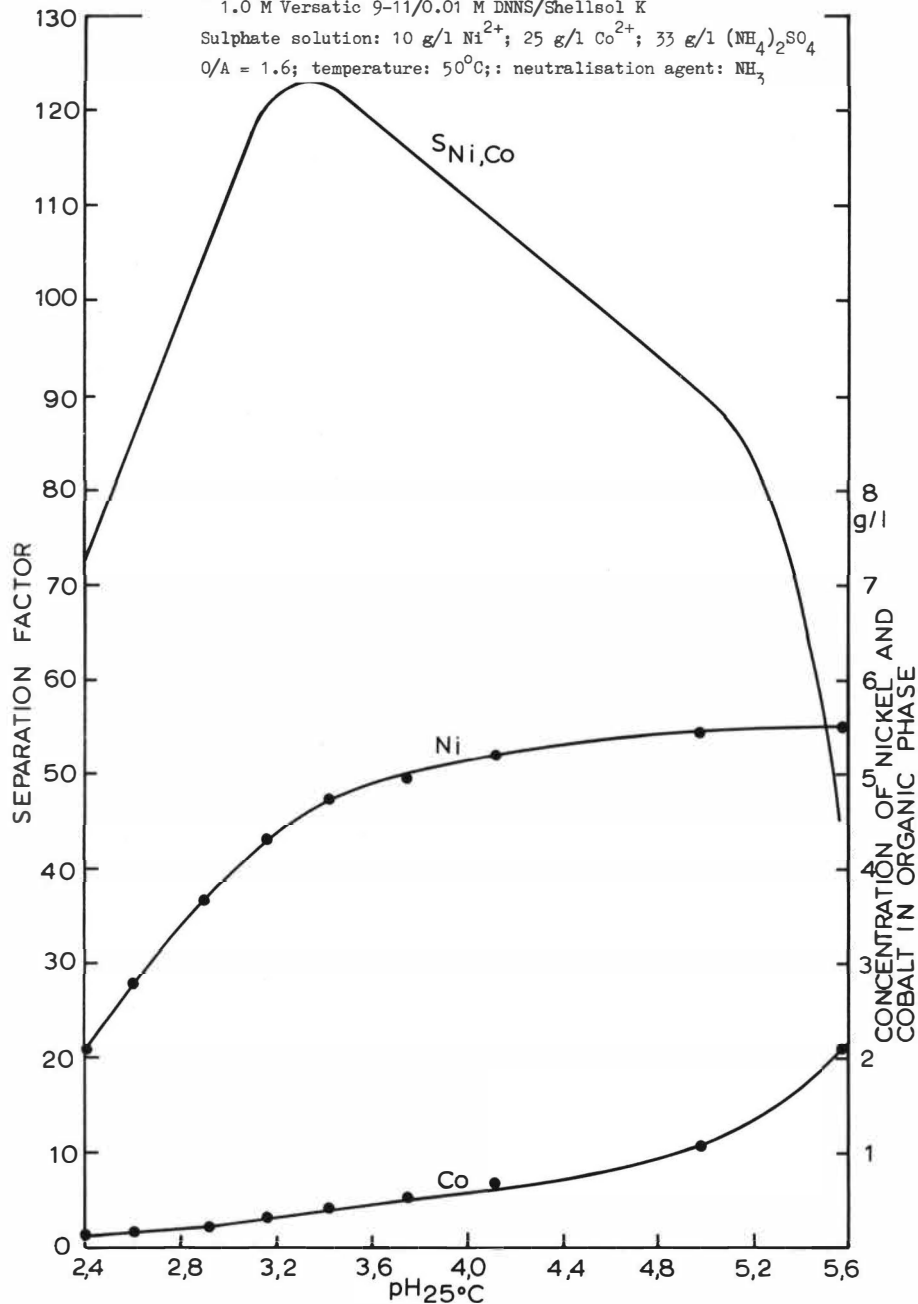
● 25 vol-% LIX-70/1.0 M Versatic 9-11/0.01 M DNNS/Shellsol K

Sulphate solution: 10 g/l Ni^{2+} ; 25 g/l Co^{2+} ; 33 g/l $(\text{NH}_4)_2\text{SO}_4$

O/A = 1.6; temperature: 50°C ; $\text{pH}_{23^\circ\text{C}} = 3.80$; neutralisation agent: air-diluted NH_3

Fig.3. Extraction of nickel and cobalt by 25 vol-% LIX-70/
1.0 M Versatic 9-11/0.01 M DNNS/Shellsol K

Sulphate solution: 10 g/l Ni^{2+} ; 25 g/l Co^{2+} ; 33 g/l $(\text{NH}_4)_2\text{SO}_4$
O/A = 1.6; temperature: 50°C; neutralisation agent: NH_3



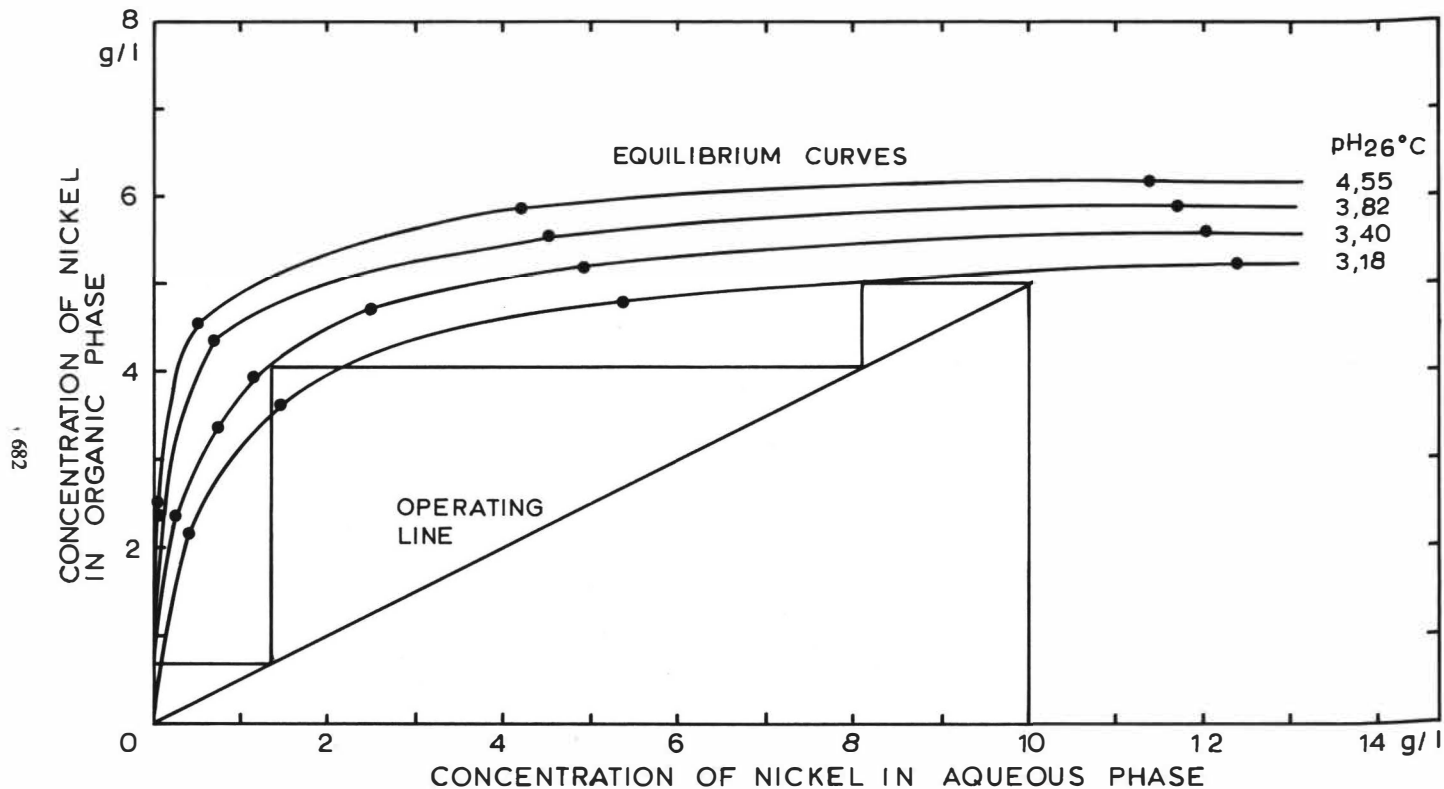


Fig.4. Graphical McCabe-Thiele construction for a pH controlled countercurrent separation of nickel(II) and cobalt(II)

Aqueous feed: 10 g/l Ni^{2+} ; 25 g/l Co^{2+} ; 33 g/l $(\text{NH}_4)_2\text{SO}_4$

Organic feed: 25 vol-% LIX-70/1.0 M Versatic 9-11/0.01 M DNNS/Shellsol K

Temperature: 50°C

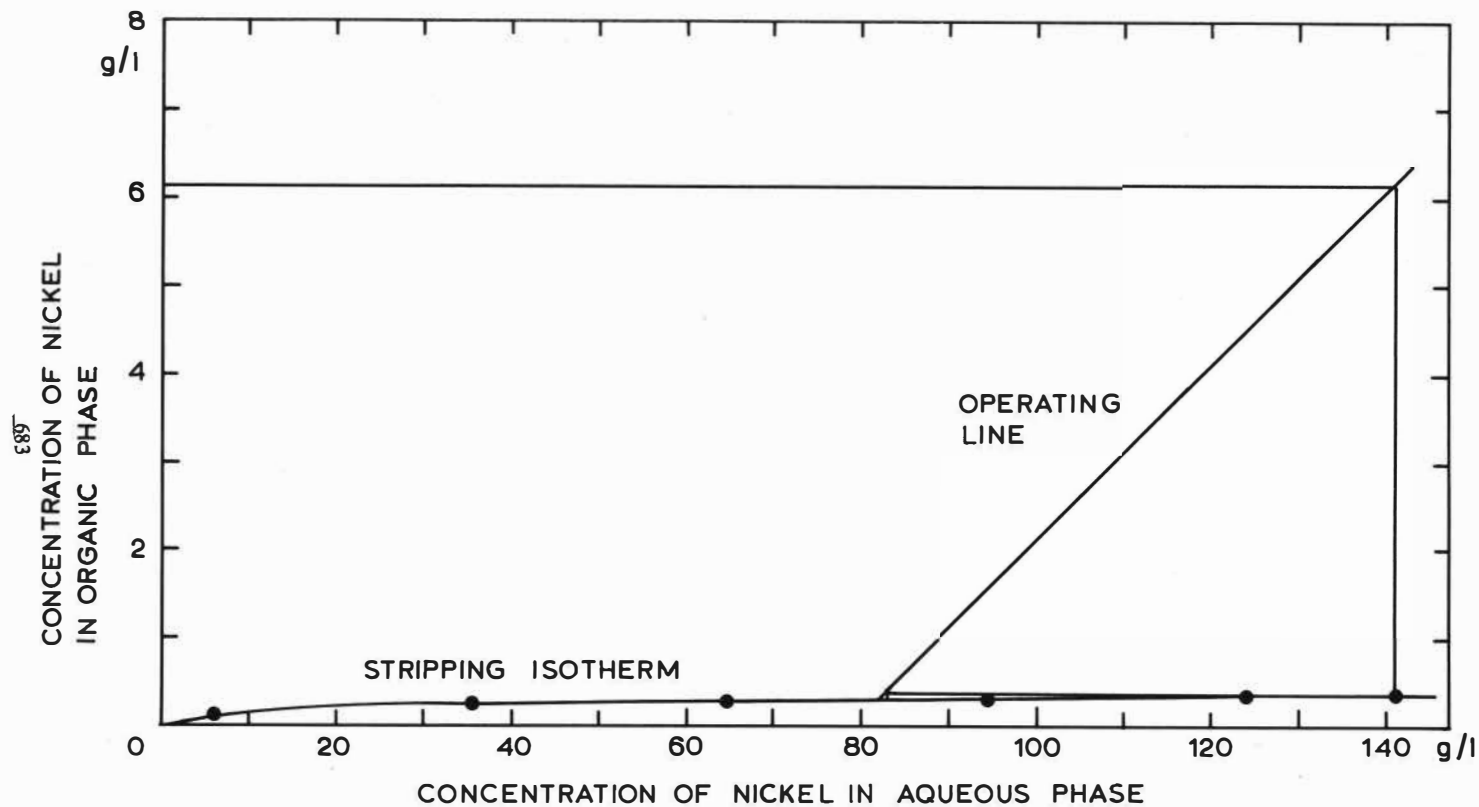


Fig.5. McCabe-Thiele strip circuit profile at a high aqueous nickel ion concentration.

Organic feed: 6.12 g/l Ni^{2+} ; 25 vol-% LIX-70/1.0 M Versatic 9-11/0.01 M DNNS/Shellsol K.
 Aqueous feed: 50 g/l H_2SO_4 Temperature: 50°C

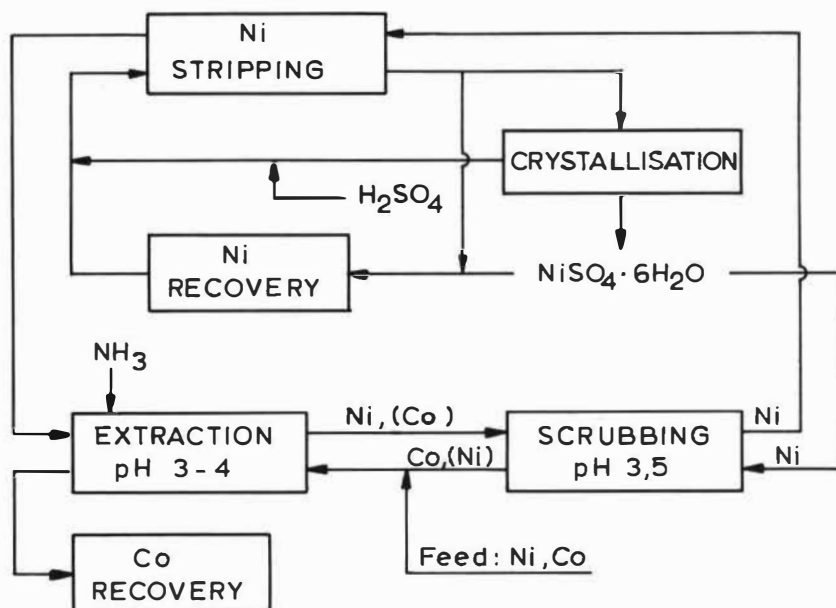


FIG.6. Proposed flowsheet

The Liquid-Liquid Extraction of Copper (II) and Iron (III)
from Chloride Solutions Using Lix 64N in Kerosene

by

P.G. Christie, V.I. Lakshmanan,^{*} and G.J. Lawson.

Department of Minerals Engineering, University of Birmingham.

Birmingham B15 2TT, U.K.

Abstract.

The behaviour of Copper (II) and Iron (III) in a solvent extraction system involving aqueous chloride solutions and Lix 64N in kerosene has been studied to assess the feasibility of a commercial process involving the recovery of copper from leach solutions containing both metals as chlorides. Logarithmic graphs of metal distribution coefficient and extraction isotherms are presented for copper concentrations ranging from $5 \times 10^{-4} \text{M}$ to those at which maximum loading of the reagent occurs and for Lix 64N concentrations between 2% and 25% (v/v) in kerosene. The effects of pH, temperature, and concentration of metal ion, chloride ion and extractant are considered, together with back extraction characteristics for copper, using hydrochloric acid as the stripping solution.

* Wolfson Secondary Metals Research Group.

Introduction

The commercial selective extractant Lix 64N, introduced by General Mills Inc., is being used in several copper recovery plants, notably in the U.S.A. and in Zambia. It is based on hydroxyoximes, ⁽¹⁻⁴⁾ the reagent normally supplied consisting of a mixture of an aliphatic hydroxyoxime, Lix 63, and an aromatic hydroxyoxime, Lix 65N, as an approximately 50% solution in a kerosene-type diluent⁽⁵⁾. The major component, Lix 65N, exhibits slow kinetics of extraction when used alone, and the small amount of Lix 63, which is chemically less stable, acts as a 'catalyst' to improve the kinetic behaviour of the mixture, Lix 64N^(6,7). The usual process based on Lix 64N involves the leaching of a low-grade source of copper with sulphuric acid, often derived from a neighbouring sulphide pyrometallurgical operation, and selective extraction of copper from the leach liquor with the reagent in kerosene-type diluent. Copper is finally recovered by stripping the organic solution with spent sulphuric acid electrolyte and subsequent electrowinning.

In a process designed to recover copper from low-grade sources such as mine tailings and some scrap materials, which may not be associated with smelting operations, there may be no immediate reason for using sulphuric acid for leaching, and indeed an alternative leaching agent such as hydrochloric acid might offer advantages. Dissolution of copper in hydrochloric acid is possible on an industrial scale⁽⁸⁾, dissolution rate being controlled by such factors as metal thickness, acid concentration, and availability of oxygen. The use of chlorine as an oxidising agent for this purpose instead of air or oxygen has been suggested⁽⁹⁾. Such a process would present leach solutions containing large concentrations of chloride ions for selective extraction; the present paper examines the behaviour of the system in which solutions of this type are extracted with Lix 64N in kerosene.

Experimental

Samples of Lix 64N were kindly supplied by General Mills Inc. and were used as received. Working solutions of the extractant were made up by volumetric dilution with kerosene as required. Kerosene was "kerosene white" supplied by Hopkins and Williams Ltd; all other reagents were of analytical grade.

Stock solutions of cupric and ferric chlorides were made up by dissolving appropriate amounts of the reagents in water to yield solutions of about 0.2M concentration, sufficient hydrochloric acid being added to prevent hydrolysis or precipitation of the metal hydroxide. The solutions were standardised by thiosulphate and dichromate titration respectively⁽¹⁰⁾.

The standard metal solutions were stored in polythene containers. For each extraction experiment a series of nine or ten solutions was made up containing identical metal concentrations, differing amounts of HCl to produce the desired range of pH and NaCl to adjust the total ionic strength to a predetermined level, usually 1.0M. For copper extractions, sufficient quantities of solutions were made up for several extractions to be carried out but for iron, where slow precipitation of the metal hydroxide was found to be a problem at pH levels above 2.0, fresh solutions were prepared for each experiment.

Equal volumes (10 or 20ml) of the aqueous and extractant solutions were pipetted into 100ml glass-stoppered conical flasks and equilibrated by shaking in a thermostatic oscillating incubator bath, maintained at $25 \pm 0.5^\circ\text{C}$ unless otherwise stated. Preliminary experiments indicated that extraction equilibrium was obtained in 20-40 minutes for copper and 45-60 minutes for iron, so a shaking time of 60 minutes was used throughout. After equilibration the two phases were separated using phase-separating paper (Whatman 1PS), and the pH of the aqueous solution was measured using a Pye Model 290 pH meter. Portions of the aqueous solutions were then diluted, and their metal contents determined, using a Perkin-Elmer model 303 atomic absorption spectrophotometer fitted with a three-slot burner for analysis of solutions of high dissolved solids content. Interference from sodium ions was found to be minimal when their concentration was 0.2M or less, so each sample concentration was diluted by at least five times to reduce the concentration below this value. The instrument was calibrated using a series of standard solutions of copper or ferric chloride; from the readings so obtained a least squares regression of the form $\ln(\text{Absorbance}) = \ln A + B \ln(\text{metal concentration})$ was calculated, and concentrations of unknown solutions were derived with the aid of the regression parameters. This procedure was facilitated by use of a Hewlett-Packard 9280 programmable calculator.

Results and Discussion

Extractions of copper (II) and iron (III) were carried out from aqueous solutions 1.0M with respect to chloride ions using solutions of Lix 64N in kerosene between 2% and 25% concentration and metal ion concentrations between 5×10^{-4} and $5 \times 10^{-3}\text{M}$, i.e. employing a large excess of extractant. Fig.1 shows typical $\log D$ vs pH relationships for $5 \times 10^{-3}\text{M}$ metal concentrations. The lines for copper have slopes of 2.0 ± 0.07 , indicating second power dependency of $\log D$ on pH and Cu^{2+} as the metal species being extracted. For iron the slopes vary from 2.95 with 2% Lix to 2.45 with 25% Lix, all significantly different from the expected value of 3.0 corresponding to extraction of Fe^{3+} ; these values cannot yet be explained, since Fe^{2+} is not reported to extract in this pH region and no evidence could be obtained for the extraction of iron chloro-complexes.

The copper extraction curves were almost independent of initial metal concentration, the $\text{pH}_{0.5}$ values increasing very slightly with aqueous metal content. The overall results were very similar to those obtained for corresponding extractions from sulphate media⁽¹¹⁾, the $\text{pH}_{0.5}$ values, ranging from 1.4 with 2% Lix to 0.75 with 25% Lix, being identical.

Lines relating $\log D$ to \log (Lix concentrations) showed slopes of 1.0 ± 0.1 for copper and ~ 1.5 for iron. Slope values of 2.0 for copper, corresponding to Lix behaving as a monomeric monobasic acid, have been reported for extraction from sulphate media with Lix 64N in toluene or xylene (6,7,11), but recent work(11), also showed slopes of 1.0 for extraction from sulphate solutions with Lix 64N in kerosene. The lower slope value would be expected if the extractant were dimerised in the organic phase; possibly the major component of Lix 64N, the aromatic hydroxyoxime Lix 65N, tends to dimerise in the essentially aliphatic kerosene while remaining monomeric in the more compatible aromatic diluents. The slopes of ~ 1.5 for ferric iron would similarly be consistent with the dimerised extractant.

Extractions of copper were carried out using comparable concentrations of metal and extractant, some under substoichiometric conditions. $\log D$ -pH curves for the experiments are shown in Fig 2, and extraction isotherms derived from the results in Fig 3. The corresponding calculated maximum copper loading values for the extractant were $6.0 \times 10^{-2}M$ and $1.5 \times 10^{-2}M$ respectively for 2% and 5% Lix 64N solutions. If it be assumed that data recently published(7) for Lix 65N as supplied commercially apply also to Lix 64N, then it is possible to calculate theoretical values for maximum copper loading; the corresponding figures are 1.25×10^{-2} and $3.1 \times 10^{-2}M$, about twice the present experimental values. If this assumption is correct, and if the extracted complex is represented by CuA_2 (where HA represents the Lix molecule), then it would appear that at saturation only about half the extractant molecules are directly involved in complex formation. Alternatively, complete utilisation of the extractant could be accommodated if the extracted complex were of the form $CuA_2 \cdot 2HA$ and the extractant were present in kerosene solution as a tetramer, but it is probably unwise to speculate when dealing with a commercial product of uncertain composition.

When copper was extracted with Lix 64N from solutions which also contained ferric ions in concentrations up to $2 \times 10^{-2}M$ the iron was found to have a negligible effect on the resulting copper extraction lines, the only change observed being a slight increase in $pH_{0.5}$ for copper in the presence of the highest concentration of iron.

Back extraction of copper from kerosene solutions of Lix 64N, previously loaded from chloride aqueous media, was readily and rapidly achieved by shaking for a few minutes with dilute hydrochloric acid. The results of two typical stripping experiments are shown in Fig 4. In parallel experiments copper was completely stripped from organic solution with either sulphuric or nitric acid; in the latter case tests with silver ions failed to show the presence of chloride in the resulting aqueous solution, indicating that chloride ions were not extracted from the original aqueous

phase as part of the extracted complex and that consequently chemical carry-over of chloride to the electrowinning stage of a process based on chloride media should not occur.

The extraction of copper with Lix 64N was examined at several temperatures between 10°C and 50°C; typical results are shown in Fig 5. Below about 35°C increase in temperature increased the distribution coefficient by an amount consistent with an endothermic process having $\Delta H \sim +5$ kcal/mole, but as higher temperatures were reached the distribution coefficient was found to decrease. This effect has not been observed with extraction from sulphate media, for which extraction enthalpy values of $\sim +6.5$ kcal/mole have been given⁽⁷⁾. An explanation may be found in the formation of chloro-complexes of copper in the aqueous phase, which can inhibit extraction. The formation of the species CuCl^+ and CuCl_2^0 is endothermic, having $\Delta H \sim +4.0$ kcal/mole^(12,13); increasing temperature would thus favour increasing formation of chloro-complexes and correspondingly reduced extraction. The relative magnitudes of the two opposing effects at any temperature have not yet been calculated; a possible alternative explanation, not yet examined, concerns the unknown temperature stability of the extractant, since if decomposition were to occur at the higher temperatures this would lead to reduced extraction. The effect of increasing temperature on back extraction was to shift the extraction lines towards higher acidities, a maximum change of +0.05 in $\log [\text{HCl}]$ being observed at $\log D = 0$ over the temperature range examined. Increased temperatures would thus appear to offer no advantages in a stripping operation.

An example of the effect of varying chloride concentration on the extraction of Cu(II) and Fe(III) is shown in Fig 6, for initial metal concentrations of $5 \times 10^{-3} \text{M}$ and aqueous phases maintained at 4.0M concentration of $\text{NaCl} + \text{NaNO}_3$. Increase in chloride ion concentration reduced the extraction of either metal; unlike sulphate ions, the major anionic species present in conventional leach solutions, chloride ions form series of complexes with transition metal ions, and in so doing compete with the chelating extractant and reduce the level of extraction⁽¹⁴⁻¹⁶⁾.

Copper forms a series of chloro-complexes CuCl^+ , CuCl_2^0 , CuCl_3^- , CuCl_4^{2-} , the first three being hexa-coordinate, with solvent molecules occupying the remaining ligand sites, and the fourth tetra-coordinate. The species CuCl_3^- is known to occur in ether extracts from strong HCl solutions^(17,18), and has been demonstrated in concentrated HCl solution^(19,20) although the main species present are the less saturated CuCl_2^0 and CuCl_3^- . The tetrahedral species is characterised by a uv-visible peak at 395nm; spectra for copper in aqueous chloride media (Fig 7) exhibit a broad peak in the

range 250-300nm, which can be assigned to species derived by substitution of Cl^- ions into $\text{Cu}(\text{H}_2\text{O})_6^{2+}$, but the peak at 395nm is evident only when the medium is strong HCl solution. Generally chloro-complexing appears somewhat less in NaCl solution than in the same concentration of HCl.

Iron (III) forms a similar series of chloro-complexes; the extreme members are again hexa- and tetra-coordinate respectively, but the point in the series at which the coordination number changes is not known⁽²¹⁾. Tetra-coordinate species have been demonstrated in strong HCl solutions⁽²²⁾.

In HCl solutions of up to 4M concentration the principal copper and iron species that exist are Cu^{2+} and CuCl^+ , and Fe^{3+} to FeCl_2^+ ⁽²³⁾. In view of the reduced complexing observed in NaCl solution it appears likely that the ions of importance in the present study are Cu^{2+} , CuCl^+ , Fe^{3+} , and FeCl^{2+} .

The effect of competing ligands present in the aqueous phase of a metal solvent extraction system has been discussed by several authors^(14-17,24) in terms of the reduction in free metal ion concentration, and consequent reduction in distribution coefficient, caused by complexing. Thus for a system in which the only extractable species formed by a metal ion M^{n+} is MA_n ,

$$D = \frac{[\text{MA}_n]}{[\text{M}^{n+}] + \sum [\text{MX}_q^{n-q+}]}$$

where $\sum [\text{MX}_q^{n-q+}]$ is the sum of the concentrations of complexes formed in the aqueous phase with ligand X. In the present study the likely chloro-complexes are $\text{MCl}^{(n-1)+}$ and $\text{MCl}_2^{(n-2)+}$, so that the equilibrium aqueous metal concentration can be written $[\text{M}] + [\text{MCl}] + [\text{MCl}_2]$, and

$$D = \frac{[\text{MA}_n]}{[\text{M}^{n+}](1 + \beta_1 [\text{Cl}^-] + \beta_2 [\text{Cl}^-]^2)}$$

where β_1 is the formation constant of the complex $\text{MCl}_i^{(2-i)+}$. Hence

$$D = K_{\text{ex}} \frac{[\text{HA}]^n}{[\text{H}^+]^n} \cdot \frac{1}{1 + \beta_1 [\text{Cl}^-] + \beta_2 [\text{Cl}^-]^2}$$

$$\text{and } \log D = \log K + n \log [\text{HA}] + n \text{pH} - \log \{1 + \beta_1 [\text{Cl}^-] + \beta_2 [\text{Cl}^-]^2\}$$

For any constant value of $[Cl^-]$ the last item above will be constant, decreasing $\log D$ by an amount proportional to $[Cl^-]$ and shifting extraction lines to higher pH values. The observed effect of increasing the chloride concentration from 0.2M - the minimum value possible when HCl is used to adjust the pH value - to 4.0M was to increase $pH_{0.5}$ by 0.2 pH units for copper and 0.24 for iron. The slopes of the $\log D$ - pH lines for copper remained at 2.0, whereas those of the iron lines decreased from about 2.9 to 2.5. The reduced slope values cannot apparently be explained by extraction of species such as $FeCl_2^+$ and $FeCl_2^+$ because back extraction with nitric acid and subsequent testing with silver ions failed to indicate the presence of chloride in the organic phase.

Conclusion

It is evident that Lix 64N in kerosene may be used to extract copper selectively from an aqueous solution containing copper and iron in the presence of chloride ions. Chloride ion concentrations of up to 4M do not cause serious hindrance to extraction. Back extraction is readily achieved, and no chloro-complexes appear to be present in the loaded organic phase. There is apparently little advantage, in terms of equilibrium distribution, to be gained from operating at temperatures above 25°C.

Acknowledgements.

Grateful acknowledgement is made to Professor S.G. Ward for his interest, to the Science Research Council for a research grant to P.G.C. and to the Wolfson Research Foundation for a generous grant in aid of research into recovery of metals from secondary sources. Thanks are also due to Dr. J.E. House of General Mills Inc. for providing a sample of Lix 64N.

References

- 1) Swanson, R.R. U.S. Patent. 3131998, May 1964.
- 2) Idem, Ibid., 3224873, Dec. 1965.
- 3) Idem, Ibid., 3428449, Feb. 1969.
- 4) Idem, Ibid., 3592775, July 1971.
- 5) Atwood, R.L. and Miller, J.D., Paper presented at Annual Meeting, A.I.M.E., San Francisco, Feb. 1972.

- 6) Flett, D.S., Okuhara, D.N., and Spink, D.R.,
J. inorg. nucl. Chem. 1973, 35, 2471.
- 7) Spink, D.R. and Okuhara, D.N. International Symposium on
hydrometallurgy, Chicago, 1973, 497.
- 8) Rigg, T. and Maflitt, W., Can. J. Chem. Eng. 1971, 35, 2471.
- 9) Brooks, P.T., Potter, G.M. and Martin, D.A. J. Metals, 1970,
Nov, 22, 25.
- 10) Belcher, R., and Nutten, A.J., "Quantitative Inorganic Analysis",
1960, 2nd Ed., London, Butterworths. 274, 250, 266.
- 11) Lakshmanan, V.I., Lawson, G.J., and Tomliens, J.L. In press.
- 12) Sillen, L.G., and Martell, A.E. "Stability Constants of Metal
Ion Complexes", 1964, London, Chemical Society Special
Publication, 17.
- 13) Idem, Ibid., 25
- 14) Diamond, R.M. and Tuck, D.G., Progress in Inorganic Chemistry, 1960.
Vol II, New York, Interscience.
- 15) Marcus, Y., and Kertes, A.S., "Ion Exchange and Solvent Extraction
of Metal Complexes", 1969, London, Wiley - Interscience.
- 16) Zolotov, Yu. A., "Extraction of Chelate Compounds", 1970,
Ann. Arbor, London, Ann. Arbor-Humphrey Science Publishers.
- 17) Morris, D.F.C., and Gardner, E.R., Electrochim. Acta. 1963, 8, 827.
- 18) Morris, D.F.C., Short, E.L. and Slater, D.N. Electrochim. Acta;
1963, 8, 259.
- 19) Lindenbaum, S. and Boyd, G.E., J. Phys. Chem., 1963, 67, 1238.
- 20) Creighton, J.A. and Lippincott, E.R., J. chem. Soc., 1963, 5134.
- 21) Freidman, H.L., J. Am. chem. Soc., 1952, 74, 5.
- 22) Myers, R.J. and Metzler, D.E., J. Am. chem. Soc., 1950, 72,
3767, 3772, 3776.
- 23) Marcus, Y. Co-ord. Chem. Rev., 1967, 2, 195, 257.
- 24) Haffenden, W.J. and Lawson, G.J. Advances in Extractive Metallurgy,
p.678. The Institution of Mining and Metallurgy, London, 1967.

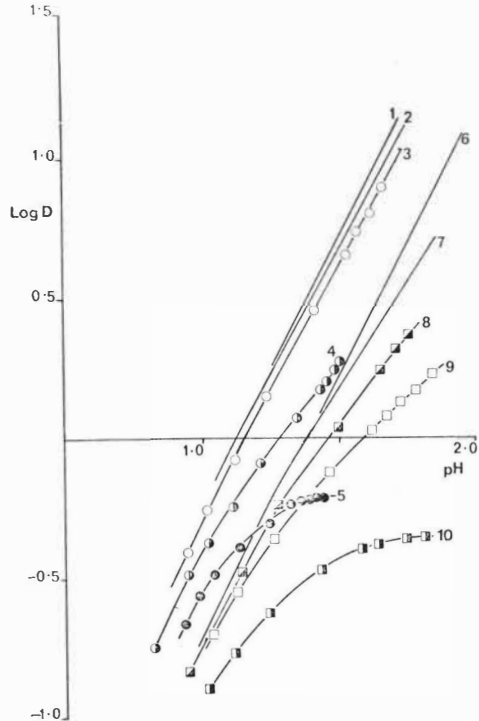


FIG. 2. SUBSTOICHIOMETRIC EXTRACTION OF Cu(II) FROM 1.0M CHLORIDE SOLUTIONS AT 25°C USING 5% LIX 64N (CURVES 1-5) AND 2% LIX 64N (CURVES 6-10) IN KEROSENE.

INITIAL COPPER CONCENTRATIONS = $2.5 \times 10^{-3}\text{M}$ (6); $5.0 \times 10^{-3}\text{M}$ (1,7); $7.5 \times 10^{-3}\text{M}$ (2,8); $1.0 \times 10^{-2}\text{M}$ (3,9); $2.0 \times 10^{-2}\text{M}$ (4,10); $4.0 \times 10^{-2}\text{M}$ (5).

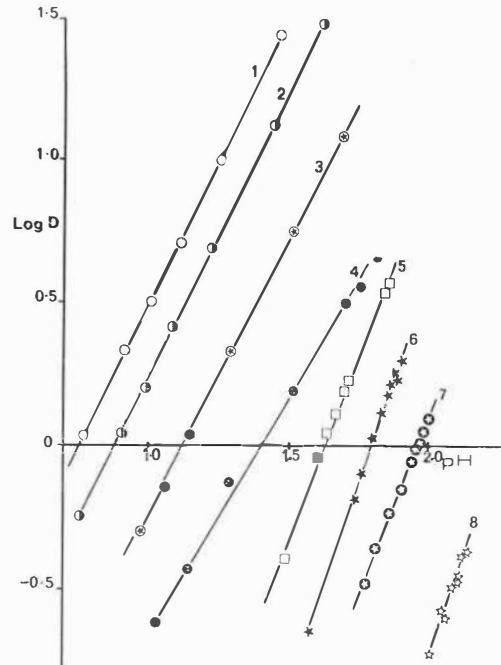


FIG. 1. LOG D vs EQUILIBRIUM pH FOR THE EXTRACTION OF $5 \times 10^{-3}\text{M}$ Cu(II) (CURVES 1-4), AND Fe(III) (CURVES 5-8), FROM 1.0M CHLORIDE SOLUTIONS AT 25°C USING LIX 64N IN KEROSENE.

LIX 64N CONCENTRATIONS: 25% (1,5); 10% (2,6); 5% (3,7); 2% (4,8).

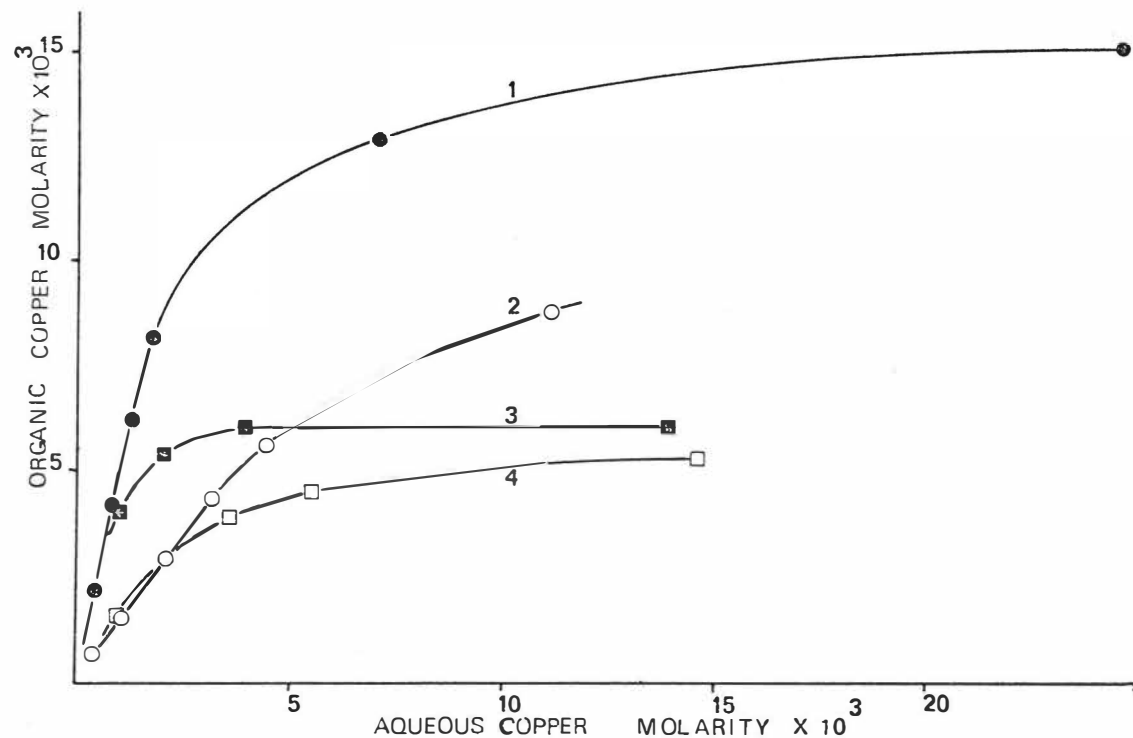


FIG.3. ISOTHERMS FOR THE EXTRACTION OF Cu(II) FROM 1.0M CHLORIDE SOLUTIONS AT 25°C USING 5% LIX 64N IN KEROSENE AT (1) $\text{pH} = 1.5$; (2) $\text{pH} = 1.2$; AND 2% LIX 64N AT (3) $\text{pH} = 1.8$; (4) $\text{pH} = 1.5$.

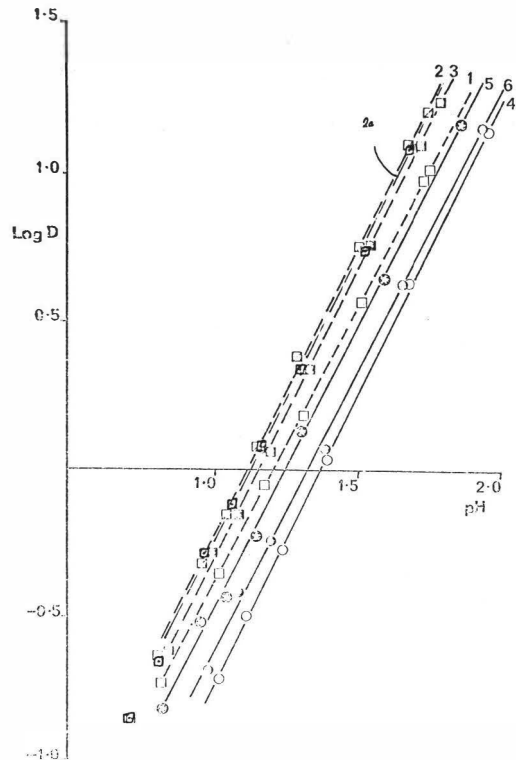


FIG. 5. EXTRACTION OF $5 \times 10^{-3}M$ Cu (II) WITH 5% LIX 64N AT
(1) $10^{\circ}C$; (2) $20^{\circ}C$; (2a) $30^{\circ}C$; (3) $45^{\circ}C$; AND
 $5 \times 10^{-4}M$ Cu WITH 2% LIX 64N AT (4) $10^{\circ}C$; (5) $25^{\circ}C$;
(6) $40^{\circ}C$.

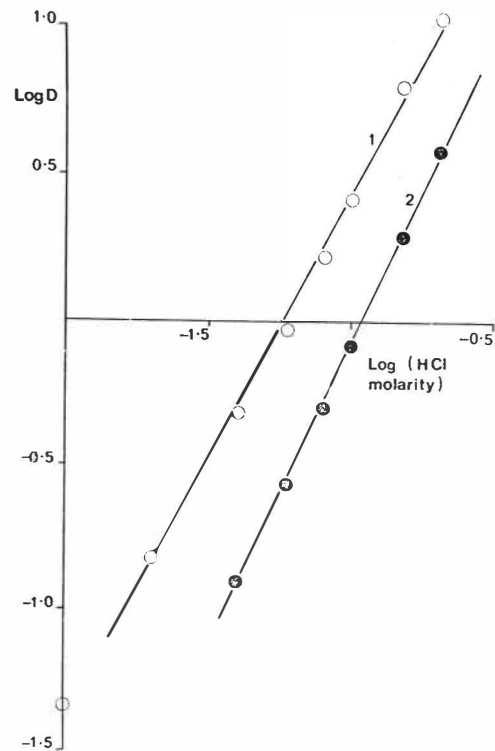


FIG. 4. BACK EXTRACTION WITH HYDROCHLORIC ACID AT $25^{\circ}C$ OF
(1) 2% AND (2) 5% LIX 64N IN KEROSENE CONTAINING
 $5 \times 10^{-3}M$ Cu (II).

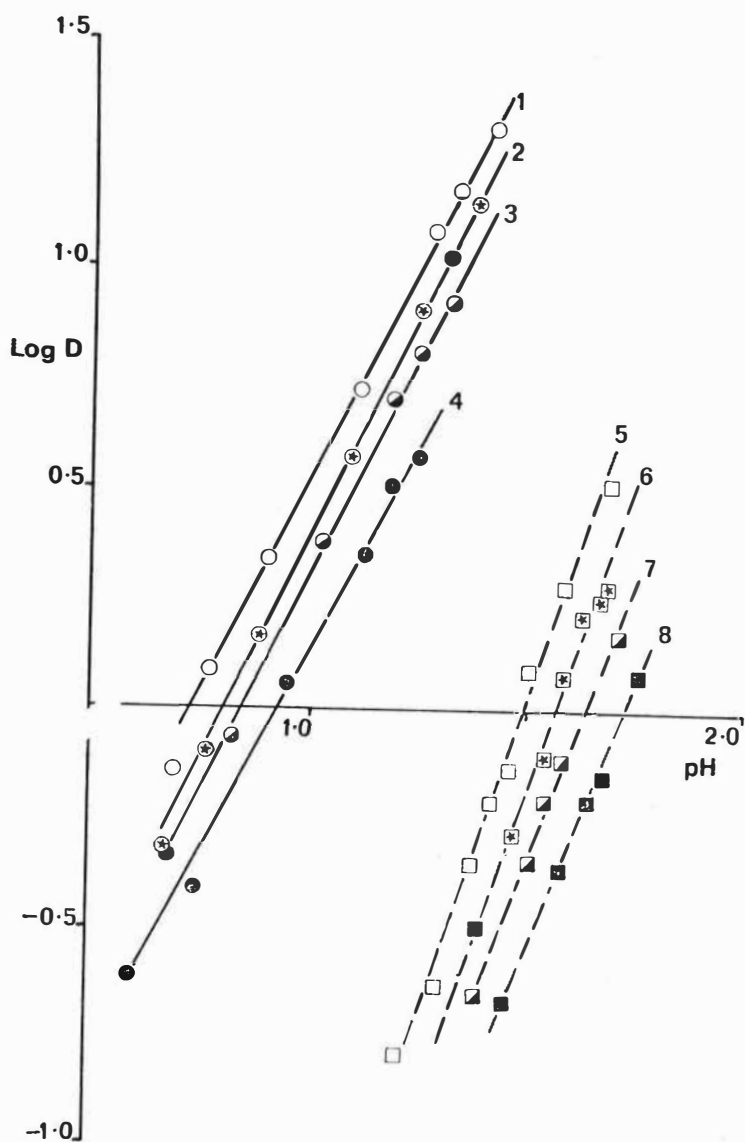


FIG.6. EFFECT OF CHLORIDE ION CONCENTRATION ON THE EXTRACTION OF $5 \times 10^{-3} \text{M Cu}$ (II) (CURVES 1-4), AND F^- (III) (CURVES 5-8). TOTAL IONIC STRENGTH MAINTAINED AT 4.0M WITH MgNO_3 , TEMP. = 25°C .

CHLORIDE CONCENTRATION = 0.2M (1,5); 1.0M (2,6); 2.0M (3,7); 4.0M (4,8).

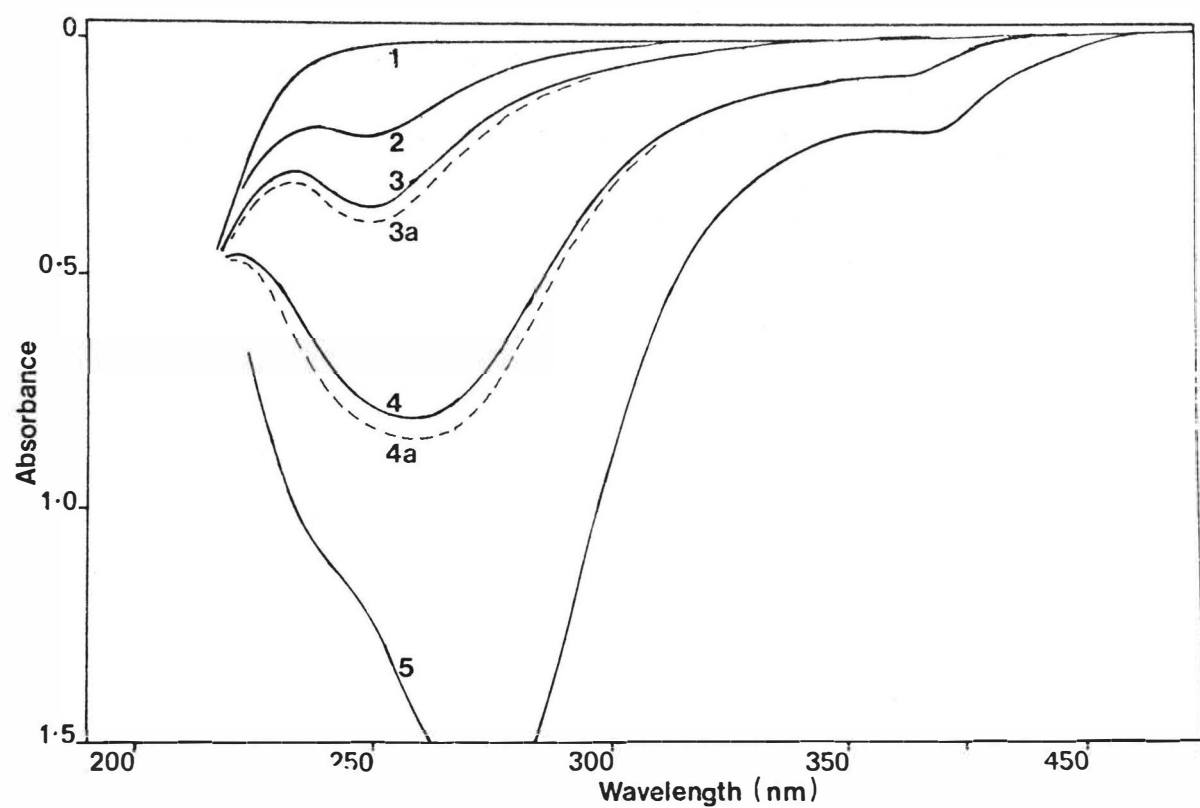


FIG. 7. UV SPECTRA OF $5 \times 10^{-4} \text{ M Cu(II)}$ IN AQUEOUS CHLORIDE SOLUTIONS.

(1) NO CHLORIDE; (2) 0.4M NaCl; (3) 1.0M NaCl; (4) 4.0M NaCl; (3a) 1.0M HCl; (4a) 4.0M HCl; (5) 5.8M HCl.

The Extraction of Copper(II) and Iron(III) with Kelex 100

from Aqueous Media containing Chloride Ions

by

V.I. Lakshmanan, G.J. Lawson and P.S. Nyholm

Wolfson Secondary Metals Research Group, Dept. of Minerals Engineering,
The University of Birmingham, Birmingham B15 2TT, U.K.

Abstract

The extraction of Copper(II) and Iron(III) from aqueous solutions containing chloride ions with Kelex 100 in kerosene has been studied to assess the applicability of this extractant to chloride leach solutions. Copper is extracted readily and reversibly from acid chloride solutions, chloride ions apparently causing little hindrance to extraction. Iron is also extracted from acid chloride solutions, but at a much slower rate, so that a separation of the two metals is possible on a kinetic basis.

Introduction

The recent introduction of selective extraction reagents for copper has led to a great increase in the use of solvent extraction for the commercial recovery of the metal. These reagents are designed particularly to extract copper while rejecting iron, and have been applied to solutions of the metals as sulphates; sulphuric acid is a good leaching agent for low-grade oxide ores and tailings, and is often readily available from an associated sulphide smelting operation. However, for leaching of non-ferrous secondary (scrap) metals, or refractory ores, or where sulphuric acid is not readily available, there may be advantages in using hydrochloric acid as an alternative, with air, oxygen or chlorine as oxidising agent when necessary. The dissolution of copper in hydrochloric acid has been⁽¹⁾, studied in this Department, and has also been reported by Rigg *et al.*⁽²⁾, and Brooks *et al.*⁽²⁾.

Dissolution in hydrochloric acid presents metals for succeeding solvent extraction as chlorides. Since both copper and iron form series of complexes with chloride ions in aqueous solution, as discussed earlier⁽³⁾, it is of interest to examine the behaviour of selective extractants with chloride solutions, to determine particularly the extent to which complexing in the aqueous phase might inhibit extraction. The present paper presents such an examination of the reagent Kelex-100, which is based on 8-hydroxyquinoline, dissolved in kerosene.

Experimental

Kelex 100 was kindly supplied by the makers, Ashland Chemical Co., Inc., and was purified before use as described previously⁽⁴⁾. Kerosene was 'kerosene white' supplied by Hopkin and Williams Limited. All other reagents were of analytical quality. Standard aqueous solutions of copper ($5.0 \times 10^{-2} \text{M}$) and iron ($2.5 \times 10^{-2} \text{M}$) were prepared by dissolving $\text{CuCl}_2 \cdot 2\text{H}_2\text{O}$, $\text{FeCl}_3 \cdot 6\text{H}_2\text{O}$ in distilled water and standardising by titration with EDTA⁽⁵⁾ or dichromate⁽⁶⁾ respectively. Sufficient hydrochloric acid was added to each solution to prevent hydrolysis.

Kelex 100 is a commercial product of undeclared composition. A small sample was purified by vacuum distillation at $160^\circ\text{C} / 0.2 \text{mm}$ to give a faintly yellow viscous liquid which was analysed by mass spectrometry and vapour phase osmometry, which showed the material to be monomeric in hexane, with a molecular weight of 311. Elementary analysis gave C, 81.3; H, 9.7; N, 4.5%. $\text{C}_{21}\text{H}_{29}\text{NO}$ requires C, 81.0; H, 9.3; N, 4.5%; M.W. 311. These measurements were kindly carried out by the Chemistry Department, University of Birmingham.

Extraction procedure. Equal volumes (10.0ml) of organic and aqueous phases were pipetted into 100ml stoppered flasks and shaken for a prescribed time in a water bath thermostatically maintained at 25°C unless stated otherwise. For dilute iron solutions polythene vessels were used instead of glass to minimise errors caused by adsorption of metal ions on the glass surface. After shaking the phases were allowed to disengage and then separated with Whatman 1PS paper. The pH of the aqueous phase was measured with a Pye Model 290 pH meter, and the metal content by atomic absorption spectrophotometry after suitable dilution. In initial experiments the metal content of the organic phase was measured similarly, after dilution with ethanol⁽⁴⁾, but, since the sum of the contents of the two phases always equalled the initial metal content, in later experiments the aqueous phase alone was measured and the organic phase metal concentration determined by difference. For copper, distribution equilibrium was established quickly, in less than 2 min., but the equilibration time for iron was much longer; accordingly a shaking time of 45 min. was adopted as standard. Organic phases were made up by dissolving Kelex 100 and dodecan-1-ol in kerosene. Aqueous phases were made up from appropriate volumes of standard Cu(II) or Fe(III) solution, hydrochloric acid to adjust the equilibrium pH value and sodium chloride and/or sodium nitrate to maintain the ionic strength of the solution. Due to the characteristics of Kelex 100 all distribution experiments were carried out in acid conditions. For each set of conditions of initial metal concentration etc., experiments at several (5 to 8) values of equilibrium pH were carried out and a graph of log D vs. pH was prepared; slope values for the resulting lines were calculated by the least squares method.

It was shown that on contact between the organic and aqueous phases transfer of the modifier to the aqueous phase (or vice versa) was negligible; consequently no pre-equilibration of phases was carried out.

Results and Discussion.

Phase disengagement and third phase formation. Early in the investigation it was found that if Kelex 100 in kerosene alone were used to extract copper a third phase formed when the aqueous phase pH was less than 0.5. This was prevented by the addition of dodecan-1-ol as a modifier, at the rate of four times the Kelex concentration for extractant concentrations up to 2%. Satisfactory two-phase disengagement was then obtained with aqueous phases even of concentrated hydrochloric acid (11.8M). Separate experiments with lower acidities and dodecanol concentrations from 0 to 8% showed that the modifier did not affect the equilibrium metal distribution. For organic phases containing 5% and 10% of Kelex the addition of 10% and 20% respectively of dodecanol was satisfactory. The use of isodecanol and nonylphenol^(8,9) with Kelex 100 has previously been reported.

Extraction of Cu(II). Extraction experiments were carried out with organic phases containing 0.5 to 10% Kelex (ca. 0.016 to 0.32M), and aqueous phases containing 5×10^{-4} to 1.25×10^{-2} M copper and maintained at an ionic strength of 1M (HCl+NaCl). From the resulting log D - pH relationships values of slope and $pH_{0.5}$ were obtained, and are presented in Table 1. Regression coefficients for the log D - pH lines were in all cases at least 0.995. Within the limits of experimental error the results showed a second power dependency of log D on pH, and that for

a given extractant concentration extraction was unaffected by initial metal concentration. In all these experiments equilibrium was reached so rapidly that no kinetic measurements were possible using the shake flask technique; this is in agreement with the measurements made by Spink et al.⁽⁹⁾ with sulphate solutions and using an AKUFVE instrument. A graph of log D vs. log (Kelex concentration) derived from the above results gave a straight line with a slope of 2.0 (Fig 1) indicating that the extracted complex contained two molecules of Kelex per atom of copper.

In a separate series of experiments an organic solution containing 2% Kelex and 8% dodecanol in kerosene was used to extract copper from aqueous phases containing $5 \times 10^{-3} M$ metal and various concentrations of chloride ions up to a maximum of 4M, the ionic strength being maintained at 4M ($HCl + NaCl + NaNO_3$). The resulting log D - pH lines were coincident for chloride ion concentrations up to 3M, but increase to 4M produced a marked reduction in extraction. This is illustrated in Fig.2, which compares a typical low-chloride line, for 1M chloride, with that for 4M chloride, and also with a line obtained for extraction under similar conditions but from an aqueous phase 1M with respect both to chloride ion and to total ionic strength. It is seen that the slope values are not reduced by alteration of the chloride ion concentration, and it is significant that the reduction in extraction caused by increase from 3M to 4M chloride at 4M ionic strength is less than that caused by reducing the ionic strength from 4M to 1M while maintaining 1M chloride ion concentration.

Extraction studies at various temperatures between 10°C and 50°C showed a small shift in the log D - pH lines with temperature, and calculations from the results indicated an extraction enthalpy of about -6 kcal/mole.

Back extraction studies showed that an organic phase loaded with copper from a chloride aqueous phase could readily be stripped with either hydrochloric or sulphuric acid. Log D - pH lines constructed from back extraction experiments agreed closely with those for forward extraction, and equilibrium was established as rapidly for stripping as for loading of the organic phase. In one case a loaded organic phase was stripped with nitric acid and the resulting aqueous solution treated with silver nitrate; no chloride ions could be detected.

The second power dependency of log D on pH shown in all the above experiments indicates that copper was being extracted as the cation Cu^{2+} , the log D - log [Kelex] relationship corresponding to a complex of the type $Cu(Kelex)_2$. From these findings and the apparent absence of chloride ions from the organic phase it is concluded that chloro-complexes of copper are not extracted; e.g. significant extraction of the first complex $CuCl^+$ would be expected to lead to a log D - pH slope less than 2.

The experiments with various chloride concentrations indicated that the effect of such complexing on extraction was small compared, for example, with the effect of ammonia as a competing ligand in the extraction of copper with a carboxylic acid⁽¹⁰⁾. This competitive effect increased with increase in aqueous phase pH, because the concentration of free ammonia increased consequently. In the present case some variation in chloride ion activity must have occurred under the more highly acid conditions; for example a solution 1M with respect to chloride ion at pH 0 would contain only hydrochloric acid, while at pH 1 most of the chloride would be present as sodium chloride, and the chloride activities in these two circumstances would differ appreciably⁽¹¹⁾. However, differences in activity of chloride, as distinct from differences in concentration, had no apparent effect on the experimented results and can be neglected.

Although the results indicate that chloride ions in concentrations up to 3M do not affect the extraction of copper by Kelex 100, it is not yet possible to explain why this is so. The equilibrium constant for the formation of the first chloro-complex,



is reported to be 630⁽¹²⁾. From this it follows that in 1M chloride the concentration of CuCl^{+} should be 630 times that of Cu^{2+} . If it were assumed that, perhaps for reasons of hydration, the possible complex $\text{CuCl}(\text{Kelex})$ would be incompatible with the organic phase or did not form at all, an explanation is still required for the lack of effect on D of apparently successful competition for copper ions by chloride. A similar situation exists in extraction of copper from chloride media with Lix 64N⁽³⁾, and both systems are being further investigated.

Extraction of Fe(III). Although the extraction of ferric iron with Kelex in the presence of chloride has not yet been examined as extensively as the extraction of copper, it presents several interesting features. Notably equilibrium is attained much more slowly with iron, as has been observed also in sulphate media^(9,13). Nevertheless Kelex 100 appears to be an 'effective' extractant for Fe(III) in that the log D - pH lines for extraction are located at low pH values; indeed, for comparable Kelex concentrations $\text{pH}_{0.5}$ for iron is less than for copper. Fig.3 shows a typical log D - pH relationship for 2% Kelex + 8% dodecanol in kerosene with $1.5 \times 10^{-3}\text{M}$ iron in 1M chloride, each point having been determined after the phases had been shaken together for 120 min.

Although the relationship shown is not so closely linear as those for copper extraction, the slope value is much closer to 3 than to 2, indicating that, as with copper, the metal was extracted substantially in the uncomplexed form. Fig. 3 also shows the variation of log D with time for the above phase combination; each experimental point corresponds to the distribution of iron between the organic phase and an aqueous phase of pH 0.9. This curve well illustrates the very slow approach to equilibrium of the iron(III)-Kelex system. Thus the Kelex - chloride system is similar to the corresponding sulphate system in that selective extraction of copper would depend on a major difference between the kinetics of extraction of copper and iron^(9,13,14). The present results indicate that, since the $pH_{0.5}$ value for iron is less than the corresponding value for copper, in a Kelex-chloride system that was allowed to reach equilibrium it should be possible to extract iron ahead of copper; however, in view of the great difference between the two metals in speed of approach to equilibrium this order of extraction would not apply in practice.

Back extraction of iron from a loaded organic phase was achieved rapidly on shaking with 2N hydrochloric or sulphuric acid, contact times of less than 1 minute being sufficient. A useful indication of the transfer of the iron to the aqueous phase was given by the discharge of the intense colour of the iron-Kelex complex; the colour was green in thin layers of loaded organic phase but was so intense as to appear black in the bulk phase volume. A visible absorption spectrum showed a strong absorption at 485nm and a subsidiary peak at 595nm, with general absorption spread over a considerable part of the spectrum. A series of back extraction experiments with aqueous phases containing various concentrations of hydrochloric acid gave a log D - pH relationship closely similar to the corresponding line for forward extraction. Back extraction with nitric acid followed by addition of silver ions indicated the absence of chloride from the loaded organic solution.

The behaviour of iron with Kelex 100 contrasts with that of cobalt, which is readily extracted but very difficult to recover by back extraction⁽⁴⁾.

Separation of copper and iron. In an experiment to examine the ease of separation of copper from iron an aqueous solution containing $1.3 \times 10^{-2}M$ Cu(II) and $1.6 \times 10^{-2}M$ Fe (III), and 1M with respect to chloride, was shaken for 4 min. with an organic phase consisting of 2% Kelex + 8% dodecanol in kerosene, the acidity being adjusted to give a final aqueous phase pH of about 0.9. Determination of the resulting metal contents in the separated aqueous solution gave log D values for copper and iron of 0.3 and -1.2 respectively, corresponding to a separation factor of about 30. This single experiment indicated that it is possible to separate the metals by extraction with Kelex 100 from chloride solution, but further work is required to determine optimum separation conditions.

Conclusions

It has been shown that both copper(II) and iron(III) can be extracted from aqueous solutions containing chloride ions at high acidities, and that a separation of the two metals may be achieved on the basis of their different extraction kinetics. Particularly in the case of copper, which has been examined more fully, the effect of chloride ions as a potential competing aqueous phase ligand was negligible for moderate chloride concentrations. Iron exhibits more complicated behaviour, further details of which will be published elsewhere.

Acknowledgements.

Grateful acknowledgement is made to Professor S.G. Ward for his interest, and to the Wolfson Foundation for the provision of a generous grant in support of this research. Thanks are also due to Dr. J.A. Hartlage of Ashland Chemical Co. Inc. for supplying a sample of Kelex 100, and to Dr. J. Hay, Dr. A. Macdonald and Dr. J. Majer of the Chemistry Department for analytical assistance.

References

1. Rigg, T. and Marflitt, W. Can. J. chem. Eng. 1971, 49, 501
2. Brooks, P.T., Potter, G.M. and Martin, D.A.
J. Metals, 1970, Nov, 22, 25
3. Christie, P.G., Lakshmanan, V.I., and Lawson, G.J.
Paper 125 to International Solvent Extraction
Conference ISEC 74, Lyon, France.
4. Lakshmanan, V.I. and Lawson, G.J. J.inorg.nucl.Chem 1973, 35, 4285
5. Vogel, A.I. "Textbook of Quantitative Inorganic Analysis",
Longmans, London, 1962, p.441.
6. Belcher, R. and Nutten, A.J. "Quantitative Inorganic Analysis",
1960, 2nd Ed., Butterworths, London. p.250.
7. Lawson, G.J. and Pridden, B.J. Paper 127 to International
Solvent Extraction Conference ISEC 74, Lyon, France.
8. U.S. Patent 3,725,046
9. Spink, D.R. and Okuhara, D.N. AIME International Symposium
on Hydrometallurgy, Chicago, 1973, 497.
10. Haffenden, W.J. and Lawson, G.J. "Advances in Extractive
Metallurgy," p.678. Institution of Mining and Metallurgy,
London, 1967.
11. Marcus, Y. and Kertes, A.S. "Ion Exchange and Solvent
Extraction of Metal Complexes", 1969,
Wiley-Interscience, London. pp.922 & 924
12. Hunt, J.P. "Metal ions in Aqueous Solution", 1963,
Benjamin, New York, p.66
13. Ritcey, G.M. CIM Bulletin, April, 1973 p.75
14. Flett, D.J. Private Communication.

		Organic Phase Composition				
Kelex 100, %		0.5	1.0	2.0	5.0	10.0
Dodecanol, %		2.0	4.0	8.0	10.0	20.0
Initial Cu(II) concn., M						
5x10 ⁻⁴	Slope	2.25	2.2	2.15	2.05	-
	pH _{0.5}	1.12	0.85	0.60	0.23	
2.5x10 ⁻³	Slope	1.95	2.1	2.2	2.15	-
	pH _{0.5}	1.17	0.87	0.55	0.20	
5x10 ⁻³	Slope	2.1	2.0	2.1	2.15	-
	pH _{0.5}	1.20	0.92	0.60	0.24	
1.25x10 ⁻²	Slope	-	2.1	2.0	2.05	2.2
	pH _{0.5}		0.92	0.65	0.28	0.00

Table 1.

Extraction of Copper(II) from 1M(HCl+NaCl) aqueous solutions with Kelex 100 in kerosene. Slope and pH_{0.5} values for log D - pH relationships with various initial copper and Kelex concentrations.

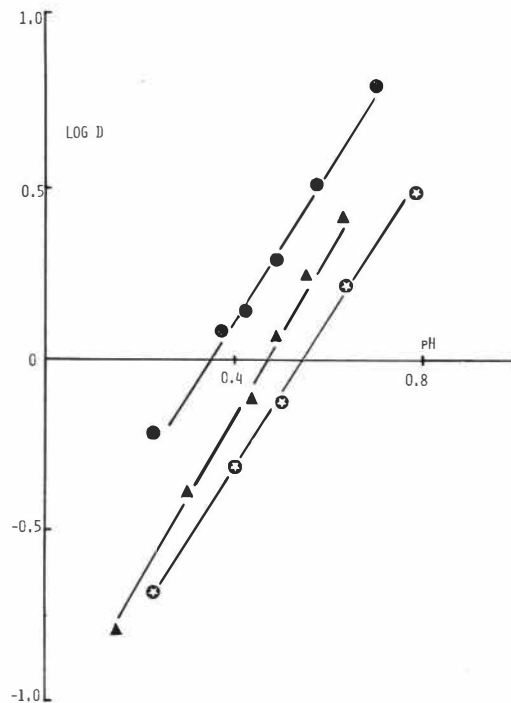


FIG. 2. EXTRACTION OF Cu (II) WITH 2% KELEX 100 IN KEROSENE, $\text{LOG D} - \text{pH}$ RELATIONSHIPS FOR INITIAL Cu (II) CONCENTRATION $5 \times 10^{-3} \text{M}$ IN VARIOUS AQUEOUS MEDIA.

- 1M CHLORIDE IN 4M ($\text{HCl} + \text{NaCl} + \text{NaNO}_3$)
- ▲ 4M ($\text{HCl} + \text{H}_2\text{O}_2$)
- ⊗ 1M ($\text{HCl} + \text{NaCl}$)

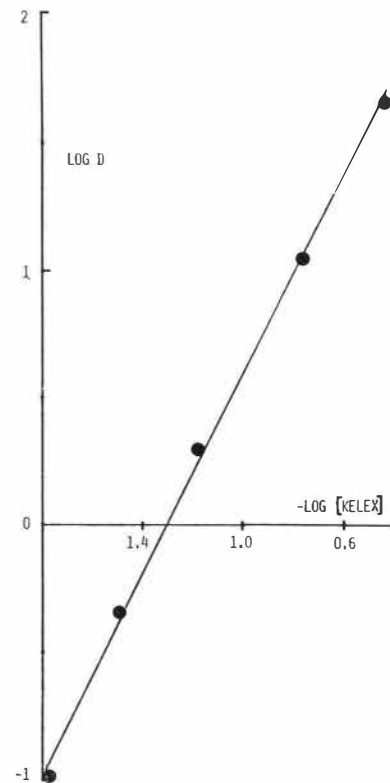


FIG. 1. EXTRACTION OF Cu (II) WITH EXCESS KELEX 100 IN KEROSENE, LOG D vs. $-\text{LOG} [\text{KELEX}]$ FOR AQUEOUS PHASES CONTAINING 1M CHLORIDE AT EQUILIBRIUM pH 0.75.

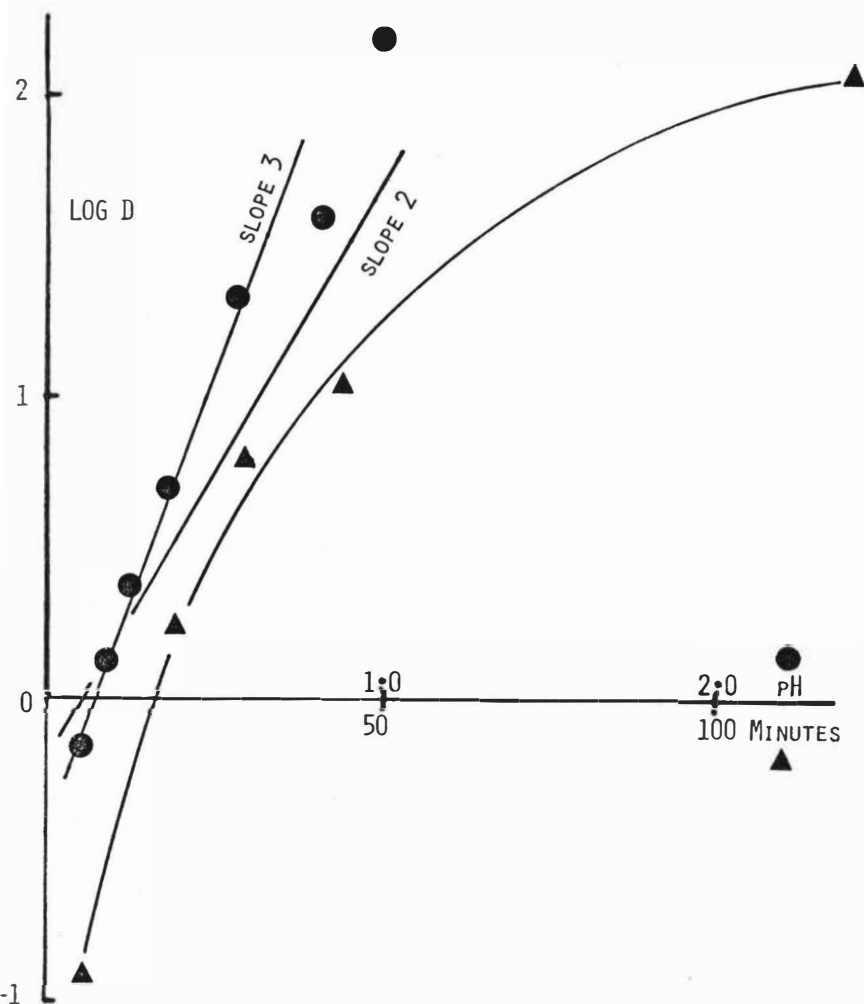


FIG. 3. EXTRACTION OF Fe (III) WITH 2% KELEX IN KEROSENE.

INITIAL Fe (III) CONCENTRATION $1.5 \times 10^{-3}\text{M}$

● - LOG D vs. pH AFTER 120 MIN. PHASE CONTACT.

▲ - LOG D vs. TIME; AQUEOUS PHASE pH 0.9 AFTER CONTACT.

Extraction of Copper, Nickel and Cobalt with Versatic Acid

from Ammoniacal Solutions

by

G.J. Lawson and B.J. Pridden

Department of Minerals Engineering, University of Birmingham
Birmingham B15 2TT, U.K.

Abstract

Earlier work has shown that the extraction of copper, nickel and cobalt with a carboxylic acid, Versatic acid, is profoundly affected by the presence of ammonium salts in the aqueous phase. The theory advanced to explain these effects in 'ideal' conditions of extraction has been modified to apply to practical conditions, and compared with experimental results. Particularly it was found that a useful separation of nickel and cobalt could be achieved.

The relationship of some deviations from theory to the possible oxidation of cobalt has been studied briefly; it has been shown that hexamminecobalt(III) may be extracted by Versatic acid, but it is not yet clear whether oxidation to the cobaltic state does occur under experimental extraction conditions.

Introduction

Earlier work in this Department showed that the extraction of Cu(II), Ni(II) and Co(II) from aqueous nitrate solutions with the carboxylic acid extractant Versatic acid (Shell Chemicals Ltd) in toluene was profoundly affected by the presence of ammonium salts in the aqueous phase. These studies were carried out under 'ideal' conditions, i.e. with small concentrations of metal ions and with a large excess of extractant, and among the effects noted when ammonium salts were present was an improvement in separation factors in certain ranges of pH. The present paper describes work undertaken to determine the behaviour of the systems, and the magnitude of the separation coefficients, under 'non-ideal' conditions.

Experimental

Versatic acid (Versatic 911) was kindly supplied by Shell Chemicals Ltd. Versatic 911 is similar to and has replaced Versatic 9, used in earlier work⁽¹⁾. All other reagents were of analytical quality. The organic phase used was prepared by dissolving Versatic 911 in toluene to give a 0.656M solution, calculated on the basis of a molecular weight of 173. Aqueous phases were prepared by dissolving appropriate nitrates in distilled water to give solutions 0.15M with respect to copper(II), nickel(II) or cobalt(II), and 2M with respect to ammonium nitrate.

Extraction procedure. Equal volumes (10.0ml) of organic and aqueous phases were transferred to 100ml stoppered flasks by means of E-mil 'Pressmatic' dispensers, and small amounts of 1M sodium hydroxide solution or, to obtain high pH values, solid sodium hydroxide, were added to give the desired equilibrium pH level; the volume of alkali was insufficient to alter the aqueous phase volume significantly. The phases were equilibrated by shaking for one hour in a water bath thermostatically maintained at 25°C; they were then separated, in a separating funnel for strongly alkaline solutions but otherwise by filtration through Whatman 1PS paper, and the pH of the aqueous phase was determined with a Pye Model 290 pH meter. The aqueous phase was then diluted with water by means of a 'Diluspense' diluter (Griffin and George Ltd.), which is capable of dilution by up to 1500 times; the metal content of the diluted solution was determined with a Perkin-Elmer 303 atomic absorption spectrophotometer. The metal content of the organic phase was determined by atomic absorption after similar dilution with ethanol; with the resulting solution the spectrophotometer showed increased sensitivity, the range of the instrument being 0-8 ppm of metal, compared with 0-25ppm for

the aqueous solutions. Dilution with ethanol proved a very satisfactory procedure and preferable to the use of ketones, which increased sensitivity so much that the instrument range was reduced to a less useful value. Organic standard solutions of metals were prepared by complete transfer of metal from an appropriate aqueous phase.

From the metal concentrations so determined the distribution coefficient D was calculated, and graphs of $\log D$ vs. pH were constructed.

Water concentrations in organic phases were measured by titration in a Karl Fischer apparatus (Radiometer Ltd). Absorption spectra were measured with a Perkin-Elmer 402 recording spectrophotometer.

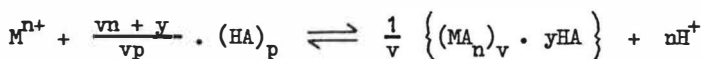
Results and Discussion

Haffenden and Lawson⁽¹⁾ studied the extraction of $Cu(II)$, $Ni(II)$ and $Co(II)$ with the commercial monocarboxylic acid Versatic 9 in toluene, and found that when ammonium nitrate was present in the aqueous phase extraction initially increased with increase in pH , as was expected with a cation-exchange extraction mechanism, but later decreased, corresponding with increase in the concentration of free ammonia. The results were interpreted in terms of hindrance of extraction of the metal due to the increasing formation of inextractable ammine complexes in the aqueous phase as the pH was increased, and a theory was developed, based on the successive formation of the ammine complexes of the three metals, by which the distribution coefficient at a particular aqueous phase pH value could be calculated. The conditions studied were 'ideal' in the sense that metal ion concentrations were small, and extractant concentrations so large as not to be altered significantly by consumption of extractant in forming Versatic-metal complexes. In a typical system examined by Haffenden⁽²⁾ a 0.2M solution of Versatic 9 in toluene was used to extract $Cu(II)$ at 2mM initial concentration from solutions containing 1.0M or 5.0M sodium or ammonium nitrate, with results shown in Fig.1. The departure of the experimental values from the theoretical curve when 5.0M ammonium nitrate was used was attributed by the author partly to inaccuracy introduced by assessing the value of z , the charge on the metal ions being extracted, and partly to inaccuracy in K_E , the extraction equilibrium constant.

It was also noted that the slopes of the experimental $\log D - \text{pH}$ curves increased beyond the expected value of 2 at low $\log D$ values at low pH, where the curves approached the lines for extraction in the absence of ammonium salts. According to the theory the slope of the parabola-type curves at any point corresponds to $z - \bar{i}$, where \bar{i} is the average number of ammonia ligands per copper atom in the aqueous phase, and in the case of copper values were assumed of $z = 2$, and $i_{\max} = 4$, the usual coordination number for copper. This latter assumption is true for smaller ammonium ion concentrations, but Bjerrum⁽³⁾ has shown that at concentrations as high as 5.0M the species $[\text{Cu}(\text{NH}_3)_5]^{2+}$ may predominate (Fig.2), leading to increased slope values at high pH ($z - \bar{i} = 2 - 5 = -3$). While such considerations may explain some deviations of experiment from theory, they do not explain the overall displacement of the experimental curve; this could however be due to the value of K_E , the effect of changing this parameter being to raise or lower the theoretical curve with respect to the pH axis. Similar displacements at high ammonium salt concentrations have also been observed recently by Ashbrook⁽⁴⁾.

Apart from the simplifications allowed by working under 'ideal' conditions, the theory assumed that both the extractant and the extracted complex were monomeric, and also that the system was ideal in the physical chemical sense. Any practical application of extraction in the presence of ammonium salts would necessitate consideration of higher metal concentrations and amounts of extractant closer to the stoichiometric requirement, and an extended theory, mentioned below but described in detail elsewhere⁽⁵⁾, has been developed for such conditions. The early work indicated that considerable variation from the simple theory might be expected, and also that in particular working in the presence of ammonium salts gave increased values of separation factor between nickel and cobalt. It was thus of interest to determine separation coefficients under 'non-ideal' conditions and to compare experimental behaviour with calculations from the new theory. Deviations were to be expected, inter alia, to result from the reduced activity coefficients consequent on operating with higher concentrations of metal ions, ammonium salt and extractant, concerning which insufficient data are available to allow them to be included in the theoretical treatment.

The extended theory considers a system in which a metal M of valency n is extracted by a polymeric acid extractant $(\text{HA})_p$ as an organic-phase complex of the form $(\text{MA}_n)_v \cdot y\text{HA}$, thus:



where v is the degree of polymerisation of the extracted complex,

y is the degree of solvation of the complex by extractant molecules,

and p is the degree of polymerisation of the extractant.

If ammonium salts are present in the aqueous phase of such a system, then it may be shown that:

$$\log D = \log (v \cdot K_E) + \left(\frac{v-1}{v} \right) \log \left[(MA_n)_v \cdot yHA \right] + \left(\frac{vn + y}{vp} \right) \log \left[(HA)_p \right] \\ - \log \sum_{i=0}^I K_i \cdot K_L^i \cdot [HL^+]^i [H^+]^{n-i} \quad \text{-----} \quad 1$$

where K_i is the successive formation constant of the ammine complex ML_i , K_L is the acid dissociation constant of the ammonium ion (HL^+) , and I is the coordination number of the metal M , and also that the gradient of the $\log D - pH$ relationship, at low values of $\log D$, is given by:

$$\left(\frac{d \log D}{dpH} \right) [HL^+], D \rightarrow -\infty (k', k'' \rightarrow 0) = v(n - \bar{i})$$

$$\text{when } k' \text{ is defined by } \frac{d \log (D+1)}{d \log D}$$

$$\text{and } k'' \text{ is defined by } \frac{d \log (fD+1)}{d \log D}$$

f is a constant and \bar{i} is the average number of ammonia ligands per metal atom in the aqueous phase. Thus at low values of pH , $\bar{i} \rightarrow 0$, and

$$\left(\frac{d \log D}{dpH} \right) [HL^+], D \rightarrow -\infty (k', k'' \rightarrow 0) = vn$$

At high values of pH , $\bar{i} \rightarrow I$, and

$$\left(\frac{d \log D}{dpH} \right) [HL^+], D \rightarrow -\infty (k', k'' \rightarrow 0) = v(n-I)$$

Extraction of Cu(II), Ni(II) and Co(II). With the aid of equation 1, families of $\log D - \text{pH}$ curves were constructed for the extraction of Cu(II), Ni(II) and Co(II) under various experimental conditions, in the presence or absence of ammonium ions, and for various values of p , v and y . From work described elsewhere⁽⁵⁾ it was concluded that under the present extraction conditions the most probable values of these parameters were $p = v = y = 2$. Fig.3 shows the theoretical curves, calculated using these values, for extraction of metal at 0.15M initial concentration in the presence of 2M ammonium nitrate with 0.656M Versatic 911 in toluene, and also the experimental $\log D - \text{pH}$ relationships for these systems. In comparing these curves it is useful to consider the slope values at high and low pH, at low values of D , and three points; these are named point R, the 'maximum' value of $\log D$ when $d \log D / d\text{pH} = 0$, and points S and T, corresponding to the low and high pH values respectively when $\log D = 0$.

The experimental curve for copper approximated to a parabola, point R occurring at pH 6.2 and $\log D \sim 2.0$ and points S and T at pH 3.95 and 8.35. The corresponding theoretical values were pH 6.0 and $\log D \sim 2.0$, and pH 3.2 and 8.1. The theoretical curve agreed reasonably with the experimental results for pH values above point R, but at lower pH values the theoretical $\log D$ values were greater than those found practically. The reason for this difference is not immediately apparent, although it may be attributable to activity effects. The experimental gradients at low and high pH values were 3.5 and ca.-2 respectively. The latter value represents $\log D$ values greater than 0, and so is probably not a true terminal slope value; it is considered that had it been possible to extend the experimental points a value of -4 or -5 might have been obtained. The colour of the organic phase was green at pH values below point R, and above this changed to blue, as was observed also by Ashbrook⁽⁴⁾, who attributed this change to the extraction of copper-ammonia complexes into the organic phase.

For nickel point R occurred at pH 7.7, while the theoretical value was about 7.2, close to that obtained by Haffenden *et al.*⁽¹⁾ for 'ideal' conditions. The gradients at low D values were 4 and -8 for low and high pH values respectively. The colour of the organic phase was bright blue up to pH values about 7.7, but beyond this a subtle change occurred in the blue colour, probably indicating a change in the organic phase complex and possibly attributable to the incorporation of ammonia into it.

The extraction curve for cobalt showed considerable displacement from the theoretical curve; pH values at point R were 8.05 and 7.8 respectively. Haffenden *et al.*⁽¹⁾ found that experimental values of log D decreased with increase of pH beyond point R more rapidly than was predicted theoretically; this was attributed to participation by ammonia molecules in the extracted complex, but Ashbrook⁽⁶⁾ has recently suggested that the deviation is caused by oxidation of cobalt(II) to cobalt(III). This point will be discussed later.

Separation of nickel and cobalt. From the experimental curves in Fig.3 it is apparent that some separation of cobalt from nickel could be achieved by extraction at pH values in the range 7.5 to 9.7. The optimum appears at about pH 8.2, when 97% of the initial cobalt would be extracted, along with 78% of the nickel, corresponding to a separation factor of about 10. Though not large, this separation warranted a study of the mixed metal system, which was carried out with 0.656M Versatic 911 in toluene and aqueous phases containing 0.075M Co(II), 0.060M Ni(II), and 2M ammonium nitrate, over the pH range 7.9 - 9.7. At pH values of 9 and greater the aqueous phase become slightly turbid, and the phases become somewhat difficult to separate, although at the highest pH levels, above 9.4, this difficulty lessened. The turbidity, which in time became a slight precipitate, was apparently associated with the nickel present, since its appearance coincided with a small but increasing 'loss' of nickel, indicated by the fact that the total of aqueous + organic metal was slightly less than the initial concentration. The recovery of cobalt was complete throughout. The results, shown in Fig.4, indicated that a separation better than had been anticipated could be obtained; between pH 8.5 and 9.1, a region free from nickel 'loss' and phase disengagement difficulties, the separation factor was about fifty, an encouraging value.

Organic phase water content. Karl Fischer titrations were carried out to determine the amount of water, if any, associated with the extracted metal complexes. Measurements on toluene, undiluted Versatic 911, and 0.656M Versatic 911 in toluene, after equilibration with aqueous phases buffered between pH 2 and 9, showed that each contained a small but constant concentration of water. Measurements on organic phases containing nickel or cobalt, in concentrations over the range covered by the extraction experiments (0 - 0.15M), showed that, after allowing for the water associated with the extractant and diluent, each atom of metal in the extracted complexes was associated with half a molecule of water. The measurements were carried out in triplicate,

and the results agreed closely over the whole concentration range. Thus each dimeric complex molecule would be associated with one molecule of water. Satisfactory results could not be obtained for copper because the metal ion reacted with the iodine present in the titration reagent.

The oxidation state of cobalt. As mentioned earlier, it has been suggested that the more rapid decrease of cobalt extraction with increase in pH in ammoniacal systems, compared with theoretical predictions, may be due to oxidation of Co(II) to Co(III). Certainly the formation of Co(III) amines is favoured; the overall formation constant for $[\text{Co}(\text{NH}_3)_6]^{2+}$ is $10^{4.39(7)}$, while that for $[\text{Co}(\text{NH}_3)_6]^{3+}$ is $10^{35.2(8)}$, so that in ammoniacal solution in the presence of oxygen oxidation to the cobaltic state would be favoured. However, although the hexamminecobalt(III) ion is undoubtedly stable, its formation requires conditions such as the presence of activated charcoal⁽⁹⁾, and work in this laboratory has confirmed that oxidation is not achieved as readily as might at first be expected. This was done by treating solutions containing Co(II) ions in various oxidising conditions and examining the oxidation state of the metal by means of visible absorption spectra, Co(II) showing an absorption peak at 512nm and Co(III) peaks at 340 and 478nm. The hexamminecobalt(III) complex would be more stable than the Versatic 911 - cobalt complex, and its formation would hinder extraction to a greater extent than formation of cobalt (II) amines, assuming that all the metal amines were inextractable. Apart from the increasing departure from theoretical prediction with increasing ammonium salt concentration, the system is complicated in other ways; at pH values above about 8.4 a brown turbidity appears in the aqueous phase during extraction experiments, as was noted also by Ashbrook⁽⁶⁾, who observed in addition that if such an aqueous phase were contacted with kerosene, and the pH adjusted to about 7.5, some cobalt could be transferred to the kerosene phase. It thus appeared that a significant concentration of the ammonium salt of Versatic 911 could be present in the aqueous medium without being visibly evident as a second phase.

To investigate further the role of Co(III) in cobalt extraction, solutions containing 0.0015M hexamminecobalt(III) nitrate were extracted with 0.656M Versatic 911 in toluene in the presence of 0.1M sodium or ammonium nitrate, over a range of pH values. The results are shown in Fig.5. With sodium nitrate 'normal' extraction appeared to occur until pH values greater than 7.5 were reached, when the organic phase became colourless and a viscous third phase formed. When this third phase was added to sodium hydroxide solution a two phase system was obtained initially but a clear single phase resulted after further addition,

indicating that the third phase, possibly consisting mainly of a salt of hexamminecobalt(III) and Versatic 911, was not completely incompatible with aqueous media. Extraction in the presence of ammonium nitrate produced a parabola-type curve, and no turbidity or third phase formation was evident. However, if an aqueous phase, equilibrated at a pH value greater than 8.4, was acidified to pH 7.5, a second phase separated, similar in viscosity to the third phase mentioned above, indicating solubility of the organic complex in aqueous media at high pH values and that the reversal of extraction was probably due to this solubility. Certainly the explanation advanced for the reversal in the case of Co(II) ions in the presence of ammonium salts cannot apply in the case of a fully complexed, stable hexamminecobalt ion, and indeed the fact that this ammine has been shown to be extracted by Versatic 911, presumably as a salt, calls into question the assumption that ammine complexes in the aqueous phase are inextractable. However the limited evidence so far obtained applies only to hexamminecobalt(III), and investigations are being continued.

Conclusions

An extended theory has been developed to describe the extraction of metals with carboxylic acids from ammoniacal solutions under 'non-ideal' conditions; predictions made from this theory agree reasonably with experimental results, although there are unexplained deviations. Some of these deviations may be useful, e.g. when a mixed nickel-cobalt solution is extracted with Versatic 911 unexpectedly high separation factors are found. It has been shown that hexamminecobalt(III) can be extracted with Versatic 911, and this brings into question the roles both of oxidation and of ammine formation in carboxylic acid systems.

Acknowledgements.

Grateful acknowledgement is made to Professor S.G. Ward for his interest, to Rio Tinto Zinc Corporation for provision of a research studentship (to BJP), and to Shell Chemicals Ltd. for a supply of Versatic 911.

References

1. Haffenden, W.J., and Lawson, G.J. In "Advances in Extractive Metallurgy", p.678, Institution of Mining and Metallurgy, London, 1967.
2. Haffenden, W.J. Ph.D. Thesis, University of Birmingham 1966.
3. Bjerrum, J. "Metal Ammine Formation in Aqueous Solution", p.287, P.Haase, Copenhagen, 1957.
4. Ashbrook, A.W. J.inorg.nucl.Chem., 1972, 34, 3523
5. Lawson, G.J., and Pridden, B.J., In Press.
6. Ashbrook, A.W. J.inorg.nucl.Chem., 1972, 34, 1721.
7. Bjerrum, J. "Metal Ammine Formation in Aqueous Solution", p.188, P.Haase, Copenhagen, 1957
8. Idem, Ibid., p.285.
9. Cotton, F.A., and Wilkinson, G. "Advances in Inorganic Chemistry", p.727, Wiley-Interscience, 1962.

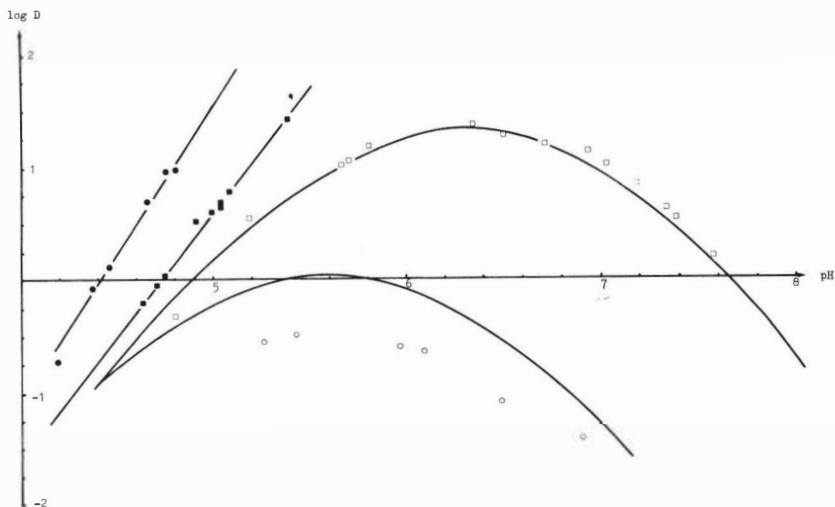


FIG.1 EXTRACTION OF Cu(II) WITH 0.200M VERSATIC 9 IN TOLUENE (HAFFENDEN⁽²⁾).
 INITIAL Cu(II) CONCENTRATION 2mM
 AQUEOUS SALT CONCENTRATIONS: \square 1M NaNO_3 , \bullet 5M NaNO_3 ,
 \circ 1M NH_4NO_3 , \bullet 5M NH_4NO_3 .
 CURVED LINES SHOW THEORETICAL RELATIONSHIPS.

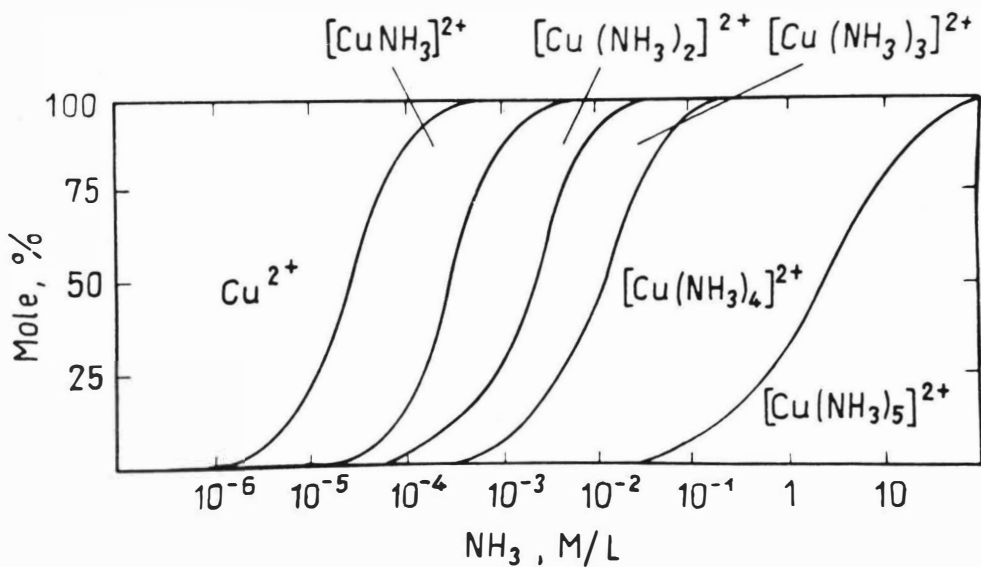


FIG.2 PROPORTIONS OF COPPER AMMINE COMPLEXES AS A FUNCTION OF AMMONIA CONCENTRATION (BJERRUM⁽³⁾).

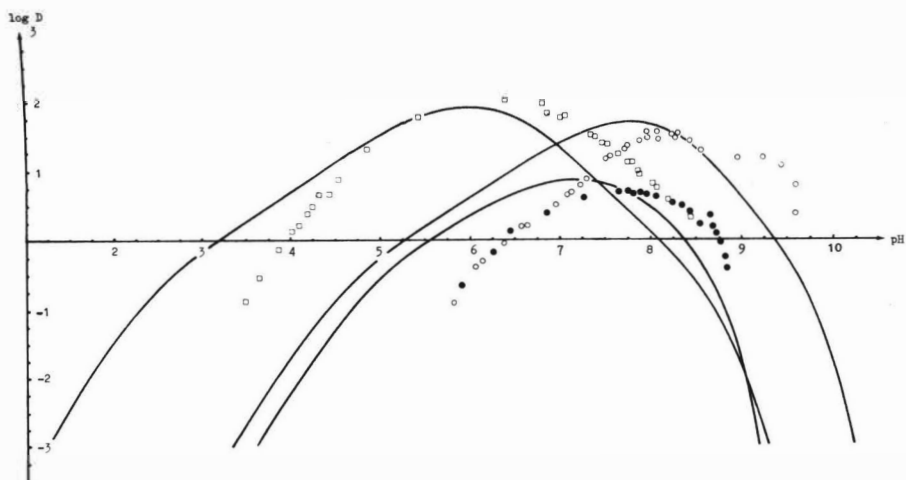


FIG.3 EXTRACTION OF Cu(II), Ni(II) AND Co(II) FROM 2M NH_4NO_3 SOLUTION
WITH 0.656M VERSATIC 911 IN TOLUENE.
INITIAL METAL CONCENTRATION 0.15M
□ Cu(II), • Ni(II), ○ Co(II).
CONTINUOUS LINES REPRESENT THEORETICAL RELATIONSHIPS.

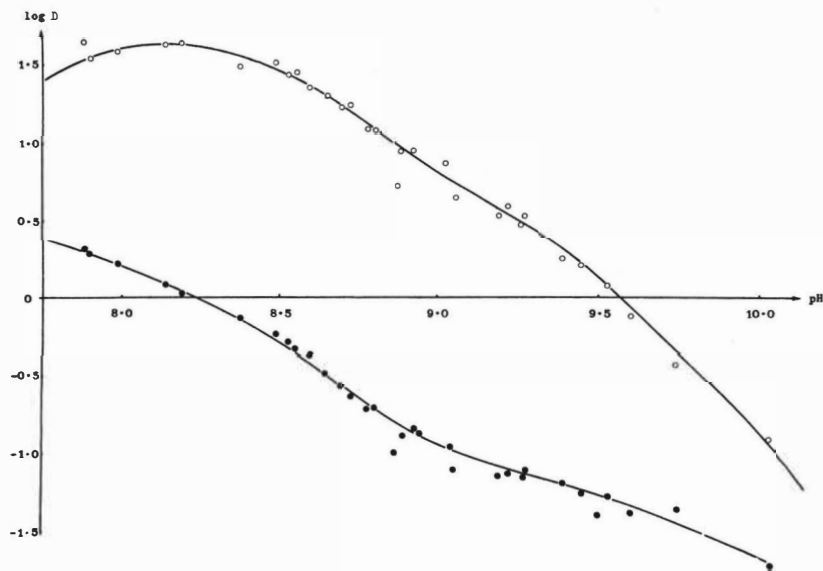


FIG.4 EXTRACTION OF MIXED Ni(II) AND Co(II) FROM 2M NH_4NO_3 SOLUTION WITH
0.656M VERSATIC 911 IN TOLUENE,
●—● Ni(II), INITIAL CONCENTRATION 0.060M
○—○ Co(II), INITIAL CONCENTRATION 0.075M.

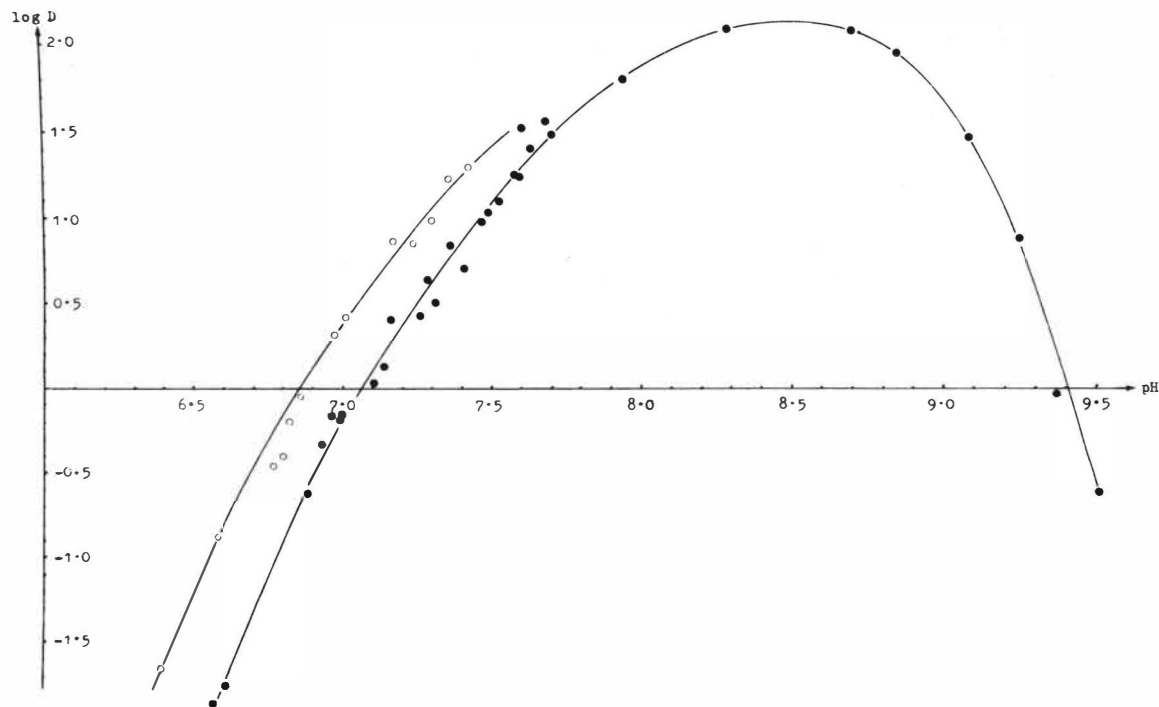


FIG.5 EXTRACTION OF HEXAMMINECOBALT (III) NITRATE WITH 0.656M VERSATIC 911
IN TOLUENE. INITIAL METAL CONCENTRATION 1.5mM.

○—○ FROM 1M NaNO_3 SOLUTION

●—● FROM 1M NH_4NO_3 SOLUTION.

USE OF HIGH DENSITY HYDROCARBONS AS DILUENTS
IN COPPER SOLVENT EXTRACTION

W. MANFROY AND T. GUNKLER

DOW CHEMICAL U. S. A.

FUNCTIONAL PRODUCTS & SYSTEMS DEPARTMENT

Summary

A series of tests was run comparing the performance of perchloroethylene with existing hydrocarbon diluents in copper solvent extraction. LIX® 64N was used as a standard extractant. Looked for were kinetics of extraction, extraction isotherms, solvent's strength, feed solution pH, iron rejection, and phase separation in the loading process. Main operating parameters on the stripping section were also investigated.

Recommendations for proper handling and recovery of the solvent are described.

In the system studied, perchloroethylene showed faster kinetics and phase disengagement, higher iron rejection and improved stripping efficiency. The relatively high cost of perchloroethylene, combined with higher evaporation losses, make it necessary to recover the diluent.

W. Manfroy
Dow Chemical U.S.A.
Chemical Engineer
Mining Chemicals Group
Functional Products & Systems
Walnut Creek, California U.S.A.

T. Gunkler
Dow Chemical U.S.A.
Part-time Student
Mining Chemicals Group
Functional Products & Systems
Walnut Creek, California U.S.A.

USE OF HIGH DENSITY HYDROCARBONS AS DILUENTS
IN COPPER SOLVENT EXTRACTION

W. MANFROY AND T. GUNKLER
DOW CHEMICAL U. S. A.
FUNCTIONAL PRODUCTS & SYSTEMS DEPARTMENT

Introduction

Solvent extraction is becoming an increasingly important process for the production of copper from low value ores, waste streams, streams, tails and dumps.

Traditionally, the organic phase of the recovery process consists of an active molecule or extractant (LIX® 64N, Kelex® 100) and a diluent. Diluents used in practice are kerosene-type cuts or similar hydrocarbons.

Very little attention has been drawn, so far, to the selection of suitable diluents. Recent availability problems of Napoleum® 470 plus some work done at the Exxon Research Laboratories¹ has created a larger interest. Exxon's work showed wide differences in the behavior of the system by simply changing the nature of the diluent. Furthermore, it also indicated that, according to the nature of the problem, an optimum diluent could be formulated.

- Napoleum® - Trademark of Kerr-McGee Chemical Corp., Oklahoma City, Oklahoma, U.S.A.
- LIX® - Trademark of General Mills Chemicals, Inc., Minneapolis, Minnesota, U.S.A.
- Kelex® - Trademark of Ashland Chemical Company, Division of Ashland Oil, Inc., Columbus, Ohio, U.S.A.

TABLE 1
PROPERTIES OF SOME HEAVY LIQUIDS³

Sp. Gr.	Compound	Formula	Boiling Point °C	Viscosity cp (25°C)
3.31	Methylene iodide	CH_2I_2	182.0	2.60
2.95	Acetylene tetrabromide	$(\text{CHBr}_2)_2$	243.5	9.60
2.75	Tribromo-fluoro methane	CBr_3F	108.0	1.50
2.48	Methylene bromide	CH_2Br_2	97.0	0.97
1.67	Pentachloro ethane	$\text{CCl}_3-\text{CHCl}_2$	161.0	2.33
1.62	Perchloroethylene	$\text{CCl}_2=\text{CCl}_2$	121.0	0.86
1.59	Carbon tetrachloride	CCl_4	76.5	0.90
1.46	Trichloroethylene	$\text{CCl}_2=\text{CHCl}$	87.1	0.55
1.33	Methyl chloroform	CCl_3-CH_3	74.1	0.80
1.25	Dichloroethane	$\text{CH}_2\text{Cl}-\text{CH}_2\text{Cl}$	83.5	0.79

Other practical considerations limit the choice considerably. To be able to use a "chemical solvent" as a diluent in solvent extraction, it has to satisfy numerous physical requirements:

- High density
- Chemically stable versus leach solution, strip solution and extractant
- Solubilize the extractant in a wide range of concentrations, in loaded and unloaded state
- Viscosity - intrinsic viscosity of diluent should be as low as possible
- Flash point $>70^\circ\text{C}$
- Toxicity - as low as possible

- Low solubility in aqueous phases
- Low volatility
- Low cost
- Available in large quantities

Also, the diluents should have a beneficial, or at least no detrimental effect on the physical handling of the solvent. Particular emphasis should be put on phase disengagement, kinetics of extraction, maximum loading and iron rejection in either the extraction or the stripping stage.

The purpose of this paper is to examine the effects of various diluents, and particularly perchloroethylene, on the solvent extraction of copper. Only a very few data have been generated on brominated compounds for the sake of comparison with the chlorinated solvents.

The perchloroethylene studied was a high grade, low impurity, specially inhibited, industrial solvent made by Dow Chemical U.S.A. Great care should be taken in selecting the type of perchloroethylene adopted because impurities and additions can greatly effect the efficiency of the diluents, as will be seen later.

Table 2 summarizes the principal physical properties of the diluents tested in this paper.

TABLE 2
PRINCIPAL CHARACTERISTICS OF DILUENT SYSTEMS

	Perchloro- ethylene	Chevron 3	Refined Kerosene	Escaid 100	Norpar 12	Methylene bromide
Manufacturer	Dow	Standard Oil of Calif.	Kerr- McKee	Exxon	Exxon	Dow
Sp. Gr. (25°C)	1.62	0.885	0.802	0.791	0.749	2.48
Solubility (mg/l)						
in water	150	ca 100	ca 100*	ca 100*	ca 100*	>100
in leach	ca 30-50					
in strip lig.	ca 30-50					
of water in	140					
Vapor density (air = 1.0)	5.76	-----	-----	-----	-----	not avail- able
Viscosity 25°C (cp)	0.86	-----	1.35	-----	-----	0.97
TLV ppm	100	-----	-----	-----	-----	100
Flash point °C	none	62	80	>65	>65	none
Kauri-Butand No.	92	88	85	-----	-----	not avail- able
Surface tension (dynes/cm)	32.3	29	28	-----	-----	-----
Vapor pressure at 20°C mm Hg.	14.3	-----	-----	-----	-----	45.3
Cost U. S. ¢/lb. (Est.)	9.0	3.0	3.0	5.6	5.6	30.0
**LIX 64N U.S. ¢/l (Est.)	63.5	51.8	51.8	53.6	53.6	85.0
% Aromatics	none	100	low	medium	low	none
Latent heat vapor (cal/g)		-----	-----	-----	-----	44.9
Density differ- ence vs. leach	0.55	0.117	0.189	0.197	0.238	1.48
vs. strip (150 g/l)	0.39	0.27	0.35	0.36	0.40	1.32

*Initial Solubility

**Extractant solution at 5% active of LIX 64N

A thorough analysis of the physical-chemical characteristics indicates that perchloroethylene could be a suitable diluent, provided the losses can be maintained at a reasonable level. Several means of controlling these losses will be discussed later.

Effect on Extraction

In order to determine the feasibility of using perchloroethylene as a diluent, its influence on the different parameters of the solvent extraction process was investigated. Parameters examined were:

- kinetics
- concentration of extractant in the solvent
- concentration of metal in aqueous feed
- temperature of contact systems
- phase separation
- mixing velocity
- pH, etc.

Except where otherwise noted, feed solutions used were 1.9 g/l copper and 1.9 g/l ferric iron, pH of 2.0. Organic solvent concentration was fixed at 10 vol. % of LIX® 64N. Extraction tests were made in a thermostatically controlled beaker at 23°C. The mixer was a lab size pump mixer developed by Davy Power Gas. Organic to aqueous phase ratio was 1/1.

Kinetics or Time Dependence

Considerable differences were seen in the copper extraction, especially at low mixing times. (See Figure 1). The tests clearly indicated Chevron 3 to be an inferior diluent (only 60% under test conditions at equilibrium versus 75-85% for all others).

It is interesting to note that in actual operations two to five minutes mixing time is provided. In this range, improvements with perchloroethylene over the hydrocarbon-type diluents were of the order of 15%. All these differences tend to fade away and even to reverse for longer mixing times (15-20 minutes). Table 3 also shows, unexpectedly, a much better iron rejection (except for Chevron 3 at equilibrium) for the chlorinated solvent, perchloroethylene.

This considerably better iron rejection with perchloroethylene has been confirmed in all following experiments. This is of particular importance because presently 5 to 10% of the actual electrolyte can be bled from the electrowinning system to control iron buildup.

Extraction Isotherms

A paper published earlier mentioned the use of perchloroethylene as a diluent in an extraction system which utilized cyclones² to gain improved organic/aqueous separation. A typical extraction isotherm taken from that reference shows perchloroethylene to be equal to, if not better than, refined kerosene. (See Figure 2).

Solvent's Strength

Very little difference was found at equilibrium between the hydrocarbon diluents and perchloroethylene for copper extraction. At high extractant concentrations, thus when more reagent is available for chelation, the iron extraction was 1.3% for perchloroethylene versus 3.5% for kerosene, an almost threefold increase. (See Figure 3).

TABLE 3
EFFECT OF DILUENTS ON IRON REJECTION - KINETICS TEST

Time (min.)	Cu/Fe Extraction Ratios				
	0.5	1.0	2.0	5.0	20.0
Carrier					
Perchloroethylene	120.0	121.6	80.4	107.1	143.5
Kerosene	51.1	36.9	58.3	73.5	66.5
Escaid 100	62.5	52.0	75.6	78.1	83.0
Norpar 12	44.0	62.1	55.8	66.7	43.0
Chevron 3	58.9	56.3	54.2	150.0	196.7

Influence of Equilibrium pH

The diluents do not seem to shift the extraction isotherms to lower pH's. All variations found were well within the experimental error, with the exception of iron. (See Table 4).

TABLE 4
IRON EXTRACTION (%)

Equilibrium pH	Escaid 100	Norpar 12	Kerosene	Perchloro- ethylene
1.3	0.55	0.45	0.7	0.40
1.4	0.75	0.75	0.9	0.40
1.5	1.10	1.30	1.3	0.35
1.6	1.50	2.50	2.5	0.40

Temperature, Mixing Speed

No significant differences were found among the diluents tested between 15° and 30°C. The same applies for variation in mixing speed. It is to be noted that mixing speed below 500 rpm ($N^3D^2 < 20$) decreases the copper extraction efficiency to a considerable extent.

Phase Separation

A series of phase separation tests was made according to a published procedure⁴. Two leach concentrations were selected, namely 5 and 1 g/l of copper. (See Table 5). The mixing time allowed the phases to be at equilibrium. Except for Chevron 3, all organics were loaded at approximately the same level (2.12 g/l copper for the 5 g/l feed, 0.95 g/l copper for the 1 g/l feed).

TABLE 5
PHASE SEPARATION
LIX 64N - 10 Vol. %; O/A Ratio 1/1.
At Equilibrium. pH of Feed 2.0.

Separation Time (Perchloroethylene = 100 in each case)		
Diluent	Cu - 5 g/l Feed	Cu - 1 g/l Feed
Escaid 100	146	---
Norpar 12	133	135
Kerosene	219	173
Chevron 3	187	133
Perchloroethylene	100	100

Results in Table 5 show that the higher the loading, the bigger the difference in settling rates. Phase disengagement with perchloroethylene was fastest in all cases with improvements between 30 and 120%. This, together with faster kinetics, could lead to reduced inventory or higher throughput for existing facilities.

Effect on Stripping

The density differences between the strip solution and the various solvents is much closer than for the extraction stage. Differences are comparable (from 0.27 to 0.40). One would thus expect no major differences in phase separation times. Surprisingly, tests did not verify this. Figure 4 shows the influence of the

acidity of strip solutions for different diluents (10 vol. % LIX 64N). Why the differences in phase separation times do not taper off with increased acid strength of the strip solution is unexplained. Tests at 2 and 20 vol. % LIX 64N showed the same trend with the difference markedly higher for 20 vol. % LIX 64N.

Kinetics of stripping was satisfactory for all diluents tried. Perchloroethylene looks slightly slower than kerosene and Norpar 12 but is comparable to Escaid 100. Stripping efficiency at equilibrium is 2% better with perchloroethylene than with the former diluents and 3% better than with the latter one. (See Figure 5).

Stripping efficiency is slightly worse at low mixing speeds and slightly better at high mixing speeds, break-even point being around 1250 rpm. (See Figure 6).

At all temperatures tested, perchloroethylene shows a slight advantage over the other diluents tested for stripping efficiency.

Solvent Losses - Recovery Systems

Even though solubility of perchloroethylene in water at 25°C is around 150 mg/l, extensive test work on solubility losses indicated losses in the 30 to 70 mg/l range. The relative initial cost of the solvent makes it economical to recover as much solvent as possible. Extensive data are available from the food and metal cleaning industries where such solvent recovery systems are widely used.^{5,6,7}

Most of the solvent losses will occur through vaporization above the mixers. The high density of perchloroethylene vapors (5.76 x heavier than air) facilitates the recovery. As most of the existing mixer-settlers are covered for dust and sun protection, fairly little additional costs are involved. Airtight structures are not a must. A good ventilation system to slowly remove the saturated vapor, coupled with a recovery system, would bring the total solvent losses by evaporation to a very low level.

Several recovery systems of perchloroethylene are acceptable.

They are based on one of the two following principles:

- condensation on cool surfaces
- adsorption on hydrophobic substances.

The latter also has the advantage of reducing losses in liquids below solubility points. It could thus be used to minimize the evaporation losses and the entrained and solubility losses.

Condensation System

All that is needed is to have an air stream going through a water-cooled jacket. The solvent is condensed and sent to a water separator, after which the solvent can be reintroduced into the circuit. Typical water separators, as used in metal cleaning, are shown in Figure 7 and Figure 8.

Adsorption System

Perchloroethylene and the additive inhibitors are readily adsorbed on activated carbon or any other hydrophobic material such as polystyrene beads or polyurethane foam. These products absorb many times their own weight in perchloroethylene. Usually a dual unit, fixed-bed system is used, one being in the adsorption cycle and the other being in the desorption cycle. Desorption is carried out by steaming or heating the loaded adsorbent. The solvent is recovered by a condenser. (See Figure 9). Typical operating costs for these units are between two and four cents per gallon of solvent recovered; thus, they are considerably below the costs of the solvent.

Materials of Construction, Toxicity, Safety

Materials of construction suitable for perchloroethylene are well known and range from steel to various plastic materials. Polypropylene, certain epoxy resins, Saran®, Kynar®, Penton®, Teflon®, and polyamides are some of these materials. Stainless steel is, of course, widely recommended.

Toxicity data on perchloroethylene show the TLV (Threshold Limit Value) to be 100 ppm. Handling of perchloroethylene does not present any particular problem except to avoid breathing the vapor repeatedly or continuously. It is already widely used in industry.

Conclusions

Preliminary batch test data show that perchloroethylene could be considered as a suitable diluent for solvent extraction of metals. It has the following main advantages:

- slightly better kinetics
- faster phase disengagement
- higher iron rejection
- better stripping efficiency
- non-flammability

Its relatively high cost, coupled with higher evaporation rates and high volatility, make it necessary to recover the solvent completely through condensation or adsorption recovery systems. Costs of recovery are estimated to be around two to four cents per gallon.

Acknowledgment

The authors wish to thank the Functional Products and Systems Management of Dow Chemical U.S.A., an operating division of The Dow Chemical Company, for the permission to present this paper and for their support in the work.

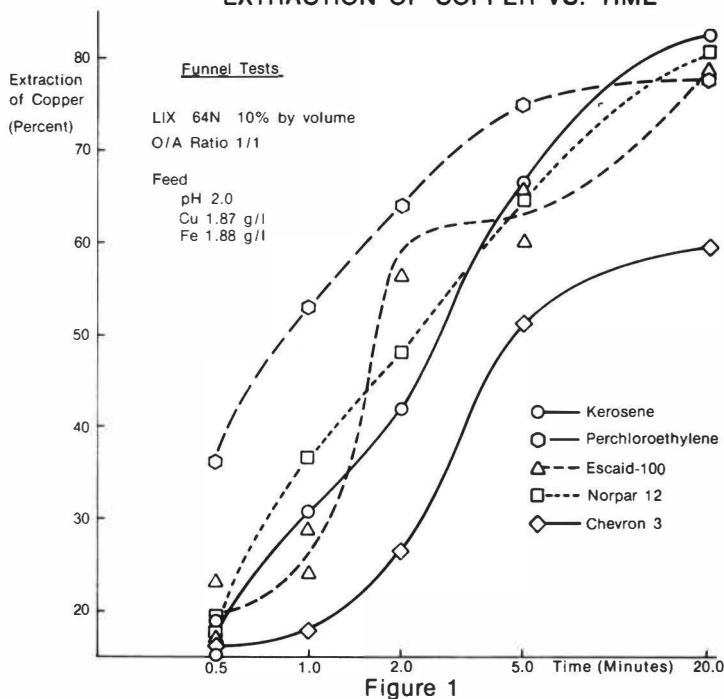
Notice

The information in this paper is presented in good faith, but no warranty, expressed or implied, is given nor is freedom from any patent owned by The Dow Chemical Company or by others to be inferred.

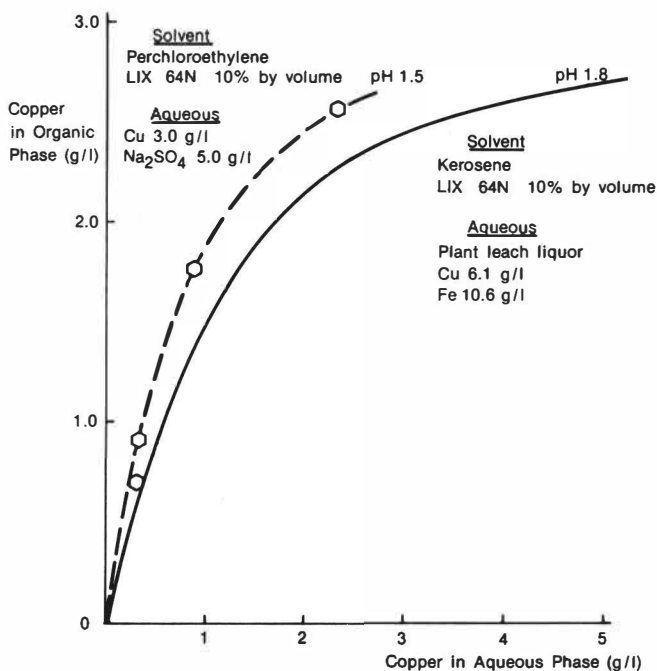
Literature References

1. Six Carrier Solvents. K. J. Murray and C. J. Bouboulis
Symposium on Solvent Ion Exchange. Arizona - 1973.
2. Cyclone Separators for Solvent Extraction in Metallurgy.
James K. Kindig, Wayne C. Hazen. Transactions of the
Society of Mining Engineers of the AIME. p. 68-71,
March 1971.
3. Heavy Liquids for Mineral Beneficiation. E. C. Tveter,
W. L. O'Connell.
4. Phase Separation Test for Liquid Ion Exchange Systems.
R. R. Swanson, L. T. Ditsch. Annual Meeting AIME, 1972.
5. Food Processing with Chlorinated Solvents. J. F.
Valle-Riestra. 33rd Annual Meeting of the Institute of
Food Technologists.
6. Dow Brochure 100-61-69 on Dow-per Solvent Cleaning.
7. Perchloroethylene Vapor Degreasing.

EXTRACTION OF COPPER VS. TIME



EXTRACTION ISOTHERMS



EXTRACTION OF IRON VS. CONCENTRATION OF EXTRACTANT

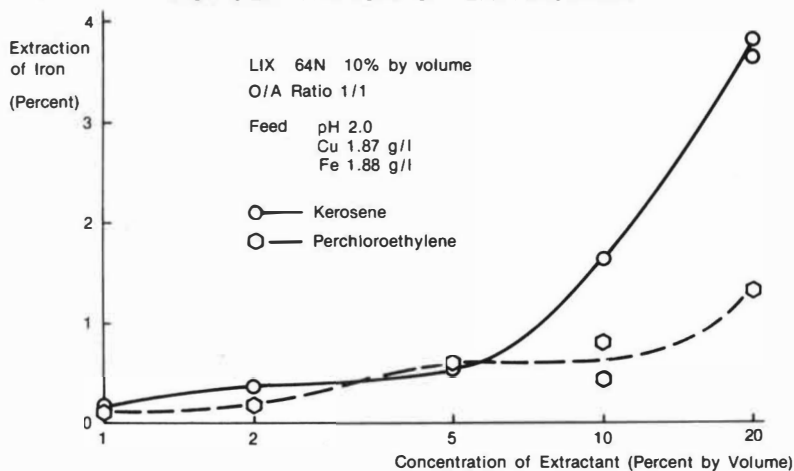


Figure 3

PHASE SEPARATION - STRIPPING

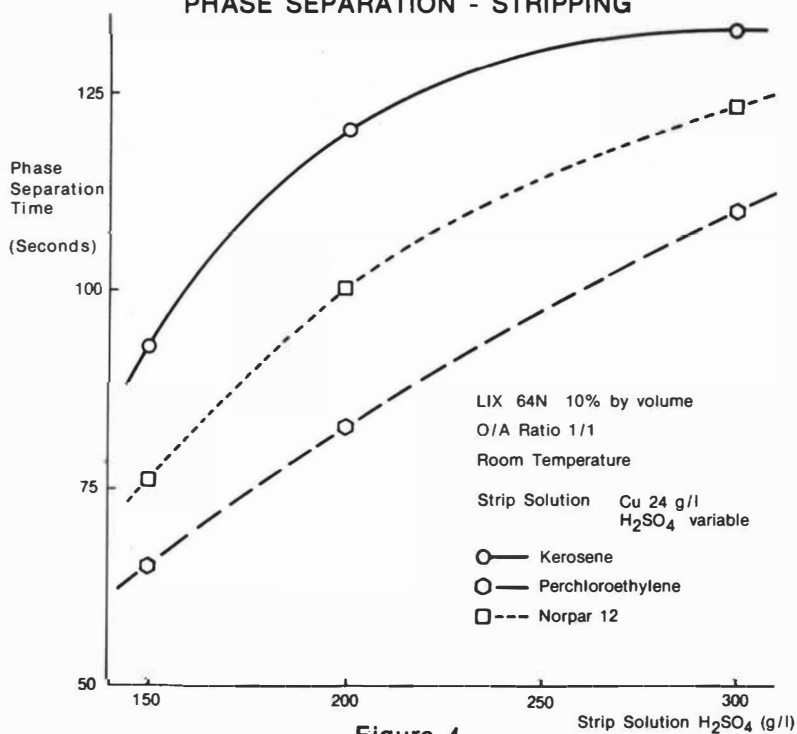


Figure 4

STRIPPING OF COPPER VS. TIME

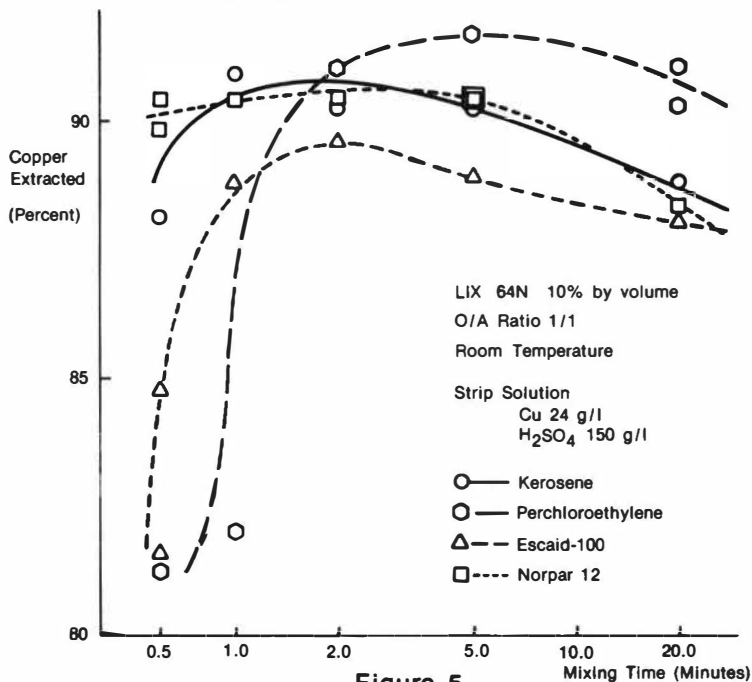


Figure 5

STRIPPING OF COPPER VS. MIXING SPEED

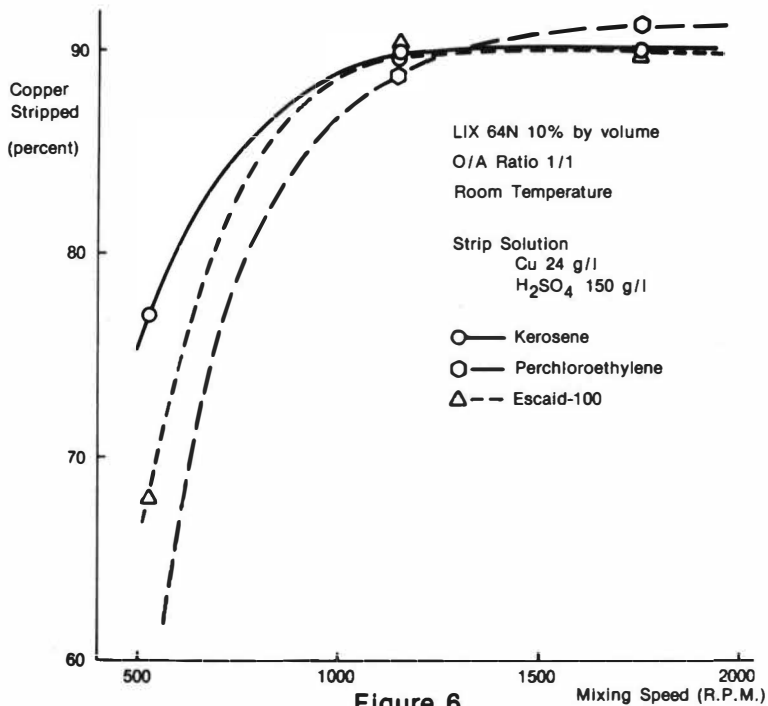


Figure 6

WATER SEPARATOR

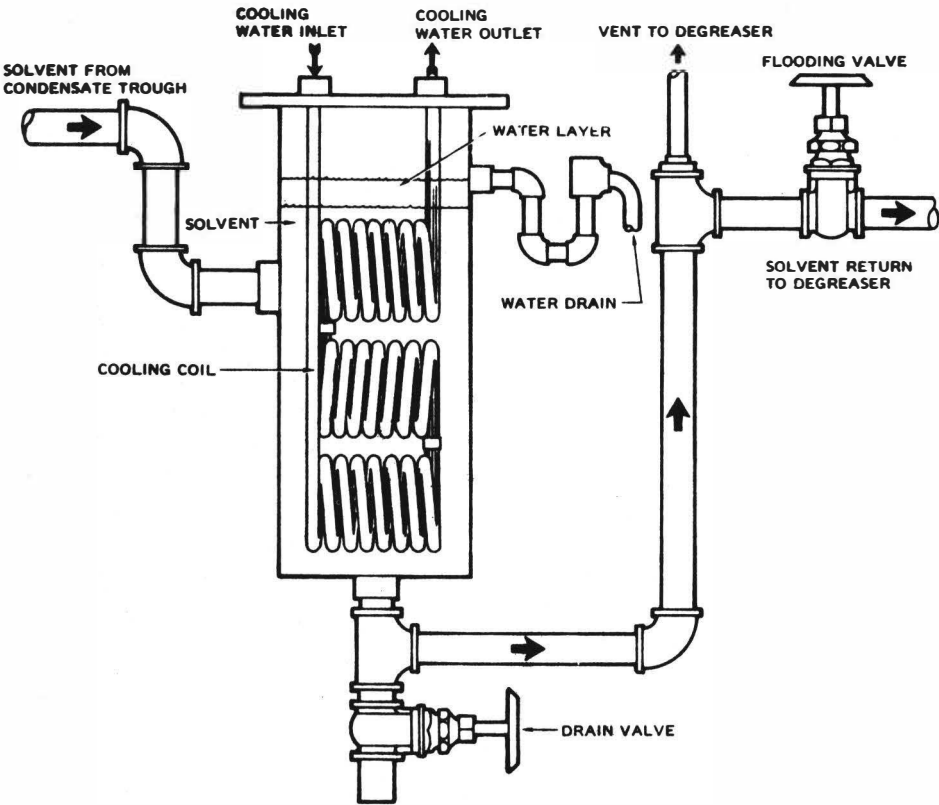
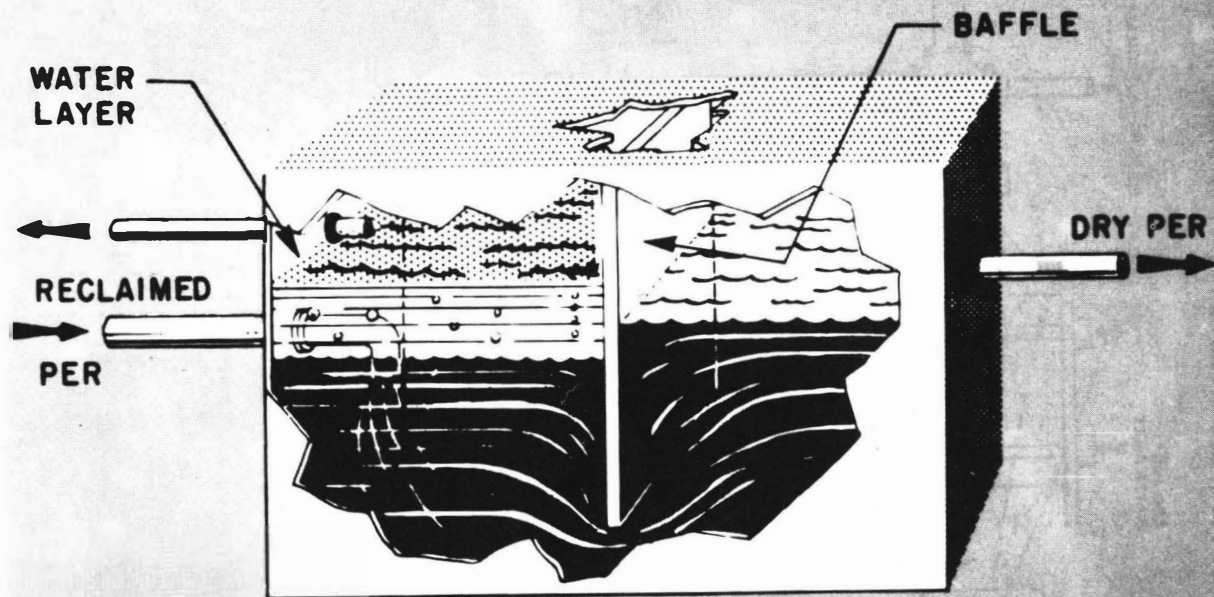


Figure 7



WATER SEPARATOR

Fig. 8

2-UNIT FIXED-BED ADSORBER

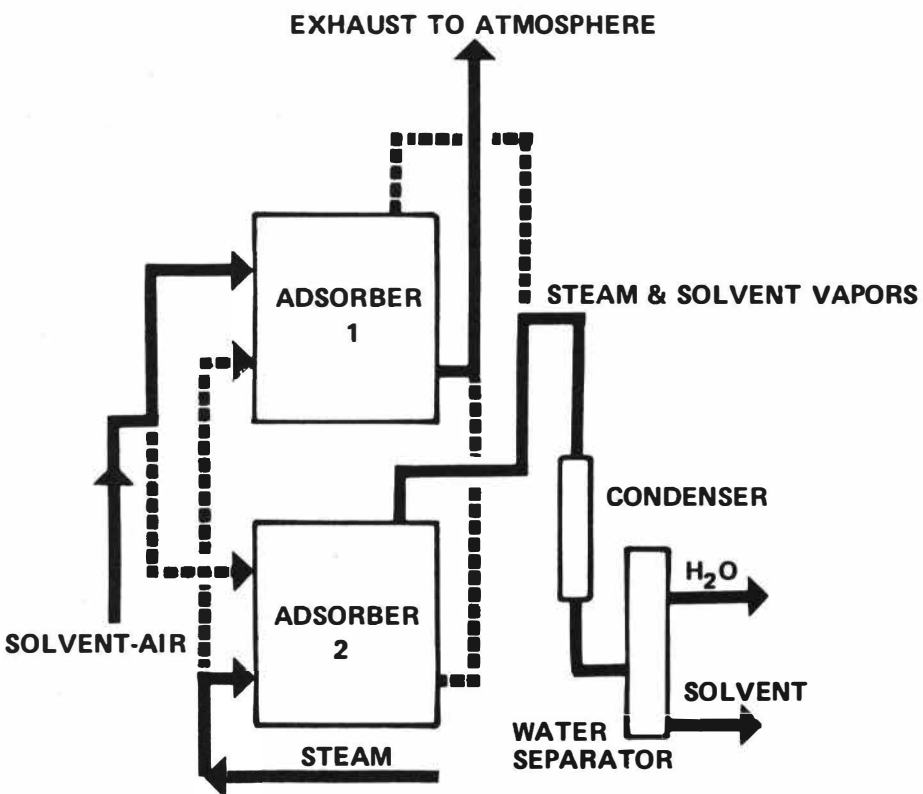


Figure 9



CORRELATION OF KELEX[®] COPPER DISTRIBUTION DATA

WITH EXTRACTION AND STRIPPING MIXER SETTLER

PERFORMANCE

J. A. Hartlage and A. D. Cronberg
Ashland Chemical Company
Research & Development
Dublin, Ohio U. S. A.

ABSTRACT

Kelex 100[®], an alkylated 8-hydroxyquinoline derivative, has been investigated to determine the effects of varying sulfuric acid concentration on copper distribution between organic and aqueous phases. The equilibria are plotted and correlated with mixer settler extraction and stripping data. Results are interpreted to explain the sulfuric acid stripping mechanism for the Kelex solvent system.

INTRODUCTION

For several years, Ashland Chemical Company has been active in studying and promoting the use of Kelex 100 as a metal extraction reagent. (1, 2) Spink and Okuhara (3) have measured distribution coefficients and have published preliminary kinetic data for Kelex. Ritcey and Lucas have investigated the use of Kelex on high copper feeds along with some preliminary data on extraction of other transition metals. (4, 5) Lakshmanan and Lawson have studied the use of a Kelex-Carboxylic acid system for extraction of nickel and cobalt. (6)

Work to date on copper feed solutions has demonstrated that the Kelex system is extremely efficient in extracting copper and, on the other hand, very efficiently stripped with sulfuric acid. This report contains results of mixer-settler studies and compares them with static extraction data in which both acid and copper equilibria are measured. Results are used to mechanistically interpret mixer-settler performance data.

EXPERIMENTAL

Reagents: Production samples of Kelex 100 were diluted with nonylphenol modifier and Escaid 100, a carrier solvent product from Exxon. Solvents for static tests were

conditioned by two 2-minute contacts with 10% sulfuric acid solution containing 0.5 gpl copper. The solvent, employed in the continuous mixer-settler operation, was circulated for the equivalent of two passes through the extraction and stripping system before profiles were measured. Copper bearing solution for the first solvent extraction test (Figure 2) was an actual vat leach solution. The other feed solutions used (Figures 3 to 5) were synthetic.

Analytical: Distribution ratios were determined by iodometric titration of aqueous copper samples. Organic copper content was measured by stripping all of the copper from the organic phase with two contacts of 10 vol % sulfuric acid, followed by iodometric titration. Organic acid concentrations were measured by scrubbing 10 ml aliquots of solvent with 3 successive 20 ml water washes. Sulfuric acid was then titrated with standardized potassium hydroxide solution.

Profile analyses for the copper extraction and stripping equilibria in continuous operation were

measured in a way similar to that described
above for static determinations.

EXTRACTION-STRIPPING COPPER DISTRIBUTIONS

A conditioned solvent of 15% Kelex 100 and 20% nonylphenol in Escaid 100 was contacted with copper solutions designed to simulate the copper content present in extraction and stripping during mixer settler operation. Figure 1 shows a plot of the copper distribution measured between 10 and 200 gpl sulfuric acid at 35° C. This plot of data obtained with 12 gpl aqueous copper for extraction and 30 gpl aqueous copper for stripping exhibits a smooth curve throughout the entire acid range studied, indicating that the copper distribution throughout the low pH region investigated is more strongly controlled by the sulfuric acid content of the aqueous phase than the copper concentration. Data points taken from mixer settler operation are also indicated on the plot to show the agreement with mixer settler data.

LABORATORY SCALE SOLVENT EXTRACTION

CIRCUIT RESULTS

Figures 2, 3, 4 and 5 show S-X circuit profiles of laboratory tests that were run on a 33 gpl copper feed as well as two additional high copper leach solutions. All tests were run using 15% Kelex -

20% nonylphenol solvent having a copper loading capacity of 12 gpl. The total flow to the extraction mixers was adjusted to 200 cc per minute in order to maintain 2-minute mixing residence time or twice the residence time required as indicated in static tests. (2) Each extraction and stripping stage was operated under organic continuous condition and no recycles were used.

The circuit profiles show the excellent copper recovery that is possible with Kelex 100 on high copper feed solutions. Note Figure 2 which demonstrates a 0.27 gpl copper raffinate from a 33 gpl copper feed is achievable. Similar excellent recovery results are indicated in Figures 3, 4 and 5. Note also, the surprisingly efficient reaction reversal achieved in stripping. Figure 4 indicates 93% of the copper was removed from loaded organic while producing 33.5 gpl copper pregnant electrolyte containing only 111 gpl sulfuric acid. Extraction and stripping stages were maintained at greater than 30°C in order to facilitate phase separation and increase the rate of approach to copper equilibrium. Most data were gathered from mixer settlers operated at $35 \pm 3^\circ \text{C}$.

Returning to Figure 1, it is evident that in spite of the potential problems of mixer channeling and variability introduced by temperature differences, the correlation between static and continuous data is fairly good. The only mixer-settler data omitted from the figure are those obtained in final extraction stages where insufficient copper was available to allow the reagent to approach copper loading equilibrium.

EXTRACTION-STRIPPING ACID DISTRIBUTION

Figure 6 shows a plot of organic acid content vs aqueous sulfuric acid for the same solvent as used for Figure 1, again using solutions designed to simulate feed and strip copper-acid concentrations. This plot illustrates that the reagent is being significantly protonated in the same acid content region of the graph as found for copper stripping. Thus, the slope of the copper distribution line of Figure 1 is steeper than would be anticipated had the reagent not been protonated. The amount of organic acid found in mixer-settler operation is represented by the numbered data points of Figure 6 and again a good correlation between static and continuous data is evidenced. Noteworthy also, from an operational standpoint, is that the greatest degree of change in protonation and copper extraction occurs in the range of 25 gpl to 150 gpl H_2SO_4 .

In order to explain the interrelation between copper and H_2SO_4 extraction from a mechanistic standpoint, a series of static equilibria were run using a 13% Kelex 100, 16% Nonyl Phenol, 71% Escaid 100 solvent. After conditioning by two acid and three water washes, 50 ml aliquots of solvent were contacted for two minutes with 50 ml aqueous solution samples containing 10.45 gpl copper and 1 gpl to 400 gpl sulfuric acid. The copper-acid distribution data were determined and plotted as shown in Figures 7 & 8.

The acid-copper dependency was similar to that found in previous tests which correlated well with mixer-settler results. When copper equivalents and acid molarities were plotted versus aqueous sulfuric acid content as shown in Figure 9, the extraction-stripping mechanism of Kelex was varified. The reagent loaded copper quite efficiently until the aqueous sulfuric acid content approached 75 gpl, at which point the reagent became increasingly protonated while the copper extraction rapidly decreased through an aqueous sulfuric acid content of 100 gpl. As the

aqueous acid concentration was again increased, the degree of reagent protonation became more complete, forcing more copper from the reagent-complexed state into the aqueous phase. As the acid concentration approached 400 gpl the 8-hydroxyquinoline derivative was completely protonated with one mole of sulfuric acid per mole of reagent.

Discussion:

From the distribution data measured and reported here it is clearly determined that the equilibrium position of the extraction equation for Kelex lies far to the right at acid concentrations less than 25 gpl H₂SO₄.

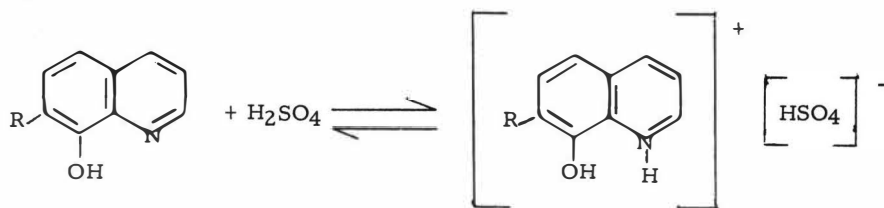
Equation:



RH = KELEX 100 = 7 alkenyl-8-hydroxyquinoline

As the acid concentration of the aqueous phase is increased, it drives the reaction to the left reducing the distribution of copper in the organic phase. In addition to this reversal of the extraction reaction, the basic nitrogen of the 8-hydroxyquinoline derivative becomes increasingly protonated at higher acid concentrations.

Equation 2:



R = C12 to C16 alkenyl

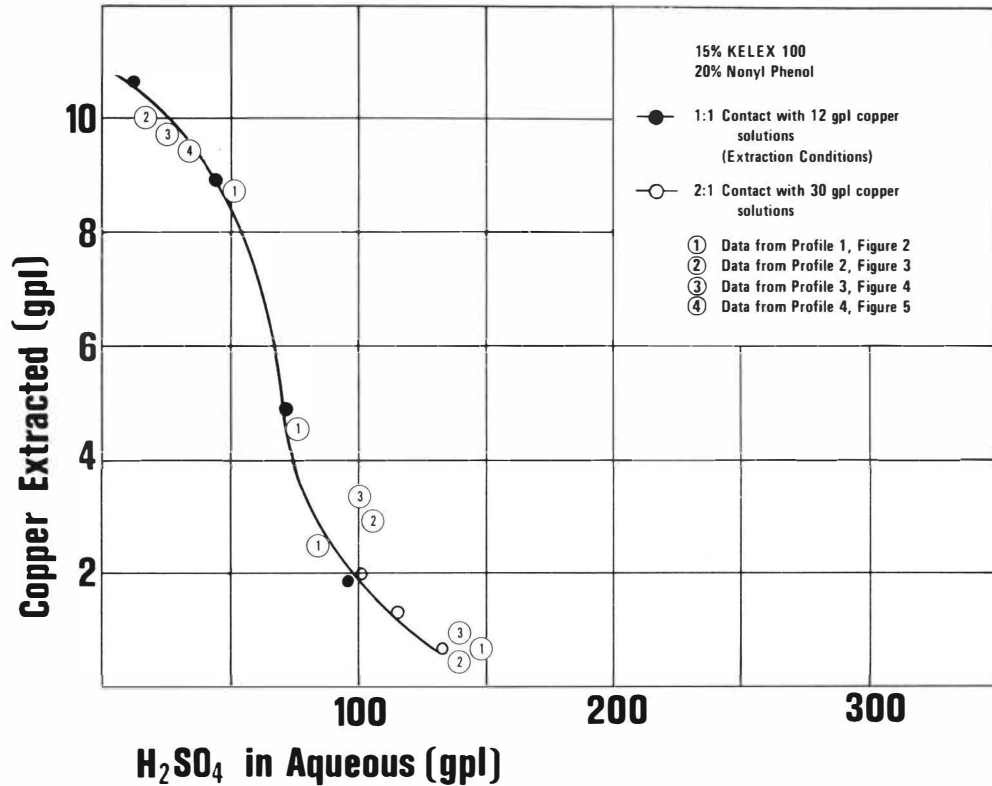
This reaction effectively reduces the RH concentration of equation 1 and drives the equilibrium of the reaction still further left. The result of protonation is that the amount of copper extracted (Equation 1) from acid solutions greater than about 50 gpl H_2SO_4 is strongly influenced by reagent protonation (Equation 2).

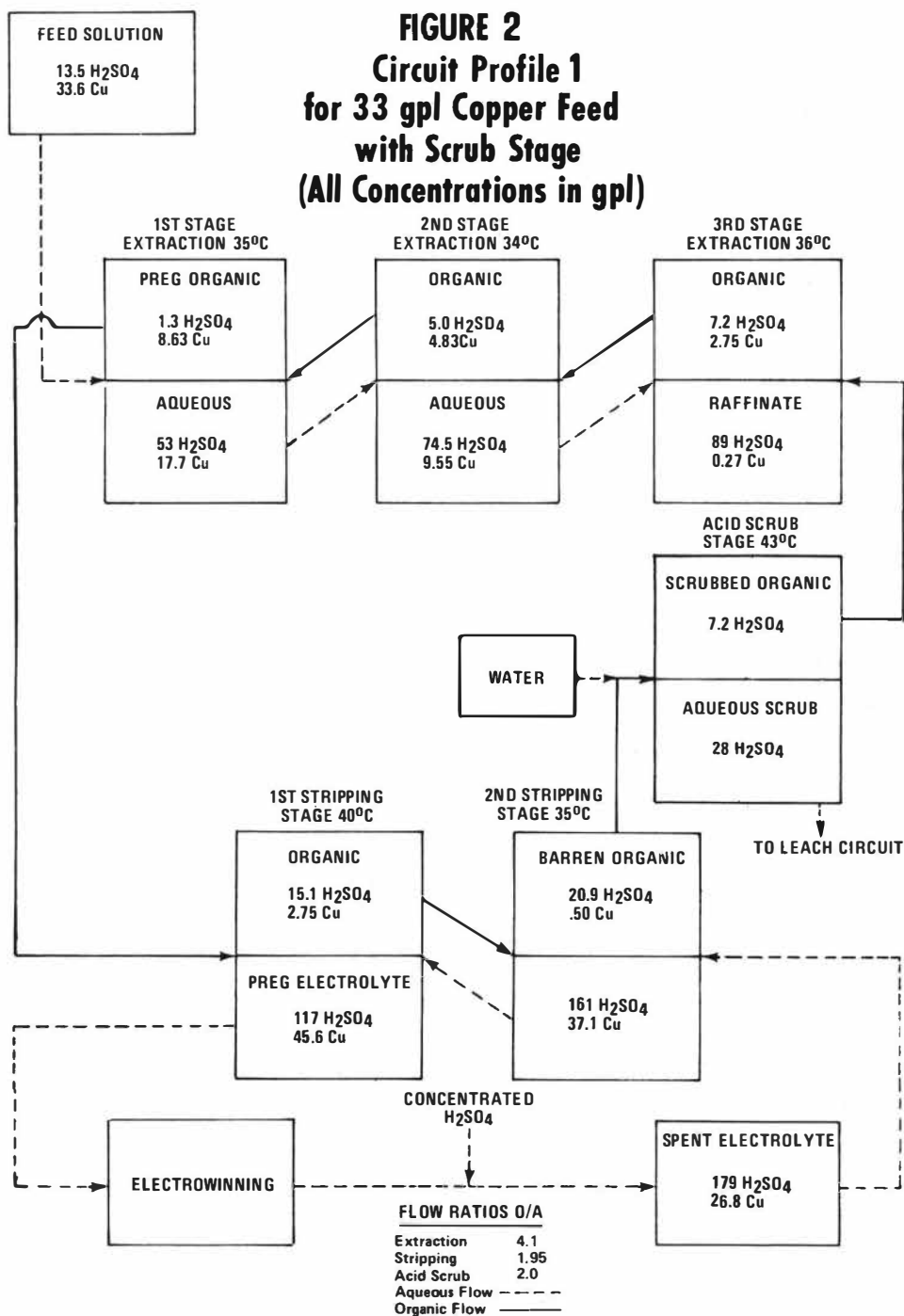
When utilized in a continuous extraction-stripping process the reagent is thus efficient in extraction until the aqueous acid concentration reaches about 75 gpl, at which point protonation becomes significant. When the equilibrium aqueous acid concentration is 125 gpl or greater the reagent is sufficiently protonated to cause efficient stripping of organic copper. Thus the reagent extracts well at low pH, but, because of protonation, is very efficiently stripped at low stripping acid levels.

REFERENCES

- 1) J. A. Hartlage, paper presented to the SME Fall Meeting, September, 1969. Salt Lake City, Utah.
- 2) Hartlage, J. A. and Cronberg, A. D. Paper presented to the Annual Conference of Metallurgists, CIMM, Quebec City, August, 1973.
- 3) D. R. Spink and D. N. Okuhara. Int. Symposium on Hydrometallurgy, AIME eds, D. J. L. Evans and R. S. Shoemaker, pp 497-534 (1973).
- 4) Ritcey, G. M., "Recovery of Copper from Concentrated Solution by Solvent Extraction using Kelex 100", presented at 2nd Hydrometallurgy Conference of the Hydrometallurgy Group of CIM, Montreal, Quebec, October, 1972.
- 5) Ritcey, G. M. and Lucas, B. H. Paper presented to the Annual Conference of Metallurgists CIMM, Quebec City, August, 1973.
- 6) Lakshmanan, V. L. and Lawson, G. J. Journal of Inorganic and Nuclear Chemistry 35, 4285 (1973).

Copper Extraction vs Aqueous Acid Using Simulated Electrolyte-Feed Copper Solutions





FEED SOLUTION

14.01 gpl Cu
2.8 gpl H₂SO₄
78 ml/min

FIGURE 3 Circuit Profile 2 14 gpl Copper Feed with Scrub Stage (All Concentrations in gpl)

TO LEACHING

1ST STAGE EXTRACTION 39°C

PREG ORGANIC

2.7 H₂SO₄
9.68 Cu

AQUEOUS

23.1 H₂SO₄
4.40 Cu

2ND STAGE EXTRACTION 43°C

ORGANIC

5.5 H₂SO₄
3.56 Cu

RAFFINATE

32.8 H₂SO₄
0.18 Cu

ACID SCRUB STAGE 54°C

SCRUBBED ORGANIC

9.4 H₂SO₄

AQUEOUS

41.1 H₂SO₄

WATER

1ST STAGE STRIPPING 35°C

ORGANIC

16.1 H₂SO₄
2.95 Cu

PREG ELECTROLYTE

107 H₂SO₄
36.7 Cu

2ND STAGE STRIPPING 33°C

PREG ELECTROLYTE

21.6 H₂SO₄
43 Cu

STRIP

147 H₂SO₄
25.7 Cu

CONCENTRATED
H₂SO₄

ELECTROWINNING

SPENT ELECTROLYTE

175 H₂SO₄
20.1 Cu

FLOW RATIOS O/A

Extraction 1.49
Stripping 1.97
Scrub 2.76
Aqueous Flow - - - - -
Organic Flow ————

FIGURE 4

Circuit Profile 3...14 gpl Copper Feed without Scrub Stage (All Concentrations in gpl)

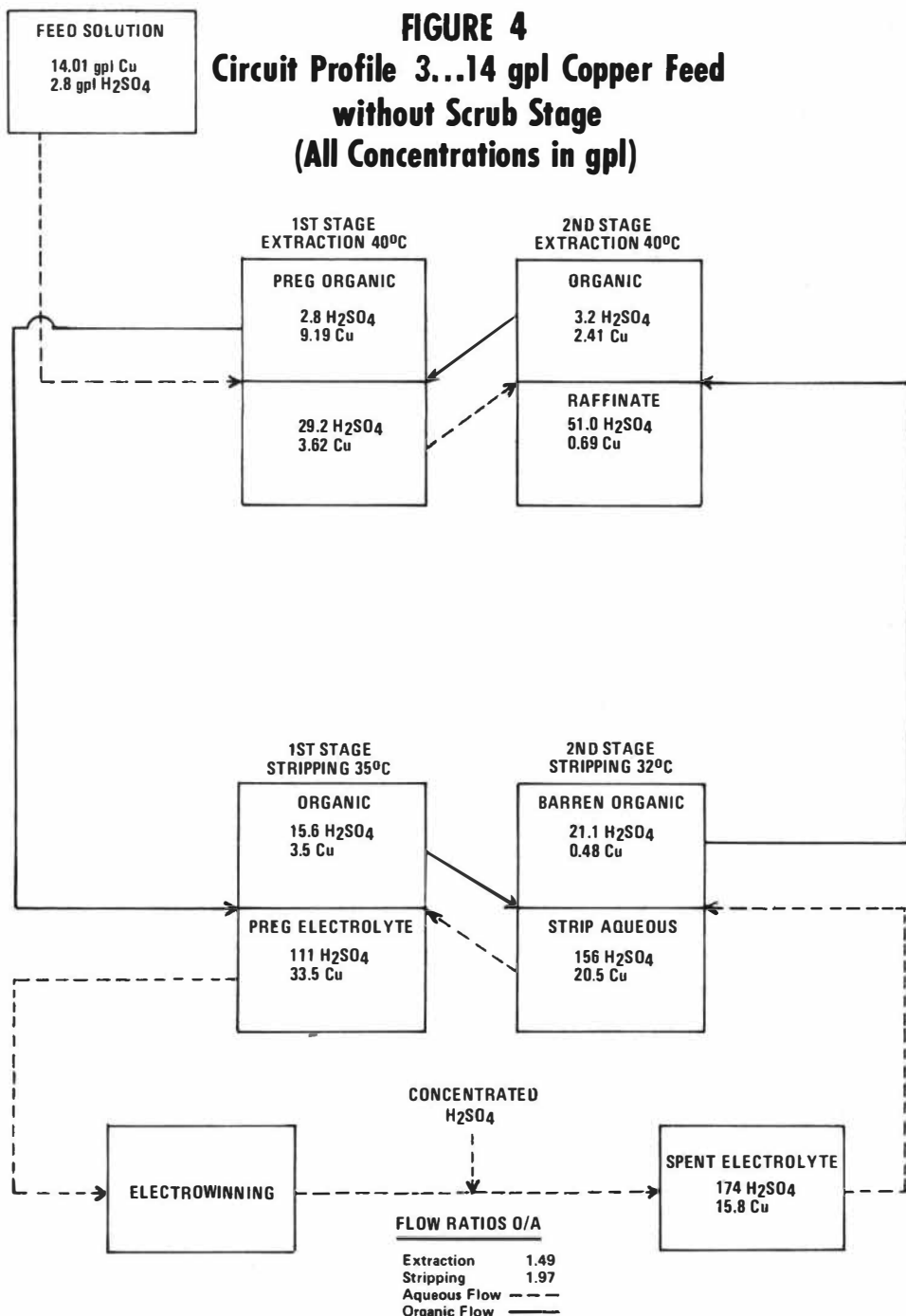
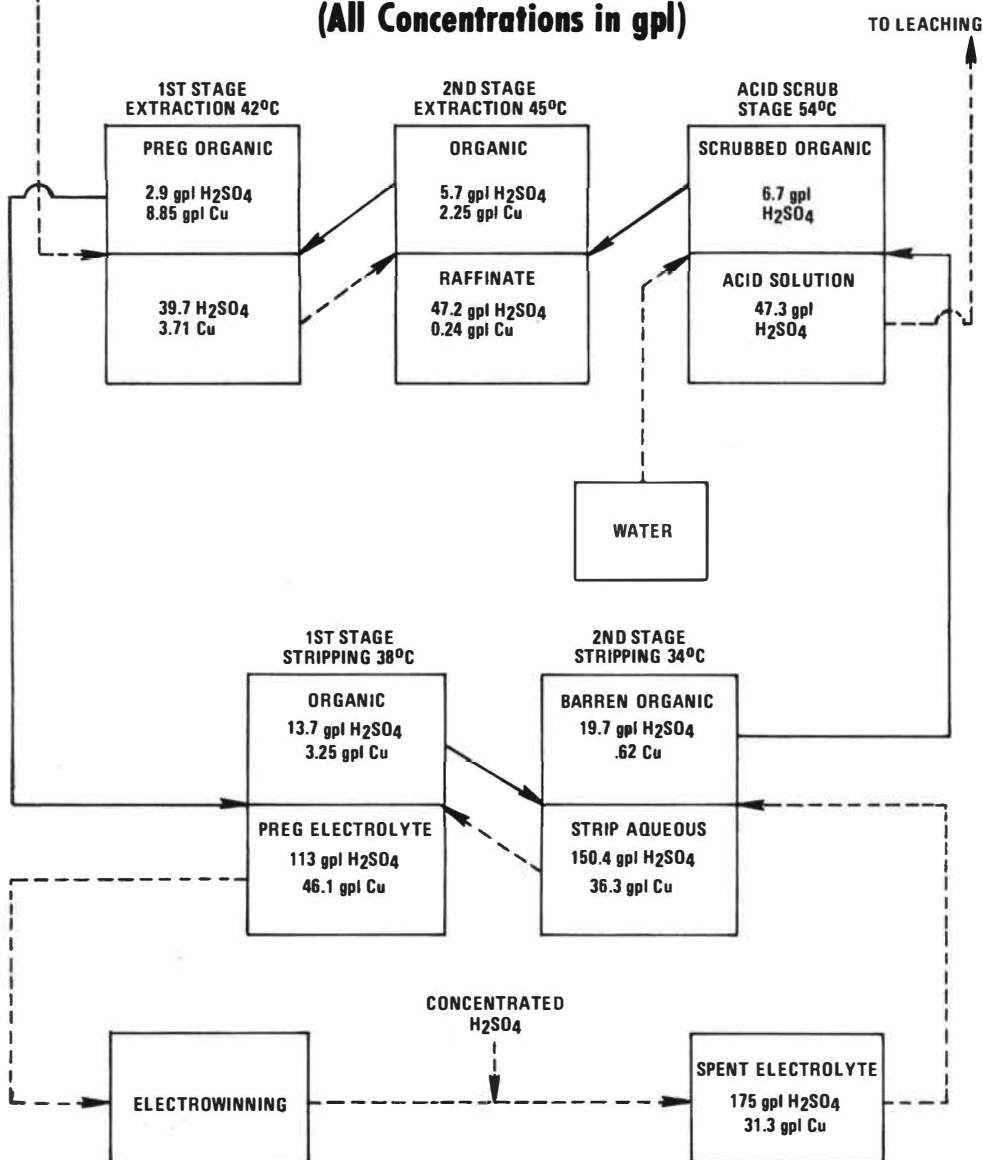


FIGURE 5
Circuit Profile 4
19.8 gpl Copper Feed
(All Concentrations in gpl)

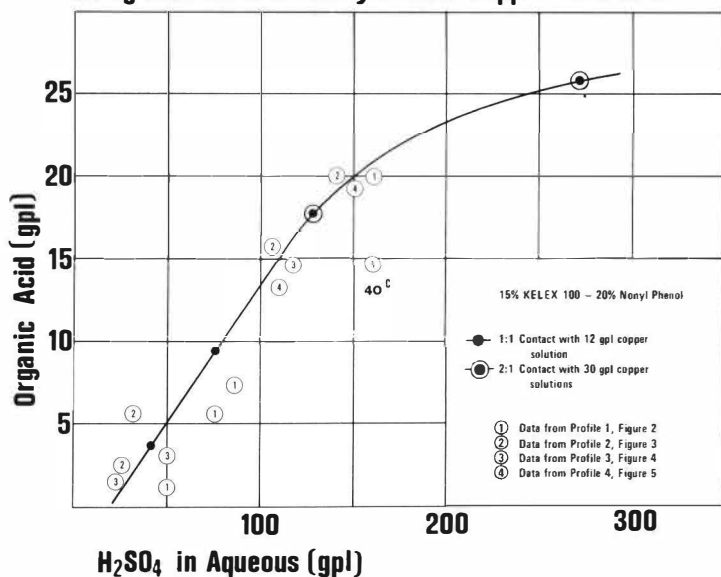


FLOW RATIOS O/A

Extraction	2.37
Stripping	2.09
Scrub	3.41
Aqueous Flow	----
Organic Flow	———

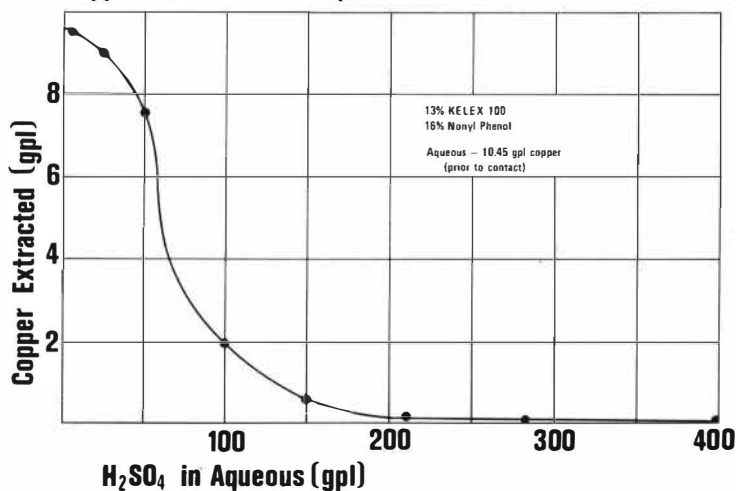
6

Organic Acid vs Aqueous Acid Using Simulated Electrolyte-Feed Copper Solutions



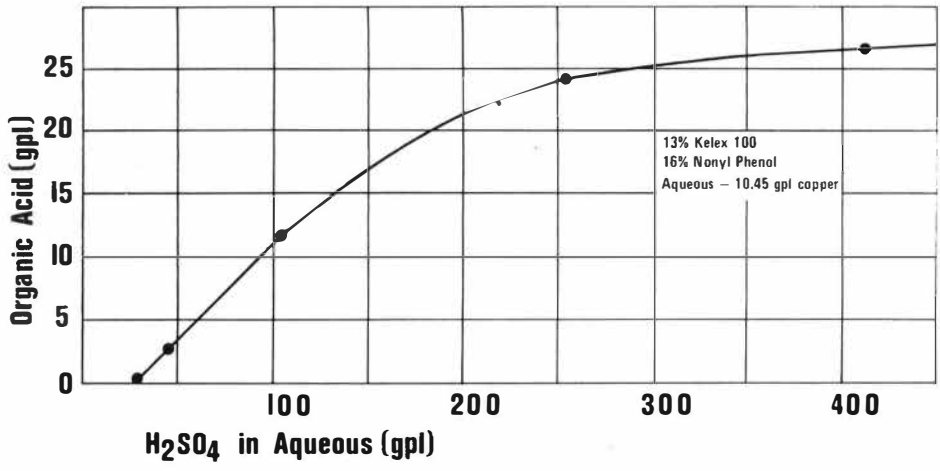
7

Copper Extraction vs Aqueous Acid



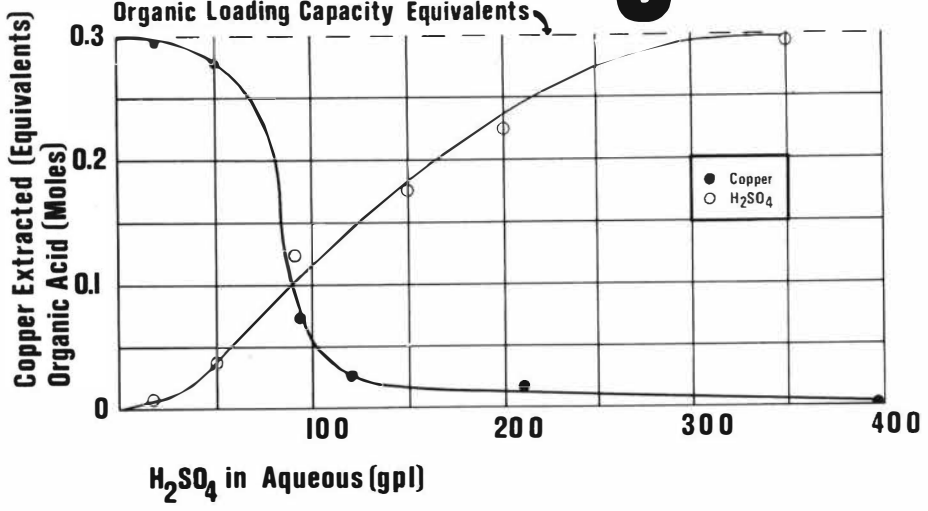
8

Organic Acid vs Aqueous Acid



9

Acid-Copper Extraction vs Aqueous Acid Organic Loading Capacity Equivalents





SESSION 7

Tuesday 10th September: 9.00 hrs

C H E M I S T R Y O F E X T R A C T I O N

(Common Metals)

Chairman:

Professor J. Rydberg

Secretaries:

Dr. G.J. Lawson

Dr. H. Latreille



ACIDIC ORGANOPHOSPHORUS EXTRACTANTS - XXII. COMPLEXES OF SOME
BIVALENT TRANSITION METALS WITH DI(2-ETHYLHEXYL) PHOSPHORIC
ACID IN HIGHLY LOADED ORGANIC PHASES

R. Grimm and Z. Kolarík

Institut fuer Heisse Chemie, Kernforschungszentrum Karlsruhe,
Federal Republic of Germany

Abstract: Macro amounts of Zn(II) and Cu(II) are extracted by di(2-ethylhexyl) phosphoric acid (HA) in aliphatic diluents up to a metal to HA ratio of 1/2. The exchange of Zn(II) and Cu(II) in the highly loaded organic phase for Cd^{2+} , Cu^{2+} , H^+ and Na^+ and the nature of extracted Zn(II) and Cu(II) complexes were studied by distribution measurements, absorption spectroscopy, vapour-pressure osmometry and Karl-Fischer titration. Complexes of the type $(\text{ZnA}_2)_n$ and $(\text{CuA}_2)_n$ are not hydrated in dodecane and at 45°C the n value of the former in n-hexane is 3, while $n = 2.4 - 3.5$ was found for the latter in dependence on its concentration. The formation of mixed complexes of the type $\underline{x}\text{ZnA}_2.\underline{y}\text{CuA}_2$ in n-dodecane is indicated by spectrometric data.

INTRODUCTION

Extractant properties of di(2-ethylhexyl) phosphoric acid (HDEHP) have been studied predominantly in systems with trace metals, where complexes of the type $\text{MA}_{\underline{z}}.\underline{x}\text{HA}$ are formed in most cases¹ (HA is the monomeric molecule of HDEHP and $\underline{z} = 1-3$). Little is known about systems with the organic phase loaded so highly that, due to the lack of free HDEHP, \underline{x} is reduced to zero. Undoubtedly, polymeric metal complexes of HDEHP are formed in such cases. Trivalent metals like lanthanides(III)

and Fe(III) deposit as solid compounds of the type $(MA_3)_n$ (see e.g.² and the literature cited therein). On the other hand, bivalent metal cations can load HDEHP solutions practically to the limiting ratio of $M(II)/HDEHP = 1/2$ without any considerable precipitation and under a viscosity increase only; this has been reported for cations as different as UO_2^{2+} 3, Sr^{2+} 4, Co^{2+} 5,6, Cu^{2+} 6,7, Zn^{2+} 7 and Ni^{2+} 6. Since information on the properties of highly loaded organic solutions of HDEHP is of importance for some applications, e.g. in hydrometallurgical processes, we attempted to contribute to the knowledge of the behaviour and nature of complexes formed by Zn(II) and Cu(II) with HDEHP in n-alkane solutions. This paper is a preliminary report on the results of a more extended study.

EXPERIMENTAL

Stock solutions of Zn(II), Cu(II) and Cd(II) perchlorates were prepared by the reaction of excess metal oxides with perchloric acid and had pH 3-4.5. To prepare solutions of Zn(II) and Cu(II) complexes of HDEHP with the metal to HDEHP ratio of 1/2, a dodecane solution of HDEHP was first shaken with excess aqueous NaOH and the two organic phases obtained were then shaken with an aqueous solution containing excess Zn(II) or Cu(II) nitrate or sulfate. A single organic phase was so obtained and shaken twice more with aqueous Zn(II) or Cu(II). To analyze the solutions, the metal was stripped from an aliquot by dilute nitric acid and determined by standard complexometric or iodometric methods, while HDEHP was titrated in the unloaded organic phase (diluted with acetone and water) with aqueous NaOH.

HDEHP was purified according to reference 8.

Distribution experiments were carried out at room temperature and in the usual manner. Samples of the rather viscous organic phase for the radioactivity measurement, as taken by automatic pipettes (Eppendorf), were not squeezed out from the one-way tips, but placed together with them in measuring flasks.

Vapour-pressure osmometric measurements were performed with an apparatus (Knauer) determining the temperature dependence between two thermistors with hanging drops, one of a solution of a metal HDEHP complex in n-hexane and the other one of pure n-hexane. The apparatus was calibrated with n-hexadecane as the standard solute.

Water was determined in n-dodecane solutions of the HDEHP complexes by the Karl-Fischer method. Visible and near infrared spectra were recorded by a Cary 17 apparatus. The radioactivity of ^{65}Zn , ^{109}Cd (both purchased from Amersham) and ^{64}Cu (obtained by the irradiation of metallic Cu with thermal neutrons) was measured by the automatic device BF 5000 G (Berthold-Friesecke) equipped with two NaI(Tl) crystals.

The total concentration of HDEHP in the organic phase, both free and bound to metals, will be denoted as \bar{C}_A and expressed in F units, i.e. monomer formula weights/l. Species and their concentrations in the organic phase will be denoted by a bar.

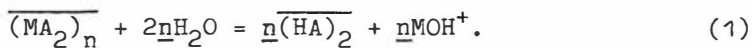
RESULTS AND DISCUSSION

To obtain data on distribution of metal species in a two-phase system with a highly loaded HDEHP solution, we used as the starting organic phase a dodecane solution of a complex $(\text{MA}_2)_n$ with $M = \text{Cu}$ or Zn . This was contacted with aqueous perchlorate solutions containing a constant amount of Na^+ and variable amounts of M^{2+} and N^{2+} , where $N = \text{Cd}$ or Cu . The star-

ting and equilibrium concentrations of single metal species in the phases are given in Table 1 for the M-N pairs Zn-Cd, Zn-Cu and Cu-Cd. The equilibrium pH value of the unbuffered aqueous phase could be only roughly estimated as ~ 5 , because no stable pH-meter reading could be achieved and an addition of a buffer would have distorted the picture by side complexing reactions. Nevertheless, the concentration of the hydrogen ions in the aqueous phase was negligible in comparison with the concentrations of metal ions M^{2+} and N^{2+} loading the organic phase, where the amount of hydrogen ions bound to HDEHP is comparable with or larger than that of N(II) and Na(I) and can be estimated by difference. The starting total amount of HDEHP could be assumed to remain in the organic phase. The aqueous solubility of $(NaA)_n$ is suppressed in the presence of sodium ions⁹ and a solubility still lower can be expected for $(MA_2)_n$.

The complex equilibrium with four mutually exchangeable ions, M^{2+} , N^{2+} , H^+ and Na^+ , cannot be treated as a simple M(II)-N(II) exchange. The separation factors $S_{M-N} = \frac{\bar{C}_M C_N}{C_M \bar{C}_N}$ are not constant with the exception of the system with M-N = Cu-Cd, where S_{Cu-Cd} seems to approach a constant value at low aqueous Cu^{2+} concentrations. It is worth noting that the extractability sequence $Zn(II) > Cd(II) > Cu(II)$ observed in a virtually noncomplexing nitrate medium with trace metals⁷ is converted here with macro amounts of the metals to $Zn(II) > Cu(II) > Cd(II)$. At $\bar{C}_A = 0.05F$ the loading of the organic phase by M(II), initially practically 100%, was lowered in the equilibrium to 80 - 95% and the corresponding amount of M(II) was then found in the aqueous phase; 1 - 2% of the loading capacity was occupied by Na(I). Since the concentration of N(II) in the organic phase was too low to fill the remaining capacity, a

fraction of HDEHP must be supposed to have existed in the acid form, most probably bound to M(II) in a complex of the type $\underline{M}_n - \underline{A}_m \underline{H}_{(m-2n)}$. The starting aqueous phase had a pH value of 3-4 and thus the hydrogen ions for the conversion of $(\underline{MA}_2)_n$ to $(\underline{HA})_2$ were most probably gained in the reaction



A small fraction of M^{2+} and N^{2+} was then hydrolyzed in the equilibrium aqueous phase, but did not exceed 5% in the system with $\text{M} = \text{Zn}$ and 6% in the system with $\text{M} = \text{Cu}$.

It is rather surprising that at $\overline{C}_A = 0.05F$ and with $\text{M} = \text{Zn}$ the organic Na(I) concentration decreases with decreasing concentration of Zn^{2+} in the aqueous phase, i.e. with increasing organic concentrations of $\text{N(II)} = \text{Cd(II)}$ or Cu(II) (Table 1). This cannot be explained so that N^{2+} substitutes not Zn(II) but Na(I) in the organic phase, because even the sum of the equivalents of N(II) and Na(I) in the organic phase decreases in the same direction as the Na(I) concentration.

A rather striking anomaly was observed with $\text{M-N} = \text{Zn-Cu}$ at $\overline{C}_A = 0.05F$: the organic Cu(II) concentration does not increase monotonously with the aqueous concentration of Cu^{2+} , but goes through a minimum (Table 1). A possible explanation would be that both Zn(II) and Cu(II) are bound in the organic phase in a mixed polymeric complex with HDEHP. Some evidence for this is given by visible and near infrared spectra of wet organic phases loaded with Cu(II) alone and Cu(II) and Zn(II) together. The absorption maximum of $0.012F (\underline{\text{CuA}}_2)_n$ in dodecane at 860 nm is shifted to 782 nm in the presence of $0.026F (\underline{\text{ZnA}}_2)_n$ and the absorption peak becomes rather flat (Fig. 1). At a constant $(\underline{\text{ZnA}}_2)_n$ concentration in dodecane, a decrease of the concentra-

tion of $(\text{CuA}_2)_n$, i.e. an increase of the Zn to Cu concentration ratio leads to an increasing shift of the absorption maximum of $(\text{CuA}_2)_n$ towards shorter wavelengths (Fig. 2).

The position of the absorption maximum of $(\text{CuA}_2)_n$ depends on the diluent nature (Fig. 3) and its wavelength increases in the order cyclohexane < carbon tetrachloride < chloroform < benzene, methyl isobutyl ketone < ethylhexyl alcohol < dodecane. A similar dependence of the absorption maximum on the diluent nature has been observed in Cu(II) complexes with complexing agents similar to HDEHP, namely carboxylic acids¹⁰. Absorption maximum of dimeric Cu(II) vinylacetate is shifted toward higher wavelengths in the sequence dichloromethane < acetone < benzene < methanol < ethanol and this has been ascribed to increasing effectiveness of the diluents as donors toward Cu(II). Molecules of the diluents are supposed to be bound to the Cu^{2+} central ion perpendicularly to the plane in which the four oxygens of the carboxyl groups are bonded to Cu^{2+} . This explanation appears to be plausible also for the spectra of $(\text{CuA}_2)_n$, with the exception of that in dodecane. Here the absorption maximum should have a similar wavelength as in the comparably inert cyclohexane, provided that $(\text{CuA}_2)_n$ has not any other configuration in dodecane than in other diluents. With dodecane diluent we found no maximum in the ultraviolet region down to 250 nm, where an absorption band characteristic for four- and five-coordinated Cu(II) should appear at about 370 nm¹¹. No effect of water on the spectrum of $(\text{CuA}_2)_n$ in benzene was observed. Let us note that our absorption maximum of $(\text{CuA}_2)_n$ in cyclohexane lies at a shorter wavelength than 755 nm, reported recently⁶.

The degree of the self-association, \underline{n} , of $(\text{ZnA}_2)_{\underline{n}}$ and $(\text{CuA}_2)_{\underline{n}}$ in n-hexane at 45°C, as determined by vapour-pressure osmometry, is given in Fig. 4 as a function of the concentration of the complexes. Whatever the reliability of the absolute \underline{n} values is, two tendencies are obvious: \underline{n} of the Cu(II) complex increases with its concentration, while the Zn(II) complex exhibits a constant \underline{n} value over the whole concentration range studied. This is in contradiction with the high viscosity of $>0.01\text{F}$ solutions of $(\text{ZnA}_2)_{\underline{n}}$ and rather low viscosity of a 0.1F solution of $(\text{CuA}_2)_{\underline{n}}$ in n-alkane diluents at the room temperature, and an extension of the vapour-pressure osmometric measurements to 25°C would be necessary to obtain a clearer picture. The value of $\underline{n} = 2.95$ should be mentioned, given for $(\text{CuA}_2)_{\underline{n}}$ in benzene⁶ without specifying the temperature and concentration.

We found no significant amounts of water coextracted with $(\text{ZnA}_2)_{\underline{n}}$ and $(\text{CuA}_2)_{\underline{n}}$ into dodecane. The absence of water in the extraction of Cu(II) as $(\text{CuA}_2)_{\underline{n}}$ with n-hexane has been already reported⁶.

REFERENCES

1. Peppard D. F. and Mason G. W., Nucl. Sci. Eng. 1963, 16, 382.
2. Harada T., Smutz M. and Bautista R. G., J. Chem. Eng. Data 1972, 17, 203.
3. Baes C. F., Jr., Zingaro R. A. and Coleman C. F., J. phys. Chem. 1958, 62, 129.
4. McDowell W. J. and Coleman C. F., J. Tenn. Acad. Sci. 1966, 41, 78.
5. Brisk M. L. and McManamey W. J., J. Appl. Chem. 1969, 19, 103.
6. Sato T. and Nakamura T., J. inorg. nucl. Chem. 1972, 34, 3721.
7. R. Grimm and Z. Kolařík, J. inorg. nucl. Chem., in press.
8. Partridge J. A. and Jensen R. C., J. inorg. nucl. Chem. 1969, 31, 2587.
9. Myers A. L. McDowell W. J. and Coleman C. F., J. inorg. nucl. Chem. 1964, 26, 2005.
10. Edmondson B. J. and Lever A. B. P., Inorg. Chem. 1965, 4, 1608.
11. Graddon D. P., J. inorg. nucl. Chem. 1961, 17, 222.

Distribution of metal species in the system $(\overline{MA_2})_n$ - dodecane - M^{2+} - N^{2+} - Na^+ - ClO_4^- - water

M	N	Starting concentrations of				Equilibrium concentrations of					
		$\overline{(MA_2)_n}$	$M(l)$	$N(l)$	$Na(l)$	$\overline{M(l)}$	$M(l)$	$\overline{N(l)}$	$N(l)$	$\overline{Na(l)}$	$Na(l)$
		\underline{F}	\underline{M}	\underline{M}	\underline{M}	\underline{M}	\underline{M}	$\underline{M} \times 10^4$	\underline{M}	$\underline{M} \times 10^3$	\underline{M}
Zn	Cd	0.025	0.100	0.100	0.40	0.0208	0.104	0.30	0.100	1.14	0.40
		0.025	0.050	0.150	0.40	0.0194	0.055	0.50	0.150	0.94	0.40
		0.025	0.030	0.170	0.40	0.0197	0.035	0.57	0.170	0.80	0.40
		0.025	0.020	0.180	0.40	0.0209	0.024	0.69	0.180	0.70	0.40
		0.025	0.0100	0.190	0.40	0.0224	0.0123	1.07	0.190	0.47	0.40
		0.0100	0.100	0.100	0.40	0.0106	0.099	0.13	0.100	0.153	0.40
		0.0100	0.050	0.150	0.40	0.0102	0.050	0.29	0.150	0.171	0.40
		0.0100	0.030	0.170	0.40	0.0099	0.030	0.32	0.170	0.20	0.40
		0.0100	0.020	0.180	0.40	0.0099	0.020	0.45	0.180	0.227	0.40
		0.0100	0.0100	0.190	0.40	0.0097	0.0101	0.70	0.190	0.058	0.40
Zn	Cu	0.025	0.100	0.100	0.40	0.0192	0.105	5.45	0.100	1.19	0.40
		0.025	0.050	0.150	0.40	0.0241	0.051	4.45	0.150	1.03	0.40
		0.025	0.030	0.170	0.40	0.0197	0.035	2.97	0.170	0.46	0.40
		0.025	0.020	0.180	0.40	0.0193	0.0254	3.11	0.180	0.32	0.40
		0.025	0.0100	0.190	0.40	0.0228	0.0119	6.4	0.190	0.19	0.40
		0.0100	0.100	0.100	0.40	0.0104	0.099	0.73	0.100	0.116	0.40
		0.0100	0.050	0.150	0.40	0.0101	0.050	0.77	0.150	0.104	0.40
		0.0100	0.030	0.170	0.40	0.0097	0.030	0.91	0.170	0.058	0.40
		0.0100	0.020	0.180	0.40	0.0096	0.0202	1.70	0.180	0.067	0.40
		0.0100	0.0100	0.190	0.40	0.0093	0.0104	2.81	0.190	0.066	0.40

Table 1 (continued)

M	N	Starting concentrations of				Equilibrium concentrations of			
		$\overline{(MA_2)}_n$ <u>F</u>	<u>M</u> M(11)	<u>M</u> N(11)	<u>M</u> Na(1)	<u>M</u> M(11)	<u>M</u> M(11)	<u>M</u> N(11)	<u>M</u> N(11)
Cu	Cd	0.025	0.100	0.100	0.40	0.0192	0.106	0.00022	0.098
		0.025	0.050	0.150	0.40	0.0164	0.059	0.0060	0.144
		0.025	0.030	0.170	0.40	0.0139	0.041	0.0094	0.161
		0.025	0.020	0.180	0.40	0.0123	0.033	0.0113	0.168
		0.025	0.0100	0.190	0.40	0.0104	0.0246	0.0137	0.176

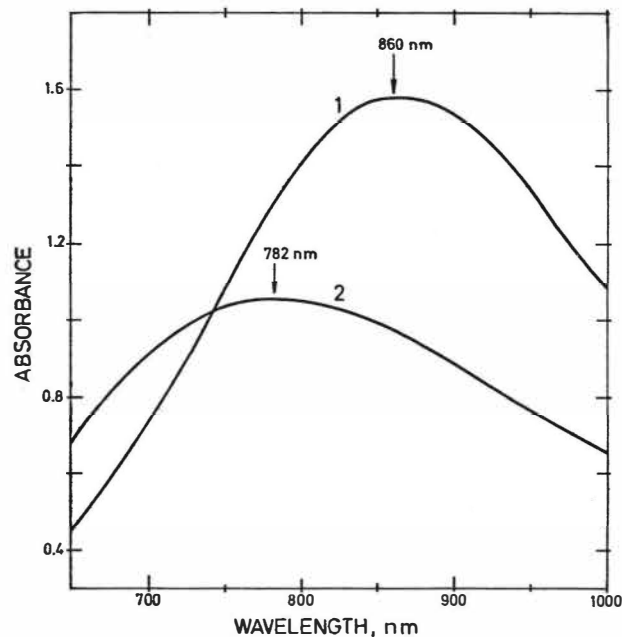


Fig. 1. Absorption spectra of $0.012F (CuA_2)_{II}$ (curve 1) and $0.012F (CuA_2)_{II} + 0.026F (ZnA_2)_{II}$ (curve 2) in n-dodecane (path length 5.00 cm).

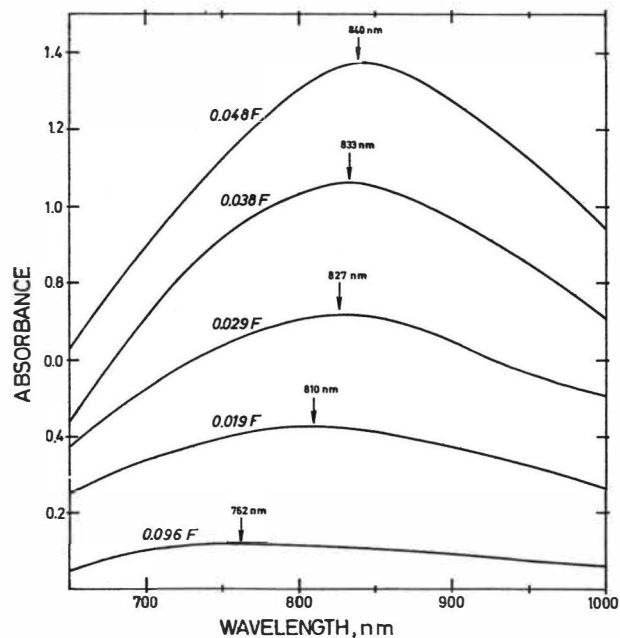


Fig. 2. Absorption spectra of $0.0205F (ZnA_2)_{II} + \text{variable } (CuA_2)_{II}$ in n-dodecane (path length 1.00 cm). Italic numerals on the curves indicate the $(CuA_2)_{II}$ concentrations.

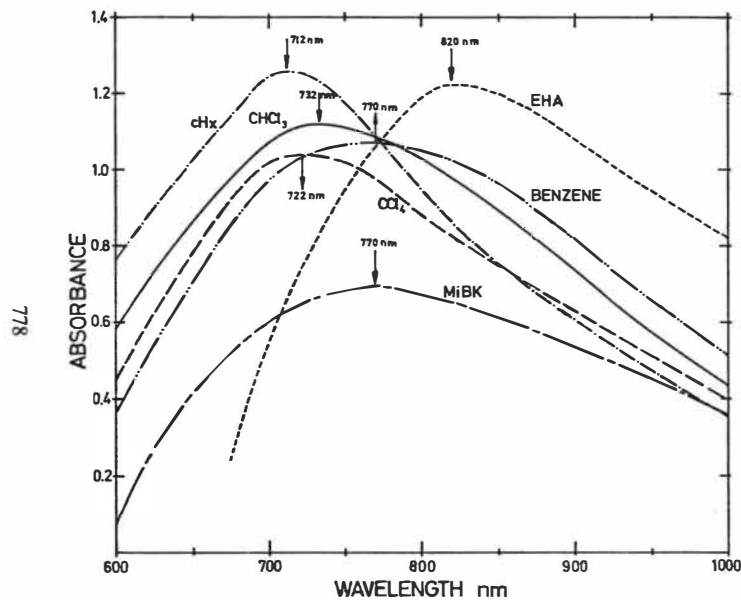


Fig. 3. Absorption spectra of $0.012F (CuA_2)_n$ in various diluents and $0.08F (CuA_2)_n$ in MiBK (path length 5.00 cm). MiBK - methyl isobutyl ketone, EHA - 2-ethylhexyl alcohol and CHx - cyclohexane.

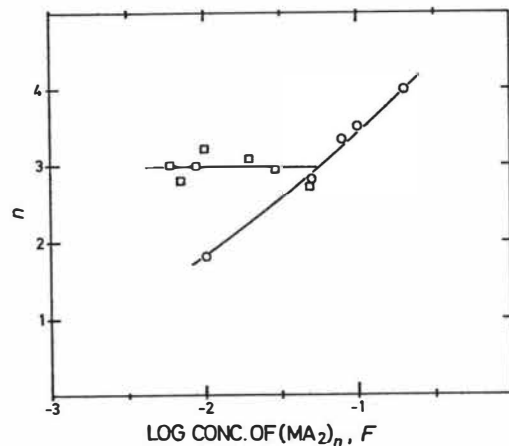


Fig. 4. The degree of self-association, \underline{n} , of $(CuA_2)_n$ (circles) and $(ZnA_2)_n$ (squares) as a function of the concentration of the complexes (monomer formula weight/l) in n-hexane at $45^\circ C$.

C. HANSON (1) AND S.L.N. MURTHY (2)

SUMMARY

A process is described for the recovery of magnesium chloride from sea water concentrates using a mixed ionic extractant comprising an equimolar mixture of Aliquat-336 and Acid-810. The sensitivity of the economics of the process to variations in the various flowsheet parameters is considered. Product evaporation and solvent losses are shown to be major cost items. Amortization charges for the solvent inventory are also significant. The capital costs of the contactors are less important. The process would not be economic if applied to the effluent from a desalination plant but might be viable for more concentrated brines such as the bitterns produced during solar evaporation of sea water for sodium chloride production.

(1) University of Bradford, U.K.

(2) Indian Institute of Technology, Bombay.



1. INTRODUCTION

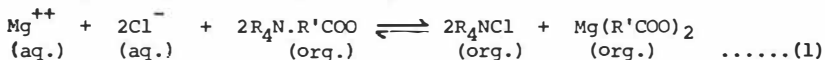
Fears of the exhaustion of the conventional sources of many non-ferrous metals have led to consideration of alternative supplies. The oceans appear particularly attractive, at first sight, since they contain virtually inexhaustible resources of most elements. The expectation of desalination being used extensively for the production of fresh water has attracted attention to the possibility of recovering minerals from the concentrated by-product brine. In addition, there is in certain parts of the world appreciable production of even more concentrated bitterns from the solar evaporation of sea water to produce sodium chloride. However, a simple economic analysis (1) has shown that very few elements (Na, K, Mg, Cl, Br) could be recovered from even these sea water concentrates at prices comparable with current levels. Production of others from such sources will not be economic unless alternative sources become exhausted, with corresponding rise in value.

Amongst metals which are already produced economically from sea water is magnesium. Recovery involves precipitation as the hydroxide by addition of some convenient form of calcium hydroxide. It is also produced from certain bitterns by crystallization routes via carnallite, a hydrated double salt with potassium chloride, although in such cases it is essentially a by-product in recovery of the potassium.

Consideration has been given to the possible use of solvent extraction for the recovery of magnesium from brines. It would have the attraction for such application of greater specificity than existing methods, leading to a purer product. However, in view of the modest value of the product, any solvent extraction process must involve a minimum of reagent costs for conditioning steps and very low solvent losses. A process using alcohols as solvent has recently been described in Israel(2).

The present authors(3,4), expanding on previous work by Grinstead and others(5), have shown that mixed ionic extractants have promise for the recovery of magnesium. Of several systems studied, the best results were obtained with an equimolar mixture of Aliquat-336 and Acid-810 as extractant. Aliquat-336, manufactured by General Mills Inc., is a mixture of quaternary ammonium chlorides approximating to the molecular formula $\{CH_3-N[-(CH_2)_nCH_3]_3\} Cl$, with n varying between 8 and 10. Acid-810, marketed by Novadel Chemicals Ltd., is essentially a mixture of iso-octanoic, iso-nonanoic and iso-decanoic acids. The mixed extractant is used as a solution (1 M suggested) in a suitable diluent. Only pure diluents were considered and toluene was found to be satisfactory. However, it may not be the best and some advantage might accrue from the use of one of the mixed aliphatic-aromatic diluents now available commercially.

The extraction of magnesium as its chloride from a brine by such a solvent may be represented by the equation:



The big attraction of such a system is the fact that both the magnesium and the chloride ions are extracted simultaneously. The potential for forward extraction, i.e. displacing equation (1) to the right, is provided by the large excess of chloride ions inevitably present in a brine derived from sea water. No additional conditioning is necessary. Similarly, the reaction can be reversed to give stripping simply by contacting the loaded solvent with water, again avoiding the need for any chemical conditioning.

Experimental determination of distribution isotherms showed these expectations to be justified, as will be seen from Figure 1. Extensive equilibrium data for the system have been presented elsewhere (3,4). While showing the technical feasibility of using such mixed ionic extractants for the recovery of magnesium chloride from brines, these studies left unanswered the question of whether such a process could be economically viable. It was therefore decided to develop a possible flowsheet, study the sensitivity of the overall economics to the various process variables, and attempt an economic analysis of the optimum combination.

2. THE FLOWSHEET

The equilibrium studies suggested a flowsheet of the form shown in Figure 2. Evaluation of this flowsheet was based on its possible use for the recovery of magnesium chloride from the by-product bittern after production of sodium chloride by solar evaporation of sea water, a process extensively used in countries having suitable climates, e.g. India. The concentrations of the principal elements in such a bittern are given in Table 1.

TABLE 1
Principal Components of Typical Bittern

<u>Element</u>	<u>Concentration (ppm)</u>
Chlorine	152,600
Sodium	34,650
Magnesium	44,750
Potassium	10,950
Bromine (approx.)	2,000

While the solvent exhibits good selectivity for magnesium over sodium, the high concentration of the latter in the feed produces some contamination in the loaded solvent leaving the extraction section and necessitates use of a scrubbing section. The most effective scrub feed in the circumstances will be an aqueous solution of magnesium chloride and some of the product from the stripping section is used for this purpose. The aqueous raffinate from the scrubbing section is combined with the main feed to the extraction section to avoid loss of magnesium chloride.

Potassium contamination is no real problem. Its partition coefficient is less than that of sodium and this fact, together with its low concentration, means that the scrubbing section can safely be designed on the basis of sodium decontamination only. This will inevitably give a product with an extremely low potassium content.

While only present in the original feed at low concentrations, calcium and bromide are preferentially extracted with the magnesium and chloride ions and are not removed in scrubbing. If the loaded solvent is completely stripped, they will appear as impurities in the product. This could be avoided by use of a two part stripping operation in which pure magnesium chloride is produced in the first by use of a low aqueous : organic flow ratio, with total stripping in the second part at a higher ratio. If stripping is not complete, calcium and bromide ions will tend to build-up in the recycled solvent.

For purposes of initial evaluation, a single stripping section has been assumed but with provision to bleed some of the recycled solvent via a clean-up operation to avoid build-up of impurities.

3. COST ESTIMATION

3.1 General Basis of Evaluation

An initial judgement of the possible viability of the process depicted in Figure 2 for the production of magnesium chloride from a bittern demands comparison of the current market value of the product with the production cost. In view of the dependence of the latter on local circumstances dictated by location, plus the difficulty of academic workers obtaining precise cost data, the latter can only be very approximate. In view of this, there is no value in using modern sophisticated methods of economic evaluation such as discounted cash flow and a traditional approach was adopted. However, it was hoped that this would yield information on the relative economic sensitivity of flowsheet variables and also give some insight into the costs to show whether a more precise economic evaluation would be justified. The cost figures used were the best generally available for the United Kingdom in 1971. While no claim is made for their absolute accuracy and many changes have since taken place, relative magnitudes should be of the right order and the sensitivity analysis should be reasonably valid.

The feed bittern is assumed to be available free of cost, i.e. its production is charged against the primary product of sodium chloride. For purposes of flowsheet optimization, labour costs can be assumed constant and independent of minor variations in the flowsheet. The production cost of magnesium chloride will then be dominated by the four major items discussed below.

3.2 Capital Cost of Solvent Extraction Plant

For a given number of stages, this will depend on the type of contactor chosen and the materials of construction. Volumetric throughputs would be considerable. Recovery of 90% of the magnesium chloride (about 40,000 tons per year) in the bitters from a typical 250,000 tons per year solar salt installation could require combined phase throughputs of the order of 750 gallons per minute. The brines are highly corrosive. Suitable materials of construction would be fibreglass-lined concrete or mild steel, with Hastelloy-B for agitators, etc.

It was decided to base estimates of capital cost on the assumed use of mixer-settlers as contactors. They would be suitable for this type of operation. In addition, flowsheet design calculations from the distribution data available had to be based on the numbers of equilibrium stages required under different conditions. These numbers could be directly related to a mixer-settler, whereas no transfer rate data were available for the system to use in the design of differential contactors.

Suitable mixer-settler units were sized on the assumption of a settler capacity of $1.5 \text{ gallons min}^{-1} \text{ ft}^{-2}$, a fairly modest figure reflecting the poor phase separation characteristics of the system, and a mixer residence time 25% that of a settler. Approximate costs for such units in fibreglass lined concrete were obtained from industry(6) and the installed cost was assumed twice the direct cost of the contactor. Amortization was taken over 15 years, at 9% per year, giving a capital cost per stage per ton of magnesium chloride produced. The exact figure was a function of the aqueous : organic flow ratio chosen.

3.3 Solvent Inventory

This was readily calculated for the different possible flowsheets using the plant sizes obtained above. The costs of the extractants were taken as £750 per ton for Aliquat-336 and £180 per ton for Acid-810, giving a total of £18 per ft.³ for a 1.0M solution.

The solvent inventory is generally treated as a capital cost upon which only interest has to be paid and the solvent is not depreciated, the assumption being that it will retain its value. However, the validity of such an assumption is doubtful in view of the rapid steps which are taking place with extractant development. It seems more realistic to make provision for extractant obsolescence and so the solvent inventory was depreciated over the same period as the plant.

3.4 Solvent Losses

Solvent loss by entrainment and solution will take place in the raffinate from the extraction section and in the product from stripping. Assuming equilibrium is established, loss by solution will be proportional to the flow rate of the aqueous phase and may be calculated from published solubility data(3,7). Entrainment losses, on the other hand, depend on contactor design and operation. Operating experience with 1.0M solutions of high molecular weight amines suggest that entrainment losses should not exceed(8) 50ppm, although Grinstead(7) has used a figure of 100ppm.

3.5 Evaporation

The cost of evaporation is made up of both the capital cost of the plant and the steam consumption during operation. Consideration of the extraction isotherm shown in Figure 1 suggests a maximum concentration of magnesium chloride in the product from the stripping section of about 1.8M ($\approx 15\%$ MgCl_2). The final product considered is a 36% solution as this represents the upper concentration limit for conventional evaporators. This allows comparison with alternative routes since all use the same method of final dehydration. It will be seen that the extent of evaporation required is appreciable and must make a significant contribution to overall costs.

4. CHOICE OF OPERATING PARAMETERS

4.1 Water Feed Rate to Stripping Contactor

The water feed rate to the stripping contactor affects four cost items: (a) the capital cost of the contactor itself, (b) the solvent inventory, (c) the amount of solvent lost in the product stream, and (d) the degree of evaporation required. In general, increase in the water flow rate will reduce the number of contacting stages required, thus decreasing (a) and (b), while giving a more dilute product with corresponding increase in (c) and (d). The variations in the costs of solvent loss and evaporation as functions of magnesium concentration in the product from the stripping section were calculated and are shown in Figure 3. It is clear that the total costs of these two items fall quite rapidly with increase in concentration in the early stages, although the rate of fall diminishes. On the other hand, the increase in the number of stages required to produce the rise in concentration is small at the lower end but begins to increase rapidly in the region of 1.8M.

4.2 Magnesium Chloride Content of Stripped Solvent

Another important parameter in the operating conditions for the stripping section is the concentration of magnesium chloride to be left in the recycled solvent. A very large number of contacting stages would be required to achieve both a concentrated aqueous product and a magnesium chloride free stripped solvent. A concentrated product is most easily produced by allowing some of the magnesium chloride to recycle in the solvent. This would reduce the capacity of the solvent in the extractor, necessitating an increase in the number of stages in that section for a given solvent/feed ratio and degree of magnesium recovery.

A balance is required between the numbers of stages in the extraction and stripping sections as a function of magnesium chloride concentration in the recycled solvent. Such calculations are conveniently performed using graphical constructions of the McCabe-Thiele type. The results are shown in Figure 4 for three product brine concentrations, assuming 90% recovery of magnesium chloride from the feed bittern. Since both the capital cost of the contactor and the solvent inventory are directly related to the number of stages, it is clear that the magnesium chloride content of the recycled solvent is a sensitive parameter for flowsheet optimization.

Allowance was not made for the need to bleed some of the recycled solvent through a thorough "clean-up" operation to prevent build-up of calcium and bromide ions in the system.

The scrubbing section does not make an important contribution to this optimization since very few stages are required under any conditions, the aqueous feed rate to the section being determined mainly by the need to have an adequate aqueous : organic flow ratio to ensure efficient contacting of the two phases.

4.3 Solvent : Feed Flow Ratio in Extraction Section

There is a minimum solvent : feed ratio for any particular magnesium content in the raffinate. Increase above this figure will reduce the number of stages required to maintain this raffinate concentration but will result in larger individual stages and a more dilute extract. These two conflicting trends result in the overall capital cost being relatively insensitive to the ratio. The figures given in section 4.2 were based on a solvent : feed ratio in the extraction section of 6.0 (approximately 1.25 times the minimum). Increase of this to 7.0, with 90% recovery of magnesium chloride and a concentration of 0.10M in the recycled solvent, would reduce the number of stages required from 6 to 5. The capital cost of each stage is equivalent to £0.014 per ton $MgCl_2$. Yet the additional cost of the larger stages with their solvent inventory would add £0.016 per ton. The difference is marginal and suggests that the precise ratio adopted will not play a significant part in any optimization.

4.4 Magnesium Chloride Concentration in Raffinate

The number of stages required in the extraction section depends on the degree of recovery demanded for the magnesium chloride in the feed. Since the latter is free and available in substantial quantities, there may appear to be a superficial case for accepting only a modest degree of recovery and compensating for this by a higher volumetric feed rate. However, any such saving through a reduction in the number of stages has to be balanced against the increase in individual stage sizes required and the increase in solvent losses in the raffinate, which are proportional to aqueous phase throughput. The extraction isotherm is such that for recoveries below 90%, large changes are required to cause any appreciable variation in the number

of stages. For greater recovery, the number starts to increase quite rapidly. The figure of 90% was therefore adopted for purposes of preliminary evaluation.

5. FLOWSHEET EVALUATION

To show the overall effect of the various cost components, values were calculated for three possible plants, all based on the flowsheet shown in Figure 2 but with different product concentrations corresponding to different numbers of stages in the stripping section. The results are summarised in Table 2. In view of the approximations involved, no great significance should be attached to the different totals of cases B and C. It is clear from the table that the principle cost items are solvent losses and product evaporation, and development work would have to aim at minimising these.

The total cost figure of approximately £8 per ton of $MgCl_2$ as a 36% solution does not include ancillary equipment, utilities, labour, overheads or interest charges on the capital. Pumping costs, while possibly considerable, have also been neglected since the magnesium recovery plant would be part of a larger operation and much would depend on the situation of the latter. It is particularly difficult to estimate these ancillary costs since the location would not be in the United Kingdom. However, the above figure is only about one-sixth of the market price of this type of product. The process would therefore appear to have a chance of proving economically viable.

The flowsheet was tested using a batch simulation of counter-current contacting. Close agreement was found between observed and predicted concentrations in each stage.

TABLE 2

Costs (£ per ton $MgCl_2$) for Process Shown in Figure 2 (Based on production of 40,000 tons per year at 90% recovery, recycled solvent containing 0.1M $MgCl_2$)

Flowsheet Parameters	Case A	Case B	Case C
Number extraction stages	6	6	6
Number scrubbing stages	2	2	2
Number stripping stages	5	7	12
Product brine concentration (M)	1.4	1.6	1.8
Cost Items			
1. Capital cost of solvent extraction contactors	0.19	0.22	0.29
2. Depreciation of solvent inventory	0.95	0.98	1.28
3. Solvent losses in (i) raffinate	2.13	2.13	2.13
(ii) product	1.52	1.36	1.22
4. Evaporation	3.53	3.15	2.80
TOTAL	8.32	7.84	7.72

6. RECOVERY OF MAGNESIUM CHLORIDE FROM DESALINATION PLANT EFFLUENTS

The concentration of magnesium chloride in the effluent from a typical desalination plant (about 0.16M) will be very much less than in a bittern. This would result in substantially higher solvent losses per ton produced since the losses are directly related to volumetric throughput. In addition, concentrations in the product will be lower, leading to higher evaporation costs, and capital costs per unit of production will be higher. A preliminary calculation indicated solvent loss costs in the region of £30 per ton $MgCl_2$ and evaporation costs of at least £20 per ton $MgCl_2$.

It is clear from this that the extraction process described could not be applied economically to a desalination plant effluent.

7. CONCLUSIONS

7.1 The use of a mixed ionic extractant comprising an equimolar mixture of Aliquat-336 and Acid-810 is promising for the recovery of magnesium chloride from the mother liquor bitterns resulting from solar evaporation of sea water to produce sodium chloride but would not be economic applied to the effluent from a desalination plant.

7.2 The major cost items would be product evaporation and solvent losses. Flowsheet design should aim at producing as concentrated an aqueous product as possible from the stripping section and at minimising throughputs of aqueous streams in the solvent extraction units.

7.3 The capital cost of the solvent extraction plant is relatively low and so the numbers of stages in the various sections should not be minimised at the expense of the requirements in paragraph 7.2

7.4 Solvent obsolescence could make a significant contribution to the overall economics of such a process.

REFERENCES

1. Hanson C. and Murthy S.L.N.: The Chemical Engineer, (264), 295 (1972).
2. Israel Patent 23760.
3. Hanson C., Hughes M.A. and Murthy S.L.N.: publication pending.
4. Murthy S.L.N.: PhD Thesis, University of Bradford (1971).
5. Grinstead R.R. and Davis J.C.: Ind.Eng.Chem.,Prod.Res.Develop., 9(1),66 (1970).
6. Private communication from Mr. G.C.I. Warwick, Davy Powergas Limited.
7. U.S. Office of Saline Water, Res.Dev.Prog.Rep. 406 (1969).
8. Private communication from Mr. G. M. Ritcey, Mines Branch, Ottawa.

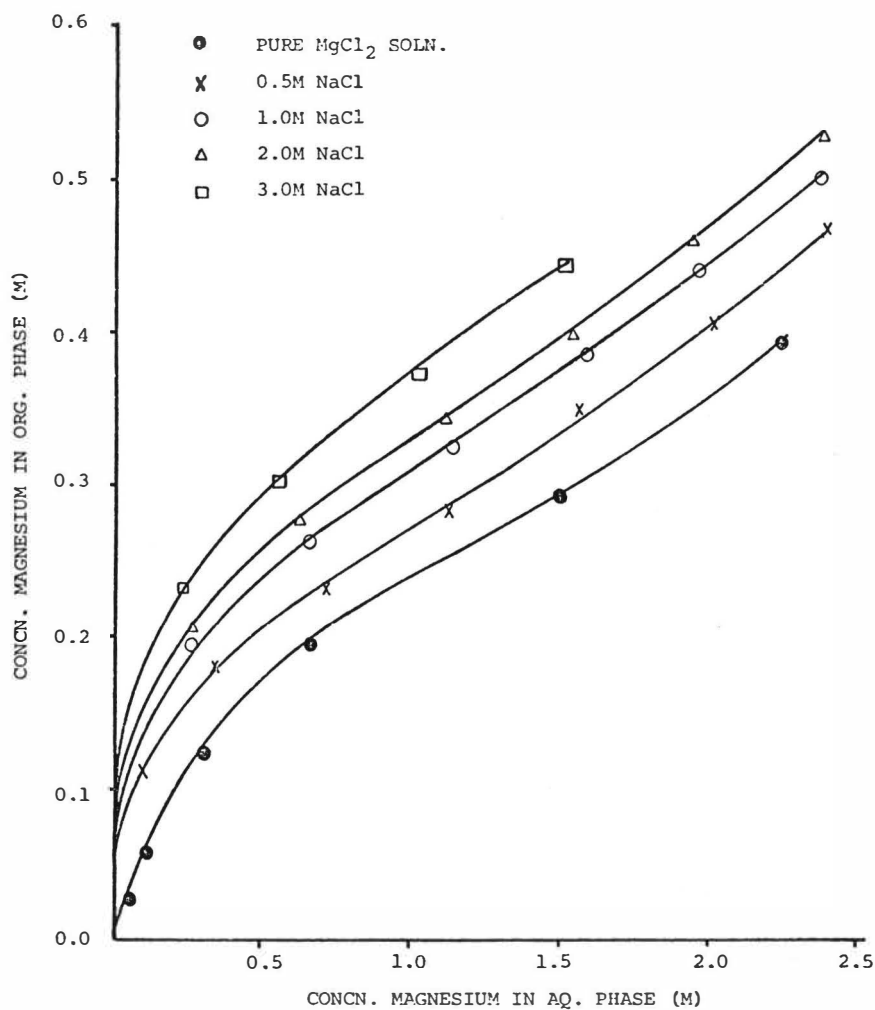


FIG. 1: EXTRACTION ISOTHERMS FOR MAGNESIUM FROM NaCl - MgCl_2 SOLNS. AT 25°C

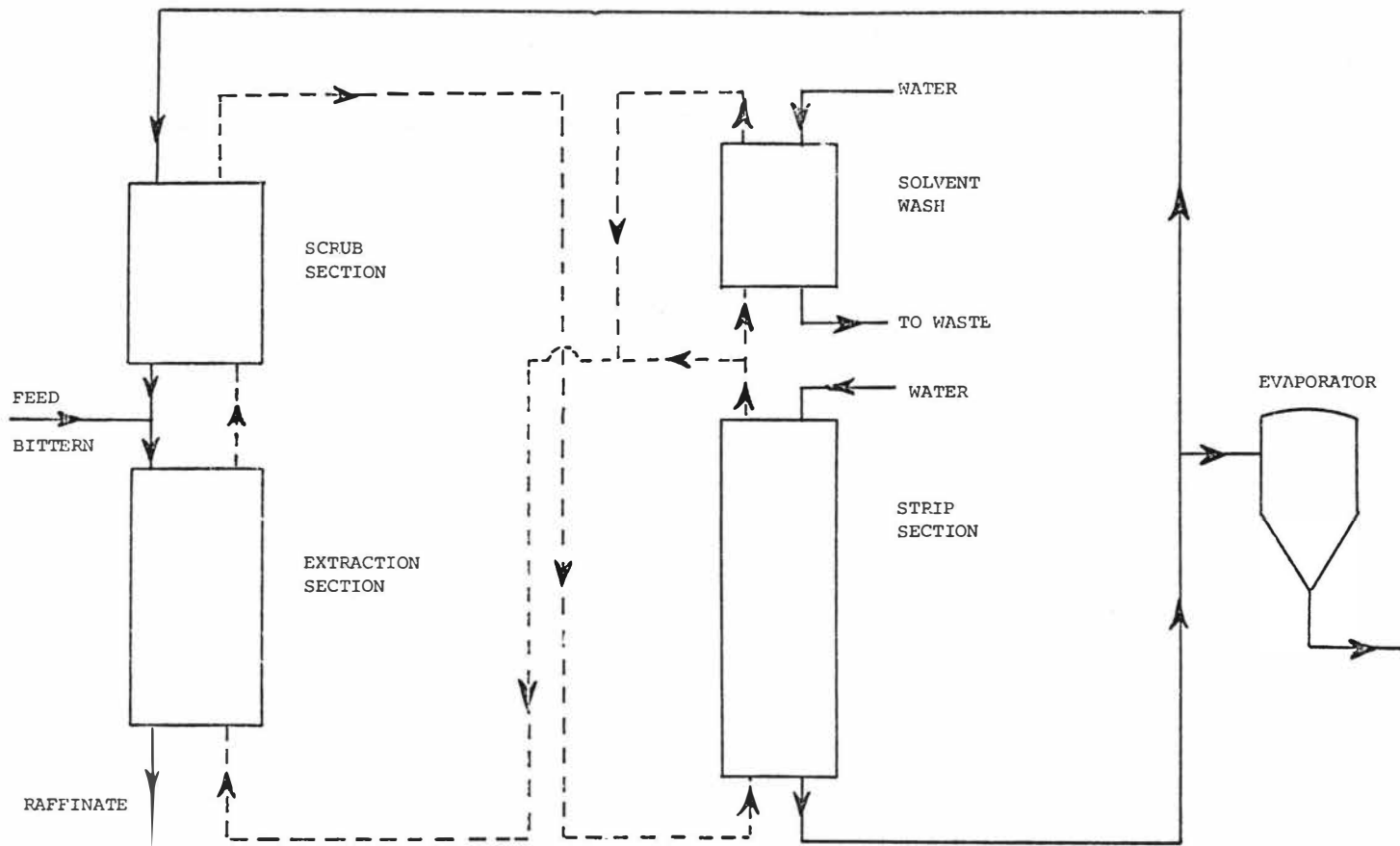


FIG. 2: PROPOSED FLOWSHEET

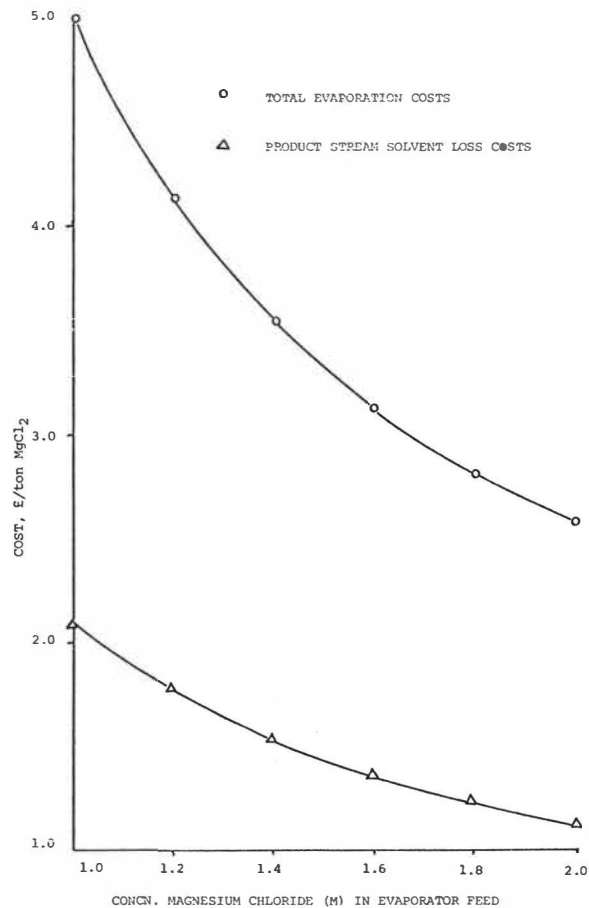


FIG. 3: VARIATION OF EVAPORATION AND PRODUCT STREAM SOLVENT LOSS COSTS WITH EVAPORATOR FEED CONCENTRATION

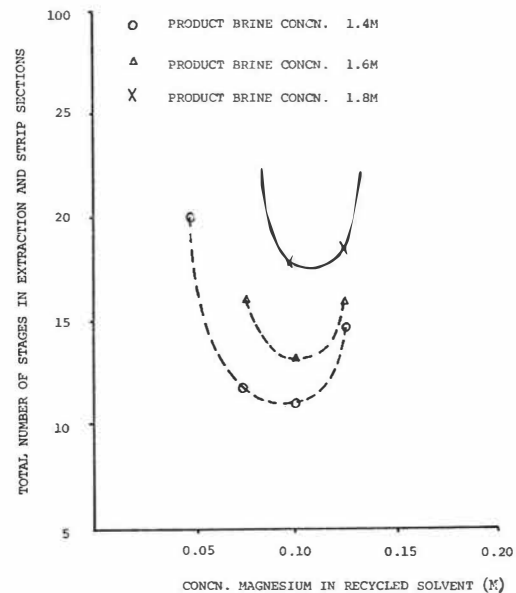


FIG. 4: EFFECT OF CONCENTRATION OF MAGNESIUM IN RECYCLED SOLVENT ON THE TOTAL NUMBER OF STAGES REQUIRED IN EXTRACTION AND STRIPPING SECTIONS

A SPECTROPHOTOMETRIC STUDY OF THE ORGANIC
PHASE COMPLEXES FORMED IN THE EXTRACTION
OF COBALT II WITH CARBOXYLIC ACIDS

H.E. Crabtree

and

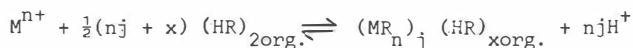
N.M. Rice

Detailed analysis of the U/V - visible and infra-red spectral properties of carboxylic acid extracts of cobalt II have been carried out using derivative spectroscopy. It has been shown that the extracts contain a number of complexes in equilibrium. The structures of some of the carboxylate complexes have been determined and the factors which control the compositions of the complexes have been examined.

Department of Mining and Mineral Sciences,
University of Leeds.
ENGLAND

INTRODUCTION

The conventional method for determining the compositions of complexes formed in the solvent extraction of metals is slope analysis. Two main methods are used to derive an extraction equation. The single equilibrium method⁽¹⁾ depicts the equilibrium between the metal and extractant present in the aqueous and organic phases as

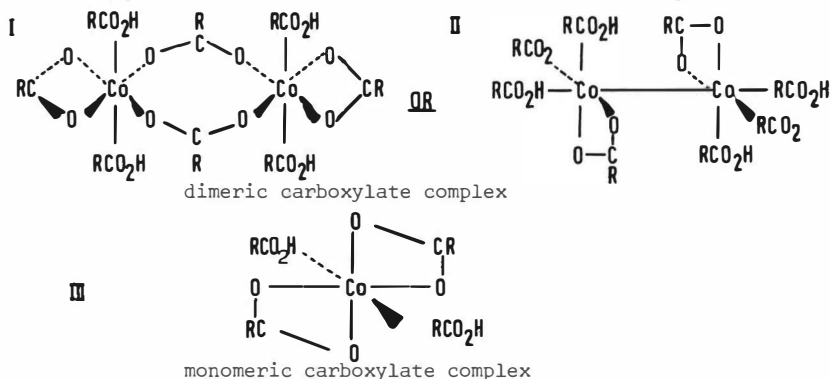


where the subscript org. refers to the organic phase. The metal, M, of valency n, exists as the ion in the aqueous phase and as a polymeric, solvated complex of generalised formula in the organic phase. The acid, HR, is assumed to exist as the dimer in the organic phase and to be insoluble in the aqueous phase.

The second method, the multiple equilibria method⁽²⁾ attempts to break down the overall equilibrium into the various equilibria which are assumed to exist in each phase and to then solve the set of subsidiary equilibrium constant equations. Thus the final extraction equation must contain, for example, terms which take into account the equilibria between monomeric and dimeric acid and the monomeric and polymeric forms of the metal complex and also the solubility of the acid and metal complex in the aqueous phase. Because insufficient information is available on the factors which control the composition of extracted complexes the method has not been developed to its full potential. In fact, to apply the technique satisfactorily, simplifications have to be introduced and under these circumstances the new extraction equation approaches that derived from the single equilibrium method. As a result the two treatments become equivalent⁽³⁾.

Irrespective of approach, slope analysis has only been applied in cases where the concentration of metal in the system is small and very much less than the concentration of extractant. Under these conditions, it has been found⁽¹⁾ that the composition of the cobalt carboxylate complex extracted with naphthenic acid has the formula $(CoR_2 \cdot 2HR)_2$. Two complexes have been detected in octanoic acid extracts⁽²⁾: at low metal concentrations ($< 10^{-4}M$) the metal is extracted as $CoR_2 \cdot 2HR$, whereas at concentrations between $10^{-4}M$ and $5 \times 10^{-3}M$ the metal is extracted as $(CoR_2 \cdot 2HR)_2$, in agreement with the naphthenate work.

In the extraction of cobalt (0.1M in 0.5M nitrate medium) with Versatic acid 911* in cyclohexane (0.1M), three distinct changes occur in the spectrum of the organic phase as the equilibrium pH increases and higher metal-loadings of the organic extract are achieved (Fig.1). At low pH, a pink extract is obtained indicative of octahedral co-ordination in the metal ion, cf. $\text{Co}(\text{H}_2\text{O})_6^{2+}$ ⁽⁴⁾. At this stage of the extraction, conditions are favourable to slope analysis and so we can write the following possible structural formulae for the metal complexes:



At pH 8.5, the amount of metal in the organic phase is high and a good proportion of the acid has been consumed in the complex. Conditions favourable to slope analysis no longer exist: metal-loadings are akin to those envisaged in industrial applications of carboxylic acid extractants⁽⁵⁾. The final stages of extraction, at pH 9.6, yield blue-grey extracts. Neither the structures nor the number of complexes responsible for the observed spectral changes are known. The present paper describes attempts to determine the complexes in the system and to provide more information about factors affecting their compositions.

The ultimate form of the carboxylate complexes may be regarded as being controlled by four factors:

- (i) the co-ordination number adopted by the metal ion,
- (ii) the co-ordinating properties of carboxylate ligands,
- (iii) the availability of other ligands,

* A synthetic mixture of tertiary carboxylic acid manufactured by Shell.

and (iv) the ability of the metal complexes to polymerise in the organic phase.

(i) Cobalt II forms mainly octahedral and tetrahedral complexes,⁽⁶⁾ although square planar⁽⁷⁾ and pyramidal⁽⁸⁾ co-ordinations have been reported. The interconversion between octahedral and tetrahedral co-ordination occurs easily and rapidly. A spectrophotometric study of complexes of the general type CoX_2S_2 ,⁽⁹⁾ where X is halide and S represents polar, organic solvating molecules, has revealed a host of charged and neutral tetrahedral species and has shown that conversion from tetrahedral to octahedral proceeds through numerous stages. The addition of carboxylic acid (S) to blue, tetrahedral cobalt carboxylate (CoX_2) extracts causes a colour-change to pink and, by analogy, this transition may also be expected to proceed through intermediate species.

The usual method for determining the compositions of complexes from electronic spectra is by the technique of continuous variation⁽¹⁰⁾. The method is, however, only applicable to mixtures of complexes when a region of the spectrum can be found in which only one of the complexes absorbs. Fig. 1 shows clearly that, in the present case, the absorptions of octahedral and tetrahedral cobaltous complexes overlap over the whole range and consequently the method cannot be applied directly.

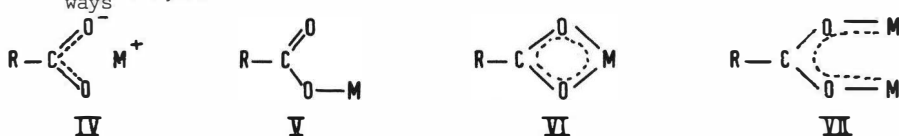
Absorption spectra arise from electronic transitions in the metal ion: a single transition gives rise to a peak of approximately Gaussian shape⁽⁴⁾. The complicated absorption spectra encountered in practice represent the sums of a number of Gaussian bands, each arising from a single transition. Recent reports^(11, 12, 13) have shown that if the spectrum of a mixture of complexes can be resolved into its Gaussian components, the latter can be analysed by the technique of continuous variation to obtain the number and types of complexes present.

A Gaussian band is characterised by three parameters: the position of its maximum absorption, its extinction coefficient at the maximum and its half-width.⁽⁴⁾ Derivative spectroscopy⁽¹⁴⁾ allows the position of the maximum to be determined: minima in the second derivative correspond with the maxima of the Gaussian components. Extinction coefficients and half-widths are less easy to obtain. They may be determined manually by a laborious process of trial and error⁽¹²⁾ or alternatively, an interactive computerised method⁽¹⁵⁾ may be employed which, nevertheless, requires a

close initial estimate if it is to be successful.

In the present work attempts to fit Gaussian components failed, due to the complicated absorption patterns of tetrahedral cobalt II complexes, and so an abridged version of the above procedure was adopted in which only derivative spectroscopy was used to determine the number of complexes responsible for a change in the spectra of extracts.

(ii) Carboxylate groups can bond to metals in any of the following ways (16,17)



and as a result octahedral complexes of the form $(\text{CoR}_2 \cdot 2\text{HR})_2$ can be drawn as either of the structures indicated earlier, (I and II.) The different modes of bonding will lead to characteristic patterns in the infra-red.

In substances of type IV the oxygen atoms are indistinguishable. The ion conforms to C_{2v} symmetry for which three fundamental vibrations are to be expected for the O-C-O system⁽¹⁸⁾. Two of these vibrations are represented by the symmetrical (ν_1) and antisymmetrical (ν_2) modes which occur between 1300 and 1700cm^{-1} . Bonding of types VI and VII also shows C_{2v} symmetry and two stretching modes are to be expected. Previous workers^(16,17) have proceeded from this group theoretical basis to interpret the effects of changes in M upon ν_1 and ν_2 and it has become common practice to regard the separation $\Delta\nu$, between them as indicative of the dentative properties of the carboxylate anion. Thus it is claimed⁽¹⁶⁾ that the larger the value of $\Delta\nu$ the more dissimilar the two C-O bonds and hence the more like structure V is the bonding. A paper on the structure of precious metal carboxylates⁽¹⁹⁾ does much to strengthen this argument.

It should be clear, however, that in bonding of type V no C_{2v} symmetry is present and the group theoretical basis breaks down. Further, if M were replaced by an alkyl group, an ester would result. Esters have only one carbonyl frequency, but they also absorb in the range $1200-1250\text{cm}^{-1}$ because of the C-OR vibrator. It follows, therefore, that carboxylates of type V will have only one absorption in the carbonyl range and that, due to the influence of the metal ion, the frequency of the vibration will be lower than in acids and esters. A further consequence is that a change from bondings of types IV, VI or VII to type V will be observed in the

infra-red as a disappearance of ν_1 .

Because the carboxylate extracts under investigation occur in cyclohexane, it can be assumed that ionic interactions of type IV are not present. Two types of bidentate behavior, chelation (VI) and bridging (VII) are to be expected along with monodentate complexing (V). In chelation, the nominal negative charge of the carboxyl group is associated with a single, doubly charged metal ion, whereas a bridging carboxyl group is associated with two divalent metal ions. The O-C-O system in VI will have a more dense electron cloud than the O-C-O system in VII and as a result the C-O bonds in VI will be of a slightly higher bond-order than those in IV and will be expected to vibrate at higher frequencies.

(iii) In addition to carboxylate anions, the systems under investigation contain other potential ligands. Reference has already been made to the probable solvating properties of carboxylic acids and close examination of the acid carbonyl stretching region of the infra-red spectra of extracts should indicate the extent to which it occurs. After carboxylic acids, water is probably the most important potential ligand in the system. It is known ⁽²⁰⁾ to be present in metal carboxylate extracts, but its role is not understood. Nitrate and hydroxyl ligands may also complex with the metal ion in the organic phase and, of these, evidence will be presented for the existence of a mixed carboxyl/hydroxyl complex of cobalt at high equilibrium pH.

(iv) The most probable route by which metal complexes polymerise is through formation of carboxyl bridges, evidence for which should appear in the infra-red spectrum. The formation of Co-Co bonds and of nitrate and hydroxyl bridges would also allow polymerisation.

The spectrophotometric study described below has been carried out on two systems, the cobaltous nitrate/Versatic 911 system and the cobaltous nitrate/octanoic acid system. Extracts have been isolated at known equilibrium pH's and have been analysed to determine acid-contents (free acid + carboxylate acid), cobalt-contents and water. The extracts have been subjected to two tests. In one series of experiments the extracts were simply diluted and the detailed changes in the visible and infra-red spectra were observed. In the second series of experiments known amounts of free acid were added to the extracts and the detailed spectral changes noted.

EXPERIMENTAL

Preparation of the extracts

Carboxylate extracts were obtained by the dropwise addition of potassium hydroxide solution (5N) to a dispersion of cobaltous nitrate solution (100 ml.; 0.1M cobaltous nitrate and 0.3M potassium nitrate) and a solution of carboxylic acid in cyclohexane (100 ml.; 0.25M). All reagents were of Analar quality. After the mixture had attained the required equilibrium pH it was allowed to equilibrate for 1h. at room temperature. The mixture was centrifuged and the organic phase was drawn off, transferred to a separate vessel and stored in darkness. The residual aqueous phase was retained for analysis. The preparation of blue Versate extracts invariably yielded an additional solid product which was preferentially wetted by the organic phase and which, being of intermediate density, resided at the interface after centrifugation. In such cases, the solid product was recovered separately and analysed.

Spectral analysis in both the visible and infra-red regions of organic extracts from replicate experiments showed that extracts could be reproduced accurately. It was found, however, that it was necessary to allow organic phases at least 16h. to achieve "internal" equilibrium. Incomplete experiments strongly suggested that water plays an important role in the attainment of the immediate equilibrium with the aqueous phase but that molecular rearrangements in the extracted complexes subsequently led to its expulsion from solution.

Determination of cobalt- and acid-contents

The cobalt - and carboxylic acid - contents of the organic and aqueous phases and of the solid product were determined by treating the samples with sulphuric acid (2M). Carboxylic acids were extracted from the acidified mixtures with cyclohexane and, after thorough washing, the acid was determined by two phase titration with standard sodium hydroxide under a nitrogen atmosphere using phenolphthalein as indicator.

Cobalt-contents were determined by atomic absorption spectrometry on Techtron AA-5 equipment (Varian Ltd.). Care was taken to ensure that test solutions and standards were alike in respect of all components other than cobalt.

Determination of water in organic extracts

Karl Fischer titrations and gas chromatography were used. The latter was carried out on Porapak P (Waters Associates) columns at 150°. Helium (20 ml/min.) was the carrier gas and a thermal conductivity detector (250°) was used to sample the effluent gases. Although both techniques failed to give accurate figures of water-contents they showed conclusively that the amount of water in the extracts was less than 0.02% and about equal to its solubility in cyclohexane, 0.01%⁽²¹⁾.

Determination of nitrate in organic extracts

Lassaigne tests and elemental analyses were carried out on the extracts examined. Both indicated the absence of nitrogen and hence nitrate can be excluded from organic phase complexes.

Ultraviolet and visible spectroscopy

Electronic spectra were recorded on a Pye Unicam SP1800 spectrophotometer. The technique of Savitzsky⁽²²⁾, using a 17-point convolute and absorbance measurements taken at 2nm. intervals, was used to obtain the 2nd derivatives of absorption spectra. To overcome excessive noise levels and to ensure reproducibility derivative spectra were, where practicable, calculated from absorption envelopes whose maximum absorbance values were around one optical density unit.

Presentation of derivative spectral data

To interpret the derivative data more easily an approximate method of Gaussian-fitting was used. The relative contributions of each component revealed in the derivative spectrum was estimated and represented by an approximately-Gaussian peak of suitable intensity in a composite diagram. Figs. 2 and 3 show the relationships between absorption spectra, second-derivative spectra and composite band diagrams.

Infra-red spectroscopy

Infra-red spectra of cobalt carboxylate solutions in variable path-length cells fitted with silver chloride windows were recorded against cyclohexane references on Pye Unicam SP200 and Grubb-Farsons Spectromaster infra-red spectrometers. Where necessary, the components making up complex absorption bands were resolved by derivative spectroscopy carried out electronically⁽²³⁾.

System (equilibrium pH)	Sample analysed	Concentration in moles/litre						
		Initial aqueous phase Cobalt	Initial organic phase Acid	Cobalt	Total acid (free acid + carboxylate)	Water+	Ratio Co: Acid	Ratio Co: Water
OCTANOATE (7.3)	Aqueous phase	0.088	-	0.004	0.065	-	-	-
	Organic phase	-	0.247	0.084	0.183	0.004	1:2.18	1:0.05
VERSATE (8.3)	Aqueous phase	0.088	-	0.008	0.020	-	-	-
	Soluble org. phase	-	0.232	0.071	0.208	0.004	1:2.93	1:0.06
	Insoluble product	-	-	(0.009)*	(0.004)*	-	1:0.45	1:0.45
VERSATE (8.6)	Aqueous phase	0.088	-	0.010	0.077	-	-	-
	Soluble org. phase	-	0.232	0.064	0.147	0.004	1:2.30	1:0.06
	Insoluble product	-	-	(0.014)*	(0.007)*	-	1:0.50	1:0.35
VERSATE (9.1)	Aqueous phase	0.088	-	0.029	0.198	-	-	-
	Soluble org. phase	-	0.232	0.023	0.016	0.004	1:0.70	1:0.25
	Insoluble product	-	-	(0.036)*	(0.017)*	-	1:0.47	1:0.11

Table 1. The compositions of the carboxylate extracts examined

+calculated on the assumption that the water-content is equivalent to that of the cyclohexane/water
azeotrope(21)

*obtained by difference

RESULTS

The course of extraction of cobalt with carboxylic acids

The spectrophotometric data given in Fig.1 do not accurately portray the course of extraction. Although pink Versate extracts are wholly soluble in the organic phase, subsequent purple-blue extracts comprise a soluble and an insoluble portion. Inspection of Table 1 indicates that the proportion of insoluble product increases with rising pH and at pH 9.1 the spectrum of the organic phase is essentially the same as that of a suspension of the insoluble complex in chloroform (see Fig. 12).

Extraction of cobalt II with octanoic acid yields only pink complexes irrespective of metal-loading and pH. At pH values in excess of ~7.4 the system forms a stable emulsion.

The effect of dilution on the spectral properties of soluble cobalt extracts

Figs. 2 and 3 show the changes in the electronic spectrum of a purple cobalt Versate extract, obtained at pH 8.3, caused by dilution. The disappearance and emergence of bands in the derivative spectra indicate that the changes occur through several complexes. Bands at 470 and 490 nm. in the neat extract are characteristic of octahedrally co-ordinated cobalt II^(4,9). Absorption in the range 520-540 nm. is common to both octahedral and tetrahedral cobalt II^(9,24). Peaks in the range 540-700 nm. are due to tetrahedrally co-ordinated species^(9,24). It can be seen, therefore, that in the most concentrated solution, cobaltous ions occupy both octahedral and tetrahedral sites, whereas in the most dilute sample only tetrahedral co-ordination is evident.

The changes in Gaussian components in passing from Versate sample 5 to sample 8 (Fig.3) are as follows. Two bands, at 475 and 495 nm. occur in the spectrum of sample 5 but not in samples 6, 7 and 8, indicating that an octahedral complex is present in 5 which disappears with further dilution. Among the bands which occur in samples 6, 7 and 8 are four, at 545, 550, 583 and 588 nm., which are characteristic of tetrahedral complexes. The intensity of the band at 545 nm. decreases in passing from sample 8 to sample 5 whereas that at 550 nm. increases in intensity. Corresponding changes in the bands at 583 and 588 nm. also occur. These observations show that the changes encountered in passing from sample 5 to sample 8 result from changes in the equilibrium between one octahedral and two tetrahedral species. The application of similar reasoning to the remaining spectra in the series leads to the conclusion that a minimum of six

complexes are responsible for the overall changes in spectral properties.

Spectral evidence (Figs. 2 and 3) shows that on diluting the cobalt octanoate extract (pH 7.3) the amount of octahedrally co-ordinated metal becomes less and eventually disappears and that three complexes can be detected. The final product is different from that obtained in the Versatic acid system. Its absorption pattern consists of only three bands, the positions of which (470-480, 520 and 560 nm.) give the extract a pink colour. Clearly, the metal is neither tetrahedrally nor octahedrally co-ordinated in the most dilute sample.

For both the Versate and octanoate extracts dilution causes profound changes in the region of the infra-red spectrum examined (Figs. 4 and 5). In the frequency range where acid carbonyl groups vibrate, $1725-1660\text{ cm}^{-1}$, both extracts show essentially two peaks. Those in the spectrum of the neat Versate extract (Fig.4) occur at 1700 cm^{-1} and 1675 cm^{-1} . A solution of Versatic acid (1M) in cyclohexane (Fig.6) absorbs strongly at 1700 cm^{-1} owing to the carbonyl vibrations of the free, dimeric acid. Increase in the intensity of hydrogen-bonding of OH groups in carboxylic acids leads to an effective reduction in bond-order, and a corresponding decrease in the frequency of the acid carbonyl band⁽²⁵⁾. The second and smaller peak in the acid carbonyl range, at 1675 cm^{-1} , would therefore appear to represent a situation in which the acid molecule finds itself more strongly H-bonded than in the dimer. Such a situation will arise for acids which solvate the metal complex by co-ordination through the carbonyl oxygen. The peak at 1675 cm^{-1} would appear therefore to correspond with solvating acid. Corresponding peaks can be detected in the spectrum of the neat octanoate extract (Fig.5) at 1710 cm^{-1} and $1700-1690\text{ cm}^{-1}$: the former coincides precisely with the carbonyl band of 0.1M octanoic acid in cyclohexane (Fig.6).

The effect of dilution on both extracts is to cause a gradual increase in the free acid vibration while the intensity of the lower frequency vibrations becomes less and finally vanishes. The observation indicates that the amount of free, dimeric acid in the system increases as the amount of solvating acid decreases.

Dilution also brings about changes in the regions of the infra-red spectrum where carboxylate groups absorb. Both neat extracts exhibit a strong and complex absorption band in the range $1660-1520\text{ cm}^{-1}$. Maximum absorption for the Versate extract is at 1580 cm^{-1} with lesser vibrations up to 1610 cm^{-1} . The higher frequency components disappear as the dilution

increases and only that at 1580 cm^{-1} remains at high dilution. A similar change occurs in the corresponding region of the octanoate extract; high frequency absorptions disappear and the most dilute sample shows only one "pure" peak at 1560 cm^{-1} .

In those regions of the infra-red spectrum where cyclohexane, the diluent, absorbs strongly much less reliance can be placed upon absorptions due to the carboxylate group. Thus, although the detailed changes in the acid carbonyl and carboxylate vibrations noted above are reliable, changes in the $1520\text{--}1300\text{ cm}^{-1}$ carboxylate range and at lower frequencies are meaningless with cell pathlengths greater than 0.5 mm . A further complication arises in that skeletal vibrations of alkyl groups also occur in the ν_1 range (Fig.6) to confuse the picture. Nevertheless it appears from the spectra of samples 1 to 5, for which short pathlengths were used, that dilution causes the disappearance of bands at 1480 cm^{-1} (Versate extract) and $1440\text{--}50\text{ cm}^{-1}$ (octanoate extract) which may be ascribed to bidentate carboxylate groups.

When considered along with data which will emerge in subsequent acid-addition experiments, the effects of dilution suggest that in both acid systems, the neat extracts contain all the types of carboxylate bonding listed earlier (with the assumed exception of type IV) and that the effect of dilution is to cause the destruction of bridging and chelating molecules and the retention of only monodentate carboxylate (type V) groups.

A further piece of information may be introduced at this point. The neat Versate and octanoate extracts are solutions of low viscosity, but whereas dilution does not change the rheological properties of the Versate extract, it causes the octanoate extract to gel. The observation is taken to indicate that, at the molecular level, cobalt octanoate complexes are able to form a more orderly arrangement than Versate complexes.

The effect of adding free acid to cobalt carboxylate extracts

From the dilution tests it is clear that the initial samples in the series of experiments in which free acid was added to carboxylate extracts, that is five times diluted specimens of the neat extracts, are mixtures of essentially two complexes. The effect of adding increasing quantities of acid to the mixtures (Figs 7 and 8) is to generate octahedrally co-ordinated complexes. Derivative spectra indicate that in the Versatic acid system the final sample, that containing a vast excess of acid, is also a binary mixture of complexes. About 4 or 5 new complexes can be detected in inter-

mediate samples and seven complexes seem to occur in the system as a whole. In three, the cobalt ion is octahedrally co-ordinated.

The final sample in the octanoic acid/octanoate specimens is also a mixture and a further three complexes can be detected in the sequential changes brought about by the addition of free acid. Of the complexes in the system, all except one exhibit octahedral co-ordination.

The addition of free acid to the carboxylate complexes of both systems brings about changes in the patterns of acid carbonyl and carboxylate absorption (Figs. 9 and 10). In the Versatic acid system, two distinct absorption bands occur in the acid carbonyl region at 1700 and 1675 cm^{-1} , and, as expected, the intensity of the higher frequency band increases with increase in acid-content. Increase in acid concentration also leads, however, to an increase in absorption at the lower frequency; samples 1 and 2 (Fig.9), containing respectively no added acid and only a small amount, show only shoulders at 1675 cm^{-1} whereas subsequent samples show distinct peaks. The observation is consistent with an increase in the amount of solvating acid in the carboxylate complexes.

Because no separate and distinct peak attributable to solvating acid appears in the spectra of mixtures of octanoic acid and cobalt octanoate it would seem, at first sight, that the pattern of behaviour is different from the Versatic/Versate case. A slight broadening towards lower frequency of the main acid carbonyl peak at 1700 cm^{-1} , however, suggests the presence of solvating acid. Additionally, a plot of optical density against concentration for the main absorption, Fig. 11, gives an S-shaped curve. That a similar plot for the experiments with Versatic acid was even more markedly S-shaped whereas the plot for pure octanoic acid over the same range of concentration was essentially linear, indicated still more forcefully that the main acid carbonyl band contained more than one absorption band and that solvating acid was present in the system.

To eliminate the possibility of water taking the place of solvating acid in the complexes, tests were repeated with a specially dried sample of octanoic acid in cyclohexane. Corresponding spectra from the "wet" and dry experiments were identical showing the influence of water to be negligible.

Changes were also brought about in the carboxyl absorption bands by the addition of free acid. For the Versate system, the immediate effect is the introduction of a new band at 1595 cm^{-1} and in the series of spectra the intensity of the new band increases markedly, apparently at the expense of

lower frequency vibration at 1580 cm^{-1} . The main peak also shifts slightly to higher frequency, 1602 cm^{-1} , probably due to the development of bands in the region of 1610 cm^{-1} . For the octanoic acid system parallel, though more noticeable changes occur in the infra-red spectrum. An absorption band at 1565 cm^{-1} decreases with increase in acid-content and is replaced by two overlapping absorptions at 1598 cm^{-1} and 1610 cm^{-1} . Infra-red evidence in the region $1650\text{-}1520\text{ cm}^{-1}$ suggests, therefore, that for both systems the effect of adding free acid to cobalt extracts is to cause a change in carboxylate-metal bonding in many ways the reverse of that brought about by diluting extracts.

Additional evidence for this conclusion is to be found in the region $1520\text{-}1300\text{ cm}^{-1}$. Despite the fact that carboxylate absorptions in this region tend to become obliterated by absorptions of alkyl chains in the free acid and in the diluent, broad bands at 1425 cm^{-1} and 1450 cm^{-1} for the Versatic acid and octanoic acid systems respectively, can be detected as the amount of acid increases, strongly suggesting the presence of bidentate carboxyl groups.

Versate extracts obtained at high pH and insoluble extracts

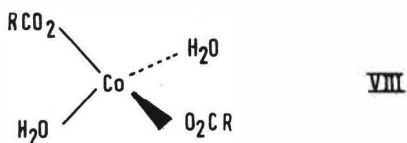
Table 1 shows that as the equilibrium pH in the extraction of cobalt with Versatic acid increases so does the proportion of insoluble product. Additionally, at pH 9.1 the soluble portion of the extract is no longer deep purple but light blue-grey. Fig. 12 shows the visible spectra of the soluble extract and of a suspension of the insoluble product in chloroform. Not only are they remarkably alike, they are also very similar to the spectrum of a solution of cobaltous hydroxide in alkali.

Because of the large pathlengths needed to obtain the infra-red spectrum (Fig. 6) of the soluble extract, 2 mm., only a limited amount of information can be obtained. Absorptions in those regions of the spectrum where the diluent does not absorb show the presence of free and solvating acid and of all types of carboxylate bonding. The lack of absorption bands below 1500 cm^{-1} can be regarded as insignificant. The other important feature of the spectrum is the presence of a large peak at 3400 cm^{-1} , not detected in other extracts, which indicates O-H bonds. Since the amount of water in the extract is in the region of 0.01%, the pronounced band must arise from hydroxyl groups in the complex.

No infra-red information was obtained for the insoluble product.

DISCUSSION

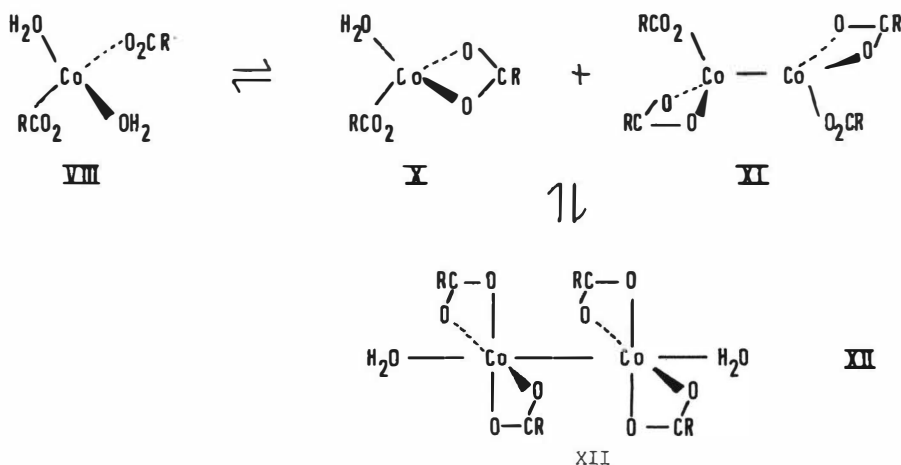
There are two points of attack from which to obtain information about the complexes responsible for the observed changes in spectral properties of the carboxylate extracts. The first is at the complexes present in the most dilute samples of Versate and octanoate extracts. In those specimens the cobalt to total acid ratios are respectively, 1:2.93 and 1:2.18. Experimental evidence has shown that no charged ligands other than carboxylate anions can be detected and free carboxylic acid is present as only dimeric acid and does not solvate the complex. The ratio of cobalt to carboxylate anion must, therefore, be 1:2. Although the formation of cobalt-cobalt bonds in the more dilute samples cannot be excluded, the fact that bridging carboxylate groups are destroyed by dilution strongly suggests that depolymerisation of the carboxylate complexes in the more concentrated solutions is occurring. Given that the most dilute samples contain sufficient water to provide more than two molecules to solvate each **cobalt ion and that the carboxylate anions have been shown to** behave as monodentate ligands it is entirely reasonable to assume that the composition of the extracts in the dilute specimens have the general formula $\text{Co}(\text{H}_2\text{O})_2\text{R}_2$. The Versate extract is a tetrahedral complex and the structural formula VIII can be drawn.



The octanoate extract is neither octahedral nor tetrahedral. Its low extinction coefficient and its pink colour suggest that it is more like octahedrally co-ordinated compounds. Because it would seem to be four-coordinate, the only other possibility is a square-planar configuration. Although the magnetic moment of the complex, 4.4 BM, is characteristic of tetrahedral and octahedral cobalt II ⁽⁶⁾, the value would equally apply to a square-planar, low field (high spin) complex. The most compelling piece of evidence for the assignment of the square-planar structure is the fact that the octanoate extract gels with great ease. Not only would the cobalt octanoate/cyclohexane/water system be expected to behave like other soap/oil/water mixtures in its ability to form smectic phases ⁽²⁶⁾, but plate-like structures of the type envisaged, IX, would readily align in solution to yield multimolecular chains responsible for gel-formation.

In progressing from the most dilute to the most concentrated extracts, experiments have indicated that, for the Versatic extract, three stages can

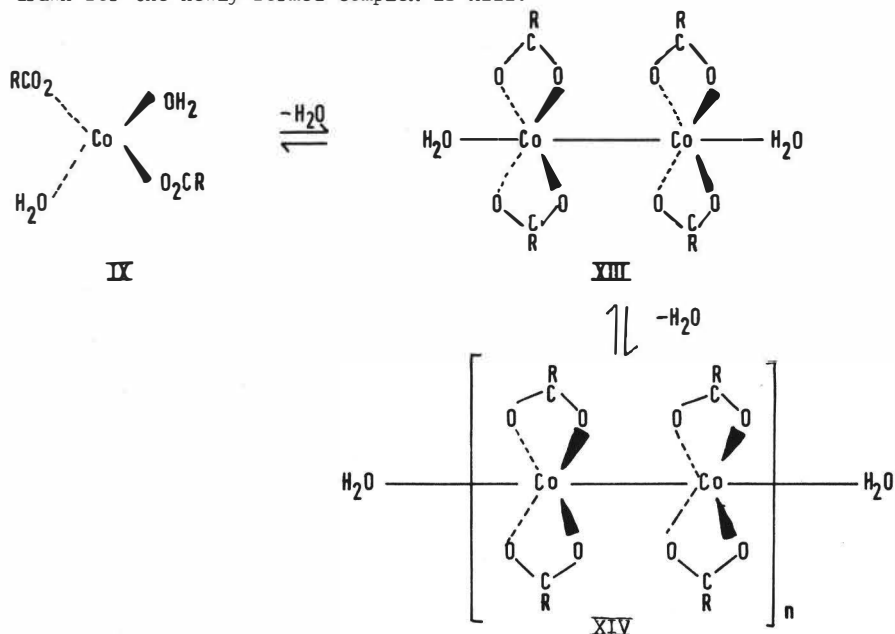
be readily detected before the pictures becomes excessively complicated and of these that occurring in more concentrated solution (Fig. 3, sample 5) is an octahedral complex. Tetrahedral complexes persist through the whole range of concentration but at high concentration (samples 1 to 5) they are accompanied by octahedral complexes. The changes which occur in the infra-red show that at intermediate concentrations (sample 5) both monodentate and bidentate chelating carboxyl groups are present, whilst at high concentrations (samples 3 to 1) the monodentate and chelating groups are also accompanied by bridging carboxylate groups and by solvating acid. Further, in sample 5 the ratio of cobalt to water is of the order 1:0.5 to 1. These observations can only be explained in terms of the following equilibria



Because of the difficulty in resolving the derivative spectra of subsequent samples and because of the introduction of solvating acid and bridging carboxyl groups at high concentration, no firm conclusions can be drawn about the remaining complexes in the system.

Three stages of complexation can be detected in the dilution experiments with cobalt octanoate, of which the two occurring at a higher concentration are octahedrally co-ordinated. Infra-red evidence shows the presence of bidentate and monodentate carboxylate groups in the more concentrated solutions, but only at very high concentration does the small amount of free acid in the system (1 molecule for every 6 cobalt II ions) become involved in solvation. Further, at intermediate concentrations the amount of water, calculated from its solubility in cyclohexane, is less than one molecule per

cobalt ion. Under these conditions, the simplest structure which can be drawn for the newly-formed complex is XIII.



A third stage, XIV, which shows the same i.r. and u.v./visible properties as XIII is envisaged, the controlling factor in its formation being the amount of water in the system. That dilute and moderately concentrated solutions of cobalt octanoate form gels lends further support for the presence of an equilibrium between complexes IX, XIII and XIV since the value of *n* and hence the ability to gel will increase as the ratio of cobalt to water becomes less.

Attempts to draw structures for the octahedral complexes present in the most concentrated solution must account for the following observations. All types of carboxylate bonding behaviour occur. The cobalt will appear to occupy only octahedral environments. Some of the free acid in the extract is involved in solvation. Coupled with these observations, the fact that the neat extract does not readily gel suggests a highly crosslinked and random system of chains similar to XIV.

The second point of attack from which to obtain information about the carboxylate complexes is under circumstances where the ratio of free acid to cobalt is high. In the experiments in which acid was added to the extracts the most extreme samples contained 0.014 M cobalt and 1.4 M free acid

in the Versate case and 0.016 M cobalt and 1.6 M free acid in the octanoate case. At these metal and extractant concentrations, conditions are favourable to slope analysis and it has been shown^(1,2) that complexes of the general formulae $(\text{CoR}_2 \cdot 2\text{HR})_2$ and $\text{CoR}_2 \cdot 2\text{HR}$ are extracted. Fig.8 indicates that the samples (Versate samples 10 and 11 and octanoate sample 7) are binary mixtures of complexes and it can be concluded that monomeric and dimeric species are present. Further evidence for this comes from the analysis of an extract from another experiment in which conditions favourable to the extraction of the monomeric⁽²⁾ species prevailed, i.e. cobalt concentration $< 10^{-4}\text{M}$ and cobalt to acid ratio of 1:500. (Fig.8. Versate sample 11).

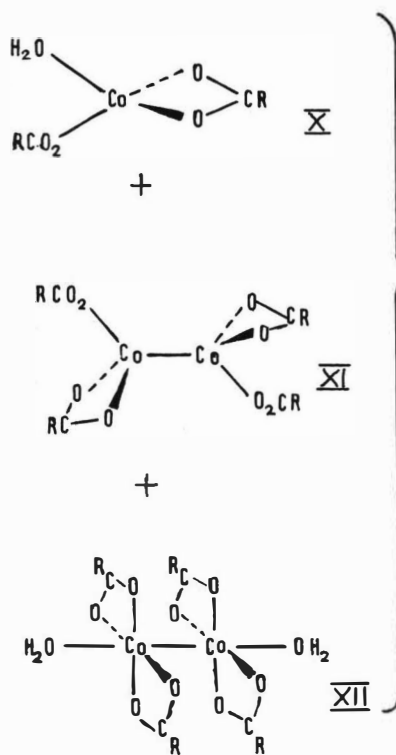
Having made this assignment it is now possible to say more about the structures of the monomeric and dimeric complexes, I, II and III. For two reasons, the configuration III is the only acceptable one for the monomeric complex. Firstly, the only two ligands in solution are carboxylate anions and carboxylic acids: the possibility of water participating in the complex has already been examined and excluded. Secondly, to satisfy the general formula $\text{CoR}_2 \cdot 2\text{HR}$ and octahedral co-ordination the carboxylate ligands must be bidentate groups. Infra-red evidence indicates that only bidentate carboxylate groups are present in samples containing large amounts of acid and not only does this agree with the assignment of the monomer as III, but the absence of monodentate carboxylate groups shows that the dimeric complex must have structure I. This last conclusion conflicts with earlier views⁽²⁾ that the dimer contains a cobalt-cobalt bond.

The initial samples in the acid addition experiments have been shown to be mixtures by dilution studies and so the overall sequence of changes which occur on treating the extracts with free acid is shown on the following page.

The scheme strongly suggests that the routes by which the products are formed simply involve the substitution of carboxylic acid for water and the expansion of co-ordination number as the amount of acid increases.

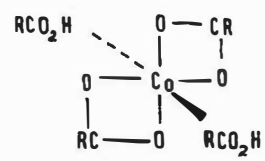
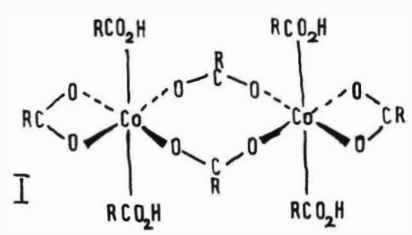
Mixed hydroxide/carboxylate complexes of cobalt

Evidence for their formation is to be found in the Versate extract obtained at pH 9.1. The strong infra-red evidence for OH groups in the soluble extract (Fig.12) finds support in the fact that the electronic spectra of soluble and insoluble products are akin to that of an alkaline solution



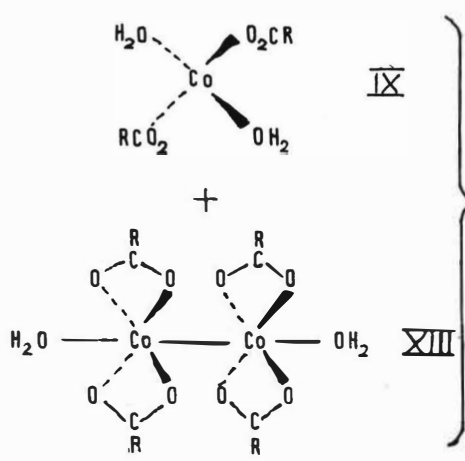
Versatic acid system

2 or 3 complexes



III

1 complex



Octanoic acid system

of cobaltous hydroxide which has been reported⁽²⁴⁾ to contain $\text{Co}(\text{OH})_4^{2-}$ and $\text{Co}(\text{OH})_3\text{H}_2\text{O}^-$. Further, analysis of the soluble fraction reveals (Table 1) more cobalt II than total acid and as a result another negatively charged ligand must be present in the complex. It would seem reasonable to propose the existence of mixed complexes of the general formula $\text{Co}_a(\text{OH})_b(\text{RCO}_2)_c(\text{H}_2\text{O})_d(\text{RCO}_2\text{H})_e$. In this way it is possible to explain the solubility behaviour of the mixed complexes and also the apparent variable pattern of carboxylate bonding and the presence of solvating acid.

Complex-forming equilibria

Thus far, the compositions and types of carboxylate complexes have been approached wholly from structural aspects. Having determined some of the complexes in the system and the factors which play a part in their formation, the results can be discussed from a thermodynamic stand-point.

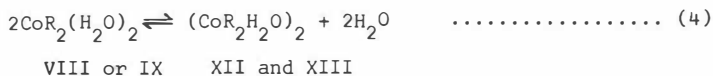
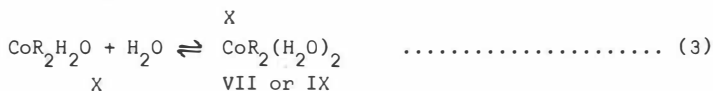
Clearly, as in the stepwise formation of complexes in aqueous media, the formation and co-existence of the various cobalt species in organic extracts is a function of the thermodynamic activities of the metal and associated ligands.

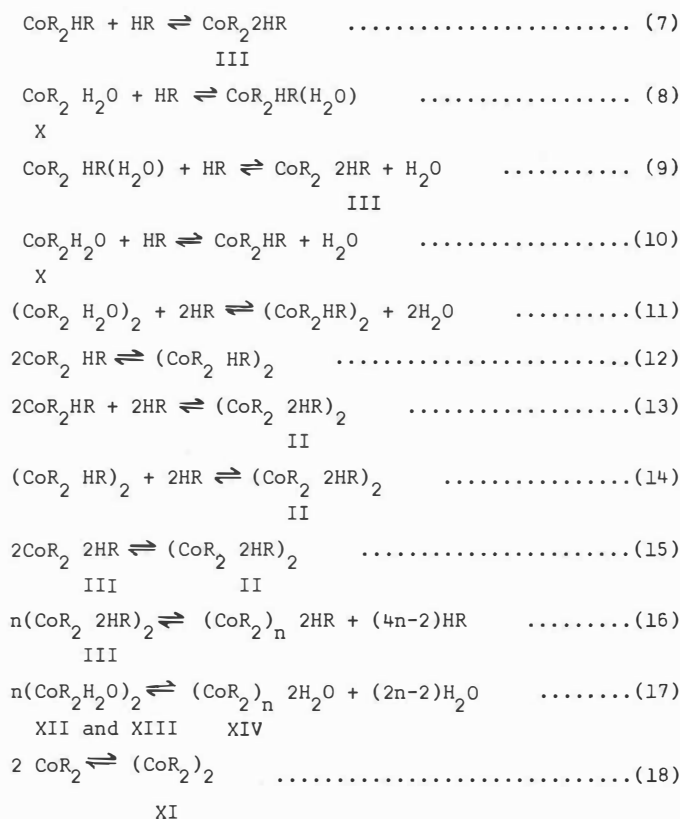
Owing to the low dielectric constant of cyclohexane, the occurrence of ionised species is extremely improbable and thus the reaction:



can be assumed to go to completion. To simplify the picture mixed hydroxide/carboxylate complexes will be omitted. The complex-forming reactions in the extract will involve solvation of CoR_2 with water or carboxylic acid (HR), nitrate having been shown to be absent, and will also involve polymerisation of the solvated species. CoR_2 can thus be regarded as the uncomplexed form of cobalt.

The following series of equilibria may then be postulated.





These equilibria are summarised diagrammatically in Fig. 13 which sets out the relationships between the various species. It should, of course, be emphasised that some of the stages may be hypothetical or may occur to such a minor extent as to be undetectable. Those species for which spectrophotometric evidence exist are clearly indicated. Other species are either necessary to satisfy the stepwise formation of the dominant complexes or else may be shown to represent thermodynamically equivalent and indistinguishable routes to the same product, e.g. reactions (5) and (3)+(4); (8)+(9) and (7)+(10).

The fraction of total cobalt in any given form will be a function of $[\text{CoR}_2]$, $[\text{H}_2\text{O}]$ and $[\text{HR}]$ and will obviously depend on the relative values of the equilibrium constants, K_2 to K_{18} , of the equilibria listed above. The two acid systems, Versatic 911 acid and octanoic acid, will have different values for $K_2 - K_{18}$.

In principle the values of K_2 to K_{18} could be calculated, but in practice data are insufficient and the system too complicated for this to be done with any confidence. However, the application of a programme such as LETAGROP VRID⁽²⁷⁾ might well give additional information on the important equilibria in the system.

Qualitatively we can make use of the equations (2) to (16) to explain the spectrophotometric observations during dilution of organic extracts with cyclohexane and addition of free carboxylic acid to them.

(i) Dilution experiments

Dilution of an extract with cyclohexane containing 0.01% water will result in a constant water activity and falling activities of free carboxylic acid and cobalt carboxylate. This will initially result in the breakdown of chain-like structures, e.g. XIV, according to (17), for which the overall formation constant is

$$\beta_{17} = [(\text{CoR}_2)_n \cdot 2\text{H}_2\text{O}] / [\text{CoR}_2]^{2n} [\text{H}_2\text{O}]^2$$

Thus the concentration of polymeric complexes is proportional to a large power of $[\text{CoR}_2]$ and highly sensitive to any decrease. Relative increases in water activity will result in the formation of the dimer, $(\text{CoR}_2 \cdot \text{H}_2\text{O})_2$ rather than a species such as $(\text{CoR}_2 \cdot \text{HR})_2$ which involves solvating carboxylic acid molecules.

Further dilution will result in the dissociation of $(\text{CoR}_2 \cdot \text{H}_2\text{O})_2$, according to equilibria (4) and (5), to four co-ordinate monomers such as IX and X. The dissociation will be governed by $[\text{CoR}_2]^2$ because the overall formation constant of the dimer (from equations (2), (3) and (4) or (2) and (5) is $\beta_4 = [(\text{CoR}_2 \cdot \text{H}_2\text{O})_2] / [\text{CoR}_2]^2 [\text{H}_2\text{O}]^2$. Lower cobalt activities will therefore favour the formation of monomeric species, lending support to assumptions made in the structural determinations carried out earlier. There is no spectral evidence for species such as $\text{CoR}_2 \cdot \text{HR}$ at high dilution so that water must satisfy the co-ordination number of cobalt and its small free concentration relative to free acid (Table 1) indicates that the equilibrium constant of reaction (3) is much greater than that of (6), i.e., that water solvates cobalt II ions much more strongly than carboxylic acid.

(ii) Acid addition experiments

Addition of free carboxylic acid to systems containing the mixtures X + XI + XII (for the Versatic acid case) and IX + XIII (for the octanoic acid case) will result in the solvation of the complexes by carboxylic acid according to reactions (8) and (11) with possible formation of mixed solvated species such as $\text{CoR}_2\text{HR}(\text{H}_2\text{O})$ by route (8) although there is no direct evidence for such a complex. The production of dimeric species such as XIII will be favoured by a decrease in water activity, by (4). This is likely to result in a mixture of species such as $(\text{CoR}_2\cdot\text{H}_2\text{O})_2$, $\text{CoR}_2\cdot\text{HR}$ and $(\text{CoR}_2\cdot\text{HR})_2$, the proportions of each depending on the actual equilibrium constants of the reactions. Further addition of free HR is likely to result in the formation of octahedrally co-ordinate monomer $\text{CoR}_2\cdot 2\text{HR}(\text{III})$ by route (7) and dimer $(\text{CoR}_2\cdot 2\text{HR})_2(\text{I})$ by reactions (13) and (14). The proportions of monomer and dimer will be controlled by $[\text{CoR}_2]$ according to equation (15). The formation of more highly polymerised species such as $(\text{CoR}_2)_n 2\text{HR}$ by (16) would not be favoured by addition of free carboxylic acid, but might result at very high cobalt-loadings due to consumption of free carboxylic acid by the cobalt.

CONCLUSIONS

Of the information obtained from UV-visible and infra-red measurements, the latter is more open to alternative interpretations. Consequently, some of the proposed structural formulae must be regarded as only tentative. Notwithstanding this uncertainty, the infra-red measurements have clearly shown that the carboxyl group can change its dentative properties to satisfy the co-ordinative requirements of the system.

The most significant point to emerge from the investigation derives, however, from the derivative work on visible spectra. It is that clear evidence now exists for the presence of multiple equilibria in the organic phase metal extract.

ACKNOWLEDGEMENTS

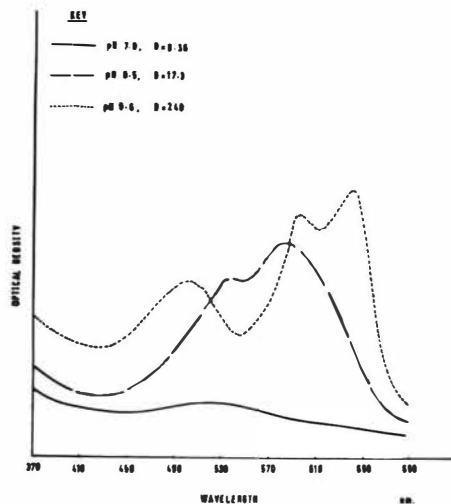
The authors wish to express thanks to Mrs R. Wright for invaluable assistance in compiling the diagrams and to Dr. J. Keighley and Mr. D. Brook for allowing the authors to use their Grubb-Parsons spectrometer. One of us (H.C.) must also thank the Science Research Council for the provision of a research fellowship.

REFERENCES

1. Fletcher, A.W., and Flett, D.S., J. Appl. Chem., Lond., 1964, 14, 250.
2. Tanaka, M., Nakasuka, N., and Goto, S., "Solvent Extraction Chemistry", (Ed. Dyrssen D., et al.), 1967, p.154 (North-Holland, Amsterdam).
3. Jaycock, M.J., and Jones, A.D., *ibid.*, p.160.
4. Jorgensen, C.K., Acta Chem. Scand, 1954, 8, 1495.
5. Ritcey, G.M., and Lucas, B.H., Proc. Int. Solv. Extraction Conf., ISEC 71, 1971 p.463, (Society of Chemical Industry, London).
6. Cotton, F.A., and Wilkinson, G., "Advanced Inorganic Chemistry", 1966, p.865, (Interscience, London).
7. Everett, G.W., and Holm, R.H., Inorg. Chem., 1968, 7, 776.
8. Orisli, P.L., Di Vaira, M., and Sacconi, L., Chem. Comm., 1965, 590.
9. Buffagni, S., and Dunn, T.M., J. Chem. Soc., 1961, 5105.
10. Ramette, R.W., J. Chem. Ed., 1967, 44, 647.
11. Tsimbler, S.M., and Grigoreva, V.V., Russ. J. Inorg. Chem., 1970, 15, 1397.
12. Yatsimirskii, K.B., and Malkova, T.V., *ibid.*, 1961, 6, 1308.
13. Yatsimirskii, K.B., and Malkova, T.V., *ibid.*, 1961, 6, 426
14. Petrakis, L., J. Chem. Ed., 1967, 44, 432.
15. Marquardt, D.W., J. Soc. Ind. Appl. Maths., 1963, 11, 431.
16. Nakamoto, K., "Infra-red Spectra of Inorganic and Co-ordination Compounds", 1963, p.222, (Wiley/Interscience).
17. Edwards, D.A., and Haywood, R.N., Can. J. Chem., 1968, 46, 3443.
18. Ito, K., and Bernstein, H.J., Can. J. Chem., 1956, 34, 170.
19. Stephenson, T.A., Morehouse, S.M., Powell, A.R., Heffer, J.P., and Wilkinson, G., J. Chem. Soc., 1965, 3632.
20. Fletcher, A.W., and Flett, D.S., "Solvent Extraction Chemistry of Metals", (Ed. McKay, et al.), 1965, p.359, (Macmillan, London).
21. Handbook of Chemistry and Physics, 53rd Edition, 1972 (Chemical Rubber Corp).
22. Savitzky, A., and Golay, M.J.E., Anal. Chem., 1964, 36, 1627.
23. Keighley, J.H., and Rhodes, P., Infra-red Physics, 1972, 12, 277.
24. Cotton, F.A., Goodgame, D.M.L., and Goodgame, M., J. Amer. Chem. Soc., 1961, 83, 4690.

25. Colthup, N.B., Daly, L.H. and Wiberley, S.E., "Introduction to Infra-red and Raman Spectroscopy, 1964, p.258, (Academic Press, London).
26. Durham, K., "Surface activity and detergency", 1961, (Macmillan, London).
27. Sillen, L.G., Acta Chem. Scand., 1964, 18, 1085.

Fig. 1 Spectral changes in the organic phase during the extraction of cobalt(II) (0.1M) with Versatic (0.1M) in cyclohexane



316

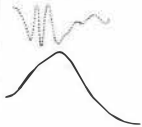
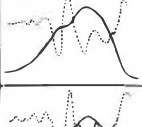
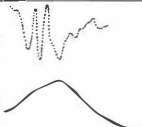
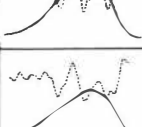
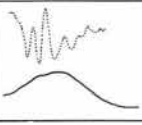
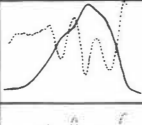

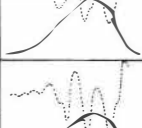
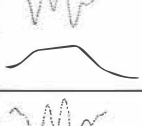
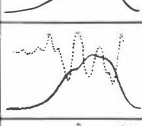
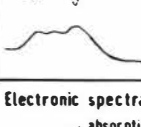
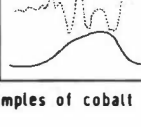
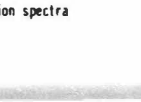
Octanoic Acid System				Versatic Acid System			
ϵ_{max}	nm	SAMPLE NUMBER	DILUTION FACTOR	ϵ_{max}	nm	SAMPLE NUMBER	DILUTION FACTOR
19		1	0	51		1	0
19.5		2	1.3	64		2	1.3
19		3	2	70		3	2
10		4	4	108		4	4
21		5	5	85		5	5
24		6	20	113		6	10
				225		7	20
				225		8	40

Fig. 2 Electronic spectra of diluted samples of cobalt carboxylate extracts

— absorption spectra

... 2nd derivatives of absorption spectra

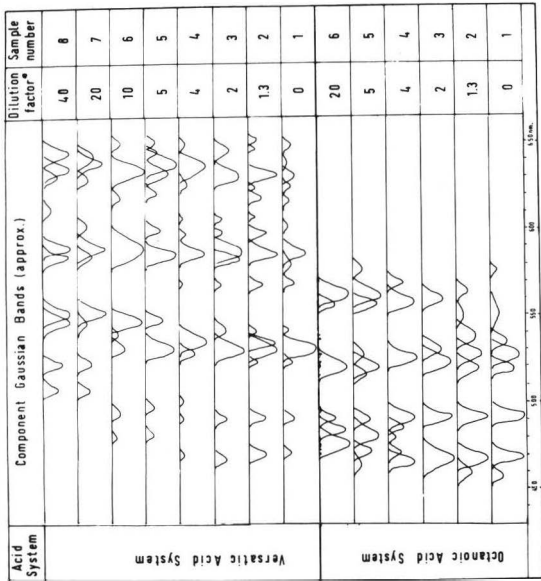


Fig.3. Composite band diagrams from the derivative spectra of diluted samples of cobalt carboxylate extract.

* Dilution factor = vol. of dilute soln. / initial volume of neat extract

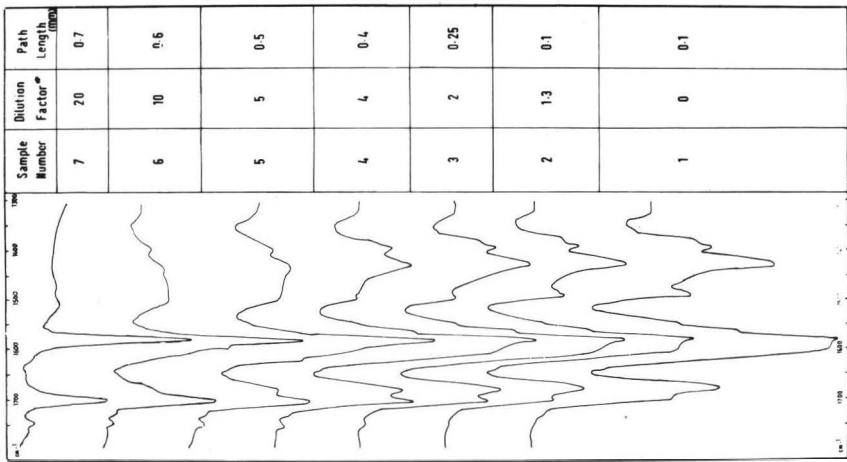


Fig. 4. Infrared spectra of dilute samples of cobalt Versate

* Dilution factor = vol. of dilute soln. / initial volume of neat extract

Fig 5 Infrared spectra of diluted samples of cobalt octanoate

* Dilution factor = vol. of diluted sample / initial vol. of neat extract

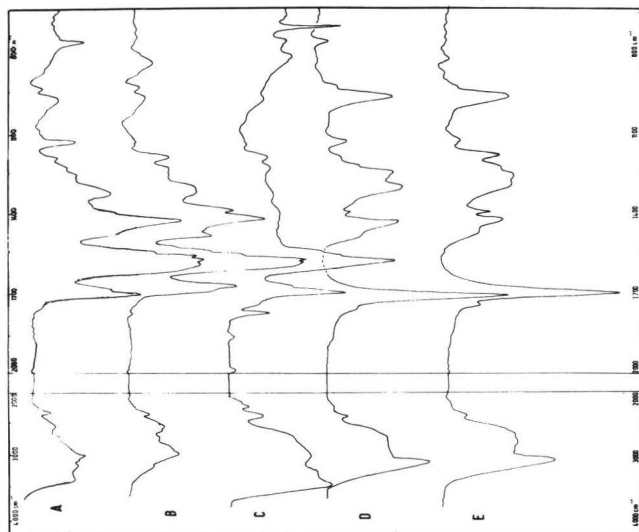
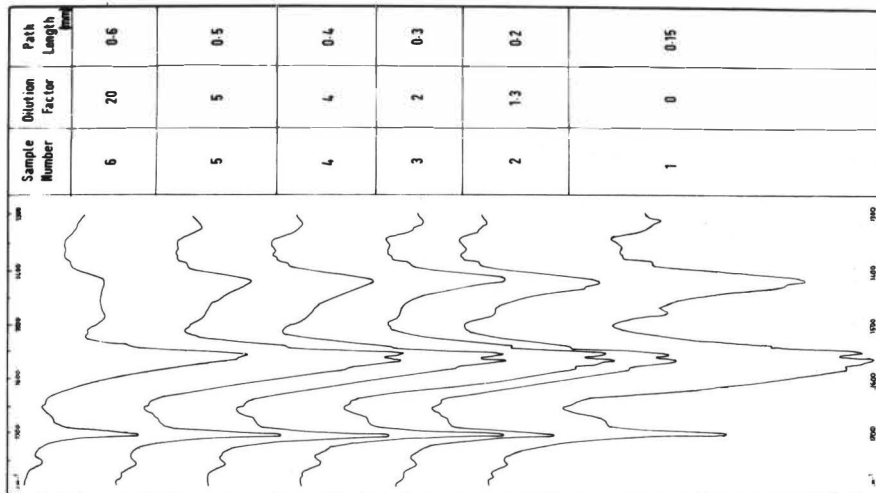


Fig.6 Infrared spectra of cobalt carboxylate extracts and carboxylic acids

- (A) Meat cobalt octanoate extract (pH 7.3) path length 0.2mm
- (B) Meat cobalt Versate extract (pH 8.3) path length 0.2mm
- (C) Meat cobalt Versate extract (pH 9.1) path length 2.0mm
- (D) 0.1M octanoic acid in cyclohexane path length 0.25mm
- (E) 0.1M Versatic 911 in cyclohexane path length 0.25mm

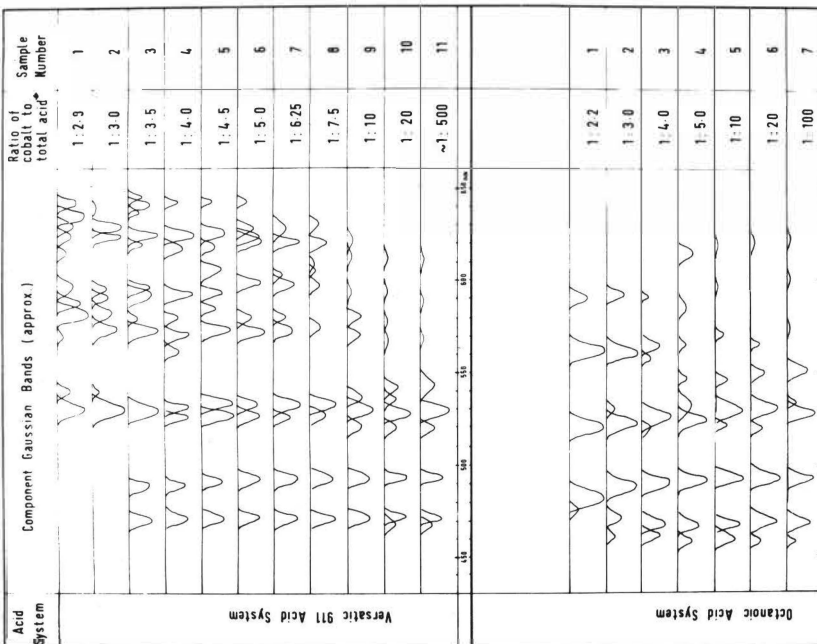


Fig. 8 Composite band diagrams from the derivative spectra of cobalt carboxylate / carboxylic acid mixtures

* Total acid = [free acid + carboxylate acid in extract] + added free acid

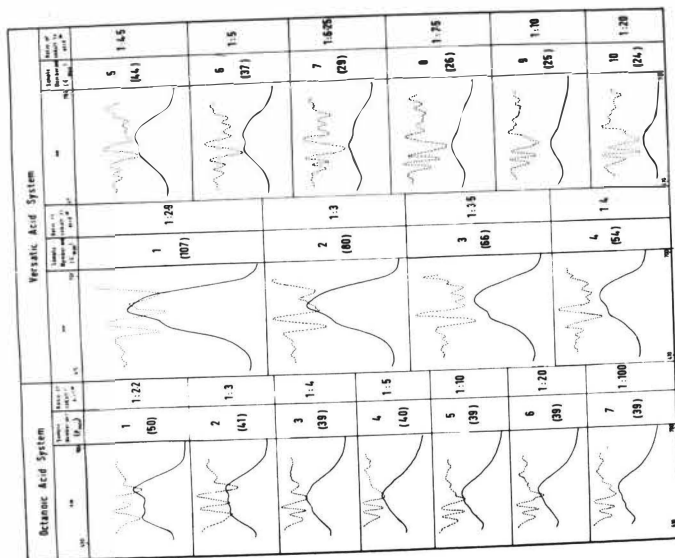


Fig. 7 Electronic spectra of mixtures of cobalt carboxylate and carboxylic acid

* Total acid = [free acid + carboxylate acid in extract] + added free acid

~ absorption spectra

~ 2nd derivative of absorption spectra

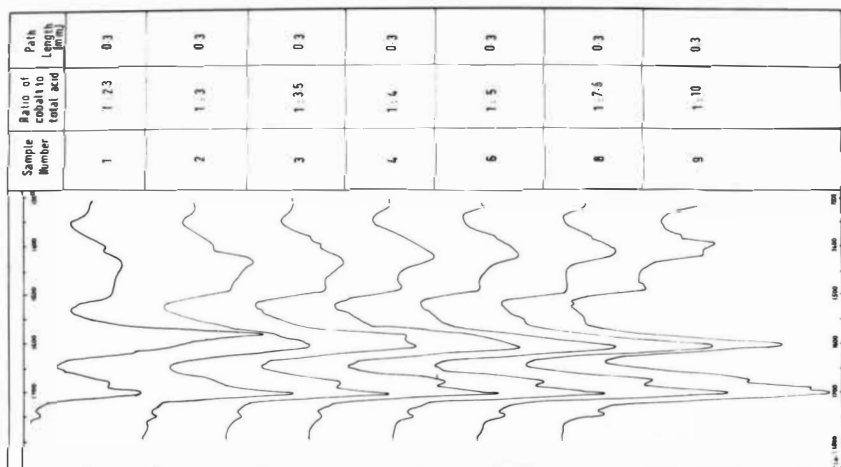


Fig. 9 Infrared spectra of mixture of cobalt Versaile extract and Versanic acid

• Total acid = [free acid + carboxylate acid in Extract] + added free acid

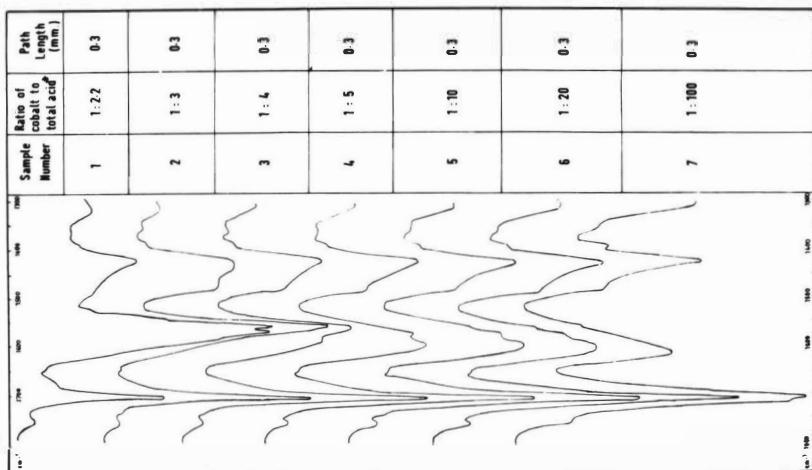


Fig. 10 Infrared spectra of mixtures of cobalt octanoate extract and octanoic acid

• Total acid = [free acid + carboxylate acid in extract] + added free acid

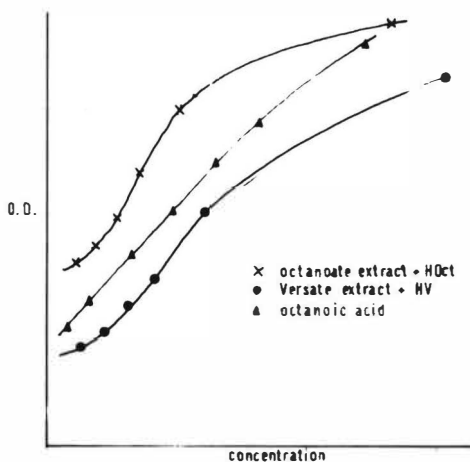


Fig. 11. O.D. vs concentration plots for the acid carbonyl peak in extract/acid mixtures.

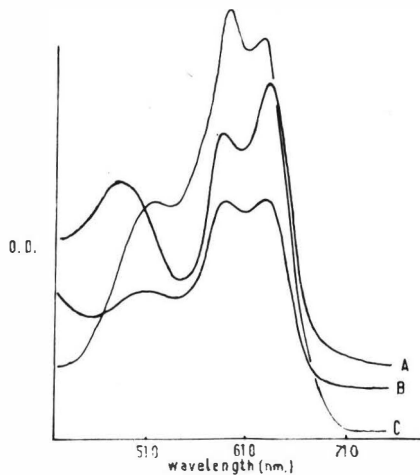


Fig. 12. U/V spectra of the insoluble extract (pH 9.1), A, the soluble extract (pH 9.1), B, an alkaline solution of Co(OH)_2 , C.

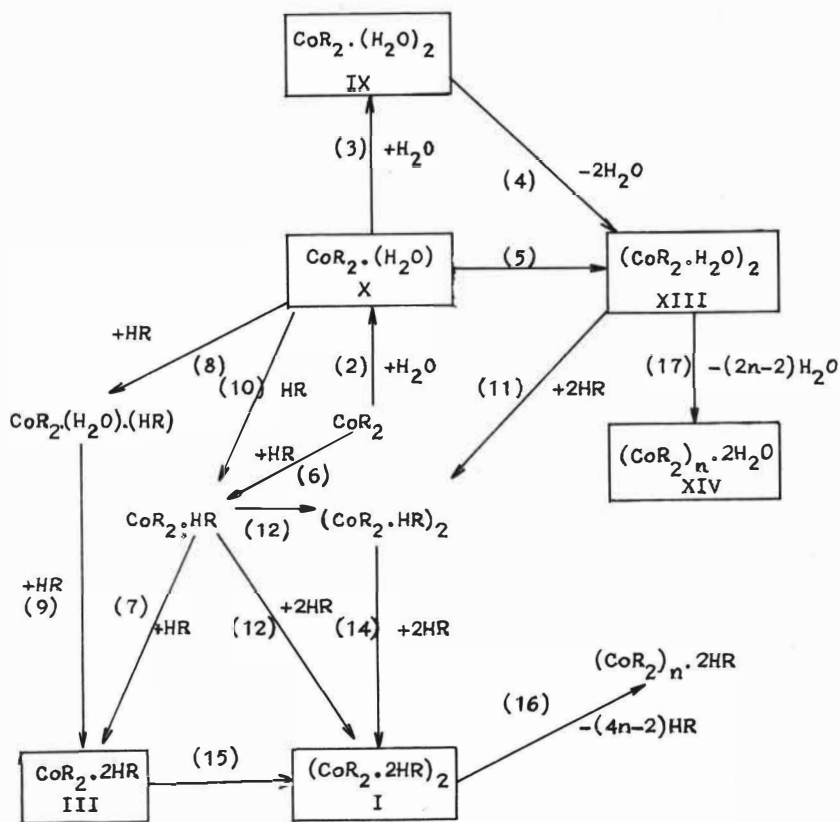


Fig. 13 Diagram showing the proposed complex-equilibria in cobalt carboxylate extracts

species for which evidence exists
 () reaction number

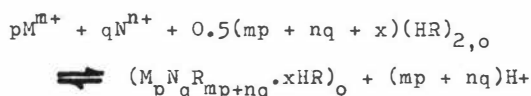
FORMATION OF MIXED METAL COMPLEXES IN THE EXTRACTION OF METALS WITH CAPRIC ACID

Noriyuki NAKASUKA, Hiromichi YAMADA* and Motoharu TANAKA

Laboratory of Analytical Chemistry, Faculty of Science,
Nagoya University, Nagoya 464, Japan

ABSTRACT

The formation of mixed metal complexes in the carboxylate extraction has been studied. The general treatment of equilibria involved is presented. Evidence is given for the mixed metal caprates in the caprate extraction of the following pairs of metal ions: nickel and cobalt; sodium and zinc; sodium and cadmium; aluminium and gallium. Extraction equilibrium of a mixed metal complex is written as:



for which the constant is denoted as $K_{ex}^{M,N}(pqx)$. The compositions and extraction constants at (25°C and an ionic strength of 0.1M NaClO₄) of the extracted mixed metal species are as follows:

$$NiCoR_4 \cdot 4HR: \quad \log K_{ex(114)}^{Ni,Co} = -19.1 \pm 0.1$$

$$ZnNaR_3 \cdot 5HR: \quad \log K_{ex(115)}^{Zn,Na} = -13.86 \pm 0.05$$

$$CdNaR_3 \cdot 5HR: \quad \log K_{ex(115)}^{Cd,Na} = -14.0 \pm 0.1$$

$$CdNaR_3 \cdot 7HR: \quad \log K_{ex(117)}^{Cd,Na} = -13.8 \pm 0.3$$

$$Al_3Ga_3R_{12}(OH)_6 \quad (\text{tentative composition})$$

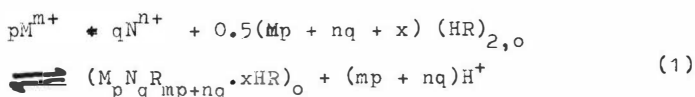
*Faculty of Engineering, Gifu University, Gifu 504, Japan

INTRODUCTION

The extraction of metal ions with carboxylic acids has been examined by several authors and has been recently reviewed by Flett and Jaycock. In the extraction of metals with capric acid coextraction is not exceptional. We have extracted species of definite composition involving two metal ions in the same molecule. This paper describes the general treatment of the equilibria involved and some examples of coextraction recently obtained in this laboratory.

EQUILIBRIUM TREATMENT

Two metal ions M^{m+} and N^{n+} are supposed to be extracted by an extractant HR as a mixed metal complex of the composition $M_p N_q R_{mp+nq} \cdot xHR$. The following equilibrium is responsible for the extraction of this species:



for which the extraction constant $K_{ex(pqx)}^{M,N}$ is defined as:

$$K_{ex(pqx)}^{M,N} = \frac{(M_p N_q R_{mp+nq} \cdot xHR)_o (H^+)^{(mp+nq)} (M^{m+})^{-p} (N^{n+})^{-q}}{x ((HR)_2)_o^{-(mp+nq+x)/2}} \quad (2)$$

The molar concentrations of metals M and N involved in the mixed metal complex (denoted as $C'_{M,o}$ and $C'_{N,o}$ respectively) are given as follows:

$$C'_{M,o} = C_{M,o} - \sum_j \sum_y j (M_j R_{mj} \cdot yHR) \quad (3)$$

$$C'_{N,o} = C_{N,o} - \sum_i \sum_z i (N_i R_{ni} \cdot zHR) \quad (4)$$

where $C_{M,o}$ and $C_{N,o}$ refer to the total concentration of metals M and N respectively, in the organic phase.

To elucidate the composition of a mixed metal species in the organic phase, the extraction behaviour of each metal ion involved must have been previously studied. From known values of extraction constants of species involving only M, terms $\sum_j j(M_j R_{mj} \cdot yHR)$ are calculable². Thus we obtain $C'_{M,o}$ and, quite similarly, $C'_{N,o}$.

The molar ratio of M and N in the mixed complex, r , is now defined by the following:

$$r = C'_{N,o} / C'_{M,o} = q/p \quad (5)$$

Combining equations (2) and (5), we have

$$\begin{aligned} \log C'_{M,o} = & p \left[\log(M^{m+}) + r \log(N^{n+}) - (m+nr) \log(H^+) \right] \\ & + 0.5(mp + nrp + x) \log((HR)_2)_o + \log K_{ex}^{M,N}(pqx) \\ & + \log p \end{aligned}$$

Thus from the slope of the plot of $\log C'_{M,o}$ against $[\log(M^{m+}) + r \log(N^{n+}) - (m + nr) \log(H^+)]$ at a fixed extractant concentration, we find the value of p .

Now m , n , r and p being known, the plot of $\log C'_{M,o} - p [\log(M^{m+}) + r \log(N^{n+}) - (m + nr) \log(H^+)]$ against $\log((HR)_2)_o$ yields a straight line with a slope of $0.5(mp + nrp + x)$. From the intercept of the plot we obtain the value of extraction constant $\log K_{ex}^{M,N}(pqx)$.

RESULTS AND DISCUSSION

Partitions were performed between water and benzene containing capric acid in a bath thermostatted at $25.0 \pm 0.1^\circ\text{C}$. The ionic strength of the aqueous phase was kept constant at 0.1 M with sodium perchlorate. The composition of the extracted species as well as values of extraction constants given below are therefore valid for these experimental conditions.

Nickel cobalt caprate²

The extraction of nickel and cobalt in the presence of each other is always higher than predicted from the extraction constants of single metal ions, the fact pointing to the formation of a mixed metal complex(es) in the organic phase.

Determination of the r values for a number of partitions of the two metals has revealed the value of r to be unity. The plot of $\log C'_{Ni,o}$ against $(\log(Co^{2+}) + \log(Ni^{2+}) - 4\log(H^+))$ at a fixed $((HR)_2)_o$ yielded a straight line with a slope of unity, i.e. $p = q = 1$. The composition of the nickel cobalt caprate is thus $NiCoR_{4.4}HR$ with the extraction constant of $\log K_{ex(114)}^{Ni,Co} = -19.0 \pm 0.1$.

Electronic spectra for the mixed metal complex are quite similar to those composed of each spectrum for dimeric caprate of single metal, that is, the additivity of spectra holds for the mixture of cobalt and nickel caprates. This fact implies that the octahedral environments around both central metal ions in the mixed metal caprate resemble closely those in their respective dimeric caprates.

Zinc sodium caprate³

The distribution ratio of zinc is proportional to the third power of aqueous hydrogen ion concentration. Flame-photometry showed the ratio $C'_{Na,o}/C'_{Zn,o}$ to be unity. From these experimental evidences we have arrived at the conclusion that the extracted mixed zinc sodium caprate contains one atom each of zinc and sodium. Finally extractant dependence of $(\log D_{Zn} + 3\log(H^+))$ revealed the composition of the extracted species to be $ZnNaR_{2.5}HR$ with the corresponding extraction constant of $\log K_{ex(115)}^{Zn,Na} = -13.86 \pm 0.05$.

Cadmium sodium caprate³

In much the same way as in the preceding case, we found the following mixed metal caprates:

$$\text{CdNaR}_{3.5}\text{HR with } \log K_{\text{Ex}(115)}^{\text{Cd,Na}} = -14.0 \pm 0.1;$$

$$\text{CdNaR}_{3.7}\text{HR with } \log K_{\text{ex}(117)}^{\text{Cd,Na}} = -13.8 \pm 0.3.$$

We have in the organic phase $\text{CdR}_2 \cdot 4\text{HR}$, dimeric and trimeric cadmium caprates as well as these mixed metal caprates.

Aluminium gallium caprate⁴

In the case of aluminium gallium caprate, of which the reaction with δ -quinolinol is much faster than that of aluminium caprate in the organic phase, the mixed metal caprate is kinetically distinguishable.

At present we would like to note only a tentative composition for this mixed metal caprate: $\text{Al}_3\text{Ga}_3\text{R}_{12}(\text{OH})_6$.

REFERENCES

1. Flett, D.S., and Jaycock, M.J., "Ion Exchange and Solvent Extraction" (J.A. Marinsky and Y. Marcus, editors), 1973, Vol. 3, pp. 1 - 50, New York, Marcel Dekker Inc.
2. Nakasuka, N., Ito, T. and Tanaka, M., Chemistry Letters, 1973, 553.
3. Nakasuka, N., Mitsuoka, Y. and Tanaka, M., J. inorg. nucl. Chem., in press. 36, 431, 1974.
4. Yanada, H., Maeda, T. and Tanaka, M., to be published.

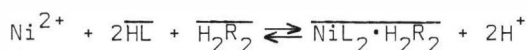


USE OF EXTRACTANT MIXTURES CONTAINING KELEX 100 FOR SEPARATION OF NICKEL(II) AND COBALT(II)

by L. Hummelstedt, H.-E. Sund*, J. Karjaluoto, L.-O. Berts and B.G. Nyman**

Inst. for Industrial Chemistry, Åbo Akademi, Åbo, Finland

Abstract The present investigation concerns the applicability of Kelex 100 (HL) and its mixtures with Versatic 9-11 (HR) to the separation of Ni(II) and Co(II). While Ni(II) is preferentially extracted by Kelex 100 in isodecanol/Shellsol K the co-extracted Co(II) apparently undergoes oxidation in the organic phase in the presence of air. This difficulty does not exist in Kelex 100/Versatic 9-11 mixtures which show synergic behaviour due to the formation of mixed complexes. Ni(II) is shown to exist as $\text{NiL}_2 \cdot \text{H}_2\text{R}_2$ while the Co(II) complex apparently has the formula $\text{CoL}_2 \cdot 2\text{H}_2\text{R}_2$. For the extraction equilibria



the concentration products K_{Ni} and K_{Co} were found to have the following values in isodecanol/Shellsol K at 25°C:

$$K_{\text{Ni}} \approx 4.2 \cdot 10^{-4} \text{ l/mole}$$

$$K_{\text{Co}} \approx 2.2 \cdot 10^{-5} \text{ l}^2/\text{mole}^2$$

The separation factor $S_{\text{Ni,Co}}$ is largest (≈ 65) at 25°C but in practice the temperature must be raised to 50°C in order to increase the extraction rate and reduce the acid uptake during stripping. Careful pH control is required in this operation in order to keep $S_{\text{Ni,Co}}$ at a satisfactory level of about 35.

*Present address: Kemira Oy, Oulu, Finland

**Present address: Metallurgical Research Centre, Outokumpu Oy, Pori, Finland

INTRODUCTION

Extractant mixtures containing hydroxyoximes (LIX reagents, General Mills Chemicals, Inc.) and carboxylic acids (Versatic 9-11, Shell Chemical Co. Ltd.) have recently been successfully utilized for the separation of nickel(II) and cobalt(II) in sulphate solutions¹. The selectivity of LIX-63/carboxylic acid mixtures for nickel(II) was discovered several years ago^{2,3} but the adverse kinetics of nickel extraction was considered likely to preclude commercial application of this extractant mixture³. This difficulty was later overcome by the addition of a small amount of dinonyl naphthalene sulphononic acid (DNNS) and a rapid and efficient separation of nickel(II) and cobalt(II) was achieved, particularly when using mixtures containing LIX-70 and Versatic 9-11 as main components¹.

The reagent Kelex 100 introduced by Ashland Chemical Co. apparently has 7-[3-(5,5,7,7-tetramethyl-1-octenyl)]-8-hydroxyquinoline as its active component⁴. It is thus a chelating agent similar to the hydroxy oximes of the LIX series and like these it has mainly been used for extraction of copper. Kane and Cardwell^{4a} have, however, proposed a method for separation of cobalt(II) and nickel(II) by selective stripping of nickel(II) with HCl from an organic phase containing 10 vol.-% Kelex 100 and 30 vol.-% isodecanol in kerosene. According to the inventors Co(II) and Ni(II) are first extracted in the pH range 3.0-4.2 from an aqueous chloride, sulphate or nitrate solution whereafter nickel(II) is stripped from the organic phase using 3-20 % HCl and cobalt(II) using more concentrated HCl. It is recommended that the stripping be performed at 30-50°C in order to reduce the uptake of acid in the organic phase.

Very recently Lakshmanan and Lawson⁵ have studied the extraction of cobalt(II) by Kelex 100 and mixtures of Kelex 100 and Versatic 9-11. Co(II) was reported to form a very stable complex with Kelex 100 in kerosene, as deduced from the fact that the metal ion could not be stripped from the organic phase even with 3.5M H₂SO₄. The complex was found to have the formula CoL₂(HL)₂ (HL = Kelex 100). Kelex 100/Versatic 9-11 mixtures extracted cobalt(II) with similar efficiency as Kelex 100 alone

but the mixed complex $\text{CoL}_2\text{H}_2\text{R}_2$ (HR = carboxylic acid) was found to be easily decomposed by stripping with dilute acid. According to these authors the Kelex 100/Versatic 9-11 mixture shows no evidence of synergic action.

By analogy with the LIX/Versatic systems¹ one may expect mixtures of Kelex 100 and Versatic 9-11 to be useful for the separation of nickel(II) and cobalt(II). The purpose of the present investigation is to explore this possibility as well as the usefulness of Kelex 100 alone as an extractant for separating cobalt(II) and nickel(II) in aqueous sulphate solutions. The studies include extraction experiments combined with spectrophotometry and vapour pressure osmometry. In this manner it has been possible to investigate extracts at concentration levels of interest in practical applications.

EXPERIMENTAL

The reagents Kelex 100 (Ashland Chemical Co.), Versatic 9-11 (Shell Chemical Co. Ltd) and dinonyl naphthalene sulphonic acid (DNNS) (R.T. Vanderbilt Co., Inc.) were used without purification. For Kelex 100 an apparent molecular weight of 321 was determined by saturating with Ni(II) at pH 9 in the presence of NH_3 . An aliphatic hydrocarbon solvent Shellsol K (Shell Chemical Co. Ltd) was used as diluent and isodecanol (Ashland Oil & Refining Company) as modifier. All organic phases with Shellsol K as diluent contained 100 g/l of isodecanol; this solvent system is referred to as isodecanol/Shellsol K.

All other solvents and chemicals used were of analytical reagent quality.

Extraction experiments were performed using a phase volume ratio of one in a 250 ml glass vessel equipped with a stirrer, glass calomel electrodes, and an inlet for gaseous ammonia diluted with nitrogen. The pH was maintained constant by means of a Metrohm E 450 control unit coupled to a magnetic valve in the ammonia line. All aqueous phases contained 0.25M $(\text{NH}_4)_2\text{SO}_4$ in order to reduce fluctuations in the ionic strength. The glass calomel electrodes immersed in the dispersion in the extraction vessel gave stable readings over long periods of time. All

equilibrium pH values were also checked with a digital pH-meter (Radiometer pHM 52) after phase separation. In experiments at elevated temperatures the final pH values were measured after cooling the aqueous phase to 25°C.

A Hitachi Perkin-Elmer Model 139 spectrophotometer was used for the photometric studies while aggregation in iso-octane solutions was measured with a Knauer vapour pressure osmometer. The mole fraction x_2 obtained from the osmometer reading ΔR according to equation (1) was used for computation of the average aggregation number for the dissolved substance according to equation (2), where C_2 is the monomeric molarity of the dissolved substance and C_1 the molarity of the solvent. The constant A was

$$x_2 = \frac{\Delta R}{A} \quad (1)$$

$$\bar{n} = \frac{C_2(1 - x_2)}{C_1 x_2} \quad (2)$$

determined for iso-octane using trioctyl amine, which is known to be monomeric in hydrocarbon solvents.

When extracted from separate solutions Ni(II) and Co(II) were determined by conventional EDTA titration. Organic phases containing both metals were stripped with 8M HCl, whereafter Co(II) was determined photometrically⁶ and the sum of Ni(II) and Co(II) by titration with EDTA.

RESULTS AND DISCUSSION

Extraction with Kelex 100

Effect of DNNS and temperature on the extraction rate in isodecanol/Shellsol K

The rate of extraction of Ni(II) with Kelex 100 in isodecanol/Shellsol K was found to be quite low at 25°C, where equilibrium was not reached even after 120 min at pH 4.72 (Fig. 1). Raising the temperature to 50°C increased the extraction rate considerably and further improvements were obtained by

adding DNNS in concentrations of 0.005 and 0.010M. At the higher DNNS-concentration equilibrium was reached in about 20 min when the temperature was 50°C.

For Co(II) the extraction rate was found to be faster than for Ni(II), about 8 min being required to attain equilibrium at 50°C in the presence of 0.005M DNNS.

The addition of DNNS was thus found to have an effect similar to but not as pronounced as that in the LIX/Versatic systems¹. All subsequent extraction experiments with Kelex 100 at 25°C were performed in the presence of 0.01M DNNS. Even with this addition contact times of the order of 1.5 h were required to reach equilibrium for Ni(II) at 25°C.

Effect of pH on extraction equilibria in isodecanol/Shellsol K

The pH-dependence of the extraction equilibria of Ni(II) and Co(II) in isodecanol/Shellsol K was studied by extracting the metal ions from separate sulphate solutions at four different concentrations of Kelex 100 (75, 100, 150 and 200 g/l). The results for the lowest and the highest extractant concentrations are shown in Fig. 2. While nickel is extracted at lower pH than cobalt at both extractant levels there are considerable differences in shape between the curves for cobalt. At 75 g Kelex 100/l (0.236M) only 85 % of the cobalt was extracted although the pH was raised to 6.5. The capacity of this extractant thus seems insufficient for complete extraction of cobalt in spite of the fact that complete extraction of nickel from a solution of roughly the same metal ion concentration was achieved at a pH of about 5.5. However, the ratio Kelex 100/cobalt is close to 2 and thus much lower than the value 4 found by Lakshmanan and Lawson⁵ in experiments at lower concentrations ($5 \cdot 10^{-5}$ M to $7.5 \cdot 10^{-3}$ M Co(II); 0.00125M to 0.125M Kelex 100). At 200 g Kelex 100/l the cobalt curve in Fig. 2 has a steep slope indicating a marked change in the system. The probable explanation for this phenomenon, which will be subject to further study, is a partial oxidation of cobalt to the trivalent state in the organic phase by exposure to air. Further support for this hypothesis was obtained from stripping experiments with an aqueous solution containing 150 g H₂SO₄/l. While 90-95 % of the nickel was stripped

in one stage cobalt was very difficult to strip, particularly when extracted at pH values higher than 5.5. However, addition of some zinc powder promoted the stripping of cobalt, obviously by reducing it to the divalent state.

A similar slow oxidation of cobalt(II) in the organic phase has been observed in certain mixtures of LIX reagents and Versatic 9-11¹, where it was easily eliminated by performing the extraction under nitrogen.

It appears that the stripping difficulty reported by Lakshmanan and Lawson⁵ might also be explained by air oxidation rather than by assuming the existence of a very stable complex of divalent cobalt.

The oxidation phenomenon prevented a meaningful slope analysis of the extraction data for cobalt, since no experiments were performed in the absence of air. The data for Ni(II) were plotted according to equation (3), where D is the distribution coefficient, HL the extractant, and K the concentration product:

$$\log D - 2 \log[\overline{HL}] = \log K + 2 \text{ pH} \quad (3)$$

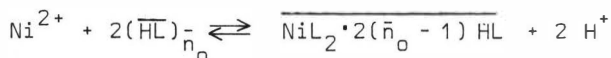
When using data for pH > 3.5 relatively good straight lines were obtained but only the lowest Kelex-concentration (75 g/l) gave a nearly theoretical slope of 2.1, lower values in the range 1.5 - 1.8 being obtained at the higher extractant levels. At pH 3.0 the values of $\log D - 2 \log[\overline{HL}]$ were higher than expected, the deviation increasing with decreasing extractant concentration. This phenomenon is probably due to the appearance of a new extraction mechanism when the organic phase begins to extract sulphuric acid.

Composition of the Ni(II)/Kelex 100 complex in iso-octane

In an attempt to find an explanation for the low pH-dependence indicated by slope analysis of data for Ni(II) extraction in isodecanol/Shellsol K some extraction experiments were also performed with solutions of Kelex 100 in iso-octane. Since these organic phases did not contain any isodecanol as modifier they could be studied by combining extraction experiments with vapour pressure osmometry.

Fig. 3 shows the mean aggregation number \bar{n}_0 at 25°C for Kelex 100 solutions of different concentrations. According to these osmometric data there is considerable interaction between the extractant molecules in spite of the fact that 8-hydroxyquinolines should have a low dimerization tendency because of intramolecular hydrogen bond formation⁷. Thus the functional groups may not be involved in the interaction.

Plots of extraction data in iso-octane according to equation (3) gave slopes in the range 1.5 - 1.6. However, comparison with osmometric data for the extracts showed that the extraction could best be represented by the reaction



where \bar{n}_0 is the average aggregation number for Kelex 100 at zero nickel concentration. This reaction formula implies that the extent of interaction between extractant molecules is the same whether they are bound to nickel or not. With this assumption one obtains equation (4), where the concentration

$$\log D - 2 \log [\overline{\text{HL}}] + 2 \log \bar{n}_0 = \log K + 2 \text{pH} \quad (4)$$

$[(\overline{\text{HL}})_{\bar{n}_0}]$ has been replaced by $[\overline{\text{HL}}]/\bar{n}_0$, $[\overline{\text{HL}}]$ being the free extractant concentration calculated as monomer. $[\overline{\text{HL}}]$ is obtained from equation (5), where $[\overline{\text{HL}}]_0$ denotes the free extractant

$$[\overline{\text{HL}}] = [\overline{\text{HL}}]_0 - 2 \bar{n}_0 [\overline{\text{Ni}}] \quad (5)$$

concentration at zero nickel concentration in the organic phase.

When the results from extraction experiments at four different concentrations of Kelex 100 were plotted according to equation (4) all the points fell very close to a straight line with a slope of 2.0 (Fig. 4). In Table 1 the experimentally determined mean aggregation numbers \bar{n}_{exp} for the extractant in the extracts are compared with computed values \bar{n}_{calc} obtained according to equation (6):

$$\bar{n}_{\text{calc}} = \bar{n}_0 \left(1 + 2 \bar{n}_0 [\overline{\text{Ni}}]/[\overline{\text{HL}}]_0 \right) \quad (6)$$

The good agreement confirms that Ni(II) forms a monomeric complex with the average composition $\text{NiL}_2 \cdot 2(\bar{n}_0 - 1)\text{HL}$, \bar{n}_0 being a constant for a given total extractant concentration.

Qualitatively, the same explanation may be assumed to be valid for the isodecanol/Shellsol K system. However, the presence of the modifier makes that solvent system more polar than iso-octane and the interaction between extractant molecules may therefore be somewhat weaker in isodecanol/Shellsol K.

Water determinations according to Karl Fischer showed the extracts to contain only negligible amounts of water. Thus the nickel complex must be unhydrated.

Extraction with Kelex 100/Versatic 9-11

Composition of the Ni(II)/Kelex 100/Versatic 9-11 complex in iso-octane

The reaction between the Ni(II)/Kelex 100 complex and Versatic 9-11 was studied photometrically at two concentration levels. Fig. 5 shows the absorbance increase ($A - A_0$) at 980 nm as a function of the molar ratio between Versatic 9-11 (calculated as monomer) and Ni(II). The sharpness of the break at a ratio of 2 indicates the formation of a stable complex containing two molecules of carboxylic acid per nickel ion. Fig. 6 illustrates the formation of the mixed ligand complex in dilute solutions of constant nickel concentration. Under these conditions the interaction between the molecules of Kelex 100 should be negligible (see Fig. 3) and the reaction with Versatic 9-11 (which in osmometric experiments was found to exist as the dimer H_2R_2 at these concentrations) may be written as follows:

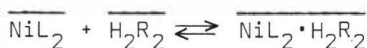


Table 2 shows the concentration product for this equilibrium, as calculated from photometric data at low concentration. The

high concentration product $(6.5 \pm 0.3) \cdot 10^3$ l/mole explains the sharp break in Fig. 5, which is based on photometric studies at higher concentrations. Under these conditions the concentration product may, however, be somewhat lower because of the solvating effect of the excess of Kelex 100 on NiL_2 .

The results of osmometric studies of some extracts at 30°C are summarized in Table 3. In these experiments the concentration level was relatively high (0.236M or 0.230M HL, 0.030M to 0.208M H_2R_2) and it may therefore be assumed that practically all carboxylic acid is bound in the mixed complex when $[\text{Ni}] \geq [\text{H}_2\text{R}_2]_0$. When $[\text{Ni}] \leq [\text{H}_2\text{R}_2]_0$ all nickel is in the mixed complex, the excess of carboxylic acid existing as dimer. Analysis of the experimental data indicates that the excess of Kelex 100 exists as $(\text{HL})_{\bar{n}_0}$ and any Ni/Kelex 100 complex as $\text{NiL}_2 \cdot 2(\bar{n}_0 - 1) \text{HL}$ while the mixed ligand complex $\text{NiL}_2 \cdot \text{H}_2\text{R}_2$ is not solvated by HL. Here \bar{n}_0 is the mean aggregation number (1.35) for Kelex 100 (0.236 or 0.230M) measured at 30°C in the absence of nickel and Versatic 9-11. With these assumptions equations (7) ($[\text{Ni}] \geq [\text{H}_2\text{R}_2]_0$) and (8) ($[\text{Ni}] \leq [\text{H}_2\text{R}_2]_0$) were derived for the calculation of the apparent mean aggregation number \bar{n}_{calc} for the extractant molecules (HL and HR) in extracts of known total concentrations $[\text{Ni}]$, $[\text{HL}]_0$ and $[\text{H}_2\text{R}_2]_0$.

$$\bar{n}_{\text{calc}} = \frac{\bar{n}_0 ([\text{HL}]_0 + [\text{HR}]_0)}{[\text{HL}]_0 + (\bar{n}_0 - 1) [\text{HR}]_0 - \bar{n}_0 [\text{Ni}]} \quad [\text{Ni}] \geq [\text{H}_2\text{R}_2]_0 \quad (7)$$

$$\bar{n}_{\text{calc}} = \frac{2 \bar{n}_0 ([\text{HL}]_0 + [\text{HR}]_0)}{2 [\text{HL}]_0 + \bar{n}_0 [\text{HR}]_0 - 4 [\text{Ni}]} \quad [\text{Ni}] \leq [\text{H}_2\text{R}_2]_0 \quad (8)$$

A relatively good agreement between \bar{n}_{exp} and \bar{n}_{calc} is evident from Table 3.

Typical results obtained in extracting Ni(II) and Co(II) from separate solutions are shown in Fig. 7. Since Versatic 9-11 alone does not extract these ions at low pH a comparison with the curves for the same concentration of Kelex 100 in Fig. 2 reveals a substantial synergic effect, contrary to the findings of Lakshmanan and Lawson⁵ at considerably lower concentration levels. In agreement with the results of the aforementioned authors cobalt was found to be easily stripped from organic phases containing Kelex 100 and Versatic 9-11. There was no indication of oxidation of Co(II) in this case.

The composition of the Co(II)/Kelex 100/Versatic 9-11 complex was not investigated separately in the present study but some conclusions may be drawn from the work of Lakshmanan and Lawson⁵. These authors assumed Versatic 9-11 to be monomeric in kerosene and therefore found the formula $\text{CoL}_2\text{H}_2\text{R}_2$ for the mixed complex. According to our experience Versatic 9-11 should occur as dimer under the experimental conditions of Lakshmanan and Lawson, and the formula thus becomes $\text{CoL}_2 \cdot 2\text{H}_2\text{R}_2$. Since the mixed Ni(II) complex is $\text{NiL}_2 \cdot \text{H}_2\text{R}_2$ extraction data for the two metals should conform to equation (9) and (10), respectively:

$$\log D_{\text{Ni}} - 2 \log [\overline{\text{HL}}] - \log [\overline{\text{H}_2\text{R}_2}] = \log K_{\text{Ni}} + 2 \text{ pH} \quad (9)$$

$$\log D_{\text{Co}} - 2 \log [\overline{\text{HL}}] - 2 \log [\overline{\text{H}_2\text{R}_2}] = \log K_{\text{Co}} + 2 \text{ pH} \quad (10)$$

Ni(II) and Co(II) were extracted from separate aqueous solutions using six different extractant mixtures. In four of them the concentration of Versatic 9-11 was kept constant at 1.00M while the concentration of Kelex 100 was 75, 100, 150 and 200 g/l, respectively. The other two mixtures were 1.50M Versatic 9-11/150 g/l Kelex 100 and 0.50M Versatic 9-11/200 g/l Kelex 100.

For Ni(II) all the six extractant mixtures yielded results in good agreement with equation (9), all points falling close to a single straight line with a slope of about 2. The Co(II) data showed more scatter but agreed fairly well with equation (10)

except for the results obtained with the mixture containing only 0.50M Versatic 9-11. In this case there would sometimes be only a small excess of carboxylic acid if all cobalt in the extracts would exist as $\text{CoL}_2 \cdot 2\text{H}_2\text{R}_2$. Probably mainly $\text{CoL}_2 \cdot \text{H}_2\text{R}_2$ is formed under these conditions, as judged from the fact that an equation analogous to (9) gives a better plot than equation (10). Fig. 8 shows the plots of equations (9) and (10) obtained by taking the average of all experimental points at given pH values.

Table 4 shows the results obtained by extracting an aqueous solution containing 9.90 g Ni(II)/l and 24.90 g Co(II)/l with an organic phase containing 200 g Kelex 100/l and 1.00M Versatic 9-11. From equations (9) and (10) one obtains the following expression for the ratio $K_{\text{Ni}}/K_{\text{Co}}$:

$$\frac{K_{\text{Ni}}}{K_{\text{Co}}} = \frac{D_{\text{Ni}}}{D_{\text{Co}}} \cdot [\text{H}_2\text{R}_2] = S_{\text{Ni,Co}} \cdot [\text{H}_2\text{R}_2] \quad (11)$$

As shown in Table 4 the three lowest pH values yield relatively constant values for $K_{\text{Ni}}/K_{\text{Co}}$, the average being 19.0M. At pH 3.04 a somewhat lower value 15.4M is obtained, probably because of the experimental uncertainty in D_{Ni} .

Using the value 19.0M for $K_{\text{Ni}}/K_{\text{Co}}$ and determining K_{Ni} by extrapolating Y_{Ni} to zero in Fig. 8 (which gives $\log K_{\text{Ni}} = -2 \text{ pH} = -3.38$) the following approximate values are found for the concentration products:

$$K_{\text{Ni}} \approx 4.2 \cdot 10^{-4} \text{ l/mole}$$

$$K_{\text{Co}} \approx 2.2 \cdot 10^{-5} \text{ l}^2/\text{mole}^2$$

An approximate expression for $S_{\text{Ni,Co}}$ is obtained directly from equation (11):

$$S_{\text{Ni,Co}} \approx \frac{19.0\text{M}}{[\text{H}_2\text{R}_2]} \quad (12)$$

Equation (12) indicates that Ni(II) and Co(II) should be separated at low $[H_2R_2]$. There is, however, a lower limit for $[H_2R_2]$ under which the complex $CoL_2 \cdot 2H_2R_2$ no longer exists.

Rate of extraction

Fig. 9 shows the time-dependence of $[Ni]$ and $[Co]$ when extracting at about 25°C and a constant pH of 2.7. Cobalt is extracted faster than nickel as shown by the maximum in the curve for $[Co]$. About 1.5 h is needed for attainment of equilibrium. Raising the temperature to 50°C decreased the time requirement to about 20 min, but at the same time the separation factor decreased from 63.0 to 44.5.

Stripping problems

Both Co(II) and Ni(II) are easily stripped with sulphuric acid at room temperature, 60 g H_2SO_4 /l being sufficient for stripping more than 90 % of the total metal content in one stage. Cobalt reacts faster than nickel, as seen from colour changes in the aqueous stripping solution.

However, the basic character of Kelex 100 creates serious difficulties. Even when using 60 g H_2SO_4 /l as strip solution Kelex 100 was largely protonated. This extraction of sulphuric acid resulted in precipitate formation in the organic phase upon standing. It also reduced the separation factor $S_{Ni,Co}$ from about 65 to 1. Treatment with basic solutions is not practical in the presence of Versatic 9-11 since considerable amounts of carboxylic acid would be lost to the aqueous phase. Stripping of Versatic-free solutions of Kelex 100 had the same adverse effect on the extraction of Ni(II).

At the present time no detailed explanation can be offered for the drastic change in $S_{Ni,Co}$. Apparently some new extraction mechanism involving H_2SO_4 becomes important under the conditions caused by stripping.

The uptake of sulphuric acid could be reduced considerably by performing the stripping at 50°C. It was also found necessary to keep the pH of the strip solution in the range 1.2 - 1.5 by

means of a regulator. Under these conditions 90 % of the metal was stripped while maintaining the separation factor $S_{Ni,Co}$ at a level of about 35.

CONCLUSIONS

Extractants containing only Kelex 100 are not well suited for separation of Ni(II) and Co(II) in the presence of air because cobalt is very difficult to strip from the loaded extractant. Apparently a very stable complex of trivalent cobalt is formed in the organic phase. This difficulty is eliminated by using mixtures of Kelex 100 and Versatic 9-11 which exhibit marked synergism in the extraction of Ni(II) and Co(II). With fresh extractant mixtures separation factors $S_{Ni,Co}$ around 65 may be obtained at 25°C but long contact times (about 1.5 h) are needed for attainment of equilibrium. At 50°C extraction is considerably faster and less acid is taken up by the organic phase during stripping. This must be performed at a controlled pH in the range 1.2 - 1.5 in order not to cause a drastic decrease in the separation factor $S_{Ni,Co}$. By such careful stripping at 50°C separation factors around 35 can be maintained.

REFERENCES

1. Nyman, B.G., Hummelstedt, L., *Proc.Int.Solvent Extraction Conf. 1974*, Society of Chemical Industry, London 1974.
2. Rainio, K., M.Sc.Thesis, Åbo Akademi 1970.
3. Flett, D.S., West, D.W., *Proc.Int.Solvent Extraction Conf. 1971*, Vol. I, 214-223, Society of Chemical Industry, London 1971.
4. Hartlage, J.A., Budde, W.M., U S Pat 3637711/1972.
5. Lakshmanan, V.I., Lawson, G.J., *J.inorg.nucl. Chem.*, 1973, 35, 4285.
6. Walker, C.R., Vita, D.A., *Anal.Chim.Acta*, 1969, 47, 9.
7. Atwood, R.L., Miller, J.D., AIME Annual Meeting, San Francisco 1972.
- 4a Kane, W.S., Cardwell, P.H., Ger. Offen. 2126233 (1971)

Table 1. Experimental and calculated average aggregation numbers at 25°C for Kelex 100 in iso-octane in the presence of Ni(II)

$\frac{[\overline{\text{HL}}]_0}{M}$	$\frac{[\overline{\text{Ni}}]}{M}$	\bar{n}_{exp}	\bar{n}_{calc}
0.142	0.0103	1.71	1.64
0.142	0.0322	2.27	2.22
0.142	0.0450	2.69	2.56
0.235	0.0102	1.61	1.60
0.235	0.0146	1.75	1.67
0.235	0.0542	2.39	2.35
0.329	0.0330	1.95	1.95
0.329	0.0512	2.25	2.20
0.329	0.0890	2.69	2.70
0.423	0.0275	1.87	1.86
0.423	0.0550	2.25	2.17
0.423	0.0777	2.50	2.43

Table 2. Computation of the concentration product K for the equilibrium $\text{NiL}_2 + \text{H}_2\text{R}_2 \rightleftharpoons \text{NiL}_2 \cdot \text{H}_2\text{R}_2$ from absorbance data at 492 nm for solutions with $[\text{Ni}] = 0.052 \cdot 10^{-3} M$

$\frac{[\overline{\text{H}_2\text{R}_2}]_{\text{tot}}}{M}$	A_{492}	$\frac{A_0 - A}{A} \left(= \frac{[\overline{\text{NiL}_2 \cdot \text{H}_2\text{R}_2}]}{[\overline{\text{NiL}_2}]} \right)$	$\frac{K}{1/\text{mole}}$
0.000	0.452		
$0.030 \cdot 10^{-3}$	0.394	0.147	$6.3 \cdot 10^3$
$0.062 \cdot 10^{-3}$	0.348	0.299	$6.0 \cdot 10^3$
$0.104 \cdot 10^{-3}$	0.288	0.569	$6.7 \cdot 10^3$
$0.209 \cdot 10^{-3}$	0.202	1.238	$6.9 \cdot 10^3$
$0.557 \cdot 10^{-3}$	0.101	3.475	$6.7 \cdot 10^3$
$0.431 \cdot 10^{-2}$	0.016	27.25	$6.4 \cdot 10^3$
$0.415 \cdot 10^{-1}$	0.000		

Table 3. Experimental and calculated average aggregation numbers at 30°C for Kelex 100/Versatic 9-11 in iso-octane in the presence of Ni(II)

$\frac{[\overline{\text{HL}}]_0}{\text{M}}$	$\frac{[\overline{\text{H}_2\text{R}_2}]_0}{\text{M}}$	$\frac{[\overline{\text{Ni}}]}{\text{M}}$	\bar{n}_{exp}	\bar{n}_{calc}
0.236	0.028	0.074	2.67	2.54
0.230	0.030	0.052	2.23	2.20
0.236	0.051	0.079	2.99	2.77
0.236	0.075	0.100	3.46	3.40
0.208	0.071	0.079	3.29	3.13
0.236	0.103	0.104	3.57	3.56
0.236	0.103	0.100	3.49	3.41
0.230	0.063	0.052	2.41	2.31
0.236	0.104	0.073	2.70	2.61
0.230	0.104	0.052	2.34	2.25
0.236	0.166	0.077	2.64	2.52
0.230	0.209	0.052	2.24	2.18

Table 4. Extraction of Ni(II) and Co(II) with 200 g/l Kelex 100/1.00M Versatic 9-11 from a solution containing 9.90 g Ni(II)/l and 24.90 g Co(II)/l. (25°C)

pH	$\frac{[\overline{\text{Co}}]}{\text{M}}$	D_{Co}	$\frac{[\overline{\text{Ni}}]}{\text{M}}$	D_{Ni}	$\frac{[\overline{\text{H}_2\text{R}_2}]}{\text{M}}$	$\frac{K_{\text{Ni}}/K_{\text{Co}}}{\text{M}}$
2.28	0.011	0.0268	0.094	1.25	0.384	17.9
2.50	0.018	0.0449	0.123	2.68	0.341	20.4
2.79	0.036	0.0941	0.146	6.23	0.282	18.7
3.04	0.056	0.153	0.154	10.00	0.234	15.4

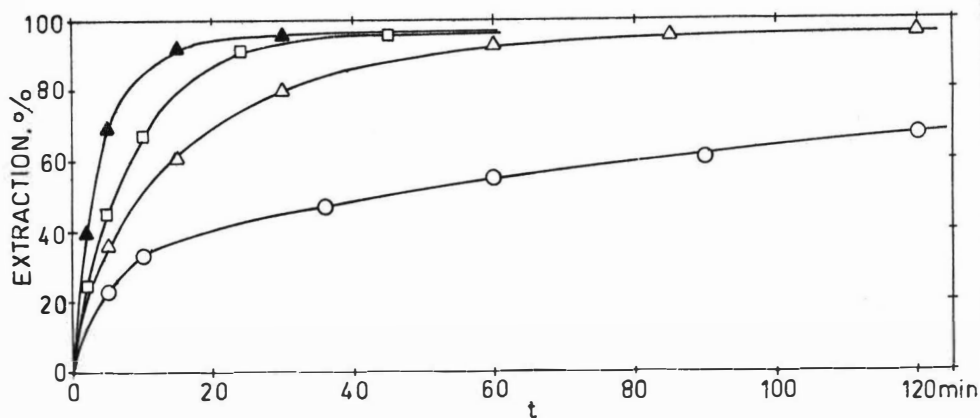


Fig. 1. Rate of Ni(II) extraction from 0.10M Ni^{2+} solutions by Kelex 100 (100 g/l) in isodecanol/Shellsol K at constant pH values ○ 25°C, pH 4.72; △ 50°C, pH 5.14; □ 50°C, pH 5.05, 0.005M DNNS; ▲ 50°C, pH 5.11, 0.010M DNNS.

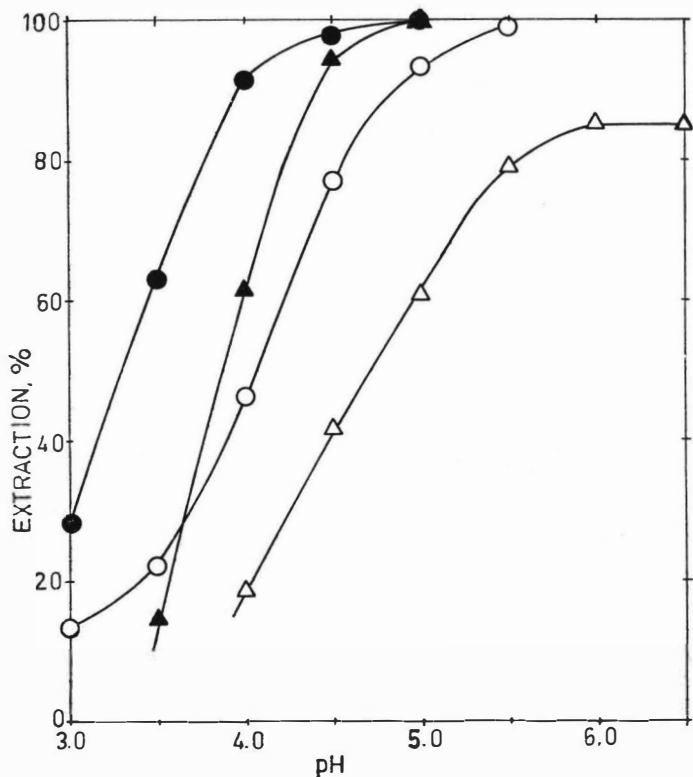
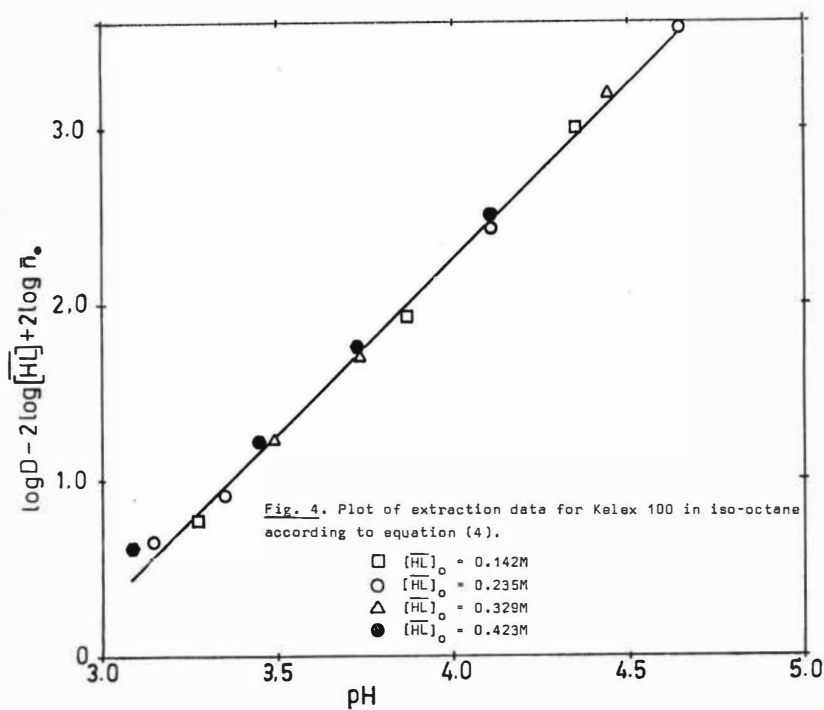
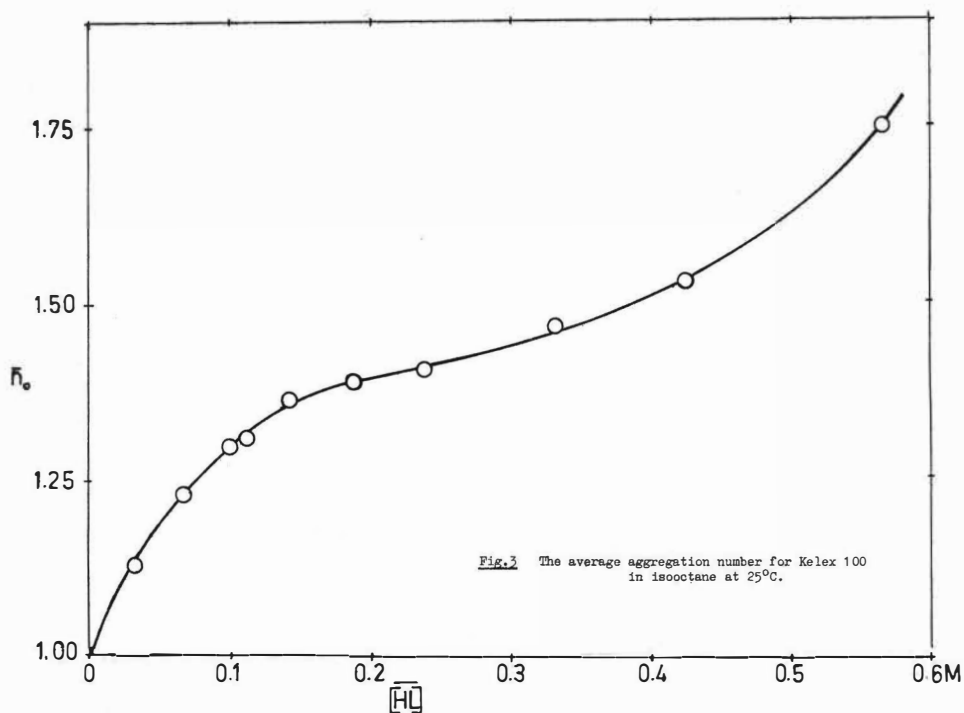


Fig. 2. Effect of pH on equilibrium extraction of Ni(II) (circles) and Co(II) (triangles) from 0.10M Ni^{2+} and 0.107M Co^{2+} solutions with Kelex 100 in isodecanol/Shellsol K at 25°C ○, △ 75 g Kelex 100/l (0.236M) ●, ▲ 200 g Kelex 100/l (0.620M).



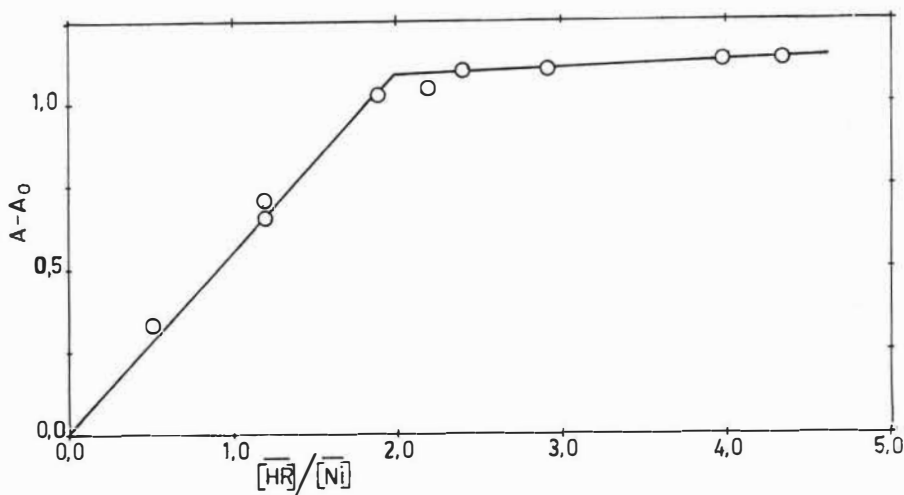
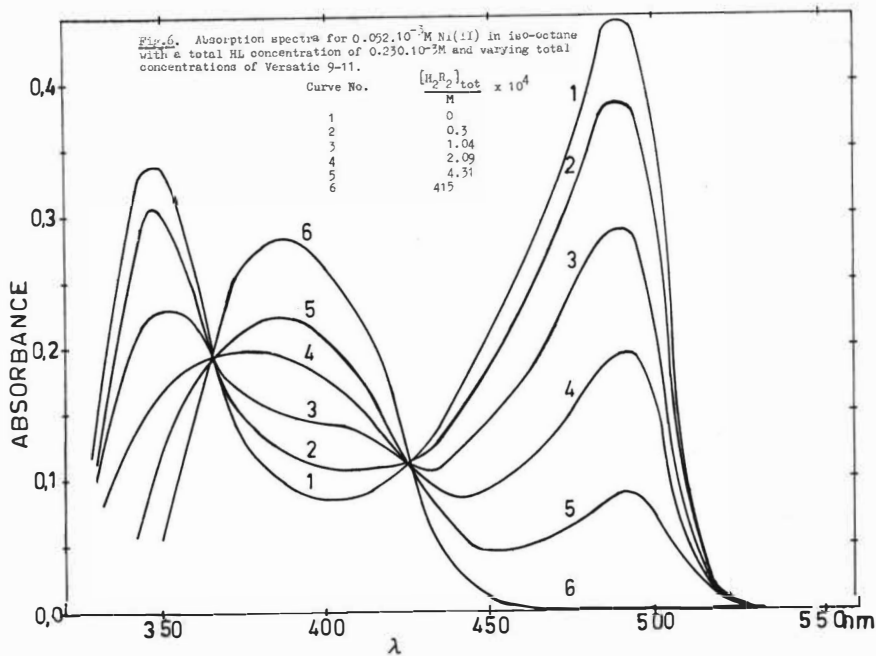


Fig. 5. The absorbance increase at 980 nm as a function of the molar ratio between Versatic 9-11 and nickel in iso-octane at constant $[Ni] = 0.052M$



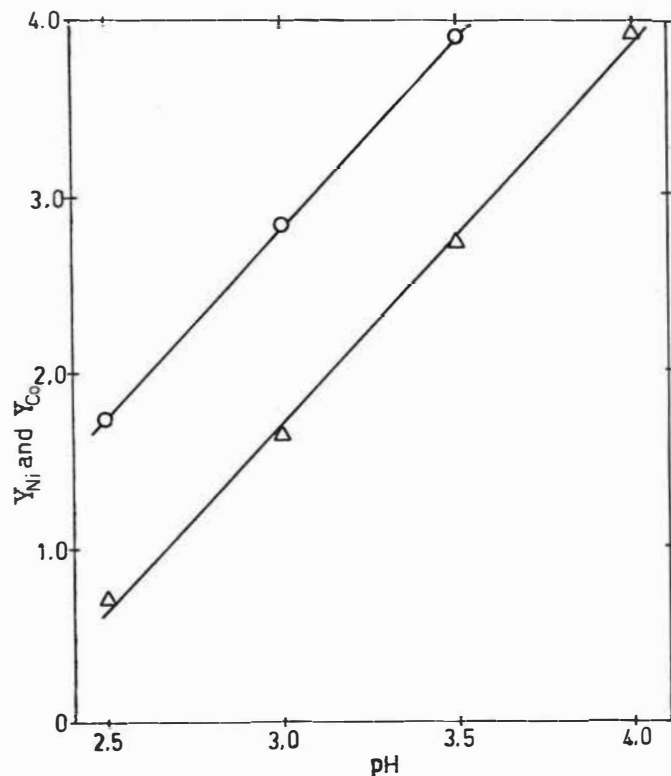


Fig. 8. Average plots of extraction data for Ni(II) (○) and Co(II) (△) according to equations (9) and (10), respectively.

$$Y_{Ni} = \log D_{Ni} - 2 \log [HL] - \log [H_2R_2]$$

$$Y_{Co} = \log D_{Co} - 2 \log [HL] - 2 \log [H_2R_2]$$

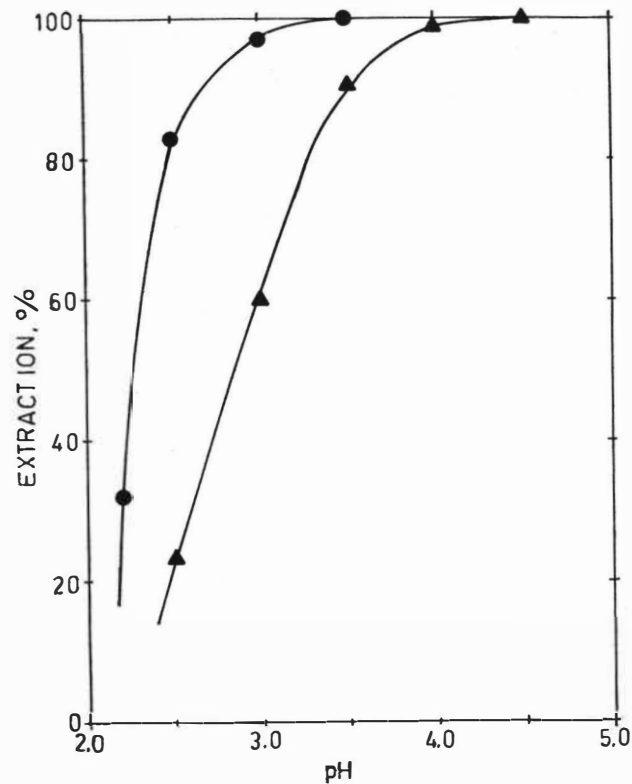


Fig. 7. Extraction of Ni(II) and Co(II) from separate 0.1M solutions with 200 g/l Kelex 100/1.00M Versatic 9-11 in isodecanol/Shellsol K at 25°C. (● Ni; ▲ Co)

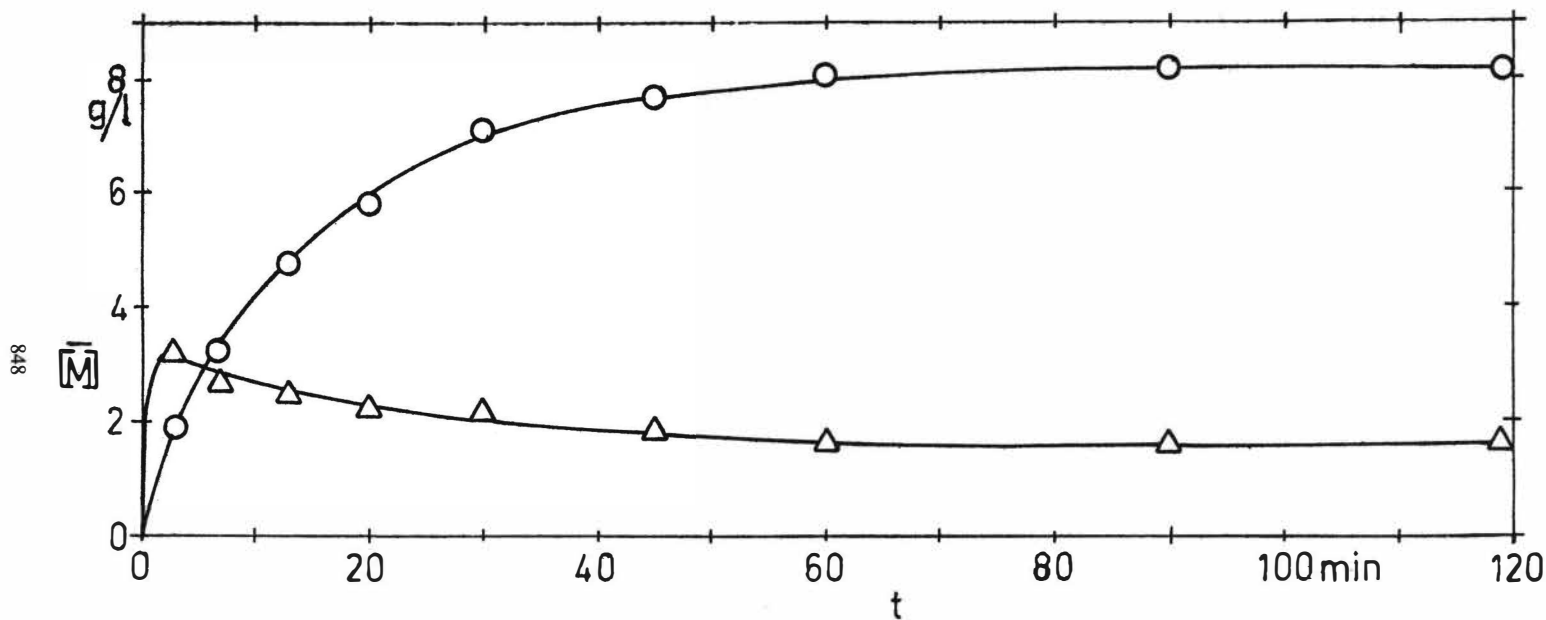


Fig. 9. Rate of extraction of Ni(II) (O) and Co(II) (Δ) at 25°C with 200 g/l Kelex 100/1.00M Versatic 9-11 in isodecanol/Shellsol K from a solution containin 9.90 g Ni(II)/l and 24.50 g Co(II)/l.

THE EXTRACTION ABILITY OF OXYGEN-CONTAINING EXTRACTANTS
OF CLASS R_nXO WITH RESPECT TO COBALT(II) CHLORIDE

by V.G.Torgov, V.A.Mikhailov, M.K.Drozdova, G.A.Mardezhova
and E.A.Gal'tsova

The extraction ability (EA) of neutral extractants of class R_nXO with respect to $CoCl_2$ is considered. By the analysis of distribution isotherms, and direct synthesis using electronic and IR-spectra it is shown that in all the cases cobalt is extracted in the form of tetrahedral complexes $[CoL_2Cl_2]$. EA of extractants considered is found to be characterized quantitatively either by the shift value of $\nu_{sym}(OH)$ due to interaction between extractants and water molecules in CCl_4 medium or by the energy of hydrogen bond $XO...H-OH$. Results of X-ray spectra investigation of XO bonds in extractants series show the existence of $p_n - d_{32}$ interaction between S and O atoms in R_2SO and more appreciable contribution of this interaction to the PO bond in R_3PO compared with XO bonds in R_3NO and R_3AsO .

Institute of Inorganic Chemistry, Novosibirsk, USSR

Introduction

The available data about dependences of EA of neutral extractants on their structures are generally related to compounds containing phosphoric group^{1,2}. As to compounds of class R_nXO where X may be N, S, As, Sb, Se, the only few works known are devoted to the place of dialkyl sulphoxides³⁻⁵, *α*-alkylpyridine N-oxides³⁻⁴, dimethylselen oxide¹ and triphenylarsine oxide^{1,6} in neutral extractants series. EA of Ph_3PO , Ph_3AsO and $(CH_3)_2SeO$ increased with increase of extractants basicity characterized by protonization constants (K_a) as was established by Krasovec and Klofutar¹. Logarithms of extraction equilibrium constants for acids HNO_3 , $HReO_4$ and $HTcO_4$

extracted as monosolvates and $\text{UO}_2(\text{NO}_3)_2$ extracted as disolvate, correlate with $\log K_a$ for such extractants as Ph_3AsO , R_3PO and Ph_3PO^2 .

In accordance with protonization constant values¹ a decrease of EA can be expected in series $\text{R}_2\text{TeO} > \text{R}_3\text{SbO} > \text{R}_3\text{NO} > \text{R}_3\text{AsO} > \text{Ph}_2\text{SeO} > \text{Ph}_3\text{AsO} > \text{R}_3\text{PO}$. However, there is no evidence for this series at least for the most effective extractants. EA of the following neutral extractants of class R_nXO in relation to CoCl_2 is compared here: tributylphosphate (TBP), triisooamylphosphine oxide (TAPO), di-n-octyl sulphoxide (DOSO), α -nonylpyridine N-oxide (α -NPO), trioctylamine N-oxide (TOAO) and trioctylarsine oxide (TOARO). The extractants above differ in their basicity to a great extent as one can judge by their ability to extract mineral acids. The choice of CoCl_2 as extracted compound was dictated by the same extraction mechanism for whole extractant series in this case (changes in extraction mechanism with increasing extractant basicity have been shown previously³;

for example, when substituting TBP or DOSO by α -NPO or TOAO such a change in uranium extraction mechanism was observed, the uranium hydroxoforms being extracted).

Experimental

Reagents

TBP and TAPO (as solution in heptane) were purified by treatment with 10 % sodium carbonate solution followed by vacuum distillation (TBP) or repeated recrystallization from heptane (TAPO)

DOSO, α -NPO, TOARO and TOAO were prepared as described elsewhere⁷⁻¹⁰ and according to thin layer chromatography data had no admixtures.

Synthesis of $[\text{CoL}_2\text{Cl}_2]$.

The compounds were prepared by mixing propyl alcohol solutions of $\text{CoCl}_2 \cdot 6\text{H}_2\text{O}$ (10mmol in 10 ml) and ligand L (20mmol in 20 ml) both heated to 50°C . In the case of α -NPO crystals were formed immediately after solution mixing, for complexes with DOSO and TAPO the elimination of part of the solvent and cooling of solutions was necessary. All the compounds were recrystallized from $\text{C}_3\text{H}_7\text{OH}$ and dried in vacuum over P_2O_5 . The complex $[\text{Co}(\text{TOARO})_2\text{Cl}_2]$ was isolated as an oil after propyl alcohol removal. The results of elemental analysis are given in Table 1. Previously the analogous compounds of CoCl_2 with methyl derivatives of pyridine N-oxide¹¹, trimethylphosphine oxide¹²⁻¹⁴, trimethylarsine oxide¹⁵, trimethylamine oxide^{14,16} and triethylamine oxide¹⁷ were synthesized.

Table 1

Composition^a and melting points of compounds $[\text{CoL}_2\text{Cl}_2]$.

Compound	% Co	% Cl	% C	% H	m.p., $^\circ\text{C}$
$[\text{Co}(\text{DOSO})_2\text{Cl}_2]$	9.64 (8.69)	11.12 (10.47)	55.75 (56.60)	9.78 (10.00)	90-95 with decomposition
$[\text{Co}(\alpha\text{-NPO})_2\text{Cl}_2]$	10.40 (10.30)	12.19 (12.41)	58.21 (58.80)	7.92 (8.04)	97 - 98
$[\text{Co}(\text{TAPO})_2\text{Cl}_2]$	9.19 (9.06)	10.63 (10.92)	55.60 (55.38)	10.26 (10.15)	147 - 148
$[\text{Co}(\text{TOARO})_2\text{Cl}_2]$	6.00 (5.95)	7.19 (7.17)	57.66 (58.18)	10.30 (10.30)	-

^aCalculated values are given in parenthesis.

When dissolving $[\text{Co}(\text{DOSO})_2\text{Cl}_2]$ in C_6H_6 and CCl_4 partial dissociation of complex with detachment of DOSO and solid phase formation is observed. In excess of L all the complex solutions are

quite stable.

Cobalt(II) chloride extraction

To establish the extraction mechanism of CoCl_2 its distribution at 25°C between water and extractants solutions in C_6H_6 and CCl_4 was studied at constant concentration of L, or at constant concentration of CoCl_2 with the concentration of L in the diluent being varied. The concentration of cobalt in organic phase was determined colorimetrically after stripping with water by means of the well-known reaction with nitroso-R-salt.

When determining the extraction equilibrium constants the concentration of extractants did not exceed 0.3M for TBP and DOSO, 0.1M for α -NPO, 0.01M for TOARO, 0.01M for TOAO in CCl_4 and 0.001M for TOAO in C_6H_6 . At higher concentrations of TOAO the extraction equilibrium constants were sharply decreased apparently due to micelle formation. Furthermore the extraction of Co was performed only with freshly prepared TOAO solutions because of slow decomposition of extractant in C_6H_6 and CCl_4 media at low concentrations with formation of N,N-dioctylhydroxylamine and octen-1.

Electronic spectra

The electronic spectra of benzene solutions of complexes $[\text{CoL}_2\text{Cl}_2]$, mixtures $[\text{CoL}_2\text{Cl}_2] + \text{L}$ and organic phases after CoCl_2 extraction were measured using spectrophotometer "Carry - 15" in the range $20,000 - 14,000 \text{ cm}^{-1}$. Concentration of cobalt was equal $1 + 2 \times 10^{-3} \text{ M}$. Spectra of $[\text{Co}(\text{DOSO})_2\text{Cl}_2]$ were measured only in the presence of an excess of L.

Infrared spectra

The IR-spectra of benzene solutions of complexes and extracts were measured by spectrophotometer UR-20 with KBr (400 - 700 cm^{-1}) and NaCl ($700 - 4,000 \text{ cm}^{-1}$) prisms in KRS-5, KBr and

NaCl cuvettes. The changes in PO and SO bands of extracts could not be observed because of too low cobalt content in organic phase.

IR-spectra of solutions of L in CCl_4 containing water were measured in the frequency range corresponding to valent vibration of OH-group. The solutions used were: 0.2M DOSO + 2.8×10^{-3} M H_2O (corresponding to water saturated solution of extractant); 0.5M d-NPO + 0.27M H_2O ; 0.5M TAPO + 0.08M H_2O ; 0.5M TOARO + 0.22M H_2O ; 0.5M TOAO + 0.38M H_2O .

X-ray K-spectra of oxygen and L-spectra of sulphur

X-ray emission spectra were measured as described earlier¹⁸ by universal X-ray spectrometer, which is adjustable to investigate the wavelength range from 3 to 100 Å. The crystal of KAR and pseudocrystal of barium stearate were used as analysers for measurements of oxygen K-spectra and sulphur L-spectra, respectively. To avoid sample decomposition due to irradiation all samples were repeatedly substituted by new ones during the exposure.

Results and discussion

Extraction stoichiometry and extraction equilibrium constants

The distribution isotherms are plotted in Fig.1 in $\log C_{\text{Co}} / (C_{\text{L}} - 2C_{\text{Co}})^2 - \log m \gamma_{\pm}$ co-ordinates, where C_{Co} is the Co concentration in organic phase (mole/l); C_{L} - initial concentration of extractant; m - molality of CoCl_2 in aqueous solution and γ_{\pm} - mean ionic molal activity coefficient of CoCl_2 in aqueous phase. The data¹⁹ on CoCl_2 aqueous solution densities were used to calculate molal concentrations from molar ones. The γ_{\pm} values were taken from a monograph²⁰ (for solutions with $m > 0.1$ these were evaluated by the expression $\log \gamma_{\pm} = -1.7615 \sqrt{m} / (1 + 2.691 \sqrt{m}) + 0.194m$, which describes well the dependence of γ_{\pm} on m in m range from 0.1 to 0.8). As is seen in the figure

linear dependences are observed over a wide range of CoCl_2 concentrations, the slope being equal to 3 for all the ligands and diluents. In the case of TOAO which is the most basic extractant among those investigated, no decrease in isotherm slopes was observed in C_L range from 1×10^{-3} to $0.1M$. This circumstance as well as constant Co to Cl ratio in organic phase equal to 1 : 2 indicates the CoCl_2 hydrolysis in the presence of TOAO to be negligible. The CoCl_2 distribution between phases is characterized by cubic dependence of C_{Co} on $m\gamma_{\pm}$ which is evidence of formation of a mononuclear complex non-electrolyte $[\text{CoL}_2\text{Cl}_2]$ in the organic phase.

The effect of C_L on cobalt extraction is illustrated by Fig.2 where $\log C_{Co} / 4(m\gamma_{\pm})^3$ is plotted against $\log(C_L - 2C_{Co})$. It follows from quadratic dependence of C_{Co} on equilibrium extractant concentration at low values of the latter, that the extracted compound contains two molecules of extractant, which is confirmed by data on saturation of TAPO, TOARO and TOAO solutions with cobalt and direct synthesis of $[\text{CoL}_2\text{Cl}_2]$ complexes. In the case of TBP, DOSO and α -NPO the Co to L ratio in organic phase is much less than 1 to 2 because of low EA of these extractants.

Thus, the distribution equilibrium of CoCl_2 may be described by the equation : $\text{Co}_{aq}^{2+} + 2\text{Cl}_{aq}^{-} + 2L_{org} \rightleftharpoons [\text{CoL}_2\text{Cl}_2]_{org}$, with the effective extraction equilibrium constant being equal to $\bar{K} = C_{Co} / 4(m\gamma_{\pm})^3 (C_L - 2C_{Co})^2$. These constants for dilute solutions of L in C_6H_6 and CCl_4 are listed in Table 2. From the data above it follows that TOAO and TOARO are quite similar in their EA and much more effective than the other extractants. According to decreasing EA value the extractants can be placed in the following series: TOAO, TOARO > TAPO > α -NPO > DOSO > TBP, the order of magnitude of \bar{K} varying by factor of 11. Benzene is a more ef-

fective diluent than CCl_4 for all the extractants.

Table 2

The effective extraction equilibrium constants^a

L	$\bar{K} (\text{C}_6\text{H}_6)$	$\bar{K} (\text{CCl}_4)$
TBP	$(6.6 \pm 0.2) \times 10^{-7}$	$(1.7 \pm 0.2) \times 10^{-7}$
DOSO	$(5.7 \pm 0.6) \times 10^{-5}$	$(4.9 \pm 0.8) \times 10^{-6}$
α -NPO	$(3.1 \pm 0.2) \times 10^{-3}$	$(1.9 \pm 0.5) \times 10^{-4}$
TAPO	$(0.2 \pm 0.02) \times 10^0$	$(3.5 \pm 0.2) \times 10^{-2}$
TOARO	$(3.9 \pm 0.3) \times 10^4$	$(7.2 \pm 0.2) \times 10^3$
TOAO	$(4.4 \pm 0.4) \times 10^4$	$(1.3 \pm 0.08) \times 10^4$

^aThe error of a constant value is given as 26 (P= 0.95).

As was mentioned above the EA of R_nXO increases with increasing L basicity. The shift $\Delta\nu(\text{OH})$ of valent vibration frequency $\nu_{\text{sym}}(\text{OH})$ in the water molecule resulting from its interaction with extractant in CCl_4 medium compared with $\nu_{\text{sym}}(\text{OH})$ for water alone in the same medium (3614 cm^{-1}) can be used to characterize EA of the oxygen atom responsible for extraction as well as the energy (E_{H}) of hydrogen bond $\text{XO} \dots \text{H}-\text{OH}$, because data on basicity of TBP, DOSO, α -NPO and octyl-derivatives of amine- and arsineoxides are absent. Previously both quantities above were used to construct correlation dependence series of neutral phosphorus-containing compounds when extracting uranium and plutonium salts²¹ so as to estimate the EA of sulfoxides²². The experimentally determined linear dependence between the displacement of OH-group frequency in phenol (when interacting with base) and the enthalpy of corresponding adduct formation^{23,24} gives foundation for selection of the magnitudes $\Delta\nu(\text{OH})$ and E_{H} as the characteristics of donor ability of an organic base

Valent vibration frequencies $\nu_{\text{sym}}(\text{OH})$, $\nu_{\text{asym}}(\text{OH})$, $\Delta\nu(\text{OH})$ values and hydrogen bond energies calculated from IR-data in accordance with the method²⁵ are presented in Table 3.

Table 3

IR-spectroscopic characteristics of interaction between extractants and water in CCl_4 as solvent.

L	$\nu_{\text{sym}}(\text{OH})$ cm^{-1}	$\nu_{\text{asym}}(\text{OH})$ cm^{-1}	$\Delta\nu(\text{OH})$ cm^{-1}	E_{H} kcal/bond
H_2O in CCl_4 ²⁶	3614	3705	-	-
TBP	-	-	149 ²⁷	4.0 ²⁸
DOSO	3440	3690	174	4.4 ^a
<i>d</i> -NPO	3415	3685	199	4.9
TAPO	3385	3695	229	5.5 ^b
TOARO	3295	3685	319	6.9
TOAO	3295	3685	319	6.9

^a For $(\text{CH}_3)_2\text{SO}$ $E_{\text{H}} = 4.3$ ²⁸, for $(\text{C}_4\text{H}_9)_2\text{SO}$ we find $E_{\text{H}} = 4.4$. ^b According Karjakin and Kriventsova²⁹ for $(\text{C}_4\text{H}_9)_3\text{PO}$ $\nu_{\text{sym}}(\text{OH}) = 3390 \text{ cm}^{-1}$ which is consistent with our value for TAPO. Nevertheless, $E_{\text{H}} = 5.0$ was given by these authors for $(\text{C}_4\text{H}_9)_3\text{PO}$.

The values of $\Delta\nu(\text{OH})$ and E_{H} increase systematically in the extractant series above. Moreover, the $\log K$ values are associated with $\Delta\nu(\text{OH})$ or E_{H} by linear proportion* (Fig.3).

In the case of CoCl_2 extraction with R_nXO in C_6H_6 solutions the values of parameters "a" and "b" in equation of regression

* The E_{H} values calculated by formula from the paper²⁵ appeared to be connected with $\Delta\nu(\text{OH})$ by the following linear equation: $E_{\text{H}}(\text{kcal/bond}) = 1.44 + 1.71 \times 10^{-2} \Delta\nu(\text{OH}) (\text{cm}^{-1})$.

$\log \bar{K} = a + b \Delta V(\text{OH})$ are -15.6 and 6.32×10^{-2} , and for solutions in CCl_4 these are -16.3 and 6.27×10^{-2} respectively. Similar linear correlations are also shown in Fig.3 for processes of $\text{UO}_2(\text{NO}_3)_2$ extraction as disolvate $\text{UO}_2(\text{NO}_3)_2 \cdot 2\text{L}_2$ ($a = -4.00$, $b = 4.1 \times 10^{-2}$), thorium nitrate extraction as trisolvate $\text{Th}(\text{NO}_3)_4 \cdot 3\text{L}_2$ ($a = -5.90$, $b = 5.70 \times 10^{-2}$) and nitric acid extraction as monosolvate $\text{HNO}_3 \cdot \text{L}$ ($a = -4.92$, $b = 2.90 \times 10^{-2}$).

The correlations above indicate that for the extractant class under consideration the $\Delta V(\text{OH})$ and E_{H} values offer a quantitative measure of the EA, which is independent either of the nature of extracted metal or of that of diluent as far as one can conclude from the available data.

This experimentally determined regularity can be interpreted in the following manner. The value of $\log \bar{K}$ for process of extraction of salt MA_p in the form $\text{MA}_p \cdot \text{L}_q$ is proportional to the standard change of free energy ΔG° . Using an ordinary thermodynamic cycle one can represent this magnitude as the sum:

$$\Delta G^\circ = -\sum \Delta G_{\text{hydr}} - q \Delta G_{\text{solv}}^{\text{L}} + (\Delta G^\circ)_{\text{vac}} + \Delta G_{\text{solv}}^{\text{e.c.}} \quad (1)$$

where $\sum \Delta G_{\text{hydr}}$ is the sum of hydration energies of reacting ions; $\Delta G_{\text{solv}}^{\text{L}}$ and $\Delta G_{\text{solv}}^{\text{e.c.}}$ - the solvation energies of extractant and extracted complex, respectively; $(\Delta G^\circ)_{\text{vac}}$ - the value of ΔG° of the reaction when it occurs in vacuum. The magnitude of $\Delta G_{\text{solv}}^{\text{L}}$ for extractants of R_nXO class can be represented approximately as a sum of contributions from XO group ($\Delta G_{\text{solv}}^{\text{XO}}$) and from hydrocarbon parts of the molecule. In the same manner $\Delta G_{\text{solv}}^{\text{e.c.}}$ is constituted from contributions corresponding to hydrocarbon parts and non-hydrocarbon part ($\Delta G_{\text{solv}}^{\text{A}}$) of extracted complex. When composing the sum (1) the contributions corresponding to the solvation of hydrocarbon radicals and determining the

most part of solvation energies $\Delta G_{\text{solv}}^{\text{L}}$ and $\Delta G_{\text{solv}}^{\text{e.c.}}$ cancel one another:

$$\Delta G^{\circ} = -\sum \Delta G_{\text{hydr}} - q \Delta G_{\text{solv}}^{\text{XO}} + (\Delta G^{\circ})_{\text{vac}} + \Delta G_{\text{solv}}^{\text{A}} \quad (2).$$

The first term in this sum is constant for given reaction series, the fourth one is independent of extractant nature (or depends on it in very small degree), for each diluent used. Thus, experimentally established linear correlation between $\log \bar{K}$ and

$\Delta V(\text{OH})$ apparently arises from linear changes of magnitudes $(\Delta G^{\circ})_{\text{vac}}$ and $\Delta G_{\text{solv}}^{\text{XO}}$ with $\Delta V(\text{OH})$. If C_6H_6 and CCl_4 are used as diluents then energies $\Delta G_{\text{solv}}^{\text{XO}}$ are small and probably weakly depend on extractant and diluent nature.

The similar slopes of lines 1 and 2 on Fig. 3 are due to this circumstance.

Let us consider the extraction of CoCl_2 with undiluted TBP. In the literature^{30,31} cobalt is believed to be extracted as dimer $(\text{CoCl}_2)_2$ in this case. The empirical linear dependence³² $\log D_{\text{Co}} = a + 0.83 \log C_{\text{Co}}$ which describes satisfactorily cobalt extraction at high concentrations has been a foundation for this, but the change in aqueous phase had not been taken into account when deriving this equation.

The distribution isotherms for CoCl_2 extraction (Fig. 1) with pure TBP and its 0.3M solutions in C_6H_6 and CCl_4 are parallel to each other, slopes being equal to 3 in all the cases. This shows cobalt to be extracted in the monomer form. The distribution isotherm for undiluted TBP plotted on literature data³² is close to that in Fig. 1 and also has the slope of 3 (at dimerization $C_{\text{Co}}^{\infty} (m\chi_2)^6$ i.e. slope would increase up to 6). When pure TBP was used the effective extraction equilibrium constant for CoCl_2 is equal to 6.8×10^{-6} (recalculation from literature data³² gives the value 1×10^{-5}).

The composition and structure of extracted compounds in organic phase

The $[\text{CoL}_2\text{Cl}_2]$ formation in organic phase is confirmed by electronic and IR-spectra of extracts and solutions of individual compounds $[\text{CoL}_2\text{Cl}_2]$ as well as their mixtures with L in C_6H_6 .

An absorption at $17,000 - 15,000 \text{ cm}^{-1}$ is observed in electronic spectra, which is independent of L nature and corresponds to the ${}^4\text{A}_2 \rightarrow {}^4\text{T}_1(\text{P}) (\gamma_3)$ transition for Co(II) ion in tetrahedral field (Table 4). In their peak positions and corresponding ϵ values the observed spectra of complexes with TAPO and TOARO in benzene do not differ substantially from those in the literature^{13,15} spectra of such complexes with $(\text{CH}_3)_3\text{PO}$ and $(\text{CH}_3)_3\text{AsO}$ in CH_2Cl_2 and CH_3NO_2 as solvents. If an excess of $(\text{CH}_3)_3\text{NO}$ is added to a solution of $\{\text{Co}[(\text{CH}_3)_3\text{NO}]_2\text{Cl}_2\}$ in CH_3CN then a change in spectrum and increase in conductivity are observed¹⁶ due to inner sphere substitution of Cl by L. The identity of studied spectra of extracts with those of complexes $[\text{CoL}_2\text{Cl}_2]$ and mixtures of $[\text{CoL}_2\text{Cl}_2]$ with L indicates the absence of this process in benzene and the conservation of tetrahedral environment of Co in a large excess of L.

The tetrahedral complexes of cobalt(II) chloride with sulphoxides and pyridine N-oxides are quite unstable in solvents of CH_3NO_2 and CH_3CN type. So $[\text{CoL}_6] [\text{CoCl}_4]$ is the most characteristic form for complexes with $(\text{CH}_3)_2\text{SO}$ ³³. If the CoCl_2 complexes with methyl derivatives of pyridine N-oxide are dissolved in CH_3CN then the tetrahedral environment of Co atom is changed to octahedral¹¹ because of the entry of two solvent molecules into the inner sphere. The low stability of $[\text{Co}(\alpha\text{-NPO})_2\text{Cl}_2]$ in benzene solution leads to the essential difference in ϵ values

Table 4

The electronic spectra of extracts, complexes $[\text{CoL}_2\text{Cl}_2]$ and mixtures $[\text{CoL}_2\text{Cl}_2] + \text{L}$ in C_6H_6 as solvent

	ν_3 , cm^{-1} and ϵ , $\text{M}^{-1}\text{cm}^{-1}$ (in parentheses)
Extract ($1.04 \times 10^{-3}\text{M}$ Co + + 0.6M TBP)	16 900(192), 15 400(318), 14 700(366)
Extract ($1.6 \times 10^{-3}\text{M}$ Co + + 0.3M DOS O)	17 050(262), 15 500(366), 14 750(409)
Mixture $[\text{Co}(\text{DOS O})_2\text{Cl}_2]$ ($2.1 \times 10^{-3}\text{M}$) + DOSO(0.1M)	17 100(266), 15 500(364), 14 700(405)
Extract ($2.3 \times 10^{-3}\text{M}$ Co + 0.1M α -NPO)	17 250(295), 16 000(381), 14 700(408)
Mixture $[\text{Co}(\alpha\text{-NPO})_2\text{Cl}_2]$ ($2.1 \times 10^{-3}\text{M}$) + α -NPO(0.2M)	17 300(289), 16 000(362), 14 700(379)
Complex $[\text{Co}(\alpha\text{-NPO})_2\text{Cl}_2]$ ($2.2 \times 10^{-3}\text{M}$)	17 300(215), 16 000(252), 14 700(283)
Extract ($1.0 \times 10^{-3}\text{M}$ Co + + 0.1M TAPO)	16 810(292), 16 260 sh , 15 500 sh , 15 810(532)
Mixture $[\text{Co}(\text{TAPO})_2\text{Cl}_2]$ ($2.1 \times 10^{-3}\text{M}$) + TAPO(0.2M)	16 810(254), 16 260 sh, 15 500 sh , 15 810(466)
Complex $[\text{Co}(\text{TAPO})_2\text{Cl}_2]$ ($2.1 \times 10^{-3}\text{M}$)	16 810(264), 16 260 sh , 15 500 sh , 15 810(493)
Extract ($2.5 \times 10^{-3}\text{M}$ Co + $7.0 \times 10^{-3}\text{M}$ TOARO)	16 950 sh , 16 000(393), 15 650(389), 14 800(489)
Mixture $[\text{Co}(\text{TOARO})_2\text{Cl}_2]$ ($2.5 \times 10^{-3}\text{M}$) + 0.05M TOARO	16 950 sh , 16 000(370), 15 700(368), 14 800(470)
Complex $[\text{Co}(\text{TOARO})_2\text{Cl}_2]$ ($2.4 \times 10^{-3}\text{M}$)	16 950 sh , 16 000(387), 15 650(360), 14 800(454)
Extract ($7.3 \times 10^{-4}\text{M}$ Co + + 0.1M TOA O)	17 250(264), 16 140(377), 14 900(354)
Mixture $[\text{Co}(\text{TOA O})_2\text{Cl}_2]$ ($2.1 \times 10^{-3}\text{M}$) + $1.6 \times 10^{-4}\text{M}$ TOAO	17 250(238), 16 250(345), 15 000(338)

between extract and $[\text{Co}(\alpha\text{-NPO})_2\text{Cl}_2]$ itself (Table 4). If $\alpha\text{-NPO}$ is added to the solution of this complex then both spectra will coincide in practice due to suppression of dissociation with ligand detachment. From the spectra obtained, the complexes with TOARO and TOAO are much less dissociated, which is in agreement with the higher EA of these extractants.

The assignment of X-O and Co-O vibrations in IR-spectra of L, $[\text{CoL}_2\text{Cl}_2]$ and extracts is given in Table 5.

Table 5
Infrared spectra of extracts and complexes $[\text{CoL}_2\text{Cl}_2]$ in C_6H_6 as solvent

	$\nu(\text{X-O})$ cm^{-1}	$\nu(\text{Co-O})$ cm^{-1}	Other peaks for L
0.4M DOSO ^a	1050s	-	-
0.2M $[\text{Co}(\text{DOSO})_2\text{Cl}_2]$ ^a	975s, 1050sh ^b	-	-
0.2M $\alpha\text{-NPO}$	1260s	-	-
Extract($5 \times 10^{-2}\text{M Co} +$ $+ 0.2\text{M } \alpha\text{-NPO}$)	1200, 1260	-	-
0.04M $[\text{Co}(\alpha\text{-NPO})_2\text{Cl}_2]$	1200s	-	-
0.5M TAPC	1173s	-	445w, 480, 490
Extract($7.1 \times 10^{-2}\text{M Co} +$ 0.15M TAPC)	1100s, 1120s	442s	480, 490
0.25M $[\text{Co}(\text{TAPC})_2\text{Cl}_2]$	1100s, 1120s	440s	480, 490
0.5M TOARO	900s	-	-
Extract($0.169\text{M Co} +$ 0.4M TOARO)	860s, br	417s, br	-
0.25M $[\text{Co}(\text{TOARO})_2\text{Cl}_2]$	855s, br	417s, br	-
0.5M TOAO ^a	940w	-	540sh
Extract($0.196\text{M Co} +$ 0.5M TOAO) ^a	938w	583m	540sh

^aSpectra were measured in CCl_4 because of benzene absorption in necessary frequency range. ^bThe shoulder arises from slow complex decomposition with sulphoxide detachment.

As in the case of electronic spectra the IR-spectra of TAPO, TOARO, TOAO (in the frequency range of XO-vibrations) and their compounds with CoCl_2 and extracts differ quite a little from those of $(\text{CH}_3)_3\text{XO}$ and $[\text{Co}(\text{CH}_3)_3\text{XO}_2\text{Cl}_2]$ ($\text{X} = \text{N}, \text{P}, \text{As}$)^{12,14,17}. The co-ordination of R_nXO molecules to cobalt atoms is performed through the oxygen, and is reflected by the shifts of X-O valence vibration bands in spectra of $[\text{CoL}_2\text{Cl}_2]$ or extracts towards lower frequencies, compared with those of extractants alone. The shift of NO band due to complex formation was not observed, in agreement with previous results^{14,17}. This fact is believed to be connected with the absence of $p_\pi - d_\pi$ interaction in the NO bond.

So, the data above in their entirety allow the conclusion that the extraction mechanism of CoCl_2 by all the investigated compounds of R_nXO class is the same one and it consists in the formation of $[\text{CoL}_2\text{Cl}_2]$ tetrahedral complexes in organic phase.

X-ray spectra investigation of XO bond nature

The previous X-ray spectra investigations³⁴⁻³⁷ of the electronic structure of extractants show their EA to depend on the electron density at the donor atom. From this view-point, for R_nXO class extractants one of the most important problems is the problem of $p_\pi - d_\pi$ interaction between O and X atoms. Theoretical calculations³⁸⁻⁴² show the significant contribution of 3d-orbitals of phosphorus and sulphur to SO and PO bonds (i.e. $p_\pi - d_\pi$ interaction) in the compounds under consideration. On the other hand the quantum mechanic calculation⁴² of measurable characteristics of the NO bond in R_3NO does not require, in contrast to that for R_3PO , the assumption about $p_\pi - d_\pi$ interaction. The delocalization of 2p-electrons of oxygen on to d-orbitals

of X atom resulting from $p_{\pi} - d_{\pi}$ interaction, reduces the ability of oxygen to behave as donor of electrons when producing the Me-O bond and reduces by this way the EA of the extractant.

The X-ray spectra allow observation of the $p_{\pi} - d_{\pi}$ interaction effects. The X-ray emission L-spectra of sulphur atom in $(CH_3)_2SO$ and $(CH_3)_2S^a$ (SL-spectra) are produced by electron transition to 2p-orbitals of a sulphur atom from occupied molecular orbitals (MO), in formation of which the appreciable contribution is given by sulphur atomic orbitals (AO). The R_2SO molecule's MO with contribution from 3d-AO's of sulphur will have the maximum energy, and the peak of the highest energy in SL-spectra will correspond to transition from this MO. The appearance of this peak in SL-spectrum (W in Fig.4) gives evidence of existence of partly populated 3d orbitals of S atoms in R_2SO due to $p_{\pi} - d_{\pi}$ interaction. This peak is absent in R_2S spectra.

The oxygen K-spectra (OK-spectra) are studied for R_3XO compounds with $X = N, P, As$ (Fig.5). The broad and intensive peaks in these spectra named as P in Fig.5 are mainly due to electron transitions from MO of e and a_1 symmetry (π - and σ -bonding orbitals between O and X) in formation of which 2p-AO's of oxygen contribute. Less probable transitions from neighbour MO of e symmetry which correspond to σ -bonds between X and R-groups give also a contribution to the peak under consideration. OK-spectra of all three compounds are similar to each other by position and form of peaks P but in the case of R_3PO peak is essentially more narrow, the decrease in its width being due to decreasing of intensity on the high energy side. This feature

^a The length of hydrocarbon radicals does not exert influence on form and line positions of the spectra.

of R_3PO OK-spectrum should be considered as effect of $p_{\pi} - d_{\pi}$ interaction. Indeed, the decrease of oxygen 2p-AO contribution to e-orbital because of increasing phosphorus 3d-AO contribution leads to decrease in the relative intensity of transition from this MO to 1s orbital of oxygen atom. In addition, the e and a_1 levels approached each other as a result of increasing e-level energy due to $p_{\pi} - d_{\pi}$ interaction, and peak P's width is decreased on its high energy side. The approximate peak P expansion for R_3PO and R_3NO , corresponding to transitions from three considered MO, is given on Fig.5 for illustration. The available data are quite insufficient to exclude any contributions from vacant d-orbitals of N and As to formation of occupied higher MO in R_3NO and R_3AsO ; however the $p_{\pi} - d_{\pi}$ interaction in these compounds is undoubtedly too weak compared with R_3PO .

So, the high and almost equal EA of R_3NO and R_3AsO is due to the similarity of electronic states of oxygen atoms in these compounds.

References

- ¹Krasovec, F., & Klofutar, C., "Solvent Extraction Chemistry", 1967, p.509 (Amsterdam: North-Holland Publishing Co.)
- ²Rozen, A.M., Nicolotova, L.N., et al., In "Khimiya protsessov ekstraktsii", 1972, p.41 (Moscow: Nauka)
- ³Torgov, V.G., Mikhailov, V.A. In "Ekstraktsiya neorganicheskikh veshchestv", 1970, p.240 (Novosibirsk: Nauka)
- ⁴Mikhailov, V.A., Torgov, V.G. et al., Proceedings International Solvent Extraction Conference 1971, 1971, vol. 2, p.1112, (London: Society of Chemical Industry)

- ⁵Mikhailov, V.A., Torgov, V.G., & Nikolaev, A.V., Izv. Sibirsk. Otd. Akad. Nauk SSSR, Ser. Khim. Nauk, 1973, No 7, vyp. 3, 3
- ⁶Rozen, A.M., & Nicolotova, L.N., Dokl. Akad. Nauk SSSR, 1968, 183, 1350
- ⁷Methoden der organischen Chemie (Houben-Weyl), 1955, Band 9, s. 213 (Stuttgart: Georg Thieme Verlag)
- ⁸Torgov, V.G., Nicolaev, A.V., Mikhailov, V.A., et al. Izv. Sibirsk. Otd. Nauk SSSR, Ser. Khim. Nauk, 1964, No 11, vyp. 3, 95
- ⁹Merijanlian, A., & Zingaro, R.A., Inorg. Chem., 1966, 5, 187
- ¹⁰Torgov, V.G., Mikhailov, V.A., et al. Dokl. Akad. Nauk SSSR, 1966, 168, 836
- ¹¹Ramaswamy, H.N., & Jomassen, H.B., J. Inorg. Nucl. Chem., 1965, 27, 740
- ¹²Cotton, F.A., Barnes, R.D., & Bannister, E., J. Chem. Soc. (A), 1960, 2199
- ¹³Brodie, A.M., Hunter, S.H., et al. J. Chem. Soc. (A), 1968, 2039
- ¹⁴Hunter, S.H., Langford, V.M., et al. J. Chem. Soc. (A), 1968, 305
- ¹⁵Brodie, A.M., Hunter, S.H., et al. J. Chem. Soc. (A), 1968, 987
- ¹⁶Herlocker, D.M., & Drago, R.S., Inorg. Chem. 1968, 7, 1479
- ¹⁷Cunningham, D.M., & Workmen, M.O., J. Inorg. Nucl. Chem., 1971, 33, 3861
- ¹⁸Mazalov, L.N., Sadovsky, A.P., Dolenko, G.N., et al. Zh. str. Khim. 1973, 14, 1048
- ¹⁹Timmermans, J., "Physico-chemical constants of binary systems", 1960, vol. 3, p. 967 (New-York: Interscience)
- ²⁰Robinson, D., & Stokes, R.N., "Electrolyte solutions", 1959 (London: Butterworths)
- ²¹Karjakin, A.V., Muradova, G.A., Zh. fiz. Khim., 1971, 45, 1054
- ²²Shanker, R., & Venkateswarlu, S., J. Inorg. Nucl. Chem., 1970, 32, 229
- ²³Josten, M.D., & Drago, R.S., J. Am. Chem. Soc., 1962, 84, 3817

- ²⁴Drago, R.S., Wayland, B., & Carlson, R.S., J. Am. Chem. Soc., 1963, 85, 3125
- ²⁵Ykhnevitch, G.V., & Karjakin, A.V., Dokl. Akad. Nauk SSSR, 1964, 156, 681
- ²⁶Karjakin, A.V., Tokhadze, V.L., & Maisuradze, G.V., Zh. analit. Khim., 1970, 25, 315
- ²⁷Nicolaev, A.V., Djadin, Yu.A., et al. Izv. Sibirsk. Otd. Acad. Nauk SSSR, Ser. Khim. Nauk, 1969, No. 7, vyp. 3, 3
- ²⁸Karjakin, A.V., & Kriventsova, G.A., Dokl. Akad. Nauk SSSR, 1973, 208, 107
- ²⁹Karjakin, A.V., & Kriventsova, G.A., "Sostoyanie vody v organicheskikh i neorganicheskikh soedineniyakh", 1973, p. 38, (Moscow: Nauka)
- ³⁰Diamond, R.M., & Tuck, D.G., "Extraction of inorganic compounds into organic solvent", Progress in Inorganic Chemistry, 1960, vol. 2 (New York-London: Interscience)
- ³¹Belousov, E.A., & Trofimov, Yu., M., Zh. neorg. Khim., 1969, 14, 1296
- ³²Chatelet, M., & Nicond, C., Compt. rend., 1956, 242, 1471
- ³³Meek, D.W., Straub, D.K., & Drago, R.S., J. Am. Chem. Soc., 1960, 82, 6013
- ³⁴Nicolaev, A.V., Mazalov, L.N., et al., Izv. Sibirsk. Otd. Akad. Nauk SSSR, Ser. Khim. Nauk, 1972, No 12, vyp. 5, 3
- ³⁵Nicolaev, A.V., Torgov, V.G., et al., Zh. neorg. Khim., 1970, 15, 1336
- ³⁶Nicolaev, A.V., Yakovleva, N.I., Galt'tsova, E.A., et al. Izv. Sibirsk. Otd. Akad. Nauk SSSR, Ser. Khim. Nauk, 1972, No 14, vyp. 6, 118

- ³⁷Nicolaev, A.V., Torgov, V.G. et al., In " Khimiya protsessov ekstraktsii ", 1972, p. 75 (Moscow: Nauka)
- ³⁸Moffit, W., Proc. Roy. Soc., 1950, 200A, 409
- ³⁹Van Wazer, J.R., & Absar, I., Sulfur Rep. Trends 3rd Annual Meeting, Gras. symp. Amer. Chem. Soc., 1971, p.23 (New-Orleans)
- ⁴⁰Hiller, J.H., & Saunders, V.R., J. Chem. Soc. (A), 1970, 2475
- ⁴¹Archibald, R.M., & Perkins, P.G., Rev. Ram. Chim., 1971, 16, 1137
- ⁴²Choplin, F., & Kaufman, G., J. Mol. Structure, 1972, 11, 381

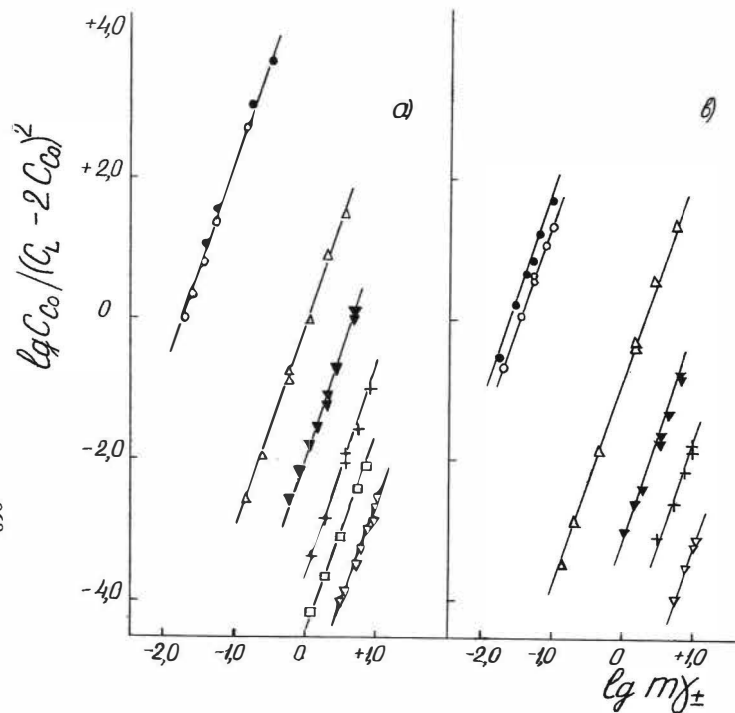


Fig. 1. Distribution isotherms for CoCl_2 extraction with R_nXO solutions in C_6H_6 (a) and CCl_4 (b) at 25°C . ∇ - TBP, \square - TBP(100 %), $+$ - DOSO, \blacktriangledown - d -NPO, \triangle - TAPO, \circ - TOARO, \bullet - TOAO.

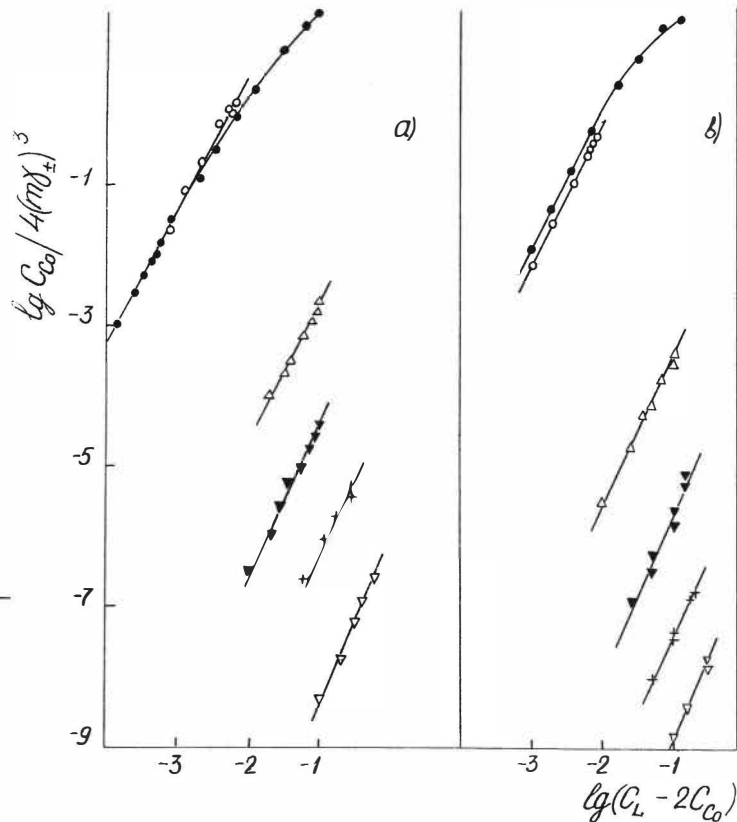


Fig. 2. Effect of R_nXO concentration in their solutions in C_6H_6 (a) and CCl_4 (b) upon CoCl_2 extraction. ∇ - TBP, $+$ - DOSO, \blacktriangledown - d -NPO, \triangle - TAPO, \circ - TOARO, \bullet - TOAO.

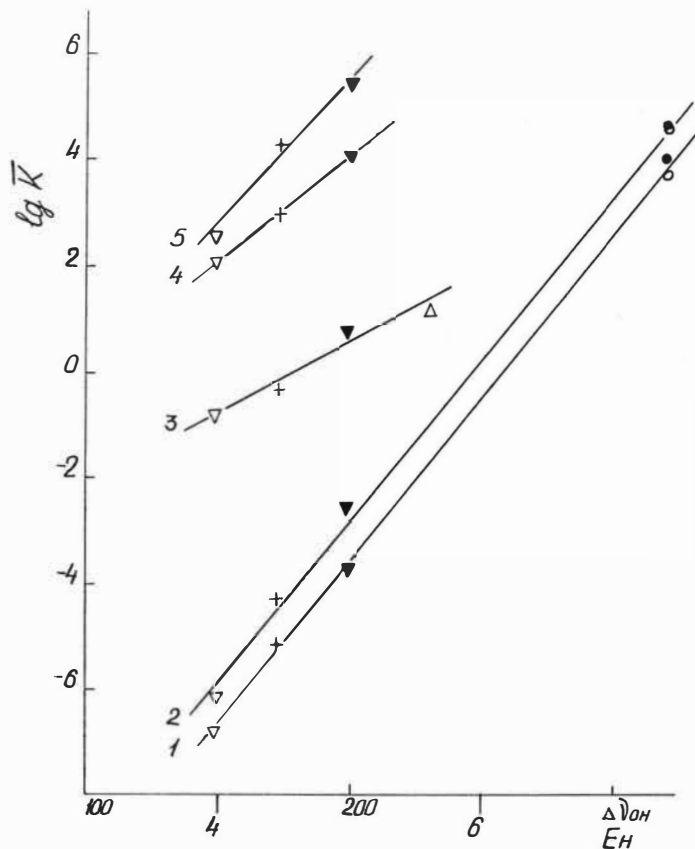


Fig. 3. Correlations between $\log \bar{K}$ and $\Delta V(\text{OH})$ (or E_H) for solutions of extractants of R_nXO class in CCl_4 (line 1) and C_6H_6 (lines 2-5): 1, 2 - CoCl_2 , 3 - HNO_3 , 4 - $\text{UO}_2(\text{NO}_3)_2$, 5 - $\text{Th}(\text{NO}_3)_4$.

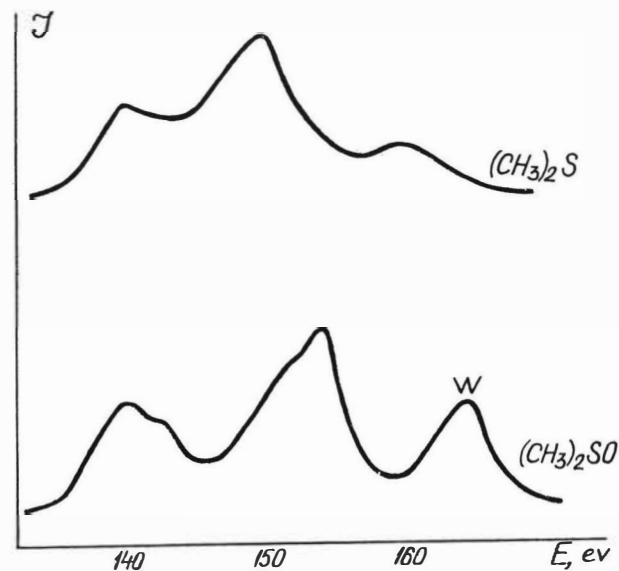


Fig. 4. X-ray emission L-spectra of sulphur in $(\text{CH}_3)_2\text{SO}$ and $(\text{CH}_3)_2\text{S}$.

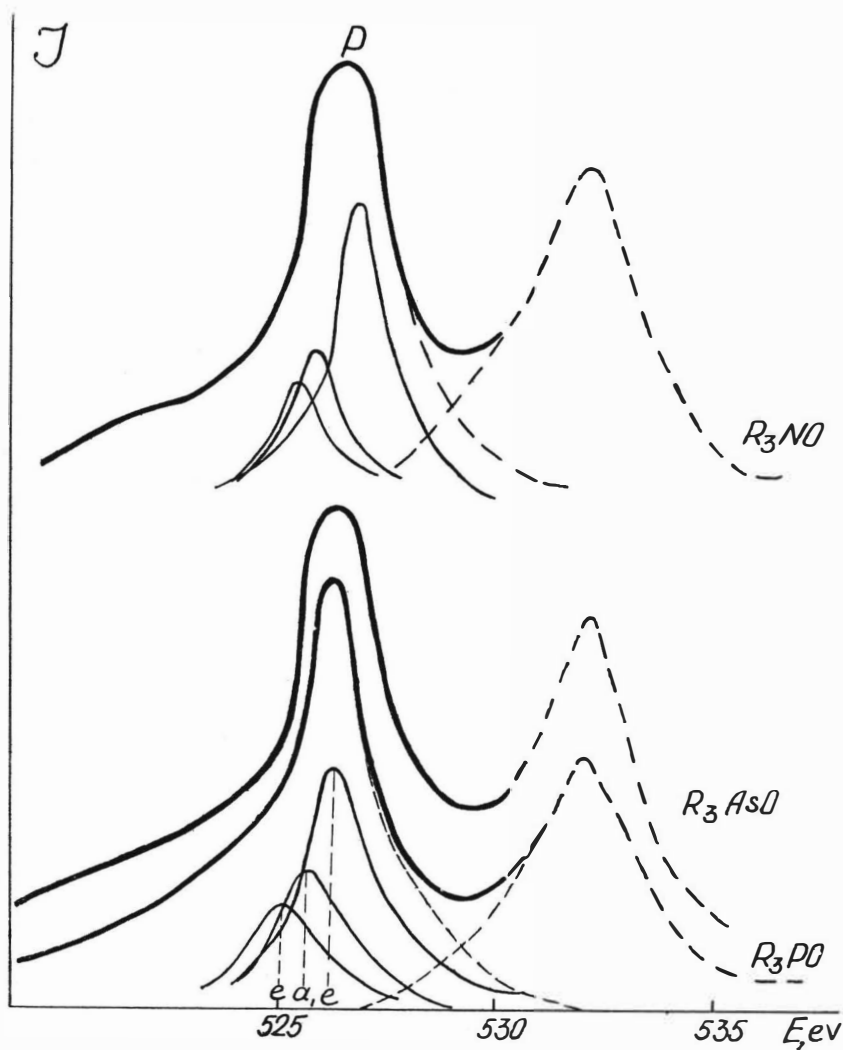


Fig.5. X-ray K-spectra of oxygen in $(C_8H_{17})_3NO$, $(C_8H_{17})_3PO$ and $(C_8H_{17})_3AsO$.

The Complexes Formed in the Divalent Metals - Hydrochloric Acid - Di-(2-Ethylhexyl)-Phosphoric Acid Extraction Systems -- Manganese (II), Iron (II), Cobalt (II), Nickel (II), Copper (II) and Zinc (II) Complexes

Taichi SATO and Masahiro UEDA

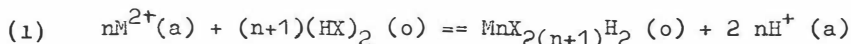
(Department of Applied Chemistry, Faculty of Engineering,
Shizuoka University, Hamamatsu, Japan.)

Abstract

The complexes formed in the extraction of divalent manganese, iron, cobalt, nickel, copper and zinc from hydrochloric acid solutions by di-(2-ethylhexyl)-phosphoric acid (DEHPA, HX) have been examined by measurements of water content, apparent molecular weight and magnetic moment, and electronic and infrared spectrophotometry. Thermal analyses have been carried out for the iron (II) and nickel complexes, and the electron spin resonance spectra have been investigated for the manganese (II) and copper (II) complexes. Consequently it is concluded that the DEHPA complexes of divalent manganese, iron, cobalt, nickel, copper and zinc exist as polymers having tetrahedral, octahedral, tetrahedral, octahedral, square-planar and tetrahedral structures with MnX_2 , $FeX_2 \cdot 2 H_2O$, CoX_2 , $NiX_2 \cdot 2 H_2O$, CuX_2 and ZnX_2 , respectively.

Introduction

In a previous paper¹⁾, it has been confirmed that the following equilibrium equation, expressed as an ion-exchange reaction governed by the formation of polymeric species, is given for the extraction of divalent metal from sulphuric acid solutions by di-(2-ethylhexyl)-phosphoric acid (DEHPA) :



where $n \geq 1$, X is the anion $(C_8H_{17}O)_2PO_2^-$, $(HX)_2$ the dimeric solvent²⁾, (a) and (o) are the aqueous and organic phases respectively. However, since the divalent metals show low extractability by DEHPA³⁾, the confirmation of Equation (1) has not been obtained by making an experiment on distribution, but by investigating the composition of the divalent cobalt, nickel and copper complexes formed in these extraction systems.

The present paper extends the work to determine the composition of the divalent manganese, iron, cobalt, nickel, copper and zinc complexes formed in the extraction from hydrochloric acid solutions by DEHPA.

Experimental

Chemicals

DEHPA (Union Carbide Corp.) was purified by the usual method⁴⁾. Aqueous solutions of divalent manganese, iron, cobalt, nickel, copper and zinc were prepared by dissolving their chlorides ($\text{MnCl}_2 \cdot 4 \text{H}_2\text{O}$, $\text{FeCl}_2 \cdot 4 \text{H}_2\text{O}$, $\text{CoCl}_2 \cdot 6 \text{H}_2\text{O}$, $\text{NiCl}_2 \cdot 6 \text{H}_2\text{O}$, $\text{CuCl}_2 \cdot 2 \text{H}_2\text{O}$ and ZnCl_2) in water. Other chemicals were of analytical reagent grade.

Extraction and analytical procedures

A solution of 0.1 M DEHPA in benzene was contacted with the aqueous solutions of divalent metal chlorides in 100 g/l and then 0.5 M sodium hydroxide solution was added dropwise. The complexes freed from benzene were prepared by drying the metal-saturated organic phases in vacuo.

Metals in the organic phase were stripped with 1 M hydrochloric acid, and determined by EDTA titration using xylenol orange^{5,6)} or Eriochrome Black T (for manganese⁷⁾) as indicator. The water content and chloride concentration of the organic phase were determined by Karl-Fischer titration and Volhard titration using nitrobenzene, respectively.

Spectrophotometry and E S R experiments

The absorption spectra were obtained on a Shimadzu Model QV-50 spectrophotometer, using matched 1.00 cm fused silica cells. The infrared spectra were measured on a Japan Spectroscopic Co. Ltd. Model IR-3, equipped with potassium chloride

prisms for measurement at 4,000-550 cm^{-1} , and IR-F, a grating model for measurement at 700-200 cm^{-1} , as a capillary film between thallium halide plates.

ESR spectra were determined on a high-sensitivity ESR spectrometer, designed in the Research Institute of Electronics, Shizuoka University and made by Shimada Rikakogyo Co. Ltd. Measurements were made in the solid state by using a super-heterodyne detection⁸⁾, as described previously¹⁾.

Measurements of apparent molecular weight and magnetic moment

The apparent molecular weight was determined in benzene on a Hitachi Model 115 isothermal molecular weight apparatus, and the magnetic moment was measured by the Gouy method⁹⁾.

Thermal analyses

Thermogravimetric and differential analyses (TGA and DTA) were carried out as described previously¹⁰⁾.

Results and discussion

In Equation (1), if we assume that the species containing chloride ion are inextractable, the extracted complexes should contain no chloride. This is supported by the fact that the infrared spectra of the complexes do not exhibit an absorption band due to the chloride group, in agreement with chemical analysis for the chloride concentration of the complexes. The data for the apparent molecular weights of the complexes are shown in Table I, compared with the theoretical values for monomeric species. This suggests that the extracted complexes exist as polymeric species. In addition the data for the water contents of the complexes are given in Table II, indicating that the iron (II) and nickel (II) complexes each contain two water molecules, but that the other complexes do not contain water

For the iron (II) and nickel (II) complexes, the nature of the bonding water was examined by thermal analysis, as shown in Fig.1. Below 240°C, the DTA curves of iron (II) and nickel (II) complexes show small endothermic reactions at 175 and 210°C, respectively. Also both complexes exhibit a sharp endothermic peak at 260°C, due to the thermal decomposition of DEHPA. These peaks correspond approximately to changes in slope of the TGA curves. On heating for three hours at 180°C, the nickel (II) complex exhibits thermochromism, showing a reversible colour change from yellow-green to violet due to the following equilibrium :



This property has also been observed for the complex formed in the nickel (II) sulphate-DEHPA system¹⁾. Accordingly it is inferred that the iron (II) and nickel (II) complexes contain coordinated water molecules.

Infrared spectra

The spectrum of DEHPA shows the P → O stretching absorption band at 1230 cm⁻¹, the OH stretching bands at 2680 and 2350 cm⁻¹ and the OH bending band at 1690 cm⁻¹, which are attributed to hydrogen bonding in the dimer²⁾, and the [P-O]-C stretching band at 1030 cm⁻¹. In the spectra of the complexes, the OH stretching and bending bands due to the formation of dimer disappear, while the original P → O absorption shifts toward lower frequency and simultaneously splits into two bands due to the POO asymmetrical and symmetrical stretching vibrations, as indicated in Table III. The splitting of the P → O band probably arises from some couplings of the metal and P → O bond in the polymeric species^{11,12)}. The infrared results thus confirm that the divalent metals extracted into

DEHPA by cation exchange are bonded to the phosphoryl oxygen atom. Additionally, the spectrum of the iron (II) complex reveals the OH stretching and bending bands at 3530 and 1650 cm^{-1} respectively, and of the nickel (II) complex at 3440 and 1635 cm^{-1} respectively, in accordance with the data for the water content.

In the region at 700-200 cm^{-1} , the spectra of the complexes exhibit the characteristic absorptions, assigned to the O-P-O bending frequency around at 600 and 500 cm^{-1} and to the M-O stretching vibration at about 400 cm^{-1} , as given in Table III. The O-P-O bending mode of DEHPA appears as the broad band centred around 485-455 cm^{-1} , but in the complexes is split into two bands, ascribed to the formation of the polymeric species. In the copper (II) complex, however, the Cu-O band is replaced by two absorptions at 360 and 300 cm^{-1} due to the asymmetrical and symmetrical stretching vibrations respectively, because of the lowering in the symmetry¹³).

Electronic spectra

The absorption spectra of the aqueous solutions of manganese (II), iron (II), cobalt (II), nickel (II), copper (II) and zinc (II) chlorides and of their DEHPA complexes in benzene were investigated. As some representative results, the spectra for cobalt (II), nickel (II) and copper (II) are illustrated in Figs.2-4.

The manganese (II) ion, with electron configuration d^5 , showing only the 6S ground state and the sextuplet state, gives the main structural types being octahedral, tetrahedral and square-planar. The spectrum shows that the typical

aquo ion species $[\text{Mn}(\text{H}_2\text{O})_6]^{2+}$ (14) is present in the aqueous solution of manganese (II) chloride. In contrast, the spectrum of the manganese (II) - DEHPA complex exhibits the broad and weak bands assigned to the transition ${}^6\text{A}_1 \rightarrow {}^4\text{T}_1$ (G) at 20000 cm^{-1} and the strong absorption due to the charge-transfer transition at above 25000 cm^{-1} . As a similar spectrum is observed for the species $[\text{MnCl}_4]^{2-}$ (15,16), it is expected that the manganese (II) - DEHPA complex is in a tetrahedral coordination.

The iron (II) ion, with electron configuration d^6 , has its ground state configuration in either an octahedral or a tetrahedral ligand field. For the aqueous solution of ferrous chloride, which is very pale blue-green in color, the spectrum shows the characteristic absorption of the species $[\text{Fe}(\text{H}_2\text{O})_6]^{2+}$ (17): the spin-allowed ${}^5\text{T}_{2g} (\text{D}) \rightarrow {}^5\text{E}_g (\text{D})$ transition occurs as a doublet around 10000 cm^{-1} , due to a Jahn-Teller effect. In the iron (II) - DEHPA complex, the spectrum exhibits the absorption at 22200 cm^{-1} , which appears as a shoulder, in addition to the charge-transfer absorption band giving the leading edge at lower frequency. However, since the magnetic moment of the iron (II) - DEHPA complex is smaller than the value of the spin-only magnetic moment, as indicated in Table IV it is considered that the absorption at 22200 cm^{-1} may be assigned to the transition ${}^1\text{A}_{1g} (\text{I}) \rightarrow {}^1\text{T}_{1g} (\text{I})$, in comparison with the spectrum of the diamagnetic species $[\text{Fe}(\text{CN})_6]^{4-}$ which reveals a similar absorption pattern (19). Thus the iron (II) - DEHPA complex is expected to be in an octahedral coordination.

The cobalt (II) ion, with the electron configuration d^7 , may have its ground state configuration in either an octahedral

or a tetrahedral ligand field. An octahedrally coordinated cobalt (II) ion should have three spin allowed d-d transitions, from the ground state ${}^4T_{1g}(F)$ to the states ${}^4T_{2g}(F)$, ${}^4A_{2g}(F)$ and ${}^4T_{1g}(P)$, while a tetrahedrally coordinated cobalt (II) ion should show the transition from the ground state ${}^4A_2(F)$ to the states ${}^4T_2(F)$, ${}^4T_1(F)$ and ${}^4T_1(P)$. In octahedral coordination, the ${}^4T_{1g}(F) \rightarrow {}^4T_{2g}(F)$ transition corresponds to the $10 Dq-3B$ value, in which B represents the Racah parameter for electron repulsion, and in tetrahedral coordination, the ${}^4A_2(F) \rightarrow {}^4T_2(F)$ transition corresponds to the $10 Dq$ value. Fig.2 indicates that the octahedral cobalt aquo ion species $[Co(H_2O)_6]^{2+}$ is present in the aqueous solution of cobalt (II) chloride, and that the cobalt (II) - DEHPA complex is in a tetrahedral coordination^{19,20}). The value of the ligand field parameter for the cobalt (II) complex may be calculated by using the elements of the matrices determined by Tanabe and Sugano²¹) : $B=769 \text{ cm}^{-1}$ and $10 Dq=4345 \text{ cm}^{-1}$. This is analogous to the value ($B=680 \text{ cm}^{-1}$ and $10 Dq=4150 \text{ cm}^{-1}$) for the complex formed in the cobalt (II)sulphate - DEHPA system¹). Accordingly it is seen that the value of $10 Dq$ in the cobalt (II) - DEHPA complex is close to the value (4130 cm^{-1}) which is four-ninths times the value of $10 Dq$ (9500 cm^{-1}) in the hexaquo cobalt (II) ion. Furthermore, the factor β in the nephelauxetic series^{21,22}), the ratio between the value of representative parameters of interelectronic repulsion in the complex and in the corresponding free ion, is estimated to be 0.69, implying that the nephelauxetic effect caused by bond formation is relatively large.

The nickel (II) ion, with electron configuration d^8 ,

commonly forms the complexes of the structural type being octahedral, tetrahedral and square-planar. In Fig.3, however, the spectra of both the aqueous solution of nickel (II) chloride and of the nickel (II) - DEHPA complex show the characteristic features of octahedral species ^{19,23}). For an octahedrally coordinated nickel (II) complex, it is expected to observe three spin-allowed transitions from the ground state ${}^3A_{2g}(F)$ to the states ${}^3T_{2g}(F)$, ${}^3T_{1g}(F)$ and ${}^3T_{1g}(P)$. In octahedral coordination, the ${}^3A_{2g}(F) \rightarrow {}^3T_{2g}(F)$ transition corresponds to the value of $10 Dq$. In the spectrum of the nickel (II) - DEHPA complex, the absorption bands at 8300, 14300 and 24400 cm^{-1} are assigned to the transitions ${}^3A_{2g}(F) \rightarrow {}^3T_{2g}(F)$, ${}^3A_{2g}(F) \rightarrow {}^3T_{1g}(F)$ and ${}^3A_{2g}(F) \rightarrow {}^3T_{1g}(P)$ respectively. Accordingly the ligand field parameter of the nickel (II) complex is obtained by considering the interaction of configuration : $B=841 \text{ cm}^{-1}$ and $10 Dq=8700 \text{ cm}^{-1}$. This also resembles the value ($B=894 \text{ cm}^{-1}$ and $10 Dq=8110 \text{ cm}^{-1}$) for the complex formed in the nickel (II) sulphate - DEHPA system¹⁾. As the nephelauxetic ratio is estimated to be 0.78, it is thought that the extent to which covalent bond formation occurs in the nickel (II) complex is lower than that in the cobalt (II) complex.

The copper (II) ion, with electron configuration d^9 , generally gives distorted octahedral and square-planar species. In Fig.4, it seems that a hexaquo copper (II) species exists in the aqueous solution of cupric chloride^{19,24}). For the copper (II) - DEHPA complex, the value of $10 Dq=12500 \text{ cm}^{-1}$ is obtained from the spectrum, but it is difficult to predict whether the species is either octahedral or square-planar since the spectrum consists of a broad band. However, this

value is similar to that ($B=13000\text{ cm}^{-1}$) for the complex formed in the cupric sulphate-DEHPA system¹⁾.

E S R spectra

The ESR spectrum of the copper (II) complex was examined as illustrated in Fig.5, compared with that of the manganese (II) complex. The spectrum of the copper (II) complex shows the typical feature due to a square-planar symmetry, and the calculated g values²⁵⁻³¹⁾ are $g_{\parallel}=2.238$, $g_{\perp}=2.046$, and average $g=2.141$. It is therefore postulated that the spin-orbit coupling constant for E terms³²⁾ reduces to 72.8 per cent of that for the free ion. In contrast, the spectrum of the manganese (II) complex reveals the feature to be isotropic in a tetrahedral symmetry, and the calculated g values are $g_{\parallel}=2.052$ and $g_{\perp}=1.956$.

Magnetic moment and structure of the complexes

The magnetic moments of the complexes and their probable structures are given in Table IV. From this it is seen that the contribution of the orbital angular momentum by ligand field is completely quenched for the complexes, except the iron (II) complex. Hence the agreement between the calculated values³³⁾, obtained by using the spin-orbit coupling constant of free ion and the $10 Dq$ value from absorption spectra, and the experimental results support the structure of the complexes deduced from the spectral studies.

Thereby it is presumed that the equilibrium expression in Equation (1) is also satisfied in the present extraction system as well as the divalent metal sulphate - DEHPA system¹⁾, because the molar ratio, $[X]/[M]$, of the complex, $M_nX_{2(n+1)}H_2$, formed in the extraction is expected to approach nearly two as the

value of n increases.

Acknowledgements

We wish to thank Professor I. Takao of the Research Institute of Electronics, Shizuoka University for the ESR spectral experiment and Mr. T. Nakamura for assistance with part of the experimental work.

References

1. Sato, T. and Nakamura, T. J. inorg. nucl. Chem., 1972, 34, 3721
2. Peppard, D.F., Mason, G.W., Maier, J.L., Driscoll, W.J. and Sironen, R.J. J. inorg. nucl. Chem., 1958, 7, 276; Mayers, A.L., McDowell, W.J. and Coleman, C.F. ibid., 1964, 26, 2005
3. Baes, C. F.. Jr. ibid., 1962, 24, 707
4. E.g., Sato, T. ibid., 1962, 24, 699
5. Kinnunen, J. and Wennerstrand, B. Chemist - Analyst, 1957, 46, 92
6. Korble, J. and Pribil, R. ibid., 1956, 45, 102
7. Flaschka, H. ibid., 1953, 42, 56
8. Hirshon, J.M. and Fraenkel, G.K. Rev. Sci. Instr., 1955, 26, 34; Misra, H. ibid., 1958, 29, 590
9. Gray, T.F. 'Chemistry of the Solid State' (Ed. W.E. Garner), p.147, London, Butterworths, 1955.
10. Sato, T. and Adachi, K. J. inorg. nucl. Chem., 1969, 31, 1395
11. Cotton, F.A., Barnes, R. and Banister, E. J. chem. Soc., 1960, p.2199
12. Ferraro, J.R. J. inorg. nucl. Chem., 1962, 24, 475
13. Rodley, G.M., Goodgame, D.M.L. and Cotton, F.A. J. chem. Soc., 1965, p.1499
14. Cotton, F.A. and Wilkinson, G. 'Advanced Inorganic Chemistry', 2nd Ed., p.840 New York, Interscience, 1966.
15. Buffagnie, S and Dunn, T.M., Nature, Lond., 1960, 188, 937
16. Furlanic, A and Furlani, C. J. inorg. nucl. Chem., 1961, 19, 51.
17. As ref. 14), p.856.
18. Konig, E. and Madeja, K. Inorg. Chem., 1968, 7, 1848
19. Gill, N.S. and Nyholm, R.S. J. chem. Soc. 1959, p.3977.
20. As ref. 14), p.869.

21. Jørgensen, C.J. 'Absorption Spectra and Chemical Bonding in Complexes', p.134, Oxford, Pergamon Press, 1962.
22. Dunn, T.M. 'Modern Coordination Chemistry' (Ed. J.Lewis and R.G. Wilkins), p.267, New York, Interscience, 1960.
23. As ref. 14), p.881.
24. As ref. 14), p.898.
25. Kneubuhr, F.K. J. chem. Phys., 1960, 33, 1074
26. Abragam, A. and Pryce, M.H.L. Proc. Roy. Soc., 1951, A205, 135.
27. Bleaney, B.; Proc. phys. Soc., 1960, A75, 621.
28. Vanngard, T. and Aasa, R. Proc. 1st. Int. Conf. Paramagnetic Resonance, Jerusalem, 1962 (Ed. W. Low) Vol.1. p.509 New York, Academic Press, 1963.
29. Willett, R.D., Loles, O.L. Jr. and Michelson, C. Inorg. Chem., 1967, 6, 1885
30. Figgis, B.N. 'Introduction to Ligand Fields', p.293, New York, Interscience, 1962.
31. Balhausen, C.J. 'Introduction to Ligand Field Theory', New York, McGraw-Hill, 1962.
32. As Ref. 30), p.276.
33. As Ref.30), p.265.

Fig.1. TGA and DTA curves of divalent metal - DEHPA complexes (A, Fe (II) ; B, Ni (II)).

(a) TGA curve ; (b) DTA curve

Fig.2. Absorption spectra of aqueous cobalt chloride solution and of Co (II) - DEHPA complex in benzene (numerals on curves are cobalt concentrations, M ; continuous and broken lines represent organic and aqueous solutions, respectively ; thickness of cell, 1.00 cm).

Fig.3. Absorption spectra of aqueous nickel chloride solution and of Ni (II) - DEHPA complex in benzene (numerals on curves are nickel concentrations, M ; continuous and broken lines represent organic and aqueous solutions, respectively ; thickness of cell, 1.00 cm).

Fig.4. Absorption spectra of aqueous copper chloride solution and of Cu (II) - DEHPA complex in benzene (numerals on curves are copper concentrations, M ; continuous and broken lines represent organic and aqueous solutions, respectively ; thickness of cell, 1.00 cm).

Fig.5. ESR spectra of Mn (II) - and Cu (II) - DEHPA complexes (continuous and broken lines represent the spectra of Cu (II) and Mn (II) complexes, respectively).

Table I. Molecular weight of divalent metal-DEHPA complexes

Metal	Complex	Mol. wt.		
		Obs.	Theor.	Obs./Theor.
Mn	MnX_2	3500	698	5.01
Fe	$\text{FeX}_2 \cdot 2\text{H}_2\text{O}$	2008	735	2.73
Co	CoX_2	3650	702	5.22
Ni	$\text{NiX}_2 \cdot 2\text{H}_2\text{O}$	3784	738	5.13
Cu	CuX_2	1263	706	1.79
Zn	ZnX_2	16869	708	23.82

Table II. Water content of divalent metal-DEHPA complexes

Metal	[Complex], M	[H ₂ O], M	Molar ratio [H ₂ O]/[Complex]
Mn	0.0610	0.0124	0.203
Fe	0.0562	0.1156	2.06
Co	0.0452	0.0079	0.175
Ni	0.0379	0.0803	2.12
Cu	0.0386	0.0187	0.474
Zn	0.0856	0.0145	0.169

Table III. Infrared spectral data for divalent metal-DEHPA complexes

Metal	ν POO		δ (O-P-O)	ν (M-O)
	asym	sym		
Mn	1190	1102	585, 480	385
Fe	1170	1100	615, 490	420
Co	1190	1100	600, 480	390
Ni	1195	1080	600, 540	360
Cu	1180	(1095)*	590, 500	360, 300
Zn	1190	1105	600, 480	400

* This is indistinct.

Table IV. Magnetic moment and probable structure of divalent metal-DEHPA complexes

$3d^n$	Complex	Structure	Ground state	Obs. μ_{eff} , B.M.	Calc. μ_{eff} , B.M.
5	MnX_2	Tetrahedral, Td	$^6\text{A}_1$	5.93	5.92
6	$\text{FeX}_2 \cdot 2\text{H}_2\text{O}$	Octahedral, Oh	$^5\text{T}_{2g}$	4.15	4.90*
7	CoX_2	Tetrahedral, Td	$^4\text{A}_2$	4.51	4.48
8	$\text{NiX}_2 \cdot 2\text{H}_2\text{O}$	Octahedral, Oh	$^3\text{A}_{2g}$	3.22	3.27
9	CuX_2	Square-planar, D_{4h}	$^2\text{B}_{1g}$	1.79	1.96
10	ZnX_2	Tetrahedral, Td	—	0.	—

* This is the value of spin-only magnetic moment.

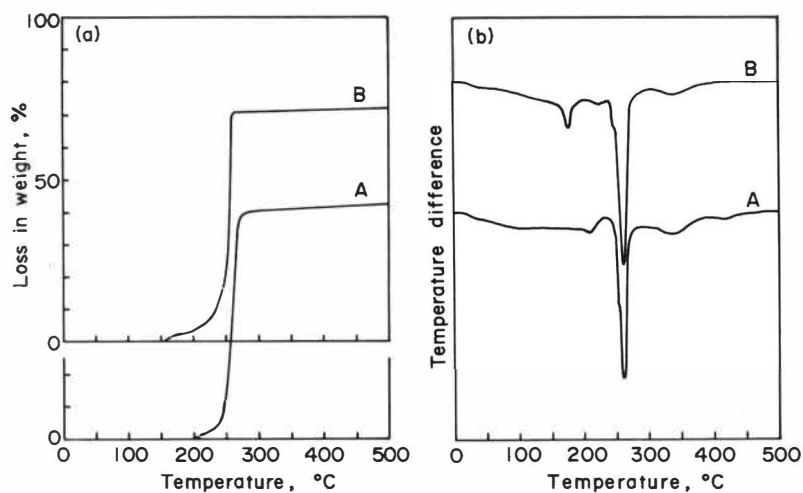


Fig. 1 TGA and DTA curves of divalent metal-DEHPA complexes (A, Fe(II); B, Ni(II)).

(a) TGA curve; (b) DTA curve

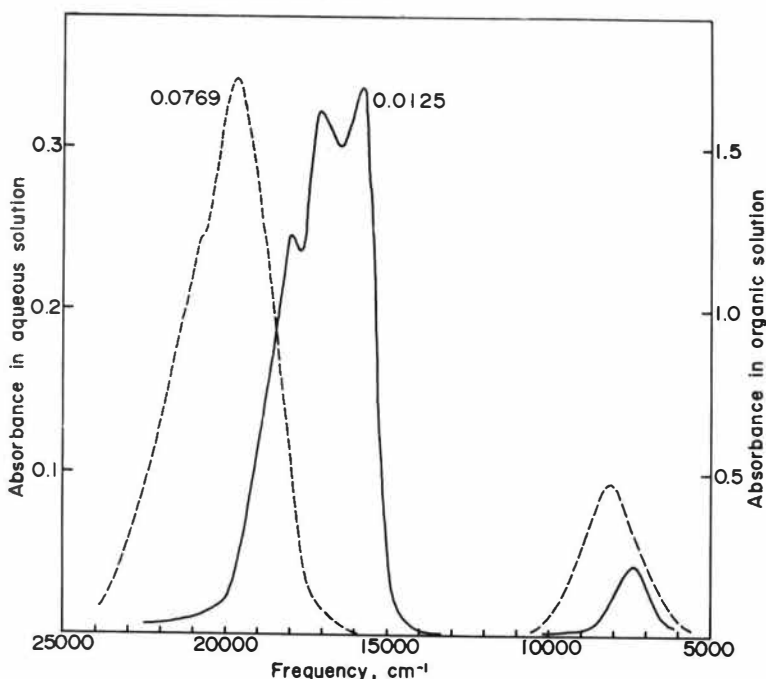


Fig. 2 Absorption spectra of aqueous cobalt chloride solution and of Co(II)-DEHPA complex in benzene (numerals on curves are cobalt concentrations, M; continuous and broken lines represent organic and aqueous solutions, respectively; thickness of cell, 1.00 cm).

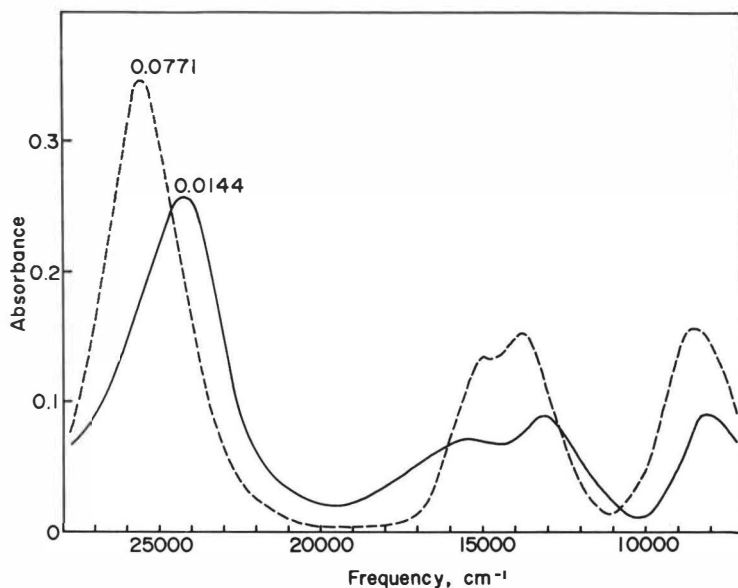


Fig. 3 Absorption spectra of aqueous nickel chloride solution and of Ni(II)-DEHPA complex in benzene (numerals on curves are nickel concentrations, M; continuous and broken lines represent organic and aqueous solutions, respectively; thickness of cell, 1.00 cm).

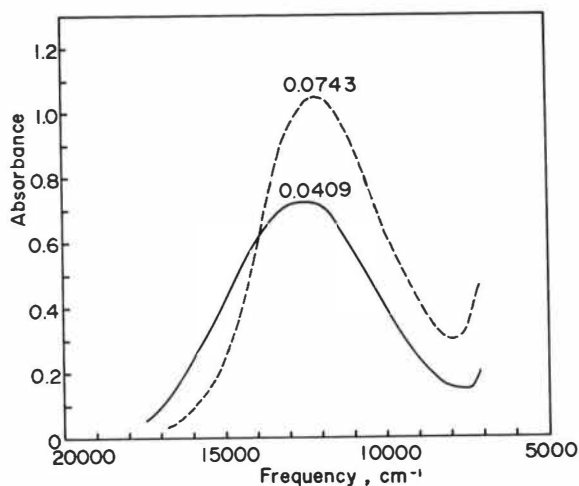


Fig. 4 Absorption spectra of aqueous copper chloride solution and of Cu(II)-DEHPA complex in benzene (numerals on curves are copper concentration, M; continuous and broken lines represent organic and aqueous solutions, respectively; thickness of cell 1.00 cm).

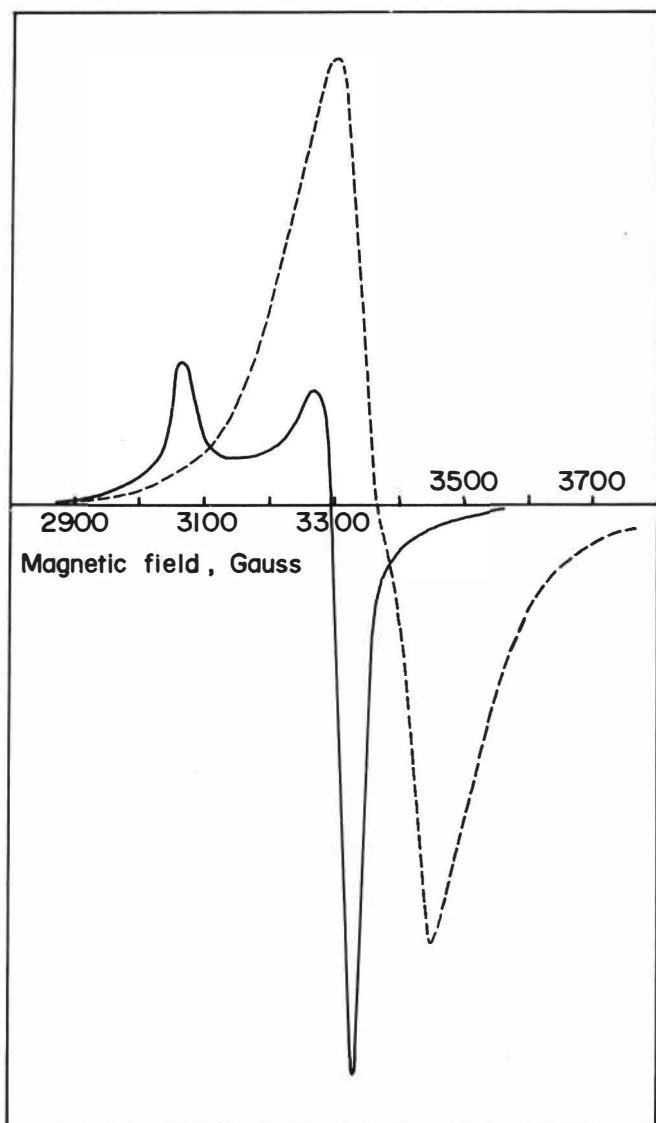


Fig. 5 ESR spectra of Mn(II)-and Cu(II)-DEHPA complexes (continuous and broken lines represent the spectra of Cu(II) and Mn(II) complexes, respectively).

SESSION 8

Tuesday 10th September: 9.00 hrs

E X T R A C T I O N T E C H N O L O G Y

(Organic Processes)

Chairman:

Professor C. Hanson

Secretaries:

Dr. P.J. Bailes

Mr. H. Van Landeghem

SEPARATION OF MIXTURES OF 2-6 LUTIDINE WITH 3- AND 4- PICOLINE BY
LIQUID-LIQUID EXTRACTION

M. M. Anwar*, S. T. M. Cook*, C. Hanson[‡], M. W. T. Pratt[‡]

Abstract

The separation of mixtures of the organic bases 2-6 lutidine, 3- and 4- picoline into the individual components by liquid-liquid extraction is described.

First, the lutidine may be extracted by a mixed organic solvent (95% v/v n-hexane, 5% chloroform) from an aqueous phase to which potassium thiocyanate has been added to increase the separation factor. The picolines may be extracted from the aqueous phase and separated by dissociation extraction with counter-current flow of an organic solvent (benzene) and an aqueous solution of sodium dihydrogen phosphate. The aqueous phase containing the 4- picoline salt is then contacted with fresh organic solvent to liberate undissociated picoline and regenerate the phosphate reagent.

Experimental data are used to outline a proposed practical separation process and the general theory of dissociation extraction is developed to cover the incomplete reaction between organic bases or acids and weakly acidic or basic salts of the type used in this process.

* Department of Chemical Engineering, Teesside Polytechnic

‡ Schools of Chemical Engineering, University of Bradford

1. Introduction

Mixtures of 2-6 lutidine, 3- and 4- picoline occur together in the ' β - picoline' fraction of coal tar distillates and their separation by common techniques is difficult. Ordinary fractional distillation is not feasible because all three components boil within 1°C of 144°C at atmospheric pressure. Separation methods suggested in the literature include azeotropic distillation with water or acetic acid⁽¹⁾ and fractional crystallisation combined with a chemical conversion of the ternary mixture into binary mixtures⁽²⁾. Liquid-liquid extraction processes, which may commonly be used to separate close boiling mixtures, have proved difficult to develop in this case because of the close chemical similarity of the components and separation attempts using single solvents have not been very successful. The most practical proposals for a compound fractional liquid extraction process for this separation have been made by Karr and Scheibel⁽³⁾ and the process now suggested is a development of their method.

As the first stage in the complete separation, the liquid-liquid extraction of 2-6 lutidine from the feed mixture will be considered. The separation of the picoline isomers is discussed in a later section and, finally, these two steps are combined in an outline description of a practical process for producing the individual components.

2. Separation of 2-6 Lutidine from the Picolines

The processes previously suggested for achieving this separation by liquid-liquid extraction have certain disadvantages and allow scope for improvement.

Columbic and Orchin⁽⁴⁾ showed that the distribution coefficient of 2-6 lutidine between chloroform and water is about 2.6 times greater than that of either 3- or 4- picoline. However, for a fractional solvent extraction process to be viable, it is not sufficient that the separation factor is favourable; the capacities of both phases for the components of the feed mixture must also be reasonably high. Otherwise, one of the streams leaving the extraction stage will contain only a very dilute solution of one or more of the feed components, the recovery of which will involve high cost: for example, in steam consumption for distillation. Use of the water/chloroform system for lutidine separation involves an aqueous/organic phase ratio of over 100 to achieve comparable quantities of the solutes in both phases, and makes necessary the recovery of 3- and 4-

picoline from a very dilute aqueous solution.

Karr and Scheibel⁽³⁾ separated 2-6 lutidine from the 'β - picoline' fraction using "Skellysolve B" (essentially n-hexane) and water as the solvents. In this system, the concentration of solute in the organic phase is about equal to that in the aqueous phase at low solute concentrations only. As the concentration of the organic bases increases, the distribution coefficients decrease, so that for the concentrated solute feeds with which any practical industrial process will be concerned, a high organic/aqueous phase ratio is required. In this case, it is the lutidine component which must be recovered from a dilute solution.

The process of dissociation extraction, with which the authors have recently been concerned^(5,6,7), is normally capable of achieving the separation of isomeric mixtures of organic acids or bases. The technique is based upon the differences in the strengths of the components as acids or bases, i.e. differences in their dissociation constants, which may be considerable even for isomers due to their differing molecular arrangements. For example, organic bases may be separated by the combination of solvent extraction with a partial neutralisation by aqueous acid. The stronger organic base, having the higher dissociation constant, tends to react forming a salt which is soluble in the aqueous phase, while the weaker base, losing the competition to react, tends to remain undissociated and soluble in organic solvents. In a multi-stage process, involving counter-current flow of organic solvent and aqueous acid, a high degree of separation of the isomers may be obtained.

Unfortunately, the application of dissociation extraction to the separation of 2-6 lutidine from the picolines is difficult. Although the dissociation constant of 2-6 lutidine is the highest (38.4×10^{-9} , compared with 4.5×10^{-9} for 3- picoline and 10.6×10^{-9} for 4- picoline) its affinity for most organic solvents is also the greatest. The first factor on its own would lead to a concentration of lutidine in the aqueous phase, but the latter causes a tendency towards the concentration of undissociated lutidine in the organic phase. The opposition of these two effects results in a separation factor which is too small for a practical process.

It was decided, therefore, to investigate the possibility of achieving the initial separation of lutidine from the picolines by more complex solvent extraction processes involving the use of mixed solvents, either alone, or in conjunction with additives to promote selectivity at high feed concentrations.

In an attempt to achieve a roughly balanced distribution of the organic bases between organic and aqueous solvent phases, the use of mixtures of two organic solvents was studied, one having a relatively high affinity for the bases, the other being a relatively weak solvent for them. A mixture of chloroform and n-hexane, as the strong and weak solvents respectively, was found to give good results at the composition: 95% v/v n-hexane, 5% chloroform.

There are many examples quoted in the literature of improved separation factors obtained by the addition to one phase of a compound which may preferentially form a weak association or complex with one or more components of the feed. It is important, of course, that the resultant molecular complex is not too strongly bound for otherwise much chemical or thermal energy will be required, after the separation, to break it down and liberate the pure feed component. In the present case, the presence of potassium thiocyanate in the aqueous phase was found to be beneficial.

The effects of the use of mixed hexane/chloroform solvent together with potassium thiocyanate addition upon separation factor are presented here.

2(i) Experimental

Equimolar mixtures were made up: (a) of 2-6 lutidine with 3-picoline and (b) of 2-6 lutidine with 4-picoline. Varying known amounts of one or other of the mixtures were added to 10 ml of the mixed organic solvent (95% v/v n-hexane, 5% chloroform) and 10 ml water in stoppered bottles suspended in a thermostat at 25°C. Equilibrium distribution was essentially established after the bottles had been shaken for 5 mins but, in practice, 15 mins were allowed to ensure that complete equilibrium had been achieved. To measure separation factors, the two phases were then separated and analysed for lutidine and picoline concentration by gas-liquid chromatography.

A Pye Series 104 Dual Flame Ionization Temperature Programmed Chromatograph, Model 24, was used. The solid support was prepared by the treatment of Chromosorb P of 80 - 100 mesh with alcoholic sodium hydroxide (6% NaOH on dried Chromosorb P) followed by evaporation of the alcohol. The stationary phase applied to the solid support was 12% diglycerol on dried Chromosorb P. The operating temperature was 90°C and the column length 5ft.

Samples of the organic and aqueous phases for analysis were injected directly and the molar ratio of the two organic bases in each phase was determined from the ratio of peak areas recorded by a Kent 'Chromolog' integrator. The amounts of bases in each of the two phases and the separation factor were calculated from the concentration ratios in each phase and the known total amount present. Separation factors were always expressed as the following ratio of mole fractions of total bases in each phase; i.e. on a solvent free basis:

$$\frac{[2-6 \text{ lutidine in organic solvent phase}]}{[2-6 \text{ lutidine in aqueous phase}]} \times \frac{[\text{picoline in aqueous phase}]}{[\text{picoline in organic solvent phase}]}$$

The concentration of each organic base was determined with a maximum error of $\pm 0.5\%$ in reproducibility.

To find the effect of temperature on separation factor, further determinations were made for equilibrium distributions established at 3° , 13° and 36°C .

To demonstrate the effect of an aqueous solution of potassium thiocyanate on the separation, 5 ml of either feed mixture (a) or (b) were distributed between 10 ml of the mixed organic solvent and 10 ml of an aqueous KCNS solution of known strength. The measurement of separation factor was made as before.

The organic bases used were obtained from British Drug Houses Ltd., and were shown to be pure by GLC analysis. 'Analar' organic solvents were employed.

2(ii) Results

Separation factors for the distribution of equimolar mixtures of 2-6 lutidine with (a) 3- picoline and (b) 4- picoline at 25°C between the mixed organic solvents and water are shown in Table 1 as a function of the volume of the feed mixture of organic bases added.

The effect of temperature on separation factor is shown in Table 2 for the distribution of 4.5 ml of the feed mixtures of organic bases between 10 ml mixed organic solvents and 10 ml water.

Measurements of separation factor when KCNS was present in the aqueous phase are given in Table 3.

TABLE 1

Separation factors for the distribution between 10 ml mixed organic solvents and 10 ml water of equimolar mixtures (a) 2-6 lutidine and 3- picoline, and (b) 2-6 lutidine and 4- picoline.

Mixture	Vol.of mixture added to system ml	Equilibrium concentration of bases in the conjugate phases					Separation Factor
		Total conc. of bases in aqueous phase ml/10ml	Organic solvent phase (molar %)		Aqueous phase (molar %)		
			lutidine	picoline	lutidine	picoline	
(a)	1.50	0.41	55.4	44.6	35.5	64.5	2.26
	2.50	0.71	55.6	44.4	35.8	64.2	2.25
	3.50	1.27	56.4	43.6	38.7	61.3	2.12
	4.50	2.09	57.3	42.7	41.6	58.4	1.88
	5.50	3.27	58.2	41.8	44.4	55.6	1.74
(b)	1.50	0.46	57.0	43.0	34.2	65.8	2.65
	2.50	0.81	57.4	42.6	34.7	65.3	2.54
	3.50	1.44	58.5	41.5	37.8	62.2	2.34
	4.50	2.31	59.6	40.4	40.9	59.1	2.13
	5.50	3.52	60.7	39.3	44.0	56.0	1.96

Variation in separation factor with temperature for 4.5 ml of mixtures (a) or (b) distributed between 10 ml mixed organic solvents and 10 ml water.

Mixture	Temperature °C	Equilibrium concentration of the bases in the conjugate phases					Separation Factor
		Total conc. in the aqueous phase ml/10ml	Organic solvent phase (molar %)		Aqueous phase (molar %)		
			lutidine	picoline	lutidine	picoline	
(a)	3.0	3.53	59.4	40.6	47.4	52.6	1.62
	13.0	2.91	59.3	40.7	44.9	55.1	1.79
	25.0	2.09	57.3	42.7	41.6	58.4	1.88
	36.0	1.31	54.4	45.5	39.0	61.0	1.87
(b)	3.0	3.27	61.7	38.3	45.6	54.4	1.92
	13.0	2.87	61.5	38.5	43.5	56.5	2.07
	25.0	2.31	59.6	40.4	40.9	59.1	2.13
	36.0	1.60	56.5	43.5	38.2	61.8	2.10

TABLE 3

The effect of KCNS concentration on separation factor. Distribution of 5 ml of mixture (a) or (b) between 10 ml mixed organic solvents and 10 ml aqueous KCNS.

Mixture	KCNS conc. grams/litre	Equilibrium concentration of the bases in the conjugate phases :					Separation Factor
		Total conc. in the aqueous phase ml/10ml	Organic solvent phase (molar %)		Aqueous phase (molar %)		
			lutidine	picoline	lutidine	picoline	
(a)	200	2.85	60.2	39.8	42.3	57.7	2.06
	360	2.99	62.1	37.9	41.9	58.1	2.28
	420	3.03	62.7	37.2	41.8	58.2	2.34
	480	3.04	62.8	37.2	41.7	58.3	2.36
	540	3.04	62.9	37.1	41.7	58.3	2.37
(b)	200	2.91	61.6	38.4	41.7	58.3	2.24
	360	2.97	62.9	37.1	41.2	58.8	2.42
	420	2.98	63.3	36.7	41.0	59.0	2.48
	480	2.98	63.4	36.6	40.9	59.1	2.50
	540	2.97	63.4	36.6	40.8	59.2	2.51

2(iii) Discussion

The separation factors for the distribution of 2-6 lutidine and the separate picoline isomers between mixed organic solvent and water decrease significantly with increase in the concentration of organic bases, as Table 1 shows, the lutidine being preferentially concentrated in the organic phase. At the highest loading of organic bases, the desired result of fairly balanced concentrations of solutes between the two phases has clearly been achieved with this mixed solvent system, for the difference between the equilibrium concentrations in the two phases does not exceed 2:1.

Table 2 confirms that the separation factor increases with temperature and the concentration of the solutes in the aqueous phase decreases. The latter observation is of great importance for a practical separation process, as the desirable reflux of 2-6 lutidine at the organic phase exit end of the contactor may be obtained simply by a reduction in temperature, thus reducing its affinity for the organic phase.

The increase in separation factor by the addition of potassium thiocyanate to the aqueous phase is significant. From Table 3, the separation factor increases with KCNS concentration and at the highest concentration used (540 g/litre) this additive produces an increase in separation factor from 1.8 to 2.36 for feed mixture (a) and from 2.0 to 2.51 for (b). The concentrations of solutes in the two phases are satisfactorily high, and in a multi-stage contactor with counter-current flow of mixed organic solvent and aqueous potassium thiocyanate solution, it should be possible to separate 2-6 lutidine from the picolines to a high degree of purity in a reasonable number of equilibrium stages, as the separation factor is close to 2.

The aqueous potassium thiocyanate solution leaving this contactor will contain the 3- and 4- picolines of the feed mixture, now essentially free from lutidine. An increase in the temperature of this stream will, as Table 2 shows, increase the affinity of the picolines for the organic phase. This fact may be used not only to provide the necessary reflux stream of picolines but also to extract the picolines from the aqueous potassium thiocyanate stream, which may then be recycled.

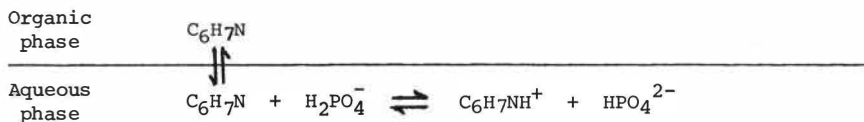
The results indicate that, at 36°C, the distribution coefficient of picolines between the mixed organic solvent and the aqueous potassium thiocyanate phase will be between 1.5 and 2.5. A second contactor working at high temperature (or a separately heated part of the first contactor) will allow most of the picolines to be transferred into the counter-current stream of organic solvent. Different organic solvents may be used to recover

the picolines for reflux and the picolines passing to their separation stage. Benzene is a more suitable solvent for the latter. Any picolines not extracted from the aqueous phase will not be lost, as they will be recycled to the first contactor in the aqueous thiocyanate stream. They will tend to reduce the efficiency of the first contactor, however, and so the amount of picolines recycled in this stream should be limited to the economic optimum.

3. Separation of 3- and 4- picolines

The process of dissociation extraction may be used to separate the 3- and 4- picoline isomers, exploiting the difference between the dissociation constants of the two bases. The generalised theory of dissociation extraction presented earlier by the present authors⁽⁵⁾ was confirmed experimentally by a study of the separation of these compounds by reaction with a deficiency of aqueous mineral acid. A later paper⁽⁷⁾ showed that the use of weakly acidic or basic reagents instead of strong acids or bases enables the dissociation reaction in the aqueous phase to be reversed after the isomers have been separated, simply by multi-stage contact with fresh organic solvent. This liberates the separated isomer in the undissociated form and regenerates the extraction reagent, which may be recycled. The separation is thus achieved without the continuous consumption of chemicals characteristic of dissociation extraction processes using strong acids or bases and should result in significantly reduced operating costs.

To illustrate this, consider the separation of the 3- and 4- picoline isomers present in an organic solvent phase by contact with an aqueous solution of the weakly acid salt, sodium dihydrogen phosphate, NaH_2PO_4 . The phosphate salt should be in a stoichiometric deficiency compared with the picolines so that in the aqueous phase there will be competition between the two isomers to react, as shown below:



The more strongly basic 4- picoline will tend to win the competition, forming a dissociated salt soluble in the aqueous phase. The picoline which does not react and so remains undissociated, containing an increased proportion of 3- picoline, will be soluble in organic solvents and

will partition between the two phases according to the distribution law. The combination of partial neutralisation and contact with an organic solvent will, therefore, achieve a partial separation of the isomers and a high degree of separation may be achieved in a multi-stage process.

The aqueous phase, containing the salt of 4- picoline, may then be contacted with a fresh organic solvent, such as chloroform, which has a high affinity for undissociated picoline. As the picoline is extracted into the organic solvent phase, the reaction equilibrium in the aqueous phase will tend to reverse, generating more undissociated picoline and regenerating the reagent dihydrogen phosphate salt. Again, a multi-stage counter-current process will achieve a high degree of reaction.

So, exploitation of the competing equilibria for reaction and distribution between the two phases enables the isomers to be separated without continuous consumption of chemicals.

A reaction in the aqueous phase of the type described, involving a weak organic base and a weakly acidic salt, will not necessarily approach completion. For example, the equilibrium constant K_E , for the reaction between picoline and dihydrogen phosphate ion is given by the relation below, neglecting activity coefficients and with terms in square brackets denoting concentrations:

$$K_E = \frac{[C_6H_7NH^+][HPO_4^{2-}]}{[C_6H_7N][H_2PO_4^-]}$$

Now, the dissociation constant for picoline, K_B , is given by:

$$K_B = \frac{[C_6H_7NH^+][OH^-]}{[C_6H_7N]} = \begin{matrix} 4.59 \times 10^{-9} & \text{for 3- picoline and} \\ 10.62 \times 10^{-9} & \text{for 4- picoline} \end{matrix}$$

The second dissociation constant for phosphoric acid, K_{A2} , is given by:

$$K_{A2} = \frac{[H^+][HPO_4^{2-}]}{[H_2PO_4^-]} = 6.23 \times 10^{-8}$$

and the dissociation constant of water, K_W , by:

$$K_W = [H^+][OH^-] = 10^{-14}$$

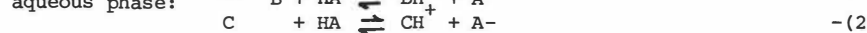
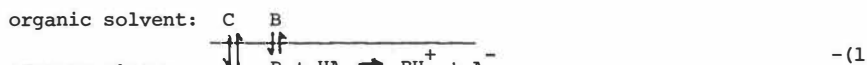
$$\text{From this, } K_E = \frac{K_B K_{A2}}{K_W}$$

Therefore, for 3- picoline, $K_E = 2.9 \times 10^{-2}$ and for 4- picoline $K_E = 6.6 \times 10^{-2}$, and the reaction in the aqueous phase will clearly be only a partial one .

Picoline is too weak a base to generate a high concentration of PO_4^{3-} ions; the equilibrium constant for the reaction $\text{C}_6\text{H}_7\text{N} + \text{HP O}_4^{2-} \rightleftharpoons \text{C}_6\text{H}_7\text{NH}^+ + \text{PO}_4^{3-}$ involves the third ionisation constant of phosphoric acid ($K_{3A} = 5.0 \times 10^{-13}$) and is of the order 5×10^{-7} . Therefore, the presence of PO_4^{3-} ions in the aqueous phase may be neglected.

3(i) General Theory of Dissociation Extraction with Incomplete Reaction in the Aqueous Phase

Previoustheories of dissociation extraction have assumed complete reaction in the aqueous phase between the organic acids or bases to be separated and the extraction reagent. For the general case of incomplete reaction between two organic bases to be separated, B and C, and weakly acidic reagent, HA, which is insoluble in the organic solvent phase, the following equilibria are established:



Assume C is the stronger base: the sum of the reactions in the aqueous phase will then be the exchange reaction:



The dissociation constants of the organic bases, neglecting activity coefficients, are defined:

$$K_B = [\text{BH}^+][\text{OH}^-]/[\text{B}] \quad (4)$$

$$K_C = [\text{CH}^+][\text{OH}^-]/[\text{C}] \quad (5)$$

The distribution coefficients of the undissociated bases are:

$$D_B = [\text{B}]_o/[\text{B}]_a \quad (6)$$

$$\text{and } D_C = [\text{C}]_o/[\text{C}]_a \quad (7)$$

where subscripts $_o$ and $_a$ denote organic solvent and aqueous phases respectively.

Overall distribution coefficients are defined as:

$$S_B = [\text{B}]_o/([\text{B}]_a + [\text{BH}^+]) \quad (8)$$

$$\text{and } S_C = [\text{C}]_o/([\text{C}]_a + [\text{CH}^+]) \quad (9)$$

and the dissociation constant of the acidic reagent:

$$K_A = [\text{H}^+][\text{A}^-]/[\text{HA}] \quad (10)$$

The equilibrium constant for reaction (1), K_1 , is given by:

$$K_1 = K_B K_A / K_W \quad (11)$$

$$\text{Similarly, } K_2 = K_C K_A / K_W \quad (12)$$

$$\text{Also, } K_3 = K_C/K_B \quad -(13)$$

showing that the equilibrium of the key exchange reaction is related to the relative strengths of the two bases.

If the above relations cover all the chemical equilibria which contribute significantly to the overall state of the system, the following two equations are derived from stoichiometry on the assumption that reactions (1) and (2) do not proceed to the state of complete consumption of the acidic reagent, HA, for which the original or feed concentration is N moles per litre.

$$\text{As one mole of } BH^+ \text{ or } CH^+ \text{ is formed for every one of HA which reacts: } [HA]_{\text{original}} = N = [HA]_{\text{eq}} + [BH^+] + [CH^+] \quad -(14)$$

where $[HA]_{\text{eq}}$ is the concentration of reagent in the aqueous phase at equilibrium which is left unreacted.

$$\text{Also, } [A^-] = [BH^+] + [CH^+] \quad -(15)$$

The separation factor for the organic bases is $\alpha_{B,C}$

$$\text{where } \alpha_{B,C} = S_B/S_C \quad -(16)$$

We require an expression for $\alpha_{B,C}$ in terms of known physical constants and measurable or controllable concentration terms. This may be derived as follows:

From equations (16), (8) and (9):

$$\alpha_{B,C} = S_B/S_C = \frac{[B]_O ([C]_a + [CH^+])}{[C]_O ([B]_a + [BH^+])} \quad -(17)$$

From equations (6), (11), (14) & (15):

$$\frac{K_B K_A}{K_W} = K_1 = \frac{[BH^+][A^-]}{[B]_a[HA]} = \frac{([BH^+] + [CH^+])[BH^+]}{([B]_O/D_B)(N - ([BH^+] + [CH^+]))} \quad -(18)$$

and, similarly, from (7), (12), (14) & (15):

$$\frac{K_C K_A}{K_W} = \frac{([BH^+] + [CH^+])[CH^+]}{([C]_O/D_C)(N - ([BH^+] + [CH^+]))} \quad -(19)$$

In equations (18) and (19), K_A , K_B , K_C and K_W are known physical constants; N, $[B]_O$ and $[C]_O$ are system variables which may be assigned any convenient value. Therefore, if D is known at the actual values of the system concentration variables, we have two equations, (18) and (19), containing only two unknowns: $[BH^+]$ and $[CH^+]$. The equations may be solved simultaneously, therefore, to yield the unknowns. However, as the equations are not linear, simple analytical solutions are not possible and

a computer programme is the most convenient method of obtaining the real and positive solution values of $[BH^+]$ and $[CH^+]$.

When $[BH^+]$ and $[CH^+]$ are found, $[HA]_{eq}$ and $[A^-]$ may be derived from relations (14) and (15) and $[B]_a$ and $[C]_a$ from equations (6) and (7). All the terms in equation (17) are now known and the required value of $\alpha_{B,C}$ may be calculated. If wanted, the values of the overall distribution coefficients may be calculated from equations (8) and (9).

A similar treatment may be used to derive the analogous relations covering the separation of organic acids by a weakly basic reagent.

The theory was tested experimentally by a study of the distribution of 3- and 4- picoline between benzene and an aqueous solution of sodium dihydrogen phosphate. Karr and Scheibel also suggested the use of this reagent for separation of the picolines, but based their theoretical treatment upon the pH of the aqueous phase, which has been shown⁽⁵⁾ to be an inconvenient concept. The distribution was measured of the separate picoline isomers and also of an equimolar mixture of the two picoline isomers between 2 molar sodium-dihydrogen phosphate solution and benzene. Experimental values of the overall distribution coefficients for the separate picoline isomers and of separation factors for the mixed picolines were compared with the corresponding values calculated on the basis of the theory presented here.

3(ii) Experimental

Varying known amounts of the separate 3- and 4- picoline isomers were distributed between 100 ml benzene and 100 ml of a 2-molar aqueous solution of sodium dihydrogen phosphate, NaH_2PO_4 . As before, equilibrium was established in stoppered bottles contained in a thermostat at 25°C with frequent shaking. The phases were then analysed by GLC as before for picoline content and the overall distribution coefficient calculated.

Similarly, varying known amounts of an equimolar mixture of 3- and 4- picoline were distributed between 100 ml of benzene and 100 ml of 2M aqueous solution of sodium dihydrogen phosphate at 25°C. The phases were analysed by GLC and the separation factor calculated. Again, the concentration percentage of each organic base was determined with a maximum error of $\pm 0.5\%$ in reproducibility.

3(iii) Results

Table 4 lists experimentally measured and computed values for the overall distribution coefficients of the separate 3- and 4- picoline isomers. In the calculated values, the distribution coefficients of the undissociated picolines are taken as 14 for 3- picoline and 10 for 4- picoline, these being the literature values⁽³⁾ for the distribution coefficients between benzene and water.

TABLE 4

Distribution of the separate picoline isomers between
100 ml benzene and 100 ml 2M NaH_2PO_4 solution at 25°C

<u>Total 3- picoline added (ml)</u>	<u>Equilibrium ml of picoline in the conjugate phases</u>		<u>Overall Distribution Coefficients</u>	
	<u>Organic</u>	<u>Aqueous</u>	<u>Experimental</u>	<u>Computed</u>
4.0	2.03	1.97	1.03	1.03
10.0	6.6	3.4	1.96	1.97
18.0	13.3	4.7	2.83	2.82
31.0	24.8	6.2	4.00	3.98
58.0	49.0	9.0	5.44	5.53

<u>Total 4- picoline added (ml)</u>	<u>Equilibrium ml of picoline in the conjugate phases</u>		<u>Overall Distribution Coefficients</u>	
	<u>Organic</u>	<u>Aqueous</u>	<u>Experimental</u>	<u>Computed</u>
2.8	0.8	2.0	0.40	0.53
5.5	2.3	3.2	0.71	0.71
9.0	4.8	4.2	1.14	1.40
15.0	9.4	5.6	1.67	1.72
26.0	18.5	7.5	2.48	2.52

In Table 5 are shown experimentally measured and computed values for the separation factors of an equimolar mixture of 3- and 4- picoline between benzene and 2M NaH_2PO_4 solution at 25°C.

TABLE 5

Distribution of an equimolar mixture of 3- and 4- picolines
between 100 ml benzene and 100 ml 2M NaH_2PO_4 solution at 25°C

<u>Total picoline mixture added (ml)</u>	<u>Equilibrium concentration of bases in the conjugate phases</u>				<u>Separation Factor</u>	
	<u>Organic Solvent Phase</u>		<u>Aqueous Phase</u>		<u>Experi- mental</u>	<u>Computed</u>
	<u>(molar %)</u>		<u>(molar %)</u>			
	<u>3- picoline</u>	<u>4- picoline</u>	<u>3- picoline</u>	<u>4- picoline</u>		
7.0	60.5	39.5	37.5	62.5	2.55	2.56
12.0	58.3	41.7	35.7	64.3	2.52	2.54
18.0	56.2	43.8	34.6	65.4	2.42	2.45
36.0	54.5	45.5	34.6	65.4	2.26	2.25

3(iv) Discussion

Both for the overall distribution coefficients of the individual isomers and for the separation factors, there is very good agreement between the experimental and computed results, even though the distribution coefficients of the undissociated isomers used were only approximate. The separation factor of 2.3 - 2.6 is adequate and should enable a high degree of separation to be obtained in a reasonable number of stages. The aqueous phase containing the separated 4- picoline salt may be contacted with chloroform, which has a higher affinity for picolines than benzene, to recover the undissociated organic base and regenerate the H_2PO_4^- ions.

4. Overall Process

The methods suggested for the extraction of 2-6 lutidine and the separation of the picolines may be combined in a process for the complete separation of the 3- component feed mixture. The flow diagram of the proposed process is shown in Figure 1.

The feed enters the first liquid-liquid contactor, in which there is a counter-current flow of mixed organic solvent (95% V/V n-hexane, 5% chloroform) and aqueous KCNS solution. The 2-6 lutidine is taken off in the organic phase and may be separated by distillation after a reflux stream has been returned to the contactor by a reduction in temperature of the organic phase. From the first contactor, the aqueous KCNS stream containing the picolines is heated so that the picolines needed for reflux pass into a counter-current stream of the mixed organic solvent and the aqueous KCNS solution may be recycled. The remainder of the picolines may be recovered in a solvent such as benzene, which is suitable for the dissociation extraction stage. The heart of this is a multi-stage contactor with counter-current streams of organic solvent and an aqueous solution of sodium dihydrogen phosphate. The dissociation extraction equilibrium established in the contactor leads to the enrichment of 3- picoline in the organic solvent stream, from which it may be recovered by distillation. Part is returned as reflux, the remainder being the 3- picoline product. The aqueous stream from the contactor containing the 4- picoline salt passes counter-currently to a chloroform stream in another multi-stage contactor. The dissociation extraction reaction is reversed and 4- picoline passes into the chloroform phase, from which it is recovered in turn by distillation and part returned as reflux. The reformed sodium dihydrogen phosphate solution is recycled.

No attempt has been made to optimise the design of the suggested process, choice of solvents or reagents. There is almost certainly room for improvement in the latter. For example, while KCNS increases the separation factor for 2-6 lutidine, other compounds might have a greater impact. Similarly, it can be seen from the results that the extent of reaction between the picoline isomers and sodium dihydrogen phosphate is modest. Thus the competition, which is the basis of separations by dissociation extraction, is limited. It would be desirable to find another reagent which would react more strongly whilst still permitting reversal of the reaction by physical means. Nevertheless, the theory and results presented do establish the basic feasibility of achieving the separation by liquid-liquid extraction. It is hoped to present a more detailed process design in a later publication.

REFERENCES

1. Coulson, A.E. and Jones, J.I., J.Soc.Chem.Ind., 1946, 65, 169.
2. Glowacki, W.L. and Winans, C.F., U.S. Patent 2,402,158, 1946.
3. Karr, A.E. and Scheibel, E.G., Ind.Eng.Chem., 1954, 46, 1583.
4. Golumbic, C. and Orchin, M.J., J.Amer.Chem.Soc., 1950, 72, 4145.
5. Anwar, M.M., Hanson, C. and Pratt, M.W.T., Trans.Inst.Chem.Engrs., 1971, 49, 95.
6. Anwar, M.M., Hanson, C., Patel, A.N. and Pratt, M.W.T., Trans.Inst. Chem.Engrs., 1973, 51, 151.
7. Anwar, M.M., Hanson, C. and Pratt, M.W.T., Proceedings of International Solvent Extraction Conference, The Hague, 1971, paper 95 (Academic Press, London).

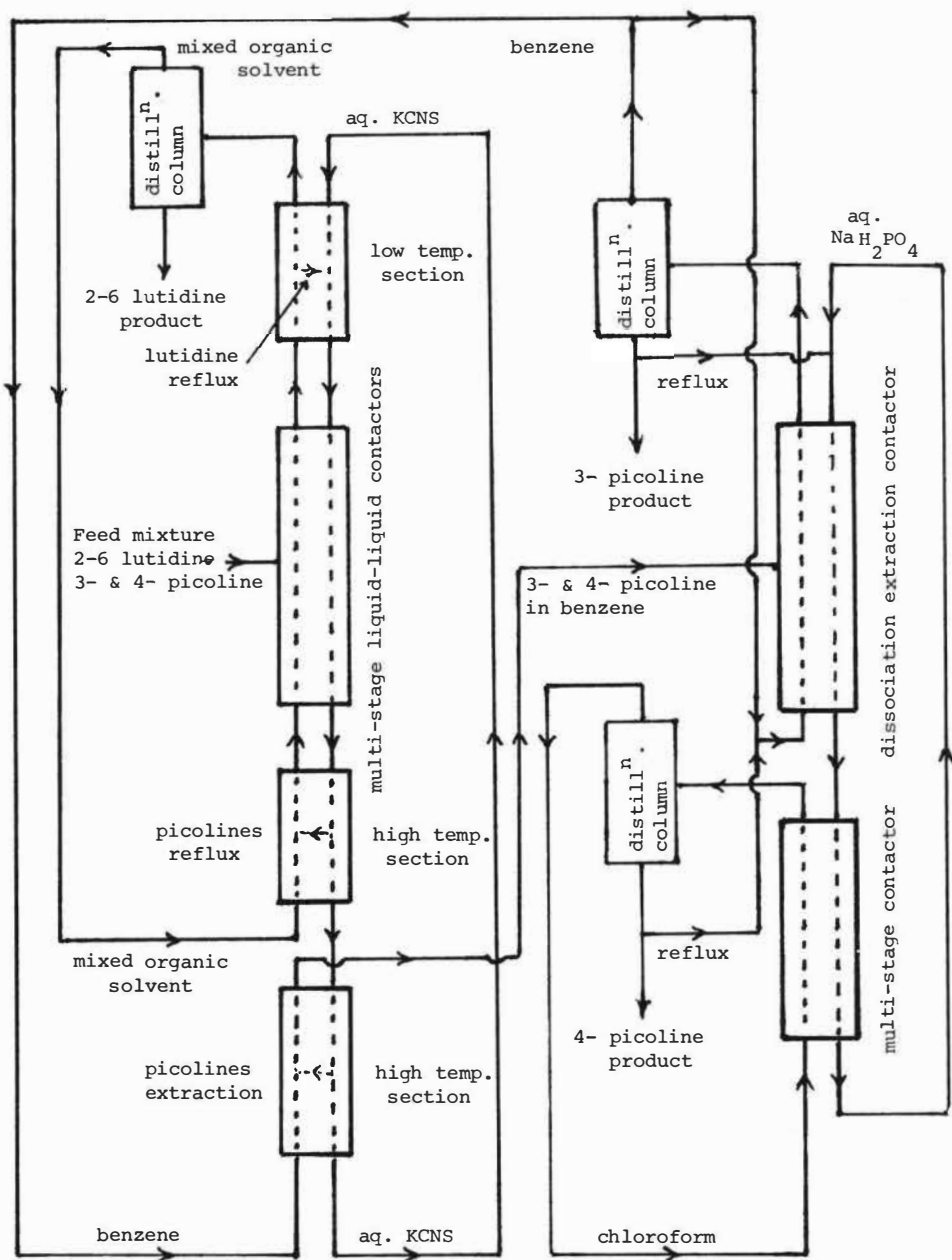


FIG. 1 Flow diagram for the Separation of Mixtures of
2-6 Lutidine, 3- and 4- Picoline

DENSE BED IN A SPRAY COLUMN AN APPLICATION TO THE
EXTRACTION OF PHENOL FROM WASTE WATER

by

J.M. CROIX, C. LABROCHE, C. LACKME, A. MERLE

SUMMARY

First is explained the hydrodynamica of the extractor where a dispersed phase and a continuous phase flow counter-currently in such a way that a dense packing is obtained. Then the principle of the design of the extractor is reported and finally the practical case of phenol extraction from waste water using di-iso-propyl-ether as solvent is dealt with.

INTRODUCTION

It is well known that a spray column can be used as an extractor (1) but the rather low surface of contact between the two phases and above all the rapidly prohibitive back mixing when the diameter of the column increases make more sophisticated extractors preferable.

However, if the spray column is so operated that the dense packing can appear, it becomes again competitive in front of much more complicated and expensive devices like pulses columns, packed beds,...

2. HYDRODYNAMICS OF A SPRAY COLUMN IN COUNTERCURRENT FLOW

If Q_C and Q_D are respectively the flowrates of the continuous and dispersed phases, α the volumetric concentration of the dispersed phase, it can be shown (2) that two regimes are possible. One is characterized by a low hold up α_L which is classically obtained, the other shows a very high value α_D , this last regime is the dense bed.

These two regimes can coexist in the column, if it is the case, they are separated by a very sharp line (Fig.1).

The two values α_L and α_D are the roots lying in the interval 0 - 1 of the equation

$$\frac{Q_D}{S\alpha} + \frac{Q_C}{S(1-\alpha)} = \frac{U_0}{1-\alpha} \quad (1)$$

Where S is the area of the section of the column and U_0 is the velocity of a swarm of drops of the dispersed phase climbing up in the quiescent continuous phase. U_0 is a function of α and of the physical properties of the phases. For practical cases, the phases are such mixtures that $U_0(\alpha)$ is generally an experimental function. Fig.2 for example shows how U_0 varies with α for drops of a kerosene-heptane mixture climbing in tap water.

As U_0 is already a graphical function, it is interesting to solve graphically equation (1). Fig.3 gives the principle of this resolution. On this figure, U_0 is plotted versus using the results of fig. 2.

A straight line joining the points H and E of respective coordinates $(0, \frac{Q_D}{S})$, and $(1, \frac{Q_C}{S})$ intersects the curve $U_0\alpha = f(\alpha)$ in two points G and F, the abscissae of which are α_1 and α_2 , solutions of equation (1).

As a matter of fact, we have

$$\frac{GB'}{HB'} = \frac{EE'}{GE'} \quad (2)$$

and in the same way

$$\frac{FF'}{HF'} = \frac{EE'}{FE'} \quad (3)$$

And therefore

$$\frac{U_0 \alpha_1 - Q_{D/S}}{\alpha_1} = \frac{Q_{C/S} - U_0 \alpha_1}{1 - \alpha_1}$$

or

$$\frac{U_0 \alpha_2 - Q_{d/S}}{\alpha_2} = \frac{Q_{C/S} - U_0 \alpha_2}{1 - \alpha_2}$$

Such that, after rewriting

$$\frac{Q_D}{S \alpha_1} + \frac{Q_C}{S(1 - \alpha_1)} = \frac{U_0}{1 - \alpha_1} \quad (4)$$

showing that α_1 and α_2 are effectively roots of equation (1)

Fig. 4 is a curve obtained from the data of Fig. 2 which will be used to illustrate the technique for predicting the hydrodynamics of the column. The points in a circle are those corresponding to the beginning of instability.

Two types of diagram may be drawn. One shows (Fig.5) the variation of α with the superficial velocity of the continuous phase, the other superficial velocity being a parameter. For purpose of comparison, experimental values of α obtained by the quick closing valves technique are indicated.

From visual inspection, it appears that the curve of fig.4 should have been drawn slightly on the left, this corresponding to an interpolated curve of Fig.2 pushed upwards relative to the experimental points.

The most interesting use of the data of Fig.2 is that of Fig.6 where the inputs of the extractor are the coordinates. In that diagram, the iso α are straight lines of slope

$$- \frac{\alpha}{1 - \alpha}$$

The order of magnitude of these slopes clearly distinguishes the dense bed from the classical light bed.

The boundary of the flooding zone where no countercurrent flow can exist corresponds to the case when HE on Fig.3 is tangent to the curve $U_0 \alpha = f(\alpha)$.

Practically the position of the flooding zone is very sensitive to the presence of impurities in the phases.

It is recommended to limit the choice of the couple $(\frac{Q_G}{S}, \frac{Q_D}{S})$ to the centre of the zone of existence of Fig.6, let us say between the lines $\alpha = 0.6$ and $\alpha = 0.7$.

To evaluate the transfer coefficient between phases, we shall need the relative velocity V_R . In the case of countercurrent flow, we have

$$V_R = \frac{Q_D/S}{\alpha} + \frac{Q_G/S}{1 - \alpha} \quad (5)$$

and from equation (1), simply

$$V_R = \frac{U_0}{1 - \alpha}$$

3. OPERATION OF A DENSE BED COLUMN

In a spray column what takes place spontaneously is a light dispersion, bubbles or drops of the front escaping from the swarm. To obtain a dense bed, it is necessary to decelerate the drops downflow so that the others are obliged to pile up behind them.

Suppose the continuous phase is the denser phase, it flows downward in the column and the dispersed phase upward.

When the column is full of light dispersion, we increase the outflow Q_{CS} of the continuous phase without changing the inflow Q_{CE} , then the interface between continuous and coalesced dispersed phase in the separator is obliged to go down. When this interface reaches the top of the column in the separator, it stops there, thus in a slice of column at this point we have $Q_{CE} < Q_{CS}$ and to ensure continuity the drops of the dispersed phase pile up leading to a congestion which propagates downward as long as $Q_{CS} > Q_{CE}$. The interface between dense bed and light bed is generally stopped about twenty centimeters above the dispersed phase injector.

4. DESIGN OF A DENSE BED EXTRACTOR

Let Q_C be the flowrate of feed to be introduced in the extractor as continuous phase, we have to determine

- the area of the section of the extractor
- the solvent flowrate
- the height of the extractor

A figure such as Fig.6 tells us that Q_C/S must be approximately 1 cm/s. It is thus easy to evaluate S . Now if we choose the line $\alpha = 0.6$ after stability consideration, the solvent flowrate is immediately known.

Then, with the specific area of contact between phases given by $a = \frac{6}{d}$, where d is the mean diameter of the drops, determined by the injector conditions (Scheele and Meister correlation for example) with, moreover, the relative velocity of Eq. 6 the use of known correlations of mass transfer enables us to compute the number of transfer units necessary to realize the wanted extraction and the height of a transfer unit. Thus the height of the extractor may be calculated.

The problem we are faced with now is to know if such a section of extractor and such a height of extractor have proper values for the formation of a dense bed. It is a double problem of extrapolation that we have studied in our laboratory for a few years.

4.1 Extrapolation in diameter

It is very easy to build a dense bed in a small column up to 75 mm in diameter. For columns of 150 mm and above, the distribution of the continuous phase at the top of the column is a very sharp problem.

The feeding of the column without special care, for example by simple overflow in a separator of the Elgin type leads to violent eddies which make the dispersed phase to coalesce and destroy the dense bed. But good design have been performed which give very stable dense beds.

Fig.7 shows as a function of the continuous phase superficial velocity the variation of the height of a theoretical plate for heat transfer in countercurrent flow, the parameter is the diameter of the column.

The efficiency of a light bed in exactly the same conditions is also plotted on this diagram. The indicated HTS's are overall values, that is to say including back mixing effect which may eventually be present.

4.2. Extrapolation in height

The laboratory columns are about two or three meters high. Depending on the difficulty of the extraction, heights of the order of ten meters may be required. The, on one hand, we must be sure that the rate of coalescence on the total height is small enough to prevent the collapse down of the dense bed. On the other hand, if the dispersed phase hold up varies all along the column, we need its variation in order to bring the desired corrections to the design computations.

Fig. 8 shows a typical result of experiments done in different conditions (3). It can be seen that over nearly nine meters there are no significant change in hold up.

5. APPLICATION OF THE DENSE BED TECHNIQUE TO THE EXTRACTION OF PHENOL FROM WASTE WATER (4)

5.1. Nature of the feed

The interval of variation of the phenol concentration in the industrial waste water was 0.5 g/l to 7.6 g/l. Some greasy solids appeared at the surface and it was necessary to design a special settler to eliminate the biggest pieces before introducing the feed at the top of the column. Even after this operation, a packed bed column would have been destroyed in a very short time. To prevent early appearance of coalescence, we are obliged to raise the pH of the feed.

5.2. Choice of the solvent

The diisopropyl ether was chosen in consideration of the great distribution coefficient that is obtained for a wide range of phenol concentration. Moreover its value is nearly a constant equal to 20. The difference in density with water is also an advantage when a spray column is to be used.

5.3. Reliability of the extractor

For a dense bed of 1 meter, a feed flowrate of 40 l/h (i.e. 1,38 cm/s) and a solvent flowrate of 20 l/h (0,69 cm/s), Fig.9 shows the performance of the extractor.

5.4. Comparison of the computed HTU with observed one

The HTU's have been computed following the method briefly indicated in § 4 and the observed one are simply the height of the extractor divided by measured number of transfer units. Fig.10 shows the comparison. The computed value is generally higher than the observed one because we suppose in a pessimistic way that the drops are always rigid and we use thus the known correlation to calculate the inside mass transfer coefficient.

6. CONCLUSION

A spray column operated in the dense bed condition seems to be^a convenient device for various extractions.

The advantages are very low investment cost and rather easy design. However the phases in presence must give reasonably stable emulsions to prevent coalescence and collapse of the dense bed it is sometimes necessary to use some additives to modify the interfacial properties of the system. The preliminary experiments, for example to plot $U_0(\alpha)$, give immediate information on this point.

REFERENCES

=====

- [1] R.E. TREYBAL
Liquid extraction
Mac Graw Hill, 1973

- [2] C. LACKME¹
Two regimes of a spray columns in countercurrent flow
Presented at the 14th AIChE-ASME National Heat Transfer Conference,
ATLANTA, Georgia, August 5-8, 1973, A.I.Ch.E preprint n° 7

- [3] A. DIGONNET, J.M. SELLA
Internal publication (C.E.A., C.E.N.G.)

- [4] J. CROIX, C. LABROCHE, C. LACKME, A. MERLE
Extraction en colonne à lit dense (et illustration par un cas
concret : les eaux résiduaires phénolées)
Communication au Salon Professionnel des Techniques Anti-Pollution,
Grenoble, 2-6 Octobre 1973

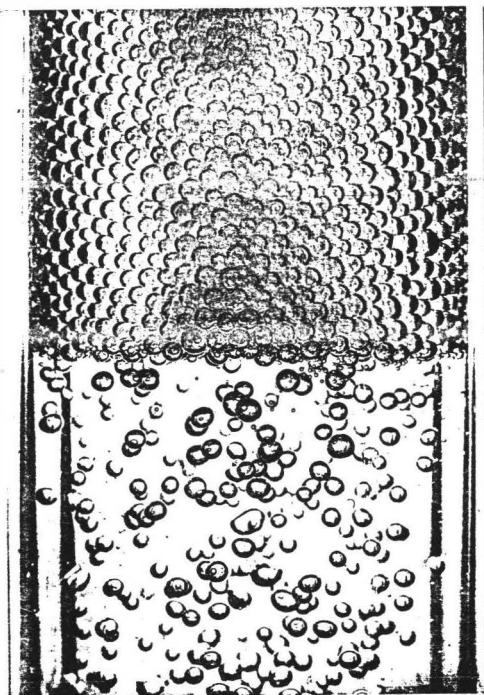


FIG 1 : Interface dense bed -light bed

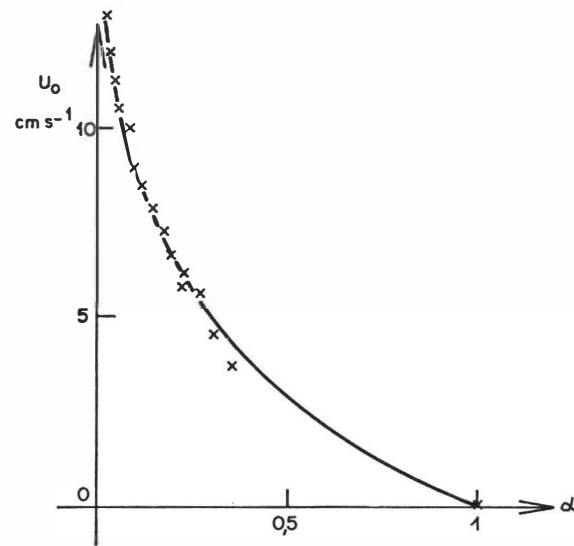


FIG2 Velocity of a swarm of Kerozene-Heptane drops in quiescent water

Fig 3_ Graphical solution of Eq - (1)

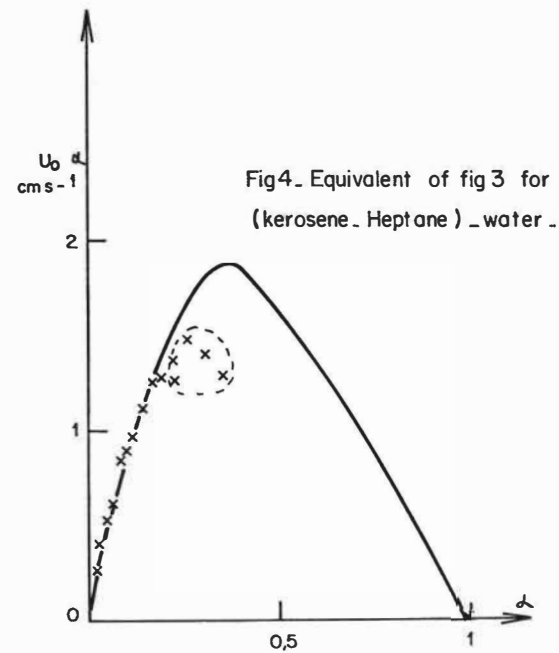
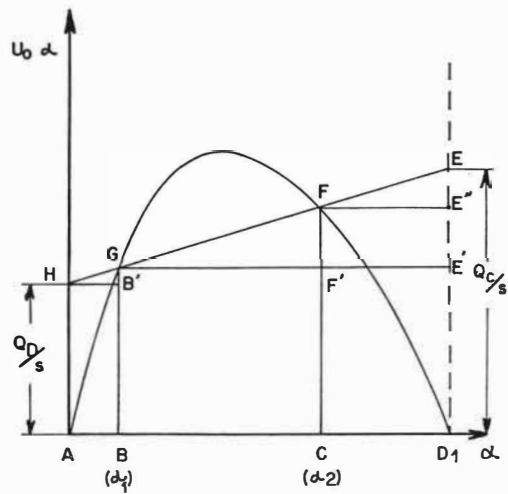


Fig 5 Estimated and experimental volumetric concentration α as a function of the flowrates

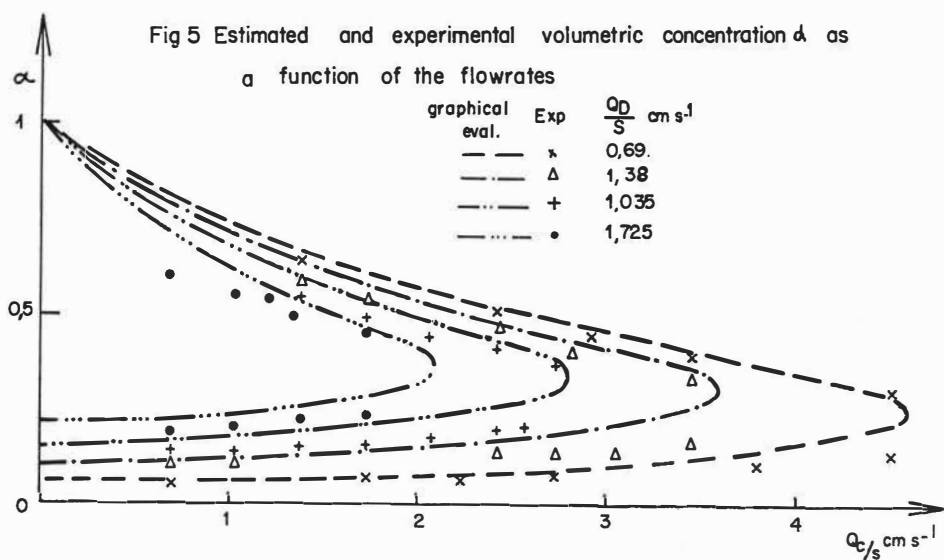


Fig:6 Working curve for designing an extractor

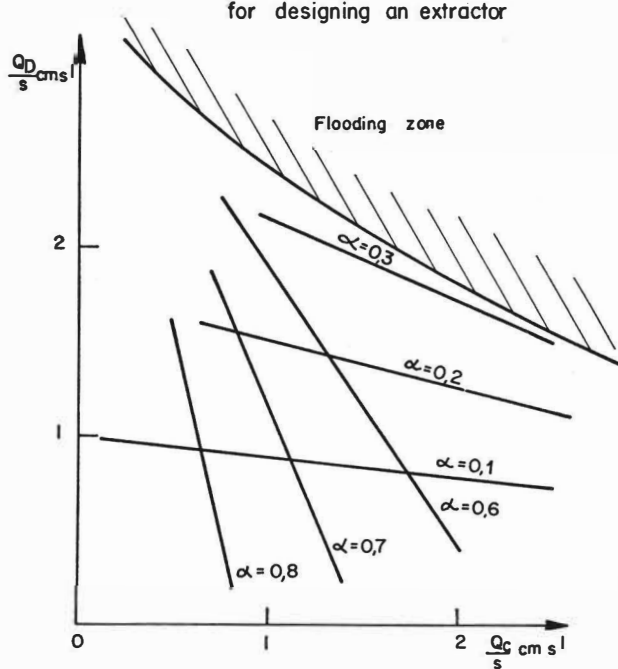


Fig 7_Variation of efficiency with the column diameter

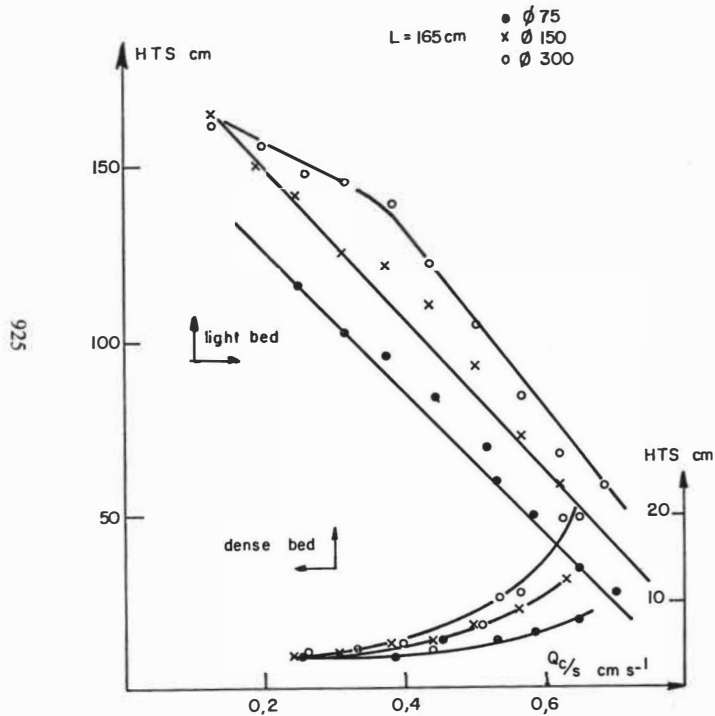


Fig 8. Variation of α with height (I.D.=32mm)

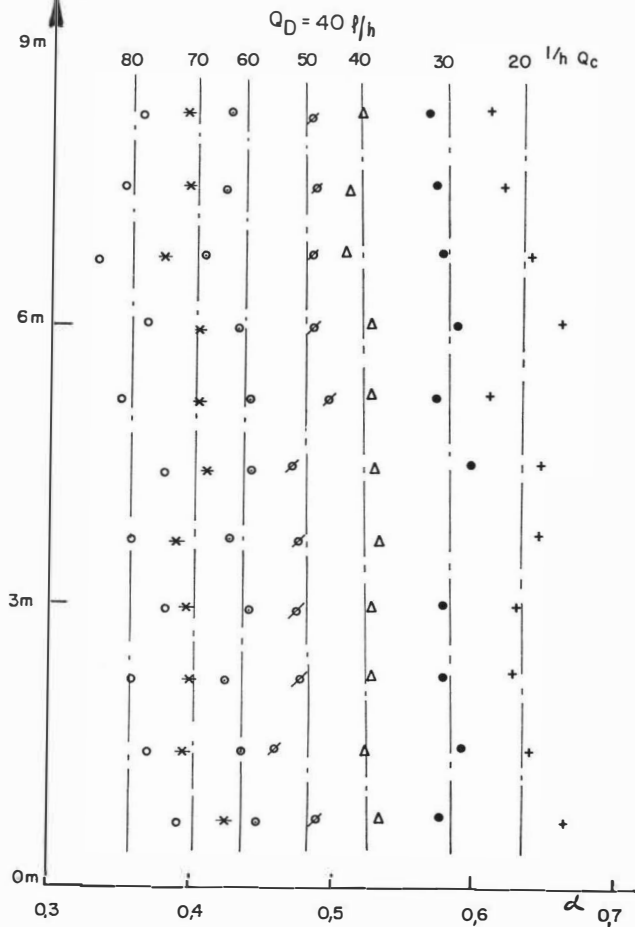


Fig 9 - Operations for hours of a dense bed extractor
for two inlet concentrations.

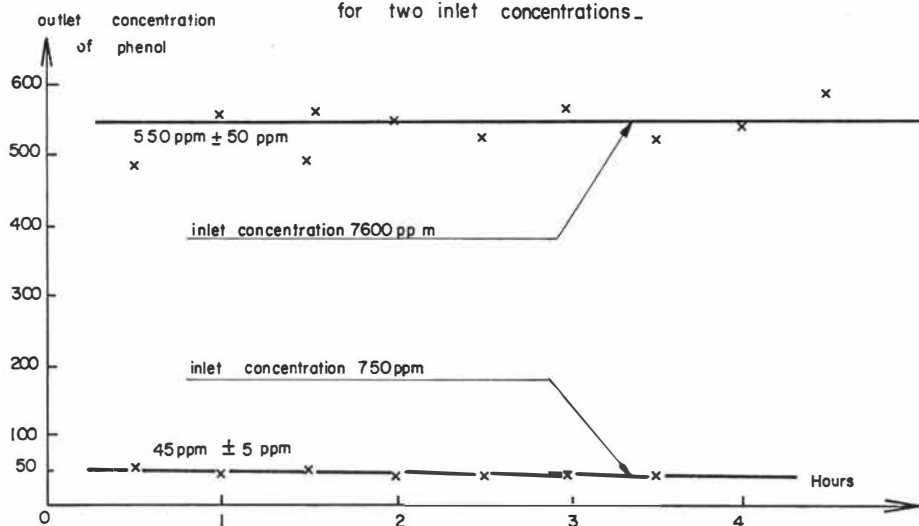
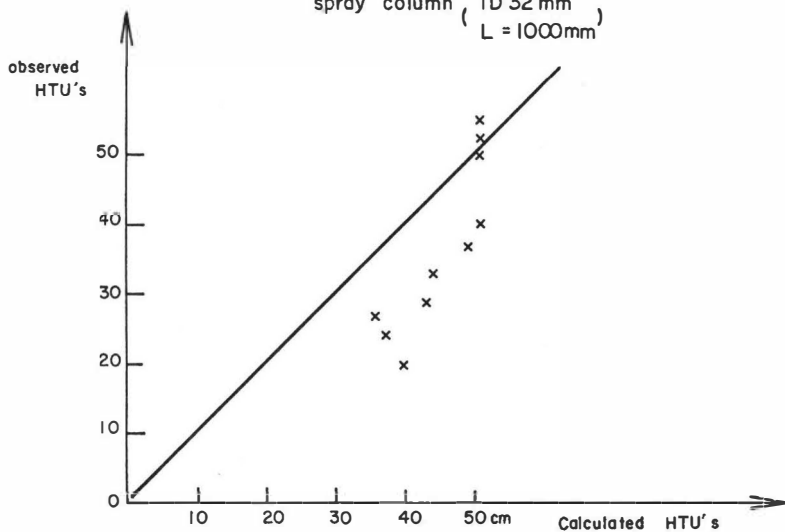


Fig 10 Comparison of estimated and observed HTU for a dense bed
spray column (ID 32 mm
L = 1000mm)



ABSTRACT

The distribution of proteins in aqueous biphasic systems containing dextran and poly(ethylene glycol) has been studied. The distribution is somewhat pH-dependent when different salts are included in the system. Depending on the salt used the distribution coefficient increases or decreases with increasing pH, or may even become pH-independent. By using poly(ethylene glycol) with covalently bound ionized groups, the pH-dependence is much enhanced. In all cases a linear relationship is found between the logarithm of the distribution coefficient of the protein and its net charge. The separatory capacity of the systems has been investigated by partition of a mixture of two proteins which can be assayed separately.

An extract from swine heart was distributed in this type of system at various pH's. The distribution of the enzymes present was strongly pH-dependent, while the distribution of protein varied somewhat. It is shown that the enzymes can be separated by using counter-current distribution. In some cases multiple forms of enzymes have been detected by this technique.

From Dept. of Biochemistry, Umeå University, S-901 87 Umeå, Sweden.

INTRODUCTION

The main methods used for separation of proteins are fractional precipitation, chromatography, electrophoresis and isoelectric focusing. Liquid-liquid extraction of proteins, on the other hand, has found only limited use due to the lack of suitable biphasic systems. In order for a biphasic system to be suitable, proteins must be highly soluble in both phases and should not be denatured. Both requirements are fulfilled by the aqueous biphasic systems formulated by Albertsson¹. They are obtained by mixing aqueous solutions of two polymers, usually poly(ethylene glycol) and dextran. These biphasic systems have been used for separation of cells, viruses, cell organelles and nucleic acids. This is possible since distribution is strongly dependent on pH and the presence of salts, and can therefore be adjusted within wide limits. The distribution of proteins, however, is usually less extreme, which makes purification by liquid-liquid extraction inexpedient. In spite of this, the aqueous systems have in some cases been used for protein purification^{2,3,4}. If a small amount of charged groups is attached to the poly(ethylene glycol), 1-2 groups per molecule, the distribution of proteins becomes strongly pH-dependent⁵. In some cases the distribution coefficient can be varied over several powers of ten.

The aim of this work has been to study the separatory capacity of the aqueous biphasic systems and investigate their usefulness for liquid-liquid extraction of proteins. Further, the data obtained have been used to verify a theoretical model published by Albertsson⁶. This model describes the effect of ionic species present in the system on the distribution of charged macromolecules, e. g. proteins.

EXPERIMENTAL

Materials

Extract from swine heart. 70 g of frozen heart from swine was cut into small pieces and ground in the cold with 140 ml of 10 mM potassium phosphate buffer pH 6.8 in a Turmix blender for 2 minutes at highest speed. The mixture was centrifuged at 2°C, 15x12 000g using a Sorvall RC-2B centrifuge with SS 34 rotor. The supernatant was filtered and centrifuged at 3°C 110x73 500g in a Beckman L2-65K centrifuge with a type 30 rotor. The supernatant was directly used in the partition experiments.

Yeast lysate was prepared from fresh Baker's yeast, obtained from Jästbolaget, Sollentuna, Sweden. The yeast was ground with an equal weight of crushed dry ice in a blender with rotating knives (Turmix) for 2 minutes. The homogenate was spread on a plastic plate to allow the dry ice to evaporate. The yeast homogenate was centrifuged at 20x15 000g. The turbid supernatant was then centrifuged at 60x160 000g using a type 65 fixed-angle rotor. The clear supernatant above the brown pellet was recovered with a Pasteur pipette, avoiding contamination from the thin white film at the meniscus. This solution was dialyzed against a phosphate buffer for 2 hours at 10°C. A length of dialysis tubing (Union Carbide) knotted at the lower end and stretched transversely over a frame made of glass tubing was used for dialysis. The frame was rotated by a motor.

CO-hemoglobin was prepared from swine blood. The blood was centrifuged 10x3 000g. The erythrocytes were washed by 4-fold suspension and centrifugation in 0.85 % (w/w) NaCl solution. They were then lysed in 3 times their volume of water. The erythrocyte ghosts were removed by centrifugation, 10x16 000g, and the supernatant was collected and saturated with carbon monoxide. The solution was dialyzed at 3°C against water. Concentration of CO-hemoglobin was determined by dry-weight analysis.

Bovine serum albumin from Sigma Chemical Co., St. Louis, fraction V, was stained with bromophenol blue in water solution 8 mg dye per g protein. No traces of free dye could be detected when the stained protein was chromatographed on Sephadex G-25.

The proteins: hen ovalbumin, grade V; lysozyme from egg white, grade I and ribonuclease-A from bovine pancreas, type I-A were all obtained from Sigma Chemical Co.,

Chemicals used were all of analytical grade. The water was double distilled in quartz.

Dextran T 500, batch No. 5996 ($M_w = 5 \cdot 10^5$) was supplied by Pharmacia, Uppsala, Sweden.

Poly(ethylene glycol), PEG, ($M_n = 6\ 000$) was obtained from Union Carbide, New York, as Carbowax 6 000.

Trimethylamino-poly(ethylene glycol), TMA-PEG, was prepared by the method published earlier⁵.

Carboxymethyl-poly(ethylene glycol), CM-PEG, was prepared from Carbowax 6 000 by oxidation with KMnO_4 . 13 g KMnO_4 dissolved in 200 ml of water was added to a solution of 250 g PEG and 0.8 g NaOH in 600 ml of water. After 15 minutes on a boiling waterbath the precipitate (MnO_2) was removed by suction filtration. The clear filtrate was adjusted to pH 2.6 by adding 1 M HCl. The water was evaporated in vacuum and the remaining polymer was dissolved in 500 ml of toluene. 100 ml toluene + water was distilled out from the solution and undissolved salts were removed by

filtration. The polymer was allowed to precipitate at 3°C overnight and collected on a filter by suction. The CM-PEG was recrystallized at 3°C from 600 ml of absolute ethanol.

Enzymes used as reagents in activity assays were lactate dehydrogenase from rabbit muscle, type I; glyceraldehydephosphate dehydrogenase from rabbit muscle and α -glycerolphosphate dehydrogenase from rabbit muscle. They were all obtained from Sigma Chemical Co., St. Louis.

Methods

Enzymic assays. Activity was measured by standard methods at 25°C, using a Unicam SP-800 B spectrophotometer with tempered 1 cm quartz cuvettes. The enzymes studied were malate dehydrogenase⁷(340 nm), fumarase⁸(240 nm), enolase⁹(240 nm), aspartate-glutamate transaminase¹⁰(280 nm), hexokinase¹¹(560 nm), pyruvate kinase¹²(340 nm), 3-phosphoglycerate kinase¹³(340 nm) and triose phosphate isomerase¹⁴(340 nm). The dependence of the distribution coefficient, D, on pH. 40 g biphasic system was made up in a glass beaker by mixing PEG or/and substituted PEG (40 % aqueous solution), dextran (20 % aqueous solution), buffer, salt solution and protein solution. All concentrations given in per cent are calculated in weight per weight. The system was stirred mechanically and pH was measured simultaneously by using a Radiometer titrigraph (Radiometer, Copenhagen). The system was titrated with either 2 M NaOH or 2 M HCl. After each addition an aliquot of 2.5 ml was taken and centrifuged 10'x 1500g. In this way a series of biphasic systems with the same polymer composition but differing in pH was obtained. 0.500 ml phase was diluted with 2.500 ml water and analyzed for protein and enzymic activity. The distribution coefficient, D, defined as the ratio between the concentration of protein or activity in the upper and lower phase was calculated. Protein concentration was measured in terms of absorbance, using a blank prepared from a system containing no protein. The wavelength was 280 nm except in the case of stained serum albumin (610 nm) and CO-hemoglobin (460 nm). When the two latter were partitioned together the relative concentration ($C_{\text{albumin}}/C_{\text{hemoglobin}}$) of each protein could be determined by the relations;

$$C_{\text{hemoglobin}} = (16.63 A^{460} - A^{610}) / 16.44$$

$$C_{\text{albumin}} = (5.36 A^{610} - A^{460}) / 5.30$$

The dependence of D on concentration of salt.

The salt concentration was varied, at constant pH, by using a 2 M salt solution instead of acid or base in the titration above.

Counter-current distribution with 9 transfers was carried out in one of the glass units of a Craig machine (Gallenkamp), shaking and transferring by hand. 1.75 or 2.00 ml upper and 1.75 ml lower phase were used. The protein mixture was introduced into the system in chamber No. 0. The shaking time was 1 min and the settling time 10 min. At the end of the experiment 4.00 ml water was added to each chamber to obtain one phase, and the enzymic activity and absorbance (using diluted blank system) was measured. The counter-current distribution diagrams were mathematically analyzed as described by Hecker¹⁵. The distribution ratio was calculated from the activity or concentration ratio in two consecutive chambers.

RESULTS

Effect of salts on the partition of serum albumin.

Bovine serum albumin was partitioned in a biphasic system containing 5 % dextran, 4 % PEG and 0.1 mole/kg salt (K_2SO_4 , potassium acetate, KCl, LiCl) at 3°C, Fig. 1. The logarithm of the distribution coefficient, D , of the protein is well proportional to its net-charge, Z . The net charge was obtained from the measured pH values via the titration curve of the albumin¹⁶. The dependence of D on Z varies from one salt to another. D either decreases (K_2SO_4 , LiCl) or increases (potassium acetate, KCl) with increasing Z .

Partition of proteins in systems containing potassium acetate.

The distribution of proteins is only slightly pH-dependent when the above system contains potassium acetate. However, the distribution coefficient differs for the different proteins. The distribution of serum albumin, ribonuclease, ovalbumin and lysozyme as a function of pH is shown in Fig. 2.

Partition of serum albumin and of CO-hemoglobin in systems containing charged PEG. The proteins were partitioned separately in systems containing either negatively charged CM-PEG or positively charged TMA-PEG at different pH's. The extraction curves obtained when log D is plotted versus pH are given in Fig. 3. Curves obtained when the respective protein was partitioned in a system containing no substituted PEG but with 25 mmole/kg NaCl present have been included in Fig. 3 for comparison. The distribution of the proteins was strongly pH-dependent in systems containing charged PEG compared with the distribution affected by NaCl. CM-PEG and TMA-PEG act in opposite ways in determining the partition. With increasing pH the distribution coefficient increases when TMA-PEG is used, while it decreases in systems containing CM-PEG.

By plotting log D versus Z a linear relationship between the two is established. The slopes of these lines are given in Table 1. The slopes at a given composition of the system (polymers, salts) are almost the same for the two proteins. The expected separatory capacity of the biphasic systems for a mixture of the two proteins can be determined from Fig. 3. It is here measured as the logarithm of the separation factor¹⁵, β . Log β is equal to the difference between the two curves in the figure at a given pH. The maximal log β values are 1.8 when CM-PEG was used and 2.3 in the case of TMA-PEG.

Partition of a mixture of serum albumin and CO-hemoglobin.

Bovine serum albumin, stained with bromophenol blue, and CO-hemoglobin were partitioned together in systems containing either CM-PEG or TMA-PEG., Fig. 4. Since the two proteins absorb light in different regions of the visible spectrum, it was possible to determine their respective concentrations by absorbance measurements. The separation factor was less than when the proteins were partitioned singly. The maximal log β values obtained are 0.65 with CM-PEG and 1.7 with TMA-PEG.

The separation factor in systems containing charged PEG is strongly affected by the presence of salts. Fig. 5 shows the variation in log β with the concentration of NaCl or potassium phosphate included in the system at constant pH. The chloride acts more strongly on TMA-PEG than on CM-PEG in diminishing the separatory efficiency of the system. Phosphate, on the other hand, shows stronger negative effect on β in a system containing CM-PEG.

Partition of heart muscle extract. The extract was included in systems containing either CM-PEG or TMA-PEG, Fig. 6. A small amount of precipitate formed a thin film at the interface and was avoided when samples were withdrawn from the phases. For some of the enzymes measured (malate dehydrogenase and enolase) the total amount of activity increased with increasing pH. This indicates that the enzyme was partly precipitated at low pH (start of extraction) and then successively dissolved. When a CM-PEG-containing system was used, the distribution coefficient decreased with increasing pH up to pH 8. At higher pH, D increased again or remained constant. With a TMA-PEG-system, D increased with pH over the whole pH interval studied. The overall distribution of proteins is less pH-dependent than the distribution of enzymatic activity.

Counter-current distribution of enzymes. The extract from swine heart and the lysate of baker's yeast were subjected to counter-current distribution in biphasic systems containing dextran and TMA-PEG. Fig. 7a shows the distribution of some enzymes and of protein (A^{280}) in the row of tubes when the heart muscle extract was used. Enolase activity behaved as a single component with $D=0.17$, fumarase appeared to be heterogeneous with 90 % of one component with $D=1.2$ and 10 % of another component with $D=5.7$. Malate dehydrogenase consisted of two components: one with $D=0.33$ (67 %) and the other with $D=2.3$ (33 %). Aspartate-glutarate transaminase also consisted of at least two forms. 53 % moved as a homogeneous substance with $D=2.2$ while the remaining 47 % of material moved with D varying from 0.1 to 0.4. The distribution of material absorbing at 280 nm was completely heterogeneous. The calculated distribution coefficients varied from about 0.15 to 6.5.

The glycolytic enzymes in yeast lysate were also partly separated by counter-current distribution. Hexokinase behaved as a single component in the system used and had $D=4.0$. Pyruvate kinase showed a tendency to separate into two components, 18 % with $D=1.2$ and 72 % with $D=2.7$. Triose phosphate isomerase and 3-phosphoglycerate kinase were both relatively well separated into two fractions. The former consisted of 67 % with $D=1.1$ (or less) and 33 % with $D=3.9$. The latter consisted of 66 % with $D=0.4$ and 34 % with $D=4.9$.

DISCUSSION

The linear relationship between the logarithm of the partition coefficient for a protein and its net charge is in agreement with the theoretical model proposed by Albertsson⁶. This model postulates the presence of an interfacial potential, ψ , which steers the partition of the protein. The potential across the interface is a result of different affinity of negative and positive ions for the two phases. If ionic species, e.g. salts, are present in excess compared with the protein, the interfacial potential is determined by the former. The partition coefficient, K_p , of the protein is related to the potential via;

$$\ln K_p = \ln K_p^0 + \psi ZF / RT$$

where K_p^0 is the partition coefficient of the protein when partitioned in a system in which the interfacial potential is zero. F is the Faraday constant,

R the gas constant, Z the protein net charge and T the absolute temperature. From the experimental data given in Fig. 1, the interfacial potential has been calculated and found to be -0.17 mV for LiCl, -0.22 mV for K_2SO_4 , +0.13 mV for potassium acetate and +0.64 mV for KCl.

Since the ions of these salts differ only slightly in their affinity for the two phases, which can be seen from the partition of the salts¹⁸, the interfacial potential is low. By choosing a suitable salt, the potential can be practically eliminated and the partition coefficient therefore will be pH-independent and equal to K_p^0 in the formula above. Under such conditions the partition of a protein is determined only by the solvation capacity of the two phases for the protein. Under these circumstances proteins may be separated according to their relative solubility in the phases, which is related to the hydrophobicity of the proteins. Since the upper, PEG-rich, phase is more hydrophobic than the lower, dextran-rich, phase¹⁹, K_p^0 would increase with increasing hydrophobic character of the protein.

On the other hand, when the system contains charged poly(ethylene glycol) the bound charged group will be predominantly in the upper phase, while the counter ion has approximately the same affinity for the two phases. This gives rise to a high potential between the phases. Since CM-PEG is negatively charged and TMA-PEG is positively charged but contains approximately the same number of charges, they will give rise to potentials of the same order but working in opposite direction. From the slopes of the straight lines, log D versus Z, the potentials have been calculated, Table 1. They are almost the same for a given system for both proteins which supports the model above.

The separation effect, β , can by aid of the model be separated into two factors. One factor depends on the difference in net charge between two proteins, the other on their relative solubility in the two phases. Designating the proteins (1) and (2) and using the formula above;

$$\begin{aligned} \log \beta &= \log K_1 - \log K_2 = \log K_1^0 + \psi F Z_1 / RT \ln 10 - (\log K_2^0 + \psi F Z_2 / RT \ln 10) = \\ &= \Delta \log K^0 + (Z_1 - Z_2) \psi F / RT \ln 10 \end{aligned}$$

From this expression it can be seen that two systems having interfacial potentials of equal strength but opposite direction have different separatory capacity when $K_1^0 \neq K_2^0$. Depending on the respective Z values, K^0 and the sign of the potential, a difference in K^0 either increases or decreases the separation factor. Albumin has a higher K^0 than hemoglobin, when taken as the D value at the respective isoelectric points, in Fig. 3. $\Delta \log K^0$ is around 0.4 if hemoglobin \equiv (2) and albumin \equiv (1). Between pH 4 and 9, $Z_2 > Z_1$. The separation factor is therefore larger when the potential is negative (TMA-PEG) than when it is positive (CM-PEG), which is in line with the experiments. This despite the somewhat higher potential arising from CM-PEG.

It is evident from the experiments in which the two proteins were partitioned together that the separation factor is negatively influenced by the proteins themselves. This behaviour indicates a weak interaction between the two proteins. The interaction may be electrostatic, since between pH 5 and 7 the two proteins bear charges of opposite sign.

If the interaction between proteins is at least partly of electrostatic nature, it ought to be diminished by addition of salt to the system. Salts, however, decrease the separation factor even at low concentrations, because the ions of the salt compete with the charged PEG in determining the interfacial potential. When a salt must be used (up to 0.015 mole/kg) it should be chosen so as to counteract the interfacial potential as little as possible. This is the case when the potentials from the salt and the charged PEG act in the same direction. NaCl induces a positive potential and can therefore be used together with CM-PEG. Potassium phosphate, on the other hand, is preferable in TMA-PEG-containing systems since both give rise to negative potentials²⁰. Proteins which show strong interaction even at moderate salt concentrations may therefore be difficult to separate by using the system containing charged PEG. However, liquid-liquid extraction can be performed with the aqueous biphasic systems using high concentrations of a salt that causes a relatively high potential. It has been shown⁴ that D of a protein is independent of the concentration of salt above a certain limiting value, 0.01-0.03 mole/kg. In addition to their use in separation, the biphasic systems can be useful for studying the interaction between proteins and in determining their association constants. Even hydrophobic interactions can be overcome by including a suitable detergent, e.g. Triton-X, in the system²¹.

The components in complex mixtures partition rather freely as illustrated by the distribution experiment using heart muscle extract. Since the distribution of enzymes often varies more with pH than does the overall protein distribution, the type of biphasic system used here is useful for liquid-liquid extraction of enzymes and other proteins. The extraction curves obtained with systems containing TMA-PEG are monotonous functions, as expected from the model. Systems containing CM-PEG, however, behave anomalously above pH 8. This is probably due to a beginning deprotonization of the dextran molecule, which becomes negatively charged²⁰. Since CM-PEG and dextran are situated in opposite phases, the dextran counteracts the effect from CM-PEG when the former becomes negatively charged. The presence of di- and tribasic acids may also interfere, since their ions increase in charge and importance in determining ψ with increasing pH.

The reason for the weak dependence of aspartate-glutamate transaminase and malate dehydrogenase on pH in the pH-region 6-8 is explained by the presence of the two forms of each enzyme. In this pH-interval one form is mainly in the upper phase while the other is mainly in the lower phase. The different forms can easily be detected by a counter-current distribution with only a few partition steps, and, by mathematical analyses of the curve, the percentage and partition coefficient of each component can be calculated. To obtain a complete separation of the isoenzymes, five additional distribution steps would suffice. The two isoenzymatic forms of the transaminase and of malate dehydrogenase are probably identical with the mitochondrial and cytoplasmatic forms respectively of these enzymes^{22,23}. The substantial difference in the counter-current distribution curves for the various enzymes assayed indicates that there was little interaction between the partitioned components. In the counter-current experiment with yeast lysate, multiple enzymatic forms were also found for three enzymes belonging to the glycolytic pathway.

The results from the extraction experiments with the crude enzyme mixtures show that the type of aqueous biphasic systems described here can be useful for protein separation. Especially interesting is the possibility of separating different isoenzymes in large quantities directly in a crude extract. The fractions can then be purified with conventional methods. The loss of isoenzymes, present in minor amounts, during purification could in this way be avoided.

ACKNOWLEDGEMENTS

We wish to express our gratitude to Prof. P. -Å. Albertsson for his kind interest in our work and we also thank Miss Eleonore Granström and Miss Maj Olsson for their technical assistance. This research has been supported by grants from STU-Swedish Board for Technical Development.

REFERENCES

1. Albertsson, P. Å. (1971) Partition of Cell Particles and Macromolecules, 2nd edn., (Stockholm, Almqvist and Wiksell, New York, Wiley)
2. Albertsson, P. Å. and Nyns, E. J., Nature (1959) 184, 1465
3. Berridge, N.J. and Svett, D. L., J. Dairy Res. (1966) 33, 277
4. Johansson, G. in Proceeding International Solvent Extraction Conference (Gregory, J. G., Evans, B. & Weslon, P. C., eds) (1971) Vol. 2, p. 928 (London, Society of Chemical Industry)
5. Johansson, G., Hartman, A. and Albertsson, P. -Å., Eur. J. Biochem. (1973) 33, 379
6. Albertsson, P. Å. (1971) Partition of Cell Particles and Macromolecules, 2nd edn, pp.67-71 (Stockholm, Almqvist and Wiksell, New York, Wiley).
7. Englard, S. and Siegel, L. (1969) In Methods in Enzymology (Lewenstein, J. M., ed) Vol. XIII, p. 99 (New York, Academic Press)
8. Kanarek, L. and Hill, R. L., J. Biol. Chem. (1964) 239, 4202
9. Warburg, O. and Christian, W., Biochem. Z. (1942) 310, 384
10. Cohen, P. P. (1955) in Methods in Enzymology (Colowick, S. P. and Kaplan, N. O., eds) Vol. II, p. 178 (New York, Academic Press)
11. Darrow, R. A. and Colowick, S. P. (1962) in Methods in Enzymology (Colowick, S. P. and Kaplan, N. O., eds) Vol. V. p. 226 (New York, Academic Press)
12. Bücher, T. and Pfleiderer, G. (1955) in Methods in Enzymology (Colowick, S. P. and Kaplan, N. O., eds) Vol. I, p. 435 (New York, Academic Press)
13. Bücher, T. (1955) in Methods in Enzymology (Colowick, S. P. and Kaplan, N. O., eds) Vol. I, p. 415 (New York, Academic Press)
14. Beisenherz, G. (1955) in Methods in Enzymology (Colowick, S. P. and Kaplan, N. O., eds) Vol. I, p. 387 (New York, Academic Press)
15. Hecker, E. (1955) Verteilungsverfahren im Laboratorium (Weinheim, Verlag Chemie, GmbH)
16. Tanford, C., Swanson, S. A. and Shore, W. S., J. Am. Chem. Soc. (1955) 77, 6414
17. Beychok, S. and Steinhardt, J., J. Am. Chem. Soc. (1959) 81, 5679.
18. Johansson, G., Biochim, Biophys. Acta (1970) 221, 387.

19. Albertsson, P. Å. (1971) Partition of Cell Particles and Macromolecules, 2nd edn., p.29 (Stockholm, Almqvist and Wiksell, New York, Wiley)
20. Johansson, G. (1973) Thesis, Umeå University, Sweden
21. Albertsson, P. Å., Biochemistry (1973) 12, 2525
22. Boyd, J. W., Biochem. J. (1961) 81, 434
23. Wieland, T., Pfeleiderer, G., Haupt, I. and Wörner, W. Biochem. Z. (1959) 331, 103

TABLE 1: Interfacial potential calculated from the linear relationship between $\log D$ and the net charge, Z , for bovine serum albumin (stained with bromophenol blue) respective porcine CO-hemoglobin. The data originate from the experiment in Fig. 3, Z of the hemoglobin was determined from its titration curve¹⁷.

Composition of the biphasic system (temp 22°C)	Protein	The slope of the straight line, $\log D$ versus Z ,	Interfacial potential, mV
8 % Dextran, 8 % PEG 25 mmole/kg NaCl	Serum albumin	0.010	0.6
	CO-hemoglobin	0.010	0.6
8 % Dextran, 4 % PEG, 4 % TMA-PEG, 2 mmole/kg NaCl	Serum albumin	-0.068	-4.0
	CO-hemoglobin	-0.064	-3.8
8 % Dextran, 4 % PEG 4 % CM-PEG 2 mmole/kg NaCl	Serum albumin	0.090	5.3
	CO-hemoglobin	0.084	5.0

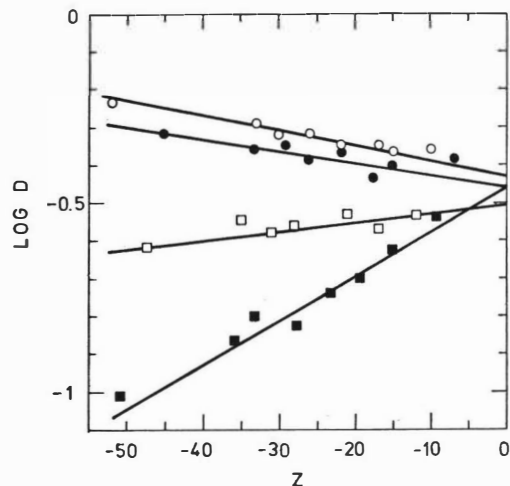


Fig. 1 Distribution coefficient, D , of bovine serum albumin (not stained) as function of its net charge, Z . The biphasic system used contained 5 % dextran, 4 % PEG, 1 g/kg albumin and salt; 50 mmole/kg K_2SO_4 , \circ ; 100 mmole/kg $LiCl$, \bullet ; 100 mmole/kg potassium acetate, \square , or 100 mmole/kg KCl , \blacksquare . Temperature, $2^\circ C$.

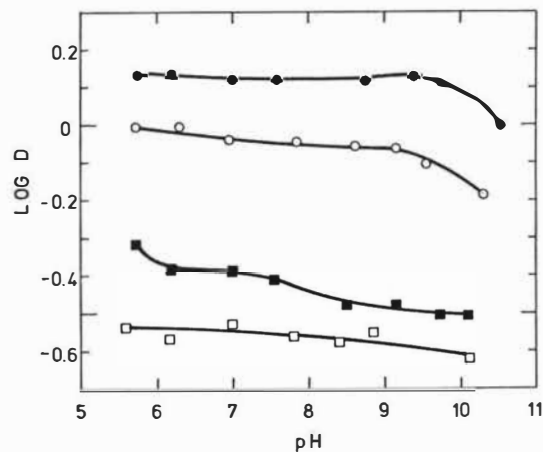


Fig. 2 Distribution coefficient, D , of some proteins as function of pH in a system containing 5 % dextran, 4 % PEG and 100 mmole/kg potassium acetate. The proteins are lysozyme, \bullet , 1 g/kg; ovalbumin, \square , 2 g/kg; ribonuclease A, \circ , 1 g/kg and bovine serum albumin, \blacksquare , 2 g/kg. Temperature, $2^\circ C$.

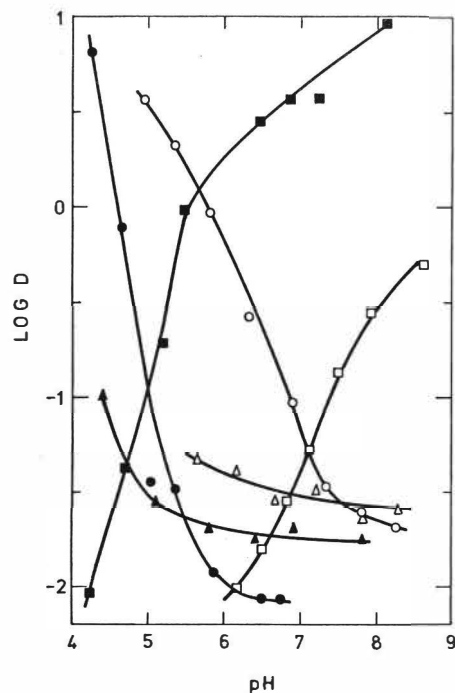


Fig. 3 Distribution of CO-hemoglobin, open symbols, and bovine serum albumin stained with bromophenol blue, filled symbols, in biphasic system containing 8 % dextran and 8 % PEG, at 22°C.

△ , systems containing 25 mmole/kg NaCl;
 □ , systems in which 50 % of the PEG was in the form of TMA-PEG
 ○ , systems in which 50 % of the PEG was in the form of CM-PEG
 Systems containing substituted PEG also contained 2 mmole/kg NaCl. The two proteins were partitioned separately. Protein concentration was 8 g/kg CO-hemoglobin and 4 g/kg albumin.

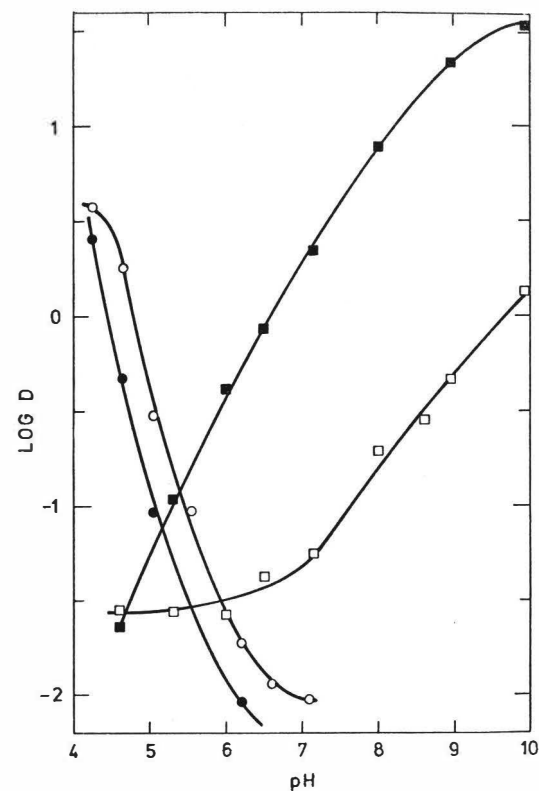


Fig. 4 Simultaneous distribution of CO-hemoglobin, open symbols, and stained bovine serum albumin, filled symbols, in the same system as in Fig. 3 containing CM-PEG, O, or TMA-PEG, □. Protein concentrations were 1.6 g/kg CO-hemoglobin and 3 g/kg albumin.

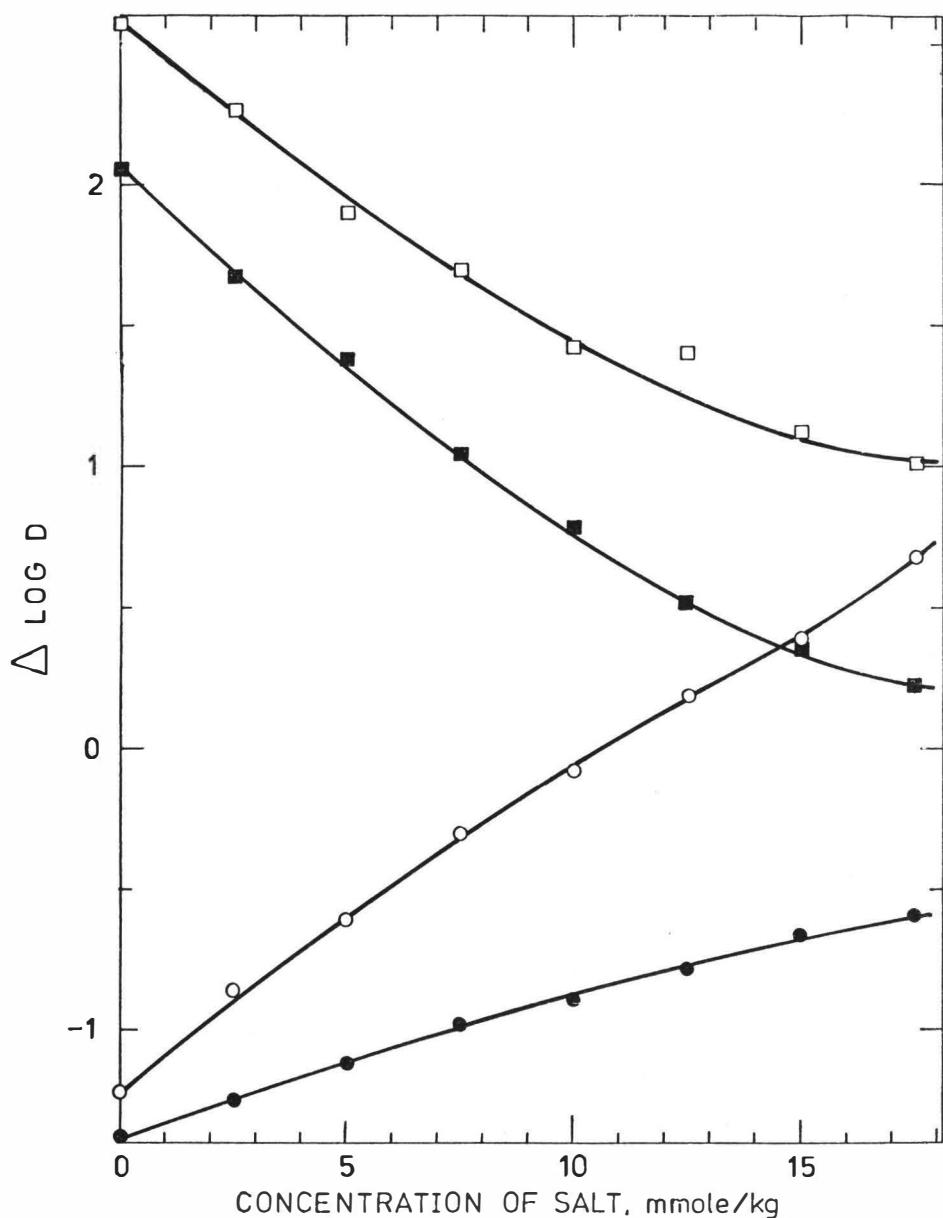


Fig. 5 The dependence of the separatory capacity, $\log D$ (albumin) - $\log D$ (hemoglobin) = $\Delta \log D$, on the concentration of salt. $|\Delta \log D| = \log \beta$ CO-hemoglobin and bovine serum albumin (stained) were partitioned in a system containing 8 % dextran, 4 % PEG and either 4 % TMA-PEG, \square , or CM-PEG, \circ . The salts used were NaCl, filled symbols, and potassium phosphate, open symbols. Protein concentrations were 1.6 g/kg hemoglobin and 3 g/kg albumin. The pI was 6.4, with TMA-PEG and 4.9 with CM-PEG. Temperature, 22°C.

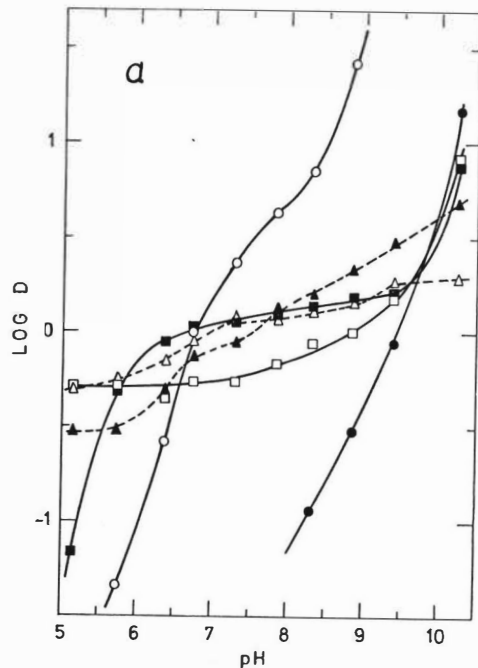


Fig. 6a Variation of the distribution of some enzymes with pH when extract from swine heart was included in a biphasic system containing 6.4 % dextran and either 6.6 % TMA-PEG, Fig. 6a, or 6.6 % CM-PEG, Fig. 6b, at 22°C. O, fumarase; ●, enolase; □, malate dehydrogenase and ■, aspartate-glutarate transaminase. The ratio between the absorbance of the upper and lower phase is used as D for material absorbing light at 280 nm, ▲, and at 260 nm, △ (broken lines). The systems contained 0.125 ml extract per g.

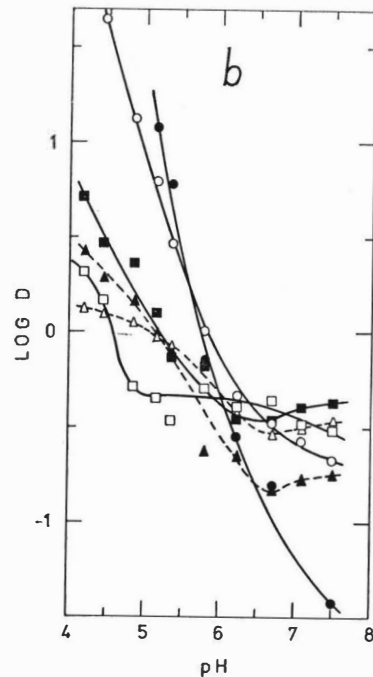


Fig. 6b Variation of the distribution of some enzymes with pH when extract from swine heart was included in a biphasic system containing 6.4 % dextran and either 6.6 % TMA-PEG, Fig. 6a, or 6.6 % CM-PEG, Fig. 6b, at 22°C. O, fumarase; ●, enolase; □, malate dehydrogenase and ■, aspartate-glutarate transaminase. The ratio between the absorbance of the upper and lower phase is used as D for material absorbing light at 280 nm, ▲, and at 260 nm, △ (broken lines). The systems contained 0.125 ml extract per g.

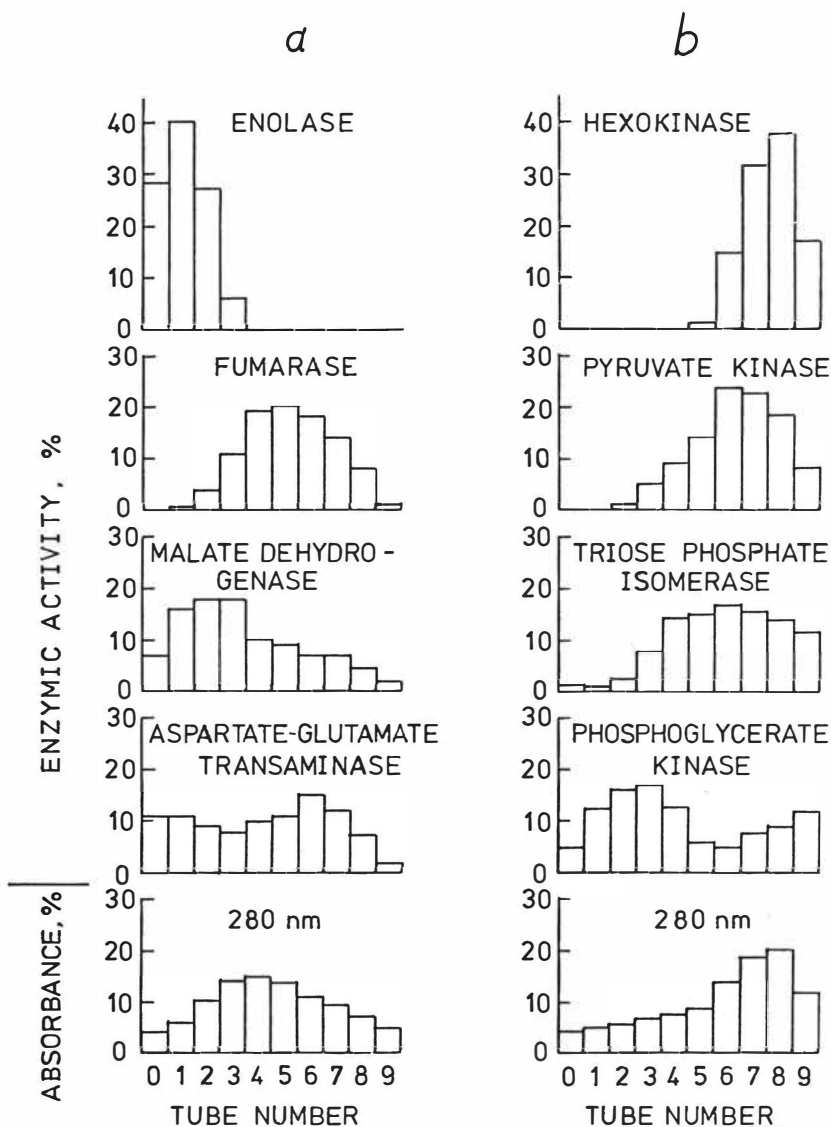


Fig. 7 Counter-current distribution with nine transfers in dextran-TMA-PEG biphasic systems. The system containing protein sample was introduced in tube no. 0 and the upper phase was transferred to the right. (a) Extract from swine heart in a system containing 6.4 % dextran, 6.6 % TMA-PEG and 2.5 mM potassium phosphate at pH 7.5. Each tube contained 1.75 ml upper phase and 1.75 ml lower phase. 0.88 ml of the extract was used. Temperature, 22°C (b) Lysate of baker's yeast in a system containing 7 % dextran, 5 % TMA-PEG and 5 mmole/kg potassium phosphate at pH 6.5. Each tube contained 2.0 ml upper phase and 1.75 ml lower phase. 0.75 ml lysate was used. Temperature, 10°C.

TREATMENT OF SOLVENT EXTRACTION RAFFINATES
FOR THE REMOVAL OF ORGANIC REAGENTS

by

G.M. Ritcey, B.H. Lucas,
and A.W. Ashbrook

INTRODUCTION

In a previous paper⁽¹⁾ the general position of the loss of solvent extraction reagents by various means was discussed, together with some effects that organic reagents can have on the environment. We shall now concern ourselves with the recovery of organic materials from solvent extraction raffinates.

As is the case regarding the environmental effects of solvent extraction reagents, little attention appears to be paid to the recovery or removal of organic materials from solvent extraction raffinates. Consequently, there are few data available on this aspect of the process. Accordingly, we are restricted to discussions mainly involving processes used in other industries, such as the chemical industry, and with the recovery of phenol and similar materials from waste aqueous streams. However, we feel that much can be learned and applied from the several processes which are now in operation in chemical plants for treating waste streams.

The objective of this paper is to attempt to relate these, and other, processes to solvent extraction operations, and to indicate, where possible, the economics and efficiencies of the different approaches.

ACTIVATED CARBON ADSORPTION

One of the most efficient methods available for the removal of organic chemicals from effluents is adsorption on activated carbon. Activated carbon has the capability to adsorb organic molecules from both liquids and gases. In a properly designed system, an effluent can be produced containing 1 ppm or less organic. The following section reviews several carbon adsorption schemes together with the regeneration procedures, for removal of organics from solutions and vapors.

Adsorption From Solutions

Phenol or cresol are organic chemicals, and, although they are not used in solvent extraction processing, they are mentioned here in the context of feasibility of carbon adsorption for their removal ⁽²⁾, and that some of the ideas and steps might be utilized to treat effluents arising from solvent extraction processing.

In a paper by Baker et al. ⁽³⁾, they describe the use of Nuchar WV-L 8 X 30 granular activated carbon for the removal of cresol from effluents. Adsorption is downflow, the cresol is recovered, and the carbon regenerated for re-use by upflow regeneration using 10% sodium hydroxide solution at 65 to 70°C.

At Midland, Mich. 144,000 gal/day of brine effluent wastes from a phenol plant are being treated by activated carbon to remove the 150 to 200 ppm phenol from the solution also

containing 18% NaCl and 2000 ppm sodium acetate ⁽⁴⁾ . Because the carbon also adsorbed the acetic acid, and because both phenol and acid are soluble in caustic, the carbon was regenerated with a caustic soda solution. Caustic regeneration is applicable only to organic chemicals whose adsorption is affected by change in pH⁽⁵⁾ .

In another process ⁽⁴⁾ , a waste stream was neutralized to pH 11.5. The decant was adjusted to pH 7, clarified, and then passed through towers containing 40-mesh granular activated carbon. Estimates of costs for a 10 million gal/day plant to produce high purity water with more than 97% chemical oxygen demand (COD) removed would cost \$4.4 million (compared to conventional tertiary treatment plant of \$8.8 million), and 26.3¢/1000 gal to operate (compared to 42.8¢/1000 gal in conventional).

As to the performance of packed beds and expanded bed columns of activated carbon, the effectiveness of organic removal was equal ⁽⁴⁾ , but there were several differences noted in the operation. In the packed beds, even with highly clarified solution, head loss increased steadily, resulting in increased pumping pressures and eventual cleaning and backwashing. The expanded beds were more efficient, with reduced labour requirements as they required no cleaning or maintenance. The flow rates remained constant without any head loss.

The Chipman Division of Rhodia Inc. process removes alcohol, phenoxyacetic acid and dissolved organic compounds that can not be removed by clarification or biological degradation ⁽⁶⁾ .

This effluent also contains sulphates and chlorides. In Figure 1 are shown breakthrough curves for the removal of phenol from clarified coke plant effluents ⁽⁷⁾. It was reported by Brunotts et al ⁽⁸⁾ that 1 gram of carbon could remove 190 mg of total organic carbon (TOC). At an influent TOC concentration of 6400 mg/l, this is equivalent to a carbon usage rate of 315 lb/1000 gal of effluent treated. The general layout for adsorption and reactivation is shown schematically in Figure 2 ⁽⁸⁾.

In the processes described above the carbon is regenerated by caustic scrubbing to recover the phenol or cresol. Occasionally, depending upon the operation, it may be cheaper to discard the loaded carbon, rather than regenerate it for re-use. In the SEC process for extraction of copper from acid solution followed by pH adjustment to the alkaline side and extraction of nickel, the nickel electrolyte prior to electro-winning is passed through carbon towers to remove about 15 ppm of soluble organics ⁽⁹⁾. When a tower becomes saturated the carbon is discarded and replaced with fresh carbon. At a throughput of 800 lb Ni/day, the cost of using the charcoal beds is about 4¢/lb Ni produced.

Removal of adsorbed organics from carbon is not always a simple matter of caustic stripping, and therefore more expensive steps are required such as steam stripping or reactivation of the carbon in a furnace. Treatment in a furnace at a controlled temperature results in burning the adsorbed organic carbon to CO₂ and leaving the activated carbon suitable for re-use.

Five recent approaches ⁽¹⁰⁾ for furnace regeneration are:

1. Westvaco process, a low temperature oxidizing gas moves spent carbon to a combustion chamber where foreign matter is burnt off.
2. Battelle Memorial Institute process uses a fluidized-bed.
3. FMC Corporation uses a transport reactor furnace.
4. Nichols Engineering and Research uses a multiple-hearth furnace.
5. Zimmerman Process uses a wet combustion method.

A system capable of desorbing a wide variety of organic chemicals has been developed which involves the desorption of organics from the carbon with a solvent phase⁽¹¹⁾. Following desorption, the solvent is separated from the organics by steam-stripping, and the vapors condensed and recycled. The solvent regenerant, containing the desorbed organics, is distilled to recover the solvent, leaving a recovered organic concentrate. The process offers promise where caustic regeneration is unsuitable, where thermal regeneration is excessive in cost, and where organics recovery is desirable.

Adsorption From Vapors

In a normal plant operation, there is a possibility of evaporation of some of the solvent mixture particularly if the operation is at elevated temperatures or in a hot climate. It may be that by proper collection of the vapors from a solvent extraction plant, the solvent can be removed from the air,

concentrated, and recovered. The effectiveness depends greatly upon the solvent concentration and boiling point; the more dilute the concentration the less efficient the process⁽¹²⁾. A fixed bed adsorber is commonly used. Although trace amounts of soluble solvents can be recovered from vapor effluents, solvents of a strongly polar nature are difficult to remove. Regeneration of the adsorbent is by heat treatment at 800 - 900°C in the presence of steam. Some typical data for adsorption of various compounds are shown in Table 7⁽¹²⁾.

In the recovery of organic solvent vapors, the sequence of operating conditions is

1. loading till breakthrough.
2. steaming-out, where live steam is blown through the bed stripping off the vapors and discharging them to a condenser and distillation unit.
3. reactivating period in which the hot moist bed is subsequently dried and cooled.

These different criteria, based on successful practice, have been recommended for determination of the optimum quantity of steam to be used in purging out a given adsorber:

1. the temperature through the bed should reach about 100°C to ensure thorough desorption of the solvent vapors⁽¹³⁾.
2. the resulting eluate batch should contain at least 26 to 27% solvent⁽¹³⁾.
3. the solvents recovery efficiency should be about 99 to 99.8%⁽¹⁴⁾.

TABLE 7

Some Typical Results of Solvent Adsorption by Carbons,
as Experienced in Solvent Recovery Practice ⁽¹²⁾

SOLVENT	CONCENTRATION (%w/w)	* INITIAL ADSORPTION (%w/w)	† CYCLIC ADSORPTION (%w/w)	**STEAM RATIO	BOILING POINT RANGE (°C)
Methylene chloride	1.0	28.3	17.3	1.4	40.5
Arklone P	0.5	44.9	20.8	1.4	47.6
Acetone	1.0	20.3	12.5	2.3	56
Tetrahydrofuran	0.5	22.0	9.0	2.0	66
Hexane	0.48	21.3	8.2	3.5	68.7
Ethyl acetate	0.5	27.6	13.6	2.1	77.2
Trichlorethylene	0.5	44.6	19.9	1.8	86.7
n-Heptane	0.12	22.4	5.9	4.3	98
Toluene	0.4	23.3	9.6	3.5	110
Methyl isobutyl ketone	0.2	22.0	9.0	3.5	115.9
Mixed rubber solvent	0.3	25.7	10.3	3.8	120-160
Shellsol E	0.3	35.6	11.9	3.7	153-193
3,3,5-trimethyl cyclohexyl acetate	0.1	36.4	7.9	4.5	206

* Initial adsorption refers to the solvent adsorbed by new carbon to 'breakpoint', i.e. when solvent can be detected in the effluent air stream. The 'slip' level at this point is normally of the order of 20ppm.

† Cyclic adsorption refers to the solvent which can be adsorbed and desorbed consistently at an economical steam consumption.

** Steam ratio refers to the total steam used to desorb the solvent from the adsorbent and is an overall figure inclusive of condensate and moisture condensed on the carbon bed.

Such conditions are meant to approximate to the most economic purging at which incremental increases in the cost of steam consumed in purging and in the distillation of more dilute mixtures is just balanced by the cost in the additional solvents recovered (12).

Conventional adsorption systems contain at least two adsorbers, one on adsorption, while the other is being regenerated with steam. The stripped solvent and steam are condensed, and the solvent is recovered by decantation or distillation. When the solvent concentration in the vapor-laden air is greater than 0.2% the carbon is usually sufficiently regenerated with 3.5 lb of steam per lb of recovered solvent⁽¹⁴⁾. With superheated steam, the requirements can be slightly lower. These systems can be expensive because of the materials of construction necessary to withstand the corrosive condition during regeneration. Therefore the large capital costs, together with high operating costs, does not appear economical for recovery of solvents at low concentration, but may be suitable for removal from solvent-rich vapors.

The Zorbacin process⁽¹⁵⁾ combines the use of carbon adsorption with air incineration. Vapor at 100°F containing organics, is passed through the carbon bed to remove the organics. Hot air is used to regenerate the carbon. A blowdown stream from the regenerating system flows to the air incinerator where the stripped organic vapor is burned. This burned vapor provides the fuel for incinerating, and the gases provide the heat for regeneration. A small amount of natural gas is also burned in the incinerator to supply the initial heat requirement. As

the regenerator temperature rises, more solvent is stripped from the carbon.

The advantages of this route are as follows:

1. the inert atmosphere produced by the incinerated gases prevents oxidation of the carbon and reduces fire hazard in the regeneration system. The oxygen required to burn the organic vapors in the blowdown stream can be supplied by make-up at the incinerator.
2. since steam is not required for regeneration (the vapors are always held above their dew point) the system will be free of corrosive condensate. This permits the use of inexpensive material of construction.

A slight modification of the Zorbcin process is the Cascade system of Mattia⁽¹⁶⁾ whereby provision is made for the removal and recovery of the solvent from vapor, rather than incinerating the vapor. When the carbon becomes saturated with organic, it is regenerated by steam-stripping, and the solvent can often be recovered by either distillation or by decantation.

MINES BRANCH TESTS ON CARBON ADSORPTION

The use of activated carbon, and other materials, have been studied at the Mines Branch for possible use for removal of soluble organic from solvent extraction process raffinates. A raffinate resulting from separation of cobalt and nickel from a sulphate solution at an equilibrium pH 6.0, using 20 vol percent DEHPA in kerosene containing 5 vol percent TBP, was used in the initial investigation. This raffinate contained

T A B L E 8

Screening Tests for Solvent Removal from a Raffinate
(56ppm DEHPA, pH 6.0)

Treatment	Quantity Used	Treated Raff. (ppm)
Pittsburgh Carbon 12 x 40	2g	<0.05
Norite Act. Carbon -8 x 20	2g	1.6
Filtrisorb 400, -12 + 40	2g	2.5
Norite 2 -12 + 40	2g	11
Lignite	2g	35
Lignite 2 -12 + 40	2g	15
Sodium Silicate	1ml	30
Silica gel -6 + 20	2g	34
VOSO ₄ ·2H ₂ O	.08g	40
Diatomaceous earth	2g	44
Air flotation		49
Ultrasonics		38
Teflon beads	4g	49
Commercial Soap Solution	1ml	18
Commercial Soap Solution	2ml	11
Commercial Soap Solution	4ml	7
Commercial Soap Solution	6ml	7
Commercial Soap Solution	8ml	7

	<u>System</u>	<u>Quantity</u> g.	<u>Raffinate (ppm)</u>	
			<u>Feed</u>	<u>Treated</u>
Filterol 62	DEHPA	10	12	6
Filterol 62	Alamine	10	39	1.2
Attapulugus Clay	DEHPA	10	14	6
Attapulugus Clay	Alamine	10	39	0.5

56 ppm DEHPA as soluble organic reagent. The results of contacting 200-ml portions of raffinate in these screening tests are shown in Table 8. Also shown are results of two additional adsorbents for amine and DEHPA. Activated carbon proved the most effective of the adsorbents tested. In Table 9 is shown the effect of variation of the amount of carbon on the removal of DEHPA.

TABLE 9

Use of Calgon Carbon Filtrasorb 400
for Removal of DEHPA
 (Feed 56 ppm DEHPA)

g Charcoal/l Treated	Treated Raff. ppm DEHPA
1.25	25
2.50	17
3.75	6
5	5
10	2.5
* 10	< .05

*The 2.5 ppm raffinate recycled once

Since the activated carbon was obviously effective for the removal of DEHPA, other process raffinate systems were studied for effectiveness in removal. Table 10 shows a few of

TABLE 10

ADSORPTION TEST ON TYPICAL PROCESS RAFFINATES

(10g Filtrasorb 400/litre treated)

SOLVENT SYSTEM		AQUEOUS SYSTEM				SOLVENT ANALYSIS		
EXTRACTANT	MODIFIER	DILUENT	METAL	ANION	pH	FEED ^{ppm} RAFF.	TREATED RAFF.	ANALYZED
Alamine 336	isodecanol	Shell 140	U	SO ₄	1.8	6.7	<0.3	Amine
Alamine 336	isodecanol	Shell 140	Cu	HCl	(6M)	100	20	Amine
Primene JMT	isodecanol	Shell 140	Th	SO ₄	2.0	990	10	Amine
DEHPA	TBP	Shell 140	U	SO ₄	1.8	1.2	0.6	DEHPA
DEHPA	TBP	Shell 140	Co-Ni	SO ₄	6.0	56	2.5	DEHPA
LIX 63	-	Shell 140	Cu-Zn-Mn	SO ₄	1.4	4.2	1.2	LIX 63
LIX 64	-	Shell 140	Cu-Zn-Mn	SO ₄	1.4	11	1.3	LIX 64
LIX 64N	-	Shell 140	Cu-Zn-Mn	SO ₄	1.4	11	1.5	LIX 64N
LIX 63	-	Shell 140	Cu-Ni-Co	(NH ₄) ₂ SO ₄	8.1	<.05	<.05	LIX 63
-	5% isodecanol	DX 3641	Cu	SO ₄	2.0	<5	<5	isodecanol
-	10% nonylphenol	Solvesso 150	Cu	SO ₄	2.0	10	<5	nonylphenol
-	5% TBP	DX 3641	Cu	SO ₄	2.0	65	15	TBP
-	5% 2-ethylhexanol	DX 3641	Cu	SO ₄	2.0	<5	<5	2-ethylhexanol
-	-	Solvesso 150	Cu	SO ₄	2.0	<5	<5	Solvesso 150
-	-	Isopar L	Cu	SO ₄	2.0	<5	<5	Isopar L
-	-	Cyclohexane	Cu	SO ₄	2.0	25	10	Cyclohexane

the data, indicating primary and tertiary amines, LIX 63, LIX 64, LIX 64N, as well as DEHPA can be removed by the carbon adsorption process. These tests were all in the acid pH range. Tests in an alkaline system, in which LIX 63 was used to extract copper from a solution containing 12 g Cu/l and 275 g $(\text{NH}_4)_2\text{SO}_4$ /l showed a solvent solubility of < 0.05 ppm LIX 63. Carbon treatment gave the same results. The data also show that the paraffinic modifiers have very little solubility, and that there was no indication of adsorption on carbon. A cyclic modifier, such as nonylphenol, was slightly soluble and was adsorbed on carbon. TBP used in the test as a modifier, and which is of course also an extractant, had high solubility and was adsorbed by carbon. Paraffinic and aromatic diluents had low solubility and no indication of adsorption on carbon. The naphthenic diluent was soluble and could be adsorbed on carbon. It would appear then that although modifiers and diluents might be adsorbed by activated carbon, that the extractant would adsorb preferentially.

Saturation loading tests were performed on Calgon carbon Filtrasorb 400, using a raffinate from uranium extraction that contained a total of 35 ppm amine. Using a 2-inch diameter column containing 0.5 lb of the carbon, 362 gallons of raffinate were processed, resulting in a loading at breakthrough of 0.14 lb amine/lb carbon. The flow rate, although not optimum was 86 gal/hr/ft². This loading compares with the phenol loadings reported in the literature of about 0.22 lb/lb carbon.

Both steam stripping and organic stripping were tested for recovery of the amine. The amine was readily removed using 1.5 lb steam/lb carbon. With organic stripping, methanol was relatively efficient, and 65% of the amine was recovered in one stage. Optimum conditions of carbon type, adsorption, and stripping, have not been determined.

Economics

In summary, activated carbon will adsorb a mixture of gases, the higher molecular weight gases in greater proportion. From liquids there is a similar tendency for adsorption of the higher molecular weight substances, as well as non-polar materials. Thus a non-polar substance, such as an oil, would be preferentially adsorbed from a polar solvent such as water.

The activated carbon must possess sufficient hardness to permit easy and effective backwashing, as well as to withstand the hydraulic and mechanical handling associated with the regeneration process.

Regeneration usually takes place at 1600 to 1800°F. Carbon losses in multi-hearth furnaces are about 5% per cycle. Operating costs for reactivation vary, depending upon the size of the plant, but is estimated in the 10¢ per lb carbon range. This includes fuel, power, labor and make-up carbon. With carbon adsorption and thermal regeneration of the carbon, the direct non-capital-related operating costs are 8¢ to 13¢/lb organic removal⁽¹⁷⁾. Capital cost is in the range of 32.5⁽¹⁸⁾ to 80.0¢/lb⁽⁶⁾ organic/year.

Operating costs to treat 150,000 gal/day of waste-water containing alcohol, and other dissolved organic compounds were stated as 35.6¢/1000 gal of treated water⁽⁶⁾ . The breakdown of the capital costs of \$300,000 is shown in Table 11.

TABLE 11

Capital Costs ⁽⁶⁾

Activated carbon system	
2 Adsorber vessels (wooden).....	\$ 13,300
2 Carbon storage vessels.....	10,400
Recycle water vessel.....	3,500
Quench tank.....	500
Pumps and eductors.....	5,900
Reactivation furnace*.....	35,400
Afterburner and stack.....	6,300
Stack gas scrubber.....	10,000
Dewatering screw.....	6,900
Piping and misc. material.....	26,500
Electrical.....	11,000
Instruments.....	5,800
Structures and foundations.....	22,800
Carbon inventory.....	18,500
Construction labor.....	31,400
Engineering.....	<u>21,800</u>
	SUBTOTAL
	\$230,000
Neutralization system.....	40,000
Water collection system.....	<u>30,000</u>
	TOTAL
	300,000

*Excluding installation

In Table 12 is shown a breakdown of operating costs for adsorption of phenol from coke plant effluents ⁽⁷⁾. Each operation may vary, depending upon specific condition such as flows and organic content, reactivation rates, and labor. In Figure 3 is shown reactivation costs vs pounds reactivated, based on costs shown in Table 12 ⁽⁷⁾.

Additional data on capital and operating costs of carbon plants have been reported by Paulson ⁽⁴⁾ and Mattia ⁽¹⁵⁾. The design of activated carbon adsorption systems has been reported showing the effects of varying feed concentrations, flow rates, or effluent composition ⁽¹⁹⁾.

TABLE 12

Operating Cost Breakdown For
Granular Carbon Process ⁽⁷⁾

Fuel	5000 BTU's/lb Carbon Reactivated \$0.75/10 BTU
Steam	1 lb steam/lb carbon \$1.00/1000 lb steam
Electricity	1.1¢/Kw. hr
Labor	12 man-hours/day \$4.00/man-hour
Make-up Carbon	5% loss per cycle 30¢/lb
Note: Maintenance costs are between 2 and 5 percent of capital investment. Usually this cost is between 0.1 and 0.2¢/lb reactivated.	

Carbon has the capacity for 15 to 30 lb of phenol per 100 lb, depending upon the influent concentration. An estimate of carbon in an average plant would be 100 lb for every 20 lb of phenol to be removed^(7,8). The type of carbon -- whether granular or powdered -- will be an important factor in determining the operating costs, because powdered carbon ranges from 9¢ to 15¢/lb compared to granular carbon costing 15¢ to 30¢/lb⁽¹⁰⁾.

With direct reference to use of activated carbon for treatment of process raffinates arising from solvent extraction processing, costs were estimated, based on the adsorption of amine from a uranium process raffinate. Basis for the cost estimation is for a 3000 tpd mill treating ore grading 0.1% U_3O_8 , and an effluent flow of 500 gal/min from solvent extraction processing, and containing 35 mg/l amine. The carbon loading was 0.14 lb amine/lb carbon, and the steam consumption was 1.5 lb steam/lb carbon. The estimated costs in Table 13 show a cost, including capital, labor, carbon loss, and steam, of 29¢/lb amine recovered, or 1.3¢/lb U_3O_8 production. The value of amine recovered per day, at \$1.00/lb amine, would be \$252, or a credit of 4.2¢/lb U_3O_8 . Based on operating costs of 1.3¢/lb U_3O_8 , the profit differential of 2.9¢/lb U_3O_8 would be equivalent to a net savings to the operation of \$52,200 per year. In addition, a potential pollutant of the environment would be eliminated.

TABLE 13

Estimated Costs for Treatment of Uranium
Solvent Extraction Raffinates by Carbon Adsorption

	Estimated Costs		
	¢/lb amine	¢/lb U	¢/1000 gal treated
Steam (1)	1.2	0.1	0.4
Carbon (2)	8.6	0.4	3.0
Labor (3)	19.1	0.8	6.7
Capital (4)	0.1	0.01	0.1
	<hr/>	<hr/>	<hr/>
	29.0	1.31	10.2

- (1) Steam consumption: 1.5 lb steam/lb carbon at \$1.00/1000 lb steam.
- (2) Carbon loading: 0.14 lb amine/lb carbon
Carbon loss of 5% at a cost of 12¢/lb carbon.
- (3) Labor: 12 hours at \$4/hr.
- (4) Capital: Installed cost of \$100,000 10-year straight line depreciation.

Mill - 3000 tpd, 0.1% U_3O_8
 500 gal/min, 35 mg/l amine.

OTHER REMOVAL METHODS

Data have been reported for the adsorption on zeolites, of butylene, propylene, ethylene, butane, propane, and ethane⁽²⁰⁾. The results indicated that equilibrium loadings, by weight, are generally lower for the saturated than for the unsaturated hydrocarbons, and that loadings increase with increasing chain length.

In addition to adsorption on activated carbon, or zeolites, numerous other methods are becoming available for the removal of soluble or entrained solvents from effluents. These developments have arisen because of the necessity of treating oil spills to meet the environment specification.

One process consists of first saturating the solution with air under pressure which coagulates the material⁽²¹⁾. From coagulation, the flow is to an inverted truncated cone inlet to a flotation column. The clear water drains downward, while coagulated waste floats to the top. The floated sludge is transferred to a dewatering tank where the solids are collected and separated in polypropylene filter bags. The water and small amounts of free oil run through the bags and the oil is recovered by skimming.

Units from 3,800 to 20,000 gal/day are available. Soluble oils up to 11,000 ppm have been removed with an efficiency of 98+%. Because of the vertical column used, the space requirement is low, at 50 sq ft of floor space and 10 ft of headroom for treatment of 10,000 gal/day.

Other units involve the use of an oil-soluble ferrofluid added to the water which mixes with the oil film, and is recovered by an electromagnet⁽²²⁾.

Coalescing devices, such as plates, have been reported for oil-water separation⁽²³⁾ as well as the use of hydrophilic membranes⁽²⁴⁾. Materials such as chemically-treated polyurethane foam and peat moss have also been used for recovery from oil spills. Surface-active agents are also available for use, and the Province of Ontario lists some approved dispersants and surface tension modifiers⁽²⁵⁾.

At the Mines Branch, tests have been carried out on the use of a coalescing device for the removal of entrained organic from solvent extraction process raffinates. This oil/water separator is marketed by Techrad, Inc., Oklahoma, and consists of a specially-designed cartridge placed inside a cylinder. The device is fitted into the raffinate discharge line. As the solution flows through the cartridge, organic is removed and coalesced, with the droplets collecting and passing out through a separate organic discharge line.

Hydrophilic membranes have been reported useful for oil-water separations⁽²⁴⁾ for possible application for shipboard use. Screening tests of several membranes indicated that a surface-hydrolyzed cellulose acetate was suitable. The effects of feed temperature, flow rate, salt concentrations, applied pressure, and type and concentrations of oil contaminants were determined in salt water containing oil. Typical rejection of oil-water mixtures are shown in Table 14, while salt rejection was essentially zero⁽²⁴⁾.

TABLE 14

Removal of Oil by Hydrolysed Cellulose Acetate Membranes⁽²⁴⁾

Type of Oil	Oil in Feed (ppm)	Oil in Treated Solution (ppm)
Lubricating Oil	10,000	1.3
Crude Oil	2,500	2 - 4
Diesel Fuel	2,500	5
Filtered bilge water	10,000	0.4

Operating pressures using the cellulose acetate membranes were stated to be in the range of 50 to 90 psi. The membrane was readily cleaned by flushing with a solution containing surfactant, such as Sterox A.J. (Monsanto). The use of a hydrophilic membrane should permit the treatment of stable emulsions, which may be difficult to coalesce in conventional coalescing equipment. Filtration rates range from 50 to 100 gallons per day per ft² membrane area⁽²⁶⁾.

CONCLUSIONS

Solvent that is soluble in the aqueous phase can be removed by activated carbon and economically recovered for re-use. Unless the solvent extraction reagents are removed from the process effluent, serious effects on aquatic life can result. If, after treatment of the raffinate with activated

carbon, some organic components remain, then it is possible that these compounds will be biodegraded to carbon dioxide and water.

Although treatment of certain effluent streams and off-gas vapors containing solvents could be costly, it may be necessary in order to meet the environment specification. The amount of solvent recovered or not recovered may be a minor aspect in the decision to remove and/or recover solvents. Today there is more of a trend to water re-use throughout the world. Each plant or operation, although seemingly similar to others as far as the operation and products are concerned, may be unique where the effluents and vapors are concerned. It is therefore essential that sufficient studies and tests be made prior to the plant flowsheet decision in order that the best method for treatment of the plant effluents for solvent removal can be selected. It is hoped that this paper has indicated the problems, areas where studies are required, and perhaps some methods which may prove useful.

ACKNOWLEDGEMENTS

The authors gratefully acknowledge the assistance of K. Price of the Solution Treatment Section for the investigations; R. Pugliese, D. MacPherson of the Chemical Analysis Section for the analysis; and D. Clugston and R. Draper of the Fuels Research Centre of EM&R for the mass spectral data.

REFERENCES

1. Ritcey, G.M., Lucas, B.H., and Ashbrook, A.W., "Some Comments on the Loss and Environmental Effects of Solvent Extraction Reagents Used in Metallurgical Processing", Paper No. , Intern. Solvent Extn. Conf., Lyon, France, Sept. 1974.
2. Painter, H.A., Chem. and Ind., No. 17, pp 818-822, Sept. 1, 1973.
3. Baker, C.D., Clark, E.W., Jeserning, W.V., and Huether, C.H., Chemical Engineering Progress, Vol. 69, No. 8, pp. 77-78, August 1973.
4. Browning, J.E., Chemical Engineering, pp. 32-34, Sept. 7, 1970.
5. Fox, R.D., Chem. Eng., Aug. 6, 1973, pp. 72-82.
6. Henshaw, T.B., Chemical Engineering, pp. 47-49, May 31, 1971.
7. Van Stone, G.R., and Mendiaino, F.F., "Physical-Chemical Treatment of Coke Plant Wastewater", Presented at the Environmental Quality Conference of AIMME, Washington, D.C., June 7, 1971.
8. Brunotts, V.A., Lynch, R.T., and Van Stone, G.R., Chemical Engineering Progress, Vol. 69, No. 8, pp. 81-84, Aug. 1973.
9. Eliassen, R.D., "The Operation of a Nickel Solvent Extraction and Electrowinning Circuit", Presented at Symposium on Solvent Ion Exchange. Arizona Section of AIChE, Tucson, May, 1973.
10. Browning, J.E., Chemical Engineering, pp. 36-40, Feb 21, 1972.
11. Smisek, M., Cerny, S., "Active Carbon-Manufacture, Properties and Applications," Elsevier Pub. Co., New York, 1970.
12. Houghton, F.R., and Wildman, J., Chem. Process Eng., (London), 52, (4), pp. 61-64, 1971.
13. Ross, T.K., and Freshwater, D.C., "Chemical Engineering Data Book", 1958, Pub. London, Leonard Hill Books.
14. Courouleau, P.H., and Benson, K.B., The Chemical Engineer, Vol. 55, p. 112, 1948.
15. Mattia, M.M., Chemical Engineering Progress, Vol. 66, No. 12, pp. 74-79, Dec. 1970.
16. Mattia, M.M., U.S. Patent 3,455,089.

17. Van Stone, G.R., *Industrial Wastes*, 23, July/August, 1972.
18. Shumaker, T.P., Zanitsch, R.H., "Physical/Chemical Treatment: A Solution to a Complex Problem", Presented at the 45th Annual Water Pollution Control Federation Conference, Atlanta, Ga., Oct., 1972.
19. Hutchins, R.A., *Chemical Engineering*, pp. 133-138, Aug 1973.
20. Youngquist, G.R., Allen, J.L., and Eisenberg, J., *Ind. Eng. Chem. Prod. Res. Develop.*, Vol. 10, No. 3, pp. 308-314, 1971.
21. Technical Editor, *Chemical Engineering*, pp. 72-73, Oct 16, 1972.
22. Technical Editor, *Chem. & Eng. News*, pp. 47-48, Feb 1, 1971.
23. Merryman, J.G., and Osterstock, E.R., "Coalescing Plates and Packs for Oil Water Separation in Various Shipboard Applications", Obtained from National Technical Information Service, Washington, No. AD-758-319, Jan, 1973.
24. Milstead, C.E., and Loos, J.F., "Study of Hydrophilic Membranes for Oil-Water Separation", Feb. 1973 (Gulf Environmental Systems, San Diego), Distributed by National Technical Info. Service, U.S. Dept. Commerce, AD-758-321.
25. Editor, *Eco/Log Report*, p. 4, June 1, 1963, Pub, Corpus Services, Toronto, Ontario.
26. Goldsmith, R.L., and Hossain, S., Abcor Inc., Mass., "Ultrafiltration Concept for Separating Oil from Water", Jan. 1973. Distributed by National Tech. Info. Service, U.S. Dept, of Commerce, AD-758-318.

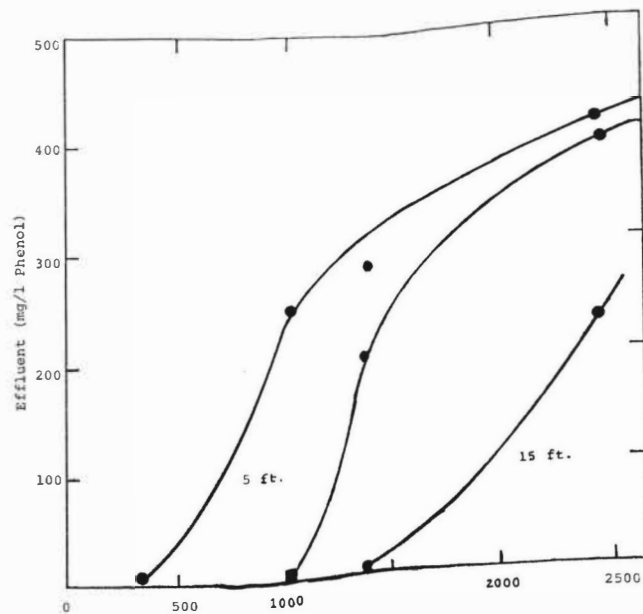
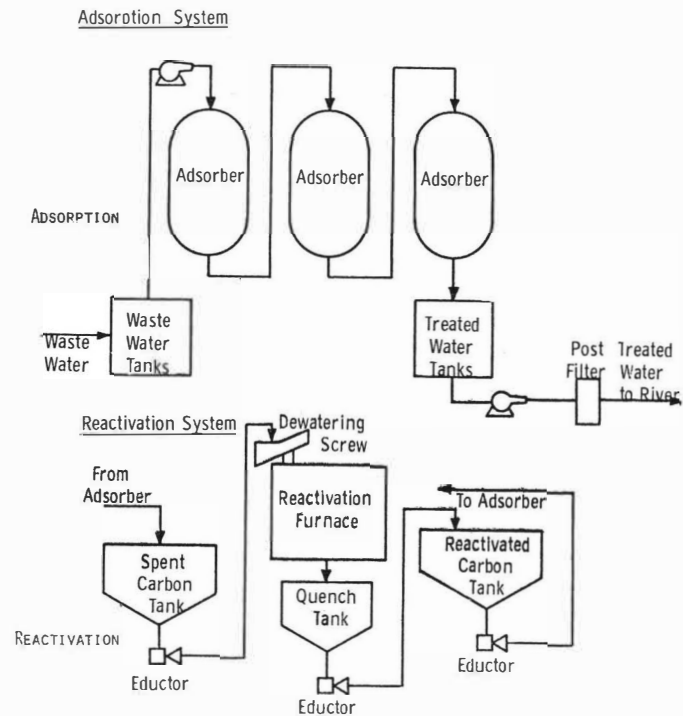
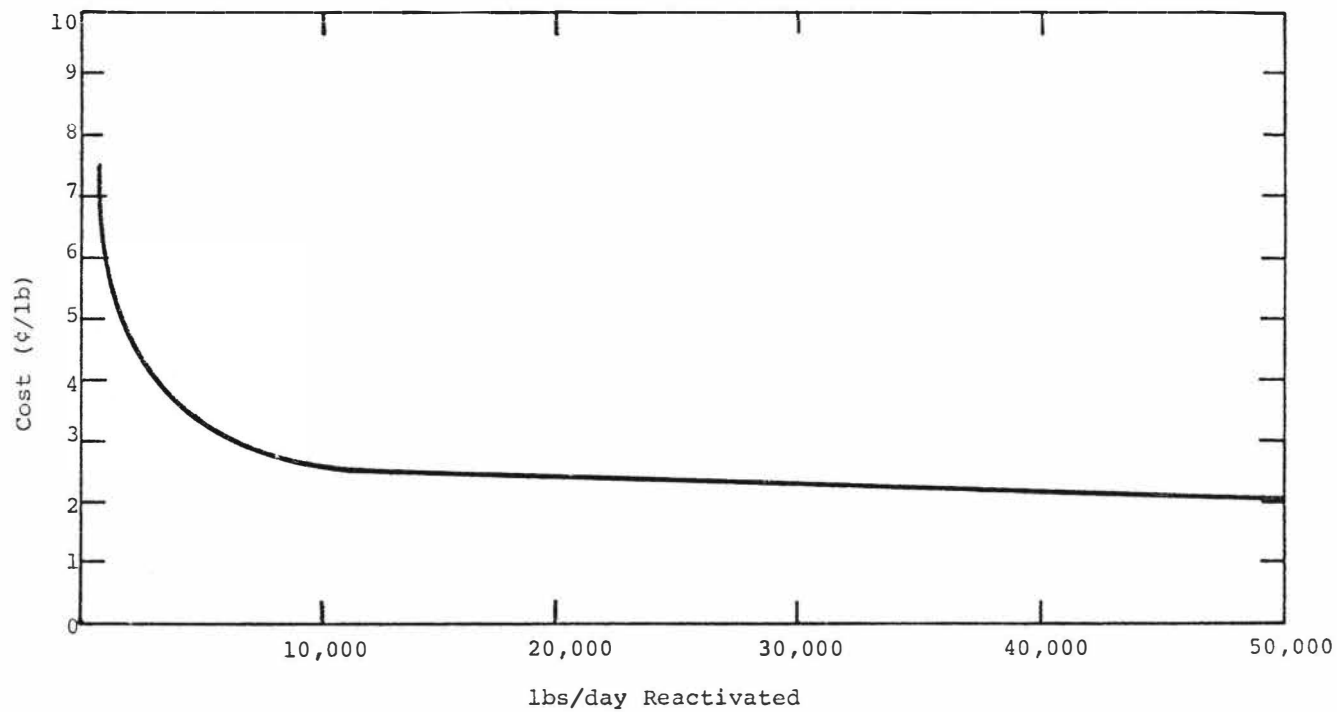


FIG. 1

FIG. 2 SCHEMATIC FOR ADSORPTION AND REACTIVATION⁽⁸⁾

FIG. 3 REACTIVATION COSTS ⁽⁷⁾

LIQUID-LIQUID EQUILIBRIUM OF TERNARY SYSTEMS HYDROCARBONS -
-FLUOROCARBON.

I.Kikic, P.Alessi

Liquid-liquid equilibrium was studied in the systems n-heptane - A - perfluorocyclic oxide (where A indicates n-hexane, 1-heptene, toluene or propionitrile) at 23°C in order to evaluate the effect of the non-ideality of the system n-heptane - A on the ternary systems. The separation factor of perfluorocyclic oxide in regard to the n-heptane - A pair was determined. A linear relationship was obtained between the natural logarithm of the separation factor and the excess free energy, both evaluated at a composition of 50 mole per cent of n-heptane in the systems.

Istituto di Chimica Applicata dell'Università degli Studi,
Trieste - Centro di Chimica Analitica Strumentale C.N.R., Bari.

Introduction

Fluorocarbon compounds are of remarkable interest as additives for increasing the surface tension of solutions and as antisolvents for the separation of hydrocarbons. Fluorocarbons containing atoms other than fluorine (for example, nitrogen or oxygen) are very important for these uses.

Mair ⁽¹⁾ points out that, with many hydrocarbons, the perfluorocyclic oxide $C_8F_{16}O$ forms azeotropes whose properties are different from those of the azeotropes formed by hydrocarbons with polar solvents.

In spite of these interesting properties, no exhaustive study which completely characterizes the behaviour of systems containing fluorocarbons is available in the literature. In fact, the papers of Scott ⁽²⁾, Kyle ⁽³⁾ and Hildebrand ⁽⁴⁾ consider binary hydrocarbon-fluorocarbons systems, and only mutual solubilities were experimentally determined for these systems.

The present Authors believe that the experimental determination of the behaviour of fluorocarbons in ternary systems is very important both for theoretical studies and for industrial applications, as these systems are similar to those involved in solvent extraction practice.

In the present work the concentrations of the two phases in equilibrium were experimentally determined for systems n-heptane (1) - A(2) - $C_8F_{16}O$ (3). Different substances were used as A (n-hexane, 1-heptene, toluene, propionitrile) to vary the non-ideality of the 1-2 binary mixture, so that its influence upon the ternary system could be studied. Non-ideality variations with temperature were also studied. The results were correlated and interpreted by NRTL equation ^(5,6).

Experimental

The hydrocarbons examined were high purity products (Fluka, BDH - 99.9 mole per cent minimum purity); when analyzed by GLC,

the impurities found did not exceed 0.05 mole per cent. The solvents propionitrile (Fluka) and $C_8F_{16}O$ (3M Minnesota) did not contain any detectable impurity.

Liquid-liquid equilibrium was established in 10 ml test tubes closed at the two ends by pierceable gaskets to allow the sampling of the two phases with a syringe. During the whole operation the test tubes were kept at constant temperature ($23^{\circ}C$ or $-40^{\circ}C$) in a liquid circulation thermostat (bath control within $0.02^{\circ}C$), which was shaken for at least 30 minutes. The time required for equilibration was more than four hours. Subsequently, the samples of the two phases were withdrawn with a syringe and immediately analyzed by GLC. Particular accuracy was devoted to the precooling of the syringe in the tests at $-40^{\circ}C$.

The mutual solubilities of the binary mixtures were determined both by GLC and by the cloud point method.

Results

The concentrations, in terms of mole fractions, of the two liquid phases in equilibrium are reported for the systems n-heptane - n-hexane - $C_8F_{16}O$, n-heptane - 1-heptene - $C_8F_{16}O$, n-heptane - toluene - $C_8F_{16}O$ and n-heptane - propionitrile - $C_8F_{16}O$ at $23^{\circ}C$ in Tables 1, 2, 3, 4, for the system n-heptane - toluene - $C_8F_{16}O$ at $-40^{\circ}C$ in Table 5.

Figure 1 presents the distribution isotherms and the tie lines for the system n-heptane - n-hexane - $C_8F_{16}O$. In the systems studied, the distribution isotherms are similar, as they all consist of two partially miscible pairs and one miscible pair (systems of type II).

Discussion

For a correct interpretation of the experimental results, these were correlated and interpreted with the non-random two liquid (NRTL) equation, which is particularly suitable to describe

liquid systems with partial miscibility.

The NRTL equation for the molar excess Gibbs energy of a multicomponent mixture is

$$g^E = RT \sum_{i=1}^N x_i \frac{\sum_{j=1}^N x_j G_{ji} \tau_{ji}}{\sum_{k=1}^N x_k G_{ki}} \quad (1)$$

where N is the number of components of the system;

$$G_{ji} = \exp\left(-\alpha_{ji} \frac{C_{ji}}{RT}\right) \quad (1a)$$

$$\tau_{ji} = \frac{C_{ji}}{RT} \quad (1b)$$

$$C_{ji} = g_{ji} - g_{ii} = C_{ji}^C + C_{ji}^T (T - 273.15) \quad (1c)$$

$$\alpha_{ji} = \alpha_{ji}^C + \alpha_{ji}^T (T - 273.15) \quad (1d)$$

The parameters α_{ji} and C_{ji} were determined from the experimental data through the minimum of the function F

$$F = \sum_{i=1}^L \sum_{j=1}^3 \left[(a_j^1)_i - (a_j^2)_i \right]^2 \quad (2)$$

where L is the number of tie lines.

The temperature dependence of C_{ji} and α_{ji} (eqs. 1c and 1d) was considered only for the systems n -heptane - $C_8F_{16}O$, n -heptane - toluene and toluene - $C_8F_{16}O$.

There was good agreement between the experimental tie lines and those calculated using the values obtained for the parameters which are reported in Table 6; the deviations are about 0.5% on the average, but never higher than 1.5%.

The values of the parameters for the binary systems n -hexane - n -heptane, n -heptane - toluene agree very well with those reported by Renon⁽⁷⁾.

From the data of Table 6 the molar excess Gibbs energies were

calculated according to eq.1 for the binary mixtures with complete miscibility. The values found for a composition of 50 mole per cent ($g_{0.5}^E$) are reported in Table 7 together with the ($C_{FC,A} - C_{FC,nC_7}$)

values ($FC = C_8F_{16}O$, $nC_7 = n$ -heptane). The five binary mixtures present different deviations from ideality: the systems n -hexane - n -heptane and n -heptane - 1-heptene are nearly ideal, while the system n -heptane - propionitrile is strongly non-ideal; the same trend is also evident for the ($C_{FC,A} - C_{FC,nC_7}$) values.

The effect of the non-ideality of the 1-2 binary systems on the ternary system appears also from a comparison of the distribution isotherms. The branch of the isotherm corresponding to the $C_8F_{16}O$ -poor phase is similar in all the systems, but with increasing ideality of the 1-2 system it gradually becomes parallel to the side of the triangular diagram relative to the 1-2 system. As can be seen from Figure 2, the branches of the isotherm which represent the $C_8F_{16}O$ -rich phase pivot on point A (solubility of n -heptane in $C_8F_{16}O$), progressively departing from the vertex (pure $C_8F_{16}O$) with increasing ideality.

From the concentration data reported in Tables 1-5 the values of the separation factor β of $C_8F_{16}O$ in regard to the solutes 1 and 2 were calculated using the equation:

$$\beta = \frac{x_1^{(2)}}{x_2^{(2)}} \cdot \frac{x_2^{(1)}}{x_1^{(1)}}$$

In Figure 3, $\log \beta$ is plotted versus n -heptane composition (reported as $\frac{x_1^{(1)}}{x_1^{(1)} + x_2^{(1)}}$).

It can be noticed that the separation factor obtained for the systems n -heptane - n -hexane, n -heptane - 1-heptene is constant and near to unity. For the other systems this separation factor varies remarkably with concentration. The β values increase with increasing non-ideality of the 1-2 binary system con-

sidered, as is confirmed by the diagram of Figure 4, where $\log \beta_{0.5}$ is plotted against $g_{0.5}^E$ (both evaluated for a composition of 50 mole per cent of n-heptane). The linear relation obtained between $\log \beta_{0.5}$ and $g_{0.5}^E$ allows the latter to be evaluated, if the separation factor in regard to the components 1 and 2 is known.

By varying the temperature it is possible to vary the non-ideality of the 1-2 binary system without changing the component 2. Therefore, the $g_{0.5}^E$ value and the separation factor of $C_8F_{16}O$ (Figure 3) were calculated for the system n-heptane - toluene - $C_8F_{16}O$ also at $-40^\circ C$. Between the $g_{0.5}^E$ and the $\log \beta_{0.5}$ values evaluated for the system at $-40^\circ C$ there is the same linear relationship found for all the systems at $23^\circ C$ (the point falls on the same straight line of Figure 4); this behaviour can be related to the peculiar solvent properties of perfluorocyclic oxide, which become more apparent in the ternary systems.

Conclusions

The results obtained in this work show that the ternary systems containing perfluorocyclic oxide are strongly dependent upon the non-ideality of the 1-2 system. It follows that liquid-liquid equilibrium in such ternary systems can be used as a method for the investigation of the binary systems in place of the classical method of liquid-vapour equilibrium.

Acknowledgment

The writers thank Prof. P. Papoff for helpful discussions.

References

- (1) Mair B.J. Analyt.Chem. 1956, 28, 52.
- (2) Scott R.L. J.phys.Chem., 1958, 62, 136.
- (3) Kyle B.G., Reed T.M.III J Amer.chem.Soc. 1958, 80, 6170.
- (4) Hildebrand J.H., Scott. R.L., "Regular Solutions" 1962
(Englewood Cliffs, N.J., Prentice-Hall).
- (5) Renon H., Prausnitz J.M., A.I.Ch.E.Journal, 1968, 14, 135.
- (6) Renon H., Prausnitz J.M., Industr.Engng.Chem.Process Design
and Development 1969, 8, 413.
- (7) Renon H., Asselineau L., Cohen G., Raimbault C. "Calcul sur
ordinateur des équilibres liquide-vapeur et liquide-liquide"
1971 (Paris, Ed. Technip).

Notation

- $(a_j^1)_1$ = activity of the component j in the phase 1 for the tie line 1
- $(a_j^2)_1$ = activity of the component j in the phase 2 for the tie line 1
- $C_{ji} = g_{ji} - g_{ii}$ (cal/mole)
- C_{ji}^C = value of the C_{ji} parameter at 273°K (cal/mole)
- g_{ji} = parameter of free energy for the j-i interaction (cal/mole)
- g_{ii} = parameter of free energy for the i-i interaction (cal/mole)
- g^E = molar excess Gibbs energy (cal/mole)
- $g_{0.5}^E$ = molar excess Gibbs energy at 50 mole per cent composition (cal/mole)
- L = number of tie lines
- N = number of components
- R = gas constant (cal/mole . °K)
- T = absolute temperature (°K)
- $x_i^{(1)}$ = mole fraction of component i in the phase 1
- $x_i^{(2)}$ = mole fraction of component i in the phase 2

Greek Letters

- $\alpha_{ji} = \alpha_{ij}$ = parameters which represent the nonrandomness of the mixture
- α_{ji}^C = value of the α_{ji} parameter at 273°K
- β = separation factor

Table 1

Composition of the two phases in equilibrium at 23°C
for the system n.heptane(1)-n.hexane(2)-C₈F₁₆O(3)

$x_1^{(1)}$	$x_2^{(1)}$	$x_3^{(1)}$	$x_1^{(2)}$	$x_2^{(2)}$	$x_3^{(2)}$
0.92590	-	0.07410	0.20070	-	0.79930
0.77338	0.15180	0.07482	0.18884	0.03951	0.77165
0.57095	0.35343	0.07563	0.14285	0.09441	0.76274
0.42711	0.49296	0.07993	0.10892	0.13509	0.75598
0.28411	0.63168	0.08420	0.07378	0.17735	0.74887
-	0.89050	0.10950	-	0.25800	0.74200

Table 2

Composition of the two phases in equilibrium at 23°C
for the system n.heptane (1)-1.heptene(2)-C₈F₁₆O(3)

$x_1^{(1)}$	$x_2^{(1)}$	$x_3^{(1)}$	$x_1^{(2)}$	$x_2^{(2)}$	$x_3^{(2)}$
0.92590	-	0.07410	0.20070	-	0.79930
0.83345	0.09330	0.07325	0.18770	0.02110	0.79120
0.60790	0.32010	0.07200	0.14450	0.07350	0.78200
0.32220	0.61190	0.06590	0.07750	0.14430	0.77820
0.08580	0.85190	0.06230	0.01940	0.19730	0.78330
-	0.92980	0.07020	-	0.21150	0.78850

Table 3

Composition of the two phases in equilibrium at 23°C
for the system n.heptane(1)-toluene(2)-C₈F₁₆O(3)

$x_1^{(1)}$	$x_2^{(1)}$	$x_3^{(1)}$	$x_1^{(2)}$	$x_2^{(2)}$	$x_3^{(2)}$
0.92590	-	0.07410	0.20070	-	0.79930
0.87950	0.04820	0.07230	0.19420	0.00950	0.79630
0.78210	0.15580	0.06210	0.17200	0.02860	0.79940
0.44950	0.51200	0.03850	0.08450	0.06050	0.85500
0.13150	0.85700	0.01150	0.03100	0.09050	0.87850
0.03970	0.95210	0.00820	0.00890	0.08650	0.90460
-	0.99500	0.00500	-	0.08670	0.91330

Table 4

Composition of the two phases in equilibrium at 23°C
for the system n.heptane(1)-propionitrile(2)-C₈F₁₆O(3)

$x_1^{(1)}$	$x_2^{(1)}$	$x_3^{(1)}$	$x_1^{(2)}$	$x_2^{(2)}$	$x_3^{(2)}$
0.92590	-	0.07410	0.20070	-	0.79930
0.67250	0.29820	0.02930	0.14520	0.02800	0.82680
0.58400	0.39130	0.02470	0.13160	0.02750	0.84090
0.20150	0.79100	0.00750	0.09000	0.02550	0.88450
0.10500	0.88790	0.00710	0.06500	0.02500	0.91000
0.06310	0.93380	0.00310	0.02750	0.01780	0.95470
-	0.99730	0.00270	-	0.01620	0.98380

Table 6

Parameter values obtained by NRTL equation for the binary systems

Systems		Parameters			Temperature
i	j	α_{ij}	C_{ij}	C_{ji}	$^{\circ}\text{C}$
n-heptane	n-hexane	0.200	428.5	-405.8	23
n-heptane	1-heptene	0.300	25.0	20.0	23
n-heptane	toluene	0.200	-177.0	511.4	23
n-heptane	propionitrile	0.250	240.0	706.0	23
n-heptane	$\text{C}_8\text{F}_{16}\text{O}$	0.2058	1574.1	332.0	23
n-hexane	$\text{C}_8\text{F}_{16}\text{O}$	0.205	1450.0	305.0	23
1-heptene	$\text{C}_8\text{F}_{16}\text{O}$	0.205	1410.0	420.0	23
Toluene	$\text{C}_8\text{F}_{16}\text{O}$	0.212	2480.0	520.0	23
Propionitrile	$\text{C}_8\text{F}_{16}\text{O}$	0.200	2589.0	1330.0	23
n-heptane	toluene	0.200	-88.8	468.2	-40
n-heptane	$\text{C}_8\text{F}_{16}\text{O}$	0.192	1710.0	1180.0	-40
Toluene	$\text{C}_8\text{F}_{16}\text{O}$	0.195	2860.0	1410.0	-40

Table 5

Composition of the two phases in equilibrium at -40°C for the system n-heptane(1)-toluene(2)- $\text{C}_8\text{F}_{16}\text{O}$ (3)

$x_1^{(1)}$	$x_2^{(1)}$	$x_3^{(1)}$	$x_1^{(2)}$	$x_2^{(2)}$	$x_3^{(2)}$
0.99300	-	0.00700	0.01580	-	0.98420
0.88910	0.10440	0.00650	0.01360	0.00140	0.98500
0.67700	0.31860	0.00440	0.01083	0.00347	0.98570
0.48340	0.51400	0.00260	0.00837	0.00484	0.98679
0.21570	0.78320	0.00110	0.00553	0.00697	0.98750
0.08170	0.91770	0.00060	0.00220	0.00774	0.99006
-	0.99990	0.00010	-	0.01060	0.98940

Table 7

Molar excess Gibbs energies for the binary systems n.heptane-A

Systems		$E_{0.5}^E$	${}^C_{FC,A} - {}^C_{FC,nC_7}$	Temperature
nC_7	A			$^{\circ}C$
n.heptane-n.hexane		-9.102	-27.0	23
n.heptane-1.heptene		11.180	88.0	23
n.heptane-toluene		71.050	188.0	23
n.heptane-propionitrile		207.150	998.0	23
n.heptane-toluene		106.950	230.0	-40

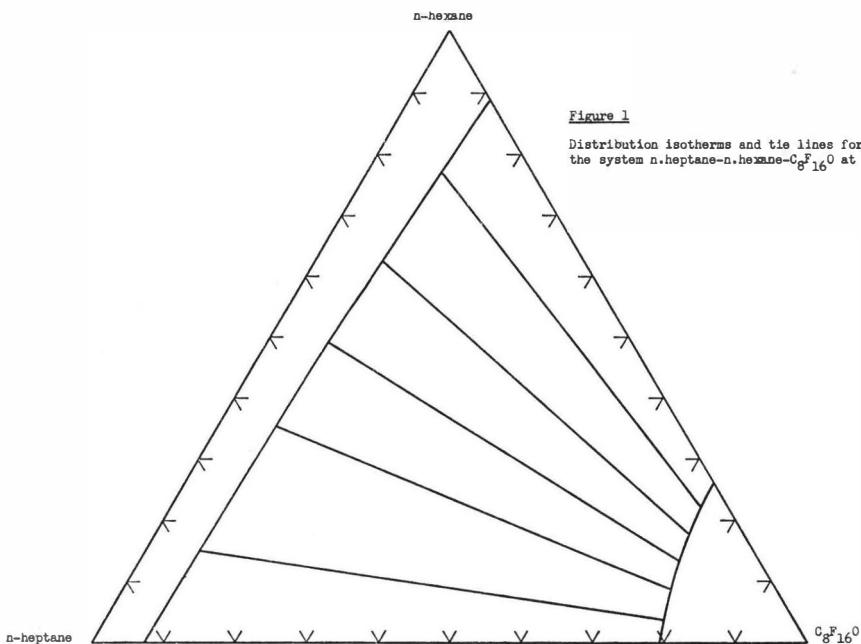


Figure 1

Distribution isotherms and tie lines for the system n-heptane-n-hexane- $C_8F_{16}O$ at $23^\circ C$

- +++++ n-heptane-n-hexane at $23^\circ C$
- n-heptane-1-heptene at $23^\circ C$
- n-heptane-Toluene at $23^\circ C$
- n-heptane-propionitrile at $23^\circ C$

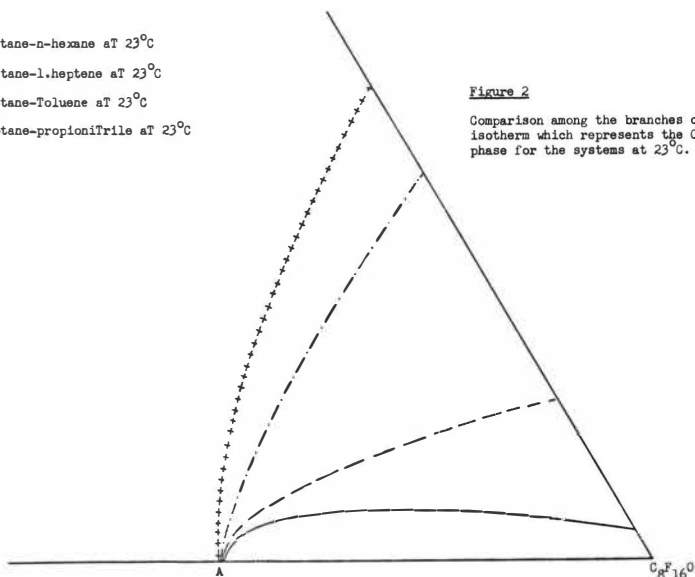


Figure 2

Comparison among the branches of the isotherm which represents the $C_8F_{16}O$ -rich phase for the systems at $23^\circ C$.

Figure 3

Separation factor variation with n.heptane composition.

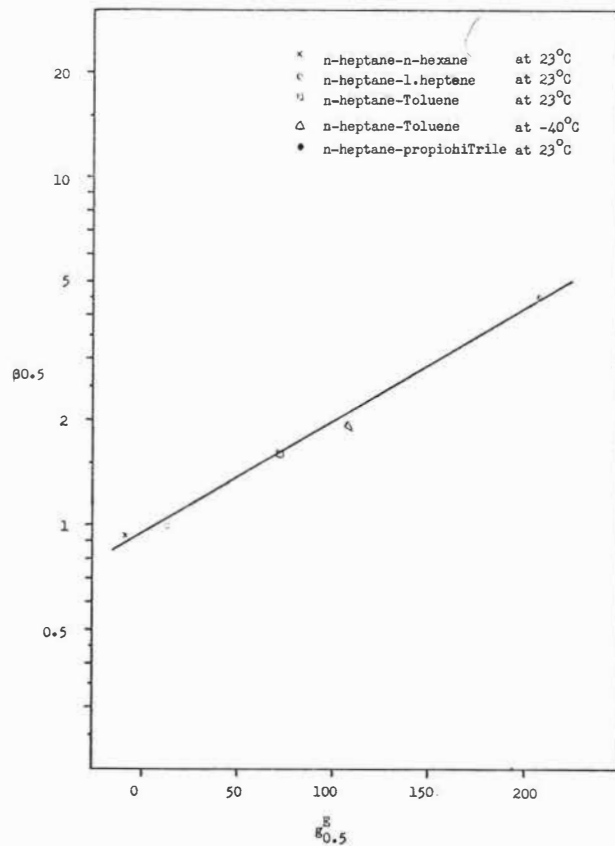
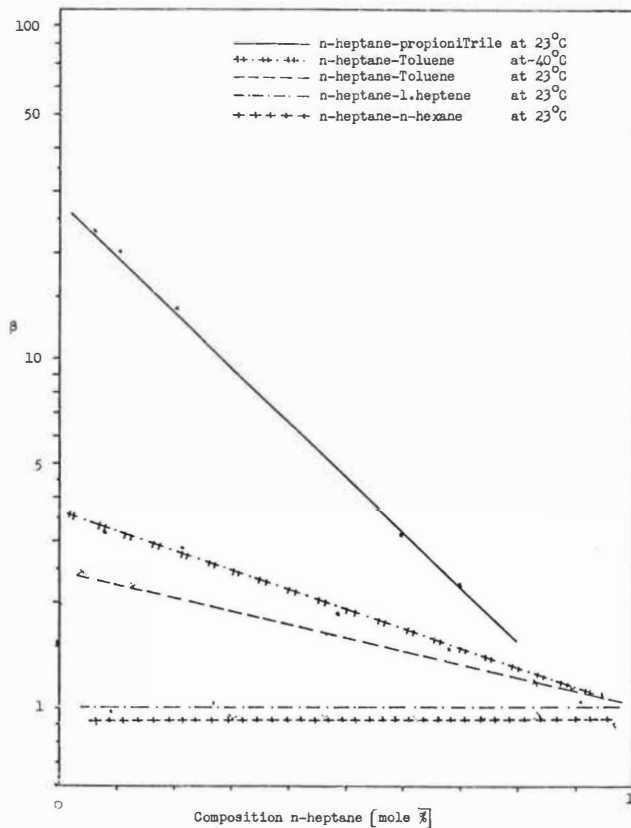


Figure 4

Relation between the separation factor and molar excess free energy at 50 mole per cent composition.

THE SEPARATION OF DICHLOROPHENOLS BY DISSOCIATION/EXTRACTION

SUMMARY

Separation of certain mixtures of dichlorophenols, difficult, if not impossible, by any other physical means was achieved by exploiting the difference in acidities in a dissociation/extraction procedure. This was accomplished by use of a Graesser Contactor, a commercial multistage counter-current extraction apparatus.

Mixtures of 2,4- and 2,5-dichlorophenols and 2,3- and 2,6-dichlorophenols were partially separated by counter-current extraction with caustic soda or, better, with sodium carbonate solution. Increased temperature had little or no effect on the efficiency of separation, but high concentrations of dichlorophenols in the solvent or alkali in water both brought about complications which diminished the efficiency.

Extracting the alkali extract of a dichlorophenol mixture with a secondary solvent was found to be an alternative and more economic method of recovering the dichlorophenols than direct acidification.

By treating the counter-current apparatus as a fractionation column it was shown that if the product isomers were recycled as reflux the purity of the products were greatly enhanced.

M. H. Milnes,
Coalite & Chemical Products Ltd.,
P.O. Box 21,
Chesterfield,
Derbyshire.

INTRODUCTION

Hydrolysis of polychlorobenzenes using caustic soda and a solvent is a convenient route to chlorophenols not accessible by normal chlorination means.¹ This method is used extensively in producing the pesticide intermediates 2,4,5-trichlorophenol and 2,5-dichlorophenol from 1,2,4,5-tetrachlorobenzene and 1,2,4-trichlorobenzene, respectively. In the case of 1,2,4-trichlorobenzene hydrolysis, the product contains all three dichlorophenols predictable from its orientation, the 2,5-isomer being the predominant one. A binary dichlorophenol mixture, consisting of the 2,3- and 2,6-isomers, arises from the hydrolysis of 1,2,3-trichlorobenzene, and the resolution of this mixture as well as the hydrolysate of 1,2,4-trichlorobenzene into pure dichlorophenols is a matter of some difficulty. The general theory of dissociation/extraction, as a method by which weak acids can be separated by their respective affinities for alkali has been already fully covered by Hanson and co-workers.² According to the work of Murray and Gordon³, and Tiessens⁴ the dichlorophenols and also the trichlorophenols possess widely varying dissociation constants, which provide a satisfactory basis for their separation, i.e.

<u>Isomer</u>	<u>K x 10¹⁰</u>
2,6-dichlorophenol	1600
2,5-dichlorophenol	450
2,3-dichlorophenol	360
2,4-dichlorophenol	180
3,5-dichlorophenol	120
3,4-dichlorophenol	41
2,3,6-trichlorophenol	7600
2,4,6-trichlorophenol	3800
2,3,5-trichlorophenol	540
3,4,5-trichlorophenol	470
2,3,4-trichlorophenol	260
2,4,5-trichlorophenol	180

These differences in acidity are much greater than for 2,4- and 2,5-xylenols which were separated on this basis by

Coleby⁵, and m- and p-cresol by Anwar et al². A method of separation of dichlorophenol isomers has now been devised⁶ using a commercial continuous counter-current process, and the efficiency of this process is enhanced by "reflux" of the isomers.

EXPERIMENTAL

(1) Materials:

The dichlorophenol mixtures were either hydrolysates of 1,2,4- or 1,2,3-trichlorobenzenes fractionally distilled to give binary dichlorophenol mixtures and leave polyglycols as distillation residues, or mother liquors from crystallisations, containing a broader mixture of dichlorophenols.

2,4-/2,5-dichlorophenol feedstocks

	<u>Percentages</u>					
	<u>2,4-</u>	<u>2,5-</u>	<u>3,4-</u>	<u>2,3-</u>	<u>2,6-</u>	<u>Pet. Ether</u>
A	37.2	39.5		Trace	Trace	
B	29.2	28.1	5.2	4.7	10.9	21.9
C	14.6	82.5				

2,3-/2,6-dichlorophenol feedstocks

	<u>Percentages</u>		
	<u>2,3-</u>	<u>2,6-</u>	<u>2,4-</u>
D	31.6	43.6	Trace
E	46.4	47.5	
F	48.8	46.2	

Aqueous Solutions

50 g/l. caustic soda solution and also solutions of sodium carbonate of 25, 50, 100 and 125 g/l. concentrations.

Reflux solutions

- (i) A toluene solution of 75 g/l. of a mixture of 95% 2,6- and 5% 2,3-dichlorophenols,

- (ii) An aqueous solution containing 50 g/l. sodium carbonate and 53 g/l. of a mixture of 95% 2,3-D.C.P. 5% 2,6-D.C.P.
- (iii) Equilibrated solutions: a toluene solution of feedstock at 300 g/l. shaken to equilibrium with 0.715 x its volume of 50 g/l. sodium carbonate solution, the phases then separated and fed per se.

(2) Equipment:

The countercurrent mixing device was either one or a combination of two laboratory Graesser contactors of five theoretical stages. The latter is described in British Patents No. 860,880; 972,035 and 1,037,573 and is a cylindrical vessel (volume 6 l.) through which the two phases flow counter-currently in a substantially horizontal direction, the vessel being provided with a rotor which serves to bring the phases into repeated contact by carrying portions of the heavier phase up into the lighter phase and vice versa.

(3) Work-up of product and analysis:

The raffinate phase was normally freed from solvent by distillation at atmospheric pressure followed by a reduction in pressure to remove the last traces. The product was substantially a mixture of dichlorophenols, except in one or two cases, when sodium dichlorophenates were present.

The dichlorophenolate phase was agitated and acidified to give dichlorophenol mixtures (unless otherwise stated). Frequently the product was a solid and this was filtered off, washed and dehydrated by distillation. In the case of liquid products, the organic phase was separated and dehydrated as before.

Analysis of the dichlorophenol mixtures was then done by gas liquid chromatography on the trimethylsilylethers, eluted in a nitrogen stream over 10% OV1 silicone on AWD MCS Chromosorb W, using a flame ionisation detector. It was normal to use an internal standard, commonly 3,5-dichlorophenol, an isomer not present in these mixtures.

RESULTS

(1) 2,4-/2,5-dichlorophenol separation

Initially a small laboratory experiment demonstrated the feasibility of this process. 500 ml of 50 g/l. feedstock A in toluene was brought to equilibrium with 100 ml of 50 g/l. caustic soda in a separating funnel (theoretical extraction 50%); the phases separated and the aqueous extract again brought into equilibrium with 500 ml of fresh 50 g/l. A in toluene. This process was repeated three times more so that the aqueous phase had undergone the equivalent of a 5 stage process. Analysis of the dichlorophenolate showed the process worked well, increasing the 2,5-D.C.P. : 2,4-D.C.P. ratio from 1.06 to 7.18, but, during the 5-stages, the trace quantities of the 2,6- and 2,3-dichlorophenols had built up appreciably.

	<u>A</u>	<u>Extract</u>
% 2,5-dichlorophenol	39.5	47.7
% 2,4-dichlorophenol	37.2	6.7
% 2,6-dichlorophenol	Trace	23.3
% 2,3-dichlorophenol	Trace	22.3

Using a Graesser contactor (rotor speed 18 r.p.m.) to pass 125 g/l. feedstock B in butyl acetate against 50 g/l. caustic soda, an extraction rate of 68% was intended. In fact only 19% of the phenols were extracted, due to high solubility of sodium dichlorophenates in the butyl acetate. Again, although separation of 2,5- and 2,4-dichlorophenols did occur,

the much more acidic 2,6- and 2,3-dichlorophenols tended to be preferentially extracted.

	<u>B</u>	<u>Raffinate</u>	<u>Dichlorophenolate</u>
% 2,5-dichlorophenol	28.1	26.2	47.1
% 2,4-dichlorophenol	29.2	29.0	18.3
% 3,4-dichlorophenol	5.2	6.3	----
% 2,6-dichlorophenol	10.9	----	20.9
% 2,3-dichlorophenol	4.7	2.2	7.6
% Pet Ether	21.9	N.E.	

It was shown that sodium carbonate solutions would preferentially extract the most acidic dichlorophenols according to the following equation:



Passing a 360 g/l. solution of C in toluene and 100 g/l. sodium carbonate solution through a Graesser contactor, at a theoretical extraction rate of 12.5%, considerable separation of the isomers was achieved:

	<u>C</u>	<u>Raffinate</u>	<u>Dichlorophenolate</u>
% 2,5-dichlorophenol	82.5	68.1	92.8
% 2,4-dichlorophenol	14.6	29.2	7.2

At higher concentrations of sodium carbonate solution the contactor became blocked due to precipitation of sodium bicarbonate in accordance with the above equation.

(2) 2,3-/2,6-dichlorophenol separation

The separation of these two isomers should be more facile than for the 2,4-/2,5-dichlorophenol system, owing to the greater difference in acidities.²

Passing a 125 g/l. solution of feedstock D in toluene counter-current to 25 g/l. sodium carbonate solution through

a Graesser contactor with rotor speed 14 r.p.m. at a theoretical extraction rate of 15% gave a good separation, viz:

	<u>D</u>	<u>Raffinate</u>	<u>Dichlorophenolate</u>
% 2,6-dichlorophenol	43.6	5.6(14.4)	75.3(58.2)
% 2,3-dichlorophenol	31.6	38.2(25.5)	5.6(35.1)
% 2,4-dichlorophenol	Trace	2.5(2.3)	---

In brackets are the figures for a straight single-stage contact of the feedstock and carbonate solutions in a separating funnel. Improved separation figures were given when the raffinate and dichlorophenolate from the last experiment were each passed through the Graesser contactor counter-current to 25 g/l. sodium carbonate and fresh 125 g/l. feed stock D in toluene, viz:

	<u>Raffinate/sodium carbonate</u>	<u>Dichlorophenolate/12.5% D in toluene</u>
	<u>Second Raffinate</u>	<u>Dichloro phenolate</u>
		<u>Dichloro phenolate</u>
% 2,6-dichlorophenol	6.4	70.2
% 2,3-dichlorophenol	62.4	29.8
		88.1
		11.9

Effect of temperature

The feeds for this experiment were heated to 50°C by means of steam bayonets in the feed drums and the Graesser contactor maintained at this temperature by steam tracing. Passing the feedstock and sodium carbonate solutions under the same conditions as experiment 1 gave products of virtually the same composition as before, showing that increased temperature brings about no material benefit in the isomer separation. There was, however, an improved phase separation under these conditions, no trace of emulsion appearing in either phase.

Utilising two Graesser contactors coupled in series, a counter-current extraction was done with 125 g/l. feedstock E in toluene flowing against 50 g/l. sodium carbonate solution at a theoretical extraction rate of 50%. The results of a snap

sample were sufficiently encouraging to do a prolonged run, which proved to be less efficient than the snap sample suggested, viz:

	<u>Snap Sample</u>			<u>Long Run (500 l. each phase)</u>	
	<u>E</u>	<u>Raffinate</u>	<u>Dichloro phenolate</u>	<u>Raffinate</u>	<u>Dichloro phenolate</u>
% 2,6-dichlorophenol	47.5	10.2	99.0	25.9	95.0
% 2,3-dichlorophenol	46.4	88.8		73.1	5.0

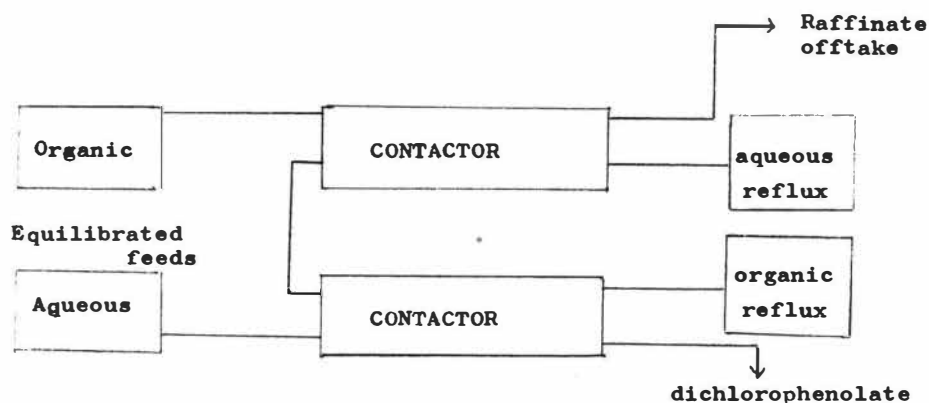
Effect of concentration

The low concentration of the required products in the output phases is a feature adverse to the commercial exploitation of this process. When high concentration of dichlorophenols in toluene (958 g/l. feedstock F in toluene) was extracted counter-current with 100 g/l. sodium carbonate a reversal of phases occurred in the contactor, the organic layer being on the bottom, but this posed no operational difficulties.

At 30% extraction, emulsification became a problem since the specific gravities of the output phases approached each other. Although a fair separation of the dichlorophenols occurred, the raffinate phase contained an unacceptably high quantity of sodium salts, solubilised by the high dichlorophenol content.

Application of the principle of reflux

Considering the counter-current equipment as a distillation column, the efficiency of separation of isomers can be enhanced by adding a reflux of the required isomer at the appropriate end at which it is removed. In the case of 2,3-/2,6-dichlorophenol separation the arrangement of feeds and apparatus was as shown in the diagram.



Initially a toluene solution of feedstock F (303 g/l.) was agitated to equilibrium with 50 g/l. sodium carbonate solution (0.715 vols: 1 vol sodium carbonate) to give an actual extraction of 50%. The equilibrated feeds were then each fed into a separate contactor counter-current to a reflux either of solvent or a solution of the isomer to be taken off in the reverse phase. In this way, mass transfer of dichlorophenols between the phases was avoided, only exchange of isomers between the phases occurring. Thus 2,6-dichlorophenol was removed as an aqueous solution of its sodium salt at point X, at the same end as a toluene solution of 2,6-dichlorophenol was introduced as a reflux. A similar situation arises at point Y, where 2,3-dichlorophenol is removed in toluene solution at the same end as it is introduced as an aqueous solution of its sodium salt.

Relatively unfavourable results were obtained when toluene and sodium carbonate solutions were used as reflux:

<u>Experiment Number</u>	<u>1</u>	<u>2</u>
Type of reflux used: organic	Toluene	Toluene
aqueous	50 g/l. Na_2CO_3	50 g/l. Na_2CO_3
Reflux ratios: organic	0.5:1	2:1
aqueous	0.5:1	2:1
Raffinate: % 2,3-dichlorophenol	81.7	72.5
% 2,6-dichlorophenol	16.2	25.3

Dichlorophenolate: % 2,6-dichlorophenol	87.9	79.5
% 2,3-dichlorophenol	12.1	20.4

Excellent results were obtained when reflux of 95% pure isomers were used (Table 1). High purity 2,3- and 2,6-dichlorophenols were removed from separate ends of the counter-current extraction system.

TABLE 1

<u>Experiment No:</u>	3	4	5	6	7	8A	8B	9	10
<u>Reflux ratios:</u>									
organic	3.22	4.36	3.22	2.43	2.50	2.88	2.88	2.50	3.67
aqueous	0.78	2.61	2.09	2.17	2.50	3.53	3.53	2.50	3.17

Raffinate:

% 2,3-DCP	86.7	98.0	95.6	81.6	92.5	95.0	99.3	97.3	82.7
% 2,6-DCP	13.3	2.0	4.3	10.6	3.0	2.1	0.7	1.6	3.8

Dichlorophenolate:

% 2,6-DCP	96.4	99.0	99.0	98.5	99.0	79.2	78.6	98.1	*
% 2,3-DCP	3.4	Trace	Trace	1.5	1.0	19.0	18.9	1.9	*

* recycled as reflux

Type of reflux used:

organic:	95% 2,6-DCP) dissolved in toluene at a rate of 5% 2,3-DCP) 75 g/l.
aqueous:	95% 2,3-DCP) dissolved at a rate of 53 g/l. in 50 g/l. 5% 2,6-DCP) sodium carbonate

DISCUSSION

The favourable distribution of dissociation constants of the dichlorophenol isomers made this system theoretically a good one for resolution by dissociation/extraction. This was proved to be factual by experiment. In the 1,2,4-trichlorobenzene hydrolysate system, the three dichlorophenol isomers formed can be easily split by distillation into a 2,4-/2,5-distillate (containing 80% of the 2,5-) and a 3,4-dichlorophenol-rich

residue. The distillate can then be split on the basis of dissociation constants into a stronger acidic extract (2,5-) and a weaker acidic raffinate (2,4-) by counter-current contacting with mild alkali, aided by reflux.

The 1,2,3-trichlorobenzene hydrolysate system yields 2,3- and 2,6-dichlorophenols in approximately equal proportions, the mixture being completely incapable of separation by fractional distillation. Distillation is however advisable in order to obtain a fraction consisting substantially of the two isomeric dichlorophenols and free from impurities (e.g. polyglycols). This mixture of isomers is easily and completely separated by dissociation extraction; using reflux of both isomers improves the purities considerably.

No discernible advantage is gained by counter-current extracting at temperature higher than atmospheric. Operating at low concentrations is essential for obtaining high purity isomers: 50 g/l. for dichlorophenols in either phase is about the highest, otherwise solubilisation of sodium salts in the organic phase vitiates the separation.

A promising line of approach to improve the economics of the process is the extraction of dichlorophenols from the aqueous sodium salt phase by secondary solvent. Although not investigated very fully, this was found both theoretically feasible, and experimentally possible. Again, an adverse factor is the solubility of sodium dichlorophenolates in the solvent. If this problem can be overcome, the process could be successfully operated without large irreversible consumption of alkali and mineral acid.

REFERENCES

1. Brit. Pat. 1,221,019
2. Anwar M.M., Hanson C., and Pratt M.W.T.
Trans Instn. Chem. Engrs. 1971, 49.
3. Murray and Gordon
J. Amer. Chem. Soc. 1935,57, 110-111
4. Tiessens,
Rec. Trav. Chim.1929 48, 1066 and 1931, 50, 112
5. Coleby J.
Paper presented to symp. on liquid-liquid extract.
Newcastle on Tyne 20.21 April, 1971.
6. Brit. Pat. 1,316,276

ACKNOWLEDGEMENTS

The author wishes to thank the Board of Coalite & Chemical Products Ltd., for permission to publish, Dr. K. R. Payne and Mr. F. R. Moore for helpful discussions, Mr. K. F. Clarke for analytical work on samples and Messrs M. P. Talbot and G. Hasman for assistance in the practical work.